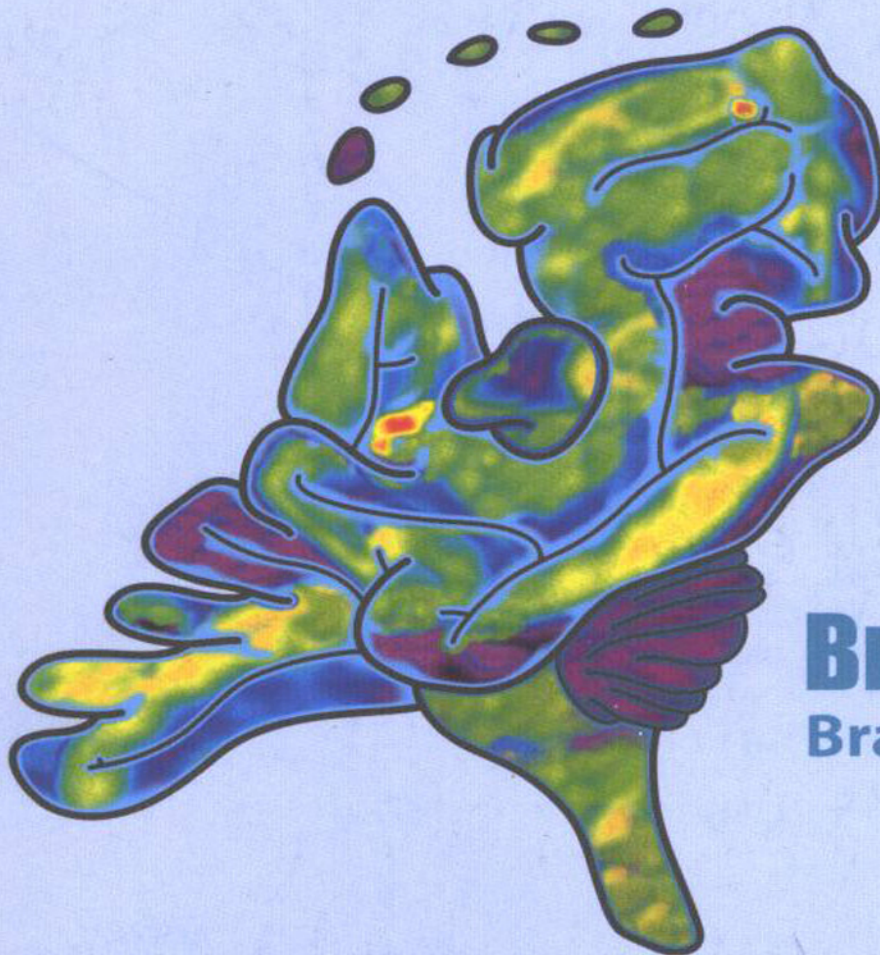


# Brain '05 & BrainPET '05

June 7 - 11, 2005

Vrije Universiteit, Amsterdam, the Netherlands



**Brain '05**  
**BrainPET '05**

XXII<sup>nd</sup> International Symposium on  
Cerebral Blood Flow, Metabolism, and Function  
&

VII<sup>th</sup> International Conference on  
Quantification of Brain Function with PET

[www.brain05.com](http://www.brain05.com)



&

## Search

Á

V@Á^æ&@Á!Áæ•dæ&Á^&ç}•Á-Á@Á[ & { ^} Á^~ã^Á[ à^Á[ àæÜ^æ^!Á  
Qnclude option for searching PDF files and accessibility support)Á Áã, Á  
ÜÖÁÁ•ÈV@•^ÁÜÖÁÁ•ÁæÁ^Á•Áã, ^áÁ•ã\*Á@Áæ•Á^!•ã}Á-Á  
Á[ à^Á[ àæÜ^æ^!Á@æÁ & á^Á] ç}Á!Á^æ&@\*ÁÜÖÁÁ•Áã áÁ  
æ&•ããÁ~]]!ÁÜ^æ^Á•ÁÜÜSÁÁÁ^æ&@•ã\*Á[~!Á^àÁ[, •^!É  
Á

Á



## LONG-TERM EFFECTS OF CHRONIC STATIN TREATMENT IN THE POST-ISCHEMIC BRAIN

**Karen Gertz**<sup>1</sup>, Golo Kronenberg<sup>1,2</sup>, Benjamin Winter<sup>1</sup>, Juri Katchanov<sup>1</sup>, Helmut Schröck<sup>3</sup>, Georg Nickenig<sup>4</sup>, Josef Priller<sup>1,2</sup>, Ulrich Laufs<sup>4</sup>, Matthias Endres<sup>1</sup>

<sup>1</sup>*Department of Neurology, Charite Berlin, Berlin, Germany*

<sup>2</sup>*Department of Psychiatry, Charite Berlin, Berlin, Germany*

<sup>3</sup>*Institute of Physiology, University of Heidelberg, Heidelberg, Germany*

<sup>4</sup>*Department of Cardiology, Saarland University, Homburg, Germany*

Pretreatment with statins, inhibitors of HMG-CoA reductase, augments cerebral blood flow during cerebral ischemia, resulting in neuroprotection via mechanisms related to the upregulation of endothelial nitric oxide synthase (eNOS). Endothelium-derived NO is also known to be essential for the growth of new vessels, and statins increase neovascularization through NO-dependent pathways. In addition, it has recently been demonstrated that statins mobilize bone marrow-derived endothelial progenitor cells, which are dependent on eNOS. Here, we investigated the long-term effects of the HMG-CoA reductase inhibitor rosuvastatin in a model of mild ischemic stroke. SV129 mice were treated by daily subcutaneous injections with rosuvastatin (2mg/kg body weight). Treatment started two weeks before 30 minutes of filamentous left middle cerebral artery occlusion (MCAo) and reperfusion and was continued for 4 additional weeks. Ischemic lesion size, functional outcome and eNOS regulation in the vasculature were determined in animals following sacrifice. Additionally, we measured absolute cerebral blood flow with the Iodo-C14-antipyrine-technique, counted capillary density via Evans blue perfusion signal and detected engraftment of bone marrow-derived progenitor cells and newly-generated endothelial cells within the ischemic lesion. We demonstrated that chronic continuous administration of rosuvastatin conferred long-term histologic and functional protection six weeks after cerebral ischemia. Upregulation of eNOS expression in the aorta was sustained until 6 weeks after onset of treatment, but neuroprotection was completely abolished when the NOS inhibitor L-NAME was co-administered. This shows that eNOS plays a role in the effect of rosuvastatin on tissue recovery. In addition, rosuvastatin augmented disc neovascularization, enhanced the engraftment of bone marrow-derived progenitor cells and the number of von-Willebrand-factor/bromodeoxyuridine double-positive cells in the lesion, indicating an angiogenic stimulus. The density of perfused vessels in the post-ischemic brain was not increased in rosuvastatin-treated animals while large increases in average caliber were observed four weeks after MCAo. Moreover, areas of enlarged vessels were associated with lower blood flow levels. In conclusion, stroke protection by chronic rosuvastatin treatment extends until weeks after the ischemic insult. While the protection is mediated by eNOS upregulation and accompanied by an angiogenic response, vessel density and absolute cerebral blood flow levels were not increased by chronic rosuvastatin treatment in the post-ischemic brain.

## MITOGEN ACTIVATED PROTEIN KINASE INHIBITION ATTENUATE CEREBRAL BLOOD FLOW REDUCTION AND ABOLISH CEREBRAL ARTERY RECEPTOR UPREGULATION AFTER SUBARACHNOID HAEMORRHAGE IN RAT

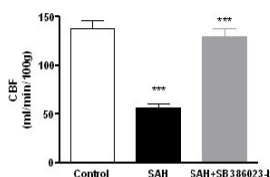
Saema Beg<sup>1,2</sup>, Jacob Hansen-Schwartz<sup>2</sup>, Lars Edvinsson<sup>1,2</sup>

<sup>1</sup>*Department of Medicine, Division of Vascular Research, Lund University, Lund, Sweden*

<sup>2</sup>*Department of Clinical Experimental Research, Glostrup University Hospital, Glostrup, Denmark*

Introduction: Previous studies have shown that endothelin type B (ETB) and 5-hydroxytryptamine type 1B (5-HT1B) receptors are upregulated following experimental subarachnoid haemorrhage (SAH). However, the intracellular pathways responsible for this upregulation remain unclear. Several studies have demonstrated an involvement of mitogen activated protein kinase (MAPK) in the pathogenesis of vasospasm after SAH, and this could possibly be an intracellular mediator of the ETB and 5-HT1B/2A receptor upregulation. The purpose of the present study was to test whether MAPK inhibition could alter the degree of SAH induced ET and 5-HT1 receptor upregulation in addition to prevent the cerebral blood flow reduction. Methods: SAH was induced by injecting 250  $\mu$ l blood into the prechiasmatic cistern. In conjunction and after the induced SAH the MAPK inhibitor SB-386023-b was injected intracisternally. Two days after the SAH basilar arteries (BA) and middle cerebral arteries (MCA) were harvested and contractile responses to endothelin-1 (ET-1; ETA and ETB receptor agonist) and 5-carboxamidotryptamine (5-CT; 5-HT1 receptor agonist) were investigated in sensitive myographs. To investigate if MAPK inhibition had an influence on the local CBF after SAH we used an autoradiographic technique. In addition, the mRNA levels of ET and 5-HT1 receptors were investigated by real time PCR. Results: SAH resulted in enhanced contraction to ET-1 and 5-CT, as well as increased levels of ETB and 5-HT1B receptor mRNA in BA and MCA. Administration of the MAPK inhibitor SB-386023-b during the SAH decreased the maximum contraction elicited by application of ET-1 and 5-CT in BA and MCA considerably compared to SAH. The MAPK inhibition downregulated ETB and 5-HT1B receptor mRNA levels compared to that seen after SAH only. No differences were observed in the ETA receptor mRNA levels. The reduction in global and regional CBF observed after SAH were significantly prevented by treatment with SB-386023-b (Figure 1). Statistical analyses were performed using the nonparametric Wilcoxon rank test, differences were considered significant at  $p \leq 0.05$ . Data are expressed as mean  $\pm$  s.e.m. Conclusion: These are the first experiments to show a close relationship between receptor upregulation in cerebral arteries following SAH and changes in cerebral blood flow. Since vasoconstriction and reduction in the CBF are a result of cerebral vasospasm our study is of high clinical relevance. Inhibition of MAPK prevented the reduction in global and regional CBF and attenuated the vasoconstriction mediated by ETB and 5-HT1B receptors in rat cerebral arteries after SAH. These results indicate that MAPK inhibition has a therapeutic potential in the treatment of cerebral vasospasm associated with SAH.

Figure 1



## ACUTE AUGMENTATION OF CEREBRAL BLOOD FLOW BY RHO-KINASE INHIBITORS IN FOCAL CEREBRAL ISCHEMIA IS DEPENDENT ON ENDOTHELIAL NITRIC OXIDE SYNTHASE

Hwa Kyoung Shin<sup>1</sup>, Andrew K. Dunn<sup>3</sup>, Phillip Jones<sup>3</sup>, David A. Boas<sup>3</sup>, James K. Liao<sup>4</sup>, Michael A. Moskowitz<sup>1</sup>, Cenk Ayata<sup>1,2</sup>

<sup>1</sup>*Stroke and Neurovascular Regulation Lab, Department of Radiology, Massachusetts General Hospital, Harvard Medical School, Charlestown, MA, USA*

<sup>2</sup>*Stroke and Neurointensive Care Unit, Department of Neurology, Massachusetts General Hospital, Harvard Medical School, Charlestown, MA, USA*

<sup>3</sup>*Martinos Center for Biomedical Imaging, Department of Radiology, Massachusetts General Hospital, Harvard Medical School, Charlestown, MA, USA*

<sup>4</sup>*Vascular Medicine Research, Brigham & Women's Hospital, Harvard Medical School, Cambridge, MA, USA*

Background: Endothelial nitric oxide synthase (eNOS) is an important enzyme regulating vascular tone, platelet aggregation and inflammatory cell migration in cerebral ischemia. Stimulation of eNOS activity is protective, whereas its inhibition or genetic knock-out is detrimental in animal models of stroke. Recent studies have identified multiple regulatory pathways, such as Rho-kinase/phosphoinositol-3-kinase/Akt, that can modulate endothelial NO production within minutes, via phosphorylation and dephosphorylation cascades, or translocation of the enzyme between subcellular compartments. Rho-kinase inhibitors stabilize eNOS mRNA, and increase eNOS protein and endothelial NO production. We previously showed that pretreatment with Rho-kinase inhibitors for 2-3 days significantly reduce infarct size in a transient middle cerebral artery occlusion model. However, it is not known whether Rho-kinase inhibitors exert their neuroprotective effects acutely by augmenting cerebral blood flow (CBF) in the ischemic brain. In this study, we investigated the acute cerebral hemodynamic effects of Rho-kinase inhibitors and whether these effects are dependent on eNOS. Methods: Two-dimensional real-time CBF imaging was performed with high spatial and temporal resolution using laser speckle flowmetry during focal cerebral ischemia in mice. Ischemia was induced by distal middle cerebral artery occlusion (dMCAO) via a temporal craniotomy, under full physiological monitoring. The areas of ischemic cortex with moderate (21-30% residual CBF, penumbra) or severe (0-20% residual CBF, core) reduction in CBF were quantified 60 minutes after dMCAO by using a thresholding paradigm. The following drugs were tested: 7-nitroindazole (7-NI, 50 mg/kg i.p.), N5-(1-Iminoethyl)-L-ornithine (L-NIO, 20 mg/kg i.p.), OH-fasudil (10 mg/kg i.p.), Y-27632 (10 mg/kg, i.p.). All drugs were administered 60 min before dMCAO; in addition, OH-fasudil was tested when administered 5 min after dMCAO. Results: Rho-kinase inhibitor OH-fasudil administered 60 minutes before dMCAO attenuated the CBF deficit, and reduced the area of core and penumbra by 60% and 25%, respectively ( $p < 0.01$ , compared to vehicle-treated controls,  $n = 5$ ). When administered 5 minutes after dMCAO OH-fasudil still reduced the area of ischemic cortex although its effect was weaker in the severely ischemic core (30% and 30% reduction in core and penumbra, respectively,  $n = 6$ ;  $p < 0.05$ ). Y-27632, another Rho-kinase inhibitor that is structurally distinct from OH-fasudil, also attenuated the CBF deficit (55% reduction in the area of ischemic core,  $n = 4$ ). eNOS knockout mice developed worse CBF deficit and larger area of ischemic cortex after dMCAO (68% and 45% increase in the area of ischemic core and penumbra, respectively,  $p < 0.05$ ,  $n = 4$ ), compared to wild-type controls. OH-fasudil completely failed to reduce the area of ischemic cortex in eNOS knockouts ( $n = 4$ ), suggesting that its beneficial CBF effects are strictly dependent on eNOS. Relatively eNOS-specific inhibitor L-NIO significantly worsened the CBF deficit (70% increase in the area of core,  $n = 5$ ;  $p < 0.05$  vs. vehicle), whereas relatively nNOS specific 7-NI did not ( $n = 4$ ), confirming the importance of eNOS for augmenting collateral CBF to the

ischemic core. Conclusions: Rho-kinase inhibition acutely augments CBF in the focal ischemic penumbra and core. This effect is dependent on eNOS. Our results suggest that rapid non-transcriptional upregulation of eNOS activity by Rho-kinase inhibitors may be a viable therapeutic approach in acute stroke.

## THE ROLE OF NEUREGULINS IN NEUROPROTECTION FOLLOWING ACUTE STROKE

**Byron D. Ford**, Zhenfeng Xu, Gregory D. Ford, Alicia Gates, Ju Jiang

*Department of Anatomy & Neurobiology, Morehouse School of Medicine, Atlanta, GA, USA*

Stroke is the third leading cause of death in the United States and the major cause of long-term disability. However, very little progress has been made in the development of treatment of acute stroke. Neuregulins are a family of growth factors implicated in a number of neuronal functions including development, plasticity, behavior and pathology. Here, we show that neuregulin-1 (NRG-1) completely blocked ischemia-induced delayed neuronal death in the brain with an extended therapeutic window. A single intra-arterial injection of NRG-1 (2.5 ng/kg) was neuroprotective if administered either before or 5.5 hours after transient middle cerebral artery occlusion (MCAO) and resulted in a significant improvement of functional neurological outcome. The neuroprotective effects of the single administration of NRG-1 were seen at least 2 weeks following treatment. NRG-1 also prevented macrophage/microglial infiltration, reactive astrogliosis, DNA fragmentation and interleukin-1 $\beta$  expression following stroke. We demonstrated by microarray analysis, that NRG-1 not only blocked interleukin-1 expression, but also attenuated the widespread pattern of pro-inflammatory and stress gene expression following ischemia. The microarray results showed that several hundred genes were significantly induced following MCAO compared to sham controls and treatment with NRG-1 attenuated the expression of these genes by 50% or more. Gene Ontology pathway analysis of the regulated genes indicated that there are genes induced by ischemia associated with multiple biological processes including inflammation, apoptosis, stress and cell cycle that were suppressed by NRG-1. Using CONFAC software that enables the high-throughput identification of conserved transcription factor binding sites, we determine that the regulatory regions of the ischemia and NRG-1 regulated genes were associated with novel transcription factors not previously associated with stroke and neuroprotection. These results demonstrate that NRG-1 can regulate ischemia-induced gene expression and may give new insight to the molecular mechanisms involved in the neuroprotective role of neuregulins in stroke.

## NIM811 PREVENTS INDUCTION OF MITOCHONDRIAL PERMEABILITY TRANSITION IN CEREBRAL ISCHEMIA

William F. Maragos<sup>1,2,3,4</sup>, Amit S. Korde<sup>1</sup>, Peter C. Waldmeier<sup>5</sup>, Susan D. Craddock<sup>1</sup>,  
L. Creed Pettigrew<sup>1,3</sup>

<sup>1</sup>Department of Neurology, <sup>2</sup>Department of Anatomy and Neurobiology,

<sup>3</sup>Sanders Brown Center on Aging, <sup>4</sup>Graduate Center for Toxicology,

University of Kentucky, Lexington, KY, USA

<sup>5</sup>Nervous System Research, Novartis Pharma Ltd, Basel, Switzerland

**Introduction:** In ischemic neurons, elevation of Ca<sup>2+</sup> levels and formation of reactive oxygen species open an intermembranous pore in mitochondria, resulting in the activation of the mitochondrial permeability transition (MPT). Cyclosporin A (CsA), an immunosuppressive agent, can block the MPT and is neuroprotective in animal models of cerebral ischemia, but its utility is hampered by limited penetration of the blood-brain barrier (BBB) and toxicity. NIM811 (Novartis Pharma, Basel, Switzerland) is a novel non-immunosuppressive derivative of CsA that is a non-toxic and specific inhibitor of MPT induction. We report the first use of NIM811 to affect infarct volume and modulate cytochrome C release. **Methods:** To determine the effect of NIM811 on infarct volume, spontaneously hypertensive rats (SHRs) underwent reversible middle cerebral artery occlusion (MCAO) for 2 hrs. After 1 hr of reperfusion, animals were treated with NIM811 (50 mg/kg) or drug-free vehicle (100% DMSO). Brain was removed *en bloc* after 24 hrs for measurement of infarct volume corrected for ischemic edema. To determine the effect of NIM811 on release of cytochrome C from mitochondria in ischemic brain, SHRs underwent MCAO for 2 hrs, were treated with 50 mg/kg NIM811 or vehicle after 1 hr of reperfusion, and samples of ischemic core and penumbra were removed and snap-frozen 1 hr after treatment. Supernatants obtained after ultracentrifugation of brain mitochondrial fractions were assayed for cytochrome C content by ELISA. To determine whether NIM811 had any effects on cerebral perfusion, Laser-Doppler Flowmetry (LDF) was performed over the exposed surface of the cortex overlying the core and penumbra in animals rendered ischemic before and after systemic administration of 50 mg/kg NIM811. **Results:** Treatment with NIM811 at 1 hr after post-ischemic reperfusion reduced infarct volume measured at 24 hrs by 40% ( $88 \pm 3.8 \text{ mm}^3$  [vehicle; n=4] vs.  $53 \pm 8.8 \text{ mm}^3$  [NIM811; n=5]; \* $p \leq 0.005$ , *t*-test). Cytochrome C levels were increased fivefold in ischemic core ( $74.4 \pm 3.9 \text{ ng/mL}$ ) and penumbra ( $68.5 \pm 3.6 \text{ ng/mL}$ ; n=4) vs. comparable areas in non-ischemic controls (sham-core  $13.6 \pm 0.56 \text{ ng/mL}$  and sham-penumbra  $14.2 \pm 0.54$ ; n=4;  $p < 0.001$  for both by ANOVA with Scheffe *post hoc*). Treatment with NIM811 after MCAO lowered the cytochrome C level to  $49.2 \pm 2.2 \text{ ng/mL}$  in ischemic core and  $42.4 \pm 2.4 \text{ ng/mL}$  in penumbra ( $p < 0.001$  compared to levels in vehicle-treated ischemic controls). During 120 min of ischemia, there was an 80% reduction in cerebral perfusion in the core and 55% reduction in the penumbra. During 60 min of reperfusion, regional perfusion increased by 10-20%. Treatment with NIM811 had no significant effect on cerebral perfusion in either region for at least 120 min following reperfusion. **Conclusion:** Our results show that NIM811 reduces infarct volume significantly after ischemia and attenuates the release of cytochrome C from distressed mitochondria into the cytoplasm of ischemic neural cells. NIM811 has no effect on cerebral perfusion suggesting that the protective effect of NIM811 was not the result of enhanced blood flow. These data support the hypothesis that activation of MPT contributes to ischemia-reperfusion injury in brain and underscore the potential value of NIM811 as novel therapy for stroke.

**Acknowledgements:** This work was supported by NIH grants NS01941 and NS42111 (WFM) and NS47395 (LCP).



## NEUROPROTECTIVE EFFECTS OF CREATINE IN A MOUSE MODEL OF STROKE: AN EXPERIMENTAL MRI STUDY

Georg Royl, Konstantin Prass, Ute Lindauer, Dirk Megow, Ulrich Dirnagl, Josef Priller

*Experimental Neurology, Charité Universitätsmedizin Berlin, Berlin, Germany*

Stroke leads to energy failure and subsequent neuronal cell loss. Creatine and phosphocreatine constitute a cellular energy buffering and transport system, and dietary creatine supplementation has been shown to protect neurons in several models of neurodegeneration. We examined whether creatine has beneficial effects in a mouse model of focal cerebral ischemia. Oral creatine administered three weeks before stroke reduced infarct sizes induced by MCA occlusion in a dose-dependent manner. However, no significant differences in the brain concentration of creatine, phosphocreatine and ATP were found in our HPLC analysis. In contrast to previous studies that linked neuroprotection with increased levels of creatine and/or phosphocreatine, we thus observed beneficial creatine effects in stroke that are independent of the concentrations of creatine and energy-rich phosphates in the brain. To investigate the role of perfusion-related protective mechanisms we measured vascular reactivity of isolated MCA and performed in vivo MR imaging (alternating Diffusion Weighted Imaging (DW-MRI) and Perfusion Weighted Imaging with FAIR (FAIR-MRI)) in the acute phase during and after MCA occlusion. At 30min after MCAO, FAIR-MRI showed the same absolute perfusion of the ipsilateral hemisphere in creatine-fed and control animals ( $0.43 \pm 0.18$  /  $0.39 \pm 0.18$  ml/g\*min respectively). However, 30min after reperfusion (90min post MCAO) ipsilateral blood flow in creatine-fed animals was significantly higher than in control animals ( $0.51 \pm 0.10$  /  $0.30 \pm 0.15$  ml/g\*min respectively,  $p=0.01$ ). DWI during ischemia at 50min after MCAO showed no difference in ipsilateral absolute ADC reduction between creatine-fed animals and controls ( $0.69 \pm 0.10$  /  $0.74 \pm 0.16 \times 10^{-3}$  mm<sup>2</sup>/s respectively). At 90min after reperfusion (150min post MCAO) ipsilateral ADC recovered significantly better in creatine-fed compared to control animals ( $0.84 \pm 0.07$  /  $0.62 \pm 0.17 \times 10^{-3}$  mm<sup>2</sup>/s respectively,  $p=0.01$ ). Our findings suggest a novel mechanism of creatine-induced neuroprotection through improvement of cerebrovascular function during cerebral ischemia.

## DIFFERENTIAL EFFECTS OF OESTROGEN IN MODELS OF PERMANENT AND TRANSIENT FOCAL CEREBRAL ISCHAEMIA

Kirsty B. Gordon, I. Mhairi Macrae, Hilary V.O. Carswell

*Division of Clinical Neuroscience, University of Glasgow, Glasgow, UK*

**Introduction:** Oestrogen's neuroprotective effect in stroke models has been challenged recently with reports of the hormone exacerbating ischaemic damage (1, 2, 3). What controls stroke outcome in the presence of oestrogen remains unclear but may relate to the severity and duration (permanent or transient) of the ischaemic insult. The present work examined the effects of oestrogen on ischaemic damage induced by either transient or maintained (permanent) focal cerebral ischaemia using the intraluminal thread (ILT) model. **Methods:** In Study 1, female, ovariectomised Sprague-Dawley rats were pre-treated with a high physiological dose of 17beta-oestradiol (0.25mg, 21-day release pellet) or placebo 14 days before 24 hours of permanent focal ischaemia using the ILT model. In Study 2, ovariectomised Lister Hooded rats received 14 days of pre-treatment with 17beta-oestradiol (0.25mg or 0.025mg) or placebo pellet then underwent transient focal ischaemia by ILT: 2 hours ischaemia and 7 days reperfusion. Infarct volume, cortical blood flow (laser Doppler) and neurological deficits were compared between 17beta-oestradiol and placebo treated groups in each study. **Results:** 17beta-Oestradiol significantly increased infarct volume by 118% 24 hours after permanent ischaemia (Figure 1) but had no effect on ischaemic blood flow or neurological deficit. Transient ischaemia produced no overall effect at either dose of 17beta-oestradiol on infarct volume (Figure 2), blood flow or neurological deficit. **Conclusion:** Oestrogen can induce detrimental effects on the ischaemic brain as displayed in Study 1. Most studies reporting neuroprotective effects of oestrogen involve models of transient ischaemia. The lack of effect of oestradiol in Study 2 may be due to detrimental effects of oestrogen (evident in the permanent ischaemia model), counteracting any beneficial effects during reperfusion, resulting in no overall influence of oestrogen on stroke outcome. The results of Study 1 clearly demonstrate that oestrogen has the capacity to promote detrimental actions in the stroke-injured brain. In line with recent large clinical trials (e.g. Womens Health Initiative), our studies reveal a detrimental influence of oestrogen on stroke and indicate the need for further research on more selective oestrogen receptor agonists and selective oestrogen receptor modulators (SERMs). **References:** 1. Bingham et al. (2005) Detrimental effects of 17beta-oestradiol after permanent middle cerebral artery occlusion *J Cereb Blood Flow Metab* (in press) 2. Harukuni et al. (2001) Deleterious effect of beta-estradiol in a rat model of transient forebrain ischemia *Brain Res* 9:137-142 3. Santizo et al. (2002) Loss of benefit from estrogen replacement therapy in diabetic ovariectomized female rats subjected to transient forebrain ischemia *Brain Res* 956:86-95 **Acknowledgements:** The authors thank Prof. DI Graham, Dr. E Irving and J McGill for their expertise. KG is supported by a Research into Ageing PhD studentship.

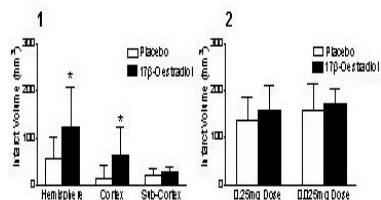


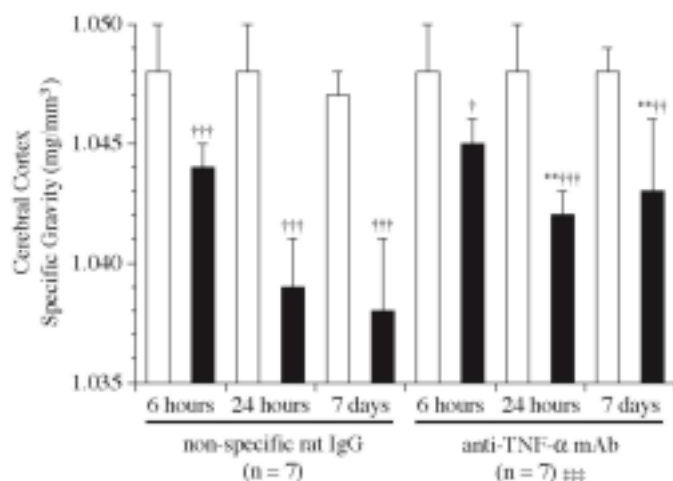
**Figure: 1)** Study 1: Infarct volumes 24 hours after permanent MCAO. 17β-Oestradiol pre-treatment significantly increased infarct volume in the hemisphere and cortex (mean ±SD, \* p<0.05, unpaired Student's t-test). **2)** Study 2: Infarct volumes after 2 hours ischaemia and 7 days reperfusion. No overall influence of 17β-oestradiol pre-treatment on infarct size (mean ±SD).

## TUMOR NECROSIS FACTOR-ALPHA NEUTRALIZATION REDUCED CEREBRAL EDEMA FOLLOWING TRANSIENT FOCAL CEREBRAL ISCHEMIA

Naohisa Hosomi, Takayuki Naya, Masakazu Kohno

*Second Department of Internal Medicine, Kagawa University School of Medicine, Kagawa, Japan*

Following focal cerebral ischemia, tumor necrosis factor- $\alpha$  deteriorates cerebral edema and survival rate. Therefore, tumor necrosis factor- $\alpha$  neutralization could reduce cerebral microvascular permeability in acute cerebral ischemia. Left middle cerebral artery occlusion for 120 min followed by reperfusion was performed with the thread method under halothane anesthesia in Sprague-Dawley rats. Anti-rat tumor necrosis factor- $\alpha$  neutralizing monoclonal antibody with a rat IgG Fc portion (15mg/kg) was infused intravenously right after reperfusion. Stroke index score, infarct volume, cerebral specific gravity, and the endogenous expression of tumor necrosis factor- $\alpha$ , matrix metalloproteinase-2, matrix metalloproteinase-9, and membrane type 1- matrix metalloproteinase in the brain tissue were quantified in the ischemic and matched contralateral non-ischemic hemisphere. In the anti-tumor necrosis factor- $\alpha$  neutralizing antibody treated rats, infarct volume was significantly reduced ( $p = 0.014$ ,  $n = 7$ ; respectively), and cerebral specific gravity was dramatically increased in cortex and caudate putamen ( $p < 0.001$ ,  $n = 7$ ; respectively) in association with a reduction in matrix metalloproteinase-9 and membrane type 1- matrix metalloproteinase upregulation. Tumor necrosis factor- $\alpha$  in the brain tissue was significantly elevated in the ischemic hemisphere 6 hours after reperfusion in the non-specific IgG treated rats ( $p = 0.021$ ,  $n = 7$ ) and was decreased in the anti-tumor necrosis factor- $\alpha$  neutralizing antibody treated rats ( $p = 0.001$ ,  $n = 7$ ). Post-reperfusion treatment with anti-rat tumor necrosis factor- $\alpha$  neutralizing antibody reduced brain infarct volume and cerebral edema, which is likely mediated by a reduction in matrix metalloproteinases upregulation.





## LATE POST-ISCHEMIC INTRACEREBRAL THROMBIN-APPLICATION REDUCES INFARCT VOLUME

Petra Henrich-Noack<sup>1</sup>, Georg Reiser<sup>1</sup>, Klaus G. Reymann<sup>2</sup>

<sup>1</sup>*Otto-von-Guericke University, Medical Faculty, Institute for Neurobiochemistry, Magdeburg,* <sup>2</sup>*Leibniz Institute for Neurobiology and Research Institute Applied Neurosciences (FAN), Magdeburg, Germany*

**Introduction:** In addition to its role in the blood coagulation cascade, the serine protease thrombin has, depending on the specific conditions, either neuroprotective or neurotoxic effects on brain tissue during cerebral ischemia. Previous data suggest that thrombin-induced protection in vivo can be achieved by preconditioning rather than by acute treatment (Masada et al., 2000, Striggow et al., 2000). In the current approach we evaluated the regenerative potency of thrombin by injecting the protease repeatedly, starting from 1 week post ischaemia. As a parameter of neural damage we quantified the infarct areas. **Materials and methods:** Male Sprague Dawley rats were used for all experiments. A guiding cannula was implanted under pentobarbitone anaesthesia 7 days before induction of ischaemia. We occluded the Middle Cerebral Artery by intracerebral injection of endothelin-1 (eMCAO) in freely moving animals. Thrombin (0.009 U/rat) was injected via the same guiding cannula intracerebrally on day 7, 8, 9 and 10 post ischaemia. Histological quantification of the infarct areas were performed 14 days post ischaemia. **Results:** Control animals, which were injected with saline on day 7, 8, 9 and 10 post ischaemia developed an average infarct volume of  $20.7 \pm 2.5$  mm<sup>3</sup>. In rats which received 4 injections of thrombin we measured a damaged area of  $12.6 \pm 1.9$  mm<sup>3</sup>. Statistical analysis revealed a significant difference between both groups (Mann-Whitney, U-test; \* $p < 0.05$ ; N=12-15). **Conclusions:** Data from literature indicate, that 7 days post eMCAO the ischaemic damage is fully developed. Therefore protection cannot be induced when we inject thrombin on day 7 post ischaemia. Also influences of thrombin on oedema are unlikely to be the cause of the reduced infarct volume, as there should be no pronounced oedema anymore on day of injection (7 d post ischaemia) or on day of decapitation (14 d post ischaemia). It has been shown that thrombin induces proliferation in astrocytes (Wang et al., 2002), but astrocytosis is defined as damaged area and therefore cannot account for the smaller infarct areas. Further studies are needed to examine the underlying mechanism of this reduction in infarct volume with late post-ischemic intracerebral injection of thrombin.

### Literature:

- Masada T, Xi G, Hua Y, Keep RF (2000): The effects of thrombin preconditioning on focal cerebral ischemia in rats. *Brain Res* 867: 173-9
- Striggow F, Riek M, Breder J, Henrich-Noack P, Reymann KG, Reiser G (2000): The protease thrombin is an endogenous mediator of hippocampal neuroprotection against ischemia at low concentrations but causes degeneration at high concentrations. *Proc Natl Acad Sci U S A* 97: 2264-9
- Wang H, Ubl JJ, Stricker R, Reiser G (2002): Thrombin (PAR-1)-induced proliferation in astrocytes via MAPK involves multiple signalling pathways. *Am J Physiol Cell Physiol* 283: C1351-1364.

## **$\beta$ -ADRENORECEPTOR ANTAGONISTS ATTENUATE BRAIN INJURY FOLLOWING TRANSIENT FOCAL ISCHEMIA IN RATS**

**Toru Goyagi, Tetsu Kimura, Toshiaki Nishikawa**

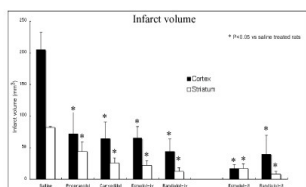
*Department of Anesthesia and Intensive Care, Akita University School of Medicine, Akita, Japan*

**Introduction:**  $\beta$ -adrenoreceptor antagonists experimentally reduce cardiac and renal injury following ischemia, and also are clinically useful for myocardial infarction [1] and severe burn [2]. In addition,  $\beta$ -adrenoreceptor antagonists have neuroprotective effects in focal cerebral ischemia in experimental settings [3]. The present study was conducted to compare the neuroprotective effects of several  $\beta$ -adrenoreceptor antagonists in the rat transient focal cerebral ischemia. **Methods:** Halothane anesthetized normothermic adult male Sprague-Dawley rats (280 – 320 g) were subjected to 2 hr of middle cerebral artery occlusion (MCAO) using the intraluminal suture technique confirmed by laser Doppler flowmetry. Rats received intravenous (iv) infusion of saline 1 ml/hr, propranolol 100  $\mu$ g/kg/min, carvedilol 4  $\mu$ g/kg/min, esmolol 200  $\mu$ g/kg/min, or landiolol 50  $\mu$ g/kg/min (n=6 in each group). Infusion was initiated 30 min prior to MCAO and continued for 24 hr. Additional rats received esmolol 50  $\mu$ g/kg/min, or landiolol 10  $\mu$ g/kg/min intrathecally (it) via cisterna magna (n=6 in each group), according to the same experimental protocol. The neurological deficit score was evaluated at 24 hr after reperfusion, and the brains were removed and stained with TTC. Data (mean $\pm$ SD) were analyzed by ANOVA, with P<0.05 being significant. **Results:** Neurological deficit scores were smaller in the rats treated with propranolol-iv (15.3  $\pm$  3.7), carvedilol-iv (13.6  $\pm$  3.3), esmolol-iv (11.3  $\pm$  6.1), landiolol-iv (9.1  $\pm$  4.0), esmolol-it (3.6  $\pm$  4.3), and landiolol-it (10.6  $\pm$  1.3), compared to saline-treated rats (27.5  $\pm$  9.8)(P<0.05). The infarct volumes of cortical and striatum were less in the rats receiving  $\beta$ -adrenoreceptor antagonists irrespective of administration route, than in saline-treated rats (P<0.05, figure). **Conclusion:** We conclude that administration of  $\beta$ -adrenoreceptor antagonists improves neurological and histological outcome following transient focal cerebral ischemia in rats. In particular, short acting  $\beta$ -adrenoreceptor antagonists provide neuroprotection independent of administration route.

### **References:**

- [1] Kloner RA, Rezkilla SH; *J Am Coll Cardiol* 44: 276-286 (2004)  
 [2] Herndon DN, Hart DW, Wolf SE, et al; *N Engl J Med* 345: 1223-1229 (2001)  
 [3] Savitz SI, Erhardt JA, Anthony JV, et al; *J Cereb Blood Flow Metab* 20: 1197-1204 (2000)

*Grant support: Supported by Grant-in-Aid for Young Scientists (B) project number 15790809*



## NEUROPROTECTIVE AND ANTI-APOPTOTIC EFFECTS OF FK506 FOLLOWING TRANSIENT FOCAL ISCHEMIA IN RATS

**Shimon Amemiya**, Tatsushi Kamiya, Toshiki Inaba, Masayuki Ueda, Kengo Kato, Chikako Nito, Satoshi Suda, Yasuhiro Nishiyama, Yasuo Katayama

*Second Department of Internal Medicine, Nippon Medical School, Tokyo, Japan*

**Introduction:** We have already demonstrated that an immunosuppressant FK506 (tacrolimus) inhibited ischemic neuronal injury [1], and that mild hypothermia enhanced the neuroprotective effect in the transient focal cerebral ischemia model [2]. However, mechanisms of the neuroprotective effects have not been clarified. The aim of the present study is to investigate anti-apoptotic effects of FK506 following transient focal ischemia in rats using immunohistochemical study. **Methods:** A transient (2hours) focal ischemia was induced by left middle cerebral artery occlusion using an intraluminal suture method [2]. FK506 (0.3mg/kg) or vehicle was intravenously administered immediately after occlusion. After 24 hours of reperfusion, hematoxylin and eosin staining for infarct volume measurement and immunohistochemistry for the detection of single strand DNA breaking (SSB) were carried out. To confirm characters of SSB positive cells, the double staining for SSB with anti-apoptotic protein Bcl-2, neuronal marker NeuN, or TUNEL were also performed. **Results:** FK506 did not affect cortical cerebral blood flow measured by a Laser Doppler flowmetry. The total infarct volume was significantly reduced in the FK506-treated group (92.2 +/- 16.02 mm<sup>3</sup>) compared with the vehicle-treated group (136.8 +/- 13.2 mm<sup>3</sup>, p<0.01). The total numbers of SSB positive cells in the ischemic hemisphere were 135.8+/-45.7 in the FK506-treated group, and 345.3+/-43.7 in the vehicle-treated group with a statistically significant difference (p<0.01). SSB positive cells were predominantly distributed in the peri-infarct area of the ischemic hemisphere. Semi-quantified analysis revealed a significant up-regulation of Bcl-2 expression in the FK506-treated group compared with the vehicle-treated group. Cells with strong cytoplasmic Bcl-2 expression did not show nuclear SSB signals in the peri-infarct area. SSB positive cells were also stained with NeuN, and several SSB positive cells were TUNEL positive. **Conclusion:** The present data demonstrated that FK506 significantly reduced infarct volume in the rat transient focal ischemia model. The neuroprotection was associated with a significant decrease in SSB positive neurones together with a significant increase in cytoplasmic Bcl-2 expression. These suggest that anti-apoptotic mechanisms are involved in the neuroprotective effects of FK506 in the model. **References:** [1] Arii T., Kamiya T., Arii K., et al. *Neurol. Res.* 23: 755-760 (2001). [2] Nito C., Kamiya T., Ueda M., et al. *Brain Res.* 1008: 179-185 (2004).



**THE IMPORTANCE OF EXTRACELLULAR CALCIUM FOR ENDOTHELIN TYPE A AND B RECEPTOR-MEDIATED CONTRACTION IN RAT BASILAR ARTERY****Roya Jamali, Lars Edvinsson***Division of Experimental Vascular Research, Department of Medicine, Lund University, Lund, Sweden*

**Aim:** The aim of the study was to evaluate the role of extracellular  $\text{Ca}^{2+}$  for endothelin type A (ETA) and B receptor (ETB) mediated contraction in rat basilar artery. **Methods:** Myographs were used for the functional studies. Intracellular calcium ( $[\text{Ca}^{2+}]_i$ ) levels were determined by the calcium indicator Fura-2 technique. Arteries were studied in three different ways: 1) Preincubation with nifedipine ( $1 \mu\text{M}$ ) for 30 min before addition of endothelin-1 (ET-1) or sarafotoxin 6c (S6c); 2) precontraction with ET-1 or S6c followed by addition of nifedipine at the maximum of contraction; 3) preincubation with or without nifedipine in  $\text{Ca}^{2+}$ -free buffer and then addition of increasing doses of  $\text{Ca}^{2+}$  ( $10 \mu\text{M}$ - $2 \text{mM}$ ). **Results:** The effect of nifedipine on ETA receptor-mediated contraction was negligible while ETB receptor-mediated contraction was reduced about 30 % ( $P < 0.005$ ). ET-1-induced vasoconstriction was reduced by nifedipine in fresh arteries, while nifedipine had little effect on S6c-induced contraction in cultured arteries. After preincubation in  $\text{Ca}^{2+}$ -free buffer, S6c induced a small contraction (10-20 % of contraction at  $2 \text{mM}$  of  $\text{Ca}^{2+}$  concentration) and an increase in  $[\text{Ca}^{2+}]_i$ . In low  $\text{Ca}^{2+}$  concentrations ( $10$  or  $100 \mu\text{M}$ ), ET-1 induced a strong contraction and an increase in  $[\text{Ca}^{2+}]_i$  that was sensitive to nifedipine. S6c had no such effect. **Conclusion:** Our study suggests that ET-receptors in rat basilar arteries mediate their effect through different mechanisms. The ETA -receptor is more sensitive to extracellular  $\text{Ca}^{2+}$  as compared to the ETB receptor. On the other hand ETB receptors are more dependent on voltage-dependent  $\text{Ca}^{2+}$  channels.

**ALPHA-LINOLENIC ACID AND RILUZOLE, ACTIVATORS OF 2 PORE-DOMAIN  
K<sup>+</sup> CHANNELS AFFORD BRAIN PROTECTION AGAINST FOCAL BRAIN  
ISCHEMIA**

**Catherine Heurteaux**, Christophe Laigle, Gisèle Jarretou, Michel Lazdunski,  
Nicolas Blondeau

*Institut de Pharmacologie Moléculaire et Cellulaire, CNRS UMR6097, Valbonne, France*

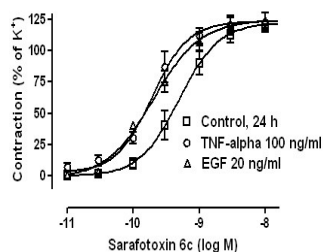
**Background and Purpose:** Alpha-linolenic acid (ALA) and riluzole (RLZ), potent activators of two-pore domain K<sup>+</sup> channel TREK-1 and TRAAK are known to be neuroprotective against forebrain global ischemia and epileptic seizures. Recent studies have revealed that TREK-1 plays a major role in neuronal excitability control and ALA-induced neuroprotection. We investigated the potential protective effect of ALA and riluzole in a model of focal ischemia clinically relevant to stroke. **Methods:** Mice were subjected to transient middle cerebral artery occlusion (MCAO, 1 hour) and reperfusion by use of intraluminal filament model. To determine the therapeutic window, mice received a single dose of 4 mg/kg RLZ or 500 nmol/kg ALA at different times of reperfusion. Then, the efficiency of a single dose of 4 mg/kg RLZ or 500 nmol/kg ALA injected 1 (RLZ) or 2 hours (ALA) after reperfusion was compared to a dose of 2 mg/kg RLZ and 250 nmol/kg ALA given 1-2, 48 and 72 hours after reperfusion or 1-2 hours after reperfusion and once each week during the next two weeks of reperfusion. A combined treatment with 2 mg/kg RLZ + 250 nmol/kg ALA injected 2 hours after reperfusion was also tested. RLZ and ALA were injected as a bolus directly in the jugular vein. Ischemic neuronal injury was evaluated 24 hours (Infarct volume, neurological deficit, counting of TUNEL-positive cells, Bax expression) and 28 days (neuronal counting on cresyl-violet sections, GFAP expression) after ischemia. The same protocol was also performed with administration of palmitic acid, a saturated fatty acid that did not activate TREK-1 and TRAAK channels. **Results:** A single dose of RLZ (4mg/kg) or ALA (500 nmol/kg) up to 3 hours after reperfusion reduced the stroke volume by 75% and 86 % (P<0.001), respectively and improved the neurological scoring. ALA- and RLZ-treatment was associated with a reduction in cytopathological features of cell injury, including cell shrinkage, DNA-fragmentation, Bax and GFAP expression both in the cortex and the caudate-putamen. In term of survival rate observed in a 28-day time, the best protection was obtained with the injection of 250 nmol/kg ALA given 2 hours after reperfusion and once each week during the next two weeks of reperfusion or with a single dose of the combined treatment (2 mg/kg RLZ + 250 nmol/kg ALA). The palmitic acid failed to induce a neuroprotective effect against focal ischemia. **Conclusion:** These results provide further evidence for a therapeutical value of a riluzole and alpha-linolenic acid treatment in brain injury resulting from focal ischemia/reperfusion.

## TNF-ALPHA AND EGF POTENTIATE THE ETB RECEPTOR MEDIATED CONTRACTION IN RAT MIDDLE CEREBRAL ARTERIES

Emelie Stenman, Marie Henriksson, Lars Edvinsson

*Department of Medicine, Experimental Vascular Research, Lund University, Lund, Sweden*

**Introduction:** We have previously shown that focal cerebral ischemia in rat upregulates contractile endothelin type B (ETB) receptors and the contractile response to angiotensin II (Ang II) in the ipsilateral middle cerebral artery. Our hypothesis is that this may be detrimental if it involves a decreased perfusion in the ischemic hemisphere. Since ischemic stroke is characterized by inflammation and remodeling of the cerebral vasculature we wanted to explore if cytokines or growth factors may influence the regulation of endothelin and angiotensin receptors. **Methods:** Male Wistar rats were anesthetized with CO<sub>2</sub> and decapitated. The middle cerebral arteries were removed from the brains and incubated for 24 hours at 37 °C in humidified 5 % CO<sub>2</sub> and air in Dulbecco's modified Eagle's medium supplemented with penicillin and streptomycin. Interleukin (IL)-1 $\beta$ , IL-2, tumor necrosis factor (TNF)- $\alpha$ , basic fibroblast growth factor (bFGF), platelet derived growth factor (PDGF) and epidermal growth factor (EGF) were added individually in different concentrations at the beginning of culture. Middle cerebral arteries cultured 24 hours without addition of cytokines or growth factors were used as controls. The contractile responses to sarafotoxin 6c (S6c; ETB receptor agonist) and Ang II in raising concentrations were examined by myographs, and the mRNA-levels for the endothelin receptors were studied by real-time PCR. Statistical analysis was performed by Kruskal-Wallis test followed by Dunn's Multiple Comparison Test, and  $P < 0.05$  was considered significant. Values are expressed as mean  $\pm$  SEM. **Results:** TNF- $\alpha$  (100 ng/ml) and EGF (20 ng/ml) increased the potency to S6c significantly as compared to control (pEC<sub>50</sub> [agonist concentration eliciting half maximal response] =  $9.74 \pm 0.09$  for TNF- $\alpha$ ;  $9.75 \pm 0.12$  for EGF and  $9.30 \pm 0.10$  for control;  $P < 0.05$ ; Figure), while the other examined cytokines and growth factors did not have any effect. No contractile responses to Ang II (with or without cAMP stimulation) could be detected with or without cytokines or growth factors, suggesting that other factors may be responsible for the enhanced Ang II-contraction seen after ischemic stroke. There was a tendency towards elevated mRNA levels for the ETB receptor in MCAs incubated with TNF- $\alpha$  (100 ng/ml) as compared to control ( $P = 0.11$ ), while the mRNA levels for the ETA receptor was significantly decreased in the same arteries ( $P < 0.05$ ). EGF (20 ng/ml) did not affect the transcription of the ET receptors. **Conclusion:** TNF- $\alpha$  and EGF have the ability to increase the contractile ETB receptor mediated responses in rat middle cerebral arteries. Since inflammation and angiogenesis are common phenomena in ischemic stroke, this may explain the enhanced ETB receptor mediated responses after focal cerebral ischemia. Previous findings have shown harmful effects of TNF- $\alpha$  and EGF in cerebral ischemia and this may partly be explained by an increased function of contractile ETB receptors.

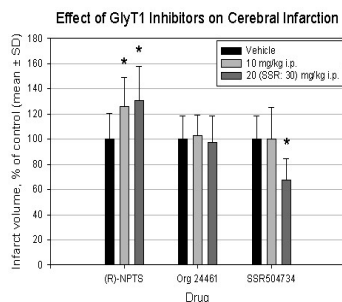


## DIFFERENTIAL EFFECT OF GLYT1 INHIBITORS ON THE DEVELOPMENT OF ISCHEMIC CEREBRAL INFARCTION

Laszlo Szabo

*Department of Pharmacology, Neuroscience Discovery Research, Abbott GmbH & Co. KG, Ludwigshafen, Germany*

**Introduction:** The enhancement of NMDA receptor-mediated glutamatergic neurotransmission has recently gained acceptance as a promising strategy for the treatment of schizophrenia. Because of obvious concerns over excitotoxicity, current research is focused on NMDA receptor activation through modulatory sites rather than the development of glutamate site agonists. In particular, inhibition of glycine reuptake at the GlyT1 transporter has been shown to upregulate NMDA receptor function via the strychnine-insensitive glycine site, but the side effect liability of this approach has not been explored. We therefore investigated the effect of three structurally different GlyT1 inhibitors (R)-NPTS [1], Org 24461 [2] and SSR504734 [3] on ischemic infarct development in the rat. **Methods:** Focal cerebral ischemia was induced in fasted male Long Evans rats under sevoflurane/nitrous oxide anesthesia by permanent distal ligation of the right middle cerebral artery just above the rhinal fissure. The rats were pretreated with a single intraperitoneal injection of the GlyT1 inhibitor either 30 min ((R)-NPTS and Org 24461) or 60 min (SSR504734) before the onset of ischemia. Twenty-two hours after vessel occlusion the animals were sacrificed and cerebral infarct volume was determined on triphenyltetrazolium chloride-stained serial coronal sections by image analysis. Each treatment group (n = 8 to 11) was compared to its own vehicle-treated controls by unpaired two-tailed t-test. Differences with P < 0.05 were considered statistically significant. **Results:** Pretreatment with 10 or 20 mg/kg (R)-NPTS led to an increase in infarct volume by 26% and 31%, respectively, without any noticeable change in the behavior of the animals. The administration of Org 24461 (10 or 20 mg/kg) had no effect on the final extent of ischemic infarction although it resulted in deep and protracted sedation. Preischemic therapy with 30 mg/kg SSR504734 reduced infarct volume by 32% while 10 mg/kg was without effect. The infarct reduction achieved by the higher dose was accompanied only by a small decrease in the volume of edema, indicating genuine neuroprotection afforded by the compound. Treatment was not associated with any obvious behavioral effects. **Conclusion:** Although the reasons for the disparate impact of GlyT1 inhibitors on infarct development is unclear at present, the findings nevertheless suggest that the pharmacologically efficacious upregulation of NMDA receptor function via inhibition of the GlyT1 transporter does not necessarily lead to an enhancement of ischemia-induced acute excitotoxic cell death. **References:** [1] Lowe JA, Drozda SE, Fisher K et al.; *Bioorg Med Chem Lett* 13:1291-1292 (2003) [2] Harsing LG, Gacsalyi I, Szabo G et al.; *Pharmacol Biochem Behav* 74:811-825 (2003) [3] Coste A, Dargazanli G, Estenne-Bouhtou G et al.; 2004 Abstract Viewer/Itinerary Planner, Washington, DC: Society for Neuroscience, Program No. 349.14 (2004)

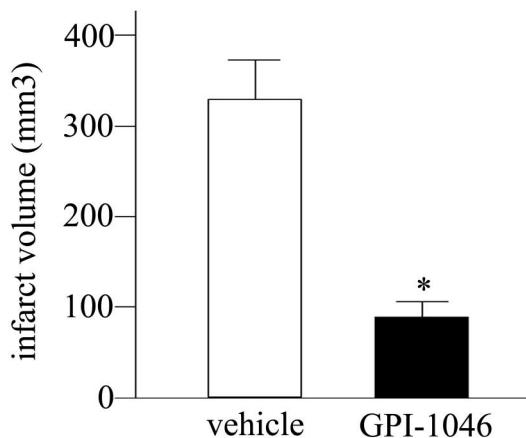


**PROTECTION AGAINST ISCHEMIC BRAIN DAMAGE IN RATS BY  
IMMUNOPHILIN LIGAND GPI-1046**

Feng Li, **Takeshi Hayashi**, Nobuhiko Omori, Guang Jin, Kentaro Deguchi, Shoko Nagotani,  
Hanzhe Zhang, Yoshihide Sehara, Xiquan Wang, Keiko Hamakawa, Isao Nagano,  
Mikio Shoji, Koji Abe

*Department of Neurology, Okayama University Graduate School of Medicine and Dentistry,  
Okayama, Japan*

<Background> FK506 inhibits ischemic neuronal cell death but its immunosuppressive property could become a problem for clinical use. GPI-1046 is one of the ligands for FK506-binding proteins, but it does not cause immunosuppression. Because this molecule has strong neuroprotective effect as FK506 does, we investigated whether this molecule actually ameliorates in vivo ischemic brain damage. <Methods> We used male Wistar rats of 11-weeks-old. Under the anesthesia with nitrous oxide and halothane, the origin of the right middle cerebral artery (MCA) was occluded using a nylon thread. Ninety minutes later, the cerebral blood flow (CBF) was restored by removal of the thread. At 2 hours before the ischemia and just after the CBF restoration, 30 mg/kg of GPI-1046 or vehicle was subcutaneously injected. At 24 hours after the CBF restoration, the brain was removed and the infarct volume was measured using triphenyltetrazolium chloride method. In order to confirm that GPI-1046 actually bound with FK506-binding protein, we measured rotamase activity which becomes decreased when FK506-binding protein binds with its ligand. We also performed immunohistochemistry for caspase-8, caspase-3, and cytochrome c, and investigated whether GPI-1046 prevents apoptotic machinery activation. <Results> Infarct volume was significantly decreased by GPI-1046 treatment (Fig, \* $p < 0.05$ ), indicating that this molecule exerts its neuroprotective property also in vivo. Rotamase activity was markedly increased by ischemia, but was partially reduced by GPI-1046 treatment, indicating that GPI-1046 ameliorated ischemic brain damage through binding with FK506-binding protein. Immunohistochemical analysis for caspase-8, caspase-3, and cytochrome c revealed that GPI-1046 prevented increased staining of these molecules, which indicated that GPI-1046 prevented activation of apoptotic machinery and thus reduced infarct volume. <Conclusion> Immunophilin ligand GPI-1046 was effective for ameliorating in vivo ischemic brain damage. As GPI-1046 does not possess immunosuppressive property, this molecule could be used for ischemic stroke in clinical situation. Inhibition of apoptotic machinery activation should be the mechanism of this molecule's neuroprotection.

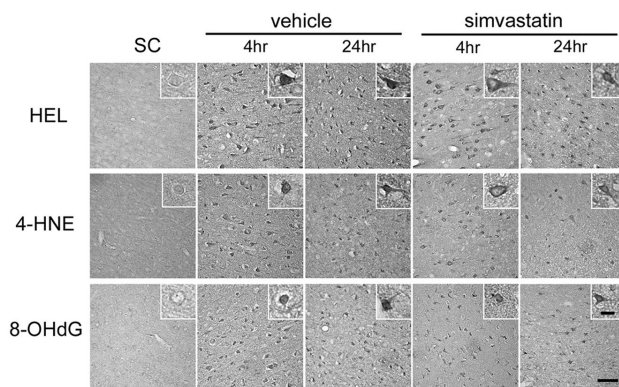


## REDUCTION OF CEREBRAL INFARCTION IN SHR-SP BY STATINS

**Shoko Nagotani**, Takeshi Hayashi, Keiko Hamakawa, Guang Jin, Kentaro Deguchi, Yoshihide Sehara, HanZhe Zhang, XiQuan Wang, Isao Nagano, Mikio Shoji, Koji Abe

*Department of Neurology, Okayama University Graduate School of Medicine and Dentistry, Okayama, Japan*

**Background and Purpose:** 3-hydroxy-3-methylglutaryl coenzyme A (HMG-CoA) reductase inhibitors (statins) have pleiotropic effects on ischemic brain. This study aimed to clarify the effect of statins against spontaneous stroke occurrence and oxidative brain damage caused by transient middle cerebral artery occlusion (tMCAO). **Methods:** Stroke-prone spontaneously hypertensive rats (SHR-SP) were treated with pitavastatin (10mg/kg), atorvastatin (20mg/kg), simvastatin (20mg/kg), or vehicle (n=5 each group) for 28 days. Physiological parameters and serum lipids were measured, and spontaneous infarct volumes were evaluated by immunohistochemical examination for MAP2. Using the simvastatin- (n=12) and the vehicle-treated (n=10) SHR-SP, we immunohistochemically detected the oxidative stress markers for lipids (HEL and 4-HNE) and DNA (8-OHdG) in their brains following 90 min of tMCAO. **Results:** In the spontaneous stroke model, body weight and blood pressure were not different among 4 groups. Statins did not affect the serum cholesterol levels. The infarct volume was significantly smaller in the atorvastatin ( $3.5 \pm 3.2$  mm<sup>3</sup>,  $P < 0.05$ )- and the simvastatin ( $3.3 \pm 1.1$  mm<sup>3</sup>,  $P < 0.01$ )-treated groups than in the vehicle-treated group ( $8.7 \pm 3.6$  mm<sup>3</sup>). In the tMCAO model, immunoreactivities for HEL, 4-HNE, and 8-OHdG in neurons were increased at 4 and 24 hr after tMCAO in the vehicle-treated animals, while simvastatin significantly reduced such inductions (Figure). **Conclusions:** Treatment with statins reduced infarct volume in the spontaneous stroke model, and ameliorated the oxidative stress in the tMCAO model. Our results suggest that the antioxidative properties of statins could be useful for preventing neuronal damage in cerebral ischemia.



Immunohistochemistry for HEL, 4-HNE and 8-OHdG after tMCAO.  
SC, sham control. Scale bars = 50  $\mu$  m (large panel), 10  $\mu$  m (inset).

**THE NEUROPROTECTIVE EFFECTS OF A NEWLY SYNTHESIZED POLY (ADP-RIBOSE) POLYMERASE (PARP) INHIBITOR (KCL-440) ON NEURONAL CELL DEATH FOLLOWING TRANSIENT FOCAL ISCHEMIA IN RAT**

**Tatsushi Kamiya, Chikako Nito, Simon Amemiya, Masayuki Ueda, Kengo Kato, Yasuhiro Nishiyama, Satoshi Suda, Toshiki Inaba, Yasuo Katayama**

*Division of Neurology, Second Department of Internal Medicine, Nippon Medical School, Tokyo, Japan*

Background and purpose: Recently, it has been reported that Poly (ADP-ribose) polymerase (PARP), a nuclear protein that participates in DNA base excision repair in response to DNA damage, is involved in the mechanism of ischemic neuronal cell death (1, 2). Over-activation of PARP-1 induced by extensive DNA damage consumes NAD<sup>+</sup> and ATP consequently, leading to necrotic cell death. PARP-1 also induces the activation of nuclear factor κB (NF-κB)-dependent gene expression that initiates cell injury, or induces the release the apoptosis-inducing factor, resulting in PARP-1-dependent apoptotic cell death. Nevertheless, the mechanism of PARP over-activation on the ischemic brain have not been fully understood. The aim of this study is, therefore, to determine whether a newly synthesized PARP inhibitor, KCL-440, which have strong inhibition of PARP-1, would prevent neuronal cell death following transient focal ischemia in rats compared to a free radical scavenger, edaravone , which is the first clinical neuroprotective agent used in Japan for the treatment of acute stroke patients. Methods: Sprague-Dawley rats were subjected to MCAo using an intraluminal suture technique for 2 hours (3). The rats were reperfused for 24 hours and decapitated for infarct and edema analysis (4). Animals were randomly divided into the following four groups. (I) vehicle-treated control group (II) low dose of KCL-440 (3.0 mg/kg)-treated group (III) high dose of KCL-440 (10.0 mg/kg)-treated group (IV) edaravone-treated group. PARP inhibitor-treated animals received a continuous injection of KCL-440 (3.0 or 10.0 mg/kg) intravenously for 6 hours after the onset of ischemia, while vehicle-treated groups received same dose of vehicle. Edaravone-treated animals received twice injection of edaravone (3.0 mg/kg) intravenously after the onset of ischemia and 30 minutes after ischemia. During ischemia, temporal muscle and rectal temperatures were monitored and maintained at 37° in the experimental animals. Neurological symptoms evaluation were performed immediately before infarct and edema analysis. Results: The cortical infarct volume (120±35 mm<sup>3</sup>) in the edaravone-treated group was significantly less than those in group I (251±42 mm<sup>3</sup>, p<0.05), while there was no significant difference in the striatum. KCL-440 (group II, III) decreased the cortical or striatal infarct volume (105±34 mm<sup>3</sup>, 31±10 mm<sup>3</sup> in group II, 64±21 mm<sup>3</sup>, 25±9 mm<sup>3</sup> in group III) significantly compared with those of groups I (251±42 mm<sup>3</sup>, 66±7 mm<sup>3</sup>, p<0.05), dose-dependently. KCL-440 also improved the cortical or striatal edema significantly compared with those of groups I (p<0.05, p<0.05, respectively). Moreover, KCL-440 significantly improved neurological symptoms (posture and hemiplegia). Conclusions: These results demonstrate that a newly synthesized PARP inhibitor, KCL-440 prevents neuronal cell death, compared to a free radical scavenger, edaravone. Furthermore, it is suggested that this PARP inhibitor may be a candidate for new neuroprotectant for the treatment of acute stroke in future. References:(1) Eliasson MJ, Sampei K, Mandir AS et al., *Nat Med* 1997;3: 1089-1095. (2) Virag L, Szabo C. *Pharmacol Rev* 2002;54:375-429. (3) Nito C, Kamiya T, Ueda M et al. *Brain Res* 2004;1008:179-185. (4) Jacewicz M, Tanabe J, Pulsinelli WA. *J Cereb Blood Flow Metab.* 1992; 12: 359-370.

## THROMBIN GENERATION AND INHIBITION IN THE MEDIATION OF ISCHEMIC NEURONAL DEATH

Marlise de Castro Ribeiro<sup>1</sup>, Jerome Badaut<sup>2</sup>, Melanie Price<sup>1</sup>, Marita Meins<sup>3</sup>,  
Julien Bogousslavsky<sup>1</sup>, Denis Monard<sup>3</sup>, **Lorenz Hirt**<sup>1</sup>

<sup>1</sup>*Neurology, Centre Hospitalier Universitaire Vaudois, Lausanne, Switzerland*

<sup>2</sup>*Neurosurgery, Centre Hospitalier Universitaire Vaudois, Lausanne, Switzerland*

<sup>3</sup>*Friedrich-Miescher Institute for Biomedical Research, Basel, Switzerland*

Thrombin is a serine protease with dual effects on cell death and survival: It mediates apoptotic cell death at high concentrations in cultured astrocytes and hippocampal neurons and induces neuroprotection at low concentrations in the same cells. Recent evidence indicates that thrombin plays a role in ischemic cell death, as rats subjected to middle cerebral artery occlusion were protected by the intracerebral injection of hirudin, a selective thrombin inhibitor. We are using an in vitro approach to further characterise the mechanisms involved. Organotypic hippocampal slice cultures were subjected to a 30 minute oxygen (10%) and glucose (1mmol/L) deprivation (OGD). 24 hours after OGD, there was a marked increase in thrombin immunoreactivity on Western blots, showing for the first time that OGD leads to the activation of prothrombin into thrombin. We could also demonstrate that this ischemia induced activation of thrombin plays an important role in ischemic neuronal death, as both recombinant hirudin and protease nexin-1, an endogenous cerebral thrombin inhibitor, significantly prevented neuronal death, when administered after OGD. Using this in vitro approach we are currently characterising the role of thrombin as a mediator of ischemic neuronal death.

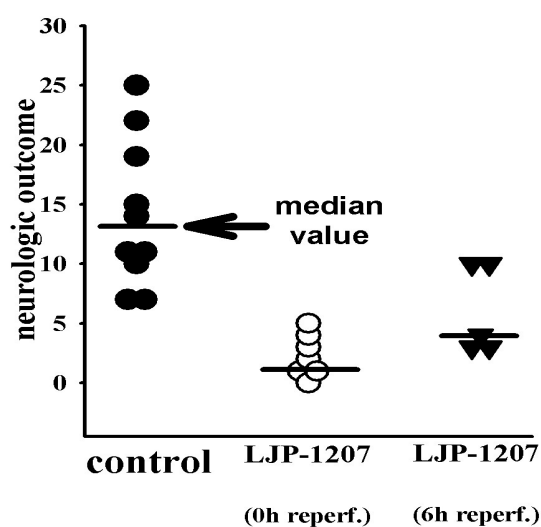
**PROLONGED THERAPEUTIC WINDOW ASSOCIATED WITH PHARMACOLOGIC BLOCKADE OF VASCULAR ADHESION PROTEIN-1 (VAP-1)-RELATED POST-ISCHEMIC LEUKOCYTE ADHESION IN DIABETIC, OVARIECTOMIZED (OVX) FEMALE RATS GIVEN CHRONIC ESTROGEN REPLACEMENT**

Dale A. Pelligrino<sup>1</sup>, Luisa Salter-Cid<sup>2</sup>, Matthew D. Linnik<sup>2</sup>, Hao-Liang Xu<sup>1</sup>

<sup>1</sup>*Neuroanesthesia Research, University of Illinois at Chicago, Chicago, IL, USA*

<sup>2</sup>*La Jolla Pharmaceutical Co., La Jolla, CA, USA*

Endothelial VAP-1 facilitates post-ischemic leukocyte adhesion and infiltration in cerebral venules (abstract-this meeting). Evidence suggests that this role of VAP-1 relates, in part, to its function as an amine oxidase and the formation of H<sub>2</sub>O<sub>2</sub> and aldehydes. In the present study, we examined whether treatment with a specific inhibitor of the enzymatic function of VAP-1 (LJP-1207) was capable of reducing the neuropathology accompanying transient forebrain ischemia (TFI). We used a model associated with a high level of post-ischemic leukocyte adhesion and infiltration—diabetic (6-8 wks post-streptozotocin) OVX female rats given 1 week of estrogen replacement therapy (ERT). The rats were allowed to recover over 3 days following 20 min TFI. We compared rats treated, either at the onset or at 6h reperfusion, with saline or LJP-1207 (30 mg/kg iv). Neurologic function was scored each day over the 3-day reperfusion period. The daily scores could range from 0 (no dysfunction) to 18 (severe dysfunction). In controls (n=10), the 3-day score was 13 ± 2; while in the VAP-1-inhibited rats, the scores were 2 ± 1 (LJP-1207 treatment @0h reperfusion [n=7]) and 6 ± 1 (LJP-1207 treatment at 6h reperfusion [n=5]) (see figure). Both treatment groups were statistically different from control. Findings from our laboratory have shown that leukocyte infiltration, in diabetic OVX females given ERT, commences at >6h reperfusion (Stroke 35:1974-8, 2004), and that this “transformation” is largely prevented by LJP-1207 (abstract-this meeting). These findings, therefore, indicate that VAP-1-mediated post-TFI leukocyte adhesion/infiltration, in diabetic OVX females given chronic ERT, contributes substantially to neuropathology. One intriguing implication of these findings is that preventing leukocyte infiltration may provide a substantial measure of neuroprotection. This could explain the finding of LJP-1207 having at least a 6-hour therapeutic window, in this model.

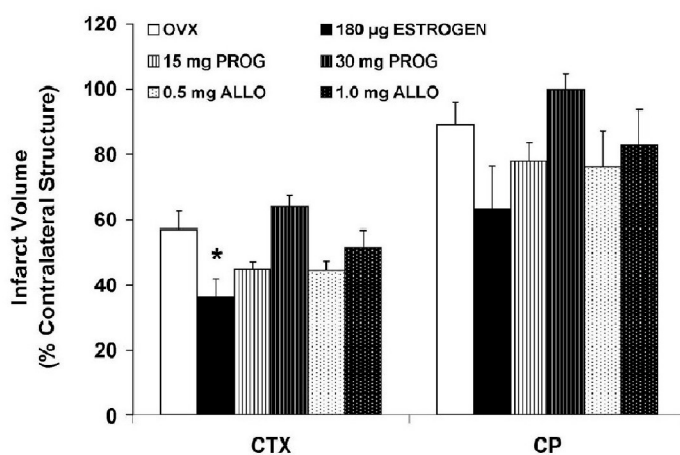


## PROGESTERONE AND ALLOPREGNANOLONE AS NEUROPROTECTANTS IN ISCHEMIC OVARIECTOMIZED MOUSE BRAIN

Susan M. Parker, Patricia D. Hurn, **Stephanie J. Murphy**

*Anesthesiology and Peri-Operative Medicine, Oregon Health and Science University,  
Portland, OR, USA*

**Introduction:** We have demonstrated that infarction following transient middle cerebral artery occlusion (MCAO) is smaller in female rats and that this protection is lost after ovariectomy (1). We have also shown that chronic progesterone administration before ischemia exacerbates striatal injury in ovariectomized rats (2) but that low dose acute progesterone treatment before and after experimental stroke is neuroprotective (3). Allopregnanolone, a progesterone metabolite, is neuroprotective in rat traumatic brain injury (4) and may mediate progesterone's neuroprotective effects. The purpose of this study was to determine in ischemic ovariectomized mouse brain if exogenous progesterone or allopregnanolone administration can be neuroprotective. **Methods:** Seven to 8 days before MCAO, C57BL/6 mice were ovariectomized and received concurrently either no hormone (OVX), 180  $\mu$ g 17 $\beta$ -estradiol (ESTROGEN) via subcutaneous silastic implant, 15 or 30 mg 21-day release commercial progesterone (PROG) pellets placed subcutaneously, or 0.5 or 1.0 mg allopregnanolone (ALLO) via subcutaneous silastic implant. Each animal subsequently underwent 90 minutes of MCAO by the intraluminal filament technique (5) followed by 22 hours reperfusion. Cortical (CTX) and caudate-putamen (CP) infarct volumes were determined by digital image analysis of sequential 2 mm thick coronal brain slices stained with 2,3,5-triphenyltetrazolium chloride. Laser-Doppler flowmetry (LDF) was used to estimate ischemic reduction of cortical perfusion at initiation of MCAO. **Results:** Rectal temperatures were maintained within normal physiological range and were equivalent among treatment groups. Results of CTX and CP infarct volumes are shown in figure. LDF (% baseline) at induction of MCAO was equivalent among treatment groups. All data are mean  $\pm$  SEM. \* $p < 0.05$  from OVX. **Conclusion:** Chronic, exogenous progesterone and allopregnanolone administration prior to MCAO at the tested doses did not significantly alter ischemic brain injury in ovariectomized female mice. **References:** [1] Alkayed NJ, Harukuni I, Kimes AS, et al.; *Stroke* 29:159-165 (1998) [2] Murphy SJ, Traystman RJ, Hurn PD; *Stroke* 31:1173-1178 (2000) [3] Murphy SJ, Littleton-Kearney MT, Hurn PD; *JCBFM* 22:1181-1188 (2002) [4] He J, Hoffman SW, Stein DG; *Restor Neurol Neurosci* 22:19-31 (2004) [5] Eliasson MJ, Sampei K, Mandir AS, et al.; *Nat Med* 3:1089-1095 (1997) **Grant Support:** Supported by NIH grants RR00163, NS33668, and NR03521.





**NEUROPROTECTIVE ACTIVITY OF GLUCOCORTICOIDS AGAINST NMDA TOXICITY IN MOUSE CORTICAL NEURON-ASTROCYTE CULTURES: POTENTIAL ROLE OF THE TPA-PAI-1 AXIS**

**Edith Debroas**, Carine Ali, Nathalie Lebeurrier, Denis Vivien, Dominic Duval

*INSERM-Avenir 'TPA in the Working Brain', Caen, France*

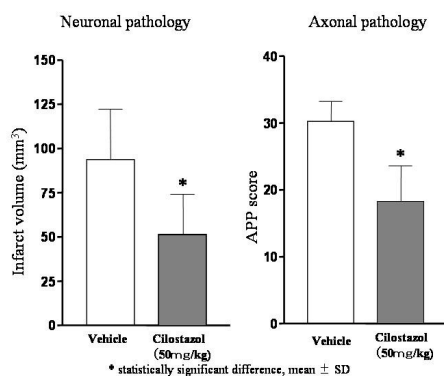
Given the potent anti-inflammatory effects exerted by glucocorticoids under various pathological situations, their use has been proposed to protect the brain against cerebral ischemia, neuro-inflammatory diseases and trauma. However, the efficiency of these treatments remains a matter of debate, since both neuroprotective and neurotoxic effects have been observed depending on the experimental models used (Ábrahám et al., J Neuroendocrinol., 13: 749, 2001). First we observed that purified neuron and astrocyte populations both express the mRNA encoding for the glucocorticoid receptor (as determined by RT PCR), suggesting that both cell type might respond to glucocorticoid. In order to further understand the role of glucocorticoids in brain tissues, we have tested the effect of dexamethasone (a potent glucocorticoid) in a model of mixed murine cultures of neurons and glia subjected to N-methyl-D-aspartate (NMDA)-induced excitotoxicity. We observed that pre-treatment of the cultures with dexamethasone significantly reduced NMDA-induced neuronal necrosis. We also described that dexamethasone (dose and time dependently) induced within 12-24 hours of treatment a significant increase in both the synthesis and secretion of type 1 plasminogen activator inhibitor (PAI-1) in astrocyte cultures. Previous experiments in the laboratory have shown in the same paradigm of NMDA-induced toxicity that tPA markedly increases the deleterious action of NMDA and that this potentiating action of tPA is abolished by PAI-1 (Buisson et al., FASEB J, 12: 1683, 1998). Since dexamethasone led to a significant decrease in t-PA activity (as assessed by zymography assay), our results suggest that glucocorticoids might exert a neuroprotective activity against NMDAR-mediated toxicity by interacting with the t-PA/PAI-1 axis.

## CILOSTAZOL PROTECTS BOTH GREY AND WHITE MATTER IN A RODENT MODEL OF PERMANENT FOCAL CEREBRAL ISCHEMIA

Fumiaki Honda, Hideaki Imai, Chisato Kubota, Tatsuya Shimizu, Nobuhito Saito

*Department of Neurosurgery, Gunma University Graduate School of Medicine, Gunma, Japan*

**Background and Purpose:** Cilostazol, an inhibitor of phosphodiesterase type 3, has been demonstrated to increase the intracellular cyclic AMP and is approved for use for treating intermittent claudication by the Food and Drug Administration. Recently cilostazol was approved by Japanese Health and Welfare Organization as the drug for prevention of lacunar infarction. The aim of this study was to determine the ability of cilostazol to reduce ischemic damage in both grey and white matter in a rodent model of permanent focal cerebral ischemia. **Methods:** Adult male Sprague Dawley rats (300- 370g) were used. The left middle cerebral artery (MCA) was occluded by electrocoagulation of the MCA using a modification of the Tamura method (1). Rats were randomly assigned into three groups to receive 30 (n=7), 50 mg/kg (n=7) cilostazol or the placebo (n=8). Cilostazol (30 or 50 mg/kg) or vehicle was administered by gavage 30 min and 4 hours after the induction of cerebral ischemia by permanent occlusion of the left MCA. Animals were killed 24 hours following MCA occlusion, and the volume of grey matter damage evaluated by quantitative histopathology. The hemispheric extent of axonal damage was determined by amyloid precursor protein (APP) immunohistochemistry. APP score was calculated by the previously reported method (2). **Results:** Treatment with the higher dose cilostazol (50 mg/ kg) significantly reduced the volume of grey matter damage in the cerebral hemisphere by 45.0 % (p< 0.05) and cerebral cortex by 48.5% (p< 0.05), respectively, compared with vehicle. Axonal damage was reduced by 39.5 % (p< 0.005) (Figure). The neuroprotective efficacy of the lower dose (30 mg/kg) was less than that of higher dose cilostazol. The volume of ischemic damage in the cerebral hemisphere was reduced by 36.8 % (p<0.05) and cerebral cortex by 40.4% (p< 0.05). Both doses of cilostazol (30, 50 mg/kg) had no therapeutic efficacy on the caudate nucleus, where ischemia was most severe in this model. **Conclusions:** The treatment with cilostazol significantly reduced grey and white matter damage with permanent ischemia. The main neuroprotective mechanism of cilostazol has been linked to its inhibition of platelet aggregation and vasorelaxant, which may contribute to beneficial action in terms of restore of cerebral blood flow in penumbra. Cilostazole was reported to dilate pial arteries and inhibit the formation of thrombosis during focal ischemia in the cat. The treatment of cilostazol is likely to be a one of the most beneficial pharmacological regimen that will minimize brain injury in acute stroke. **Reference:** (1) A Tamura et al (1981) *J Cereb Blood Flow and Metab* 1:53-60. (2) H Imai et al (2002) *J Cereb Blood Flow and Metab* 22: 1080-1089.



**ATORVASTATIN REDUCES CEREBRAL INFARCTION VIA INHIBITING NADPH OXIDASE-DERIVED SUPEROXIDE IN TRANSIENT FOCAL ISCHEMIA**Hua Hong<sup>1,2</sup>, Jin-Sheng Zeng<sup>2</sup>, Yong-Yuan Guan<sup>3</sup>, **Alex F. Chen**<sup>1</sup><sup>1</sup>*Departments of Pharmacology, Neurology and Neuroscience, Michigan State University, East Lansing, MI, USA*<sup>2</sup>*Department of Neurology and Stroke Center, The First Affiliated Hospital, Sun Yat-Sen University, Guangzhou, China*<sup>3</sup>*Department of Pharmacology, Sun Yat-Sen University, Guangzhou, China*

Introduction: Statins have recently been shown to exert neuronal protection in ischemic stroke. Reactive oxygen species (ROS) including superoxide anion formed during early phase of reperfusion in ischemic stroke augments neuronal injury, and NADPH oxidase is a key enzyme for superoxide production. The present study tested the hypothesis that atorvastatin reduces cerebral infarct size via inhibiting NADPH oxidase-derived superoxide in transient focal ischemia. Methods: Focal ischemia (2 hours) was created in halothane-anesthetized adult male Sprague-Dawley rats (250-300 g) by middle cerebral artery occlusion (MCAO). Atorvastatin (Lipitor™, 10 mg/kg) was administrated subcutaneously 48, 24 and 2 hrs prior to MCAO. Infarct volume was determined by triphenyltetrazolium chloride staining. NADPH oxidase enzymatic activity and superoxide levels were quantified in both ischemic core and penumbral regions by lucigenin (5 μM)-enhanced chemiluminescence assay. Expression of NADPH oxidase membrane subunit gp91phox and cytosolic subunit p47phox was measured by Western blot analysis. Results: NADPH oxidase enzymatic activity was increased following reperfusion and peaked within 2 hours of reperfusion in the penumbra, but not core, of MCAO rats (31.9±5.5 vs. 16.8±0.8 nmol/min/mg protein in control, p<0.01, n=4-5), which was prevented by atorvastatin pretreatment (21.2±1.3, p<0.05, n=4-5). Furthermore, atorvastatin treatment significantly reduced superoxide levels (0.3±0.07 vs. 0.6±0.04 nmol/min/mg protein in control, p<0.001, n=3-4), impeded the expression of NADPH oxidase membrane subunit gp91phox (73±3 vs. 104±9% in control, p<0.01, n=3) and the translocation of cytosolic subunit p47phox to the membrane (78.8±1.5 vs. 239.5±78.9% in control, p<0.05, n=6-7) in the penumbra 2 hrs after reperfusion in MCAO rats. Consequently, cerebral infarct volume was significantly smaller in atorvastatin-treated compared to non-treated control MCAO rats 24 hours after reperfusion (11±3 vs. 22±1% in control, p<0.01, n=6). Conclusions: These results demonstrate that atorvastatin reduces cerebral infarct size via inhibiting NADPH oxidase-derived superoxide in transient focal ischemia. (Supported by American Heart Association grants #0130537Z and #0455594Z (to AFC), China Medical Board (CMB) grant #00730 and the National Natural Sciences Foundation of China grants #39940012 and #30271485 (to JSZ and YYG).

**STROKE PROTECTION BY ATORVASTATIN TREATMENT IN STROKE-PRONE SPONTANEOUSLY HYPERTENSIVE RATS (SHRSPS):1. RATE OF MORBIDITY AND MORTALITY OF STROKE, AND SERUM ASYMMETRIC DIMETHYL ARGININE (ADMA)**

**Noriko Tanaka**, Toshiya Katsumata, Tatsuo Otori, Yutaka Nishiyama, Hidenori Nakamura, Yasuo Katayama

*Internal Medicine 2, Nippon Medical School, Tokyo, Japan*

**Purpose** Previous studies have demonstrated neuronal protective effects of statin treatment. ADMA is an inhibitor of endogenous nitric oxide, which regulates blood circulation to adjust vascular diameter, and is considered to inversely correlated with nitric oxide production. The objective of the present study was to determine whether atorvastatin treatment to SHRSPs protects against stroke. Serum biochemical examinations including ADMA were also examined. **Methods** Male 8 weeks SHRSPs were treated orally daily with atorvastatin suspension at a high dose of 20mg/kg (n=10, A group) or a low dose of 2mg/kg (n=10, B group). Vehicle male 8 weeks SHRSPs were treated orally daily with same amount of suspension without atorvastatin (n=10, V group). Body weight was measured every day after treatment started, and blood pressure and heart rate were measured at the age of 8 and 17 weeks. To determine a morbidity of stroke, neurological score was examined every day. Biochemical examinations including cholesterol and ADMA were measured at the age of 19 weeks. **Results** Each mean survival times were 76 (A group), 64 (B group) and 50 (V group) days from the day of treatment started (Kaplan-Meier method). Survival period in A group was significant longer than that in V group (logrank test). Each mean period of stroke morbidity were 42 (A group), 39 (B group) and 35 (V group) days from the day of treatment started (Kaplan-Meier method). The period of stroke morbidity in A group was significant longer than that in V group (logrank test). There were no significant differences in body weight, blood pressure and heart rate among three groups (Dunnett test). ADMA was significantly lower in A group ( $0.61 \pm 0.06$ ) than V group ( $0.81 \pm 0.18$ ) (mean  $\pm$  SD, Dunnett multiple comparison test), whereas there were no significant differences in biochemical examinations of serum cholesterol, renal and liver functions and creatinine phosphokinase. **Conclusions** It was demonstrated that atorvastatin treatment reduced morbidity and mortality of stroke in SHRSPs. It was suggested that this protection was mediated by up regulation of nitric oxide production by atorvastatin treatment.

## MAPPING OF GLIAL METABOLISM IN INTACT RAT BRAIN USING 14C-ACETATE

Rie Hosoi<sup>1</sup>, Yuto Kashiwagi<sup>1</sup>, Shin-ichiro Hirose<sup>1</sup>, Koji Abe<sup>1</sup>, Jun Hatazawa<sup>2</sup>, Antony Gee<sup>3</sup>, Osamu Inoue<sup>1</sup>

<sup>1</sup>*Course of Allied Health Sciences, Graduate School of Medicine, Osaka University, Osaka, Japan*

<sup>2</sup>*Department of Diagnostic Medicine, Osaka University Graduate School of Medicine, Osaka, Japan*

<sup>3</sup>*GlaxoSmithkline, Clinical Research Unit, Cambridge, UK*

**Introduction** Exogenous acetate is preferentially taken in astrocytes by monocarboxylate transporter-1 (MCT1) mediated process. Recently, we found that 14C-acetate uptake in the rat brain appears to occur in parallel with glial energy metabolism and reflects glial conditions. In this study, we examined in vivo 14C-acetate uptake after ischemia/reperfusion of middle cerebral artery (MCA). Effects of microinjection of excitotoxic amino acid into rat striatum were also studied. **Methods** Male Wistar rats (8-9 weeks old) were used, and middle cerebral artery occlusion (MCAO) was made under halothane anesthesia. After 3, 10, 30 and 90 minutes of MCAO, the intraluminal suture was removed for reperfusion. Immediately after the reperfusion, rats were given an intravenous bolus injection of 14C-acetate, 14C-IMP, or 14C-deoxyglucose (DG) and decapitated 5 minutes, 0.5 minute, or 45 minutes after the tracer injection. Coronal sections (20 µm) were prepared and autoradiograms were obtained. The radioactivity concentrations in regions of interest (ROIs) were determined as the photo-stimulated luminescence (PSL) values and expressed as the proportion of the value on the ischemic side to that on the contralateral side. For excitotoxic amino acid experiments, rats were microinjected with ibotenic acid (16 µg/2 µl) into the left striatum. At 3, 24 hours and 2 weeks after the microinjection, autoradiograms for 14C-acetate and 14C-DG were prepared by the same method. The sections were stained with cresyl violet for estimating cell injury. **Results and Discussion** The brain uptake of 14C-acetate was very sensitive to brain ischemia. Immediately after the 3 minutes-MCAO and reperfusion, 14C-acetate uptake showed a significant reduction (50%) in the rat striatum (ischemic core). In contrast, 14C-DG uptake was almost unaltered by 3 minutes-MCAO and reperfusion. By 90 minutes occlusion, 14C-acetate uptake in the striatum was reduced to 30%, whereas 14C-DG uptake was decreased to 70%. The reduction areas were expanded to cerebral cortex (penumbra) with increase in occlusion period. A significant increase in regional blood flow was seen in the striatum and cerebral cortex in rat brain occluded for 10 and 30 minutes, which indicated 14C-acetate uptake was independent on changes in blood flow. Transient down regulation of MCT-1 function or glial metabolism is the mechanism for sensitive reduction in 14C-acetate uptake in ischemic rat brain. Ibotenic acid caused significant reduction in 14C-acetate uptake at 3, 24 hours and 2 weeks after the microinjection. An increase in 14C-DG uptake was seen at 3 hours after the ibotenic acid injection, however decreases in glucose metabolism were observed at 24 hours and 2 weeks after the microinjection. These results indicated that excitotoxic amino acid might have important roles on regulation of 14C-acetate uptake in intact rat brain. In conclusion, 14C-acetate is a very sensitive probe to detect glial dysfunction in ischemic rat brain.

## NEUROPROTECTIVE EFFECTS OF DEXMEDETOMIDINE-HYPOTHERMIA AFTER ASPHYXIAL CARDIAC ARREST IN RATS

**Tetsu Kimura**, Toru Goyagi, Makoto Tanaka, Yoshitsugu Tobe, Yoko Masaki,  
Toshiaki Nishikawa

*Department of Anesthesia and Intensive Care Medicine, Akita University School of Medicine,  
Akita, Japan*

Background: Dexmedetomidine and hypothermia are known to reduce brain injury following ischemia. We examined whether dexmedetomidine would enhance the neuroprotective effects of hypothermia after asphyxial cardiac arrest in rats. Methods: Male Sprague-Dawley rats, anesthetized with halothane, were assigned to one of four groups (n = 7 for each group); control (C, saline 1 ml/kg and temporal muscle temperature 37.5°C), dexmedetomidine (D, dexmedetomidine 10 µg/kg and 37.5°C), hypothermia (H, saline 1 ml/kg and 35.0°C), and dexmedetomidine - hypothermia (DH, dexmedetomidine 10 µg/kg and 35.0°C) groups. After obtaining predetermined temporal muscle temperature, either dexmedetomidine or saline was administered intraperitoneally 30 min before insult. Cerebral ischemia was induced with asphyxia of 5 min, which led to cessation of circulation at about 3 min of apnea, resulting in cardiac arrest of about 2 min. Spontaneous circulation was restored by external cardiopulmonary resuscitation and intravenous epinephrine. Neurological deficit score (worst = 0; best = 18) was assessed at 24, 48, and 72 hours after return of spontaneous circulation, and then the brain was fixed and stained with hematoxylin and eosin. Results: Percentages of intact neurons in hippocampal CA1 were smaller in the group C than the other groups (C, D, H, and DH: 26 ± 14, 53 ± 9, 61 ± 5, and 58 ± 21 (mean ± SD), respectively (P < 0.05), whereas percentages of intact neurons in cerebellar Purkinje cells were similar among the groups. Neurological deficit scores were similar among the groups. Conclusions: Our results suggest that intraperitoneal dexmedetomidine 10 µg/kg and hypothermia have the neuroprotective effects after asphyxial cardiac arrest respectively, whereas the addition of dexmedetomidine to hypothermia does not enhance the neuroprotective effects of hypothermia.

**HYPERGLYCEMIA INCREASES PROTEIN KINASE C (PKC) ACTIVITY AND MYOGENIC TONE OF PENETRATING BRAIN PARENCHYMAL ARTERIOLES AND IS ASSOCIATED WITH DIMINISHED POSTISCHEMIC REPERFUSION AND ENHANCED INFARCTION**

**Marilyn J. Cipolla**, Lisa Vitullo, Nicole Hoyniak, Rachael Hannah

*Department of Neurology, University of Vermont, Burlington, Vermont, USA*

Background: Preexisting hyperglycemia is associated with enhanced injury in the postischemic brain, including a significantly higher incidence and severity of cerebral infarction and edema formation. Because elevated glucose is known to have a significant effect on vascular function, including myogenic tone and reactivity, we hypothesized that elevated glucose influences stroke outcome through a direct effect on cerebral blood flow (CBF) and the extent of postischemic reperfusion. Methods: Male Wistar rats that were either normoglycemic (n=19; glucose=158±12mg/dL) or hyperglycemic (n=17; glucose=348±41mg/dL; p<0.01) by injection of 50mg/kg streptozocin (STZ) for 3 days, underwent middle cerebral artery occlusion (MCAO) for 1 hour followed by 30 min. of reperfusion. Neurologic deficit score (out of 32), infarction score (0-4) after TTC staining, and percent of CBF recovery were compared between groups. In separate groups of animals that did not undergo MCAO, microvessels were isolated and PKCβII activity determined by Western analysis of phospho-PKCβII. Lastly, the percent of myogenic tone was determined in isolated and pressurized parenchymal arterioles. Results: Hyperglycemic animals had significantly worsened stroke outcome compared to normoglycemic controls, including neurologic deficit score (32.0 ± 0.0 vs. 4.5 ± 1.5; p<0.01), infarct score (3.5 ± 0.5 vs. 1.5 ± 0.4; p<0.01) and extent of CBF recovery (58 ± 12% vs. 87 ± 13%; p<0.05). Further, high serum glucose negatively correlated with decreased reperfusion after ischemia (r= 0.5; p=0.02). In cerebral microvessels, PKCβII activity was significantly elevated in hyperglycemic animals compared to controls (Western ratio = 2.7 ± 0.3 vs. 3.8 ± 0.8; p<0.01) that was associated with increased myogenic tone (% tone at 40mmHg= 38 ± 2% vs. 54 ± 8%; p<0.01). Conclusions: These results demonstrate that preexisting hyperglycemia significantly worsens stroke outcome, including enhanced infarction and neurologic deficit, possibly through a direct effect on the vasculature that diminishes postischemic reperfusion. Increased PKCβII activity in cerebral microvessels is likely due to enhanced flux of glucose through the glycolytic pathway that increases diacylglycerol accumulation, the primary activator of PKC. This pathway has been shown to be a major contributor to diabetic vascular complications. In addition, since PKC activity is known to underlie myogenic activity, it is possible that its enhanced activation under hyperglycemic conditions contributes to the greater myogenic tone in those animals, an effect that would serve to diminish CBF reperfusion and worsen stroke outcome. In conclusion, it appears that the cerebrovasculature is a potential therapeutic target for protection during hyperglycemic stroke, possibly by preventing the glucose-induced increase in PKCβII activation and/or enhanced myogenic tone. Supported by NIH NS40071 and Totman Medical Research Trust.

## PROTECTIVE EFFECT OF MINOCYCLINE TREATMENT ON STRIATAL ISCHEMIA IN RATS

Huijin Yan<sup>1</sup>, Richard Buist<sup>1</sup>, Dale Corbett<sup>2</sup>, James Peeling<sup>1,3</sup>

<sup>1</sup>*Department of Radiology, University of Manitoba, Winnipeg, Canada*

<sup>2</sup>*Department of Basic Medical Sciences, Memorial University, St. John's, Newfoundland, Canada*

<sup>3</sup>*Department of Pharmacology and Therapeutics, University of Manitoba, Winnipeg, Canada*

We demonstrated previously that minocycline is neuroprotective in a rat model of collagenase-induced intrastriatal hemorrhage through depression of inflammation. Minocycline treatment significantly reduced necrotic damage and apoptotic cell death, suppressed monocyte activation, and downregulated MMP-12 (matrix metalloproteinase) expression. The present study examined the effect of minocycline treatment in an intrastriatal ischemia (ISI) model in rat. Twenty-four male SD rats received an intrastriatal injection of endothelin-1 (ET-1, 400 pmol in 1 $\mu$ L saline) under halothane anesthesia. Minocycline was given intraperitoneally at a dose of 45 mg/kg 1 hour before or 3 hours after ISI, and on days 1, 2, and 3, and 22.5mg/kg on day 4 and 5. Control rats received equivalent injections of saline at the same times. Behavioral tests (forelimb postural reflex, spontaneous circling, and beam walking) were conducted before and 2, 4, 7, and 21 days after ISI. Rats in both treatment groups showed a significant improvement in behavioral scores ( $p < 0.05$ ) as early as day 2 after ISI, and this was maintained until day 21 ( $p < 0.01$ ). The cylinder test, which measures any asymmetrical usage of the forelimbs during postural support, was conducted before and at 1 and 3 weeks after ISI. Rats in the control group displayed more reliance on the ipsilateral limb, while those in both treatment groups showed a nearly normal pattern ( $p < 0.05-0.01$ ), after ISI. Delaying the initiation of minocycline treatment to 3 hr after ISI was as effective as starting treatment before ISI. All rats underwent MRI examination for brain perfusion 1 hour after ISI, and T2-MRI 2 days and 21 days after ISI. The size of the ischemic lesion at 2 days was not different significantly between groups, nor was there a difference in blood flow in the lesion region of interest. The final volume of histological injury was correlated with MRI estimates of damage. The results showed that the neurobehavioral outcome was significantly improved with minocycline treatment after ISI, even though there was no marked difference in the size of the ischemic lesion, and that there appears to be a clinically useful window for minocycline treatment. (Supported by the Canadian Stroke Network).

## PROTECTIVE EFFECT OF THE FREE RADICAL SCAVENGER (EDARAVONE) AGAINST THE PHOTOCHEMICALLY INDUCED CEREBRAL INFARCTION IN THE MICE

Shinji Nakajima<sup>1</sup>, Syoujiroh Sawada<sup>1</sup>, Yuhji Morimoto<sup>3</sup>, Souichiroh Nomura<sup>2</sup>

<sup>1</sup>First Internal Medicine, NDMC, Tokorozawa, Japan

<sup>2</sup>Neurology/Psychiatry, NDMC, Tokorozawa, Japan

<sup>3</sup>Medical Engineering, NDMC, Tokorozawa, Japan

Introduction: Edaravone is a potent free radical scavenger, which is known to reduce the size of infarction in animal experiments and clinical applications. The aim of this study is to observe sequentially the effect of this unique antioxidant against the photochemically induced cerebral infarction in the non-invasive way using the higher magnetic field MRI device. Methods: C57BL/6J mice (25-30g) were anesthetized by the intraperitoneal injection of chloralose and urethane mixture, keeping the rectal temperature at 37.5 degrees on the thermo-regulated heating pad (Nihon Kohden, ATB-1100). Photothrombosis (PT) was created in the right parietal lobe by the stereotactic illumination of the laser-diode light (532 nm, 5 mW) for 30 minutes after the injection of rose-bengal solution via the tail vein. Cerebral blood flow was measured on the right parietal lobe using the laser-Doppler flow meter (Advance, ALF21), and the mean arterial pressure with heart rate was monitored throughout the experiment from the tail artery (Muromachi, MK-2000). Animals were divided into the ischemic control (C) group (N=6), and edaravone (E) group (N=6) treated twice (3 mg/kg iv, each time), immediately before and after PT. Cerebral images were taken by the 9.4 T MRI (Bruker, AVANCE400WB) at 1- and 3-hour, 1- and 3-day, and 1-week after PT in individual mice. Ischemic changes were measured sequentially in T1+Gd-DTPA (PWI), Diffusion (DWI), and T2 weighted images (20mm FOV, 256x128 matrix, coronal slice) by the ROI analysis program. Small numbers of mice were used for the videomicroscopic observation through the cranial window and the morphological analysis. Results: Microscopic observation through cranial windows showed diffuse cortical vessel occlusions by homogenous thrombi in the C group, indicating the enough ischemic insult by 30-minutes irradiation of green light laser. In the C group, MR images showed moderate ischemic changes in PWI and DWI at 1-hour. T2 changes appeared at 3-hour, further enlarging in size at 1- and 3-day, and then subsided at 1-week. These edematous changes apparently reduced in the E group. The cross-sectional size of ischemic T2 changes occupied  $36.2 \pm 1.9$  % ( $M \pm SEM$ ) of the ipsilateral hemisphere at 3-day in the C group, and it decreased to  $9.6 \pm 2.6$  % ( $p < 0.05$ ) in the E group. Conclusion: Free radical scavenger, edaravone, markedly decreased the size of ischemic changes induced by photothrombosis. One mechanism of protection may be due to the reduction of the post-ischemic inflammatory process through blocking the dissociation of NFkB and Ikb by free radicals. Another mechanism might be the attenuation of blood brain barrier disruptions by interfering free radical reactions initiated by singlet oxygen molecules generated photochemically at endothelium (1). Further analysis will be required. References: (1) Dietrich WD et al., Acta Neuropathol (Berl) 1987; 72: 315-325

**3-METHYL-PHENYL-2-PYRAZOLIN-5-ONE (EDARAVONE), A NOVEL FREE RADICAL SCAVENGER: EDARAVONE INHIBITS THE INCREASE OF PLASMA OXLDL AND S100B IN PATIENTS WITH ACUTE CORTICAL INFARCTION**

Atsuhiko Suzue<sup>1</sup>, Masaaki Uno<sup>1</sup>, Keiko T. Kitazato<sup>1</sup>, Kazuhito Matsuzaki<sup>1</sup>, Hiroyuki Itabe<sup>2</sup>, Shinji Nagahiro<sup>1</sup>

<sup>1</sup>*Department of Neurosurgery, Institute of Health Biosciences, The University of Tokushima Graduate School, Tokushima, Japan*

<sup>2</sup>*Department of Biological Chemistry, School of Pharmaceutical Sciences, Showa University, Tokyo, Japan*

Objective: MCI-186 inhibits both nonenzymatic lipid peroxidation and lipid oxygenase pathway of the arachidonate cascade. This agent has several neuroprotective effects by inhibiting vascular endothelial cell injury and ameliorating neuronal damage in ischemic brain models. Clinically it represents a neuroprotective efficacy and potentially useful for treating acute ischemic stroke, since it can exert significant effect on functional outcome as compared with placebo. However, to date, there is no assessment regarding any efficacy of MCI-186 based on the plasma biomarkers. Previously we first demonstrated that plasma oxidized low-density lipoprotein (OxLDL) reflects the brain oxidative damage in acute cerebral infarction. And also S100B levels in the plasma have been reported to correlate with the brain damage. The aim of this study is to investigate whether the efficacy of MCI-186 is reflected by the plasma biomarkers of brain damage. Material and Methods: Our study population consisted of 43 patients (27 men and 16 women) who had suffered an ischemic cerebral infarct. Based on the location of the ischemic lesions, they were divided into two groups; G1(n=23) had cortical lesions, G2(n=20) lesions in the basal ganglia or brain stem. MCI-186 was administered for initial 14 days from admission for 26 patients (G1a, n=12, G2a, n=14). The initial use of the drug was within 6h after the stroke onset. The efficacy was compared with patients not treated by MCI-186 (G1b, n=11, G2b, n=6). Plasma OxLDL was determined by a sandwich ELISA. S100B and MnSOD were measured using commercial kits. Neuronal deficits were evaluated by NIH stroke scale (NIHSS) on admission and discharge. Results: In G1 group, admission plasma OxLDL was significantly higher than G2 group ( $p < 0.01$ ). The elevated plasma OxLDL in G1a on admission was significantly decreased after MCI-186 treatment ( $p < 0.05$ ). On the contrary, G1b patients had a persisted increase in plasma OxLDL until 3 days after the insult. Although there was significant difference between G1a and G1b on third days, both G2a and G2b patients had similar plasma OxLDL. The plasma level of S100B and MnSOD in G1a was significantly lower than in G1b 3 days after the treatment ( $p < 0.05$ , respectively). NIHSS in G1a and G2a tended to be lower than in G1b and G2b, the difference was not significant. Conclusions: This is the first evidence that indicated the efficacy of MCI-186 via plasma biomarkers. Our findings indicated that MCI-186 may be useful for the reduction of oxidative damage in the cortical infarction but not the other lesion, and suggested that this effect contributes to the decrease of brain damage, resulting in the decrease of S100B level.

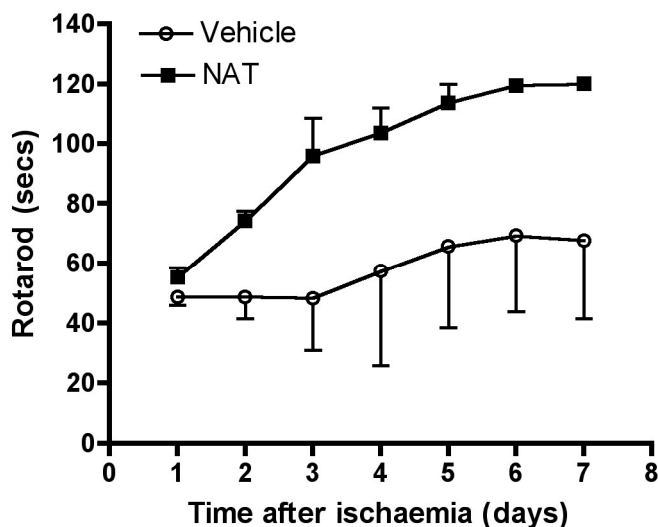
## A SUBSTANCE P ANTAGONIST IMPROVES OUTCOME FOLLOWING REVERSIBLE MIDDLE CEREBRAL ARTERY OCCLUSION IN RATS

Renee J. Turner<sup>1</sup>, Peter C. Blumbergs<sup>1,2</sup>, Robert Vink<sup>1,2</sup>

<sup>1</sup>*Department of Pathology, University of Adelaide, Adelaide, Australia*

<sup>2</sup>*Hanson Institute Centre for Neurological Diseases, Adelaide, Australia*

Previous results from our laboratory (1) have shown that neurogenic inflammation is associated with traumatic brain injury. This neurogenic inflammation was characterized by increased substance P (SP) immunoreactivity, and could be attenuated with administration of SP antagonists with a resultant decrease in functional deficits. The present study examines SP immunoreactivity following experimental stroke in rats and characterizes the effects of a substance P antagonist on functional outcome. Experimental stroke was induced in halothane anesthetized Sprague-Dawley rats using a reversible thread model of right middle cerebral artery occlusion (2) where occlusion was maintained for 2 h and the thread retracted to allow reperfusion. Animals not exhibiting anti-clockwise circling behaviour at 2 h after commencement of reperfusion were excluded from the study. In a subgroup of animals, either 25 mg/kg n-acetyl-tryptophan or equal volume saline was administered i.v. at this timepoint, and their motor function subsequently assessed for 7 days using a rotarod device. Untreated animals were reanesthetized at 24 h and their brains perfusion fixed with 10% formalin, removed and blocked in paraffin wax. Increased SP immunoreactivity relative to the contralateral (non-infarcted) hemisphere was observed in perivascular, neuronal and glial tissue within the penumbra of the infarcted hemisphere. This increased SP immunoreactivity was not as apparent in the infarct core. In animals receiving treatment, administration of the SP antagonist resulted in a significant improvement in rotarod score as compared to vehicle treated animals. We conclude that neurogenic inflammation, as reflected by increased SP immunoreactivity, occurs in the ischemic penumbra following experimental stroke, and that it may be associated with the development of functional deficits. As such, inhibition of neurogenic inflammation may represent a novel therapeutic target for the treatment of reversible, ischemic stroke. (1) Vink R (2004) New developments in the pharmacologic management of posttraumatic edema. 7th Int. Neurotrauma Symp. Medimond, Bologna, pp 55-60. (2) Anderson MF, Nilsson M, Eriksson PS, Sims NR (2004) Glutathione monoethyl ester provides neuroprotection in a rat model of stroke. *Neurosci. Lett.* 354,163-165.



## DO CYCLOSPORIN A AND INSULIN SYNERGISTICALLY PROTECT AGAINST ISCHEMIC SPINAL CORD INJURY IN RABBITS?

Shyunsuke Tsuruta, **Mishiya Matsumoto**, Yumika Koizumi, Shiro Fukuda, Takefumi Sakabe  
*Department of Anesthesiology, Resuscitology Yamaguchi University School of Medicine, Ube, Japan*

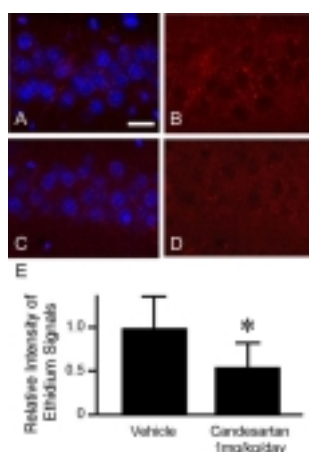
**Introduction:** Cyclosporin A (CsA) has been reported to protect against ischemic brain injury by inhibiting calcineurin and blocking the mitochondrial permeability transition pore. In the present study, we sought to determine whether CsA protects against ischemic spinal cord injury in rabbits. In the preliminary study, we observed CsA-induced hyperglycemia. Therefore, insulin was administered to control blood glucose concentrations. Also, spinal cord microinjury (SCI) was made to facilitate the delivery of CsA to the spinal cord. **Methods:** Thirty New Zealand white rabbits were assigned to one of the five groups (six in each). Group A: sham operation of SCI & vehicle; Group B: SCI & vehicle; Group C: SCI & CsA; Group D: SCI & vehicle & insulin; Group E: SCI & CsA & insulin. SCI was made by insertion of a 0.35 mm steel needle into the spinal cord (2 mm in depth) bilaterally at the level of L 4-5 and L 5-6 interlamina space under general anesthesia four days before ischemia. CsA (10 mg/kg) was administered intravenously daily for three days before ischemia (two days, one day, and just before ischemia). Spinal cord ischemia was induced in all groups for 13 min by occlusion of the abdominal aorta. Hind limb motor function was assessed using five-point grading scale for 4 days after reperfusion as follows: 4 = normal; 3 = ability to hop, but not normally; 2 = inability to hop, but good antigravity strength; 1 = weak antigravity movement only; 0 = paraplegia. Then, the lumbar spinal cord was examined morphologically (HE staining). Data are expressed as mean  $\pm$  SD. \* & #: significant difference ( $P < 0.05$ ) from Group A and B, respectively. **Results:** Blood glucose concentrations just before ischemia were  $163 \pm 19$ ,  $179 \pm 37$ ,  $237 \pm 71$ ,  $120 \pm 21^{*#}$ ,  $115 \pm 15^{*#}$  mg/dl in Group A, B, C, D, and E, respectively. Average motor function scores at 96 h after reperfusion were  $1.3 \pm 0.5$ ,  $1.3 \pm 0.5$ ,  $1.3 \pm 0.5$ ,  $3.3 \pm 1.0^{*}$  # and  $4^{*#}$ , in Group A, B, C, D, and E, respectively. The number of normal neurons in the anterior spinal cord at the L5 level was  $29 \pm 13$ ,  $35 \pm 9$ ,  $33 \pm 8$ ,  $67 \pm 28^{*}$ ,  $73 \pm 8^{*#}$ , in Group A, B, C, D, and E, respectively. **Discussion:** CsA and insulin protected against ischemic spinal cord injury, whereas CsA itself did not have any protective effect even in the animals pretreated with spinal cord microinjury to facilitate the drug delivery to the spinal cord. CsA-induced hyperglycemia may have offset the protective effects of CsA. Insulin itself showed protective effects. SCI might have strengthened the protective effects of insulin. Further investigation would be encouraged to determine the interaction between CsA and insulin as well as the mechanism for protective effects against ischemic spinal cord injury. **References:** 1) Uchino H, et al. *Acta Physiol Scand* 1995;155:469-71 2) Nakao Y, et al. *J Thorac Cardiovasc Surg* 2001;122:136-43

**PRETREATMENT WITH ANGIOTENSIN TYPE II RECEPTOR BLOCKER  
CANDESARTAN REDUCES SUPEROXIDE PRODUCTION AND SUBSEQUENT  
ISCHEMIC NEURONAL INJURY AFTER GLOBAL CEREBRAL ISCHEMIA**

**Taku Sugawara**, Hiroyuki Kinouchi, Masaya Oda, Hidehiko Shoji, Tomoya Omae,  
Suguru Yamaguchi, Kazuo Mizoi

*Neurosurgery, Akita University School of Medicine, Akita, Japan*

**INTRODUCTION** Excessive superoxide production after cerebral ischemia is known to mediate neuronal injury. Angiotensin type 1 receptor (AT1R) activation is a source of superoxide, but whether blockade of AT1R leads to reduction of superoxide and subsequent neuronal injury after ischemia remains unclear. **METHODS** Normotensive rats were treated with daily administration of the AT1R blocker candesartan (0.1---10 mg/kg) or vehicle from days 1 to 12. Global cerebral ischemia was induced for 5 minutes on day 7 and the animals were sacrificed on day 12 for evaluation of morphological injury to the vulnerable hippocampal CA1 neurons. Production of superoxide in these cells in the early stage after ischemia was also examined. **RESULTS** Candesartan 0.5 and 1 mg/kg/day protected approximately 30% of the hippocampal CA1 neurons, whereas only 2% of neurons survived in vehicle-treated animals. There was significantly less superoxide production in these vulnerable neurons in candesartan-treated animals than in vehicle-treated animals (Fig 1: Photomicrographs taken under a confocal microscope of the hippocampal CA1 pyramidal cell layer (A---D) and quantitative study of ethidium signals (E). Numerous punctate superoxide signals were observed in the cytosol of hippocampal CA1 neurons in vehicle-treated animals (A, B), whereas less numerous and less intense signals were observed in the 1 mg/kg/day candesartan-treated animals (C, D). Ethidium signals are shown in panels B and D and nuclear counterstaining overlapped in panels A and C. Quantitative analysis confirmed the differences between these two groups (E, n = 4 each, \*p < 0.05). Scale bar = 20  $\mu$ m.). **CONCLUSIONS** AT1R may be involved in superoxide production and subsequent injury in the vulnerable neurons after global cerebral ischemia.



**INFLUENCE OF ANAESTHESIA ON THE NEUROPROTECTIVE EFFECT  
ELICITED BY 3-AMINOBENZAMIDE, A POLY(ADP-RIBOSE) POLYMERASE  
INHIBITOR, IN A MOUSE MODEL OF TRANSIENT FOCAL CEREBRAL  
ISCHEMIA**

Jérôme Couturier, Elisabeth Letellier, Bruno Palmier, Michel Plotkine, **Isabelle Margail**

*Laboratoire de Pharmacologie, Université Paris 5, Paris, France*

Introduction: We and others reported the neuroprotective effect of 3-aminobenzamide (3-AB), a poly(ADP-ribose) polymerase (PARP) inhibitor in cerebral ischemia (1,2). The aim of this study was to evaluate the effect of 3-AB in transient focal cerebral ischemia performed in mice under two distinct anaesthetics: chloral hydrate (CH) and ketamine/xylazine (KX). Materials: Male Swiss mice (27-32 g) anaesthetized i.p with ketamine (50 mg/kg) + xylazine hydrochloride (6 mg/kg) or with chloral hydrate (400 mg/kg) were subjected to a 1 h-intraluminal occlusion of the left middle cerebral artery (MCAo) followed by reperfusion. Ischemia was controlled by measuring cerebral blood flow in the MCA territory (using MoorLab® laser doppler flowmeter). Treatments with 3-AB at 40 mg/kg or with its vehicle (saline) were administered i.p 15 min prior to reperfusion and again 3 h after its onset. The functional outcome (neurological score, grip test, loss of weight) were examined 24 h after MCAo and infarct volumes were measured after triphenyltetrazolium chloride staining. In a second experiment, PARP activation was evaluated by western blotting of poly(ADP-ribose) polymers 6 hours after ischemia in the ipsilateral brain parenchyma of sham-operated animals (undergoing all the surgery except the filament insertion) and of ischemic mice given 3-AB or its vehicle. Results: The drop in cerebral blood flow (68-72%) did not statistically differ among the four groups. The infarct volume of mice anaesthetized with CH (n=6) was increased by 27% (P<0.05) as compared with mice anaesthetized with KX (n=6). In “CH” mice, 3-AB reduced by 26% the infarct volume (n=6, P<0.05). By contrast, 3-AB (n=8) was devoid of effect in “KX” animals. None of the functional outcome was improved by 3-AB whatever the anaesthetic. In “KX” mice, ischemia induced a 2-fold increase in the level of poly(ADP-ribose) polymers in comparison with sham-operated animals (122±13 arbitrary units (n=6) vs 61±4 arbitrary units (n=6), P<0.01). This PARP activation was inhibited by 90% by 3-AB (67±11 arbitrary units (n=6), P<0.01). Conclusion: One hour MCAo led to larger infarct volumes in mice anaesthetized with chloral hydrate. In this model, 3-AB is neuroprotective suggesting a deleterious role of PARP in cerebral ischemia. By contrast, 3-AB failed to reduce the infarct volume in ketamine+xylazine anaesthetized mice although it completely blocked PARP activation. Thus anesthesia altered the role of PARP in cerebral ischemia. References: 1.Couturier J, Ding-Zhou L, Croci N, Plotkine M, Margail I (2003) 3-Aminobenzamide reduces brain infarction and neutrophil infiltration after transient focal cerebral ischemia in mice. *Exp Neurol* 184: 973-980 2. Virag L, Szabo C (2002) The therapeutic potential of poly(ADP-ribose) polymerase inhibitors. *Pharmacol Rev.* 54: 375-429.

## TEMPORARY CEREBRAL ISCHAEMIA UPREGULATES THE 5-HT(1) RECEPTOR IN THE MIDDLE CEREBRAL ARTERY

Jacob Hansen-Schwartz<sup>1,2</sup>, Flemming F. Johansen<sup>2</sup>, Lars Edvinsson<sup>1,3</sup>

<sup>1</sup>*Department of Experimental Research, Glostrup University Hospital, Glostrup, Denmark*

<sup>2</sup>*Institute of Molecular Pathology, University of Copenhagen, Copenhagen, Denmark*

<sup>3</sup>*Department of Internal Medicine, University of Lund, Lund, Sweden*

Stroke gives rise to an immediately infarcted area surrounded by an area of critically perfused neural tissue ('area at risk'); the fate of this tissue being dependent on increased perfusion subacutely. Using experimental temporary occlusion of the middle cerebral artery (MCA) in the rat we studied the possible upregulation of the 5-HT(1) receptor in the MCA. Experimental stroke: The MCA of an anaesthetised rat was exposed and temporarily occluded with a hook for 120 mins. Afterwards the rat was revitalised. In vitro pharmacological examination: After two days the rat was killed and the MCA's were harvested and suspended on wires for measurement of contractile properties. Selective 5-HT(1) agonists and antagonists were used to study contractile responses. Contractile responses to 5-HT(1) stimulation were clearly enhanced after stroke (compared to the contralateral MCA). This receptor upregulation implies an increased sensitivity towards the endogenous agonist 5-hydroxytryptamine. It has earlier been shown that temporary occlusion leads to upregulation of a contractile ET(B) receptor. The combined upregulation of contractile receptors may further reduce the blood supply to the area at risk, thus, increasing the infarct size with subsequent increased neurological disability. Fig. 1: Concentration-contraction curves showing the effect of the 5-HT1 receptor agonist 5-Carboxamidotryptamine (5-CT) on isolated middle cerebral artery (MCA) segments from a rat model of temporary MCA occlusion. In the ipsilateral MCA (MCAi), i.e. the MCA subjected to occlusion, there is an enhanced response to 5-CT compared to the contralateral side (MCAc). Fig. 2: Concentration-contraction curve showing the effect of the ETB receptor agonist Sarafotxin 6c (S6c). This confirms the findings of Stenman et al (Stroke 2002) showing a contractile response in the MCAi (see fig. 1), not noted in MCAc. In addition we found a spatial relationship with a marked upregulation in the segment adjacent to the site of occlusion (MCAi/dist) compared to the segment closer to the circle of Willis (MCAi/prox).

**MECHANISMS OF NEUROPROTECTION BY ACETYL-L-CARNITINE****Nina J. Solenski<sup>1</sup>, Gary M. Fiskum<sup>3</sup>, Santina A. Zanelli<sup>4</sup>, Robert E. Rosenthal<sup>2</sup>**<sup>1</sup>*Department of Neurology, University of Virginia, Charlottesville, VA, USA*<sup>2</sup>*Trauma Center, Department of Surgery, University of Maryland, Baltimore, MD, USA*<sup>3</sup>*Department of Anesthesiology, University of Maryland, Baltimore, MD, USA*<sup>4</sup>*Department of Pediatrics, University of Virginia, Charlottesville, VA, USA*

Background: Acetyl-L-carnitine (ALCAR) is neuroprotective in animal models of focal and global cerebral ischemia. Several mechanisms of action have been proposed, including 1) oxidative metabolism of the acetyl group of ALCAR to compensate for impaired pyruvate dehydrogenase activity, 2) stimulation of cerebral blood flow and, 3) direct antagonism of glutamate excitotoxicity. This study tested each of these hypotheses using a combination of an in vivo model of ischemic brain injury and an in vitro model of excitotoxic neuronal death. Methods: A canine model of 10 min ventricular fibrillation cardiac arrest followed by open chest CPR and electrical defibrillation was used as a clinically relevant model of global cerebral ischemia and reperfusion. Animals were either administered ALCAR at 100 mg/kg i.v. or the drug vehicle (buffered sodium bicarbonate) immediately after restoration of spontaneous blood flow. Relative cerebral blood flow velocity was monitored prior, during and following the cardiac arrest with an Oxford Optronix Oxy Flo laser Doppler probe inserted approximately 0.5 cm deep into the right frontal cortex. Glucose utilization and lactate production was measured in cortical tissue slices taken from vehicle-treated animals prior to cardiac arrest and at 2 hr reperfusion. Slices in suspension were incubated for 60 min at 37°C in the absence and presence of 1 mM ALCAR. Initial and final glucose and lactate concentrations were determined spectrophotometrically. The in vitro model of excitotoxicity consisted of exposing primary cultures of rat cortical neurons (10-15 day in vitro) to 100 µM NMDA for 30 min then measuring cell death using the calcein-AM/propidium iodide (live/dead) assay immediately following exposure to NMDA in the absence and presence of 1 mM ALCAR. Results: Consistent with other measures of CBF, the laser Doppler probe qualitative measurements of blood flow velocity after cardiac arrest and resuscitation demonstrate an initial period of hyperemia lasting 15-30 min followed by a period of hypoperfusion that continues over the 2 hr experimental period. This period of hypoperfusion was much shorter (<30 min) in animals treated with ALCAR. In the metabolic measurements, exposure of cortical slices from 2 hr reperfused animals to ALCAR in vitro significantly reduced the rate of glucose utilization and tended to reduce lactate formation. Exposure of cortical neurons to NMDA for 30 min resulted in a significant, greater than 50% acute cell death that was completely blocked by the presence of 1 mM ALCAR. Conclusions: 1. ALCAR improves postischemic CBF; however, the hypoperfusion associated with this model is likely not the primary determinant of neuronal cell death and neurologic impairment. 2. The inhibition of brain tissue glucose utilization and lactate formation by ALCAR in vitro is consistent with its ability to be oxidatively metabolized both in vitro and in vivo. ALCAR protects against acute excitotoxic neuronal death, suggesting a distinctly different mechanism of action involving either the NMDA receptor or downstream events such as mitochondrial calcium overload or secondary neuronal calcium influx through other channels. Acknowledgments: This work was supported by NIH P01 HD16596 and by Sigma-Tau Research, Inc.

**VELCADE®, A FIRST-IN-CLASS PROTEASOME INHIBITOR, IS EFFICACIOUS IN RAT PERMANENT MIDDLE CEREBRAL ARTERY OCCLUSION**

Nancy E. Stagliano<sup>1</sup>, JingMei Ren<sup>2</sup>, William Riordan<sup>1</sup>, Seth P. Finklestein<sup>2</sup>

<sup>1</sup>*Millennium Pharmaceuticals, Inc., Cambridge, MA, USA*

<sup>2</sup>*Biotrofix, Inc., Needham, MA, USA*

**Background and Introduction:** Although a variety of agents targeting a single mechanism have been studied as stroke therapies, the majority of these have failed. Many reasons can be attributed to the lack of successes, both pre-clinically and clinically, but one likely cause is the redundancy of pathways in the brain that lead to neuronal death. Novel therapies are clearly needed to overcome the multitude of cell death processes rapidly activated after cerebral ischemia. VELCADE® is a first-in-class, novel proteasome inhibitor which is approved for the treatment of relapsed, refractory multiple myeloma. Its specific target is the 26s proteasome. Proteasomes are highly conserved multicatalytic enzyme complexes which are essential for the ubiquitin-dependent proteolysis of the majority of cellular proteins. By targeting the proteasome, a host of cellular effects are possible and the balance of these results in different phenotypes, depending on the cellular milieu. In rodent models of ischemia, there is an emerging body of evidence suggesting beneficial effects of proteasome inhibition (1). Possible mechanisms of this protection include decreased NF- $\kappa$ B activation, upregulation of eNOS and HIF1 $\alpha$  and decreases in inflammation. **Methods:** In the setting of stroke, we evaluated the effect of proteasome inhibition with VELCADE® on a rat model of permanent middle cerebral artery occlusion (MCAO) using the intraluminal suture method. Male Wistar rats (n=10 per group) were treated with saline or VELCADE®, given as an i.v. bolus (0.2 mg/kg) one hour post-occlusion. Whole blood samples were drawn one hour after drug or vehicle injection for the determination of blood proteasome inhibition using an ex vivo fluorogenic pharmacodynamic assay (2). At 24h after ischemia, rats were assessed for neurologic dysfunction using a Neurological Rating Scale Score (NRSS). Rats were then sacrificed and brains were extracted for TTC staining and quantification of infarcts. Data are expressed as mean+SE and were analyzed using a paired t-test. **Results and Conclusions:** A single dose of VELCADE® given 1h post-MCAO, resulted in a 40% decrease in infarct volume (% infarction: 35.9+2.6 vs. 21.7+5.0; p<0.05) and a 38% decrease in neurologic deficits (NRSS: 2.6+0.163 vs. 1.625+0.183; p<0.01). There was no difference in body weight between the two groups. The functional and histopathologic protection was accompanied by a 67% inhibition of whole blood proteasome activity, a level of inhibition which is commonly achieved in cancer patients in the clinic (3). Additional infarct volume and behavioral data will be presented assessing the dose-response of VELCADE® at 1h post-stroke. Our study suggests that proteasome inhibition is beneficial in rat ischemic injury and that blocking ubiquitin-dependent proteolysis may be desirable in the acute setting following a stroke. **References:** 1. Wojcik C, Di Napoli M. Ubiquitin-proteasome system and proteasome inhibition: new strategies in stroke therapy. 2004 *Stroke* 35:1506-18. 2. Lightcap, ES, McCormack, TA, Pien, CS et al., Proteasome inhibition measurements : Clinical application. 2000 *Clinical Chemistry* 46 : 673-683. 3. Orłowski, RZ, Stinchcombe, TE, Mitchell, BS et al., Phase I trial of the proteasome inhibitor PS-341 in patients with refractory hematologic malignancies. 2002 *Journal of Clinical Oncology* 20: 4420-4427.

**INCREASED ACTIVATION OF NF-KB AND ERK1/2 AFTER PERMANENT FOCAL ISCHEMIA IS ABOLISHED BY SIMVASTATIN PRE-TREATMENT**

**Mauro Cimino**<sup>1</sup>, Cristina Banfi<sup>2</sup>, Maura Brioschi<sup>2</sup>, Paolo Gelosa<sup>2</sup>, Elena Nobili<sup>2</sup>,  
Anita Gianella<sup>2</sup>, Elena Tremoli<sup>2</sup>, Luigi Sironi<sup>2</sup>

<sup>1</sup>*Institute of Pharmacology and Pharmacognosy, University of Urbino, Urbino, Italy*

<sup>2</sup>*Department of Pharmacological Sciences, University of Milano, Milan, Italy*

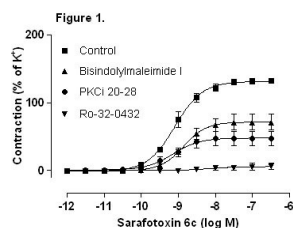
The role of inflammation in ischemic brain damage has been reported in human and in different animal models of stroke. Since statins (3-hydroxy-3-methylglutaril (HMG)-coenzymeA (CoA) reductase inhibitors), besides their lipid lowering action, exert also anti-inflammatory activity we sought to investigate the effect of simvastatin treatment on the expression of interleukin-1beta (IL-1beta), monocyte chemoattractant protein-1 (MCP-1), NF-kB activity and on signaling pathways related with NF-kB activation in a rat model of permanent middle cerebral artery occlusion (pMCAO). Unilateral pMCAO was carried out in anesthetized Sprague-Dawley rats using a microbipolar coagulator to permanently occlude the right middle cerebral artery. Expression of IL-1beta and MCP-1 was determined in cerebral cortex using RT-PCR. NF-kB DNA binding activity was assessed with Trans-AM NF-kB p65 transcription factor assay kit using cortical nuclear extracts. Binding of NF-kB to DNA was visualized by anti-p65 antibody that specifically recognizes activated NF-kB. MAP kinases were revealed by immunoblotting. Intravenous administration of a specific MEK (MAPK/ERK kinase) inhibitor, U0126 (150 mg/kg), was used to evaluate the causal relationship between anti-inflammatory actions and the neuroprotective activity. Expression of IL-1b and MCP-1 was enhanced by pMCAO and this effect was inhibited by administration of simvastatin before ischemia. We then investigated the ability of NF-kB p65 subunit to bind DNA at different time after pMCAO. The cerebral cortex ipsilateral to the occlusion displayed an increase in binding activity which reached its peak 16 hours after the ischemic insult. In order to determine whether simvastatin could interfere with pMCAO-induced activation of NF-kB, animals were treated for 3 days with 20 mg/kg of statin before permanent occlusion of the artery or 2 hours after pMCAO. Pre-treatment with simvastatin abolished the activation of NF-kB observed in vehicle-treated animals. In contrast, an acute administration of the drug, after induction of permanent ischemia, did not show any inhibitory effect on NF-kB activation. The effect of simvastatin was specific for NF-kB since other transcription factors such as Jun, Fos and NF-YA were not affected by the treatments. Following the same schedule of treatment, we have also evaluated the modulation of different signal transduction pathways such as ERK 1/2, SAPK/JNK 46/54 and p38. Under our experimental conditions, only the expression of ERK1/2 was enhanced by ischemia and this activation was prevented by prophylactic, but not post-ischemic, administration of simvastatin. Administration of U0126, after pMCAO, reduced the ischemic damage, inhibited NF-kB activation and reduced the activation of inflammatory markers. These results provide evidence for the role of simvastatin in the protection of ischemic brain damage and suggests that this effect is mediated by inhibition of ERK1/2 pathway.

## UPREGULATION OF CONTRACTILE ETB RECEPTORS IN MIDDLE CEREBRAL ARTERIES IS DEPENDENT ON PKC

Marie Henriksson, Emelie Stenman, Lars Edvinsson

*Department of Medicine, Division of Experimental Vascular Research, Lund University, Lund, Sweden*

**Introduction:** This study is designed to examine the involvement of protein kinase C (PKC) in the upregulation of endothelin type B receptors (ETB) induced by organ culture of rat middle cerebral arteries (MCA). In previous studies we have shown that contractile ETB receptors are upregulated after organ culture and that this upregulation is dependent on the MAP kinases ERK1/2 and possibly PKC. The results in the present study confirm the importance of PKC on both functional and transcriptional levels. **Methods:** To measure the contractile ETB receptor mediated responses, middle cerebral arteries from male Wistar rats were incubated for 24 hours at 37 C in humidified 5% CO<sub>2</sub> and air in Dulbecco's modified Eagle's medium. Before incubation, the PKC inhibitors bisindolylmaleimide I (10 $\mu$ M), Ro-32-0432 (10 $\mu$ M) or PKC inhibitor 20-28 (0.1 mM) were added to the medium. Segments of the vessels were thereafter mounted in myographs and the contractile response to sarafotoxin (S6c; ETB receptor agonist) was measured. Concentration-response curves for S6c were obtained by cumulative application (10-12-10-6.5 M) and the contractile responses were calculated as percentage of the contractile capacity of 63.5 mM K<sup>+</sup>. As control, we used vessel segments that were incubated in Dulbecco's modified Eagle's medium for 24 hours without inhibitors. To measure the ETB mRNA levels in the vessels, we used real-time PCR. MCAs were incubated in the same manner as for the contractile experiments. Total RNA was extracted and reverse transcribed to cDNA. Primer pairs for genes of interest were designed and the mRNA levels of the genes were compared to an internal standard. Statistical analyses were performed with Kruskal-Wallis test and  $p < 0.05$  was considered significant. The results are expressed as mean  $\pm$  SEM. **Results:** The three inhibitors each inhibited the sarafotoxin induced contraction as compared to control (Fig.1; Emax [maximal contraction] = 71 %  $\pm$  11 % for bisindolylmaleimide I, 47 %  $\pm$  10 % for PKC inhibitor 20-28, 6 %  $\pm$  5 % for Ro-32-0432 and 132 %  $\pm$  3 % for control vessels,  $p < 0.05$ ). In the real-time PCR experiments, the effect of Ro-32-0432 and bisindolylmaleimide on the ETB receptor mRNA levels was evaluated. Both inhibitors decreased the ETB receptor mRNA levels, although for bisindolylmaleimide I, it was not significant (0.117  $\pm$  0.009 for control, 0.043  $\pm$  0.004 for bisindolylmaleimide I and 0.033  $\pm$  0.002 for Ro-32-0432 as compared to an internal standard,  $p < 0.01$  for Ro-32-0432). **Conclusions:** These findings confirm that PKC is involved in the upregulation of ETB receptors after organ culture. A similar vascular alteration has been shown in an experimental model of ischemia, where the upregulation may lead to decreased perfusion in the ischemic hemisphere. The next step will therefore be to inhibit the ETB receptor upregulation in experimental cerebral ischemia, by adding inhibitors to PKC and ERK1/2.



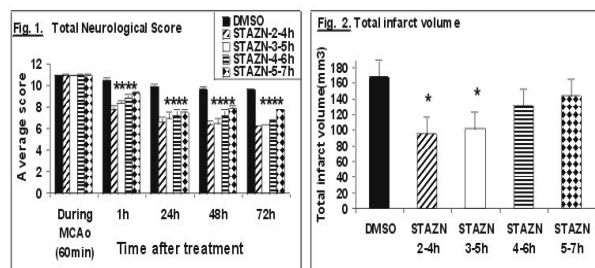
## NEUROPROTECTIVE EFFECT OF STAZN IN FOCAL CEREBRAL ISCHEMIA: A THERAPEUTIC-WINDOW STUDY

Ludmila Belayev<sup>1</sup>, Larissa Khoutorova<sup>1</sup>, Alexey Vigdorichik<sup>1</sup>, Jim J. Ley<sup>1</sup>, David A. Becker<sup>2</sup>, Weizhao Zhao<sup>1</sup>, Raul Busto<sup>1</sup>, Myron D. Ginsberg<sup>1</sup>

<sup>1</sup>Department of Neurology, University of Miami School of Medicine, Miami, FL, USA

<sup>2</sup>Department of Chemistry, Florida International University, Miami, FL, USA

Background: Stilbazulenyl nitron (STAZN) is a second-generation azulenyl nitron with markedly enhanced antioxidant properties compared to conventional alpha-phenyl nitrones such as the experimental stroke drug NXY-059.1 We have recently shown that STAZN therapy confers marked neurological and histological protection in cerebral ischemia and brain trauma in rats.<sup>2,3</sup> The purpose of this study was to define its therapeutic window in focal cerebral ischemia. Methods: Male Sprague-Dawley rats (280-359g) were anesthetized with halothane and subjected to 2 h of transient MCAo by retrograde insertion of an intraluminal nylon suture coated with poly-L-lysine.<sup>4</sup> Heating lamps were used to maintain rectal and temporalis muscle temperatures at 37.0 to 37.8 C. The drug (STAZN, 0.6 mg/kg) was administered at 2 and 4h (n=11), 3 and 5h (n=10), 4 and 6h (n=10) or 5 and 7h (n=7) after onset of stroke (i.e., 0 to 5 h after onset of reperfusion). Control rats received vehicle (DMSO; n=6) at 3 and 5 h. Additional doses were given at 24 and 48h. Neurological status was evaluated during MCAo, at 1, 24, 48 and 72h; a grading scale of 0-12 was employed, as previously described.<sup>4</sup> 72 hours after MCAo, brains were perfusion-fixed and infarct volumes and brain swelling were determined.<sup>4</sup> Results: Rectal and cranial temperatures, blood pressure, plasma glucose and blood gases in the 44 animals of this study showed no significant differences between groups. STAZN significantly reduced the neurobehavioral deficit in all treated groups compared to the DMSO group (Fig. 1). Treatment with STAZN also significantly reduced total infarct volume (Fig. 2) and cortical and subcortical infarction at multiple levels, when administered at 2 and 4h and 3 and 5h compared to the DMSO group. When administration of STAZN was delayed to 4-5h after onset of MCAo, histological protection was lost. Brain edema was not affected by STAZN. Conclusions: These results strongly support the beneficial effect of STAZN therapy in transient focal ischemia when administered up to 5 hours after onset of the MCAo, and support its possible utility in treating patients with acute ischemic stroke. Supported by NIH Grants NS46294 and NS05820. 1Becker DA et al (2002), J. Am. Chem. Soc., 124: 4678-4684. 2Ginsberg MD et al (2003) Annals of Neurology, 54: 330-342. 3Belayev L, et al, (2002) J. Neurosurgery, 96, 1077-1083. 4Belayev L et al (1996) Stroke, 27:1616-1623.



**TWO SODIUM/CALCIUM EXCHANGER GENE PRODUCTS, NCX1 AND NCX3,  
PLAY A MAJOR ROLE IN THE DEVELOPMENT OF PERMANENT FOCAL  
CEREBRAL ISCHEMIA**

Giuseppe Pignataro, Rosaria Gala, Ornella Cuomo, Anna Tortiglione, Lucia Giaccio,  
Pasqualina Castaldo, Rossana Sirabella, Carmela Matrone, Adriana Canitano,  
Salvatore Amoroso, Gianfranco Di Renzo, **Lucio Annunziato**

*Dipartimento di Neuroscienze, Universita' 'Federico II' Napoli, Naples, Italy*

In the brain, there are 3 different genes, *ncx1*, *ncx2*, *ncx3*, coding for 3 different proteins: NCX1, NCX2, and NCX3 [1]. These proteins are neuronal plasmamembrane exchangers, which, by mediating Ca<sup>2+</sup> and Na<sup>+</sup> fluxes in a bidirectional way across the synaptic plasma membrane, may play a relevant role in brain ischemia, in which the homeostasis of these ions is altered [2]. Previous studies showed that the compromission of NCX activity may be detrimental in the development of cerebral injury induced by permanent middle cerebral artery occlusion (pMCAO) [3]. The aim of this study was to determine whether the different isoforms of NCX might play a differential role in cerebral ischemia. NCX1, NCX2, and NCX3 protein expression was evaluated, by Western blotting, in the ischemic core and in the remaining ipsilateral non-ischemic area of the affected hemisphere at different time intervals starting from ischemia induction. The role of the three isoforms was also assessed by knocking out each of them with specific antisense oligodeoxynucleotides (ODNs). These ODNs were continuously intracerebroventricularly infused by an osmotic minipump (1 microliter/h) for 48 hours, starting from 24 hours before pMCAO. The results showed that, after pMCAO, in the ischemic core all three NCX proteins were downregulated, although NCX2 was only halved; in the peri-infarctual area only NCX3 decreased, whereas NCX1 and NCX2 were unchanged. The ODNs for NCX1 and NCX3 gene products increased the extent of ischemic lesion and worsened neurological scores, whereas the NCX2 ODN did not change the extent of ischemia and the neurological outcome. The results of this study suggest that in the neuroprotective effect exerted by NCX during ischemic injury, the major role is prevalently exerted by NCX1 and NCX3 gene products [4]. Therefore, the use of substances able to activate these two isoforms specifically could represent an important perspective in the future treatment of cerebral ischemia. **ACKNOWLEDGMENTS** This work was supported by MIUR-Cofin 2002, FIRB 2002RBNE01E7YX\_007 (to L.A.), and Regione Campania (POP and Legge 41; to LA). **REFERENCES** [1] Papa M, Canitano A, Boscia F, Castaldo P, Sellitti S, Porzig H, Tagliatela M and Annunziato L (2003) Differential expression of the Na<sup>+</sup>-Ca<sup>2+</sup> exchanger transcripts and proteins in rat brain regions. *J Comp Neurol.* 461: 31-48. [2] Annunziato L, Pignataro G, Di Renzo GF (2004) Pharmacology of brain Na<sup>+</sup>/Ca<sup>2+</sup> exchanger: from molecular biology to therapeutic perspectives. *Pharmacol Rev.*; 56:633-54 [3] Pignataro G, Tortiglione A, Scorziello A, Giaccio L, Secondo A, Severino B, Santagada V, Caliendo G, Amoroso S, Di Renzo GF and Annunziato L (2004) Evidence for a protective role played by the Na<sup>+</sup>/Ca<sup>2+</sup> exchanger in cerebral ischemia induced by middle cerebral artery occlusion in male rats. *Neuropharmacology* 46:439-448. [4] Pignataro G, Gala R, Cuomo O, Tortiglione A, Giaccio L, Castaldo P, Sirabella R, Matrone C, Canitano A, Amoroso S, Di Renzo GF and Annunziato L (2004) Two sodium/calcium exchanger gene products, NCX1 and NCX3, play a major role in the development of permanent focal cerebral ischemia. *Stroke* 35:2566-70.

## **NORMOXIC RESUSCITATION AFTER CARDIAC ARREST PROTECTS AGAINST HIPPOCAMPAL OXIDATIVE STRESS, METABOLIC FAILURE, AND NEURONAL DEATH**

**Robert E. Rosenthal**<sup>1,2</sup>, Viktoria Vereczki<sup>2</sup>, Erica M. Martin<sup>2</sup>, Gary Fiskum<sup>2</sup>

<sup>1</sup>*Department of Surgery, Program In Trauma, University of Maryland School of Medicine, Baltimore, MD, USA*

<sup>2</sup>*Department of Anesthesiology, University of Maryland School of Medicine, Baltimore, MD, USA*

Background: Animal models of global cerebral ischemia and reperfusion indicate that neurologic outcome is improved using normoxic compared to hyperoxic resuscitation; however the molecular basis for this improvement is unknown. This study tested the hypothesis that normoxic ventilation (21% O<sub>2</sub>) during the first hour after 10 min cardiac arrest in dogs protects against oxidative protein tyrosine nitration and loss of the critical metabolic enzyme complex pyruvate dehydrogenase (PDHC) in the hippocampus, an area selectively vulnerable to delayed neuronal cell death. The study also tested the hypothesis that normoxic resuscitation also improves oxidative cerebral energy metabolism early during reperfusion and protects against delayed neuronal cell death. Methods: Chloralose-anesthetized adult beagles underwent 10 min ventricular fibrillation cardiac arrest, followed by electrical defibrillation and ventilation with either 21% or 100% O<sub>2</sub>. At 1 hr post-resuscitation, the ventilator was adjusted to maintain normal blood gas levels in both groups. Brains were perfusion-fixed at 2 hr reperfusion and used for semi-quantitative immunohistochemical measurements of nitrotyrosine and pyruvate dehydrogenase (E1 alpha subunit). In other animals, mitochondria were isolated from the hippocampi of unfixed brains. Pyruvate dehydrogenase activity was measured spectrophotometrically and pyruvate-dependent mitochondrial respiration measured polarographically. Other animals were provided with constant critical care for 24 hr, then perfusion fixed for quantitative neuropathology using stereologic analysis of hippocampal neuronal cell death based on morphological changes apparent with cresyl violet stained tissue. Results: In hyperoxic ventilated dogs, E1 alpha immunostaining diminished by approximately 90% in CA1, CA3, and dentate gyrus compared to sham-operated dogs, while neuronal PDHC staining in normoxic animals was not significantly different from non-ischemic dogs. Protein nitration in hippocampal pyramidal neurons of hyperoxic animals was 2-3 times greater than either sham-operated or normoxic resuscitated animals at 2 hr reperfusion. In 2 hr hyperoxic animals, hippocampal mitochondrial PDHC enzyme activity was 35% less, and ADP-stimulated respiration was 50% less than non-ischemic controls, whereas these activities in normoxic animals were not significantly different from controls. Stereologic quantification of neuronal death at 24 hr reperfusion demonstrated a significant reduction in the percentage of dying neurons  $\pm$  s.d. using normoxic compared to hyperoxic resuscitation (CA1:  $32 \pm 8\%$  vs.  $48 \pm 2\%$ ; CA3:  $27 \pm 6\%$  vs.  $49 \pm 3\%$ ;  $p < 0.05$ ). Conclusions: These results indicate that postischemic hyperoxic ventilation promotes oxidative stress that exacerbates prelethal loss of pyruvate dehydrogenase, respiratory dysfunction, and delayed hippocampal neuronal cell death. Moreover, these findings indicate the need for clinical trials comparing the effects of low and high ventilatory oxygen levels on neurologic outcome after cardiac arrest. Supported by grants NIH R01NS34152 and U01NS49425 References: 1) Liu Y, Rosenthal RE, Haywood Y, Miljkovic-Lolic M, Vanderhoek JY, Fiskum G. Normoxic ventilation after cardiac arrest reduces oxidation of brain lipids and improves neurologic outcome. *Stroke* 1998;29:1679-86. 2) Martin E, Rosenthal RE, Fiskum G. Pyruvate dehydrogenase complex: Metabolic link to ischemic brain injury and target of oxidative stress. *J Neurosci Res* 2005;79:240-7.

## DEFEROXAMINE REDUCES CSF FREE IRON LEVELS FOLLOWING INTRACEREBRAL HEMORRHAGE IN RATS

Shu Wan<sup>1</sup>, Guohua Xi, Richard Keep, Julian Hoff, **Ya Hua**

*Department of Neurosurgery, University of Michigan, Ann Arbor, MI, USA*

**Introduction:** Iron is essential for normal brain function, but iron overload may have devastating effects. It has been reported that iron overload contributes to many kinds of brain injury including Alzheimer's disease and Parkinson's disease. Our previous studies have found that brain iron overload occurs after intracerebral hemorrhage (ICH) [1] and an iron chelator, deferoxamine, attenuates perihematomal brain edema and oxidative stress [2]. The present study investigated whether deferoxamine reduces free iron levels in the CSF following ICH. **Methods:** Under pentobarbital anesthesia (50 mg/kg, i.p.), a total of 70 male Sprague-Dawley rats received an intracerebral infusion of 100- $\mu$ l autologous whole blood into the right basal ganglia. Rats were treated with deferoxamine (100 mg/kg, i.p., administered 2 hour after ICH and then at 12-hour intervals for up to 7 days) or vehicle, and were killed at 1, 3, 7, 14 and 28 days for free and total iron measurements. Behavioral tests including forelimb placing test, forelimb use asymmetry test and corner turn test were preformed. **Results:** Free iron levels in normal CSF were very low in the rat. After ICH, free iron levels in CSF were increased significantly at the first day ( $8.5 \pm 1.3 \mu\text{M}$ , mean  $\pm$  S.D.) and peaked at the third day ( $14.2 \pm 5.0 \mu\text{M}$ ). CSF free iron remained at high levels for at least 28 days ( $6.2 \pm 1.1 \mu\text{M}$ ). Deferoxamine given 2 hours after ICH reduced free iron in CSF at all time points (e.g. day 3:  $6.7 \pm 2.0 \mu\text{M}$  vs.  $14.2 \pm 5.0 \mu\text{M}$  in the vehicle-treated group,  $p < 0.05$ ) and reduced ICH-induced neurological deficits ( $p < 0.05$ ). The levels of brain total iron were also increased after ICH ( $p < 0.05$ ). However, deferoxamine failed to reduce brain total iron levels in the ipsilateral hemisphere ( $p > 0.05$ ). **Conclusions:** ICH results in iron accumulation in the brain. CSF free iron levels are high and are not cleared at least for 28 days after ICH. Deferoxamine reduces free iron levels and improves functional outcomes in the rat ICH model indicating that it may be a potential therapeutic agent for ICH patients. **References:** [1] Wu J, Hua Y, Keep RF, Nakamura T, Hoff JT, Xi G. Iron and iron handling proteins in the brain after intracerebral hemorrhage. *Stroke* 34:2964-2969 (2003) [2] Nakamura T, Keep RF, Hua Y, Schallert T, Hoff JT, Xi G. Deferoxamine-induced attenuation of brain edema and neurological deficits in a rat model of intracerebral hemorrhage. *J Neurosurg.* 100:672-678 (2004) Supported by NIH NS 17760, NS 39866, NS 47245 and AHA 0435354Z.

## EFFECT OF ERYTHROPOIETIN ON NEONATAL HYPOXIA-ISCHEMIA ENCEPHALOPATHY

Changlian Zhu<sup>1</sup>, Wenqing Kang<sup>2</sup>, Xiaoyang Wang<sup>1</sup>, Hong Xiong<sup>2</sup>, Xiuyong Cheng<sup>1</sup>

<sup>1</sup>*Department of Pediatrics, The Third Affiliated Hospital, Zhengzhou University, Zhengzhou, China*

<sup>2</sup>*Department of Pediatrics, Zhengzhou Children's Hospital, Zhengzhou, China*

**Objective:** The neuroprotective effect of erythropoietin has been proven in several brain injury models. It has not been evaluated in the neonatal hypoxia-ischemia encephalopathy (HIE). The purpose of this study was to evaluate the clinical effect of erythropoietin on neonatal HIE by systemic injection.

**Methods:** Fifty-eight asphyxiated newborns were enrolled this study in our neonatal section who fulfilled the criteria of moderate to severe HIE, with the exception of gestation age <37 week's, body weight <2.5 kg, severe congenital abnormalities and hemorrhage. The infants were randomized to either EPO-treated group with the dosage of 300 U/kg/time or control group without EPO treatment. The recombinant human erythropoietin (r-hu-EPO) was injected intravenously for each other day with 3 times each week for 2 weeks. The supportive care was same among the groups. The short-term effect of EPO was evaluated by Neonatal Behavioral Neurological Assessment (NBNA) on day 7, 14 and 28. The long-term effect was evaluated by measuring neurodevelopment quote on 3 and 6 months of age.

**Results:** There were 29 cases in EPO-treated group and 29 cases in control group. There were no differences in gestation age, birth weight, sex and clinical symptoms between two groups ( $P>0.05$ ). The scoring of NBNA showed a significant difference between EPO treated groups and control group ( $P<0.05$ ). The DQ scores at the 3<sup>rd</sup> and 6<sup>th</sup> month in low dose EPO-treated group ( $89.17\pm 7.11$ ,  $90.85\pm 9.14$ ) were significantly higher than that of control group ( $77.38\pm 10.97$ ,  $78.92\pm 11.24$ ) ( $P<0.05$ ).

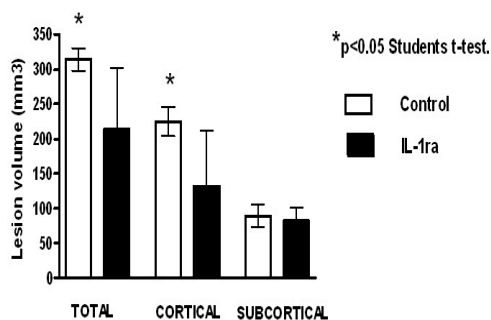
**Conclusion:** EPO treatment could promote neurological recovery, improve long-term neurobehavioral development.

## PERIPHERAL ADMINISTRATION OF INTERLEUKIN-1 RECEPTOR ANTAGONIST (IL-1RA) REDUCES ISCHAEMIC BRAIN DAMAGE IN THE RAT

Simon R. Clark, Allan Stuart, Rothwell J. Nancy

*Faculty of Life Sciences, University of Manchester, Manchester, UK*

Introduction Pro-inflammatory cytokines such as interleukin-1 (IL-1) have been strongly implicated in the pathogenesis of ischaemic brain damage. After all forms of cerebral ischemia the expression of IL-1 is rapidly up-regulated. Furthermore, exogenous IL-1, given via the intracerebroventricular (icv) route, has been shown to markedly increase ischaemic brain damage. In contrast, the naturally occurring IL-1 receptor antagonist (IL-1ra), which binds to the IL-1R1 and blocks actions of IL-1, has been shown to be effective in reducing lesion volume when given either directly into the brain parenchyma or icv1. Clinically, it is not feasible to deliver IL-1ra directly into the brain of patients suffering brain ischemia. However, some clinical studies have shown that peripherally administered IL-1ra does indeed cross the blood brain barrier in patients suffering from subarachnoid haemorrhage, which likely involves cytokines in the pathogenesis of the cerebral ischaemia that develops2. To date such studies have been too small to show efficacy and the aim of this study therefore was to examine the efficacy of intravenous IL-1ra on ischaemic brain damage in rodents. Methods Experiments were performed on Sprague-Dawley rats (310-380g). Cerebral ischaemia was induced in anaesthetised rats according to the intraluminal filament occlusion model3. Briefly, the right carotid artery and its branches were exposed. A monofilament was advanced until resistance was felt at around 20mm, to block the origin of the right middle cerebral artery. After 90 minutes, the filament was withdrawn to allow reperfusion. Immediately prior to induction of ischaemia, a bolus of 10mg of IL-1ra was given via an external jugular cannula and an osmotic minipump (8ul/hr- to deliver 0.8mg/h for 24h) filled with IL-1ra (100mg/ml) was connected to the tubing. Controls received identical volumes of NaCl (0.9%). After 24h of IL-1ra infusion, animals were sacrificed. Brains were removed, processed and infarct volumes calculated using an image analysis program, the final volumes being adjusted for oedema. Groups were compared using an unpaired students T-test. Results Intravenous delivery of IL-1ra for a period of 24h after the onset of middle cerebral artery occlusion resulted in a significant decrease in both total ( $313 \pm 9 \text{mm}^3$  vs.  $216 \pm 92 \text{mm}^3$   $p < 0.05$ ) and cortical ( $229 \pm 18 \text{mm}^3$  vs.  $140 \pm 78 \text{mm}^3$   $p < 0.05$ ) lesion volumes. The subcortical lesion was not affected by IL-1ra treatment ( $85 \pm 17 \text{mm}^3$  vs.  $86 \pm 22 \text{mm}^3$   $p > 0.05$ ). Conclusion IL-1ra reduces ischaemic damage as measured by lesion volumes after transient MCAO when given intravenously. Further work will determine plasma levels and corresponding CSF levels of IL-1ra required for neuroprotection, in support of pharmacokinetic data in subarachnoid haemorrhage patients. This is further evidence to support the use of IL-1ra in the clinical setting as a neuroprotective agent. References 1. Rothwell, N. Brain, Behaviour and Immunity 17, 152-157 (2003). 2. Dumont, A. S. et al. Neurosurgery 53, 123-133 (2003). 3. Zea Longa, EL et al. Stroke 20, 84-91 (1989).





**PLASMA KALLIKREIN INHIBITOR DX-88 PROTECTS AGAINST BRAIN ISCHEMIA/REPERFUSION INJURY**

**Emanuela Rossi**<sup>2</sup>, Claudio Storini<sup>1</sup>, Diana Maiocchi<sup>2</sup>, Maria Grazia De Simoni<sup>1</sup>,  
Luigi Bergamaschini<sup>2</sup>

<sup>1</sup>*Mario Negri Institute, Neuroscience Department, Milan, Italy*

<sup>2</sup>*Department of Internal Medicine, Geriatric Unit, University of Milan, Ospedale Maggiore IRCCS, Milan, Italy*

We have investigated the involvement of the kinin system in ischemia/reperfusion brain injury in mice by using the new specific plasma kallikrein inhibitor DX-88 (Dyax Corp., Cambridge, MA). We first analysed whether DX-88 was able to cross the blood-brain barrier and found that thirty minutes after treatment with 30µg/mouse iv, a marked inhibitory activity was present in cerebrospinal fluid. Ischemia was induced by occlusion of the middle cerebral artery, using a 6-0 monofilament. At the end of the 30 min ischemic period, the filament was removed and reperfusion allowed. Mice received DX-88 iv at the beginning of the ischemic period or at the end of it (ie at reperfusion), or 1h after the beginning of the ischemic period. Twenty four hours after ischemia, neurological deficits and infarct size were evaluated. While saline treated mice showed stable scores, those who received of DX-88 at the beginning of the ischemic period had significantly reduced general (by 37.5%) and focal (by 50.0%) deficits scores. In these mice the ischemic volume was also significantly reduced by 50.9%. When given at reperfusion, DX-88 was similarly effective in improving general (by 38% ) and focal (by 50.1% ) deficits scores as well as the ischemic volume that was reduced by 58%. The inhibitor lost its neuroprotective action when administrated 1h after the beginning of the ischemic period. This study shows that: i) this specific kallikrein inhibitor can rapidly cross the intact blood-brain barrier and thus possibly reach brain tissue in its active form; ii) it has a marked neuroprotective effect indicating an important role of kallikrein in brain ischemia/reperfusion injury. This study was partially supported by Dyax Corp., Cambridge, MA.

**C1-INHIBITOR PROTECTS AGAINST BRAIN ISCHEMIA/REPERFUSION INJURY VIA INHIBITION OF CELL RECRUITMENT AND INFLAMMATION**

**Claudio Storini<sup>1</sup>, Emanuela Rossi<sup>2</sup>, Veronica Marrella<sup>1</sup>, Luigi Bergamaschini<sup>2</sup>,  
MariaGrazia De Simoni<sup>1</sup>**

*<sup>1</sup>Mario Negri Institute, <sup>2</sup>Department of Internal Medicine, Geriatric Unit, University of Milan, Ospedale Maggiore IRCCS, Milan, Italy*

C1-inhibitor (C1-INH), a major inhibitor of complement and contact-kinin systems, is neuroprotective in cerebral ischemia (1,2). Actually C1-INH induces a reduction of the ischemic volume up to 73% and 90% in CD1 and C57 mice respectively. Furthermore C1-INH is able to prevent neurodegeneration and significantly lowers general and focal neurological deficits. These data showed that C1-INH has a potent neuroprotective effect in ischemia/reperfusion injury. In order to clarify the mechanism of this action we evaluated in the present study the expression of neurodegeneration and inflammation related factors in CD1 mice, treated with C1-INH (15U) or saline and subjected to 2h of ischemia and 2 or 46h of reperfusion. mRNA expression was measured by RT-PCR in brain cortex. Ischemia was induced by occlusion of the middle cerebral artery (MCAO) using a nylon monofilament introduced into the internal carotid artery and advanced so as to block the origin of the MCA. At the end of the ischemic period, the filament was removed and reperfusion allowed. C1-INH significantly dampened the mRNA expression of the adhesion molecules P-selectin and ICAM-1 induced by the ischemic insult. These data has been confirmed by immunohistochemistry analysis: C1-INH markedly inhibited the activation and/or recruitment of microglia/macrophage, as well as the infiltration of leukocyte. It significantly decreased the pro-inflammatory cytokine (TNF $\alpha$ , IL-18) and increased the protective cytokine (IL-6, IL-10) gene expression. C1-INH treatment prevented the decrease of NFH gene, a marker of cellular integrity and counteracted the increase of pro-caspase 3, an apoptosis index. In conclusion, C1-INH exerts an anti-inflammatory and anti-apoptotic action on ischemia/reperfusion injury. Our present and past data support a major effect of C1-INH on cell recruitment from the vasculature to the ischemic site. 1. De Simoni MG, Storini C, Barba M, Catapano L, Arabia AM, Rossi E, Bergamaschini L. (2003) Neuroprotection by complement (C1)-inhibitor in mouse transient brain ischemia. *J Cereb Blood Flow Metab*, 23: 232-239. 2. De Simoni M G, Rossi E, Storini C, Pizzimenti S, Echart C, Bergamaschini L. (2004) The powerful neuroprotective action of C1-inhibitor on brain ischemia-reperfusion injury does not require C1q. *Am J Pathol.*, 164: 1857-1863.

## **PEROXISOME PROLIFERATOR-ACTIVATED RECEPTOR ALPHA ACTIVATION PROMOTES NEUROLOGICAL RECOVERY AND EXERTS ANTI-EDEMATOUS EFFECT IN A MODEL OF TRAUMATIC BRAIN INJURY**

Valerie C. Besson, Xiaoru R. Chen, Michel Plotkine, Catherine Marchand-Verrecchia

*Laboratoire de Pharmacologie de la Circulation Cérébrale, UPRES EA2510, Faculté des Sciences Pharmaceutiques et Biologiques, Paris, France*

### **INTRODUCTION**

The neuroinflammatory response following traumatic brain injury (TBI) leads to the formation of edema, the production of cytokines, the induction of NOS2 and COX2, the parenchyma infiltration by leukocytes [1,2] and a deleterious oxidative stress [3]. As it has been demonstrated that inflammatory markers and antioxidant enzymes could be modulated by the activation of Peroxisome Proliferator-Activated Receptor  $\alpha$  (PPAR $\alpha$ ) [4], this led us to study the effect of fenofibrate, a PPAR $\alpha$  agonist, on the consequences caused by TBI.

### **MATERIALS**

Male Sprague Dawley rats were randomised in five groups: non-operated (n=8), sham-operated (n=8), TBI + vehicle (n=8), TBI + fenofibrate 50 mg/kg (n=8) and TBI + fenofibrate 100 mg/kg (n=8). TBI was induced by lateral fluid percussion of the temporoparietal cortex [5]. Sham-operated rats underwent the same surgery except for percussion. Rats were given fenofibrate (50 and 100 mg/kg) or its vehicle (water containing 0.2% methylcellulose) by gavage 1h and 6h after TBI. A first neurological evaluation was performed 6h post-TBI (score ranging from 0=worst to 9=best). The rats were then given the second administration of fenofibrate or its vehicle. The second neurological evaluation was performed at 24h, then animals were killed for brain edema determination. Brain edema was obtained with the brain water content (BWC) measured by the wet weight/dry weight method [2].

### **RESULTS**

Neurological scores of non-operated and sham-operated rats were not different. TBI led to a decrease in the neurological score at 6h ( $6.0 \pm 0.5$  vs  $8.6 \pm 0.4$  for sham-operated rats,  $P < 0.01$ ) that persisted at 24h post-injury ( $5.1 \pm 0.7$ ,  $P < 0.001$ ). Six hours post-TBI, both doses of fenofibrate did not modify the neurological score (50 mg/kg:  $6.4 \pm 0.9$ ; 100 mg/kg:  $6.6 \pm 0.7$ ). Twenty-four hours post-injury, fenofibrate at 50 mg/kg improved the neurological score without reaching the statistical significance ( $7.1 \pm 0.7$ ,  $P=0.09$ ). At 100 mg/kg, we observed a significant increase of the score demonstrating a neurological recovery ( $7.6 \pm 0.5$ ,  $P<0.05$ ). The brain water contents of non-operated and sham-operated were not different. TBI led to an increase of the BWC ( $84.9 \pm 0.5$  % vs  $80.6 \pm 0.2$  % for sham-operated rats,  $P<0.001$ ) showing brain edema formation, which is reduced by the two doses of fenofibrate ( $82.7 \pm 0.8$  %,  $P < 0.05$  and  $83.3 \pm 0.9$  %,  $P < 0.05$ ).

### **CONCLUSION**

The present study shows that fenofibrate, a PPAR $\alpha$  agonist, promotes neurological recovery and exerts anti-edematous effect in the early phase after TBI. The activation of receptor PPAR $\alpha$  may be beneficial by counteracting the deleterious neuroinflammatory response following TBI. This suggests that PPAR $\alpha$  activation could be a potential therapeutic strategy for TBI.

### **REFERENCES**

[1] Ray S.K. *et al.* (2002). *Histol. Histopathol.*, 17: 1137-1152. [2] Hellal F. *et al.* (2004). *Neurosci. Lett.*, 357: 21-24. [3] Mésenge C. *et al.* (1998). *J. Pineal Res.*, 25:

41-46. [4] Chinetti G. *et al.* (2000). *Inflamm. Res.*, 49: 497-505. [5] Besson V.C. *et al.* (2003). *Brain Res.*, 989: 58-66.

## EFFECT OF THREE INDUCIBLE NOS INHIBITORS ON CEREBRAL EDEMA FORMATION AND NEUROLOGICAL DEFICIT IN A RAT MODEL OF TRAUMATIC BRAIN INJURY

Gaëlle Louin, **Catherine Marchand-Verrecchia**, Bruno Palmier, Michel Plotkine, Mehrnaz Jafarian-Tehrani

*Université René Descartes Laboratoire Pharmacologie EA, Paris, France*

**Introduction:** The role of NO produced by inducible nitric oxide synthase (iNOS) following traumatic brain injury (TBI) remains a subject of debate. Deletion of iNOS and treatment with iNOS inhibitors could be either beneficial or detrimental suggesting a dual role for iNOS in TBI 1-4. The aim of the present study was to clarify whether iNOS could be a therapeutic target in TBI. Therefore, the effect of three iNOS inhibitors was evaluated on cerebral edema formation and functional outcome in a rat model of TBI. **Methods:** Fluid percussion brain injury was performed on male Sprague-Dawley rat anesthetized with chloral hydrate (400 mg/kg, i.p.)<sup>3</sup>. In order to design an appropriate treatment protocol, kinetics of brain water content (BWC) and neurological score were studied. In the first treatment protocol, a single administration of vehicle (NaCl 0.9%) or iNOS inhibitor, aminoguanidine (AG) (100 mg/kg, i.p.), L-N-iminoethyl-lysine (L-NIL) (20 mg/kg, i.p.), or N-[3-(aminomethyl)benzyl]acetamide (1400W)(20 mg/kg, s.c.) was started at 6h post-TBI. In the second treatment protocol, 1400W (20 mg/kg, s.c.) was administered at 5 min, 8 and 16h post-TBI. Cerebral edema and neurological score were evaluated at 24h. **Results:** Trauma caused a significant increase in BWC at 6h ( $81.8 \pm 0.6\%$ , vs  $79.1 \pm 0.4\%$  in corresponding sham-operated rats,  $P < 0.001$ ) and 24h ( $82.2 \pm 0.9\%$  vs  $79.9 \pm 0.1\%$ ,  $P < 0.01$ ) following TBI. The neurological score of naive rats was 9 and was reduced after TBI with a minimum at 24h ( $4.5 \pm 0.3$ ,  $P < 0.01$ ). In the first treatment protocol, the neurological score was improved by AG ( $6.4 \pm 0.3$  vs  $5.6 \pm 0.3$  in vehicle-treated rats,  $P < 0.01$ ), L-NIL ( $6.6 \pm 0.4$  vs  $5.0 \pm 0.4$ ,  $P < 0.01$ ), and 1400W ( $6.2 \pm 0.3$  vs  $5.3 \pm 0.3$ ,  $P < 0.05$ ). However, only AG was able to significantly reduce the post-traumatic increase in BWC ( $80.3 \pm 0.2\%$  vs  $81.6 \pm 0.5\%$ ,  $P < 0.01$ ). In the second treatment protocol, 1400W administered even early improved the neurological score ( $6.0 \pm 0.2$  vs  $4.5 \pm 0.3$ ,  $P < 0.001$ ), with still no effect on the cerebral edema. **Conclusion:** Our results provide evidence that the three iNOS inhibitors improve the post-traumatic neurological function and therefore strengthen the notion that an early induction of iNOS is detrimental to functional outcome following TBI. The fact that only AG was able to reduce the cerebral edema suggests that the anti-edematous effect 1) is not the origin of the functional improvement and 2) does not related to the inhibition of iNOS. In conclusion, iNOS inhibitors are able to reduce the post-traumatic neurological deficit without reducing the cerebral edema. The large therapeutic window of iNOS inhibitors could allow their use in the treatment of functional deficit following TBI. **References:** 1. Wada K et al. (1998) *Neurosurgery* 43: 1427-1436. 2. Jones NC et al. (2004) *J Neuropathol Exp Neurol* 63:708-720. 3. Jafarian-Tehrani M et al. (2005) *Nitric Oxide* (in press). 4. Sinz EH et al. (1999) *J Clin Invest* 104: 647-656.

**DELAYED ADMINISTRATION OF DEFEROXAMINE REDUCES BRAIN  
INFARCTION AND IMPROVES FUNCTIONAL RECOVERY AFTER TRANSIENT  
FOCAL CEREBRAL ISCHEMIA IN THE RAT**

**Thomas Freret<sup>1,2</sup>, Samuel Valable<sup>1</sup>, Laurent Chalzaviel<sup>1</sup>, Eric T. MacKenzie<sup>1</sup>, Edwige Petit<sup>1</sup>,  
Myriam Bernaudin<sup>1</sup>, Michel Boulouard<sup>1</sup>, Pascale Schumann-Bard<sup>1,2</sup>**

<sup>1</sup>*CNRS UMR 6185, Caen, France*

<sup>2</sup>*CERMN EA3915 Pharmacology Faculty of Caen, Caen, France*

**Introduction:** The mechanisms underlying functional recovery after stroke are poorly understood. Hypoxia Inducible Factor 1 (HIF-1), a transcription factor regulated by the oxygen levels, has been reported to be increased after focal ischaemia in the rat (1). Since HIF-1 regulates the expression of several beneficial genes in cerebral ischaemia such as erythropoietin (EPO) (2), its activation could trigger endogenous adaptive mechanisms promoting tissue viability, reparation and/or functionality, thereby contributing to recovery after ischaemia. In order to strengthen these endogenous mechanisms and evaluate their effect on functional recovery, we investigated the effect of deferoxamine (DFX), an iron chelator known to activate HIF-1a, on the functional deficits induced by focal ischaemia in the rat. **Materials and methods:** Anesthetized male Sprague Dawley rats were subjected to transient (60 min) intraluminal occlusion of the middle cerebral artery or to sham operation. DFX treatment (300 mg/Kg s.c.) or its vehicle, started 24h after ischaemia and continued 2 times per week during 2 months. Functional recovery was evaluated in four sensorimotor tests performed regularly during two months. After euthanasia, the volume of the lesion was determined histologically on coronal brain sections. **Results:** Ischaemia resulted in a large cortico-striatal lesion in the vehicle-treated animals ( $210 \pm 35$  mm<sup>3</sup>, n=8). DFX decreased significantly the extent of the lesion ( $146 \pm 59$  mm<sup>3</sup>, p<0.05, n=8) and improved significantly the behavioural deficits. Indeed, the neurological score, as well as the sensorimotor performances in the adhesive removal test, recovered earlier in the DFX-treated animals. Moreover, the long lasting, skilled paw reaching, deficits observed in the Montoya's staircase have been decreased by the administration of DFX. **Discussion:** Our results suggest that DFX, administered chronically, decreases the infarct volume and improves functional recovery after ischaemia in the rat. Several hypotheses can be drawn to explain this beneficial effect. First, by chelating iron, DFX may exert an antioxidant effect that could limit the expansion of the lesion. Second, by activating HIF-1a, DFX could increase the expression of beneficial genes, such as EPO (2,3), glucose transporters-1 (GLUT-1) (4) and vascular endothelial growth factor (VEGF) (5). Although further experiments are needed to clarify the mechanisms underlying its beneficial effects, our preliminary data suggest that a delayed administration of DFX could represent an interesting therapeutical approach to treat ischaemia. **References:** (1) Bergeron M et al. Induction of hypoxia-inducible factor-1 (HIF-1) and its target genes following focal ischaemia in rat brain. *Eur J Neurosci* (1999) 11:4159-4170. (2) Bernaudin M et al. A potential role for erythropoietin in focal permanent cerebral ischemia in mice. *J Cereb Blood Flow Metab.* (1999) 19:643-651. (3) Shingo T et al. Erythropoietin regulates the in vitro and in vivo production of neuronal progenitors by mammalian forebrain neural stem cells. *J Neurosci* (2000) 21:9733-9743 (4) Lawrence MS et al. Overexpression of the glucose transporter gene with a herpes simplex viral vector protects striatal neurons against stroke. *J Cereb Blood Flow Metab.* (1996) 16:181-185 (5) Sun Y et al. VEGF-induced neuroprotection, neurogenesis, and angiogenesis after focal cerebral ischemia. *J Clin Invest* (2003) 111: 1843-1851.

**ROLE OF AKT1 IN ESTROGEN-MEDIATED NEUROPROTECTION**Nabil J. Alkayed, Staphanie J. Murphy, Sharon M. Graham, **Patricia D. Hurn***Anesthesiology & Peri-Operative Medicine - Research Division/Oregon Health & Science University, Portland, OR, USA*

**INTRODUCTION:** Estrogen is protective in experimental cerebral ischemia, but the mechanism of neuroprotection remains unknown. In cultured cortical neurons, estradiol enhances Akt phosphorylation, and pharmacological inhibition of Akt phosphorylation prevents protection by estradiol against glutamate-induced neurotoxicity (1). Phosphorylation via phosphatidylinositol 3-kinase (PI3-K) activates Akt, which promotes neuronal survival. There are three isoforms of Akt. It is not known, however, which isoform is involved in estradiol-mediated neuroprotection. Akt1 has been implicated in cellular growth, development, and survival (2). Therefore, we tested the hypothesis that Akt1 gene deletion abrogates the neuroprotective effect of estradiol in vivo, and to evaluate AKT and ischemia when estrogen is low. **METHODS:** Female homozygous Akt1 knockout (KO) and wild-type mice (18-25 g) were ovariectomized and implanted subcutaneously with Silastic capsules containing 180 mg 17 $\beta$ -estradiol (E2) or vehicle for 7 days. Male Akt1 KO and WT mice were also included in the study for comparison. Mice were subsequently subjected to 2-hour MCA occlusion via the intraluminal filament technique (3), followed by 22 hours reperfusion. Cortical, caudate-putamen and total hemispheric infarct volumes were determined by digital image analysis of sequential 2-mm thick coronal brain slices after staining with 2,3,5-triphenyltetrazolium chloride. Laser-Doppler perfusion was monitored to estimate the relative drop in cortical perfusion at initiation of occlusion and restoration of blood flow at reperfusion. Body temperature was monitored and regulated during surgery by warming blankets. **RESULTS:** Body temperature was maintained within normal physiological range and was equivalent among groups. Laser-Doppler perfusion was reduced to less than 20% of baseline after MCA occlusion, and recovered to at least 55% of pre-occlusion baseline after reperfusion. Estradiol replacement increased plasma E2 from  $20 \pm 2$  to  $47 \pm 3$  pg/ml WT, and from  $18 \pm 1$  to  $50 \pm 3$  pg/ml in Akt1 KO mice. Estradiol significantly reduced infarct size in the cerebral cortex ( $13.8 \pm 3.5\%$  compared to  $26.8 \pm 4.6\%$  in vehicle-treated mice,  $n=11$  per group,  $p<0.05$ , mean  $\pm$  sem) and caudate-putamen ( $49.2 \pm 5.7\%$  compared to  $70.5 \pm 4.7\%$ ,  $n=11$  per group,  $p<0.05$ ) in WT mice. Estradiol replacement also reduced infarct size in Akt1 KO ( $9.6 \pm 1.9\%$  total hemispheric infarct in E2-treated vs.  $18.9 \pm 5.3\%$  in vehicle-treated mice,  $n=10$  per group,  $p>0.05$ ). Both male and female Akt1 KO mice sustained smaller infarcts after MCA occlusion compared to WT mice ( $14.2 \pm 4.1\%$  in male KO vs.  $35.1 \pm 5.5\%$  in male WT,  $n=10$  per group,  $p<0.05$ ,  $18.9 \pm 5.3$  in female KO,  $n=10$  vs  $29.2 \pm 4.5$  in female WT,  $n=11$ ,  $p<0.05$ ). **CONCLUSION:** Akt1 KO mice are paradoxically protected from ischemic brain injury. The protection by estradiol does not seem to be mediated via Akt1. **REFERENCES:** [1] Honda K et al. J Neurosci Res. 2000;60:321-7. [2] Cho H et al. J Biol Chem. 2001;276:38349-52. [3] Sampei K et al. Stroke. 2000;31:738-43

## EFFECT OF NUCLEAR FACTOR-KAPPA B ON CELL SURVIVAL OF SOD1 TG ASTROCYTES AFTER OXYGEN GLUCOSE DEPRIVATION

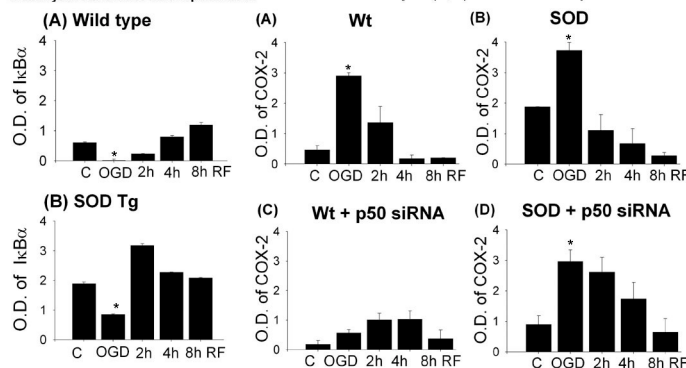
Yong-Sun Lee<sup>1</sup>, Yun Seon Song<sup>1</sup>, Jian Wang<sup>2</sup>, Rona G. Giffard<sup>1,2</sup>, Pak H. Chan<sup>1</sup>

<sup>1</sup>Department of Neurosurgery, Stanford University School of Medicine, Stanford, CA, USA

<sup>2</sup>Department of Anesthesia, Stanford University School of Medicine, Stanford, CA, USA

Purpose: NFκB is activated in brain cells after various insults, including cerebral ischemia. In cytoplasm, NFκB is tightly associated with inhibitory protein, IκBα. On activation by H<sub>2</sub>O<sub>2</sub>, IκBα is phosphorylated and degraded, exposing the nuclear localization signals on NFκB heterodimer. Cyclooxygenase (COX2) is known as an NFκB-inducible gene, expressed in leukocytes and brain. It is an important mediator of cell injury in inflammation. We investigated the effect of oxygen glucose deprivation (OGD) on IκBα phosphorylation, NFκB activation, COX2 expression and the relation of OGD to cell survival in SOD1 transgenic (Tg) mice. Methods : Primary astrocytes from postnatal day 2-3 SOD1 Tg and wild type (Wt) mice were cultured for 14 days. Cells were subjected to OGD for 4 hrs and collected for the indicated time points. Small interfering RNAs (siRNA) of NFκB p50 were used to suppress the gene expression. NFκB p50, IκBα, phospho-IκBα and COX2 antibodies were used for immunoblotting. Cell death was measured by LDH assay. Results: In Wt and SOD1 Tg astrocytes, IκBα level decreased rapidly after OGD, and recovered to basal level by 4 hr of reperfusion (Fig.1). Phospho-IκBα was highly expressed after OGD and 2h reperfusion in both cell types, which corresponded with the decreased level of IκBα at these time points. Cytosolic level of NFκB p50 in Wt gradually increased after OGD and decreased by 3.7-fold during reperfusion. NFκB p50 level increased by 1.9-fold after OGD in SOD1 Tg astrocytes. The reduced cytosolic NFκB p50 was consistent with for the increase in nuclear translocation. SOD1 transfected astrocytes exhibited enhanced elevation of NFκB at 2 hr of OGD. COX2 level was induced by 6-fold and 1.9-fold after OGD in Wt and SOD1 Tg astrocytes (Fig.2). SOD1 Tg cells were 3.3-fold more protected than Wt cells after OGD (p<0.05, n=6). However, SOD1 Tg cells transfected with siRNA showed 8-fold higher cell death rates and elevated COX2 expression. Immunostaining showed similar results. Conclusions: After OGD, IκBα was rapidly phosphorylated, leading to decreased IκBα and translocation of NFκB into the nucleus. NFκB had a protective role in cell survival after oxidative injury. However, blocking NFκB p50 expression by siRNA led to attenuation of COX2 expression in Wt, but enhanced COX2 expression and cell death in SOD1 Tg astrocytes. These results suggest that the transcriptional mechanism involved in COX2 gene expression may be different in SOD1 Tg astrocytes after OGD. Supported by P50NS14543, PN5037520, RO1NS25372, RO1NS36147, RO1NS38653 and AHA Bugher Foundation.

Fig.1. IκBα protein levels in Wt and SOD astrocytes after OGD and reperfusion. Fig.2. COX-2 levels in Wt (A), SOD(B) and siRNA transfected astrocytes (C, D) after OGD and reperfusion.



## ROLES OF THE C-TERMINAL PEPTIDE BINDING DOMAIN OF HUMAN INDUCIBLE HSP70 IN FOCAL ISCHEMIC BRAIN INJURY

Yunjuan Sun, Yibing Ouyang, Lijun Xu, **Rona G. Giffard**

*Department of Anesthesia, Stanford University, Stanford, CA, USA*

The inducible heat shock protein 70 (Hsp70) is a molecular chaperone that is expressed primarily in response to stress, including heat shock, ischemia and glucose deprivation. Hsp70 consists of a 44 kDa amino terminal ATPase domain, an 18 kDa peptide or substrate binding domain, and a 10 kDa carboxy terminal domain. While a large number of proteins interact with Hsp70, only in some cases has the domain with which they interact been identified. Although it is accepted that Hsp70 can protect cells from ischemic injury, the mechanism is not known. Possible protective effects include prevention of protein aggregation, refolding denatured proteins and reduction of apoptosis. The relative importance of the ATP-binding domain compared to the peptide binding domain of HSP70 in ischemic protection is unknown. To explore this question we tested whether two Hsp70 mutant proteins could protect against ischemia-like injury of primary cultured murine astrocytes and reduce focal ischemic injury induced by transient (2h) middle cerebral artery occlusion (MCAO). The two mutants studied were 1) Hsp70 K71E, a point mutation that abrogates ATP binding and renders the protein deficient in folding ability and 2) Hsp70 381-640 a deletion mutant lacking the ATP binding domain. Hsp70 wild type (WT), -K71E, -381-640 and vector plasmid LXSXN were expressed in primary murine astrocyte cultures using retroviral mediated transfection. After G418 selection, more than 95% of cells expressed these proteins by immunostaining. Cultures were then subjected to combined oxygen-glucose deprivation (OGD) and cell survival was assessed by MTT assay or PI staining and cell counting. Astrocytes overexpressing Hsp70 -WT, -K71E or -381-640 were all significantly protected from 4h OGD (cell viability was increased about 50%,  $p < 0.05$ ). We then tested the ability of these mutant proteins to protect rats from transient focal ischemic injury. Plasmids encoding Hsp70 -K71E, -381-640, or the control backbone plasmid LXSXN were stereotactically injected into the left lateral ventricle 24 h prior to MCAO. These mutant proteins were expressed in both astrocytes and neurons as determined by double immunostaining. Animals that overexpressed either of these two mutant proteins had significantly better neurological scores and smaller infarct volumes (30-35%) assessed at 24 hr (infarction volume (mm<sup>3</sup>): 233.5±38.6 in control group; 152.25±43.95 in Hsp70 K71E group; and 162.71±32.5 in Hsp70 381-640 group,  $P < 0.05$  compared to control,  $n=8$  in each group). Protection by both mutants was associated with reduced protein aggregation and apoptosis, as assessed by ubiquitin immunohistochemistry and Klenow staining. Both the point mutant and the deletion mutant were found to reduce ischemic injury. Since the carboxy terminal half of the protein is sufficient for protection, interaction with protein partners that bind the aminoterminal half of the protein are not essential to ischemic protection. Also, since neither mutant can facilitate folding, their efficacy against ischemia suggests that inhibiting protein aggregation is sufficient to reduce ischemic injury and apoptotic cell death. 'Supported in part by GM49831 and NS37520'

**NEUROPROTECTIVE EFFECTS OF DIKETOPIPERAZINES, POTENTIAL  
CLINICAL APPLICATION OF SMALL CYCLIC FORM OF NEUROPEPTIDE  
FOLLOWING ISCHEMIC BRAIN INJURY**

**Jian Guan<sup>1</sup>**, Sam Mathai<sup>1</sup>, Frank Sieg<sup>3</sup>, Thorsten Gorba<sup>1</sup>, Margaret Brimble<sup>2</sup>,  
Peter Gluckman<sup>1</sup>

<sup>1</sup>*The Liggins Institute, FMBS, University of Auckland, Auckland, New Zealand*

<sup>2</sup>*Medicinal Department, SBS, University of Auckland, Auckland, New Zealand*

<sup>3</sup>*Neuren Pharmaceuticals Limited, Auckland, New Zealand*

Introduction: A considerable number of neuropeptides have been shown to be neuroprotective tested in various animal models with ischemic brain injuries. However the central delivery of peptide has always been problematic due to their large molecular weight and potential mitogenic effect after being administered into the peripheral circulation. Diketopiperazine (DKP)s are a group of cyclic forms of dipeptides, naturally occurring in the central nervous system. The current experiment examined the neuroprotective effects of a native DKP and its analogues, modified to improve its potency on neuroprotection. Methods: An analogue of DKP was modified to improve the potency of neuroprotection. The effects of neuronal survival of both a native DKP and its analogue following glutamate + 3NP neurotoxicity were first examined in cerebellar neuronal culture. The neuroprotection of the native DKP and its analogue were also tested in adult rats with hypoxic-ischemic brain injury. Results: Both the native DKP and its analogue prevented cerebellar neuronal death from glutamate/3-NP induced neurotoxicity in a dose dependent manner. The effect of the analogue on neuronal survival was more potent (10pM-1nM) compared to that of native DKP (1-100nM). Central administration of either native DKP (200ng/rat, icv) or its analogue (2-20ng/rat, icv) reduced neuronal loss in the lateral cortex, hippocampus and striatum, also in a dose dependent manner. Peripheral administration of the analogue significantly improved neuronal outcome 7 days after HI injury, however the degree of neuroprotection was not as strong compared to that after central administration. Discussion: Current study demonstrated for the first time that the cyclic form of proline containing dipeptides were neuroprotective. The data suggest a potential pharmaceutical development for treating ischemic brain injury.

**PHARMACOLOGICAL CORRECTION OF THE HEMORHEOLOGICAL PROFILE  
CHANGES UNDER, CEREBRAL ISCHAEMIA-REPERFUSION INJURY BY  
IMIDAZOBENZIMIDAZOLE DERIVATIVE**

**Alexey V. Stepanov**, Alexander A. Spasov, Natalia V. Arjkova, Maria P. Samokhina,  
Ludmila V. Naumenko, Vitalij N. Kotov, Tatjana V. Goncharova, Darya M. Maltzeva,  
Ivan N. Tjurenkov, Miroslav N. Bagmetov, Andrey V. Voronkov, Ludmila E. Borodkina,  
Jakov Tivon, Vera A. Anisimova

*Volgograd State Medical University, Volgograd, Russia*

Previously, hemorheological screening of 162 bi- and tricyclic benzimidazole and xantine derivatives has been performed. The most active substances were evaluated in class of N9-imidazobenzimidazoles, which activity exceed widely used drugs (pentoxifylline, gliclazide etc.). The most potent agent - AKS-17 has been taken out for further examination. Total cerebral ischaemia was induced by common carotid arteries occlusion (1h) under hypovolemic hypotension conditions (blood samples were used for evaluation of initial hemorheological parameters), followed by reperfusion. Intravenous injection of AKS-17 (5 mg/kg) or pentoxifylline (equalmolar dose 4 mg/kg) or saline (control groups - ischaemic and sham-operated) had been performed before operation. Blood samples were taken from abdominal aorta 1h after reperfusion onset. Blood rheology properties were tested using rotational viscosimetry, micropore filtration system, light microscopy, light transmission aggregometry, coagulation parameters were evaluated, DSM+ RBC fluorescence rates were determined. Regional cerebral blood flow (CBF) in cortex supplied by the right middle cerebral artery was measured by Doppler flowmetry during ischemia period. ANOVA was used to analyze statistical differences among groups, with significance level at  $P < 0.05$ . Significant increase of blood viscosity at low and high shear-rates (11% at 300 and 39.36% - 3s-1), RBC aggregation index - 15.85% (associated with decrease of DSM+ fluorescence (33,84%) - negative surface charge diminishment - 'exhausted' aggregation mechanism), as well as decreased RBC deformability (40.54%) and osmotic fragility (73.1%) were evaluated in ischaemic versus control (sham-operated) rats. AKS-17 or pentoxifylline reduced blood viscosity at high shear rates (21,93 and 12,48%, respectively) as well as at low shear rates (40,79% and 19,31%, respectively). AKS-17 decreased RBC aggregation index (24,35% versus 11% - pentoxifylline), RBC filtration rate (exceed pentoxifylline in 61.85%), viscosity of RBC suspensions (24.29% versus 13.36% - pentoxifylline). AKS-17 significantly decreased platelets aggregation parameters and improved hypercoagulable state. Local CBF decreased in 1.9 times after bilateral CCA occlusion and was stable up to 1 hour. In a group, receiving AKS-17 reduction was only 23,7% and returned to initial level to 10 minute of ischaemia. So, preventive AKS-17 administration leads to improvement of the microcirculation parameters so it may be useful for a new cerebroprotective agent creation.

## NEUROPROTECTIVE OF SESAME SEED AND ITS COMPONENT SESAMIN ON THE BRAIN ISCHEMIA IN RATS

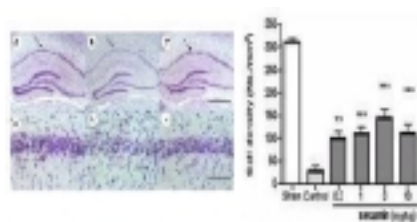
Hocheol Kim<sup>1</sup>, Eunbang Lee<sup>3</sup>, Youngmin Boo<sup>2</sup>, Minjung Kong<sup>1</sup>, Seungju Rho<sup>1</sup>, Nina Ha<sup>1</sup>, Hayoung Lee<sup>1</sup>, Miyeon Kim<sup>1</sup>, Dalseok Oh<sup>1</sup>, Donghwan Lee<sup>1</sup>, Sungin Hong<sup>1</sup>

<sup>1</sup>Department of Herbal Pharmacology, KyungHee University, Seoul, Korea

<sup>2</sup>Department of Herbal Pharmacology, Woosuk University, Jeonbuk, Korea

<sup>3</sup>Korea Institute of Science and Technology for Eastern Medicine, NeuMed, Seoul, Korea

**Introduction:** Sesame seeds (Ss; *Sesamum indicum* Linn, Pedaliaceae), has been widely used in traditional Korean medicine for anti aging. Ss contains significant amount of lignan, such as sesamin. It is known to have many biological activities. The aims of this study were to do investigation of neuroprotective effect of Ss and its component sesamin on brain ischemia using 4-vessel occlusion (4-VO) rat model. **Method:** Ss was extracted with methanol. We analyzed the content of sesamin by HPLC. We fractionated the extract repeatedly from vacuum silica gel column chromatography and isolated the component, sesamin. We investigate the The neuroprotective effect of samples on CA1 hippocampal neurons was evaluated by measuring the neuronal cell density in CA1 hippocampal region at 7 days after 10min ischemia. Ss treated group (at a dose 500 mg/kg) were orally administered at 0 min and 60 min after ischemia. Sesamin (0.3, 1, 3, 10 mg/kg) was dissolved in 100% DMSO and intraperitoneally injected at 0 and 90 min after ischemia. We investigated the neuroprotective effect on 2 hr of oxygen glucose deprivation (OGD) in primary neuronal culture. As mechanisms, we investigated the effect of sesamin on NO production in BV2 cell line after LPS treatment. We also investigated the inhibitory effects of sesamin on RNA and protein expression of COX-2, iNOS, IL-1 $\beta$  and TNF- $\alpha$  by RT-PCR, immunohistochemistry and western blot analysis, after 4-VO. **Results:** We confirmed that Ss contained 3% of sesamin. Oral administration of Ss methanol extract (500 mg/kg) showed 29% of neuroprotective effect While, intraperitoneal injection of sesamin (3 mg/kg) protected 42.5% in neuronal death in hippocampal CA1 neurons at 7 days after 4-VO without changing of body temperature. Sesamin (1 mg/kg) protected 40% after OGD 2 hr in primary neuronal cells. It also inhibited NO production in BV-2 cell after LPS treatment. Sesamin inhibited COX-2 and microglial activation in the CA1 of hippocampus after 4-VO. Sesamin (1, 3 mg/kg) suppressed iNOS induction and blocked the enhancement of IL-1 $\beta$  and TNF- $\alpha$  levels. **Conclusion:** Sesame seed including sesamin reduced neuronal cell density in global cerebral ischemia in rat by ant-inflammatory effects. and these results lead to the possibility that Sesame seed and its ingredient including sesamin may be available for treatment of brain ischemia patients. **References:** [1] Kim HC. Herbal Pharmacology Seoul; Jipmoondang, 432-433(2001). [2] Pulsinelli WA, Brierley JB ; Stroke, 10:267-272 (1979). **Grant support:** supported by a grant (PF0320201-00) from Plant Diversity Research Center of 21st Century Frontier Research Program funded by Ministry of Science and Technology of Korean government.



The neuroprotective effect of sesamin on 4 vessel occlusion rat model. A, B and C in left photos is the hippocampus of sham, control and sesamin treated rat. a, b and c is CA1 of A, B and C, respectively. Scale bar is 1 mm (A,B,C) and 100 $\mu$ m (a,b,c).



**ANTIOXIDANT PROTECTIVE EFFECTS OF STOBADINE AGAINST ISCHEMIA/REPERFUSION (I/R) INDUCED ALTERATIONS OF MUSCULAR AND ENDOTHELIAL FUNCTIONS OF RAT MIDDLE CEREBRAL ARTERIES (MCA)**

Michèle Bastide<sup>1</sup>, Olivier Pétrault<sup>1</sup>, Maud Laprais<sup>1</sup>, **Thavarak Ouk**<sup>1</sup>, Svorad Stolc<sup>2</sup>, Régis Bordet<sup>1</sup>

<sup>1</sup>*Laboratoire de Pharmacologie, Faculté de Médecine, Lille, France*

<sup>2</sup>*Institute of Experimental Pharmacology, Slovak Academy of Sciences, Bratislava, Slovak Republic*

The reperfusion step during cerebral I/R is known to be responsible for the generation of free radicals which play significant role in the development of alterations of cerebral tissue and vessels. The aim of our study was to investigate the effects of stobadine (STO), a pyridolindole derivative, previously experienced in different models of pathologies for its scavenging effects towards free radicals<sup>1</sup>. Rats were ischemized for 1 h then allowed to reperfusion for 24 h. STO (1 mg/kg) or vehicle (VEH) was administered (IV) at t=0 and 5 h of reperfusion. Brain infarct volumes were quantified and MCA studied either with patch-clamp technique for KIR2.1 of smooth muscle cells (SMC), either by vasomotricity for endothelium and smooth muscle functions (Halpern myograph). STO reduced brain infarct volumes from 238±9 mm<sup>3</sup> on VEH-treated rats (n=18) to 182±9 mm<sup>3</sup> (p<0.005, n=21). KIR2.1, an inward rectifier potassium current of SMC was drastically reduced after I/R. Tested on SMC of I/R STO-treated rats, the KIR2.1 density was significantly preserved (-1.06±0.17 pA/pF, n=9, p<0.05) compared to -0.48±0.07 pA/pF (n=6) in I/R VEH-treated rats and -1.23±0.11 pA/pF in SHAM VEH-treated rats (n=9). The endothelial-dependent vasorelaxation was induced by ACh (3.10-5M) on serotonin-precontracted (10-6M) MCA. The percentage of diameter increase induced by ACh was 22.20±1.60% (n=11) on sham-VEH MCA but was significantly reduced to 12.31±1.42% (n=6) on I/R VEH-treated MCA. After STO treatment, endothelium-dependent vasodilation was significantly preserved on I/R MCA (20.73±2.63%, p<0.01, n=6). Concerning the smooth muscle dependent relaxation induced by KIR2.1 activation, stobadine pretreatment didn't allow any protection towards the I/R induced reduction of this vasodilation. Application of 15 mM KCl allowed SHAM VEH-treated MCA to relax to a 25.53±2.25% increase of its basal tone (n=15). Same application on I/R VEH-treated MCA induced only 5.00±1.35% of increase basal diameter (n=8). After STO treatment, vasodilation reached 11.45±2.28% (n=11) on SHAM MCA and 6.24±2.18% (n=8) on I/R MCA. These data revealed the potent protective effects of the antioxidant agent stobadine towards neuronal tissue (i.e. reduction of infarct size) in parallel to endothelial vascular function. Smooth muscle KIR2.1 density is also protected while the relaxation depending on is still altered. This result suggested another step between KIR2.1 activation and the triggering of the smooth muscle dependent relaxation. However stobadine appeared to be a promising tool to reveal new therapeutic strategies against cerebral ischemia.

1- Horakova & Stolc, 1998, *Gen Pharmac*, 32 : 627-638. 2- Bastide et al, 1999, *J Cereb Blood Flow Metab*, 19 : 1309-1315.

## ACUTE TREATMENT BY A PPAR- $\alpha$ AGONIST DECREASES CEREBRAL INFARCT VOLUME AND PREVENTS POST-ISCHEMIC ENDOTHELIUM AND KIR 2.1 IMPAIRMENT

Thavarak Ouk<sup>1</sup>, Olivier Pétrault<sup>1</sup>, Sophie Gautier<sup>1</sup>, Patrick Gelé<sup>1</sup>, Maud Laprais<sup>1</sup>, Patrick Duriez<sup>2</sup>, Michèle Bastide<sup>1</sup>, Régis Bordet<sup>1</sup>

<sup>1</sup>Laboratoire de Pharmacologie, Faculté de Médecine, Lille, France

<sup>2</sup>Laboratoire de Physiologie, Faculté de Pharmacie, Lille, France

Introduction Chronic pre-treatment by Peroxysome Proliferator-Activated Receptor- $\alpha$  agonist induces a neuroprotective effect in experimental model of focal cerebral ischemia by both anti-inflammatory and anti-oxidant mechanisms (1). The aim of our study is to demonstrate if an acute activation of PPAR- $\alpha$  could also induce cerebral protection during cerebral ischemia as well as a prevention of post-ischemic endothelium and Kir 2.1 smooth muscle impairment, which are mediated by oxidative stress. Materials Male Wistar rats were subjected to a 60 minutes middle cerebral artery occlusion (MCAo). Vehicle or fenofibrate (50 or 200 mg/kg per day), a PPAR- $\alpha$  activator, was administered by gavage twice a day during 72 hours after onset of ischemia. The infarct volume was determined at 72 hours of reperfusion. The ipsilateral MCA was removed and mounted in a small vessel arteriograph. The endothelium and smooth muscle reactivity was then studied. Results Fenofibrate at 50 and 200 mg/kg induced a significant decrease in infarct volume by 21% and 32 %, respectively ( $p < 0.05$  versus vehicle). Acute administration of fenofibrate at 50 mg/kg prevented the ischemia/reperfusion-impairment of endothelium relaxation ( $21.6 \pm 5.0\%$  versus  $12.9 \pm 2.9\%$ ,  $p < 0.05$ ) but not at 200 mg/kg ( $9.8 \pm 1.8\%$ , NS). KCl-induced smooth muscle relaxation was reduced in ischemic animals compared to control ( $12.1 \pm 1.5\%$  versus  $26.0 \pm 2.4\%$ ,  $p < 0.05$ ) whereas fenofibrate administration at 50 mg/kg prevented the post-ischemic impairment of smooth muscle Kir 2.1 relaxation ( $22.6 \pm 2.9\%$ ,  $p < 0.05$  versus ischemic animals) and not at 200 mg/kg ( $14.8 \pm 4.4\%$ , NS versus ischemic animals). Endothelium-independent relaxation to sodium nitroprusside was similar in all groups. Conclusion Acute administration of PPAR- $\alpha$  agonist induces a significant neuroprotection. But our results show also a discrepancy between the neuroprotection and the vasculoprotection level according to the dose, suggesting that the vascular wall should not be considered as the only pharmacological target in the treatment of stroke. References 1. Deplanque D, Gelé P, Pétrault O, Six I, Furman C, Bouly M, Nion S, Dupuis B, Leys D, Fruchart JC, Cechelli R, Staels B, Duriez P, Bordet R (2003) Peroxisome Proliferator-Activated Receptor- $\alpha$  as a mechanism of preventive neuroprotection induced by chronic fenofibrate treatment. *J Neurosci* 23(15):6264-6271.

**TALAMPANEL, A NON-COMPETITIVE AMPA-ANTAGONIST IMPROVES THE FUNCTIONAL RECOVERY AFTER FOCAL CEREBRAL ISCHEMIA IN RATS - A 30-DAY FOLLOW UP STUDY**

**Franciska Erdo, Pál Berzsenyi, Ferenc András**

*Department of Pharmacology, IVAX Drug Research Institute Ltd., Budapest, Hungary*

Background and aim of the study: The beneficial effect of the anti-epileptic talampanel was previously shown in acute focal cerebral ischemia models in rats and mice. The compound (6 x 2 mg/kg i.v.) reduced the infarct size by 49% (in rats) and 44.5% (in mice) after 1 h ischemia and 24 h recirculation. The aim of present study was to test the therapeutic potential of talampanel under clinically more relevant conditions, in a chronic model of stroke with not only morphological but also functional assessments. Methods: Three groups of male CDBR rats (sham operated, ischemic control and talampanel treated) were used for the experiments. Transient middle cerebral artery occlusion (tMCAO) was produced by intraluminal filament technique. On the day of the operation the animals were treated with talampanel (10 mg/kg i.p.) or vehicle (saline containing 0.5 % Tween 80) six times (30 min, 1.5 h, 2.5 h, 3.5 h, 4.5 h and 5.5 h post-occlusion). The functional deficit was measured on the days 1, 2, 3, 4, 7, 15, 22 and 29 after the tMCAO. Survival rate, body weight, neurological status, locomotor activity, spontaneous rotation, muscle strength, motor coordination, balancing and reaction time following forepaw stimulation were monitored. At the end of the 30-day observation period the brain tissues were histologically analysed after hematoxylin eosin staining. Results and conclusions: Due to the restitutive capacity of the rat brain a spontaneous improvement of motor deficit was observable in several behavioral tests during the 30 days in the ischemic control animals. Talampanel treatment improved the survival rate, the stroke-induced rotation, the failure of the motor coordination, the balancing disturbances and the prolongation of the reflex time at every timepoint comparing with the ischemic control. The effects were statistically significant in rotometer, rotarod and beam walking tests. Analysing the size and structure of the infarcted area of the brain tissue no remarkable differences were found between the vehicle and talampanel treated animals at 30 days after the ischemia. These results suggest that the size of the infarction and the severity of the sensorimotor deficit is not necessarily correlate. In conclusion our results indicate that talampanel is able to attenuate the long-term neurological and motor dysfunctions following stroke in rats. However, a spontaneous recovery of the behavioral functions is detectable in the ischemic control animals as well. The complex functional monitoring applied in the present study is unique in the literature and may serve as a relevant approach to predict the anti-ischemic effect of the drug before a possible clinical investigation. Acknowledgements: The authors are grateful to Mária Szaniszló, Zsuzsa Doma, Krisztina Kürti, Ágnes Háda and Mónika Csatári for the excellent technical assistance.

## TIME-LAG COMBINATION THERAPY FOR CEREBRAL ISCHEMIA USING THE FNK PROTEIN TRANSDUCTION TECHNOLOGY AND AN IMMUNOSUPPRESSANT, I: IN VIVO STUDY

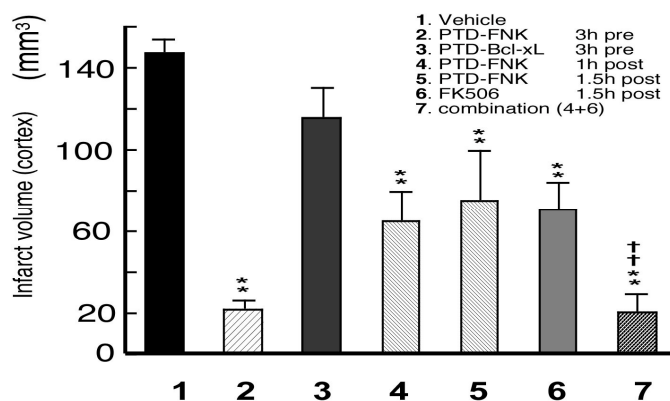
Ken-ichiro Kasura<sup>1</sup>, Megumi Watanabe<sup>1</sup>, Kumiko Takahashi<sup>1</sup>, Genki Mizukoshi<sup>1</sup>, Seiji Ohkubo<sup>1</sup>, Hironaka Igarashi<sup>1</sup>, Takashi Mori<sup>3</sup>, Sadamitsu Asoh<sup>2</sup>, Shigeo Ohta<sup>2</sup>, Yasuo Katayama<sup>1</sup>

<sup>1</sup>The Second Department of Internal Medicine, Nippon Medical School, Tokyo, Japan

<sup>2</sup>Department of Biochemistry and Cell Biology, Institute of Development and Aging Sciences, Graduate School of Medicine, Nippon Medical School, Kawasaki, Japan

<sup>3</sup>Saitama Medical Center/School, Kawagoe, Saitama, Japan

Background and purpose: Ischemic cerebral infarction is a major cause of death. However, few practical therapies have been explored for clinical applications. We show here a potential combination therapy in a rat focal ischemic model to improve neurological symptoms as well as reduces the infarct volume at the maximum level. Methods: As reported previously (1), we applied a protein transduction technology using super anti-cell death FNK protein (artificially modified Bcl-xL protein, ref 2) fused with a protein-transduction-domain peptide from HIV Tat protein (PTD-FNK). Focal ischemia was produced by intraluminal occlusion of the left middle cerebral artery (MCA) with a nylon monofilament for 1.5 h. Results: When PTD-FNK (0.25mg/kg) was administered intravenously at 1 hr after initiating ischemia, the infarct volume were reduced down to 50% of the vehicle treated group. Furthermore, if FNK post treatment was followed by an intravenous injection of an immunosuppressant FK506 (1mg/kg) with 30 min interval, the infarct volume of the cortex was markedly reduced down to 14%. This procedure not only reduced the infarct volume but also markedly improved the neurological symptoms. All ischemic rats post-treated with the combination of PTD-FNK and FK506 could walk smoothly whereas untreated ischemic rats could not walk at all. The therapeutic time windows for PTD-FNK alone treatment was until 3h after ischemia and the combination therapy elongated the timewindow to at least 4.5h after ischemia. Conclusions: Protein therapy with cell penetrating technology such as using Tat-PTD is quite effective for cerebral ischemia. Furthermore the combination with FK506 synergistically enhanced the protective effect. Since PTD-FNK localizes around Mitochondria and FK506 will influence the ER function, mechanisms of additive therapeutic effects of PTD-FNK and FK506 could be due to protection of both mitochondria and ER. References 1. Asoh et al. (2002) Proc. Natl. Acad. Sci. USA. 99, 17107-17112. 2. Asoh et al., (2000) J. Biol. Chem., 275, 37240-37245.



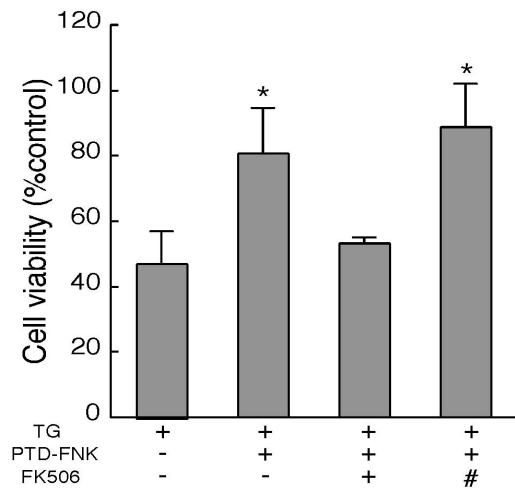
**TIME-LAG COMBINATION THERAPY FOR CEREBRAL ISCHEMIA USING THE  
FNK PROTEIN TRANSDUCTION TECHNOLOGY AND AN  
IMMUNOSUPPRESSANT, II: IN VITRO STUDY**

**Megumi Watanabe<sup>1</sup>, Ken-ichiro Katsura<sup>1</sup>, Genki Mizukoshi<sup>1</sup>, Ikuroh Ohsawa<sup>2</sup>,  
Sadamitsu Asoh<sup>2</sup>, Shigeo Ohta<sup>2</sup>, Yasuo Katayama<sup>1</sup>**

*<sup>1</sup>The Second Department of Internal Medicine, Nippon Medical School, Tokyo, Japan*

*<sup>2</sup>Department of Biochemistry and Cell Biology, Institute of Development and Aging  
Sciences, Graduate School of Medicine, Nippon Medical School, Kawasaki, Japan*

**Background and purpose** We applied a protein transduction technology using super anti-cell death FNK protein (artificially modified Bcl-xL) fused with a protein-transduction-domain peptide from HIV Tat protein (PTD-FNK)(Ref1,2). We present strong protective effects with rat middle cerebral artery occlusion model in this meeting. When PTD-FNK administration was followed by administration of an immunosuppressant FK506 with 30 min interval, the protective effect was markedly enhanced. We tried to explore protective mechanisms of the combination therapy for cerebral ischemia using in vitro cell death system. Methods Neuroblastoma SH-SY5Y cells were cultured, and PTD-FNK and/or FK506 were administered. Then, thapsigargin (TG), a potent inhibitor of endoplasmic reticulum calcium-ATPase, was added. After 24hours, viable cells were counted under a microscope. For determination of intracellular free Ca<sup>2+</sup> ([Ca<sup>2+</sup>]<sub>i</sub>), the fluorescence Ca<sup>2+</sup> indicator Fluo-3 AM was added at first, and pretreated with PTD-FNK and/or FK506, and further stimulated with TG. Results Cell viability was lost to 47.3% in the treatment with TG. PTD-FNK and FK506 showed 80.9% and 72.5% cell viability, respectively. The combination of PTD-FNK and FK506 with 30 min interval showed 88.7% cell viability(right most column of figure), however, the simultaneous treatment did not have protective effect. [Ca<sup>2+</sup>]<sub>i</sub> increased after the addition of TG. After the addition of FK506, [Ca<sup>2+</sup>]<sub>i</sub> also increased. In contrast, the increase of [Ca<sup>2+</sup>]<sub>i</sub> was suppressed with PTD-FNK and the combination of PTD-FNK and FK506 with 30 min time lag. If PTD-FNK and FK506 were added simultaneously, [Ca<sup>2+</sup>]<sub>i</sub> increased to similar level of TG alone treatment. Conclusions These experiments suggest that the combination treatment of PTD-FNK and FK506 with 30 min interval affects the movement of calcium ions, leading to protection against cell death. It is reported FK506 can cause an inhibition of endoplasmic reticulum calcium-ATPase which could increase cytosolic calcium level. Furthermore, FK506 was reported to strip FKBP12 from 1,4,5-triphosphate receptor or ryanodine receptor, making those channels “leaky” for calcium. If PTD-FNK were treated before FK506 administration, the adverse effect of FK506 (increase cytosolic calcium level) decreased and the protective effect appeared more effectively, leading to synergistic protection References 1.Asoh et al., (2002) Proc. Natl. Acad. Sci. USA. 99, 17107-17112 2.Asoh et al., (2000) J. Biol. Chem. 275, 37240-37245



**STROKE PROTECTION BY ATORVASTATIN TREATMENT IN STROKE-PRONE SPONTANEOUSLY HYPERTENSIVE RATS (SHRSPS):2. MEASUREMENT OF REGIONAL CEREBRAL BLOOD FLOW (RCBF) BY AUTORADIOGRAPHY**

**Tatsuo Otori**, Toshiya Katsumata, Noriko Tanaka, Yutaka Nishiyama, Hidenori Nakamura, Yasuo Katayama

*Internal Medicine 2, Nippon Medical School, Tokyo, Japan*

**Purpose** We are reporting in the first study that daily atorvastatin treatment in SHRSPs demonstrated stroke protection and decreasing mortality. In the second study, to reveal the protective mechanism from the aspect of cerebral blood circulation, SHRSPs were treated daily with atorvastatin, and rCBF were measured by autoradiography at premorbid period of stroke. **Methods** Male 8 weeks SHRSPs were treated daily orally with atorvastatin suspension at a dose of 20mg/kg (n=5, A group). Vehicle male 8 weeks SHRSPs were treated daily orally with same amount of suspension without atorvastatin (n=5, V group). RCBF were measured by autoradiography (Sakurada et al) at age of 13 weeks, which was considered at premorbid period of stroke from the result of the first study. Briefly, rats were anesthetized with a mixture of halothane, oxygen and balance of nitrous oxide. Catheters were placed into femoral artery and vein, and physiological variables were monitored, such as blood pressure and arterial blood gas. After recovered from anesthesia, 150 $\mu$ Cu/kg of [14C]-iodoantipyrine (IAP) was infused into the vein, and 10 blood samples were obtained from the arterial catheter. RCBF were calculated from brain sample and blood samples. Region of interest was set for 15 sites bilaterally (cingulate, frontal, temporal, parietal, occipital, rhinal and entorhinal cortex, caudoputamen, globus pallidus, thalamus, hypothalamus, substantia nigra, CA1 and CA3 hippocampus and dentate gyrus). Averages of both hemispheres from each regions were used for rCBF, and values were indicated as mean $\pm$ SD. Differences between A and V groups were tested for statistical significance using unpaired t-test. A P value less than 0.05 was considered statistically significant. **Results** There were no significant differences in physiologic variables between A and V groups. RCBF was significant larger in A group in cingulate cortex (A:128 $\pm$ 14, V:96 $\pm$ 21), and there were larger tendency in the other cortex, caudoputamen and globus pallidus. There were no significant difference between A and V groups in thalamus, hypothalamus, substantia nigra, CA1 and CA3 hippocampus and dentate gyrus. **Conclusions** Atorvastatin treatment increased rCBF in many region of interest especially cingulate cortex at premorbid period of stroke without changing physiologic variables. It was considered that higher cerebral blood flow at premorbid period contribute to stroke prevention.

**INTENSIVE INSULIN THERAPY IS ASSOCIATED WITH REDUCED  
EXTRACELLULAR GLUCOSE AND INCREASED OXYGEN EXTRACTION  
FRACTION AFTER SEVERE TRAUMATIC BRAIN INJURY**

Paul Vespa<sup>1</sup>, Marvin Bergsneider<sup>1</sup>, David McArthur<sup>1</sup>, H.M. Wu<sup>3</sup>, S.C. Huang<sup>3</sup>, Jeffrey Alger<sup>2</sup>,  
Thomas Glenn<sup>1</sup>, David Hovda<sup>1</sup>

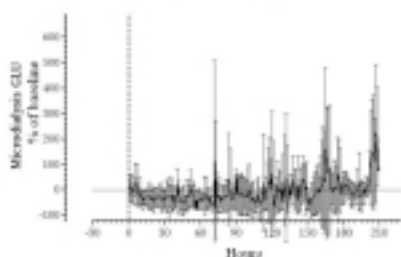
<sup>1</sup>Neurosurgery, UCLA, Los Angeles, CA, USA

<sup>2</sup>Radiology, UCLA, Los Angeles, CA, USA

<sup>3</sup>Nuclear Medicine, UCLA, Los Angeles, CA, USA

Intensive Insulin Therapy is Associated with Reduced Extracellular Glucose and Increased Oxygen Extraction Fraction after Severe Traumatic Brain Injury Introduction: Reductions in extracellular glucose after traumatic brain injury (TBI) is associated with poor outcome and may be related to substrate limitation. Intensive insulin therapy is a commonly used treatment in intensive care and is considered to be crucial in limiting brain damage and brain lactic acidosis after a TBI. Hypothesis: Intensive Insulin therapy (IIT) to maintain normoglycemia may provoke reductions in available brain glucose and precipitate changes in oxidative metabolism. Methods: Nineteen patients with severe TBI underwent cerebral microdialysis (1 $\mu$ L/min) in normal appearing brain tissue before and during insulin infusion aimed at maintaining glucose levels in normal range (5-7 mM). Serial hourly changes in extracellular glucose, lactate and pyruvate were tracked. Single session oxidative positron emission tomography (PET) was obtained in each subject during spontaneous uncontrolled states of glycemia. Regional and whole brain quantitative rates of oxygen extraction fraction (OEF) were determined and compared with serum glucose and extracellular glucose values. Results: During IIT, extracellular glucose decreased by 70%  $\pm$  11% of hyperglycemic baseline in 2/3 of patients (responders). In responders, the extracellular glucose decreased to low levels (< 0.2 mmol/l) in 31% of samples with a corresponding increase in the lactate/pyruvate ratio > 40 in 61% of samples. In nonresponders, the total duration of elevated lactate/pyruvate was nonsignificantly less than that of the responders (p < 0.06). Regional PET OEF correlated poorly with extracellular glucose (-0.03) but whole brain OEF negatively correlated with serum glucose (-0.61, r = 0.01). Serum glucose values of 5-5.5 mM (the goal of IIT) were associated with the highest PET OEF, ranging from 0.5-0.8. These effects were independent of severity of injury. Conclusion: During IIT, the brain exhibits signs of metabolic distress with decreases in extracellular glucose, elevation of lactate/pyruvate ratio and increases in OEF.

Mean reduction in MD glucose during  
insulin infusion



## TRANSLATIONAL COMPLEX AGGREGATION AFTER TRANSIENT CEREBRAL ISCHEMIA

Chunli Liu, Maryann Martone, Pengfei Ge, Fan Zhang, Shaoyi Chen, **Bingren Hu**

*Department of Neurology, University of Miami School of Medicine, Miami, FL, USA*

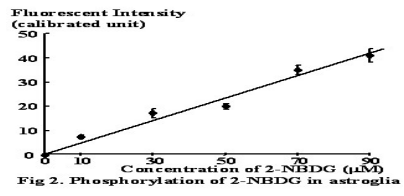
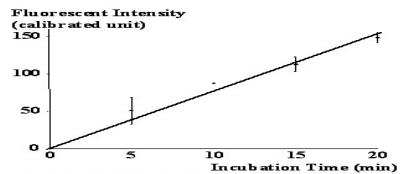
Background: Transient cerebral ischemia followed by reperfusion causes delayed neuronal death selectively in ischemic vulnerable neurons after 48 h of reperfusion. Despite the fact that neuronal ATP production is gradually recovered in neurons destined to undergo delayed neuronal death after ischemia, inhibition of the overall rate of protein translation continues. Irreversible inhibition of protein biosynthesis is a most accurate indicator for delayed neuronal death after transient cerebral ischemia, but the underlying mechanism remains unknown. A brief eIF-2 $\alpha$  phosphorylation is responsible, at least in part, for the transient depression of translation in ischemia-surviving neurons, but cannot account for irreversible translational inhibition in ischemia-vulnerable neurons. This study suggests that translational complex aggregation destroys protein synthesis machinery and contributes to delayed neuronal death after ischemia. Methods: This study utilized a 15 or 20 min of transient cerebral ischemia followed by 30 min, 4 and 24 h of reperfusion in rats to investigate whether irreversible translational inhibition is due to aggregation of translational complex, i.e., the ribosomes and their associated newly synthesized polypeptides, protein biosynthesis initiation factors, translation-coupled folding-chaperones and degradation enzymes after ischemia. Translational complex aggregation and delayed neuronal death were studied by electron and confocal microscopy, as well as by biochemical analyses. Results: Both conventional osmium-uranyl-lead and the EPTA-ribosome-selective EM staining methods clearly show that ribosomes are clumped into large aggregates only in the cytoplasm of neurons destined to undergo delayed neuronal death after brain ischemia. The translational complex components consisting of ribosomal small subunit protein S6, large subunit protein L28, co-translational chaperones HSC70 and HSP40, translational initiation factor eIF-3 $\eta$ , and co-translational ubiquitin ligase CHIP, are all deposited into a detergent/salt-insoluble protein aggregate-containing fraction in vulnerable neurons after ischemia. Sedimentation analysis further confirms that these translational complex components are aggregated into higher densities of protein aggregate fractions in a sucrose density gradient. Immuno-fluorescence of ubiquitin, CHIP, S6, L28, and HSC70 under confocal microscopy gradually disappears only in neurons destined to undergo delayed neuronal death after ischemia. These results clearly demonstrate that translational complex is clumped into large abnormal aggregates, resulting in destruction of protein synthesis machinery after brain ischemia. Discussion: Translational complex aggregation in ischemic vulnerable neurons may represent a new mechanism underlying permanent inhibition of protein synthesis and delayed neuronal death after transient ischemia. An ischemia-induced cascade of energy failure and changes in intracellular homeostasis cumulatively disable ATP-dependent protein quality control machinery for co-translational folding and folding-coupled degradation after brain ischemia. As a result, nascent polypeptides on ribosomes are unable to fold. Consequently, unprocessed nascent polypeptides, together with their associated chaperones, initiation factors, degradation enzymes and ribosomes, are irreversibly aggregated. Translational complex aggregation-induced damage accumulates over time, and when it reaches a critical degree, may eventually lead to delayed cell death after ischemia. Supported by: NS040407.

## GLUCOSE UTILIZATION IN NEURONS IN RAT BRAIN EVALUATED WITH FLUORESCENT ANALOGUE OF DEOXYGLUCOSE

Yoshiaki Itoh, Rie Takaoka, Takato Abe, Norio Tanahashi, Norihiro Suzuki

*Department of Neurology, Keio University School of Medicine, Tokyo, Japan*

**BACKGROUND:** Glucose is the major energy source the adult brain utilizes under physiological conditions. Recent findings, however, have suggested that neurons obtain most of their energy from the oxidation of extracellular lactate derived from astroglial metabolism of glucose transported into the brain from the blood. In the present studies we have used a fluorescent analogue of 2-deoxyglucose, which is often used to trace glucose utilization in neural tissues, to examine glucose metabolism in neurons in vivo. **METHODS:** Utility of 2-[N-(7-nitrobenz-2-oxa-1,3-diazol-4-yl)amino]-2-deoxy-D-glucose (2-NBDG) to evaluate glucose metabolism was assessed through in vitro study. We incubated cultured neurons and astroglia with 2-NBDG for predetermined time and washed unmetabolized dye out. Phosphorylated 2-NBDG remaining in the cells was measured with a fluorescent microscope, a CCD camera, and an image analysis system. To determine glucose utilization in neurons in vivo, Sprague-Dawley rats were intravenously injected with a pulse bolus of 2-NBDG and decapitated 45 minutes later. After recording the distribution of phosphorylated 2-NBDG, the brain section was further stained immunohistologically. **RESULTS:** In neurons as well as in astroglia, fluorescence intensity increased proportionately to incubation time (fig 1). These findings reconfirmed previous in vitro reports that both types of brain cells utilize glucose as their energy source (1). Phosphorylation of 2-NBDG was linearly dose-dependent up to 90 micro-M (fig 2), suggesting that hexokinase which phosphorylates glucose was not saturated with the tracer at these concentrations. The metabolized dye remained in the cells at least 60 min after wash. The finding is in good agreement with previous reports that both neurons and astroglia contain negligible, if any, amount of glucose-6-phosphatase (2), an important fact when measuring glucose utilization in the brain using 2-deoxyglucose. These results indicated that, similar to 2-deoxyglucose, 2-NBDG is useful to determine glucose uptake in the brain cells. Examination of hippocampus sections of rats revealed that phosphorylated 2-NBDG accumulated in anti-NeuN positive neurons in the pyramidal cell layer and that GFAP-positive astroglial contribution to overall 2-NBDG accumulation was minor. Sagittal sections of the cerebellum demonstrated that 2-NBDG accumulated in molecular layer, Purkinje cell layer and granular cell layer. Immunostaining for calbindin showed that Purkinje cells in the section all contained metabolized 2-NBDG. Sections at the parietal cortex also suggested the 2-NBDG phosphorylation in neurons as well as astroglia but we could not identify the cells in these sections. **CONCLUSION:** This is the first study demonstrating in vivo glucose uptake and metabolism in neurons in rat brain under physiological conditions. Even though astroglial contribution to overall glucose consumption seemed minor, further studies are needed to confirm the extent of glucose utilization compared to lactate in neurons in vivo. **REFERENCE:** 1. Itoh Y, Esaki T, Shimoji K et al., Proc Natl Acad Sci USA. 100 (8):4879-84,2003 2. Gotoh J, Itoh Y, Kuang TY et al., J Neurochem. 2000 Apr;74(4):1400-8.



## GLUCOSE UPTAKE AND METABOLISM IN THE HUMAN BRAIN DURING HYPOGLYCAEMIA ASSESSED BY IN VIVO MAGNETIC RESONANCE

Marinette van der Graaf<sup>1</sup>, Bastiaan E. de Galan<sup>2</sup>, Dennis W.J. Klomp<sup>1</sup>, Laura M. Parkes<sup>3</sup>, Cees J.J. Tack<sup>2</sup>, Arend Heerschap<sup>1</sup>

<sup>1</sup>*Department of Radiology, Radboud University Nijmegen Medical Center, Nijmegen, The Netherlands*

<sup>2</sup>*Department of Medicine, Radboud University Nijmegen Medical Center, Nijmegen, The Netherlands*

<sup>3</sup>*F.C. Donders Center for Cognitive Neuroimaging, Radboud University Nijmegen, Nijmegen, The Netherlands*

Introduction: In type-1 diabetes, iatrogenic hypoglycaemia is a serious complication of intensive insulin therapy that primarily endangers brain function. Little is known about the effect of hypoglycaemia on brain glucose uptake and metabolism. Magnetic Resonance (MR) provides several non-invasive methods to investigate these factors in the human brain in vivo, i.e. <sup>13</sup>C MR spectroscopy (MRS) to follow uptake and metabolism of <sup>13</sup>C-labeled glucose, <sup>1</sup>H MRS to determine local glucose concentrations, <sup>31</sup>P MRS to assess high energy phosphate compounds and pH, and arterial spin labeling (ASL) to measure blood flow. Aim of the study: To test the feasibility of the application of these MR methods on the human brain under euglycaemic and hypoglycaemic conditions for the assessment of local changes in glucose uptake and (energy) metabolism. Methods: Eleven healthy volunteers (9F/2M, 21.9 ± 1.6 years) underwent a hyperinsulinaemic (60-120 mU×m<sup>-2</sup>×min<sup>-1</sup>) euglycaemic (~ 5.3 mmol/L; 60 min.) – hypoglycaemic (~ 2.9 mmol/L; 60 min.) glucose clamp [1]. Measurements included: <sup>13</sup>C MRS using <sup>13</sup>C-1-glucose isotopic enrichment to determine cerebral glucose uptake and subsequent metabolism (n=6), <sup>1</sup>H MRS to determine cerebral glucose content (n=5), <sup>31</sup>P MRS to measure global cerebral energy demand (n=2), and ASL to measure cerebral perfusion (n=3). In one subject undergoing <sup>13</sup>C MRS, a 100% <sup>13</sup>C-enriched glucose solution was used during the hypoglycaemic phase of the clamp. All experiments were performed on a sophisticated 3T Siemens Trio MR spectrometer using extended tubing. Results: Cerebral glucose content, measured by <sup>1</sup>H MRS, averaged 1 mmol/L under euglycaemic conditions, but was undetectable during hypoglycaemia. Plasma <sup>13</sup>C isotopic enrichment (determined by hf <sup>1</sup>H-NMR) was 29±1% during euglycaemia and 25±1% during hypoglycaemia, except in the subject receiving 100% <sup>13</sup>C-enriched glucose where it increased to 68%. <sup>13</sup>C MRS resulted in spectra of good quality allowing monitoring of brain glucose uptake and time-dependent conversion to metabolites under both glycaemic conditions. The experiment using 100% <sup>13</sup>C-enriched glucose revealed ongoing cerebral glucose uptake and subsequent metabolism under hypoglycaemic conditions. Overall brain perfusion measured by ASL was 47.5±5.8 mL×min<sup>-1</sup>×100mL<sup>-1</sup> brain tissue during euglycaemia and 46.9±4.6 mL×min<sup>-1</sup>×100mL during hypoglycaemia (P=NS). The <sup>31</sup>P MRS experiments resulted in spectra with clearly resolved resonances of phosphomonoesters, phosphodiesteres, intracellular inorganic phosphate (Pi), phosphocreatine (PCr), and alpha,beta,gamma-ATP. Upon changing the glycaemic condition to hypoglycaemia, PCr/ATP remained unaltered, but Pi resonance shifted slightly equaling an intracellular pH increase in the order of ~0.01-0.02. Conclusion: Hyperinsulinaemic euglycaemic-hypoglycaemic clamp conditions can be safely applied in a 3T MR magnet. Acute hypoglycaemia results in a lower glucose content in the human brain, but does not affect cerebral blood flow or global cerebral energy demand and does not abolish cerebral glucose metabolism. All MR methods worked sufficiently to allow implementation of these techniques for future studies on hypoglycaemia in diabetic patients. Reference: [1] De Galan BE, et al., Diabetes 51 (2002). Acknowledgements: We thank Aarnout Jansen van Rosendaal for assistance during the hyperinsulinemic euglycemic-hypoglycemic clamps and financial support by the Dutch

Diabetes Research Foundation (Grants 2002.11.009 and 2004.00.012) and NIH (Grant 1 R21 DK069881-01).

## METABOLIC ABNORMALITIES PRECEDE PATHOLOGIC CHANGES IN THE G93A SOD1 MOUSE MODEL OF ALS

Jon-Paul P. DiMauro, Lichuan Yang, Sara W. Fuller, **Susan E. Browne**

*Department of Neurology, Weill Medical College of Cornell University, New York, NY, USA*

Amyotrophic lateral sclerosis (ALS) is a devastating neurodegenerative disease characterized by selective loss of CNS motor neurons, leading to rapidly progressing muscle weakness, wasting, paralysis, and ultimately death. Multiple cell death pathways have been implicated in ALS pathogenesis, but the causal event remains unknown. One hypothesis is that metabolic dysfunction underlies pathogenesis, since alterations in energy metabolism and mitochondrial function occur in patients. In addition, expression of mutant Cu,Zn-superoxide dismutase (mSOD1), associated with approximately 25% of patients with familial ALS (fALS), can induce mitochondrial abnormalities. To determine whether metabolic defects contribute to disease onset *in vivo*, we examined the association between energetic defects and the onset of symptoms and pathologic events in fALS transgenic mice over-expressing the G93A SOD1 mutation. We measured glucose use rates in 49 brain regions and 9 spinal cord regions in conscious 60 and 120 day-old G93A mice (n=6/group) and wild-type littermates (n=9/group) by quantitative [<sup>14</sup>C]-2-deoxyglucose autoradiography. Glucose utilization rates were impaired in multiple brain components of the motor system in G93A mice as early as 60 days of age. This precedes the first detectable pathologic changes in G93A mice (in spinal motor neuron mitochondria at 70-80 days), and symptom onset (hind-limb weakness at 90-100 days; mice die at 130-150 days). At 60 days, glucose use was reduced in components of the corticospinal projection, notably primary motor cortex (Fr1) layers I-III (innervation sites) and V (projection zones) (-19%, p<0.005, Student's unpaired t-test). A pattern of hypometabolism also emerged in several areas synaptically associated with Fr1, including the pontine nuclei (-25%, p<0.05) and the pontine reticular formation (-17%, p<0.05) of the bulbospinal pathway, and in several thalamic relay nuclei. In contrast, within the rubrospinal pathway glucose use was significantly reduced in the red nucleus only at 120 days (-28%, p<0.005), and sensorimotor cortical regions showed no alterations. In the spinal cord, generally regarded as the crucial site of neurodegeneration in ALS, glucose metabolism remained normal at 60 days, but was markedly impaired in cervical and thoracic grey matter by 120 days. In an additional experiment, 21 month-old mice overexpressing human wildtype SOD1 showed no alterations in cerebral or spinal cord glucose use with age, implying that the changes detected in G93A mice are due to the SOD1 mutation rather than SOD1 overexpression. We also examined metabolite levels in G93A brain and spinal cord. HPLC revealed depletions in ATP levels in the cerebral cortex of G93A mice concomitant with glucose use changes, which was partially rescued by administration of creatine. Further, cortical ATP levels were reduced by >40% as early as 30 days of age, implying that reduced neuronal energy generation is an extremely early consequence of mSOD1 expression. In conclusion, these studies demonstrate that energetic defects occur earlier than any other pathogenic processes reported to date in G93A mice, and suggest that dysfunction within the corticospinal projection may precede alterations in spinal neurons in this ALS model. Overall, results support a critical role for metabolic dysfunction in the pathogenesis of ALS.

## FUNCTIONAL DISTINCTIONS AMONG BASELINE, CONTROL, AND DEFAULT MODES OF BRAIN OPERATION

Manouchehr S. Vafaei, Albert Gjedde

*Center of Functionally Integrative Neuroscience, PET Center, Aarhus University Hospital, Aarhus, Denmark*

Background: Functional neuroimaging studies generally discard the control state in comparisons with an activation state. The difference is said to be the work associated with an incremental cognitive task. To ignore the activity of a control state is then meaningful only if the brain truly is at rest in that condition. However, in principle, the restful baseline state is equal neither to a default state of absent experimentation, nor to an arbitrary control state of a given experimental comparison. Although blood flow (CBF) is the conventional marker of brain activity, oxygen consumption (CMRO<sub>2</sub>) is a better index of energy turnover. Raichle et al (PNAS, 2001) define the default mode as the state consistent with the globally average oxygen extraction (EO<sub>2</sub>). To assign labels of baseline, control or default state to experimental conditions of awake volunteers, we contrasted CBF, CMRO<sub>2</sub> and EO<sub>2</sub> in two PET studies. Materials and Methods: In the first study, 12 volunteers underwent PET motor activation studies with control CBF as the first scan of the first session and control CMRO<sub>2</sub> as the first scan of the second session. Eyes were closed with an eye-patch. In the second study, 12 subjects fixated a cross-hair during all scans. Absolute magnitudes of CMRO<sub>2</sub> and CBF were determined with two-compartment weighted-integration and mean subtracted image volumes were converted to z-statistic volume. Results: Subtraction of the state of eyes-closed from the state of eyes-open yielded significant bilateral CBF increases in medial frontal gyrus, insula, thalamus, anterior cingulate, superior parietal lobe, lateral front-orbital cortex, right precentral gyrus, lateral occipitotemporal gyrus, cuneus, and extrastriate visual cortex, while CMRO<sub>2</sub> increased significantly at sites in right lingual gyrus (BA 17/18), precentral gyrus, and superior parietal lobe that did not coincide with the sites of CBF increase. Discussions: The direction of change of EO<sub>2</sub> from 40% is said to be the index of a functional state's relation to the default state. In the present study, however, EO<sub>2</sub> declined at the sites of CBF increase, and increased at the separate sites of CMRO<sub>2</sub> increase. Thus, during the control state of eyes-closed, neurons in middle frontal gyrus, occipitotemporal area, and cingulate cortex went to rest in terms of CBF, while other neurons in striate cortex and precentral gyrus went to rest in terms of CMRO<sub>2</sub> when not in the state of eyes-open. Therefore, the condition of having closed eyes is likely to be a more inactive state and hence a baseline in most brain regions involved. In contrast, the default state of striate cortex and precentral gyrus appears to be the condition of having open eyes, while the default state of the middle frontal gyrus, occipitotemporal area, and cingulate cortex is likely to be the condition of closed eyes. We interpret this to mean that little information is transmitted from primary visual cortex to these regions in the default mode.

**ACTIVITY-DEPENDENT OXYGEN TRANSIENTS IN RAT CEREBELLAR CORTEX  
ARE BLOCKED BY SYNAPTIC INHIBITION****Kirsten Caesar<sup>1</sup>, Martin Lauritzen<sup>2</sup>**<sup>1</sup>*Department of Medical Physiology, University of Copenhagen, Copenhagen, Denmark*<sup>2</sup>*Department of Clinical Neurophysiology, Glostrup Hospital, Glostrup, Denmark*

Introduction: One of the most exciting issues in neuroscience is the exploration of the complex interaction between excitatory and inhibitory activity in activated brain regions and the associated vascular and metabolic signals. In this study we explored the effect of tonic synaptic inhibition on activity-dependent rises in oxygen consumption evoked by stimulation of the excitatory, glutamatergic climbing fiber system in the rat cerebellum. Materials and Methods: Experiments were carried out in male  $\alpha$ -chloralose-anesthetized Wistar rats (250-350g). Synaptic activity, measured as local field potentials (LFPs), was recorded with a glass microelectrode. Tissue pO<sub>2</sub> was recorded with a modified Clark-type polarographic oxygen microelectrode. Muscimol, a selective GABA A receptor antagonist, was used to induce tonic inhibition of Purkinje cells (PCs). Excitation was evoked by stimulation of climbing fibers (CF) at 5, 7.5 and 10 Hz for 15 s. To express neuronal activity in terms of synaptic activity produced by one stimulation train, the summed LFP ( $\sum$  LFP) were calculated. Results: Control stimulations of CFs at 5, 7.5 and 10 Hz evoked  $\sum$  LFPs of 26.5, 35.5 and 44.2 mV, respectively. The tpO<sub>2</sub> responses were either mono- or biphasic, composed of an initial negative phase and at higher frequencies also of a late positive phase (n=5). During control stimulations the area of the negative phase amounted to  $-26\pm 9\%$ ,  $-31\pm 10\%$ , and  $-51\pm 7\%$ , respectively (n=5), indicating that oxygen consumption increased proportional to the increase in synaptic activity. After application of muscimol, the negative areas decreased markedly to  $4\pm 3\%$ ,  $2\pm 2\%$  and  $1\pm 1\%$ . This finding was unexpected and indicated that synaptic inhibition strongly attenuated oxygen consumption evoked by excitation. The averaged LFP amplitudes increased from  $5.2 \pm 0.7$  mV to  $7.1 \pm 0.9$  mV for stimulations at 10 Hz (n=5), suggesting an increased work load on the PCs. The increase in LFP amplitude can be explained by an increased driving force for the transmembrane synaptic currents, due to the hyperpolarization that is produced when the GABA A receptors are activated. The shape of the LFPs also changed - the late positive wave, which indicates the occurrence of a calcium-activated potassium efflux was abolished suggesting that the rise in intracellular calcium which normally accompanies activity at the climbing fiber-Purkinje cell synapse was blocked. Conclusion: Abrogation of oxygen consumption by synaptic inhibition is a previously unknown mechanism for the regulation of brain oxidative metabolism. We hypothesize that oxygen consumption under normal conditions may be evoked by synaptic excitation, and controlled by signalling processes related to increases in intracellular Ca<sup>2+</sup> that are sensitive to synaptic inhibition.

## THE STRESS HORMONE CORTICOSTERONE INHIBITS GLUCOSE-, BUT NOT LACTATE-SUPPORTED HIPPOCAMPAL LTP

Ralphiel S. Payne, Avital Schurr

*Anesthesiology & Perioperative Medicine, University of Louisville School of Medicine,  
Louisville, KY, USA*

**Introduction:** Long-term potentiation (LTP), accepted cellular correlate of memory and learning, is compromised by hypoglycemia without altering basal synaptic transmission in rats [1]. When glucose utilization is compromised, other sources of energy may be beneficial in maintenance of neuronal function important for basal synaptic transmission as well as for more sensitive functions such as learning and memory. We previously reported that acute exposure of rat hippocampal slices to stress levels of the glucocorticoid (GC) corticosterone (CT) exacerbates ischemic neuronal damage in vitro [2]. The present study was designed to investigate differences between glucose- and lactate-supported LTP in the presence of CT.

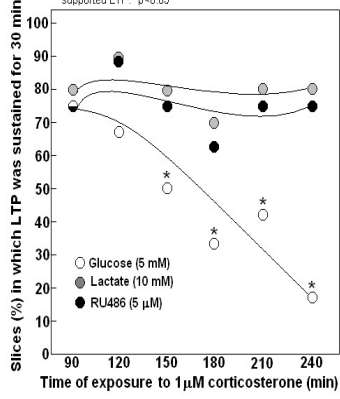
**Methods:** Hippocampal slices (400  $\mu\text{m}$ ) were prepared from ether-anesthetized rats as described elsewhere [3], placed in an interface incubation/recording chamber, perfused with aCSF containing either glucose (5 or 10 mM) or lactate (10 mM) and maintained at 34°C under 95% O<sub>2</sub>/5% CO<sub>2</sub> atmosphere. After 90 min incubation, extracellular recordings of orthodromically-evoked CA1 population spike (PS) were ensued. Upon establishing a stabilized baseline of neuronal activity (PS) at maximal stimulus strength (~10 V), the stimulating voltage was reduced to produce PS amplitudes approximately 50% of maximum (5-6 mV). LTP was induced by a 2 s-long 100 Hz train of electrical pulses at the reduced voltage. We considered a PS amplitude >125% of baseline to be a successful LTP induction. When LTP was induced, it was monitored for 30 min. A slice in which LTP could not be maintained for 30 min was counted as one that failed to exhibit LTP. Statistical analysis of data on slice function between groups (N=6/group) was performed using paired t-test. Changes within and between groups were considered statistically significant when the P value was equal or smaller than 0.05. All data are expressed as the mean  $\pm$  SEM.

**Results:** The ability to induce and maintain LTP in glucose-supplemented (5 mM) slices exposed to CT (1  $\mu\text{M}$ , for 90 to 240 min) was significantly diminished compared to lactate-supplemented (10 mM) slices ( $p < 0.001$ ). Moreover, the sensitivity of glucose supported LTP to CT was ameliorated by treatment with RU486 (5  $\mu\text{M}$ ), a potent CT receptor antagonist ( $p < 0.01$ ), demonstrating that the effect of CT on LTP is receptor-specific (Figure 1). When glucose level was raised to 10 mM, the observed deleterious effects of CT on LTP were abolished.

**Conclusion:** This study indicates that chronic elevation in CT levels compromises glucose-, but not lactate-supported LTP. Therefore, we concluded that lactate is a viable energy substrate capable of sustaining sensitive brain functions involved in neuronal plasticity when glucose metabolism is compromised.

**References:** [1] Izumi et al., *Neurosci Lett* 232:17-20, 1997; [2] Payne et al., *Neuroreport* 12:1261-1263, 2001; [3] Schurr et al., *J Neurosci* 19(1):34-39, 1999.

The effects of corticosterone (CT) on glucose- and lactate-supported LTP. RU486 antagonized CT effect of glucose-supported LTP. \* $p < 0.05$



**A ROLE OF LACTATE IN NEURONAL ENERGY METABOLISM:  
INVESTIGATION WITH DYNAMIC LIVING BRAIN SLICE IMAGING SYSTEM**

Mikako Ogawa<sup>1</sup>, Hiroshi Watabe<sup>2</sup>, Noboru Teramoto<sup>2</sup>, Takuya Hayashi<sup>2</sup>, Yoshinori Miyake<sup>2</sup>,  
Hidehiro Iida<sup>2</sup>, Yasuhiro Magata<sup>1</sup>

<sup>1</sup>*Photon Medical Research Center, Hamamatsu University School of Medicine, Hamamatsu,  
Japan*

<sup>2</sup>*Department of Investigative Radiology, National Cardiovascular Center, Osaka, Japan*

**Background and Purpose:** Glucose has been thought as the principal metabolic substrate of the brain. However, Magestritti et al. proposed an astrocyte-neuron lactate shuttle hypothesis, which claims the metabolic role of lactate in the brain, especially in neurons(1). This model hypothesizes that neuronal activation stimulates the anaerobic production of lactate in neighboring astrocytes. The produced lactate in astrocytes is then transferred to the neuron, which then uses the lactate as an energy substrate aerobically. However, this hypothesis has not been clearly elucidated yet. Therefore, in this study, the role of lactate was evaluated by “Bioradiography” system with 2-deoxy-2-[18F]fluoro-D-glucose ([18F]FDG.), which is a positron emitting radiotracer for glucose metabolism measurement. “Bioradiography” is the dynamic living brain slice imaging system for positron-emitter labeled compounds. We investigated the brain energy metabolism under steady state and neural activated conditions. **Methods:** The “Bioradiography” was performed according to the method of Murata et al.(2). Two groups of rat brain slices were incubated with [18F]FDG in oxygenated Krebs-Ringer solution (including 10 mM glucose) for 150min. To the one group, 0.5 mM of lactate transporter inhibitor, alpha-cyano-4-hydroxycinnamate (4-CIN), was loaded (4-CIN group, n=8), and to the other group, this inhibitor was not added (control group, n=7). 4-CIN inhibits the lactate transport to neuron via monocarboxylate transporter-2 (MCT2). After 60min incubation, 50 mM KCl was added to both groups to activate the neuronal metabolism. During the incubation, serial [18F]FDG images of the slices were obtained on imaging plates at every 10min. [18F]FDG uptake rate (R) was obtained from the slope of time activity curve. The lactate concentration of the incubation medium was also measured in every 20min. **Results:** [18F]FDG uptake increased with time in both 4-CIN added and control conditions. No significant difference was observed in the [18F]FDG uptake rate between both conditions before KCl addition (R=0.013 min<sup>-1</sup> for both 4-CIN and control group). These observations suggest that neurons do not use exogenous lactate as a dominant energy substrate in steady state. On the other hand, KCl elevated the uptake rate in both 4-CIN and control group, but increased extent was significantly larger for the 4-CIN added condition (R=0.075 min<sup>-1</sup> for 4-CIN and 0.040 min<sup>-1</sup> for control group). This indicates that activated neuron consume lactate for energy substrate. The lactate concentration in the incubation medium was increased with KCl treatment in both groups and the extent was slightly greater in 4-CIN group. **Conclusion:** These results suggested that: 1. The brain mainly uses glucose, not lactate, as an energy substrate in steady state. 2. When neuron is stimulated, excess amounts of lactate are produced in astrocytes and the lactate is mobilized as an energy substrate. **References:** P. J. Magistretti et al. *Science* 1999;283(5401):496-7. T. Murata et al. *J Neurol Sci* 1999;164(1):29-36.

## REDUCED REGIONAL CMRGLUC SUPPRESSION IN NEWBORN PIGLETS DURING THIOPENTAL-INDUCED BURST SUPPRESSION

Reinhard Bauer<sup>1</sup>, Bernd Walter<sup>2</sup>, Frank Füchtner<sup>3</sup>, Rainer Hinz<sup>3</sup>, Hiroto Kuwabara<sup>4</sup>,  
Peter Brust<sup>5</sup>

<sup>1</sup>*Institute of Pathophysiology and Pathobiochemistry, Universitätsklinikum Jena, Friedrich Schiller University, Jena, Germany*

<sup>2</sup>*Department of Neurosurgery, Universitätsklinikum Jena, Friedrich Schiller University, Jena, Germany*

<sup>3</sup>*Institute of Bioinorganic and Radiopharmaceutic Chemistry, Research Center Rossendorf, Dresden, Germany*

<sup>4</sup>*Department of Radiology and Radiological Science, Johns Hopkins University, Baltimore, MD, USA*

<sup>5</sup>*Institute for Interdisciplinary Isotope Research, Leipzig, Germany*

**INTRODUCTION:** In the adult brain cerebral energy metabolism has been functionally compartmentalized using the barbiturate thiopental into active part, associated with electroencephalographic (EEG) activity, and the balance, basal component, associated with the maintenance of neuronal viability. It has been shown that whole-brain estimation in adult monkeys showed an active:basal distribution of approximately 50:50 for CMRO<sub>2</sub>, 40:60 for CBF, and 60:40 for CMRGluc. However, similar studies have not been done in the immature brain. Moreover, we asked whether or not regional differences exist. **METHODS:** Experiments were performed on 14 newborn (age: 2 – 5 days) and 11 juvenile (age: 6 – 7 weeks) pigs. Animals were anesthetized and artificially ventilated. Several arterial, venous and sagittal sinus catheters were inserted for taking blood pressure measurements and obtaining blood samples. ECoG recording was performed using 2 screw electrodes, inserted above the parietal cortex bilaterally. A left thoracotomy was performed through the third intercostal space and a catheter was inserted into the left auricle for injection of colored microspheres for regional CBF measurement. CMRO<sub>2</sub> was calculated as forebrain CBF x avDO<sub>2</sub>. Regional CMRGluc was estimated by 18FDG and positron emission tomography. 7 newborn and 5 juvenile pigs served as sham-operated control. In remaining animals and after an initial measurement of CBF and CMRO<sub>2</sub> under baseline conditions, burst suppression (BS) ECoG was induced by infusion of thiopental (TP, 50 mg/ml; 0,2 ml/ min x kg b.w.). 30 min later 18FDG (100 –250 MBq) was infused in all animals and regional CMRGluc was estimated for 60 min. **RESULTS:** Under baseline conditions, CBF of newborn pigs was increased by ~20% (p < 0.05), whereas CMRO<sub>2</sub> was similar in both age groups. Regional CMRGluc, however, was markedly reduced in all brain regions between 22% and 30% in newborn piglets (p < 0.01). BS induced a similar reduction in CBF (by ~50 %) and CMRO<sub>2</sub> (~56-61%) in both groups (p < 0.05). Juvenile pigs exhibited a comparable CMRGluc reduction in all brain regions studied, with the most pronounced suppression in forebrain regions (~63%), whereas midbrain and cerebellum showed a diminished reduction of 73 and 80% of control (p < 0.05). In contrast, newborn piglets showed a BS-induced suppression of CMRGluc only in the forebrain regions, whereas brain stem and cerebellum did not show changes in CMRGluc. In addition the amount of CMRGluc suppression in newborn piglets was markedly diminished in all brain regions compared with the older animals (p < 0.05). **CONCLUSION:** There is a regional difference in active:basal distribution of brain cerebral energy metabolism even in the mature brain as estimated by regional CMRGluc under normal conditions vs. BS. Brain immaturity aggravates these regional differences, because brain stem and cerebellum does not respond with CMRGluc reduction during thiopental-induced BS. Thus, compartmentalization is less developed in early postnatal period, possibly due to an immature state of dendritic development and synaptogenesis. It can be speculated

that neuroprotective procedures which influence prominently the basal component of brain energy metabolism may be preferred in the immature brain.

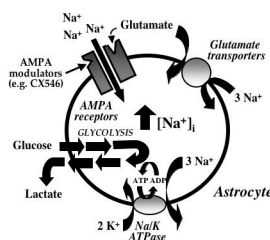
## AMPAKINE CX546 BOLSTERS ENERGETIC RESPONSE OF ASTROCYTES: A NOVEL TARGET FOR COGNITIVE-ENHANCING DRUGS ACTING AS AMPA RECEPTOR MODULATORS

Luc Pellerin<sup>1</sup>, Pierre J. Magistretti<sup>2</sup>

<sup>1</sup>*Department of Physiology, University of Lausanne, Lausanne, Switzerland*

<sup>2</sup>*Brain and Mind Institute, Ecole Polytechnique Fédérale de Lausanne (EPFL) and Centre de Neurosciences Psychiatriques, CHUV, Université de Lausanne, Lausanne, Switzerland*

Introduction Development of cognitive enhancing drugs for the treatment of conditions ranging from mild cognitive impairment to Alzheimer's disease represents a valuable task. A family of compounds known as ampakines are potential candidates. Despite clear-cut effects on excitability, their influence on brain energy metabolism has not been explored. Methods Deoxyglucose uptake and lactate release were measured in primary cultures of mouse astrocytes prepared from cortex, hippocampus or cerebellum. Immunocytochemistry was performed with primary antibodies targeted against each AMPA receptor subunit type and revealed by epifluorescence microscopy. Results and Discussion Glutamate was previously shown to enhance aerobic glycolysis i.e. increase glucose utilization and lactate production with no change in oxygen levels, in mouse cortical astrocytes by a mechanism involving glutamate uptake. It is reported here that a similar response is produced in both hippocampal and cerebellar astrocytes. Application of the cognitive-enhancing drug CX546 promoted further enhancement of glucose utilization by astrocytes from each brain area upon glutamate exposure. AMPA receptors represent the purported molecular target of cognitive-enhancing drugs like CX546 and the presence of AMPA receptor subunits GluR1-4 was evidenced in astrocytes from all three regions by immunocytochemistry. AMPA itself did not stimulate aerobic glycolysis but in presence of CX546 a strong enhancement of glucose utilization and lactate production was obtained in cortical, hippocampal and cerebellar astrocytes. The effect of CX546 was concentration-dependent with an EC<sub>50</sub> of 93.2  $\mu$ M in cortical astrocytes. AMPA-induced glucose utilization in presence of CX546 was prevented by the AMPA receptor antagonist CNQX and the negative modulator GYKI 52466. In addition, the metabolic effect of CX546 in presence of AMPA was mimicked by the AMPA receptor modulator cyclothiazide. Our data suggest that astrocyte energetics represents a novel target for cognitive-enhancing drugs acting as AMPA receptor modulators



## THE CENTRAL ROLE OF ASTROCYTES IN NEUROMETABOLIC COUPLING : A DECADE'S PERSPECTIVE

Pierre J. Magistretti<sup>1</sup>, Luc Pellerin<sup>2</sup>

<sup>1</sup>*Brain and Mind Institute, Ecole Polytechnique Fédérale de Lausanne (EPFL) and Centre Hospitalier Universitaire Vaudois (CHUV), Lausanne, Switzerland*

<sup>2</sup>*Department of Physiology, University of Lausanne, Lausanne, Switzerland*

The coupling between synaptic activity and glucose utilization (neurometabolic coupling) is a central physiological principle of brain function which has provided the basis for 2-deoxyglucose-based functional imaging with PET (1). About ten years ago we provided experimental evidence indicating a central role of astrocytes in neurometabolic coupling (2). The basic mechanism in neurometabolic coupling is the glutamate-stimulated aerobic glycolysis in astrocytes, such that the sodium-coupled reuptake of glutamate by astrocytes and the ensuing activation of the Na-K-ATPase triggers glucose uptake and its glycolytic processing, resulting in the release of lactate from astrocytes. Lactate can then contribute to the activity-dependent fuelling of the neuronal energy demands associated with synaptic transmission (3). Analyses of this coupling have been extended in vivo (4,5), and recently have also defined the modalities of coupling for inhibitory neurotransmission as well as its spatial extent in relation to the propagation of metabolic signals within the astrocytic syncytium (6,7). On the basis of a large body of experimental evidence (for a recent review see 8,9) we have proposed an operational model, 'the astrocyte-neuron lactate shuttle' (10,11), which has stimulated discussions in the field (12,13). Recently a series of results obtained by independent laboratories has provided further support for this model (14 -16). This body of evidence provides a molecular and cellular basis for interpreting data obtained with functional brain imaging studies. 1) Sokoloff L, Reivich M, Kennedy C, Des Rosiers MH, Patlak CS, Pettigrew KD, Sakurada O, Shinohara M. (1977) *J Neurochem* 28:897-916. 2) Pellerin, L. and Magistretti, P.J. (1994) *Proc Natl Acad Sci (USA)* 91:10625 – 10629 3) Magistretti, P.J. and Pellerin, L. (1999) *Phil Trans R Soc London B* 354:1155-1163. 4) Cholet, N., Pellerin, L., Welker, E., Lacombe, P., Seylaz, J., Magistretti, P. and Bonvento, G. (2001) *J Cereb Blood Flow Metab* 21:404 – 412 5) Voutsinos-Porche, B., Bonvento, G., Tanaka, K., Steiner, P., Welker, E., Chatton, J.-Y., Magistretti P.J. and Pellerin, L. (2003) *Neuron* 37:1-20. 6) Chatton, J.-Y., Pellerin, L. and Magistretti, P.J. (2003) *Proc Natl Acad Sci USA* 100:12456-12461 7) Bernardinelli, Y., Magistretti, P.J., Chatton, J.-Y. (2004) *Proc Natl Acad Sci USA* 101:14937-14942. 8) Pellerin, L. and Magistretti, P.J. (2003) *J Physiol.* 546:325. 9) Pellerin, L. and Magistretti, P.J. (2004) *J Cereb Blood Flow Metab* 11:1240-1241. 10) Bittar, P., Charnay, Y., Pellerin, L., Bouras, C. and Magistretti, P.J. (1996) *J Cereb Blood Flow Metab* 16:1079-1089. 11) Pellerin, L., Pellegrini, G., Bittar, P.G., Bouras, C., Martin, J.-L., Stella, N. and Magistretti, P.J. (1998) *Dev Neurosci.* 20:291 - 299. 12) Gjedde, A., Marrett, S. and Vafae, M. (2002) *J Cereb Blood Flow Metab* 22:1-14 13) Chih and Roberts (2003) *J Cereb Blood Flow Metab* 23:1263-1281 14) Porrás, O.H., Loaiza, A. and Barros, L.F. (2004) *J Neurosci.* 24:9669-9673 15) Serres, S., Bezançon, E., Franconi, J.M. and Merle, M. (2004) *J Biol Chem* 279:47881-47889 16) Kasischke, K.A., Vishwasrao, H.D., Fisher, P.J., Zipfel, W.R. and Webb, W.W. (2004) *Science* 305:99-103

**THEORETICAL SUPPORT FOR THE ASTROCYTE-NEURON LACTATE SHUTTLE  
HYPOTHESIS. I. MODELING NEURONAL AND ASTROCYTIC NADH/NAD<sup>+</sup>  
KINETICS**

Agnès Aubert<sup>1</sup>, **Luc Pellerin**<sup>1</sup>, Pierre J. Magistretti<sup>3</sup>, Robert Costalat<sup>2</sup>

<sup>1</sup>*Department of Physiology, University of Lausanne, Lausanne, Switzerland*

<sup>2</sup>*UMRS 678, Université Pierre et Marie Curie, Paris, France*

<sup>3</sup>*Brain and Mind Institute, EPFL, Lausanne, Switzerland*

Introduction The question of the compartmentalization of brain energy metabolism has been the subject of intense debate for the past decade, with the astrocyte-neuron lactate shuttle (ANLS) hypothesis, proposed by Pellerin and Magistretti [1], which assumes that astrocytes can provide lactate as an energy fuel to neurons. Some authors challenged this hypothesis, defending the classical view that glucose is the major energy substrate of neurons, at rest as well as in response to a stimulation [2]. An important aspect of this discussion is the role that NADH might play in brain energy metabolism, since it is produced by glycolysis and both consumed by lactate dehydrogenase-catalyzed reaction and by mitochondria. In order to assess neuronal and astrocytic NADH/NAD<sup>+</sup> ratio changes and then test the ANLS hypothesis from a theoretical point of view, we developed a mathematical model of compartmentalized energy metabolism between neurons and astrocytes [3]. Method On the basis of a previously validated model [4], which describes the relationships between brain activation, energy metabolism and hemodynamics within the brain tissue, we distinguished between neuronal, astrocytic, extracellular and vascular compartments. We adopted hypotheses highly unfavorable to ANLS, e.g. we assumed that at steady state neurons do not take up lactate and the regulation of mitochondrial activity is the same in both neurons and astrocytes. Most variable and parameter values were chosen to be the same for neurons and astrocytes, except a moderate lactate efflux from astrocytes at rest, and a slightly higher NADH/NAD<sup>+</sup> ratio in astrocytes at rest. Results and Discussion Simulation results can be divided between two groups, depending on the relative neuron versus astrocyte stimulation. If this ratio is low, ANLS is observed during all the stimulus and post-stimulus period (continuous ANLS), but a high ratio induces ANLS only at the beginning of the stimulus and during the post-stimulus period (triphasic behavior). Finally, our results show that (i) current experimental data on brain lactate kinetics [5;6] are compatible with the ANLS hypothesis, and (ii) occurrence of ANLS may greatly depend on the neuronal and astrocytic NADH/NAD<sup>+</sup> ratio changes. These theoretical results are fully consistent with the recent experimental data of Kasischke et al. [7], who used a two-photon fluorescence imaging of NADH in hippocampal slices. These authors showed that, in response to a short activation, dendrites undergo an early oxidation, followed by a significant reduction in astrocyte cytoplasm. This sequence of events agrees with a net lactate transfer between astrocytes and neurons as predicted by the ANLS. This work was supported by the Fondation pour la Recherche Médicale and the ACI 'Neurosciences Intégratives et Computationnelles' (French Ministry of Research). Reference 1. Pellerin and Magistretti (1994) Proc. Natl. Acad. Sci. USA 91:10625 2. Chih and Roberts (2003) J. Cereb. Blood Flow Metab. 23:1263 3. Aubert and Costalat (2005) J. Cereb. Blood Flow Metab., in press 4. Aubert and Costalat (2002) NeuroImage 17:1162 5. Hu and Wilson (1997) J. Neurochem. 69:1484 6. Mangia et al. (2003) Neurosci. 118:7 7. Kasischke et al. (2004) Science 305:99

**BIPHASIC METABOLIC ADAPTATION TO HYPOXIA IN RAT ASTROCYTES****Celine Vega**<sup>1,2</sup>, Leroy Sachleben<sup>2</sup>, David Gozal<sup>2</sup>, Evelyne Gozal<sup>2</sup><sup>1</sup>*Laboratoire Hypoxie et Ischémie Cérébrales Développementales,  
Université P. & M. Curie-CNRS, UMR NPA 7102, Paris, France*<sup>2</sup>*Kosair Children's Hospital Research Institute Baxter Biomedical Research Building,  
Louisville, KY, USA*

Oxygen deprivation, a major characteristic of ischemia, leads to complex metabolic changes, and is likely to play a central role in the pathogenesis of cerebrovascular diseases. Our work focuses on the mechanism of cultured astrocytes response to an acute exposure to chronic hypoxia (one day), or to a long term hypoxic environment (3 weeks), in terms of energy metabolism. To examine the mechanisms of astrocytes regulation of energy metabolism during hypoxic conditions, cells were exposed to two different experimental conditions: (1) acute hypoxia by exposing astrocytes to one day of chronic hypoxia (5% O<sub>2</sub>), and (2) the adaptation of astrocytes to hypoxia by exposing the cells to chronic hypoxia for three weeks. Our results showed: (1) Astrocytes subjected to one day of chronic hypoxia increased glucose consumption. In addition, overall protein synthesis was decreased without decrease of cells number. (2) In contrast, astrocytes subjected to chronic hypoxia during 3 weeks decreased their glucose consumption. In addition, overall protein synthesis was decreased without decrease of cells number. (3) Increased glucose uptake after one day hypoxia is not inhibited by the sodium-independent transport inhibitor cytochalasin B, suggesting a role for the sodium glucose-linked transporter SGLT1 in this increased uptake. Our study shows for the first time SGLT1 expression in astrocytes. Quantitative RT-PCR showed that expression of both the facilitative glial glucose transporter GLUT1 and SGLT1 correlates with glucose consumption during hypoxia. In addition, expression of GLUT1 and SGLT1 mRNA in astrocytes was decreased following 3 weeks hypoxia. (4) Lactate production was also affected depending on the duration of exposure to hypoxia. The relatively short-term exposure to hypoxia (one day) resulted in increased lactate release that could provide energy to neurons. In contrast, decreased lactate release was detected after a long exposure to hypoxia, with less lactate available to neurons as an energy substrate. This finding suggests that hypoxia-induced lactate deficiency in astrocytes may results in neuronal energy deprivation. Hypoxia-induced energy metabolism alteration in astrocytes first increases lactate release followed by a decrease of lactate availability impairing both astrocytic and neuronal survival. Future studies in our laboratories will explore potential disruption of neuronal-astrocytic interactions and other aspects of brain energetic and metabolism that could contribute to hypoxia-induced neurodegeneration.

**EFFECTS OF PRO-INFLAMMATORY CYTOKINES AND BETA-AMYLOID PEPTIDE ON GLUCOSE METABOLISM IN PRIMARY CULTURES OF ASTROCYTES**

**Mathilde Gavillet, Igor Allaman, Luc Pellerin, Pierre J. Magistretti**

*Department of Physiology, University of Lausanne, Lausanne, Switzerland*

Local alterations of brain energy metabolism one of the features of neurodegenerative disorders, notably of Alzheimer's disease (AD), for which both amyloid peptide and inflammation have been shown to play a significant role. The aim of the present study was to investigate the effects of pro-inflammatory cytokines (TNF $\alpha$  and IL-1 $\beta$ ) and beta-amyloid (A $\beta$ ) on glucose metabolism in primary cultures of mouse cortical astrocytes. We observed that TNF $\alpha$  (0.25ng/ml) increases glucose utilization, as assessed by the [3H]2-deoxyglucose uptake technique. This effect was detectable within hours, thus after 48 hours of stimulation (reference time) the increase reached +80%. TNF $\alpha$  induced a decrease in lactate release (-40%). Beta-amyloid (A $\beta$ 25-35, 25 microM) produced a different metabolic pattern: it caused a lesser increase in glucose utilization (+40%) and a slight increase of lactate release (+20%). Very similar effects were observed with IL-1 $\beta$  (20ng/ml), another pro-inflammatory cytokine. When combined, TNF $\alpha$ , IL-1 $\beta$  and A $\beta$  acted synergistically on glucose utilization (+220%). No effect on lactate release was observed. Under these conditions treatment of either pro-inflammatory cytokines or Abeta peptide were not toxic to astrocytes as assessed by MTT oxidation and LDH release assays. Taken together these results suggest that both pro-inflammatory cytokines and beta-amyloid peptide strongly modulate astrocyte glucose metabolism. Moreover the observation of different metabolic patterns induced by these factors could indicate alternative fates for glucose.

## OXYGEN METABOLISM, ELECTROPHYSIOLOGICAL ACTIVITY AND CEREBRAL BLOOD FLOW IN RAT SENSORY CORTEX

Pia Enager<sup>1,2</sup>, Nikolas Offenhauser<sup>1</sup>, Martin Lauritzen<sup>1,2</sup>

<sup>1</sup>*Department of Medical Physiology, University of Copenhagen, Copenhagen, Denmark*

<sup>2</sup>*Department of Clinical Neurophysiology, Glostrup Hospital, Copenhagen, Denmark*

**Introduction:** The mechanisms underlying the coupling between neuronal activation and changes in cerebral metabolism and cerebral blood flow (CBF) are still incompletely understood. There is still a debate regarding the relation of increases in cerebral metabolic rate of oxygen (CMRO<sub>2</sub>) and CBF changes during functional activation. We here examined the influence of infraorbital nerve stimulation on the relationship between oxygen metabolism, synaptic activity and CBF in rat sensory cortex. Our working hypothesis was that attenuation of the evoked CBF responses would unmask the initial dip in the tissue oxygen tension produced by increases in synaptic activity. This was based on the assumption that increases in CBF during activation clouds the initial dip by acutely increasing oxygen supply to the tissue. **Methods:** Partial pressure of tissue oxygen (tpO<sub>2</sub>) was measured using a Clark-type O<sub>2</sub> microelectrode (tip diameter between 3–4 μm). CBF was recorded by laser-Doppler flowmetry. Electrophysiological recordings of local field potentials and spike activity were made using glass microelectrodes. All experiments were carried out using an open cranial window preparation in isoflurane and α-chloralose anaesthetized adult male Wistar rats. We used stimulation trains of 4s duration at increasing frequencies from 0.25 to 6 Hz at 1.5mA. Evoked CBF responses were attenuated by the combined use of nitric oxide synthase (NOS) inhibition with 7-Nitroindazole (7-NI) and the non-selective cyclooxygenase (COX1 and COX2) inhibitor (Indomethacin, INDO). **Results:** Stimulation consistently increased synaptic excitatory activity as evidenced by an increase in the summed LFP amplitudes (ΣLFP). At the same time CBF increased frequency-dependently. The stimulus-induced tpO<sub>2</sub> responses were extremely variable. The changes in tpO<sub>2</sub> often consisted only of a positive peak, on other occasions the tpO<sub>2</sub> responses were biphasic with both an initial decrease in tissue pO<sub>2</sub> followed by a longer lasting positive peak. Pure oxygen dips were not observed. 7NI and INDO significantly attenuated the evoked CBF responses and the positive peak of the pO<sub>2</sub> signals. Surprisingly, abolition of the CBF responses did not enhance or produce oxygen ‘dips’. In contrast, negative tpO<sub>2</sub> signals, if present before drug treatment, were attenuated. **Conclusion:** The initial ‘dip’ of tpO<sub>2</sub> in the sensory cortex is independent of the accompanying rise in CBF. In comparison, oxygen ‘dips’ are common in the cerebellar cortex, and in this brain region changes in tpO<sub>2</sub> depends strongly on CBF. This may point to differences in capacity and regulation of oxygen consumption among brain regions. **Grant support:** Supported by the Lundbeck Foundation and the NOVO-Nordisk Foundation.

## NEUROENERGETIC BASIS OF REGIONAL TEMPERATURE DYNAMICS IN BRAIN

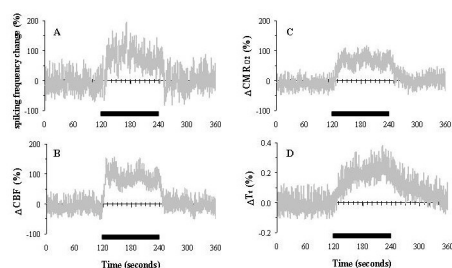
Hubert K.F. Trübel<sup>1,2</sup>, Laura I. Sacolick<sup>3</sup>, **Fahmeed Hyder**<sup>1,3</sup>

<sup>1</sup>*Diagnostic Radiology, Yale University, New Haven, CT, USA*

<sup>2</sup>*HELIOS Klinikum Wuppertal, University Witten/Herdecke, Wuppertal, Germany*

<sup>3</sup>*Biomedical Engineering, Yale University, New Haven, CT, USA*

Maintaining near constant brain temperature ( $T_t$ ) over a wide range of metabolic activity is critical for normal brain function [1]. However brain temperature is an often ignored parameter in neuroscience and clinical studies. Time-dependent variations in  $T_t$  are likely to be caused by fluctuations of CBF and CMRO<sub>2</sub>, both of which are seemingly coupled to alterations in neuronal activity. To this end, we combined magnetic resonance, optical imaging, temperature sensing, and electrophysiological methods in  $\alpha$ -chloralose anesthetized rats to obtain multi-modal measurements during forepaw stimulation. Localized changes in neuronal activity were co-localized with regional increases in  $T_t$  (by  $\sim 0.2\%$ ), CBF (by  $\sim 95\%$ ), and CMRO<sub>2</sub> (by  $\sim 73\%$ ). The time-to-peak for  $T_t$  ( $42 \pm 11$  s) was significantly longer than those for CBF and CMRO<sub>2</sub> ( $5 \pm 2$  and  $18 \pm 4$  s, respectively). Net heat ( $Q_{net}$ ) in the region of interest (ROI) was modeled as being dependent on the sum of heats attributed to changes in CMRO<sub>2</sub> ( $Q_m$ ) and CBF ( $Q_f$ ) as well as conductive heat loss from the ROI to neighboring regions ( $Q_c$ ) and to the environment ( $Q_e$ ). Although tissue cooling due to  $Q_f$  and  $Q_c$  can occur and are enhanced during activation, the net increase in  $T_t$  corresponded to a large rise in  $Q_m$ , whereas effects of  $Q_e$  can be ignored. The study shows that  $T_t$  increases slowly (by  $\sim 0.1$  C) during physiologic stimulation in  $\alpha$ -chloralose anesthetized rats. Since the potential cooling effect of CBF depends on the temperature of blood entering the brain,  $T_t$  is mainly affected by CMRO<sub>2</sub> during functional challenges. While the importance of the “uncoupling” between changes in CMRO<sub>2</sub> and CBF and the temperature of arterial blood for the cooling efficiency of the brain are obvious, our current experimental and theoretical results reveal the significance of the resting CBF and more importantly resting CMRO<sub>2</sub> for temperature regulation in the brain. Although the changes in brain temperature recorded for the entire study were spread over a wide range, the stimulation-induced change of  $\sim 0.1$  C in the ROI was significant for the majority of the experiments. The small changes in  $T_t$  were reproducibly measured from layer 4 of the rat’s somatosensory cortex where the highest neural activity changes (induced by forepaw stimulation) were localized. The current temperature measurements from the brain are in accord with previous functional studies in animals [2,3]. This is the first study which provides a neuroenergetic basis of regional temperature changes in the brain. The results have implications for functional studies and temperature regulation. Supported by NIH (DC-003710, MH-067528) and NSF (DBI-0095173) grants. [1] Baker MA (1982) *Ann Rev Physiol* 44:85-96. [2] McElligott JG, Melzack R (1967) *Exp Neurol* 17:293-312. [3] Melzack R, Casey KL (1967) *Exp Neurol* 17:276-292.



## **HYPEROXIDATION OF NAD(P)H REDOX STATE AFTER ANOXIA AND REOXYGENATION: EFFECTS OF NITRIC OXIDE AND PARP-1 INHIBITION**

**Sibel Kahraman, Gary Fiskum**

*Department of Anesthesiology, University of Maryland School of Medicine,  
Baltimore, MD, USA*

Background: A detailed description of acute changes in neuronal mitochondrial metabolism during and after anoxia is essential for understanding how metabolic dysfunction contributes to the pathogenesis of ischemia/reperfusion. Studies with cultured neurons are typically performed under relatively high PO<sub>2</sub> values that do not simulate clinical ischemic conditions. We established a fluorescence microscopy perfusion system that induces true metabolic anoxia, as validated by measurements of the autofluorescence of endogenous reduced NAD(P)H (1). This system was used to test the hypothesis that metabolic anoxia and reoxygenation is associated with hyperoxidation of NAD(P)H, an event that can limit neuronal energy metabolism and impair detoxification of reactive oxygen species. Methods: Primary cultures of rat cortical neurons were placed in a closed micro-perfusion chamber (2) and subjected to oxygen-glucose deprivation for 30-45 min at 37°. Oxygen was displaced by continuous infusion of ultra-high purity argon in the perfusate and the chamber. The PO<sub>2</sub> of the perfusate in the chamber was monitored continuously by a Optronix Oxylite fiber-optic microprobe. When added, DETA-NO (25 μM) was present in the perfusate as a NO donor to increase the K<sub>m</sub> of cytochrome oxidase for O<sub>2</sub>. NAD(P)H autofluorescence was measured at 355 nm excitation and 460 nm emission wavelengths using a ORCA-ER cooled digital CCD camera (Hamamatsu Photonics, Hamamatsu, Japan) mounted on a Nikon Eclipse TE2000-S inverted microscope (Nikon Corp., Japan). Results: Perfusate PO<sub>2</sub> values fell to < 0.4 mm Hg within 5 min after the chamber was exposed to argon and the argon-flushed perfusate. This level of hypoxia was associated with an increase in NAD(P)H fluorescence to a level equivalent to the maximum obtained in the presence of 1 mM KCN. Fluorescence remained high in the presence of glucose; however, when glucose was substituted with 2-deoxyglucose, fluorescence declined toward the minimum value observed in the presence of the respiratory uncoupler FCCP. While the presence of 25-200 μM DETA-NO alone had no effect on NAD(P)H fluorescence, 200 μM DETA-NO exacerbated the decline observed during chemical anoxia induced with KCN. Subsequent removal of KCN, or reoxygenation of cells after oxygen/glucose deprivation caused a further NAD(P)H hyperoxidation. This hyperoxidation observed in the absence or presence of DETA-NO and the accelerated decline in fluorescence observed during KCN treatment with DETA-NO was diminished by exposure of cells with a specific PARP-1 inhibitor, DPQ. Conclusions: 1. True metabolic anoxia in vitro, as defined by a maximum reduced shift in NAD(P)H redox state, requires a very low PO<sub>2</sub> and (or) a level of NO sufficient to severely limit the consumption of oxygen by cytochrome oxidase. 2. Maintenance of reduced NAD(P)H during anoxia is dependent on glycolysis. 3. Hyperoxidation of NAD(P)H is exacerbated by NO, possibly due to PARP-1 dependent degradation of pyridine nucleotides. Acknowledgments: Supported by NIH R01NS34152 and HD16596 References: 1. Chance B. *Methods Enzymol*, 2004; 385: 361-370 2. Ince C, Beekman RE, Verschragen G. *J Immunol Methods*, 1990; 128: 227-234

**ACTIVITY-INDUCED TISSUE OXYGENATION CHANGES IN RAT CEREBELLAR CORTEX: INTERPLAY OF POSTSYNAPTIC ACTIVITY AND CEREBRAL BLOOD FLOW**

Nikolas Offenhauser<sup>1</sup>, Kirsten Thomsen<sup>1</sup>, Kirsten Caesar<sup>1</sup>, Martin Lauritzen<sup>1,2</sup>

<sup>1</sup>*Department of Medical Physiology, Copenhagen University, Copenhagen, Denmark*

<sup>2</sup>*Department of Clinical Neurophysiology, Glostrup Hospital, Glostrup, Denmark*

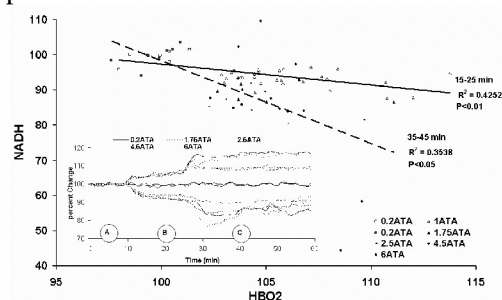
Neuronal activity, cerebral blood flow, and oxygen consumption are all strongly coupled, although the mechanisms behind remain unclear. We examined this coupling in rat cerebellar cortex by simultaneously recording local field potentials, tissue oxygen partial pressure (tpO<sub>2</sub>), and CBF using laser-Doppler flowmetry. Stimulation of the monosynaptic, excitatory climbing fiber system evoked activity-dependent increases in synaptic activity and blood flow, and biphasic tissue pO<sub>2</sub> responses. Relating parameters of the initial negative tpO<sub>2</sub> response to changes in synaptic activity revealed that the disappearance rate of oxygen in the tissue varied as a linear function of synaptic activity, while the area of the negative tpO<sub>2</sub> response saturated at high levels of synaptic activity. Following the initial oxygen dip, tpO<sub>2</sub> increased as a non-linear function of synaptic activity, paralleling the steep rise in blood flow at high levels of synaptic activity. Attenuation of the activity-dependent rise in blood flow by nNOS inhibition enlarged the negative tpO<sub>2</sub> response and decreased the positive tpO<sub>2</sub> response. These findings imply that the activity-induced reduction in tpO<sub>2</sub> is counteracted by an increase in oxygen supply due to the rise in CBF. They also support the hypothesis that the positive tpO<sub>2</sub> response is an overshoot caused by the evoked increase in CBF. Blockade of glutamatergic AMPA receptors with CNQX abolished synaptic activity, and CBF and tpO<sub>2</sub> responses. We suggest, that in the cerebellum activity-dependent increases in oxygen consumption can be recorded as the disappearance rate of oxygen in the tissue, and that oxygen consumption increases as a linear function of activity in postsynaptic cellular elements without evidence for a threshold. Our results provide new fundamental insights into the regulation of oxygen consumption during activation, showing direct coupling of activity in postsynaptic AMPA receptors to oxygen consumption.

## RELATIONSHIP BETWEEN BRAIN MICROCIRCULATORY BLOOD FLOW, HEMOGLOBIN OXYGENATION AND MITOCHONDRIAL NADH UNDER HYPERBARIC OXYGENATION

Elhanan Meirovithz, Judith Sonn, Avraham Mayevsky

*Faculty of Life Sciences, The Leslie & Susan Gonda, Multidisciplinary Brain Research Center, Bar-Ilan University, Ramat-Gan, Israel*

Background: Real time evaluation of brain mitochondrial function using NADH fluorometry In vivo is widely documented. Nevertheless, the identification of the exact NADH redox state status in the brain In vivo was never determined. Also, the relationship between microcirculatory blood flow, hemoglobin oxygenation (HbO<sub>2</sub>) and mitochondrial NADH was rarely measured. The availability of such data will add significant information to the understanding of brain energy metabolism. Objective: In this study we tested the effect of maximal In vivo oxygenation of hemoglobin in brain microcirculation, induced by hyperbaric oxygenation (HBO), on mitochondrial NADH redox state In vivo. The tested hypothesis was that the NADH is not fully oxidized in the normoxic brain In vivo. Methods: The monitoring system includes time-sharing fluorometer reflectometer for NADH and HBO<sub>2</sub> measurement combined with Laser Doppler Flowmetry for CBF monitoring. The rats located, after the operation, in the hyperbaric chamber connected to the monitoring system by a combined fiber optic probe inserted via the wall of the hyperbaric chamber. After 4 hours of recovery from the operation a total of 35 awake rats were exposed to 0.2,1,1.75,2.5,4.5 and 6 absolute atmospheres (ATA) for a total of 60 minutes of continues monitoring. Results: The results show that cerebral blood flow (CBF) measured by LDF was not significantly affected by hyperbaric oxygenation at all levels. The total backscattered light (reflectance) increased during HBO and may represent the decrease in blood volume due to the vasoconstrictive response to oxygen. As seen in the figure HbO<sub>2</sub> and NADH were inversely affected by the increased HBO levels, namely the microcirculatory HbO<sub>2</sub> was significantly more oxygenated leading to oxidation signal of NADH. Each line represents an average of 7 rats. Statistical analysis of this correlation was done in three timing points A, B and C representing the steady state of the signals. Point A (0.2ATA) represent the levels of 0-10 minutes, point B (1ATA) was calculated under 100% O<sub>2</sub> at 10-25 minutes, point C represents the level of signals measured at 1.75, 2.5, 4.5 and 6 ATA in the time interval 35-45 minutes after the beginning of monitoring. When the NADH values were plotted against the HbO<sub>2</sub> levels of the 2 sets of results (B and C) two different regression lines were evaluated and found to be statistical significant. Conclusions: 1. At the microcirculation level, the HbO<sub>2</sub> oxygenation was affected significantly by hyperbaric oxygenation reaching maximal levels at 2.5ATA. 2. The intramitochondrial NADH redox state was not maximally oxidated at air breathing conditions. 3. Increase of HBO levels led to the oxidation of NADH (decrease fluorescence) reaching plateau on minimal level at 2.5ATA.



## PERTURBATION OF HUMAN CEREBRAL ENERGETICS WITH CHRONIC KETOSIS

Jullie W. Pan<sup>1</sup>, C.J. Segal-Isaacson<sup>2</sup>, Monika Jamrozek<sup>1</sup>, Brandy Cowell<sup>2</sup>, Anne Obertance<sup>2</sup>

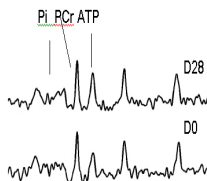
<sup>1</sup>Department of Neurology, Albert Einstein College of Medicine, New York, NY, USA

<sup>2</sup>Department of Epidemiology & Population Health, Albert Einstein College of Medicine, New York, NY, USA

Introduction: It is well known that the human brain switches from its primary fuel of glucose to (largely) ketones under conditions such as fasting, certain diets and severe exercise. Whether this switch is accompanied by cerebral metabolic and energetic shifts is unknown. This question is relevant, particularly given the increasing frequency with which such diets are encountered in the population, as well as the fact that ketotic diets have been shown to affect brain function in several disorders, e.g., the success of the ketogenic diet to treat epilepsy and improve Parkinsons' symptomatology and the Atkins' diet in also improving seizure control in epilepsy (1-3). Methods: We used high field <sup>31</sup>P whole brain spectroscopic imaging to study healthy moderately obese human (n=5, mean age 36.0±10.4years) subjects, examining them prior to initiating a very low carbohydrate diet and after 4 weeks of sustaining this diet. For optimum diet control, meals from a licensed caterer were provided to the subjects, and the macronutrient distribution of the diet was 65% fat: 30% protein: 5% carbohydrate. The mean body mass index at baseline was 34.2±3.1, and after 4 weeks of the diet was 30.7±2.4. Weight loss was achieved by all volunteers, averaging 8.4±1.8kg. <sup>31</sup>P spectroscopic imaging was performed at 4Tesla (Varian Inova, whole body MR system) using a pulse acquire acquisition utilizing a three-dimensional spherical sampling scheme (13x13x13, FOV = 24x24x24cm, ref. 4). Including scout imaging and calibrations, the duration of the <sup>31</sup>P study was ~75min. The <sup>31</sup>P acquisition has an effective sampling radius of 1.4cm; previous studies have shown the reproducibility of the <sup>31</sup>P acquisition is 10%. Analysis was performed using single voxel reconstructions, with curve fitting for 9 resonances including PCr,  $\gamma$ -ATP, Pi, phosphomonoesters, phosphodiesteres. Quantification was performed accounting for tissue volume, coil loading and relaxation. Results: A moderate ketosis was achieved in all subjects, with plasma BHB rising from 0.24±0.05 to 1.64±0.93. Spectra from subject #3 (hypothalamus) is shown in the figure, showing PCr, ATP and inorganic phosphate Pi. Data and loci of spectral analysis are shown in the Table. The ATP concentrations in the thalamus, hypothalamus and hippocampus rose significantly between D0 to D28. The hypothalamus increased from 2.68±0.24mM to 3.18±0.33mM ATP. Conclusions: Cerebral energetics changed with use of a ketotic diet, with increased ATP concentrations in the hypothalamus, thalamus and hippocampus. In this limited group no significant changes were detected in PCr concentrations. The largest change was seen in the hypothalamus, and is consistent with a view that lower structures demonstrate greater energetic sensitivity to fuel selection. References: 1. Huttenlocher PR. Ped Res 10:536-540 1976. 2. Van Itallie et al in press Neurology 2005. 3. Kossoff E et al Neurology 61(12):1789-91 2003. 4. Pan JW and Takahashi K, Ann Neurol 65(1):92-97 2005.

Table: mM concentrations before and during diet

	ATP D0	ATP D28	PCr D0	PCr D28
Hypothal	2.68±0.24	3.18±0.33*	1.51±0.43	1.49±0.30
Thalamus	2.53±0.15	2.78±0.21*	3.24±0.29	3.58±0.14
Hippo	2.33±0.14	2.49±0.22*	2.74±0.18	2.95±0.29
Occipital GM	2.52±0.18	2.70±0.24*	2.93±0.17	3.02±0.12



D0, baseline; D28 after 4weeks on diet  
\* Significantly different between D0 and D28, p<0.05, two tailed t-test

## IS OXYGEN INSUFFICIENCY COMPENSATED DURING ACUTE ISCHEMIA? - A PET STUDY IN AN ISCHEMIC MODEL OF NON-HUMAN PRIMATES

Rishu Piao, **Takuya Hayashi**, Nobuyuki Kudomi, Noboru Teramoto, Yoichiro Ohta, Hedehiro Iida

*Department of Investigative Radiology, National Cardiovascular Center, Research Institute, Suita, Japan*

Insufficient delivery of oxygen to tissue is the central core of ischemia. A large number of observations in rodents revealed that compensatory responses against ischemia occurs at cellular or biochemical level, however, there is a lack of *in vivo* evidences of biological responses to fulfil oxygen demand. Among them, vascular response to maintain the delivery (e.g. vasodilatation) and transport efficiency of metabolic substrates from blood to tissue assumed to be fundamental (Hayashi et al. 2003). Here, we show using PET whether there is response in vasculature or in the diffusion efficiency of oxygen in an acute stroke model in non-human primates. We used four adult male macaque monkeys (*macaca fascicularis*, body weight = 5 kg). The study was approved by the local committee of animal experiments. Experiments were performed under general anesthesia using propofol. A single PET scan with dual tracer/integration (DTI) method for CBF/CMRO<sub>2</sub> and a PET scan for CBV were repeatedly performed before and 360 min after the artificial embolization of intracerebral artery. Embolization was produced by injecting autologous blood clot through a thin catheter placed at middle cerebral artery or internal carotid artery. “Ischemic” regions of interest (ROI) were defined by searching voxels with the highest values in the oxygen extraction fraction (OEF) images at the time point of 5 min or 180 min after embolization. CBF, CMRO<sub>2</sub> and CBV values were also obtained by placing the same ROI to the corresponding images. CBV values were used for the assessment of vascular response, whereas effective oxygen diffusibility (EOD) that was calculated from measured CBF, OEF and arterial haemoglobin content (Hb) and oxygen saturation fraction (Sa) was used as a marker of efficiency of oxygen transport from blood to brain tissues (Hayashi et al. 2003). The values were normalized by ROI values in cerebellum for each image and by the values at the time point of pre-embolization for each subject to minimize measurement- and subject-specific variability. The mirror regions contralateral to the “ischemic” ROI were used for control. “Ischemic” regions (n = 7) showed decrease in CBF (-30%, -32% at 5 min and 180 min, respectively) and CMRO<sub>2</sub> (-18%, -10%) and increase in OEF (+18%, +26%) compared to the control. CBV values showed no change (+1%, +2%) whereas EOD decreased (-12%, -11%). When the “ischemic regions” were divided in two categories by the final tissue outcome (non-infarcted or infarcted), significant decreases in CBF, CMRO<sub>2</sub> and EOD were found in the regions of final infarcted, but no difference in CBV were seen between the two categories. Similar results were also obtained in the other time points (30, 60, 120, 210 and 360 min post embolization). These results reveal that in acute ischemic regions there is little response in vasculature and that change in diffusion efficiency of oxygen does not act as a compensatory response rather passively depends on the metabolic demand, although oxygen extraction fraction is increased. The findings indicate that brain tolerance for oxygen insufficiency is not so large that oxygen metabolism during ischemia correlates final tissue outcome.

**OXYGEN CONSUMPTION BY SPIKING ACTIVITY IN RAT CEREBELLUM****Kirsten Thomsen<sup>1</sup>, Martin Lauritzen<sup>2</sup>***<sup>1</sup>Department of Medical Physiology, Panum Institute, University of Copenhagen, Copenhagen, Denmark**<sup>2</sup>Department of Clinical Neurophysiology, Glostrup Hospital, Copenhagen, Denmark*

**Introduction:** The mechanisms coupling neuronal activity, cerebral metabolism and cerebral blood flow (CBF) during activation as well as in the basal state (rest) are not clear. The type of neuronal activity, i.e., synaptic input or action potential output (spiking activity), responsible for energy consumption is under debate. We here examined the effect of basal spiking activity per se on oxygen consumption in the cerebellar cortex in rats. **Methods:** Spiking activity, as well as field potentials, and tissue oxygen tension (tpO<sub>2</sub>) were measured at the same cortical depth using glass microelectrodes (tip diameter 2 mm) and Clark-type oxygen electrodes (tip diameter 3-4 μm), respectively. CBF was recorded with laser-Doppler flowmetry. All experiments were carried out using an open cranial window preparation placed over the cerebellar vermis in a-chloralose-anaesthetized adult male Wistar rats (n = 6). Basal measurements were performed in control conditions and after superfusion of the cerebellum with the GABAA antagonist, bicuculline (0.2 mM). Parallel fiber stimulation with 30 s stimulation trains at 0.5, 5, 10, and 15 Hz was given before and after bicuculline application. **Results:** As we have shown previously, application of bicuculline caused basal spiking activity to increase 3-4 fold without influencing either basal CBF or mean arterial blood pressure. Maximal effect of bicuculline on spike rate was achieved after 3 – 12 minutes of exposure to the GABAA antagonist. PO<sub>2</sub> was measured directly before bicuculline application and when maximal spike rate occurred. In 5 of 6 rats, pO<sub>2</sub> decreased, while remaining unchanged in the sixth. Averaging results from all rats, pO<sub>2</sub> decreased by 25% at maximal spike rate and this decrease was maintained during the 30 minute observation period. In the parallel fiber system, the magnitude of field potential amplitude, representing synaptic input, appeared to increase in the presence of bicuculline (control: 0.082 mV vs bicuculline: 0.116 mV) without reaching significance (p = 0.1522). **Conclusion:** We conclude that basal spiking activity per se increases cerebellar oxidative metabolism. We have previously shown that synaptic input via the climbing fibers is not influenced by GABAA antagonism. In the parallel fiber system, however, increased synaptic input via the parallel fibers may be a contributing factor to both spiking activity and brain metabolism. **Grant support:** Supported by the Lundbeck Foundation and the NOVO-Nordisk Foundation.

## EFFECTIVELY TRUNCATED TCA CYCLE DURING PROFOUND HYPOGLYCEMIA

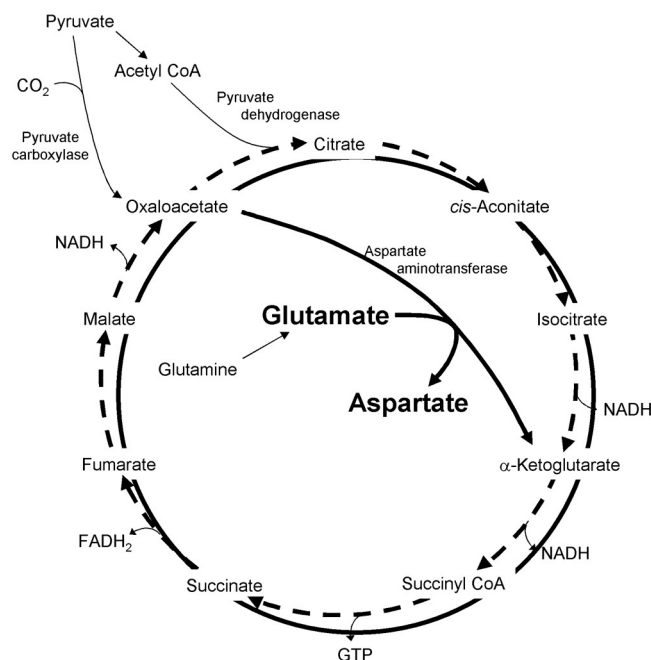
Roland N. Auer<sup>1,2,3</sup>, Randy L. Tyson<sup>3</sup>, Garnette R. Sutherland<sup>1,3</sup>

<sup>1</sup>*Clinical Neurosciences, Calgary, AB, Canada*

<sup>2</sup>*Pathology & Laboratory Medicine, Calgary, AB, Canada*

<sup>3</sup>*Hotchkiss Brain Institute, Calgary, AB, Canada*

**BACKGROUND** In the medical, scientific and legal communities, it is now widely understood that hypoglycemic brain damage occurs in the presence of coma (flat EEG), a prerequisite for brain damage signaled by excitatory amino acid release. Alterations must take place, however, allowing most brain tissue to survive hypoglycemic coma. **METHODS** Brain metabolism was interrogated in rats during and following recovery from 40 min of profound hypoglycemia using *ex vivo* <sup>1</sup>H MR spectroscopy. **RESULTS** A time-dependent increase in aspartate was equaled by a reciprocal decrease in glutamate/glutamine. The kinetics of aspartate formation during the first 30 min ( $0.36 \pm 0.03 \mu\text{mol g}^{-1} \text{min}^{-1}$ ) showed that glutamate, via aspartate aminotransferase, becomes the primary source of carbon when glucose-derived pyruvate is unavailable. Oxaloacetate is produced directly from  $\alpha$ -ketoglutarate, so that reactions involving the six-carbon intermediates of the tricarboxylic acid cycle are bypassed (figure). **CONCLUSIONS** We demonstrate for the first time that the Krebs cycle is effectively truncated from a tricarboxylic to a dicarboxylic acid cycle during hypoglycemia, allowing it to still turn. This fundamental alteration in basic metabolic pathways explains the partial preservation of energy charge during periods of glucose deficiency. The results may explain how most brain neurons, and all glia, survive profound hypoglycemia accompanied by electrocerebral silence.



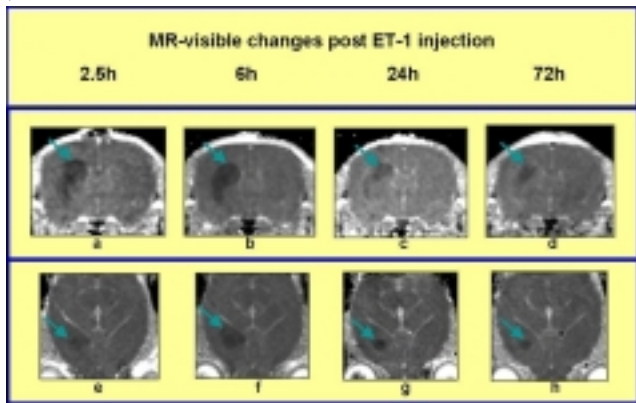
## MRI & 31P MRS STUDIES OF BRAIN ENERGETICS IN A MODEL OF CEREBRAL VASOCONSTRICTION

Raman Saggy<sup>1</sup>, John P. Lowe<sup>1</sup>, Andrew M. Blamire<sup>1</sup>, Daniel C. Anthony<sup>2</sup>, Peter Styles<sup>1</sup>, Nicola R. Sibson<sup>1</sup>

<sup>1</sup>*Experimental Neuroimaging Group, Department of Biochemistry, University of Oxford, Oxford, UK*

<sup>2</sup>*Experimental Neuropathology Laboratory, Department of Pharmacology, University of Oxford, Oxford, UK*

Ischaemic brain events necessitate prompt diagnosis and clinical intervention if the ischaemia is to be reversed. At present, MR is unable to distinguish between reversibly and irreversibly damaged tissue. Although apparent diffusion coefficient (ADC) MRI is established as a sensitive indicator of acute ischaemia, an unresolved challenge is to non-invasively distinguish between reversibly and irreversibly damaged tissue early in the ischaemic event. Endothelin-1 (ET-1) produces a potent and prolonged vasoconstrictive effect on the brain vasculature and has been used as a model of low flow ischaemia in the rat brain. We hypothesise that a focal striatal injection of ET-1 creates a graduated lesion consisting of both reversibly and irreversibly damaged tissue. A longitudinal study of MR-visible changes following intrastriatal ET-1 injection in the juvenile rat brain was conducted and correlated with the metabolic status of brain tissue using phosphorus (31P) MRS. Male Wistar rats (50-55g) were anaesthetised by inhalation using 2% isoflurane in 70% N<sub>2</sub>O:30% O<sub>2</sub>. Using a minimally-invasive stereotaxic procedure, 160pmoles of ET-1 was injected in a volume of 1.0 µl of sterile saline into the striatum (n=8). Animals were positioned in a purpose-built head restraint system and a 2cm-diameter single-turn circular surface phosphorus coil was placed over the animal's head. Anaesthesia was maintained in the magnet using 1% isoflurane in 70% N<sub>2</sub>O:30% O<sub>2</sub>. T1 and T2-weighted images, DWI and 31P spectra were obtained using a 7T horizontal bore magnet (MagneX Scientific) interfaced to a Varian/SISCO spectrometer (Varian, Palo Alto, CA, USA). We observed a significant decrease in the ADC around the site of injection at 2.5h post-injection [Figure 1a. & e.]. MRI was repeated at 6, 24 and 72 hrs over which time ADC changes resolved in the periphery of the lesion, but remained low at the core. These findings suggest that the tissue at the core of the lesion may be irreversibly damaged whereas normalisation of ADC in the periphery may be indicative of reversibly damaged tissue. 31P spectra from the whole of the injected hemisphere did not detect any reductions in the PCr to ATP ratio. Significant changes in these metabolites may only occur in the speculated irreversibly damaged core of the lesion, which constitutes less than 25% of the 31P MRS voxel. The inclusion of a significant volume of healthy tissue in the 31P MRS voxel may explain the absence of a change in metabolite levels. Ongoing studies are investigating the perfusion changes in the core and peripheral regions of ET-1-induced focal lesions and their correlation with ADC changes.



## TURNOVER OF EXTRA-CELLULAR GLUCOSE AND LACTATE IN THE RAT STRIATUM ESTIMATED BY EQUILIBRIUM MICRO-DIALYSIS

Maria M. Rhemrev-Boom<sup>1</sup>, Gea M.R. Leegsma-Vogt<sup>1,2</sup>, **Jakob Korf**<sup>1,2</sup>, Folkert Postema<sup>1</sup>, Kor Venema<sup>1</sup>

<sup>1</sup>*Department of Psychiatry UMCG Groningen, Groningen, The Netherlands*

<sup>2</sup>*Behavioral & Cognitive Neurosciences, University of Groningen, Groningen, The Netherlands*

**Introduction:** Intercellular trafficking of substrates is essential to meet the energy demand of the brain. Accordingly, neuronal energy consumption may depend on trafficking of glucose and lactate through the brain intercellular space (ICS, about 18% of tissue) to neurons. We report here estimates of ICS steady state levels ( $C_{ss}$ ) and the relative amounts of lactate or glucose (indicated here as R%) that diffuse via the ICS of the striatum of conscious and freely moving rats.

**Methods:** We applied equilibrium microdialysis (eMD), that is very slow microdialysis (100 nL = 0.1  $\mu\text{L}\cdot\text{min}^{-1}$ ). eMD allows the estimation of  $C_{ss}$  and the turnover rates in the ICS. Various concentrations of lactate and glucose were continuously infused and measured in the perfusate with miniature bio-sensors. The difference between the amounts infused and collected per time unit reflects the sum of diffusion and consumption of the substrates in the ICS surrounding the eMD-probe. The cellular transporters of lactate and glucose are bi-directional, so the rate of disappearance is predominantly due to metabolism at steady state perfusion. Rats were provided with conventional micro-dialyses probes and studied at various days post-surgery. eMD, animals, surgery, sensors, equipment and probes were done as reported [1,2].

**Results:**  $C_{ss}$  of glucose (n = 10) and lactate (n = 6) were measured up to 6 days following the implantation of the probe. The lowest levels ( $\pm$  SEM) of glucose were measured at days 2, 3 and 4 and were  $0.35 \pm 0.07$ ,  $0.18 \pm 0.04$  and  $0.31 \pm 0.05$  mM, respectively. The lactate levels did not significantly vary over 4 days; these levels were at day 2, 3 and 4,  $0.64 \pm 0.03$ ,  $0.68 \pm 0.03$  and  $0.58 \pm 0.02$  mM, respectively. At day 3 and 4 the turnover rates of glucose (n = 6) and lactate (n = 6) were estimated by infusing glucose (0.5, 1.0, 2.0, 2.5 or 5.0 mM) or lactate (1.5, 2.5, 3.0, 4.0 or 5.0 mM). At day 3 six rats were studied either with lactate (3 rats) or with glucose (3 rats); the same rats were studied next day, but now with the other substrate. The turnover rate of lactate was  $0.13 \pm 0.03$   $\mu\text{Mol/g/min}$  and that of glucose  $0.03 \pm 0.01$   $\mu\text{Mol/g/min}$ . R% is less than 10%.

**Conclusions:** The relative amount of glucose diffusing through the ICS is far smaller than that of lactate (<1% versus > 7% of total energy consumption) and are in line with [3]. Our data do not support the idea that the majority of brain energy need is provided by the glutamate-recycling shuttle, but they emphasize that lactate, rather than glucose, is the major trafficking energy substrate.

### References:

- [1] Rhemrev-Boom MM, Jonker MA, Venema K, Jobst G, Tiessen R, Korf J. *Analyst.*, 2001; 126: 1073-1079.
- [2] Rhemrev-Boom MM, Korf J, Venema K, Urban G, and Vadgama P. *Biosensors Bioengineering* 2001;16: 839-847.
- [3] Attwell D, Laughlin SB. *J Cereb Blood Flow Metab.* 2001; 21: 1133-45

*Grant support:* Dutch technology Foundation (STW) and European Commission (EC).

## SLEEP-DEPENDENT CHANGES IN THE CEREBRAL METABOLIC RATE OF OXYGEN CONSUMPTION IN NEWBORN LAMBS

Alessandro Silvani<sup>1</sup>, Valentina Asti<sup>1</sup>, Chiara Berteotti<sup>1</sup>, Tijana Bojic<sup>1</sup>, Vera Ferrari<sup>1</sup>, Carlo Franzini<sup>1</sup>, Daniel A. Grant<sup>2</sup>, Pierluigi Lenzi<sup>1</sup>, Adrian M. Walker<sup>2</sup>, Giovanna Zoccoli<sup>1</sup>

<sup>1</sup>*Dipartimento di Fisiologia Umana e Generale, Università di Bologna, Bologna, Italy*

<sup>2</sup>*Ritchie Centre for Baby Health Research, Monash University, Clayton, Australia*

Aim of this study was to determine whether REM sleep during early postnatal development is already characterised by a high cerebral oxygen uptake. In adults, cerebral blood flow (CBF) and cerebral metabolic rate of oxygen consumption (CMRO<sub>2</sub>) decrease from wakefulness to non-rapid-eye-movement (non-REM) sleep and return during REM sleep to values similar to those in wakefulness, especially in subcortical regions (cf. (1)). No study addressed the issue of cerebral metabolism during REM sleep in newborn life, when REM sleep duration is at a lifetime maximum, while CBF is at a lifetime minimum. In this respect, a high CMRO<sub>2</sub> during REM sleep could represent a metabolic challenge for newborns, and a situation of risk owing to the strong dependency of CBF dynamics on fluctuations in arterial blood pressure in this sleep state (2). Six Merino/Border-Leicester cross lambs 2-5 day old were anaesthetised (halothane / N<sub>2</sub>O) and instrumented with electroencephalographic and electromyographic electrodes for determining the sleep state and with a transit-time ultrasonic flow probe around the superior sagittal sinus to measure CBF (3). Non-occlusive catheters were inserted into the carotid artery and in the superior sagittal sinus for blood sample withdrawal. Studies began at least 72 hours after surgery: each animal was recorded for 2-4 days, and every day blood samples (2 ml) were obtained simultaneously from the carotid artery and the superior sagittal sinus during uninterrupted epochs of wakefulness, non-REM sleep and REM sleep. Samples were collected in heparinised syringes and immediately analysed. The arterovenous difference in oxygen content, computed from the concentration and saturation of haemoglobin in the arterial and venous blood, was multiplied by CBF to yield estimates of CMRO<sub>2</sub>. Average data were obtained for each lamb and state. Data are presented as mean ± SEM. Cerebral oxygen arterovenous difference (mM) was 1.9 ± 0.1 in wakefulness, 1.9 ± 0.1 in non-REM sleep, and 1.7 ± 0.1 in REM sleep. CBF (ml/min) was 21.2 ± 2.1 in wakefulness, 18.5 ± 2.3 in non-REM sleep, and 25.0 ± 2.8 in REM sleep. The oxygen arterovenous difference correlated negatively with CBF ( $r = -0.44$ ,  $p < 0.01$ , Pearson correlation computed on z-scores from 54 samples). Nonetheless, CMRO<sub>2</sub> (micromol/min) was significantly higher ( $p < 0.05$ , Friedman test and Wilcoxon test) in REM sleep (42.4 ± 4.7) and in wakefulness (39.8 ± 5.0) than in non-REM sleep (34.6 ± 4.3). Data thus demonstrate that in newborn lambs, cerebral oxygen uptake in REM sleep is higher than in non-REM sleep and similar to that in wakefulness. In lambs, the superior sagittal sinus mainly drains from the frontal and anterior parietal lobes (3). Therefore, these data suggest that in newborn life CMRO<sub>2</sub> is high during REM sleep even in cortical regions, in which changes in CMRO<sub>2</sub> among wake-sleep states are inconstant in adults (1). (1) Zoccoli et al. *Sleep Med Rev* 2002; 6: 443-455 (2) Silvani et al. *Sleep* 2004; 27: 36-41 (3) Grant et al. *Am J Physiol* 1995; 269: R274-R279

## THE BLOOD-BRAIN UPTAKE OF 3-O-METHYL D-GLUCOSE MAY BE MAINLY INTERSTITIAL OVER TIMES LESS THAN 45 SECONDS

Joseph D. Fenstermacher<sup>1,2</sup>, Ling Wei<sup>1,2</sup>, Daniel Bereczki<sup>1</sup>, Tadahiro Otsuka<sup>1</sup>,  
Jiann-Liang Chen<sup>1</sup>, Franz-Josef Hans<sup>1</sup>, Virgil Acuff<sup>1</sup>, Clifford S. Patlak<sup>1</sup>

<sup>1</sup>Anesthesiology, Henry Ford Health System, Detroit, MI, USA

<sup>2</sup>Neurosurgery, State University of New York, Stony Brook, NY, USA

Introduction: The equilibrium distribution space of 3-O-methyl-D-glucose (3OMG), a non-metabolizable analog of D-glucose, is around 50 ml/100 g tissue (50%) in most brain areas [1]. The 3OMG space is considerably larger than the extracellular space (18%) but much less than the water space (78% in gray matter; 65% in white matter). In the past we [2, 3] and others have assumed that the 3OMG after crossing the blood-brain barrier instantly mixes in a 50% space in brief (e.g., 30 sec) experiments. This assumption was tested by short-term, ramp infusions of <sup>14</sup>C-3OMG in Sprague-Dawley (SPD), spontaneously hypertensive (SHR), and Wistar-Kyoto (WKY) rats. Methods: Young adult SPD, SHR, and WKY rats were intravenously infused with <sup>14</sup>C-3OMG with a schedule that yielded a continuously rising plasma concentration. Blood was continuously sampled, and experiments terminated at 15 sec (n=4/rat strain), 30 sec (n=3), and 45 sec (n=3). Radioactivity was determined in plasma by liquid scintillation counting and in 7 regions of interest (ROIs) by quantitative autoradiography. The ROIs were sensorimotor (SMC) and occipital (OCC) cortex, caudate-putamen (CPU), medial geniculate (MGT), inferior colliculus (IC), genu of the corpus callosum (GCC), and median eminence (ME). The resulting set of multi-time data (n=10) were inserted into a two compartment (plasma and tissue) model, and the influx (K<sub>i</sub>) and effective tissue distribution space (eV) for the 15 - 45 sec interval were obtained for each ROI by compartmental analysis. The difference between eV and 0.5 ml/g were considered significant at p<0.05 level. Results: Among the three strains, plasma glucose concentrations were comparable, and the rates of 3OMG influx were lowest for GCC (white matter; K<sub>i</sub> ~0.08 ml/g/ml) and highest for the ME (a circumventricular organ with leaky capillaries; K<sub>i</sub> = 0.72 - 1.05 ml/g/ml). The differences in K<sub>i</sub> for any ROI were not significant among the three strains. In SMC, OCC, CPU, MGT, IC, and GCC of SPD rats, eV (±SE of the estimate) ranged from 0.07±0.02 ml/g (GCC) to 0.18±0.05 ml/g (IC). In these ROIs, eV was significantly less than 0.5 ml/g and approximated the extracellular space. For these six ROIs, comparable values of eV were found in WKY, and the differences between eV and 0.5 ml/g were significant. For the ME, eV was >0.5 ml/g for SPD (p>0.05) but only 0.28 ±0.07 ml/g for WKY (p<0.05). For each of the seven ROIs, eV values in SHR were 2 or more times higher than in either SPD or WKY and not statistically significantly different than 0.5 ml/g. Conclusions: The assumption of rapid mixing of 3OMG in a 50% tissue space was not upheld for gray and white matter of SPD and WKY rats. The distribution of 3OMG was completely and strangely different in SHR, suggesting considerable variations in the glucose transporter systems of neurons and/or glia among the three strains. References: 1.Namba et al. J Appl Physiol 252:E299-303 (1987) 2.Chen et al. Microvas Res 48:190-211 (1994) 3.Chen et al. Microcirc 1:35-47 (1994) Grant support: NIH grants HL-35791, NS-21157, and NS-26004.

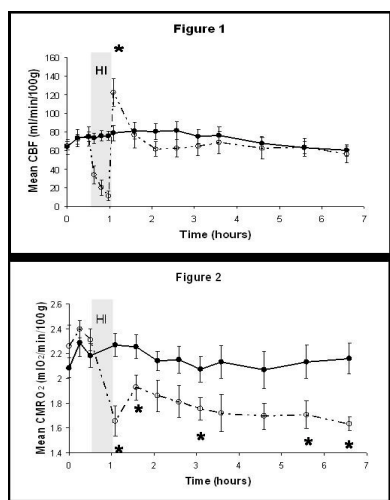
## NEAR-INFRARED SPECTROSCOPY MEASUREMENTS OF CEREBRAL BLOOD FLOW AND OXYGEN CONSUMPTION FOLLOWING HYPOXIA-ISCHEMIA IN NEWBORN PIGLETS

Kenneth M. Tichauer<sup>1,2</sup>, Derek W. Brown<sup>1,2</sup>, Jennifer Hadway<sup>1,2</sup>, Ting-Yim Lee<sup>1,2</sup>,  
Keith St. Lawrence<sup>1,2</sup>

<sup>1</sup>Imaging Division, Lawson Health Research Institute, London, ON, Canada

<sup>2</sup>Imaging, Robarts Research Institute, London, ON, Canada

**Introduction** Impaired oxidative metabolism after hypoxia-ischemia (HI) is believed to be an indicator of delayed brain injury (1). We have recently developed a near-infrared spectroscopy (NIRS) technique that could be used to measure the cerebral metabolic rate of oxygen (CMRO<sub>2</sub>) at the bedside of the critically ill newborn. The CMRO<sub>2</sub> measurement requires a combination of indocyanine green-based measurements of cerebral blood flow (CBF) and measurements of cerebral deoxy-hemoglobin concentration (2-3). The objective of this experiment was to investigate the ability of NIRS to measure changes in CMRO<sub>2</sub> following HI in newborn piglets as a prerequisite to clinical investigation. **Methods** Nine piglets were subjected to 30 minutes of HI by occluding both carotid arteries and reducing the fraction of inspired oxygen to 8 %. An additional nine piglets served as sham-operated controls. Measurements of CBF and CMRO<sub>2</sub> were acquired at baseline, every 30 minutes for the first 2 hours after the insult, and on the hour for the following 4 hours. **Results** Figures 1 and 2 display the CBF and CMRO<sub>2</sub> measurements, respectively, for each group of piglets throughout the experiment. The solid line represents the control group, the dashed line represents the hypoxic-ischemic group and the shaded region represents the duration of HI. Only CMRO<sub>2</sub> showed a persistent change following HI. Five minutes after reoxygenation, there was a 28 +/- 12 % decrease in CMRO<sub>2</sub> and a 72 +/- 50% increase in CBF compared to baseline ( $p < 0.05$ ). CBF returned to baseline by 30 minutes post-insult and did not change for the remainder of the study, whereas, CMRO<sub>2</sub> was depressed for the remainder of the study. **Conclusion** We have demonstrated that NIRS can measure persistent decreases in CMRO<sub>2</sub> following HI, despite the return of CBF to baseline within 30 minutes post-insult. The results infer a potential for NIRS to be used in the neonatal intensive care unit to detect early signs of delayed brain injury. **Acknowledgements:** This work was funded by the Canadian Institutes of Health Research. **References** [1] Hagberg H; J Bioenerg and Biomembr 36, 369-373 (2004) [2] Brown DW, et al.; Pediatr Res 51, 564-570 (2002) [3] Brown DW, et al.; Pediatr Res 56, 861-867 (2003)



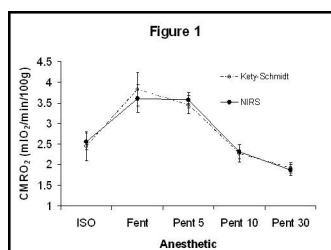
## NEAR-INFRARED SPECTROSCOPY MEASUREMENT OF CEREBRAL OXIDATIVE METABOLISM: A VALIDATION STUDY

Kenneth M. Tichauer<sup>1,2</sup>, Jennifer Hadway<sup>1,2</sup>, Ting-Yim Lee<sup>1,2</sup>, Keith St. Lawrence<sup>1,2</sup>

<sup>1</sup>*Imaging Division, Lawson Health Research Institute, London, ON, Canada*

<sup>2</sup>*Imaging, Robarts Research Institute, London, ON, Canada*

**Introduction:** The measurement of the cerebral metabolic rate of oxygen (CMRO<sub>2</sub>) is an important indicator of tissue viability following ischemic injury in the neonatal brain (1). Current methods of measuring CMRO<sub>2</sub> such as PET and MRS are unsuitable for use in newborns from neonatal intensive care units due to their unstable conditions. Our group has recently developed a minimally invasive technique using near-infrared spectroscopy (NIRS) for measuring CMRO<sub>2</sub> at the bedside. The technique uses cerebral blood flow (CBF) measurements – obtained with the tracer indocyanine green – combined with measurements of cerebral deoxy-hemoglobin concentration to determine CMRO<sub>2</sub> (2, 3). This technique was recently used to measure changes in CMRO<sub>2</sub> following hypoxia-ischemia in a piglet model (4). The purpose of this study was to validate our NIRS measurements of CMRO<sub>2</sub> by comparison with measurements obtained using a gold standard technique (the Kety-Schmidt technique). **Methods:** Measurements were obtained on piglets 0-3 days of age. Five different states of cerebral oxidative metabolism were created in each piglet by using a range of anesthetics: 1% isoflurane, 0.04 mg/kg/h fentanyl infusion coupled with 70% nitrous oxide, and three levels of pentobarbital (5, 10, and 30 mg/kg) added to the fentanyl/nitrous oxide mixture. Each level of anesthetic was maintained for roughly 30 minutes. At each level, measurements of CMRO<sub>2</sub> were taken using the NIRS technique as well as the Kety-Schmidt technique. Both methods are based on the Fick Principle:  $CMRO_2 = CBF \cdot \text{arteriovenous } O_2 \text{ difference (AVO}_2)$ . For the Kety-Schmidt technique, AVO<sub>2</sub> was determined from blood samples collected from the sagittal sinus and a femoral artery. For the NIRS technique, AVO<sub>2</sub> was measured indirectly from measurements of cerebral deoxy-hemoglobin concentrations. At each anesthetic level, CBF was determined using NIRS and the contrast agent indocyanine green (2). **Result** A total of 4 piglets were studied (3 females, 1 male, mean age of 1.1 days and mean weight of 1.57 kg). Figure 1 displays the measurements of CMRO<sub>2</sub> from both methods at the five levels of anesthesia. The Data points are expressed as averages over all piglets and error bars are standard error. The correlation between the two methods obtained from these preliminary results yielded an  $R^2 = 0.56$ . **Conclusion:** This preliminary study demonstrated that the NIRS technique of measuring CMRO<sub>2</sub> correlates well with the gold standard. The results imply that NIRS could be used to rapidly and accurately measure CMRO<sub>2</sub> at the bedside of the newborn as an indicator of brain injury. **Acknowledgements:** This work was funded by the Canadian Institutes of Health Research. **References:** [1] Hagberg H; *J Bioenerg and Biomembr* 36, 369-373 (2004) [2] Brown DW, et al.; *Pediatr Res* 51, 564-570 (2002) [3] Brown DW, et al.; *Pediatr Res* 56, 861-867 (2003) [4] Tichauer KT, et al.; *Brain05* (submitted)



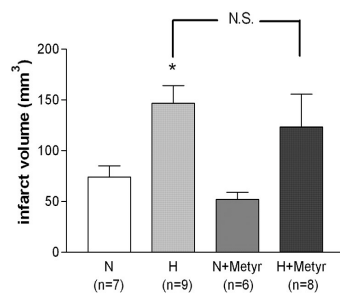
## THE ADVERSE EFFECTS OF HYPERGLYCEMIA DURING TRANSIENT FOCAL ISCHEMIA IN RATS ARE NOT ATTRIBUTABLE TO INCREASED PLASMA CORTICOSTEROIDS OR NEUTROPHIL INFILTRATION

Abraham Martín<sup>1</sup>, Angel Chamorro<sup>2</sup>, Anna M. Planas<sup>1</sup>

<sup>1</sup>Department of Pharmacology & Toxicology, IIBB-CSIC, IDIBAPS, Barcelona, Spain

<sup>2</sup>Stroke Unit, IMSN, Hospital Clínic, IDIBAPS, Barcelona, Spain

**Introduction:** Hyperglycemia adversely affects the outcome of stroke<sup>1,2</sup>. A raise in plasma corticosteroids is thought to be involved in this effect after transient global ischemia<sup>3</sup>. Here we investigated the harmful effects of hyperglycemia after transient middle cerebral artery (MCA) occlusion in rats and whether these are dependent on plasma corticosteroids. **Methods:** One-hour intraluminal MCA occlusion was induced in adult male Sprague-Dawley rats (n=159). Sham-operated and non-operated rats were used as controls (n=20). Acute hyperglycemia was induced by i.p. injection of dextrose (25%) 30 min prior to MCA occlusion. Corticosteroid synthesis was inhibited by injecting i.p. metyrapone (100 mg/Kg). Plasma corticosteroids were measured by radioimmunoassay. Neutropenia was induced with vinblastine (0.5 mg/Kg i.p.) 4 days prior to ischemia, and neutrophils in plasma were determined. The neurological function was assessed at 24h, then rats were killed and infarct volume was measured. Neutrophil infiltration was evaluated with the mieloperoxidase assay (MPO), and matrix metaloproteinase-9 (MMP-9) content was determined by gel zymography. Measuring Evans blue extravasation at 48h assessed blood-brain barrier leakage. **Results:** Hyperglycemia (H) significantly increased infarct volume (p<0.01) (Fig. 1), it worsened the neurological score (p<0.001), and it enhanced the ischemia-induced rise in MPO (p<0.001) and MMP-9 (p<0.01) in tissue and the Evans blue extravasation (p<0.001), compared with normoglycemic (N) rats. Metyrapone maintained plasma corticosterone under the basal level. Infarct volume in hyperglycemic rats receiving metyrapone (H+Mety) was not significantly different from hyperglycemic rats not receiving the drug (H) (Fig. 1). Metyrapone did not prevent the increased MPO and MMP-9 in hyperglycemic rats compared to the normoglycemic groups. Vinblastine caused neutropenia in hyperglycemic rats and prevented the increase in MPO and MMP-9 in brain tissue after ischemia, but it did not reduce infarct volume at 24h. **Conclusion:** Hyperglycemia exacerbated the outcome of ischemia as infarct volume was larger and the neurological outcome was worst that in normoglycemic rats. Subsequently, neutrophil infiltration, MMP-9, and BBB leakage were higher. Inhibiting the synthesis of corticosteroids did not prevent the adverse effects of hyperglycemia. Also, neutrophils were not responsible for the worst outcome of ischemia in hyperglycemic rats. Hyperglycemia during transient focal cerebral ischemia has per se adverse effects that are not attributable to increased plasma corticosteroids or neutrophil infiltration. **References:** 1. Toni et al., 2004. *Cerebrovasc Dis.* 17 (Suppl 2):30-46 2. Parsons et al., 2002. *Ann Neurol.* 52:20-28. 3. Payne et al., 2003. *Brain Res.* 971:9-17 Supported by the Comisión Interministerial de Ciencia y Tecnología (CICYT SAF2002-01963)



\* p< 0.05 vs N

## THEORETICAL SUPPORT FOR THE ASTROCYTE-NEURON LACTATE SHUTTLE HYPOTHESIS. II. MODELING BRAIN LACTATE KINETICS

Agnès Aubert<sup>1</sup>, Robert Costalat<sup>2</sup>, Pierre J. Magistretti<sup>3</sup>, **Luc Pellerin**<sup>1</sup>

<sup>1</sup>*Department of Physiology, University of Lausanne, Lausanne, Switzerland*

<sup>2</sup>*UMR\_S 678, Université Pierre et Marie Curie, Paris, France*

<sup>3</sup>*Brain and Mind Institute, EPFL, Lausanne, Switzerland*

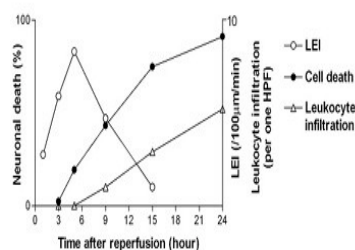
**Introduction** A critical issue in the actual debate around the astrocyte-neuron lactate shuttle hypothesis is whether lactate produced within the brain by astrocytes can be taken up and metabolized by neurons upon activation. Although there is ample evidence that neurons can efficiently use lactate as an energy substrate, at least in vitro [1], few experimental data exist to indicate that it is indeed the case in vivo [2]. In order to address this question, we used a modeling approach to determine which parameters are essential and sufficient to explain typical brain lactate kinetics observed upon activation. **Method** On the basis of a previously validated model taking into account the compartmentalization of energy metabolism [3], we derived a mathematical model of brain lactate kinetics, including cellular lactate production or consumption, regional cerebral blood flow, exchanges through the blood brain barrier and extracellular pH variation. This model was applied to published data describing the changes in extracellular lactate levels following activation [4]. **Results and Discussion** Results show that the initial dip in the extracellular lactate concentration observed at the onset of stimulation requires a rapid uptake within a cellular compartment which is most likely neurons. Moreover, an increase in uptake occurring with repetitive stimulation explains the more pronounced dip observed as the extracellular lactate concentration reaches higher levels due to activation of astrocytic glycolysis. In contrast, neither increased lactate washout, due to the enhancement of blood flow, nor diffusion parameters could explain such patterns. It is concluded that instead of being a major fact against the ANLS hypothesis, the initial dip in brain lactate levels, observed both in animals [4] and in humans [5], strongly suggests that lactate consumption by neurons occurs from the very start of stimulation. These data concur with recent demonstrations of a net lactate transfer between astrocytes and neurons in vivo. This work was supported by the Fondation pour la Recherche Médicale and the Action Concertée Incitative 'Neurosciences Intégratives et Computationnelles' (French Ministry of Research). **Reference** 1. Bouzier-Sore et al. (2003) *J. Cereb. Blood Flow Metab.* 23:1298 2. Serres et al. (2004) *J. Biol.Chem.* 279:47881 3. Aubert and Costalat (2005) *J. Cereb. Blood Flow Metab.*, in press 4. Hu and Wilson (1997) *J. Neurochem.* 69:1484 5. Mangia et al. (2003) *Neurosci.* 118:7

## ADHESION OF LEUKOCYTES TO CEREBRAL ENDOTHELIUM IS SUFFICIENT TO TRIGGER DELAYED NEURONAL CELL DEATH FOLLOWING FOCAL CEREBRAL ISCHEMIA

Hiroharu Kataoka, Seong-Woong Kim, Nikolaus Plesnila

*Laboratory of Experimental Neurosurgery, Institute for Surgical Research, University of Munich, Munich, Germany*

**Introduction:** Although it seems to be clear that leukocytes contribute to brain damage after cerebral ischemia, it is still under debate how and when cells of the immune system mediate post-ischemic cell death. The aim of the current study was therefore to investigate the temporal and causal relationship of leukocyte-endothelium interactions, leukocyte migration into brain parenchyma, and neuronal cell death following reperfusion from focal cerebral ischemia. **Materials & Methods:** 129/Sv mice were subjected to 45 minutes of transient middle cerebral artery occlusion by an intraluminal filament. Leukocyte-endothelium interactions were assessed by intravital microscopy (IVM) 40 min, 1, 2, 3, 5, 9, and 15 hours after reperfusion. Neuronal cell death and leukocytes migrated into the brain were quantified in the same tissue volume by histology and immunohistochemistry using the pan-leukocyte marker CD45, respectively, at the same time points. For inhibition of leukocyte-endothelium interactions an anti-CD18 antibody was injected into the left common carotid artery immediately after reperfusion. **Results:** We show that interactions of leukocytes with cerebral endothelium peaked 5 hours after reperfusion following 45 minutes of transient middle cerebral artery occlusion in mice ( $P < 0.01$  vs. control). In the same area of the brain, neuronal cell death occurred between 5 and 24 hours after reperfusion while infiltration of leukocytes into the brain parenchyma was limited and started to be detectable only 9 hours after reperfusion (Figure). Inhibition of CD18, a leukocyte adhesion molecule, reduced adherence of leukocytes to cerebral endothelium by 60% ( $P < 0.01$ ) and increased the number of viable neurons by more than 5-fold ( $P < 0.01$ ), but did not affect the number of leukocytes in the brain parenchyma. **Summary & Conclusion:** Our results show that intravascular interaction of leukocytes with cerebral endothelium seems to be sufficient for the induction of neuronal cell death after transient focal cerebral ischemia, while infiltration of leukocytes into post-ischemic brain tissue occurs too late to be responsible for this process. Despite the large number of publications dealing with the role of inflammatory cells for post-ischemic neuronal cell death, this is the first report suggesting that rather transendothelial signaling of intravascular leukocytes than physical interaction of leukocytes with neurons is responsible for cell death after cerebral ischemia. We believe that our data may help to explain previous contradicting results on the role of inflammatory cells for the pathophysiology of cerebral ischemia and may serve as a basis for future research on transendothelial signaling.



## CONTRIBUTION OF VASCULAR ADHESION PROTEIN-1 (VAP-1) TO POST-ISCHEMIC CEREBRAL VENULAR LEUKOCYTE ADHESION AND INFILTRATION IN DIABETIC, OVARIECTOMIZED (OVX) AND ESTROGEN-TREATED FEMALE RATS

Hao-Liang Xu<sup>1</sup>, Matthew D. Linnik<sup>2</sup>, Luisa Salter-Cid<sup>2</sup>, Dale A. Pelligrino<sup>1</sup>

<sup>1</sup>Neuroanesthesia Research, University of Illinois-Chicago, Chicago, IL, USA

<sup>2</sup>La Jolla Pharmaceutical Co., La Jolla, CA, USA

We examined the role of VAP-1 in the increased leukocyte adhesion seen in cerebral venules during the reperfusion period following transient forebrain ischemia (TFI). We used a model associated with a high level of post-ischemic leukocyte adhesion and infiltration—diabetic (6-8 wks post-streptozotocin) OVX females given 1 week of estrogen replacement therapy (ERT). The behavior of rhodamine 6G-labeled leukocytes in pial venules was monitored through a closed cranial window, using intravital microscopy and digital videometry. The rats were observed over 10h reperfusion after 20 min TFI. We compared rats treated (at 0h or 6h reperfusion) with saline or the novel and selective VAP-1 blocker, LJP-1207 (30 mg/kg iv). Since results in the 2 control groups were indistinguishable, the data was pooled (n=6). In controls, increased neutrophil adherence was observed within 1h of reperfusion onset. The intravascular accumulation of adherent leukocytes was seen to gradually rise up to the point where neutrophil infiltration commenced (at >6h, in 83% of controls—fig. 1). Not counting extravasated cells, neutrophil adhesion reached ~17% of the viewed venular area at 6-10h (fig. 2). In the rats treated with LJP-1207 at the onset of reperfusion (0h, n=5), limited neutrophil adhesion, and no infiltration, was observed over the entire 10h period of post-ischemic observation (fig. 1), with the level of adhesion rising only to ~5% of the venular area (fig. 2). In rats treated at 6h reperfusion (n=4), the pattern of neutrophil adhesion was similar to that of the control group up to 6h, but subsequent infiltration was much more limited vs controls (fig. 1), and the level of adhesion actually declined (from ~14% to ~9%) when going from 6-10h reperfusion (fig. 2). These findings indicate that VAP-1, presumably on cerebral vascular endothelium, plays a major role in the process of leukocyte adhesion, as well as infiltration, in diabetic OVX females provided with chronic ERT.

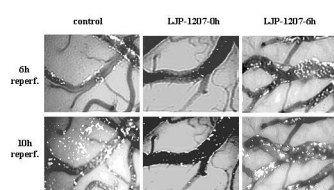


FIG. 1

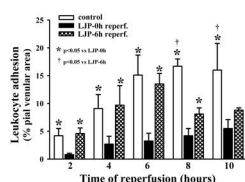


FIG. 2

## SOLUBLE EPOXIDE HYDROLASE GENE DELETION REDUCES INFLAMMATION AFTER STROKE

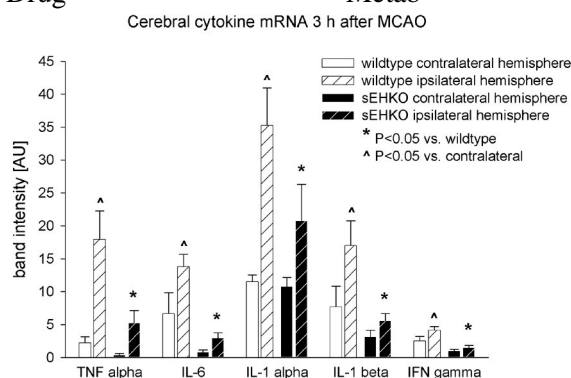
Ines P. Koerner<sup>1</sup>, Wenri Zhang<sup>1</sup>, Patricia D. Hurn<sup>1</sup>, Dennis Koop<sup>2</sup>, Nabil J. Alkayed<sup>1</sup>

<sup>1</sup>Department of Anesthesiology and Peri-Operative Medicine, Oregon Health & Science University, Portland, OR, USA

<sup>2</sup>Department of Physiology and Pharmacology, Oregon Health & Science University, Portland, OR, USA

The brain's inflammatory response to stroke exacerbates ischemic damage [1]. Epoxyeicosatrienoic acids (EETs) are cytochrome P450 metabolites of arachidonic acid that are produced in brain [2] and exhibit anti-inflammatory properties [3]. Mice with targeted deletion of soluble epoxide hydrolase (sEH), a key enzyme in EETs breakdown, are protected from ischemic brain injury [4]. We tested the hypothesis that inflammatory cytokine expression after MCA occlusion is blunted in sEH knockout (sEHKO) mice due to higher brain EETs. Methods: Adult male sEHKO and wild type (WT) C57/Bl6 mice (n=7 per group) were anesthetized with halothane and subjected to 2-hour MCA occlusion using the intraluminal filament technique. Laser-Doppler perfusion was monitored over parietal cerebral cortex during occlusion and reperfusion, and body temperature was monitored and regulated during surgery by warming blankets. Brains were harvested at 3 hours of reperfusion, and total RNA was extracted from ischemic and contralateral hemispheres. Cytokine mRNA expression was assessed after MCA occlusion by multi-probe RNase protection assay, and sEH protein expression was examined in non-ischemic WT and sEHKO mice by immunoblotting. EETs levels in sEHKO and WT mouse brains were examined by liquid chromatography/mass spectrometry. Differences in cytokine expression were evaluated by two-way analysis of variance (ANOVA). Results: Strong immunoreactivity for sEH was detected in brains of WT, but not sEHKO mice. A clear peak corresponding to 14,15-EET was detected in brains from both mouse strains. As illustrated in attached figure, the level of mRNA expression for the following cytokines was highly induced in ischemic vs. contralateral hemispheres of WT, but not sEHKO mice: tumor necrosis factor alpha (TNF $\alpha$ , 18-fold), interleukin-6 (IL-6, 10-fold), interleukin-1 alpha (IL-1 $\alpha$ , 3-fold), interleukin-1 beta (IL-1 $\beta$ , 3-fold), and interferon gamma (IFN $\gamma$ , 3-fold). Conclusion: The inflammatory response in brain to cerebral ischemia is attenuated in sEHKO mice, likely due to higher brain EETs. These findings suggest that protection in sEHKO mice may in part be linked to EETs-mediated suppression of brain's inflammatory response to cerebral ischemia, and that pharmacological inhibition of sEH may serve as a novel neuroprotective strategy against stroke damage. References: [1] Boutin H et al. J Neurosci 2001, 21:5528 [2] Shivachar AC et al. J Neurochem 1995, 65:338 [3] Node K et al. Science 1999, 285:1276 [4] Liu M et al. Curr

Drug Metab 2004, 5:225



**PPAR- $\gamma$  AGONIST ROSIGLITAZONE DECREASES FOCAL CEREBRAL ISCHEMIA-INDUCED INFLAMMATION AND BRAIN DAMAGE IN ADULT MICE**Kudret Tureyen, Ramya Sundaresan, Kellie Bowen, **Raghu Vemuganti***Department of Neurological Surgery, University of Wisconsin, Madison, WI, USA*

Acute inflammation contributes to brain damage after focal cerebral ischemia. Although several transcription factors are known to be upregulated in the post-ischemic brain, the role of transcriptional events in controlling cerebral inflammation is not evaluated in detail. Peroxisome proliferation activated receptor- $\gamma$  (PPAR- $\gamma$ ) is a ligand activated transcription factor of nuclear hormone receptor superfamily. When a ligand binds to PPAR- $\gamma$ , it dimerizes with retinoic acid-X-receptor (RXR) to form a heterodimeric complex that binds to the cis-acting sequences (peroxisome proliferator response elements) on DNA to modulate the transcription of target genes. Thiazolidinediones rosiglitazone and pioglitazone are potent exogenous agonists of PPAR- $\gamma$ . Rosiglitazone and pioglitazone are currently FDA-approved for the treatment of type-2 diabetes. PPAR- $\gamma$  agonists were shown to control inflammation associated with gut, myocardial and lung ischemia by blocking microglia/macrophage activation and pro-inflammatory gene expression. We evaluated the efficacy of rosiglitazone in preventing brain damage following transient middle cerebral artery occlusion (MCAO) in adult C57/BL6 mice. Real-time PCR analysis showed significant increases (by 2.7 to 4.2 fold;  $p < 0.05$ ;  $n$  of 6/group) in the PPAR- $\gamma$  and RXR mRNA expression in the ipsilateral cortex compared to the contralateral cortex of mice at 6h to 72h of reperfusion following a 2h transient MCAO. Compared to vehicle treated controls, 2 mg/Kg rosiglitazone pretreated mice (2 doses; at 4h before MCAO and start of reperfusion) showed significantly smaller infarcts (by 57% $\pm$ 9%,  $p < 0.05$ ;  $n$  of 10 mice/group). A 2 dose post-treatment (at 1 min and 2h of reperfusion) also decreased the infarct volume by 52% $\pm$ 8% ( $p < 0.05$ ;  $n$  of 9 mice/group) compared to vehicle control. Neuroprotection was also observed with a 1 dose rosiglitazone (2 mg/Kg) injected at either 1 min (by 46% $\pm$ 8%,  $p < 0.05$ ;  $n$  of 10 mice/group) or 2h of reperfusion (by 37% $\pm$ 7%,  $p < 0.05$ ;  $n$  of 9 mice/group). In these mice, post-ischemic neurological deficits estimated on a 6-point scale were none to mild in the rosiglitazone groups compared to moderate to severe neurological deficits observed in the vehicle groups. Real-time PCR analysis showed a significant decrease in the post-ischemic mRNA expression of the pro-inflammatory transcription factors Egr-1 and c-EBP- $\beta$  and inflammatory genes IL-1 $\beta$ , IL-6, MCP-1, ICAM-1 and iNOS in the ipsilateral cortex of rosiglitazone-treated mice compared to vehicle treated controls ( $n$  of 6/group). Furthermore, the ipsilateral cortex of the rosiglitazone treated mice (2 mg/Kg at 5 min reperfusion) showed significantly decreased numbers of activated macrophages/microglia (identified by ED-1 and CD11b immunostaining), compared to vehicle treated mice. These studies showed that PPAR- $\gamma$  activation by its ligand is a potent anti-inflammatory mechanism that can decrease the post-ischemic brain damage. Rosiglitazone potassium salt used in these studies was purchased from the Cayman Chemicals USA. These studies were funded by an RO1 grant from the United States National Institute of Health to RV.

**PARP-1 PROMOTES MICROGLIAL ACTIVATION, PROLIFERATION, AND MMP-9 - MEDIATED NEURON DEATH****Tiina M. Kauppinen**, Raymond A. Swanson*UCSF/VAMC, Neurology, San Francisco, CA, USA*

Activated microglia contribute to cell death in ischemic and neurodegenerative disorders of the central nervous system. Microglial activation is regulated in part by NF- $\kappa$ B, and the nuclear enzyme poly(ADP-ribose) polymerase-1 (PARP-1) enhances NF- $\kappa$ B binding to DNA. Here, the role of PARP-1 in microglia-mediated neurotoxicity was assessed using microglia from wild type (wt) and PARP-1<sup>-/-</sup> mice. Cultured microglia were incubated with tumor necrosis factor  $\alpha$  (TNF $\alpha$ ), a cytokine that is upregulated in many neurological disorders. When stimulated with TNF $\alpha$ , wt microglia proliferated, underwent morphological changes characteristic of activation, and killed neurons placed in co-culture. The effects of TNF $\alpha$  were markedly attenuated both in PARP-1<sup>-/-</sup> microglia and in wt microglia treated with the PARP enzymatic inhibitor 3,4-dihydro-5-[4-(1-piperidinyl)butoxy]-1(2h)-isoquinolinone (DPQ). These effects were also blocked by (E)-3-(4-methylphenylsulfonyl)-2-propenenitrile (BAY 11-7082), which inhibits translocation of NF- $\kappa$ B to the nucleus. TNF $\alpha$  also upregulated microglial release of matrix metalloproteinase-9 (MMP-9), an enzyme with potential neurotoxic properties that is transcriptionally regulated by NF- $\kappa$ B. This upregulation was blocked in PARP-1<sup>-/-</sup> microglia and in wt microglia by the PARP inhibitor DPQ. Microglia from MMP-9<sup>-/-</sup> mice were used to evaluate the contribution of MMP-9 to microglial neurotoxicity. MMP-9<sup>-/-</sup> microglia treated with TNF $\alpha$  showed substantially reduced neurotoxicity relative to the wt microglia. TNF $\alpha$ -stimulated wt microglia treated with the MMP inhibitor ilomastat also showed reduced neurotoxicity. These findings suggest that PARP-1 activation is required for both TNF $\alpha$  - induced microglial activation and the neurotoxicity resulting from TNF $\alpha$  - induced MMP-9 release.

## HSP70 PROTECTS AGAINST EXPERIMENTAL STROKE THROUGH THE INHIBITION OF POSTISCHEMIC INFLAMMATORY REACTION

Zhen Zheng<sup>1</sup>, Yanli Qiao<sup>2</sup>, Nina Dunphy<sup>2</sup>, Joyce Ma<sup>2</sup>, Jong Eun Lee<sup>3</sup>, M.A. Yenari<sup>1</sup>

<sup>1</sup>Neurology, UCSF/VAMC, San Francisco, CA, USA

<sup>2</sup>Department of Neurosurgery, Stanford University School of Medicine, Stanford, CA, USA

<sup>3</sup>Yonsei University, Seoul, Korea

We and others previously showed that the inducible 70 kDa heat shock protein (HSP70) confers neuroprotection in the brain from ischemia. While the mechanism of such protection is believed to be through reduced protein misfolding and aggregation, recent evidence suggests that HSP70 may also modulate the inflammatory response in certain of pathological settings. Whether this is relevant following ischemic insults is unclear, however. Here we evaluated the effects of HSP70 overexpression on glial cell activation and nuclear factor kappa-B (NFκB) activity using in vivo and in vitro ischemia models. Primary cultures of astrocytes and microglia were prepared from neonatal pups and subjected to simulated ischemia (oxygen-glucose deprivation), then assessed for cell death. Sister cultures were activated by exposure to lipopolysaccharide (LPS) and assessed for NFκB translocation and nitric oxide (NO) production. Transgenic mice overexpressing rat HSP70 or wildtype mice underwent 2 hours of middle cerebral artery occlusion (MCAO) plus 24 hours of reperfusion (n=6/group), or were given 5 mg/kg lipopolysaccharide (LPS) intraperitoneally (n=6/group). Infarct size was assessed by using cresyl violet stains; the neurological deficit was evaluated using a semiquantitative scale (Bederson et al, 1986); microglial activation was assessed using isolectin B4 (IB4) and an antibody against MHC-classII. The DNA-binding capacity of NFκB was assayed using the Trans-AM NFκB p65 transcription factor assay kit (Active Motif, Carlsbad, CA). Phosphorylation of IκB was detected using western blots; nuclear NF-κB translocation was assessed by fluorescent immunohistochemistry. In transgenic mice, compared to wildtype, infarct size was significantly reduced by 48% (P<0.01) after experimental stroke and this effect was related to 51% reduction of activated microglia (P<0.01). In LPS-treated transgenic mice, microglia activation was also decreased by 32% (p<0.05), compared with wildtype. HSP 70 transgenic mice had improved neurological deficits compared with wildtype littermates 24 h after ischemia onset (p<0.05). Chemiluminescent detection revealed that the DNA-binding capacity of NFκB was significantly decreased in ischemic brain regions among transgenic mice compared with wildtype mice (p<0.05). Western blots showed that HSP70 overexpression did not change IκB expression, but IκB phosphorylation was remarkably inhibited among HSP70 transgenic mice. Co-immunoprecipitation of HSP70 and NFκB p65 subunit indicated that the two proteins were bound to one another, especially within the cytosol. In cultures, HSP70 overexpression led to improved survival of both transgenic astrocytes and microglia (90% and 48% reduced cell death, respectively, P<0.01). Transgenic astrocyte cultures also expressed 82% less NO following LPS stimulation (P<0.05) and suppressed nuclear NF-κB translocation. These data suggest that HSP70 protects against ischemia and simulated ischemia followed by reperfusion, and this protection may be associated with the inhibition of the postischemic inflammatory response. Support Contributed By: NINDS and AHA Postdoctoral Fellowship Award (0325089Y)

**BLOOD LYMPHOCYTES INDICATE ON DIFFERENT ROLE OF TGF-B AND PDGF-AB AT CEREBRAL AND CORONARY ATHEROSCLEROSIS.****Andrei I. Teplyakov***Research Institute for Ecopathology and Occupational Disease, Mogilev, Belarus*

We hypothesized that proatherogenic T cells are controlled by cytokines network balance. Among them, TGF-b has been implied in atherogenesis, but its mechanism of action remains unclear. Taken together, abrogation of TGF-b signaling in T cells able to accelerate the atherosclerosis and permit to suggest that TGF-b reduces atherosclerosis by dampening T cell activation. Inhibition of T cell activation may therefore represent a strategy for antiatherosclerotic therapy. Goal: to analyze the possible evidence for TGF-b action on lymphocytes functions (Go chromatin topography changes) in vitro at cerebral and coronary atherosclerosis. Object: 29 patients. The original research technique has been used: adding TGF-b to achievements the final concentration: 0.05, 0.5 and 5.0 ng/ml in whole blood sampled PDGF-AB for achievement final concentration in whole blood sample: 0.5, 5.0 and 10.0 ng/ml (without separation procedure to goal to do not disturb the "habitual" cell-cell coordination additionally, i.e. approximated the conditioning in vivo) with following incubation in plastic tube for each sample. The lymphocytes chromatin nuclei behavior was estimated after 30, 60 and 360 min for each samples. The chromatin of lymphocytes nuclei was studied using Computer TV Morphodensitometry System "DiaMorph" (Russia) in the smears dyed especially for DNA. Results are contraindicated to habitual opinions about common atherogenic mechanisms without evaluation of organ-target influence. At first sight, it seem to be possible that mechanisms of sensitivity to PDGF have switched on (i.e. PDGF at cerebral atherosclerosis acted in other manner or in assembly to other factor, which are could be known). However, more complex manner of chromatin changes of lymphocytes, implicated in atherogenesis, have shown, that they have underwent by most of involved components of cytokines network factors, which are reversed timely. The main detected features at cerebral in comparison to coronary atherosclerosis have consist of initial hetero- and euchromatin rebuilding. Obtained results have conflicted to becoming fixed opinion that cerebral and coronary atherosclerosis are common process, unified any atherosclerosis without locations evaluation. So it is possible, that the detected changes have resulted more disseminated vascular implication in cerebral atherosclerosis in comparison to coronary ones. Conclusion. Obtained results are controversial to described the dampening lymphocytes activation, induced by TGF-b. We have no satisfied results, evidenced the TGF-b suppressive manner on lymphocytes functioning at atherosclerosis. Received results, in our opinion, reflects the more complicated interaction between TGF-b and lymphocytes functioning changes. It has been confirmed by the facts, that G0 lymphocytes chromatin (dependent from concentration and exposition time) have changed its portrays on biphasic manner after PDGF-AB adding: initially at short period of time we detected the same nuclear activation (and gene expression activation, correspondingly) with following stable chromatin topography changes, reflected the stable lymphocytes functioning changes on pathologic manner, which is needed to more detail investigation.

**NEUROGENESIS IN ORGANOTYPIC HIPPOCAMPAL SLICE CULTURES  
INHIBITED BY INFLAMMATION EARLY AFTER OXYGEN-GLUCOSE  
DEPRIVATION IS RESTORED AT LATER TIME POINT**

**Olga Chechneva<sup>1</sup>, Klaus M. Dinkel<sup>1,2</sup>, Klaus G. Reymann<sup>1,2</sup>**

<sup>1</sup>*Leibniz Institute for Neurobiology, Project Group Neuropharmacology, Magdeburg,  
Germany*

<sup>2</sup>*Institute for Applied Neuroscience (FAN GGmbH), Magdeburg, Germany*

The neurogenesis in the dentate gyrus (DG) of the hippocampus is regulated by many factors including the pathological conditions like stroke, epilepsy, traumatic injury or inflammation. Increase of neurogenesis occurring in response to injury has been reported and considered as a mechanism of regeneration after neuronal loss. We studied the neurogenesis in organotypic hippocampal slice cultures (OHCs) after oxygen and glucose deprivation (OGD). 14 days old OHCs from P7-9 rats were exposed to 40 min of OGD. OGD caused the neuronal damage that reached the significant level at 6h as revealed by propidium iodide uptake. At the same time point activation and increase in number of microglial cells was observed that resulted in the development of inflammatory reaction in the system. Application of anti-inflammatory drug indomethacine (10 $\mu$ M) prevented neuronal degeneration. Upregulation of pro-inflammatory cytokines was found 8h after OGD. qPCR showed 4 fold increase in the IL-1 $\beta$  and 2 fold increase in TNF- $\alpha$  mRNA. To label proliferating cells the OHCs were treated with bromodeoxyuridine (BrdU) and increase in cell proliferation was revealed by BrdU immunohistochemistry at 16h after OGD. Newly generated neurons were detected with early neuronal markers doublecortin (DCX) and  $\beta$ -III Tubulin. The neurogenesis (DCX immunostaining) was restricted in the dentate gyrus where the BrdU/DCX+ neurons could be found already at day 3 after first BrdU application with further increase to day 6. At early time point (3d) after OGD very few BrdU/DCX+ cells might be observed in DG however at 6d the number of BrdU/DCX+ neurons increased and some of the newly generated neurons expressed  $\beta$ -III Tubulin. Our data indicate that OGD results in the neuronal degeneration and activation of inflammatory reactions that inhibit the basal neurogenesis in the DG at early time point. However neurogenesis seems to restore later on.

**NEUROPROTECTIVE ROLE OF FC GAMMA RECEPTOR IN ISCHEMIA-REPERFUSION INJURY USING FC GAMMA RECEPTOR KNOCKOUT MICE****Takao Urabe, Miki Komine-Kobayashi, Ning Zhang, Yoshikuni Mizuno***Department of Neurology, Juntendo University School of Medicine, Tokyo, Japan*

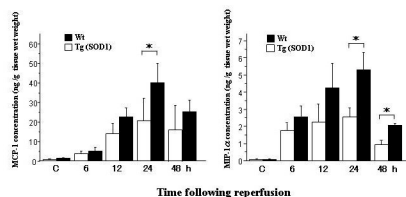
Background and Purpose: Cerebral ischemia-reperfusion injury is associated with the development of inflammatory response including pathologic contributions by vascular leukocytes and endogenous microglia. Expression of Fc receptors (FcRs) on macrophages and microglia is thought to be involved in the inflammatory cascade. The present study assessed the role of FC gamma receptor in ischemia-reperfusion injury, using Fc gamma receptor knockout (FCgR<sup>-/-</sup>) mice and bone marrow chimera FCgR<sup>-/-</sup> mice, which express enhanced green fluorescent protein (EGFP). Methods: Studies were conducted in 8-week old FCgR<sup>-/-</sup> and C57BL/6 (wild-type, WT) (n=50/group) mice of the same genetic background. Mice underwent occlusion of the middle cerebral artery for 60 minutes, followed by reperfusion. We generated the FcγR<sup>-/-</sup>/EGFP transgenic model by bone marrow transplantation of EGFP into FcγR<sup>-/-</sup> mice and induced transient cerebral ischemia in these animals 6 weeks later. At 6, 12, 24, 72 h, or 14 days post-reperfusion, the mice were anesthetized by intraperitoneal injection of 50 mg/kg pentobarbital (n=5/group) and decapitated. Infarct volume and mortality was calculated at several time points after ischemia. To clarify the function and distribution of microglia/macrophages, immunohistochemical staining and immunoblotting of ionized calcium-binding adapter molecule 1 (Iba-1), inducible nitric oxide synthase (iNOS), and nitrotyrosine were performed. Results: FCgR<sup>-/-</sup> mice showed significantly reduced mortality (20%) and smaller infarcts (P < 0.001) than wild-type (WT) mice at 72 hours post-reperfusion. FcγRI staining was detected in glial cells, which morphologically resembled microglia. However, no specific FcγRI staining was noted in the brain of FcγR<sup>-/-</sup> mice. In FcγR<sup>-/-</sup> mice, microglial activity in the transition area was weak compared with WT mice. In WT mice, induction of iNOS in microglia of peri-ischemia area reached a peak level at 48-72 h post-reperfusion. On the other hand, in FCgR<sup>-/-</sup> mice, iNOS was only detected in endothelial cells of the ischemic core area. Western blotting revealed that microglial activation (P < 0.002) and induction of iNOS (P < 0.005) was reduced in FCgR<sup>-/-</sup> mice compared with WT mice. At 7 days post-reperfusion, sections double-immunostained for EGFP and Iba-1 showed less activation and migration of EGFP-positive bone marrow-derived macrophages in FCgR<sup>-/-</sup> chimera mice than WT mice. In WT/EGFP chimera mice, induction of nitrotyrosine in microglia of transition area was detected and nitrotyrosine-staining was observed in the luminal surface of vessels at ischemic lesion, while there were few nitrotyrosine-positive cells in FCgR<sup>-/-</sup>/EGFP chimera mice. These nitrotyrosine-positive microglia did not stain for EGFP. Conclusions: In this study, we demonstrated that FcγR deficiency decreased the inflammatory responses through microglial activation, iNOS induction and bone marrow-derived macrophage infiltration after transient focal cerebral ischemia/reperfusion. Therefore, Our results demonstrated that the neuroprotective effect of FcγR deficiency in our model might be primarily attributed to the suppression of activation and infiltration of inflammatory cells. Our data showed that anti-inflammatory therapy through the FcγR might be useful for neuroprotection after cerebral infarction.

## SOD1 OVEREXPRESSION REDUCES MCP-1 AND MIP-1 $\alpha$ EXPRESSION AFTER TRANSIENT FOCAL CEREBRAL ISCHEMIA

Tatsuro Nishi, Carolina M. Maier, Hidenori Endo, Hiroshi Kamada, Pak H. Chan

*Department of Neurosurgery, Department of Neurology and Neurological Sciences, and Program in Neurosciences, Stanford University School of Medicine, Stanford, CA, USA*

**Introduction:** Proinflammatory cytokines and chemokines are quickly upregulated following ischemia/reperfusion (I/R) injury. However, the relationship between I/R-induced oxidative stress and cytokines/chemokine expression has not been elucidated. Overexpression of some of these molecules has been shown to exacerbate ischemic injury, while their deficiency has been shown to confer neuroprotection. Our hypothesis is that, if oxidative stress is involved in cytokine/chemokines-induced neuronal death, then we should observe the upregulation of these inflammatory molecules in the ischemic brain. Furthermore, reducing the oxidative stress should also lessen the cytokine/chemokine expression. To test our hypothesis, we first investigated the temporal profile of cytokine and chemokine gene expression in transient focal cerebral ischemia using cDNA array technology. Based on those results, we then proceeded to compare the gene and protein expression profiles of monocyte chemoattractant protein 1 (MCP-1) and macrophage inflammatory protein 1  $\alpha$  (MIP 1 $\alpha$ ) between wild-type (Wt) mice and copper/zinc-superoxide dismutase (SOD1) transgenic (Tg) mice. **Method:** Male CD-1 mice (SOD1 Tg and Wt) were anesthetized with 1.5% isoflurane (68.5% nitrous oxide, 30 % oxygen), underwent MCA occlusion (60 min) and were reperused for 6, 12, 24, or 48 h ( n = 4 per group & per time point). We monitored the physiological variables prior, during and after the surgery. Body temperature was maintained at 37 C throughout the surgical procedure. MCP-1 and MIP-1 $\alpha$  gene expression was investigated by real-time quantitative RT-PCR, and protein expression was examined by immunohistochemistry and ELISA. **Result:** MCP-1 and MIP-1 $\alpha$  gene expression was significantly upregulated at 6 to 12 hours of reperfusion. In SOD1-Tg mice, however, MCP-1 and MIP-1 $\alpha$  mRNA expression was significantly decreased 12 hours post-insult. MCP-1 immunoreactivity, observed throughout the cellular cytoplasm, was more intense in the striatum (ischemic core) compared with the cortex in Wt animals. MCP-1 immunopositive staining was observed at 12 to 48 hours of recirculation with peak intensity observed at 24 hours. SOD1-Tg mice showed less MCP-1 immunoreactivity even within the ischemic core. MIP-1 $\alpha$  immunopositivity was observed in the ischemic penumbra at 6 to 48 hours in both Wt and SOD1-Tg mice; however, the latter showed qualitatively less immunoreactivity than their Wt littermates. ELISA results showed that SOD1-Tg mice had significantly lower MCP-1 and MIP-1 $\alpha$  levels at 24 hours of reperfusion compared with Wt animals. Double-immunohistochemistry showed that MCP-1 was expressed in neurons, astrocytes and endothelial cells, while MIP 1 $\alpha$  was colocalized only activated microglia. **Conclusions:** These results suggest that MCP-1 and MIP-1 $\alpha$  expression is influenced by the I/R-induced oxidative stress that occurs following a transient focal stroke. Supported by NIH grants NS 14543, NS25372, NS36147, NS 38653 and Bugher Award from AHA



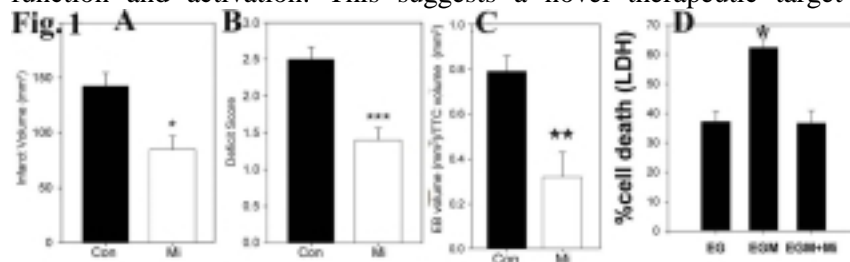
## MICROGLIA POTENTIATE INJURY TO THE BLOOD BRAIN BARRIER: REVERSEAL BY MINOCYCLINE

Xian N. Tang<sup>1</sup>, Yanli Qiao<sup>2</sup>, Lijun Xu<sup>2</sup>, Rona Giffard<sup>2</sup>, Midori A. Yenari<sup>1</sup>

<sup>1</sup>*Department of Neurology, University of California, San Francisco & SF VAMC,  
San Francisco, CA, USA*

<sup>2</sup>*Department of Anesthesia, Stanford University, Stanford, CA, USA*

**Background and Purpose-** Microglial function is a double edged sword. Under normal circumstances, it supplies neurons with trophic factors, contributes to the rearrangement of neural connections and plasticity of normal brain tissue. But after stroke, microglia are activated and may potentiate ischemic injury. Blood-brain barrier (BBB) disruption can complicate stroke due to edema and hemorrhage. Minocycline is a semisynthetic second-generation tetracycline known to inhibit microglial activation. In this study, we examined the influence of microglia on blood brain barrier (BBB) components and whether this could be reversed by minocycline treatment. **Methods-** In vitro, neocortical astrocytes (G), endothelial cells (E) and microglia (M) were isolated from postnatal Swiss Webster mice. Primary EG or EGM mixed cultures were prepared. Cultures were subjected to oxygen & glucose deprivation followed by reperfusion. In vivo, 28 C57BL/6J male mice (25~30 grams) were subjected to 1.5 h middle cerebral artery occlusion followed by 22.5 h reperfusion. Mice were treated with minocycline (Mi) (n=16) or vehicle (n=12). **Results-** When microglia were added to cocultures, cell death nearly doubled compared to cocultures lacking microglia (\*P<0.01). The increase in cell death in the presence of microglia could be reversed by minocycline (\*P<0.05) (Fig 1D). Infarct volume (Fig. 1A, \*P<0.01), Evans blue extravasation (Fig. 1C, \*\*P<0.001) and neurological deficit scores (\*\*\*P<0.001, Fig. 1B) decreased significantly in the minocycline treated mice compared with the vehicle treated group. Minocycline also prevented the occurrence of gross cerebral hemorrhage (P<0.05). Fewer microglia and MHC Class II positive cells were found within the penumbra in minocycline treated mice (P<0.001, P<0.05, respectively). **Conclusions-** Minocycline can reduce BBB disruption and decrease injury to BBB components after ischemia by inhibiting microglial function and activation. This suggests a novel therapeutic target for stroke treatment.



**OSTEOPONTIN MEDIATES NEUROPROTECTION VIA INHIBITION OF INDUCIBLE NITRIC OXIDE SYNTHASE****Sebastian Jander<sup>1</sup>, Michael Schroeter<sup>1</sup>, David T. Denhardt<sup>2</sup>**<sup>1</sup>*Department of Neurology, Heinrich-Heine University, Düsseldorf, Germany*<sup>2</sup>*Department of Cell Biology and Neuroscience, Rutgers University, Piscataway, NJ, USA*

Neurodegeneration following ischemic stroke extends from the ischemic infarct to nonischemic subcortical regions such as the ipsilateral thalamus. At both sites, inflammation with activation of resident microglia/brain macrophage ensues and may exacerbate the degenerative process. Osteopontin (OPN) is a macrophage-derived secreted glycoprotein with cytokine-like and chemoattractant properties mediated via RGD-binding integrin receptors and CD44. OPN exerts proinflammatory effects in autoimmune conditions, but also participates in beneficial wound healing responses. Here, we addressed the role of OPN in ischemic brain injury using OPN knock-out (KO) mice in models of cortical stroke. Compared to wild-type (WT) animals, OPN KO mice exhibited unaltered infarct development at the primary injury site but greatly increased secondary neurodegeneration of the ipsilateral thalamus. Thalamic neurodegeneration in OPN-deficient mice was associated with excessive microglia activation and inflammatory gene expression and could be attenuated via pharmacologic blockade of the inducible nitric oxide synthase (iNOS). Thus, OPN provided neuroprotection through down-regulation of microglia activation and iNOS. OPN-dependent pathways may represent a new target of neuroprotective therapy in neurodegenerative diseases and stroke. Supported by the Deutsche Forschungsgemeinschaft (Ja 690/5-1).

**TEMPORAL PROGRESSION OF SEIZURES-INDUCED  
AMYGDALOALLOCORTICAL MICROVASCULAR INFLAMMATION LEADING  
TO EDEMA AND MULTIFOCAL MICROHEMORRHAGIC STROKE IN THE RAT**

Sima Mraovitch<sup>1,2</sup>, Angélique Régnier<sup>1,2</sup>, Yolande Calando<sup>1</sup>, Eric Vicaut<sup>2</sup>

<sup>1</sup>*Laboratoire de Recherche Cérébrovasculaire, CNRS, FR2363, Faculté de Médecine  
Université Paris VII, Paris, France*

<sup>2</sup>*Laboratoire D'Etude de la Microcirculation (EA 3509), Faculté de Médecine Université  
Paris VII, Paris, France*

Introduction: We have recently demonstrated that generalized convulsive seizures (GCS) induced by cholinergic stimulation of the thalamus provoke a focal post-seizures amygdaloallocortical neurovascular injury characterized by neuronal loss, microvascular TNF $\alpha$  and IL-1 $\beta$  expression and gliosis, followed by atrophy (1). Here we report the temporal progression and spatial specificity of the seizures-induced neurovascular amygdaloallocortical injury. Methods: Adult Wistar rats were injected stereotaxically with carbachol (55nmol in 100nl PBS) under halothane anesthesia unilaterally in the ventroposterolateral and reticular thalamic nuclei as previously described (2). Behavioral alterations were observed for 2 hours. After at least one episode of GCS, animals were sacrificed at 3h (n=2), 6h (n=3), 12h (n=2), 24h (n=3), and 72h (n=3). Brain sections immunohistochemically processed for COX-2, TNF $\alpha$  and IL-1 $\beta$  staining were examined with a camera lucida. Edema and microhemorrhage sites were estimated on digital photographs of fresh frozen tissue using an image analyser. Results: Three hours after the initial GCS, neuronal COX-2 induction was observed bilaterally throughout the brain. However, as compared to the contralateral side, the ipsilateral side was devoid of neuronal COX-2 expression in the insular and perirhinal cortices, in the amygdaloid complex including the basolateral, the posteromedial cortical amygdaloid nuclei and the amygdalohippocampal area. At approximately 6h after the initial GCS, the TNF- $\alpha$  and IL-1 $\beta$  staining was clustered in the COX-2 devoid area including the rostral part of the amygdaloallocortical area, the claustrum and the dorsal endopiriform nucleus, the piriform cortex and the basolateral, central and medial amygdaloid nuclei, as well as in the internal capsule. Between 12h and 24h, IL-1 $\beta$  induction was also seen in microglia/macrophage-like cells throughout the allocortex and amygdala, particularly the insular cortex, the perirhinal cortex, the upper layer of the piriform cortex, the posteromedial, posterolateral cortical amygdaloid nuclei and the amygdalopiriform transition. Edema, seen as a gray area on fresh frozen tissue coronal sections, appeared at 24h after the initial GCS along the rostro-caudal amygdaloallocortical axis and remained relatively unchanged up to 72h. Rostrally to the anterior commissure, edema was observed in the insular cortex, the piriform cortex, the dorsal endopiriform nucleus and the claustrum representing  $6\pm 0.2\%$  (n=5) of the total coronal surface area. Caudally, edema was observed in the perirhinal cortex, the basolateral and the centromedial amygdala, the anterior cortical amygdaloid nucleus and amygdalopiriform transition reaching  $11\pm 0.1\%$  (n=5) of the total coronal surface area. Edema was associated with multifocal microhemorrhage scattered along the rostro-caudal amygdaloallocortical axis. Conclusion: We conclude that generalized convulsive seizures elicited by cholinergic stimulation of the thalamus are at the origin of amygdaloallocortical microvascular inflammatory processes leading to edema and multifocal microhemorrhage. The spatial distribution of multifocal microhemorrhages was shown to correlate with microvascular and glial-like cells expressing TNF- $\alpha$  and IL-1 $\beta$  within the amygdaloallocortical area characterized by reduced and/or absent neuronal COX-2 expression. References: (1) Mraovitch S. Isocortical hyperemia and allocortical inflammation and atrophy following generalized convulsive seizures of thalamic origin in the rat. *Cell Molec Neurobiol* 23 (4/5) 773-791, 2003. (2) Mraovitch S., Calando Y. Limbic and/or generalized convulsive seizures elicited by specific sites in the thalamus. *Neuroreport*. 6: 519-23, 1995.



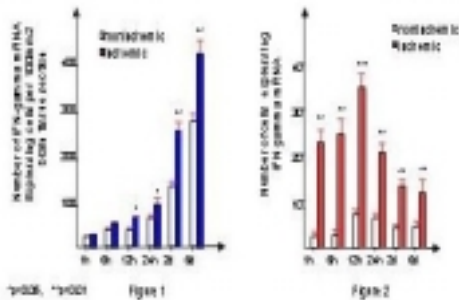
## INTERFERON-GAMMA EXPRESSING IN FOCAL RABBIT CEREBRAL ISCHEMIC INJURY

Xiaoping Wang<sup>1</sup>, Fengcai Tang<sup>2</sup>

<sup>1</sup>*Division of Neonatal-Perinatal Medicine, Emory University, Atlanta, GA, USA*

<sup>2</sup>*Harbin Medical University, Department of Neurobiology, Harbin, China*

**Introduction:** Interferon , a proinflammatory cytokine which has traditionally been associated with inflammatory CNS, may be involved in the mechanisms of cerebral ischemia. To investigate a potential role of interferon-gamma on brain injury caused by focal cerebral ischemia (FCI), we investigated the expression of interferon-gamma mRNA in the cortex at various times after FCI. **Methods:** FCI was induced by inserting a nylon monofilament suture embolus into the right external carotid artery to occlude the middle cerebral artery (MCA) in New Zealand white rabbits[1]. At various periods (1, 6, 12, 24h, 2d, and 6d) after FCI, the brains were obtained, and frozen sections were prepared for INTERFERON-GAMMA mRNA in situ hybridization(n=6). interferon-gamma mRNA in peripheral blood was also measured(n=6). **Results:** In ischemic brain tissues, interferon-gamma mRNA began to increase from 1 h after FCI and peaked 6d after FCI (Fig. 1). In contrast, in the non-ischemic cortex, interferon-gamma mRNA also increased from 2d to 6d after FCI. When compared to the non-ischemic side, interferon-gamma mRNA was significantly increased in the ischemic hemisphere from 12h to 6d after FCI. (Fig.1). Additionally, in peripheral blood, interferon-gamma mRNA significantly increased at various times after FCI (Fig. 2). **Conclusion:**These results suggested that interferon-gamma might involve in the inflammation progress after cerebral ischemia and cause brain injury. **Reference:**1. Longa, E.Z., Weinstein, P.R., Carlson, S., Cummins, R., 1989. Reversible middle cerebral artery occlusion without craniectomy in rats. *Stroke* 20, 84-91

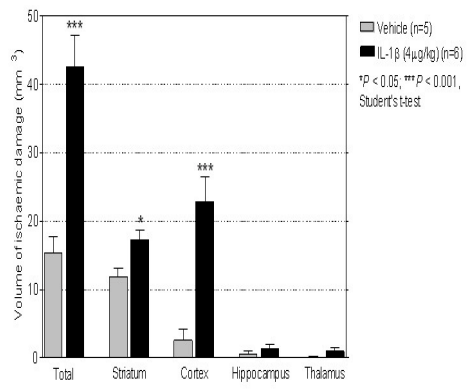


## PERIPHERAL ADMINISTRATION OF INTERLEUKIN-1 $\beta$ EXACERBATES ISCHAEMIC BRAIN DAMAGE AFTER TRANSIENT FOCAL ISCHAEMIA IN MICE

Barry W. McColl, Nancy J. Rothwell, Stuart M. Allan

*Division of Neuroscience, Faculty of Life Sciences, University of Manchester, Manchester, UK*

**Introduction** Interleukin-1 $\beta$  (IL-1 $\beta$ ) is a proinflammatory cytokine implicated in the pathogenesis of ischaemic brain damage. In experimental models of cerebral ischaemia, IL-1 $\beta$  expression is up-regulated and administration of IL-1 $\beta$  intracerebroventricularly or into the brain parenchyma exacerbates ischaemic damage. Conversely, administration of the IL-1 receptor antagonist is neuroprotective (1). IL-1 $\beta$  expression is also elevated in systemic inflammatory conditions, such as atherosclerosis, and acute infection (2), which are risk factors for stroke (3). However, the effects of increased systemic IL-1 $\beta$  levels on ischaemic brain damage have not been studied. The present study determined the effects of peripheral IL-1 $\beta$  administration on outcome after transient focal ischaemia in mice. **Methods** Transient focal ischaemia (30min) was induced in C57Bl/6J mice (25 – 28g) by intraluminal filament occlusion. Anaesthesia was induced with 3% halothane in 70% N<sub>2</sub>O and 30% O<sub>2</sub> and maintained with 1.5 – 2% halothane in the same mixture. A 6-0 nylon monofilament, coated at the tip (2mm; 180 $\mu$ m diameter) with “thermo-melting” glue, was positioned to occlude the middle cerebral artery. At the onset of occlusion, mice received an intraperitoneal injection of vehicle (0.5% bovine serum albumin in PBS; n = 5) or recombinant human IL-1 $\beta$  (4 $\mu$ g/mg; n = 6). The filament was withdrawn after 30min to allow reperfusion. Neurological deficit (4) was assessed at 4h and 24h after occlusion. Brains were removed 24h after occlusion and frozen in isopentane (-42°C). Coronal sections (20 $\mu$ m) were cut at 200 $\mu$ m intervals, stained with cresyl violet and the volume of ischaemic damage measured as described (5). **Results** Peripheral IL-1 $\beta$  treatment significantly increased the total volume of ischaemic damage compared to vehicle treatment (43  $\pm$  5mm<sup>3</sup> vs. 15  $\pm$  3mm<sup>3</sup>, P < 0.001). IL-1 $\beta$  treatment also significantly increased the volume of ischaemic damage in the striatum (17  $\pm$  1mm<sup>3</sup> vs. 12  $\pm$  1mm<sup>3</sup>, P < 0.05) and cerebral cortex (23  $\pm$  3mm<sup>3</sup> vs. 3  $\pm$  2mm<sup>3</sup>, P < 0.001). The neurological deficit score was greater at 4h and 24h after occlusion in the IL-1 $\beta$ -treated group compared to the vehicle-treated group, although this reached statistical significance only at 24h (2  $\pm$  0.3 vs. 1  $\pm$  0.2, P < 0.05). **Conclusions** These data show that peripheral IL-1 $\beta$  administration exacerbates ischaemic brain damage and neurological deficit after transient focal ischaemia and suggest that the systemic inflammatory status may be an important modulator of outcome to ischaemic brain injury. Further characterisation of the peripheral inflammatory response after cerebral ischaemia may reveal novel targets for therapeutic intervention. **References** (1) Rothwell NJ. *Brain Behav Immun* 2003, 17: 152-157. (2) Perry VH et al. *Nat Rev Neurosci* 2003, 4: 103-112 (3) Emsley HC and Tyrrell PJ. *J Cereb Blood Flow Metab* 2002, 22: 1399-1419 (4) Bederson JB et al. *Stroke* 1986, 17: 472-476 (5) Touzani O et al. *J Neurosci* 2002, 22: 38-43



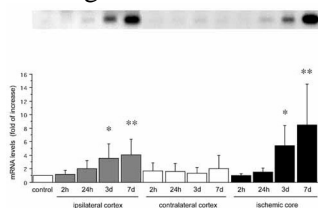
## EXPRESSION OF CYCLOPHILIN C-ASSOCIATED PROTEIN AND CYCLOPHILIN C MRNAS IN FOCAL CEREBRAL ISCHEMIA

Tatsuya Shimizu<sup>1</sup>, Hideaki Imai<sup>1</sup>, Koji Seki<sup>1</sup>, Shinichiro Tomizawa<sup>1</sup>, Mitsunobu Nakamura<sup>1</sup>, Fumiaki Honda<sup>1</sup>, Nobutaka Kawahara<sup>2</sup>, Nobuhito Saito<sup>1</sup>

<sup>1</sup>Department of Neurosurgery, Gunma University Graduate School of Medicine, Maebashi, Japan

<sup>2</sup>Department of Neurosurgery, University of Tokyo Graduate School of Medicine, Tokyo, Japan

**Background and Purpose:** Immunophilin ligands, such as cyclosporin A and FK506, have neuro-protective effects in experimental stroke models, although the precise mechanism is unclear. Cyclophilin C-associated protein (CyCAP) is a natural cellular ligand for the immunophilin, cyclophilin C, and has a protective effect against endotoxins by down-modulating the proinflammatory response. The present study examined the pattern of expression of CyCAP and cyclophilin C mRNA within the ischemic hemisphere using Northern blotting and *in situ* hybridization at several time points (at 2 hours, 24 hours, 3 days, and 7 days) after focal cerebral ischemia. **Methods:** Permanent middle cerebral artery occlusion model (Tamura model) was employed in halothane anesthetized adult Sprague Dawley rats (300-330g, n= 30). Rats were decapitated at 2 hours, 24 hours, 3 days, and 7 days after ischemia. Sections of 20  $\mu$ m thickness were cut on a cryostat and were stained with hematoxylin and eosin, and examined by light microscopy. For *in situ* hybridization, these sections were applied by Digoxigenin -labeled antisense cRNA for CyCAP and cyclophilin C probes. For Northern blot analysis, total RNA was isolated from dissected region such as ipsilateral remote cortex, ischemic core cortex, and contralateral cortex. The [ $\alpha$ -<sup>32</sup>P] UTP-labeled cRNA probes for CyCAP and cyclophilin C were used. **Results:** Both CyCAP and cyclophilin C mRNAs were ubiquitously distributed in the neurons of the normal brain. Expression increased in neurons of the peri-infarct zone up to 7 days after MCA occlusion. The neuronal distribution was confirmed by counter-immunostaining of NeuN. Both mRNAs were predominantly expressed in microglia of the ischemic core at 7 days, confirmed by immunostaining with the microglial marker, ED1. The quantification of CyCAP and cyclophilin C mRNAs at 7 days by Northern blot analysis showed the 8.5 fold increase ( $P<0.005$ , n=6) and 6.8 fold increase ( $P<0.005$ , n=6), respectively, in ischemic core compared with control. **Conclusions:** The observed changes in CyCAP and cyclophilin C mRNA expression in response to permanent focal cerebral ischemia strongly suggest that these molecules participate in intrinsic tissue protection by providing neuroprotection as a mimic of cyclosporin A; by recruiting microglia/macrophages to remove potentially deleterious debris, promote tissue repair by secreting growth factors, and facilitate the return to tissue homeostasis; and by suppressing pro-inflammatory cytokines in response to ischemia. Preservation of these effects could represent a novel pharmacological approach to counter the inflammatory reaction triggered by cerebral ischemia. In addition, overexpression of CyCAP in the penumbra suggests a role in cell survival, an intriguing possibility that deserves further investigation.



**INNATE IMMUNE SIGNAL TRANSDUCTION MEDIATED  
HYPERPHOSPHORYLATION OF TAU AND INFLAMMATORY CHANGES IN  
HUMAN SH-SY5Y NEUROBLASTOMA CELLS**

**Nurun N. Begum<sup>1</sup>**, Toshihisa Tanaka, Golam Sadik, Md. Ashik B. Ansar, Takashi Kudo,  
Masatoshi Takeda

*Osaka University Graduate School of Medicine, Department of Psychiatry and Behavioral  
Proteomics Course of Advance Medicine, Osaka, Japan*

Immunological and inflammatory changes and hyperphosphorylation of Tau protein are observed in the pathogenesis of taupathies like Alzheimer's disease as well as Subacute Sclerosing Panencephalitis being caused by measles virus. However these pathological changes are yet to be interlinked in a common explainable background. In this study the relevance of mechanisms on phosphorylation of tau protein and up regulation of interleukins as a mediator of inflammation were investigated in relation with an innate immune signal transduction system. Toll-like receptors (TLRs) are the basic signaling receptors of the innate immune system. They are activated by molecules associated with pathogens or injured host cells and tissue. Toll like receptor-3 (TLR-3) has been shown to respond to double-stranded (ds) RNA, a replication intermediary for many viruses. Expression of TLR-3 in brain has been already reported. Activation of TLR-3 was known to transduce its signal into intracellular transduction pathway, leading to activation of JNK and p38 MAPK and also NF- $\kappa$ B; a transcription activator of various inflammatory mediators. Method and results: Total RNA was isolated from SH-SY5Y cells by using with an RNeasy kit (Qiagen) and the structural integrity of RNA was evaluated by observing the sharpness of 28s and 18s r RNA band. 2.8  $\mu$ gm of isolated RNA had been used to perform RT-PCR of TLR-3 in human neuroblastoma, SH-SY5Y cells. Thus the endogenous expression of TLR-3 in SH-SY5Y cells was initially confirmed at mRNA level by RT-PCR. Finally, expression of TLR-3 was confirmed at protein level by western blot analysis. Then the cells were treated with 50ug/ml of polyinosinic-polycytidylic acid (pIpC), a synthetic analogue of dsRNA and changes of phosphorylation of tau protein were investigated. Further the level of phosphorylation of tau protein was investigated when cells had been previously treated with 10 ng/ml of lipopolysaccharide (LPS) for 6 hours to induce over-expression of TLR-3. Increased phosphorylation of tau protein at PHF-1 site (Ser396/404) and activated JNK and p38 MAPK were observed in cells treated with pIpC. and these effects were enhanced when cells were pre-treated with LPS, a known transducer of TLR-3. We also evaluated the level of interleukin 6, one of the inflammatory mediator regulated by NF- $\kappa$ B in the down stream signal transduction of TLR-3. Conclusion: In this study for the first time, we evaluated the expression of TLR-3 and its functional consequences upon activation, in human SH-SY5Y neuroblastoma cells. These data suggest that Toll like receptor 3, an innate immune molecule might be a potential link between hyperphosphorylation of tau protein and inflammatory changes in neurodegenerative processes of Alzheimer's disease and other taupathies like Subacute Sclerosing Panencephalitis.

## THE TNFALPHA-TRANSGENIC RAT: A NEW MODEL OF CYTOKINE-MEDIATED ISCHEMIC BRAIN INJURY

L. Creed Pettigrew<sup>1,2</sup>, Mary L. Holtz<sup>1,2</sup>, Mark S. Kindy<sup>3,4</sup>, Thomas C. Foster<sup>5</sup>,  
David S. Grass<sup>6</sup>, Susan D. Craddock<sup>1</sup>

<sup>1</sup>*Department of Neurology and Sanders-Brown Center on Aging, University of Kentucky,  
Lexington, KY, USA*

<sup>2</sup>*Department of Veterans Affairs Medical Center, Lexington, KY, USA*

<sup>3</sup>*Department of Veterans Affairs Medical Center, Charleston, SC, USA*

<sup>4</sup>*Department of Physiology and Neuroscience, Medical University of South Carolina,  
Charleston, SC, USA*

<sup>5</sup>*McKnight Brain Institute, University of Florida, Gainesville, FL, USA*

<sup>6</sup>*Xenogen Biosciences, Cranbury, NJ, USA*

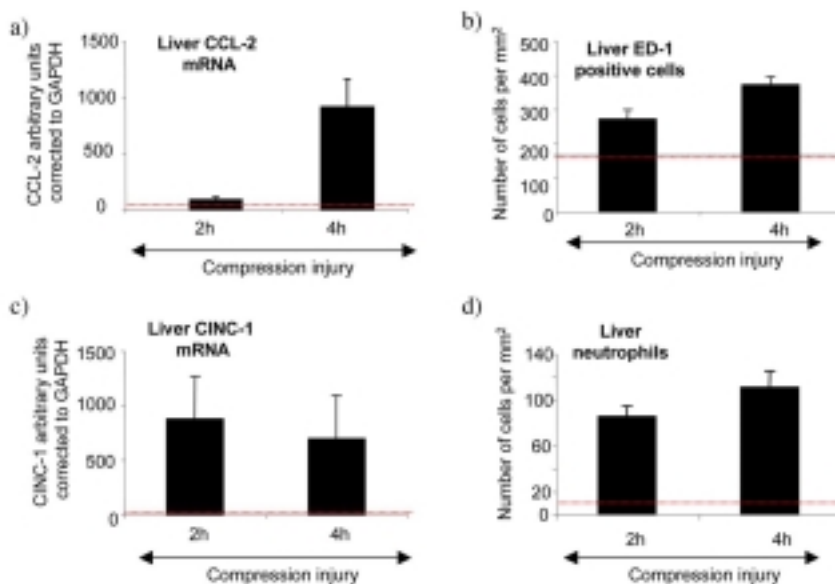
Introduction: Tumor necrosis factor-alpha (TNF $\alpha$ ) is a pleiotropic cytokine suspected to enhance or deter cellular survival by activation of signal transduction cascades. Brain tissue levels of TNF $\alpha$  are increased after middle cerebral artery occlusion (MCAO). We describe a new model of ischemic brain injury in a transgenic (Tg) rat overexpressing the murine TNF $\alpha$  gene. We tested the hypothesis that chronic elevation of TNF $\alpha$  in the brain of the Tg rat will expand infarct volume after MCAO and cause impairment of spatial discrimination compared to wild type (WT) controls, without affecting post-ischemic reperfusion. Methods: We constructed a Tg rat overexpressing the murine TNF $\alpha$  gene with its own promoter. Levels of TNF $\alpha$  protein were quantified in tissue homogenates prepared from Tg rats and WT controls. Parallel groups of Tg and WT rats underwent MCAO for 1 h before assessment of percent infarct volume 24 h or 7 d afterward. Animals rendered ischemic and sustained for 7 d underwent a spatial discrimination task in a Morris water maze before measurement of infarct volume. Cortical perfusion was monitored by laser-Doppler flowmetry (LDF) during and after MCAO. Results: TNF $\alpha$  protein in brain was fivefold higher in non-ischemic Tg vs. WT rats ( $57 \pm 12$  [SD] vs.  $10 \pm 3$  pg/100 mg protein;  $n=3$  per group;  $p \leq 0.01$ ; unpaired t test). At 24 h, mean %infarct volume was greater in Tg animals ( $32 \pm 11\%$ ;  $n=7$ ) than in WT controls ( $17 \pm 10\%$ ;  $n=9$ ;  $p \leq 0.01$ ; unpaired t test). Both groups learned a spatial discrimination task before ischemia (decrease in escape latencies over 5 trial blocks: WT  $34.4 \pm 16.3$  to  $8.7 \pm 7.2$  sec [ $n=10$ ];  $p=0.0002$ ; Tg  $44.3 \pm 10.9$  to  $25.8 \pm 22$  sec [ $n=6$ ];  $p=0.0012$ ; ANOVA /Fisher's test). No significant differences between non-ischemic groups were detected except in the fifth trial block ( $p=0.02$ ). Post-ischemic WT rats ( $n=7$ ) showed differential search strategy by spending more than 25% of allotted time in the goal quadrant ( $39.9 \pm 14\%$ ;  $p=0.03$ ; t-test). Tg rats ( $n=6$ ) failed to demonstrate preference for the goal quadrant that exceeded chance. No significant difference was detected in mean percent infarct volume measured at 7 d between post-ischemic WT ( $18 \pm 8\%$ ) and Tg ( $21 \pm 7\%$ ) rats. There were no significant differences between Tg and WT rats ( $n=10$  per group) in mean cortical perfusion measured by LDF at pre-ischemic baseline, during 1 h of ischemia, or during 30 min of post-ischemic reperfusion. Conclusion: TNF $\alpha$  protein was elevated selectively in brain of Tg rats and remained low in serum and external organs. Overexpression of TNF $\alpha$  in brain had no effect on cortical perfusion during and after MCAO, but probably contributed to greater observed infarct volume in Tg animals at 24 h. The difference in infarct volume between WT and Tg animals observed after 24 h was not apparent after 7 d of post-ischemic reperfusion. This may indicate time-related amelioration of acute inflammatory reactions. Both groups of non-ischemic animals performed successfully in cognitive assessment tasks. Ischemic WT rats maintained spatial discriminatory skills while Tg rats failed to persist in the goal quadrant appropriately, perhaps due to the effect of chronic TNF $\alpha$  expression on synaptic architecture.

## THE HEPATIC CHEMOKINE RESPONSE TO SPINAL CORD INJURY - A NEW TARGET FOR THERAPEUTIC INTERVENTION

Sandra J. Campbell, Daniel C. Anthony

*Department of Pharmacology, University of Oxford, Oxford, UK*

Following acute inflammation in the rodent brain, one of the earliest events is the hepatic release of regulatory acute phase proteins (APP), which occurs before there is any evidence of an inflammatory response in the brain. We have found that one of the first APPs to be released from the liver in response to interleukin-1 beta (IL-1 $\beta$ )-mediated experimental brain inflammation is the CXC chemokine, cytokine-induced neutrophil chemoattractant-1 (CINC-1). We now show that the hepatic chemokine response to injury is not restricted to the CXC chemokines and is a significant feature of the APR in a rodent model of spinal cord injury. CCL-2 and CINC-1 mRNA and protein, are rapidly expressed and released by the liver in response to injury. This hepatic chemokine response controls monocyte and neutrophil mobilisation and recruitment to the spinal cord and to the liver. Elevated CCL-2/CINC-1 mRNA and protein were observed in the liver as early as 2h following a mild compression injury in the spinal cord compared to a sham operation with laminectomy. Intravenous injection of anti-CINC-1 alone was sufficient to inhibit the mobilisation of blood neutrophils and to inhibit the recruitment neutrophils to the injured cord and to the liver. CINC-1 inhibition also reduced lesion volume and preserved axon integrity. Thus hepatic chemokine production may regulate the CNS response to inflammation by controlling leukocyte recruitment to the injured spinal cord. Figure: A partial laminectomy was carried out at T8, and a controlled spinal cord compression injury was performed. Taqman RT-PCR (a, c) was used to assess the (a) CCL-2 and (c) CINC-1 mRNA levels in the liver 2h and 4h post-injury. Immunohistochemistry (b,d) was used to assess the number of activated kupffer cells/recruited monocytes (ED-1-positive cells) (b) and recruited neutrophils (d) in the liver post-spinal cord injury. Dashed red lines represent levels of mRNA and liver cells in naïve animals of the same age.

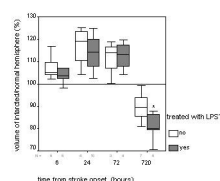


## SYSTEMIC ADMINISTRATION OF LIPOPOLYSACCHARIDE DURING TRANSIENT FOCAL CEREBRAL ISCHEMIA LEADS TO CHRONIC CNS INFLAMMATION

Kyra J. Becker, Darin L. Kindrick, Mark P. Lester, Connor P. Shea

*Department of Neurology, University of Washington School of Medicine, Seattle, WA, USA*

**Background:** Patients who become infected after stroke have worse neurological outcome than those who remain infection free. The nature of this association is unclear. We sought to determine the effects of lipopolysaccharide (LPS) administration during middle cerebral artery occlusion (MCAO) on neuropathology one month later. **Methods:** Male Lewis rats were subjected to 3 hours of MCAO. At the time of reperfusion, a subset of animals was injected intraperitoneally with LPS (1 mg/kg). Animals were sacrificed at various time points after stroke for histological and immunocytochemical analysis. Temperature and behavioral outcome were monitored. **Results:** Initial infarct size at 6, 24, and 72 hours did not differ between LPS(+) and LPS(-) animals. One month after MCAO, the ischemic hemispheres of LPS(+) animals were more atrophic than that of LPS(-) animals (Figure 1;  $P < 0.05$ ) and there were more apoptotic neurons in this hemisphere ( $P = 0.03$ ). LPS(+) animals also had evidence of ongoing CNS inflammation with more CD8+ cells in the ischemic hemisphere ( $P = 0.02$ ) and more neutrophils in the ischemic core ( $P = 0.04$ ). **Discussion:** We show that injection of LPS 3 hours after MCAO onset leads to long-term pathological changes in the brain consistent with chronic inflammation. Exposure to inflammatory stimuli after clinical stroke may similarly enhance the CNS inflammatory response and neuronal cell death in patients, which might be expected to lead to worse clinical outcome.





## EFFECTS OF INTRAUTERINE INFLAMMATION ON DEVELOPING MOUSE BRAIN

Xiaoyang Wang<sup>1</sup>, Carina Mallard<sup>1</sup>, Bo Jacobsson<sup>2,3</sup>, Henrik Hagberg<sup>1,2</sup>

<sup>1</sup>*Perinatal Center, Department of Physiology, Goteborg, Sweden*

<sup>2</sup>*Department of Obstetrics and Gynecology, Sahlgrenska Academy, Goteborg, Sweden*

<sup>3</sup>*North Atlantic Neuro-Epidemiology Alliances (NANEA), University of Aarhus, Aarhus, Denmark*

**OBJECTIVE** Clinical and experimental evidence indicate that the presence of intrauterine inflammation in pregnancy is not only a cause of preterm birth but is also associated with perinatal brain damage and long-term neurological handicap. In the present study, preterm delivery was induced using a recently developed model in C57BL/6 mice through intrauterine administration of lipopolysaccharide (LPS), and the neuropathological outcome was investigated in surviving pups. **METHODS** C57BL/6 mice were subjected to intrauterine infusion (between the amniotic and chorionic membranes) of LPS (250 µg/mouse or 125µg/mouse) or saline, at a time corresponding to 70% of average gestation (gestational day 15). Fetuses that survived after LPS administration were allowed to deliver and were sacrificed on postnatal 14 days (PND 14) at a time in development when myelination has started. Brain injury was examined in parallel sections stained with H & E, Lectin, microtubule associated protein 2 (MAP2), myelin basic protein (MBP) and glial fibrillary acidic protein (GFAP). **RESULTS** The brain weight of LPS-exposed pups (n=12) were significantly lower than that of saline-exposed pups (n=21) at PND14 (brain weight LPS  $0.278 \pm 0.008$  g vs. control  $0.303 \pm 0.005$ g,  $p=0.017$ ). In all LPS-exposed brain sections examined (n =12), 8 displayed various abnormalities that were not observed in any of the saline-exposed animals. Three brains displayed enlarged ventricles as determined in H&E stained sections. Four brains exhibited decreased MBP density in the white matter indicating hypomyelination. Focal cerebral white matter cysts surrounded by activated astrocytes were detected in 5 of the LPS-exposed pups. A focal cortical gray matter lesion was detected by MAP2 immunostaining. The infarct and border zone area was infiltrated with activated microglia and astrocytes. The wedge-like form of the injured area in combination with a vessel located centrally proximal to the lesion suggested a thrombotic infarction. None of these pathologies were detected in sham-treated animals. **CONCLUSIONS** LPS impaired brain development and various brain lesions were produced in both the white and gray matter in a clinically relevant model of preterm birth in mice. We suggest that some of this brain damage might be related to LPS-induced perturbation of coagulation. The mechanism by which LPS induces injury in the developing brain needs to be further explored.

**GONADAL HORMONES MODULATE LPS-INDUCED INFLAMMATORY MARKERS IN RAT CEREBRAL BLOOD VESSELS****Rayna Gonzales, Ali Razmara, Lorraine Sunday, Diana Krause, Sue Duckles***Pharmacology, University of California Irvine, Irvine, CA, USA*

Following ischemic injury, activation of inflammatory mechanisms plays a significant role in cerebrovascular pathogenesis. In the rodent model, previous studies suggest that endogenous female sex steroids attenuate cerebral ischemia/reperfusion injury following experimental stroke. Because sex hormones modulate the outcome of ischemic injury in brain tissue, we investigated the impact of chronic in vivo estrogen or testosterone administration on cerebrovascular inflammation induced by the potent endotoxin, lipopolysaccharide (LPS). We hypothesized that estrogen will suppress, while testosterone will exacerbate the induction of cyclooxygenase-2 (COX-2) and inducible nitric oxide synthase (iNOS), important mediators of vascular inflammation contributing to the onset of cerebral tissue injury. The localization of LPS-induced COX-2 and iNOS protein was confirmed in both the endothelial and vascular smooth muscle layers of cerebral blood vessels using antibody specific staining and confocal microscopy. Initial experiments were performed to establish peak induction of COX-2 and iNOS protein levels in cerebral vessel homogenates from female and male rats using Western blot. Protein levels of COX-2 and iNOS were greatest at 6 hours post LPS (2 mg/kg i.p.) injection; thus this time point was selected to determine the effect of estrogen or testosterone on LPS-induced inflammation in cerebral blood vessels. Fischer-344 rats were gonadectomized and implanted with hormone filled pellets for 3 weeks. Orchiectomized male rats were treated without (ORX) or with either testosterone propionate (ORX+T) or 17 beta-estradiol (ORX+E). Ovariectomized female rats were treated without (OVX) or with 17 beta-estradiol (OVX+E). LPS treatment increased protein levels of both COX-2 and iNOS in cerebral blood vessels from all groups compared to saline (6 hr) injected controls. However, the induction of COX-2 and iNOS protein by LPS was significantly attenuated in cerebral vessels from OVX+E and ORX+E compared to OVX and ORX controls, respectively. In contrast, there was a marked increase in LPS-induced COX-2 and iNOS protein levels in cerebral vessels from ORX+T compared to ORX controls. In conclusion, it is likely that opposing actions of testosterone and estrogen to modulate cerebrovascular inflammation may contribute to the well-known gender differences clinically observed in stroke incidence and outcome. Supported by NIH grant HL-50775 and AHA Postdoctoral Fellowship (RG).

## INTERLEUKIN-6 TRIGGERS HUMAN CEREBRAL SMOOTH MUSCLE CELL PROLIFERATION

Jinghua S. Yao<sup>1</sup>, Zheng Xue<sup>1</sup>, William L. Young<sup>1,2,3</sup>, **Guo-Yuan Yang**<sup>1,2</sup>

<sup>1</sup>*The Center for Cerebrovascular Research, Departments of Anesthesia and Perioperative Care, University of California, San Francisco, CA, USA*

<sup>2</sup>*Department of Neurological Surgery, University of California, San Francisco, CA, USA*

<sup>3</sup>*Department of Neurology, University of California, San Francisco, CA, USA*

Introduction: Interleukin-6 (IL-6), a pleiotropic cytokine, is proposed to play a crucial role in inflammatory response (ref). Further study shows that IL-6 also plays important roles during angiogenesis and vascular remodelling, depending upon cell types. We investigated the effects of IL-6 on a major cell type crucial for remodelling, human cerebral vascular smooth muscle cells (HCSMCs). Methods: HCSMCs were grown to confluence on gelatin coated 35mm dishes and then treated with IL-6 protein at different concentrations (25-200ng/ml). HCSMC proliferation was determined using a BrdU assay kit, and migration was determined using a HCSMC invasion assay. Expression of vascular endothelial growth factor (VEGF) and VEGF receptor, the kinase insert domain-containing receptor (KDR), and matrix metalloproteinase (MMP)-3, -9 protein and mRNA levels were determined using Western blot analysis, ELISA, and real time-polymerase chain reaction (RT-PCR) assay, respectively. MMP-9 activity was determined using MMP zymography. Results: VEGF had a minimal mitogenic effect on HCSMCs. However, IL-6 induced HCSMC proliferation and migration in a dose dependent manner. To explore the signal transduction pathway for the effect of IL-6 on HCSMC proliferation, we studied the downstream factor expression in HCSMCs (VEGF, MMP-3, -9). IL-6 significantly enhanced VEGF, MMP-3, -9 both mRNA and protein expression levels in HCSMCs compared with the control (without IL-6 treatment,  $p < 0.05$ ), respectively. Neutralizing or inhibiting IL-6 and/or VEGF using antibodies or inhibitors could block IL-6 induced HCSMC proliferation. Importantly, we demonstrated that IL-6 directly activated KDR phosphorylation in the IL-6 treated HCSMCs. Blocking KDR abolished IL-6 induced HCSMC proliferation. Conclusion: Our results indicate that the IL-6 treatment accelerated HCSMC proliferation through stimulation of the VEGF-KDR-MMP signal pathway. We provide the first evidence that IL-6, by triggering KDR phosphorylation, plays an important role in IL-6 induced HCSMC proliferation. HCSMC-derived MMPs could be an additional source of proteases to digest vascular basement membranes, potentially providing a key step in the initial stage of brain angiogenesis. MMPs may also contribute to HCSMC migration in angiogenesis. References: [1] He Wang and Joan A Keiser; *Circ Res* 83 832 - 840 (1998) Supported by NIH grants: PO1 NS and RO1 NS27713 (WLY) and R21 NS45123 (GY)

**THE INFLAMMATORY CELLS AND TNF, TGF IN HUMAN INFARCTED BRAIN****Yupu Guo<sup>1</sup>, Qingjie Zhao<sup>2</sup>***<sup>1</sup>Neurological Department, PUMCH, Beijing, China**<sup>2</sup>Neurological Department, Harbin Medical University Hospital, Harbin, China*

Objective: To study the relationship between inflammation and infarction, protect or damage?  
Method: seven infarcted autopsy brain were enrolled in our study with different ischemia time, we observed the active microglia and macrophage by CD68, and the others including LCA, GFAP, TNF and TGF, still about the cytoskeleton, NF100 and MAP2. All of them finished by immunohistochemistry. Results: from 10 hours to 48 hours after ischemia there are the activated microglia in the centre of the infarct area. From the third day to two weeks the activated microglia are in the surrounding area, the edge of the infarction and the neighbor responsive area. The astrocyte disappear in the necrosis centre of the infarction and astrocytosis appear in the surrounding area from the ischemia 10 hours to two weeks. The longer of the ischemia time, the more far from the centre of infarction, the astrocytosis distribution is. The activated astrocyte also show the shape from rod with branch to protoplasm. The macrophage appear in the centre of infarction at 27 hours after ischemia, and much more were seen two days later. All the LCA are negative in infarcted brain, but they are positive in the hemorrhage brain. The TNF distribution are same to the microglia at the early time and same to the astrocyte at the late time. The TNF are expressed mainly by astrocyte, only a little by vessels and neurons. After 27 hours, some isolate area, the hippocampus have a lot of TNF expression, and in four cases, the opposite hippocampus have a lot TNF expression. TGF expressed in the surrounding area. Conclusion: The microglia have more relationship with the infarction mature. The function of astrocytosis seems partly same to the TNF. They may both have the function of damage and repair.

## PREDICTING EFFECTS OF THROMBOLYTIC THERAPY IN ACUTE STROKE PATIENTS USING MR IMAGING

Ona Wu<sup>1,2</sup>, Søren Christensen<sup>1</sup>, Niels Hjort<sup>1</sup>, Rick M. Dijkhuizen<sup>2</sup>, Thomas Kucinski<sup>3</sup>, Jens Fiehler<sup>3</sup>, Joachim Rother<sup>4</sup>, Leif Ostergaard<sup>1</sup>

<sup>1</sup>Center for Functionally Integrative Neuroscience, Århus University Hospital, Aarhus, Denmark

<sup>2</sup>Image Sciences Institute, University Medical Center Utrecht, Utrecht, The Netherlands

<sup>3</sup>Department of Neuroradiology, University Hospital Hamburg-Eppendorf, Hamburg, Germany

<sup>4</sup>Department of Neurology, University Hospital Hamburg-Eppendorf, Hamburg, Germany

**Introduction:** Predicting response to treatment strategies for stroke patients prior to therapy can aid the clinical decision making process and improve patient outcome. Algorithms combining multiple MRI parameters accurately predict tissue infarction in patients imaged <12h from symptom onset who did not receive thrombolysis [1]. This study extends application of these algorithms to patients imaged at the hyperacute stage who were treated with thrombolytic therapy. **Methods:** Acute stroke patients who received diffusion-weighted (DWI) and perfusion-weighted (PWI) MRI within 6 h of symptom onset and a follow-up after 5-8 days (F/U) [2] were retrospectively analyzed. Patients either received standard medical treatment (Group 1; n=12), or thrombolysis (Group 2; n=29). All thrombolysed patients were imaged prior to drug administration. Apparent diffusion coefficient (ADC), T2-weighted images, isotropic DWI, CBF, CBV, mean transit time (MTT) and transit delay maps were calculated, coregistered, normalized with respect to contralateral normal white matter values and used to train a predictive algorithm which outputs infarction risk on a voxel-wise basis [1]. Model parameters were trained using regions of infarcted and non-infarcted tissue outlined on the F/U. Model 1 was trained from all Group 1 data. Model 2 was developed using Group 2 data and applied using jackknifing. Predicted lesion volumes (PLV) were defined as tissue with > 50% infarction risk. PLV were compared to the measured lesion volumes (MLV) that had been used for training. Patients exhibiting complete reperfusion on F/U according to modified TIMI criteria [2] were classified as reperfusers and others as non-reperfusers. **Results:** Absolute differences between PLV and MLV were larger for Model 1 (105±57 cm<sup>3</sup>) than Model 2 (78±49 cm<sup>3</sup>) (p<.001). The calculated infarction risk was greater for Model 1 than Model 2 (p<.001). Model 2 infarction risk was lower for reperfusers than non-reperfusers (p=.04). Fig 1 shows an example where, using the same input data, significantly lower infarction risk is predicted if the patient were to receive thrombolysis. **Discussion:** The results show that infarction risk on a voxel-wise basis is predicted to be reduced by thrombolysis, demonstrating the potential of these algorithms for prospectively identifying effect of a therapeutic intervention. In addition, statistical algorithms may provide an objective measure for identifying patients most likely to respond favorably to intervention. Furthermore, the spatial heterogeneity of predicted risk values likely reflects varying degrees of existing tissue injury and salvageability within the PLV. **References:** 1. Wu O, et al. Stroke. 2001; 32, 933-42. 2. Fiehler J, et al. Stroke. 2002; 33, 79-86.

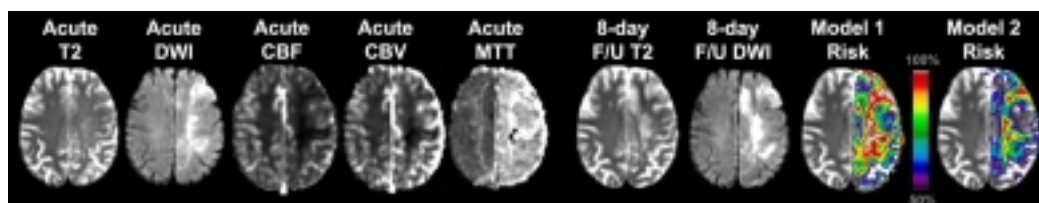


Fig 1: Example input and output for a patient imaged 4.5 h after symptom onset.

## ULTRASOUND-AUGMENTED THROMBOLYSIS IMPROVES OUTCOME IN HYPERGLYCAEMIC STROKE

Sharyl Martini<sup>1,2</sup>, Michael D. Hill<sup>3</sup>, Andrei V. Alexandrov<sup>4</sup>, Carlos A. Molina<sup>5</sup>,  
Thomas A Kent<sup>1,2</sup>

<sup>1</sup>*Department of Neurology, Baylor College of Medicine, Houston, TX, USA*

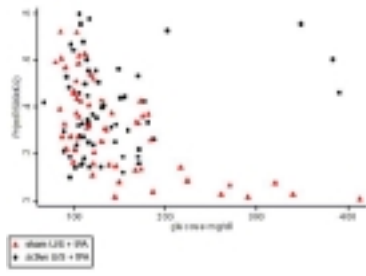
<sup>2</sup>*VAMC Stroke Program, Houston, TX, USA*

<sup>3</sup>*Department of Clinical Neurosciences, University of Calgary, Calgary, AB, Canada*

<sup>4</sup>*Stroke Treatment Team, University of Texas-Houston Medical School, Houston, TX, USA*

<sup>5</sup>*Neurovascular Unit, Vall D'Hebron Hospital, Barcelona, Spain*

**Introduction:** Human and animal studies indicate that hyperglycaemia worsens outcome in acute ischemic stroke, especially after reperfusion or thrombolysis. No treatment has been shown to overcome its detrimental effects. The mechanism by which hyperglycaemia worsens stroke outcome is not established. Prior work indicated that reperfusion vascular injury rapidly impairs eNOS resulting in a contractile phenotype, impairing reperfusion blood flow and worsening the ischemic deficit. Intriguingly, therapeutic ultrasound can rapidly increase perfusion of ischemic tissue, possibly via phosphorylation of eNOS. The CLOTBUST trial (Alexandrov et al NEJM 2004;351(21):2170-8) demonstrated enhanced lytic activity of tPA when augmented with diagnostic pulsed wave Doppler ultrasound. We hypothesised that hyperglycaemic stroke subjects might benefit from ultrasound therapy and that this effect would not be solely due to enhanced recanalisation. **Methods:** 126 acute MCA ischemic stroke subjects treated within 3 hours with tPA were randomised to either sham or active continuous ultrasound therapy of the MCA. Primary outcome was 90 day modified Rankin Scale score of 0-2. We sought an interaction between glucose and active ultrasound treatment in a simple logistic regression model, subsequently searching for potential confounding variables using backwards elimination. Age and baseline NIHSS were included in the final model. The interaction term was tested using a likelihood ratio test. **Results:** 32% of controls and 33% of active ultrasound subjects had baseline serum glucose levels >140mg/dL. High glucose levels predicted a lower probability of functional independence in the control but not the active ultrasound group, as demonstrated by a statistically significant interaction between glucose and treatment group (p=0.043). This beneficial effect of ultrasound on outcome was particularly prominent at high glucose levels (Figure). Of subjects with admission glucose >200 mg/dl, none of the controls recanalised at 2 hours, compared to 24% in the active ultrasound group (NS, p=0.417). None of these controls were functionally independent at 90 days, compared to 75% of the active ultrasound subjects (p=0.024), even though no early recanalisation was demonstrated in half of the active ultrasound subjects. **Discussion:** Ultrasound exposure overcame the negative effect of hyperglycaemia on outcome. This is the first therapy that has improved functional outcome in hyperglycaemic stroke subjects. Additional analyses supported our hypothesis that the mechanism of benefit is not due to enhanced or earlier recanalisation, suggesting that ultrasound may act through other mechanisms, including beneficial vasodilatory actions within the vessel wall and downstream. Future planned studies will test this hypothesis prospectively.



## ALBUMIN THERAPY FOR NEUROPROTECTION IN ISCHEMIC STROKE: ALIAS I TRIAL

Myron D. Ginsberg<sup>1</sup>, Michael D. Hill<sup>2</sup>, Yuko Y. Palesch<sup>3</sup>, Karla J. Ryckborst<sup>2</sup>,  
Diego Tamariz<sup>1</sup>

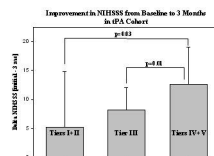
<sup>1</sup>Department of Neurology, University of Miami School of Medicine, Miami, FL, USA

<sup>2</sup>Department of Clinical Neurosciences, University of Calgary, Calgary, AB, Canada

<sup>3</sup>Department of Biostatistics, Bioinformatics and Epidemiology, Medical University of South Carolina, Charleston, SC, USA

Human albumin (ALB) therapy is highly neuroprotective in preclinical models of cerebral ischemia. Multiple mechanisms underlie ALB's efficacy: fatty-acid and transition-metal binding, antioxidant and oncotic actions, and salutary microcirculatory effects. Design: In this dose-escalation trial, ALB (25% solution) was administered within 16 h of stroke onset to subjects with acute ischemic stroke and NIH Stroke Scale scores (NIHSS)  $\geq 6$ . Two cohorts were assessed: 1) those also receiving IV tPA; and 2) those not given tPA. Seventy subjects have been enrolled into 5 ALB dose-tiers: I [0.34 g/kg; n=9 (tPA) and 8 (non-tPA)]; II [0.68 g/kg; n=5 and 6], III [1.03 g/kg; n=6 and 6]; IV [1.38 g/kg; n= 9 and 9]; and V [1.71 g/kg; n=6 and 6]. Mean age ( $\pm$  SD) was  $66 \pm 15$  years; 38 were male. ASPECTS CT-scan score was  $8.1 \pm 2.3$ . The 2-h ALB infusion was begun at  $8.2 \pm 3.7$  h after stroke onset. Post-discharge assessments (modified Rankin (mRS), Barthel, NIHSS) were conducted at 1 and 3 months.

Safety: Six of the 70 subjects died; all had severe strokes (NIHSS 23-38). Pulmonary edema occurred in 3 subjects of tier IV (but in none of tier V, when prophylactic administration of furosemide was encouraged). One serious adverse event (SAE) (congestive failure with prolonged hospitalization) in tier III was possibly ALB-related. No tier IV or V subject had ALB-related SAE's. Clinical course: Mean NIHSS was  $13.7 \pm 6.6$  initially;  $8.8 \pm 8.6$  at 72h; and  $5.4 \pm 6.6$  at 3 mo. In both cohorts, NIHSS tended to improve more extensively over time at higher ALB dose-tiers, particularly in the tPA cohort (Figure). Overall, mean NIHSS declined from 14.1 (initial) to 7.8 (3 mo) in tier I, from 16.1 (initial) to 3.4 (3 mo) in tier IV, and from 8.7 (initial) to 3.6 (3 mo) in tier V. Of note, the tier IV and tier V ALB doses (1.37 and 1.71 g/kg) exceeded the highly-protective per-kg dose in preclinical focal-ischemia studies (1.25 g/kg). In the tPA subgroup (n=35), tPA was given at  $2.3 \pm 0.9$  h post-stroke onset, and i.v. ALB was started at  $6.6 \pm 3.2$  h. By contrast, in the non-tPA subgroup, i.v. ALB was started 3 hours later ( $9.6 \pm 3.5$  h). In the tPA subgroup, significantly greater improvement in NIHSS was observed at the higher ALB dose-tiers (IV + V) than at lower dose-tiers (Figure). Conclusions: ALB therapy is well tolerated, and data suggest that higher-dose ALB may improve neurological outcome. We are planning to implement a randomized multicenter, placebo-controlled Phase III trial of this therapy – the ALIAS Trial. Supported by NIH Grants NS40406 and NS48784.



**INITIAL EVIDENCE FOR PERI-INFARCT DEPOLARIZATION OR CORTICAL SPREADING DEPRESSION AS A CAUSE OF NEUROLOGICAL DETERIORATION IN PATIENTS WITH SUBARACHNOID HAEMORRHAGE**

Robin Bhatia<sup>1</sup>, Martyn G. Boutelle<sup>2</sup>, Parastoo Hashemi<sup>2</sup>, Martin Fabricius<sup>3</sup>, Martin Lauritzen<sup>3</sup>, Susanne B. Fuhr<sup>3</sup>, Lisette Willumsen<sup>4</sup>, **Anthony J. Strong**<sup>1</sup>

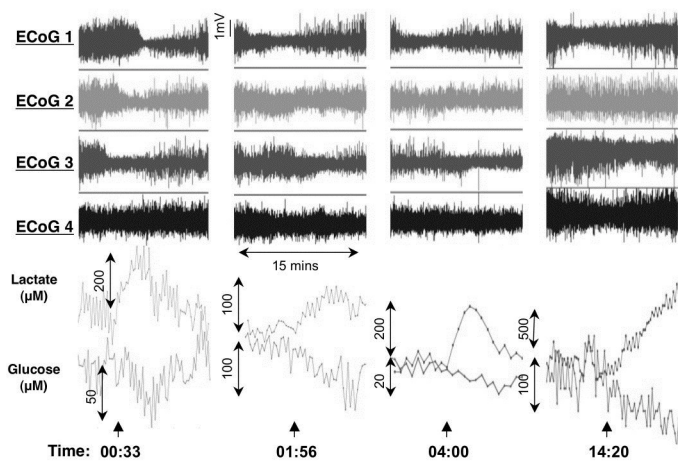
<sup>1</sup>*Department of Clinical Neurosciences, King's College London, London, UK*

<sup>2</sup>*Department of Chemistry, King's College London, London, UK*

<sup>3</sup>*Department of Clinical Neurophysiology, Glostrup Hospital and University of Copenhagen, Copenhagen, Denmark*

<sup>4</sup>*Department of Neurosurgery, Glostrup Hospital and University of Copenhagen, Copenhagen, Denmark*

**Introduction** Non-haemorrhagic neurological deterioration occurs in some 20% of patients with aneurysmal subarachnoid haemorrhage (SAH), is maximal in days 3-8 post SAH and associated with ischaemia, is difficult to treat, and is linked with worse outcome. It has been attributed to adverse effects on the cerebral microcirculation of products of erythrocyte lysis in the subarachnoid space, and superfusion of model post-SAH cerebrospinal fluid over the brain in rats induces spreading ischaemia resembling a peri-infarct depolarisation{1}. Here we report findings compatible with a similar mechanism in the human brain. **Methods** With ethics approval, 2 patients undergoing surgery for ruptured middle cerebral (1) or anterior communicating (1) aneurysms were enrolled in the COSBID study ( www.cosbid.org ). We monitored electrocorticogram (ECoG){2}, and in the first patient, microdialysate glucose and lactate{3}, each at 30 second intervals, for a minimum of 2 days following surgery. **Results** In patient 1, recurrent waves of depression of the cortical activity propagated along the electrode strip (middle temporal gyrus) at 2-5 mm/min. 33 events were recorded between 9 and 28 hours after surgery (12 days after SAH), 18 of them associated with stereotyped, coupled transient reductions in dialysate glucose and increases in lactate (Figure). Focal neurological deficit increased during this period. In patient 2, 3 episodes of depression occurred, propagating at 4-5 mm/min. The patient was comatose and ventilated during the entire period of monitoring. **Discussion** To our knowledge this is the first report of spreading depression-like events occurring in patients after SAH: in one there was simultaneous neurological deterioration, and the associated metabolic transients closely resemble those observed experimentally in the penumbra{3}. The capacity of peri-infarct depolarisations to reduce cortical perfusion and to increase infarct size suggests that a clear mechanism for deterioration and target for treatment in poor grade SAH patients is now emerging. **References** 1. Dreier JP et al. J. Neurosurgery: 93: 658-666, 2000. 2. Strong AJ et al. Stroke: 33: 2739-2744, 2002. 3. Hopwood SE et al. J Cereb Blood Flow Metab, in press.



## A PANEL OF BIOMARKERS MAY SUCCESSFULLY PREDICT ACUTE STROKE DIAGNOSIS

**Joan Montaner**, Anna Rosell, Pilar Delgado, Marc Ribo, Francisco Purroy, Anna Penalba, Israel Fernandez-Cadenas, Carlos Molina, Jose Alvarez-Sabin

*Neurovascular Research Laboratory, Stroke Unit, Vall D'Hebron Hospital, Barcelona, Spain*

**Background-** At present, the absence of a widely available diagnostic test for acute cerebral ischemia remains a significant limitation in the diagnosis (mostly made on clinical grounds and CT) and management of stroke. Moreover, the relationship between blood biomarkers and brain tissue expression of those markers following ischemic or hemorrhagic stroke remains largely unknown. **Purpose and methods-** To examine the prognostic value of a diagnostic panel of blood-borne biochemical markers of cerebral ischemia, consecutive patients with acute focal neurological deficit within the last 24 hours attended by neurologists were evaluated. Blood samples were drawn at arrival. CT, ultrasonography and other tests were done to make precise etiologic diagnosis. Patients were classified as “real strokes (strokes)” or “other causes mimicking stroke (mimics)”. Tested biomarkers were CRP, D-dimer, RAGE, MMP-9, s-100b, BNP, NT-3, Caspase-3, Chimerin and Secretagogin (assayed by ELISA). Healthy controls (n=99) were studied to obtain biomarkers normality values. In a subgroup of deceased stroke patients, biomarkers expression was studied in the brain parenchyma (ischemic core, penumbra and contralateral areas in ischemic strokes and perihematoma and contralateral areas in hemorrhagic strokes) by means of Western Blot and Zymographic techniques. **Results-** The complete protocol was achieved in 1005 patients (915 were strokes and 90 were mimics). Most biomarkers were higher among stroke patients compared to controls (CRP, D-dimer, MMP-9, BNP and Caspase-3,  $p<0.05$ ) except for lower levels of Secretagogin ( $p=0.017$ ). Main independent predictors of stroke versus mimics were: Caspase-3  $>1.96$  (OR=3.32; 1.88-5.88,  $p<0.0001$ ), D-dimer  $>0.27$  (OR=2.97; 1.72-5.16;  $p=0.0001$ ), RAGE  $>0.91$  (OR=2.19; 1.26-3.83,  $p=0.006$ ), Chimerin  $>1.11$  (OR=0.4; 0.19-0.81,  $p=0.011$ ), Secretagogin  $>0.24$  (OR=0.51; 0.27-0.97,  $p=0.041$ ) and MMP-9 $>199$  (OR=1.66; 1.01-2.73,  $p=0.046$ ). The odds to predict stroke when those six biomarkers are above/below these cut-offs is 99.01% (0% mimics and 0% healthy controls had such a combination). Similar results were obtained for patients attended  $<6$  hours of symptoms onset. Best specificity was for Caspase-3=73% and sensitivity for D-dimer=81%. Combinations (i.e. Caspase-3+D-dimer+MMP-9) gained specificity (92.8%) but lost sensitivity (32.7%). The utility of these biomarkers to identify stroke subtypes will be discussed. Regarding brain tissue, we identified maximal MMP-9 expression in the ischemic core and areas of hemorrhagic transformation and active forms of Caspase-3 appeared to be over expressed in the ischemic penumbra. **Conclusions-** A combination of biomarkers including caspase-3, an apoptosis related biomarker, seems promising to make an urgent biochemical diagnosis of stroke. This approach will permit rapid referral of stroke patients to hospitals where acute treatments are available.

**BILIRUBIN PRODUCTION AND OXIDATION IN CSF OF PATIENTS WITH CEREBRAL VASOSPASM AFTER SUBARACHNOID HEMORRHAGE**

Gail Pyne-Geithman<sup>1</sup>, Chad Morgan<sup>2</sup>, Kenneth Wagner<sup>1</sup>, Janice Carrozzella<sup>1</sup>, Daniel Kanter<sup>1</sup>, Elizabeth Dulaney<sup>1</sup>, Mario Zuccarello<sup>2</sup>, **Joseph Clark**<sup>1</sup>

<sup>1</sup>*Department of Neurology, University of Cincinnati, Cincinnati, OH, USA*

<sup>2</sup>*Department of Neurosurgery, University of Cincinnati, Cincinnati, OH, USA*

Delayed cerebral vasospasm after subarachnoid hemorrhage (SAH) remains a significant cause of mortality and morbidity, however, the etiology is, as yet, unknown, despite intensive research efforts. Research in this laboratory indicates that bilirubin and oxidative stress may be responsible by leading to formation of bilirubin oxidation products (BOXes), so we investigated changes in bilirubin concentration and oxidative stress in vitro, and in cerebral spinal fluid (CSF) from SAH patients. Non-SAH CSF, a source of heme oxygenase I (HO-1), and blood were incubated, and in vitro bilirubin production measured. CSF from SAH patients was collected, categorized using stimulation of vascular smooth muscle metabolism in vitro (CSFv and CSFc for with vasospasm and without vasospasm respectively). CSF was analyzed for hemoglobin, total protein and bilirubin, BOXes, malonyldialdehyde and peroxidized lipids (indicators of an oxidizing environment), and HO-1 concentration. The study patients comprised 7 males and 5 females. The median age was 46, and the ages ranged from 32 to 72 years old at time of hemorrhage. The CSFc samples averaged  $0.92 \pm 0.31$  g/dL total protein and  $0.39 \pm 0.06$  g/dL hemoglobin, compared with  $0.94 \pm 0.37$  g/dL and  $0.41 \pm 0.07$  g/dL in the CSFv samples. HO-1 concentrations are significantly higher ( $p < 0.05$ ) in CSFv, compared with CSFc. When bilirubin concentration is compared for patients with and without clinical vasospasm, there is significantly greater bilirubin in the vasospasm patients ( $5.6 \pm 0.93$  vs.  $29.4 \pm 3.9$  umols/L). We found that total peroxidized lipids (LOOH) is significantly elevated in vasospasm patients compared to control ( $18.24 \pm 4.4$  vs.  $7.5 \pm 0.53$  umols/L respectively). We have found that the concentration of BOXes in CSFv of patients following SAH is significantly elevated compared to CSFc ( $1.33 \pm 0.07$  versus  $0.02 \pm 0.004$  uM respectively). Bilirubin, BOXes, HO-1 and peroxidized lipid content were significantly higher in CSF from SAH patients with vasospasm, compared with non-vasospasm SAH CSF, and correlated with occurrence of vasospasm. We conclude that vasospasm may be more likely in patients with elevated BOXes. The conditions necessary for the formation of BOXes are indeed present in CSF from SAH patients with vasospasm, but not CSF from SAH patients without vasospasm.

## EARLY PROTEOMIC MARKERS OF VASOSPASM CAN BE IDENTIFIED IN CEREBRAL MICRODIALYSATES OF PATIENTS WITH SUBARACHNOID HEMORRHAGE

Martin H. Maurer<sup>1</sup>, Daniel Haux<sup>2</sup>, Oliver W. Sakowitz<sup>2</sup>, Robert E. Feldmann<sup>1</sup>,  
Andreas W. Unterberg<sup>2</sup>, Wolfgang Kuschinsky<sup>1</sup>

<sup>1</sup>*Department of Physiology and Pathophysiology, University of Heidelberg, Heidelberg, Germany*

<sup>2</sup>*Department of Neurosurgery, University of Heidelberg, Heidelberg, Germany*

**Introduction:** A major complication of aneurysmal subarachnoid hemorrhage (SAH) is delayed cerebral ischemia (delayed ischemic neurological deficit [DIND], also called symptomatic vasospasm) several days after SAH, affecting about 30% of the patients. It is unknown why symptomatic vasospasm develops in some patients after SAH and does not in others. In this study, we hypothesized that one or more proteins might be detected in the brain parenchyma of patients before they develop vasospasm and that these proteins do not show up in SAH patients without vasospasm. Therefore, we searched for protein markers in human brain microdialysates which might be related to developing vasospasm. **Patients and Methods:** We investigated 10 patients with SAH, 5 developing vasospasm and 5 others without vasospasm. Informed consent was obtained from the patient or legal representative. After the initial surgery, flexible microdialysis probes (CMA 70 custom probes, CMA Microdialysis, Solna, Sweden) were inserted into fronto-temporal cortex for later-on metabolic monitoring in neuro-intensive care. The probes were perfused at 0.3  $\mu\text{L}/\text{min}$  with sterile Ringer's solution. We analyzed proteomic profiles of the microdialysate 24 hours and 5-6 days after insertion of the probes by two-dimensional gel electrophoresis. Proteins were separated in the first dimension according to their isoelectric point, and in the second dimension according to their molecular weight. Polyacrylamide electrophoresis gels were silver-stained and analysed by the Phoretix 2D Elite software (Nonlinear Dynamics, Newcastle-upon-Tyne, UK). Proteins were identified by mass spectrometry (Center for Molecular Biology, University of Heidelberg). We compared protein expression profiles by hierarchical clustering using the EMBL online tool EPCLUST, version 0.9.23 beta, at <http://ep.ebi.ac.uk>. **Results:** We found an average of 57  $\pm$  22 protein spots in the individual gels, ranging from 37 to 149. Thirty-three spots consistently appeared in at least 50% of the gels analyzed. of these, 20 protein spots were differentially expressed ( $P < 0.05$ ), of which we could identify 15. Glyceraldehyde-3-phosphate dehydrogenase (GAPDH, 4 isoforms) was increased by a factor of  $3.7 \pm 1.1$  ( $n=33$  vasospastic;  $n=47$  non-vasospastic, means  $\pm$  sd) in the vasospasm group, whereas the concentration of Heat shock protein 73 (HSP73, 9 isoforms) was decreased to  $0.47 \pm 0.2$  ( $n=88$  vasospastic;  $n=101$  non-vasospastic). These protein changes occurred  $2.4 \pm 2.1$  days before vasospasm developed. Cluster analysis of the proteome data revealed a close relationship of GAPDH and HSP73 in the context of cell death and apoptosis. **Conclusions:** Patients who develop cerebral vasospasm after SAH show a pattern of proteins in their brain microdialysate which is different from that of SAH patients who do not develop vasospasm. Since these differences in the protein pattern are evident as soon as 2 days before the development of vasospasm, they may potentially be used as early prognostic markers for the development of vasospasm after SAH, enabling selective early therapeutic intervention in this high risk group of patients. **Acknowledgement:** Supported by the German National Genome Research Network NGFN-2 of the German Ministry of Education and Research (BMBF) (to MHM and WK).

**CHANGES IN SUPERFICIAL TEMPORAL ARTERY BLOOD FLOW AND  
CEREBRAL HEMODYNAMICS OF MOYAMOYA DISEASE AFTER  
EXTRACRANIAL-INTRACRANIAL BYPASS SURGERY**

**Shigeru Fujimoto<sup>1</sup>**, Kazunori Toyoda<sup>1</sup>, Tooru Inoue<sup>2</sup>, Yoko Yokoyama<sup>1</sup>, Juro Jinnouchi<sup>1</sup>,  
Koh Nakachi<sup>1</sup>, Seiji Goto<sup>1</sup>, Kotaro Yasumori<sup>3</sup>, Setsuro Ibayashi<sup>4</sup>, Yasushi Okada<sup>1</sup>

<sup>1</sup>*Department of Cerebrovascular Disease, National Hospital Organization Kyushu Medical Center, Fukuoka, Japan*

<sup>2</sup>*Department of Neurosurgery, National Hospital Organization Kyushu Medical Center, Fukuoka, Japan*

<sup>3</sup>*Department of Neuroradiology, National Hospital Organization Kyushu Medical Center, Fukuoka, Japan*

<sup>4</sup>*Department of Medicine and Clinical Science, Graduate School of Medical Sciences, Kyushu University, Fukuoka, Japan*

Introduction: Recently, Japanese extracranial-intracranial (EC-IC) bypass trial has revealed a benefit of EC-IC bypass for preventing stroke in patients with cerebral artery occlusive disease and severe cerebral hemodynamic failure. We previously reported that flow velocity of the superficial temporal artery (STA) was predictive of the extent of bypass flow or the improvement in the regional cerebral blood flow (rCBF) after EC-IC bypass surgery (1, 2). The purpose of the present study is compare post-surgical changes in STA blood flow and cerebral hemodynamics between patients with atherothrombotic carotid occlusive disease and moyamoya disease. Methods: This study included 37 consecutive patients with atherothrombotic carotid occlusive disease (Athero-Group) and 11 consecutive patients with moyamoya disease (Moya-Group) who underwent EC-IC bypass. We adopted the inclusion criteria using single photon emission computed tomography (SPECT) as follows: rCBF <32ml/100g/min (80% of the mean value in the normal control subjects) and acetazolamide (ACZ) reactivity <10% in the ipsilateral middle cerebral artery (MCA) territory. STA duplex ultrasonography (STDU) was performed to measure the flow velocity and diameter of the operated STA before and 14 days and 3 months after EC-IC bypass surgery. Relationships between STA mean flow velocity (MFV) 14 days after EC-IC bypass and various clinical and radiological factors were investigated. Changes in parameters of STDU and SPECT were compared between Athero-Group and Moya-Group. Results: STA MFV was correlated with the rCBF in the ipsilateral MCA territory 14 days after EC-IC bypass surgery ( $R=0.51$ ,  $p<0.0001$ ) 14 days after EC-IC bypass. There was no significant difference in any baseline STDU and SPECT parameters between Athero-Group and Moya-Group. Two patients in Moya-Group showed a hemispheric hyperperfusion syndrome within 14 days after EC-IC bypass. In Athero-Group, hyperperfusion syndrome was not observed. Between Moya-Group and Athero-Group, there was a significant difference in STA MFV 14 days after EC-IC bypass ( $73.2\pm 20.9$  vs  $55.1\pm 16.7$  cm/sec,  $p<0.01$ ). The rCBF of the ipsilateral MCA territory was also higher in Moya-Group than Athero-Group 14 days after EC-IC bypass ( $40.0\pm 8.3$  vs  $34.6\pm 5.8$  ml/100g/min,  $p<0.05$ ). These differences were not observed 3 months after EC-IC bypass. There was no difference in STA diameter 14 days and 3 months after EC-IC bypass between the 2 groups. Changes in STA MFV ( $42.2\pm 23.7$  vs  $29.3\pm 13.9$  cm/sec,  $p<0.05$ ) and rCBF ( $8.7\pm 4.9$  vs  $5.3\pm 4.3$  ml/100g/min,  $p<0.05$ ) before and 14 days after EC-IC bypass were also higher in Moya-Group than Athero-Group. Conclusions: In patients with severe cerebral hemodynamic failure, STA MFV is a highly sensitive parameter for predicting rCBF in the ipsilateral MCA territory after EC-IC bypass. In moyamoya disease, changes in STA MFV as well as rCBF were higher than those in atherothrombotic carotid occlusive disease after EC-IC bypass. Hyperperfusion syndrome was observed only in patients with moyamoya disease. References: [1] Arakawa S, Kamouchi M, Okada Y, et al; AJNR 24:886-891 (2003) [2] Hirai Y, Fujimoto S, Toyoda K, et al; J Cereb Blood Flow Metab 23(suppl.1):553 (2003)



**COMBINATION THERAPY OF RT-PA AND G-CSF****Rainer Kollmar**, Nils Henninger, Christian Urbanek, Stefan Schwab*University of Heidelberg, Department of Neurology, Heidelberg, Germany*

Thrombolysis is so far the only successful therapy for ischemic stroke, but essentially limited by side effects. Therefore, combination therapy with neuroprotective substances is warranted. We investigated whether Granulocyte colony-stimulating factor (G-CSF) alone or in combination with rt-PA is neuroprotective in a thromboembolic stroke model. Male Wistar rats (n=59) were subjected to thromboembolic occlusion (TE) of the middle cerebral artery (MCA). G-CSF (60µg/kg body weight) was administered intravenously 60 min after TE. Thrombolysis was performed 3 hours after TE with intravenous rt-PA (10 mg/kg body weight). Experimental groups included control (C), G-CSF, thrombolysis (Th), and G-CSF plus thrombolysis (com). Animals were investigated by MRI and silver infarct staining (SIS) and perfusion status. 70% of the animals in the Th group died within 24 hours, whereas the mortality in remaining groups ranged between 30% and 40%. G-CSF alone or in combination with rt-PA significantly decreased infarct volume after 24 hours in T2 and DWI as compared to the control and Th groups ( $p < 0.05$ ). MRI data showed that late thrombolysis (Th) alone led to an increase of relative regional cerebral blood volume (rrCBV) above normal values. G-CSF possesses neuroprotective properties when administered alone or in combination with rt-PA. Further studies need to investigate long-term outcome after combination therapy.

## EVALUATION OF CEREBRAL METABOLISM BY MULTI-VOXEL PROTON MAGNETIC RESONANCE SPECTROSCOPY IMAGING BEFORE AND AFTER STA-MCA BYPASS

Kazunori Akaji<sup>1</sup>, Hideichi Takayama<sup>1</sup>, Masahito Kobayashi<sup>3</sup>, Yoshio Tanizaki<sup>1</sup>,  
Kenji Hiraga<sup>1</sup>, Sadao Suga<sup>4</sup>, Ban Mihara<sup>2</sup>

<sup>1</sup>*Department of Neurosurgery, Mihara Memorial Hospital, Iseaki, Japan*

<sup>2</sup>*Department of Neurology, Mihara Memorial Hospital, Iseaki, Japan*

<sup>3</sup>*Department of Neurosurgery, Keio University School of Medicine, Tokyo, Japan*

<sup>4</sup>*Department of Neurosurgery, Tokyo Dental College Ichikawa General Hospital, Ichikawa, Japan*

Introduction: Proton magnetic resonance spectroscopy (1H-MRS) is a useful method to evaluate cerebral metabolism directly and non-invasively. We examined 1H-MRS in the patients with major cerebral artery occlusive diseases and hemodynamic cerebral ischemia to study whether cerebral metabolism can improve after STA-MCA bypass. Methods: The subjects were 11 patients. The age of the patients varies between 47-74 years. Six patients had internal carotid artery occlusion. Two patients had middle cerebral artery occlusion. Three patients had internal carotid artery severe stenosis. We examined Xenon-CT including acetazolamide challenge to evaluate the regional cerebral blood flow (CBF) and examined multi-voxel 1H-MRS using SE-2D-CSI method placed axially above the lateral ventricle before and at 6 months after STA-MCA bypass. Results: The patency of STA-MCA bypass was good in 10 patients. In 8 of the 10 patients, percentile changes of regional CBF after acetazolamide challenge in the affected cortex were less than +10%. In 5 of the 8 patients, the regional CBF was normalized (more than +10%) after STA-MCA bypass. In 3 of the 8 patients, N-acetyl aspartate/creatine (NAA/Cr) ratios in the affected cortex were normal. In 5 of the 8 patients, NAA/Cr ratios were less than the lower limit (mean-2×standard deviation). In all 8 patients at the range of less than +10% in percentile change of regional CBF after acetazolamide challenge in the affected cortex, NAA/Cr ratios increased after STA-MCA bypass. Conclusion: Cerebral metabolism improved after STA-MCA bypass in the patients with the impaired cerebrovascular reserve capacity in the affected cortex.

**MELATONIN REVERSES TISSUE-PLASMINOGEN ACTIVATOR (T-PA)-INDUCED  
BRAIN INJURY AFTER INTRALUMINAL MIDDLE CEREBRAL ARTERY  
OCCLUSION: ROLE OF INDUCIBLE NO SYNTHASE AND PHOSPHATIDYL  
INOSITOL-3 KINASE/ AKT**

**Ertugrul Kilic, Ülkan Kilic, Claudio L. Bassetti, Dirk M. Hermann**

*Department of Neurology, University Hospital Zurich, Zurich, Switzerland*

**Purpose:** In vivo studies showed that t-PA may aggravate neuronal injury after focal cerebral ischemia (1-3). We hypothesized that therapeutically delivered t-PA might impair survival-promoting cell signalling in the ischemic brain, which may be reversed by an anti-oxidative neuroprotectant, the neurohormone melatonin. **Methods:** We examined the effects of t-PA (10 mg/kg, i.v.), administered alone or in combination with melatonin (4 mg/kg, i.p.) immediately after reperfusion onset, on ischemic injury, inducible NO synthase (iNOS) expression and Akt, Bcl-XL and caspase-3 signalling following 90 minutes of intraluminal middle cerebral artery (MCA) occlusion in mice, followed by 24 hours of reperfusion. **Results:** t-PA, delivered immediately after reperfusion onset, increased infarct volume at 24 hours after MCA occlusion, in accordance with previous findings. Melatonin reduced infarct size, when administered alone, and reversed the t-PA-induced brain injury. Immunohistochemical studies showed an accumulation of iNOS+ cells in ischemic brain areas after t-PA treatment, which was abolished after co-delivery of melatonin. Western blots revealed that t-PA decreased phosphorylated Akt levels, but did not influence Bcl-XL expression and caspase-3 activity in ischemic brain lysates. Co-treatment with melatonin restored phosphorylated Akt levels, increased Bcl-XL expression and reduced caspase-3 activity. **Conclusions:** We provide evidence that t-PA-induced brain injury is accompanied by an activation of iNOS and inhibition of phosphatidylinositol-3 kinase/ Akt. Our observation that melatonin reverses the signalling changes and brain injury evoked by t-PA makes this indole attractive as add-on treatment with thrombolytics.

**References:**

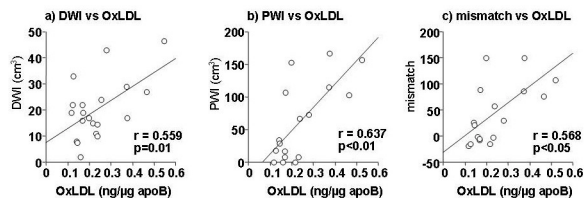
1. Y.F. Wang, S.E. Tsirka, S. Strickland, P.E. Stieg, S.G. Soriano, S.A. Lipton (1998) *Nature Med.* 4: 228-231.
2. E. Kilic, M. Bähr, D.M. Hermann (2001) *Stroke* 32: 2641-2647.
3. E. Kilic, Ü. Kilic, C.M. Matter, T.F. Lüscher, C.L. Bassetti, D.M. Hermann (2005) *Stroke*: in press.

**ELEVATION OF PLASMA OXIDIZED LDL IN ACUTE STROKE PATIENTS IS ASSOCIATED WITH ISCHEMIC LESION DEPICTED BY DWI AND PREDICTIVE OF INFARCT ENLARGEMENT**

Masaaki Uno, Keiko Kitazato, Atsuhiko Suzue, Kyoko Nishi, Shinji Nagahiro

*Department of Neurosurgery, The University of Tokushima, Tokushima, Japan*

Oxidized low-density lipoprotein (OxLDL) plays a major role in atherosclerosis. In our previous study, we used specific antibody against oxidized phosphatidylcholine (FOH1a/DLH3) by which OxLDL is recognized, and first demonstrated the significant association between raised plasma OxLDL and acute cerebral infarction, especially cortical infarction. We undertook the present study to clarify the relationship between plasma OxLDL and the ischemic volume. We used ELISA to determine plasma OxLDL levels and performed diffusion- and perfusion-weighted MRI (DWI, PWI) to measure the ischemic volume in 44 ischemic stroke patients. Based on the location of the ischemic lesion, they were divided into 3 groups: Group I (GI, n=21) had cortical lesions, Group II (GII, n=17) had lesions in the basal ganglia or brain stem, and Group III (GIII, n=6) had massive lesions that involved one entire hemisphere. In GI, but not GII and GIII, plasma OxLDL was significantly higher than in 19 age-matched controls ( $p<0.01$ ) and was significantly correlated with the initial ischemic volume visualized on DWI ( $p=0.01$ ), PWI ( $p<0.01$ ), and the DWI-PWI mismatch ( $p<0.05$ ) (Figure a-c)). A persistent increase in plasma OxLDL was associated with enlargement of the ischemic lesion in the early phase after the insult. These findings suggest that elevated plasma OxLDL levels are associated with moderate ischemic damage in patients with cortical lesions (GI) but not those with massive hemispheric lesions (GIII) which may be irreversible. In addition, elevated plasma OxLDL may represent a predictor of enlargement of the ischemic lesion.



## ACTIVATION OF THE JAK-STAT SIGNALING PATHWAY IN BASILAR ARTERY AFTER SUBARACHNOID HEMORRHAGE

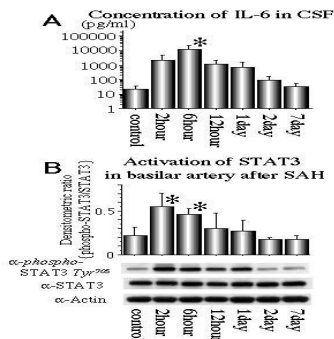
Koji Osuka<sup>1</sup>, Yasuo Watanabe<sup>2</sup>, Nobuteru Usuda<sup>3</sup>, Ayami Nakazawa<sup>3</sup>, Jun Yoshida<sup>1</sup>

<sup>1</sup>Department of Neurosurgery, Nagoya University Graduate School of Medicine, Nagoya, Japan

<sup>2</sup>Department of Cell Physiology, Kagawa University Faculty of Medicine, Kagawa, Japan

<sup>3</sup>Department of Anatomy II, Fujita Health University School of Medicine, Aichi, Japan

**Introduction:** Janus kinases (JAK) and signal transducers and activators of transcription (STAT) are those of transcription factors that function as a major signal transduction pathway in cytokine signaling. Subarachnoid hemorrhage (SAH) produces proinflammatory cytokines in CSF. The roles of this signaling pathway in cerebral artery after SAH still remain to be elucidated. This paper describes the chronological and spatial expression of this signaling pathway after SAH *in vivo*. **Methods:** We used a one-hemorrhage SAH model in Sprague-Dawley rats. Autologous arterial blood (300  $\mu$ L) was injected into the cisterna magna. Basilar arteries and CSF were collected at 2, 6, 12, 24, 48, and 168 hours after SAH (n=4 series). Basilar arteries and CSF without injection of blood were used as controls. The concentration of interleukin-6 (IL-6) in CSF was measured by ELISA. STAT3, phosphorylated STAT3, JAK1, phosphorylated JAK1, and Actin were identified by Western blot analysis. IL-6 (2  $\mu$ g / 2  $\mu$ L) was injected into the cisterna magna and basilar artery was removed one hour later. Tris-HCl (pH 7.6, 2  $\mu$ L) was used as control vehicle. Western blot analysis using STAT3, phosphorylated STAT3, and Actin antibodies were performed. The band intensities were quantitated by densitometric scanning using the NIH IMAGE program. Immunohistochemical expression of STAT3 and phosphorylated STAT3 were studied in basilar artery at 2 hours after SAH and control. **Statistical significance** was less than 0.05. **Results:** The concentration of IL-6 in CSF increased immediately after SAH, peaked at 6 hours, and decreased thereafter (Fig A). Western blot analysis showed constant expression of Actin, JAK1, and STAT3, while phosphorylated JAK1 and STAT3 at Tyr705 significantly increased at 2 hours after SAH (Fig B). Injection of IL-6 significantly increased the phosphorylation of STAT3 compared with control. Phosphorylated STAT3 was detected in the endothelial and smooth muscle cells of basilar artery at 2 hours after SAH, while that was hardly detected in control basilar artery. **Conclusion:** These results suggest that SAH produces proinflammatory cytokine IL-6, which may activate JAK-STAT signaling pathway in the basilar artery immediately after SAH. This signaling pathway may be involved with immediate early gene transcription in the basilar artery and play an important role in cerebral vasospasm after SAH.



**NITRIC OXIDE-BASED PATHOMECHANISM OF DELAYED CEREBRAL VASOSPASM AFTER SAH****Ryszard Pluta<sup>1</sup>**, Carla Jung<sup>2</sup>, Brian Iuliano<sup>3</sup>, Edward Oldfield<sup>1</sup><sup>1</sup>*Surgical Neurology Branch, NINDS, NIH, Bethesda, MD, USA*<sup>2</sup>*Department of Neurosurgery, Johann-Wolfgang Goethe University, Frankfurt, Germany*<sup>3</sup>*Department of Neurologic Surgery, Mayo Clinic, Rochester, Minnesota, MN, USA*<sup>4</sup>*Surgical Neurology Branch, NINDS, NIH, Bethesda, MD, USA*

Nitric oxide (NO) is produced by endothelial NOS (eNOS) in the intima and by neuronal NOS (nNOS) in the adventitia of cerebral vessels. It dilates the arteries in response to a shear stress, metabolic demands, and chemoregulation. Subarachnoid hemorrhage (SAH) interrupts this regulation; oxyhemoglobin and deoxyhemoglobin, gradually released ( $p < 0.05$ ) from the subarachnoid clot enveloping the conductive arteries, destroy nNOS-containing neurons. This deprives the arteries of NO, leading to initiation of delayed vasospasm (PHASE I). However, the narrowing of the vessel stimulates eNOS through increased shear stress, which normally would lead to an increased production of NO and dilation of arteries. However, this does not happen due to transient eNOS dysfunction evoked by an increase of endogenous competitive NOS inhibitor, asymmetric dimethyl-arginine (ADMA) in CSF in response to the presence of bilirubin-oxidized fragments (BOXes). This eNOS dysfunction sustains vasospasm (PHASE II). ADMA levels are closely correlated with the degree and a time-course of vasospasm in humans ( $p < 0.002$ ) and in primate model ( $p < 0.01$ ) and when ADMA levels decrease vasospasm resolves (PHASE III;  $p < 0.05$ ). Increased levels of ADMA is evoked by its decreased elimination due to decreased presence of ADMA-hydrolyzing enzyme dimethylamine-dimethyl-L-arginine hydrolase (DDAH II;  $p < 0.05$ ) in the arteries in spasm. Thus, inhibition of the L-arginine-methylating enzyme (IPRMT3) or stimulation of the DDAH II may provide new therapeutic venues. We will present 1) experimental data confirming endothelial and neuronal NO synthases dysfunction during vasospasm, 2) experimental and clinical data supporting the hypothesis that BOXes are responsible for eNOS dysfunction during vasospasm and pre-clinical data on 3) probucol influence on ADMA production by endothelial cells exposed to hemoglobin and BOXes in vitro ( $p < 0.05$ ) and 4) in vivo data of a double-blind placebo-controlled primate SAH study of probucol to prevent vasospasm ( $p = 0.09$ ). Despite being negative, the results of this study support the hypothesis that pharmacological lowering of the CSF ADMA levels may prevent development of post-hemorrhagic delayed cerebral vasospasm.

## IMBALANCE BETWEEN OXIDANT/ANTIOXIDANT SYSTEMS CONTRIBUTES TO PLAQUE VULNERABILITY IN PATIENTS UNDERWENT CAROTID ENDARTERECTOMY

Kyoko Nishi<sup>1</sup>, Masaaki Uno<sup>1</sup>, Keiko T. Kitazato<sup>1</sup>, Atsuhiko Suzue<sup>1</sup>, Hao Liu<sup>1</sup>, Hiroyuki Itabe<sup>2</sup>, Shinji Nagahiro<sup>1</sup>

<sup>1</sup>*Department of Neurosurgery Institute of Health Biosciences, The University of Tokushima Graduate School, Tokushima, Japan*

<sup>2</sup>*Department of Biological Chemistry, School of Pharmaceutical Sciences Showa University, Tokyo, Japan*

Objective: Reactive species of oxygen and nitrogen mediate the oxidative modification of low-density lipoprotein (LDL). Oxidation of LDL is inhibited by endogenous radical scavenging enzymes such as MnSOD and Cu/ZnSOD that catalyze dismutation of O<sub>2</sub><sup>-</sup> to H<sub>2</sub>O<sub>2</sub>. Cu/ZnSOD but not MnSOD is inactivated by H<sub>2</sub>O<sub>2</sub>. Low molecular antioxidants such as uric acid regulate this inactivation. As the reduction of SOD activity progresses, superoxide could react more easily with NO to produce peroxynitrite, resulting in an increase in OxLDL. Here we evaluated whether a focal imbalance between pro- and antioxidant systems induces plaque vulnerability in patients with carotid stenosis. Methods and Results: Carotid plaques from 35 patients who underwent carotid endarterectomy were classified as vulnerable or stable based on histopathological findings. In vulnerable plaques, OxLDL, measured by sandwich ELISA was significantly higher ( $p < 0.01$ ) and the SOD activity significantly lower than in stable plaques ( $p < 0.05$ ). The plaque and plasma OxLDL level were inversely correlated with plaque SOD activity ( $p < 0.01$ ). There was a significant correlation between plaque and plasma OxLDL levels ( $p < 0.01$ ). The physiological uric acid level in all plaques was one-fourth to one-eighth of that in plasma and appeared to be unable to protect Cu-ZnSOD from degradation by H<sub>2</sub>O<sub>2</sub>. Immunohistochemical methods disclosed increased peroxynitrite and OxLDL in vulnerable plaques. The present findings suggest that once the oxidative status overwhelms the antioxidative defense system, the oxidation progresses rapidly. Although more patients with vulnerable plaques were symptomatic than patients with stable plaques, the difference was not statistically significant, and also their stenosis was almost similar. However, plaque and plasma OxLDL levels in symptomatic patients ( $n=13$ ) with vulnerable plaque were significantly higher than those in asymptomatic patients ( $n=9$ ) with stable plaque ( $31.9 \pm 19.4$  ng/ $\mu$ g of apoB and  $0.26 \pm 0.063$  vs  $3.96 \pm 2.14$  and  $0.142 \pm 0.036$ ;  $p < 0.01$ ). On the other hand, plaque SOD activity in symptomatic patients with vulnerable plaque were significantly lower than in asymptomatic patients with stable plaque ( $48.2 \pm 8.1$  % vs  $73.3 \pm 6.6$  %;  $p < 0.01$ ). Conclusion: Our results suggest that a focal imbalance between pro- and antioxidant defense systems in patients with carotid plaques induces an increase in plaque OxLDL levels and consequent plaque instability, and contributes to the high levels of plasma OxLDL.

**MUTIVARIATE STATISTICAL DIFFERENTIATION OF HEMODYNAMIC FACTORS IN CHRONIC OCCLUSIVE CEREBROVASCULAR DISEASE WITH POSITRON EMISSION TOMOGRAPHY. –ANALYSIS OF 100 PATIENTS WITH MOYAMOYA DISEASE**

Tadashi Nariai<sup>1</sup>, Yoji Tanaka<sup>1</sup>, Iwae Yu<sup>3</sup>, Motoki Inaji<sup>1</sup>, Kikuo Ohno<sup>1</sup>, Kiichi Ishiwata<sup>2</sup>, Michio Senda<sup>4</sup>, Kenji Ishii<sup>2</sup>

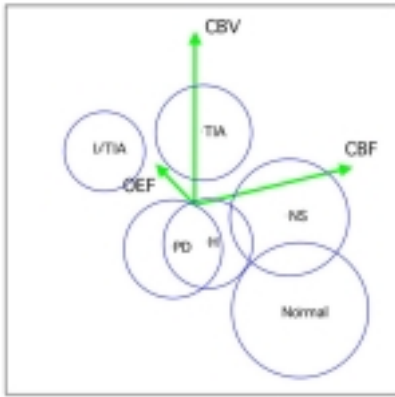
<sup>1</sup>*Department of Neurosurgery, Tokyo Medical and Dental University, Tokyo, Japan*

<sup>2</sup>*Positron Medical Center, Tokyo Metropolitan Institute of Gerontology, Tokyo, Japan*

<sup>3</sup>*Department of Neurosurgery, Tokyo Metropolitan Toshima Hospital, Tokyo, Japan*

<sup>4</sup>*Department of Image Based Medicine, Institute of Biomedical Research and Innovation, Kobe, Japan*

Introduction: Positron emission tomography (PET) is a powerful method that enables the simultaneous analysis of multiple hemodynamic factors. In the analysis of occlusive cerebrovascular diseases, various combinations of cerebral blood flow (CBF), metabolism, and blood volume (CBV) are observed depending on the severity of hemodynamic stress. Nonetheless, there have been no appropriate analyses to interpret the combination of factors in multivariate space. In this report, we differentiated the distribution of multiple PET-measured hemodynamic factors of patients with moyamoya disease, as a representative of chronic occlusive cerebrovascular disease, to examine if such analysis is useful to clarify the pathophysiology of the disease. Methods: Data of 100 patients with moyamoya disease (mean of age 31.3, range 12-58) that were obtained from 1991-2004 were retrospectively analyzed. PET measurement of CBF, CBV, cerebral metabolic rate for oxygen (CMRO<sub>2</sub>), and oxygen extraction fraction (OEF) were performed with inhalation of <sup>15</sup>O labeled gases and with continuous arterial blood sampling. Patients were classified into 5 groups depending on clinical presentation as presented previously (1); non-symptomatic (NS) patients, patients presenting transient ischemic attack (TIA group), those with infarction associated with TIA (I/TIA), those with a permanent deficit with infarction (PD), and those with hemorrhagic onset (H group). Values of patients groups were compared with a normal group (Norm). Results: 1) In earlier 57 patients, multivariate analysis of covariance to test the distribution of three dimensional (CBF, CBV, OEF) vector was performed, indicating that the significant difference of distribution existed between every possible pair out of six groups except NS vs. H, and H vs. PD among the frontal cortex (figure 1). 2) Using the data of these earlier patients, a multivariate discriminant was obtained and applied for the prediction of clinical presentation of latter patients using three factors (CBF, CBV, OEF) in frontal cortex. In more than 85 percent of patients, clinical type was correctly determined by this method, but such prediction was impossible by using single factor. 3) Significant alteration of factors in three dimensional space was detected before and after surgical revascularization in each patient. Conclusions: Multi-variate statistical differentiation of hemodynamic factors could provide useful information that cannot be obtained in single factor analysis. This method was even useful in the determination of hemodynamic stage in single patient. Reference: (1) Nariai T et al. Severe hemodynamic stress in selected subtypes of patients with moyamoya disease – A positron emission tomography study-. *J Neurol Neurosurg Psychiatry* 2005 (in press).



## DYNAMIC CT PERFUSION IMAGING IN SUBARACHNOID HEMORRHAGE RELATED VASOSPASM

Amanda M. Laslo<sup>1,2,3</sup>, James D. Eastwood<sup>4</sup>, Fang Chen<sup>1,2,3</sup>, Ting-Yim Lee<sup>1,2,3</sup>

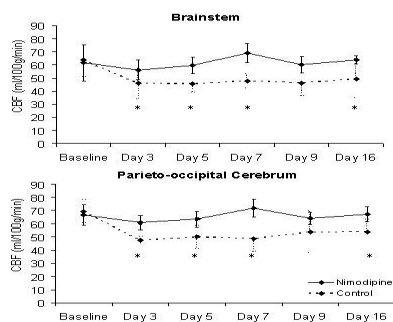
<sup>1</sup>Department of Medical Biophysics, University of Western Ontario, London, ON, Canada

<sup>2</sup>Imaging Research Laboratories, Robarts Research Institute, London, ON, Canada

<sup>3</sup>Imaging Division, Lawson Health Research Institute, London, ON, Canada

<sup>4</sup>Duke University Medical Center, Durham, NC, USA

Vasospasm (VSP) and changes in cerebral blood flow (CBF) are complications of subarachnoid hemorrhage (SAH) that can lead to delayed ischemic deficits (DID). In many institutions, nimodipine is the standard treatment used to prevent DIDs subsequent to SAH. However, there are discrepancies regarding the ability of nimodipine to improve outcome in all SAH patients. As new therapies become available for the treatment of DIDs associated with SAH, it will be necessary to develop a method to assess the need for, and the response to, therapy. In response to this need, we attempt to demonstrate the feasibility of using a functional computed tomography (CT) imaging protocol to quantify the effects of nimodipine on VSP and CBF in a rabbit model of SAH. SAH was induced by injecting autologous blood into the cistern magna in New Zealand White rabbits randomized to two groups: nimodipine (n=14) or control (n=12). Subcutaneous nimodipine (2.5 mg/kg) was given one hour after SAH, and every 24 hours after this for the duration of the study. CT Perfusion (CTP) and CT angiography (CTA) were used to measure CBF and basilar artery (BA) diameter at baseline, 10, 30, and 60 minutes after SAH, and on day 3, 5, 7, 9, and 16. Neurological assessments were performed by a blinded observer on each day of scanning. There was no difference in the incidence or severity of VSP between the control and nimodipine groups ( $p > 0.05$ ). When  $VSP > 15\%$ , nimodipine significantly increased CBF in the brainstem, cerebellum, parieto-occipital cerebrum, and subcortical regions ( $p < 0.05$ ) (See figure). Nimodipine had no effect on CBF when all degrees of VSP were included in the analysis. The degree of neurological deficit was less in the nimodipine group compared to the control group ( $p < 0.05$ ). We demonstrated that CTP and CTA imaging can quantify arterial VSP and CBF changes in a rabbit SAH model and that these techniques may be useful for evaluating the potential of new therapies for SAH compared to, or in the presence of, nimodipine. Specifically, we showed that nimodipine improves neurological outcome and increases CBF in the presence of moderate or severe VSP.



**ROLE OF C-JUN N-TERMINAL KINASE IN CEREBRAL VASOSPASM OF SUBARACHNOID HEMORRHAGE**

Hiroshi Yatsushige<sup>1,3,4</sup>, Mitsuo Yamaguchi<sup>1</sup>, Changman Zhou<sup>1</sup>, John H. Calvert<sup>1</sup>,  
Austin R.T. Colohan<sup>2</sup>, **John H. Zhang**<sup>1,2</sup>

<sup>1</sup>*Department of Physiology, Loma Linda University School of Medicine, Loma Linda, CA, USA*

<sup>2</sup>*Division of Neurosurgery, Loma Linda University Medical Center, Loma Linda, CA, USA*

<sup>3</sup>*Section of Neurosurgery, Tokyo Medical and Dental University Graduate School, Tokyo, Japan*

<sup>4</sup>*Department of Neurosurgery, National Hospital Organization Disaster Medical Center, Tokyo, Japan*

**Background and Purpose:** We have previously investigated several signaling pathways of cerebral vasospasm after subarachnoid hemorrhage (SAH). This study explored a pivotal role of c-Jun N-terminal kinase (JNK) in inflammation and cerebral vasospasm. **Method:** Twenty-seven dogs were randomly assigned to 5 groups: control, SAH without treatment, SAH+dimethyl sulfoxide (DMSO), SAH+JNK inhibitor SP600125 (10  $\mu\text{mol/L}$ ), and SAH+SP600125 (30  $\mu\text{mol/L}$ ). SAH was induced by the injection of the autologous blood into cisterna magna on day 0 and day 2. Angiograph was performed on Day 0 and Day 7. Neurobehavioral scores were evaluated daily. Activation of JNK pathway, the infiltration of leukocytes, and the production of cytokines were examined by morphology, Western blot and ELISA. **Results:** Severe cerebral vasospasm was observed in the basilar artery accompanied by the activation of JNK pathways in SAH without treatment and DMSO treated dogs. The JNK inhibitor SP600125 reduced angiographic and morphological vasospasm and improved behavior scores with a concomitant reduction of the activation of JNK, the infiltrated leukocytes and the IL-6 production. **Conclusions:** These results indicated that the JNK inhibitor attenuated cerebral vasospasm through suppression of inflammatory response, which may provide a novel therapeutic target for cerebral vasospasm.

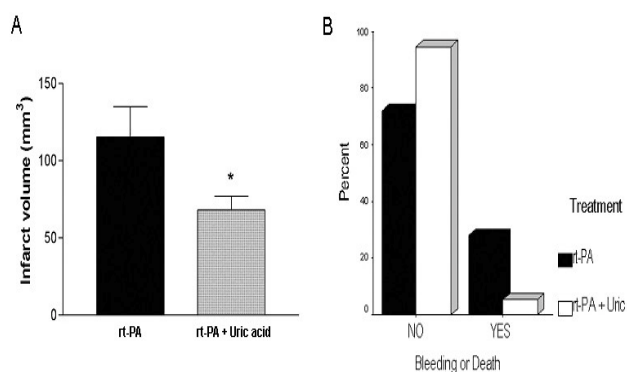
## URIC ACID IMPROVES THE BENEFICIAL EFFECTS OF RT-PA IN A RAT MODEL OF THROMBOEMBOLIC ISCHEMIA

Eduardo Romanos<sup>1,2</sup>, Anna M. Planas<sup>1</sup>, Angel Chamorro<sup>2</sup>

<sup>1</sup>Department of Pharmacology & Toxicology, IIBB-CSIC, IDIBAPS, Barcelona, Spain

<sup>2</sup>Stroke Unit, IMSN, Hospital Clínic, IDIBAPS, Barcelona, Spain

**Objectives:** Thrombolysis with rt-PA is the only treatment of stroke with proven benefit in randomized clinical trials. Most neuroprotective agents added to rt-PA have proved so far clinically ineffective. Uric acid is a natural antioxidant that reduces infarct volume after middle cerebral artery (MCA) occlusion in rats<sup>1</sup>, and recent clinical studies have described an association between increased uric acid plasma levels and improved neurological outcome after stroke <sup>2,3</sup>. Here we sought to confirm the neuroprotective effects of uric acid in a thromboembolic model of brain ischemia in the rat, and to investigate whether it increases the global benefits of thrombolysis. **Methods:** Male adult Sprague-Dawley rats (n=88) were anesthetized (halothane) and ischemia was induced using a thromboembolic model of MCA occlusion. Thrombin-blood clots were injected into the internal carotid artery using our own modification of previously described procedures <sup>4</sup>. Uric acid (16 mg/Kg) was dissolved in Locke's buffer and was injected i.v. 20 min after the induction of ischemia. At 3h, rats were anesthetized and received rt-PA (10 mg/Kg) that was given as an i.v. bolus (10%) followed by a 1-hour i.v. perfusion (90%). At 24h rats animals were killed and infarct volume was measured in the following treatment groups: controls (n=16), uric acid (n=15), rt-PA (n=16); and uric acid + rt-PA (n=16). **Results:** Uric acid significantly reduced infarct volume at 24h (p<0.05). rt-PA given at 3h caused a very strong and significant reduction of infarct volume (p<0.001). As shown in Fig. 1, uric acid + rt-PA reduced infarct volume more than rt-PA alone (p<0.05). Nonetheless, the protective effect of combined therapy was restricted to the cortex. Combined therapy also showed a trend to significance (p=0.058) in the reduction of fatal and non-fatal bleeding compared with rt-PA alone (Fig.2). **Conclusions:** Uric acid given early after thromboembolic ischemia is neuroprotective and improves the safety profile of rt-PA. This combined therapy deserves further clinical investigation. **References:** 1. Yu ZF, et al.(1998) *J Neurosci Res* 53:613-625 2. Chamorro A et al. (2002) *Stroke* 33:1048-1052 3. Chamorro A, Planas AM (2004) *Stroke* 35:e11-12 4. Busch E et al. (1998) *J Cereb Blood Flow Metab* 18:407-418 **Acknowledgment:** Supported by grants from the Comisión Interministerial de Ciencia y Tecnología (CICYT SAF2002-01963).



**SUBARACHNOID HEMORRHAGE IN RATS – NEUROPROTECTIVE EFFICACY OF BRADYKININ B2 RECEPTOR BLOCKADE**

**Stefan Zausinger**<sup>1</sup>, Sporer Sonja<sup>1</sup>, Thal Serge<sup>2</sup>, Plesnila Nikolaus<sup>1</sup>, Schöller Karsten<sup>1</sup>, Schmid-Elsaesser Robert<sup>1</sup>

<sup>1</sup>*Klinikum Der Universität München-Grosshadern, Department of Neurosurgery, Munich, Germany*

<sup>2</sup>*Johannes Gutenberg-Universität, Department of Anesthesiology, Mainz, Germany*

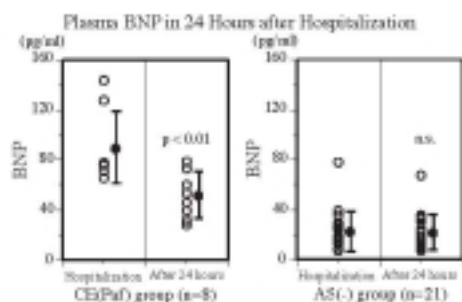
**Objective:** Increased ICP and decreased CBF leading to global cerebral ischemia are the primary causes of death after severe subarachnoid hemorrhage (SAH). One reason for dramatic initial increase of ICP is the rapidly developing cerebral edema as a result of breakdown of cerebral autoregulation and the blood-brain barrier, constituting an independent risk factor for mortality and poor outcome. Bradykinin, an active peptide of the kallikrein-kinin system has been found to enhance brain edema formation, mediated by bradykinin B2-receptors. LF 16-0687, a novel bradykinin B2 receptor antagonist decreased brain swelling in various models of traumatic and ischemic brain injury. We investigated the influence of LF 16-0687 in a rat model of SAH on ICP, CBF, neurological recovery and evolution of brain edema. **Method:** 28 rats were subjected to SAH by an endovascular filament. ICP and bilateral CBF were continuously recorded by a parenchymal probe and Laser Doppler flowmetry. Animals were randomly assigned to 3 groups: (a) vehicle, (b) LF 16-0687 s.c. (3 mg/kg), given 30 min before and 6 hours after SAH or (c) LF 16-0687 s.c. (3 mg/kg), given 30 min and 6 hours after SAH. Cerebral water content and functional recovery were assessed 24 hours after SAH at the maximum of brain edema evolution. **Results:** SAH resulted in an immediate increase of ICP up to ~60 mmHg initially and ~30 mmHg for the following 90 min without significant differences between groups. Bilateral CBF fell by over 80% with partial recovery without differences between groups. Blockade of bradykinin B2 receptors with treatment started before SAH (group b) afforded significant attenuation of brain water content after 24 hours ( $79.1 \pm 0.07$  % vs. control:  $79.8 \pm 0.3$  %). Furthermore, this group exhibited significantly better neurological recovery after 24 hours ( $5 \pm 0$  pts. vs. control:  $24 \pm 7$  pts.). **Discussion:** The present findings provide evidence for an involvement of the kallikrein-kinin system and of bradykinin, its active metabolite, in evolution of brain edema after SAH. Our results demonstrate that blocking of bradykinin B2 receptors by LF 16-0687 before SAH attenuates increase of brain water content. Furthermore, pretreatment improved neurological recovery in the early post-SAH period. Failure of treatment started after SAH warrants further experiments with higher dosage or i.v. application.

## PLASMA BRAIN NATRIURETIC PEPTIDE ON THE DIAGNOSIS OF CARDIOEMBOLIC STROKE DUE TO PAROXYSMAL ATRIAL FIBRILLATION

Takayuki Naya, Kazushi Yukiiri, Naohisa Hosomi, Tsutomu Takahashi, Masakazu Kohno

*Second Department of Internal Medicine, Division of Stroke, Kagawa University School of Medicine, Kagawa, Japan*

**Objective:** When ischemic stroke patient had sinus rhythm in hospitalization, it is difficult to differentiate cardioembolic stroke from atherosclerotic stroke (atherothrombotic stroke and lacunar stroke). The plasma brain natriuretic peptide (BNP) was evaluated for the discrimination of cardioembolic stroke. **Methods:** Ninety-four consecutive patients with acute cerebral infarction were admitted to Kagawa University Hospital from January 1, 2000 to December 31, 2003. The patients with valve disease, cardiomyopathy, or heart failure were excluded from the evaluation ( $n = 23$ ). The mean age of the study sample was 69.6 years and 49 patients were men and 22 were women. The patients were categorized into cardioembolic stroke (CE) or atherosclerotic stroke (AS) using echocardiography, brain computed tomography, magnetic resonance imaging, magnetic resonance angiography, and carotid ultrasonography by two stroke specialists. In the same time, atrial fibrillation was diagnosed as permanent atrial fibrillation (Af), paroxysmal atrial fibrillation (PAf), or sinus rhythm (-) with electrocardiography. The plasma BNP was evaluated at their hospitalization in these patients. **Results:** Plasma BNP was significantly higher in CE(Af), AS(Af), CE(PAf) group than in AS(-) group ( $112 \pm 29$  ( $n = 16$ ),  $91 \pm 18$  ( $n = 7$ ),  $90 \pm 29$  ( $n = 8$ ) vs.  $27 \pm 14$  ( $n = 40$ ),  $p < 0.01$ ; respectively). Furthermore, plasma BNP at hospitalization was the strong independent predictor of cardioembolic stroke among plasma BNP at hospitalization, E/A at hospitalization, and left atrium dimension with multivariate analysis ( $F_{3,47} = 44.1$ ,  $p < 0.001$ ,  $n = 48$ ). In all patients of CE(PAf) group and 21 patients of AS(-) group, plasma BNP was evaluated again in 24 hours after hospitalization. Plasma BNP in CE(PAf) group has decreased significantly in 24 hours after hospitalization from  $90 \pm 29$  pg/ml to  $52 \pm 19$  pg/ml ( $p < 0.01$ ). In AS(-) group, there was no significant change on BNP in 24 hours after hospitalization. **Conclusion:** From the present study, it was shown that cardioembolic stroke patients with PAf showed high plasma BNP even they had sinus rhythm at hospitalization. In addition, plasma BNP did not change in atherosclerotic stroke patients, but decreased in cardioembolic stroke patients with PAf. Therefore, it was shown that cardioembolic stroke with PAf and atherosclerotic stroke patients were differentiable with plasma BNP evaluation.



**BIOCHEMICAL MARKERS OF ACUTE ISCHEMIC STROKE PATIENTS**

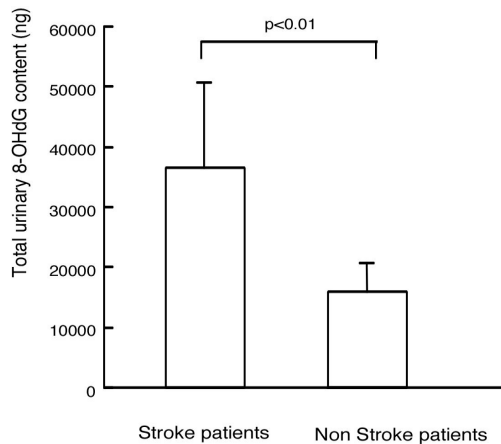
**Genki Mizukoshi**, Ken-ichiro Katsura, Megumi Watanabe, Yasuo Katayama

*Second Department of Internal Medicine, Nippon Medical School, Tokyo, Japan*

**Background and purpose:** Early predictors of prognosis in patients with acute ischemic stroke may help therapeutic decisions. Several studies have been made on several biochemical markers of ischemic stroke, however 8-hydroxy-2-deoxyguanosine (8OHdG), a novel marker of oxidative DNA stress, has never been studied in human yet. We investigated whether measurements of urinary 8OHdG can predict the course of acute ischemic stroke of middle cerebral artery (MCA) territory. At the same time we measured serum S100 $\beta$ , the astroglial protein which is reported to be correlated to cerebral infarct volume and prognosis, and compared with 8OHdG.

**Methods:** 23 patients were divided into an edaravone-treated group (n=16) and an edaravone non-treated group (n=7). We evaluated efficacy of edaravone by calculating urinary 8-OHdG and plasma S100 $\beta$  per unit volume of cerebral infarction. Urine was collected for 24h for 8-OHdG measurement and plasma was sampled for S100 $\beta$  analysis at the 3rd, 4th, 5th, 7th, and 14th day after onset. All patients were treated similarly except for edaravone use.

**Result;** Total urinary 8-OHdG content during the 3rd to 5th day was significantly higher in stroke patients than in non-stroke patients ( $p<0.01$ , Figure). The total urinary 8-OHdG contents showed significant correlation to volume of infarction ( $p<0.05$ ), modified Rankin Scale ( $p<0.05$ ), and plasma S100 $\beta$  values ( $p<0.05$ ). Edaravone treatment did not show significant effects on delta 8-OHdG values divided by volume of infarction. In contrast, S100 $\beta$  index (individual S100 $\beta$  values minus value at 14th day divided by volume of infarction) showed significant reduction in the edaravone-treated group ( $p<0.05$ ).



## MAPPING OF ADC ABNORMALITIES ASSOCIATED TO ACUTE SPONTANEOUS INTRACEREBRAL HEMATOMA AS EVALUATED BY DIFFUSION-WEIGHTED IMAGING

Enrico Fainardi<sup>1</sup>, Stefano Ceruti<sup>1</sup>, Massimo Borrelli<sup>1</sup>, Andrea Saletti<sup>1</sup>,  
Roberta Schivalocchi<sup>2</sup>, Cristiano Azzini<sup>3</sup>, Monia Russo<sup>3</sup>, Michele Cavallo<sup>2</sup>,  
Arturo Chierigato<sup>4</sup>, Riccardo Tamarozzi<sup>1</sup>

<sup>1</sup>Neuroradiology Unit, Arcispedale S. Anna, Ferrara, Italy

<sup>2</sup>Neurosurgery Unit, Arcispedale S. Anna, Ferrara, Italy

<sup>3</sup>Neurology Unit, Arcispedale S. Anna, Ferrara, Italy

<sup>4</sup>Neurointensive Care Unit, Ospedale M Bufalini, Cesena, Italy

**Objectives.** Accumulating experimental evidences suggest that acute spontaneous intracerebral hemorrhage (SICH) is surrounded by a zone of perihematomal brain edema. However, data coming from human studies based on the assessment of perihemorrhagic regional Apparent Diffusion Coefficient (rADC) changes by using Diffusion-Weighted Imaging (DWI) are still controversial. Thus, in this study we sought to quantify rADC values around SICH in order to clarify the effective presence of perilesional edema. **Patients and Methods.** DWI was performed on a 1-Tesla Magnetic Resonance Imaging (MRI) unit equipped for isotropic DWI. Axial images covering the whole brain were obtained by single-shot echo-planar spin-echo sequences in 45 patients (22 male and 23 female; mean age =  $64.1 \pm 10.4$ ) with supratentorial acute SICH at admission CT scans and having a Glasgow Coma Scale at entry ranging from 9 to 15. Mean hematoma volume was  $18.3 \pm 12.7$  cm<sup>3</sup>. ADC maps were generated for each patient by using an imaging workstation. rADC values were measured in four different regions of interest (ROI) drawn freehand on the T2-weighted images at b 0 mm<sup>2</sup>/s on every section in which hematoma was visible and including: 1) the perihematomal hyperintense area; 2) 1 cm of normal appearing brain tissue surrounding the perilesional hyperintense rim; 3) an area mirrored the region including the clot and perihematomal hyperintense area placed in the contralateral hemisphere. rADC values within the hemorrhagic core were not evaluated due to the well-known presence of susceptibility artifacts. rADC levels were expressed in mm<sup>2</sup>/s. rADC values lower than  $70 \times 10^{-5}$  and higher than  $80 \times 10^{-5}$  mm<sup>2</sup>/s were considered as suggestive of cytotoxic and vasogenic edema, respectively. All DWI studies were obtained within 48 hours after symptom onset. Statistical analysis was performed by Mann-Whitney U test and Spearman rank correlation coefficient test. **Results.** rADC mean values were higher in perihematomal hyperintense and in contralateral than in normal appearing areas ( $p < 0.001$ ). The analysis of absolute values revealed that rADC mean levels were increased in perihematomal hyperintense ( $111.6 \pm 36.7 \times 10^{-5}$ ), in normal appearing ( $93.1 \pm 11.1 \times 10^{-5}$ ) and in contralateral areas ( $105.9 \pm 20.1 \times 10^{-5}$ ). No definite correlations were observed between perihematomal rADC mean levels and hematoma volume. **Conclusions.** rADC values reflecting vasogenic edema were found in perihematomal area and in normal appearing brain tissue located both ipsilaterally and contralaterally to hematoma, with less pronounced values in non-injured area located around the periclot T2 hyperintense rim. In addition, the edema formation in perilesional T2 high signal area seems to be independent from hematoma size. These findings suggest that acute SICH is associated to both local and global edematous brain responses and indicate that DWI with analysis of rADC values represents a powerful tool for the evaluation of early edema development occurring around an acute hemorrhagic focal lesion.

## CONTRACTILE AND CYTOSKELETAL PROTEIN CHANGES IN RABBIT BASILAR ARTERY 7 DAYS AFTER SUBARACHNOID HEMORRHAGE AND EFFECTS OF DEXAMETHASONE TREATMENT

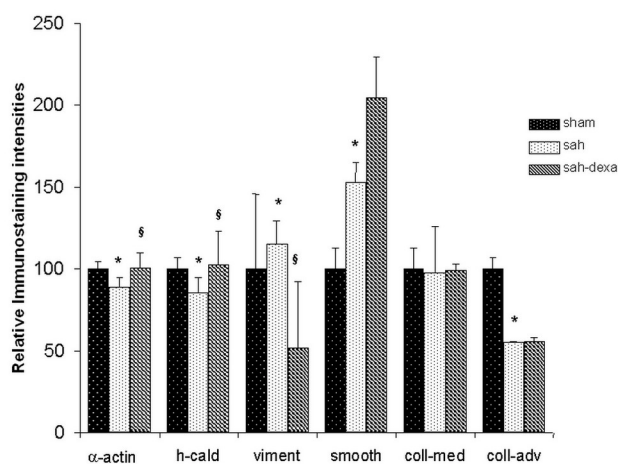
Philippe Gomis<sup>1,3</sup>, Yves-Roger Tran Dinh<sup>1,2</sup>, Christine Sercombe<sup>1</sup>, Richard Sercombe<sup>1,2</sup>

<sup>1</sup>CNRS UPR 646, Paris, France

<sup>2</sup>Laboratory for Microcirculation Research (EA3509), Faculté de Médecine Lariboisière-St Louis, Université Paris VII, Paris, France

<sup>3</sup>Department of Anesthesia, Centre Hospitalier Universitaire, Reims, France

**Object.** Following subarachnoid hemorrhage (SAH), cerebral arteries undergo morphologic and functional modifications. We aimed to study the perturbations of the expression of four smooth muscle cytoskeletal and contractile proteins and an extracellular protein, collagen-I, after SAH, and the possible preventive effects of an anti-inflammatory drug, dexamethasone. **Methods.** Using a one-hemorrhage rabbit model (autologous blood injection into the cisterna magna), we studied, first, the effects of SAH on the expression of alpha-actin, h-caldesmon, vimentin, smoothelin-B, and collagen-I, and second, whether post-SAH systemic administration of dexamethasone (3 daily injections of 5.6 mg/kg i.m.) corrected the alterations induced by the SAH. Measurements were made at day 7 after SAH. The proteins were studied by indirect immunohistochemical staining of 20 $\mu$  frozen artery sections using a laser-scanning confocal microscope and attached software to determine the relative protein staining densities. **Results.** Compared to sham arteries, the staining density of the media of SAH arteries was reduced for alpha-actin (-11%,  $p = 0.01$ ) and for h-caldesmon (-15%,  $p = 0.06$ ), but increased for vimentin (+15%,  $p = 0.04$ ) and smoothelin-B (+53%,  $p = 0.04$ ). Compared to arteries of the SAH group, those from the dexamethasone-treated SAH group showed higher values of density for alpha-actin (+13%,  $p = 0.05$ ) and h-caldesmon (+20%,  $p = 0.01$ ), and lower values for vimentin (-55%,  $p = 0.05$ ) and non-significantly different values for smoothelin-B. The density of collagen-I in the adventitia decreased significantly after SAH (-45%,  $p = 0.01$ ), but dexamethasone treatment was without effect on this decrease. These results are summarized in the figure. **Conclusions.** Thus, SAH-induced alterations in the density of 3 out of 4 smooth muscle proteins were reversed by dexamethasone treatment; two of these are directly related to contraction. This drug may potentially be useful to prevent certain morphological and functional changes in cerebral arteries after SAH. **Figure legend.** Means and SD of immunostaining intensities expressed relative to values in sham animals. Coll-med=medial collagen; coll-adv=adventitial collagen. \*  $p < 0.05$  between sham and sah groups ( $p = 0.06$  for h-cald). §  $p < 0.05$  between sah and sah dexa groups.





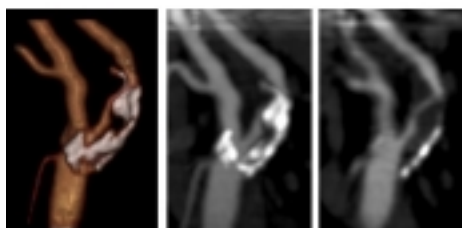
**PERIOPERATIVE EVALUATION OF CAROTID ENDARTERECTOMY BY 3D-CT ANGIOGRAPHY WITH REFINED RECONSTRUCTION: PRELIMINARY EXPERIENCE OF CEA WITHOUT CONVENTIONAL ANGIOGRAPHY**

**Hiroyuki Katano<sup>1</sup>, Kojiro Kato<sup>2</sup>, Atsushi Umemura<sup>1</sup>, Kazuo Yamada<sup>1</sup>**

*<sup>1</sup>Department of Neurosurgery and Restorative Neuroscience, Nagoya City University Graduate School of Medical Sciences, Nagoya, Japan*

*<sup>2</sup>Department of Neurosurgery, Kamiida Daiichi General Hospital, Nagoya, Japan*

Object: For preoperative studies in cases of carotid endarterectomy (CEA), conventional arterial angiography has been used as a golden standard to evaluate extent of carotid stenosis. Three-dimensional computed tomography angiography (3D-CTA) has been developed and utilized in visualization of various cerebral lesions. Here we present a preliminary report of our experience with CEA using perioperative 3D-CTA in place of selective angiography for evaluation of carotid stenosis. Methods: A total of 62 carotid arteries were examined before and after CEA, 26 with an early 3D-CT system and 36 with a multidetector helical CT allowing sophisticated reconstruction by personal workstation. In addition to patients who had undergone conventional angiography at other institutes, ten subjects underwent CEA on the basis of 3D-CTA findings alone. Results: Three D-CTA provided detailed information with an excellent view of carotid stenoses. Volume rendering images comprehensively visualized lesions and surrounding structures as well as calcifications, which were also well depicted by maximum intensity projection images (Fig.). With postoperative evaluation, amelioration of stenosis of carotid arteries and disappearance of calcifications on walls were obviously displayed in 3D images. Evaluation of the cerebral circulation is one problem that still requires solution, although cerebral vessels were delineated by 3D-CTA. One patient experienced transient hemiparesis but no significant permanent deficit. Conclusions: Our preliminary experience of CEA on the basis of 3D-CTA without conventional angiography indicates that this approach with a high-performance workstation provides detailed images with satisfactory preoperative information for CEA. We conclude that 3D-CTA is a safe and accurate modality which is a practical alternative to conventional perioperative angiography.



**PREDICTING THE FATE OF ACUTE ISCHEMIC LESION WITH CT-PERFUSION**

**Hiroshi Hagiwara**, Hidenori Nakamura, Hironaka Igarashi, Tatsushi Kamiya,  
Yasuo Katayama

*The Second Internal Medicine, Nippon Medical School, Tokyo, Japan*

**Purpose:** To clarify whether CT-Perfusion (CTP) derived maps, namely regional cerebral blood flow (rCBF) map, regional cerebral blood volume (rCBV) map, and regional mean transit time (rMTT) map, provide feasible information to predict the fate of the ischemic tissue on acute stage of ischemia, and, if so, which is a best predictor among three. **Methods:** 13 patients with the obstruction of major artery were recruited. CTP was taken within six hours of onset in all cases. Seven regions of interest (ROI) were set on ischemic hemisphere at the level of basal ganglia. The value of rCBF, rCBV and rMTT in these ROI were calculated. Besides, ratio of these three parameters against the mirrored region on non-ischemic hemisphere, namely CBF ratio, CBV ratio and MTT ratio, were also calculated. Then discriminant analyses were performed to access whether threshold for the fate of ischemic tissue (infarcted or salvaged) can be established on these six parameters. Then ROC analyses were taken to evaluate the sensitivity, specificity, and likelihood ratio on each parameter. **Results:** Thresholds by discriminant analyses were 27.9ml/100g/min for rCBF, 0.63 for CBF ratio, 1.69ml /100g for rCBV, 0.85 for CBV ratio, 6.53s for rMTT, and 2.2 for MTT ratio, respectively. Evaluated by sensitivity, the best predictor was 0.91 for each rCBF and CBF ratio; the other sensibilities were 0.84 for rCBV, 0.69 for CBV ratio, 0.86 for rMTT, and 0.88 for MTT ratio. Evaluated by specificity, the best predictor was 0.89 for MTT ratio; the other specificities were 0.75 for rCBF, 0.71 for CBF ratio, 0.59 for rCBV, 0.71 for CBV ratio, and 0.86 for rMTT. The highest likelihood ratio was 8.167 for MTT ratio; the other likelihood ratios were 3.625 for rCBF, 3.383 for CBF ratio, 2.054 for rCBV, 2.406 for CBV ratio, and 5.906 for rMTT. Areas under the ROC curve(mean±S.E) were almost equal for rCBF, CBF ratio, rMTT, and MTT ratio, these were  $0.92 \pm 0.03$ ,  $0.93 \pm 0.03$ ,  $0.93 \pm 0.03$ , and  $0.91 \pm 0.03$ , respectively, and larger than  $0.77 \pm 0.06$  for rCBV,  $0.80 \pm 0.06$  for CBV ratio. **Discussion:** These results suggest that parameters of CTP (namely rCBF, CBF ratio, rMTT, and MTT ratio) can predict the fate of cerebral ischaemia. There are some limitations that the range of slab is limited by width of detector, and because of using non-diffusible tracer, measured value is influenced by cardiac function and presence of vascular structure, but CTP enables the evaluation of cerebral circulation in a short time, and is feasible for therapeutic decision, particularly in determining the necessity of thrombolytic therapy for hyper acute cerebral ischemia.

**STRUCTURE AND FUNCTION OF CEREBRAL MICROCIRCULATION AFTER SUBARACHNOID HEMORRHAGE CAUSED BY PUNCTURE OF THE BIFURCATION OF THE INTERNAL CAROTID ARTERY IN THE RAT**

Katarzyna Borcuch<sup>1</sup>, Radoslaw Michalik<sup>1</sup>, Anna Domasiewicz<sup>1</sup>, Zbigniew Czernicki<sup>1</sup>, Michal Walski<sup>2</sup>, Malgorzata Frontczak-Baniewicz<sup>2</sup>, **Ewa Kozniowska<sup>1</sup>**

<sup>1</sup>*Department of Neurosurgery, Medical Research Center, Polish Academy of Sciences, Warsaw, Poland*

<sup>2</sup>*Department of Ultrastructure of The Nervous System, Medical Research Center, Polish Academy of Sciences, Warsaw, Poland*

Introduction: Acute response to subarachnoid haemorrhage (SAH) is a severe, reversible ischemia which in case of the rat model persists for about one hour. Our hypothesis is that this early ischemia results in long lasting impairment of vascular responses which eventually may participate in the development of late vasospasm. The aim of this study was to assess: i) reactivity of cerebrocortical microcirculation to arterial CO<sub>2</sub> changes, to intravenous administration of papaverine or acetylcholine and to inhibition of nitric oxide synthesis, ii) structural changes of the middle cerebral artery (MCA), basilar artery (BA) and ipsilateral cerebral cortex 24, 48 and 96 hours after SAH. Methods: Male Sprague-Dawley rats (n=54) weighing from 280-320 g were anaesthetized with chloral hydrate (40 mg/kg ip). They were divided into six groups. Group 1 of 20 rats underwent sham surgery, in groups 2-6 (n = 8, 6, 7, 7 and 6, respectively) SAH was induced by endovascular puncture of the bifurcation of the internal carotid artery (Veelken JA et al., Stroke 1995; Bederson JB et al., Stroke 1995). Microflow (LDF) in cerebral cortex was measured bilaterally before, during and, for at least 1 hour, after SAH using two channels laser Doppler flowmeter. In group 2 reactivity of microcirculation was tested at 3 hours following SAH. In groups 3-5 it was assessed at 24, 48 and 96 hours after SAH, respectively. Group 6 and 6 rats from group 1 were perfused transcardially with 4% buffered glutaraldehyde. Fragments of cerebral cortex, MCA's and BA were carefully removed and processed for electron microscopy. Results: Following SAH reactivity of LDF to CO<sub>2</sub>, papaverine and acetylcholine in the ipsilateral cortex was severely impaired up to 48 hours. At 96 hours slight recovery of LDF responses was noted. On the contralateral site impairment of the reactivity to all tested vasodilators was observed only at 24 hours after SAH. The response to L-NAME was well preserved on both sites at all times. Electron microscopy demonstrated edema of the ipsilateral cerebral cortex. In ipsilateral MCA and in BA damage of endothelial cells and rearrangement of the contractile elements was observed. Conclusion: This study demonstrates that vasodilatory capacity of microcirculation is severely impaired following SAH. Moreover, preservation of LDF response to L-NAME and lack of the response to acetylcholine suggest deficiency of the NO/cGMP system. Structural changes observed in MCA and BA suggest remodelling of the vessel wall.

## PROTEIN KINASE C INHIBITION BLOCKS UPREGULATION OF ETB AND 5-HT1B RECEPTORS AND REVERSE CEREBRAL BLOOD FLOW REDUCTION IN SUBARACHNOID HAEMORRHAGE OF RATS

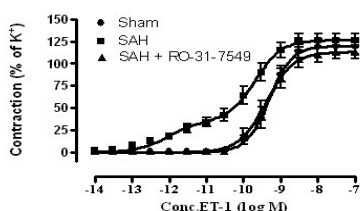
Saema Beg<sup>1,2</sup>, Jacob Hansen-Schwartz<sup>2</sup>, Lars Edvinsson<sup>1,2</sup>

<sup>1</sup>Department of Medicine, Division of Experimental Vascular Research, Lund, Sweden

<sup>2</sup>Department of Clinical Experimental Research, Glostrup University Hospital, Glostrup, Denmark

Introduction: Despite many years of research the pathogenesis of vasospasm after subarachnoid haemorrhage (SAH) still remains elusive and no specific treatment exists to alleviate the condition. Previous studies have shown that endothelin type B (ETB) and 5-hydroxytryptamine type 1B (5-HT1B) receptors are upregulated following experimental SAH. However, the intracellular pathways responsible for this receptor upregulation remains unclear. The purpose of the present study was to investigate the involvement of protein kinase C (PKC) in an experimental induced SAH model. We also wanted to test whether PKC inhibition could alter the degree of SAH induced ET and 5-HT1 receptor upregulation in addition to prevent the cerebral blood flow reduction. Methods: SAH was induced by injecting 250  $\mu$ l blood into the prechiasmatic cistern. In conjunction and after the induced SAH the PKC inhibitor RO-31-7549 was injected intracisternally. Two days after the SAH basilar arteries (BA) and middle cerebral arteries (MCA) were harvested and contractile responses to endothelin-1 (ET-1; ETA and ETB receptor agonist) and 5-carboxamidotryptamine (5-CT; 5-HT1 receptor agonist) were investigated by sensitive myographs. ETA, ETB and 5-HT1B receptor mRNA levels were analyzed by real-time PCR. In addition the regional CBF in sham, SAH and SAH treated with PKC inhibitor was evaluated by an autoradiographic technique. Results: The PKC inhibitor RO-31-7549 decreased the maximum contraction elicited by application of ET-1 in BA and MCA as compared to SAH. A sigmoidal curve was obtained with an Emax of  $113 \pm 8\%$ , and a pEC50 of  $9.42 \pm 0.16$  (Fig.1). Interestingly there was no significant difference in the contractile response between sham and RO-31-7549 treated rats. Treatment with RO-31-7549 also decreased the maximum contraction elicited by application of 5-CT considerably as compared to SAH. In parallel the PKC inhibition downregulated ETB and 5-HT1B receptor mRNA levels. No differences were observed in the ETA receptor mRNA levels. The reduction in global and regional CBF observed after SAH was significantly prevented with treatment with RO-31-7549 (SAH:  $56.5 \pm 4.0$  and RO:  $116.6 \pm 7.3$  ml/min/100g). Statistical analyses were performed using the nonparametric Wilcoxon rank test, differences were considered significant at  $p \leq 0.05$ . Data are expressed as mean  $\pm$  s.e.m. Conclusion: Our study suggests that PKC plays an important role in the pathogenesis of cerebral vasospasm. Inhibition of PKC prevented the reduction in the perfusion of global and regional CBF. It also attenuated the vasoconstriction mediated by ETB and 5-HT1B receptors and decreased the receptor mRNA levels in rat cerebral arteries after SAH. These results indicate that PKC may be an important intracellular mediator for receptor upregulation and via its inhibition we can prevent the cerebral vasospasm associated with SAH.

Figure 1.



## DETERMINATION OF THE TIME COURSE OF EXPERIMENTAL CEREBRAL VASOSPASM IN THE RAT DOUBLE SUBARACHNOID HEMORRHAGE MODEL BY NEUROLOGICAL SCORE, SELECTIVE VERTEBRO-BASILAR ANGIOGRAPHY, AND PERFUSION WEIGHTED MAGNET RESONANCE IMAGING

**Hartmut Vatter**<sup>1</sup>, Stefan Weidauer<sup>2</sup>, Juergen Konczalla<sup>1</sup>, Edgar Dettmann<sup>2</sup>,  
Michael Zimmermann<sup>1</sup>, Friedhelm E. Zanella<sup>2</sup>, Volker Seifert<sup>1</sup>

<sup>1</sup>*Department of Neurosurgery, Johann Wolfgang Goethe-University, Frankfurt am Main, Germany*

<sup>2</sup>*Institute of Neuroradiology, Johann Wolfgang Goethe-University, Frankfurt am Main, Germany*

### Object:

The double hemorrhage model in the rat is widely accepted to represent a reasonable simulation of delayed cerebral vasospasm (CVS) after subarachnoid hemorrhage (SAH). A neurological and angiographic characterization of this CVS, however, was not available so far and is provided in the present investigation. Additionally, perfusion weighted imaging (PWI) at 3 tesla magnet resonance (MR) tomography was implemented for determination of cerebral blood flow (CBF) and volume (CBV).

### Methods:

In a prospective experimental setting CVS was induced by application of 0.2 ml of autologous blood in the Cisterna magna done twice. Surviving rats were examined on the days 2, 3, 5, 7 and 9. Animals were neurologically graded between 0 and 3, followed by MRI, and selective digital subtraction angiography (DSA). The relative regional (rr) CBF and rrCBV was set in relation to the perfusion (MBF) and the blood volume of the masseter muscle (MBV).

### Results:

Neurological condition was significantly reduced on day 2, 3, and 5 (medians) (Figure 1). Basilar artery (BA) diameter, however, was not significantly reduced until day 5 reaching  $0.15 \pm 0.02$  mm (SAH) versus  $0.32 \pm 0.01$  mm (sham) (mean  $\pm$  SEM). In correlation the rrCBF/rrMBF ratio ( $2.5 \pm 0.8$  (SAH);  $9.2 \pm 1.3$  (sham)) and the rrCBV/rrMBV ( $3.2 \pm 0.5$  (SAH);  $8.5 \pm 1.3$  (sham)) was also significantly decreased on day 5 (Figure 2). Correlation between BA diameter and rrCBF/rrMBF was 0.70 and 0.77 for rrCBV/rrMBV.

### Conclusion:

A valid and reproducible CVS in the rat double hemorrhage model was proven by neurological score, DSA, and PWI on day 5. Additionally, our data demonstrate the practicability and validity of MR PWI for the monitoring of CVS in a rat SAH model.

Figure 1

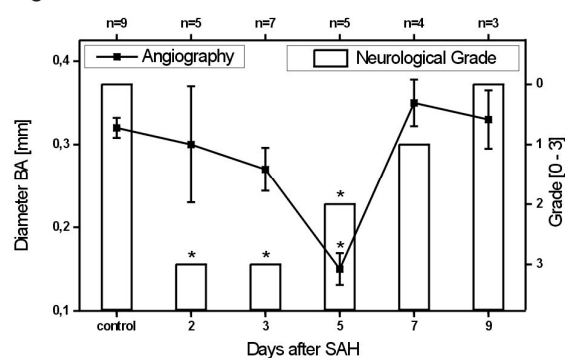
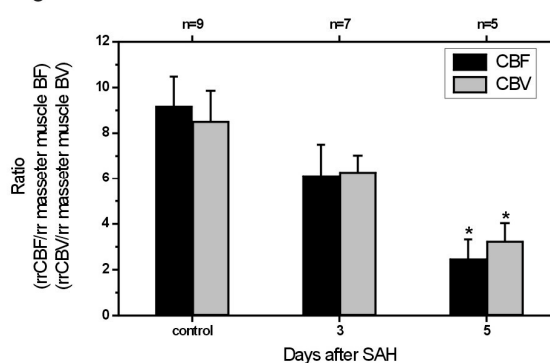


Figure 2



**TISSUE-TYPE PLASMINOGEN ACTIVATOR CROSSES THE INTACT BLOOD-BRAIN BARRIER BY LRP-MEDIATED TRANSCYTOSIS : A PHENOMENON THAT IS SWITCHED DURING OXYGEN GLUCOSE DEPRIVATION TO AN INCREASED AND LRP-INDEPENDENT PROCESS**

Karim Benchenane<sup>1</sup>, Carine Ali<sup>1</sup>, Julien Brillault<sup>2</sup>, Vincent Berezowski<sup>2</sup>,  
Monica Fernandez-Monreal<sup>3</sup>, Jose P. Lopez-Attalaya<sup>1</sup>, Julien Chuquet<sup>3</sup>, Andre Nouvelot<sup>3</sup>,  
Eric T. MacKenzie<sup>3</sup>, Marie-Pierre Dehouck<sup>2</sup>, Romeo Cecchelli<sup>2</sup>, Denis Vivien<sup>1</sup>,  
Omar Touzani<sup>3</sup>

<sup>1</sup>*INSERM-Avenir Cyceron Center, Caen, France*

<sup>2</sup>*Laboratoire de la BHE, EA 2465, Université D'Artois, Lens, France*

<sup>3</sup>*UMR CNRS 6185, Cyceron Center, Caen, France*

Despite uncontroversial benefit from its thrombolytic activity, the documented neurotoxic effect of tissue plasminogen activator (tPA) raises an important issue: the current emergency stroke treatment might not be optimum, if exogenous tPA can enter the brain and thus add to the deleterious effects of endogenous tPA within the cerebral parenchyma. Here, we aimed at determining whether vascular tPA crosses the blood-brain barrier (BBB) during cerebral ischemia, and if so, by which mechanism. We have first evidenced that brain lesions induced by intra-striatal injection of NMDA were enhanced either when tPA was co-infused in the striatum or when intravenously injected. In addition, co-infusion of PAI-1 with NMDA in the striatum prevented the deleterious effect of intravenous injection of tPA. No BBB alteration was observed in any of these conditions, as assessed by confocal microscopy analysis of FITC-Dextran (77kDa) extravasation. Altogether, these data suggest that tPA (69 kDa) has to cross the intact BBB to potentiate neuronal death within the parenchyma. By using biotinylated tPA, we have shown by immunohistochemistry, that tPA crossed the BBB in vivo in control and NMDA-injected animals. Moreover, tPA can be detected in the cerebrospinal fluid after its intravenous injection. In order to characterize the mechanism of this passage, we used a cellular model of BBB. Although tPA did not influence the integrity of the BBB by itself, tPA was capable to cross the BBB. Its passage was blocked at 4 C and was saturable, suggesting a transendothelial and receptor-mediated mechanism. As the low-density lipoprotein receptor related protein (LRP) and mannose receptor have been already shown to bind tPA, we investigated whether one of these two receptors could be involved in this passage. Although mannose had no effect on the passage of tPA, RAP (receptor-associated protein, an antagonist of LRP) blocked the passage of tPA. We next investigated whether oxygen and glucose deprivation (OGD) could influence the mechanism of the passage of tPA. OGD led to an exacerbation of tPA passage, and switched the mechanism to a LRP-independent process. These data suggest two mechanisms by which tPA can cross the BBB, a moderate receptor-mediated transcytosis in control conditions and an exacerbated and unsaturable passage involving an unspecific transcellular pathway after ischemic conditions. Preventing the interaction of tPA with LRP could thus be an interesting strategy to block the deleterious effect of tPA in vivo, but only as long as the integrity of the BBB is not altered. These data show the importance of taking the side effects of blood derived tPA into account, and offer bases to improve the current thrombolytic strategy for stroke treatment.

**IN VITRO EVALUATION OF THE CEREBROVASCULAR EFFECTS OF  
CLAZOSENTAN, THE FIRST CLINICALLY EFFECTIVE ENDOTHELIN-  
RECEPTOR ANTAGONIST FOR THE TREATMENT OF CEREBRAL VASOSPASM  
AFTER SUBARACHNOID HEMORRHAGE**

**Hartmut Vatter**<sup>1</sup>, Michael Zimmermann<sup>1</sup>, Veronika Tesanovic<sup>1</sup>, Andreas Raabe<sup>1</sup>,  
Volker Seifert<sup>1</sup>, Lothar Schilling<sup>2</sup>

<sup>1</sup>*Department of Neurosurgery, Johann Wolfgang Goethe-University, Frankfurt am Main,  
Germany*

<sup>2</sup>*Faculty of Clinical Medicine Mannheim, University of Heidelberg, Department of  
Neurosurgery, Division Neurosurgical Research, Mannheim, Germany*

**Object:**

A disturbed balance of the cerebrovascular nitric oxide (NO)-Endothelin (ET)-1 network, seems to play an important role in the development of cerebral vasospasm (CVS) after subarachnoid hemorrhage (SAH). The ET-1 effect mediated by the dominant smooth muscular ET(A)-receptor seems to represent the contractile part of this network. Activation of the endothelial ET(B)-receptor, however, results in a release of NO, which may imply a neuroprotective effect by vasodilatation. Accordingly, an ET(A)-receptor selective antagonist may be the most promising approach for treatment of CVS. Clazosentan is a putatively high selective ET(A)-receptor antagonist and the first drug that provides clinical prove of ET-1 being involved in the pathogenesis of CVS. Aim of the present investigation was, therefore, to provide the pharmacological properties of clazosentan including its actual selectivity to the ET-receptors in the cerebrovasculature in a functional approach.

**Methods:**

Isometric force measurements were performed in rat basilar artery (BA) ring segments with (E+) and without (E-) endothelial function. Concentration effect curves (CEC) were constructed by cumulative application of ET-1, Sarafotoxin S6c (S6c), or bigET-1 in the presence or absence of clazosentan ( $10^{-9}$ M -  $10^{-6}$ M). To characterize the contractile, ET(A)-receptor segments under resting tone were used. To evaluate the vasodilatory component segments were pre-contracted with prostaglandin F<sub>2 $\alpha$</sub> .(PGF F<sub>2 $\alpha$</sub> ). The inhibitory potency of clazosentan was determined by the pA<sub>2</sub>-value.

**Results:**

CECs for the contraction by ET-1 and bigET-1 were shifted to the right in the presence of clazosentan dose dependently and in a parallel manner, which indicates competitive antagonism. The pA<sub>2</sub>-values for ET-1 were 7.8 (E+) and 8.6 (E-) compared to the values for bigET-1 of 8.6 (E+) and 8.3 (E-), respectively. The relaxation by S6c, ET-1 and bigET-1 was also inhibited by clazosentan in a competitive manner, yielding pA<sub>2</sub>-values of 7.1, 6.7 and 6.5, respectively. The selectivity to the ET(A)-receptor in the cerebrovascular system was, therefore, approximately two logarithmic units.

**Conclusion:**

The present data characterize clazosentan as a potent competitive antagonist on the ET(A)-receptor mediated constriction of the cerebrovasculature by ET-1 and its precursor bigET-1. A competitive inhibition of ET(B)-receptor mediated relaxation in cerebral vessels by clazosentan in therapeutically relevant concentrations, however, is suggested by our data. Therefore, evaluation of its concentration in the cerebrospinal fluid should be performed in further clinical trials. The present data may additionally be taken to describe the pharmacological properties for an ET-receptor antagonist specifically tailored for the treatment of pathological conditions of impaired cerebral blood flow.

**CEREBRAL HEMODYNAMICS AND OXYGEN METABOLISM IN OCCLUSIVE CEREBROVASCULAR DISEASE: COMPARISON BETWEEN “MISERY PERFUSION” AND “MATCHED REDUCTION IN CBF AND CMRO2”**

Ken Okada<sup>1</sup>, Hiroshi Ito<sup>1</sup>, Eku Shimosegawa<sup>2</sup>, Kentarou Inoue<sup>1</sup>, Ryoui Goto<sup>1</sup>, Shigeo Kinomura<sup>1</sup>, Yasuyuki Taki<sup>1</sup>, Shuichi Miura<sup>2</sup>, Hiroshi Fukuda<sup>1</sup>

<sup>1</sup>*Department of Nuclear Medicine and Radiology, Institute of Development, Aging and Cancer, Tohoku University, Sendai, Japan*

<sup>2</sup>*Department of Radiology and Nuclear Medicine, Akita Research Institute of Brain and Blood Vessels, Akita, Japan*

Introduction: Measurement of cerebral blood flow (CBF), cerebral blood volume (CBV), cerebral oxygen extraction fraction (OEF), and cerebral metabolic rate of oxygen (CMRO<sub>2</sub>) by PET is widely used for investigation into the pathophysiology of occlusive cerebrovascular disease. Decreased cerebral perfusion pressure below the lower limit of cerebral autoregulation causes a decrease in CBF with an increase in OEF for maintenance of CMRO<sub>2</sub>, that is called as “misery perfusion”. On the other hand, decrease in CBF with decrease in CMRO<sub>2</sub> is often observed in brain regions suffered from occlusive cerebrovascular disease without any organic lesions on MRI (“matched reduction”). However, cerebral hemodynamics in matched reduction has not been elucidated. In the present study, we have investigated cerebral hemodynamics and oxygen metabolism using PET in both groups of misery perfusion and matched reduction. Methods: CBF, CBV, OEF, CMRO<sub>2</sub>, and vascular responses to hypercapnia and acetazolamide stress were measured by PET with H<sub>2</sub>15O, C15O, and 15O<sub>2</sub> in 22 patients with stenocclusive lesions in unilateral major cerebral arteries on 2-6 weeks after onset. All patients were divided into two groups, misery perfusion group (n=6) and matched reduction group (n=16), by ipsilateral/contralateral ratio of OEF (misery perfusion group: OEF ratio > 1.05, matched reduction group: OEF ratio < 1.05). Results: In both groups, CBF in ipsilateral side was significantly decreased as compared with contralateral side. CMRO<sub>2</sub> in ipsilateral side was significantly decreased as compared with contralateral side in the matched reduction group, but not in the misery perfusion group. In the misery perfusion group, CBV and vascular mean transit time (MTT, MTT=CBV/CBF) in ipsilateral side were significantly increased, and vascular responses to hypercapnia and acetazolamide stress in ipsilateral side were significantly decreased as compared with contralateral side. In the matched reduction group, no changes in CBV, MTT, and vascular responses to hypercapnia and acetazolamide stress were observed in ipsilateral side as compared with contralateral side. Conclusion: In the misery perfusion group, increase in CBV and decrease in vascular responses to hypercapnia and acetazolamide stress were observed, indicating decrease in cerebral vascular reserve, as reported previously. On the other hand, in the matched reduction group, no changes in CBV, MTT, and vascular responses to hypercapnia and acetazolamide stress were observed, indicating preserved cerebral vascular reserve. Reduction of CMRO<sub>2</sub> with preserved cerebral vascular reserve in matched reduction indicates that hypoperfusion in this lesion might be caused secondary. It can be speculated that lesions showing matched reduction might have microscopic lesions such as neuronal damage that can not be detected by MRI, or remote effects from other ischemic lesions.

## IPSI LATERAL THALAMIC DIASCHISIS IN PATIENTS WITH CORTICAL INFARCTION: LOGISTIC REGRESSION ANALYSIS

Komaba Yuichi<sup>1</sup>, Masahiro Mishina<sup>2</sup>, Shiro Kobayashi<sup>3</sup>, Yasuo Katayama<sup>1</sup>

<sup>1</sup>*The Second Department of Internal Medicine, Nippon Medical School, Tokyo, Japan*

<sup>2</sup>*Department of Neurology, Neurological Institute, Nippon Medical School, Chiba-Hokusoh Hospital, Chiba, Japan*

<sup>3</sup>*Department of Neurosurgery, Neurological Institute, Nippon Medical School, Chiba-Hokusoh Hospital, Chiba, Japan*

Introduction: Ipsilateral thalamic diaschisis (ITD) refers to reduced metabolism and blood flow in the ipsilateral thalamus to a cerebral lesion. We performed single-photon emission computed tomography (SPECT) in patients with cortical infarction to identify regions independently related to ITD, controlling for possible confounding effects. Methods: Patients with unilateral cortical infarction (n=113; 75 male, 38 female; mean age±SD, 66±13 years) underwent SPECT of the brain with N-isopropyl-p-[123I] iodoamphetamine (123I-IMP). Regional cerebral blood flow (rCBF) was measured autoradiographically. Asymmetry indices (AI) were calculated based on ratios representing symmetric rCBF in the thalamus and 16 cerebral regions. ITD was defined as AI<sub>thalamus</sub> exceeding 0.1. AI for 16 cerebral regions were considered as both dichotomous and continuous variables for analysis concerning ITD occurrence using backward logistic regression. Results: Considering dichotomized variables, hypoperfusion of inferior frontal (OR=6.24; 95% CI, 2.187 to 17.800), anterior cingulate (OR=3.91; 95% CI, 1.017 to 15.031), and postcentral (OR=6.372; 95% CI, 2.226 to 17.979) regions independently influenced ITD. Considering continuous variables, hypoperfusion of posterior midfrontal (OR=1.047; 95% CI, 1.012 to 1.082) regions, anterior cingulate (OR=1.046; 95% CI, 1.003 to 1.092), and postcentral (OR=1.042; 95% CI, 1.019 to 1.066) regions independently influenced ITD.

**QUALITY OF PRECLINICAL EVIDENCE FOR NEUROPROTECTION IN STROKE**

**Tori O'Collins**<sup>1,2</sup>, Malcolm Macleod<sup>2,3</sup>, Laura Horky<sup>2,4</sup>, Dennis Young<sup>2</sup>, Geoffrey Donnan<sup>2</sup>,  
David Howells<sup>1,2</sup>

<sup>1</sup>*Department of Medicine, University of Melbourne, Melbourne, Australia*

<sup>2</sup>*National Stroke Research Institute, Melbourne, Australia*

<sup>3</sup>*School of Molecular and Clinical Medicine, University of Edinburgh, Edinburgh, UK*

<sup>4</sup>*Salk Institute, La Jolla, CA, USA*

**BACKGROUND:** The gap between expectations and outcomes in clinical stroke trials of neuroprotection has brought into question the validity and sufficiency of preclinical evidence. **OBJECTIVE:** A review was undertaken in order to identify therapies tested experimentally in animal models of neuroprotection and to assess the quality of experimental evidence supporting the use of such agents in acute stroke patients. Furthermore, to better understand the currently preferred experimental model of stroke - the focal ischemia model (STAIR, 1999) - a meta-analysis was conducted using data from the focal ischemia experiments. **DATA SOURCES:** Experimental acute stroke treatments and studies were identified from PubMed, from clinical trials databases and by cross-reference. For each drug, a PubMed search was conducted using the terms (drug name) AND (neuroprotection OR cerebral ischemia OR stroke). **STUDY SELECTION:** Studies measuring treatment efficacy in controlled culture and in vivo models of neuroprotection were selected for analysis. **RESULTS:** Over 1000 experimental treatments were identified, of which, about 100 have been administered to acute stroke patients. Using a ten-point quality-of-evidence scale based on the Stroke Therapy Academic Industry Roundtable recommendations (1999), the general level of preclinical experimentation fell short of these drug development standards. Whilst the quality of evidence from animal experiments was found to be higher in those drugs that have gone to clinical trial, extensive testing of these drugs in animals was frequently undertaken only after treatments had already been given to patients. Further, the average protection afforded by clinically tested treatments did not differ significantly from those still in the experimental phase (30% vs. 25% respectively). **CONCLUSION:** With hindsight, it is not evident that the best drugs have been selected for clinical trial. More rigorous preclinical testing and a greater understanding of experimental models will assist in the evaluation of promising therapies for clinical trial.

## CEREBROVASCULAR ALTERATION IN ALCOHOLIC PATIENTS

Piroska Szalay<sup>1</sup>, Kornel Sipos<sup>1</sup>, Attila Szucs<sup>2</sup>, **Michael Bodo**<sup>3</sup>

<sup>1</sup>*Faculty of Physical Education and Sport Sciences, Semmelweis University, Budapest, Hungary*

<sup>2</sup>*Bács-Kiskun County Hospital, Kecskemét, Hungary*

<sup>3</sup>*Walter Reed Army Institute of Research, Silver Spring, MD, USA*

For most people who drink alcohol, the substance is viewed as a pleasant accompaniment to social activities. Moderate alcohol use (in general, two drinks per day for men and one drink per day for women and older people) is not harmful and protects against arteriosclerosis. However, uncontrolled alcohol consumption causes mental and somatic problems (1). Psychological and somatic variables were measured to establish possible correlations with cerebrovascular alterations due to alcoholism. Cerebrovascular alteration was estimated by rheoencephalography (REG) (2), a noninvasive bio-impedance technique acknowledged by the U.S. Food and Drug Administration as a tool for estimating cerebral blood flow (3). Jenkner (4) established the arteriosclerotic standard of REG. Our hypothesis was that uncontrolled alcohol consumption may cause cerebrovascular damage detectable by REG. The test subjects were 48 alcoholic patients in Hungary; the control group consisted of 12 drug-addicted and depressed patients in Hungary and 13 healthy male subjects in the United States. Subjects were subdivided into young and older subgroups (below and above 40 years). A REG anacrotic time above 180 ms was considered pathological. Four additional subgroups were formed according to smoking habits and average daily alcohol dose. Compared to alcoholic subjects, drug-addicted patients showed significantly shorter REG anacrotic time. Twelve alcoholics showed a pathological REG value. ANOVA showed that daily alcohol consumption and smoking were significantly higher in alcoholics than in drug patients or patients with depression. Factor analysis of variables showed gender differences. Three factors were found both for males (cumulative%= 64.86) and females (75.56): factor 1 - age and REG anacrotic time (males) and age with vegetative indexes (females); factor 2 - daily alcohol and cigarette consumption for both genders; factor 3 - REG and vegetative index (males). Longer REG anacrotic time was correlated with higher daily alcohol consumption ( $r = 0.683$ ,  $p = 0.007$ ) in a subgroup ( $n = 12$ ). For all subjects, physiological cerebrovascular aging was expected to show an identical slope with age. However, in the Hungarian alcoholic group, the sharper REG slope: 36.68 vs. age: 0.56 (ratio: 64.39) reflected the pathological impact of alcohol abuse. The U.S. control sample showed a nearly identical slope for both REG (1.79) and age (3.45; ratio: 0.52). The correlation of increased REG and daily alcohol consumption supports the accelerated cerebrovascular aging (arteriosclerosis) of the alcoholic subjects. Further study will be performed to exclude greater Hungarian cardiovascular risk factors, which may influence the increased REG anacrotic time.

1. Anonymous, The National Institute on Alcohol Abuse and Alcoholism, Bethesda, MD. <http://www.niaaa.nih.gov/publications/booklet.htm>

2. Bodo et al, A complex cerebrovascular screening system (Cerberus). *Medical Progress through Technology*, 21(2):53-66. 1995.

3. Anonymous 1997 Rheoencephalograph. Code of Federal Regulations, Title 21, Volume 8, Sec. 882.1825. (Washington DC: U.S. Government Printing Office).

4. Jenkner FL. *Clinical rheoencephalography*. Ertldruck, Vienna, 1986.

**BEDSIDE MONITORING OF CEREBRAL BLOOD FLOW (CBF) IN PATIENTS WITH CEREBRAL VASOSPASM AFTER SUBARACHNOID HEMORRHAGE****Regina Mudra<sup>1</sup>, Peter Niederer<sup>1</sup>, Emanuela Keller<sup>2</sup>**<sup>1</sup>*Institute of Biomedical Engineering ETH/UNIZH, Zurich, Switzerland*<sup>2</sup>*Department of Neurosurgery, University Hospital of Zurich, Zurich, Switzerland*

**Introduction:** Cerebral injured and patients with severe stroke are at high risk for secondary ischemic brain damage, due to intracranial hypertension and cerebral vasospasm (CVS). Established methods for measurement of cerebral blood flow (CBF) are technically difficult or need a transport of the patient. Transports for perfusion magnet resonance imaging (Perfusion-MR), computer tomography (CT), positron emission tomography (PET) or single photon emission computed tomography (SPECT) are high risk situations for the patients. To avoid such situations of risk a bedside cerebral monitoring approach is necessary. Recently, conventional near infrared spectroscopy (NIRS) for oxymetry has been extended with an indocyanine green (ICG) dye dilution method. This non-invasive approach of NIRS used with ICG can be applied at the bedside to determine mean transit time (mtt), cerebral blood volume (CBV) and cerebral blood flow (CBF) of the patient based on the observed dye dilution curve of ICG. The modified NIRS method has been validated with perfusion-MR in a healthy volunteers study (Keller et al., Neuroimage, 2003, 20:828-39). **Methods:** Further validation of the NIRS ICG dye dilution technique is done by correlating the results with clinical events e.g. intracranial pressure (ICP) crisis or brain herniation. The patient status is observed using transcranial doppler (TCD) to measure the blood flow velocities, angiography and Perfusion-CT to estimate the occurrence of delayed ischemic neurological deficits (DIND). In parallel NIRS used with ICG is done. 4 NIRS optodes are placed bilaterally on the forehead (NIRS-system Oxymon, Nijmegen). Central venous injections of 0.5mg/kg ICG are performed and the dye dilution curves are recorded to extract mtt, CBV and CBF. NIRS measurements were performed with the occurrence of CVS immediately before and after intraarterial spasmolysis. **Results:** A case report will be presented of a 42 years old woman with subarachnoid hemorrhage (SAH) Hunt &Hess 2, Fisher 3, with ruptured left sided aneurysm of the middle cerebral artery (MCA). The mtt's in both hemispheres are detected with mttleft 7.2sec and mttright 6.6sec. Day 7 hemiplegia and aphasia occurred. With the diagnosis of CVS, between day 7-14 triple h (hypertensive, hypervolemic hemodilution) therapy has been applied and three times spasmolysis with intraarterial papaverine instillation was performed. With persistent CVS, additionally, the patient was treated with hypothermia and barbiturate coma until day 14. Before papaverine instillation mtt over the left hemisphere (with CVS) has increased while the mtt over the right hemisphere remained (mttleft 8.8sec to mttright 6.6sec). After papaverine instillation into the left MCA mttleft decreased to 8sec, whereas the mtt values over the right hemisphere remained unchanged. Also the leftsided values for CBV and CBF decreased after spasmolysis (before CBVleft 1.5ml/100g and CBFleft 14ml/100g/min; after papaverine instillation CBVleft 2.5 ml/100g and CBFleft 20ml/100g/min). Day 14, the rewarming was started based on the results of the perfusion-CT. The NIRS results correlated with the trend in the perfusion-CT (mttleft=mttright). **Conclusion:** Mtt values may be the most important values to observe treatment effects of CVS with increasing brain edema. The new methodology could be a powerful tool in detection and treatment of CVS.

**ADULT-ONSET MOYAMOYA DISEASE WITH ANGIOGRAPHICALLY VERIFIED PROGRESSION**

**Yasuyuki Ezaki, Keisuke Tsutsumi, Naoki Kitagawa, Izumi Nagata**

*Department of Neurosurgery, Nagasaki University Graduate School of Medicine, Nagasaki, Japan*

**Background:** The clinical course of Moyamoya disease (MMD) is different in pediatric and adult patients. MMD seemed to progress with aging in childhood and then stabilized in adulthood. However, a few reports have indicated the dynamic angiographic change even in adult-onset MMD. Thus, in this study, we reviewed adult cases with progress in angiographic stage and report our case of adult-onset MMD with progression confirmed by cerebral angiography. **Methods:** We reviewed the clinical and radiographic records obtained in previous published reports of adult-onset (over 20 years) MMD with progression. This study encompassed only 19 cases; our case and 18 which were previously reported in the literature. We could divide these cases to two groups by angiographic appearance (unilateral or bilateral lesion at diagnosis). In these two groups, there was subgroup in which progression was found after surgical procedure. Angiographic stage was graded using Suzuki's classification. **Results:** The age at onset was 21 - 68 years (mean,  $39.8 \pm 13.3$ ) with age peaks in third decade. Females were more commonly involved (78.6%) than males. Ischemic stroke was the most common initial presentation, and there were only two cases with hemorrhagic stroke. The mean period until follow-up angiography was 35.3 months, and almost cases (84.2%) have advanced stage within 5 years. Moreover, about half (42.9%) of patients were asymptomatic, when angiographic progression was confirmed. Our case was a symptomatic 43-year-old Japanese woman with right hemispheric TIA. There was no familial and medical history. Cerebral angiography revealed MMD (stage III bilaterally according to Suzuki). Antiplatelet medication with aspirin (100mg/day) was begun. When she was 45 years old, she was readmitted to our hospital for surgical treatment because of repeated ischemic episodes. Cerebral angiography demonstrated the progressive appearance (stage V bilaterally). **Conclusions:** To our knowledge, our study is the first review for progressive adult-onset moyamoya disease in the English-language literature. There seem to be more cases with adult-onset MMD with progression than previously report. Our review indicates that 'adult-onset MMD with progression' includes the several different pathological patterns. We suggested that careful observation for at least 5 years is required even if in adulthood.

## RELATIONSHIPS BETWEEN VERTEBRAL ARTERY DIAMETER AND DISSECTING ANEURYSM FORMATION

Yoko Yokoyama<sup>1</sup>, **Shigeru Fujimoto**<sup>1</sup>, Kazunori Toyoda<sup>1</sup>, Tooru Inoue<sup>2</sup>, Juro Jinnouchi<sup>1</sup>, Koh Nakachi<sup>1</sup>, Seiji Gotoh<sup>1</sup>, Daisuke Fukui<sup>1</sup>, Kotaro Yasumori<sup>3</sup>, Yasushi Okada<sup>1</sup>

<sup>1</sup>*Department of Cerebrovascular Disease, National Hospital Organization Kyushu Medical Center, Fukuoka, Japan*

<sup>2</sup>*Department of Neurosurgery, National Hospital Organization Kyushu Medical Center, Fukuoka, Japan*

<sup>3</sup>*Department of Neuroradiology, National Hospital Organization Kyushu Medical Center, Fukuoka, Japan*

**Introduction:** It is well known that dissection in the vertebrobasilar (VB) systems shows various clinical features such as aneurysmal dilatation and consequential hemorrhagic stroke, or occlusive change and consequential ischemic stroke [1]. These features have close relationships with the clinical outcome. The purpose of the present study was to clarify which factors had an influence on aneurysm formation in patients with dissection in the VB system. **Methods:** This study included 20 consecutive patients with a dissection in the VB system. All patients underwent cerebral digital subtraction angiography (DSA), MRI including diffusion weighted image (DWI), MR angiography (MRA), and duplex ultrasonography. We adopted the diagnostic criteria for VB dissection as follows: 1) intimal flap, double lumen, pearl and string sign, or string sign was observed in DSA, MRA, or duplex ultrasonography, or 2) pearl sign or tapered occlusion was observed in DSA and changes in these findings were documented in the serial studies. In DWI, sites and number of infarct were evaluated. In duplex ultrasonography, diameter and flow velocity of the cervical portion of the vertebral artery (VA) were measured. Dominant VA was defined when diameter ratio (ipsilateral/contralateral) was more than 1.4 [2] or when contralateral VA had occluded. According to the criteria, dissecting VA was classified into 3 groups: dominant VA, non-differentiated VA, and hypoplastic VA. We investigated the relationships between the clinical and radiological factors and dissecting aneurysm formation. **Results:** On DWI, brain infarction was observed in 14 patients; 12 in the posterior inferior cerebellar artery (PICA) territory (cerebellum in 10 and the lateral medulla in 6), 2 in the medial medulla, 1 in the pons, 1 in the cerebellum of the superior cerebellar artery territory, and 1 in the posterior cerebral artery territory. One patient had dissection in the bilateral VAs. The remaining 19 patients had the unilateral dissection. Sites of dissection were VA before branching PICA in 16, VA after branching PICA in 3, and PICA in 2. Dominant VA was dissected in 5 patients, non-differentiated VA in 11, and hypoplastic VA in 4. Dissecting aneurysm was observed in 5 patients (1 in dominant VA and 4 in non-differentiated VA). Aneurysmal change was absent in the patients with dissection in hypoplastic VA. The remaining 15 patients had VA or PICA occlusive lesions due to the dissection. The diameter ratio of the VA tended to be higher in patients with dissecting aneurysm than in patients with occlusive lesions ( $1.25 \pm 0.43$  vs  $0.88 \pm 0.32$ ,  $p < 0.1$ ). Patients with VA dissection in the thicker side tended to more frequently have aneurysm formation than patients with VA dissection in the narrower side (50% vs 20%,  $p < 0.1$ ). **Conclusions:** VA diameter or dominancy evaluated using duplex ultrasonography may be an important factor for aneurysm formation in patients with VA dissection. **References:** [1] Nakagawa K, et al: J Neurosurg 2000;93:19 [2] Saito K, et al: Stroke 2004;35:1068

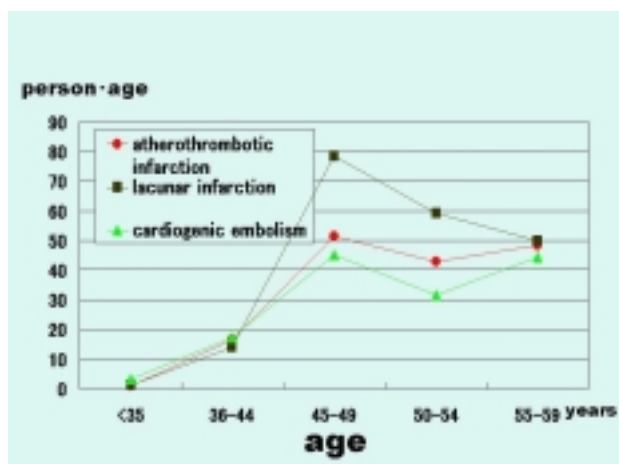
## DISEASE BURDEN OF ISCHEMIC STROKE ON FUNCTIONAL ABILITY OF WORKING

**Shigeharu Takagi**, Sari Sekiyama, Kentaro Tokuoka, Hiroyuki Mandokoro,

Tomohide Onuki, Ryuya Kumazawa, Satoko Kobori, Tsuyoshi Uesugi, Takashi Yasuda

*Department of Neurology, Tokai University School of Medicine, Isehara, Japan*

**Purpose :** To clarify the load of various subtypes of cerebrovascular disease on the functional ability of workers. **Materials and Methods :** (1) From the database of Japanese acute cerebrovascular disease, we studied modified Rankin Scale (mRS) at discharge of 1298 patients with atherothrombotic infarction, 1252 with lacunar infarction, and 1149 with cardiogenic embolism. These subjects were classified into age classes with range of 5 years. (2) We studied the patients with the first-ever ischemic stroke who were younger than 65 years when they admitted to Tokai University Hospital from April 2001 to March 2002. We evaluate mRS of these subjects at discharge, and their functional ability of working by the questionnaire. Functional disability ratio is expressed as the ratio of subjective disability to their ability before their onset of ischemic stroke. (3) Disease burden from cerebral infarction of various clinical categories with various age of onset was calculated as follows.  $\text{disease burden} = \text{occurrence rate} \times \text{functional disability ratio} \times \text{expected workable years until 65}$ . **Results and Discussion :** As shown in Figure, disease burden from lacunar infarction is the highest among the three clinical categories of cerebral infarction due to the highest incidence of occurrence rate among these categories under age of 65. Also as shown in Figure, disease burden is the highest on workers with age rank of 45-49, in all of clinical categories, because they have relatively long expected workable years until 65. **Conclusion :** From the standpoint of disease burden on working, lacunar infarction in young subjects is most important and needs strengthened efforts of prevention.



## CLINICAL DIFFERENCES BETWEEN MONOPARESIS AND HEMIPARESIS IN PURE MOTOR STROKE

Kiminobu Yonemura<sup>1</sup>, Yoichiro Hashimoto<sup>1</sup>, Makoto Uchino<sup>2</sup>

<sup>1</sup>*Department of Neurology, Kumamoto City Hospital, Kumamoto, Japan*

<sup>2</sup>*Department of Neurology, Graduate School of Medical Science, Kumamoto University, Kumamoto, Japan*

Background: Pure motor stroke is the most common of any lacunar syndrome and is of clinical use for the diagnosis of lacunar stroke.[1] However in this syndrome, pure motor monoparesis (PMM) is unusually considered to be almost due to a nonlacunar stroke.[2] We sought to clarify the clinical characteristics of ischemic stroke with PMM compared with those with pure motor hemiparesis (PMH). Methods: We analyzed 201 consecutive patients (118 men and 83 women with age of  $72\pm 11$  years) with first-ever acute ischemic stroke who presented with pure motor syndrome admitted between April 2000 and December 2004. Subjects were divided into 2 groups; patients with weakness restricted to one part of face, arm, or leg (PMM group,  $n = 50$ ), and those with weakness involving more than two parts on the same side (PMH group,  $n = 151$ ). Sex, age, vascular risk factors including hypertension, diabetes mellitus, hyperlipidemia and smoking, arterial occlusive disease in responsible cerebrovascular system, emboligenic heart disease, neurological symptoms, and infarct size and location on diffusion-weighted MR imaging were compared between the groups. Results: The PMM group showed more noticeable predominance of women (56% versus 36%,  $P < 0.05$ ) than the PMH group. Age, other vascular risk factors, and occlusive cerebral artery diseases did not significantly differ between the two groups, but emboligenic heart diseases were more frequently detected in the PMM group than in the PMH group (30% versus 9%,  $P < 0.0005$ ). 54% of patients in the PMM group harbored an emboligenic heart disease and/or an occlusive cerebral artery disease, which was a greater proportion than 31% of patients in the PMH group ( $P < 0.005$ ). The PMM group also had more frequently an abrupt onset of neurological symptoms (66% versus 33%,  $P < 0.0001$ ) and cortical infarcts on diffusion-weighted MR imaging (58% versus 21%,  $P < 0.0001$ ) than the PMH group. Multiple logistic regression analysis demonstrated that emboligenic heart disease (OR 4.895, 95% CI 2.020-11.862,  $P < 0.0005$ ) were independently associated with the PMM group. Conclusions: There were some clear differences between PMM and PMH in patients with first-ever acute ischemic stroke. PMM was independently associated with emboligenic heart disease and may be caused predominantly by embolic stroke as compared with PMH. References 1. Arboix A, Martí-Vilalta JL, Garcia JH. Clinical study of 227 patients with lacunar infarcts. *Stroke*. 1990;21:842-847. 2. Melo TP, Bogousslavsky J, van Melle G, Regli F. Pure motor stroke: a reappraisal. *Neurology*. 1992;42:789-795.

**THE ACUTE AND LONG-TERM PROGNOSIS OF CEREBRAL INFARCTION ON THE BASIS OF THE CLINICAL CLASSIFICATION OF THE OXFORDSHIRE COMMUNITY STROKE PROJECT**

**Katsunori Isa**, Takashi Tokashiki, Koichiro Okumura, Kunitoshi Iseki, Shuichi Takishita

*3rd Internal Medicine, University of the Ryukyus, Okinawa, Japan*

Background: The Oxfordshire Community Stroke Project (OCSP) clinical classification of subtypes of cerebral infarction reported to be simple and practicable. The large database of cerebral infarction is available in Okinawa, Japan. Purpose: The aim of the study was to evaluate acute and long-term prognosis of cerebral infarction registered in Okinawa prefecture in 1998-1991 according to the OCSP classification. Method: We divided total 2126 patients with cerebral infarction into the following 4 OCSP categories: total anterior circulation infarcts (TACI), partial anterior circulation infarcts (PACI), lacunar infarcts (LACI), and posterior circulation infarcts (POCI). Relative risks of death were examined by multivariate Cox proportional hazard analysis after adjusting age and sex. Result: The subjects comprised 202 patients (9.5%) with TACI, 558 (26.2%) with PACI, 1188 (55.9%) with LACI, and 178 (8.4%) with POCI. The adjusted hazard ratio (95% CI) for the risk of death in 10-year observation was 1.07 (0.85-1.34) for POCI, 1.24 (1.16-1.33) for PACI, and 1.43 (1.35-1.53) for TACI, when compared to that in patients with LACI (1.00). The mortality rates within 28 days after the onset were 37.1% for TACI, 6.1% for PACI, 1.85% for LACI, and 5.6% for POCI. Conclusion: The acute mortality rate of TACI was extensively high. The long-term prognosis of cerebral infarction differed among OCSP subgroups. Reference: Bamford J, Sandercock P, Denis M, et al.: Classification and natural history of clinically identifiable subtypes of cerebral infarction. *Lancet*, 337: 1521-1526, 1991. Tei H, Uchiyama S, Ohara K, Kobayashi M, Uchiyama Y, Fukuzawa M. Deteriorating ischemic stroke in 4 clinical categories classified by the Oxfordshire Community Stroke Project. *Stroke*, 31:2049-2054. 2000.

## DYNAMIC CHANGES OF THE PYRAMIDAL TRACT AFTER ISCHEMIC STROKE DETECTED BY MR TRACTOGRAPHY

Mette Møller<sup>1,2</sup>, Jesper Frandsen<sup>1</sup>, Grethe Andersen<sup>3</sup>, Albert Gjedde<sup>1,2</sup>,

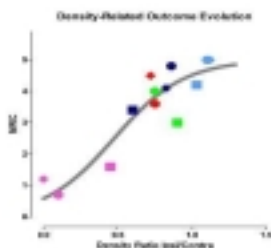
Peter Vestergaard-Poulsen<sup>1</sup>

<sup>1</sup>Center of Functionally Integrative Neuroscience, Aarhus University, Aarhus, Denmark

<sup>2</sup>PET-Centre, Aarhus University Hospital, Aarhus, Denmark

<sup>3</sup>Department of Neurology, Aarhus University Hospital, Aarhus, Denmark

**INTRODUCTION:** After ischemia the adult brain can regenerate and compensate for motor deficits by plastic change, including an initial recruitment of motor pathways in the intact hemisphere, and in patients with good recovery, return of activity to the ipsi-lesional side. Diffusion tensor axonal fiber tracking reveals the correlation between brain plasticity and recovery of motor function during rehabilitation. However, the reorganization of fiber tracks was not previously mapped in a longitudinal study of humans during recovery from stroke. We used diffusion tensor imaging (DTI) with 3D fiber tracking to test the relationship between density ratio (number of tracked fibres per unit volume) of the ipsi- and contral-lesional pyramidal tract fibres and motor function. We hypothesized that bilateral increase in fiber density underlies good recovery, whereas a persistent low ratio is associated with poor outcome. **METHODS:** Five right-handed patients with subcortical ischemic infarcts were tested with a battery of neurological motor scales acutely, and at one and three months post-stroke. Serial DTI was performed using a birdcage head-coil and double spin echo single shot EPI at 1.5 T, employing 17 isotropically-distributed directions, and a b-factor of 1000 s/mm<sup>2</sup>, with additional b-factor=0 s/mm<sup>2</sup> images. Maximum gradient strength was 36 mT/m. 50 slices of 3.3 mm thickness were acquired, covering a 24 cm FOV in a 128x128 matrix. TR/TE =17000/84 ms. The sequence was repeated four times for a total 22 min acquisition time. The eigensystem was calculated from the diffusion tensor in each voxel using diagonalization. Fiber tracking was calculated with the FACT algorithm. **RESULTS** The figure shows temporal evolution of the density ratio in relation to motor function (Medical Research Council=MRC), with squares representing acute studies. Overall, fiber density ratio in the ipsi-lesional pyramidal tract increased in the four patients with good outcome (MRC $\geq$ 4). Transiently increased contral-lesional fiber density ratio appeared to predict better outcome (not shown). **DISCUSSION:** The novel finding of fiber density related progression of outcome from ischemic stroke is based on preliminary data and more studies are needed to validate the method. The present results in a group of five stroke patients suggest that DTI fiber tracking detects changes in fiber density correlated with motor recovery within three months post-stroke. Bilateral increases in fiber density suggest plastic changes in both pyramidal tracts during recovery from hemiparesis.



**PHARMACOLOGICAL NEUTROPENIA REDUCES THROMBOLYSIS-ASSOCIATED HEMORRHAGIC COMPLICATIONS AFTER FOCAL ISCHEMIA IN RATS**

Sophie Gautier, **Thavarak Ouk**, Olivier Pétrault, Maud Laprais, Jacques Caron, Régis Bordet

*Laboratoire de Pharmacologie, Faculté de Médecine, Lille, France*

**Introduction** This study investigated whether in neutropenia conditions induced by vinblastine (Vb), we could prevent the intracerebral complications, the infarct volume increase and the postischemic endothelial dysfunction induced by thrombolysis. **Materials** A cerebral ischemia-reperfusion by endoluminal occlusion of middle cerebral artery (MCA) was performed 4 days after intravascular administration of vinblastine (0.5 mg/kg) or vehicle (saline solution 0.9%), on male spontaneously hypertensive rats (SHR) with 1 hour ischemia then followed by perfusion intravenously 5 hours later either saline or rtPA associated with thrombus lysis products (TLP). Hemorrhage severity and brain infarct volume measurement were evaluated by histomorphometric analysis. In addition, MCA reactivity was assessed using Halpern myograph. **Results** Neutropenia induced a neuroprotective effect as demonstrated by a significant decrease of brain infarct size in animals perfused by rtPA+TLP solution ( $127.68 \pm 13.11$  versus  $174.76 \pm 9.81$  mm<sup>3</sup> in NaCl TLP group;  $p < 0.05$ ). No effect of neutropenia was observed on cerebral infarct volume in animals perfused by saline solution 0.9 % ( $144.09 \pm 10.21$  mm<sup>3</sup> in Vb NaCl group and  $144.44 \pm 7.53$  mm<sup>3</sup> in NaCl NaCl group). The neutropenia-induced decrease of infarct volume was associated with a decrease of both hemorrhage severity ( $4.5 \pm 1.3$  versus  $9.6 \pm 2.1$  petechiae in NaCl TLP group) and post-ischemic impairment of MCA endothelium-dependent relaxation ( $24.55 \pm 5.64$  versus  $9.08 \pm 0.56$  in NaCl TLP group;  $p < 0.05$ ). The fully relaxation of smooth muscle response to sodium nitroprusside did not change in all groups. **Conclusion** In parallel to its neuroprotective effect, vinblastine-induced neutropenia prevents the post-ischemic impairment of MCA endothelium-dependent relaxation in TLP-perfused animals. Moreover this vascularprotection leads to limit the intracerebral hemorrhages.

**STATISTICAL PARAMETRIC ANALYSIS OF CEREBRAL BLOOD FLOW IN VASCULAR DEMENTIA DUE TO SMALL-VESSEL DISEASE USING <sup>99m</sup>Tc-HMPAO SPECT**

**Hiroki Kato**<sup>1</sup>, Takuya Yoshikawa<sup>2</sup>, Naohiko Oku<sup>1</sup>, Katsufumi Kajimoto<sup>1</sup>, Yasuyuki Kimura<sup>1</sup>, Makiko Tanaka<sup>3</sup>, Kazuo Kitagawa<sup>3</sup>, Masatsugu Hori<sup>3</sup>, Jun Hatazawa<sup>1</sup>

<sup>1</sup>*Department of Nuclear Medicine and Tracer Kinetics, Osaka University Graduate School of Medicine, Osaka, Japan*

<sup>2</sup>*Department of Internal Medicine, Kobe Ekisaikai Hospital, Hyogo, Japan*

<sup>3</sup>*Department of Internal Medicine and Therapeutics, Osaka University Graduate School of Medicine, Osaka, Japan*

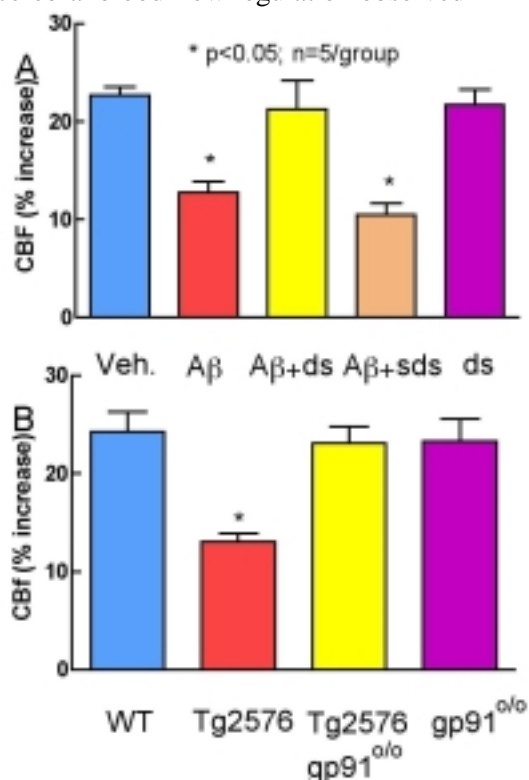
**Background** In our previous study, a vascular dementia (VaD) due to small-vessel disease showed more heterogeneous cerebral blood flow distribution than healthy controls.1) In the present study, we investigated whether or not regional cerebral blood flow (rCBF) in patients with VaD due to small-vessel disease is locally reduced in particular brain areas compared with normal healthy controls. **Subjects and method** The subjects consisted of 17 right handed patients with VaD due to small-vessel disease (age(y):  $69.5 \pm 8.5$ , MMSE:  $18.6 \pm 4.5$ ) (VaD group) and 20 healthy volunteers (age(y):  $62.9 \pm 11.3$ , MMSE:  $26.5 \pm 2.6$ ) (control group). The diagnosis of VaD due to small-vessel disease was made on the basis of the NINDS–AIREN criteria 2) and a full clinical examination including history, neuropsychological tests, neurological examination, and brain MRI. The SPECT was performed with <sup>99m</sup>Tc-hexamethyl-propyleneamine oxime. The images were reconstructed without a correction for tracer-washout. The SPM99 was employed for the analysis. In the SPM99, a threshold masking value was set to be 0.6 for the control and VaD group. **Results** In the VaD group, rCBF of right thalamus and left parietal cortex was significantly lower than that in normal group ( $p < 0.05$ , uncorrected). **Discussion** Thalamus has a projection pathway to association area of cerebral cortices responsible to higher cognitive functions.3) Left parietal cortex is also one of such areas. The present results suggested a possibility that impairment of cognition / higher neurological functions in patients with VaD due to small vessel disease is partly caused by dysfunction of thalamus and parietal cortex. **References** 1) Yoshikawa T, et al. J Nucl Med. 2003; 44(4): 505-11. 2) Roman GC, et al. Neurology 1993; 43(2): 250-60. 3) Schmahmann JD, Stroke. 2003; 34(9): 2264-78.

## NADPH OXIDASE-DERIVED FREE RADICALS MEDIATE NEUROVASCULAR DYSFUNCTION IN MODELS OF ALZHEIMER'S DISEASE

Costantino Iadecola<sup>1</sup>, Laibaik Park<sup>1</sup>, Josef Anrather<sup>1</sup>, George Carlson<sup>2</sup>

<sup>1</sup>Division of Neurobiology, WCMC, New York, NY, <sup>2</sup>MacLaughlin Research Institute, Great Falls, MT, USA

Overproduction of the amyloid  $\beta$  (A $\beta$ ) peptide is a key factor in the pathogenesis of Alzheimer's disease (AD), but the mechanisms of its pathogenic effects have not been defined. Patients with AD have cerebrovascular alterations attributable to the deleterious effects of A $\beta$  on cerebral blood vessels. Furthermore, mice overexpressing the amyloid precursor protein (APP) have marked alterations in the cerebrovasodilation produced by neural activity (functional hyperemia). Experimental evidence suggests that these cerebrovascular alterations are mediated by reactive oxygen species (ROS). However, the source of the ROS mediating the dysfunction has not been defined. NADPH oxidase has recently emerged as a major source of ROS at the vascular level. In this study we tested the hypothesis that NADPH-derived ROS mediate the vascular dysfunction produced by A $\beta$ . Methods: The increases in somatosensory cortex cerebral blood flow (CBF) induced by stimulation of the facial whiskers were monitored in urethane-chloralose anesthetized mice using laser-Doppler flowmetry. ROS production in the somatosensory cortex was monitored by the hydroethidine technique. The cerebrovascular effects of A $\beta$  were studied either by A $\beta$ 1-40 superfusion on the exposed neocortex, or in mice overexpressing APP (Tg2576). Results: The alterations in functional hyperemia induced by A $\beta$  (fig. A) were abrogated by the NADPH oxidase peptide inhibitor gp91ds-tat (ds; fig. A), but not by its scrambled control (sds). CBF responses to adenosine were not affected by A $\beta$  (28 $\pm$ 2%) or A $\beta$ +ds (30 $\pm$ 3; n=5; p>0.05). The ds peptide blocked ROS production (n=5/group). Furthermore, the cerebrovascular dysfunction and ROS upregulation observed in wild-type mice (WT) did not occur in double-transgenic mice overexpressing the amyloid precursor protein but lacking the critical NADPH oxidase subunit gp91phox (Tg2576 gp910/0; fig. B). Conclusions: A gp91phox-containing NADPH oxidase is the critical link between A $\beta$  and cerebrovascular dysfunction, which may underlie the alteration in cerebral blood flow regulation observed in AD patients.





**CEREBRAL VASCULAR EFFECTS OF ANGIOTENSIN II: NEW INSIGHTS FROM GENETIC MODELS**

Frank M. Faraci<sup>1,2</sup>, Mary L. Modrick<sup>1</sup>, Kathryn G. Lamping<sup>1,2</sup>, Curt D. Sigmund<sup>1,3</sup>,  
Sean P. Didion<sup>1</sup>

<sup>1</sup>*Internal Medicine, University of Iowa, Iowa City, IA, USA*

<sup>2</sup>*Pharmacology, University of Iowa, Iowa City, IA, USA*

<sup>3</sup>*Physiology, University of Iowa, Iowa City, IA, USA*

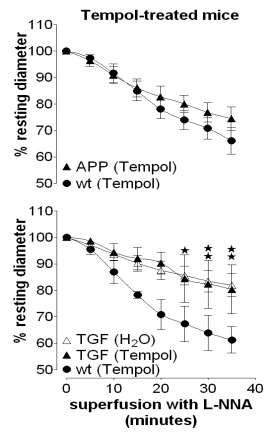
Angiotensin II (Ang II) has been implicated as a major cause of oxidative stress and vascular dysfunction in the peripheral circulation. Although chronic hypertension is a major risk factor for cerebral vascular disease, stroke and vascular cognitive impairment, very little is known regarding mechanisms of action of Ang II or effects of chronic Ang II-dependent hypertension in the cerebral circulation. In initial studies, we tested the hypothesis that Ang II produces constriction of cerebral arteries that is mediated by activation of the AT1a receptors and Rho kinase. Basilar arteries (baseline diameter ~130  $\mu\text{m}$ ) from control (C57BL/6) mice were isolated, cannulated and pressurized in order to measure vessel diameter. Ang II constricted arteries from male mice beginning at 0.01 nM with a maximum decrease in diameter of  $25\pm 2\%$  (mean $\pm$ SE) at 1 nM Ang II. In contrast, Ang II had very modest effects in arteries from female mice ( $-3\pm 1\%$  at 1 nM Ang II). In male mice, vasoconstriction in response to Ang II was completely prevented by an inhibitor of Rho kinase (Y27632, 3  $\mu\text{M}$ ). In contrast, constriction of the basilar artery to KCl was similar in males and females and was not inhibited by Y27632. Vasoconstrictor responses to Ang II were almost eliminated in male mice deficient in expression of AT1a receptors (AT1a  $-/-$ ). Recent pharmacological studies suggest that intact Ang II-mediated signaling is important in maintaining endothelial function in cerebral arteries. We found that responses of the basilar artery to acetylcholine (ACh, an endothelium-dependent agonist) were similar in AT1a  $+/+$  and AT1a  $-/-$  mice. In a second series of studies, we examined effects of Ang II using a chronic model of hypertension, mice which overexpress human renin (R+) and human angiotensinogen (A+). ACh produced dilation of cerebral arteries in control mice that was eliminated by an inhibitor of nitric oxide synthase. Responses to ACh were markedly impaired in R+A+ mice: 1  $\mu\text{M}$  ACh dilated the arteries by  $41\pm 6$  vs  $9\pm 5\%$ , ( $P < 0.01$ ) in control and R+A+ mice, respectively. A23187 (0.1  $\mu\text{M}$ , another endothelium-dependent agonist), produced vasodilation in control mice ( $35\pm 7\%$ ) but vasoconstriction in R+A+ mice ( $-8\pm 5\%$ ). Impaired responses to ACh in R+A+ mice were restored to normal by the superoxide scavenger PEG-superoxide dismutase. In contrast, dilation of the basilar artery in response to a NO donor (NONOate) was similar in R+A+ mice and controls ( $P > 0.05$ ). Thus, Ang II is a potent constrictor of cerebral arteries and this effect is mediated by AT1a receptors and activation of Rho kinase. There are marked, but selective, gender differences in cerebral vascular responses to Ang II. Our findings provide direct evidence that endothelial function is not affected by deletion of AT1a receptors. Finally, endothelial function is greatly impaired in mice made chronically hypertensive by expression of renin and angiotensinogen. The mechanism of this impairment involves increased oxidative stress.

**REVERSAL OF FULLY DEVELOPED CEREBROVASCULAR DYSFUNCTIONS IN TWO TRANSGENIC MOUSE MODELS OF ALZHEIMER'S DISEASE**

Nektaria Nicolakakis, Xin-Kang Tong, Edith Hamel

*Lab. of Cerebrovascular Research, Montreal Neurological Institute, McGill University, Montréal, Canada*

Introduction: Recent studies suggest that cerebrovascular dysfunctions occur early in Alzheimer's disease (AD), as reflected primarily by regional decreases in cerebral perfusion that, often, precede the neurological deficits (Iadecola 2004, *Nat Rev Neurosci* 5: 347). Oxidative stress induced by amyloid beta (A $\beta$ ) and cerebrovascular fibrosis associated with increased levels of the transforming growth factor-beta 1 (TGF- $\beta$ 1) have been proposed to underlie these dysfunctions. In the present study, we attempted to reverse cerebrovascular alterations in vivo in order to better understand their underlying mechanisms. Methods: Transgenic mice overexpressing mutated forms of the amyloid precursor protein (APP mice) or TGF- $\beta$ 1 (TGF mice) were treated when cerebrovascular dysfunctions were fully developed, together with their respective wild-type littermates. Mice (n=3-6/group) received the antioxidant Tempol (1mM in drinking water, 6 weeks) or N-acetyl-L-cysteine (NAC; 100mg/kg/day i.p., 4 weeks), or pioglitazone (Actos, 20mg/kg/day in chow, 6 weeks) which exhibits anti-inflammatory, -oxidant and -angiogenic properties. The ability of isolated and pressurized middle cerebral artery (MCA) segments to dilate to calcitonin gene-related peptide (CGRP) and/or constrict in response to nitric oxide synthase (NOS) inhibition (10 $\mu$ M L-NNA) was determined by in vitro videomicroscopy. Changes in cortical and hippocampal microvessels were evaluated by immunocytochemical staining of the oxidative stress marker manganese superoxide dismutase (MnSOD) or structural components of the blood vessel wall. Results: APP and TGF mice exhibited impaired dilatations to CGRP ( $\downarrow$ 56% and 69%, respectively,  $p < 0.05$ ) and constrictions to NOS inhibition ( $\downarrow$ 54% and 53%, respectively,  $p < 0.05$ ). Tempol and NAC fully restored cerebrovascular responsiveness in APP mice. In contrast, Tempol had no beneficial effects in TGF mice and NAC only normalized the NO-mediated response, but not the CGRP-mediated dilatation, indicating that increased TGF- $\beta$ 1 levels differentially affect these two pathways. Interestingly, pioglitazone fully restored cerebrovascular functions in both mouse models. Preliminary immunocytochemical data suggest that Tempol and NAC normalize the perivascular MnSOD upregulation selectively observed in APP mice. Conclusion: These results show that the apparently similar cerebrovascular dysfunctions in APP and TGF mice are mediated by different pathogenic mechanisms. They also show that perivascular oxidative stress-mediated deficits in APP mice can be fully reversed even at an advanced stage of the pathology. In contrast, other pathogenic factors are involved in TGF mice as antioxidants could not fully restore cerebrovascular functions. The efficacy of pioglitazone warrants additional work so that we may elucidate the molecular and cellular mechanisms leading to recovery from A $\beta$  and TGF- $\beta$ 1 pathologies, both present in AD. This may offer a means to re-establish brain hemodynamics in AD patients with cerebrovascular deficits. Supported by CIHR (MOP-64194 (EH), studentship (NN)) and Alzheimer Society of Canada.



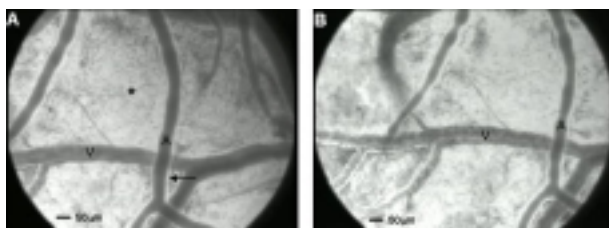
## THE USE OF OPS IMAGING TO DETECT MICROVASCULAR DISTURBANCES IN CEREBRAL ISCHEMIA

Frits A. Pennings<sup>1</sup>, Can Ince<sup>2</sup>, Gerrit J. Bouma<sup>1</sup>

<sup>1</sup>*Department of Neurosurgery, Academic Medical Center, Amsterdam, The Netherlands*

<sup>2</sup>*Department of Physiology, Academic Medical Center, Amsterdam, The Netherlands*

**Introduction** Microcirculatory function of the brain is essential for providing adequate oxygen to the tissue cells. In neurovascular diseases disturbances of the cerebral microcirculation possibly plays a role in the development of cerebral ischemia. Until recently, the in-vivo observation and quantitative functional assessment of the human cerebral microcirculation were limited by the absence of appropriate investigational techniques. This limitation have been overcome with the introduction of orthogonal polarization spectral (OPS) imaging. We used OPS imaging on the brain cortex during aneurysm surgery and resection of an arteriovenous malformation (AVM) to directly observe the small cortical blood vessels and quantify the contractile properties and changes in microvascular flow (MFI) and functional capillary density (FCD). **Method** In 22 patients undergoing aneurysm surgery the diameter changes of small cortical vessels (15 - 180  $\mu\text{m}$ ) were observed using OPS imaging. Fifteen patients were operated early (within 48 hours after bleeding) and 7 underwent late surgery. Immediately after dura opening, the response to hyperventilation (n=16) and papaverin (n=6) of arterioles and venules was observed with OPS imaging under sevoflurane anesthesia. Furthermore, images of the cerebral microcirculation were obtained in two patients undergoing microsurgical removal of an AVM. Eight patients undergoing craniotomy for a disease not affecting the cortical microcirculation served as controls. **Results** In the presence of subarachnoid blood a severe disturbed reaction of the microvessels was observed. More specifically, hyperventilation resulted in a  $39 \pm 15\%$  ( $p < 0.05$ ) decrease in arteriolar diameter with a "bead string" constriction pattern occurring in 60% of patients (figure 1a and 1b). The topical application of papaverin resulted in an increase in arteriolar diameter of  $> 50\%$ . These reactions were not seen in the absence of subarachnoid blood (late surgical patients and controls). In the cerebral cortex surrounding an AVM, MFI and the FCD were decreased to 2 (moderate flow) respectively  $1.4 \pm 1.3 \text{ cm}^2/\text{mm}^2$ . After AVM excision a substantial increase in MFI to 4 (high flow) was seen accompanied by an increase in FCD to  $2.1 \pm 0.8 \text{ cm}^2/\text{mm}^2$ . **Conclusions** OPS imaging allows direct in vivo observation and quantitative functional assessment of the cerebral microcirculation. Thus, microvascular reactivity and hemodynamic changes in the human brain at the microcirculatory level can be readily assessed and correlated with metabolic and clinical parameters. This new tool may contribute to a better understanding of the pathophysiology of cerebral ischemia.



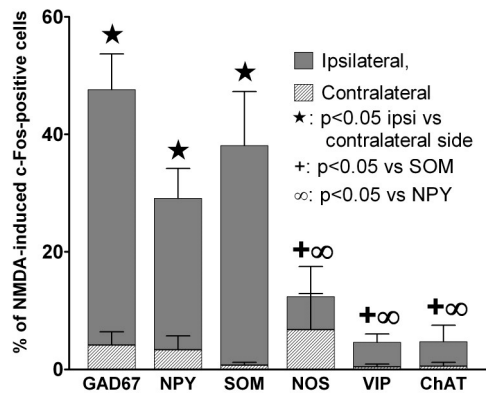
**CHEMICAL OR ELECTRICAL STIMULATION OF BASAL FOREBRAIN NEURONS  
ACTIVATES SPECIFIC SUBSETS OF CORTICAL GABA-INTERNEURONS IN  
PARALLEL WITH INCREASES IN CORTICAL CEREBRAL BLOOD FLOW**

Ara Kocharyan<sup>1</sup>, Priscilla Fernandes<sup>1</sup>, Nella Serluca<sup>1</sup>, Elvire Vaucher<sup>2</sup>, Edith Hamel<sup>1</sup>

<sup>1</sup>*Montreal Neurological Institute, McGill University, Laboratory of Cerebrovascular  
Research, Montréal, QC, Canada*

<sup>2</sup>*École d'Optométrie de L'Université de Montréal, Montréal, QC, Canada*

**Introduction:** Basal forebrain (BF) neurons project to cortical microvessels and GABA-interneurons and, upon stimulation, induce increases in cortical cerebral blood flow (CBF). The identity of the different subsets of GABA-interneurons activated by BF stimulation under conditions of increased cortical CBF was determined by double-immunocytochemistry of c-Fos (a marker of cell activation) and peptides (somatostatin (SOM), neuropeptide Y (NPY), vasoactive intestinal polypeptide (VIP)) or enzymes (nitric oxide synthase (NOS), choline acetyltransferase (ChAT)) co-localized with glutamate decarboxylase (GAD67) in GABA interneurons. **Methods:** Cortical CBF was measured bilaterally using Laser Doppler flowmetry during and 20 min after a unilateral BF stimulation. This was achieved by BF microinjection of sodium glutamate (NaGlut, 100nmol/100nl over 1min), NMDA (5nmol/100nl over 1min), or saline (control, 100nl over 1 min), or by electrical stimulation (100Hz 1sec, 50  $\mu$ A, on/1sec off, 5 min) in Sprague Dawley rats (3-4/group) previously implanted in the right BF (4-6 days earlier) with guide cannula or stimulating electrode. Activated cells (c-Fos-positive) were identified in different cortical areas or layers in brains fixed 60 min after the end of the stimulation. **Results:** NaGlut, NMDA and electrical BF stimulations elicited ipsilateral cortical CBF increases ( $p < 0.05$ , t-test) corresponding to 62.6, 65.4 and 96.1% from baseline, respectively. All paradigms of BF stimulation elicited similar patterns of interneurons activation, although the extent of activation differed between them. Overall, BF stimulation induced a significant increase in the number of NPY, SOM and GAD67 interneurons immunolabelled for c-Fos in the ipsilateral as compared to the contralateral parietal cortex, without activation of VIP, NOS or ChAT interneurons. A larger proportion of NPY, SOM and GAD67 activated neurons (26.9, 51.6, 42.4%, respectively,  $p < 0.001$ ) was obtained with NMDA (Figure), while electrical stimulation resulted in activation of a smaller proportion of these same interneurons (10.5, 10.9, 6.6%,  $p < 0.05$ ). All c-Fos-positive neurons in layer I of the rat cerebral cortex co-stained only for GAD67, and these were activated in the ipsilateral parietal cortex after NMDA, NaGlut and electrical BF stimulation (40, 26 and 8.6%, respectively,  $p < 0.001$ ). Saline injection had no effect on either CBF or c-Fos. **Conclusions:** These results show that increased cortical perfusion following BF stimulation is accompanied by activation of GABA interneurons and, specifically, those containing SOM and/or NPY, two peptides with vasoconstrictive properties. We suggest that these subsets of GABA interneurons might regulate cortical perfusion, possibly by limiting the extent of the vasodilatation induced by cortical release of acetylcholine and nitric oxide from activated basalcortical fibres. Supported by CIHR grant (MOP-53334, EH).

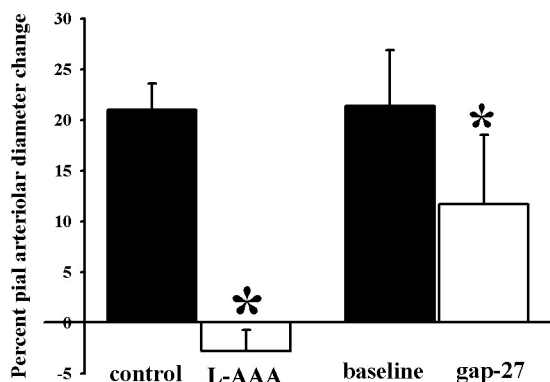


## ROLE OF ASTROCYTES AND GAP JUNCTIONS IN SEIZURE-INDUCED PIAL ARTERIOLAR DILATIONS IN RATS

Hao-Liang Xu, Dale A. Pelligrino

*Neuroanesthesia Research, University of Illinois at Chicago, Chicago, IL, USA*

Cerebral arterioles and astrocytes are physically and physiologically linked to one another. Indeed, astrocyte-related factors appear to make a significant contribution to the local regulation of CBF. For example, in recent studies we reported that topical application of L-alpha-aminoadipic acid (L-AAA), an astroglial toxin which selectively damaged the glia limitans (without affecting vascular smooth muscle, endothelium, or neurons), was associated with a reduced pial arteriolar reactivity to selected vasodilating stimuli (e.g., hypercapnia and ADP; but not acetylcholine or NO). In the present study, we examined whether the pial arteriolar dilation accompanying seizure (topical bicuculline [BC]) was influenced by L-AAA-induced glial injury. In addition, we tested whether gap junctions influence the vascular response. These experiments employed topical applications of the gap junction inhibitory peptide, gap 27. To ensure that changes in the vasodilatory magnitude were not related to reduced brain activity, the local EEG activity (total EEG power) was monitored. We used anesthetized rats, with closed cranial windows inserted 24h prior to study. L-AAA (or aCSF, 300 ul each) was introduced into the periarachnoid space immediately after window placement. BC (100 uM) was suffused over 15 min and pial arteriolar diameters measured every minute. Arteriolar responses in L-AAA- and aCSF-treated rats were compared. To assess gap junction contributions, the rats were exposed to two BC exposures (separated by 2h). Gap 27 was topically applied for 1h prior to the 2nd evaluation. In controls, the gap 27 was omitted. No differences in the magnitude of the EEG power increase were observed when comparing L-AAA or gap 27-treated rats to their controls. The arteriolar responses are summarized in the figure. The 20-25% increase in diameter that is normally seen during seizure was completely lost in L-AAA-treated rats. Topical blockade of gap junctions was associated with a 50% reduction in pial arteriolar dilation. These results indicate that astrocytes, and, to a lesser extent, gap junctions, contribute greatly to the cerebrovasodilation accompanying seizure.



## INTERACTION OF ADENOSINE AND CYTOCHROME P450 EPOXYGENASE PATHWAYS IN NEUROVASCULAR COUPLING DURING WHISKER STIMULATION

Yanrong Shi<sup>1</sup>, John R. Falck<sup>2</sup>, David R. Harder<sup>3</sup>, **Raymond C. Koehler<sup>1</sup>**

<sup>1</sup>*Department of Anesthesiology, Johns Hopkins University, Baltimore, MD, USA*

<sup>2</sup>*Department of Biochemistry, University of Texas Southwestern Medical Center, Dallas, TX, USA*

<sup>3</sup>*Cardiovascular Research Center, Medical College of Wisconsin, Milwaukee, WI, USA*

**Introduction:** Adenosine has been implicated in mediating functional hyperemia, but the role of specific adenosine receptors is unknown. Cerebrovascular effects of exogenous adenosine are largely mediated by adenosine A2A and A2B receptors (1, 2). In addition, A2A and A2B receptor activation can increase Ca in astrocytes, which may mobilize arachidonic acid. Epoxyeicosatrienoic acid (EETs) are synthesized from arachidonic acid in astrocytes by cytochrome P450 epoxygenase and open KCa channels on cerebrovascular smooth muscle, leading to dilation. Epoxygenase inhibitors MS-PPOH and miconazole reduce functional hyperemia (3). Presently, the epoxygenase pathway was further investigated with the recently described EETs antagonists 14,15-EEZE and its methylsulfonylimide derivative 14,15-EEZE-sMI (4). The potential interaction of the adenosine and EETs pathways were investigated by combining treatments of 14,15-EEZE or MS-PPOH with the adenosine A2A receptor antagonist ZM241385 or the A2B antagonist alloxazine to determine if there was an additive inhibitory effect on the blood flow response to whisker stimulation. **Methods:** The percent change in laser-Doppler flow (LDF) over whisker barrel cortex during 60 s whisker stimulation was measured in chloralose-anesthetized rats at baseline, at 1 h of cortical superfusion of a single antagonist, and after an additional hour of either single or combination antagonist superfusion. Responses were compared within groups by repeated measures ANOVA and paired t-test. **Results:** ZM241385 (1 mg/kg iv + 1  $\mu$ M CSF superfusion) had no effect on the increase in LDF during whisker stimulation (from 17 $\pm$ 4% to 16 $\pm$ 5% at 1h and 17 $\pm$ 5% at 2h;  $\pm$ SD; n=6). In contrast, alloxazine (1 mg/kg iv + 1  $\mu$ M superfusion; n=6) reduced the LDF response from 17 $\pm$ 4% to 10 $\pm$ 4% at 1h and to 12 $\pm$ 4% at 2h of superfusion. Superfusion of 14,15-EEZE (n=6) reduced the LDF response from 14 $\pm$ 4% to 7 $\pm$ 3% at 1 h and to 5 $\pm$ 2% at 2h. Similar reductions were obtained with 30  $\mu$ M 14,15-EEZE-sMI and 20  $\mu$ M MS-PPOH. In another group (n=8) in which alloxazine was found to reduce the response from 15 $\pm$ 2% to 9 $\pm$ 3%, subsequent superfusion of both alloxazine and 14,15-EEZE failed to significantly reduce the LDF response further (8 $\pm$ 5%). Likewise, addition of alloxazine with MS-PPOH failed to reduce the response further (9 $\pm$ 3%) compared to MS-PPOH alone (11 $\pm$ 4%; n=6). 14,15-EEZE still reduced the response (8 $\pm$ 4%) in the presence of ZM241385 compared to ZM241385 alone (13 $\pm$ 3%; n=6). **Conclusions:** We conclude 1) that adenosine A2B receptors, rather than A2A receptors, play a significant role in coupling cortical blood flow to neuronal activity, 2) that the role of EETs previously supported by the use of epoxygenase inhibitors is strengthened by new evidence with EETs antagonists, and 3) that the epoxygenase and adenosine A2B receptor signaling pathways are not functionally additive. **References:** 1. Ngai et al. (2001) *Am J Physiol Heart Circ Physiol* 280: H2329-H2335. 2. Shin et al. (2000) *Am J Physiol Heart Circ Physiol* 278: H339-H344. 3. Peng et al. (2002) *Am J Physiol Heart Circ Physiol* 283: H2029-H2037. 4. Gauthier et al. (2004) *Pharmacol Res* 49: 515-524. Supported by NIH grant HL59996

**FLOW-INDUCED CEREBRAL VASODILATATION INVOLVES ACTIVATION OF PI3-KINASE AND PRODUCTION OF REACTIVE OXYGEN SPECIES****Christopher G. Sobey<sup>1</sup>, Grant R. Drummond<sup>2</sup>, Tamara M. Paravicini<sup>1</sup>**<sup>1</sup>*Department of Pharmacology, University of Melbourne, Parkville, Australia*<sup>2</sup>*Department of Pharmacology, Monash University, Clayton, Australia*

Reactive oxygen species (ROS) such as superoxide and hydrogen peroxide are known to be cerebral vasodilators. A major source of ROS in the vasculature is the flavin-containing enzyme NADPH-oxidase. We have previously demonstrated that activation of NADPH-oxidase leads to dilatation of the basilar artery in vivo, via a mechanism involving production of hydrogen peroxide from superoxide dismutase. The endogenous stimuli for this unique vasodilator mechanism are yet to be characterised, however shear stress is known to activate phosphatidylinositol 3-kinase (PI3-K) and NADPH-oxidase in cultured cells. This study investigated whether increased intraluminal blood flow could induce cerebral vasodilatation via the activation of PI3-K and/or NADPH-oxidase. A cranial window preparation in anaesthetised rats was used to examine vasomotor responses of the basilar artery in the absence and presence of inhibitors of ROS production and breakdown. Bilateral occlusion of the common carotid arteries to increase basilar artery flow resulted in reproducible dilatations of this vessel ( $77\pm 2\%$  of maximum,  $n=39$ ) that were rapidly reversed when normal flow was restored. Flow-dependent dilatation was profoundly inhibited following treatment with the PI3-K inhibitor wortmannin ( $1\mu\text{M}$ ). Treatment of the basilar artery with the NADPH-oxidase inhibitor diphenyleneiodonium at  $0.5$  and  $5\mu\text{M}$  also caused a significant reduction in flow-dependent dilatation ( $54\pm 9\%$  and  $37\pm 7\%$  of maximum) without affecting nitric oxide-mediated dilatations to acetylcholine. Treatment with the hydrogen peroxide scavenger catalase also reduced flow-dependent dilatation from  $79\pm 7\%$  to  $55\pm 7\%$ , indicating a role for NADPH-oxidase-derived hydrogen peroxide in this response. The nitric oxide synthase (NOS) inhibitor L-NAME caused a small reduction (from  $83\pm 8\%$  to  $57\pm 6\%$ ) in flow-dependent dilatation. Furthermore, combined treatment with a ROS inhibitor (diphenyleneiodonium or catalase) and L-NAME caused a greater reduction in flow-dependent dilatation than seen with inhibition of either pathway alone. Thus, flow-dependent cerebral vasodilatation in vivo involves production of both ROS and nitric oxide, and is dependent on PI3-K activation.

## IS THE VASCULAR TREK-1 POTENTIALLY INVOLVED IN PUFAS-INDUCED NEURONAL

Nicolas Blondeau<sup>1</sup>, Gisèle Jarretou<sup>1</sup>, Pierre Gounon<sup>2</sup>, Valérie Giordanengo<sup>1</sup>,  
Michel Lazdunski<sup>1</sup>, Catherine Heurteaux<sup>1</sup>

<sup>1</sup>*Institut de Pharmacologie Moléculaire et Cellulaire, CNRS-UMR 6097, Valbonne, France*

<sup>2</sup>*Université de Nice Sophia-Antipolis, INSERM U627, Nice, France*

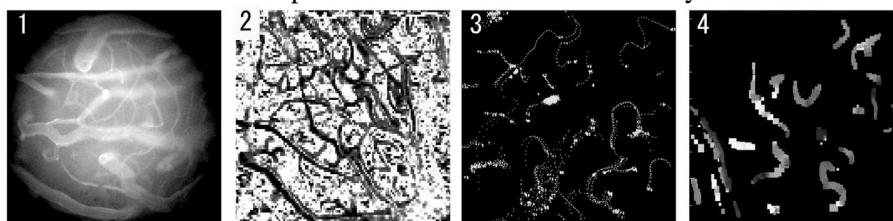
Introduction: Fatty acids are critical for the development and function of all organisms, in particular, very long chain of polyunsaturated fatty acids, such as alpha-linolenic acid (ALA) are necessary for the health and maintenance of mammals. ALA is a potent activator of some background 2P-domain K<sup>+</sup> channels, TREK and TRAAK, involved in the regulation of cell excitability. We have shown that (1) ALA is a powerful neuroprotector in acute cerebral ischemia and is a preconditioning inductor of delayed tolerance to cerebral ischemia; (2) TREK-1-KO mice are more sensitive to cerebral ischemia and not protected by ALA. Altogether this indicates that TREK-1 is a crucial mediator of the neuronal protection. Although there is some evidence that TREK-1 is expressed in neurons as well as in some vessels, little is known on the role of the vascular TREK-1 in the resistance to ischemia. We have therefore analyzed the brain vessel distribution of TREK-1 mRNA using RT-PCR, in situ hybridization and electron microscopy, as well as TREK-1 protein localization by immunohistochemistry. Moreover, we are investigating the role of this channel in association with cerebral blood flow and ALA-induced acute cerebral protection. Methods: RT-PCR was performed on different mouse and rat vessel mRNAs and visualized on 2% agarose gel. For in situ hybridization, the oligonucleotide probe (CAC AAT GGT CCT CTG GGA AAT CTC CTG AGG) was DIG-dUTP labelled. TREK-1 mRNA was detected with a Fluorescein-conjugated anti-DIG antibody. For electron microscopy, probes were immunogold-labeled with an anti-DIG antibody and silver enhanced. Ultrathin sections were examined using a JEOL 6700F field emission scanning electron microscope. For immunostaining, small fixed arteries were detected with an anti-TREK-1 primary antibody (Alomone) and observed using an epifluorescence microscope. Monoclonal mouse anti-CD31 antibody and Hoechst, a blue-fluorescent nuclei acid stain, were used to determine which cell type expresses TREK-1. To assess the effect of a neuroprotective dose of ALA on the CBF, we monitored it using a laser-Doppler in WT and TREK-1-KO animals within the protection window described for a single dose of 500nM ALA. Results: This study shows that TREK-1 channel is present throughout all the mouse vessels and more abundant in brain arteries. In situ techniques using epifluorescence and electron microscope combined with immunohistochemistry provide compelling evidence for the expression of these channels throughout the vessels in both myocytes and endothelial cell layers. CBF-monitoring shows that an injection of ALA increased the CBF in rats as well as in WT mice. Further experiments on TREK-1 KO should establish if TREK-1 account for the vasodilatation and CBF increase induced by ALA. Conclusion: These results provide evidence for the presence of two-pore domain K<sup>+</sup> channels, TREK-1 in rat and mice brain arteries, in both myocytes and endothelial cells and for a modulation of the LIN-induced CBF at a dose known to be neuroprotective. Collectively, they strongly suggest that activation of vascular TREK-1 channels by ALA is most likely to participate to the brain protection observed versus ischemia, in association with the neuronal activation of this channel.

## SPATIAL AND TEMPORAL HETEROGENEITY OF SINGLE CAPILLARY PLASMA FLOW AND RBC TRACKING IN THE RAT CEREBRAL CORTEX

Minoru Tomita, Istvan Schiszler, Hidetaka Takeda, Yutaka Tomita, Takashi Osada, Miyuki Unekawa, Norio Tanahashi, Norihiro Suzuki

*Department of Neurology, School of Medicine, Keio University, Tokyo, Japan*

We present a new high-speed (125-500 frames per sec) confocal fluorescence microscopy and image analysis system employing Matlab and our own KEIO-IS1 and KEIO-IS2 software to visualize plasma flow and RBC tracking in single capillaries in the living rat cerebral cortex. Wistar rats with a cranial window were given fluorescein isothiocyanate (FITC)-dextran and FITC-labeled red blood cells (RBC) intravenously as a bolus to visualize single capillaries and RBC in the capillaries (Seylaz et al., JCBFM 19:863,1999). FITC-Dextran was also used to measure local plasma flow changes along single capillaries by applying the hemodilution principle in individual pixels. Reciprocal mean transit times calculated with KEIO-IS1 were displayed on a 2-D flow map as reported previously (Am J Physiol 279, H1291, 2000). After the microvessels were vitally stained, FITC-RBCs were injected. The bright RBCs were observable flowing through single capillaries over a dark background. A video clip at a speed of 250-500 frames per sec was taken for a 10 sec interval, and analyzed with KEIO-IS2 to document tracking of all RBCs, which were individually numbered, and to calculate automatically individual RBC velocities on a spreadsheet (Excel). The software further created a map of neighboring trains of peaks due to RBC passage in all pixels. Fig. 1 shows a microphotograph taken with a digital camera of intraparenchymal microvessels, including capillaries, which are vitally stained with FITC-dextran. Fig. 2 shows the microvascular network in situ, constructed by connecting pixels showing passage of RBC spike trains along the time axis, using KEIO-IS1 (correlation coefficient, 0.8). Fig. 3 presents total RBCs (small dots) tracked at a depth of 60  $\mu$ m below the pia by the video at 250 frames per sec for 10 sec. RBCs are automatically numbered (KEIO-IS2) and their velocities are calculated and expressed on a 2-D velocity map (Fig. 4). Heterogeneous optical density implies variation in RBC velocity even in straight capillaries. Single, double, and multiple tracking of RBCs can be seen, suggesting independent periodic passage of RBCs. Some capillaries show a swinging movement due probably to vasomotion occurring within 10 sec. Preliminary data based on 26 rats show spatial and temporal heterogeneity of plasma flow along single capillaries and its change with time, together with capillary vasomotion seen as local winding and translocation. RBC tracking was not parallel to the plasma flow. The plasma flow was present (slow or fast) continuously, while RBC passage was periodic (RBC recruitment). The possible regulation of RBC flow in response to neuronal activity remains to be studied.



## A COMPACT PHYSIOLOGICAL MODEL OF THE AUTOREGULATION OF CEREBRAL BLOOD VESSELS

Alexander B. Rowley<sup>1</sup>, Christopher J. Stephens<sup>2</sup>, Stephen J. Payne<sup>2</sup>

<sup>1</sup>*Computational Biology Research Group, Oxford University Computing Laboratory, Oxford, UK*

<sup>2</sup>*Biomedical Signal Processing Research Group, Department of Engineering Science, Oxford, UK*

[Introduction] Current mathematical models of the processes known as cerebral autoregulation consist of a lumped parameter approximation to the cerebral vasculature with autoregulation being represented as a simple feedback mechanism, based on changes in flow. A realistic physiologically-based model of cerebral autoregulation, however, would allow for quantitative interpretation of a number of existing clinical tests. We present here a compact model of blood vessels that includes the main chemical feedback pathways and integrates them with the mechanical behaviour of the vascular smooth muscle to simulate the myogenic autoregulatory response. This model is comparable in size to current feedback models but developed with reference to the underlying physiology. [Method] The primary feedback mechanisms are based upon the production of the endothelium-derived relaxing factor Nitric Oxide (NO) in response to shear stress and variations in intracellular calcium (Ca<sup>2+</sup><sub>i</sub>) due to pressure. A simple model of the vascular smooth muscle cell membrane relates the potential, Ca<sup>2+</sup><sub>i</sub> and pressure, based on stretch-sensitive channels, in which NO and Ca<sup>2+</sup><sub>i</sub> are signalling pathways activating and inactivating the vascular smooth muscle respectively. The smooth muscle behaviour is determined by a simple mechanical model, using the Hai-Murphy kinetic model to describe myosin phosphorylation and latch bridge formation. Mechanical equilibrium is then used to balance pressure and stress, allowing the inner area of the vessel to be set in response to changes in pressure. This compact system of only 7 non-linear ordinary differential equations allows the autoregulatory behaviour of the vessel to be determined, both in steady state and under dynamic conditions in response to changes in Arterial Blood Pressure (ABP). The compactness of the model allows the system equations to be solved very rapidly. The number of coefficients within the model is small, allowing the behaviour of the model to be analysed simply. The autoregulation model can also be incorporated into a lumped parameter model of the cerebral vasculature to simulate the response of Cerebral Blood Flow in response to changes in ABP. [Results] Steady state solutions of the model equations show good agreement with results obtained from in vitro tests on rat cerebral arteries: a key advantage of this model is that the available measured parameters (in particular Ca<sup>2+</sup><sub>i</sub> and membrane potential) are predicted by this model. The model response when coupled to an existing lumped parameter approximation to the human cerebral vasculature casts doubt upon the accuracy of the response predicted by existing models. It is hoped that the insights into cerebral autoregulation provided by this new model will allow the work to be extended to consider integrating autoregulating vessels within a geometrically accurate model of the cerebral vasculature, in a similar way to those already proposed for the heart. This would allow for simulations of the fMRI response, which can show how consumption by neuronal cells changes the local flow distribution. It is hoped that this may provide greater insight into the origin of the BOLD response in fMRI studies and predict how this is altered in diseased cases such as stroke and dementia.

## **IMPLICATION OF NOCICEPTIN IN ALTERATIONS IN CEREBRAL BLOOD FLOW REGULATION FOLLOWING POSTNATAL EXPOSURE TO ETHANOL IN RATS**

**Won Suk Lee, Su Yeon Ko, Jeong Hee Kim, Dong Hwan Cho**

*Department of Pharmacology, College of Medicine, Pusan National University, Busan, South Korea*

This study aimed to investigate whether nociceptin is implicated in the alterations in cerebral blood flow regulation following postnatal exposure to ethanol in Sprague-Dawley rats. Animals received ethanol (2.5 g/kg, s.c.) twice a day, 2 hours apart, on postnatal 6, 7 and 8 days. The changes in regional cerebral blood flow (rCBF) in response to the changes in mean arterial blood pressure were determined at 4-, 8-, and 12-weeks of age by laser-Doppler flowmetry. Hypotension was induced by the gradual withdrawal of blood from arterial catheter, and the reversal of blood pressure was produced by the reinfusion of blood. Expression of nociceptin-like immunoreactivity was determined in dura mater and cerebral cortex using immunohistochemistry. Postnatal exposure to ethanol almost abolished the autoregulation of rCBF in all age groups. Pretreatment with nociceptin (0.138 µg/kg, i.p.) but not with [Nphe1]nociceptin(1-13)NH<sub>2</sub> (1.38 µg/kg, i.p.), a selective competitive nociceptin receptor antagonist, 5 minutes prior to ethanol administration preserved the autoregulation of rCBF in all age groups. Postnatal exposure to ethanol markedly increased the expression of nociceptin-like immunoreactivity in dura mater, which was significantly inhibited by pretreatment with 7-nitroindazole monosodium salt (7-NINA, 50 mg/kg, i.p.) as well as aminoguanidine (1 mg/kg, i.p.) 5 minutes prior to ethanol administration in all age groups. Postnatal exposure to ethanol markedly increased the expression of nociceptin-like immunoreactivity in cerebral cortex, which was significantly inhibited by pretreatment with 7-NINA as well as aminoguanidine 5 minutes prior to ethanol administration in all age groups. The values of arterial blood gas analysis were not significantly different from the basal levels in all groups. These results suggest that nociceptin is deeply implicated in the compensatory mechanisms for the nitric oxide-dependent alterations in CBF autoregulation following postnatal exposure to ethanol.

### PERTURBATION OF INTRAPARENCHYMAL ARTERIOLES DURING K<sup>+</sup>-INDUCED CORTICAL SPREADING DEPRESSION IN CATS

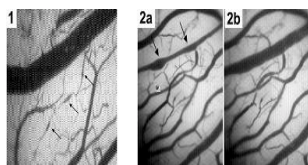
Takashi Osada<sup>1</sup>, Minotu Tomita<sup>1</sup>, Norio Tanahashi<sup>1</sup>, Hidetaka Takeda<sup>1</sup>, Masahiro Kobari<sup>2</sup>,  
Manabu Ohtomo<sup>3</sup>, Norihiro Suzuki<sup>1</sup>

<sup>1</sup>*Department of Neurology, School of Medicine, Keio University, Keio, Japan*

<sup>2</sup>*Kyosai Tachikawa Hospital, Tokyo, Japan*

<sup>3</sup>*National Sanatorium Higashi Saitama Hospital, Saitama, Japan*

During K<sup>+</sup>-induced cortical spreading depression (CSD) in the rat cerebral cortex, we previously observed repetitive wave-ring spread of oligemia/hypoperfusion followed by hyperemia/hyperperfusion. The oligemia/hypoperfusion occurred before upstream feeding arteriolar changes, suggesting that the capillary changes of the oligemia/hypoperfusion was of neuronal origin (Tomita M et al (2005) J CBF & M, in press). In this communication, we examined intraparenchymal arteriolar changes in the early phase of tissue oligemia. Six cats were used. Under  $\alpha$ -chloralose-urethan anesthesia, a skull window was opened in the parieto-temporal region. The dura was removed and the cerebral cortex was exposed. An optical fiber of 150  $\mu$ m in diameter was inserted into the brain tissue obliquely from 3 mm behind the skull window, so that the light source was positioned at the center of the ROI 1 mm below the pia. Intraparenchymal 20-40  $\mu$ m arterioles were both trans-illuminated in silhouette from below and epi-illuminated from above. They were monitored with a Canon video camera, and images were taken into a computer through a Scion frame grabber card (LG-3). When K<sup>+</sup> was microinjected into the cortex at a site near the ROI, oligemic wave-ring spread was reproduced as reported previously (Tomita Y et al (2002) Neurosci Lett:322,157). We found that capillary flow in the oligemic area became very slow, with clustered RBCs passing through small vessels like ants marching. During oligemia/hypoperfusion, we noticed in all cases segmental constriction/dilatation of arteriole(s), forming a sausage-string shape (Fig. 1 and Fig. 2a) which had never been seen in other series of experiments. Chronological changes of arteriolar diameter were seen; for example, in 2 cases, a part of the arteriole suddenly contracted by 50% for about 1 to 1.5 sec and then dilated to 250% at 10 sec and remained dilated for more than 1 min (Fig. 2b). In the remaining cases, the time courses of constriction/dilatation of arteriole(s) were rather slow. In one case, the vascular dilatation occurred at a branching site and moved peripherally along the arteriole, like the movement of an egg swallowed by a snake. Despite these events, subtraction pictures revealed that the majority of the epi-cortical pial arteries did not change their diameter in this early phase. Based on these observations, we speculate that arterioles were perturbed by discrepant controls of high K<sup>+</sup> concentration in the extracellular fluid, unknown feedback signals from oligemic tissue, and autonomic ganglionic regulation. Fig. 1: Sausage-string-like change of an intraparenchymal arteriole of ca. 25  $\mu$ m during K<sup>+</sup>-induced CSD. Fig. 2a: Sausage-string-like change of ca. 50  $\mu$ m followed by marked dilatation (Fig. 2b).



## STELLATE CELLS RELEASE NO AND INDUCE VASODILATION OF INTRAPARENCHYMAL BLOOD VESSELS IN RAT CEREBELLAR SLICES

Armelle Rancillac<sup>1</sup>, Manon Guille<sup>2</sup>, Xin-Kang Tong<sup>3</sup>, H el ene Geoffroy<sup>1</sup>, St ephane Arbault<sup>2</sup>, Edith Hamel<sup>3</sup>, Christian Amatore<sup>2</sup>, Jean Rossier<sup>1</sup>, Bruno Cauli<sup>1</sup>

<sup>1</sup>*Lab de Neurobiologie, CNRS, UMR 7637, ESCPI, Paris, France*

<sup>2</sup>*Lab D'Activation Mol culaire et R activit s Electrochimiques, CNRS, UMR 8640, ENS, Paris, France*

<sup>3</sup>*Lab Cerebrovascular Res, Montreal Neurol Inst, McGill University, Montr al, QC, Canada*

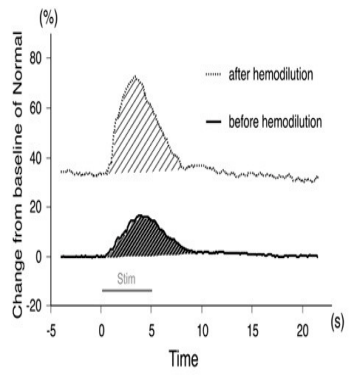
**Introduction:** The tight coupling between neuronal activity and local perfusion, known as functional hyperemia, is central to normal brain function. In the cerebellum functional hyperemia depends almost exclusively on nitric oxide (NO), a potent vasodilator. The neuronal isoform of nitric oxide synthase (nNOS), a NO synthesizing enzyme, is expressed by different neuronal types in the cerebellum, among which stellate cells are suspected to be critical for neurovascular coupling. **Methods:** To demonstrate this functional role, we applied the NO donor diethylamine NONOate (DEA-NONOate) in rat cerebellar acute slices. NO was detected by amperometry with a platinized carbon NO probe (poised at E = 650 mV vs Ag/AgCl) placed in the molecular layer. Cerebellar microvessel diameter changes were monitored by infrared videomicroscopy. Stellate cells characterization was achieved by patch-clamp recordings and single-cell reverse transcriptase-multiplex PCR (RT-mPCR), and their associations with responsive microvessels identified by confocal microscopy following biocytin labeling and immunodetection of blood vessel laminin. **Results:** Bath application of DEA-NONOate (100  $\mu$ M) produced NO flux (84.8  $\cdot 10^7$  molecules/s) and vasodilation (86 %) of intraparenchymal blood vessels. Similarly, neuronal stimulation with NMDA (100  $\mu$ M) induced NO flux (99.8  $\cdot 10^6$  molecules/s) and microvessel vasodilatations (42 %) that were completely abolished by TTX (1  $\mu$ M) or by L-NAME (1 mM), a NOS inhibitor. In patch clamp recordings the evoked firing of single stellate cells also induced NO flux (22.5  $\cdot 10^6$  molecules/s) and dilatation (10 %) of neighboring intraparenchymal microvessels. Molecular and morphological characterization of stimulated stellate cells by single cell RT-PCR and confocal microscopy revealed the expression nNOS mRNAs and the association of stellate cell neurites with responsive blood vessels. **Conclusions:** These ex vivo results confirm a functional role of stellate cells in neurovascular coupling mediated by NO release. Further, these data demonstrate that single interneurons activation is sufficient to alter the tone of local microvessels, emphasizing their role in the regulation of local perfusion. Supported by CNRS (JR, BC, AR), CIHR (MOP-53334, EH), and FRSQ-INSERM exchange program (EH and BC).

**LOCAL OXYGEN DELIVERY EVOKED BY HINDPAW STIMULATION IS THE SAME BEFORE AND AFTER ISOVOLEMIC HEMODILUTION IN RAT SOMATOSENSORY CORTEX**

**Masakatsu Ureshi, Iwao Kanno**

*Akita Research Institute for Brain and Blood Vessels, Department of Radiology and Nuclear Medicine, Akita, Japan*

Introduction: Isovolemic hemodilution causes decreased blood viscosity and arterial oxygen content (CaO<sub>2</sub>). It is also known that isovolemic hemodilution increases the baseline local cerebral blood flow (LCBF) and this phenomenon has been interpreted as maintaining the baseline oxygen delivery. However, the changes in evoked local oxygen delivery with stimulation have not been reported during isovolemic hemodilution. The aim of the present study is to investigate this relationship. Methods: Twenty Sprague-Dawley rats (12 for LCBF and 8 for field potential) were used in this study. The tail artery and femoral vein were cannulated for blood pressure monitoring, blood gas sampling and drug injection. Rats were anesthetized with  $\alpha$ -chloralose during the experiments and were fixed in a stereotactic frame. The parietal bone was thinned to translucency over the left somatosensory cortex. The cortex was activated by electrical stimulation of the hind paw with 5 Hz pulses (0.1 ms width) applied at a current of 2.0 mA for 5 s. LCBF was measured using Laser-Doppler flowmetry. To confirm that the neurological activity was unchanged, the field potential was recorded with a tungsten microelectrode inserted into the cortex. Isovolemic hemodilution was performed by drawing 9ml of blood from the tail artery and infusing the same volume of hetastarch through the femoral vein. Blood pressure was kept constant by infusing methoxamine after isovolemic hemodilution. Results: Hematocrit decreased from  $37.2 \pm 3.1\%$  to  $20.3 \pm 2.0\%$  and CaO<sub>2</sub> decreased from  $17.5 \pm 1.4\text{ml/dl}$  to  $9.8 \pm 0.9\text{ml/dl}$  after isovolemic hemodilution. The summed field potentials did not change after isovolemic hemodilution. Figure 1 shows the evoked LCBF before and after isovolemic hemodilution. Both curves were normalized by the baseline level before isovolemic hemodilution. The local oxygen delivery was calculated as the product of the integrated evoked LCBF and CaO<sub>2</sub>. The local oxygen delivery after isovolemic hemodilution was a factor of 0.88 (0.69 – 1.12) (median (25-75%)) times that before isovolemic hemodilution despite an increase in integrated evoked LCBF by a factor of 1.48 (1.31 – 1.85). The change in evoked local oxygen delivery was not significant ( $p > 0.05$ ). Discussion: This is the first report to investigate evoked oxygen delivery after isovolemic hemodilution. Despite a 50% increase in evoked LCBF, the evoked local oxygen delivery is kept constant. Thus, evoked LCBF maintains a constant local oxygen delivery even in the transient condition although its vascular mechanism is yet to be elucidated. Grant support: Science and Technological Research Fellowship of Japan Society for the Promotion of Science (JSPS) and National Institute of Health MH57180 Fig.1. LCBF responses before and after isovolemic hemodilution. Both were normalized by the baseline LCBF before isovolemic hemodilution.



**INTRAMICROVASCULAR BEHAVIOR OF PLATELETS IN RAT BRAIN  
OBSERVED BY HIGH-SPEED LASER CONFOCAL FLUORESCENCE  
MICROSCOPY**

**Norio Tanahashi**, Hidetaka Takeda, Takasi Osada, Kouichi Ohki, Miyuki Unekawa,  
Minoru Tomita, Norihiro Suzuki

*Department of Neurology, School of Medicine, Keio University, Tokyo, Japan*

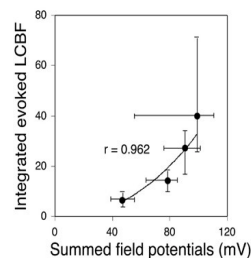
Although abundant data are available on in vitro platelet behavior, in situ studies in the brain microvasculature, especially in the intraparenchymal vessels, have not previously been possible because of methodological difficulties. We used our newly developed high-speed (125-1000 frames per sec) confocal fluorescence microscopy and image analysis system employing Matlab and our own KEIO-IS1 and KEIO-IS2 software to visualize platelet flow, tracking individual platelets in the microvasculature in living rat cerebral cortex. The program exploits the light intensity difference between the dark background and the light platelets in the visual field of the microscope to detect the platelets automatically. A small cranial window was trephined in the parietal region of urethane-anesthetized Wistar rats (n=10). Fluorescein isothiocyanate (FITC)-dextran (70 kDa) was injected intravenously to stain the microvessels. Subsequently, carboxylfluorescein succinimidyl ester (CFSE) was also injected intravenously to label platelets. Platelets in circulating blood became visible as bright particles in the intraparenchymal microvessels. In the veins, platelets were seen flowing slowly along endothelial cell walls (rolling) with a standard video camera at 30 frames per sec for a couple of minutes after the CFSE injection. In the arteries/arterioles, flowing platelets were detected only at high speed settings (125-1000 frames per sec). Contrary to expectation, platelet flow was well mixed in the circulating blood, and did not occur preferentially in the peripheral layer. However, transient contact of platelets with endothelial cells and detachment (stoth and go h phenomenon) were occasionally observed in the pial arteries. Flowing platelets in the capillaries were by no means stationary. For documentation of platelet tracking, video clips taken at 250-500 frames per sec for a 10 sec interval were analyzed with KEIO-IS2 (see Schiszler et al. Brain 05). The software automatically assigned individual numbers to platelets, calculated their velocities, and presented the results on a spreadsheet (Excel). The velocities were  $2.72 \pm 0.52$  mm/sec for arterioles,  $0.75 \pm 0.3$  mm/sec for single capillaries and  $0.21 \pm 0.07$  mm/sec for venules. In the later stage of experiments (5-10 min after CFSE injection), platelets began to adhere to the wall of venules, occasionally forming large platelet aggregates, probably owing to some toxic effect of CFSE itself on the endothelial cells. The high-speed laser confocal fluorescence microscope is a promising tool for investigating hemodynamic changes at the vessel wall, including formation of platelet clots and their resolution with therapeutic agents.

## NONLINEAR CORRELATION BETWEEN EVOKED LOCAL CEREBRAL BLOOD FLOW AND FIELD POTENTIAL IN RAT SOMATOSENSORY CORTEX AS A FUNCTION OF STIMULUS CURRENT

Masakatsu Ureshi, Iwao Kanno

*Akita Research Institute for Brain and Blood Vessels, Department of Radiology and Nuclear Medicine, Akita, Japan*

**Introduction:** It is known that the local cerebral blood flow (LCBF) in rat somatosensory cortex demonstrates transient changes in response to peripheral stimulation. However, the mechanism responsible for the transient evoked LCBF has yet to be determined. As the change in LCBF is almost certainly coupled to neuronal activity, the correlation between evoked LCBF and field potential (FP) as a function of the characteristics of the stimulus is important to understanding this mechanism. In the present study, we examined the relationship between local cerebral blood flow (LCBF) and field potential (FP) evoked by hindpaw stimulation in rat somatosensory cortex while changing the stimulus current. **Methods:** Twenty Sprague-Dawley rats were used in this study. The tail artery and femoral vein were cannulated for blood pressure monitoring, blood gas sampling and drug injection. Rats were anesthetized with  $\alpha$ -chloralose during the experiments and were fixed in a stereotactic frame. The parietal bone was thinned to translucency with a drill and the thinned region covered an area of  $3 \times 3 \text{ mm}^2$  over the left somatosensory cortex centred 2.5 mm caudal and 2.5 mm lateral to the bregma. The cortex was activated by electrical stimulation of the hind paw with 5 Hz pulses (0.1 ms width) applied at currents of 1.0, 1.5, 2.0 and 2.5 mA for 5 s. LCBF was measured using Laser-Doppler flowmetry and the FP was recorded by a tungsten microelectrode inserted into the cortex. **Results:** The peak value of the LCBF and integrated evoked LCBF increases linearly with stimulus current. On the other hand, the gradient of the summed FP decreases at higher currents. Consequently, the relationship between integrated evoked LCBF and summed FP was nonlinear and a least-squares fit of a power-law to the data gave  $y = a x^b$ ,  $a = 1.05 \times 10^{-3}$ ,  $b = 2.25$  ( $R = 0.962$ ). **Discussion:** There are two possible reasons for the nonlinear correlation between the integrated evoked LCBF and summed FP. One possibility is a mismatch in the size of the fields-of-view of the measurement probes. The second possibility is that the measure of neural activity, SFP, did not include the slower, low amplitude contributions to the FP by unmyelinated nerve fibers at higher currents. It isn't yet clear which of these possibilities is more likely. **Grant support:** Science and Technological Research Fellowship of Japan Society for the Promotion of Science (JSPS) and National Institute of Health MH57180 Fig.1. The relationship between the integrated evoked LCBF and summed field potentials.

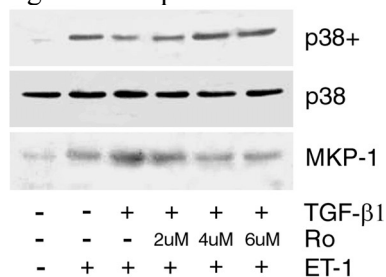


**TRANSFORMING GROWTH FACTOR- $\beta$ 1 (TGF- $\beta$ 1) ALTER ENDOTHELIN-1 (ET-1)-INDUCED CONTRACTION IN BRAIN VESSELS VIA UPREGULATION OF MITOGEN-ACTIVATED PROTEIN KINASE PHOSPHATASE 1 (MKP-1) AND INACTIVATION OF P38 MITOGEN-ACTIVATED PROTEIN KINASE (P38 MAPK)**

Xin-Kang Tong, Edith Hamel

*Laboratory of Cerebrovascular Research, Montreal Neurological Institute, McGill University, Montréal, QC, Canada*

**Introduction:** Increased levels of TGF- $\beta$ 1 have been implicated in the cerebrovascular dysfunctions that accompany Alzheimer's disease. Transgenic mice that overexpress TGF- $\beta$ 1 exhibit perivascular accumulation of amyloid and basement membrane proteins, thinner endothelial cells, decreased local cerebral blood flow (Buckwalter et al., 2002, Ann NY Acad Sci 997, 87) and, as we recently found in middle cerebral arteries (MCAs) from such aged mice, a reduced contractile response to ET-1 (Tong et al., submitted). As ET-1 is an important regulator of cerebrovascular tone and homeostasis, we tested if chronic overproduction of TGF- $\beta$ 1 could decrease contraction to ET-1 via inactivation of its signal transduction pathway. **Methods:** ET-1-induced contractions were measured in isolated and pressurized MCAs from aged (>16 months) TGF- $\beta$ 1 transgenic and wild-type littermate controls (n=3/group), or young C57Bl/6 (n=10) mice in the presence or absence of 25 $\mu$ M SB-203580 (p38 MAPK inhibitor) or 10 $\mu$ M U0126 (extracellular signal-regulated kinase (ERK1/2) kinase or MEK inhibitor). Primary cultures of rat brain microvascular smooth muscle (SMC) cells were generated from 112  $\mu$ m mesh-harvested cortical microvessels. Cells were exposed (3 days) to TGF- $\beta$ 1 (3ng/ml) in the absence of serum, and then stimulated with ET-1 (10-7M, 10 min) with or without pre-incubation (1 hr) with SB-203580 (25 $\mu$ M) or U0126 (10 $\mu$ M). Alternatively, cells were exposed to TGF- $\beta$ 1 (2 days) and, on the 3rd day, to both TGF- $\beta$ 1 and Ro-31-8220 (2-6 $\mu$ M, an inhibitor of MKP-1 expression), before ET-1 stimulation. Cell lysates were separated by SDS-PAGE, transferred to nitrocellulose filters, probed with antibodies against ETA and ETB receptors, MKP-1, cyclo-oxygenase-2 (COX-2, marker of cell activation) or phosphorylated-MKK3/6, -ERK1/2, or -p38 MAPK. **Results:** MCAs from aged TGF- $\beta$ 1 transgenic mice had reduced contractions to ET-1 as compared to wild-type littermates ( $\downarrow$ 39%, p<0.01). Similarly, MCAs from young mice treated with SB-203580 showed severely impaired contractions to ET-1 ( $\downarrow$ 68%, p<0.001) while U0126 exerted a much smaller effect ( $\downarrow$ 32%, ns), indicating that p38 MAPK is the main transduction pathway in this response. In SMC cells, chronic exposure to TGF- $\beta$ 1 increased COX-2 expression, had no effect on levels of ETA and ETB receptors, MKK3/6, but significantly decreased ( $\downarrow$ 18.5%, p<0.05) phosphorylated p38 MAPK levels while increasing those of MKP-1 protein, indicating selective inhibition of the down-stream ET-1 transduction pathway at the p38 phosphorylation step. Further, SMC cells treated with TGF- $\beta$ 1 and Ro-31-8220 showed normalized levels of phosphorylated p38 MAPK and decreased MKP-1 protein levels (Figure). **Conclusion:** These results demonstrate that chronic high levels of TGF- $\beta$ 1 induce MKP-1 expression in cerebrovascular SMC cells, which leads to the inactivation of p38 MAPK and altered capacity of the brain vessels to constrict in response to ET-1. TGF- $\beta$ 1 may thus exert detrimental effects on cerebrovascular tone and homeostasis by promoting MKP-1, a negative regulator of p38 MAPK activity. Supported by CIHR (MOP-64194) and Alzheimer Society of Canada.





**VASCULAR FIBROSIS VERSUS AMYLOID BETA (A $\beta$ )-INDUCED OXIDATIVE STRESS IN THE CEREBROVASCULAR PATHOLOGY ASSOCIATED WITH ALZHEIMER'S DISEASE (AD)**

**Xin-Kang Tong, Nektaria Nicolakakis, Edith Hamel**

*Laboratory of Cerebrovascular Research, Montreal Neurological Institute, McGill University, Montreal, QC, Canada*

**Introduction:** Recent studies indicate that cerebrovascular pathologies, ranging from structural alterations, atherosclerotic lesions and impaired hemodynamic responses, are another if not a primary feature of Alzheimer's disease (AD). Oxidative stress mediated by amyloid beta (A $\beta$ ) and chronic inflammation associated with increased levels of transforming growth factor-beta 1 (TGF- $\beta$ 1), have been implicated in these dysfunctions. Using transgenic mice of different ages (4, 12 and/or 18/21 months) that overexpress A $\beta$  or TGF- $\beta$ 1, we studied the age-related changes in cerebrovascular responsiveness, assessed their relationships with alterations in specific proteins, tested in vitro their reversibility at an advanced stage of the pathology, and compared them to changes seen in cortical microvessels, including from neuropathologically confirmed cases of AD. **Methods:** Responsiveness of the middle cerebral artery to increasing concentrations of serotonin (5-HT), endothelin-1 (ET-1), or calcitonin gene-related peptide (CGRP), and to NOS inhibition (10 $\mu$ M L-NNA) was assessed in vitro in transgenic APP (Swedish and Indiana mutated forms of the amyloid precursor protein) and TGF- $\beta$ 1 mice. Underlying mechanisms were explored by i) measuring, by Western blot, changes in protein levels of markers of inflammation, oxidative stress, angiogenesis, or blood vessel wall components, ii) localizing, by immunohistochemistry, changes in some of these or other markers in cortical microvessels of transgenic mice and AD brains, and iii) pharmacologically attempting to reverse cerebrovascular deficits in vitro by MCA superfusion (30-60 min) with superoxide dismutase (SOD) or catalase (120 or 1000U/ml). Wild-type littermate mice and non-demented elderly brains served as controls. **Results:** Middle cerebral arteries from both APP and TGF- $\beta$ 1 mice showed age-impaired ability to dilate to CGRP and constrict upon NOS inhibition. The contractile responses to 5-HT and ET-1 were preserved except in aged TGF- $\beta$ 1 mice. SOD normalized the response to NOS inhibition in APP mice but SOD and catalase had no beneficial effect in TGF- $\beta$ 1 mice. Protein changes in pial and intracortical vessels of APP mice were limited to upregulation in manganese SOD (MnSOD) that typically distributed in cuffs along and around penetrating and small intracortical microvessels at all ages, being more salient in aged mice. In contrast, TGF- $\beta$ 1 mice exhibited no change in MnSOD but increases in vascular content of VEGF, total collagen and collagen type IV together with a decrease in eNOS protein and alkaline phosphatase activity. In AD brains, there was no perivascular upregulation of MnSOD, but increased microvascular collagen content and decreased alkaline phosphatase activity that occurred independently from vascular A $\beta$  plaques. **Conclusion:** Increased vasocontractile tone, as seen in APP and TGF- $\beta$ 1 mice, can result from different underlying mechanisms. Oxidative stress, mediated primarily by superoxide anions, was the main culprit in APP mice, while structural changes in the vessel wall, exemplified by decreased eNOS and alkaline phosphatase activity and increased VEGF and collagen content, characterized TGF- $\beta$ 1 mice and, also, AD cortical microvessels. We suggest that pathological vascular remodeling – and not oxidative stress – is a key determinant in AD cerebrovascular dysfunctions, and that it may be an attractive therapeutic target for AD. CIHR (MOP-64194, EH) and Alzheimer Society of Canada.

### CHANGES OF FLOW VELOCITY AND RBC TRACKING IN SINGLE CAPILLARIES AND CAPILLARY DENSITIES DURING SEVERE HYPOTENSION IN RAT BRAIN

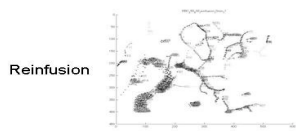
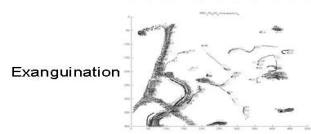
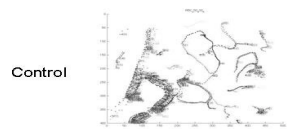
Hidetaka Takeda<sup>1</sup>, Minoru Tomita<sup>1</sup>, Istvan Schiszler<sup>2</sup>, Yutaka Tomita<sup>3</sup>, Takashi Osada<sup>1</sup>,  
Kouichi Ohki<sup>1</sup>, Miyuki Uekawa<sup>1</sup>, Norio Tanahashi<sup>1</sup>, Norihiro Suzuki<sup>1</sup>

<sup>1</sup>*Department of Neurology, School of Medicine, Keio University, Tokyo, Japan*

<sup>2</sup>*Torokbalint, Hungary*

<sup>3</sup>*Laboratoire de Biologie et Physiologie Moléculaire du Vaisseau INSERM U 541, Paris,  
France*

Cerebral blood flow is autoregulated in a certain range of blood pressure (BP), but below the lower threshold, flow starts to decrease and cerebral metabolism and function become impaired. However, little is known about changes of cerebral blood flow outside the autoregulation range, e.g., in severe hypotension. The purpose of this communication is to examine intraparenchymal capillary blood flow during severe hypotension (BP = 40-50 mmHg) by employing a new high-speed (125-500 frames per sec) confocal fluorescence microscopy and image analysis system. Urethane-anesthetized Wistar rats (n=12) with a cranial window were given fluorescein isothiocyanate (FITC)-dextran (MW = 70 kDa) intravenously as a bolus to detect capillaries and obtain dye dilution curves, and FITC-labeled red blood cells (RBCs) to track RBCs in the capillaries. A video recording of a region of interest in the somatosensory area was taken at a speed of 250 frames per sec for 10 sec before and during hypotension induced by 8-10 ml exanguination and after reinfusion of the blood. The video clip was analyzed with KEIO-IS1 software for plasma flow and KEIO-IS2 (see Schiszler et al., Brain 05) to document tracking of all RBCs, which were individually numbered, and to calculate automatically individual RBC velocities. We found that capillary density was decreased during exanguination. i.e., some capillaries were collapsed and less dense, but increased just after reinfusion, and each capillary reached maximal dilation at 10 minutes after reinfusion. Consequently, the distribution of capillaries changed slightly during exanguination and reinfusion of the blood. The hypotension did not cause much change in plasma flow or RBC tracking. The control velocity of RBC in the capillaries was  $2.2 \pm 1.1$  mm/sec. Capillaries had different numbers of RBC passages per 10 sec, e.g., some had one RBC passage and others had up to three passages per 10 sec. The hypotension produced a decrease of RBC velocity which was maximum just after the end of blood exanguination (RBC velocity decreased to  $40 \pm 18$  % of the control), but recovered slightly to  $77 \pm 40$  % of the control at 10 minutes after blood loss. The RBC velocity showed an overshoot to  $134 \pm 90$  % just after the reinfusion of the blood, and the increase of RBC velocity persisted for 15 minutes thereafter ( $148 \pm 15$  %). It is concluded that decreases in capillary density and RBC perfusion aggravate the brain tissue damage due to severe hypotension, although plasma flow in the remaining capillaries is unchanged.



## CEREBRAL PERFUSION PRESSURE OR ARTERIAL PRESSURE ONLY: HOW TO ASSESS DYNAMIC CEREBRAL AUTOREGULATION MORE ACCURATELY ?

Piotr Smielewski, Phil Lewis, Marek Czosnyka, John D. Pickard

*Academic Neurosurgery, Addenbrooke's Hospital, Cambridge, UK*

Objective: Dynamic tests of cerebral autoregulation are becoming increasingly popular in clinical practice. The clinical usefulness of cerebral autoregulation is believed to depend on its close association with outcome; impaired autoregulation in the post-injury period implies a poorer outcome (1). Various methods based on time-domain or frequency-domain analysis of blood flow velocity fluctuation (measured non-invasively using Transcranial Doppler Ultrasonography), in response to spontaneous or provoked variations of arterial blood pressure (ABP) or cerebral perfusion pressure (CPP) have been described in the literature. The main advantage of such a methodology is that the test does not require any pharmacological alteration of ABP and the state of autoregulation can be monitored virtually continuously – as long as transcranial doppler probes may remain in place. Our objective was to investigate the clinical utility of two indices of dynamic autoregulation. One of them is based on changes in arterial pressure and the other, changes in cerebral perfusion pressure

Methods: One hundred and eighty anaesthetised and ventilated head injured patients with intracranial pressure, arterial pressure and MCA blood flow velocity recorded intermittently (for periods of 10 minutes up to two hours) were studied. Indices of dynamic autoregulation were calculated as a moving correlation coefficient of 60 samples (total time 3 minutes) of 6 second mean values of blood flow velocity and arterial pressure (Mxa) or blood flow velocity and cerebral perfusion pressure (Mx), recomputed every 3 seconds. Values of Mx and Mxa were averaged over multiple recordings in each patient and correlated with outcome at 6 months post injury. Results. Pearson's correlation coefficient between Mx and Mxa was significantly positive ( $R=0.85$ ;  $p<0.000001$ ). Mxa was significantly greater than Mx ( $0.22\pm 0.22$  versus  $0.062\pm 0.28$ ;  $p<0.000001$ ). The difference between Mx and Mxa significantly decreased with impaired autoregulation ( $R= -0.39$ ;  $p < 0.000001$ ) and with greater ICP ( $R= -.26$ ;  $p<0.0005$ ). Mx showed a significant correlation with outcome while the correlation between Mxa and outcome was much weaker and non-significant ( $R= 0.25$ ;  $p<0.0008$  versus  $R= 0.14$ ;  $p<0.07$  (NS)). Both indices correlated positively with ICP and negatively with CPP but this dependence was stronger for Mx than Mxa. Conclusion. Although both indices are relatively well correlated with each other, differences between them may be considerable. The observation that the differences between indices decrease when ICP increases, contradicts the opinion that CPP rather than ABP should be taken into account only in cases when ICP is already elevated. When ICP is recorded, CPP rather than ABP should always be used in calculations. After head injury, the index based on cerebral perfusion pressure correlates more strongly with outcome than the index using arterial pressure alone, and therefore is clinically far more useful. REFERENCE 1. Czosnyka M, Smielewski P, Piechnik S, Steiner LA, Pickard JD. Cerebral autoregulation following head injury. *J Neurosurg.* 2001 Nov;95(5):756-63

**EVALUATION OF CRITICAL HEMODYNAMIC STATUS INDUCED BY  
ACETAZOLAMIDE CHALLENGE IN PATIENTS WITH CEREBROVASCULAR  
DISEASE: ASSESSMENT OF REGIONAL PERFUSION PRESSURE**

**Hidehiko Okazawa<sup>1</sup>, Tatsuro Tsuchida<sup>2</sup>, Yoshikazu Arai<sup>3</sup>, Tetsuya Mori<sup>1</sup>,**

**Masato Kobayashi<sup>1</sup>, Fumiko Tanaka<sup>1</sup>, Yoshiharu Yonekura<sup>1</sup>**

<sup>1</sup>*Biomedical Imaging Research Center, <sup>2</sup>Department of Radiology, <sup>3</sup>Department of  
Neurosurgery, University of Fukui, Japan*

Introduction: Autoregulatory mechanism to keep cerebral blood flow (CBF) and perfusion pressure may be impaired in patients with cerebrovascular disease (CVD). To investigate the critical hemodynamic status in the impaired cerebral circulation, changes in regional CBF (rCBF) and arterial-to-capillary blood volume (V<sub>0</sub>) induced by acetazolamide (ACZ) were measured in CVD, as well as changes in hemodynamic parameter defined by rCBF/V<sub>0</sub> ratio, which is expected to be proportional to the regional perfusion pressure. Method: Thirty-nine patients (mean age = 64.5±9.3 y) with unilateral major cerebral arterial occlusive disease underwent O-15 water PET at baseline and 10 min after ACZ administration. The mean interval between an ischemic event and the PET examination was 5.7±7.4 months. Dynamic PET data were acquired to calculate rCBF, V<sub>0</sub> and rCBF/V<sub>0</sub> ratio using the 3-weighted integral method. The hemodynamic parameters in the territories of bilateral middle cerebral arteries were obtained and compared between the 2 hemispheres and 2 conditions. Results: Following ACZ administration, the group of patients who had a diminished rCBF response in the ipsilateral hemisphere (reduced vasodilatory capacity group = RVC; 22 patients) showed a significant V<sub>0</sub> increase in the same region. Thus, the rCBF/V<sub>0</sub> ratio decreased significantly after ACZ administration in the ipsilateral hemisphere of RVC. This ratio did not change in the contralateral hemisphere of this group nor in the other group with normal vasodilatory capacity (NVC; 17 patients), suggesting that its reduction represented severe hemodynamic impairment and dysfunction of autoregulation for regional perfusion pressure. The significant decrease in rCBF/V<sub>0</sub> ratio was associated with strokes in patients of RVC (Table). Eight patients in RVC (36%) and 15 in NVC (88%) had suffered strokes. Twelve patients in RVC (56%) had a history of TIA, whereas only one in NVC had suffered from TIA (5.9%). The incidence of past history of stroke and TIA was significantly different between the two groups (p<0.005, Chi-square test). Conclusion: The lack of rCBF increase after ACZ challenge does not necessarily reflect the exhaustion of vasodilatory capacity in patients with severely impaired cerebral circulation. Decrease in the rCBF/V<sub>0</sub> ratio after ACZ challenge is presumed to represent altered regional cerebral perfusion pressure reflecting a critical hemodynamic status in patients with CVD because post-ACZ reduction of this ratio was closely associated with hemodynamic deficiency in RVC. References: [1] Okazawa H, et al. J Nucl Med 2003;44:1875-1883. [2] Ohta S, et al. J Cereb Blood Flow Metab 1996;16:765-780.

Table: Comparing of rCBF/V<sub>0</sub> ratio (min<sup>-1</sup>) among different symptoms in RVC and all NVC

	RVC Ipsilateral		NVC Ipsilateral
	Stroke (n = 8)	TIA (n = 12)	(n = 17)
Baseline	25.7 ± 6.9	24.1 ± 5.0	20.9 ± 4.3
Post-ACZ	16.9 ± 4.9 <sup>†</sup>	21.5 ± 4.5	20.8 ± 4.7
% Change	-8.8 ± 5.2 <sup>†</sup>	-2.6 ± 2.3	-0.1 ± 2.7

<sup>†</sup>p < 0.05, <sup>††</sup>p < 0.01, comparing the 3 groups (one-way ANOVA and post-hoc Scheffe's F-test).

**'ECSTASY' AS A RISK FACTOR IN STROKE: A LABORATORY INVESTIGATION OF 3, 4-METHYLENEDIOXYMETHAMPHETAMINE-INDUCED CEREBROVASCULAR DYSFUNCTION**

Linda Ferrington<sup>1</sup>, Douglas E. McBean<sup>2</sup>, Henry J. Olverman<sup>1</sup>, **Paul A.T. Kelly<sup>1</sup>**

<sup>1</sup>*Division of Neuroscience, University of Edinburgh, Edinburgh, UK*

<sup>2</sup>*School of Health Sciences, Queen Margaret University College, Edinburgh, UK*

Background and Purpose: “Ecstasy” (3,4-methylenedioxyamphetamine; MDMA) is a popular recreational drug which is widely perceived to be “safe” by many users and some commentators. However, a growing body of clinical evidence suggests that MDMA use is a risk factor for cerebrovascular accident (CVA) in otherwise healthy young people (1), although the mechanism by which MDMA might effect these pathological changes remains to be fully elucidated. In order to identify the mechanism by which MDMA might induce cerebrovascular dysfunction, we have examined the cerebrovascular effects of a single acute exposure to MDMA in Dark Agouti (DA) rats. Methods: Conscious, lightly restrained adult DA rats were injected i.p. with either 15mg.kg<sup>-1</sup> MDMA or saline (both n=10). Local cerebral blood flow (LCBF) and glucose utilization (LCMRglu) were measured in equal numbers from each group, 25 and 15 minutes post-MDMA respectively, in 62 brain areas using [14C]- iodoantipyrine and [14C]-2-deoxyglucose quantitative autoradiography respectively. Mean arterial blood pressure (MABP) and rectal temperature were monitored throughout. Data (mean±s.e.m.) were analysed using appropriate t-tests (p<0.05). Results: MDMA produced significant increases in rectal temperature (37.7±0.2 to 39.5±0.2oC) and MABP (142±3 to 182±4 mmHg). MDMA produced significant increases in LCMRglu in 21 brain areas, most markedly in the motor system (globus pallidus; +82%; medial striatum; +71%). Conversely no significant increases in LCBF were measured. Significant decreases in LCBF were observed in 20 brain areas, most markedly in the limbic system (anterior thalamus; -34%; dorsal subiculum; -30%). Global analysis of all 62 areas revealed a close correlation (r=0.86) between LCMRglu and LCBF with an overall ratio of 1.46 in controls. Despite the divergence of LCMRglu (increases) and LCBF (decreases) in MDMA treated groups, there was a similar close correlation (r=0.82), however the overall ratio was decreased to 1.07. In the whole brain, LCBF was coupled to metabolism in both groups, but the equations defining the best-fitting straight line for the data-points demonstrate that the gradient was decreased in the MDMA group, indicating a downward re-setting of the flow-metabolism relationship. Taking the brain areas individually the ratio of flow to metabolism was found to decrease in all but two. Conclusions: This study indicates that acute MDMA exposure may radically alter the fundamental relationship between cerebral perfusion and metabolic demand. The local uncoupling of flow from underlying metabolism and the global re-setting of this relationship may result from the vasoconstrictor action of MDMA-induced acute 5-HT efflux, and the relative oligoemia produced might provide the mechanism for CVA in human users. Although this phenomenon may be more limited in the human brain, deficits in brain function that parallel the cognitive decline seen in multi-infarct dementia have been found in persistent MDMA users and with the scale of current 'Ecstasy' usage this has the potential to develop into a healthcare problem in the future. McEvoy AE et al (2000) *BMJ* 320; 1322–1324. This study was funded by EC Grant No. QLG3-CT-2002-00809.

## NOS INHIBITOR ATTENUATES VASODILATATION BY TRIGEMINAL STIMULATION

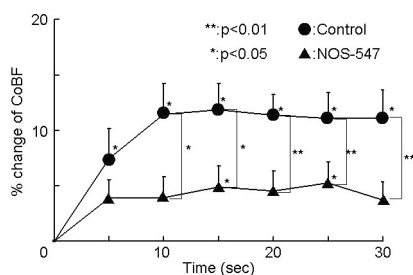
Michinari Fukuda<sup>1</sup>, Shinya Tsukahara<sup>1</sup>, Kenzo Koizumi<sup>1</sup>, Shigeyoshi Maruyama<sup>2</sup>,  
Norihiro Suzuki<sup>3</sup>, Fumihiko Sakai<sup>1</sup>

<sup>1</sup>Department of Neurology, Kitasato University, Sagamihara, Japan

<sup>2</sup>Department of Laboratory Animal Science, Kitasato University, Sagamihara, Japan

<sup>3</sup>Department of Neurology, Keio University, Tokyo, Japan

**Introduction:** The mechanism of the blood flow increase by trigeminal activation is an important issue in terms of the pathophysiology of migraine and ‘vascular headache’. We have previously demonstrated that 5-HT<sub>1B/1D</sub> receptor agonist and CGRP receptor antagonist abolished the blood flow increase elicited by trigeminal activation (1, 2) and that NK<sub>1</sub> receptor antagonist and leukotriene receptor antagonist failed to attenuate this flow increase. Yet, the precise neurotransmitter-receptor mechanism of the trigeminal neurogenic vasodilatation is unclear. It has been proposed that nitric oxide (NO) may be the causative molecule of ‘vascular headache’. The purpose of this study is to investigate the role of NO in the trigeminal neurogenic vasodilatation utilizing selective nNO-synthase inhibitor. **Methods:** Seven male Sprague-Dawley rats, weighing 350-400 gram, were anesthetized with  $\alpha$ -chloralose and urethane, and ventilated mechanically with room air. Parietal cortical blood flow (CoBF) on the right side was continuously monitored with the Laser-Doppler flow meter system. The nasociliary nerve (NCN) - a cerebrovascular branch of the trigeminal nerve in the rat - was carefully approached from the orbit in the right side. The post-ganglionic nerves from the pterygopalatine ganglion were gently eliminated from the ethmoidal foramen (EF). NCN was stimulated electrically near its entrance to EF through a bipolar platinum electrode with an electrical stimulator (5-25  $\mu$ A, 0.5 ms duration, 10 Hz, 30 sec stimulation). CoBF were measured during and after electrical stimulation of NCN under intravenous injection of 1.0 ml saline followed by nNO-synthase inhibitor, NOS-547 (100  $\mu$ g/kg in 1.0 ml saline). The flow data were analyzed by one-way ANOVA followed by Bonferroni/ Dunn adjustment for multiple comparisons and repeated measures ANOVA. **Results:** No significant change in physiological parameters was observed during and after electrical stimulation. CoBF was significantly increased upon electrical NCN stimulation at 20 sec, 25 sec, 30 sec from the initiation of stimulation by 11.3 $\pm$ 1.9 %, 11.1 $\pm$ 2.4 %, 11.1 $\pm$ 2.5 %, respectively in control state. This increase was significantly suppressed after NOS-547 administration to 4.5 $\pm$ 1.8 %, 5.3 $\pm$ 1.9 %, 3.7 $\pm$ 1.7 % at 20 sec, 25 sec, 30 sec, respectively. The amount of blood flow increase when NOS-547 was given was significantly less than the control data. **Conclusion:** NO-synthase inhibitor attenuated the blood flow increase upon trigeminal nerve stimulation. NO is one of the most important neurotransmitter molecule in the trigeminal neurogenic vasodilatation. **References:** [1] Suzuki N, Fukuda M, Dobashi K, Maruyama S, Kitamura A, Sakai F; J Cereb Blood Flow Metab 21: S249 (2001) [2] Fukuda M, Suzuki N, Tsukahara S, Maruyama S, Sakai F; J Cereb Blood Flow Metab 23: S18 (2003)

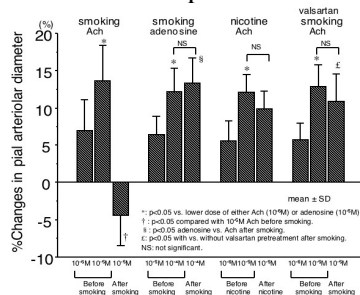


## ANGIOTENSIN II TYPE 1 (AT1)-RECEPTOR BLOCKER PREVENTS IMPAIRMENT OF ENDOTHELIUM-DEPENDENT CEREBRAL VASODILATION BY ACUTE CIGARETTE SMOKING IN RATS

Mami Iida<sup>1,3</sup>, Hiroki Iida<sup>2</sup>, Motoyasu Takenaka<sup>2</sup>, Hisayoshi Fujiwara<sup>1</sup>, Shuji Dohi<sup>2</sup>

<sup>1</sup>2nd Dept. of Internal Medicine (Cardiology), <sup>2</sup>Dept. of Anesthesiology & Pain Medicine, Gifu University Graduate School of Medicine, <sup>3</sup>Dept. of Health & Nutrition, Faculty of Home Economics, Gifu Women's University, Gifu, Japan

[Background and purpose] A number of previous studies have shown that both cigarette smoking and smoke extract impair the nitric oxide synthase (NOS)-dependent reactivity of peripheral blood vessels, but not clearly shown in cerebral vessels. It is possible that antagonizing the action of angiotensin II might limit or prevent the endothelial dysfunction induced by free radicals that is associated with cigarette smoking. Our aim is to test whether the response of cerebral arterioles to acetylcholine (Ach; endothelium-dependent vasodilation) is altered (a) after brief inhalation of cigarette smoke or (b) by administration of nicotine itself. In addition, we investigated the effects of an angiotensin II type 1 (AT1)-receptor blocker (valsartan) on the impairment of endothelium-dependent vasodilation in cerebral arterioles induced by acute cigarette smoking. [Materials and methods] In pentobarbital-anesthetized, mechanically ventilated Sprague-Dawley rats (350g ~ 400g), we used a closed cranial window preparation to measure changes in pial vessel diameters. We initially examined the response of arterioles to an endothelium-dependent vasodilator [Ach (10-6M and 10-5M)] and also to an endothelium-independent vasodilator [adenosine (10-5M and 10-4M)] before smoking (n=6, each). Then, 1 hour after smoking had been performed we again examined the responses of arterioles to the larger doses of Ach and adenosine. In experiment 2, we examined the effects of acute infusion of nicotine on the reactivity of cerebral arterioles to Ach (n=6). Then, in experiment 3, after intravenous valsartan pretreatment we reexamined the pial vasodilator response to topical Ach (before and after cigarette smoking; n=6). [Results] Under control conditions, cerebral arterioles were dilated by 6.9±4.2% and 13.6±4.8% by topical Ach (10-6M and 10-5M, respectively) and by 6.4±2.5% and 12.2±3.1% by topical adenosine (10-5M and 10-4M, respectively). One hour after a 1-min inhalation of mainstream smoke (1mg-nicotine cigarette), 10-5M Ach constricted cerebral arterioles (-4.4±4.1%), while 10-4M adenosine dilated them by 13.4±3.4%. One hour after a 1-min nicotine infusion (0.05mg), 10-5M Ach dilated cerebral arterioles by 9.9±2.4%. Thus, vasodilator response to topical Ach was impaired after smoking, whereas that to adenosine was unaffected. However, the vasodilator response to Ach was unaffected by intravenous nicotine. Valsartan pretreatment did not change the responses to topical Ach application obtained before smoking. One hour after a 1-min inhalation of mainstream smoke, 10-5M Ach dilated cerebral pial arteries by 10.9 ± 3.7% in the valsartan pretreatment group, a response that was significantly different from that obtained without valsartan pretreatment. Thus, valsartan completely prevented the smoking-induced impairment of Ach-induced vasodilation. [Conclusion] Acute single-cigarette smoking causes a dysfunction of endothelium-dependent, but not endothelium-independent, vasodilation of rat cerebral vessels *in vivo*, and the effect was not mimicked by intravenous nicotine. AT1-receptor blockade prevented the above smoking-induced impairment of endothelium-dependent vasodilation.





## CEREBRAL VASCULAR MITOCHONDRIAL EFFICIENCY IS INCREASED BY ESTROGEN TREATMENT

Chris Stirone<sup>1</sup>, Diana N. Krause<sup>1</sup>, Vincent Procaccio<sup>2</sup>, **Sue P. Duckles**<sup>1</sup>

<sup>1</sup>*Department of Pharmacology, School of Medicine, University of California, Irvine, CA, USA*

<sup>2</sup>*Center for Molecular and Mitochondrial Medicine and Genetics, School of Medicine, University of California, Irvine, CA, USA*

We have previously demonstrated that estrogen, either endogenous or exogenous, increases the production of endothelial vasodilators in the cerebral vasculature. Since mitochondria are thought to play a vital role in vascular dysfunction we have investigated the impact of estrogen treatment on cerebral vascular mitochondrial electron transport and formation and metabolism of reactive oxygen species. We now show that treatment in vivo with 17beta-estradiol also modulates cerebral vascular mitochondrial function and protein expression. Mitochondria were isolated from cerebral blood vessels obtained from ovariectomized female rats, with and without estrogen replacement for three weeks. Plasma levels achieved by estrogen replacement mimicked those seen in intact, cycling females. Estrogen receptor, ER-alpha, but not ER-beta, was detected in mitochondrial fractions, and ER-alpha protein was increased following estrogen treatment. Levels of mitochondrial cytochrome c, manganese superoxide dismutase, and subunits I and IV of complex IV also were increased in vessels from estrogen-treated rats. These findings correlated with functional increases in mitochondrial citrate synthase and complex IV activities in vessels from estrogen-treated animals. In contrast, hydrogen peroxide production, measured using succinate in vitro, was decreased in mitochondria from vessels of estrogen-treated animals. Surprisingly, PGC-1alpha expression was significantly decreased, and NRF-1 protein levels were unchanged following estrogen exposure, suggesting that estrogen acts independently of these previously defined modulators. Together, these novel findings suggest that vascular protection by estrogen is mediated, in part, by modulation of mitochondrial function resulting in greater energy producing capacity, more efficient coupling of electron transport, and decreased reactive oxygen species production.

## AGE INCREASES OVERALL COMPLEXITY OF HUMAN SPONTANEOUS CBV FLUCTUATIONS

Andras Eke, Peter Herman, Marton Hajnal

*Institute of Human Physiology and Clinical Experimental Research, Faculty of Medicine,  
Semmelweis University, Budapest, Hungary*

**Background and Purpose:** Complexity of spontaneous CBV fluctuations - earlier demonstrated by us in young adults<sup>1</sup> — can emerge from random, fractal<sup>2</sup> or chaotic processes<sup>3</sup>. Our aims were to define the contribution of these patterns to the observed complexity and to evaluate the effect of age and gender on it. **Methods:** Total hemoglobin content as the measure of CBV was monitored by near infrared spectroscopy (NIRS) on volunteers (male n=19, age=20-78 years; female n=23, age=21-79 years). Random and fractal pattern was distinguished by the spectral index ( $\beta$ )<sup>2</sup>. Chaos was identified by the surrogate analysis of correlation dimension and largest Lyapunov exponent<sup>4</sup>. **Results:** In spontaneous CBV fluctuations both fast random and slow fractal dynamics are present as demonstrated in the power spectral density of the CBV fluctuations (Fig. 1), where they are separated by a cutoff frequency,  $f^*$ . Below  $f^*$  the pattern is fractal (self-similar), in that power rises inversely with frequency as  $1/f^*$ . Above  $f^*$  the pattern is of white noise with <sup>high</sup> $\beta$  around 0.  $f^*$  decreases with age in both genders. Neither in pre- nor in postmenopause age groups (group 1 and 2, respectively) shows <sup>low</sup> $\beta$ , the slope across the power estimates at the low frequencies, gender difference (female<sub>group1</sub>:1.23±0.25 vs. male<sub>group1</sub>:1.14±0.22, p=0.329, female<sub>group2</sub>:1.39±0.26 vs. male<sub>group2</sub>:1.17±0.20, p=0.089, respectively). The range of fluctuation amplitudes produced by the slow fractal dynamics is always larger than that of the fast random fluctuations, which difference significantly (p=0.013) decreases with age in women, only. Surrogate analysis demonstrated that CBV dynamics cannot be characterized on grounds of deterministic chaos. **Conclusions:** Fractals are an ordered form of complexity due to their special autocorrelation structure. The complexity of random (white) noise is maximal in that it is without any correlation structure or order. Age affects the balance between the orderly and disorderly forms of CBV complexity rendering the overall pattern more complex.

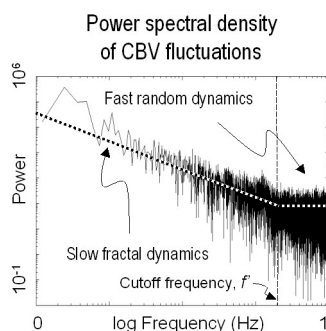
(This study was supported by OTKA Grant T34122.)

<sup>1</sup>Eke, A. and P. Hermán, *Adv Exp Med Biol* 471: 49-55, 1999.

<sup>2</sup>Eke *et al.*, *Pflügers Arch — Eur J Physiol* 439: 403—415, 2000.

<sup>3</sup>Griffith, T. M., *Cardiovasc Res*, 31:342-358, 1996.

<sup>4</sup>Bassingthwaighe, J. B. *et al.*, *Fractal Physiology*. Oxford University Press, 1994.



**ESSENTIAL CEREBRAL DISTRIBUTION OF CARDIAC OUTPUT IN INFANTS****Takashi Kusaka<sup>1</sup>, Kenichi Isobe<sup>2</sup>, Kensuke Okubo<sup>2</sup>, Keiko Nagano<sup>2</sup>, Susumu Itoh<sup>2</sup>**<sup>1</sup>*Maternal and Perinatal Center, Faculty of Medicine, Kagawa University, Kitagun, Japan*<sup>2</sup>*Department of Pediatrics, Faculty of Medicine, Kagawa University, Kitagun, Japan*

Introduction: The major regulatory mechanisms for CBF in infants are autoregulation, arteriolar CO<sub>2</sub>, oxygen delivery, blood glucose and neural activity. Furthermore, the cardiovascular system regulates CBF through variation in cardiac output (CO) and distribution of blood flow. In this study, the usefulness of multi-channel near-infrared spectroscopy (MNIRS) and pulse dye densitometry with indocyanine green (ICG) for determining CBF and left ventricle CO in infants was investigated. Subjects and methods: We measured CBF and CO in 17 infants (mean gestational age  $\pm$  SD:  $32.9 \pm 4.3$  weeks) without neural abnormalities on day 0 to day 82 after birth. A bolus of ICG (0.2 mg/kg) was injected into the peripheral vein of each infant. Changes in the cerebral ICG concentration in a 6 cm X 6 cm field of the parieto-temporal region were recorded using MNIRS. Simultaneously, pulse dye densitometry, using the general principles of pulse oximetry, was used to measure the arterial blood concentration of ICG. The CBF was calculated using Fick's equation. CO was calculated from the first dilution curve on a dye densitogram. Results and Discussion: CO and CBF in the parieto-temporal region were  $202.8 \pm 90.6$  mL/kg/min (mean  $\pm$  SD) and  $15.3 \pm 4.2$  mL/100 g/min, respectively. The relationship between CO and CBF was  $CBF = 0.03 CO + 8.71$  ( $r = 0.70$ ,  $p = 0.002$ ). The blood flow distribution to the brain of left ventricular CO is estimated to be 11% if the brain weight is assumed to be 15% of body weight. When CO was high (300 mL/kg/min) the CBF was 20.1 mL/100 g /min, which calculated to 7.8% of CO. When CO fell to  $\sim$ 100 mL/kg/min, CBF also fell (to 12.0 mL/100 g /min), the percentage of CBF to CO was calculated to 21.2%. The brain is considered an essential organ defined as one whose blood supply is preferentially maintained during periods of reduced CO. We conclude that control of CO important for regulation of CBF during the acute phase of illness in infants. Acknowledgement: We thank Professor William Meadow (The University of Chicago) for his critical comments regarding our studies. Refereces: Kusaka T, Isobe K, Nagano K, et al.; Neuroimage 13: 944-952 (2001) Kusaka T, Okubo K, Nagano K et al.; Arch Dis Child Fetal Neonatal Ed. 90: F77-78 (2005) Nagano K, Kusaka T, Okubo K, et al.; Paediatric Anaesthesia: (in press) Meadow WL, Rudinsky BF, Bell A, et al.; Pediatr Res 35:649-656. (1994)

**CEREBRAL HAEMODYNAMICS ASSESSED BY TRANSCRANIAL DOPPLER  
ULTRASONOGRAPHY DURING ORTHOTOPIC LIVER TRANSPLANT. A  
PRELIMINARY REPORT**

**Eric A. Schmidt<sup>1,3</sup>, Marek Czosnyka<sup>1</sup>, David Tew<sup>2</sup>, John R. Klink<sup>2</sup>, Marcella Balestreri<sup>1,2</sup>,  
John D. Pickard<sup>1</sup>, Basil F. Matta<sup>2</sup>**

<sup>1</sup>*Department of Neurosurgery, Addenbrooke's Hospital, Cambridge, UK*

<sup>2</sup>*Department of Anaesthesiology, Addenbrooke's Hospital, Cambridge, UK*

<sup>3</sup>*Federation de Neurochirurgie, Hôpital Purpan, Toulouse, France*

Background: Autoregulation is known to be altered in patients with acute liver failure [1,2]. Transcranial Doppler is considered as an appropriate technique to gauge cerebral haemodynamics during hepatic failure and liver transplantation [3,4]. We aimed at assessing dynamic autoregulation [5] and non invasive cerebral perfusion pressure estimation (nCPP) [6] during an orthotopic liver transplantation (OLT). Methods: OLT was performed in 10 patients suffering from chronic liver disease. General anesthesia was performed according to a standardized technique. During the surgery, as a routine clinical procedure, arterial blood pressure (ABP) was invasively measured and cerebral blood flow velocity was assessed using transcranial Doppler (TCD Intraview Rimed™) in the middle cerebral artery. Analog signal was digitized, and stored in a computer using a dedicated in-house software. Off line, the correlation coefficient between ABP and FV, termed mean Mxa, was calculated [5]. Mxa close to +1 denotes that slow fluctuations in ABP produce synchronized slow changes in FV indicating defective autoregulation. In anesthetized patients, Mxa<0.4 indicates a preserved autoregulation [7]. nCPP was also calculated as followed: nCPP=(ABPm\*FVd/FVm)+14 [6]. During every surgery, we defined three time periods: the dissection phase ie from surgical start till portal vein has been clamped, the anhepatic phase when the portal vein is clamped and at least the reperfusion phase when the portal vein is released until the completion of the surgery. All haemodynamic indices were calculated for each time period and averaged. Results: ABP was relatively stable during the surgery. nCPP followed passively the changes in ABP. Autoregulation significantly weakens in the course of the surgery, and deteriorates significantly whilst anhepatic (p<0.01) the reperfusion phase (p<0.001). Blood flow velocity increased significantly during reperfusion phase (p<0.05). Conclusion: We have been able to gauge non invasively cerebral haemodynamics during OLT. Our results indicate an alteration of dynamic autoregulation during the liver transplantation, and autoregulation deteriorates pari passu. During the reperfusion phase, autoregulation is severely deranged, indicating cerebral vasodilation. During liver transplant, nCPP looks maintained within a rather normal range, but further investigations are mandatory to assess the validity of this method during liver dysfunction. References: 1 Larsen et al Hepatology 1995;22:730-736 2 Pott et al Clinical physiology 1995;15:119-30 3 Sidi et al Anesth analg 1995;80:194-200 4 Dobljar et al J Clin Anesth 1993;5:479-85 5 Czosnyka et al Stroke 1996;27(10)1829-34 6 Czosnyka et al J Neurosurg 1998;71:673-80 7 Lang EW et a IJ Neurol Neurosurg Psychiatry 2002;72(5):583-586

	Dissect on (n=10)	Anhepatic (n=10)	Reperfusion (n=9)
ABP (mmHg)	78.4±9.7	72.4±7.3	66.9±9.3
nCPP (mmHg)	59.4±12.1	60.1±10.4	53.5±10.1
FV (cm/s)	43.2±16.9	46.1±14.4	56.6±25.4*
Mxa	0.39±0.18	0.49±0.17**	0.63±0.16*

**CEREBRAL AUTOREGULATION IN ACUTE AND CHRONIC HYPOXIA****Robert Roach**, Julia Dober, Paige Sheen, Vaughn Browne, Andrew Subudhi*CCAMP, Division of Emergency Medicine, Departments of Surgery & Anesthesiology,  
UCHSC, Aurora, CO, USA*

Impaired cerebral autoregulation (CA) in hypoxia may allow harmful perturbations in arterial blood pressure to damage the blood-brain barrier leading to vasogenic cerebral edema. We studied the dynamic CA response in acute hypoxia during spontaneous breathing and after thigh cuff deflation in volunteers breathing room air (NX) or hypoxia (12% O<sub>2</sub>, HX, barometric pressure ~622 Torr). Methods: In random order, 14 volunteers repeated the cuff deflation protocol 6 times, 3 each while NX or HX. Resting supine data were collected for 6 mins prior to second trial with NX and HX for spectral analysis. Mean ABP (MABP) and transcranial Doppler for CBF velocity (CBFv) were recorded. Dynamic CA was assessed during spontaneous breathing by cross-spectrum analysis of beat-to-beat changes in ABP and CBFv, and from the cuff deflation protocol by calculation of the rate of regulation (ROR). Results. HX caused a 17% drop in arterial SaO<sub>2</sub>% ( $p < 0.001$ ) and 12% drop in PETCO<sub>2</sub> ( $p < 0.001$ ), and a 10% rise in CBFv ( $61.8 \pm 2.9$  vs  $68.1 \pm 3.2$ , NX vs. HX,  $p < 0.01$ , all values mean  $\pm$  SEM). Resting MABP was similar (NS,  $92.0 \pm 2.9$  vs  $92.9 \pm 2.9$  (NX vs. HX). Cross spectrum analyses of MABP and CBFv at very low frequencies (0.02-0.07 Hz) revealed that MABP (mmHg<sup>2</sup>/Hz) rose from NX to HX ( $3.75 \pm 1.05$  to  $6.76 \pm 1.79$ , NX vs. HX,  $p < 0.05$ ), and CBFv (cm<sup>2</sup>/s<sup>2</sup>/Hz) was elevated from NX to HX ( $5.94 \pm 2.06$  vs.  $12.83 \pm 3.44$ , vs. HX,  $p < 0.05$ ). After cuff deflation, MABP dropped  $14.7 \pm 3.4$  mmHg in NX and  $14.9 \pm 3.1$  mmHg in HX (NS). ROR fell 18.6% from NX to HX ( $0.7 \pm 0.04$  vs  $0.5 \pm 0.06$ ,  $p < 0.03$ ). Conclusions: Acute exposure to poikilocapnic hypoxia leads to increased ABP and CBFv oscillations, and impairs dynamic CA assessed by two independent methods in young, healthy human volunteers. Further research is necessary to determine the role of impaired CA in chronic hypoxia, and its relationship to altitude illness. Supported, in part, by NIH-HL-070362.

**DELIVERY OF A DELTAPKC INHIBITOR PEPTIDE IMPROVES STROKE SURVIVAL IN A RAT MODEL OF HYPERTENSION, AND INCREASES CEREBRAL BLOOD FLOW FOLLOWING TRANSIENT FOCAL ISCHEMIA IN NORMOTENSIVE RATS**

**Rachel Bright**<sup>1</sup>, Koichi Inagaki<sup>1</sup>, Midori A. Yenari<sup>3</sup>, Gary K. Steinberg<sup>2</sup>,  
Daria Mochly-Rosen<sup>1</sup>

<sup>1</sup>*Department of Molecular Pharmacology, Stanford University School of Medicine, Stanford, CA, USA*

<sup>2</sup>*Department of Neurosurgery, Stanford University School of Medicine, Stanford, CA, USA*

<sup>3</sup>*Department of Neurology, University of California, San Francisco, and San Francisco VA Medical Center, San Francisco, CA, USA*

**Introduction:** Chronic arterial hypertension shifts the autoregulation curve of cerebral blood flow (CBF), increasing the risk of cerebrovascular events such as ischemic and hemorrhagic stroke. These acute events also cause fluctuations in CBF, contributing to ischemic/reperfusion damage. Therefore maintaining adequate flow is a priority for reducing damage from compromised cerebrovascular function. Recent work has demonstrated a role for protein kinase C (PKC) isozymes in mediating arterial tone. Additionally, we have previously shown that delivery of a deltaPKC-specific inhibitor peptide, deltaV1-1-TAT47-57 (deltaV1-1-TAT), reduces cerebral damage when delivered following stroke. We therefore sought to determine whether chronic delivery of deltaV1-1-TAT improves survival from stroke in a chronic hypertensive rat model, and whether protection in this model may be due to deltaPKC-mediated effects on CBF, both in hypertensive animals, and in a transient focal ischemia model. **Methods:** Dahl salt-sensitive rats were fed 8% salt diet from 6 weeks old to induce systemic hypertension. Rats were treated continuously with deltaV1-1-TAT (n=16), TAT (n=21) or saline (n=22) between 11 and 15 weeks of age using a subcutaneously implanted osmotic pump (5µL/hr, 1mM). There was no change in average blood pressure by peptide treatment. Animals were monitored for signs of stroke, and cerebral infarctions were confirmed at death by histological examination. To examine the role of deltaPKC in modulating cerebrovascular activity, we determined the effect of acute treatment with deltaV1-1-TAT peptide on CBF in a normotensive rat model of transient focal ischemia, and in a chronic hypertension model. **Acute stroke model;** normotensive, male Sprague-Dawley rats underwent 2hr MCA suture occlusion. Following ischemia CBF was monitored (n=9). **Hypertensive rat model;** CBF was measured at age 9 weeks, 3 weeks following salt diet onset (n=10). In both models, a burr hole was drilled 1mm posterior and 6mm lateral to bregma (corresponding to ischemic territory in the MCAo model). CBF was measured using laser Doppler. Following a baseline period of 20-30 minutes following reperfusion onset, TAT control peptide or deltaV1-1-TAT peptide was injected by intraperitoneal bolus (0.2 mg/kg), and CBF was monitored for an additional 20-30 minutes. **Results:** Chronic treatment with deltaV1-1-TAT improved survival rate from stroke in the hypertensive rat model; 12.5% of deltaV1-1-treated rats, 38.1% of TAT-treated rats and 40.9% of saline-treated rats died from stroke by 15 weeks old (P<0.05 deltaV1-1-TAT vs. TAT or saline). We found that delivery of deltaV1-1-TAT increased CBF following transient ischemia by 18+/-8% (P<0.05), but did not alter flow in sham-treated non-ischemic animals. In hypertensive rats, however, CBF responses were variable following delivery of deltaV1-1-TAT peptide; 50% of animals showed an increase in flow (of these, CBF increased by 24+/-4%). The source of this variation is currently under investigation. **Conclusion:** Chronic treatment with deltaV1-1-TAT improves stroke survival in a rat model of chronic hypertension. This may be due to a reduction in ischemic injury related to increased blood flow. In addition, an increase in CBF was observed following delivery of deltaPKC inhibitor in a stroke model in normotensive rats, suggesting that deltaPKC is involved in improving cerebral blood flow following stroke.

**CIRCADIAN PERIODICITY IN CEREBRAL BLOOD FLOW: STUDIES IN  
NORMOTENSIVE AND TRANSGENIC HYPERTENSIVE RATS**Constantin A. Wauschkuhn<sup>1</sup>, Klaus Witte<sup>2</sup>, Stefan Gorbey<sup>2</sup>, Björn Lemmer<sup>2</sup>,**Lothar Schilling<sup>1</sup>**<sup>1</sup>*Division of Neurosurgical Research, Department of Neurosurgery, University Hospital  
Mannheim, University of Heidelberg, Heidelberg, Germany*<sup>2</sup>*Department of Pharmacology and Toxicology, Faculty of Clinical Medicine Mannheim,  
University of Heidelberg, Heidelberg, Germany*

Cardiovascular parameters such as arterial blood pressure (ABP) and heart rate display pronounced circadian variation. In addition, evidence has been presented in favor of diurnal changes of perfusion in the heart, skin, kidney, and skeletal muscle. The present study was performed to detect whether there is a circadian periodicity in the regulation of cerebral perfusion. Normotensive Sprague Dawley rats (SDR, appr. 15 weeks old) and hypertensive (mREN2)27 transgenic rats (TGR, approximately 12 weeks old) were equipped in the abdominal aorta with a blood pressure sensor coupled to a telemetry system for continuous recording of systolic and diastolic ABP, heart rate, and locomotor activity. Five to twelve days later, a laser-Doppler flowmetry (LDF) probe was attached to the skull by means of a guiding device to measure changes of cerebral blood flow (CBF). After recovery from anesthesia, continuous measurements were taken for 3 - 5 days. The time series were analyzed with respect to the MESOR (midline estimating statistic of rhythm, i.e. the mean value of a given period), amplitude, and acrophase (i.e. the phase angle corresponding to the peak of a given period) of the 24h period and subharmonics including 12h, 8h, 4.8h and 4h period length. All data are given as mean±SD with the time indicated in 24 hour format. The circadian rhythm was the most prominent one for each parameter throughout the experiments. In SDR the acrophases of systolic and diastolic ABP were at 04:12 h ± 42 min and 02:24 h ± 42 min, respectively. In the TGR the ABP signal showed its typical inverse pattern with the maximum of the ABP occurring during light on (acrophase of systolic ABP, 09:48 h ± 108 min; acrophase of diastolic ABP, 09:54 h ± 144 min), i.e. during the resting phase of the animals. The peak of the circadian periodicity in the LDF signal occurred around midnight in both, SDR (23:54 h ± 114 min) and TGR (00:48 h ± 78 min), i.e. during the subjective activity phase of the animals. The acrophase position of the LDF signal was consistently prior to that of the locomotor activity (SDR, 01:42 h ± 18 min; TGR, 1:18 h ± 66 min). The present data suggest the presence of a circadian periodicity in the regulation of cerebral perfusion. The generator of this periodicity is not yet known. The circadian rhythm in the LDF signal is independent from that of the ABP since it did not follow the inverse periodicity in TGR. It is probably also independent from locomotor activity since its peak occurred consistently prior to that of the locomotor activity. The presence of a circadian periodicity in the CBF may have implications for the occurrence of diurnal alterations of cerebrovascular events with a morning peak observed in humans.

## FRACTAL PROPERTIES OF NEUROPHYSIOLOGIC SIGNALS IN RAT SOMATOSENSORY CORTEX

Peter Herman<sup>1,2</sup>, Shaun A. Wahab<sup>2,3</sup>, Andras Eke<sup>1</sup>, Fahmeed Hyder<sup>2,4</sup>

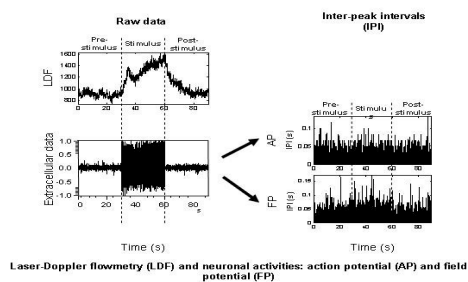
<sup>1</sup>*Institute of Human Physiology and Clinical Experimental Research, Semmelweis University, Budapest, Hungary*

<sup>2</sup>*Diagnostic Radiology, Yale University, New Haven, CT, USA*

<sup>3</sup>*Physiology, Michigan State University, East Lansing, MI, USA*

<sup>4</sup>*Biomedical Engineering, Yale University, New Haven, CT, USA*

While it is generally accepted that alternations in neuronal activity influence changes in CBF [1,2], the common analytical approaches usually neglect the small time-dependent variations in the neurophysiological signals and treat them as noise. It remains to be verified whether or not the measured fluctuations or variations (i.e., inhomogeneities) in neuronal activity can affect noise-like fluctuations in CBF. The inhomogeneities in the neuronal and vascular signals can emerge from independent events, but the possibility of non-linear correlations cannot be excluded. To identify these possibilities in the neuronal and vascular fluctuations, scaled windowed variance (SWV) method [3] was applied to characterize variations of neurophysiological signals measured from layer 4 of rat somatosensory cortex [4]. Artificially ventilated rats (male, Sprague-Dawley, n=15) were anesthetized with  $\alpha$ -chloralose (40 mg/kg/hour). Dynamic changes in CBF and electrical activity were measured by laser Doppler flowmetry (LDF) and extracellular Tungsten microelectrodes, respectively, during rest and forepaw stimulation (0.3ms, 2mA, 3Hz, 30s). The extracellular signals were filtered appropriately to be separated into field and action potentials (FP, AP) and were represented by inter-peak intervals for SWV analysis (see figure). The perfusion data were analyzed by amplitude variations [4]. We hypothesized that fluctuations in these multi-modal signals could be either random or time-scale invariant (i.e., fractal). The fractal nature of the signal, obtained from SWV analysis [4], was characterized by the Hurst coefficient (H). The CBF signals were fractal and anti-persistent (i.e., the step-by-step changes in the signal were anti-correlated with  $H < 0.5$ ) for all conditions ( $0.39 \pm 0.18$ ,  $0.40 \pm 0.17$ ,  $0.39 \pm 0.18$ , respectively). The AP signals proved to be fractal as well but with a positive correlation ( $H > 0.5$ ) for all conditions ( $0.71 \pm 0.13$ ,  $0.61 \pm 0.1$ ,  $0.71 \pm 0.13$ , respectively). In contrast the FP signals proved to be random ( $H = 0.5$ ) during pre- and post-stimulus conditions ( $0.51 \pm 0.06$ ,  $0.52 \pm 0.07$ , respectively) and during stimulation the signals became anti-correlated ( $H = 0.41 \pm 0.11$ ). In summary, during sensory stimulation the fractal properties were partly modified for the electrical signals but not in the blood flow response. The CBF and AP signals appeared more consistent in their deterministic behavior and may be important for physiological modeling [1,2]. These results demonstrate that the apparently random fluctuations in local CBF are related to the neuronal signals, and FP and AP are in fact realizations of complex processes of specific correlation structure [5] that are influenced by sensory-induced functional activity of the brain. Supported by NIH (DC-003710, MH-067528), NSF (DBI-0095173), and OTKA (T34122) grants. [1] Smith AJ et al (2002) PNAS-USA 99:10765-10770 [2] Lauritzen M (2001) J Cereb Blood Flow Metab 21:1367-1383 [3] Cannon MJ et al (1997) Physica A 241:606-16. [4] Eke A et al (2000) Pflügers Arch - Eur J Physiol 439:403-415 [5] Eke A et al (2002) Physiol Meas 23:R1-R38.





## INTERACTIONS BETWEEN THE HEME OXYGENASE, CYCLOOXYGENASE AND NITRIC OXIDE SYNTHASE PATHWAYS IN THE REGULATION OF THE RESTING HYPOTHALAMIC BLOOD FLOW

Béla Horváth<sup>1</sup>, László Hortobágyi<sup>1</sup>, Péter Sándor<sup>1</sup>, **Zoltán Benyó**<sup>2</sup>

<sup>1</sup>*Institute of Human Physiology and Clinical Experimental Research, Semmelweis University, Budapest, Hungary*

<sup>2</sup>*Institute of Pharmacology, Ruprecht-Karls-University, Heidelberg, Germany*

The heme-oxygenase (HO) – carbon monoxide (CO) pathway has been reported to evoke direct vascular effects and to influence other vasoregulatory mechanisms like the cyclooxygenase (COX) and nitric oxide synthase (NOS) systems. Since the hypothalamus expresses relatively high HO, COX and NOS levels compared to other brain regions, we have hypothesized interactions among these pathways in the regulation of the resting local hypothalamic tissue blood flow (HBF). Therefore, we have investigated whether inhibition of the COX and NOS pathways influences the alterations of the HBF that develop after HO blockade. Adult male Wistar rats were anaesthetized with 1.3 g/kg urethane. The femoral arteries were cannulated for measurement of the mean arterial pressure (MAP) and for blood sampling. HBF was measured by use of the hydrogen gas-clearance method. HO-blockade was induced by ip. injection of 45  $\mu\text{mol/kg}$  zinc deuteroporphyrin 2,4-bis glycol (ZnDPBG). In the first group of the animals HBF, MAP and blood gas measurements were performed under physiological conditions. In the second and third experimental groups the animals received diclofenac (10 mg/kg iv.) or NG-nitro-L-arginine methyl ester (L-NAME, 50 mg/kg iv.) pretreatment in order to inhibit prostanoid- or NO-synthesis, respectively. In the fourth group the animals received combined diclofenac and L-NAME pretreatment. In all groups HBF values were determined before and after the pretreatment as well as after the induction of HO-blockade. Baseline arterial pO<sub>2</sub>, pCO<sub>2</sub> and pH values were within the physiological range and did not change throughout the experiments. In animals pretreated with L-NAME or with diclofenac+L-NAME the MAP was significantly higher (143 $\pm$ 5 mmHg and 138 $\pm$ 6 mmHg, respectively) than in controls (99 $\pm$ 5 mmHg) or after diclofenac pretreatment alone (95 $\pm$ 7 mmHg). ZnDPBG administration, however, did not influence the MAP in any of the experimental groups. L-NAME and diclofenac+L-NAME pretreatments markedly reduced the HBF (from 0.90 $\pm$ 0.10 to 0.55 $\pm$ 0.09 ml/g/min and from 0.79 $\pm$ 0.11 to 0.44 $\pm$ 0.11 ml/g/min, respectively) while diclofenac alone had no significant effect (0.84 $\pm$ 0.09 vs. 0.88 $\pm$ 0.10 ml/g/min). ZnDPBG administration in control animals did not influence the HBF (-0.3 $\pm$ 4.1 %), but significantly increased it by 15.5 $\pm$ 2.9 % after diclofenac pretreatment. In contrast, ZnDPBG induced a marked reduction (-20.6 $\pm$ 5.6 %) of the HBF in animals pretreated with L-NAME. In animals receiving both diclofenac and L-NAME pretreatment the HBF remained unchanged after ZnDPBG administration (+5.9 $\pm$ 5.4 %). Our observations indicate that the HO pathway interacts with both the COX and the NOS systems in the regulation of the hypothalamic circulation. Endogenous CO production appears to increase the HBF via a COX-dependent mechanism, but at the same time suppresses NOS activity which leads to the reduction of HBF. These effects of CO may neutralize each other under physiological conditions. In pathophysiological states, however, which are associated with altered COX or NOS activity, the HO pathway may significantly influence the resting CBF. Supported by the Hungarian OTKA (T037386, T037885) and the German DFG. Z. B. was supported by a Marie Curie Individual Fellowship.

## EVALUATION OF THE MATHEMATICAL ASSUMPTION UNDERLYING NUMERICAL IDENTIFICATION MODELING OF CEREBROVASCULAR PRESSURE TRANSMISSION

Michael L. Daley<sup>1</sup>, Charles W. Leffler<sup>2</sup>, Marek Czosnyka<sup>3</sup>, John D. Pickard<sup>3</sup>

<sup>1</sup>*Department of Electrical and Computer Engr., The University of Memphis, Memphis, TN, USA*

<sup>2</sup>*Department of Physiology, University of Tennessee Health Science Center, Memphis, TN, USA*

<sup>3</sup>*Academic Neurosurgical Unit, Addenbrooke's Hospital, Cambridge, UK*

**Introduction:** To both evaluate cerebrovascular autoregulation and provide on-going insight into cerebrovascular pathophysiology of patients with brain injury we have been exploring the development of a numerical identification modeling technique which uses arterial blood pressure (ABP) and intracranial pressure (ICP) recordings. This numerical technique requires an assumed mathematical structure for the physical process of cerebrovascular pressure transmission. We have based our assumption on a previously proposed analog circuit model of ICP dynamics. Just as the modal frequencies, critical vibration modes, of a tuning fork reflect its structural properties; the modal frequencies of cerebrovascular pressure transmission reflect the structural properties of the cerebrovascular bed. To conveniently quantify cerebrovascular pressure transmission, we chose to evaluate the highest modal frequency (HMF) which represents the highest critical vibration frequency of transmission. The purpose of this study was to test the validity of our mathematical assumption required for numerical identification modeling by comparing the simulations of the analog model with those obtained by identification modeling technique generated from the same clinical pressure recordings. **Methods:** Pressure recordings were obtained from 6 patients with traumatic brain injury, a group (n=3) with mean cerebral perfusion pressure (CPP) > 50 mmHg and a group (n=3) with mean CPP < 30 mmHg. Values of HMF were computed by two methods: 1) derivation by the numerical identification autoregressive moving average technique; and 2) derivation from the analog circuit model of ICP dynamics. For each simulation we used a clinical ABP recording as the applied pressure source and manipulated the parameters of the analog model to obtain a match of the: 1) simulated and numerically derived values of HMF within 0.3 Hz; and 2) clinical and simulated ICP recordings. **Results:** All simulations of ICP generated by the analog circuit model visually match the corresponding clinical ICP recording. The group of patients with CPP >50 mmHg were assumed to have intact autoregulation with a mean cerebral blood flow (CBF) at approximately 750 ml/min. The other patients were assumed to have impaired autoregulation with a significantly lower mean CBF. Simulated values of intracranial compliance were found to increase with cerebral hypoperfusion. Simulated mean values of CPP, HMF, and intracranial compliance (IC), and CBF are given in Table 1. **Conclusions:** The findings of this study are: 1) simulations of ICP produced by the analog circuit model match clinical ICP recordings for equivalent values of simulated and numerically derived HMF; and 2) the simulated value of IC increases during impaired regulation with cerebral hypoperfusion. These findings support the validity of the mathematical assumption required for the proposed numerical identification modeling technique of cerebrovascular pressure transmission.

Table 1: Summary of Means ( $\pm$  S.D.) of Simulated HMF, Arterial Resist., IC, and CBF

	N	CPP (mmHg)	HMF (Hz)	Sim. intracranial compliance (mmHg)	Sim. cerebral blood flow (ml/min)
Intact regulation	3	56.8 ( $\pm$ 5.6)	3.5 ( $\pm$ 0.54)	0.25 ( $\pm$ 0.16)	746.7 ( $\pm$ 19.2)
Impaired regulation	3	19.8 ( $\pm$ 3.1)	0.85 ( $\pm$ 0.22)	0.58 ( $\pm$ 0.22)	371.9 ( $\pm$ 167.8)
Degree of Significance		p < 0.005	p < 0.005	p < 0.00	p < 0.025



## INHIBITION OF THE CANNABINOID-1 RECEPTOR ENHANCES THE CEREBROCORTICAL HYPEREMIC RESPONSE TO HYPOXIA/HYPERCAPNIA

Miriam Ishiguro<sup>1</sup>, Zsombor Lacza<sup>1</sup>, Eszter M. Horváth<sup>1</sup>, Zoltán Járαι<sup>2</sup>, Péter Sándor<sup>1</sup>,

**Zoltán Benyó<sup>1</sup>**

<sup>1</sup>*Institute of Human Physiology and Clinical Experimental Research, Semmelweis University, Budapest, Hungary*

<sup>2</sup>*Department of Internal Medicine, Semmelweis University, Budapest, Hungary*

Activation of cannabinoid-1 (CB1) receptors may evoke diverse vascular effects under physiological conditions: it has been shown to induce vasodilation but also to increase the vascular tone by inhibition of the endothelium-derived hyperpolarizing factor (EDHF). However, the role of CB1 receptors in certain pathophysiological states is obscure. We hypothesized that activation of the CB1 receptors may influence the cerebral hyperemic response to hypoxia/hypercapnia (H/H). Therefore, we investigated the effect of the CB1-antagonist AM-251 on H/H-induced vasodilation in the cerebral cortex. Adult male Wistar rats were anesthetized with intraperitoneal injection of 1.3 g/kg Urethane. Femoral arteries were cannulated for monitoring arterial blood pressure and for measuring arterial blood gas and acid-base parameters. CBF was measured in the parietal cortex simultaneously on both sides by laser-Doppler (LD) flowmetry. H/H was induced by inhalation of different gas mixtures. In the first step, during mild H/H, animals inhaled a gas mixture of 10% O<sub>2</sub>-10% CO<sub>2</sub>-80% N<sub>2</sub>, which produced arterial pO<sub>2</sub> of 75-85 mmHg and pCO<sub>2</sub> of 50-60 mmHg. In the second step, during moderate H/H, animals inhaled a gas mixture of 5% O<sub>2</sub>-20% CO<sub>2</sub>-75% N<sub>2</sub>, which produced arterial pO<sub>2</sub> of 55-65 mmHg and pCO<sub>2</sub> of 80-90 mmHg. In the third step, during severe H/H, animals inhaled a gas mixture of 0% O<sub>2</sub>-20% CO<sub>2</sub>-80% N<sub>2</sub>, which produced arterial pO<sub>2</sub> of 45-50 mmHg and pCO<sub>2</sub> of 90-100 mmHg. In the first experimental group, animals were subjected to these three steps of H/H, then brought back to physiological conditions. After steady state obtained, 10 mg/kg AM-251 was injected intravenously, followed by repetition of the stepwise H/H. In the second, control group the same protocol was performed, but between the two series of H/H only the vehicle (ethanol and emulphor, dissolved in saline) was administered intravenously. Inhalation of the different gas mixtures induced similar changes of the blood gas tensions and acid-base parameters before and after administration of AM-251 or its vehicle. Application of AM-251 did not alter baseline LD flow or arterial blood pressure. AM-251 has significantly increased, however the H/H-induced hyperemia in each step: by 30% during mild H/H, by 22% during moderate H/H, and by 14% during severe H/H. In contrast, vehicle of AM-251 had no significant effect. H/H did not change significantly the mean arterial pressure of the untreated or vehicle-treated animals, but it has induced slight hypertension (11±6 mmHg) following AM-251 treatment. The observed enhancement of the cerebrocortical hyperemic response to H/H after blockade of the CB1 receptors indicates that during hypoxia/hypercapnia the activation of CB1 receptors attenuates the vasodilation in the cerebral cortex. A possible explanation of these results is that endothelial CB1 receptors suppress the production of EDHF or other vasodilator mediators during H/H. If this is the case, increased cannabinoid levels during H/H limit the magnitude of reactive hyperemia in the brain tissue. Alternatively, activation of neuronal CB1 receptors may also affect the cerebrocortical blood flow during H/H by influencing the cerebral metabolic rate or the neural regulatory mechanisms of the cerebrovascular tone. Supported by the Hungarian OTKA (T037386, T037885, D045933) and ETT (248/2003)).

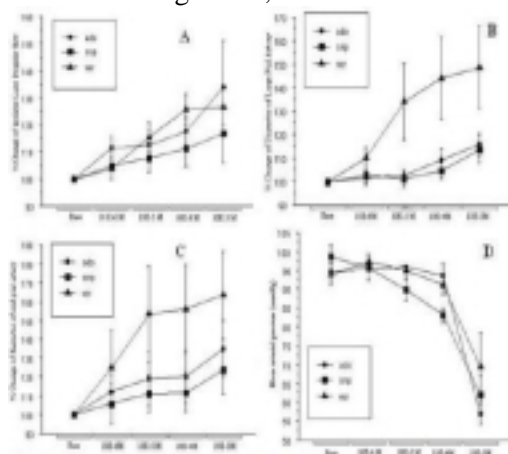
## COMPARATIVE MICROCIRCULATORY EFFECTS OF INTRACAROTID VASODILATORS

Mei Wang, Joshua Etu, Shailendra Joshi

*Department of Anesthesiology, Columbia University Medical Center, New York, NY, USA*

**Introduction:** In vitro studies suggest that, the small cerebral arteries are more sensitive to nitric oxide synthesis inhibition<sup>1</sup>. We have observed that, intracarotid nitroprusside (NP) fails to augment cerebral blood flow (CBF) in baboons and human subjects<sup>2,3</sup>. In contrast, NO independent drug, such as adenosine (ADO), has a profound effect<sup>3</sup>. We therefore hypothesized that, based on their predominant mechanism of action, NO donors (such as NP) will selectively augment diameters of proximal middle cerebral artery (MCA) branches while NO independent drug (such as ADO) will preferentially affect the diameter of the end-pial arteries (EPAs). Non-selective drugs, such as Ca<sup>++</sup> channel blocker (verapamil, VER) will increase the diameter of both the proximal-MCA branches and EPAs. **Methods:** Acute cranial windows were implanted just behind the bregma over the right temporal-parietal region of New Zealand white rabbits. The dura was reflected to expose the proximal-MCA branches. The arterial images were captured by custom build microscope with Dage CCD camera. Hemodynamic, CBF (laser Doppler) and EEG data was captured in real-time using a Powerlab system. All animals randomly received increasing doses of intracarotid drugs, from 0 to 10-3M. Each infusion lasted for one minute. Peak changes in arterial diameters and CBF were measured immediately after the cessation of infusion. There was a 45 minute period of rest between drug challenges. **Results:** All three vasodilators produced a dose-dependent increase in laser Doppler blood flow, Fig. A. There was a dose-dependent increase proximal-MCA and EPA diameters with all three drugs (Fig. B&C). The increase in arterial diameter was more robust with VER than with ADO and NP, but there was no difference between ADO and NP. Intracarotid injection of all three drugs resulted in significant hypotension at the highest concentration (10-3 M, Fig. D). **Discussion and Conclusions:** This study reveals that intracarotid delivery of ADO, NP and VER produces a dose-dependent increase in CBF as measured by laser Doppler technique. VER had a more profound effect on cerebral microcirculation than ADO and NP. However, the increase in arterial diameters did not always translate into equally proportional increase in CBF as would be suggested by arterial diameter changes. CBF increase after intracarotid vasodilator is affected by several factors besides their direct effect, such as effect of re-circulating drug on systemic parameters (such as arterial pressure and cardiac output), the effect of autoregulation triggered cerebrovascular responses, and the effect of CBF changes on intracarotid drug kinetics.

(1) Faraci FM: Am J Physiol : 1991, 261:H, 1038-42 (2) Joshi S et al: Stroke 1997; 28:1115-22 (3) Joshi S et al: Anesth & Analg: 2002; 94: 393-399



Figures: Percent Change in ipsilateral laser Doppler flow (A), the diameter of the large pial arteries (proximal-MCA branches) (B), the diameter change of the end-pial arteries (C) and mean arterial pressure (D) by three intracarotid drugs (ADO: Adenosine, Ver: Verapamil and NP: Sodium Nitroprusside) in different concentrations (base, 10<sup>-3</sup> M to 10<sup>-1</sup> M)



## CEREBRAL BLOOD FLOW AFFECTS THE DOSE REQUIREMENTS OF INTRACAROTID PROPOFOL FOR EEG SILENCE

Shailendra Joshi<sup>1</sup>, Mei Wang<sup>1</sup>, Joshua Etu<sup>1</sup>, John Pile-Spellman<sup>2</sup>

<sup>1</sup>*Department of Anesthesiology, Columbia University Medical Center, New York, NY, USA*

<sup>2</sup>*Departments of Radiology and Neurological Surgery, Columbia University Medical Center, New York, NY, USA*

**Introduction:** Intracarotid (IC) drugs have been used to treat a variety of brain diseases such as malignant tumors, cerebral vasospasm, thrombo-embolic strokes, severe infections, and intractable raised intracranial pressure. However, except in diagnostic neuroradiology, IC drug delivery is not routinely used in clinical practice. Dedrick et al, based on computer simulations, proposed that IC drug delivery would be particularly suitable in low regional blood flow states. <sup>1</sup> We therefore hypothesized that, cerebral blood flow (CBF) changes will affect the dose of IC-propofol required to produce EEG silence.<sup>2</sup> **Methods:** We tested our hypothesis on three groups of New Zealand White rabbits. Surgical preparation included ear vein, femoral and internal carotid artery cannulations; placement of laser Doppler probes and EEG leads. In the first group (n=9) we determined the dose of IC-propofol required to produce 10 min. of EEG silence during: (i) normoventilation, (ii) hyperventilation, and (iii) hypoventilation. In the second group (n=14) we determined the dose of IC-propofol required to produce a similar duration of EEG silence, with or without IC-verapamil pretreatment. IC-verapamil (0.4 mg) pretreatment was aimed to increase CBF by 75-100% during EEG silence. The third group of rabbits (n=8) received bolus IC-propofol during (i) normotension, (ii) severe systemic hypotension (with IV esmolol 20 mg and adenosine 30 mg) aimed to decrease CBF to  $\approx 25\%$  of the resting value, and (iii) after hemodynamic recovery. **Results:** In the first group, there was a linear correlation between dose of IC-propofol and the %-change in CBF from the baseline due changes in the minute ventilation, total dose ( $y$ ) =  $0.17 + 0.012 X$ ,  $n=27$ ,  $r=0.76$ ,  $P<0.0001$ . In the second group, the dose of IC-propofol was also a function of CBF change after verapamil pretreatment, total dose ( $y$ ) =  $0.98 + 0.1 * \% \Delta \text{ CBF} (x)$ ,  $n=14$ ,  $r=0.75$ ,  $P<0.002$ . In the third group, the duration of EEG silence after IC-propofol (3 mg) was significantly increased when it was injected during cerebral hypoperfusion, compared to pre- and post- hypoperfusion values ( $141 \pm 38$  vs.  $19 \pm 24$  and  $16 \pm 12$  s., respectively,  $P<0.0001$ ). **Conclusions:** We conclude that changes in CBF have a significant effect on the dose of IC-propofol required to produce EEG silence. Clinically CBF could be modulated mechanically by intraarterial balloon occluding catheters, severe systemic hypotension or by altering ventilation. These adjuvant CBF modulating methods may be useful in enhancing the efficacy of IC drugs. **References:** 1. Dedrick RL: Journal of the National Cancer Institute 1988; 80:84-9. 2. Wang M et al: Anesthesiology 2003; 99:904-10.

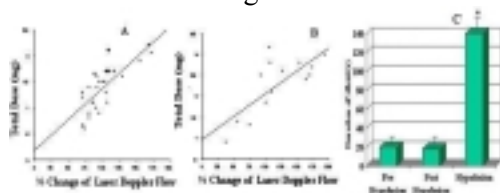


Figure: A & B: Changes in dose requirements of intracarotid propofol required to produce 10 minutes of EEG silence as a function of CBF from baseline after altering minute ventilation (A), and intraarterial infusion of verapamil a potent vasodilator (B). Figure C: shows duration of EEG silence after intracarotid injection of 3 mg of propofol during cerebral hypoperfusion and before and after the hypoperfusion challenge (C).

## MEDULLARY EPITHELIAL SODIUM CHANNELS (ENAC) PARTICIPATE IN CEREBRAL BLOOD FLOW (CBF) AUTOREGULATION

Eugene Golanov<sup>1,2</sup>, Heather Drummond<sup>2</sup>, Jasleen Shant<sup>1</sup>, Benjamin Clower<sup>3</sup>, Betty Chen<sup>1</sup>

<sup>1</sup>*Department of Neurosurgery, University of Mississippi Medical Center, Jackson, MS, USA*

<sup>2</sup>*Department of Physiology, University of Mississippi Medical Center, Jackson, MS, USA*

<sup>3</sup>*Department of Anatomy, University of Mississippi Medical Center, Jackson, MS, USA*

Introduction: Mechanical stimulation of the medulla oblongata produces sympathoexcitation and increase in arterial pressure (AP) [1] triggering Cushing reflex targeted for the maintenance of adequate brain perfusion pressure and cerebral blood flow (CBF). While mechanisms of autoregulation of cerebral blood flow (CBF) remain elusive, data indicate participation of medullary structures [2]. These findings suggest that medullary neurons may possess mechanosensitive properties. Since epithelial sodium channels (ENaC) have been proposed to participate in barosensing of arterial pressure (AP) [3], we hypothesized that mechanosensitive properties of the medulla are due to the presence of ENaCs, which also may contribute to CBF autoregulation. Methods: Deeply anesthetized Sprague Dawley rats (230-270 g) were transcidentally perfused, brains were removed and sectioned coronally. Medullary sections from the rostral pole of the facial nerve nucleus to 1 mm caudal to the obex were processed for ENaC beta subunit (affinity purified polyclonal antibodies, n=5) and tyrosine hydroxylase immunoreactivity (IR). To establish involvement of ENaCs in CBF autoregulation rats were anesthetized, artificially ventilated, while body temperature and blood gases were monitored and maintained at normal levels. Parietal cortex CBF was recorded using laser Doppler flowmeter. Autoregulatory curves were reconstructed by observing CBF changes while AP was varied from ~60 to ~140 mmHg by continuous i/v infusion of nitroprusside or phenylephrine, resp. Blockers of ENaCs (amiloride or benzamil) were microinjected into medulla using micropipettes with subsequent histological identification of the injection sites. Results: ENaC IR, mostly associated with large neuronal cells, was observed in nucleus of the solitary tract, gigantocellular and hypoglossal nuclei, and rostral ventrolateral medulla (RVLM). To establish whether ENaC IR-positive cells are catecholaminergic neurons we analyzed colocalization of ENaC IR and TH-IR. Catecholaminergic neurons of the caudal RVLM demonstrated ENaC IR. To establish possible involvement of ENaCs in CBF autoregulation we microinjected amiloride (1.5  $\mu$ M/100 nl, n=3) or benzamil (1  $\mu$ M/100 nl, n=5), bilaterally into caudal RVLM. Microinjections of ENaC blockers did not affect baseline levels of CBF or AP. However as a result of the microinjections the slope of CBF autoregulatory curve increased significantly ( $p < 0.05$ ) indicating attenuation of the autoregulatory response. Conclusions: Our experiments demonstrated the presence of ENaCs in the medullary nuclei, including nucleus of solitary tract, which is known to be involved in autoregulation [2] and RVLM, which is involved in CBF regulation [4]. In RVLM ENaC positive neurons were also TH positive indicating that RVLM catecholaminergic neurons, which participate in AP regulation, may possess mechanosensitive properties. Attenuation of the autoregulatory responses by specific ENaC blockers suggests involvement of mechanosensitive channels in CBF autoregulation. We conclude that ENaC proteins might be expressed in medullary neurons and participate in the autoregulatory control of CBF and medullary mechanosensitivity. 1. Dickinson, C.J. Clin. Sci. 79, 543-550. 1990. 2. Talman, W.T., Dragon, D.N. Brain Research 931, 92-95. 2002. 3. Drummond, H.A., Welsh, M.J., Abboud, F.M. Ann. NY Acad Sci. 940, 42-47, 2001. 4. Golanov, E. V., Ruggiero, D. A., Reis, D. J. J. Physiol. 529, 413-429. 2000.

**TRANSCRIPTIONAL AND TRANSLATIONAL MECHANISMS FOR THE  
RECIPROCAL CONTROL OF INOS AND ENDOTHELIN 1 EXPRESSION IN BRAIN  
MICROVESSELS AFTER TRAUMATIC BRAIN INJURY TBI**

Christian Kreipke, Jose Rafols, **Theodor Petrov**

*Wayne State University School of Medicine, Department of Anatomy and Cell Biology,  
Detroit, MI, USA*

Previously we demonstrated in a rat model (Marmarou's) that in vivo inhibition of iNOS gene expression (not observed in the intact brain and a source of abnormally high levels of nitric oxide (NO)) results in upregulation of the endothelin 1 (ET-1) gene and protein expression at the microvascular wall<sup>1</sup>. We attributed the exacerbated hypoperfusion and enhanced vasoconstriction to increased synthesis and release of ET-1, a powerful vasoconstrictor. In addition, we have shown that iNOS and ET-1 are synthesized in the same endothelial cells that form the microvascular wall<sup>2</sup>. Recently we observed, post TBI, induction of c-fos expression (the immediate early gene whose expression is essential for the activation of the AP-1 cascade and the ET-1 gene). Also, we showed and increased synthesis of the phosphorylated form of eukaryotic initiation factor 2 alpha (eIF2aP phosphorylation of the a subunit of causes inhibitor of translation of protein synthesis)<sup>3</sup>. Here we test the hypothesis that c-fos and eIF2aP are temporally associated with the enhanced expression of ET-1 after TBI and that iNOS expression and inhibition plays a role in regulating their synthesis. We used combinations of double immunocytochemistry and in situ hybridization to detect expression of ET-1, iNOS, c-fos and eIF2aP in cortex and hippocampus of male Sprague-Dawley rats at 4, 24 and 48h post TBI. Other animals were pretreated with antisense iNOS oligodeoxynucleotides (ODNs) to block the mRNA synthesis. In the latter group expression of c-fos was increased in ET-1 positive cells (endothelial cells, pericytes, neurons and astroglia) by ~25% in comparison to brains from animals that were not pretreated with antisense ODNs. In the same group, the number of cells that coexpressed iNOS and eIF2aP was reduced by ~32% and the intensity of eIF2aP immunoreactivity decreased by ~38%. The effectiveness of the iNOS knockout was confirmed with in situ hybridization and Western blotting. The results suggest that further upregulation of ET-1 synthesis in animals subjected to TBI and pretreated with antisense iNOS ODNs is related to: 1) disinhibition of AP-1 since NO is known to suppress its expression at several levels including c-fos and c-jun, the protein product of the latter forming a dimer with c-fos (the protein) that binds to AP-1 and, 2) by reducing the amount of eIF2aP since previous in vitro work has shown, that NO is a phosphorylating molecule. Therefore, by decreasing the synthesis of NO we may have disinhibited protein synthesis including ET-1. In addition, our finding that c-fos is localized in the nucleus, while eIF2aP is observed in both nucleus and cytoplasm, suggests that NO can influence their synthesis at the transcriptional and translational level. 1. Steiner et al., (2004) Nitric Oxide, 10:162-169. 2. Rafols et al., (2004). Neurosci. Lett., 326:154-157. 3. Petrov et al., (2001) J. Neurotrauma, 18: 799-812. Supported by NIH Grant 39860.

## A SIMPLE FEADBACK MODEL OF CEREBRAL BLOOD FLOW DEPENDENCE ON ARTERIAL BLOOD PRESSURE

**Alexander Gersten**

*Department of Physics, Ben-Gurion University, Beer-Sheva, Israel*

The autoregulation of cerebral blood flow (CBF), or the independence of CBF on changes of mean arterial blood pressure (MABP) in a wide range of MABP (the so called "plateau"), is considered to be a well established fact. But looking carefully at the existing experimental data we could not find even one publication, which gives an adequate experimental support for the existence of the plateau of the autoregulation. The first publication, seemingly proving autoregulation in humans, was that of Lassen (1959). However the data at different points on the plateau were taken from different people (Lassen, 1959). As individual differences are quite important, the above procedure is not accurate and may serve as an indication only. Harper (1966) has done experiments with 12 dogs, measuring CBF for a wide range of MABP. However he presented and discussed results taken together on 8 normocapnic animals and 4 hypercapnic ones. Fortunately he tabulated the experimental data for each dog separately. Harper's data are the only published data, which describe for each animal separately the dependence of the CBF on MABP in a wide range of MABP. We shall use Harper's data and re-analyze their content using a new feedback model. The dependence of the cerebral blood flow (CBF) on mean arterial blood pressure (MABP) is described using a simple model:  $CBF(MABP) = S \cdot MABP - b \cdot F(MABP) \cdot CBF(MABP)$ , (where  $S$  is the initial linear slope of the CBF,  $F$  is a feedback function and  $b$  its slope. Below certain MABP (denoted as MABP1) there are no autoregulatory or feedback mechanisms influencing CBF ( $b=0$ ). Between MABP1 and MABP2 (MABP at which breakthrough occurs) there is a linear (on MABP) dependent feedback with a slope (a feedback parameter  $b$ ) depending very much on the individual considered. The classical autoregulation model with a plateau in between MABP1 and MABP2 is a particular case of this model (with a feedback parameter  $b=1$ ). New effect of decreased CBF (the feedback parameter  $b>1$ ), while increasing MABP, was observed in two dogs. For hypercapnic dogs there was no autoregulation ( $b \sim 0$ ) at all. The model describes well the experiments performed on dogs (Harper, 1966), for which the individual feedback slope parameters varied to great extent (from a weak feedback  $b=0.29$  to an over-strong feedback  $b=1.37$  for the normocapnic dogs), indicating the importance of measurements on individuals against averaged measurements (or measurements on different individual). (Our results may have practical importance in neuroimaging, neurosurgery and in the treatment of hypertension.

References:

- Harper AM (1966), " Autoregulation of cerebral blood flow: influence of the arterial blood pressure on the blood flow through the cerebral cortex ," J. Neurol. Neurosurg. Psychiat. 29:398-403.
- Lassen NA (1959), " Cerebral blood flow and oxygen consumption in man ," Physiol. Rev. 39:183-238.

**COMBINED MEASUREMENTS OF CEREBELLAR BLOOD FLOW, LOCAL FIELD POTENTIALS AND GLUCOSE UTILIZATION DURING CLIMBING FIBRES STIMULATION: EFFECT OF POSTSYNAPTIC EXCITATORY ACTIVITY**

Aïcha Douhou<sup>1</sup>, Kirsten Caesar<sup>2</sup>, Nikolas Offenhauser<sup>2</sup>, Martin Lauritzen<sup>2</sup>, **Gilles Bonvento**<sup>1</sup>

<sup>1</sup>*CEA CNRS URA 2210, Hôpital D'Orsay- Service Hospitalier Frédéric Joliot, Orsay, France*

<sup>2</sup>*Department of Medical Physiology, The Panum Institute, University of Copenhagen, Copenhagen, Denmark*

**Introduction:** The aim of this study was to determine the influence of glutamatergic transmission for activity-dependent cerebellar glucose use (CeGU) and blood flow (CeBF). The experiments tested the hypothesis that increases in glucose in response to activation originate in postsynaptic cellular elements. **Materials and Methods:** Experiments were carried out in 26 male  $\alpha$ -chloralose-anesthetized Wistar rats (250-350g). CeGU was quantitatively measured in all rats using the [14C]-2-deoxy-glucose (2-DG) autoradiographic technique. At end of experiment, brains were immediately removed, frozen in isopentane (-40 C) and cut into 20- $\mu$ m coronal sections. Sections were collected on glass slides and autoradiographed together with [14C] standards on x-ray film for 5-6 days (Sokoloff et al., 1977). CeBF was recorded with a double-wavelength Laser Doppler Flowmetry probe using green laser light to record CeBF in the upper 0-250  $\mu$ m of the cerebellar cortex and red laser light to record CeBF in deeper layers. Glutamatergic neurotransmission was increased by stimulation of cerebellar climbing fibres (CF) at the level of the inferior olive (IO) in the brain stem. Local field potentials (LFP) were recorded with glass microelectrodes. CeGU was measured in cerebellar lobules 5 and 6, i.e. at the same site at which CeBF and LFPs were recorded. CNQX, a selective AMPA receptor antagonist, was used to block the excitatory postsynaptic potentials. The protocol included 4 groups of rats: (i) sham rats (ii) CF stimulated rats (iii) CF stimulated rats + CNQX, (iv) sham rats + CNQX. The IO was continuously stimulated at 5 Hz for 45 min. **Results:** Continuous IO stimulation evoked a sustained and robust CeBF increase (mean of 167% for the green probe, mean of 215% for the red probe) associated with increased LFP amplitudes (mean amplitude =  $4.46 \pm 0.62$  mV), stable for the entire 45 min stimulation period. The AMPA receptor antagonist CNQX significantly attenuated CeBF increases evoked by IO stimulation by up to 80% and induced a marked decrease of LFP amplitudes by up to 90%. CNQX did not affect basal CeGU in sham + CNQX animals. The increase of postsynaptic activity of Purkinje cells was associated with a modest, heterogeneous change in CeGU that appeared to depend on the accompanying rise in CeBF. A large rise in CeBF was associated with a low change in CeGU value and vice versa. This relationship was lost when CNQX was applied. **Conclusion:** Overall, our data indicate that CeGU changes do not seem to parallel CeBF variations and that postsynaptic excitatory activity is responsible for a functional link between CeBF and CeGU changes during activation of the CF system.

## INVESTIGATION OF THE CHANGES IN CEREBRAL TISSUE OXYGENATION MEASURED WITH NEAR INFRARED SPECTROSCOPY IN RESPONSE TO MODERATE HYPERCAPNIA

Ilias Tachtsidis<sup>1</sup>, Holie Jones<sup>2</sup>, Caroline Oliver<sup>2</sup>, Dave T. Delpy<sup>1</sup>, Martin Smith<sup>2</sup>, Clare E. Elwell<sup>1</sup>

<sup>1</sup>University College London, Medical Physics and Bioengineering, <sup>2</sup>The National Hospital for Neurology & Neurosurgery, Department of Neuroanaesthesia & Neurocritical Care, London, UK

**Introduction:** The arterial partial pressure of carbon dioxide (PaCO<sub>2</sub>) has a major influence on cerebral blood flow (CBF). Cranial near-infrared spectroscopy (NIRS) can monitor the resulting *changes* in cerebral haemodynamics and recent technical advances enable *absolute* measurements of tissue oxygenation using spatially resolved spectroscopy (SRS). This mixed (arterial, venous) oxygenation signal has been termed the tissue oxygenation index (TOI). TOI can be related to the arterial saturation (SaO<sub>2</sub>), oxygen consumption (CMRO<sub>2</sub> in ml of O<sub>2</sub>/min), CBF (in ml/min) and arterial (Va), venous (Vv) blood volume per unit mass of tissue (in l/g) by Eq. 1: where [Hb] is the haematocrit (g/dl) and k is the oxygen combining power (~1.306 ml O<sub>2</sub>/g Hb). The aim of this study is to investigate the association between the cerebral TOI and systemic physiological changes during hypercapnia.

**Methods:** 12 healthy volunteers (mean ± SD age 32 ± 4 years) were investigated. A Hamamatsu NIRO 300 system recorded *changes* in oxyhaemoglobin ([HbO<sub>2</sub>]) and deoxyhaemoglobin ([HHb]) concentrations and *absolute* TOI. End tidal CO<sub>2</sub> (EtCO<sub>2</sub>) values were monitored continuously via a face mask and non-invasive beat-to-beat blood pressure with a Portapres® system. Data were recorded as the volunteers (i) breathed room air and (ii) during inspiration of 5% CO<sub>2</sub>.

**Results:** Average values of each signal were calculated for 1 minute periods at the end of rest and hypercapnia. A statistically significant increase during hypercapnia was observed in EtCO<sub>2</sub> (7±4mmHg), cerebral TOI (2.7±1.4%) and total haemoglobin [HbT]=[HbO<sub>2</sub>]+[HHb] (2.4±1.7µmol/l) (paired t-test, p<0.001). Correlation analysis showed that the *changes* in EtCO<sub>2</sub> were associated with the *changes* in [HbT] (r=0.54, p=0.03) but not the changes in [TOI] (r=0.46, p>0.05). However association analysis between the *absolute* values of TOI and EtCO<sub>2</sub> during hypercapnia show a substantial correlation (r=0.63, p=0.01). Multi-regression analysis between hypercapnic *absolute* values of EtCO<sub>2</sub>, MBP and TOI revealed a relationship with r=0.74 and p<0.05.

**Discussion:** We have investigated cerebrovascular reactivity to induced hypercapnia observing a consistent increase in [HbT] and TOI confirming results of others [1,2]. Significant association was found between the *absolute* values of TOI and the *absolute* EtCO<sub>2</sub> and MBP values during hypercapnia suggesting that the *absolute* TOI value is dependent on the baseline state of these two variables. This might imply a relationship between CBF and TOI, which has already been shown in neonates [3]. Our data shows that the *changes* in TOI are not linearly related to the *changes* in [EtCO<sub>2</sub>]. Clearly the relationship between TOI, CBF and the arterial:venous volume fraction requires further investigation particularly in studies where CBF is measured directly. These data have implications for the interpretation of changes in TOI during clinical monitoring.

### References:

- [1] Smielewski P, Kirkpatrick P, Minhas P, Pickard JD, and Czosnyka M; *Stroke* **26**, 2285-2292 (1995)
- [2] Yoshitani K, Kawaguchi M, Tatsumi K, Kitaguchi K, and Furuya H; *Anesth Analg* **94**, 586-590 (2002)
- [3] Elwell CE, Henty JR, Leung TS, Austin T, Meek JH, Delpy DT, and Wyatt JS; *Adv.Exp.Med.Biol.* In press 2005

$$(1) \text{ TOI} = \text{SaO}_2 - \left( \frac{V_v}{V_a + V_v} \right) \cdot \left( \frac{\text{CMRO}_2}{k \cdot \text{CBF} \cdot [\text{Hb} \cdot 10^{-2}]} \right)$$



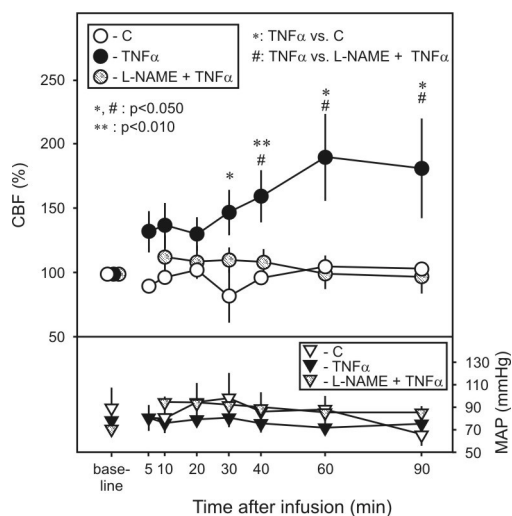
## CIRCULATING TUMOR NECROSIS FACTOR- $\alpha$ ALTERS CEREBRAL BLOOD FLOW AND MICROVASCULAR ULTRASTRUCTURE THROUGH NITRIC OXIDE RELEASE IN THE RAT BRAIN

Eszter Farkas<sup>1</sup>, Peter Antal<sup>2</sup>, Valeria Toth-Szuki<sup>2</sup>, Ibolya G. Farkas<sup>1</sup>, Andras Mihaly<sup>1</sup>, Ferenc Bari<sup>2</sup>

<sup>1</sup>Department of Anatomy, <sup>2</sup>Department of Physiology, School of Medicine, University of Szeged, Hungary

Tumor necrosis factor- $\alpha$  (TNF $\alpha$ ), a proinflammatory cytokine can play a prominent role in CNS injury putatively in part through cerebrovascular dysfunction. The aim of our study was to demonstrate how cerebral blood flow and microvascular morphology are affected by circulating TNF- $\alpha$ .

Fifty male Wistar rats were anesthetized with chloral hydrate (400 mg/kg, i.p.). Five animals were administered by 2.5  $\mu$ g/kg TNF $\alpha$  (in 1 ml saline) infused unilaterally to the left common carotid artery. Control animals received 1 ml saline (n=5). Another group of rats received L-nitroarginine methyl ester (20 mg/kg/0.5ml/2min, L-NAME), a nitric oxide synthase (NOS) inhibitor into the right femoral vein prior to TNF $\alpha$  or saline infusion (n=5/group). Mean arterial pressure (MAP) was monitored through a tail artery cannula, while cerebrocortical blood flow (CBF) was recorded by a laser-Doppler probe positioned above the frontoparietal cortex. In a next set of experiments, rats were infused with TNF $\alpha$  or saline, and were sacrificed for electron microscopic analysis at various survival times (45 min, 4 h and 8 h post-infusion, n=5/group). While MAP values did not differ between groups, TNF $\alpha$  significantly increased cortical CBF with the progress of time to 190 % of baseline at 60 min after TNF $\alpha$  infusion. The administration of L-NAME prevented TNF $\alpha$ -induced CBF elevation. Damage to the blood-brain barrier (BBB) was observed in the form of perivascular edema. Approximately 50 % of cerebrocortical capillaries demonstrated severe swelling of astrocytic endfeet at 45 min, while about 65 % of the vessels were damaged at 8 h post-infusion. The average lumen diameter of investigated capillaries decreased gradually from 4.5  $\mu$ m to 3.6  $\mu$ m by 8 h after TNF $\alpha$  infusion. Our results demonstrate that circulating TNF $\alpha$  is a vasoactive compound in the CNS. It affects cerebral blood vessels both at functional and morphological levels. Since NOS inhibition could prevent CBF increase, TNF $\alpha$  action is suggested to be mediated by NO from an unclarified source. Further, our data support the notion, that circulating TNF $\alpha$  can impose morphological damage at the BBB and can lead to CNS complications. Acknowledgements: The project was supported by the Hungarian Scientific Research Fund (OTKA F042803, T32566 and T046531), and the Bolyai János Research Scholarship of the Hungarian Academy of Sciences to E.F.





## FRactal PATTERNS OF LOCAL AND GLOBAL CBF IN RAT BRAIN DURING HYPOTENSION

Peter Herman<sup>1,2</sup>, Hubert Trübel<sup>2,3</sup>, Fahmeed Hyder<sup>2,4</sup>, Andras Eke<sup>1</sup>

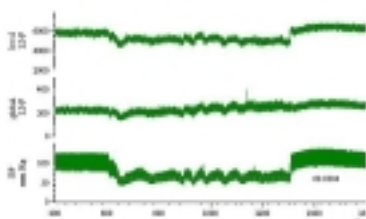
<sup>1</sup>*Institute of Human Physiology and Clinical Experimental Research, Semmelweis University, Budapest, Hungary*

<sup>2</sup>*Diagnostic Radiology, Yale University, New Haven, CT, USA*

<sup>3</sup>*HELIOS Klinikum Wuppertal, University Witten/Herdecke, Wuppertal, Germany*

<sup>4</sup>*Biomedical Engineering, Yale University, New Haven, CT, USA*

CBF as measured by laser-Doppler flowmetry (LDF) in rat brain has been demonstrated to contain spontaneous fractal fluctuation patterns during normotension [1,2]. In this study we characterized to what extent during hypotension does perfusion autoregulate and fluctuations in local and global CBF maintained. Artificially ventilated rats (male, Sprague-Dawley, n=17) were anesthetized with urethane (1.3 g/kg). Dynamic changes in global and local CBF were measured by LDF probes of different sizes (Perimed and Oxford Optronix, respectively) placed superficially and in deeper cortical layers. The interoptode distances of the two probes were 1.0 and 0.2 mm, respectively. The local and global CBF were measured on opposite sides of the cortex. The local LDF signal was localized to layer 4 and the global LDF signal was comprised of superficial layers in a small region of that hemisphere. The hypotensive steps (of 80, 60, and 40 mmHg) were maintained by a computer-controlled negative lower body pressure method (figure) [3]. The duration of each hypotensive step was ~10 minutes and after each step the pressure was let to rise back spontaneously. Spontaneous fluctuations were characterized by fractal analysis where the Hurst exponent (H) ranging from 0 to 1 corresponded to very rapidly changing hence noisy signal to a very slowly changing, smooth signal, respectively. The value of H=0.5 is a random pattern. The H values of the spontaneous fluctuations in local CBF were  $0.30 \pm 0.04$ ,  $0.29 \pm 0.05$  and  $0.30 \pm 0.05$  before each hypotensive step of 80, 60 and 40 mmHg. During hypotension these values (for local CBF) were significantly increased ( $p < 0.05$ ) in every step (H:  $0.32 \pm 0.06$ ,  $0.32 \pm 0.07$  and  $0.33 \pm 0.1$ ) and the local CBF changed according to autoregulation ( $\Delta$ CBF: 93.9%, 90.3% and 72.4% of local CBF under normotension). On the contrary there were no significant differences in values of H for global CBF between the three hypotension levels. The values of H for global CBF did not show significant changes as pressure dropped from the spontaneous level (H:  $0.43 \pm 0.06$ ,  $0.39 \pm 0.08$  and  $0.40 \pm 0.08$ , respectively) to the levels of hypotension (H:  $0.44 \pm 0.06$ ,  $0.41 \pm 0.09$ ,  $0.42 \pm 0.14$ ) and the global CBF changed only slightly according to autoregulation ( $\Delta$ CBF: 99.1%, 98.8%, 79.3% of global CBF under normotension). Fractal analysis reveals that local LDF signal is sensitive to hypotension challenges probably because local CBF is controlled in the deep cortical layers with a unique mechanism that alters the pattern of local CBF fluctuations. In contrast this hypotension-induced change in the fractal pattern of the global LDF signal was not detected probably because the fluctuations in global CBF can be obscured by integration of layer-specific CBF signals. These results suggest different analytical treatments of local and global CBF data for quantitative neuroimaging methods like fMRI and PET. Supported by NIH (DC-003710, MH-067528) and OTKA T34122. [1] Eke A et al (1997) Adv. Exp Med Biol, 428:703-709 [2] Eke A et al (2000) Pflügers Arch., 439:403-415 [3] Dirnagl U et al (1993) Neurol Res 15:126-130



Computer controlled hypotensive step (80 mmHg) with the lower body negative pressure method



## EVOKED POTENTIALS AND ACTIVATION FLOW COUPLING IN ENDOTOXIN MEDIATED SEPSIS SYNDROME IN RATS

Bernhard Rosengarten<sup>1</sup>, Mirko Hecht<sup>1</sup>, Ardeschir Ghofrani<sup>2</sup>, Manfred Kaps<sup>1</sup>

<sup>1</sup>*Department of Neurology, JLU Giessen, Giessen, Germany*

<sup>2</sup>*Department of Internal Medicine, JLU Giessen, Giessen, Germany*

During sepsis progression microcirculatory dysfunction precedes macrocirculatory failure partly explaining occurrence of early organ dysfunction. The matter concerning microcirculatory dysfunction in the brain under septic conditions is less clear. Activation-flow coupling denotes a principle adapting local cerebral blood flow in accordance to the metabolic needs of the neurons. We utilized a rat model of endotoxic shock and investigated the activation flow coupling under sepsis progression. Chloralose-anesthetized rats (n=10) were subjected to electric forepaw stimulation. Over the somatosensory cortex electrical activity and flow responses were recorded with surface electrodes and laser Doppler. After baseline recordings 5mg/kg lipopolysaccharide from *E. coli* was given i.v. and activation flow coupling, blood pressure, and blood gases were investigated at regular time points up to 270min. At the end lactate, glucose, NSE and S-100B levels were measured. All rats developed signs of septic shock. SEP amplitudes and latencies as well as evoked flow responses changed significantly. Changes in evoked flow responses preceded SEP reductions leading to a sigmoid rather than linear relationship between signals indicating insufficient blood supply. Dividing rats into two groups one with more and one with less severe changes in pH ( $7.40 \pm 0.04$  vs.  $7.35 \pm 0.06$ ), blood pressure ( $77 \pm 14$  vs.  $55 \pm 13$  mmHg) and lactate levels ( $1.4 \pm 0.5$  vs.  $3.3 \pm 0.6$  mmol/L) it appeared that occurrence of cerebral hyperemia (+40% for both groups) and NSE-levels ( $1.9 \pm 0.4$  vs.  $2.2 \pm 0.3$  ng/ml) were identical between groups. SEP latencies ( $10 \pm 0.6$  vs.  $12 \pm 0.8$  ms) and S-100B ( $5.3 \pm 2.3$  vs.  $13.5 \pm 1.3$  ng/ml) were significantly higher in the severe sepsis group whereas SEP amplitudes (270min:  $13 \pm 2.1$  vs.  $8 \pm 4.2$   $\mu$ V) and evoked flow responses (270min:  $10 \pm 8$  vs.  $6 \pm 5$  AUC [area under the curve]) showed only a trend to lower values. More or less independent from the severity of the sepsis syndrome microcirculatory dysfunction precedes changes in electrical parameters leading to an insufficient blood supply of active neurons. This finding contrasts with occurrence of cerebral hyperemia during sepsis progression and is in line with concepts of microcirculatory failure explaining occurrence of early septic encephalopathy. The constellation of higher S-100B rather than NSE levels might be explained by a disruption of astrocytic end feet due to blood brain barrier leakage. Since astrocytes are involved in the activation flow coupling further studies are needed to investigate a possible relation.

## CEREBRAL BLOOD FLOW AUTOREGULATION IN A RAT MODEL OF SUBARACHNOID HEMORRHAGE AS DETERMINED WITH LASER DOPPLER FLOWMETRY AND THE INTRA-ARTERIAL <sup>133</sup>XENON METHOD

Jan Tonnesen<sup>1</sup>, Erik H. Larsen<sup>2</sup>, John Hauerberg<sup>1</sup>, Olaf B. Paulson<sup>1</sup>, Gitte M. Knudsen<sup>1</sup>

<sup>1</sup>Neurobiology Research Unit, Rigshospitalet, <sup>2</sup>August Krogh Inst, University of Copenhagen, Denmark

**Introduction:** Laser Doppler flowmetry (LDF) has proven useful for assessment of relative changes in cerebral blood flow (CBF) and the CBF autoregulation lower limit (LL) mean arterial blood pressure (MABP) in rats (Tonnesen et al, accepted). The aim of this study was to validate the LDF method against the <sup>133</sup>xenon method for determination of cerebral autoregulation lower limit in a rat model of subarachnoid hemorrhage (SAH). **Methods:** Male SPRD rats were used. SAH was induced 48 h prior to autoregulation studies by injecting 0.07 mL freshly drawn autologous arterial blood into the cisterna magna. Rats were anaesthetized with isoflurane in 70/30 % N<sub>2</sub>O/O<sub>2</sub> and autoregulation lower limit was challenged by controlled systemic hemorrhage. Before systemic hemorrhage in xenon measurement experiments, noradrenaline (NA) was infused to raise systemic blood pressure ~10-15 mmHg to broaden the autoregulatory plateau. In two groups (SAH and control) autoregulation was determined by LDF only and in another two groups (SAH and controls) autoregulation was determined simultaneously both with LDF and the xenon method.

**Results:** Data are shown in the table; lower limit units are mmHg (MABP), LDF units are given as percent of baseline values. In SAH rats that were *not* given NA, CBF autoregulation LL as determined with LDF was found to be significantly higher than in control rats (63±1.7 and 58±1.8 mmHg, p=0.04, two-tailed t-test). All rats had preserved CBF autoregulation (Figure). In SAH rats administered NA, the CBF autoregulation LL as determined by LDF was substantially higher, (75±4.4 mmHg). Even though the two techniques were applied simultaneously, the xenon method, however, showed a substantial right-shift (105±5.9 mmHg). By contrast, controls rats investigated under NA infusion showed preserved autoregulation as determined by LDF (57±4.9 mmHg) and abolished based on the xenon method (119±11.2 mmHg). **Discussion:** To our surprise we were unable to reproduce earlier findings of loss of CBF autoregulation in SAH rats conducted in our laboratory with the Xe-technique (e.g., Springborg et al. 2002). Our LDF data showed that CBF autoregulation was preserved in SAH with the LL being increased by only 5 mm Hg in comparison to control rats. In simultaneous measurements of CBF autoregulation LL by two different methods we found that in SAH and control animals that NA administration – leading to a targeted increase in MABP of about 10-15 mmHg – apparently has a large impact on the LL. In this respect, the xenon method seems to be more susceptible to this influence of NA than LDF. The small increase in MABP by NA administration is well below the upper limit of autoregulation. Our findings are suggestive of an unpredictable effect of NA that needs to be considered in future studies.

References: Springborg et al. Br J Pharmacol 135(3):823-9. 2002.

Tonnesen et al. Exp Phys. Accepted.

## EFFECT OF CAFFEINE ON THEOPHYLLINE ON CEREBRAL BLOOD FLOW RESPONSE TO BRAIN ACTIVATION: *IN VITRO* AND *IN VIVO* STUDIES

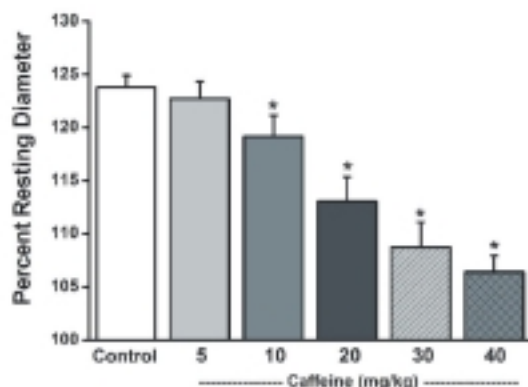
Joseph R. Meno<sup>1,2</sup>, Thien-son K. Nguyen<sup>2</sup>, Elise M. Jensen<sup>2</sup>, G. Alexander West<sup>2,3</sup>, Leonid Groysman<sup>1</sup>, David K. Kung<sup>1</sup>, Al. C. Ngai<sup>2</sup>, Gavin W. Britz<sup>2</sup>, **H. Richard Winn**<sup>1</sup>

<sup>1</sup>*Department of Neurosurgery, Mount Sinai School of Medicine, New York, NY, USA*

<sup>2</sup>*Department of Neurological Surgery, University of Washington, Seattle, WA, USA*

<sup>3</sup>*Oregon Health & Science University, Department of Neurological Surgery, Portland, OR, USA*

Despite its wide consumption and well-documented psychoactive effects, little is known regarding the effects of caffeine, an adenosine receptor antagonist, on neurovascular coupling. In the present study, we evaluated the effects of caffeine on intracerebral arterioles *in vitro* and on the pial circulation *in vivo* during cortical activation induced by contralateral sciatic nerve stimulation (SNS). In our *in vitro* studies, we utilized isolated intracerebral arterioles to determine the effects of caffeine (10 or 50 $\mu$ M) on vasodilatation induced by extraluminal application of adenosine. Adenosine caused dose-dependent dilations. Pretreatment with caffeine alone, at either of the concentrations tested, had no effect on resting diameter. The higher concentration (50 $\mu$ M) of caffeine resulted in significant attenuation of adenosine-induced vasodilatation ( $p < 0.05$ ,  $n = 5$ ), whereas 10 $\mu$ M had no effect. We utilized reverse-phase HPLC to quantify *in vivo* CSF caffeine concentrations. Intravenous administration of 5 mg/kg caffeine led to CSF concentrations of approximately 3 $\mu$ M, whereas higher doses (10 and 40 mg/kg), resulted in CSF caffeine accumulations of more than 10 and 60 $\mu$ M, respectively ( $n = 18$ ). To study the effect of caffeine on neurovascular coupling, we created a close cranial window in anesthetized, ventilated and temperature-regulated rats. Pial arteriolar response to contralateral sciatic nerve stimulation (SNS) was then evaluated before and after intravenous administration of caffeine (5, 10, 20, 30 & 40 mg/kg). Contralateral SNS resulted in a 23.8% increase in pial arteriolar diameter in the hindlimb sensory cortex under control conditions. Intravenous administration of caffeine at the lowest dose (5 mg/kg), equivalent to ~2 cups of brewed coffee, had no effect on resting arteriolar diameter but slightly suppressed the arteriolar response to somatosensory stimulation. This trend, however, did not reach statistical significance. At all of the higher doses (10, 20, 30 & 40 mg/kg, *i.v.*), caffeine significantly attenuated the cerebral blood flow responses to contralateral SNS (Figure 1;  $p < 0.05$ ;  $n = 6$ ). Caffeine administration also significantly reduced resting arteriolar diameter. In contrast, hypercarbic vasodilatation was unaffected by caffeine at any of the doses tested. The results of the present study demonstrate that caffeine significantly reduces cerebrovascular responses to both adenosine and to somatosensory stimulation and supports a role of adenosine in the regulation of CBF during functional neuronal activity.





**REGIONAL VARIABILITY IN THE CBF RESPONSE TO MILD HYPOTENSION  
CORRELATES WITH HETEROGENEOUS CBF AFTER FOCAL CEREBRAL  
ISCHEMIA**

Alexander Kharlamov, Stephen C. Jones

*ASRI, Anesthesiology Department, AGH, Pittsburgh, PA, USA*

Regional variability in cerebral blood flow (CBF) during mild hypotension has been demonstrated (Kharlamov et al, *Neurosci Lett* 368:151-156, 2004). We hypothesize that regional changes in CBF in response to hypotension can predict the CBF changes in the same brain after focal ischemia. Male Sprague/Dawley rats (n=4) were intubated and mechanically ventilated (0.5-1.5% isoflurane, 70% N<sub>2</sub>O balance O<sub>2</sub>). An 8-mm diameter closed cranial window was placed between bregma and lambda. Focal ischemia was produced by transection of the left MCA and bilateral common carotid artery occlusion (MCAT). Laser speckle flowmetry (LSF) allowed simultaneous measurement of CBF in different cortical regions. CBF was measured in at least 70 separate regions of interest (ROI, 310 microns diameter): a) before blood withdrawal at a mean arterial pressure (MAP) of 100 mmHg, CBF<sub>1</sub>; b) during hemorrhagic hypotension, MAP 70 mmHg, CBF<sub>2</sub>; c) after blood re-infusion and before MCAT at MAP 100 mmHg, CBF<sub>3</sub>; d) after MCAT at MAP 100 mmHg, CBF<sub>4</sub>. In each ROI, the response to hypotension and MCAT were expressed as %CBF<sub>70</sub> [100\*(CBF<sub>2</sub>/CBF<sub>1</sub>)] and %CBF<sub>MCAT</sub> [100\*(CBF<sub>4</sub>/CBF<sub>3</sub>)], respectively. Using these percentages, ROIs were divided into three types (LF, NF, and HF) with the boundaries of 85% and 120%, and 45% and 120%, respectively. For each ROI, we analyzed changes in the CBF response from hypotension to MCAT between the categories LF, NF, and HF as presented in the Table. Analysis of CBF in individual animals demonstrated that in rats #1 and #2 (see Table) the total % of ROIs with the same level of response were 55 and 57%, respectively. In most of those ROIs the flow after ischemia remained in the NF category (53%). In another two rats the hypotension LF ROIs remained as LF after MCAT (61% and 42%). At 2 h after MCAT 59±15% (n=4, mean ± STD) of ROIs remained in the same category as during mild hypotension, and 25±15% (n=4, mean ± STD) reduced from NF ROIs during hypotension to LF after MCAT. ROIs with HF during hypotension either stayed in the same category or reduced to NF after MCAT, but never became LF. Therefore, regional changes of CBF during mild hypotension were predictive of the flow changes in the ischemic brain. AHA-Bugher grant

Rat #2		CBF <sub>70</sub>		
		LF ROI (%)	NF ROI (%)	HF ROI (%)
CBF <sub>MCAT</sub>	LF ROI (%)	3	29	0
CBF <sub>MCAT</sub>	NF ROI (%)	7	53	2
CBF <sub>MCAT</sub>	HF ROI (%)	0	5	1

## EFFECTS OF VOLATILE AGENTS ON NEUROPHYSIOLOGY IN $\alpha$ -CHLORALOSE ANESTHETIZED RATS

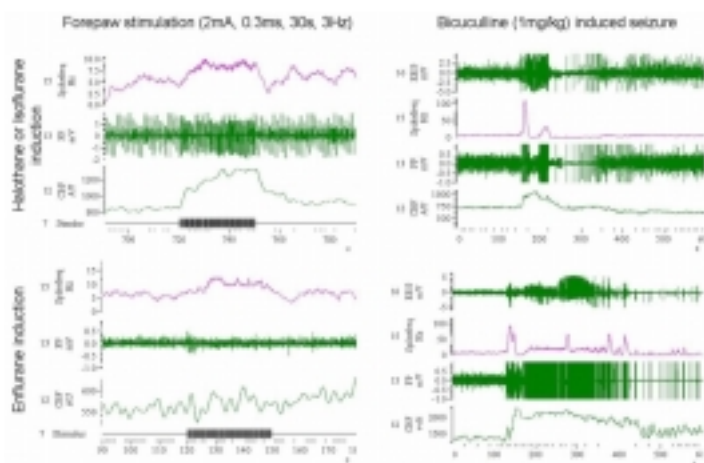
Basavaraju G. Sangannahalli<sup>1</sup>, Peter Herman<sup>1,2</sup>, Fahmeed Hyder<sup>1,3</sup>

<sup>1</sup>*Diagnostic Radiology, Yale University, New Haven, CT, USA*

<sup>2</sup>*Institute of Human Physiology and Clinical Experimental Research, Semmelweis University, Budapest, Hungary*

<sup>3</sup>*Biomedical Engineering, Yale University, New Haven, CT, USA*

The mechanisms by which volatile anesthetics reduce neuronal activity in the mammalian central nervous system still need to be clarified [1,2]. Previous studies have shown that volatile anesthetics reduced neuronal activity in various parts of the CNS [3,4]. A mechanism that may contribute to neuronal depression concerns the effects on GABAA receptors [5]. The extent to which an increase in GABAA mediated synaptic inhibition contributes to the decreased neuronal firing must be explored further. In the present work, we have compared the effects of induction with volatile anesthetic agents halothane, isoflurane, and enflurane on neuronal activity and CBF of somatosensory cortical neurons *in vivo* for  $\alpha$ -chloralose (40 mg/kg/hr) anesthetized rats, in the absence and presence of the competitive GABAA antagonist bicuculline (1 mg/kg). Sprague-Dawley rats were tracheotomized and artificially ventilated (70% N<sub>2</sub>O, 30% O<sub>2</sub>). During the animal preparation halothane (0.7%) / isoflurane (0.5%) / enflurane (0.5%) were used for induction. The figure shows changes in CBF and neuronal activity obtained during forepaw stimulation (2mA, 3Hz, 30s) of rat in the somatosensory cortex (left panel) and during bicuculline induced seizure (right panel) under halothane/isoflurane or enflurane induction. With sensory stimulation there were increases in neuronal spiking frequency, local field potential, and CBF responses both when halothane and isoflurane were used for induction. In contrast enflurane-induction failed to produce very significant CBF responses to the same stimulation paradigm. To compare the effectiveness of the above-mentioned volatile induction agents in reducing neuronal activity and CBF, experiments were performed in presence of bicuculline. In the case of halothane and isoflurane induction, the patterns of the induced seizure were similar. On the contrary enflurane-induction showed a different pattern of seizure activity. Our results indicate that the above-mentioned volatile induction agents increased GABAA mediated synaptic inhibition and acted differently on GABAA receptors. In view of these findings we suggest that even mild exposure to volatile induction agents can have varied effects on GABAA receptors, which consequently affected stimulation-induced changes in neuronal activity and CBF responses. Supported by NIH (DC-003710, MH-067528) and NSF (DBI-0095173) grants. [1] Franks et al., Nature 367:607-14, 1994 [2] Langmoen, Eur J Anesth 12:51-58, 1995 [3] Nicoll et al., Science 217:1055-1057, 1982 [4] Antkowiak et al., Anesthesiology 88:1592-1605, 1998 [5] Campagna et al., N Engl J Med 348:2110-2124, 2003.





**CELL-SPECIFIC EXPRESSION AND FUNCTION OF IKCa CHANNELS IN  
CEREBRAL ENDOTHELIAL CELLS BUT NOT SMOOTH MUSCLE CELLS:  
RELEVANCE TO THE MECHANISM OF EDHF-MEDIATED DILATION**

Christina Hatfield<sup>1</sup>, Marrelli Sean<sup>1,2</sup>

<sup>1</sup>*Department of Anesthesiology, Baylor College of Medicine, Houston, TX, USA*

<sup>2</sup>*Department of Molecular Physiology and Biophysics, Baylor College of Medicine, Houston, TX, USA*

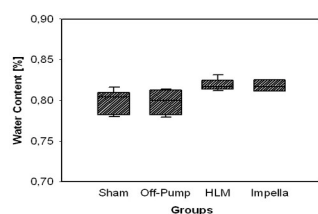
Background: We recently hypothesized that EDHF-mediated dilations in cerebral arteries and arterioles involves hyperpolarization of the endothelium by activation of intermediate-conductance Ca<sup>2+</sup>-sensitive K channels (IKCa) as a critical initiating step. Whole vessel studies are consistent with this hypothesis in the rat middle cerebral artery (MCA). However, the specific cell type(s) that express functionally relevant IKCa channels remains to be demonstrated. Here we provide direct evidence for the cell-specific location of IKCa channels within rat cerebral arteries. Methods: Freshly dispersed smooth muscle or endothelial cells (10 to 20 cells) were harvested and evaluated by RT-PCR. Two rounds of PCR with nested primers were used to determine cell-specific expression of eNOS, SM22 $\alpha$ , GAPDH, and IKCa. The initial assignment of cell type was based upon morphological criteria at the time of cell harvesting. Confirmation of this assignment was based upon the expression (or lack of expression) of cell specific markers. Protein was evaluated by Western from whole vessel preparations and by immunofluorescence in freshly dispersed cells. KCa channel function (IKCa and BKCa) was evaluated by whole-cell patch clamp in freshly dispersed endothelial and smooth muscle cells. Cultured cells were not used in these studies given that KCa channel expression has been shown to be significantly altered by cell culture. Results: In general, cells that were initially identified as endothelial expressed eNOS but not SM22 $\alpha$ , whereas the reverse was true for cells initially identified as smooth muscle. Results were discarded from samples in which GAPDH was not expressed. IKCa message was found in endothelial cells but not in smooth muscle cells. Western analysis demonstrated IKCa immunoreactivity at the predicted size from MCA protein extracts. The cell-specific origin of the immunoreactivity was assessed in freshly dispersed MCA cells by immunofluorescence. Anti-IKCa immunofluorescence appeared on clusters of small rounded cells that were identified as endothelium in separate experiments. Whole-cell voltage clamp recordings from endothelial cells demonstrated Ca<sup>2+</sup>-sensitive outward current that was blocked by TRAM-34, a selective IKCa channel blocker. Smooth muscle cells did not demonstrate TRAM-34 sensitive current, although they did possess significant current that was sensitive to BKCa channel blockers, iberiotoxin (IbTx 0.1  $\mu$ M) or tetraethylammonium (TEA 2 mM). Conclusions: We conclude that IKCa channels are present and functionally relevant in the endothelium (but not smooth muscle) within cerebral arteries. This cell-specific location of IKCa channels is consistent with the hypothesis that activation of endothelial IKCa channels is 1) capable of hyperpolarizing the endothelium and 2) critical to the mechanism of EDHF-dependent dilation of cerebral arteries. These studies were supported by AHA 0230353N and 0270110N.

## THE EFFECT OF CEREBRAL EMBOLI FORMATIONS AFTER CONVENTIONAL, OFF-PUMP AND ASSISTED BEATING HEART MYOCARDIAL REVASCULARISATION ON REGIONAL CEREBRAL PERFUSION AND WATER CONTENT IN AN ADULT PORCINE MODEL

Benjamin O. Bierbach<sup>1</sup>, Matthias Meier<sup>3</sup>, Walter Kasper-Koenig<sup>1</sup>, Axel Heimann<sup>3</sup>, Beat Alessandri<sup>3</sup>, Georg Horstick<sup>2</sup>, Christian F. Vahl<sup>1</sup>, Oliver Kempfski<sup>3</sup>

<sup>1</sup>Department of Cardiothoracic and Vascular Surgery, <sup>2</sup>II. Medical Department, <sup>3</sup>Institute of Neuropathophysiology, University Hospital Mainz, Germany

**Objectives:** Emboli generation during cardiac surgery is known to contribute to postoperative neurocognitive outcome. Cardiopulmonary bypass (CPB) seems to be a major cause for both intraoperative microemboli generation and cerebral hypoperfusion. In opposition to cardiopulmonary bypass off-pump coronary artery bypass grafting (OPCAB) reduces microemboli generation. On the other hand OPCAB carries the risk for hemodynamic instability due to manipulation on the beating heart. Hemodynamic impairment during surgical revascularisation causes postoperative morbidity and mortality. Therefore an intracardiac left ventricular microaxial bloodpump was used to augment cardiac output during beating heart myocardial revascularisation in this adult porcine model. The effect of these three different operative techniques on emboli generation, cerebral perfusion and water content was studied. **Methods:** In 27 swines a bypass from the internal mammary artery to left anterior descending coronary artery was constructed using CPB with cardioplegic arrest (n=9), OPCAB surgery (n=9) or Impella microaxial bloodpump supported OPCAB (n=9). 9 animals received a sham operation. Emboli count in the right common carotid artery was monitored. Regional cerebral perfusion (RCP) was assessed in 21 biopsies from the Cortex cerebri, Mesencephalon, Hippocampus, Thalamus, Hypothalamus, Medulla oblongata, Pons and Cerebellum with 15µm fluorescent microspheres. Mean arterial pressure (MAP), cardiac output (CO), left ventricular dp/dt (LV dp/dt), LV ejection fraction (LVEF) and arterial blood gases were recorded. These variables were analysed 30 minutes before, several times during the procedure and four hours postoperatively. Four hours after surgery the brain was removed and the water content in a part of the frontal lobe was determined. **Results:** During CPB and Impella assistance a significant amount of embolies were registrated. A minimal amount of cerebral embolies was counted during OPCAB surgery and in control animals. During CPB regional cerebral perfusion was unaffected, but afterwards RCP showed reactive hyperemia during early reperfusion in all observed areas. During and after OPCAB RCP remained unchanged and showed low flow during and after Impella pump-run (p<0.05). Cerebral water content was significantly increased after CPB and Impella assistance. There was no difference in cerebral water content between control and OPCAB animals. MAP significantly decreased during revascularisation in all groups staying below preoperative values thereafter (p<0.05). After CPB norepinephrine was administered to maintain MAP. CO, LVdp/dt and LVEF were impaired more distinct during OPCAB than Impella (p<0.05) with subsequent recovery. Arterial bloodgases remained stable throughout all experiments. **Conclusions:** Highflow normothermic CPB with cardioplegic arrest led to emboli generation with consecutive cerebral reactive hyperemia although cardiac output, mean arterial pressure and arterial bloodgases stayed in uncritical ranges resulting in a signifcant increase in cerebral water content. OPCAB surgery did not generate significant cerebral emboli load. However hemodynamic depression without adverse effects on RCP was observed. Hemodynamic depression can be reduced by the Impella bloodpump. On the other hand regional cerebral blood flow is decreased by massive emboli formations resulting in the most pronounced increase in cerebral water content.





## MYOGENIC STRETCH OF OVINE CEREBRAL ARTERIES INDUCES BOTH MLC PHOSPHORYLATION AND THIN-FILAMENT ACTIVATION IN AN AGE-DEPENDENT MANNER

Renan Sandoval, Melody M. Chang, James M. Williams, **William J. Pearce**

*Center for Perinatal Biology, Loma Linda University, Loma Linda, CA, USA*

**Introduction** As we've shown previously, myofilament calcium sensitivity is upregulated in fetal compared to adult cerebral arteries, particularly in response to G-protein receptor agonists. Myogenic reactivity, however, has been suggested to be depressed in immature compared to mature arteries. The present experiments explore the hypothesis that myogenic reactivity is depressed in immature arteries due to attenuation of stretch-induced calcium influx. **Methods** Posterior communicating arteries from term fetal and non-pregnant adult sheep were mounted in vitro for measurement of contractility and exposed to graded stretch between 1.3 and 2.3 times unstressed diameter. In one segment from each animal, the time course of the effects of rapid stretch on cytosolic calcium were determined via Fura-2 photometry. In the remaining segments, the effects of rapid stretch on myosin light chain phosphorylation were determined using urea gels and immunoblotting for myosin light chain. **Results** The magnitude of maximum myogenic tone as a percentage of the maximum contractile response to potassium was similar in adult ( $26\pm 5\%$ ) and fetal ( $24\pm 7\%$ ) arteries, although peak myogenic tone occurred at a lower stretch ratio in fetal (2.1) than adult (2.3) arteries. Graded stretch increased cytosolic calcium significantly more in adult ( $\Delta R=0.292$ ) than in fetal ( $\Delta R=0.108$ ) arteries. Unexpectedly, stretch increased %myosin phosphorylation to similar peak values in fetal ( $45\pm 8\%$ ) and adult ( $41\pm 7\%$ ) arteries. Basal phosphorylation levels were also similar in fetal ( $14\pm 3\%$ ) and adult ( $11\pm 3\%$ ) arteries. The stretch ratios at which peak phosphorylation was observed were far less in both the fetus (1.9) and adult (1.9) than were required to produce maximum myogenic tone. Plots of %myosin phosphorylation against stretch yielded a sigmoidal relation in adult arteries, indicating stretch-induced thin filament activation. This relation was absent in fetal arteries. **Discussion** The present results refute the idea that myogenic tone is depressed in immature cerebral arteries, when tone is normalized relative to maximum potassium-induced contractile capacity. Stretch-induced increases in cytosolic calcium were indeed significantly less in fetal than adult arteries, but the extent of stretch-induced myosin phosphorylation was similar in both age groups. This suggests either that the ability of calcium to activate myosin light chain kinase is greater in fetal than adult arteries and/or that myosin phosphatase activity is attenuated in immature relative to mature arteries, particularly during graded stretch. Our finding of a direct relation between %myosin phosphorylation and myogenic tone also suggests a possible mechanism coupling stretch to thin-filament activation. Because this relation was observed in adult but not fetal arteries, it may help explain why myogenic length-tension relations operate over a greater range in mature arteries, and why peak myogenic tone develops at stretch ratios greater than required to produced peak myosin phosphorylation. Whereas the mechanisms coupling stretch to thin filament activation clearly merit further study, it is clear that fetal artery responses to stretch are mediated by a different mix of mechanisms that those governing mature arteries. Regardless, fetal arteries exhibit a well-developed myogenic responses to stretch that no doubt contribute to cerebral autoregulation in the fetus and neonate. Supported by NIH HD31226 and HL54120.

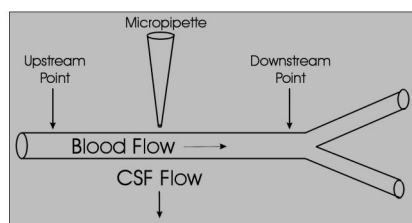
## ROLE OF GAP JUNCTIONAL COMMUNICATION IN PIAL ARTERIOLE DILATION DURING SOMATOSENSORY STIMULATION

Al C. Ngai<sup>1</sup>, Jeffrey J. Iliff<sup>1</sup>, Gavin W. Britz<sup>1</sup>, H. Richard Winn<sup>2</sup>

<sup>1</sup>*Department of Neurological Surgery, University of Washington School of Medicine, Seattle, WA, USA*

<sup>2</sup>*Department of Neurological Surgery, Mount Sinai School of Medicine, New York, NY, USA*

Pial arterioles supplying the hindlimb somatosensory cortex dilate in response to electrical stimulation of the contralateral sciatic nerve. The mechanism of this response is not well understood. One possibility involves the cell-to-cell conduction of dilator signals via gap junctions from parenchymal to pial vessels. To test the hypothesis that sciatic nerve stimulation (SNS)-induced dilation of pial arterioles involves gap junctional communication, we determined if pharmacological gap junction blockers may prevent the dilation response. We performed a craniotomy over the somatosensory cortex of adult chloralose-anesthetized rat to create an open cranial window. A surface electrode was placed in the same area for somatosensory evoked potential (SEP) recording. Through the craniotomy, a segment of a pial arteriole overlying the hindlimb somatosensory cortex was chosen for study (Figure 1). Microscopic streams of the gap junction blockers octanol (4 mM) and carbenoxolone (75 microM) were applied continuously onto a segment of the chosen pial arteriole by pressure-ejection using micropipettes, while vessel diameter was monitored at sites upstream and downstream from the site of application relative to the direction of blood flow (Fig. 1). Warmed mock cerebrospinal fluid was continuously superfused to disperse drugs applied by micropipette. At the upstream site, octanol (n=6) and carbenoxolone (n=6) reversibly attenuated SNS-induced dilation to ~35% and ~30% of the baseline response, respectively. The gap junction blockers did not alter the dilation response at the downstream site. Moreover, the blockade was not due to nonspecific impairment of the response by octanol and carbenoxolone, because 1) dilation to hypercapnia remained intact at both upstream and downstream sites, and 2) SEP did not change. In addition, we evaluated the effect of connexin mimetic peptides homologous to extracellular loop motifs of vascular connexins, on SNS-induced pial dilation. The gap junction peptides, Gap27(37,43) [SRPTEKTIFIL, 250 microM, n=5] and Gap26(37,40) [VCYDQAFPISHIR, 250microM, n=5], were superfused over the pial surface for 120 minutes while the dilation response to SNS was observed at 15-minute intervals. Both peptides significantly reduced SNS-induced dilation (by ~70% and 50%, respectively), without affecting SEP. These results suggest that the dilation response of pial arterioles to somatosensory stimulation involves the conduction of dilator signals via gap junctions along the vascular wall.



## NADPH-OXIDASE ACTIVITY AND FUNCTION IS ENHANCED IN THE CEREBRAL CIRCULATION AND INFLUENCED BY GENDER

Christopher G. Sobey<sup>1</sup>, Grant R. Drummond<sup>2</sup>, Alyson A. Miller<sup>1</sup>

<sup>1</sup>*Department of Pharmacology, University of Melbourne, Parkville, Australia*

<sup>2</sup>*Department of Pharmacology, Monash University, Clayton, Australia*

NADPH-oxidase is now regarded as the major source of reactive oxygen species (ROS) in the vasculature, and sustained high levels of ROS such as superoxide ( $O_2^-$ ) are known to exert damaging, pro-constrictor effects in blood vessels. However, ROS can also act as endogenous signalling molecules within some blood vessels, especially when generated acutely in low levels. In particular, hydrogen peroxide ( $H_2O_2$ ) generated following activation of NADPH-oxidase is an effective cerebral vasodilator *in vivo*, raising the possibility that this enzyme could play a physiological role, at least in the cerebral circulation. However, it is unknown whether NADPH-oxidase activity and function varies between vascular beds. Hence, the first aim of this study was to compare NADPH-oxidase activity in arteries from the rat intracranial (basilar, BA; middle cerebral, MCA) and systemic (carotid, CA; mesenteric, MA; renal, RA; aorta, AO) circulations of Sprague-Dawley rats. Furthermore, although the activity of NADPH-oxidase is reportedly suppressed in the systemic circulation of females, it is unknown whether such gender differences exist in cerebral blood vessels. Therefore, a second aim was to test whether female gender is associated with lower NADPH-oxidase activity and function in the cerebral circulation. NADPH (100  $\mu\text{mol/L}$ )-stimulated  $O_2^-$  production was measured by lucigenin-chemiluminescence. Additionally, ring segments of BA, AO, CA and MA were mounted in a wire myograph or organ bath for recording of isometric tension. NADPH-stimulated  $O_2^-$  production by BA (5312 $\pm$ 431) and MCA (11336 $\pm$ 1020) was 10-80-fold greater than levels generated by AO (534 $\pm$ 40), CA (140 $\pm$ 18), MA (238 $\pm$ 42) and RA (287 $\pm$ 32) ( $P < 0.001$ ). In all vessels NADPH-dependent  $O_2^-$  production was abolished by the NADPH-oxidase inhibitor, diphenyleneiodonium (5  $\mu\text{mol/L}$ ). Either NADPH (10-100  $\mu\text{mol/L}$ ) or  $H_2O_2$  (10-1000  $\mu\text{mol/L}$ ) relaxed precontracted arteries with variable efficacy: BA>MA>AO=CA. Endothelial removal inhibited NADPH-induced relaxation of BA by >50%, whereas it increased relaxation of AO, CA and MA in response to NADPH. Treatment with the  $H_2O_2$  scavenger catalase (1000 units/ml) also prevented NADPH-induced relaxation of BA. Finally, both relaxation of BA and production of  $O_2^-$  in response to NADPH was ~50% smaller in females ( $P < 0.05$ ), whereas relaxation responses to  $H_2O_2$  were similar between genders. Studies in ovariectomized female rats treated with either vehicle or 17 $\beta$ -estradiol (10  $\mu\text{g/kg}$  per d, 14 d) revealed that the gender difference in NADPH-oxidase activity was estrogen-dependent. Thus, NADPH-oxidase activity is profoundly higher in intracranial versus systemic arteries of the rat. Intracranial arteries are also more sensitive to the vasodilator effects of endogenous or exogenous  $H_2O_2$ , consistent with the possibility that ROS derived from NADPH-oxidase play a physiological role as vasodilators in the cerebral circulation. NADPH-oxidase activity and function is suppressed in the female cerebral circulation due to an effect of estrogen.

## ADAPTATION OF THE HYPOTHALAMIC BLOOD FLOW TO CHRONIC NITRIC OXIDE SYNTHASE BLOCKADE

László Hortobágyi<sup>1</sup>, Béla Kis<sup>2</sup>, András Hrabák<sup>3</sup>, Béla Horváth<sup>1</sup>, Péter Sándor<sup>1</sup>,

David W. Busija<sup>2</sup>, **Zoltán Benyó**<sup>1</sup>

<sup>1</sup>*Institute of Human Physiology and Clinical Experimental Research, Semmelweis University, Budapest, Hungary*

<sup>2</sup>*Department of Physiology and Pharmacology, Wake Forest University Health Sciences, Winston-Salem, NC, USA*

<sup>3</sup>*Department of Medical Chemistry, Molecular Biology and Pathobiochemistry, Semmelweis University, Budapest, Hungary*

Nitric oxide (NO) plays an essential role in the maintenance of the resting cerebrovascular tone and CBF. During chronic NO synthase (NOS) blockade, however, the CBF is normalized [1] indicating the activation of compensatory mechanisms. One possibility for the adaptation could be the hyperreactivity of cerebral vessels to NO, since previous studies indicated a remnant 10% cerebral NOS activity during chronic NOS inhibition [1,2] accompanied by a recovery of acetylcholine-induced cerebrovascular relaxation [2]. Another potential compensatory mechanism could be upregulation of vasodilator prostanoids. We attempted to clarify the contribution of these mechanisms to the adaptation of the hypothalamic blood flow (HBF) to chronic NOS blockade. HBF was measured in anesthetized (urethane 1.3 g/kg) male Wistar rats and ex vivo hypothalamic NOS activity was determined as described previously [1]. Chronic NOS inhibition was induced by 1 mg/ml NG-nitro-L-arginine methyl ester (L-NAME) administration in the drinking water. Urinary and CSF concentrations of stable metabolites of vasodilator prostaglandins (PGI<sub>2</sub>, PGE<sub>2</sub> and PGD<sub>2</sub>) were measured by enzyme immunoassay. Semiquantitative RT-PCR analysis of hypothalamic cyclooxygenase mRNA expression was performed as described [3]. One week of L-NAME pretreatment resulted in marked arterial hypertension, but HBF remained unchanged in spite of the significantly reduced hypothalamic NOS activity. Steady state arterial blood gas and acid-base parameters showed no significant differences between control and L-NAME pretreated animals. Reversal of the chronic NOS blockade by intravenous L-arginine infusion (10 mg/kg/min) normalized the blood pressure and at the same time evoked marked hypothalamic hyperemia indicating the presence of a compensatory vasodilator mechanism in the cerebrovascular bed. However, this compensation was independent of the remnant NO production, since intravenous administration of high dose (50 mg/kg) L-NAME after chronic NOS blockade did not influence the HBF. With regard to vasodilatory prostanoids, urinary PGI<sub>2</sub> excretion increased significantly during chronic L-NAME treatment. On the other hand, CSF levels of PGI<sub>2</sub>, PGE<sub>2</sub>, PGD<sub>2</sub> metabolites were similar in control animals and after chronic NOS blockade. Although all three known cyclooxygenase enzymes (COX-1, COX-2 and COX-3) were found to be expressed constitutively in the hypothalamus, none of them showed upregulation during chronic NOS inhibition. General COX blockade by indomethacin (5 mg/kg, iv.) but not specific COX-2 inhibition by diclofenac (10 mg/kg, iv.) decreased the HBF in control rats. Neither of these COX-inhibitors, however, showed an altered response after chronic L-NAME treatment. We conclude that the adaptation of the hypothalamic circulation to the reduction of NO synthesis is independent of the remnant NO production or upregulation of the cerebral vasodilatory prostanoid mechanisms. Constitutive COX-1 or COX-3 activity appears to contribute to the maintenance of the HBF both under physiological conditions and during chronic NOS inhibition. (Supported by the Hungarian OTKA (T037386, T037885, T043075) and ETT (213/2003).) References 1. Benyó Z, Szabó C, Stuijver BT, Bohus B, Sándor P (1995) *Neurosci Lett* 198: 127-30 2. Sercombe R, Issertial O, Seylaz J, Pinard E (2001) *Life Sci* 69: 2203-16 3. Kis B, Snipes JA, Toyohi I, Nagy K, Busija DW (2003) *J Cereb Blood Flow Metab* 23: 1287-92.



**ALLOSTERIC RELEASE OF NITRIC OXIDE FROM HEMOGLOBIN DOES NOT  
MEDIATE NEUROVASCULAR COUPLING**

**Christoph Leithner**<sup>1</sup>, Heike Sellien<sup>1</sup>, Benjamin Rohrer<sup>1</sup>, Georg Roysl<sup>1</sup>, Dirk Megow<sup>1</sup>,  
Jens Steinbrink<sup>1</sup>, Matthias Kohl-Bareis<sup>2</sup>, Ulrich Dirnagl<sup>1</sup>, Ute Lindauer<sup>1</sup>

<sup>1</sup>*Experimental Neurology, Charite Universitätsmedizin, Berlin, Germany*

<sup>2</sup>*University of Applied Sciences Koblenz, RheinAhrCampus, Remagen, Germany*

Neuronal activation leads to an increase in regional cerebral blood flow (rCBF) and blood oxygenation (rCBO). The underlying mechanisms of neurovascular coupling are poorly understood. Recently a new model of activity induced vascular regulation was proposed by Stamler et al. (1997) based on the fact that nitric oxide (NO), a potent vasodilator, binds to hemoglobin in the oxygenated state (oxy-Hb) but is released upon deoxygenation of hemoglobin (deoxy-Hb). It was suggested that during cellular activity oxygen consumption locally increases which causes deoxygenation of hemoglobin and release of NO. Indeed it has recently been shown that red blood cell-bound NO mediates hypoxic vasodilation in vitro, and transpulmonary gradients of hemoglobin-bound NO are evident in patients with congestive heart failure (Datta et al., 2004). According to this elegant model of combined oxygen and NO release, blood flow will be directly matched to tissue oxygen demands. To test this model as a physiological mechanism of neurovascular coupling in the brain, we measured rCBF and rCBO responses to functional activation under hyperbaric oxygenation (3 ATA, FiO<sub>2</sub> 1.0) in the anesthetized rat. During hyperbaric oxygenation oxygen supply to tissue is entirely provided through physically dissolved oxygen. During activation no deoxygenation of hemoglobin and thus no allosteric release of NO occurs. Laser Doppler flowmetry combined with microfiber Hb-spectroscopy was performed through the thinned skull in rats to measure relative changes in rCBF and rCBO and cortical hemoglobin saturation. Averaged rCBF and rCBO responses to electrical forepaw stimulation (3 Hz, 10 s stimulation period) were recorded under normobaric normoxia and compared with responses during hyperbaric hyperoxygenation. Hyperbaric hyperoxygenation increased hemoglobin saturation within the microcirculation from  $44 \pm 2$  to  $103 \pm 3$  %. The deoxy-Hb decrease normally occurring during functional activation disappeared. The oxy-Hb increase was unchanged, and the rCBF response to functional activation was increased but not decreased under hyperbaric hyperoxygenation compared with control responses. In most animals the observed increase in the rCBF response was paralleled by an increase in the amplitude of somatosensory evoked potentials. Our results suggest that in contrast to the in-vitro situation and to pathophysiological conditions of severe hypoxia rCBF regulation during physiological neuronal activation involves other mechanisms than oxygen-dependent delivery and release of NO from hemoglobin.

## QUANTIFICATION OF SMALL MICROVASCULAR SYSTEM MORPHOLOGY IN FIVE RAT BRAIN AREAS

Joseph D. Fenstermacher<sup>1,2</sup>, Shinn-Zong Lin<sup>1</sup>, Joseph A. De Maro<sup>1</sup>, Jia-Yi Wang<sup>1</sup>,

Wendy Akmentin<sup>1</sup>, Gyongyi Gesztelyi<sup>1</sup>, Ling Wei<sup>1,2</sup>

<sup>1</sup>Neurosurgery, State University of New York, Stony Brook, NY, USA

<sup>2</sup>Anesthesiology, Henry Ford Health System, Detroit, MI, USA

**Introduction:** The local microvascular system consists of small arterioles, capillaries, and small venules. In the main, it is this system that is involved when investigating microvascular physiology by quantitative autoradiography (QAR) and other imaging modalities. In a previous animal study, this system was divided into small, medium, and large components based on luminal diameter [1]. The purpose of the present work was to analyze the ultrastructure of these same three groups of microvessels in tissue samples from the previous study, correlate luminal diameter with microvessel type (arteriole, capillary, and venule), and calculate luminal (blood) volumes and surface area of arterioles, capillaries, and venules for five representative brain area. **Methods:** Brain tissue from 5 spontaneously hypertensive (SHR) and 5 Wistar-Kyoto (WKY) rats were fixed; regions of interest (ROIs) were embedded in EPON resin, cut into 2 micron thick sections, and stained with 1% Toluidine blue as described before [1]. Using these sections for guidance, sets of ultrathin sections from five ROIs were prepared. Small microvessels were chosen at random within them and viewed by electron microscopy. The microvessels were sized as: small,  $d \leq 7.5 \mu\text{m}$ ; medium,  $7.5 < d \leq 12 \mu\text{m}$ ; and large,  $12 < d \leq 50 \mu\text{m}$ . The ROI's were the sensorimotor cortex (SMC), inferior colliculus (IC), paraventricular nucleus of the hypothalamus (PVN), the genu of the corpus callosum (GCC), and the subfornical organ (SFO), one of the brain areas with leaky capillaries. **Results:** First, there were no differences between SHR and WKY rats for any of the measured end points, and the data from the two strains have been combined. Of the 181 small microvessels studied in all five ROIs, only one had a bit of discontinuous vascular smooth muscle and appeared to be arteriolar. All the rest (99% of those with  $d \leq 7.5 \mu\text{m}$ ) were capillaries. Pericytes were visible within the basal lamina in 80% of these capillaries. For the SMC, IC, PVN, and GCC, 25% of the 72 medium-sized microvessels examined had vascular smooth muscle and were, thus, arterioles. The remaining 75% of these microvessels ( $7.5 < d \leq 12 \mu\text{m}$ ) were classified as very small venules; pericytes were present in the walls of 84% of them. For these same four ROIs, 23% of the 39 large microvessels ( $12 < d \leq 50 \mu\text{m}$ ) studied were muscular and were, therefore, arterioles. The rest were venules, of which 85% were pericytic. As for the SFO, both the medium ( $n=14$ ) and large ( $n=9$ ) microvessels lacked smooth muscle and were venules. **Conclusions:** Essentially all of the microvessels with  $d \leq 7.5 \mu\text{m}$  are capillaries. Approximately 80% of surface area and 65% of the "blood" volume of the small microvascular system is in the capillaries [1]. About 75% of the medium and large microvessels of this system are venules; the rest are arterioles. These two populations of microvessels have 35% of the morphological blood volume and 20% of the surface area, with 75% of both being venular. **Reference:** Gesztelyi G et al. Brain Res 611:249-257 (1993) Grant support: NIH grants HL-35791 and NS-21157.

**PHYSICAL ACTIVITY PROMOTES ANGIO- AND VASCULOGENESIS IN THE POST-ISCHEMIC BRAIN**Karen Gertz<sup>1</sup>, Josef Priller<sup>1,2</sup>, Golo Kronenberg<sup>1,2</sup>, Helmut Schröck<sup>3</sup>, Ulrich Laufs<sup>4</sup>,**Matthias Endres<sup>1</sup>**<sup>1</sup>*Department of Neurology, Charite Berlin, Berlin, Germany*<sup>2</sup>*Department of Psychiatry, Charite Berlin, Berlin, Germany*<sup>3</sup>*Department of Physiology, University of Heidelberg, Heidelberg, Germany*<sup>4</sup>*Department of Cardiology, Saarland University, Homburg, Germany*

Clinical and experimental evidence supports the notion that regular physical activity up regulates endothelial nitric oxide synthase, improves endothelium-dependent vasorelaxation, and protects from vascular disease. Here, we demonstrate that continuous voluntary training on running wheels via up regulation of endothelial nitric oxide synthase improves neo-vascularization and long-term recovery following mild brain ischemia induced by 30 min filamentous occlusion of the left middle cerebral artery followed by reperfusion in the mouse. Experiments were performed under isoflurane anesthesia in 129/SV wild-type mice or chimeric mice that were transplanted with bone marrow from transgenic mice that express the lacZ gene under control of the endothelial promotor Tie2. In ischemic animals, physical activity conferred up regulation of endothelial nitric oxide synthase in the vasculature and of endothelial progenitor cells in the spleen and bone marrow as measured by FACS analysis and cell culture techniques. This was associated with higher numbers of circulating endothelial progenitor cells in the blood, enhanced neo-vascularization in a disc angiogenesis model, and increased engraftment of Tie2/lacZ positive bone marrow-derived cells in the ischemic brain. Six weeks after the insult, trained animals had higher numbers of newborn endothelial cells in the brain (as determined by bromodesoxyuridine/von Willebrand factor double immunostaining and confocal microscopy) and increased density of perfused vessels with apparent normal morphology (as determined by tiled-field mapping of Evans Blue perfused brains). This conferred sustained augmentation of absolute regional cerebral blood flow in the ischemic lesion in trained vs. sedentary mice at 6 weeks after the insult (as determined by 14-C iodoantipyrine autoradiography). In fact, exercised mice had smaller ischemic lesion sizes (determined on NeuN-immunostained coronal brain sections by computer assisted volumetry), improved functional scores (Bederson test, wire hanging) and better performance in the Morris water maze when compared to sedentary animals. Co-administration of the nitric oxide synthase inhibitor L-NAME in the drinking water not only inhibited up regulation of endothelial progenitor cells by physical activity but also completely abrogated the stroke-protective effects of exercise. In conclusion, voluntary physical activity enhances regeneration in the ischemic brain by endothelial nitric oxide-dependent mechanisms leading to improved neo-vascularization and increased cerebral blood flow.

**ENRICHED ENVIRONMENT AND LEARNING ENHANCES NEUROGENESIS AND PERI-INFARCT NEURONAL DENSITY AFTER CEREBRAL FOCAL ISCHEMIA**Yasuhiko Matsumori<sup>1,4</sup>, Shwuhuey M. Hong<sup>1</sup>, Yang Fan<sup>1</sup>, Zhengyan Liu<sup>1</sup>,Philip R. Weinstein<sup>1</sup>, Chung Y. Hsu<sup>2,3</sup>, **Jialing Liu**<sup>1</sup><sup>1</sup>*Department of Neurosurgical Service, University of California, and VA Medical Center, San Francisco, CA, USA*<sup>2</sup>*Taipei Medical University, Taipei, Taiwan*<sup>3</sup>*Department of Neurology, Washington University, St. Louis, MO, USA*<sup>4</sup>*Department of Neurosurgery, Yamagata University School of Medicine, Yamagata, Japan*

**Background and purpose:** Enriched environment (EE) has been shown to increase neurogenesis in normal adult rodents. Likewise, numerous studies have also shown that cerebral ischemic insult induces neurogenesis. In light of our recent finding suggesting that neurogenesis might contribute to functional recovery after cerebral ischemia, we intend to maximize neurogenesis by increasing the survival of newborn cells in the hippocampus. The aim of this study was to determine the effect of EE and learning on neurogenic activity and the survival of newborn neurons in the dentate gyrus (DG) following ischemic stroke. The effect of running on the treadmill, a widely used rehabilitation therapy, was also explored in rats with focal stroke. **Methods:** Rats were subjected to 90-min right distal middle cerebral artery occlusion (MCAO) and sham surgery, and labeled with BrdU on days 4-7 after MCAO. NMDA was microinjected into layer V cortex to study the effect of excitotoxicity on dentate gyrus progenitor cell proliferation. One to two weeks following MCAO, rats were then placed in standard environment (SE), EE, or subjected to 30-min daily treadmill running for various periods of time from 2 weeks to 2 months. In all groups, the number of BrdU, Ki67 and double cortin immunoreactive cells were quantified in the subgranular zone (SGZ) and granule cell layer (GCL). The number of new neurons was also determined by quantifying the cells double positive for BrdU and NeuN immunostaining. Neuronal density was determined in the ischemic penumbra medial to cortical lesion by unbiased stereology. **Results:** Cerebral focal ischemia induces a transient increase of cell proliferation and neuroblasts in both ipsilateral and contralateral DG SGZ. NMDA microinjected into layer V of cerebral cortex also triggers an increase of cell proliferation in the DG SGZ to a lesser extent compared to MCAO. Majority of the newborn cells induced by cerebral ischemia in the SGZ and GCL died within 2 weeks following cell division with approximately two thirds of the surviving new cells expressing neuronal marker NeuN. An increased survival of newborn cells after MCAO is observed in both EE and running groups, compared to SE. However, EE but not running, restores the total number of neuroblasts after MCAO compared to sham operation. EE also results in the highest newborn neurons compared to running or SE. Furthermore, EE but not running, significantly increases the neuronal density in the ischemic penumbra. DG progenitor cell proliferation induced by running is fast and transient compared to the effect of EE. At 2 months following treatment, running no longer increases progenitor cell proliferation, whereas EE still significantly increases the number of Ki67 immunoreactive cells in the SGZ of both MCAO and sham rats. **Conclusions:** EE enhances neurogenesis, restores neuroblast production, and promote neuronal survival in the ischemic penumbra after MCAO, while running only increases newborn neuron survival. Further study is needed to delineate the mechanisms mediating EE and running enhanced neurogenesis.

**TRANSGENIC VEGF INDUCES POST-ISCHEMIC NEUROPROTECTION, BUT FACILITATES HEMODYNAMIC STEAL PHENOMENA**

Hugo H. Marti<sup>1</sup>, Yaoming Wang<sup>2</sup>, Ertugrul Kilic<sup>2</sup>, Ülkan Kilic<sup>2</sup>, Claudio L. Bassetti<sup>2</sup>, Dirk M. Hermann<sup>2</sup>

<sup>1</sup>*Institute of Physiology and Pathophysiology, University of Heidelberg, Heidelberg, Germany*

<sup>2</sup>*Department of Neurology, University Hospital Zurich, Zurich, Switzerland*

Introduction Vascular endothelial growth factor (VEGF) is a major regulator of new blood vessel growth (angiogenesis) and is required for the ability of the mature vasculature to adapt to tissue hypoxia. In addition, recent reports suggest that VEGF also has neurotrophic and neuroprotective functions. Therapeutic angiogenesis with VEGF is a clinically promising strategy in ischemic disease. The pathophysiological consequences of enhanced vessel formation, however, are poorly understood. In addition, the use of VEGF as a therapeutic agent is hampered by the fact that VEGF is also a major inducer of vascular permeability leading to brain edema. In an attempt to dissect the molecular pathways in vivo between angiogenesis, neuroprotection, and vascular permeability inducing properties of VEGF in the brain we generated transgenic mice overexpressing VEGF specifically in the brain. The aim of the present study was to define the pathophysiological consequences of brain-selective VEGF overexpression in ischemic stroke. Methods Mice expressing human VEGF165 under a neuron-specific promoter were established, which exhibited an increased density of brain vessels under physiological conditions [1]. These mice were submitted to focal cerebral ischemia, as induced by 90 or 30 minutes of intraluminal middle cerebral artery (MCA) occlusion, followed by 24 (90 min) or 72 (30 min) hours of reperfusion [2]. Cerebral blood flow (CBF) was measured using the 14C-iodoantipyrine technique. Results Transgenic mice overexpressing VEGF165 under control of the rat neuron-specific enolase (NSE) promoter are viable and fertile. Transgenic VEGF expression was predominantly found in neuronal cells of the hippocampus, dentate gyrus and cortex while the endogenous mouse VEGF gene is mainly expressed in astrocytes. Analysis of new vessel growth revealed a significant increase in the capillary density in all brain areas analyzed. After transient focal ischemia, transgenic VEGF significantly alleviated neurological deficits and infarct volume and reduced disseminated neuronal injury and caspase-3 activity. Furthermore, Akt activity was increased, confirming earlier in vitro observations that VEGF has neuroprotective properties. Brain swelling was not influenced by VEGF expression, while sodium fluorescein extravasation was moderately increased; suggesting that the higher VEGF levels in transgenic animal induced a mild blood brain barrier leakage. To elucidate whether enhanced angiogenesis improves regional cerebral blood flow in the ischemic brain, 14C-iodoantipyrine autoradiography was performed. Autoradiographies revealed that VEGF induces hemodynamic steal phenomena with reduced blood flow in ischemic areas and increased flow values only outside the MCA territory. Conclusions Our data demonstrate that VEGF protects neurons from ischemic cell death by a direct phosphatidylinositol-3 kinase/ Akt-dependent neurotrophic action rather than by promoting angiogenesis. Our results suggest that strategies aiming at increasing vascular density in the whole brain, e.g. by VEGF overexpression, may worsen rather than improve cerebral hemodynamics after stroke. References [1] Vogel J, Gehrig M, Kuschinsky W, Marti HH (2004) *J Cereb Blood Flow Metab* 24: 849-859. [2] Wang Y, Kilic E, Kilic Ü, Weber B, Bassetti CL, Marti HH, Hermann DM (2005) *Brain* 128: 52-63. Key words vascular endothelial growth factor, angiogenesis, neuroprotection, permeability stroke.

## NEUROTRANSMITTER SYNTHESIS IN NEWBORN NEURONS IN ADULT RAT CEREBRAL CORTEX AFTER PHOTOTHROMBOTIC RING STROKE WITH SPONTANEOUS REPERFUSION

Chao Gu<sup>1</sup>, Per Wester<sup>1</sup>, Wei Jiang<sup>1</sup>, Weigang Gu<sup>1,2</sup>

<sup>1</sup>*Umea Stroke Center, University of Umea, Umea, Sweden*

<sup>2</sup>*Department of Neuroscience and Neurology, University of Umea, Umea, Sweden*

Under physiological conditions, neurons are not regenerated in the cerebral cortex in most mammalian species in the adult brain. However, neurogenesis occurs in the cerebral cortex in adult rats exposed to photothrombotic ring stroke (1) and in the penumbral cortex and ipsilateral striatum in adult rats after middle cerebral artery suture occlusion (2). The functional status of the post stroke cortical neurogenesis is unknown. In our previous studies, newborn neurons were seen to extend neurite like structures, which suggests that these cells might be potentially functional in the post stroke cortex and striatum. Whether or not the newborn neurons may synthesize neurotransmitters is unknown. The present study aimed to explore possible neurotransmitter synthesis during post stroke cortical neurogenesis. The adult male wistar rats, weighing 280-320g, were used for the induction of photothrombotic ring stroke with spontaneous reperfusion and morphological recovery in the cortical region at risk (3). The DNA duplication marker BrdU was intraperitoneally injected (10 mg/kg body weight) repeatedly, which ended at day 7th post stroke. The rats were sacrificed at day 2nd, day 7th and day 30th post stroke. Coronal brain sections were processed for single/double immunohistochemistry and single/double immunofluorescent cell labeling. To identify the newborn cells, mouse anti-BrdU was used. To detect the neurotransmitters in cortical neurons, rabbit anti-Ach, GABA and glutamate were chosen. To examine the acetylcholine synthesizing enzyme, rabbit anti-ChAT (choline acetyl transferase) was used. DAPI was used to counterstain the nuclear DNA. The double/triple immunofluorescently labeled brain sections were analyzed by 3-D confocal microscope. Numerous BrdU immunolabeled cells appeared in the cortical region at risk at post stroke day 2nd, day 7th and day 30th. Under double immunohistochemistry, some of the cortical cells immunolabeled by BrdU in the nuclei were double labeled by Ach, GABA, glutamate or ChAT in the cytoplasm as examined under high magnification light microscope. The double labeled cells were randomly distributed in the cortical layer II to VI, more in the region at risk than in the adjacent cortex. Under 3-D confocal analysis, the BrdU immunolabeled cell nuclei were colocalized with Ach, GABA, glutamate or ChAT in the same cortical cells at various times post stroke. This study suggests that newborn neurons in the post stroke cortex were capable of synthesizing Ach, GABA and glutamate, a process which is of fundamental importance for the new neurons to function in the post stroke adult brains. References: 1. Gu et al. *J Cereb Blood Flow Metab* 2000, 20: 1166 2. Jiang et al. *Stroke* 2001, 32: 1201 3. Gu et al. *Exp Brain Res* 1999, 125: 163

## TRANSFORMATION OF DIFFUSE BETA-AMYLOID PRECURSOR PROTEIN AND BETA-AMYLOID DEPOSITS TO PLAQUES IN THE THALAMUS FOLLOWING TRANSIENT OCCLUSION OF THE MIDDLE CEREBRAL ARTERY IN RATS

Thomas van Groen<sup>1</sup>, Kirsi Puurunen<sup>1</sup>, Hanna-Mari Mäki<sup>1</sup>, Juhani Sivenius<sup>2</sup>,

**Jukka Jolkkonen<sup>1</sup>**

<sup>1</sup>*Department of Neuroscience and Neurology, University of Kuopio, Kuopio, Finland*

<sup>2</sup>*Department of Neurology, University Hospital of Kuopio, and Brain Research and Rehabilitation Center Neuron, Kuopio, Finland*

Cerebral ischemia leads to a transient upregulation and accumulation of  $\beta$ -amyloid precursor protein (APP). For example, APP staining and expression are detected in the subcortical white matter and adjacent to the boundary of the ischemic lesion in the grey matter following transient occlusion of the middle cerebral artery (MCAO). Previous studies, however, have used only short survival periods ranging from days to weeks. The aim of the present study was to assess possible long-term accumulation of APP and A $\beta$  during a 9-month follow-up in rats subjected to transient MCAO. Male Wistar rats were subjected to transient middle cerebral artery occlusion (MCAO) for 2 hours. Sensorimotoric outcome was assessed using a tapered/ledged beam-walking task following operation. The distribution of APP and A $\beta$  was examined immunohistochemically at 1 week, 1 month, and 9 months after MCAO. Histologic analysis revealed severe corticostriatal damage in all MCAO rats. MCAO caused a long-lasting deficit in forelimb and hindlimb function assessed using the beam-walking test. In MCAO rats that survived 1 week, APP staining was present around the ischemic area, in the corpus callosum in crossing axons, in descending axons leaving the lesioned area, and in the terminal zone of these axons in the thalamus. There was staining for both N- and C-terminal APP. Similarly, there was positive A $\beta$  staining in all of these areas. After 1 month survival, some N- and C-terminal APP staining was present around the ischemic area, but most APP was present at the terminal zone of the deafferented axons in the thalamus. Most N-terminal APP was extracellular, in contrast to the C-terminal APP, which was predominantly intracellular. A $\beta$  was stained in a similar pattern in these areas; most A $\beta$  was extracellular, but some staining was present in axons. At 9 months following the MCAO, APP staining was not present around the lesioned area, in the corpus callosum, or in descending axons leaving the lesioned area. In the thalamus in the terminal zone of the deafferented corticothalamic axons, however, there were large, dense deposits, that resembled plaques and consisted of N-terminal APP. These deposits were also positively stained for A $\beta$ , but not for C-terminal APP. In conclusion, C- and N-terminal APP and A $\beta$  staining was present in areas adjacent to the infarct, the corpus callosum, and the thalamus for 1 week after MCAO. The staining of these proteins later disappeared from the cortical areas and white matter, but was still evident in the thalamus 9 months after MCAO. The N-terminal APP and A $\beta$  staining in the thalamus was diffuse acutely after the infarct, but accumulated, leading to dense plaque-like deposits in the ventroposterior lateral and ventroposterior medial nuclei, a finding that has not been reported previously. It is suggested that following focal cerebral ischemia APP and A $\beta$  are transported through corticothalamic axons and secreted at terminals where they form diffuse deposits, which over time develop into plaque-like structures.

**POST-STROKE NEUROGENESIS AND THE NEUROVASCULAR NICHE: NEWLY BORN NEUROBLASTS LOCALIZE TO PERI-INFARCT CORTEX IN CLOSE ASSOCIATION WITH THE VASCULAR ENDOTHELIUM**

**S. Thomas Carmichael, John Ohab, Jimmy Nguyen**

*Geffen School of Medicine At UCLA, Department of Neurology, Los Angeles, CA, USA*

Stroke induces a process of neurogenesis, whereby newly born neuroblasts migrate to areas of injury. This process may provide for endogenous neural replacement after stroke if properly harnessed. Previous studies have defined post-stroke neurogenesis using rat models of large hemispheric stroke, in which the infarct borders the subventricular zone or adjacent medial striatum. We used a model of small cortical stroke in the mouse to study the molecular mechanisms of long distance post-stroke neuroblast migration and localization to peri-infarct cortex. Systemic BrdU injections (i.p.) label doublecortin- and PSA-NCAM-positive neuroblasts predominantly in white matter at day 3 and predominantly in cortex at 7 day post-stroke. BrdU injections into the subventricular zone (SVZ) label doublecortin-positive neuroblasts migrating through white matter to peri-infarct cortex. Stereological quantification of doublecortin-positive neuroblasts in peri-infarct cortex shows that there are no doublecortin positive cells in control cortex, 468 $\pm$ 231 neuroblasts at day 3 and 4304 $\pm$ 1545 doublecortin positive neuroblasts by day 7 post-stroke. By three weeks post-stroke there are many cells that express NeuN that are BrdU positive. These are being quantified. These data show that stroke induces a robust process of migration of newly born neuroblasts from SVZ to peri-infarct cortex over the first week post-stroke, and that a portion of these cells survive and express more mature neuronal markers. In the SVZ neuroblasts develop within close relationship to vascular endothelial cells in an environment termed the neurovascular niche. Because stroke alters the molecular makeup of peri-infarct microvasculature, we hypothesized that stroke induces neuronal migration and localization of neuroblasts through the induction of a novel neurovascular niche in peri-infarct cortex. Mice were given a stroke and allowed to survive 5 days, an intermediate time point for neuroblast migration in this model. Brain sections were stained for two markers of migratory neuroblasts, doublecortin and PSA-NCAM; and three markers of the vascular endothelium: laminin, PE-CAM and intravascularly-perfused *Lycopersicon esculentum* (tomato lectin). Laminin staining visualizes the basal lamina surrounding blood vessels. PE-CAM is expressed by endothelial cells. Tomato lectin, when administered intravascularly prior to sacrifice, labels all endothelial cells that receive blood flow. Neuroblasts closely associate with vascular endothelial cells. Confocal microscopy with three dimensional reconstruction of image stacks shows that neuroblasts wrap around vascular endothelial cells in peri-infarct cortex. In sections stained for PE-CAM, and visualized with intravascular tomato lectin, doublecortin-positive neuroblasts associate with blood vessels at the border of normally perfused and hypoperfused cortical tissue near the infarct. At this site, neuroblasts express  $\alpha$  v integrin, a receptor for laminin, and Tie-2, an angiopoietin receptor. These data indicate that stroke induces neuroblast migration to peri-infarct cortex in close association with vascular endothelial cells in a microenvironment that involves specific vascular growth factors and adhesion molecules.

**ENRICHED ENVIRONMENT ENHANCES THE EXPRESSION OF GENES ASSOCIATED WITH LIPID SYNTHESIS AND TRANSPORT, AND IMPLICATES A NOVEL TREATMENT OF STROKE**

**Tadeusz Wieloch<sup>1</sup>, Donna Oksenberg<sup>2</sup>, Mattias Rickhag<sup>1</sup>, Mehrdard Shamloo<sup>2</sup>, Scott Lohr<sup>2</sup>, Joseph Murray<sup>2</sup>, Morten Krogh<sup>1</sup>, Barbro Johansson<sup>1</sup>, Karoly Nikolich<sup>2</sup>, Roman Urfer<sup>2</sup>**

<sup>1</sup>*Wallenberg Neuroscience Center, Lund University, Lund, Sweden*

<sup>2</sup>*AGY Therapeutics Inc., San Francisco, CA, USA*

The lack of success in finding a neuroprotective treatment against ischemic stroke has directed brain ischemia research towards finding therapies that enhance functional recovery of the surviving brain tissue after the ischemic insult. Clinical experience and experimental evidence have demonstrated that a challenging and stimulating environment enhance neurological recovery after stroke. We employed a genomic approach to elucidate the mechanism of enhanced recovery after stroke, which is provided by housing rats in an enriched environment (Stroke. (1995) 26:644-9). The aim of this study was to identify processes activated during exposure to an enriched environment and that could aid in developing novel stroke treatments particularly directed to stimulate functional recovery. Male SHR rats (Harlan, UK), weighing 243-293 g were used, and permanent occlusion of the middle cerebral artery was performed (Stroke. (1982),13:855-859). Two days after occlusion the rats were tested on the rotating pole (Neuroscience (2003),119:643-52), and rats that were not able to transverse the pole due to neurological deficit were included in the study. The rats were then either housed in a standard housing cages or in cages with ladders, chains, rods and toys for 14 or 60 days. Rats housed in the enriched environment recovered significantly better as has shown earlier. The rats were decapitated and the frontal, middle and caudal cortices, ipsilateral to the lesion, were dissected out. Using nitrocellulose based microarray technology, changes in the levels of mRNA transcripts in the brains from rats exposed to MCAO and housed in standard cages and in an enriched environment, respectively, were analyzed. Rigorous statistical comparison among experimental and control groups was performed, and the expression profile of the individual genes among different brain regions and the two time points were compared using cluster analysis. In one cluster, genes associated with lipid transport and synthesis were enriched, among others the sigma 1- receptor. The increase in gene expression in brains from rats exposed to enriched environment following ischemia was confirmed using in situ hybridization and the level of proteins analyzed by immunohistochemistry using a specific sigma-1 receptor antibody. The sigma-1 receptor was mainly found in astrocytes and oligodendrocytes, where it is known to participate in lipid transport to plasma membrane rafts, but found also in neurons. A ligand to the sigma-1 receptor, AGY 94806, given daily to male SHR rats for 4 weeks starting at 2 days after permanent occlusion of the middle cerebral artery, significantly enhanced recovery of function on the rotating pole test compared to vehicle treated rats. The improvement was of similar magnitude as that of enriched environment when compared to rats housed in standard cages. The sigma-1 receptor ligand stimulated neurite outgrowth in dissociated cortical and pyramidal neurons. We propose that the sigma-1 receptor participates in functional recovery after stroke by supporting axonal outgrowth, stimulating spinogenesis and enhancing synaptic function. The sigma-1 receptor, AGY-94806, may prove beneficial in the treatment of stroke patients starting at 2 days after stroke onset.

**PREMATURE CELLULAR PROLIFERATION FOLLOWING CORTICAL INFARCT  
IN AGED RATS**Aurel Popa-Wagner<sup>1</sup>, Irina Badan<sup>1</sup>, Ivona Dinca<sup>1</sup>, Yalikus Suofu<sup>1</sup>, Raluca Vintilescu<sup>3</sup>,Lary Walker<sup>2</sup>, **Christoff Keesler**<sup>1</sup><sup>1</sup>*Department of Neurology, University of Greifswald, Germany*<sup>2</sup>*Yerkes National Primate Research Center, Emory University, Atlanta, GA, USA*<sup>3</sup>*University of Medicine and Pharmacy, Craiova, Romania*

Old age is associated with an enhanced susceptibility to stroke and poor recovery from brain injury, but the cellular mechanisms underlying such phenomena are not known. Using BrdU-labeling, quantitative immunohistochemistry and 3D-reconstruction of confocal images in a rat model of mild cerebral ischemia, we found that aged rats are highly susceptible to develop an early infarct that is associated with premature cellular proliferation originating from the vascular tree. In aged rats we also found a rapid delimitation of the infarct area by capillary-derived neuroepithelial cells and an early incorporation of these cells into the glial scar. Since most proliferating cells at the infarct site are microglia or nestin-positive cells derived from the vascular wall, we conclude that the vasculature plays a hitherto unrecognized role as a source of proliferating neuroepithelial cells after stroke. Age-associated alterations in the timing and origin of the cytogenic response to cerebral ischemia may underlie the poor functional recovery from stroke. Clarifying the molecular basis of these phenomena could yield novel approaches to enhancing neurorestoration in the elderly.

**POST-ISCHEMIC GENE THERAPY USING THE HEPARIN-BINDING EPIDERMAL GROWTH FACTOR-LIKE GROWTH FACTOR (HB-EGF) GENE PROMOTES FUNCTIONAL RECOVERY AFTER FOCAL CEREBRAL ISCHEMIA IN RATS**

**Shiro Sugiura**, Kazuo Kitagawa, Kenichi Todo, Emi O. Matsuoka, Tsutomu Sasaki,  
Yoshiki Yagita, Takuma Mabuchi, Kohji Matsushita, Masatsugu Hori

*Division of Strokeology, Department of Internal Medicine and Therapeutics (A8), Osaka University Graduate School of Medicine, Suita City, Osaka, Japan*

**Background and Purpose** Recent studies have demonstrated that neurotrophic factors promote neurogenesis following cerebral ischemia. However, as most of them do not pass through the blood-brain barrier and their half-lives are relatively short, continuous or repeated intracerebral or intraventricular infusion would be necessary. Meanwhile, intracerebral gene transfer can result in efficient local production of therapeutic molecules for a longer period by a single injection. Previous studies have indicated that intraventricular administration of heparin-binding epidermal growth factor-like growth factor (HB-EGF), a hypoxia-inducible neuroprotective protein, stimulates neurogenesis in the subventricular zone (SVZ) in both normal and ischemic brains. However, it is still unknown whether proliferating neuronal precursors can differentiate into mature neurons. Moreover, although the implication of HB-EGF in angiogenesis has been reported *in vitro* and in the cornea, there are few reports about the effects of HB-EGF on angiogenesis after cerebral ischemia. Here, we examined the efficacy of intraventricular injection of a recombinant adenovirus expressing HB-EGF (Ad-HB-EGF) on neurogenesis, angiogenesis and functional outcome after cerebral ischemia.

**Methods** Transient focal ischemia was induced by the occlusion of the middle cerebral artery (MCAO) for 80 minutes with a nylon filament in 32 Wistar rats (250 – 300 g). Three days after MCAO, Ad-HB-EGF or Ad-LacZ as a control vector (n = 16, each) was injected into the lateral ventricle on the ischemic side. Bromodeoxyuridine (BrdU; 50mg / kg) was injected intraperitoneally twice daily on the 6th and 7th day. On the 8th or 28th day after MCAO, we evaluated infarct volume, neurogenesis and angiogenesis histologically. Motor function was serially evaluated by the rotarod test after MCAO.

**Results** Adenovirus-mediated gene expression was detected mainly in the ependymal cells at the periventricular area. The EGF-receptor was expressed by the neuronal stem/progenitor cells in the SVZ. There was no significant difference in infarct size between Ad-HB-EGF- and Ad-LacZ-treated rats on the 8th and 28th day after ischemia. Treatment with Ad-HB-EGF significantly increased the number of BrdU-positive cells in the SVZ on the 8th day, compared with Ad-LacZ ( $406 \pm 110$  vs  $236 \pm 92$  cells / mm<sup>2</sup>,  $p < 0.05$ ). In the Ad-HB-EGF-treated rats, some BrdU-positive cells differentiated into mature neurons in the striatum on the ischemic side on the 28th day. To the contrary, newborn mature neurons were seldom observed in the Ad-LacZ-treated rats. Increases in the number of BrdU/laminin-positive cells of microvessels at the peri-infarct striatum were also observed on the 8th day in Ad-HB-EGF-treated rats ( $36 \pm 16$  vs  $6 \pm 6$  cells / mm<sup>2</sup>,  $p < 0.05$ ). Treatment with Ad-HB-EGF significantly improved functional outcome on the 14th, 21st and 28th day after ischemia.

**Conclusions** Our data demonstrated that gene therapy using Ad-HB-EGF contributes to functional recovery following ischemic stroke by promoting neurogenesis and angiogenesis.

## HEMATOPOIETIC CYTOKINES INDUCE REGENERATION IN RAT BRAIN AFTER STROKE

Shunya Takizawa<sup>1</sup>, Hiroshi Kawada<sup>2</sup>, Mitsuyo Tsuma<sup>2</sup>, Tomomi Takanashi<sup>2</sup>, Yuko Morita<sup>1</sup>, Tsuyoshi Uesugi<sup>1</sup>, Tomomitsu Hotta<sup>2</sup>, Shigeharu Takagi<sup>1</sup>, Yukito Shinohara<sup>1</sup>

<sup>1</sup>*Division of Neurology, Department of Internal Medicine, Tokai University School of Medicine, Kanagawa, Japan*

<sup>2</sup>*Division of Hematology, Department of Internal Medicine, Divisions of Hematology, Tokai University School of Medicine, Kanagawa, Japan*

**Introduction:** In the bone marrow (BM), in addition to hematopoietic stem cells and supportive stromal cells, there are multipotent adult progenitor cells, which can differentiate, not only into mesenchymal cells, but also into cells with visceral mesoderm, neuroectoderm and endoderm characteristics in vitro. The purpose of this study is to clarify whether BM-derived cells can differentiate into neuron, astrocyte, microglia and endothelium in response to cerebral focal ischemia, and whether hematopoietic cytokines enhance neurogenesis from intrinsic neural stem cells. Further, we evaluate the effect of cytokines on brain functions. **Methods:** BM cells sampled from the long bone in male C57 Black/6 green fluorescent protein (GFP)-expressing transgenic mice, were transplanted into female C57 Black/6 mice. One month later, the left middle cerebral artery was occluded under halothane anesthesia. Mice were injected subcutaneously with human recombinant granulocyte colony-stimulating factor (G-CSF) + stem cell factor (SCF) from day 1 to 10 (group A; n=6) or day 11 to 20 (group B; n=6) after occlusion for 10 consecutive days, or vehicle alone (control group; n=12). At 4 weeks after occlusion, brain functions were examined using the rotor rod test and the Morris water maze test, and mice were then sacrificed. GFP epifluorescence was directly detected by confocal microscopy. To identify the cell types derived from BM, double-labelling studies were performed with the use of primary antibodies to neurons (Neu N), astrocytes (GFAP), microglia (F4/80) and endothelial cells (CD31). Separately, we intraperitoneally administered the cell proliferation-specific marker, bromodeoxyuridine (BrdU), to C57 Black/6 mice with focal ischemia that had received G-CSF+SCF (n=6) or no cytokines (n=6), then sacrificed them at 21 days after occlusion. Brain sections processed with double-immunofluorescent staining were scanned by confocal microscopy. **Results:** 1) GFP-expressing cells, considered to be bone marrow-derived, were observed in the perivascular position, ependyma and parenchyma, in the peri-infarct and infarct areas. 2) GFP-expressing cells were identified mainly as microglia, and partly as neurons and endothelial cells. 3) BrdU-positive cells in the infarct area were increased by cytokine treatment. 4) The rotor rod test result in group B was significantly better than that in group A or the control group ( $p < 0.05$  and  $p < 0.01$ , respectively). The water maze test result in group B was also significantly better than that in the control group ( $p < 0.0001$ ). **Conclusions:** Administration of hematopoietic cytokines in the late phase of focal ischemia (day 11 to 20) significantly improved motor and cognitive functions. This result may be partly caused by regeneration of impaired brain tissues with BM-derived cells, and mainly by the enhancement of neurogenesis from intrinsic neural stem cells. This finding may suggest a new therapeutic strategy to enhance neurogenesis after stroke in the clinical field.

## EXPRESSION OF NEUROCAN AFTER TRANSIENT MIDDLE CEREBRAL ARTERY OCCLUSION IN ADULT RAT BRAIN

Kentaro Deguchi<sup>1,2</sup>, Mikiro Takaishi<sup>2</sup>, Takeshi Hayashi<sup>1</sup>, Atsuhiko Oohira<sup>3</sup>, Shoko Nagotani<sup>1</sup>, Guang Jin<sup>1</sup>, HanZhe Zhang<sup>1</sup>, XiQuan Wang<sup>1</sup>, Yoshihide Sehara<sup>1</sup>, Isao Nagano<sup>1</sup>, Mikio Shoji<sup>1</sup>, Masahiro Miyazaki<sup>2</sup>, Nam-ho Huh<sup>2</sup>, Koji Abe<sup>1</sup>

<sup>1</sup>Department of Neurology, Graduate School of Medicine and Dentistry, Okayama University, Japan

<sup>2</sup>Department of Cell Biology, Graduate School of Medicine and Dentistry, Okayama University, Japan

<sup>3</sup>Department of Perinatology, Institute for Developmental Research, Aichi, Japan

**Background:** Neurocan is one of the major chondroitin sulfate proteoglycans in the nervous tissues, whose expression and proteolytic cleavage are developmentally regulated. Full-length neurocan (275 kD) is cleaved to yield C-terminal (150 kD) and N-terminal (130 kD) fragments in the adult brain. Both full-length and N-terminal neurocan inhibit axonal extension or regeneration, indicating their important roles in the brain after ischemia. In the present study, therefore, we investigated the expression of neurocan in the brain after ischemia. **Methods:** We used male Wistar rat of 12-weeks old. Under the anesthesia with nitrous oxide and halothane, the origin of the right middle cerebral artery (MCA) was occluded using a nylon thread. Ninety minutes later, the cerebral blood flow (CBF) was restored by removal of the thread. The animal was decapitated at 1, 2, 4, 10 and 20 days after the reperfusion and the brain was used for the immunohistochemical and Western blotting analysis as described below. The distribution of neurocan overexpression was investigated by immunohistochemical analysis. We carried out double staining of neurocan and glial fibrillary acidic protein (GFAP) in order to investigate the relationship between neurocan expression and reactive astrocytes. The temporal profile of neurocan expression was investigated by Western blot analysis (n=3 for each time point). **Results:** Immunohistochemical analysis showed that a strong signal for neurocan appeared 4 days after reperfusion in the peri-ischemic region of cerebral cortex and caudate (Fig. 1). Double fluorescence study showed that many GFAP-positive cells existed in the area of strong neurocan expression, indicating that neurocan should be produced by reactive astrocytes. Western blot analysis showed that the full-length neurocan appeared in the peri-ischemic region from 1 to 20 days after reperfusion with a peak at 4 days (Fig. 2). **Conclusion:** Full-length neurocan was increased at the peri-ischemic region of ischemic brain. Accumulation of the full-length neurocan produced by reactive astrocytes may be one of the processes for tissue repair and reconstruction of neural networks after focal brain ischemia as well.

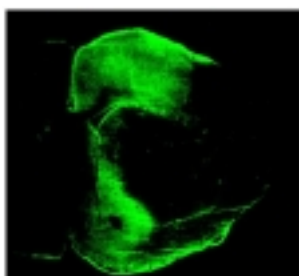


Fig.1 Immunohistochemistry for neurocan

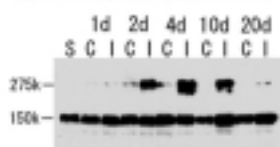


Fig.2 Western blot analysis for full-length (275 kD) and C-terminal (150 kD) neurocan  
S, sham operated; C, contralateral cortex  
I, ipsilateral cortex



## VASCULAR AND HAEMODYNAMIC RESPONSE FOLLOWING CHRONIC HYPOPERFUSION IN THE DEVELOPING AND MATURE RAT

Mankin Choy<sup>1</sup>, Mark F. Lythgoe<sup>1</sup>, Vijeya Ganesan<sup>2</sup>, David L. Thomas<sup>3</sup>, John S. Thornton<sup>1</sup>, Ted Proctor<sup>1</sup>, Louise van der Weerd<sup>1</sup>, David G. Gadian<sup>1</sup>

<sup>1</sup>*RCS Unit of Biophysics, Institute of Child Health, London, UK*

<sup>2</sup>*Radiology and Physics, Institute of Child Health, London, UK*

<sup>3</sup>*Department of Medical Physics and Bioengineering, University College London, London, UK*

Arterial occlusion is one of the main mechanisms leading to hypoperfusion. Vascular growth and collateral circulation can compensate for arterial occlusion and reduce the effects of hypoperfusion. Aberrations in blood flow due to arterial occlusion have been identified in childhood pathologies, yet there have been limited experimental investigations in the vascular response of the developing brain. Therefore we have investigated the chronic vascular and morphological changes following bilateral common carotid occlusion (BCCAO) in both the mature and developing brain using MRI and histology. Four adult male rats were studied in experiments where CBF was measured before and immediately after BCCAO surgery. For chronic experiments 8 adult rats and 8 newborn pups (3-day old) were subjected to BCCAO or sham surgery. Single slice coronal images were obtained 3.3mm from bregma on a 2.35T SMIS system using dedicated sequences to measure CBF, T1, T2 and ADC. A high-resolution SE anatomical scan was obtained with 128 x 128 pixels, 1mm slice thickness, 17 slices, FOV 30mm. MR angiography (MRA) of the neck was done with 128 x 128 x 128 pixels, FOV 25 x 25 x 30mm and visualisation by maximal intensity projection (MIP) software. To visualise the cerebro-vascular structure papaverine hydrochloride was injected intravenously to induce maximal dilatation and India ink was subsequently injected. There were significant reductions in CBF immediately after BCCAO surgery in the cortices and hippocampi (~50%) and a 20% decrease in the thalami, but no reduction in the apparent diffusion coefficient (ADC) was observed, therefore oligoemic hypoperfusion was established. However, 6 months following surgery, CBF was restored in both adults and pups. No changes were observed in the ADC, T1 or T2 values 6 months post-surgery. To investigate the underlying mechanism for the return of CBF to control values, we performed MRA of the neck. As expected, signal from the common carotid arteries was present in the sham-operated rats, but was absent in the BCCAO animals. Interestingly, signal from the vertebral arteries appeared to be enhanced and the presence of collateral formation was evident. Two observers blinded to the experiment evaluated the MRA images and reported more tortuous vertebral arteries in the BCCAO adults and more midline collaterals in the BCCAO pups indicating different extracerebral modes of adaptation dependent on the age at onset of the insult. Furthermore, the vessel diameters of various arteries which make up the circle of Willis were measured 6 months after surgery. Highly significant ( $p < 0.001$ ) differences were seen between sham-operated and BCCOA animals in the basilar, posterior cerebral, posterior communicating arteries and in the internal carotid and anterior cerebral arteries ( $p < 0.01$ ). Interestingly, no significant differences were observed between adult and neonatal age-groups for any of the vessels measured (2-way ANOVA). Our studies suggest that the developing and mature animal exhibit different patterns of arteriogenesis and that the BCCAO hypoperfusion model will be useful for investigating responses to vaso-occlusive disease. Further, non-invasive MRI measurements of cerebral haemodynamics may provide a useful indicator of the homeostatic responses to chronic hypoperfusion.

## CEREBRAL ISCHEMIA DISRUPTS THE EXPRESSION OF REGULATORS OF SYNAPTIC CELL ADHESION IN SYNAPTOSOMES

Willard Costain, Arsalan Haqqani, Ingrid Rasquinha, Edward Preston, Jaqueline Webster, Danica Stanimirovic

*Institute for Biological Sciences, National Research Council, Ottawa, ON, Canada*

**Introduction:** Dramatic and rapidly reversible structural changes are observed in dendritic spine morphology following excitotoxic or hypoxic stress(1). However, morphological and biochemical alterations in post-synaptic densities persist for up to 24 hours following transient ischemia. This suggests that the synapse may be the origin of signals that propagate toward the cell body and instigate delayed post-ischemic neuronal death. Synaptically localized cell adhesion molecules are important regulators of synaptic plasticity and synaptogenesis. Regulation of cell adhesion and cytoskeletal structure in dendritic spines is necessary for the maintenance of mature synaptic connections. Therefore, we examined the effects of transient cerebral ischemia on the expression of synaptic proteins 20 hours post-ischemia. **Methods:** Adult male C57 mice were subjected to a transient (60 min) middle cerebral artery occlusion (MCAO) followed by 20 h of reperfusion. Synaptosomes were prepared from both the contralateral and ipsilateral hemispheres using the density gradient centrifugation method and characterized by electron microscopy. Synaptosomal cell adhesion molecule expression was determined using western blots. Synaptosomal proteins were ICAT-labeled, digested and analyzed by nanoLC-MS mass spectrometry. In-house software was used to identify differentially expressed paired ICAT peaks, which were then sequenced by nanoLC-MS/MS. **Results:** Using western blot, it was found that Agrin and Catna2, but not GluR2, were significantly reduced 20 hours after MCAO (Figure 1). ICAT protein profiling experiments (Table 1) revealed the prominent over-expression of the actin binding protein dystrophin as well as various forms of tubulin. Several mitochondrial proteins were prominently under-expressed indicating substantial mitochondrial damage. **Conclusions:** Cerebral ischemia has a lasting effect on the expression of proteins that regulate synaptic plasticity, in particular cytoskeletal proteins including the actin interacting proteins Catna2 and Dmd and the tubulin subunits. These findings indicate that a prominent re-organization of the synaptic cytoskeletal architecture occurs following cerebral ischemia. This is accompanied by a decrease in the metabolic capacity of the perisynaptic area, as evidenced by the decrease in mitochondrial enzymes. This study demonstrates that the synaptic proteome is dramatically affected by cerebral ischemia and indicates the occurrence of extensive synaptic remodeling. 1. J. S. Park, et al., *Neurobiol Dis* 3, 215-27 (1996).

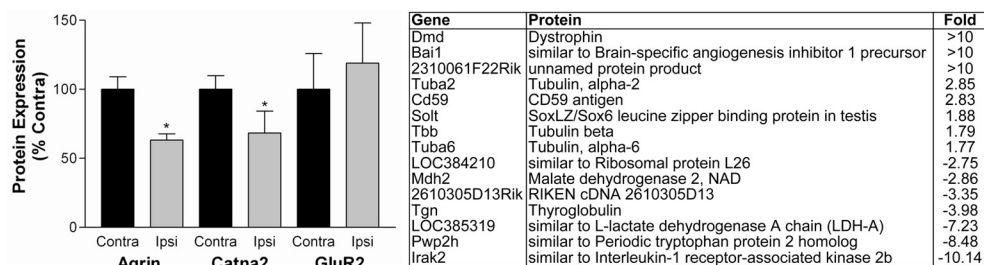


**Figure 1.** Cerebral ischemia alters synaptosomal protein expression as determined by western blot.

Gene	Protein	Fold
Dmd	Dystrophin	>10
Bai1	similar to Brain-specific angiogenesis inhibitor 1 precursor	>10
2310061F22Rik	unnamed protein product	>10
Tuba2	Tubulin, alpha-2	2.85
Cd59	CD59 antigen	2.83
Solt	SoxLZ/Sox6 leucine zipper binding protein in testis	1.88
Tbb	Tubulin beta	1.79
Tuba6	Tubulin, alpha-6	1.77
LOC384210	similar to Ribosomal protein L26	-2.75
Mdh2	Malate dehydrogenase 2, NAD	-2.86
2610305D13Rik	RIKEN cDNA 2610305D13	-3.35
Tgn	Thyroglobulin	-3.98
LOC385319	similar to L-lactate dehydrogenase A chain (LDH-A)	-7.23
Pwp2h	similar to Periodic tryptophan protein 2 homolog	-8.48
Irak2	similar to Interleukin-1 receptor-associated kinase 2b	-10.14

**Table 1.** Focal cerebral ischemia induces alterations in synaptosomal protein expression (partial list) as determined by ICAT nanoLC-MS/MS.

**EFFECT OF CILOSTAZOL ON NEURONAL REGENERATION FOLLOWING PERMANENT MIDDLE CEREBRAL ARTERY OCCLUSION IN MICE**

**Hiroyuki Nishimura<sup>1</sup>**, Toshio Takaoka<sup>1</sup>, Takayuki Nakagomi<sup>1</sup>, Hisao Tachibana<sup>1</sup>,  
Hiroo Yoshikawa<sup>1</sup>, Mari Fukunaga<sup>3</sup>, Tatsuya Yamashita<sup>3</sup>, Makoto Ishikawa<sup>3</sup>,  
Akihiro Taguchi<sup>2</sup>, Tomohiro Matsuyama<sup>1</sup>

<sup>1</sup>*Department of Internal Medicine, Hyogo College of Medicine, Nishinomiya, Japan*

<sup>2</sup>*National Cardiovascular Center, Suita, Japan*

<sup>3</sup>*Ohtsuka Pharmaceutical Company, Tokushima, Japan*

**Background:** Cilostazol, a specific phosphodiesterase-3 inhibitor, has been used for atherosclerotic stroke. Another anti-platelet agent, aspirin, is strongly recommended for treating acute ischemic stroke, but the effect of cilostazol has not been approved for use in the acute stage. In the current study, we sought to examine the potential effects of cilostazol on the cerebral infarction and on the functional outcome by using a newly developed mouse model of cerebral infarction which appeared neurogenesis after stroke (1). The model is highly reproducible and survives for more than twelve weeks, and allows us to estimate the effect of cilostazol given immediately after the onset on the chronic phase of stroke. **Methods:** Adult male severe combined immune deficiency (SCID) mice were used in this study. One hour after permanent left middle cerebral artery (MCA) occlusion, cilostazol (60 mg/kg, n=8) and aspirin (60 mg/kg, n=9) suspended with Arabian gum was administrated orally five times within 48 hours. Arabian gum only (n=9) were given as controls. All mice were reared under the free eating baits mixed with each drug (1% of concentration) during the whole post-stroke period. Brain damage was assessed continuously with brain MRI. Brain function was assessed behaviorally at 35 days after MCA occlusion. To examine the neuronal regeneration, mice were perfused with fixative at day 42, and brain was removed. Immunohistochemistry for MAP2, NeuN and PSA-NCAM was performed using vibratome sections. **Results:** The brain damage of all mice examined was restricted to cerebral cortex, when judged by ADC and T2-weighted MRI image. The infarct volume was almost same among three groups until day 3 of post-stroke (day 0: 40 mm<sup>3</sup>, day 1: 50 mm<sup>3</sup>, day 3: 30 mm<sup>3</sup>). The residual volume of ipsilateral cortex also was same among the groups on day 14 and 28, but on day 28 the volume of ipsilateral striatum of mice treated with cilostazol was significantly increased compared with those of other two groups (6.5 vs. 5.7 mm<sup>3</sup>) (P<0.05). Mice treated with cilostazol showed significantly lower locomotor activity than other two groups. Water maze test revealed impaired working memory in all groups of mice at 35 days post-stroke, but mice treated with cilostazol showed significantly better memory than mice treated with aspirin. Immunohistochemistry revealed the expression of small NeuN-positive neuronal progenitor cells located in the corpus callosum of post-stroke brain on day 14 and 28. The number of these cells was higher in cilostazol groups, suggesting that treatment with cilostazol after stroke enhanced neurogenesis. **Conclusion:** These data suggest that administration of cilostazol in acute phase of ischemic stroke is potentially useful as a therapeutic maneuver through the improvement of local cerebral blood flow and acceleration of neurogenesis. Our previous data have shown that neovascularization by transfusion of endothelial stem cells (CD34+) enhances neurogenesis in the same model of infarction (1). Although the precise mechanism is unclear, it is suggested that an increase in cAMP level in endothelial cells contributes to this effects. (1) Taguchi A, et al (2004) *J Clin Invest* 114:330-338.

## ESTROGEN TREATMENT POST EXPERIMENTAL STROKE DOES NOT INFLUENCE RECOVERY OF FUNCTION

Tracy D. Farr<sup>1</sup>, Hilary V.O. Carswell<sup>1</sup>, Lindsay Gallagher<sup>1</sup>, Barrie Condon<sup>2</sup>,

Andrew J. Fagan<sup>1</sup>, Jim Mullin<sup>2</sup>, I. Mhairi Macrae<sup>1</sup>

<sup>1</sup>Wellcome Surgical Institute and 7T MRI Facility, University of Glasgow, Glasgow, UK

<sup>2</sup>Department of Clinical Physics and Bioengineering, Southern General Hospital, Glasgow, UK

**Introduction:** Stroke is the leading cause of disability worldwide. Consequently, the development of therapeutic intervention to aid recovery is essential. The ovarian hormone estrogen has both beneficial and detrimental effects on infarct volume in rodent stroke models. Estrogen has a number of beneficial effects beyond neuroprotection that may make it a candidate for stroke rehabilitation therapy. Specifically, estrogen has been shown to promote synaptogenesis (1), and enhance behavioural performance (2). It may be possible to harness these effects to promote recovery following experimental stroke. This study was designed to assess whether estrogen treatment, administered after infarct evolution is complete, improves recovery of function post-stroke. **Materials and Methods:** Female Lister Hooded rats were ovariectomized and tested for limb asymmetry using the spontaneous forelimb use (cylinder) test. Fourteen days after ovariectomy rats received a diathermy-induced middle cerebral artery occlusion (MCAO). Since infarct size is maximal by 48 hours in this model, at this time infarct volumes were manually delineated through the use of a RARE T2 weighted magnetic resonance imaging (MRI) scan (TR/TE of 5086/73msec, 600µm slice thickness) on a 7T/30 Bruker BioSpec system and corrected for edema (3). Rats were also implanted with high dose slow release pellets of either 17β-estradiol (0.25mg, n=7) or placebo (n=6). Animals were tested for functional recovery at days 4, 18 and 28 post-MCAO. **Results:** There were no differences in infarct size between the groups prior to treatment (unpaired t-test P=0.81): estrogen 29%± 2.4 and placebo 31%± 4.1 (mean± SEM of hemispheric volume). A repeated measures ANOVA revealed significant behavioural deficit post MCAO in the cylinder (Figure 1). Rats increased use of their intact (ipsilateral) forelimb from 20% pre-surgically to 40% post-surgically (F(3,36)=21.729, P<0.001) at the expense of the impaired (contralateral) forelimb (from 20–10%). These deficits remained at 28 days, indicating no recovery of function over time. Estrogen treatment had no significant influence on limb use (F(1,11)=2.827, P=0.9869). **Conclusions:** This is the first study to assess the effects of post-stroke estrogen treatment on recovery. Estrogen had no significant influence on behavioural deficit, indicating that in this form and dose, estrogen does not provide a potential therapy for improving recovery. **Acknowledgements:** This work was supported by a Research Development Grant from SHEFC, and a University of Glasgow PhD studentship, ORS, and Canadian Stroke Network MSc studentship to TDF. **References:** (1)Woolley, C.S. 1998. Estrogen-mediated structural and functional synaptic plasticity in the female rat hippocampus. *Horm Behav.* 34(2): 140-48 (2) Sandstrom, N.J. and C.L. Williams. 2001. Memory retention is modulated by acute estradiol and progesterone replacement. *Behav Neurosci.* 115(2): 384-93 (3)Gerriets, T., E. Stolz, M. Walberer, C. Müller, A. Kluge, A. Bachmann, M. Fisher, M. Kaps and G. Bachmann. 2004. Noninvasive quantification of brain edema and the space-occupying effect in rat stroke models using magnetic resonance imaging. *Stroke.* 35: 556-571

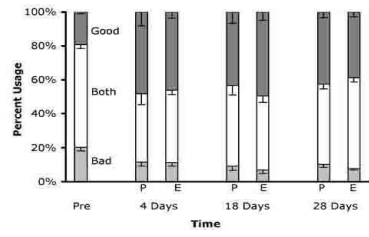


Figure 1. Percent use of each forelimb (ipsilateral-good- dark gray, contralateral-bad- light gray), and a combination of the two limbs (both- white), prior to and at 4, 18 and 28 days post MCAO (means± SEM). P= placebo and E= estrogen-treated animals.

**ISCHEMIC PRECONDITIONING PROMOTES NEUROGENESIS AND ANGIOGENESIS AFTER FOCAL CEREBRAL ISCHEMIA****Seung-Hoon Lee<sup>1</sup>**, Young-Ju Kim, Kyung-Mi Lee, Manho Kim, Byung-Woo Yoon*<sup>1</sup>Department Of Neurology, Seoul National University Hospital, Seoul, Korea*

**Background and Purpose:** A brief cerebral ischemic insult (ischemic preconditioning [IPC]), which is not harmful by itself, results in a temporary protective adaptation in the brain against a subsequent ischemic episode that would otherwise be lethal. Although numerous studies have focused on the underlying protective mechanism, there have been no studies on whether IPC may enhance endogenous neurogenesis and angiogenesis after experimental stroke. **Methods:** Adult Sprague-Dawley rats were preconditioned by a single 10-min occlusion of the middle cerebral artery. After a 48-hour reperfusion, rats were subjected to a 2-hour focal ischemia. All animals received daily intraperitoneal injections of bromodeoxyuridine (BrdU, 100mg/kg), and were sacrificed on 4, 7, 14, or 28 days after focal ischemia. Infarct volume was measured, and a battery of functional tests was also performed. Immunohistochemistry was performed to identify cell proliferation (BrdU), TUJ1, NeuN, GFAP, and vWF. **Results:** Compared to the focal ischemia alone, IPC reduced infarct volume by 35%, and improved neurological performance, which persisted for at least 28 days. At 4 and 7 days, the number of BrdU/TUJ1 double-labeled cells indicating neuroblasts was significantly increased about 3.2-fold in the subventricular zone of the rats treated with IPC. The proportion of neuronal differentiation (BrdU/NeuN double-labeled cells) was also enhanced 2.3 and 3.1-fold at 14 and 28 days, respectively. In addition, IPC significantly promotes angiogenesis at 7 days as indicated by vWF staining. **Conclusions:** We conclude that IPC confers neuroprotection, and promotes endogenous neurogenesis and angiogenesis after focal cerebral ischemia. Biochemical mediators of IPC-induced neurogenesis/angiogenesis remain to be identified for future clinical application.

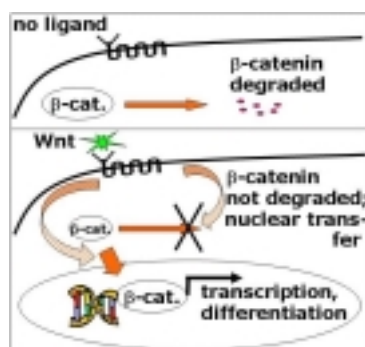
## FUNCTIONAL RELEVANCE OF THE WNT SIGNALING PATHWAY IN ADULT NEURAL STEM CELLS

Martin H. Maurer<sup>1</sup>, Robert E. Feldmann<sup>1</sup>, Fatemeh Sabouri<sup>1</sup>, Heinrich F. Bürgers<sup>1</sup>, Armin Schneider<sup>2</sup>, Wolfgang Kuschinsky<sup>1</sup>

<sup>1</sup>Department of Physiology and Pathophysiology, University of Heidelberg, Heidelberg, Germany

<sup>2</sup>Axaron Bioscience AG, Heidelberg, Germany

**Introduction:** Neural stem cells can be isolated from the adult rat brain. The mechanisms of their proliferation, self-renewal, and differentiation need clarification. We have used proteomic screening to identify new pathways critical to neurogenesis. In this context, a potential pathway is the canonical Wnt signaling pathway. It is known to be activated during embryonic development and neural crest formation. We hypothesize that the Wnt pathway becomes activated in adult neural stem cells when they differentiate into neurons and glia (see figure). **Material and Methods:** Two groups of adult neural stem cells were compared: undifferentiated vs. in vitro differentiated cells. Protein extracts were separated by two-dimensional gel electrophoresis and identified by MALDI-TOF mass spectrometry (Proteosys, Mainz, Germany). RT-PCR was performed for specific sequences of the Wnt signaling pathway and its target genes. Immunostaining was used to determine the degree of the differentiation. Astrocytes were detected by anti-GFAP staining (1:500, BD Biosciences, Heidelberg, Germany), neurons were detected by anti-Map2b and anti-tubulin-IIIbeta staining (1:100, Chemicon, Temecula, CA, USA). Nuclei were counterstained with propidium iodide. The microscope images were analyzed by cell counting where the ratio of marker positive cells and total cell number was compared between the two groups. **Results:** We were able to verify specific sequences of the Wnt signaling pathway and its target genes on the protein level by two-dimensional gel electrophoresis, Western blotting, and immunohistochemistry, and on the mRNA level by RT-PCR. Proteomic comparison of the undifferentiated vs. the in vitro differentiated neural stem cells identified the up-regulated expression of several members of the Wnt signaling pathway including the beta-catenin-binding protein Pontin 52, the Adenomatosis Polyposis Coli binding protein Eb1, and the Rho-binding protein C87222, and the down-regulation of some proteasome subunits. Western Blotting showed a decreased cytoplasmic concentration of beta-catenin in the differentiated neurospheres. RT-PCR confirmed the differential expression of Wnt signaling molecules and respective target genes, including the down-regulation of *bmp4* and *msx1*, and the up-regulation of *GFAP*. Immunostaining showed an increased number of cells positive for the astrocytic marker protein *GFAP*, and the neuronal marker proteins *MAP2b* and *tubulin-IIIbeta* after in vitro differentiation. **Conclusions:** These data are in accordance with the hypothesis that the Wnt signaling pathway is activated during in vitro differentiation of adult neural stem cells, resulting in an increased differentiation into neurons and astrocytes. The data indicate that the canonical Wnt signaling pathway is a main regulatory element for neural stem cell differentiation. **Acknowledgement:** Supported by the German National Genome Research Network NGFN-2 of the German Ministry of Education and Research (BMBF) (to MHM and WK).





**PLASTIC CHANGES IN THE CEREBRAL CORTEX CONTRALATERAL TO AN ISCHEMIC CORE AFFECT MAINLY LAYER III: CONNECTIVITY IS THE KEY****Adriana M. Medina, Martha I. Escobar***Centro de Estudios Cerebrales Universidad del Valle, Cali, Colombia*

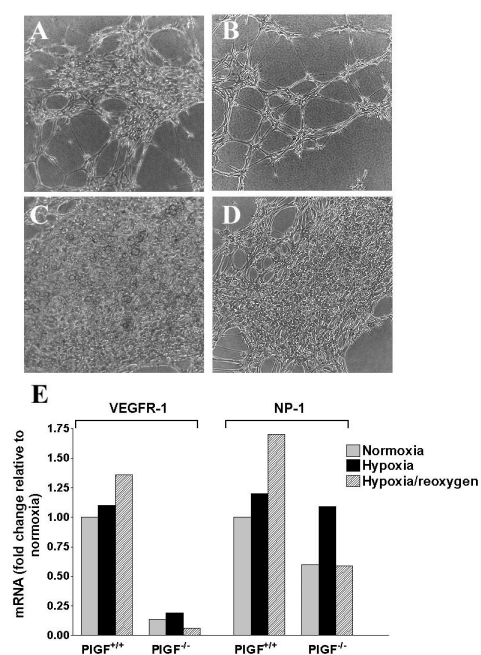
To achieve the presence of changes in the cerebral cortex contralateral to an ischemic core, we used a middle cerebral artery occlusion by intraluminal suture method to induce focal cerebral ischemia in rats. After different survival times (control subjects, 24h, 72h, n=5 each group) the animals were sacrificed by intracardiac perfusion and coronal sections of the brains were processed using an immunohistochemistry protocol with antibodies against the calcium binding proteins parvalbumin and calbindin and the glial glutamate transporter Glt1. To perform the analysis, we selected coronal sections that contain the fronto-parietal transition area, using as a reference the anterior white commissure and the striatum; these structures correspond to the coordinates interaural 9.2 mm bregma 0.2 mm of the Paxinos rat brain atlas. Microscope images were digitalized for cell counting. The results were evaluated using ANOVA statistical analysis. Results. In all periods of survival analyzed, changes in the expression of parvalbumin, calbindin and Glt1 were found in the cerebral cortex contralateral to the ischemic core. These changes were specially notorious on the intermediate layers of the cerebral cortex. Parvalbumin expression is increased from the earlier period of survival time, whereas calbindin expression in layer III is diminished in the acute period of time and then it raises again to reach levels around or beyond normal values. The altered expression of parvalbumin and calbindin may be related to an enhanced excitatory neurotransmission in the cerebral cortex contralateral to the ischemic core, and this hyperexcitability is perhaps facilitated by a decreased glutamate uptake due to the diminishment in Glt1 expression. There are notorious differences in the behavior of cortical layers, and this variation could be associated with specific connectivity pattern of each layer, specially the distribution of callosal terminals arriving from the ischemic core. These axons originate in pyramidal glutamatergic neurons from the ischemic side that make their synapses mainly on basket cells located on layers II, III and IV, inducing transcallosal inhibition. Therefore, when that transcallosal stimulation over this gabaergic cells is diminished or lost due to pyramidal cell death on the ischemic core, an increase of excitatory activity is detected on the contralateral hemisphere. Focal cerebral ischemia induce neural tissue alterations that extend beyond the ischemic core and penumbra and reach distant areas that have synaptic connections with the directly affected neurons. These distant zones are called exofocal, and they must be considered when performing a global analysis of focal ischemia and its consequences.

## ROLE OF PLGF IN HYPOXIA-INDUCED BRAIN ANGIOGENESIS

Moises Freitas- Andrade, Danica Stanimirovic, Maria Moreno

*Institute for Biological Sciences, National Research Council of Canada, Ottawa, ON, Canada*

**Introduction:** Vascular endothelial growth factor (VEGF) mediator family and their receptors are involved in co-ordinated regulation of angiogenesis and neurogenesis after stroke (1). We have recently shown that placenta-derived growth factor (PlGF), a ligand for both VEGFR1 and neuropilin-1 (NP-1), plays a permissive role for VEGF- and astrocyte-induced angiogenic responses of human brain endothelial cells (BEC) (2). The role of PlGF in hypoxia-induced angiogenesis remains unclear. **Methods:** The role of PlGF in hypoxia-induced brain angiogenesis was investigated using cultured BEC and astrocytes (AST) from PlGF wild-type (PlGF<sup>+/+</sup>) and knockout mice (PlGF<sup>-/-</sup>). Cells were subjected to either 3-h or 6-h hypoxia alone or followed by a 16-h reoxygenation. Capillary-like tube (CLT) formation by BEC grown in Matrigel<sup>TM</sup> (an in vitro measure of angiogenesis) was determined as described (2). The expression of PlGF and VEGF/PlGF receptor mRNA was determined by quantitative PCR. **Results:** PlGF mRNA increased >2 fold in both BEC and AST from PlGF<sup>+/+</sup> animals subjected to hypoxia, but returned to control levels after 16 h of reoxygenation. PlGF<sup>+/+</sup> BEC exposed to 3 (Fig 1A) or 6 (Fig 1B) h hypoxia followed by 16 h reoxygenation formed increasing number of CLTs, whereas PlGF<sup>-/-</sup> BEC failed to respond to hypoxia by angiogenic conversion (Fig.1C-D). VEGFR1 (Fig. 1E) and neuropilin-1 (NP-1, Fig. 1E) mRNA expression was significantly lower (~10 and 2-fold, respectively) in PlGF<sup>-/-</sup> compared to PlGF<sup>+/+</sup> BEC. A significant up-regulation of both VEGFR1 and NP-1 mRNAs in PlGF<sup>+/+</sup> BEC was noted during reperfusion, whereas NP-1 mRNA was transiently up-regulated during hypoxia in PlGF<sup>-/-</sup> BEC (Fig 1E). VEGFR-2 expression was not detected in BEC of either genotype. **Conclusions:** The results suggest that PlGF may be important regulator of hypoxia-induced angiogenic transformation of BEC, since both BEC and AST up-regulate PlGF mRNA in response to hypoxia and PlGF<sup>-/-</sup> BEC fail to respond to hypoxia by forming CLTs. The lower basal and hypoxia/reoxygenation-induced VEGFR1 and NP-1 expression in PlGF<sup>-/-</sup> BEC likely contribute to poor angiogenic response of PlGF<sup>-/-</sup> BEC. **References:** 1. Sun Y et al. (2003) *J Clin Invest.* 111:1843-51. 2. Autiero et al. (2003) *Nat Med.* 9:936-43.





## **HYPOTHERMIA FOLLOWING CEREBRAL ISCHEMIA PROVIDES NEUROPROTECTION BUT IS NOT BENEFICIAL TOWARD NEUROGENESIS**

Zonghang Zhao<sup>1</sup>, Jaspreet Kaur<sup>1</sup>, Ping Sun<sup>1</sup>, Lisa Hoyte<sup>1</sup>, Rose Geransar<sup>2</sup>, **Alastair Buchan**<sup>2,3</sup>

<sup>1</sup>*Department of Clinical Neurosciences, Hotchkiss Brain Institute, University of Calgary, Calgary, AB, Canada*

<sup>2</sup>*University of Calgary, Calgary, AB, Canada*

<sup>3</sup>*Oxford University, Oxford, UK*

**Background** Mild post-ischemic hypothermia provides robust protective effects on ischemic brain tissue. There is enhanced neurogenesis following stroke. We tested the effects on neurogenesis of mild hypothermia following cerebral ischemia. **Materials and Methods** Adult male SHR rats were subjected to 90 minutes MCA occlusion and adult male Wistar rats were subjected to 10 min of 4 vessel occlusion. One hour after reperfusion from either focal or global ischemia, rats were randomized to two groups: normothermia and hypothermia. Rats were cooled slowly to 33°C and maintained for 24 h, then slowly warmed to 36~37°C for 48 h. BrdU (50mg/kg) was given i.p. daily starting at day 4 post-ischemia until sacrifice (7 or 28 days). Coronal sections were taken for H&E staining. Immunofluorescent staining with BrdU and NeuN and immunochemistry staining with terminal deoxynucleotidyl transferase-mediated biotinylated UTP nick end labeling (TUNEL) were performed on adjacent sections. BrdU labelling co-localized to the DNA marker DAPI confirmed mitotic proliferation. **Results** In the focal ischemia experiment the total infarct volume was  $33.6 \pm 15$  mm<sup>3</sup> in the normothermic group while hypothermia significantly reduced this damage to  $8.7 \pm 2.9$  mm<sup>3</sup>. There were significantly less BrdU and NeuN double-labelled cells in the hypothermic group compared to the normothermic group ( $61 \pm 45$ /region vs.  $92 \pm 78$ /region,  $p = 0.04$ ). Spearman's correlation test showed a positive correlation between infarct volume and the number of double-labelled cells ( $r = 0.709$ ,  $p = 0.022$ ). A similar phenomenon was observed in the global ischemia experiment. **Conclusion** Our data suggests that mild post-ischemic hypothermia provides neuroprotection but is not beneficial toward neurogenesis.

## NEURAL STEM CELLS DIVISION, MIGRATION, AND DIFFERENTIATION IN NEONATAL RAT BRAIN AFTER ISCHEMIC/HYPOXIC INJURY

Masanori Iwai<sup>1</sup>, Tomoaki Ikeda<sup>2</sup>, Takeshi Hayashi<sup>1</sup>, Guang Jin<sup>1</sup>, Kentaro Deguchi<sup>1</sup>, Shoko Nagotani<sup>1</sup>, Hanzhe Zhang<sup>1</sup>, Yoshihide Sehara<sup>1</sup>, Isao Nagano<sup>1</sup>, Mikio Shoji<sup>1</sup>, Tsuyomu Ikenoue<sup>2</sup>, Koji Abe<sup>1</sup>

<sup>1</sup>*Department of Neurology, Okayama University Graduate School of Medicine and Dentistry, Okayama, Japan*

<sup>2</sup>*Department of Obstetrics and Gynecology, Miyazaki University School of Medicine, Miyazaki, Japan*

**Introduction:** Ischemia/hypoxia (I/H) causes severe perinatal and neonatal brain injury such as periventricular leukomalacia and hypoxic/ischemic encephalopathy. Neural stem cell research can lead to a potential treatment for such disorders. In order to elucidate the dynamic changes of neural stem cells in the neonatal brain after I/H, we investigated new cells proliferation in the subventricular zone (SVZ) and subsequent migration and differentiation of these cells to the injured area. **Methods:** Seven-day-old Wister rats were subjected to ligation of the left carotid artery followed by 2 hours of hypoxic stress (8%O<sub>2</sub> and 92%N<sub>2</sub>, at 33°C). Newly proliferated cells were confirmed by incorporation of bromodeoxyuridine (BrdU). At first, in order to elucidate the dynamic change of neural stem cells in SVZ, single BrdU (50mg/kg) was administered at 1, 7, 14, and 21 days after I/H. Sham control pups received BrdU in the same schedule as the I/H treated pups except for the section of the left carotid artery and the subsequent hypoxia. Brains were retrieved 2 hours after BrdU administration. Next, in order to elucidate migration and differentiation of newly proliferated cells to the injured area, BrdU was administered twice per day at 5-7 days after I/H. Brains were retrieved at 7 (for migration research) 14, and 28 (for differentiation research) days after I/H. Immunohistochemical and immunofluorescent studies were carried out on the lateral ventricle level coronal sections for BrdU, doublecortin (migrating neuronal precursor), NG-2 (oligodendroglial progenitor), Iba-1 (microglia), NeuN (mature neuron) and GFAP (astrocyte). **Results:** The number of BrdU-labeled cells in SVZ both of ipsilateral side and contralateral side of I/H were as twice as sham control level at 7 days after I/H, which returned to sham control level at 21 days. Because it is considered that 7 days is the maximal time of I/H induced cell proliferation, we injected BrdU between 5 and 7 days after I/H and elucidated cell migration and differentiation. Dramatically increased BrdU and DCX double positive cells located at just beneath SVZ where the progenitor cells reside and to the injured area at 7 days after I/H. BrdU and GFAP, NG-2, and Iba1 double positive cells were also increased at the same time. 14 days after I/H, BrdU and NeuN double positive cells were observed sparsely in the peri-injured area of the cortex but not striatum at 14 days after I/H. BrdU and GFAP double positive cells were observed sparsely in the peri-injured area of the striatum but not cortex at 14 days after I/H. There were no such double-positive cells 28 days after I/H. **Conclusion:** Neural stem cells proliferation is enhanced by I/H. Newly proliferated neuronal precursor cells migrate to the infarct region in order to compensate the lost neural cells. However, these neuronal precursor cells hardly survive and differentiate into mature neuron in injured area. The limit of this potential approach for stem cell therapy of neonatal I/H appears to be poor differentiation from neuronal precursors to mature neurons. New strategies to overcome this limitation will be needed.

## QUANTIFICATION OF CEREBRAL HEMOGLOBIN AS A FUNCTION OF OXYGENATION USING NEAR-INFRARED TIME-RESOLVED SPECTROSCOPY IN A PIGLET MODEL

Takashi Kusaka<sup>1</sup>, Sonoko Ijichi<sup>2</sup>, Kenich Isobe<sup>2</sup>, Susumu Itoh<sup>2</sup>

<sup>1</sup>*Maternal and Perinatal Center, Faculty of Medicine, Kagawa University, Kitagun, Japan*

<sup>2</sup>*Department of Pediatrics, Faculty of Medicine, Kagawa University, Kitagun, Japan*

**Introduction:** Near-infrared spectroscopy (NIRS) has been used for measurement of cerebral hemoglobin (Hb) concentrations in neonates to study cerebral oxygenation and hemodynamics. In this study, measurements by portable three-wavelength NIR time-resolved spectroscopy (TRS) were performed in a piglet hypoxia model with various degrees of oxygenation to estimate the absorption coefficient ( $\mu_a$ ) and reduced scattering coefficient ( $\mu'_s$ ) of the head. **Methods:** Measurements of absolute values of  $\mu_a$  at three wavelengths enable estimation of Hb concentration and Hb oxygen saturation in the head (SO<sub>2</sub>). However, there is a problem of which background absorption should be used for estimation of Hb concentration in the head derived from  $\mu_a$  at three wavelengths because it is different from a simple in vitro model. Therefore, we used two different background absorption values with the assumption that background absorption is due only to 85% (by volume) water or that background absorption is equal to absorption of the piglet head with blood exchange transfusion by fluorocarbon (FC), and we compared SO<sub>2</sub> measured by TRS with arterial Hb oxygen saturation (SaO<sub>2</sub>) and sagittal sinus venous Hb oxygen saturation (SvO<sub>2</sub>) measured by a co-oximeter at several inspired fractional O<sub>2</sub> (FIO<sub>2</sub>) concentrations. **Results and Discussions:** It was found that SO<sub>2</sub> values using the absorption of the piglet head with blood exchange transfusion by FC (abs of the head with BET by FC) were not significantly different from SO<sub>2</sub> values using the water only background at FIO<sub>2</sub> in the range of 15% to 100% but that the values using abs of the head with BET by FC were lower than the values using the water only background at FIO<sub>2</sub> in the range of 12 to 4%. The SO<sub>2</sub> values calculated from the water only background were higher than those of SaO<sub>2</sub> at FIO<sub>2</sub> in the range of 10% to 4%. However, SO<sub>2</sub> values using the abs of the head with BET by FC were between those of SaO<sub>2</sub> and SvO<sub>2</sub> over the whole range of FIO<sub>2</sub>. Therefore, abs of the head with BET by FC is more useful for estimation of the absolute values of oxyHb and deoxyHb of the piglet head. **References** Ijichi S, Kusaka T, Isobe K, et al.; *Pediatric Research* 2005 (in press) Ijichi S, Kusaka T, Isobe K, et al; *J Biomed Opt* 2005 (in press) Kusaka T, Hisamatsu Y, Kawada K et al.; *Optical Rev.* 10:466-469 ( 2003)

**DEVELOPMENTAL CHANGES OF OPTICAL PROPERTIES IN INFANTS DETERMINED BY NEAR-INFRARED TIME-RESOLVED SPECTROSCOPY**

Sonoko Ijichi<sup>2</sup>, **Takashi Kusaka**<sup>1</sup>, Kenichi Isobe<sup>2</sup>, Kensuke Okubo<sup>2</sup>, Saneyuki Yasuda<sup>2</sup>,  
Kou Kawada<sup>1</sup>, Susumu Itoh<sup>2</sup>

<sup>1</sup>*Maternal and Perinatal Center, Faculty of Medicine, Kagawa University, Kitagun, Japan*

<sup>2</sup>*Department of Pediatrics, Faculty of Medicine, Kagawa University, Kitagun, Japan*

**Introduction:** During the perinatal period, the brain undergoes anatomical, functional, and metabolic changes. The anatomical changes include neuronal proliferation, migration, organization and myelination, and the metabolic changes match the process of initial overproduction and subsequent elimination of excessive neurons, synapses, and dendritic spines known to occur in the developing brain. Noninvasive assessment of cerebral anatomical changes and of oxygen delivery and utilization is useful for evaluating the effectiveness of therapy and for preventing oxygen toxicity in seriously ill neonates. Near-infrared spectroscopy (NIRS) has been used for measurement of changes in cerebral hemoglobin (Hb) concentrations in infants to study cerebral oxygenation and hemodynamics.

**Methods:** In this study, measurements by time-resolved spectroscopy (TRS) were performed in 22 neonates to estimate the values of light absorption coefficient and reduced scattering coefficient ( $\mu$ 's), cerebral Hb oxygen saturation (ScO<sub>2</sub>), cerebral blood volume (CBV), and differential pathlength factor (DPF), and the relationships between postconceptional age and  $\mu$ 's, ScO<sub>2</sub>, CBV, DPF were investigated. A portable three-wavelength TRS system (TRS-10, Hamamatsu Photonics K.K.) with a probe attached to head of the neonate was used.

**Results and Discussions:** The mean  $\mu$ 's values at 761, 795 and 835 nm in neonates were estimated to be  $6.46 \pm 1.21$  (mean  $\pm$  SD),  $5.90 \pm 1.15$  and  $6.40 \pm 1.16$  /cm, respectively. There was a significant positive relationship between postconceptional age and  $\mu$ 's at those three wavelengths. The mean ScO<sub>2</sub> value was calculated to be  $70.0 \pm 4.6\%$ , and postconceptional age and ScO<sub>2</sub> showed a negative linear relationship. The mean value of CBV was  $2.31 \pm 0.56$  ml/100g. There was a significant positive relationship between postconceptional age and CBV. The mean DPF values at 761, 795 and 835 nm were estimated to be  $4.58 \pm 0.41$ ,  $4.64 \pm 0.46$  and  $4.31 \pm 0.42$ , respectively. There was no relationship between postconceptional age and DPF at those three wavelengths. The results demonstrated that our near-infrared TRS method can be used to monitor  $\mu$ 's, ScO<sub>2</sub>, CBV and DPF in the neonatal brain at the bedside in an intensive care unit.

**References** Ijichi S, Kusaka T, Isobe K, et al; *Pediatric Research* 2005 (in press) Ijichi S, Kusaka T, Isobe K, et al; *J Biomed Opt* 2005 (in press) Kusaka T, Hisamatsu Y, Kawada K et al.; *Optical Rev.* 10:466-469 (2003)

## ADMINISTRATION OF HEMATOPOIETIC CYTOKINES PROVIDES A FAVORABLE MICROENVIRONMENT FOR NEUROGENESIS AFTER STROKE

Yuko Morita<sup>1</sup>, Shunya Takizawa<sup>1</sup>, Tsuyoshi Uesugi<sup>1</sup>, Hiroshi Kawaguchi<sup>2</sup>, Saori Kohara<sup>1</sup>, Yoshiko Shinozaki<sup>2</sup>, Sigeharu Takagi<sup>1</sup>, Yukito Shinohara<sup>1</sup>

<sup>1</sup>*Division of Neurology, Department of Internal Medicine, Tokai University School of Medicine, Tokai, Japan*

<sup>2</sup>*Teaching and Research Support Center, Tokai University School of Medicine, Tokai, Japan*

Introduction: Several studies [1,2], including ours (to be published), have demonstrated that administration of hematopoietic cytokines enhanced the availability of circulating hematopoietic stem cells to the brain, as well as their capacity for neurogenesis and angiogenesis in rats with cerebral ischemia. However, the mechanisms involved in this process are not fully understood. In this study, we investigated whether administration of hematopoietic cytokines influences the microenvironment, such as mRNA expression of tissue cytokines, within ischemic brain. Methods: Focal ischemia was produced by occluding the left middle cerebral artery in male C57 Black/6 mice under halothane anesthesia. Mice were injected subcutaneously with human recombinant granulocyte colony-stimulating factor (G-CSF) + stem cell factor (SCF) from day 1 to 3 (cytokines-treated group; n=5), or non-injected (control group; n=7). Mice were sacrificed at 4 days after occlusion, and the parts of brain tissues corresponding to the core of infarct, peri-infarct, and non-infarct regions were sampled. In each sampled brain region, we checked mRNA expressions of IL-6 and TNF as pro-inflammatory cytokines, IL-10, TGF- $\beta$ 1, TGF- $\beta$ 2 and TGF- $\beta$ 3 as anti-inflammatory cytokines, G-CSF and SCF as hematopoietic cytokines, and iNOS, using RT-PCR. Results: In both control and cytokines-treated groups, the expression of TGF- $\beta$ 1 in the core of infarct and peri-infarct regions, and the expression of TNF in the core of infarct region were significantly higher than those in non-infarct region. However, mRNA expression of TNF in peri-infarct region was suppressed in cytokines-treated group, compared with that in control group. mRNA expressions of IL-6, IL-10, TGF- $\beta$ 2, TGF- $\beta$ 3, G-CSF, SCF and iNOS in any regions did not differ between the two groups. Conclusions: Our results showed that mRNA expression of tissue cytokines within ischemic brain rapidly increased, at least, by 4 days after stroke, and that administration of hematopoietic cytokines suppressed the rise of pro-inflammatory cytokine, TNF in peri-infarct region. Therefore, it is concluded that administration of hematopoietic cytokines may provide a more favorable environment for neurogenesis, especially in peri-infarct region, in addition to its direct effects on bone marrow-derived cells and intrinsic neural stem cells. References: [1] Corti S, et al. Modulated generation of neuronal cells from bone marrow by expansion and mobilization of circulating stem cells with in vivo cytokine treatment. *Exp Neurol* 177:448-52,2002. [2] Shyu WC, et al. Functional recovery of stroke rats induced by granulocyte colony-stimulating factor-stimulated stem cells, *Circulation* 110:1847-54,2004.

## NEUROGENESIS AND DIFFERENTIATION AFTER DOMOIC ACID INDUCED NEURODEGENERATION IN ADULT RAT HIPPOCAMPUS

Kengo Kato<sup>1,2</sup>, Tatsushi Kamiya<sup>1</sup>, Kuniko Shimazaki<sup>2</sup>, Hidenori Yokota<sup>3</sup>, Keiji Oguro<sup>3</sup>, Takahiro Miyawaki<sup>3</sup>, Cikako Nito<sup>1</sup>, Simon Amemiya<sup>1</sup>, Yasuhiro Nishiyama<sup>1</sup>, Satoshi Suda<sup>1</sup>, Toshiki Inaba<sup>1</sup>, Masayuki Ueda<sup>1</sup>, Yasuo Katayama<sup>1</sup>

<sup>1</sup>*Division of Neurology, Second Department of Internal Medicine, Nippon Medical School, Tokyo, Japan*

<sup>2</sup>*Department of Physiology, Jichi Medical School, Tochigi, Japan*

<sup>3</sup>*Department of Neurosurgery, Jichi Medical School, Tochigi, Japan*

**Background and purpose:** Domoic acid (DA), a potent neurotoxin, is structurally related to glutamate analogue kainic acid, called excitotoxins. Administration of DA evokes seizures accompanied by neuronal damage especially in the CA3 hippocampal area. The hippocampus has an important role for memory and learning. Therefore, the injury of this hippocampal area causes memory and learning disturbance, resulting dementia. In the present study, we examined neuronal damage and neurogenesis following administration of DA in the hippocampus in rats. **Methods:** Adult male Wistar rats (6 week) were treated intraperitoneally with DA at dose of 3.5 mg/kg. Rats were perfused with 4% paraformaldehyde and decapitated at 48, 72 hours for TUNEL staining, and at 7 days for HE staining after DA injection. On the regeneration study, BrdU was intraperitoneally administered 24, 48 hours and weekly after DA injection (3.5 mg/kg). 10 weeks after DA injection, rats were sacrificed for BrdU immunohistochemical staining. Double labelling for NeuN, GFAP, MAP2 were also performed. **Results:** DA can more easily transverse through the blood-brain barrier than glutamate. Several peculiar behavioral effects such as epileptic seizures, scratching and autophagia were observed after DA injection. On the histological study, the most extensive damage was observed in the CA3 area of the hippocampus (approximately 60-80%). In the other regions of hippocampus, lesser damage were observed at 7 days postinjection (CA4>CA1>CA2>DG). TUNEL positive cells were observed throughout the hippocampus, especially in the DA area. The distribution of BrdU positive cells was not correlated to the degree of neuronal damage. The BrdU positive cell proliferation was marked in the dentate gyrus subgranular layer. Double staining for NeuN, a marker for mature nerve cells, and BrdU labelling showed that some newly born cells changed to mature neuron. Double staining for GFAP, a marker for glial cells, and BrdU labelling was also observed in the same regions. **Conclusions:** The most extensive neuronal damage was observed in the CA3, with lesser damage observed in the other regions (CA4>CA1>CA2>DG) on the HE stained sections at 7 days after DA injection. TUNEL positive cells did not proceed parallel with neuronal loss. The distribution of the BrdU positive cells were most abundant in dentate gyrus subgranular layer and not correlated to the degree of the neuronal damage.

## UP-REGULATION OF LOW-DENSITY LIPOPROTEIN RECEPTOR EXPRESSION AFTER TRANSIENT MCA OCCLUSION IN RATS

Hiroshi Kamada<sup>1,2</sup>, Takeshi Hayashi<sup>1</sup>, Koji Abe<sup>1</sup>, Pak H. Chan<sup>2</sup>

<sup>1</sup>Department of Neurology, Okayama University, Okayama, Japan

<sup>2</sup>Department of Neurosurgery, Department of Neurology and Neurological Sciences, and Program in Neurosciences, Stanford University School of Medicine, Stanford, CA, USA

**Introduction:** Low-density lipoprotein (LDL) receptor is involved in regulation of cholesterol homeostasis by uptake or removal of apolipoprotein E (ApoE)-containing lipoprotein within the CNS. ApoE plays an important role in the regenerative neural process following brain ischemia. Thus, LDL receptor expression may be related to the changes in cholesterol metabolism and ApoE distribution after brain ischemia. We examined changes in LDL receptor expression after 90 min of transient middle cerebral artery (MCA) occlusion in rats. **Methods:** Male Wistar rats (250-280 g) were used. Under inhalation of a nitrous oxide/oxygen/isoflurane mixture (69%:30%:1%), the right MCA was occluded by insertion of a 4-0 nylon thread. After 90 min of ischemia, cerebral blood flow was restored by removal of the nylon thread. For immunohistochemical studies, the brains were removed 1, 7, 21, and 56 days after reperfusion (n= 6 at each time point, including a sham-operated group). We performed immunohistochemical staining for the LDL receptor, and double staining for the LDL receptor plus microtubule-associated protein 2 (MAP2) or ApoE. **Results:** In the ischemic core, the LDL receptor became positive 1 day after transient MCA occlusion, was not double-positive for MAP2 or ApoE, and disappeared at 7 and 21 days. In the peri-ischemic area, the LDL receptor was observed at 7 days, peaked at 21 days, and was mostly double-positive for MAP2. The number of LDL receptor and ApoE double-positive cells increased at 7 days, and decreased at 21 days, with the shift of LDL receptor immunoreactivity from the cytoplasm at 7 days to dendrites at 21 days in the peri-ischemic area. **Conclusions:** These results suggest that the LDL receptor, interacting with ApoE, is profoundly involved in lipid transport in the CNS for repair of tissue destined to survive in the peri-ischemic area after brain ischemia. We conclude that the LDL receptor and ApoE are molecular markers for neuronal repair in the surviving ischemic tissue. **Grant support:** Grant-in Aid for Scientific Research (B) 15390273, (Hoga) 15659338, and National Project on Protein Structural and Functional Analyses from the Ministry of Education, Scientific, Culture and Sports of Japan, grants from the Ministry of Health and Welfare of Japan, NIH grants P50NS14543, RO1 NS25372, RO1 NS36147, and RO1 NS38653, and the AHA Bugher Foundation.

Table 1. Staining for LDL receptor in cytoplasm (c) or dendrites (d) of rat brain neurons after transient MCAO.

Animal No.	Ischemic core				Peri-ischemic area			
	1	2	3	4	1	2	3	4
Sham control	..	..	..	..	..	..	..	..
1 day	..	..	..	..	..	..	..	..
7 day	..	..	..	..	..	..	..	..
21 day	..	..	..	..	..	..	..	..
56 day	..	..	..	..	..	..	..	..

The symbols .., ., and 21 represent no (0%), slight (10-30%), moderate (50%) and strong staining (80-100%), respectively.

## COMPARISON OF THE REGENERATIVE CAPACITY OF THE CEREBRAL CORTEX IN NEONATAL MICE FOLLOWING TRAUMATIC OR ISCHEMIC INJURY

Richard H. Dyck<sup>1,2</sup>, Kimberley A. Maxwell<sup>3</sup>, Nimet A. Maherali<sup>1</sup>, Jens R. Coorsen<sup>4</sup>

<sup>1</sup>*Psychology, University of Calgary, Calgary, AB, Canada*

<sup>2</sup>*Cell Biology & Anatomy, University of Calgary, Calgary, AB, Canada*

<sup>3</sup>*Neuroscience, University of Calgary, Calgary, AB, Canada*

<sup>4</sup>*Biochemistry & Molecular Biology, University of Calgary, Calgary, AB, Canada*

We have previously shown that the murine medial frontal cortex (MFC) regenerates, anatomically and functionally, when it is removed by aspiration during the early postnatal period. The cells that repopulate the aspirated MFC arise from progenitor cells in the lateral ventricles that migrate into the lesion site rather than to their normal target, the olfactory bulbs. The possibility that the postnatal brain is capable of large-scale neuronal replacement has obvious implications for pathological conditions that result in large areas of cell death, however, this has not been directly addressed. In the present study we assessed whether the neonatal MFC was equally capable of regeneration when it is damaged using a clinically relevant model of injury - stroke. We also set out to identify the molecular factors that affect regeneration following brain injury. We adopted a model of stroke for use in the neonatal mouse that is relatively non-invasive and very reliable in producing an area of injury identical to that provided by the aspiration method. In this model, the photoreactive dye, rose bengal, was injected systemically (50 mg/kg; i.p) on postnatal day (PD) 7 and the MFC was irradiated through the intact skull with laser light (532 nm; 20mW; 90s). This reaction causes platelets to aggregate and a thrombus to form in the laser-exposed blood vessels. The regenerative capacity of the MFC in these animals was compared to that of animals experiencing aspiration lesions on PD7. All animals were administered BrdU (50mg/kg once daily for 2 or 3 days post-lesion) and were allowed to survive from 2 to 8 days post-lesion, after which the brains were removed for anatomical evaluation. The number and phenotypes of cells occupying the aspiration and ischemic lesion area were compared using BrdU, and neuron- and glia-specific antibodies. A proteomics approach was used to investigate the molecular factors affecting regeneration, where we compared the proteins expressed in and around the lesion area from both modes of injury using two-dimensional polyacrylamide gel electrophoresis (2D-PAGE). We found that, unlike aspiration lesions, regeneration of the MFC did not occur following damage induced by focal ischemia. Using 2D-PAGE we were able to resolve and compare the expression of over 1200 proteins in the lesion area; 174 that were unique to aspiration-injury, and 100 that were unique to ischemic injury. The characterization of these proteins will allow us to identify those factors that facilitate or prevent regeneration following injury induced in the neonatal brain.

**FUNCTIONAL RECOVERY AND INCREASED PSA-NCAM EXPRESSION  
FOLLOWING DELAYED ADMINISTRATION OF AN ANTI-MAG ANTIBODY POST  
STROKE IN THE RAT**

**Robert I. Grundy**, Sarah Collier, Colin A. Cambell, Kevin L. Wilson, Jenny C. Roberts,  
Mary Vinson, John B. Davis, Elaine A. Irving

*Neurodegeneration Department, Neurology & GI CEDD, GlaxoSmithKline Pharmaceuticals,  
Harlow, UK*

Stroke often renders its victims functionally impaired for long periods of time if not permanently. Inhibition of regeneration by molecules found in CNS myelin such as myelin-associated glycoprotein (MAG) and Nogo are thought to limit recovery post-stroke. We have previously demonstrated that an anti-MAG antibody, SB680949 administered 1 hour post transient middle cerebral artery occlusion (tMCAO) in the rat results in improved function and neuroprotection (1). In this study we have investigated the potential time window for intervention using this antibody. In addition, we investigated expression of PSA-NCAM, a cell surface macromolecule whose expression is associated with neurogenesis and synaptic plasticity. tMCAO (90 mins) was induced in male Sprague-Dawley rats (300-350g) as described previously (2). Two doses of SB680949 were administered intracerebroventricularly 24 hours apart, starting at 1, 6 or 24 hours following tMCAO. Control animals were dosed with IgG1 control antibody at 24 and 48 hours. Functional ability was assessed weekly using a 32 point composite neuroscore (3) and the cylinder test of forepaw placement (4). At 8 weeks, animals were deeply anaesthetised and perfused fixed with ice cold 4% paraformaldehyde and brains processed for histological assessment. Administration of SB680949 starting at 1 hour, but not at other time points, reduced lesion volume relative to animals injected with control antibody ( $12.3 \pm 2.1$  versus  $20.4 \pm 2.9$  % of contralateral hemispheric volume  $P < 0.05$ ). Administration of SB680949 at 1 hour improved function in the right (impaired) forepaw in the cylinder test at 1, 5 ( $P < 0.05$ ), 7 ( $P < 0.01$ ) and 8 weeks ( $P < 0.01$ ). Administration of SB680949 starting at 24 hour improved function in the right forepaw at 2, 5, 6 ( $P < 0.05$ ), 7 and 8 weeks ( $P < 0.01$ ). When SB680949 administration was started at 6 hours, no beneficial effect was seen in the cylinder test. SB680949 did not positively affect function as assessed by 32 point neuroscore. PSA-NCAM expression increased in the M1 region of the cortex in animals treated with SB680949 starting at 1 hour ( $20.7 \pm 2.5$  PSA-NCAM positive neurones in the non lesioned hemisphere of SB680949 treated animals versus  $13.7 \pm 1.5$  in the non lesioned hemisphere of control treated animals,  $P < 0.05$ ) and 24 hours ( $18.7 \pm 4.5$  PSA-NCAM positive neurones in the non lesioned hemisphere of SB680949 treated animals versus  $11.9 \pm 1.8$  in the lesioned hemisphere of anti-MAG treated animals,  $P < 0.05$ ). These data confirm that early administration of SB680949 results in neuroprotection and improved function. Although when administered 24 hours post stroke anti-MAG treatment fails to offer neuroprotection, the degree of functional recovery is comparable. Increased expression of PSA-NCAM in the motor cortex in the groups displaying improved motor function supports the hypothesis that anti-MAG treatment enhances functional recovery through an increase in neurogenesis and enhanced plasticity. 1) Irving EI, Vinson M. et al., *J. Cereb. Blood Flow and Metab.* in press 2) E. Z. Longa, Weinstein S. et al., *Stroke*, 1989, 20: 84-91. 3) Hunter AJ, Hatcher et al., *Neuropharmacology* 2000, 39: 806-816. 4) T. Schalert, S.M. Fleming et al., *Neuropharmacology* 2000, 39: 777-787.

## IMPACT OF CHRONIC PRENATAL INTERMITTENT HYPOXIA ON NEURONAL MIGRATION

Jennifer Zechel, Michael Buczek, Jorge L. Gamboa, Michelle Puchowitz, W. David Lust

*Neurological Surgery, Case Western Reserve University, Cleveland, OH, USA*

Introduction: Hypoxic-ischemic brain injury is an important cause of morbidity and mortality in the perinatal period, second only to hyaline membrane disease as a major cause of death in pre-term infants<sup>1</sup>. Recent epidemiological studies point to chronic prenatal hypoxia as the most important factor in neurodevelopmental outcome, and that it is associated with mental retardation, SIDS and cerebral palsy. In order to better understand the underlying mechanisms by which intermittent hypoxia (IH) affects prenatal neurological development, we examined neuronal migration and components of peroxisomes, which have recently been implicated in neuronal migration. Methods: Timed pregnant Sprague-Dawley rats were exposed to either normoxia (21% O<sub>2</sub>) or IH (7% O<sub>2</sub> for 8min/hr for 10 hrs) from E3 to parturition. Dams were weighed throughout the gestational period, and offspring were weighed at P1, P5 and P46. To examine neuronal migration, dams were injected i.p. with 0.1mg/g body weight BrdU three times at E18, and pups were culled at P2, 6 and 9. Samples for immunohistochemistry (IHC) were prepared by perfuse-fixation with 4% paraformaldehyde, cryoprotection in 30% sucrose, and then 18 micron sections were taken and immunostained using standard techniques for BrdU and catalase. Catalase activity in brain homogenates ( $x \pm SEM$ ) was measured using the Amplex® Red Catalase Assay Kit (Molecular Probes). Results: Although there were no significant differences between birthweights of pups from control or IH treatments ( $6.44 \pm 0.1g$  and  $6.63 \pm 0.14g$  respectively, mean  $\pm$  SEM); significant differences are apparent at P5 ( $15.1 \pm 0.4g$  for controls and  $13.7 \pm .3g$  for IH) and continued to P46 in both males ( $256.5 \pm 3.2g$  controls;  $230.0 \pm 4.7g$  IH) and females ( $227.5 \pm 18.5g$  controls;  $172.4 \pm 3.7g$  IH). Examination of BrdU injected control animals at P2 shows that cells labeled on E18 have moved from the neuroepithelium into the layers of the cortical plate, but animals from the IH group have a significant number of BrdU positive cells present in the intermediate zones (i.e., layer 5-6) , suggesting a comparatively slower rate of migration in this group. By P6 there are fewer positive cells in the intermediate zones of the IH group, however there are significantly more BrdU positive cells in the cortex of IH animals ( $131.3 \pm 5.5$  cells/field) compared to control animals ( $47.6 \pm 3.6$ ), and by P9 this trend begins to disappear (data not shown). Catalase IHC shows more positive staining in the parietal cortex of IH animals at P6 than control animals, and their catalase activity in brain homogenates is significantly elevated in IH animals at P2 ( $212.8 \pm 13.4$  % of control) and P6 ( $197.5 \pm 18.7$  % of control). Conclusion: Prenatal exposure to intermittent hypoxia has a long term effect on the ability of offspring to thrive as seen by diminished weight gains. We also observed a short term delay in neuronal migration as seen by BrdU labeled cells, possibly as a result of the altered peroxisome function evidenced by elevated catalase activity levels. Prenatal intermittent hypoxia results in certain non-lethal abnormal development abnormalities. 1. Papile, L. A. 'The management of hypoxic-ischemic encephalopathy.' *Pediatr. Ann.* 17.8 (1988): 524-26. Grant support: Supported in part by the Philip Morris External Research Program

**PAIRED-PULSE FACILITATION ANALYSIS OF POST-TETANIC POTENTIATION  
IN THE MURINE HIPPOCAMPAL CA1 REGION****Christian H. Lange-Asschenfeldt<sup>1</sup>, Matthias M.W. Riepe<sup>2</sup>**<sup>1</sup>*University of Ulm, Ulm, Germany*<sup>2</sup>*University of Berlin Charite, Berlin, Germany*

Introduction: Paired-pulse facilitation (PPF) and long-term potentiation (LTP) are different forms of activity-dependent synaptic plasticity common to most chemically transmitting synapses. PPF is observed for short time spans (usually up to hundreds of milliseconds) and believed to be of presynaptic origin whereas LTP may predominantly be postsynaptic and persists for a long time. The initial period of synaptic enhancement in LTP is often particularly strong and is referred to as post-tetanic potentiation (PTP). Interactions of PTP and PPF were studied to clarify the role of presynaptic factors in PTP. Methods: Field excitatory postsynaptic potentials (fEPSP) were evoked from Schaffer collateral-CA1 synapses in acute murine hippocampal slices. LTP was generated by high frequency stimulation (HFS). Paired pulses of different intensity (threshold to maximum fEPSP response), pulse width (20 to 200  $\mu$ s) and interpulse interval (25 to 500 ms) were elicited before and within 5 min after HFS. PPF magnitude was expressed as the ratio of fEPSP slope between the second and the first pulse. Results: HFS resulted in an increase of fEPSP slope of  $174 \pm 26$  % compared to baseline (n=6). The PPF ratio was maximal at interstimulus intervals of 50-125 ms (ranging from 1.4 to 2.5). During PTP, the PPF ratio was significantly attenuated only at the lowest stimulus intensity (15% of maximum intensity,  $p < 0.01$ ) and the shortest pulse duration (20  $\mu$ s,  $p > 0.05$ ) sufficient to evoke fEPSPs. Otherwise, the PPF ratio was not affected by the induction of PTP across a range of stimulus intensities and pulse durations. Conclusions: These findings suggest a mainly postsynaptic locus of PTP. However, as interference with PPF at low intensities and short pulse durations occurred, a limited presynaptic involvement is conceivable.

## THE HEMATOPOIETIC FACTOR G-CSF IS A NEURONAL LIGAND THAT DRIVES NEUROGENESIS

Armin Schneider<sup>1</sup>, Carola Krüger<sup>1</sup>, Tobias Steigleder<sup>2</sup>, Daniela Weber<sup>1</sup>, Claudia Pitzer<sup>1</sup>, Martin Maurer<sup>3</sup>, Nikolaus Gassler<sup>4</sup>, Rainer Kollmar<sup>2</sup>, Stefan Schwab<sup>2</sup>, Hans-Georg Kuhn<sup>5</sup>, **Wolf-R. Schäbitz<sup>6</sup>**

<sup>1</sup>*Axaron Bioscience AG, Heidelberg, Germany*

<sup>2</sup>*Department of Neurology, University of Heidelberg, Heidelberg, Germany*

<sup>3</sup>*Department of Physiology, University of Heidelberg, Heidelberg, Germany*

<sup>4</sup>*Department of Pathology, University of Heidelberg, Heidelberg, Germany*

<sup>5</sup>*Arvid Carlsson Institute for Neuroscience, Gothenburg, Sweden*

<sup>6</sup>*Department of Neurology, University of Münster, Münster, Germany*

**Introduction:** Granulocyte-colony-stimulating factor (G-CSF) is a potent hematopoietic factor that enhances survival and drives differentiation of myeloid lineage cells resulting in the generation of neutrophilic granulocytes. Recently, we have shown that G-CSF reduces infarct volume after acute middle cerebral artery occlusion. Here we focused on a potential recovery enhancing effect of G-CSF in the chronic phase after stroke. **Methods:** G-CSF and G-CSF receptor expression in the brain was studied by immunohistochemistry and PCR of dissected brains and microdissected neurons of the frontal cortex. Neural stem cells were obtained from the hippocampus or subventricular zone of 4-6 week old male Wistar rats and cultivated. Differentiation markers in vitro were assessed by quantitative PCR and FACS analysis. Photothrombotic ischemia was induced in the rat parietal cortex. A battery of behavioral tests was performed to measure functional outcome (rotarod, adhesive removal, beam-balance, neurological severity score). Progenitor activity and neurogenesis were visualized by immunofluorescence and quantified. **Results:** Both G-CSF and its receptor are widely expressed by neurons in the CNS, and their expression is induced by ischemia, suggesting an autocrine protective signalling mechanism. Surprisingly, the G-CSF receptor was also expressed by adult neural stem cells, and G-CSF induced neuronal differentiation in vitro. G-CSF markedly improved long-term behavioural outcome after cortical ischemia while stimulating neurogenesis in vivo, providing a link to functional recovery. **Conclusion:** G-CSF is an endogenous ligand in the CNS that has a dual activity beneficial both to acute neuronal degeneration and long-term plasticity after cerebral ischemia. We therefore propose G-CSF as an ideal new drug for stroke and neurodegenerative diseases.

## INHIBITION OF CYCLOOXYGENASE-2 REDUCES PROLIFERATION OF ENDOGENOUS NEURAL PROGENITORS AND AMELIORATES THE EPILEPTOGENIC PROCESS

Soon-Tae Lee<sup>1</sup>, Kon Chu<sup>1,2</sup>, Keun-Hwa Jung<sup>1</sup>, Seung U. Kim<sup>3,4</sup>, Manho Kim<sup>1</sup>, **Jae-Kyu Roh**<sup>1</sup>

<sup>1</sup>*Stroke & Neural Stem Cell Laboratory in Clinical Research Institute, Department of Neurology, Seoul National University Hospital, Seoul National University, Seoul, Korea*

<sup>2</sup>*Center for Alcohol and Drug Addiction Research, Seoul National Hospital, Seoul, Korea*

<sup>3</sup>*Division of Neurology, Department of Medicine, UBC Hospital, University of British Columbia, Vancouver, BC, Canada*

<sup>4</sup>*Brain Disease Center, Ajou University, Suwon, Korea*

Cyclooxygenase-2 (COX-2), the principal isoenzyme in the brain, modulates inflammation, glutamate-mediated cytotoxicity, and synaptic plasticity. Its major metabolite, PGE<sub>2</sub>, exerts the action via EP1-4 receptor. Status epilepticus (SE) induces the epileptogenic process through the generation of ectopic hilar granule cells, and COX-2 is upregulated during this period. In this study, we investigated whether celecoxib, a selective COX-2 inhibitor, can prevent the epileptogenic process in the pilocarpine-induced SE. Experimental SE was induced with lithium-pilocarpine injection, and celecoxib (20mg/kg, p.o.) were treated at 2 hours after SE and afterwards for 7 or 35 days. BrdU was injected for 7 or 14 days after SE. Spontaneous recurrent seizure (SRS) were video-monitored. BrdU immunohistochemistry was used for the spatial and temporal analysis of hippocampal cell proliferation, and double labellings using NeuN, calbindin or GFAP antibodies were performed. For in vitro study, cultured human neural stem cells (NSCs, F3 cell) were treated with celecoxib, PGE<sub>2</sub>, or EP2 receptor agonist butaprost, and analyzed in means of BrdU / Ki-67 labeling index, cell cycle analysis and MTT assay. Celecoxib treatment reduced neural damage at 7 and 42 days after status epilepticus (esp. CA1, CA3 and Hilar damage) and reduced microglial infiltration after SE. In addition, celecoxib treatment reduced the proliferation of neural progenitors in subgranular layer of dentate gyrus, and reduced BrdU+ /Calbindin+ /NeuN+ cells in hilar areas. No hilar ectopic granule cell can be found in celecoxib-treated group (ectopic granule neurons: 45% of hilar BrdU+ cells in epilepsy-only group vs. 0% in epilepsy-celecoxib group). Most of the BrdU-labeled cells in the hilar area are positive to GFAP. Celecoxib treatment reduced reactive COX-2 expression in the SE-damaged brain, especially in the early period (days 1-7), with a decrease in SRS formation (days 28-42; p<0.05). In vitro analysis showed that celecoxib dose-dependently inhibited proliferation of NSCs with a decrease in BrdU/Ki-67 labeling index and in a proportion of S phase by cell cycle analysis. In contrast, PGE<sub>2</sub> or butaprost treatment increases NSCs proliferation. COX-2 inhibition interfered with cell cycle propagation of NSCs. Taken together, we provide evidences that inhibition of COX-2 prevents the epileptogenic process, which might be due to the neuroprotective and anti-inflammatory effects, and suppression of abnormal neural progenitor proliferation.

## CEREBRAL BLOOD FLOW SPET AND RESPONSE TO ACETAZOLAMIDE CHALLENGE IN PREMATURE CRANIOSYNOSTOSIS BEFORE AND AFTER SURGERY

Mayuki Uchiyama<sup>1</sup>, Hiroshi Nishimoto<sup>2</sup>, Kumiko Nozawa<sup>3</sup>, Eiji Oguma<sup>3</sup>

<sup>1</sup>*Department of Radiology, Jikei University Kashiwa Hospital, Chiba, Japan*

<sup>2</sup>*Department of Neurosurgery, Saitama Children's Medical Center, Saitama, Japan*

<sup>3</sup>*Department of Radiology, Saitama Children's Medical Center, Saitama, Japan*

**Objectives:** The aim of this study was to compare cerebral blood flow single-photon emission tomography (CBF SPET) and vascular reserve in patients with premature craniosynostosis before and after surgery using regional CBF on anatomically standardized resting and acetazolamide (ACZ)-challenged CBF SPET images, which were obtained using 3DSRT, fully automated ROI analysis software. **Method:** Twenty patients with premature craniosynostosis from 5 months to 5 years of age were treated in Saitama Children's Medical Center, 1 patient with cloverleaf skull associated with hydrocephaly, 3 patients with oxycephaly, 7 patients with brachycephaly, 4 patients with scaphocephaly, 3 patients with trigonocephaly, 1 patient with plagiocephaly and 1 patient with lamboid synostosis. Tc-99m ECD brain SPET with ACZ challenge were performed before and after surgery on all patients. The SPET images were anatomically standardized using SPM99 followed by quantification of 318 constant ROIs, grouped into 12 segments in each hemisphere to calculate segmental CBF as the area-weighted mean value for each of the respective 12 segments based on the regional CBF in each ROI. The percent change in CBF following the administration of ACZ was computed for each of the 12 segments. **Results:** Only 1 patient with cloverleaf skull showed abnormal CBF distribution on resting CBF SPET image before surgery, decreased CBF in bilateral parietal, occipital lobes and cerebellum. After surgery, abnormal CBF distribution was not detected in this patient. There was no abnormal CBF distribution on resting CBF SPET image in 19 patients. Sixteen patients showed poor vasodilatory reactivity to ACZ in whole cerebral cortex, with under 10% of the percent change, before surgery. Four patients with 1 scaphocephaly, 1 trigonocephaly, 1 plagiocephaly and 1 lamboid synostosis were confirmed good reactivity to ACZ, with over 20% of the percent change, before surgery. After surgery, 13 patients in 15 patients with poor vasodilatory reactivity (86.7%) showed improvement of vasodilatory reactivity to ACZ in whole cerebral cortex, in 9 patients with over 20% of the percent change. Three patients with 1 cloverleaf skull, 1 brachycephaly and 1 scaphocephaly were not confirmed improvement of reactivity to ACZ after surgery. **Conclusion:** Patients with usual premature craniosynostosis without cloverleaf skull associated with hydrocephaly did not show abnormal CBF distribution or definite decreased CBF in cerebral parenchyma, however 78.9% (15/19) were confirmed poor vasodilatory reactivity to ACZ in cerebral cortex. After surgery, 86.7% (13/15) showed improvement of vasodilatory reactivity. ACZ-activated quantitative SPET images showed diffuse cerebral impairment of vascular reserve before surgery and improvement after surgery in usual premature craniosynostosis. In severe premature craniosynostosis i.e. cloverleaf skull associated with hydrocephaly, hypoperfusion was detected in cerebral and cerebellar cortex before surgery and improvement of resting perfusion was showed with limited vasodilatory potential after surgery.

**THERAPEUTIC INDUCTION OF RESISTANCE VESSELS GROWTH INCREASES BLOOD SUPPLY IN HYPOPERFUSED RAT BRAIN AFTER TREATMENT WITH GRANULOCYTE-MACROPHAGE COLONY-STIMULATING FACTOR****Johannes Woitzik<sup>1</sup>, Ulf Schneider<sup>1</sup>, Helmuth Schroeck<sup>2</sup>, Lothar Schilling<sup>1</sup>**<sup>1</sup>*Department of Neurosurgery, University Hospital Mannheim, Mannheim, Germany*<sup>2</sup>*Department of Physiology, University of Heidelberg, Heidelberg, Germany*

Background: Experimental and clinical data have shown an increase of collateral vessel growth in hindlimb ischemia and cardiovascular disease after treatment with cytokins affecting proliferation or survival time of monocytes. Recently, this concept of “arteriogenesis” was also adapted to the cerebrovascular system by measuring an increase of the left posterior cerebral artery after three-vessel occlusion in rats and treatment with granulocyte-macrophage colony-stimulating factor (GM-CSF). Since it remained questionable to what extent this increase of the vessel diameter does contribute to a better collateral circulation, we investigated whether the observed normalization of brain perfusion was also based on growth of resistance vessel. Methods: Male Sprague-Dawley rats received after bilateral internal carotid artery (ICA) occlusion a daily injection for 7 weeks of 10 µg/kg GM-CSF (GM-CSF group) or isotonic saline in control animals. To evaluate the effect of bilateral ICA occlusion a sham group was added. Cerebral blood flow (CBF) was repeatedly measured by laser-Doppler flowmetry scanning under resting conditions and after acetazolamide application. At the end of the observation period resting CBF was measured by iodo[14C]antipyrine autoradiography. Vessel density was evaluated on brain sections 7 weeks after bilateral ICA occlusion as was the number of precapillary microvessels detected by  $\alpha$ -smooth muscle actin ( $\alpha$ -SMA) immunohistochemistry. Results: Resting CBF was not affected by bilateral ICA occlusion (GM-CSF group: 102±14 ml/100g/min, control group: 90±8 ml/100g/min, sham group: 100±9 ml/100g/min). However, the response to acetazolamide was abrogated in saline-treated control animals 2 weeks (2.0±4.0 %, sham: 7.8±6.1 %) and 5 weeks (2.2±3.7 %, sham: 10.8±8.4 %) after bilateral ICA occlusion. GM-CSF treatment resulted in a normalization of the CBF response to acetazolamide after 5 weeks of treatment (17.2±9.3 %). This recovery was accompanied by a slight increase in the number of cortical capillaries counted in individual observation fields (GM-CSF group: 95.1±3.2, control group: 92.6±6.1 and sham group: 92.5±2.9) and a significant increase of  $\alpha$ -SMA positive vessels in individual observation fields (GM-CSF group: 101±52, control group: 50±33 and sham group: 50±38,  $p<0.05$ ). Conclusions: The increase in the number of small resistance vessels after GM-CSF treatment under conditions of mild hypoperfusion might well explain the normalization of brain perfusion. Thus, GM-CSF treatment seems to be a promising therapeutic approach in patients with chronic impairment of CBF.

## MINOCYCLINE ENHANCES NEUROGENESIS AND FUNCTIONAL RECOVERY AFTER STROKE INJURY

Zhengyan Liu, Yang Fan, Shwuhuey M Hong, **Jialing Liu**

*Department of Neurosurgical Service, University of California, and VA Medical Center, San Francisco, CA, USA*

**BACKGROUND AND PURPOSE:** Our recent evidences suggest that neurogenesis following ischemic brain injury might not only lead to the replacement of damaged cells but can also contribute to functional recovery, thereby supporting the notion that strategies which augment endogenous neurogenesis may hold clues for the development of stroke therapy. It is known that activated microglia localized in close proximity to the newly formed neurons compromise the survival of new hippocampal neurons, and blocking inflammation has been shown to restore hippocampal neurogenesis after cranial irradiation and seizure. The aim of our current study is to determine the effect of minocycline on neurogenesis and functional recovery after focal cerebral ischemia. **METHODS:** Adult male rats underwent 60 minutes of middle cerebral artery occlusion (MCAO) via the intraluminal suture method. Minocycline was administered intraperitoneally (i.p.) starting at 6h (early treatment) or 5d (delayed treatment) after reperfusion for a continuous period of 4 weeks. During the first week of minocycline injection, animals received a daily dose of 50mg/kg, followed by daily 25mg/kg for the remaining period. BrdU (50mg/kg) was administered twice daily on days 5-8 after MCAO. The number of surviving BrdU-labeled cells, Ki67 and ED1 positive cells were quantified in the dentate gyrus (DG) or hilus following immunohistochemistry, and the phenotype of newborn cells was determined by confocal microscopy. Infarct volume was evaluated by unbiased stereology using the Cavalieri's principal based on NeuN staining. Motor and cognitive functions were evaluated by open field, cylinder, horizontal ladder, rotor rod and Morris water maze tests on a separate group of animals receiving the delayed treatment paradigm. **RESULTS:** Among the early treatment groups (6h after reperfusion), infarct volume was significantly reduced in minocycline treated MCAO rats (McI) ( $72.6 \pm 8.4$  mm<sup>3</sup>) with a concurrent decrease in progenitor cell proliferation and neurogenesis (BrdU:  $128.8 \pm 20.2$ /DG), compared to rats with MCAO alone (I) (infarct volume:  $34.5 \pm 12.3$  mm<sup>3</sup>; BrdU:  $217.0 \pm 43.0$ /DG). On the other hand, delayed treatment (5d after reperfusion) of minocycline did not result a difference in infarct size, but caused a significant decrease in the number of activated microglia in DG (McI:  $14.4 \pm 2.1$ /DG) compared to vehicle treatment (I:  $53.1 \pm 4.7$ /DG). Although there was no statistical difference in the number of total surviving new cells in the DG between minocycline and vehicle treated MCAO rats, minocycline significantly increased the number of surviving newborn neurons that co-expressing BrdU and NeuN (McI:  $165.0 \pm 27.5$ /DG; I:  $90.2 \pm 24.4$ /DG). Furthermore, minocycline did not affect progenitor cell proliferation at the SGZ, consistent with previous reports. Behavioral testing showed that there was no difference in spontaneous activity in an open field, however, minocycline significantly improved motor coordination on the rotor rod, reduced the preferential use of the unaffected limb, reduced the frequency of footfalls in the affected limb when traveling on a horizontal ladder, and improved spatial learning and memory. **CONCLUSION:** Our data suggest that minocyclin reduces functional impairment after cerebral focal ischemia, and the improved function is associated with enhanced neurogenesis in the DG.

## HEMISPHERIC DIFFERENCES IN UNILATERAL RECOGNITION MEMORY NETWORKS IN TEMPORAL LOBE EPILEPSY: A STUDY WITH INTRACAROTID AMOBARBITAL TEST AND [18F]FDG-PET

Nozomi Akanuma<sup>1</sup>, Laurence J. Reed<sup>3</sup>, Paul K Marsden<sup>2</sup>, Jozeph Jarosz<sup>1</sup>, Naoto Adachi<sup>4</sup>, William A. Hallett<sup>2</sup>, Gonzalo Alarcon<sup>1</sup>, Robin G. Morris<sup>3</sup>, Michael Koutroumanidis<sup>1</sup>

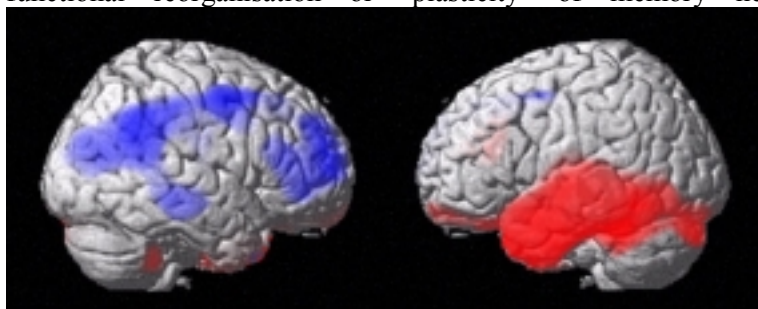
<sup>1</sup>*Department of Clinical Neurophysiology and Epilepsies & Divisions of Clinical Neurosciences, Guy's, King's and St Thomas' School of Medicine, London, UK*

<sup>2</sup>*PET Imaging Centre, Radiological Sciences and Medical Engineering, Guy's, King's and St Thomas' School of Medicine, London, UK*

<sup>3</sup>*Division of Psychological Medicine, Institute of Psychiatry, King's College, London, UK*

<sup>4</sup>*Adachi Mental Clinic, Sapporo, Japan*

**Introduction:** Temporal lobe epilepsy (TLE) is recognised to be associated with impaired memory function, particularly especially in the hemisphere bearing the epileptic focus. We hypothesised that the memory impairment associated with TLE may arise by the effect of seizure epileptic foci upon structures crucial to memory function, particularly those within the limbic regions including the hippocampus, entorhinal cortex and retrosplenial cortices. An alternative hypothesis suggests that memory function may show plasticity in the presence of seizure epileptic foci impinging on these structures and be distributed to extra-limbic structures. **Methods:** To discriminate these hypotheses, we studied associations between recognition memory performance on verbal, visual and facial items measured assessed by the intracarotid amobarbital test (IAT or Wada test) and cerebral metabolism measured using 18 F-fluorodeoxyglucose positron emission tomography in 62 patients with unilateral TLE (35 left and 27 right), grouped according to laterality of the language dominance (50 left and 12 non-left) or age at epilepsy onset (33  $\leq$  5 years of age, 29  $>$  5 years) using complementary voxel based mapping and region of interest (ROI) methods. **Results:** Considering left hemisphere function, correlation analysis identified hypometabolism within a contiguous volume including left hippocampus, inferior temporal and extra-temporal regions as being associated with lower total IAT scores. This pattern was maintained when considering verbal and visual but not facial sub-scores separately. In contrast, correlational analysis showed total right IAT scores right hemisphere function to be subserved by an entirely distinct network involving dorsolateral prefrontal and parietal cortical regions in the right hemisphere, with no involvement of medial temporal structures. This pattern of association was maintained when the verbal and visual but not facial categories of memory item were considered separately, and by ROI analysis. **Discussion:** These data demonstrate that memory performance on the IAT is subserved by hemispherically distinct networks, the left involving limbic putative long-term memory networks, the right employing fronto-parietal putative working memory networks. Considering non-left language dominant and early early-onset seizure epilepsy groups, the pattern of associations with total IAT scores were reversed, providing evidence of functional reorganisation or 'plasticity' of memory networks in these subjects.



## SPATIO-TEMPORAL PATTERNS OF MRI-DETECTED MANGANESE-ENHANCEMENT IN THE SENSORIMOTOR NETWORK OF RAT BRAIN AFTER STROKE

Jet van der Zijden, Ona Wu, Annette van der Toorn, Rick M. Dijkhuizen

*Image Sciences Institute, University Medical Center Utrecht, Utrecht, The Netherlands*

**Introduction:** Acute loss of function and subsequent spontaneous recovery after stroke have been associated with alterations in neuronal connections. Manganese-enhanced MRI allows in vivo mapping of disruption of neuronal tracts after stroke [1], however the temporal pattern of manganese enhancement has not yet been fully characterized. The aim of this study was to track changes in connectivity within the sensorimotor network in rat brain after stroke by repeated manganese-enhanced MRI measurements. **Methods:** Transient focal cerebral ischemia was induced in six male Wistar rats by 90 minutes intraluminal occlusion of the right middle cerebral artery. After 2 weeks, 0.2 ml 1M MnCl<sub>2</sub> solution was injected into the spared ipsilesional sensorimotor cortex. MnCl<sub>2</sub> was also injected in the sensorimotor cortex of six control rats. MRI measurements were done at 2 days before and at 6 h, 24 h, 2 days, 4 days, 6 days and 8 days after MnCl<sub>2</sub> injection. T2-weighted images were acquired for lesion assessment and anatomical details. T1-weighted MRI was performed to quantify T1 shortening by manganese in four ipsi- and contralateral regions-of-interest (ROIs) within the sensorimotor network (i.e., sensorimotor cortex (SMCX), caudate putamen (CPu), thalamus (Th) and substantia nigra (SN)). Data were statistically analyzed using a two-way repeated measures ANOVA with a post-hoc Bonferroni t-test. **Results:** In all rats, the cortico-striatal-nigral pathway was identified by T1 shortening after MnCl<sub>2</sub> injection (Fig 1). In stroke rat brains, however, T1 shortening was significantly reduced in the ipsilateral thalamus and substantia nigra, as compared to control rat brains ( $P < 0.05$ ). No significant differences were found for other ROIs. Maximal T1 shortening was observed at day 2 or 4 after manganese injection. T1 shortening was significantly reduced after 6 and 8 days as compared to the time-point of maximal T1 shortening in all ROIs except for the ipsilesional thalamus and substantia nigra in stroke rats. **Discussion:** Different spatial and temporal pattern of manganese enhancement in ipsilesional sensorimotor network after stroke suggests disturbed neuronal connections and transport dynamics. MRI mapping of the spatio-temporal distribution of the neuronal tracer manganese can provide unique in vivo information on neuronal connectivity that may aid in elucidating mechanisms of functional loss and recovery after stroke. **References:** Allegrini PR and Wiessner C. *NMR Biomed* 16:252-6 (2003).



Fig 1. T1 maps of 3 adjacent coronal brain slices of an ischemic rat brain 2 days after injection of manganese chloride. The ischemic lesion is characterized by a prolonged T1.

## SPATIAL DIFFERENCES OF NEURONAL CELL PROLIFERATION AFTER FOCAL ISCHEMIA: NEUROGENESIS IS ENHANCED IN DENTATE GYRUS, BUT SUPPRESSED IN THE SUBVENTRICULAR ZONE

Ansgar M. Brambrink, Yulia Ivashkova, Kamila Vagnerova, Wenri Zhang, Patricia D. Hurn

*Department of Anesthesiology and Peri-Operative Medicine, Oregon Health & Science University, Portland, OR, USA*

Contrary to previous beliefs, the brain has a potential to regenerate itself. Neurogenesis, i.e. the cell division of neuronal precursor cells in the adult brain, and their subsequent differentiation to neurons, has been observed particularly in two areas of the brain, the subgranular zone [SGZ] of the dentate gyrus and the subventricular zone [SVZ] [1]. Neurogenesis appears to be stimulated by various noxious insults, e.g. ischemia, seizures, suggesting that it is part of an endogenous repair mechanism of the brain. However, stress, e.g. inflammation, radiation, can also disrupt neurogenesis [2;3], and the overall significance of the phenomenon in relation to brain damage remains unclear. We investigated the differential effects of a well defined focal ischemic insult on neurogenesis in two remote germinal areas of murine brains. Methods: Anesthetized male C57/B16 mice (n=4 per group) were subjected to 90-min of MCAO using the intraluminal filament technique. Continuous Laser-Doppler measurements verified ischemia and reperfusion. Body temperature was monitored and controlled to physiologic levels throughout the procedure. During reperfusion, animals were pulse-injected with the thymidine analogon BrdU (50mg/kg; 3x/d) 24 hr before sacrifice. At designated times (48hr, 72hr, 96hr after MCAO) animals were transcardially perfused using 4% paraformaldehyde, brains were carefully removed and further processed for cryosections (40 $\mu$ m). Free-floating sections were immunostained using antibodies against BrdU and various cellular markers (doublecortin, Tuj1, NeuN, GFAP). Cy2- and Cy3-labeled secondary antibodies allowed evaluation of cell proliferation/maturation using confocal microscopy and digital image analysis (Image J, NHI). Differences in cell proliferation between the survival times were determined by ANOVA. Results: With the applied insult, cell proliferation (BrdU+ cells) in ipsilateral SGZ increased continuously, beginning 48hr after MCAO to more than six-fold at 96hr (382 $\pm$ 87/mm<sup>2</sup> at baseline vs. 2092 $\pm$ 1189/mm<sup>2</sup> at 96hr, p<0.05). At the same time, the contralateral SGZ did not show a significant increase in BrdU+ cells. The majority of the proliferating cells were positive for doublecortin, but negative for any of the other markers used, thus representing newborn neurons. Cell proliferation in SVZ, in contrast, showed an opposite pattern: in ipsilateral SVZ cell proliferation progressively declined to about 50% of baseline during the first 96hr after MCAO (7033 $\pm$ 60/mm<sup>2</sup> at baseline vs. 4076 $\pm$ 118/mm<sup>2</sup>, p<0.05). The contralateral SVZ showed 25% more BrdU+ cells at 48hr than at baseline. Again, most BrdU+ cells were doublecortin co-labeled. Conclusion: The cell proliferatory response to focal cerebral ischemia appears to differ between SGZ and SVZ early after the insult. One possible explanation is the relative distance between respective germinal areas and the infarct core. This may result in more severe stress and less trophic support in the SVZ, which is located closer to the infarct, after MCAO. Accordingly, the SGZ would show enhanced, and the SVZ suppressed proliferation. Different levels of cellular stimulation/stress after brain ischemia seem to have opposite effects on the neuroregenerative response to ischemia. This observation has relevance for future therapeutic strategies to enhance neurogenesis after brain insults, and warrants further investigation. References: [1] J Neurosci 1998,18:7768 [2] Proc Natl Acad Sci USA 2003,100:7919 [3] Ann Neurol 2004,55:381

**LONG-TERM MOTOR DEFICIT FOLLOWING PERIVENTRICULAR  
HEMORRHAGE IN NEONATAL RATS: A POTENTIAL MODEL FOR HUMAN  
CEREBRAL PALSY**

Janani Balasubramaniam, Mengzhou Xue, **Marc Del Bigio**

*Department of Pathology, Winnipeg, Manitoba, Canada*

**Introduction:** Periventricular hemorrhage (PVH) in the premature infant brain is often associated with developmental delay and persistent motor deficits (cerebral palsy). We hypothesized that hemorrhagic damage to the periventricular germinal region in neonatal rats would lead to immediate and long-term behavioral changes. **Materials and Methods:** Tail blood from newborn rats (1 day old) or saline was injected into the periventricular region of the cerebrum. Magnetic resonance imaging was used to define the extent of the hematoma. Rats with hemorrhage, as well as saline and intact controls, underwent behavior tests until 10 weeks of age by a blinded observer. Then the brains were subjected to histological and biochemical tests. **Results:** Rats in the PVH group displayed significant impairment in tests of motor development (ambulation, righting response, and negative geotaxis) to 22 days of age. In maturity they demonstrated impaired ability to stay on a rotating rod and impaired ability to reach for food pellets with the contralateral forelimb. Magnetic resonance imaging at the end of the experiment demonstrated subsets of rats with normal appearing brains, focal cortical infarcts, or mild hydrocephalus. Gross structural defects were associated with greater behavioral deficits. There was a good correlation between MR imaging and histological appearance. Only rare iron-containing macrophages could be identified in the white matter. Some rats exhibited periventricular heterotopia. Golgi impregnation demonstrated stunting of cortical neurons. **Conclusion:** Blood injection into the periventricular tissue of neonatal rat results in both immediate and long-term behavioral abnormalities. We conclude that the rat model of neonatal periventricular / intraventricular hemorrhage is a good model of human cerebral palsy.

## **INDOMETHACIN DECREASES IMMUNE CELL ACTIVATION AND IMPROVES CELL SURVIVAL AND NEUROGENESIS FOLLOWING STROKE, BUT DOES NOT IMPROVE FUNCTIONAL RECOVERY**

**Benjamin D. Hoehn**, Theo D. Palmer, Dave W. Schaal, Gary K. Steinberg

*Department of Neurosurgery, Stanford University, Stanford, CA, USA*

**Introduction:** New cells from the subventricular zone (SVZ) may help repair the brain after injury, but their long-term survival may be inhibited by inflammation. We investigated if treatment with the non-steroidal anti-inflammatory drug indomethacin (INDO) improves cell survival following focal cerebral ischemia. **Methods:** Ischemia was induced in adult rats by middle cerebral artery occlusion for 2 h. INDO-treated and control animals received daily BrdU injections for 6 days and were sacrificed on day 7, 14, or 28. Brains were immunostained for BrdU and lineage-specific markers and examined under a confocal microscope. Western blots were run for COX-2 and ppar-gamma. Behavioral testing was conducted on separate groups of animals at one week intervals starting 7 d before ischemia. **Results:** We observed an unexpected, marked decrease in labeling by the proliferation marker bromo-deoxyuridine (BrdU) at the time of reperfusion in the SVZ. BrdU-labeled migrating neuroblasts appeared within the neighboring parenchyma along with increases in BrdU-labeled cells within the neighboring striatum and overlying cortex. Co-labeling with BrdU and a lineage-specific marker (DCX, NG2, GFAP, NeuN, or nestin) in high-GFAP regions of the cortex and striatum (ischemic penumbra; n=12) showed that the proportion of BrdU+ cells expressing all lineages was increased compared to controls in INDO-treated animals at 14 and 28 days post-ischemia. The increase in co-labeling in the cortex was greatest with nestin (5.2 fold) and NG2 (6.4 fold). Few BrdU+/NeuN+ cells were seen even 28 days after stroke. Western blots showed decreased COX-2 at 0 and 7 d and increased ppar-gamma at 7 d with a concurrent decrease in immune cell activation in ischemic animals treated with INDO. There was no effect of INDO on behavioral recovery at any time point. **Conclusions:** Indomethacin improved cell survival and neurogenesis following stroke by increasing ppar-gamma and decreasing COX-2 and immune cell activation. These effects were not accompanied by reduced infarct sizes or improvement in behavioral recovery, however, which may reflect the severity of the injury. These data contribute to a growing literature indicating that reducing inflammation after brain injury may be beneficial.

## HEMATOPOIETIC CYTOKINES INDUCE REGENERATION IN MOUSE BRAIN AFTER STROKE

Shunya Takizawa<sup>1</sup>, Hiroshi Kawada<sup>2</sup>, Mitsuyo Tsuma<sup>2</sup>, Tomomi Takanashi<sup>2</sup>, Yuko Morita<sup>1</sup>, Tsuyoshi Uesugi<sup>1</sup>, Tomomitsu Hotta<sup>2</sup>, Shigeharu Takagi<sup>1</sup>, Yukito Shinohara<sup>1</sup>

<sup>1</sup>*Division of Neurology, Department of Internal Medicine, Tokai University School of Medicine, Kanagawa, Japan*

<sup>2</sup>*Division of Hematology, Department of Internal Medicine, Divisions of Hematology, Tokai University School of Medicine, Kanagawa, Japan*

**Introduction:** In the bone marrow (BM), in addition to hematopoietic stem cells and supportive stromal cells, there are multipotent adult progenitor cells, which can differentiate, not only into mesenchymal cells, but also into cells with visceral mesoderm, neuroectoderm and endoderm characteristics in vitro. The purpose of this study is to clarify whether BM-derived cells can differentiate into neuron, astrocyte, microglia and endothelium in response to cerebral focal ischemia, and whether hematopoietic cytokines enhance neurogenesis from intrinsic neural stem cells. Further, we evaluate the effect of cytokines on brain functions. **Methods:** BM cells sampled from the long bone in male C57 Black/6 green fluorescent protein (GFP)-expressing transgenic mice, were transplanted into female C57 Black/6 mice. One month later, the left middle cerebral artery was occluded under halothane anesthesia. Mice were injected subcutaneously with human recombinant granulocyte colony-stimulating factor (G-CSF) + stem cell factor (SCF) from day 1 to 10 (group A; n=6) or day 11 to 20 (group B; n=6) after occlusion for 10 consecutive days, or vehicle alone (control group; n=12). At 4 weeks after occlusion, brain functions were examined using the rotor rod test and the Morris water maze test, and mice were then sacrificed. GFP epifluorescence was directly detected by confocal microscopy. To identify the cell types derived from BM, double-labelling studies were performed with the use of primary antibodies to neurons (Neu N), astrocytes (GFAP), microglia (F4/80) and endothelial cells (CD31). Separately, we intraperitoneally administered the cell proliferation-specific marker, bromodeoxyuridine (BrdU), to C57 Black/6 mice with focal ischemia that had received G-CSF+SCF (n=6) or no cytokines (n=6), then sacrificed them at 21 days after occlusion. Brain sections processed with double-immunofluorescent staining were scanned by confocal microscopy. **Results:** 1) GFP-expressing cells, considered to be bone marrow-derived, were observed in the perivascular position, ependyma and parenchyma, in the peri-infarct and infarct areas. 2) GFP-expressing cells were identified mainly as microglia, and partly as neurons and endothelial cells. 3) BrdU-positive cells in the infarct area were increased by cytokine treatment. 4) The rotor rod test result in group B was significantly better than that in group A or the control group ( $p < 0.05$  and  $p < 0.01$ , respectively). The water maze test result in group B was also significantly better than that in the control group ( $p < 0.0001$ ). **Conclusions:** Administration of hematopoietic cytokines in the late phase of focal ischemia (day 11 to 20) significantly improved motor and cognitive functions. This result may be partly caused by regeneration of impaired brain tissues with BM-derived cells, and mainly by the enhancement of neurogenesis from intrinsic neural stem cells. This finding may suggest a new therapeutic strategy to enhance neurogenesis after stroke in the clinical field.

## ASSESSMENT OF THE BLOOD-TO-BRAIN TRANSFER CONSTANT FOR GD-DTPA IN ISCHEMIC BRAIN TISSUE: COMPARISON OF MRI AND QAR METHODS USING A CONTINUOUS INFUSION PROCEDURE

Robert A. Knight<sup>1</sup>, Tavarekere N. Nagaraja<sup>2</sup>, Vijaya Nagesh<sup>3</sup>, James R. Ewing<sup>1</sup>, Polly A. Whitton<sup>1</sup>, Kelly A. Keenan<sup>2</sup>, Susan C. Fagan<sup>4</sup>, Joseph D. Fenstermacher<sup>2</sup>

<sup>1</sup>Department of Neurology, <sup>2</sup>Department of Anesthesiology, Henry Ford Health System, Detroit, <sup>3</sup>Department of Radiation Oncology, Univ of Michigan, Ann Arbor, MI, <sup>4</sup>Pharmacy, Univ of Georgia, Augusta, GA, USA

**Introduction:** Pathological changes in brain tissue during and after stroke may involve injury to the blood-brain barrier (BBB). In this study, changes in BBB permeability in ischemic tissue were assessed in a rat model of transient focal ischemia that produces BBB injury acutely and hemorrhagic transformation at 24 hours. Changes in the blood-to-brain transfer constant (Ki) were measured by both magnetic resonance imaging (MRI) and quantitative autoradiographic (QAR) methods using identical non-labeled and radiolabeled gadolinium-diethylenetriaminepentaacetic acid (Gd-DTPA) preparations, respectively. **Methods:** Transient ischemia was induced in male Wistar rats (n=5) by intraluminal suture occlusion of the middle cerebral artery and withdrawal of the occluding filament after 3 hrs. MRI studies were performed at 7 Tesla. Quantitative MRI assessment of ischemia induced BBB permeability changes was performed approximately 2 hrs after reperfusion using Look-Locker based T1-weighted imaging to generate estimates of Ki via the Patlak plot methodology<sup>1</sup>. MRI localization of areas with BBB opening was performed by tracking contrast enhancement changes produced by Gd-DTPA administration using a Look-Locker T1 sequence. The Gd-DTPA injection was delivered using a stepped down continuous i.v. infusion protocol that maintained a relatively constant plasma Gd-DTPA concentration for approximately 20 minutes. After MRI, the rats were infused with 14C-labeled Gd-DTPA using the same infusion procedure, and then sacrificed for QAR. Both versions of the Gd-DTPA preparation were homemade and identically prepared. Tissue sections were prepared for QAR for confirmation of BBB leakage areas and to provide quantitative blood-to-brain transfer constant (Ki-QAR) estimates. The ischemic area regions of interest (ROIs) with BBB opening were segmented from normal tissue using ISODATA segmentation<sup>2</sup> in conjunction with the serially acquired Look-Locker T1 maps. The MRI defined ROIs were superimposed onto the 14C-labeled Gd-DTPA autoradiograms for measurements of BBB permeability. **Results:** Acute BBB disruption was detected in the preoptic area and/or striatum in all rats by Gd-DTPA enhanced MRI and corresponded closely with areas identified by 14C-Gd-DTPA QAR. Estimates of Ki by both MRI and QAR methods were significantly elevated after reperfusion as compared to brain regions with intact BBB function. A scatterplot of the MRI versus QAR estimates of Ki, for the non-labeled and radiolabeled Gd-DTPA are shown in the Figure. Post-reperfusion BBB changes between MRI and QAR were highly correlated in areas with BBB disruption (p=0.002). **Conclusion:** The correlation of blood-to-brain transfer constants for non-labeled and radiolabeled Gd-DTPA preparations using a continuous infusion schedule for both MRI and QAR methods provides a one-to-one validation of the Patlak methodology for estimating BBB permeability in reperfused ischemic infarct. With further substantiation, this approach may have potential application in the clinical setting for assessing acute BBB injury that may precede later hemorrhagic transformation. **References:** 1.Ewing et al. Magn Reson Med (2003);50:283-292. 2.Bezdek, J. IEEE (1980):2:1-8. Grant support: Supported in part by NIH RO1NS38540 and AHA 0270176N

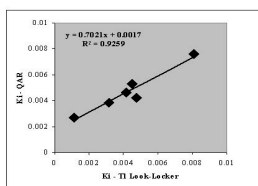


Figure: Scatterplot plot of Ki estimates as measured by MRI using T1 estimates plotted as a function of Ki estimates as measured by QAR methods.



**BRAIN AQUAPORIN 9 (AQP9) REGULATION BY SYSTEMIC INSULIN IN RAT****Jerome Badaut**<sup>1</sup>, Jean-Marie Petit<sup>2</sup>, Jean-François Brunet<sup>1</sup>, Pierre J. Magistretti<sup>2</sup>, Luca Regli<sup>1</sup><sup>1</sup>*Department of Neurosurgery, CHUV, Lausanne, Switzerland*<sup>2</sup>*Life Science, EPFL, Lausanne, Switzerland*

Background: AQP9 is a water channel that facilitates the diffusion of water and also of glycerol and monocarboxylates (for review see Badaut et Regli, 129(4), 969, Neuroscience 2004). Recent reports have shown that the expression of AQP9, is negatively regulated by insulin in hepatocytes. Brain AQP9 is expressed in catecholaminergic neurons and in astrocytes. Interestingly, insulin has been shown to cross the blood-brain barrier and bind specific receptors in the brain, which may be implicated in energy balance. Based on the above evidence, we examined whether brain AQP9 can be regulated by insulin. Methods and Results : This hypothesis has been tested in the rat, in brain stem slices in vitro and in streptozotocin (STZ) treated animals in vivo; a diabetes model in the rat. The use of brainstem culture eliminates the influence of circulating insulin. By double immunolabeling experiments, we show the presence of Tyrosine Hydroxylase-positive neurons exhibiting AQP9 staining in brain stem slices. In these slices, there is a significant decrease in AQP9 levels 6h after treatment with 2 mM of insulin (41 % of the control,  $P < 0.05$ , ANOVA,  $n=6$ ) measured by Western blot and AQP9 levels return to control values at 24 hours. In STZ treated rats (diabetic rats), the level of AQP9 expression is significantly increased in the liver (138 % of control,  $p < 0.05$ ). In the brain, AQP9 is also significantly increased in the nucleus of solitary tract (240 % of control rats,  $P < 0.005$ , ANOVA,  $n=4$ ), in the locus coeruleus (180 %,  $P < 0.05$ , ANOVA,  $n=4$ ) and in the substantia nigra (200 % of control rats,  $P < 0.005$ , ANOVA,  $n=8$ ). In contrast, AQP9 expression is not modified in the cerebellum where AQP9 is expressed on astrocytes. AQP9 immunoreactivity is significantly increased in dopaminergic neurons in the substantia nigra of STZ rats (126 versus 36 arbitrary units for control rats,  $P < 0.005$ ,  $n=3$ , ANOVA). In the cerebellum, no significant difference was observed between control and STZ rats. Conclusion : These results show that in the brain AQP9 expression on catecholaminergic neurons is regulated by the systemic insulin. This result supports the hypothesis that AQP9 may be implicated in brain metabolism as a channel for glycerol and monocarboxylates.

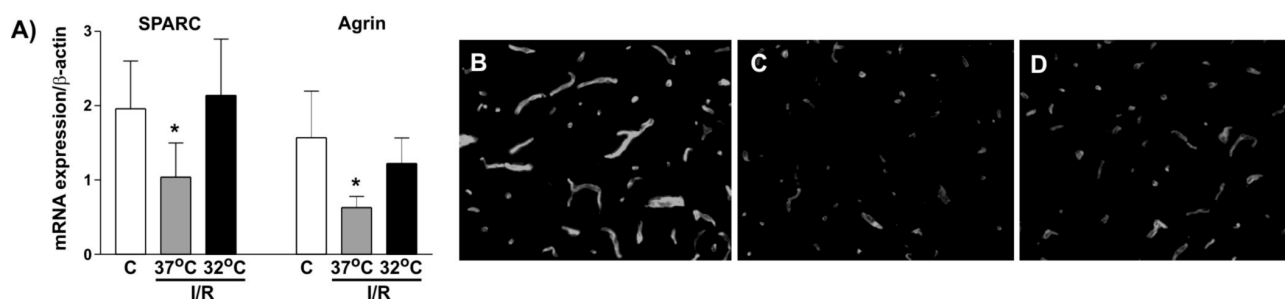
## POSTISCHEMIC HYPOTHERMIA PROTECTS AGAINST LOSS OF AGRIN AND SPARC FROM THE VASCULAR BASEMENT MEMBRANE IN GLOBAL CEREBRAL ISCHEMIA

Danica Stanimirovic<sup>1</sup>, Ewa Baumann<sup>1</sup>, Edward Preston<sup>1</sup>, Ingolf Blasig<sup>2</sup>, Reiner Haseloff<sup>2</sup>

<sup>1</sup>*Institute for Biological Sciences, National Research Council of Canada, Ottawa, ON, Canada*

<sup>2</sup>*Department of Signal Transduction and Molecular Medicine, Institute for Molecular Pharmacology, Berlin, Germany*

**Introduction:** Vascular basement membrane (BM) stabilizes brain vessels and inhibits endothelial cell cycle. Cerebral ischemia causes BM breakdown with the loss of structural BM components including collagens and laminins and subsequent endothelial cell activation and proliferation [1]. However, the fate and role of BM proteoglycans and non-structural BM constituents, including SPARC (BM-40, osteonectin), in ischemic blood-brain barrier (BBB) pathophysiology remains unknown. **Methods:** A transient 20 min forebrain ischemia followed by 24 h of reperfusion was induced in adult Sprague-Dawley rats by combined bilateral common carotid artery occlusion and hypotension (42-45 mmHg) [2]. In a separate group of animals, a mild (32°C) post-ischemic hypothermia was induced for 6 h. RNA from ~300 brain vessels (20-100 μm) extracted by laser-capture microdissection (LCM) microscopy as described [3] was used to determine the expression of BM constituents, laminin, proteoglycan agrin and SPARC mRNAs by quantitative PCR (Q-PCR). Protein expression was determined by immunohistochemistry in adjacent tissue sections. BBB permeability was assessed using 3H-sucrose as a tracer [2]. **Results:** A transient global brain ischemia resulted in a significant (ANOVA,  $p < 0.05$ ; 6 animals/group) reduction in SPARC and agrin mRNAs in LCM-captured brain vessels 24 h after reperfusion (Fig. 1A). A time-dependent loss of SPARC (not shown) and agrin (Fig 1B-C) from the BM during reperfusion was also observed by immunochemistry. A 6-h postischemic hypothermia reduced SPARC and agrin mRNA (Fig 1A) and protein loss (Fig 1D) from BM, and also reversed increased BBB transfer constants for 3H-sucrose seen at 24 h after reperfusion (basal –  $1.75 \pm 0.20$ ; I/R-  $13.88 \pm 1.59$ ; I/R-hypo –  $4.84 \pm 0.34$  nl/g/s). **Conclusions:** A transient post-ischemic hypothermia appears to stabilize brain vessels and reduce BBB leakage in part by preventing proteolytic degradation of regulatory BM constituents, SPARC and agrin. [1] del Zoppo GJ and Mabuchi T. (2003) *J Cereb Blood Flow Metab.* 23:879-894. [2] Preston E et al (1993) *Neurosci Lett.* 149:75-78. [3] Mojsilovic-Petrovic J et al. (2004) *J Neurosci Methods* 133:39-48.



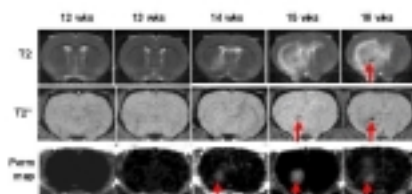
## VASCULAR PERMEABILITY MAY SPATIALLY PREDICT SUBSEQUENT HEMORRHAGES IN STROKE-PRONE SPONTANEOUS HYPERTENSIVE RATS

Guihua Zhai<sup>1</sup>, **Weili Lin**<sup>1</sup>, Qingwei Liu<sup>1</sup>, Liansheng Chang<sup>1</sup>, Jin-Moo Lee<sup>2</sup>

<sup>1</sup>University of North Carolina at Chapel Hill, Chapel Hill, NC, USA

<sup>2</sup>Washington University, St. Louis, MO, USA

Increases of vascular extravasations of MR contrast agent have been implicated to be predictive of hemorrhagic transformation in acute stroke patients. However, systemic studies are lacking. In this study, we aim to determine how the increased vascular extravasations of MR contrast agent can be used to predict the presence of subsequent hemorrhages in Stroke-prone spontaneous hypertensive rats (SHRsp). SHRsp rats (n=12), fed a high-salt low-protein diet after weaning, were imaged weekly on a 3T SIEMENS Allegra head-only scanner beginning at 12 week of age and continuing for five weeks. Three sequences were used to acquire images, including a T2-weighted, a T2\*-weighted, and a turboFLASH sequence. The acquired T2-weighted images provided anatomical data as well as an indication of brain edema. T2\*-weighted images allowed assessment of hemorrhage and were acquired using a 3D gradient echo sequence (TE=25ms). To obtain estimates of vascular permeability, the Look-Locker (L-L) technique employing the T-one by multiple read-out pulses (TOMROP) sequence (1) was used for pixel-by-pixel estimates of T1. The TOMROP sequence was repeated 10 times post-contrast. Finally, the PATLAK approach was utilized with the images acquired using the TOMROP sequence for obtaining permeability maps for each rat (2). All 12 rats developed asymmetric T2 hyperintensities by 14 weeks of age; 5 rats developed 7 regions of intracerebral hemorrhage (detected by T2\*) at later time-points. Four hemorrhages were located within the striatum; three were located in the cortex. All rats that developed spontaneous hemorrhages demonstrated concurrent or prior vascular permeability (determined by Gd as described above) at the site of the hemorrhage. In 4 of the 7 hemorrhages, evidence of vascular permeability was found prior to the detection of hemorrhage, preceding it by up to 2 weeks. The remaining three temporally coincided with the hemorrhage. The temporal evolution of vascular permeability, T2 and T2\* images of a representative rats are shown in Fig. 1. It is immediately evident that the presence of vascular leak precedes the hemorrhage by one week. Although blood-brain-barrier (BBB) breakdown, cerebral edema, and hemorrhage have been well-described in this model, the spatial and temporal relationship between these events has not been well-delineated. Although increased vascular permeability did not precede 3 of 7 hemorrhages but rather appeared concurrently, we believe that this may be due to the poor temporal resolution of our imaging scheme. These data suggest that hypertensive intracerebral hemorrhage is preceded by focal vasculopathy resulting in breakdown of the BBB.



**MALIGNANT BRAIN EDEMA AFTER MCA INFARCTION IS DETERMINED BY THE SEVERITY OF ISCHEMIA WITHIN THE INFARCTION****Bert Bosche**<sup>1,2</sup>, Christian Dohmen<sup>1,2</sup>, Rudolf Graf<sup>1</sup>, Norbert Galldiks<sup>1,2</sup>, Jan Sobesky<sup>1,2</sup>,Lutz Kracht<sup>1</sup>, Fritz G. Lehnhardt<sup>2</sup>, Wolf-Dieter Heiss<sup>1,2</sup><sup>1</sup>*Max-Planck-Institute for Neurological Research, Cologne, Germany*<sup>2</sup>*Department of Neurology University of Cologne, Cologne, Germany*

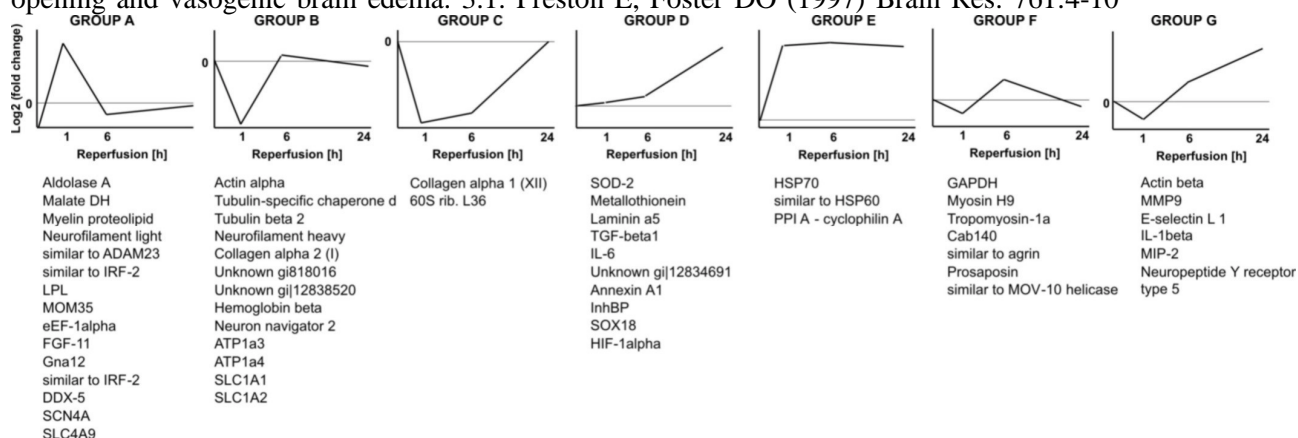
Objective: Malignant brain edema is a serious complication after MCA-infarction. For reasonable implementation of invasive therapies like hemicraniectomy, probability of malignant brain edema has to be anticipated. However, pathophysiology of edema formation after MCA-infarction is poorly understood and identification of patients finally developing such edema is difficult. Experimental studies have shown maximal edema formation when CBF was deeply reduced to <6 ml/100g/min [1,2]. Primary endothelial damage and/or a blood brain barrier break-down have been discussed to result from such deep ischemia [3]. We semiquantitatively investigated CBF in patients with large MCA-infarction by using 11-C-Flumazenil-PET [4] in order to predict malignant brain edema. Methods: We included 16 patients with clinical signs of MCA infarction and involvement >50% of MCA territory in early CT or MRI (<12 h). PET was performed within 15.9±6.4 h hours after symptoms onset. The ischemic core was defined as the volume of perfusional deficit <50% of the average within the contralateral hemisphere, corresponding to a CBF of approximately <14 ml/100g/min. Within the ischemic core subregions with different ischemic CBF values were investigated. Subregions were defined as the volume of perfusional deficit <40, <30, <20, <10% of the average within the contralateral hemisphere, corresponding to a CBF of approximately <12, <8, <6, <4 ml/100g/min. As a correlate of final edema formation, we measured maximal midline-shift on follow-up CTs at the level of the septum pellucidum. Regarding the clinical course and follow-up CT-findings, patients were post hoc divided into a malignant (n=7) and a benign group (n=9). We calculated correlations between ischemic volumes derived from subregional analysis and maximal midline shift in CT. Results: Volumes of ischemic core showed significant differences between both groups (malignant group 149.8±24.9 vs. benign group 51.5±35.8 ccm, p<0,01). Volumes of all subregions with deep ischemia were significantly larger in the malignant group than in the benign group (e.g. CBF<20% 83.1±29,8 vs. 15.0±26,1 ccm; CBF<10% 40.4±25,7 vs. 5,2±8,9 ccm; p<0,0001). The volume of these two subregions within the ischemic core was 55,5% respectively 26,9% of the total ischemic core volume in the malignant group and only 29,1% respectively 10,1% in the benign group. Volumes of regions with deep ischemia showed the best correlations with maximal midline shifts for CBF<20% Rho=0,74, p<0,005 and for CBF<10% Rho=0,76, p<0,005. Conclusion: Subregions with deep ischemia seem to be relevant for massive edema formation in human stroke. Ischemic endothelial damage may lead to a primary blood brain barrier break-down and subsequent vasogenic edema. PET imaging is able to detect the magnitude of these deeply ischemic regions at an early stage and may thereby guide the indication for early hemicraniectomy. References: 1. Crockard et al. Stroke 1980 2. Bell et al. J Neurosurgery 1985 3. Ayata and Ropper J Clin Neuroscience 2002 4. Thiel et al. J Comput Assist Tomogr 2001 The study was supported by the BMBF (Competence Network Stroke)

## CHARACTERIZATION OF VASCULAR PROTEIN EXPRESSION PATTERNS IN CEREBRAL ISCHEMIA/REPERFUSION USING LASER CAPTURE MICRODISSECTION AND ICAT-LC-MS/MS

Arsalan Haqqani, Ewa Baumann, Edward Preston, John Kelly, **Danica Stanimirovic**

*Institute for Biological Sciences, National Research Council of Canada, Ottawa, ON, Canada*

**Introduction:** Ischemic stroke causes profound anatomical and functional changes in the neurovascular unit. Molecular effectors of these changes were investigated in laser-capture microdissection (LCM)-extracted ischemic brain vessels using ICAT-based proteomics adapted to small tissue samples. **Methods:** A transient 20-min forebrain ischemia followed by 1, 6 or 24 h of reperfusion was induced in Sprague-Dawley rats by bilateral common carotid artery occlusion and hypotension (42-45 mmHg) (1). Proteins extracted from ~300 LCM captured microvessels (<100  $\mu$ m) were ICAT-labeled and analyzed by nanoLC-MS. In-house software was used to identify paired ICAT peaks, which were then sequenced by nanoLC-MS/MS. The proteins were clustered using k-means clustering method in Matlab 7.0 software and categorized according to their function using Panther Classification system. **Results:** Pattern analyses classified 57 differentially expressed proteins in 7 distinct dynamic patterns (Fig.1). Early reperfusion was characterized by down-regulation of ion pumps, nutrient transporters and cell structure/motility proteins, and the up-regulation of transcription factors, signal transduction and proteins involved in carbohydrate metabolism. In late reperfusion (6-24 h) up-regulation of inflammatory cytokines, proteins involved in the extracellular matrix remodeling and anti-oxidative defence were observed. The up-regulation of IL-1 $\alpha$  and TGF-1 $\beta$  in ischemic brain vessels was confirmed by ELISA and immunohistochemistry. **Conclusions:** Observed protein expression profiles in brain vessels after a transient global ischemia can be 'mapped' to and possibly causally associated with functional vascular responses previously reported in the same model (2) including a biphasic (1 h and 24 h) BBB opening and vasogenic brain edema. 3.1. Preston E, Foster DO (1997) Brain Res. 761:4-10



**CHRONIC BLOOD-BRAIN BARRIER INSUFFICIENCY AND CYTOTOXIC  
FRAGMENT OF AMYLOID PRECURSOR PROTEIN ACTIVITY IN WHITE  
MATTER FOLLOWING ISCHEMIA-REPERFUSION BRAIN INJURY IN LONG-  
LIVED ANIMALS**

**Ryszard Pluta**, Sławomir Januszewski, Marzena Ułamek

*Department of Neurodegenerative Disorders, Medical Research Centre, Polish Academy of  
Sciences, Warsaw, Poland*

**Introduction:** The profile of white matter neuropathology that is observed in brain ischemia shares probably a commonality with the same changes in Alzheimer's disease brain. These types of changes have been implicated in the neuropathogenesis of dementias and are often seen in the periventricular and subcortical regions. Periventricular white matter injury in ischemic brain and Alzheimer's disease referred to as leukoariosis. This type of lesion is responsible for cognition, behavior and function. A variety of vascular risk factors such as diabetes, hypertension and arteriosclerosis suggest that functional vascular defect contributes to Alzheimer's disease process. Because it is not clear whether the blood-brain barrier (BBB) in ischemic white matter is altered in long-lived animals we take into consideration investigation of BBB dysfunction and amyloid precursor protein (APP) staining in perivascular space. Additionally we will focus on the question of whether or not the neuropathological mechanism(s) observed in ischemic white matter changes is the same as that observed in Alzheimer's disease. **Materials and Methods:** Using female Wistar rats (n=8), BBB dysfunction [1], distributions of APP around BBB vessels [2] and platelets pathology [3] were examined in white matter after 10 min brain ischemia [4] with 1-year survival. Rat brains were perfusion fixed for light and electron microscopic analysis [1]. **Results:** Postischemic brains demonstrated chronic insufficiency and random and spotty BBB changes which dominated periventricularly. Peroxidase extravasations involved BBB neurovessels. Plenty of cytotoxic fragments of APP deposits were associated with the BBB vessels. Perivascular deposits of cytotoxic proteins from APP took the same form as extravasated peroxidase. Additionally our study revealed numerous platelet aggregates in- and outside arterioles, veins, venules and microcirculation. Platelet aggregates like BBB changes and C-terminal of APP deposits were focal, random and dispersedly. C-terminal of APP deposits and platelet aggregation/pathology correlated very well with BBB insufficiency. **Conclusions:** Chronic BBB changes and platelets in the perivascular space with cytotoxic fragments of APP accumulation may be involved in the gradual maturation of injurious process in ischemic white matter leading over a lifetime to severe and progressive dementia. Progressing damage of the white matter after ischemia may be caused not only by a degeneration of axons of neurons destroyed during ischemic injury, but also by pathological changes in BBB vessels with deposition of cytotoxic fragments of APP. We further examine the role of cerebral ischemia injury with an alternative hypothesis that proposes that repetitive microischemic-reperfusion insults may form the basis for development of chronic neurodegenerative disorders such as Alzheimer's disease. This process may occur by increasing the sensitivity of neurons and white matter to amyloid formation and aberrant APP processing. On the other hand brain ischemia provides a bridge between experimental and clinical research that greatly facilitates the interpretation of complex disease processes i.e. in Alzheimer-type dementia. **References:** [1] Pluta R et al. *Brain Res.*, 633, 41-52, 1994. [2] Pluta R et al. *Brain Res.*, 649, 323-328, 1994. [3] Pluta R et al. *J Brain Res.*, 35, 463-471, 1994. [4] Pluta R et al. *Acta Neuropathol.*, 83, 1-11, 1991.

**GLIAL ACTIVATION IN WHITE MATTER INJURY FOLLOWING ISCHEMIA IN THE NEONATAL P7 RAT BRAIN**

Valerie Biran<sup>1,2</sup>, Luc-Marie Joly<sup>1,3</sup>, Jean Mariani<sup>1,2</sup>, Sylvain Renolleau<sup>1,2</sup>,  
**Christiane Charriaut-Marlangue<sup>1,2</sup>**

<sup>1</sup>*Université Pierre et Marie Curie (P6), Paris, France*

<sup>2</sup>*UMR-CNRS 7102, Paris, France*

<sup>3</sup>*CHU Rouen, France*

Introduction : Neonatal hypoxic-ischemic white matter (WM) damage is a major contributor to chronic neurological dysfunction. Immature oligodendrocytes (OLs) are known to be highly vulnerable to ischemia. As little is known about the loss and restoration of myelin basic protein (MBP) as well as repair mechanisms in neonates, we studied cell outcome in the white matter (cingulum and external capsule) after MCA electrocoagulation and transient homolateral CCA occlusion. Methods : Seven day-old rat pups were anesthetized with intraperitoneal injection of chloral hydrate (300 mg/kg) and underwent left middle cerebral artery electrocoagulation associated with 50 minutes left common carotid artery occlusion [1]. They were killed at various times (between 6 h and 15 days) after reperfusion. Loss and restoration of MBP were studied by MBP protein and O4 antigen labeling. TUNEL and Fluoro-Jade B are used to label cell death. Proliferation was demonstrated by the Ki-67 marker, a nuclear protein expressed in dividing cells for the entire duration of their mitotic process and expressed in all mammalian species. Microglial activation was followed with Griffonia simplicifolia I isolectin B4 marker. Results : In P7-injured rat pups, a marked reduction in MBP immunostaining, corresponded to numerous pyknotic immature OLs as early as 12 hours and a few dying mature OLs. Several GFAP-TUNEL-positive astrocytes were also observed ipsilaterally in the external capsule. In contrast, a substantial restoration of MBP occurred in the cingulum at 48 and 72 hours of recovery. Cell proliferation, demonstrated by the Ki-67 immunostaining, revealed a first peak of new generated cells in the dorsolateral SVZ at 72 hours of reperfusion. However, no double-stained O4 and Ki-67 OLs were detected, suggesting a functional recovery of injured mature OLs. New bipolar OL progenitors are generated between 7 to 15 days of recovery in the dorsolateral SVZ, compared to the contralateral side, indicating cell migration. Microglial-macrophage infiltration occurs over days following ischemia in the cingulum and also in the subcortical white matter where they were shown to engulf immature OLs, leading to impairment of repair. These deleterious events contribute to WM cystic formation. Conclusion : The overall results suggest that the persistent activation of microglia/macrophages implicates a chronic component of immunoinflammation, which overwhelms repair processes and contributes to cystic growth. The use of drugs that modulate microglial activation can be proposed as candidate therapeutic agents. References [1] Renolleau et al., Stroke 29, 1954-1961 (1998).

## ABSENCE OF THE MDR1A P-GLYCOPROTEIN IN MICE SHOWS NEUROPROTECTION IN TRANSIENT FOCAL CEREBRAL ISCHEMIA

Michihiro Murozono, Shohei Matsumoto, Naoko Takeda, Mao Miyamoto, Seigo Watanabe

*Department of Anesthesiology, Tokyo Medical University, Tokyo, Japan*

**Introduction:** P-glycoprotein(P-gp) is expressed not only in tumor cells but also in some normal tissues including brain capillary endothelium. The mouse *mdr1a* gene encoding P-gp is predominantly expressed in the brain. P-gp can protect the organs against toxic xenobiotic compounds which are excreted into urine, bile, and the intestinal lumen, and also can prevent their accumulations in critical organs such as brain and testis. However, there are few studies to search for the function of P-gp related to brain ischemia. We investigated the functional effects of P-gp on focal cerebral ischemia using *mdr1a* knockout (ko) mice. **Methods:** *Mdr1a* ko mice and FVB wild mice were used. We prepared the middle cerebral artery occlusion model for 30 min by using a 6-0 siliconized filament in all mice. The anesthesia was maintained with isoflurane in N<sub>2</sub>O and O<sub>2</sub> by an inhalation mask during the surgical procedure. In order to monitor regional cerebral blood flow (rCBF) continuously, a laser-Doppler flowmetry probe was fixed to the intact skull. Forty eight hours after reperfusion, all mice were deeply anesthetized with isoflurane. Then thoractomies were performed to expose the heart. The brain was fixed with 4% paraformaldehyde through the heart. After that, 40 $\mu$  coronal sections were made from the brain. Those sections were stained with monoclonal mouse antibody against mouse neuronal nuclei (NeuN) for identification of the infarct area. For measuring the infarcted volumes, 5 sections at approximately 0.7mm distance chosen, immunostained with antibody against NeuN, scanned and infarcted areas were measured using NIH image version 1.55. Infarcted volumes were calculated using by the three-dimensional reconstruction. The direct arterial blood pressure was measured using a cannula inserted into the tail artery connected with a transducer and micropump in some *mdr1a* ko mice and FVB wild mice. Heart rate was calculated from arterial pressure pulses. Arterial blood samples were obtained from the same line and analyzed for the partial PaO<sub>2</sub>, PaCO<sub>2</sub>, Base Excess and hemoglobin before ischemia and 30 min after reperfusion. In order to evaluate differences in cerebrovascular anatomy between *mdr1a* ko mice and FVB wild mice, thoracotomy was performed on anesthetized animals and India ink was injected. **Results:** The mean infarction volumes seen in *mdr1a* ko mice and FVB wild mice were 25% and 40%, respectively. Infarction volume of *mdr1a* ko mice group was significantly smaller than that seen in FVB wild mice group. rCBF, blood pressure and heart rate did not differ between groups. There are no significant differences in PaO<sub>2</sub>, PaCO<sub>2</sub>, Base Excess and hemoglobin before ischemia and 30 min after reperfusion. India ink staining of cerebrovascular anatomy of the circle of Willis demonstrated that there were no gross anatomic differences in the vascular pattern of the cerebral circulation, with intact posterior communicating arteries in both groups. **Conclusion:** This study demonstrated that the neuronal damage of mutant mice without P-gp encoded by *mdr1a* was significantly smaller than that of wild mice. These results indicate that P-gp leads to exacerbate cerebral infarction in brain ischemia.

## A ROLE OF ASTROCYTIC AQUAPORIN4 ON THE TRAUMATIC BRAIN EDEMA AND A HYPOTHERMIC EFFECT UPON THE AQUAPORIN4 EXPRESSION

Akira Watanabe, **Kazuo Kataoka**, Kiyoshi Tsuji, Toshihisa Sumii, Yoshifumi Teramoto, Mamoru Taneda

*Department of Neurosurgery, Kinki University, School of Medicine, Osaka-Sayama, Japan*

**INTRODUCTION** Prevention of traumatic brain edema leads to the brain protection. Water channel protein located in cell membranes was found and named aquaporin (AQP). AQP4 is abundantly present on astrocytic end-feet in contact with brain vessels. Osmolarity of injured brain tissues increases after brain trauma. According to this osmotic gradient, water moves to the injured brain tissues. An osmotic change in injured brain tissue may influence the AQP expression of astrocytes, because astrocytes maintain water homeostasis in the brain. Hypothermia is effective for the brain protection, and may modify astrocytic AQP expression.

**METHODS** Adult male C57/BL6 mice were anesthetized with 400 mg/kg chloral hydrate, i.p., and the head was fixed in a stereotaxic instrument. A burr hole was drilled in the skull on the right side. A stainless needle (26G) was placed 10 times in the right cortex at a depth of 2 mm from the surface to produce multiple cortical stab wounds. One, 2, 3, 5, 8, and 12 days thereafter, the mice were deeply anesthetized with 1000 mg/kg chloral hydrate, i.p., then their brains were removed. The brains were quickly frozen in liquid nitrogen, or were measured the weight. Total RNA was isolated from the frozen brains, and quantitative RT-PCR was performed on a fluorescence temperature cycler (LightCycler; Roche Diagnostics) for the determination of AQP4 mRNA and  $\beta$  actin mRNA. Using the other brains, brain water contents were evaluated by means of wet-dry weight measurements. Astrocyte cultures were prepared from new-born C57/BL6 mice. The astrocyte cultures were maintained at 37C and 5% CO<sub>2</sub> in DMEM/F12 (300mOsm) containing 10% fetal bovine serum. The standard culture medium of 300 mOsm was replaced by hyperosmolar medium of 375 mOsm, and were maintained at the temperature of 29C, 32C, 34C, and 37C. Cellular mRNA was isolated from the cell cultures, and quantitative RT-PCR was performed on the LightCycler for the determination of AQP4 mRNA and  $\beta$  actin mRNA.

**RESULTS** Significant increases in water contents of the injured hemisphere were observed 2 days (80.2%), 3days (80.8%), and 5 days (80.1%) after the injuries. Brain water content of the sham control was 78.6%. The ratio of copies of AQP4 mRNA / copies of  $\beta$  actin mRNA in the injured cortex was significantly increased 2 days (160% of sham control), 3 days (150%), 5 days (193%), 8 days (200%), and 12 days (191%) after the injuries. The hyperosmolar stimulation to astrocyte cultures caused a significant rise (155% of control) of the AQP4 mRNA expression (AQP-4 mRNA /  $\beta$  actin mRNA) 48 hours after the stimulation. The hypothermic conditions (29C, and 32C) eliminated the rise of AQP4 mRNA by the hyperosmolar stimulation.

**CONCLUSION** Our study suggests that an increase of osmolarity in injured brain tissues triggers overexpression of AQP4 in astrocytes. According to the osmotic gradient, water moves to the injured brain through the water channel AQP4 that is excessively expressed. Hypothermia inhibits this overexpression of astrocytic AQP4. This inhibition may be benefit for the injured brain to prevent the brain edema.

## CARDIAC ARREST INDUCES VASCULAR ENDOTHELIAL LEAKAGE IN THE BRAIN STEM

Jeff W.M. Bulte<sup>1</sup>, Julia Kofler<sup>2</sup>, Jiangyang Zhang<sup>1</sup>, Susumu Mori<sup>1</sup>, Richard J. Traystman<sup>2</sup>

<sup>1</sup>*Department of Radiology, Johns Hopkins University School of Medicine, Baltimore, MD, USA*

<sup>2</sup>*Department of Anesthesiology and Perioperative Medicine, Oregon Health and Science University, Beaverton, OR, USA*

**Introduction:** Neurologic and neuropsychologic deficiencies are commonly found following cardiac arrest and cardiopulmonary resuscitation (CPR). Subtle changes in blood-brain barrier (bbb) permeability have been known to occur in experimental animal models (1). It has previously been shown, using a cortical freezing injury model, that iron oxide nanoparticles can accumulate in damaged endothelial cells following i.v. injection, allowing mapping of the disrupted BBB-area by MR imaging (2). We assessed whether these iron oxide contrast agents would allow MRI detection of endothelial permeability changes in the brain following cardiac arrest. **Materials and Methods:** Cardiac arrest was induced in C57/BL6 mice by i.v. injection of KCl, with body cooling to 27 C and heating of the brain at 39 C. After 10 min of cardiac standstill, CPR was initiated and MION-46L nanoparticles were administered (1 mmole Fe/kg) immediately following CPR (n=3). As controls, two sham-operated and one normal animal received the same dose of MION-46L, and one cardiac arrest/CPR animal received no contrast agent. After 24 hrs following injection, the brains were removed for high-resolution MR imaging. Imaging was performed on a 9.4 Tesla instrument, using T2- and T2\*-weighted imaging with a resolution of 70x66x63  $\mu\text{m}$ . Histopathological correlation was performed using DAB-enhanced Prussian Blue staining for iron. **Results:** For all injured animals receiving MION-46L, numerous hypointense lesions were visible throughout the brain stem (Figure 1A), but not in other parts of the cerebrum or cerebellum. The lesions appeared substantially larger on the T2\*-weighted images due to the iron-induced magnetic susceptibility effects. Histology revealed many dilated vessels in the brain stem containing endothelial cells that were uniformly filled with iron-positive magnetic nanoparticles (Figure 1B). No such lesions, either on MRI or histology, were observed in the four different controls (Figure 1C). **Discussion:** We conclude that cardiac arrest followed by resuscitation can lead to a hitherto unreported damage of brain stem endothelial cells. We hypothesize that a transient high blood pressure (from a no-flow status) induces a loss of endothelial cell membrane integrity, resulting in leakage and uptake of the iron oxide nanoparticles. It is not known why the brain stem appears primarily affected, but it may be related to the predominant occurrence of vasogenic edema in the brain stem of patients with essential hypertension, often referred to as hypertensive encephalopathy (3). **References** 1. C.L. Schleien et al., *Stroke* 22, 477-483 (1991). 2. J.W.M. Bulte et al., *Magn. Reson. Med.* 23, 215-223 (1992). 3. J. de Seze et al., *Am. J. Neuroradiol.* 21, 391-394 (2000).



## INTRACEREBRAL HEMORRHAGE IN COMPLEMENT C3 DEFICIENT AND SUFFICIENT MICE

Shuxu Yang<sup>1</sup>, Takehiro Nakamura<sup>1</sup>, Ya Hua<sup>1</sup>, Richard Keep<sup>1</sup>, John Younger<sup>2</sup>, Julian Hoff<sup>1</sup>,  
Guohua Xi<sup>1</sup>

<sup>1</sup>*Department of Neurosurgery, University of Michigan, Ann Arbor, MI, USA*

<sup>2</sup>*Department of Emergency Medicine, University of Michigan, Ann Arbor, MI, USA*

**Introduction:** The complement cascade is activated after intracerebral hemorrhage (ICH) [1]. Systemic complement inhibition and depletion reduce perihematomal brain edema in rats [2]. The development of mice deficient in elements of the complement system has enabled investigators to study the role of different complement components in systemic injury. Recently we have developed an ICH model in mice [3]. The present study investigated ICH-induced brain injury in complement C3 deficient and sufficient mice. **Methods:** This study was divided into two parts. Male C3 deficient and sufficient mice (Jackson Laboratory) received an intracerebral infusion of 30- $\mu$ l autologous whole blood into the right basal ganglia. In the first part, mice were killed at three days for brain water content measurement. Behavioral tests including forelimb use asymmetry and corner turn tests were also performed before and after ICH. In the second part, brain hemoxygenase-1 (HO-1) was measured by Western blot analysis and immunohistochemistry at day 3. **Results:** Brain water content in the ipsilateral basal ganglia 3 days after ICH was less in C3 deficient mice compared to C3 sufficient mice ( $79.45 \pm 0.41$  vs.  $80.55 \pm 1.00$  %, mean  $\pm$  S.D.,  $n=6$ ,  $p < 0.05$ ). The reduced edema in the C3 deficient mice was associated with a less accumulation of sodium and loss of potassium than in C3 sufficient mice ( $P < 0.05$ ). There was no significant difference in water or ion content in the contralateral basal ganglia and the cerebellum between C3 deficient and C3 sufficient mice. The C3-deficient mice had less ICH-induced forelimb use asymmetry deficits compared with C3-sufficient mice ( $p < 0.05$ ), although there was no significant difference in corner turn test score. Western blot analysis showed that HO-1 contents were significant lower in C3 deficient mice (day 3:  $4830 \pm 1044$  vs.  $6953 \pm 513$  pixels in the C3 sufficient mice,  $p < 0.05$ ). **Conclusions:** ICH causes less brain edema and behavior deficits in complement C3 deficient mice. These results suggest complement C3 is a key factor contributing to brain injury following ICH. Further studies should clarify whether C3 deficient mice have less cell lysis and less inflammatory response than C3 sufficient controls. **References:** [1] Hua Y, Xi G, Keep RF, Hoff JT. Complement activation in the brain after experimental intracerebral hemorrhage. *J Neurosurg* 92:1016-1022 (2000) [2] Xi G, Hua Y, Keep RF, Younger JG, Hoff JT. Systemic complement depletion diminishes perihematomal brain edema. *Stroke* 32:162-167 (2001) [3] Nakamura T, Xi G, Hua Y, Schallert T, Hoff JT, Keep RF. Intracerebral hemorrhage in mice: Model characterization and application for genetically modified mice. *J Cereb Blood Flow Metab* 24:487-494 (2004) Supported by NIH NS 17760, NS 39866, NS 47245 and AHA 0435354Z.

## BLOOD BRAIN BARRIER IMPAIRMENT IN THE STROKE-PRONE SPONTANEOUSLY HYPERTENSIVE RAT (SHRSP) 28 DAYS AFTER STROKE

Jetta K. McGill<sup>1</sup>, David I. Graham<sup>2</sup>, William Stewart<sup>2</sup>, Elaine I. Irving<sup>3</sup>,

Anna F. Dominiczak<sup>4</sup>, I. Mhairi Macrae<sup>1</sup>

<sup>1</sup>*Division of Clinical Neurosciences, Wellcome Surgical Institute, Glasgow University, Glasgow, UK*

<sup>2</sup>*Division of Clinical Neurosciences, Southern General Hospital, Glasgow, UK*

<sup>3</sup>*Department of Neurodegeneration, Neurology and GI CEDD, GlaxoSmithKline, Harlow, UK*

<sup>4</sup>*Division of Cardiovascular and Medical Sciences, Western Infirmary, Glasgow University, Glasgow, UK*

**Introduction:** SHRSP show an impaired ability to recover compared to their reference control strain, Wistar Kyoto (WKY), up to 28 days following middle cerebral artery occlusion (MCAO), even when MCAO is controlled to induce comparable ischaemic damage in the two strains (McGill et al, 2005). It is well documented that blood-brain barrier (BBB) breakdown and oedema occur in the acute phase after stroke, but this is thought to resolve within 2 weeks (Hatashita et al, 1990). Following MCAO and a recovery period of 28 days, swelling of the ipsilateral hemisphere is evident in SHRSP but not WKY. Since this indicates oedema and possibly BBB breakdown, this has been investigated further. **Methods:** Fourteen and 28 days following MCAO rats were transcardially perfused with heparinised saline followed by paraformaldehyde and brains removed for tissue processing. Coronal sections (6 micrometres) at the level of the anterior commissure from SHRSP & WKY were stained with haematoxylin and eosin (H&E) for assessment of neuropathology. BBB integrity was analysed with albumin immunohistochemistry (polyclonal antibody, Abcam, 1:1000). Albumin immunoreactivity was scored as follows: 2=widespread dark staining, 1= focal lighter staining, 0=no staining. Scores were analysed using a Mann-Whitney test. **Results:** Obvious ipsilateral hemispheric swelling was evident in 6/11 SHRSP and 1/9 WKY (Figure 1). H&E stained sections revealed that the majority of SHRSP displayed protein exudate in the brain parenchyma, indicative of BBB breakdown. This was confirmed by evidence of widespread albumin extravasation in the majority of SHRSP at 28 days post MCAO (7/11) compared to just 1/9 WKY ( $p=0.03$ ) at the same time point (Figure 2). **Conclusions:** Ongoing or delayed BBB breakdown and oedema formation in SHRSP could be a contributory factor in impaired functional recovery after stroke. **References:** 1. McGill JK et al. Impaired recovery after stroke in the SHRSP. *Stroke*. 2005;36(1):135-141. 2. Hatashita et al. Brain edema and cerebrovascular permeability during cerebral ischemia in rats. *Stroke*. 1990;21:582-588. **Acknowledgements:** JK McGill is supported by an MRC CASE award.

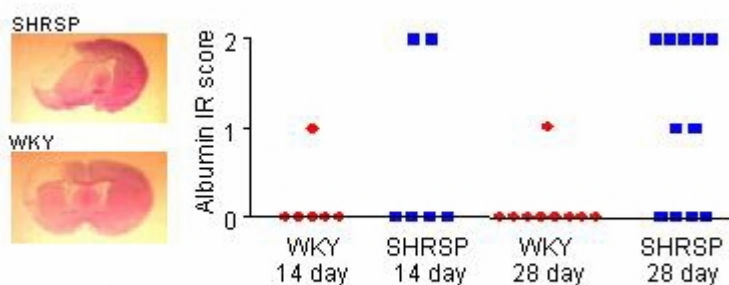


Figure 1

Figure 2

## MICROVASCULAR BASAL LAMINA DAMAGE AFTER SUBARACHNOID HEMORRHAGE (SAH) IN RATS

**Karsten Schöller**<sup>1</sup>, Andreas Trinkl<sup>1</sup>, Mariusz Kłopotowski<sup>1</sup>, Serge Thal<sup>2</sup>, Nikolaus Plesnila<sup>1</sup>, Robert Schmid-Elsaesser<sup>1</sup>, Stefan Zausinger<sup>1</sup>

<sup>1</sup>*Klinikum der Universität München-Grosshadern, Dept. of Neurosurgery, Munich, Germany*

<sup>2</sup>*Klinikum der Johannes Gutenberg-Universität, Dept. of Anesthesiology, Mainz, Germany*

**Purpose:** Mechanisms of early cerebral edema following SAH are poorly understood. Previously, we demonstrated a peak of edema evolution at 24 hours after experimental SAH in rats. Furthermore, brain water content correlated with neurological deficits of animals. In focal cerebral ischemia, alteration of the microvascular basal lamina, a constituent of the blood-brain barrier, and its relevance for development of cerebral edema and hemorrhagic transformation has previously been demonstrated. The present study was designed to demonstrate microvascular basal lamina damage in the context of blood-brain barrier dysfunction as a potential target for therapeutical interventions to reduce vasogenic brain edema following SAH. **Methods:** 54 rats were subjected to SAH by an endovascular filament. Animals were randomly assigned to 1 sham (n=9) and 4 SAH groups (n=9 each; 6, 24, 48, and 72h survival). Microvascular basal lamina alteration was quantified by anticollagen type IV immunochemistry with subsequent counting of stained cerebral microvessels/region of interest (ROI) in cortex and subcortical regions of both hemispheres; Western Blot was used to define the collagen type IV protein content. Bovine serum albumin (BSA) extravasation was quantified by Western Blot technique to assess blood-brain barrier permeability. **Results:** Significant ( $p<0.001$ ) reduction of Collagen Type IV stained microvessels/ROI occurred in all SAH groups with the most pronounced decline until 24 hours following SAH. Consistently, Collagen type IV protein content was significantly reduced after 6 and 24 hours. Microvascular damage was found within the cortex bilaterally with predominance of the ipsilateral hemisphere. There was no alteration of the microvascular basal lamina in subcortical regions (hippocampus, basal ganglia, brain stem, cerebellum), neither evaluated by immunohistochemistry nor by Western Blot for collagen type IV. BSA Western Blot revealed maximum and significant extravasation 24 hours after SAH, correlating with microvascular damage. **Conclusion:** This is the first study to demonstrate that microvascular basal lamina injury after experimental SAH is linked to blood-brain barrier permeability in a time-dependent manner. Documented loss of basal lamina integrity might contribute to the development of vasogenic brain edema. Consequently, proteolytic systems that are known to be involved in the digestion of basal lamina antigens after focal cerebral ischemia need to be investigated and their role as targets for therapeutic interventions to prevent development of cerebral edema following SAH need to be defined.

## TIME COURSE OF EDEMA FORMATION AND BRAIN AQUAPORIN EXPRESSION AFTER TRANSIENT FOCAL CEREBRAL ISCHEMIA IN MICE

Marlise de Castro Ribeiro<sup>1</sup>, Lorenz Hirt<sup>1</sup>, Julien Bogousslavsky<sup>1</sup>, Luca Regli<sup>2</sup>,

Jerome Badaut<sup>2</sup>

<sup>1</sup>*Department of Neurology, CHUV, Lausanne, Switzerland*

<sup>2</sup>*Department of Neurosurgery, CHUV, Lausanne, Switzerland*

Background: Cerebral edema contributes significantly to morbidity and death associated with brain ischemia. Recently, aquaporin 1, 4 and 9 have been identified as the three main water channels in the rodent brain (Badaut et al., 2002, *J Cereb Blood Flow Metab*; 22(4):367). Different studies show that AQP4 and 9 could be implicated in water movements during the formation and resolution of the brain edema after stroke. The role of each AQP in the water movement in the edema formation and resolution is still unclear and debated. To clarify the role of the AQPs in the edema formation after ischemia, we have compared the time course of the expression of AQP1, 4, and 9 with the edema formation after a transient focal brain ischemia in mouse. Methods: This investigation was realised by immunocytochemistry on mouse brain slices after focal transient ischemia (30min) induced by occlusion of the middle cerebral artery by a silicon coated filament. Brain sections were stained by antibodies against AQP1, 4, 9 (Chemicon), GFAP (sigma) and MAP2 (sigma). The staining was done at 1h, 6h, 24h, 48h and 7days after the occlusion. The edema was evaluated by measuring the swelling of the ischemic hemisphere on haematoxylin-eosin stained slices. The levels of expression of AQPs were quantified in the core of ischemia and in the border of the lesion ("penumbra") delimited on MAP2 stained slices. Results : The brain swelling was maximal at 1hour (hemispheric volume increased by  $8.4\% \pm 3$ ) and at 48hours (by  $10.1\% \pm 2.5$ ) after the ischemia. The size of the ischemic hemisphere was decreased ( $-3.5\% \pm 1$ ) 7days after the occlusion. AQP1, mainly expressed on the choroid plexus, did not show a modification of expression after ischemia. AQP4 expression, present on astrocytic endfeet, was increased 1h ( $117\% \pm 20$ ,  $n=3$ ,  $P<0.05$ , T-test) after occlusion and returned to the basal level at 24h ( $95\% \pm 16$ ,  $n=3$ ) in the core and penumbra. In the penumbra, 48h after the occlusion, the AQP4 expression was increased on the whole cell, without the normal polarization, ( $112\% \pm 10$ ,  $n=3$ ,  $P<0.05$ , T-test). After 7days, the AQP4 level was the lowest  $91\% \pm 10$ . AQP9, supposedly implicated in the glycerol and lactate diffusion, showed a significant induction with  $24 \pm 6$  positive astrocytes in the penumbra versus  $5 \pm 1$  in the contralateral hemisphere. This expression was increased with time and there were  $69 \pm 24$  positive astrocytes at 7days (versus,  $3 \pm 2$  in the contralateral hemisphere). Neuronal AQP9 expression was not modified. Conclusions : The variations of the level of AQP4 were correlated in time with the variations in brain swelling, in contrast with the AQP9 expression that increased gradually with time. AQP9 was highly expressed on all reactive astrocytes 7days after ischemia. This study suggests that AQP4 could play a major role in the edema formation and resolution in contrast with AQP1 and 9. AQP9, as suggested by our previous studies, could be implicated in the elimination of the excess of lactate or glycerol.

**RECURRENT SPREADING DEPRESSION (SD) CAUSES EARLY OPENING OF THE BLOOD-BRAIN BARRIER (BBB)****Sebastian Major**<sup>1</sup>, Alon Friedman<sup>2,3</sup>, Jens P. Dreier<sup>1</sup><sup>1</sup>*Experimental Neurology, Charité University Medicine Berlin, Berlin, Germany*<sup>2</sup>*Johannes-Müller-Institute of Physiology, Charité – University Medicine Berlin, Berlin, Germany*<sup>3</sup>*Department of Neurosurgery, Zlotowski Center for Neuroscience, Ben-Gurion University, Beer-Sheva, Israel*

SD is a depolarization wave propagating at a rate of about 3 mm/min in the cerebral cortex. It is characterized by an amplitude reduction of the electrocorticographic activity, a rise of the extracellular potassium to 60 mM and a reduction of the extracellular volume. Typical changes of cerebral blood flow (CBF) accompany SD, which consist of a short lasting “spreading hyperemia” followed by a long lasting “spreading oligemia”. SD is triggered by electrical, mechanical or toxic factors and is probably involved in the pathogenesis of migraine, focal ischemia, head trauma and cerebral hemorrhage. SD is assumed to be the pathophysiological correlate of the migraine aura. We have recently observed a patient with familial hemiplegic migraine (FHM) type II and a long-lasting migraine aura with fluctuating neurological symptoms. Quantitative analysis of early gadolinium-enhanced MR images revealed a left-hemispheric, cortical blood brain-barrier (BBB) disruption preceding delayed cortical edema in this ATP1A2 mutation carrier. As we know from the work by Strong et al. repetitive SDs can occur in the human brain tissue, which could explain the fluctuating symptoms in our FHM patient. Additionally, a recent publication by GURSOY-OZDEMIR et al. showed a delayed enhancement of BBB permeability and subsequent cortical oedema following a single SD. Based on these observations, we studied here whether recurrent SD causes early BBB disruption in the rat cortex in vivo. We triggered SD with artificial cerebrospinal fluid (ACSF) containing a potassium concentration ([K<sup>+</sup>]ACSF) of 130 mM at an open parietal cranial window. SDs were monitored with an intracortical potassium sensitive microelectrode and laser-Doppler flowmetry. We also recorded the propagation of SDs to a distant closed frontal cranial window using an epidural Ag-AgCl electrode. BBB integrity was evaluated quantitatively by analyzing fluorescence in brain sections following the peripheral injection of Evan’s Blue or Lucifer yellow. At the occipital window, [K<sup>+</sup>]ACSF evoked several SDs in all animals. In the first group (n = 10), one or more SDs propagated to the frontal window. In contrast, in the second group (n = 9), pretreatment with MK-801 (5mg/kg BW i.v.), abolished SD propagation. Within two hours after the onset of the first SD, significantly enhanced fluorescence intensity at the frontal cortex was only measured in animals from group 1 with multiple propagated SDs. In conclusion, we provide evidence that repetitive SDs significantly increase blood-brain barrier permeability within two hours after the onset. Keywords: spreading depression, blood-brain barrier, migraine, MK-801

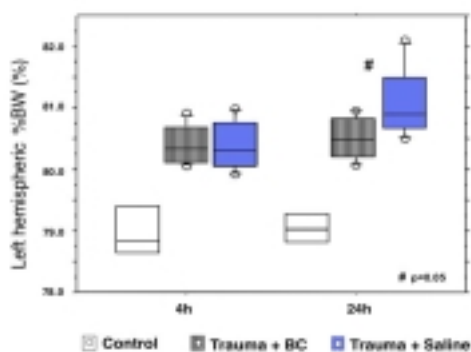
## EFFECT OF BOSWELLIA CARTERII ON BRAIN EDEMA FOLLOWING CONTUSION INJURY

Martin U. Schuhmann<sup>1</sup>, Maryam Mokhtarzardeh<sup>2</sup>, Marco Skardelly<sup>1</sup>, Matthias Jaeger<sup>1</sup>, Frank M Gutzki<sup>2</sup>, Dirk. O. Stichtenoth<sup>2</sup>

<sup>1</sup>Klinik Und Poliklinik für Neurochirurgie, University of Leipzig, Leipzig, Germany

<sup>2</sup>Institut für Klinische Pharmakologie, Hannover Medical School, Hannover, Germany

Objective: Following Controlled Cortical Impact Injury (CCI) a perifocal brain edema develops within the first 24 to 48 hours, which is restricted to the injured hemisphere and has mainly cytotoxic as well as some vasogenic edema components. Leukotrienes, which strongly augment vascular permeability and promote vasoconstriction, are generated following the posttraumatic arachidonic acid release and increase in CSF with a maximum in the first 6h. We investigated in a controlled study following cortical contusion injury the effect of *Boswellia carterii* (BC), a known natural non-redox 5-lipoxygenase inhibitor, on the development of posttraumatic brain edema and on the post-traumatic cysteinyl-leukotrienes (LT) levels in CSF. Methods: 34 male Sprague Dawley rats were studied. Animals of Group I (n=17) received 400mg/kg p.o. BC 1h prior to controlled cortical impact injury. 6 of them received another dose 12 h later. Animals of Group II (N=17) received an equal amount of saline. 5 animals per group received a sham operation and served as baseline. 12 animals per treatment group received controlled cortical impact injury (2.5mm, 4m/s, 5mm Impactor). 6 animals each were sacrificed at 4h and 24h, respectively. Left hemispheric brain water content (%BW) and left hemispheric swelling (%HS) was assessed by wet-dry weight method. After purification of CSF, LTC<sub>4</sub>, LTD<sub>4</sub> and LTE<sub>4</sub> fractions were separated by HPLC and levels determined quantitatively (pg/100µl) with tandem gas chromatography-mass spectrometry. Differences between groups were determined using Mann-Whitney test. A p value of <0.05 was required to reject the null hypothesis of equivalence. Results: At 4h brain water content (%BW) and hemispheric swelling (%HS) increased in both groups versus baseline significantly and to a comparable extent. At 24h %BW and %HS of Group I did not progress any further and were significantly (p<0.05) below Group II, where both parameters further increase. LTC<sub>4</sub> levels in CSF of Group I were significantly below Group II at 4 hours. At 24h no difference could be detected. LTD<sub>4</sub> and LTE<sub>4</sub> levels did not differ at any time point. Conclusions: These first data suggest, that BC can attenuate the posttraumatic pericontusional oedema formation. This effect is possibly mediated by the documented partial inhibition of the posttraumatic LTC<sub>4</sub> production. To further investigate a possible therapeutic role of *Boswellia carterii* and its main effectors, boswellic acids, in traumatic brain injury, future studies need to confirm these preliminary results also in comparison to the effects of synthetic 5-LO inhibitors.



## ACCUMULATION OF 4-HYDROXY-2-NONENAL-MODIFIED PROTEINS IN THE WHITE MATTER DAMAGE IN CHRONIC CEREBRAL HYPO-PERFUSION RAT MODE

Terubumi Watanabe, Yoshiko Yanagi, Takao Urabe, Yoshikuni Mizuno

*Department of Neurology, Juntendo University School of Medicine, Tokyo, Japan*

(PURPOSE) Cerebral white matter damages are often observed in human ischemic cerebrovascular disease and have been thought to contribute to cognitive impairment. This damage can be induced in rat brains under chronic cerebral hypo-perfusion by the permanent occlusion of both internal carotid arteries. However it remains uncertain how the oxidasive stress damages the white matter in chronic cerebral hypo-perfuion. Therefore, we investigated that the oxidative stress contributed to the white matter damages in chronic cerebral hypo-perfusion in rat model, using immunohistochemistry for 4-hydroxy-2-nonenal (HNE) of the oxidative stress marker. We observed the relationships of phosphorylated cyclic AMP responsive element binding protein (p-CREB) for the progression of white matter damage. (METHOD) Studies were conducted in 7~8weeks old male Wister rat. (n=3/group) Rat underwent permanently ligation of the bilateral internal carotid arteries. Cerebral blood flow (CBF) was measured using echo doppler method. 7, 14, 21, 28 days after the ischemia, the brains were perfusion-fixed 4% paraformaldehyde in 0.1M phosphate buffer. The fixed brains were 20-micrometers thick coronal sections were prepared in a cryostat. To clarify the distribution and function of glial cells, staining of H-E, Kluver-Barrela, and immunohistochemical staining of glial fibrillary acid protein (GFAP), ionized calcium binding adapter molecule 1 (Iba-1), GST-pi, HNE, and p-CREB were performed. For behavioral study, Morris's water maze test was performed at 7, 14, 21, 28 days after the ischemia. (RESULT) After the operation, CBF was decreased about 50% compared with pre-operation. However 14 days after the ischemia, CBF appeared to be slightly recovered. White matter damages were observed as the impairment of nerve fibers by H-E and Kluver-Barrela stain. Immunoreactivity for GFAP and Iba-1 were observed at 7days after ischemia and GFAP positive astrocyte and Iba-1 positive microglia were observed until 28 days after the ischemia. GST-pi and HNE were observed at 7days after the ischemia, marked increase in GST-pi positive oligodendroglia and HNE positive cells were observed at 14 days. These cells were gradually decreased in a time dependent manner. Immunoreactivity for p-CREB was observed at 7days after the ischemia, gradually decreased in time course. Morris's water maze test in chronic hypo-perfusion group showed impairment of spatial learning compared with sham group. ( $p < 0.05$ ) (CONCLUSION) These results demonstrated that the accumulation of HNE-modified proteins and the suppression of p-CREB might be an important role of white matter damage for the chronic cerebral hypo-perfusion.

## CHRONIC CEREBRAL HYPOPERFUSION INDUCES WHITE MATTER LESIONS AND COGNITIVE ABNORMALITIES; A COMPARISON BETWEEN MOUSE AND RAT MODELS FOR VASCULAR DEMENTIA

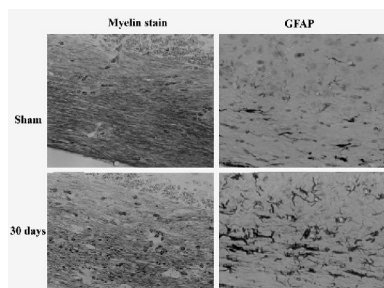
Hidekazu Tomimoto<sup>1</sup>, Masunari Shibata<sup>1</sup>, Kayoko Nakaji<sup>1</sup>, Masafumi Ihara<sup>1</sup>, Makoto Noda<sup>2</sup>, Nobuyuki Yamasaki<sup>3</sup>, Tsuyoshi Miyakawa<sup>3</sup>

<sup>1</sup>*Department of Neurology, Kyoto University Graduate School, Kyoto, Japan*

<sup>2</sup>*Department of Molecular Oncology, Kyoto University Graduate School, Kyoto, Japan*

<sup>3</sup>*Horizontal Brain Research Organization, Kyoto University, Kyoto, Japan*

We designed a mouse model of chronic cerebral hypoperfusion, which invariably exhibits white matter lesions. In the present study, we present histological and behavioral changes after chronic cerebral hypoperfusion in the mouse, and compare the advantages and disadvantages between the rat and mouse models. Application of this model to knockout or transgenic strategies is also discussed. Methods; Chronic cerebral hypoperfusion was induced by applying microcoils with diameters of 0.18mm to the bilateral common carotid arteries (CCAs) in the mouse. Rat model was prepared by clipping the bilateral CCAs. The mouse model was subjected to a set of behavioral assessment tests; rotarod test, open field, light/dark transition, prepulse inhibition, Porsolt forced swim and 8-arm radial maze test. Astroglia and microglia were examined with immunohistochemistry for glial fibrillary acidic protein (GFAP) and MHC class I antigen, respectively. The severity of white matter lesions was graded in myelin staining. Since matrix metalloproteinase 2 (MMP2) is known to be involved in the pathogenesis of white matter lesions, chronic cerebral hypoperfusion was applied to the MMP2 (-/-) mice and wild type mice. Results; Until 14 days after the operation, CBF ranged between 32-59% in the rats and 69-81% in the mice. Astroglia and microglia were markedly proliferated in the white matter of the both species after chronic cerebral hypoperfusion. White matter rarefaction developed after 14 days in the rats and after 30 days in the mice. Degeneration of the visual pathway was observed exclusively in the rats. Among the set of behavioral assessment scales, the mouse model showed a significant abnormality only in 8-arm radial maze test. Chronic cerebral hypoperfusion induced marked rarefaction of the white matter and activation of glial cells in wild type mice, but not in MMP2 (-/-) mice. Discussion; We successfully developed a mouse model of chronic cerebral hypoperfusion, which shows cognitive abnormalities without a significant damage to the visual system. Although behavioral abnormalities in the rat model have been reported previously, we did not examine the behavioral tests, since degeneration of the visual system seem to compromise the results. The rat model is more suitable for drug evaluation, because of more prompt emergence of white matter lesions and availability of osmotic minipump. The mouse model is easily applicable to genetically modified animals and also has advantages over the rat model in cognitive evaluation.



## ACTIVATION OF RHO/RHO KINASE SYSTEM AFTER FOCAL CEREBRAL ISCHEMIA

**Yoshiki Yagita**, Kazuo Kitagawa, Tsutomu Sasaki, Shiro Sugiura, Kenichi Todo, Emi Omura-Matsuoka, Kohji Matsushita, Masatsugu Hori

*Division of Strokeology, Department of Internal Medicine and Therapeutics, Osaka University Graduate School of Medicine, Osaka, Japan*

**Background and Purpose:** After ischemic brain injury, glial and inflammatory cells migrate into the lesion and vascular function is perturbed in the lesion. These changes can affect the lesion maturation (1). Small GTPase-Rho plays a crucial role in the cell motility and polarization via Rho kinase activation. Rho/Rho kinase system may work as a key signal to mature the ischemic lesion. In this study, we investigated the change of Rho/Rho kinase system and its effector molecule in the brain ischemia. **Methods:** Adult Wistar rats were subjected to permanent middle cerebral artery occlusion by intraluminal suture. Rectal temperature was monitored and was maintained at 37.0±0.5 degree. Brains were removed 1 or 2 days after ischemia for following analysis. Ischemic and non-ischemic hemispheres of forebrain were homogenated and subjected to Western blot to observe the expression change of RhoA protein. To assess Rho/Rho kinase activation, we performed the immunohistochemistry of phospho-adducin, an effector molecule of Rho/Rho kinase, in the ischemic brain. Zamboni's solution (2% paraformaldehyde and 0.2 % picric acid in phosphate buffer) fixed-brains were frozen after cryo-protection and 10µm coronal sections were prepared for immunohistochemistry. **Result:** Western blot showed that RhoA protein expression in the sham-operated brain. Twenty-four hours after ischemia, expression of RhoA protein was increased in the ischemic hemisphere. In order to show the evidence of Rho/Rho kinase system activation and reveal the localization of activated Rho/Rho kinase, phospho-adducin immunohistochemistry was carried out. Phospho-adducin signals were expressed mainly in the neuronal cells in the sham-operated brain. In the ischemic hemisphere, phospho-adducin signals were increased in the glial cells or macrophages at the margin of the infarct area. After 2 days, signals were decreased in the infarct core, whereas many cells still expressed phospho-adducin at the margin of the infarct area. In these regions, brain microvessels were also expressed phospho-adducin strongly. Signals were not increased in the microvessels of the contra-lateral hemisphere. **Conclusion:** We demonstrated up-regulation and activation of small GTPase-Rho following cerebral ischemia. It may be involved in the maturation of ischemic brain injury via inflammatory cell infiltration and perturbation of vascular function. **Reference:** (1) Mabuchi T. et al., *Stroke* 2000, 31, 1735-1743

**MOLECULAR REGULATION OF ION CHANNELS AND GAP JUNCTION IN BRAIN AND ASTROCYTE OF MOSSAMBICUS TILAPIA****Shang Lin Chang, Ching Feng Weng***Institute of Biotechnology, National Dong-Hwa University, Hualien, Taiwan*

When euryhaline teleost (*Mossambicus tilapia*) goes from hyper osmotic (Seawater; SW) to hypo-osmotic (Freshwater; FW) media, the osmolarity and the sodium and chloride concentrations in CSF are raised. However, the regulating mechanism of tilapia brain during acute SW transfer is still unclear. This study was to investigate whether the mRNA expression of ion channels and gap junction in tilapia brain during FW transfer to 25 ppt SW (1, 2, 4, 8, 16 or 24 hrs). By using Semi-quantitative RT-PCR, the mRNA expressions of Na-K ATPase, Na and Cl channel, and connexin (Cx)43 were increased during SW transfer, but not in K channel and Cx35. The Na-K ATPase mRNA expression in primary astrocytes (GFAP positive) treated with 170 mM NaCl (550 mOsmol/kg) was early than that of 270 mM mannitol (550 mOsmol/kg) treatment. The mRNA expressions of Na-K-2Cl co-transporter and Cl channel were expressed the highest levels at 8 hr in NaCl and mannitol treatments. The expression of Cx43 mRNA was a time-dependent manner in both treatments, but Cx35 mRNA was not induced. The results suggest that the cellular communication of tilapia brain under ionic and osmotic stress is mediated through gap junction Cx43.

**NA-K-2CL COTRANSPORTERS CONTRIBUTES TO IL-1-INDUCED NEURONAL DAMAGE DURING TRAUMATIC BRAIN INJURY**Kwok-Tung Lu<sup>1</sup>, Chang-Yen Wu<sup>2</sup>, **Yi-Ling Yang**<sup>2</sup>*Department of Life Science, National Taiwan Normal University, Taipei, Taiwan**<sup>2</sup>Institute of Biotechnology, National Chia-Yi University, Chia-Yi, Taiwan*

Traumatic brain injury (TBI) is one of the most prevalent causes of morbidity and mortality all over the world. One characteristic feature of patients with severe TBI is brain edema. The cerebral spinal fluid (CSF) is secreted by the epithelial cell of the choroid plexuses and Na<sup>+</sup>-K<sup>+</sup>-2Cl<sup>-</sup> cotransporter (NKCC1) has a major role in the secretory process in the CSF secretion. Our previous results demonstrated that IL-1 plays an important role in TBI-induced neuronal loss. This study assessed the effect of NKCC1 on TBI-induced brain edema and neuron damage and the relationship between NKCC1 and IL-1 induced neuronal loss. TBI model was induced by the calibrated weight-drop device (450 g weight, 2 m height) and the animals were divided into sham operation and different time course after TBI (0h, 2h, 4h, 8h, 12h, 24h, 48h, 96h). The infarction volume and neuronal damage was verified by hematoxylin and eosin staining and TTC staining. NKCC1 and IL-1 mRNA expression was detected by RT-PCR and the protein expression was measured by Western blot. IL-1 antagonist or antibody and NKCC1 blocker, bumetanide were locally injected into lateral ventricle to elucidate the effect of NKCC1 on IL-1 induced neuronal loss. In this study, we found that NKCC1 and IL-1 mRNA expression in choroid plexus started to detect at 2 h after TBI and lasted for 24 h after TBI. NKCC1 protein significantly elevated after TBI 2 h and lasted for 24 h. After TBI, animals displayed severe brain edema and neuron loss. There is a sustained up-regulation of NKCC1 in choroid plexus was detected from 2 h to 24 h after TBI. Infarction volume was significantly increased after TBI and bumetanide treatment significantly decreased infarct volume after TBI. Administration of IL-1 antibody significantly reduced the NKCC1 expression. These results evidenced that NKCC1 plays an essential roles in IL-1 induced neuron damage in TBI.

## **PACAP GENE OF ASTROCYTE IN TILAPIA BRAIN RESPONDING TO ACUTE SALINITY CHALLENGE**

**Chi Wei Lo, Ching Feng Weng**

*Institute of Biotechnology, National Dong Hwa University, Hualien, Taiwan*

Pituitary adenylate cyclase-activating polypeptide (PACAP), hypothalamic neuropeptide, is a pleiotropic hormone for multiple physiological functions. Our previous study, tGHRH and tPACAP38 (t denoted tilapia) were expressed in tilapia (*Oreochromis mossambicus*) brain and pituitary. The full-length nucleotide sequence of tGHRH-tPACAP gene was completed by using 5'- and 3'-RACE. In the present study, the existence of PACAP in astrocyte of tilapia brain was demonstrated and two messengers of tPACAP were all detected in the tilapia brain, pituitary and astrocyte by using RT-PCR. The short form was more abundant in astrocyte. The short product (166 bps) with exon skipping encodes tPACAP38 only while the long form (271 bps) encodes both tPACAP38 and tGHRH. Primary tilapia astrocyte culture treated with ovine PACAP38 or dibutyryl-cAMP (db-cAMP) showed that both exogenous PACAP38 and db-cAMP induced the mRNA expression of PACAP in a dose-dependent manner. The addition of high-salinity (170 mM NaCl, 550 mOsmol/kg) at various times (0, 4, 8, 16 or 24 h) in astrocyte culture, tPACAP expression was significantly stimulated within 4 h and maintained to 24 h by using semi-quantitative RT-PCR. The mRNA expression of short form (encodes only tPACAP38) was higher after high-salinity treatment than that of long form but the stimulating effect did not occur in high-osmolarity (270 mM Mannitol, 550 mOsmol/kg) treatment. The results suggest that the function of PACAP in tilapia astrocyte might be related to the regulation of high-salinity adaptation when the fish face to seawater environment.

**HYPERBARIC OXYGEN REDUCES BLOOD-BRAIN BARRIER DAMAGE AND EDEMA AFTER TRANSIENT FOCAL CEREBRAL ISCHEMIA****Roland Veltkamp<sup>1</sup>, Li Sun<sup>1</sup>, Dirk A. Siebing<sup>1</sup>, Katja Bieber<sup>2</sup>, Sabine Heiland<sup>3</sup>,****Hugo H. Marti<sup>2</sup>,  
Stefan Schwab<sup>1</sup>, Markus Schwaninger<sup>1</sup>**<sup>1</sup>*Department of Neurology, University Heidelberg, Heidelberg, Germany*<sup>2</sup>*Department of Physiology, University Heidelberg, Heidelberg, Germany*<sup>3</sup>*Department of Neuroradiology, Heidelberg, Germany*

Hyperbaric oxygen (HBO) has been shown to protect the brain parenchyma against transient focal cerebral ischemia but its effects on the ischemic microcirculation are largely unknown. We examined the potential of HBO to reduce postischemic blood-brain barrier (BBB) damage using repetitive MR-imaging and Na-Fluorescein uptake during 72 h of reperfusion and measured the effect of HBO on postischemic edema. Wistar rats and C57/Bl6 mice underwent focal ischemia for 2 h induced by filament occlusion of the middle cerebral artery (MCAO). Forty minutes after filament introduction, animals were placed in a HBO chamber and breathed either 100% O<sub>2</sub> at 3.0 atmospheres absolute (ata; HBO group) or at 1.0 ata (control) for 1 h. In rats, MR-images were obtained 15 min after MCAO, and after 15 min, 3, 6, 24, 72 h of reperfusion. Volume of T1w postcontrast enhancement and an interhemispheric quotient of mean gray values (MGV) in T1w images were calculated for estimation of BBB damage. In ischemic mice, BBB permeability for Na-Fluorescein was measured fluoroscopically after 24 h of reperfusion. Physiological parameters and ischemic MR-perfusion did not differ between groups. Increased postischemic BBB permeability on postcontrast T1w images had a biphasic pattern and was located within the hyperintense areas on DWI and T2w images, respectively. HBO reduced volume of early and delayed BBB damage on postcontrast T1w images. Mean abnormal enhancing volumes at the various time points were at 15 min of reperfusion: 29±7 mm<sup>3</sup> (control) vs. 19±6 mm<sup>3</sup> (HBO); at 3 h: 38±11 mm<sup>3</sup> vs. 28±7 mm<sup>3</sup>; at 6 h: 49±16 mm<sup>3</sup> vs. 31±8 mm<sup>3</sup>; at 24 h: 51±14 mm<sup>3</sup> vs. 35±8 mm<sup>3</sup>; at 72 h: 97±28 mm<sup>3</sup> vs. 68±17 mm<sup>3</sup> (p<0.05 for 6, 24, 72 h). The quotient of MGV was significantly lower in the HBO treated animals at all time points: at 15 min of reperfusion: 1.73±0.11 (control) vs. 1.57±0.07 (HBO); at 3 h: 1.74±0.07 vs. 1.60±0.06; at 6 h: 1.77±0.07 vs. 1.62±0.06; at 24 h: 1.79±0.10 vs. 1.60±0.05; at 72 h: 1.81±0.10 vs. 1.62±0.07. Reduction of postischemic BBB damage by HBO was confirmed in mice. After 24 h of reperfusion, mean interhemispheric quotient (ischemic/nonischemic) of relative fluorescence units was significantly larger in control (1.56±0.50) than in HBO (1.11±0.16) treated mice. Effect of HBO on ischemic focal brain edema was estimated by two ways. First, volume of hyperintensity on T2w images, which represent both parenchymal damage and brain edema in the ischemic hemisphere, was significantly larger in control than in HBO treated animals at 72 h after MCAO. Second, on histological sections, volume attributable to focal edema was 72±29 mm<sup>3</sup> in the control and 41±14 mm<sup>3</sup> in the HBO group (p<0,05). In conclusion, early administration of HBO reduces rapid and delayed BBB damage and brain edema after transient focal cerebral ischemia. The molecular and cellular targets of this HBO effect and its potential implications for reduction of secondary microvascular complications are currently under investigation. Supported by Deutsche Forschungsgemeinschaft (VE 196/2-1)

## DELAYED CHRONIC ENDOTHELIAL DAMAGE AFTER BRIEF GLOBAL FOREBRAIN ISCHEMIA IN THE RAT

Baowan Lin<sup>1</sup>, Weizhao Zhao<sup>1,2</sup>, Raul J. Busto<sup>1</sup>, Myron D. Ginsberg<sup>1</sup>

<sup>1</sup>*Department of Neurology, University of Miami School of Medicine, Miami, FL, USA*

<sup>2</sup>*Department of Biomedical Engineering, University of Miami, Coral Gables, FL, USA*

We have previously shown that 10- and 12.5-min (but not 7-min) of global ischemia induces secondary brain damage, including incomplete infarcts in striatum and hippocampal CA1 sector associated with endothelial degeneration and microvascular thrombosis over 4-10 weeks. 1-3 12.5-min ischemia also induces cerebral amyloid b-peptide (Ab) deposition at 8-10 weeks, concentrated in the basal cortex. Peri-vascular neuronal shrinkage degeneration coincides with evident Ab deposition.<sup>2, 3</sup> The present study investigated endothelial degeneration in cortex in an effort to understand the relationship to brain Ab deposition. Methods: Male Wistar rats (265-390g) were subjected to 10- or 12.5-min norothermic ischemia by 2-vessel occlusion and systemic hypotension (40-50 mmHg). Rats were allowed to survive for 8 weeks in 12.5-min group; and for either 1, 2, 4, 8, or 10 weeks in the 10-min group. Brains were perfusion-fixed in FAM (formaldehyde, acetic acid, methanol). Sections at level ~3.3 mm posterior to bregma were reacted with 2 monoclonal antibodies: Ab was detected by NCL-b-Amyloid (6F/3D) (Vector Lab). Normal endothelia were quantitatively assessed by Anti-EBA (Sternberger Monoclonals, Lutherville, MD), directed against endothelial barrier antigen (EBA).<sup>4,5</sup> Results: 1. The fractional area of normal blood vessels in the basal portion of cortex, Pir (piriform cortex) and AIP (agranular insular cortex) decreased in ischemic brains (Table 1) at 8 weeks and beyond. Ab accumulation initiated neuronal shrinkage (Fig 1. a-f) and disappearance (Fig 1. g,h), and perivascular Ab deposition was evident (Fig. 2). 2. Significant endothelial damage was seen between 2 and 10 weeks after a 10-min ischemic insult (Table 2). Conclusion: The results indicate delayed cerebral endothelial degeneration in the basal cortex after an ischemic insult. Abnormal cerebral Ab accumulation appears related to blood vessels. References: [1] Lin B et al (1998) Acta Neuropathol 95:511-523. [2] Lin B et al (1999) Acta Neuropathol 97:359-368. [3] Lin B, Ginsberg MD. (2000) Pharmacology of Cerebral Ischemia 2000, pp. 37-53. [4] Lin B, Ginsberg MD. (2000) Brain Res 865:237-244. [5] Lin B et al (2001) Neurotrauma 18:389-397. Grant support: NCCAM/NIH Grant 1 R21 AT001598-01A1 (B.L.) and NIH Grant NS 05820 (M.D.G.)

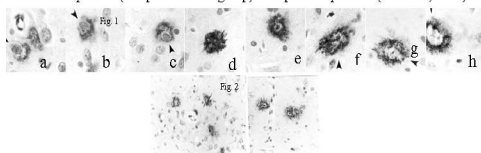
**Table 1 Fractional area occupied by normal endothelia in brains at end of 8 weeks**

Region	Sham n=4	10-min Ischemia n=5	12.5-min Ischemia n=5
AIP	3.2 ± 0.5 %	2.1 ± 1.3 %	2 ± 0.6 %*
Pir	2.1 ± 0.2 %	1.3 ± 0.5 %*	0.95 ± 0.4 %*

**Table 2 Proportion of normal endothelia after 10-min ischemia**

Region	Sham n=4	1 week n=5	2 weeks n=4	4 weeks n=4	8 weeks n=5	10 weeks n=5
AIP	3.2 ± .5 %	2.5 ± .5%	2.5 ± 1%	2.5 ± .6%	2.1 ± 1.3%	2.2 ± .6%*
Pir	2.1 ± .2 %	2.2 ± .3%	1.8 ± .4%*	1.7 ± .5% <sup>§</sup>	1.3 ± .5%*	1.4 ± .2%*

\* indicates  $p < 0.05$  (compare to sham group). <sup>§</sup> represents  $p = 0.05$  (ANOVA, t-test).



## **CHANGES IN ATTENTION AND CONCENTRATION AMONG SURVIVORS OF PEDIATRIC BRAIN TUMORS: A LOOK AT THE CURRENT BODY OF KNOWLEDGE**

**Lloyd Taylor**

*Departments of Clinical Services, Pediatrics, and Neurosurgery, Medical University of South Carolina, Charleston, SC, USA*

Advances in the medical treatment of childhood cancer have led to decreases in the mortality of children diagnosed with brain tumors. Currently, as many as 60% of children diagnosed with cancer are cured of their illness through various innovative medical treatment procedures. Today, large numbers of children, previously diagnosed with cancer, survive and experience the routine demands of childhood and adolescence. The long-term effects (i.e., cognitive late effects) of cancer treatment on learning, academic, psychological, and social functioning had been irrelevant for children with brain tumors due to the previous high mortality rate in this population. However, the improved prognosis for this group of children designates this new area of management of cognitive late effects for brain tumors a national public health concern. Investigations by Mulhern and colleagues (2001) have provided valuable information to support the notion that observed declines in cognitive performance and behavioral problems in survivors of childhood cancer are attributable to abnormally low white matter volume as revealed on radiographic studies of these children (c.f., Mulhern et al., 2001). In previous years, it had often been assumed that cognitive and behavioral declines in children with brain tumors were largely a function of the prophylactic therapies (e.g., radiation, chemotherapy) that these children had received (c.f., Mulhern et al., 2001). As Mulhern (1994) has astutely observed, however, it is actually difficult to determine whether symptoms are directly associated with the tumor itself, the CNS involvement associated with the tumor, or the general cancer experience. This investigation (1 F32 NS046944-01A1) represents one of the first studies devoted to exploring the impact of pediatric brain tumors on markers of attention and concentration and exploring potential interventions. While recruitment and data analysis is ongoing, preliminary findings suggest difficulties among domains of cognitive flexibility, memory, and concentration among pediatric survivors of brain tumors and these findings are consistent regardless of treatment employed. Additionally, this investigation has begun to explore the role of the RAS as it relates to attention and concentration among pediatric survivors of brain tumors. The proposed poster and/or paper presentation would highlight the findings of this investigation to date and would additionally provide investigators/researchers/clinicians information regarding the efficacy and effectiveness of interventions aimed at ameliorating these difficulties among pediatric populations.

## MRI MEASURES OF CHANGES IN THE TRANSFER CONSTANT OF GADOMER AFTER DEXAMETHASONE IN 9L RAT CEREBRAL TUMOR

James R. Ewing<sup>1</sup>, Stephen R. Brown<sup>2</sup>, Jamie R. Churchman<sup>1</sup>, Swayamprava R. Panda<sup>1</sup>,  
Ramesh R. Paudyal<sup>1</sup>, Joseph R. Fenstermacher<sup>3</sup>

<sup>1</sup>Neurology, Henry Ford Hospital, Detroit, MI, USA

<sup>2</sup>Radiation Oncology, Henry Ford Hospital, Detroit, MI, USA

<sup>3</sup>Anesthesia, Henry Ford Hospital, Detroit, MI, USA

**Introduction:** We used Gadomer (Schering AG), a magnetic resonance contrast agent (MRCA), and magnetic resonance imaging (MRI) measures of  $T_1$  to estimate changes in tumor vascular permeability after the administration of dexamethasone.

**Methods:** Five male Fischer 344 rats weighing 250 to 300 g were implanted with 10,000 9L tumor cells using methods previously described<sup>2,3</sup>; the resultant population of animals with cerebral tumor was studied about 14 days post-implantation using MRI and Gadomer, a dendritic gadolinium (Gd) chelate with an effective molecular weight of about 33 kD. MRI studies were carried out at 7 Tesla, using a Bruker console. Following established procedures<sup>4</sup>, a TOMROP<sup>5</sup> sequence was used to measure  $R_1$  ( $R_1 = 1/T_1$ ) at baseline, and at 145 s intervals following injection of the MRCA. Matrix size was 128X64, FOV 32 mm, three 2 mm slices. Changes in  $R_1$  were assumed to reflect changes in MRCA concentration.

Prior to the administration of MRCA, two baseline TOMROP studies were obtained, after which the next TOMROP sequence was started and Gadomer was administered in a slow push (250  $\mu$ mol/kg in a 0.3 ml volume in about 1 minute). During and after the administration of Gadomer, 10 iterations of TOMROP were run to follow the tissue concentration of MRCA across a 25 min period. Intravascular dexamethasone (2.4 mg/kg in 0.15 ml) was administered, and, after an interval of about 90 minutes, a second series of TOMROP images was run. Using a standard analysis<sup>1,2</sup>, the parameters vascular volume ( $v_d$ ), transfer constant ( $K_1$ ) and efflux constant,  $k_b$  were computed. The extravascular, extracellular space ( $V_{EES}$ ) was estimated from the ratio  $K^{trans}/k_b$ . Both region-of-interest (tumor), as well as pixel-by-pixel whole brain estimates, were generated.

Results and Discussion:

Changes in permeability parameters are summarized in the table and compared to the work of Nakagawa et al<sup>6</sup>, in which Radioiodinated serum albumin (RISA) was used to study the effect of dexamethasone on the RG-2 cerebral tumor. In every animal, the transfer constant decreased after the administration of dexamethasone. Gadomer should approximate RISA when used as a measure of vascular permeability. Despite the differences in tumor type, administration schedule, and measurement technique, the agreement between these two studies is striking, particularly the numerical agreement in the change of  $V_{EES}$ .

**Literature Cited:** 1. Tofts, P.S., et al., JMRI, 1999. 10(3): p. 223. 2. Kim, J.H., et al., Int'l J Rad Onc Bio Phys, 1995. 33: p. 861. 3. Brown, S., et al., Int'l J Rad Onc Bio Phys, 1999. 43(3): p. 627. 4. Ewing, J.R., et al., MMR, 2003. 50: p. 283. 5. Brix, G., et al., MRI, 1990. 8: p. 351. 6. Nakagawa, H., et al., J CBFM, 1987. 7: p. 687.

Mean Vascular Leakage Parameters, pre- and post-dexamethasone					
Parameter*	Pre-Dex	Post-Dex	Paired t-test p-value	RISA Values**	
				Pre	Post
$v_d$ [ml/ml]	0.0261 $\pm$ 0.00724	0.0191 $\pm$ 0.0242	NS	0.030 $\pm$ 0.24	0.018 $\pm$ 0.0091
$K_1$ [min <sup>-1</sup> ]	0.0122 $\pm$ 0.00724	0.00591 $\pm$ 0.00429	p = 0.001	0.0236 $\pm$ 0.0089	0.0083 $\pm$ 0.0029
$V_{EES} = K^{trans}/k_b$	0.110 $\pm$ 0.0291	0.0765 $\pm$ 0.0555	p < 0.05	0.140 $\pm$ 0.02	0.08 $\pm$ 0.02

\*MRI units \*\* 'Radiological' units, scaled to MRI units by tissue density

## BARRIER DISRUPTION FOLLOWING EXCITOTOXIC LESIONS IN THE BRAIN OF THE ANAESTHETIZED RAT

Jérôme Toutain, Xavier Jaglin, Didier Divoux, Laurent Chazalviel, Omar Touzani, Eric T MacKenzie

*Université de Caen, CNRS UMR 6185, Cyceron, France*

### Introduction

Consolidated ischaemic brain lesions are invariably associated with lesions of the blood brain barrier (BBB) and increased permeability of tracers of almost all molecular sizes. In contrast to necrosis, excitotoxic brain lesions are often thought not to involve, at least, early changes in the cerebral vasculature.

The object of this preliminary investigation was to study the kinetics of evolution of the brain lesions and the BBB properties following the injection of an excitotoxic agent (NMDA) into the striatum.

### Methods

Under sevoflurane anaesthesia, female Sprague dawley rats were placed in a stereotaxic frame and a cannula was inserted into the ventral striatum (coordinates 0 mm posterior, 3 mm lateral, 6 mm ventral to the bregma). NMDA (75 nmol) was injected in a 3  $\mu$ l volume of PBS. In control animals, only PBS was administered into the striatum. Euthanasia was performed 3, 6, 24 and 48 hours after the administration of NMDA. Two hours before euthanasia, each animal received an intravenous injection of 1 ml of a 2% solution of Evans blue which binds to albumin (EBA, 65 KDa). The brains were cut in 20  $\mu$ m sections using a cryostat, and 2 adjacent sections in every 40 were collected, one for quantification of the lesion and the other for evaluation of Evans blue extravasation, an indicator of changes in BBB permeability.

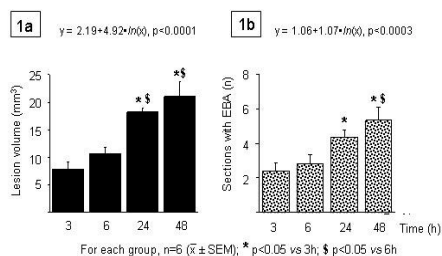
### Results

The administration of NMDA into the striatum induced well demarcated areas not stained with thionin, as early as 3 hours following the injection. The volume of this lesion displayed a significant and progressive enlargement during, at least the first 24 hours (figure 1a). The administration of the vehicle did not induce any discernable lesion at all the time points examined. The extravasation of Evans blue was visible even 3 h following the administration of NMDA and also displayed a progressive evolution with a temporal profile not dissimilar to that of the excitotoxic lesion (figure 1b)

### Conclusions

The findings indicate that in rat, NMDA-induced extravasation of Evans blue evolves in parallel to the volume of neuronal loss. Many points remain to be resolved: the molecular size of non-permeable tracers; the degree of plasma binding; the ultrastructural basis of the changes in BBB permeability. Nonetheless, the use of this model of brain lesion should take into account these alterations in the cerebral vasculature.

NMDA-induced striatal lesions and extravasation as a function of time



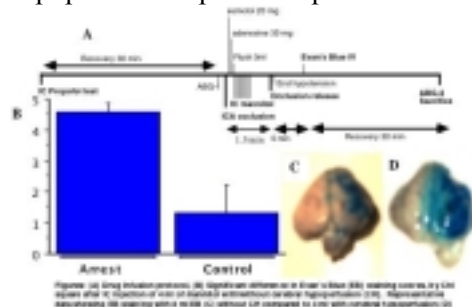


## CEREBRAL HYPOPERFUSION ENHANCES EFFECTIVENESS OF INTRACAROTID MANNITOL

Joshua J. Etu, Mei Wang, **Shailendra Joshi**

*Department of Anesthesiology, Columbia University Medical Center, New York, NY, USA*

**Introduction:** Intracarotid (IC) mannitol (20-25%) has been used to disrupt the blood brain barrier (BBB)<sup>1</sup>. IC mannitol has been used to enhance delivery of chemotherapeutic agents for treating brain tumors<sup>2</sup>. Mannitol disrupts the BBB primarily by dehydrating the endothelial cells, thus enlarging the endothelial tight junctions. We hypothesized that administration of IC mannitol in low cerebral blood flow (CBF) states would enhance the efficacy of the treatment. **Material and Methods:** We tested our hypothesis in New Zealand White rabbits that have a primate like separation of the internal (ICA) and external carotid arteries. Surgical preparation included cannulation of the ear lobe vein, femoral and ICA cannulations, placement of laser Doppler Probes and bilateral EEG monitoring. Cerebral hypoperfusion (CBF  $\approx$  25% baseline) was produced by IV injection of esmolol 20mg and adenosine 30mg and contralateral ICA occlusion. The breach of the BBB was judged by injection of 2% Evans Blue (EB, 4ml/kg, IV). Staining was graded from 0-5 on a standardized scale. **Experiments** were conducted on three groups of animals: (i) Initial dose-response studies were conducted in eight animals who received 0,2,4,6,8 ml of mannitol over 1 minute with or without cerebral hypoperfusion. (ii) Comparison of 4ml of mannitol with and without flow arrest in 12 animals. (iii) Establish the time duration of arrest by EB injection at 5, 15, 30, 60 minute after 4ml of mannitol injection during cerebral hypoperfusion 4 animals. **Staining Scale:** 0: No staining or staining limited to laser Doppler probe sites. 1: Surface staining with no deep staining and unrelated to laser Doppler Probes. 2: Staining limited to  $\leq$  30 % coronal sectional area. 3: Staining between 30-60% sectional area. 4: Staining  $\geq$  60% sectional area. 5: Extra 1- point for deep staining. **Results:** The dose of mannitol required to disrupt the BBB without flow arrest was 8 ml however BBB could be disrupted with 4ml of mannitol when injected during hypoperfusion. Comparison of 4ml of mannitol with out without flow arrest revealed a significant difference in the staining scores. The disruption of the BBB lasted for at least 60 minutes after intraarterial mannitol injection. **Conclusions:** Results suggest that the efficacy of intraarterial mannitol can be enhanced by the injection of drugs in states of cerebral hypoperfusion. The dose of intraarterial mannitol required to breach the BBB in this animal species was 8ml and was similar to that reported in literature<sup>1</sup>. The breach of the BBB could be achieved with a 50% dose reduction when delivered during cerebral hypoperfusion. In clinical settings CBF can be altered by mechanical means such as balloon occluding catheters, altering ventilation, or by severe transient systemic hypotension. These techniques could be used to enhance the efficacy of intraarterial mannitol. **References:** 1. Perkins and Strausbaugh: Antimicrobial Agents and Chemotherapy, Sept.1983 339-342 2. Rapoport: Expert Opin Investig Drugs, Oct. 2001 10(10) 1809-1818



## ROLE OF ARGININE VASOPRESSIN V1 AND V2 RECEPTORS FOR BRAIN DAMAGE AFTER TRANSIENT FOCAL CEREBRAL ISCHEMIA

Abedin Vakili, Hiroharu Kataoka, **Nikolaus Plesnila**

*Laboratory of Experimental Neurosurgery, Institute for Surgical Research, University of Munich, Munich, Germany*

**Introduction:** Brain edema formation is one of the most important mechanisms responsible for brain damage following ischemic stroke. Despite considerable efforts, no specific therapy is available yet. Arginine vasopressin (AVP) regulates cerebral water homeostasis and has been involved in brain edema formation. In the current study we investigated the role of AVP V1 and V2 receptors on brain damage, brain edema formation, and functional outcome after transient focal cerebral ischemia, a condition comparable to that of stroke patients undergoing thrombolysis. **Materials & Methods:** C57/BL6 mice were subjected to 60 min MCAo followed by 23 h of reperfusion. Five minutes after MCAo 100 or 500 ng of [deamino-Pen(1), O-Me-Tyr(2), Arg(8)]-vasopressin (AVP V1 receptor antagonist) or [adamantaneacetyl(1), O-Et-D-Tyr(2), Val(4), Abu(6), Arg(8,9)]-vasopressin (AVP V2 receptor antagonist) were injected into the left ventricle. **Results:** Inhibition of AVP V1 receptors reduced infarct volume in a dose dependent manner by 54 and 70% (to  $29 \pm 13$  and  $19 \pm 10$  mm<sup>3</sup> vs.  $63 \pm 17$  mm<sup>3</sup> in controls;  $p < 0.001$ ), brain edema formation by 67% (to  $80.4 \pm 1.0$  vs.  $82.7 \pm 1.2$  % in controls;  $p < 0.001$ ), blood brain barrier disruption by 75% ( $p < 0.001$ ), and functional deficits 24 h after ischemia, while V2 receptor inhibition had no effect. **Summary & Conclusion:** The current findings indicate that AVP V1 but not V2 receptors are involved in the pathophysiology of secondary brain damage after focal cerebral ischemia. Although, further studies are needed to clarify the mechanisms of neuroprotection, AVP V1 receptors seem to be promising targets for the treatment of ischemic stroke.

## EVOLUTION OF BRAIN EDEMA AFTER SUBARACHNOID HEMORRHAGE (SAH) IN RATS

Serge C. Thal<sup>1</sup>, Sonja Sporer<sup>2</sup>, Nikolaus Plesnila<sup>2</sup>, Karsten Schoeller<sup>3</sup>,

Robert Schmid-Elsaesser<sup>3</sup>, Stefan Zausinger<sup>3</sup>

<sup>1</sup>*Department of Anaesthesiology, Johannes Gutenberg University, Mainz, Germany*

<sup>2</sup>*Institute for Surgical Research, Ludwig Maximilians University, Munich, Germany*

<sup>3</sup>*Department of Neurosurgery, Ludwig Maximilians University, Munich, Germany*

**Objective:** Global cerebral edema is an independent risk factor for early mortality and poor outcome after SAH in humans. Little is known about time course and extent of brain edema evolution in the most widely used experimental SAH model, the rat filament model. We therefore investigated cerebral water content and brain swelling at various time points after SAH, investigating the course of CBF, ICP, evolution of cerebral edema and neurological deficits. **Method:** 42 rats were subjected to SAH by an endovascular filament. ICP and bilateral CBF were continuously recorded by a parenchymal probe and Laser Doppler flowmetry. Animals were randomly assigned to 3 control (1h, 24h, 48h survival) and 3 SAH (1h, 24h, 48h survival) groups (n=7 each). Brain water content was measured at the end of the observation time, neurological deficits at 24h and 48h after SAH. **Results:** SAH resulted in an immediate increase of ICP up to ~60 mmHg initially and ~30 mmHg for the following 30 min without significant differences between these groups. In all groups the bilateral CBF fell by over 80% with partial recovery to 50-60% baseline after 30 min. The brain water content was significantly increased at 24 (SAH: 80.2±0.4% vs. control: 79.2±0.07%) and 48 hours (SAH: 79.8±0.2% vs. control: 79.3±0.07%) after SAH, primarily within the ipsilateral hemisphere. Neuroscore was significantly worse within the SAH groups 24 hours after SAH compared to controls (24h SAH: 33±15 pts. vs. controls: 5±0 pts.), strongly correlating with extent of brain edema (r=0.96, p<0.001). There was no correlation between brain edema and ICP and bilateral CBF. **Discussion:** Experimental SAH in rats, utilizing the filament model with puncture of the internal carotid artery, leads to mainly ipsilateral brain edema peaking 24h after SAH, comparable with the situation in humans. Extent of brain edema showed strong correlation with resulting neurological deficits. The filament SAH model seems to be well suited to investigate early pathophysiological changes as brain edema formation.

## MAST CELL BLOCKING IMPROVES OUTCOME AFTER EXPERIMENTAL INTRACEREBRAL HEMORRHAGE

Daniel Strbian<sup>1,2</sup>, Turgut Tatlisumak<sup>1,2</sup>, Marja-Liisa Karjalainen-Lindsberg<sup>3</sup>,

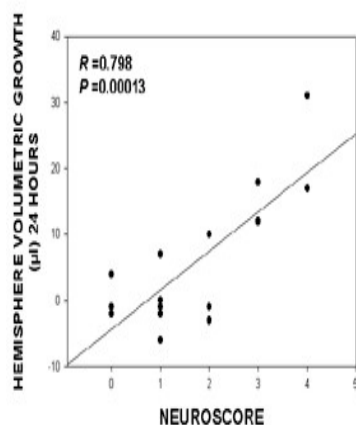
Usama Abo-Ramadan<sup>2</sup>, Perttu J. Lindsberg<sup>1,2</sup>

<sup>1</sup>*Department of Neurology, Helsinki University Central Hospital, Helsinki, Finland*

<sup>2</sup>*Neuroscience Program, Helsinki University Central Hospital, Helsinki, Finland*

<sup>3</sup>*Department of Pathology, Helsinki University Central Hospital, Helsinki, Finland*

Intracerebral hemorrhage (ICH) accounts for 15 % of all strokes and is associated with high mortality and disability, because of mass effect and brain swelling. This study was based on our previous finding of 50 % reduction of ischemic brain edema by mast cell (MC) blocking. In autologous blood injection model we treated one group (n=11) with a MC stabilizer, and the control group (n=11) with saline 5 minutes before induction of ICH. One hour later, MRI was performed. 24 hours later we scored the neurological score and repeated MRI in survivors. Neurological score in the treatment group were statistically significantly better than in the control group ( $P < 0.001$ ). There was a 55 % mortality rate in the control group and no deaths in the treatment group ( $p < 0.01$ ) by 24 hours. There was statistically significant difference in growth of brain edema between the groups ( $P < 0.001$ ). We found highly significant correlation between neurological score and hemisphere volumetric growth during 24 hours ( $R = 0.8$ ,  $P < 0.001$ , Fig. 1). There was statistically significant difference in hematoma volume at 24 hours ( $P < 0.001$ ), while hematoma volumes were not significantly different at baseline ( $P = 0.97$ ). MC blocking significantly improved clinical outcome and reduced mortality in experimental ICH. We found 4 times less brain swelling and 1.5 times lesser hematoma volume in the treatment group at 24 hours. MC contain potent vasoactive and proteolytic substances and their functional inhibition should be further studied as a potential pharmacological approach to limit tissue injury and fatal outcomes after ICH. References: 1, Mayo NE et al. Hospitalization and case-fatality rates for stroke in Canada from 1982-1991. *Stroke*, 27: 1215-1220, 1996 Grant support: This study was supported by Sigrid Juselius and Finnish Medical Foundations



## EFFECT OF AGE ON BLOOD BRAIN BARRIER TRANSPORT FUNCTION STUDIED WITH [11C](R)-VERAPAMIL AND PET

Jan R Toornvliet<sup>1</sup>, Bart NM van Berckel<sup>2</sup>, Gert Luurtsema<sup>2</sup>, Mark Lubberink<sup>2</sup>, Ab A Geldof<sup>2,3</sup>, Tessa M Bosch<sup>4</sup>, Adriaan A Lammertsma<sup>2</sup>, Eric JF Franssen<sup>5</sup>

<sup>1</sup>Pharmacy, VU University Medical Centre, Amsterdam, The Netherlands

<sup>2</sup>Nuclear Medicine & PET Research, VU University Medical Centre, Amsterdam, The Netherlands

<sup>3</sup>Urology, VU University Medical Centre, Amsterdam, The Netherlands

<sup>4</sup>Pharmacy, Slotervaart Ziekenhuis, Amsterdam, The Netherlands

<sup>5</sup>Pharmacy, Onze Lieve Vrouwe Gasthuis, Amsterdam, The Netherlands

**Introduction:** It has been hypothesised that the blood brain barrier (BBB) integrity might decrease during ageing. In addition, it has been postulated that loss of P-glycoprotein (P-gp) function with age may be one factor in the development and progression of neurodegenerative diseases. Verapamil is a substrate for P-gp, located in the BBB. The volume of distribution of [11C](R)-verapamil in the brain (inversely) reflects P-gp function in the BBB(1). This tracer can, therefore, be used to assess P-gp function in neurodegenerative diseases. For correct interpretation of results obtained in those studies, however, the effects of normal ageing on P-gp function need to be known. **Aim:** The aim of the present pilot study was to assess the role of ageing on P-gp function in the BBB using [11C](R)-verapamil and PET. **Methods:** Five young (age 21-27 years) and 5 elderly (age 59-68 years) healthy volunteers were included in this study. A dynamic 3D emission scan with a total scan duration of 60 minutes was acquired following intravenous injection of ~370 MBq [11C](R)-verapamil. During the scan arterial blood was monitored continuously and, at set times, additional samples were taken for metabolite analysis in order to generate a metabolite corrected input function. Volume of distribution (Vd) images were generated using Logan analysis. These images were segmented based on co-registered MRI data, resulting in whole brain grey matter Vd values. **Results.** Whole brain grey matter verapamil Vd as function of age is shown in figure 1. Average ( $\pm$ SD) Vd for young and elderly volunteers was 0.61 ( $\pm$  0.06) and 0.75 ( $\pm$  0.07), respectively. This difference was significant ( $p < 0.01$ ). **Conclusion:** This prospective study showed significantly decreased P-gp activity, i.e. reduced integrity of the BBB transport function, during ageing. reference: (1)Bart J, Willemsen AT, Groen HJ, van der Graaf WT, Wegman TD, Vaalburg W, de Vries EG, Hendrikse NH. Quantitative assessment of P-glycoprotein function in the rat blood-brain barrier by distribution volume of [11C]verapamil measured with PET. Neuroimage. 2003 Nov;20(3):1775-82.

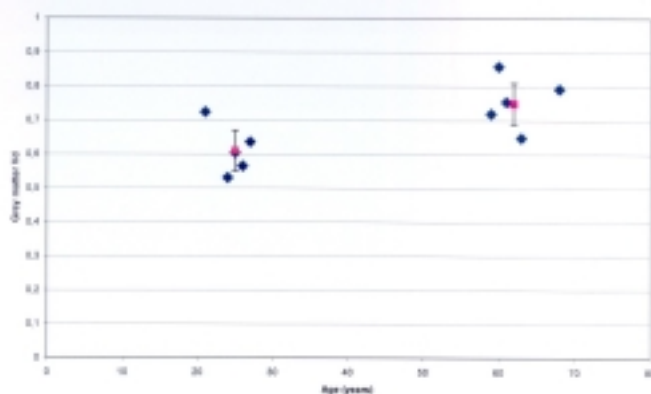


Figure 1. Grey matter [11C](R)-verapamil Vd as function of age

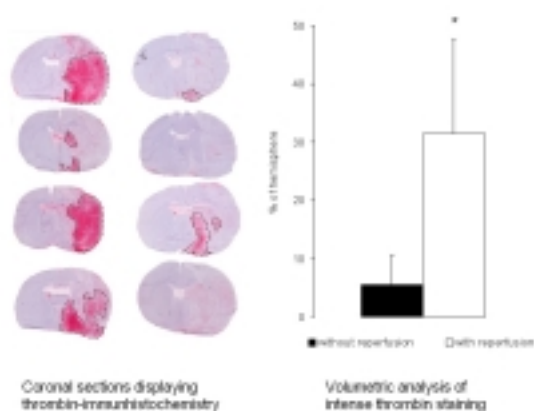


## ULTRAEARLY REPERFUSION INDUCES BLOOD BRAIN BARRIER DISRUPTION DURING FOCAL ISCHEMIA IN RATS

Johannes Woitzik, Axel Hohenstein, Nina Weinzierl, Lothar Schilling

*Department of Neurosurgery, University Hospital Mannheim, Mannheim, Germany*

Background: Unintentional reperfusion is considered a complication in a number of ischemic models. In the following study we evaluated whether this short-term reperfusion affects ischemic volume and blood brain barrier (BBB) integrity after permanent focal ischemia in rats. Methods: Focal brain ischemia was induced in male SD rats using the intraluminal filament method. In groups 1, 2, and 3 a 20 second reperfusion period was allowed 0.5, 2 and 10 minutes after thread occlusion. In control animals reperfusion was omitted. Twenty-four hours after permanent middle cerebral artery occlusion animals were killed and the infarct volume and swelling examined on serial coronar silver nitrate stained sections. Vascular leakage was determined by immunohistochemical staining for the plasma protein thrombin. Expression of vascular endothelial growth factor (VEGF) and matrix-metalloproteinases (MMP) 2 and 9 was investigated using RT-PCR and zymography methodology. Results: Short reperfusion already two minutes after thread occlusion lead to a significant increase of the ischemic volume and swelling (control animals:  $423 \pm 32$  mm<sup>3</sup> /  $12.4 \pm 8.5\%$ , group 1:  $428 \pm 62$  mm<sup>3</sup> /  $24.7 \pm 7.0\%$ \*, group 2:  $547 \pm 48$  mm<sup>3</sup> /  $36.7 \pm 4.8\%$ \*, group 3:  $592 \pm 74$  mm<sup>3</sup> /  $33.8 \pm 4.9\%$ \*, ischemic volume / swelling, respectively, \*  $p < 0.05$  vs. control animals). There was a severe leakage of the plasma protein thrombin determined immunohistochemically (Fig. 1). Quantifying the volume with the most severe thrombin leakage showed significant more leakage in animals with a short reperfusion after 10 minutes of MCA occlusion. The ratios of ipsilateral /contralateral VEGF mRNA expression and MMP 9 protein content tended to result in increased values (VEGF: group 4:  $1.67 \pm 0.44$  vs control:  $1.06 \pm 0.10$ ,  $p < 0.1$ ; MMP 9: group4:  $4.40 \pm 1.54$  vs control:  $2.42 \pm 0.87$ ,  $p < 0.1$ ). Conclusions: Early transient reperfusion may be causal for increased disruption of the BBB in permanent ischemia. Similar reperfusion episodes during early ischemia in patients - due to incomplete clot adherence or clot distal movements - could be causal for increased BBB damage and hemorrhagic conversion in individual patients. Thus, screening for mechanisms of intermittent reperfusion injury may be worthwhile to detect patients at risk for BBB damage before initiating reperfusion therapy, which is associated with a high risk of further disruption of the BBB and subsequent intracerebral bleeding.



**NOVEL ROLE OF 'ENTOURAGE' MONOACYLGLYCEROLS IN FUNCTION OF HUMAN CEREBRAL MICROVASCULAR ENDOTHELIAL CELLS**

Richard McCarron<sup>1</sup>, Esther Shohami<sup>2</sup>, Ye Chen<sup>1</sup>, Alois Strasser<sup>3</sup>, Raphael Mechoulam<sup>2</sup>,  
Joliet Bembry<sup>3</sup>, **Maria Spatz**<sup>3</sup>

<sup>1</sup>*Resuscitative Medicine Department, Naval Medical Research Center, Silver Spring, MD, USA*

<sup>2</sup>*School of Pharmacy, Hebrew University, Jerusalem, Israel*

<sup>3</sup>*Stroke Branch, NINDS, NIH, Bethesda, MD, USA*

2-arachidonoyl-glycerol (2-AG) is one of the monoacylglycerols which is a known endocannabinoid produced in various organs including brain and gut. It is recognized as a neuromodulatory, cytoprotective and vasodilatory agent. The 2-AG (isolated from brain) was shown to be accompanied by other monoacylglycerols, primarily the 2-acyl-glycerol esters, 2-linoleoyl-glycerol (2-Lino-G) and 2-palmitoyl-glycerol (2-Palm-G). These two monoacylglycerols, which were referred to as 'entourage' substances, were not shown to be active by themselves. However, they were demonstrated to enhance the function of 2-AG. Lately, we reported that 2-AG functioned as an agonist for both of the cannabinoid receptors CB1 and CB2, as well as the vanilloid receptor, TRPV1. All of these receptors were shown to be constitutively expressed on human cerebrovascular endothelial cells (HBEC). Here we characterize the effects of all three monoacylglycerols on intracellular Ca<sup>2+</sup>-levels on HBEC using a fluorescent probe Fluo-3/AM. It was observed that treatment with 2-AG stimulated Ca<sup>2+</sup>-levels in HBEC. Interestingly, treatment with 2-Lino-G and 2-Palm-G also stimulated Ca<sup>2+</sup>-levels in HBEC. The effects of all three of these endogenous fatty acid glycerol esters were almost completely abolished in the presence of Ca<sup>2+</sup>-free medium containing EDTA. In addition, 2-Lino-G (100 μM) and 2-Palm-G (50 μM) augmented (344.5 ± 13% and 263.1 ± 42%, respectively) the level of Ca<sup>2+</sup> induced by 2-AG (10 μM). Although inhibition of 2-AG-induced effects with selective receptor antagonists for CB1 (SR141716A) and TRPV1 (capsazepine) was previously shown, treatment with both antagonists also inhibited Ca<sup>2+</sup> influx induced by 2-Palm-G (46 ± 10% and 37 ± 2%, respectively) and 2-Lino-G (75 ± 4% and 44 ± 2%, respectively). Significant inhibition by SR141716A and capsazepine of augmented Ca<sup>2+</sup>-influx was also observed in HBEC exposed to combined treatments (2-AG with either of these two monoacylglycerols). Treatment with inhibitors of protein kinase C (PKC; bisindolylmaleimide) and protein kinase A (PKA; H-89 Dihydrochloride) also blocked Ca<sup>2+</sup>-influx induced by 2-Lino-G and 2-Palm-G. These results indicate that 2-Lino-G and 2-Palm-G not only function as active entourage agents, but are also capable of directly affecting Ca<sup>2+</sup>-influx and modulating 2-AG-induced effects. These findings also implicate both PKC and PKA in the signal transduction mechanism(s) associated with this phenomenon. In conclusion, these substances may actively participate in the endothelium-dependent regulation of microcirculation in the brain.

## VON WILLEBRAND FACTOR ENDOTHELIAL DEPOSITION: A NEW HYPOTHESIS OF ISCHEMIC SMALL VESSEL DISEASE

Sharyl R. Martini<sup>1,2</sup>, Thomas A. Kent<sup>1,2</sup>

<sup>1</sup>Department of Neurology, Baylor College of Medicine, Houston, TX, USA

<sup>2</sup>Michael E. DeBakey VAMC Stroke Program, Houston, TX, USA

**Introduction:** Unlike other subtypes of strokes for which there is definitive preventative therapy, small vessel cerebrovascular disease (SVD) remains particularly vexing since it is relatively resistant to usual risk factor management. The clinical course is often highly recurrent despite usual anti-platelet therapy. Evidence from the NINDS tPA trial that small vessel stroke responds as well as thrombo-embolic to thrombolysis was surprising given the prevailing wisdom that lacunar stroke is not caused by usual thrombotic pathways. We have generated a new hypothesis that can explain both the underlying pathology of chronic ischemia and this pattern of aspirin insensitivity and thrombolytic efficacy. Similarities between the subendothelial deposits in lacunar disease and thrombotic thrombocytopenic purpura (TTP), a disease associated with increased von Willebrand Factor (VWF) monomers, led us to hypothesize that hypertension and other risk factors lead to VWF deposition and the characteristic patterns of SVD seen in post-mortem brains of humans and animal models. **Methods:** Brains from 15 week old salt-loaded Stroke Prone Spontaneously Hypertensive rats (SHR/SP) were studied. SHR/SP rats begin to show lacunar-like pathology at 10 weeks if salt-loaded. Rats were euthanized and brain slices processed for light microscopy in 10% formalin followed by successive dehydration and paraffin embedding. This method preserved the relationship between vessel morphology and luminal contents. VWF was visualized by immunohistochemical detection; controls were visualized without primary antibody. Platelet aggregates were identified by immunostaining for GpIIb/IIIa antigen. Our initial efforts focused on the extent of endothelial VWF deposition and its association with luminal platelet deposition. **Results:** We found dramatic deposition of VWF and luminal obstruction in vessels throughout the striatum, in almost all cases associated with platelet aggregation (Figure, left panel). Vessels from unaffected regions demonstrated thinner walls and unobstructed lumens (Figure, right panel). **Discussion:** Our preliminary results indicate an association between platelet aggregates and endothelial VWF accumulation. VWF monomers can initiate an aspirin-insensitive platelet aggregation that is responsive to fibrinolytics. Increased circulating levels of VWF have been observed in SVD patients, but interpreted as a marker of endothelial injury. Our hypothesis considers whether VWF can itself be causative. The strong association seen in SHR/SP brains supports the relationship between VWF and platelet aggregation. Examination of SHR/SP and SHR stroke resistant rats at earlier time points are underway, as are VWF overexpression studies in mice. These studies will indicate whether VWF overexpression alone is sufficient to result in small vessel thrombosis, or whether additional factors are required. Our studies suggest a novel role of VWF in SVD and, if confirmed, will open additional preventative and therapeutic opportunities for this condition.

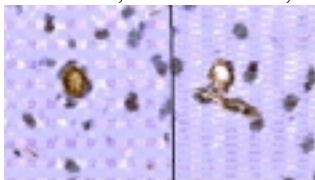


Figure 1. The photomicrograph on the left shows a fully occluded cerebral arteriole presenting early in a 10 week old SHR/SP rat. The right photomicrograph shows a control arteriole of similar diameter in the same brain. The dark, granular material particularly in both specimens is VWF. Platelets that are easily identified by staining associated with VWF are seen both in the left and right panels.



**RLIP-76: A NOVEL MECHANISM OF DRUG RESISTANCE IN EPILEPSY**

**Kerri L. Mancini**, Vince Fazio, Sanjay Awasthi, Sharad Singhal, Luca Cucullo,  
Gabriele Dini, Damir Janigro

*Cerebrovascular Research, Cleveland Clinic Foundation, Cleveland, OH, USA*

**Rationale:** We and others have shown that the drug efflux protein P-glycoprotein (P-gp or MDR1) protects the brain from xenobiotics, but other transporters that may be involved in multiple drug resistance to antiepileptic drugs may also play a role. Unlike other selective transporters, P-gp recognizes a wide range of substrates, including AED. However, there is a significant overlap between molecules transported by MDR1 and the non-ABC transporter RalA Binding Protein 1 (RLIP-76). **Methods:** We used a combination of immunohistochemistry, western blot analysis, and pharmacokinetic assays to measure levels of expression of RLIP-76; co-localization with MDR1; and relative contribution to AED extrusion. Data were obtained from 15 epileptics, age ranging from 3 months to 61 years. **Results:** While MDR1 immunoreactivity was observed in neurons, glia and endothelial cells, RLIP-76 was only found in endothelium and not in parenchymal cells. Experiments of drug extrusion using antibodies capable of selective inhibition of MDR1 or RLIP-76 revealed that the latter mechanism was responsible for 72 $\pm$ 8 % of 14C-phenytoin extrusion by epileptic BBB endothelial cells; MDR1 contributed to only 27 $\pm$ 8 % of ATP-dependent drug extrusion. These findings are in agreement with the fact that transport of P-gp substrates in these cells is only weakly inhibited by specific MDR1 blocker XR9576. **Conclusion:** Our findings suggest that RLIP-76 and not MDR1 is the main multiple drug resistance mechanism at the blood-brain barrier of drug-resistant epileptic patients.

## IN A RAT MODEL OF TRANSIENT ISCHEMIA, ACUTE ALBUMIN LEAKAGE ACROSS THE BLOOD-BRAIN BARRIER IS OFTEN FOLLOWED BY RAPID CELLULAR UPTAKE

Tavarekere N. Nagaraja<sup>1</sup>, Kelly A. Keenan<sup>1</sup>, **Joseph D. Fenstermacher<sup>1</sup>**, Robert A. Knight<sup>2</sup>

<sup>1</sup>Anesthesiology, Henry Ford Health System, Detroit, MI, USA

<sup>2</sup>Neurology, Henry Ford Health System, Detroit, MI, USA

Introduction: Evans blue-tagged albumin (EBA) is often used as a marker of blood-brain barrier (BBB) opening. Following cold injury and transient ischemia, EBA crosses the BBB and is taken up by neurons, and DNA fragmentation occurs within such neurons [1]. In view of this, it was hypothesized and tested in a model of transient ischemia and subsequent hemorrhagic transformation (HT) that EBA crosses the leaky BBB and is rapidly taken up by brain cells during the acute phase of reperfusion. Methods: In adult male Wistar rats (275-300g), one middle cerebral artery (MCA) was occluded by suture for 3 hr. After suture withdrawal and 3 hr of reperfusion, EBA was intravenously injected. After 5 min (n=4) or 20 min (n=4), rats were sacrificed, and brains quickly removed and prepared for laser scanning confocal microscopy (LSCM). Three-dimensional LSCM reconstructions (30  $\mu$  thick) were made of EBA fluorescence in both sides of the brain at 5 sites within the preoptic area (POA), striatum (STR), and parietal cortex (CTX). The LSCM system was set to yield volumes of EBA fluorescence (Vf) on the contralateral side equal to the normal radiolabeled albumin distribution volume [2]. At that setting, Vf was determined on the ischemic side and expressed as volume percent (%). The interstitial, neuronal and microglial distribution of EBA was evaluated in all 3D reconstructions. Results: Normal capillary EBA distribution patterns were seen in 39 of the 40 reconstructions from the ipsilateral CTX; some EBA leakage and neuronal uptake was noted in one case. The ipsilateral side data for the STR were similar to those of the CTX. In the ipsilateral POA, however, EBA leakage (BBB opening) was detected in 31 of the 40 POA reconstructions. Cellular uptake of EBA was evident in the ipsilateral POA in all animals of the 5 min group. Among the 40 reconstructions from both time groups, 25 showed neuronal and 24, microglial uptake of EBA. For the POA, Vf (mean  $\pm$ SD) was 0.05 $\pm$ 0.2% on the contralateral side and 2.7 $\pm$ 1.5% and 13.7 $\pm$ 13.7 on the ipsilateral side at 5 and 20 min, respectively. The large SD values indicate the great variability in EBA distribution among the 40 ischemic side reconstructions. Conclusions: Supporting the hypothesis, appreciable uptake of leaked EBA by neurons and microglia occurred by 5 min in the POA. The lack of EBA (MW=68,000 Da) leakage in the STR was striking. In this model, much smaller MR contrast agent Gd-DTPA (MW=551 Da) and sucrose (342 Da) both pass across the BBB within the STR [3]. At this stage, opening of the BBB in STR, and possibly CTX, may only be to smaller molecules and the neurons and microglia are "protected" from albumin uptake by a semi-intact BBB. Tightening the BBB in such areas may be a way to prevent further damage and progression to HT. References: 1. Murakami et al. J Neurotrauma 15:825-835 (1998) 2. Bereczki et al. Am J Physiol 264:H1360 (1993) 3. Ewing et al. Mag Res Med 50:283 (2003) Grant support: RO1NS38540 and AHA-Bugher Foundation Award (0270176N).

**PROTEOMICS ANALYSIS IN TRANSGENIC MICE OVER-EXPRESSING  
ENDOTHELIN-1 IN ASTROCYTES AFTER TRANSIENT FOCAL CEREBRAL  
ISCHEMIA**

**Amy C.Y. Lo, Marco M.K. Tsui, Victor K.L. Hung, Lai Ping Yaw, Qing-Yu He,  
Jen-Fu Chiu, Stephen S.M. Chung, Sookja K. Chung**

*Institute of Molecular Biology, The University of Hong Kong, Hong Kong*

Stroke patients have increased levels of endothelin-1 (ET-1), a strong vasoconstrictor, in their plasma, cerebrospinal fluid or brain tissue biopsy. Our previous results showed that transgenic mice over-expressing endothelin-1 in astrocytes (GET-1) display more severe neurological deficits and increased infarct with further increased cerebral edema as well as water content after middle cerebral artery occlusion (MCAO). Correspondingly, more severe blood-brain barrier breakdown and increased aquaporin 4 expression in astrocytic end-feet were also observed. To further understand the signaling pathway of astrocytic ET-1-induced cerebral edema formation in ischemic stroke, proteomics and Western analyses were performed. The expression of a transcription factor, osmotic response element binding protein (OREBP) which is upregulated and translocates to the nucleus in osmotically challenged cells, showed a significant decrease in GET-1 ipsilateral brain after MCAO by one-dimensional Western blot. One of its transcriptional targets, aldose reductase (ALR2) which is also an osmoregulatory protein, was increased after MCAO. The expression of HSP70, another target of OREBP, was significantly increased in both NTg and GET-1 brains with a higher level in GET-1 brains. The protein expression profile of GET-1 ischemic brains was further analyzed by two-dimensional gel electrophoresis and matrix-assisted laser desorption/ionization-time of flight mass spectroscopy. Our results showed that the level of transthyretin, an acute phase response protein after transient focal ischemia, was altered in GET-1 ischemic brains after MCAO, suggesting its involvement in astrocytic ET-1-induced brain water imbalance after ischemic stroke.

## NEGATIVE CORRELATION BETWEEN CIRCULATING ENDOTHELIAL PROGENITOR CELLS (EPC) AND HOMOCYSTEINE LEVELS

Umar Shuaib<sup>1</sup>, Abdul Salam<sup>1</sup>, Tom Jeerakathil<sup>1</sup>, Usman Ghani<sup>1</sup>, Abdul M. Naseer<sup>1</sup>,  
Brenda Schwindt<sup>1</sup>, Kathryn Todd<sup>2</sup>, **Ashfaq Shuaib<sup>1</sup>**

<sup>1</sup>*Stroke Research Unit, Division of Neurology, Faculty of Medicine and Dentistry, University of Alberta, Edmonton, AB, Canada*

<sup>2</sup>*Department of Psychiatry, Faculty of Medicine and Dentistry, University of Alberta, Edmonton, AB, Canada*

**Abstract** Background Recent evidence suggests that circulating endothelial progenitor cells (EPCs) may be associated with endothelial repair following ischemic injury. The number of EPCs is inversely correlated to the presence of vascular risk factors. Increasing serum levels of homocysteine may result in endothelial injury and one theory is that they affect EPC levels. The relationship between homocysteine levels and EPCs has not yet been studied. Objective To investigate the relationship between fasting homocysteine, and circulating EPC's in patients with transient ischemic attacks (TIAs), acute ischemic stroke and control. Method We recruited patients with stable cerebrovascular disease, acute stroke, and controls without any history of cerebrovascular disease and evaluated EPC levels and stroke risk factors. Results There were one hundred and two patients [Mean age 63.8 years (SD  $\pm$  12.99), 65 (63.7%) male and 37 (36.3%) female]. EPC count differed significantly ( $p = 0.001$ ) between acute [median 4.75; range 0-33], stable [median 7.275; range 0-43], and control subjects [median 15.525; range 4.3-71]. There was a significant inverse correlation between EPC level and homocysteine ( $\rho = -0.335$ ;  $p < 0.001$ ). In univariate analysis homocysteine was significantly associated with EPCs as were age, acute stroke status, stable stroke status, HDL, history of hypertension and Framingham coronary risk score (FCRS). Multiple linear regression confirmed an inverse relationship between homocysteine and EPCs ( $p$ -value = 0.013) after controlling for age, and type of subject. Conclusion Increasing homocysteine levels are associated with lower numbers of circulating EPCs suggesting another mechanism by which hyperhomocysteinemia increases the risk of atherosclerosis and vascular thrombosis. Running Head: Homocysteine, EPC

Key words: Homocysteine, endothelial progenitor cells, correlation

## THE POSITIVE CORRELATION BETWEEN ENDOTHELIAL PROGENITOR CELL AND HDL-CHOLESTEROL LEVELS IN PATIENTS WITH CEREBROVASCULAR DISEASE

Abdul Salam<sup>1</sup>, **Ashfaq Shuaib**<sup>1</sup>, Umar Shuaib<sup>1</sup>, Tom Jeerakathil<sup>1</sup>, Muzaffar Siddiqui<sup>1</sup>, Usman Ghani<sup>1</sup>, Brenda Schwindt<sup>1</sup>, Kathryn Todd<sup>2</sup>

<sup>1</sup>*Stroke Research Unit, Division of Neurology, Faculty of Medicine and Dentistry, University of Alberta, Edmonton, AB, Canada*

<sup>2</sup>*Department of Psychiatry, Faculty of Medicine and Dentistry, University of Alberta, Edmonton, AB, Canada*

**Background** Endothelial progenitor cells (EPCs), derived from bone marrow, may improve endothelial function and are inversely correlated to cardiovascular risk, as calculated by Framingham risk score. The blood levels of EPCs may be reduced in patients with increased LDL cholesterol and increase with statin treatment. There are however no reports of a relationship of HDL cholesterol to EPC levels. **Objective** To investigate a possible association of HDL levels and circulating EPCs in a clinical study population. **Methods and results** We recruited 82 patients with cerebrovascular disease and 20 controls without any history of cerebrovascular disease. All patients had evaluation of vascular disease risk factors, blood level of cholesterol, c-reactive proteins, homocysteine, carotid Doppler and cranial CT scans. The patients were divided into three groups based on their circulating EPC levels. The mean age was 63.8 years (SD  $\pm$ 12.9). Of the one hundred and two subjects in the sample, sixty five (63.7%) were male and thirty seven (36.3%) were female. The mean total cholesterol, LDL-cholesterol, triglycerides, fasting glucose, HbA1c, c-reactive proteins and creatinine were not statistically different among the three groups. Similarly, the presence of smoking and hyperlipidemia were also not significantly different. The HDL levels was directly related to EPC colony count after controlling for statin use ( $\beta = 8.14$ ,  $p = 0.002$ ). The HDL was significantly lower in individuals with low EPCc levels (below  $1.09 \pm 0.26$  mM,) compared with intermediate ( $1.28 \pm 0.29$  mM) and high HDL levels ( $1.57 \pm 0.85$  mM) ( $p = 0.027$ ) for those who were not on statin therapy. An additional 28 patients were on statins at the time of assessment and there appeared to be no difference in EPC levels in relationship to HDL levels in these individuals. **Conclusion** Our results indicate a very strong positive association between the circulating EPC levels and the blood levels of HDL cholesterol. This was significant only in patients who were not on statin therapy. In addition to the other known protective effects of HDL on vascular healing, the increase in EPCs may be an additional mechanism for its endothelial effects. **Running Head:** HDL cholesterol and EPC **Key words:** HDL cholesterol, Endothelial Progenitor cells (EPC's), Association

## PARTIAL REPLACEMENT OF $K^+$ WITH $Rb^+$ IN THE RAT BRAIN IN VIVO DOES NOT CHANGE THE TISSUE POTASSIUM DYNAMICS AFTER FOCAL CEREBRAL ISCHEMIA AND IS DETECTABLE BY $^{87}Rb$ MRI

Victor E. Yushmanov<sup>1</sup>, Alexander Kharlamov<sup>1</sup>, Eli J. Wasserman<sup>2</sup>, Fernando E. Boada<sup>2</sup>, **Stephen C. Jones<sup>1</sup>**

<sup>1</sup>Department of Anesthesiology, Allegheny General Hospital, <sup>2</sup>Department of Radiology, MR Research Center, University of Pittsburgh, Pittsburgh, PA, USA

**Introduction:** An abrupt change in brain tissue potassium concentration,  $[K^+]_{br}$ , has been suggested as an index of progression of ischemic damage [1]. MRI has a potential to study  $Na^+$  homeostasis in brain [2]. To monitor  $K^+$  by MRI, partial  $Rb/K$  replacement has been proposed [3] based on the properties of  $Rb^+$  as a congener for  $K^+$  in tissues and its much better MR-sensitivity. It is not known, however, to what extent such substitution would influence ion balance in ischemic brain. **Methods:** Five normally-fed male Sprague-Dawley rats (240-300 g) were given 30-60 mM  $RbCl$  in the drinking water for 12-19 days. Focal cerebral ischemia was induced by MCA transection (MCAT) [4], and was maintained during 2.5 (n=3) or 5 (n=2) hours. Samples of cortical brain of 1-mm diameter were punched from the ischemic core and contralateral areas [5] using the change in surface reflectivity of ischemic cortex as a guide [6].  $Na$ ,  $K$  and  $Rb$  content in the brain were determined by emission flame photometry at 589, 766 and 791 nm for  $Na$ ,  $K$  and  $Rb$ , respectively, and corrected for the mutual interference effects. **Results:** The total of  $[K^+]_{br} + [Rb^+]_{br}$  perfectly fits our previous data on the time course of  $[K^+]_{br}$  after focal ischemia featuring a sharp drop at 3.5 hours in animals without  $Rb/K$  substitution [1].  $[K^+]_{br}$  and  $[Rb^+]_{br}$  were pooled together, because the degree of  $Rb/K$  replacement (i.e., the  $Rb/(K+Rb)$  ratio) varied between 0.12 and 0.20 for different animals. As expected,  $[Na^+]_{br}$  concentration increased with time after ischemia onset. The  $Rb/(K+Rb)$  ratio increased over time in ischemic areas (normalized to the contralateral brain):  $1.057 \pm 0.007$  at 2.5 hours and  $1.15 \pm 0.01$  after 5 hours post MCAT ( $p < 0.05$ ). This suggests that the  $Rb^+$  efflux from the injured tissue is slower than the  $K^+$  efflux. **Conclusion:**  $Rb^+$  loading does not significantly change the pattern of  $[K^+]_{br}$  decrease in the ischemic brain over time. Therefore, the animals with partial  $Rb/K$  substitution are suitable for  $^{87}Rb$  MRI studies of  $K^+$  homeostasis in ischemia.

### References:

1. Jones SC et al., Abstract # 309.3, New Orleans, LA: Soc. Neurosci. (2003).
2. Thulborn KR et al., *Radiology* **213**: 156-166 (1999).
3. Kupriyanov VV et al., *Magn. Reson. Med.* **40**: 175-179 (1998).
4. Chen ST et al., *Stroke* **17**: 738-743 (1986).
5. Hu W et al., *Brain Res.* **868**: 370-375 (2000).
6. Kharlamov A et al., *J. Neurosci. Methods* **111**: 67-73 (2001).

Support: NIH grant R01 NS 30839

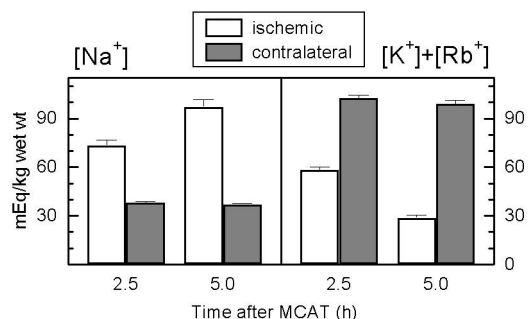


**Figure.** Concentrations of monovalent cations (average  $\pm$  SEM over all animals in the corresponding time groups) in the rat brain cortex after MCAT.



## BLOOD-BRAIN BARRIER BREAKDOWN AND MATRIX METALLOPROTEINASE ACTIVATION FOLLOWING THROMBOLYSIS IN AN AGED MODEL FOCAL CEREBRAL ISCHEMIA

Melissa A. Kelly<sup>1</sup>, Ashfaq Shuaib<sup>2</sup>, Kathryn G. Todd<sup>1,2,3</sup>

<sup>1</sup>*Center for Neuroscience, University of Alberta, Edmonton, AB, Canada*

<sup>2</sup>*Department of Neurology, University of Alberta, Edmonton, AB, Canada*

<sup>3</sup>*Department of Psychiatry, Edmonton, AB, Canada*

Stroke is the third leading cause of death in North America. Currently, the only approved treatment for stroke is thrombolysis - most commonly achieved through the use of tissue plasminogen activator (tPA). The devastating side effects of tPA include an increased risk of hemorrhage and brain swelling. It is the breakdown of structural components of the blood-brain barrier (BBB) that is thought responsible for the increased susceptibility to hemorrhage. Matrix metalloproteinases (MMPs) have been implicated in the destruction of structural proteins that comprise the BBB – these include laminin and fibronectin (Lo et al., 2003). Proteases, such as tPA, may promote the activation of MMPs, thereby conferring a mechanism for the breakdown of the BBB. MMP-2 and -9 have been shown to exhibit increased expression in the hours to days following an ischemic event in animal models of stroke and in humans (Lo et al., 2003). To date, no study has examined the effects of tPA on the aged brain, despite the increased vulnerability that aging poses on the cerebrovascular system. For the present study, aged rats older than one year will be used and compared to rats aged 3 months, considered to be young adult. This study is intended to reveal a possible mechanism for the increased vulnerability of the aged brain following administration of tPA in the treatment of focal cerebral ischemia. Male Sprague-Dawley rats assigned to one of four groups (Ischemia-tPA, Ischemia-vehicle, Sham-tPA, Sham-vehicle) are anesthetised using a halothane mixture with oxygen and nitrous oxide. One hour post-ischemia, tPA (10 mg/mL) or saline is administered via tail vein infusion. At 24 hours following ischemia, brains are removed and placed in a brain block. The brain is divided into two parts, one 2 mm section is immersed in TTC for quantification of infarct size. The second block of brain is flash-frozen in ice-cold isopentane and retained for further analysis including immunostaining and zymographic techniques. Immunohistochemistry includes the co-localization of MMP-2 and -9 to specific cell type. This also determines the extent of BBB breakdown by examining the structural components of the BBB, substrates for MMP activity. Zymographic analyses include gelatin zymography and in situ zymography. The former allows for quantification of the gelatinolytic activity of MMPs in homogenate while the latter is a means to regionally localize the MMP activity in tissue sections. Results: TTC infarct area is miniscule and therefore unmeasurable, though behavioural testing eludes to a significant amount of damage. Closer histological examination reveals small areas of brain tissue that are metabolically compromised in the territory of the middle cerebral artery, including striatum and cortex. Laminin and fibronectin immunohistochemistry as well as IgG extravasation show severely compromised vasculature even in animals which do not demonstrate a large area of ischemic damage. This is found to be more significant in those animals treated with tPA. In comparing a study with rats aged 3 months (young adult), these results indicate that tPA administration to an aged animal may lead to significantly more BBB breakdown than in the young adult.

**17BETA - ESTRADIOL TREATMENT IMPROVES NEUROHISTOPATHOLOGICAL OUTCOME AFTER CARDIAC ARREST AND CARDIO PULMONARY RESUSCITATION IN MALE MICE**

**Ruediger R. Noppens<sup>1</sup>**, Julia Kofler<sup>1</sup>, Marjorie R. Grafe<sup>1,2</sup>, Patricia D. Hurn<sup>1</sup>,  
Richard J. Traystman<sup>1</sup>

<sup>1</sup>*Department of Anesthesiology & Peri-Operative Medicine, Oregon Health & Science University, Portland, OR, USA*

<sup>2</sup>*Department of Pathology, Oregon Health & Science University, Portland, OR, USA*

Introduction: Cardiac arrest (CA) claims approximately 500,000 lives in the US alone. Despite recent advances in CPR, outcome remains poor. 17beta - estradiol, the principal mammalian estrogen, has been shown to reduce infarction size in experimental stroke[1]. Postischemic estrogen improves recovery of cerebral blood flow after stroke in rats[2]. The purpose of this study was to determine if chronic treatment with 17beta - estradiol (E2) after experimental cardiac arrest / cardio pulmonary resuscitation (CA/CPR) improves neuronal survival in male mice and if the E2 loading dose is important to alter outcome. Methods: With institutional approval 60 male C57/Bl6 mice (22-26g) were anesthetized with halothane, the jugular vein was catheterized, ECG was monitored, the trachea was intubated and controlled ventilation was performed throughout the experiment. CA was induced by i.v. injection of KCl. After 10 min, CPR was initiated by chest compressions (~300/min), administration of iv epinephrine (8 mg) and ventilation with 100% oxygen, as previously described[3]. 1.5 min after return of spontaneous circulation (ROSC) iv injection of either vehicle, 0.5 or 2.5mg E2 (loading dose) was performed. Animals received additional s.c. silastic oil implants or hormone implants (12 mg E2) 30 min after ROSC, according to treatment group. Animals were re-anesthetized three days after ROSC, blood samples for E2 serum levels were taken followed by transcardial perfusion fixation (formalin 10%). Brains were removed for standard injury quantification in hippocampus (CA1) and caudoputamen (CP; hematoxylin-eosin staining, light-microscopy). Statistical analysis was performed using ANOVA. Results: Physiologic variables, epinephrine dose and duration of CPR were not different between groups. 13 animals of the vehicle group, 16 of the 0.5+12 E2 and 17 of the 2.5+12 E2 group survived the three- day observation period. E2 serum levels were: vehicle= 28±2, 0.5+12 E2=165±10 and 2.5+12 E2=153±11 pg/ml (p<0.001; mean±SE). Neuronal injury in rostral CP was less with 0.5+12 E2 (41±5% injured neurons) and 2.5+12 E2 (36±6%) administration, compared to vehicle (68±2%, p<0.001). Both E2 groups had improved neuronal survival in the caudal CP (0.5+12 E2: 46±5%, 2.5+12 E2: 35±5%), compared to vehicle (69±2%, p<0.05). CA1 injury was similar in all groups. Conclusion: 17b - estradiol application after CA/CPR improves neuronal survival in male mice. Protection is equally robust with both loading doses used. E2 treatment might play an important role in brain resuscitation after cardiac arrest / CPR in humans. [1] Hurn PD et al., Stroke 2003 [2] McCullough LD et al., Stroke 2001 [3] Kofler J et al., J.Neurosci.Methods 2004

**HYPOTHERMIA REDUCES INFLUENCE OF MATRIX METALLOPROTEINASE INDUCTION BY EMMPRIN IN EXPERIMENTAL FOCAL CEREBRAL ISCHEMIA**Dorothe Burggraf<sup>1</sup>, Helge K. Martens<sup>1</sup>, Gerhard F. Hamann<sup>2</sup><sup>1</sup>*Ludwig-Maximilians-University, Klinikum Grosshadern, Neurology, Munich, Germany*<sup>2</sup>*Department of Neurology, HSK Dr. Horst-Schmidt-Klinik, Wiesbaden, Germany*

Background: Microvascular basal lamina damage is a regular result of experimental focal cerebral ischemia. Recombinant tissue plasminogen activator (rt-PA) is successfully used in human ischemic stroke. The main drawback is the development of hemorrhage. Hypothermia was proven to be able to reduce the basal lamina damage by almost 50%. The combination of hypothermia and rt-PA completely preserves the microvascular basal lamina following experimental focal cerebral ischemia. Matrix metalloproteinases (MMP) are critically involved in the degradation of the basal lamina after ischemia. Animals treated with rt-PA but not with hypothermia developed a dramatic increase in MMP-2, MMP-9. Hypothermia reduced the levels of both proteases, they did not differ between the groups of animals treated with or without rt-PA in combination with hypothermia. EMMPRIN, as a MMP inducer protein, was shown to be relevant in cerebral ischemia. The aim of this study was to test the influence of hypothermia and the combination of hypothermia and rt-PA to the MMP activator protein EMMPRIN. Methods: Using the suture model, we subjected 30 rats to 3 hours of focal ischemia and 24 hours of reperfusion. Each six rats received post-ischemic normothermia (37°C) with and without rt-PA (i.v. administered 18 mg/kg bw at the end of ischemia), hypothermia (32-34°C) for the reperfusion period with and without rt-PA; a group of six sham operated animals with hypothermia was used as control. EMMPRIN expression was measured by Western blot of the ischemic and non-ischemic basal ganglia and cortex separately. Gelatine-zymography was used to detect MMP-2. Results: With immunohistochemistry it was shown that EMMPRIN was present on cerebral microvessels in the rat. A significant increase of the MMP-inducer protein was demonstrated by Western blot analysis with anti-EMMPRIN antibody in the ischemic basal ganglia area after I3R24. Compared with the contralateral area, EMMPRIN expression was significantly increased in the ischemic hemisphere. Hypothermia reduces significantly the level of EMMPRIN: in basal ganglia 94±13% (hypothermia) vs. 169±29% (normothermia), and in cortex 83±7% vs. 109±26% (p<0.05). EMMPRIN expression parallels to MMP-2 expression: in basal ganglia 71±28% (hypothermia) vs. 107±4% (normothermia), and in cortex 53±11% vs. 121±5% (p<0.05) (all data are presented as ratio ischemic vs. contralateral nonischemic side). Discussion: It was recently shown that additionally given exogenous rt-PA after the period of ischemia caused an significant increase of MMP-2 under hypothermic and normothermic conditions. However the amount of EMMPRIN was not significantly increased by administration of rt-PA. These results confirm that the expression of EMMPRIN may be responsible for the known increase of MMPs following cerebral ischemia and reperfusion. Following hypothermia there was less EMMPRIN in the ischemic brain tissue. Calculating the ratio protease (MMP-2) to its possible activator (EMMPRIN) showed a lower ratio under hypothermic conditions. This also points towards a lower influence of EMMPRIN in hypothermia. Conclusions: Hypothermia provides a microvascular protection, this can be seen in the significant reduction of MMP-2. One explanation can be seen in the reduction of the MMP inducer protein EMMPRIN under hypothermic conditions.

**TRANSGENIC ERYTHROPOIETIN PROTECTS FROM FOCAL CEREBRAL ISCHEMIA BY A DUAL PATHWAY INVOLVING BOTH ERK-1/-2 AND AKT**Ülkan Kilic<sup>1</sup>, Ertugrul Kilic<sup>1</sup>, Jorge Soliz<sup>2</sup>, Claudio L. Bassetti<sup>1</sup>, Max Gassmann<sup>2</sup>,Dirk M. Hermann<sup>1</sup><sup>1</sup>*Department of Neurology, University Hospital Zurich, Zurich, Switzerland*<sup>2</sup>*Institute of Veterinary Physiology, Vetsuisse Faculty, University of Zurich, Zurich, Switzerland*

Purpose: Apart from its hematopoietic function, erythropoietin (Epo) exerts neuroprotective activity upon brain hypoxia or ischemia. We here examined the mechanisms mediating Epo's neuroprotective activity in vivo, making use of a transgenic mouse line, tg21, that constitutively expresses human Epo in the brain without inducing polycythemia (1). Methods: Adult tg21 animals and their wild-type controls were submitted to 90 or 30 minutes of intraluminal middle cerebral artery occlusion. Brain injury and cell signalling were assessed at 24 (90 min) or 72 (30 min) hours of reperfusion. Cell signalling inhibitors for MAP kinase/ERK-1/-2 (PD98059) and phosphatidyl inositol-3 kinase/ Akt (Wortmannin) were i.c.v. applied. Results: We show that human Epo is expressed in the cerebral cortex and striatum of tg21 mice and that cortical and striatal neurons carry the Epo receptor. After middle cerebral artery occlusion, transgenic Epo potently protected brains of tg21 mice against ischemic injury, both whether longer-lasting (90 min) and mild (30 min) ischemias were imposed. Histochemical studies revealed that Epo induced an activation of Jak-2, ERK-1/-2 and Akt signalling in the ischemic brain, which was associated with elevated Bcl-XL and decreased NO synthase (both neuronal and inducible) levels. STAT-5 activity, on the other hand, was not increased. I.c.v. injections of PD98059 or Wortmannin showed that both ERK-1/-2 and Akt were required for Epo's neuroprotective activity, antagonization of either pathway completely abolishing tissue protection. Inhibition of ERK-1/-2, but not Akt largely reversed the inhibition of inducible NO synthase (iNOS) in tg21 mice, while that of the neuronal NO synthase (nNOS) isoform was not influenced, indicating that ERK-1/-2 but not Akt is responsible for iNOS inhibition. Conclusions: The dual activation of ERK-1/-2 and Akt is crucial for Epo's neuroprotective function. References: 1. Ü. Kilic, E. Kilic, J. Soliz, C.L. Bassetti, M. Gassmann, D.M. Hermann (2004) FASEB J.: Epub Nov 19.

**CORTICAL SPREADING DEPRESSION ELEVATES MRNAS ENCODING  
FEEDBACK INHIBITORS OF INFLAMMATION: A NOVEL MECHANISM OF  
INDUCED TOLERANCE TO ISCHEMIA**

Katalin Kariko, Hiromi Muramatsu, **Frank A. Welsh**

*Department of Neurosurgery, University of Pennsylvania, Philadelphia, PA, USA*

**Introduction:** The molecular mechanisms by which preconditioning stimuli induce tolerance to ischemia remain poorly understood. Preconditioning with cortical spreading depression (CSD) increases the expression of proinflammatory cytokines, which themselves have been shown to induce tolerance to ischemia. Expression of cytokines is normally linked to upregulation of feedback inhibitors of inflammation, a negative feedback loop that limits the severity, duration, and spatial dissemination of inflammation (1). The objective of the present study was to determine whether CSD increases the expression of feedback inhibitors of inflammation that may protect the brain against ischemia-induced inflammatory damage. **Methods:** Multiple episodes of CSD were evoked in Sprague-Dawley rats (n=9) by applying 2 M KCl to the frontal cortex of one hemisphere for 2 hr. At various times after CSD, mRNAs encoding feedback inhibitors of inflammation were measured in several regions of the cerebral cortex using Northern blot analysis. **Results:** CSD caused rapid and robust elevation of mRNA encoding tristetraprolin (TTP), a protein that promotes the degradation of transcripts encoding inflammatory cytokines. Cortical levels of TTP mRNA increased 2.9-fold ( $p<0.01$ ) at the end of the KCl-application period and 1.8-fold ( $p<0.01$ ) after recovery for 2 hr. CSD also caused a marked elevation in mRNA encoding SOCS3 (suppressor of cytokine signaling-3), a protein that suppresses inflammatory signal transduction by binding and blocking Janus kinases. Levels of SOCS3 mRNA increased 3.2-fold ( $p<0.01$ ) at the end of the KCl-application period, 1.8-fold ( $p<0.01$ ) after recovery for 2 hr, and 2.2-fold ( $p<0.01$ ) after recovery for 24 hr. The elevation of both TTP and SOCS3 mRNAs was greatest in the frontal cortex (site of KCl application). **Conclusions:** These results demonstrate that CSD elevates mRNAs encoding TTP and SOCS3, proteins that suppress inflammation. Upregulation of these endogenous feedback inhibitors would be expected to suppress the inflammatory response to a subsequent episode of ischemia and, thus, diminish the overall extent of ischemic brain damage. Induced suppression of inflammation by blocking inflammatory cytokine production and their signal transduction is a novel mechanism that may contribute significantly to the induction of tolerance to ischemia after CSD and other preconditioning stimuli. Reference: 1. Karikó K, Weissman D, Welsh, FA. *J Cereb Blood Flow Metab* 24:1288-1304, 2004.

## ISCHEMIC PRECONDITIONING PREVENTS TRANSLATIONAL COMPLEX AGGREGATION AFTER TRANSIENT CEREBRAL ISCHEMIA

Chinli Liu, Shaoyi Chen, **Bingren Hu**

*Department of Neurology, University of Miami School of Medicine, Miami, FL, USA*

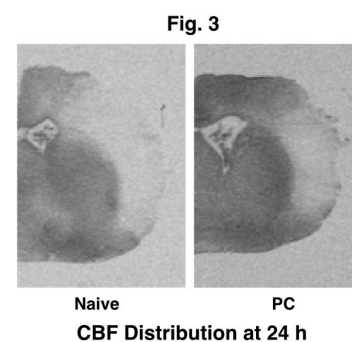
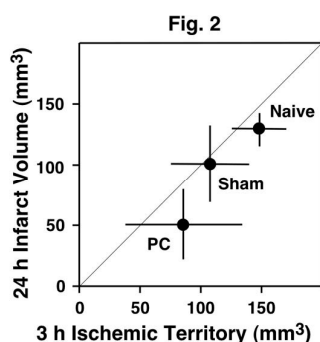
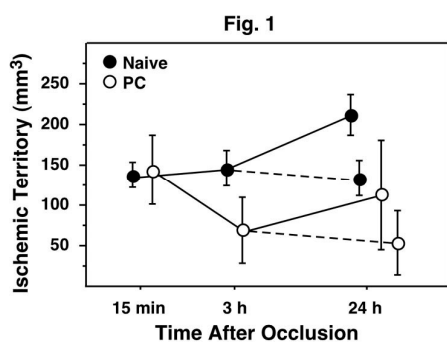
**Background:** Although definitive mechanisms underlying ischemic tolerance remain incompletely understood, activation of endogenous cellular defense machinery has been proposed to contribute to the acquisition of ischemic tolerance. Molecular chaperones and the ubiquitin-proteasomal system defend virtually all cell types from diverse pathological conditions by preventing proteotoxicity from newly synthesized polypeptides and denatured proteins, and by eliminating irreparably damaged proteins. Despite the fact that neuronal ATP production is gradually recovered during reperfusion, inhibition of the overall rate of protein translation continues. Irreversible inhibition of protein biosynthesis after ischemia is a most accurate indicator for delayed neuronal death, and is most probably caused by translational complex aggregation-mediated destruction of molecular chaperone-mediated translational folding and folding-coupled degradation. Despite such close ties between preconditioning and translational complex aggregation, it has not been studied whether ischemic preconditioning is able to prevent translational complex aggregation, thereby protecting neurons from ischemia. **Methods:** Ischemic preconditioning was introduced by 3 min of sublethal ischemia followed by 48 h of recovery. Brains with either ischemic preconditioning or sham-surgery were subjected to a second 7 min of ischemia followed by 30 min, 4, 24, 48 and 72 h of reperfusion. Translational complex aggregation and neuronal death were studied by electron and confocal microscopy, as well as by biochemical analyses. **Results:** The EPTA-ribosome-selective EM staining in brain sections clearly show that ribosomes are clumped into large aggregates only in the cytoplasm of neurons destined to undergo delayed neuronal death after brain ischemia. The translational complex components consisting of ribosomal small subunit protein S6, large subunit protein L28, co-translational chaperones HSC70 and HSP40, and co-translational ubiquitin ligase CHIP, are all highly deposited into a detergent/salt-insoluble protein aggregate-containing fraction in vulnerable neurons after ischemia. Immunofluorescence of ubi-proteins becomes highly aggregated only in neurons destined to undergo delayed neuronal death after ischemia. Ischemic preconditioning abolishes ribosomal aggregation after lethal ischemia under EM and ubi-protein aggregation under confocal microscopy, and reverses deposition of translational complex components into the detergent/salt-insoluble protein aggregate-containing fraction in vulnerable neurons after ischemia. **Discussion:** Translational complex aggregation in ischemic vulnerable neurons may account for irreversible inhibition of protein biosynthesis which is a most accurate indicator for delayed neuronal death after ischemia. Ischemic preconditioning activates endogenous molecular chaperones and the ubiquitin-proteasomal defense systems to counter ischemia-mediated disabilities of molecular chaperone-mediated translational folding and folding-coupled degradation, thereby preventing translational complex aggregation after ischemia. Supported by: NS040407.

## EARLY CBF RECOVERY PREDICTS INFARCT REDUCTION BY ISCHEMIC PRECONDITIONING IN A MODEL OF PERMANENT MIDDLE CEREBRAL ARTERY OCCLUSION IN SPONTANEOUSLY HYPERTENSIVE RATS

Liang Zhao, Thaddeus S. Nowak, Jr.

*Department of Neurology, University of Tennessee, Memphis, TN, USA*

**Introduction:** Preconditioning (PC) can be strikingly protective in focal ischemia models. Acute CBF evaluations following test occlusions have largely discounted a role of perfusion changes in PC [1,2]. This issue was reinvestigated by evaluating the distribution and time course of CBF after permanent ischemia in naïve and PC Spontaneously Hypertensive Rats (SHR). **Methods:** Preconditioning was induced by 10 min surgical occlusion of the right middle cerebral and common carotid arteries [3,4] under halothane anesthesia. In sham animals the vessels were exposed but not occluded. Permanent occlusions were done 24 h later using the same approach in sham (n=29), PC (n=37) and naïve rats (n=26), after which CBF was evaluated by quantitative C-14 iodoantipyrine autoradiography at 15 min, 3 h and 24 h. Infarct volume was assessed by hematoxylin/eosin staining of the same sections and corrected for edema. **Results:** The initial volume of flow deficit was identical in naïve and PC animals (Fig. 1). However, PC rats showed a rapid decrease in severely ischemic territory (CBF < 30 ml/100g/min). Ischemic tissue volume at 3 h was maintained at 24 h when corrected for edema (points connected by dotted lines). Ischemic territory at 3 h predicted edema-corrected lesion size at 24 h across the three groups (Fig. 2; points show mean  $\pm$  SD, line indicates identity). CBF images at 24 h are illustrated for representative animals (Fig. 3). **Conclusions:** Protection in this model is completely explained by early recovery of CBF in the margin of the MCA territory, resulting in a smaller volume of tissue below the perfusion threshold for infarction. [1] Chen et al., *J. Cereb. Blood Flow Metab.* 16:566-577 (1996) [2] Dawson et al., *J. Cereb. Blood Flow Metab.* 19:616-623 (1999) [3] Brint et al., *J. Cereb. Blood Flow Metab.* 8:474-485 (1988) [4] Barone et al., *Stroke* 29:1937-1951 (1998) Supported by USPHS grant NS42267



## CASPASE-3 DEPENDENT PROTEOLYTIC CLEAVAGE OF $\epsilon$ PKC AFTER ISCHEMIC PRECONDITIONING IN THE ORGANOTYPIC HIPPOCAMPAL SLICES

Kunjan R. Dave, Ami P. Raval, Miguel A. Perez-Pinzon

<sup>1</sup>*Cerebral Vascular Disease Research Center, Department of Neurology, University of Miami School of Medicine, Miami, FL, USA*

**Introduction:** In an earlier report we established that the epsilon protein kinase c ( $\epsilon$ PKC) played a key role in ischemic preconditioning (IPC) (1). Using an in vivo model of cerebral ischemic tolerance, activation of caspase-3 in preconditioned brain was reported (2). Recent reports also suggest that proteolytic activation of  $\epsilon$ PKC by caspases is associated with its anti-apoptotic functions (3). The goal of the present study was to determine whether caspase-3 is activated after IPC and whether this activation leads to cleavage of  $\epsilon$ PKC with a consequent neuroprotection in the organotypic hippocampal slices. **Methods:** The organotypic hippocampal slices from rat pups (9-11 day old) were used as a model for ischemia and IPC (1, 4). The cleavage of  $\epsilon$ PKC was determined at 24h of reperfusion after IPC by Western blot analysis using  $\epsilon$ PKC specific antibody. The Western blots were quantified by densitometric analysis. The effect of caspase-3 activation on cleavage of  $\epsilon$ PKC was determined by pharmacological blockade of caspase-3 using cell permeable inhibitor DMQD-CHO during and after IPC. Cell death was assessed by the propidium iodide (PI) fluorescence technique (1, 4). **Results:** PI fluorescence at 24 h after lethal OGD was  $35.85 \pm 2.57$  % (n = 3) in the IPC group, as compared to  $54.59 \pm 3.1$  (n = 3) in non-preconditioned slices (p<0.05). Superfusion with 50  $\mu$ M of the caspase-3 inhibitor during IPC and up to 3h of reperfusion completely blocked neuroprotection afforded by IPC (p<0.05) (PI fluorescence values:  $56.50 \pm 5.31$  %, n =7, after combined IPC and caspase-3 inhibitor treatment). These results show that activation of caspase-3 is required for tolerance afforded by IPC. In the next set of experiments, we found that the ratio of uncleaved to cleaved  $\epsilon$ PKC in control slices was  $1.61 \pm 0.21$  (n = 3). In the slices from the IPC group, because of the high levels of cleaved  $\epsilon$ PKC, the ratio of uncleaved to cleaved  $\epsilon$ PKC decreased 61 % (p<0.05) ( $0.63 \pm 0.08$ , n = 3) as compared to the control group ( $1.61 \pm 0.21$ , n = 3). The ratio of uncleaved to cleaved  $\epsilon$ PKC in the IPC group where the caspase-3 inhibitor was administered during IPC and for an additional 3h of reperfusion was higher by 62 % ( $1.02 \pm 0.03$ , n = 2) as compared with the IPC alone group. **Conclusion:** Our study shows that mild activation of caspase-3 following IPC is neuroprotective, perhaps in part due to cleavage of  $\epsilon$ PKC. This is supported by the anti-apoptotic role of cleaved  $\epsilon$ PKC in other models of apoptosis. We suggest that a better understanding of the mechanisms by which cleaved  $\epsilon$ PKC acts as anti-apoptotic molecule after IPC may shed light into the mechanisms of IPC induced tolerance. **Grant support:** Supported by PHS grants NS34773, NS045676 and NS05820. **Reference:** 1) Raval et al. (2003) J Neurosci. 23, 384-91. 2) McLaughlin et al. (2003) Proc Natl Acad Sci USA. 100, 715-20. 3) Basu et al. (2002) J Biol Chem. 277, 41850-6. 4) Xu et al. (2002) Brain Res. 952, 153-8.

**A-TYPE POTASSIUM CURRENTS AND NEUROPROTECTION AFTER ISCHEMIA**Ping Deng<sup>1</sup>, Zhi-Ping Pang<sup>1</sup>, Zhigang Lei<sup>1</sup>, Sojin Shikano<sup>2</sup>, Qiaoxi Xiong<sup>2</sup>, Min Li<sup>2</sup>,**Zao C. Xu<sup>1</sup>**<sup>1</sup>*Department of Anatomy & Cell Biology, Indiana University School of Medicine,  
Indianapolis IN, USA*<sup>2</sup>*Department of Neuroscience, The Johns Hopkins University School of Medicine, Baltimore,  
MD, USA*

**INTRODUCTION:** Medium spiny (MS) neurons in the striatum are highly vulnerable while large aspiny (LA) neurons are resistant to transient cerebral ischemia. The mechanisms of such selective cell death following ischemia remain under active investigation. Excitotoxicity is one of the major causes of cell death and potassium currents regulate the neuronal excitability. To reveal the role of potassium currents in neuronal injury after ischemia, the present study examined the A-type potassium currents (IA) in striatal neurons using *in vivo* and *in vitro* preparations. **METHODS:** *In vivo*: Transient forebrain ischemia was induced using 4-VO method. Brain slices were prepared before ischemia and at different intervals following reperfusion. Whole-cell patch-clamp recording was performed on visually identified striatal neurons under infrared-DIC microscopy. *In vitro*: Primary neuronal culture was prepared from the striata of embryos of 18 d gestation. Neurons were subjected to oxygen/glucose deprivation (OGD) after 10-12 d in culture. Kv 1.4 and Kv 4.2 channels were transfected into the culture using FuGENE 6. **RESULTS:** The amplitude of IA in LA neurons was significantly increased after ischemia whereas the IA in MS neurons remained unchanged. Immunohistochemical studies indicated that LA neurons expressed Kv1.4 and Kv4.2 channels, both of which contribute to IA. However, expression of Kv 1.4 channels in LA neurons were significantly increased after ischemia while the Kv 4.2 channels remained at the same level. To test the hypothesis that the increase of IA might be involved in postischemic neuronal survival, IA was enhanced in striatal neurons by over-expression of Kv1.4 and/or Kv4.2 channels in culture and then underwent 4 hr OGD. The neuronal viability in neurons over-expressed IA was significantly higher than that in control ones after OGD. Application of IA blocker 4-AP increased the cell death after OGD in a dose dependent manner. To reveal the mechanisms underlying the up-regulation of IA, the action of protein kinases, the important modulators of potassium channels, was examined. Activation of protein kinase C (PKC), but not PKA or tyrosine kinase, significantly increased the amplitude of IA in LA neurons after ischemia. PKCa, rather than PKCg or PKCe, was positively identified in LA neurons and was translocated from the cytosol of control neurons to the cell membrane after ischemia. In HEK cells transfected with Kv 1.4 or Kv 4.2 channels, intracellular infusion of PKCa increased the Kv 1.4 currents but not the Kv 4.2 currents. **CONCLUSIONS:** The present study has demonstrated that IA is increased in ischemia-resistant LA neurons after ischemia. Up-regulation of IA increases while the blockade of IA decreases cell viability after OGD. The enhancement of IA in LA neurons after ischemia is through the Kv 1.4 channels by activation of PKCa and is associated with the translocation of PKCa to the cell membrane. These results suggest that the enhancement of IA might have neuronal protective effects against cerebral ischemia.

**ANTI-S100B INCREASES IN VITRO STRETCH-INDUCED NEURONAL INJURY  
AND EXOGENOUS S100B REDUCES INJURY****Earl F. Ellis<sup>1</sup>**, Karen A. Willoughby<sup>1</sup>, Andrea Kleindienst<sup>2</sup><sup>1</sup>*Department of Pharmacology and Toxicology, Virginia Commonwealth University,  
Richmond, VA, USA*<sup>2</sup>*Department of Neurosurgery, University of Goettingen, Goettingen, Germany*

S100B is a calcium binding protein found in brain where it is contained mainly in astrocytes. Previous studies have shown that S100B release is an indicator of injury, while more recent studies also suggest that the post-traumatic release of S100B may act to reduce neuronal injury or promote recovery. The purpose of these experiments was to determine the effects of S100B and S100B antibody on normal and injured neurons in rat cortical neuronal plus glial cultures. Cells were injured by a well-established in vitro model in which cells cultured on a silicone membrane are strain-injured by a 50 msec deformation of the membrane (J. Neurotrauma 12: 325-329, 1995). Injury was assessed by uptake of the nuclear dye propidium iodide (PrI), which is impermeable to normal cells. We have previously shown that after stretch injury astrocytes immediately take up PrI but recover their ability to exclude PrI by 24 hr whereas neurons do not have increased PrI until 24-48 hr post-stretch injury. S100B (10-100 nM) when given at 6 or 24 hr after injury decreased neuronal PrI uptake at 48 hr by one-half, indicating a protective effect. Commercially available S100B antibody, dialyzed to remove its toxic sodium azide preservative, increased PrI uptake in uninjured and injured neurons and prevented the protective effect of exogenous S100B, indicating a tonic release of S100B and an increased release in response to trauma. These studies, along with recent in vivo studies by Kleindienst et al. (J. Neurotrauma 21: 541-547, 2004), suggest that exogenous or endogenous S100B reduces injury and promotes neuronal recovery. The effectiveness of S100B when given at later post-injury time points suggests its relevance to post-injury administration in humans. Supported by NS-27214, HL-57869 and NS-12587.

**ERYTHROPOIETIN REGULATED BY HYPOXIA-INDUCIBLE FACTOR-1 AND RECOMBINANT HUMAN ERYTHROPOIETIN PROTECT CULTURED NEURONS FROM HYPOXIC AND REOXYGENIC INJURY**

**Ruiqin Liu, Asuka Suzuki, Yoshikuni Mizuno, Takao Urabe**

*Department of Neurology, Juntendo University School of Medicine, Tokyo, Japan*

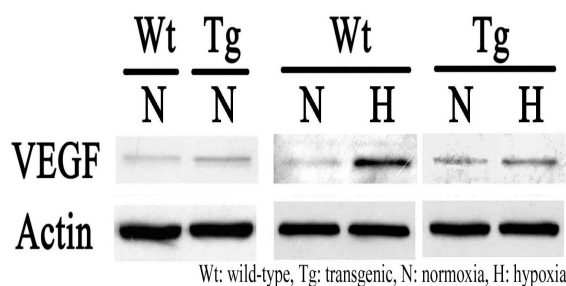
Objective: Recently, Erythropoietin (EPO) has emerged as a potent neuroprotectant against ischemic/hypoxic injury. In this study, we attempt to detect the expression of EPO regulated by hypoxia-inducible factor-1 $\alpha$  (HIF-1 $\alpha$ ) in astrocytes and neurons, and investigate the neuroprotective effect of endogenous EPO and exogenous recombinant human Erythropoietin (rhEPO) against in vitro 'ischemia'-hypoxia by use of primary pure neuronal culture and mixed neuronal/astrocytic culture models. Methods: Primary pure neuronal culture and mixed neuronal/astrocytic culture were obtained from embryos (E 16~17) of wistar rats. On Day 8, cultures were placed into a hypoxic incubator (2% O<sub>2</sub>) for 30min~ 48h. We detected the localization of EPO and EPO receptor (EPOR) in astrocytes or neurons by immunocytochemical staining and double-immunofluorescence staining. The expression of HIF-1 $\alpha$  and EPO between mixed cultures and pure neuronal cultures compared by western blot and reverse transcription-polymerize chain reaction (RT-PCR). After hypoxia, neuronal survival between mixed and pure neuronal culture was assessed by means of staining with the dye presidium iodide (PI) and fluoresce indiacetate (FDA). Recombinant human Erythropoietin (rhEPO) was applied 1~48h before hypoxia, at the start of hypoxia and after onset of re-oxygenation, and the neuronal survival was assessed. Results: Immunoreactive EPO was prominent in astrocytes, especially in the cytoplasm, and also observed in neurons with weaker staining after 3 to 48h hypoxia. EPOR was strongly detected in neurons. Western Blot analysis showed that the EPO band of neuron cultures was weaker than that of mixed neuronal/astrocytic cultures. HIF-1 $\alpha$  mRNA expression was observed after 30 minutes hypoxia preceding EPO expression coincident with protein level. Re-oxygenation completely degraded the expression of HIF-1 $\alpha$  and EPO. Neurons cultured together with astrocytes were significantly rescued by endogenous EPO compared with pure neuronal cultures. Both EPO and EPOR antibody (2.5  $\mu$ g/ml) were able to reduce the endogenous neuroprotection (P< 0.0001). Administration of rhEPO (0.1U/ml) within 6h before hypoxia or after onset of reoxygenation significantly increased neuronal survival compared with hypoxia or hypoxia-reoxygenation alone (p<0.0001). Conclusion: Our findings indicated that HIF-1 $\alpha$  target gene EPO released by astrocytes acts as an essential mediator of neuroprotection, suggested a critical role of EPO in cerebral ischemia and promote the possible therapeutic application and beneficial effect for the treatment of stroke patients. Furthermore, imitation of brain endogenous protective mechanisms may be another novel strategy to future successful approaches to neuroprotection against hypoxic/ischemic injury.

## HYPOXIC INDUCTION OF VASCULAR ENDOTHELIAL GROWTH FACTOR IS SELECTIVELY IMPAIRED IN MICE CARRYING MUTANT SOD1 GENE

Tetsuro Murakami<sup>1</sup>, Tetsuya Nagata, Isao Nagano, Takeshi Hayashi, Mikio Shoji, Koji Abe

*Department of Neurology, Okayama University Medical School, Okayama, Japan*

<Background> Spinal motor neurons are one of the most vulnerable cells to hypoxia/ischemia, and are also selectively damaged in amyotrophic lateral sclerosis (ALS), a fatal neurodegenerative disease. Recently, mice with deletion of the hypoxia-response element (HRE) in the vascular endothelial growth factor (VEGF) promoter gene have been generated. The mice showed late-onset progressive and selective motor neuron degeneration reminiscent of human ALS, and therefore, the vulnerability of motor neurons against hypoxia has been argued as the possible mechanism of the disease. <Methods> Localization and hypoxic induction of VEGF was examined in the spinal cord of transgenic mice carrying a mutation (G93A) in the superoxide dismutase 1 gene, an animal model of ALS. Animals were exposed to hypoxia (7% oxygen) for 2 hours, and sacrificed 6 hours after hypoxia. Immunohistochemical, immunofluorescent, and immunoblotting analyses were performed in transgenic (Tg) mice and wild-type (Wt) littermates (n=6, respectively) under normoxia and hypoxia. <Results> Immunohistochemical and immunofluorescent study demonstrated that VEGF is mainly expressed in motor neurons before and after hypoxia. In immunoblotting, baseline expression of VEGF was higher in Tg mice than in Wt littermates. However, VEGF was hardly induced after hypoxia in Tg mice, whereas Wt mice showed approximately a 9-fold increase. Impaired VEGF induction was obvious in Tg mice at 12 weeks of age, when they were still presymptomatic. In contrast, baseline and hypoxic expression of brain derived neurotrophic factor and glial cell line-derived neurotrophic factor did not differ between Tg and Wt mice. <Conclusion> The present study demonstrated that hypoxic induction of VEGF in Tg mice is selectively impaired from an early stage, suggesting profound involvement in the pathogenesis of motor neuron degeneration in hypoxia, as well as ALS.

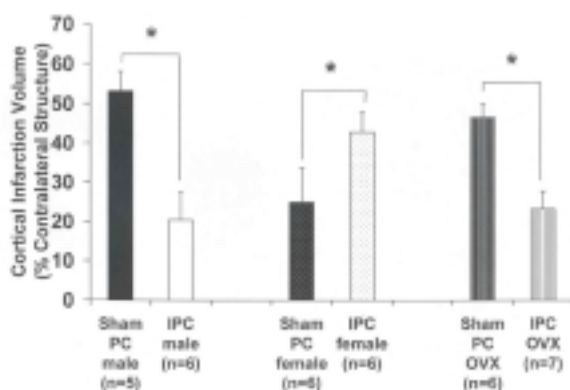


## GENDER DIFFERENCES IN ISOFLURANE PRECONDITIONING AND EXPERIMENTAL STROKE

Hideto Kitano, Patricia D. Hurn, Stephanie J Murphy

*Anesthesiology & Peri-Operative Medicine, Oregon Health & Science University, Portland, OR, USA*

**Introduction:** In male rats (1) and mice (2), pretreatment with isoflurane 24 hours before experimental stroke was shown to be neuroprotective. However, it is unknown if males and females respond differently to anesthetic preconditioning (AP) in the context of cerebral ischemia. There are some reported gender differences in terms of clinical and experimental responses to specific anesthetics but sex differences in anesthetic applications have been understudied. The choice of anesthetic in clinical patients would be important in cases where CNS damage is anticipated peri-operatively, such as in neurosurgery or cardiac bypass surgery. AP may therefore prevent or even delay neurological complications, thereby increasing the therapeutic window for other prospective neuroprotective agents. In this study, we determined if there is a gender difference in isoflurane preconditioning (IPC) of the brain before transient focal cerebral ischemia. **Methods:** Mice were preconditioned for 4 hours with 1% isoflurane (IPC) or no anesthetic (sham PC) in an air tight, temperature-controlled chamber. Animals were then recovered for 24 hours. Each animal subsequently underwent 120 minutes of MCAO by the intraluminal filament technique (3) followed by 22 hours reperfusion. Cortical (CTX), caudate-putamen (CP), and total hemispheric (TTL) infarct volumes were determined by digital image analysis of sequential 2 mm thick coronal slices of brain stained with 2,3,5-triphenyltetrazolium chloride. Laser-Doppler flowmetry (LDF) was used to estimate ischemic reduction of cortical perfusion at initiation of occlusion and restoration of blood flow during reperfusion. **Results:** Rectal temperatures were maintained within normal physiological range and were equivalent among groups. Results of CTX infarct volumes are shown in figure. CP and TTL infarct volumes showed a similar pattern of results between treatment groups. LDF at induction of MCAO and at initiation of reperfusion were equivalent among treatment groups. All data are mean  $\pm$  SEM. \* $p < 0.05$ . **Conclusions:** Isoflurane preconditioning is protective in ischemic male mouse brain but worsened infarct outcome in females. Ovariectomized female mice had comparable neuroprotection from isoflurane preconditioning as the males, suggesting that female sex steroids may alter ischemic outcome in response to isoflurane preconditioning. **References:** [1] Kapinya KJ, Löwl D, Fütterer C, et al.: *Stroke* 33:1889-1898 (2002) [2] Kapinya KJ, Prass K, Dirnagl U: *NeuroReport* 13:1431-1435 (2002) [3] Eliasson MJ, Sampei K, Mandir AS, et al.: *Nat Med* 3:1089-1095 (1997) **Grant Support:** Supported by NIH grant RR00163



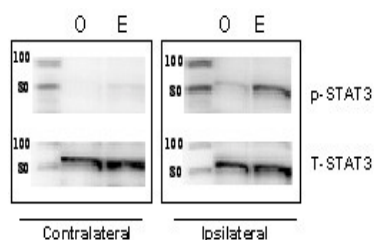
## ESTRADIOL INCREASES SIGNAL TRANSDUCER AND ACTIVATOR OF TRANSCRIPTION (STAT3) PHOSPHORYLATION AND DNA BINDING IN BRAIN NUCLEAR EXTRACT AFTER MCA OCCLUSION

Suzan Dziennis, Jennifer M. Young, Vanessa R. Anderson, Patricia D. Hurn, Nabil J. Alkayed

*Department of Anesthesiology & Peri-Operative Medicine, Oregon Health & Science University, Portland, OR, USA*

**Introduction:** Estradiol is neuroprotective in animal models of cerebral ischemia (1). Although the precise mechanisms are unknown, estrogen's beneficial properties are, in part, linked to rapid activation of signal transduction pathways that lead to the transcription of neuroprotective genes (2). We tested the hypothesis that estradiol's neuroprotective effects are partially mediated via signal transducer and activator of transcription 3 (STAT3). STAT3 resides in the cytoplasm in a latent form, but is rapidly activated by tyrosine-705 phosphorylation in response to extracellular stimuli (3), including estrogen (4). Upon activation, STAT3 translocates to the nucleus where it binds to and upregulates neuroprotective genes, such as bcl-2 (5). **Methods:** Seven days prior to MCAO occlusion, ovariectomized (O) female Wistar rats were implanted subcutaneously with 25 mg 17 $\beta$ -estradiol (E). Rats were subjected to 2-hour MCAO and sacrificed after 3 hours of reperfusion. Laser-Doppler perfusion, body and head temperatures and arterial blood pressure were monitored and kept within normal range. Blood was taken from the heart at the time of euthanasia for measurement of plasma estradiol. The neocortex from the ipsilateral and contralateral hemispheres (between coronal levels 2 and -3 mm from Bregma) was dissected and homogenized to prepare nuclear and cytosolic protein extracts. Equal protein amounts from each fraction were probed with anti-phosphotyrosine(705)-STAT3 (p-STAT3) and anti-total STAT3 (T-STAT3) antibodies. Optical density from phospho-STAT3 was normalized to total STAT3 to calculate the degree of STAT3 phosphorylation. STAT3 promoter binding was assessed by electrophoretic mobility shift assay (EMSA) in nuclear extracts. **Results:** Ischemia strongly induced phospho-STAT3 (5.85  $\pm$  1.96 fold, mean  $\pm$  sem) in the ipsilateral neocortex at 3 hours of reperfusion. Estradiol increased STAT3 phosphorylation in the ischemic side by 2.6  $\pm$  0.92 fold, mean  $\pm$  sem. STAT3 was observed in the nuclear, but not in the cytosolic fractions after MCAO, suggesting that estradiol enhances cytosolic to nuclear translocation of STAT3 after ischemia. EMSA revealed binding to a consensus STAT3 binding element in brain nuclear extracts from estradiol-treated animals. **Conclusion:** Estradiol enhances STAT3 phosphorylation, translocation and DNA binding in brain nuclear extracts after MCAO. Increased STAT3 phosphorylation by estradiol may contribute to its neuroprotective effect by upregulating neuroprotective genes.

**Reference List** (1) Alkayed, N. J., Harukuni, I., Kimes, A. S., London, E. D., Traystman, R. J., and Hurn, P. D. (1998) *Stroke* 29, 159-165 (2) Alkayed, N. J., Goto, S., Sugo, N., Joh, H. D., Klaus, J., Crain, B. J., Bernard, O., Traystman, R. J., and Hurn, P. D. (2001) *J. Neurosci.* 21, 7543-7550 (3) Darnell, J. E., Jr., Kerr, I. M., and Stark, G. R. (1994) *Science* 264, 1415-1421 (4) Bjornstrom, L. and Sjoberg, M. (2002) *Mol. Endocrinol.* 16, 2202-2214 (5) Grad, J. M., Zeng, X. R., and Boise, L. H. (2000) *Curr. Opin. Oncol.* 12, 543-549. Grant Support: Supported by PO1 NS049210





**CHRONIC MILD REDUCTION OF CEREBRAL PERFUSION PRESSURE INDUCES ISCHEMIC TOLERANCE IN FOCAL CEREBRAL ISCHEMIA****Kazuo Kitagawa, Yoshiki Yagita, Tsutomu Sasaki, Emi Omura, Kenichi Todo,****Kohji Matsushita, Masatsugu Hori***Department of Internal Medicine and Therapeutics, Osaka University Graduate School of Medicine, Suita, Japan*

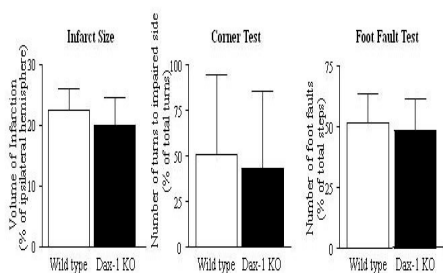
**Background:** Neurons acquire tolerance to ischemic stress when preconditioning ischemia occurs a few days beforehand. Because collateral circulation through leptomeningeal vessels may determine the severity of ischemic injury after occlusion of middle cerebral artery (MCA) in stroke patients, we focused on collateral development after mild reduction of perfusion pressure to find an endogenous response of the vascular system that contributes to development of ischemic tolerance. **Methods:** After attachment of a probe with dental cement to the intact skull 3.5 mm lateral to the bregma, the left common carotid artery (CCA) of C57BL/6 mice was occluded with halothane anesthesia. The left middle cerebral artery (MCA) was subsequently occluded permanently with a microbipolar electrocoagulator just proximal to the point where the olfactory branch came off, on days 0, 1, 4, 14 and 28 (n=8 each). Body temperature was maintained at 37°C during surgery. The change in cortical perfusion during MCA occlusion was recorded. A sham group of mice received only exposure of the CCA and MCA occlusion 14 days later. In apoE-knockout mice, the MCA was occluded 14 days after CCA occlusion or sham CCA surgery. Four days after MCA occlusion, mice were examined for neurological deficits and then their brains were removed, fixed and embedded in paraffin. Tissue sections (5  $\mu$ m) were obtained every 1 mm, beginning at the frontal pole, and were examined after HE staining for measurement of infarct size. **Results:** Unilateral occlusion of the left CCA resulted in 40-70% of baseline microperfusion over the MCA area in most mice. However, in 6 mice, cortical microperfusion was reduced to less than 35% of baseline. Only mice that had 45 to 65% of baseline perfusion after CCA occlusion were used in the subsequent experiments. Cortical perfusion after MCA occlusion was significantly preserved in day 14 (47+16%) and day 28 (46+7%) groups compared with day 0 (28+8%) and sham groups (32+9%). Infarct size and neurologic deficits were also attenuated in day 14 and day 28 groups compared with day 0 and sham groups. In apoE-knockout mice, there was no significant difference in perfusion (36.4+11.8 % compared to 30.2+7.8%,  $P=0.23$ ), neurologic deficits and infarction size (31.5+8.2 mm<sup>3</sup> compared to 37.0+5.3 mm<sup>3</sup>,  $P=0.14$ ) between groups with and without CCA occlusion. **Conclusion:** Our results demonstrated that unilateral CCA occlusion treatment given 14 days before MCA occlusion preserved cortical perfusion and reduced infarct size after MCA occlusion. Chronic mild reduction of perfusion pressure may lead to collateral development and brain protection after focal cerebral ischemia. These responses of collaterals were impaired in apoE-knockout mice.

## BRAIN AROMATASE OVEREXPRESSION DOES NOT REDUCE ISCHAEMIC DAMAGE NOR IMPROVE LONG TERM FUNCTIONAL OUTCOME AFTER EXPERIMENTAL STROKE: A MAGNETIC RESONANCE IMAGING AND BEHAVIOURAL STUDY

Hilary V.O. Carswell<sup>1</sup>, Kirsty Gordon<sup>1</sup>, Tracy Farr<sup>1</sup>, Jim M. Mullin<sup>1</sup>, Lindsay Gallagher<sup>1</sup>, Barrie Condon<sup>2</sup>,  
I. Mhairi Macrae<sup>1</sup>

<sup>1</sup>7T Experimental MRI Facility & Wellcome Surgical Institute, Division of Clinical Neuroscience, University of Glasgow, <sup>2</sup>Dept. of Clinical Physics & Bioengineering, Southern General Hospital, Glasgow, UK

**Introduction:** 17beta-Oestradiol, the female sex hormone, which has neuroprotective properties, is synthesised in the brain by the enzyme aromatase. We have recently reported that aromatase expression is increased after experimental stroke with implications for reducing ischaemic damage and improving behavioural outcome by local synthesis of oestrogens (Carswell et al, 2004). **Aims:** The present study investigates if aromatase overexpression reduces ischaemic brain damage and /or improves long term functional outcome after experimental stroke. **Methods:** Dax-1 (dosage-sensitive sex reversal adrenal hypoplasia congenita region on the X-chromosome, gene-1) knock out (KO) mice are a unique strain that overexpress aromatase. Stroke was induced by permanent middle cerebral artery occlusion (MCAO) in male Dax-1 KO (n=8) and wild-type (n=8) mice. Magnetic Resonance Imaging (MRI) (7 Tesla Bruker Biospec) was used to measure infarct size 48 hours post-MCAO using a RARE T2 weighted sequence (TR/TE 5086/73 msec, 117 micron in plane resolution, 600 micron slice thickness). The infarct areas were delineated and integrated to calculate the volume of infarction using Paravision software. At 8 weeks post-MCAO, animals underwent two long term functional outcome tests (Corner Test and Foot-Fault Test) to assess deficits in Dax-1 KO and wild type mice. These sensorimotor tests were chosen specifically since they are reported to be sensitive enough to pick up and evaluate chronic (e.g. 8 weeks) sensorimotor impairments post-MCAO in mice (Zhang et al, 2002). For the Foot Fault Test, the number of incorrect forepaw placements on a grid (foot fault) on impaired side were counted and presented as a % of total steps. All data are presented as mean±SD. **Results:** Plasma 17beta-oestradiol levels in wild type and Dax-1 KO mice were 8.7± 4.8 and 14.8± 6.3 pg/ml respectively (p=0.037, one tailed unpaired t-test). Infarct volumes were not significantly different between Dax-1 KO and wild type mice and sensorimotor deficits were similar between the two groups for both behavioural tests (Figure). **Conclusion:** The present study provides no evidence for an influence of aromatase overexpression on stroke outcome in Dax-1 KO mice. This is contrary to our hypothesis, and may be due to insufficient additional oestrogen production to exert significant neuroprotection in Dax-1 KO mice or because MCAO induces optimal aromatase overexpression in wild type mice. **References:** Carswell, H.V.O., et al. Brain aromatase (estrogen synthase) expression is increased after experimental stroke. Society for Neuroscience 34th Annual Meeting, Abstract Number 101.4 Zhang L, et al. A test for detecting long-term sensorimotor dysfunction in the mouse after focal cerebral ischemia. J Neurosci Methods. 2002;117(2):207-14 **Acknowledgements:** The authors acknowledge the grant support of Research into Ageing (grant number 230); Dr Larry Jameson Northwestern Memorial Hospital, Chicago, for supplying the Dax-1 KO mice and Dr Eric McKenzie and colleagues University of Caen, France, for their advice and expertise on the murine model of MCAO.





**ERYTHROPOIETIN PREVENTS SPINAL CORD DAMAGE AND AFFECTING ENZYME LEVELS OF BRAIN-DERIVED NEUROTROPHIC FACTOR AFTER TRANSIENT SPINAL CORD ISCHEMIA IN RABBITS**

Hiroaki Kokubo<sup>1</sup>, Masahiro Sakurai<sup>2</sup>, Koji Abe<sup>3</sup>, Yasuto Itoyama<sup>4</sup>, Koichi Tabayashi<sup>1</sup>

<sup>1</sup>*Department of Cardiovascular Surgery Tohoku University Graduate School of Medicine, Sendai, Japan*

<sup>2</sup>*Department of Cardiovascular Surgery National Hospital Organization Sendai Medical Center, Sendai, Japan*

<sup>3</sup>*Department of Neurology, Okayama University Graduate School of Medicine, Okayama, Japan*

<sup>4</sup>*Department of Neurology, Tohoku University Graduate School of Medicine, Sendai, Japan*

Objective: The mechanism of spinal cord injury has been thought to be related to the vulnerability of spinal motor neuron cells against ischemia. We have examined whether recombinant human erythropoietin (rhEPO), which is reported to have potent neuroprotective activity against a variety of potential brain injuries such as ischemia and reperfusion, can protect against ischemic spinal cord damage. Methods: After induction of ischemia, rhEPO(800U/kg) or vehicle was injected intravenously. Cell damage was analyzed by counting the number of motor neurons. To investigate the mechanism by which rhEPO prevents ischemic spinal cord damage, we observed the immunoreactivity of brain-derived neurotrophic factor (BDNF), and its receptor trkB. Results: rhEPO eased the functional deficits and increased the number of motor neurons, following ischemia. BDNF and trkB were induced at 8 hours of reperfusion following a 15-min ischemia in vehicle treated group (Group I), and about 70% of motor neuron cells showed selective cell death after 7 days of reperfusion. On the other hand, large populations of the motor neuron cells survived at 7 days in rhEpo treated group (group E), and BDNF and trkB were induced persistently in motor neurons as compared with group I Conclusion: These results suggest that rhEPO may protect motor neurons from ischemic injury by increasing induction of BDNF and trkB. RhEPO could be a potent candidate for a use as a therapeutic agent in the treatment of ischemic spinal cord injury.

## A SMALL CORTICAL LESION INCREASES THE EXPRESSION OF FEEDBACK INHIBITORS OF PROINFLAMMATORY CYTOKINE-SIGNALING

Hiromi Muramatsu, Katalin Karikó, Frank A Welsh

*Department of Neurosurgery, University of Pennsylvania School of Medicine, Philadelphia, PA, USA*

**Introduction:** Previously, we have shown that tolerance to ischemia is induced by applying hypertonic NaCl to the cerebral cortex (1). Application of hypertonic NaCl causes a small lesion without evoking cortical spreading depression (CSD). However, little is known about the molecular mechanisms by which a cortical lesion induces tolerance in the absence of CSD. Lesions to the central nervous system are known to trigger an inflammatory response, including expression of TNF, which itself has been shown to induce tolerance to ischemia. Inflammation is normally controlled by counter-regulatory pathways, which include the induction of feedback inhibitors of proinflammatory cytokine-signaling. The objective of the present study was to determine whether application of hypertonic NaCl upregulates the expression of mRNAs encoding TNF and its feedback inhibitors, tristetraproline (TTP), suppressors of cytokine signaling 3 (SOCS3), IL-1 receptor-associated kinase-M (IRAK-M), and toll-interacting protein (TOLLIP). **Methods:** A small cortical lesion was made in the left frontal cortex in anesthetized Sprague-Dawley rats by applying 5 M NaCl to the intact dura for 2 hr. After recovery for 0, 2, 4, and 24 hr (n=4 animals per time point), the animals were sacrificed, and the brains were removed for sampling. The brain was sectioned in the coronal plane 5, 10 and 15 mm behind the frontal pole. Tissue samples from the frontal cortex of both hemispheres were extracted for total RNA, and the extracts were analyzed on northern blots for mRNAs encoding TNF, TTP, SOCS3, IRAK-M and TOLLIP. **Results:** TNF and SOCS3 mRNAs were significantly elevated 2, 4, and 24 hr following NaCl application in the frontal cortex of the ipsilateral hemisphere, relative to the contralateral hemisphere. TTP mRNA was significantly elevated in the ipsilateral hemisphere at all times tested. There were no significant differences in IRAK-M and TOLLIP mRNAs between the hemispheres at any time point. **Conclusions:** These results demonstrate that a small cortical lesion increases the levels of mRNAs encoding the proinflammatory cytokine, TNF, and its feedback inhibitors, TTP and SOCS3. TTP is a proline-rich protein that binds to the AU-rich element present in the 3'-untranslated region of mRNAs encoding proinflammatory cytokines, including TNF (2). SOCS3 is one member of a family of proteins that suppresses signal transduction of cytokines, thereby inhibiting inflammation (3). Cerebral ischemia evokes a progressive inflammatory response that is believed to exacerbate ischemic damage (4). Thus, the present results suggest that the expression of feedback inhibitors of cytokine-signaling may contribute to the tolerance to ischemia induced by a small cortical lesion. **References:** [1]. Muramatsu H, Karikó K, Welsh FA; *J Cereb Blood Flow Metab* 24:1167-1171 (2004) [2]. Carballo E, Lai WS, Blackshear PJ; *Science* 281:1001-1005 (1998) [3]. Kubo M, Hanada T, Yoshimura A; *Nat Immunol* 4:1169-1176 (2003) [4]. Barone FC, Arvin B, White RF, et al. ; *Stroke* 28:1233-1244 (1997)

## MITOCHONDRIAL $K^+$ ATP CHANNEL OPENING INITIATE ISCHEMIC PRECONDITIONING IN ORGANOTYPIC HIPPOCAMPAL SLICE CULTURES

Miguel A. Pérez-Pinzón, Ami P. Raval

*Cerebral Vascular Disease Research Center, Department of Neurology and Neuroscience,  
University of Miami School of Medicine, Miami, FL, USA*

Introduction: Ischemic preconditioning (IPC) is an intrinsic adaptive condition that results in tolerance in different organs when they are subjected to mild ischemic insults prior to a 'lethal' ischemic insult. In heart, the mitochondrial ATP dependent potassium (mtK<sup>+</sup>ATP) channel activation has been reported to mediate preconditioning protection. However, in brain role of mtK<sup>+</sup>ATP channel in the IPC induction is still not clearly understood. Additionally, our previous studies demonstrated that IPC induce neuronal survival in CA1 region of hippocampus required epsilon protein kinase C ( $\epsilon$ PKC) activation (1, 2). Thus, the goal of the present study was to define whether mtK<sup>+</sup>ATP channel activation is required during triggering phase of IPC. Further, we hypothesize that  $\epsilon$ PKC mediated neuroprotection require mtK<sup>+</sup>ATP channel activation. Methods: Hippocampal slices were obtained from 9-11 days old Sprague Dawley rats and cultured for 14-15 days before experiments. Slices exposed to oxygen/glucose deprivation (OGD) for 40 min ('test' ischemia) were used as the ischemia group. Slices exposed to OGD for 15 min (or a pharmacological agent), 48 h prior to 'test' ischemia were used as the IPC/pharmacological preconditioned (PPC) groups. Propidium Iodide (PI) fluorescence images were obtained using a SPOT CCD camera and were digitized using SPOT advanced software. Percentage of relative optical intensity was used as an index of cell death. Results are expressed, as mean  $\pm$  SD. Statistical significance was determined with an ANOVA test followed by a Bonferroni's post-hoc test. Results: We confirm our previous findings that IPC induce neuroprotection in CA1 region of hippocampus in organotypic slice cultures. PI fluorescence of 'test' ischemic and IPC groups were  $54.8 \pm 14.8\%$  (n = 12) and  $28.5 \pm 13.0\%$  (n = 8), respectively (p<0.001). To test the hypothesis that mtK<sup>+</sup>ATP channel opening mimic IPC induced neuroprotection, we exposed slices to the mtK<sup>+</sup>ATP channel agonists (diazoxide 50  $\mu$ M/pinacidil 10  $\mu$ M). PI fluorescence of diazoxide and pinacidil treated groups were  $16.8 \pm 7.6\%$  (n = 8) and  $31.9 \pm 5.1\%$  (n = 5), respectively (p < 0.001, compared to ischemia). To further characterize role of mtK<sup>+</sup>ATP channel in IPC and after  $\epsilon$ PKC agonist ( $\psi\epsilon$ RACK peptide 0.02  $\mu$ M) mediated PC, slices were treated with the mtK<sup>+</sup>ATP channel antagonist 5-hydroxydecanoic acid (HD, 100  $\mu$ M). This treatment abolished IPC/ $\epsilon$ PKC mediated neuroprotection. PI fluorescence of HD treated and IPC groups were  $58.13 \pm 15.9\%$  (n =12) and  $29.7 \pm 15.7\%$  (n =8), respectively (p < 0.001). Similarly, PI fluorescence values of  $\epsilon$ PKC agonist and  $\epsilon$ PKC agonist plus HD treated groups were  $33.5 \pm 6.7\%$  (n = 5), and  $54.3 \pm 3.3\%$  (n = 5), respectively. Conclusion: The signal transduction pathway that ensues following IPC/ PPC require opening of mtK<sup>+</sup>ATP channel. It is possible however, that the plasma K<sup>+</sup>ATP may also play a role in the IPC-induced neuroprotection. References: 1. Raval AP, Dave KR, Mochly-Rosen D, Sick TJ, Perez-Pinzon MA. (2003) J Neurosci. 23(2):384-91. 2. Lange-Asschenfeldt C, Raval AP, Dave KR, Mochly-Rosen D, Sick TJ, Perez-Pinzon MA. (2004) J Cereb. Blood Flow Metab. 24(6):636-45. Grant support: Supported by PHS grants NS34773, NS05820, NS045676

### QUANTITATIVE EVALUATION OF THE NEUROPROTECTIVE EFFECTS OF THIOPENTAL SODIUM, PROPOFOL AND HALOTHANE ON BRAIN ISCHEMIA IN GERBILS: USE OF A LOGISTIC REGRESSION CURVE

Motomu Kobayashi, Yoshimasa Takeda, Ken Takata, Hisami Aoe, Kiyoshi Morita

*Department of Anesthesiology and Resuscitology, Okayama University Medical School, Okayama City, Japan*

Although some investigators have shown a comparison of the neuroprotective effects of thiopental sodium and propofol, those comparisons were not quantitative. Therefore, in the present study, the neuroprotective effects of thiopental sodium, propofol, and halothane (for a control) were quantitatively evaluated. With use of a logistic regression curve, P50, which is the ischemic time and the duration of ischemic depolarization necessary for causing 50% neuronal damage in CA1 neurons, was estimated. Methods Sixty-three male gerbils were used. In the thiopental group (n=21), thiopental sodium was continuously infused intravenously at a rate of 2.0 mg kg<sup>-1</sup> min<sup>-1</sup>, which produced a burst suppression pattern of electroencephalography in 25.3±3.4 mins. The infusion was stopped when reperfusion was initiated. In the propofol group (n=21), propofol was continuously infused intravenously at a rate of 2.0 mg kg<sup>-1</sup> min<sup>-1</sup>, which produced a similar pattern of burst suppression in 29.7±11.5 mins. The infusion was continued until 30 mins after the reperfusion because of the shorter half-life of propofol than that of thiopental sodium. In the halothane group (n=21), halothane anesthesia was maintained at 1%. After confirmation of a burst suppression pattern, brain ischemia was initiated by occlusion of bilateral common carotid arteries for a pre-determined duration (3, 5 or 10 minutes, in 7 animals for each duration). During the experimental period, direct current (DC)-potentials were measured in bilateral CA1 regions, in which histological evaluation was performed 5 days later. Brain-surface and rectal temperature were monitored and maintained at 37.0±0.5 C. Results Percentages of neuronal damage following 5 minutes of ischemia in the thiopental, propofol and halothane groups were 3.3±4.7%, 22.7±25.2% and 62.7±25.1%, respectively. The logistic regression curves showed close relationships between percentage of neuronal damage and ischemic time (halothane, r<sup>2</sup>=.71, p<.0001; propofol, r<sup>2</sup>=.86, p<.0001; thiopental, r<sup>2</sup>=.88, p<.0001). With use of these curves, P50 of ischemic time in the halothane, propofol and thiopental groups were estimated to be 5.1 minutes, 6.5 minutes and 8.4 minutes, respectively. Onset time of ischemic depolarization was significantly prolonged in both the thiopental group (2.3±0.3 minutes, p<.0001) and propofol group (2.4±0.4 minutes, p<.0001) groups compared with that in the halothane group (1.8±0.3 minutes). The logistic regression curves also showed close relationships between percentage of neuronal damage and duration of ischemic depolarization (halothane, r<sup>2</sup>=.77, p<.0001; propofol, r<sup>2</sup>=.85, p<.0001; thiopental, r<sup>2</sup>=.86, p<.0001). With use of these curves, P50 of ischemic depolarization in the halothane, propofol and thiopental groups were estimated to be 6.4 minutes, 7.7 minutes and 9.6 minutes, respectively. Conclusions We quantitatively evaluated the neuroprotective effects of thiopental sodium, propofol, and halothane on brain ischemia. P50 of ischemic time was prolonged by 3.3 minutes and 1.4 minutes in the thiopental and propofol groups, respectively, compared with that in the halothane group. Onset time was prolonged by 0.5 minutes and 0.6 minutes in the thiopental and propofol groups, respectively, compared with that in the halothane group. P50 of ischemic depolarization was prolonged by 3.2 minutes and 1.3 minutes in the thiopental and propofol groups, respectively, compared with that in the halothane group.

## IMPROVED REGIONAL CEREBRAL BLOOD FLOW MEDIATES TOLERANCE AFFORDED BY ISCHEMIC PRECONDITIONING

Lisa C. Hoyte<sup>1</sup>, Alastair M. Buchan<sup>1,2</sup>

<sup>1</sup>*Calgary Stroke Program, Hotchkiss Brain Institute, University of Calgary, Calgary, AB, Canada*

<sup>2</sup>*Department of Clinical Geratology, Nuffield Department of Clinical Medicine, Oxford University, Oxford, UK*

Background: Ischemic preconditioning is a phenomenon by which a short duration of cerebral ischemia provides protection from a more severe, injurious ischemia. The exact mechanism for this neuroprotection is unknown, theories include: increased activity of heat shock proteins, decreased caspase activity and cell death, and upregulation of genes important for hibernation and metabolism. Hypothesis: Ischemic preconditioning causes tolerance to injurious cerebral ischemia due to an increase in regional cerebral blood flow (rCBF). Materials and Methods: The effects of preconditioning were evaluated using laser doppler flowmetry and magnetic resonance imaging (MRI). Mice were assigned to one of five groups: 1) preconditioned with injurious ischemia 72 hours later, 2) injurious ischemia alone, 3) preconditioned alone, 4) preconditioned followed by injurious ischemia 2 weeks later or 5) control. These animals were temperature regulated. Mouse surgical model: Mice had radio telemetry probes embedded into the peritoneal cavity one week prior to middle cerebral artery occlusion (MCAo), and at 24 hours prior to MCAo were placed on receivers to monitor temperature. Imaged mice were temperature regulated using a rectal temperature probe. The MCAo had a duration of either 15 minutes (pre-conditioning ischemia), or 45 minutes (injurious ischemia). Local blood flow velocity was measured using laser doppler flowmetry (LDF) throughout ischemia; another cohort of mice were imaged using MRI to observe perfusion deficits during occlusion. Results: Mice were euthanized at 24 hours post-ischemia and the brain sectioned and affixed to slides. These sections were stained with hematoxylin and eosin and infarct volume analysis conducted. The blood flows were evaluated from LDF and perfusion/diffusion mismatch was calculated from the MRI data to quantify rCBF. Blood flow velocity was less than 20% in naïve mice, whereas induction of injurious ischemia in preconditioned mice had observed flows 35-40% of baseline. As well, there was a greater trace variability in the form of frequent spikes of low flow velocity in preconditioned mice as compared to naïve mice. Infarcts were significantly smaller in preconditioned mice; naïve mice had 16.75±3.6% of the brain infarcted, while preconditioned mice had 1.25±2.5% of the brain infarcted. The final infarct size was correlated to the rCBF calculated from the flow velocities of LDF. Flow drops of greater than 30% of baseline were necessary to cause a large infarction. Preconditioned mice consistently had flows of greater than 30% of baseline. Evaluation of the rCBF using 9.4T MRI is currently underway. The mice will be imaged using T1, T2, arterial spin labelling (for perfusion) and apparent diffusion coefficient (ADC). The perfusion deficit will be observed during the injurious ischemia occlusion in both preconditioned and naïve mice. A perfusion/diffusion mismatch will be calculated to evaluate the difference in rCBF between preconditioned and naïve mice. Conclusion: Mice that have been preconditioned showed smaller infarcts following injurious ischemia as compared to naïve mice, and preconditioned mice had better rCBF during injurious ischemia. A correlation between rCBF and infarct size was observed; preconditioned mice had blood flows of greater than 30% during injurious ischemia.

**ROLE OF P450 AROMATASE IN SEX-SPECIFIC ASTROCYTE CELL DEATH****Mingyue Liu<sup>1</sup>**, Patrica D. Hurn<sup>1</sup>, Charles E. Roselli<sup>2</sup>, Nabil J. Alkayed<sup>1</sup><sup>1</sup>*Department of Anesthesiology & Peri-Operative Medicine, Oregon Health & Science University, Portland, OR, USA*<sup>2</sup>*Department of Physiology and Pharmacology, Oregon Health & Science University, Portland, OR, USA*

Introduction: Female animals are less susceptible to ischemic brain injury than males (1). However, the sex difference in ischemic brain injury is abolished by ovariectomy and restored by 17 $\beta$ -estradiol, suggesting that protection is mediated in part via ovarian estrogen. Estradiol is also produced locally in brain via the P450 aromatase, and aromatase gene deletion exacerbates brain injury in female mice (2). Moreover, P450 aromatase is induced in brain after ischemia specifically in cortical astrocytes (3). However, it is not clear if P450 aromatase is differentially expressed in male vs. female cortical astrocytes, and if this contributes to the observed sex difference in response to ischemia. We tested the hypothesis that female astrocytes are less susceptible to ischemic injury than male astrocytes, in part due to higher aromatase expression in female vs. male astrocytes. Methods: Primary cultured cortical astrocytes were prepared from 1-3-day old male and female rat pups separately and grown to confluency in estrogen-free medium. Confluent monolayers (10-14 days in vitro) were incubated under 1% oxygen in glucose free medium for 6 hours (oxygen-glucose deprivation, OGD), and then returned to normoxia and glucose-containing medium for 24 hours. Cell death was assayed by propidium iodide (PI) staining, and surviving cells were identified by calcein-AM. Aromatase activity was measured in male and female astrocytes using a radiometric technique that quantifies the incorporation of tritium from [1 $\beta$ -<sup>3</sup>H]androstenedione into <sup>3</sup>H-labeled water. To determine the role of aromatase in astrocyte cell death, male and female cultures were treated with aromatase inhibitor Arimidex (100nM) and aromatase product 17 $\beta$ -estradiol (10 nM). Results: Female cortical astrocytes sustained significantly less cell death after 6-hour OGD compared to male astrocytes (19 $\pm$ 4%, n=13 compared to 41 $\pm$ 5%, n=7, respectively, p<0.05). Estradiol treatment reduced cell death in both male (from 41 $\pm$ 5% to 18 $\pm$ 8%, n=7, p<0.05) and female astrocytes (from 19 $\pm$ 4% to 10 $\pm$ 3%, n=6, p<0.05). Transfer of culture medium from male to female cells had no effect on the magnitude of cell death. However, media transfer from female to male cells significantly reduced cell death from 41 $\pm$ 5% (n=7) to 4 $\pm$ 1% (n=3). Arimidex abolished the difference in OGD-induced cell death between male and female astrocytes (40 $\pm$ 2%, n=10 in female astrocytes compared to 42 $\pm$ 1%, n=10 in male cells, p>0.05). Aromatase activity was higher in female (25 $\pm$ 5 fmoles <sup>3</sup>H<sub>2</sub>O/mg/hr, n=11) compared to male astrocytes (13 $\pm$ 3 fmoles <sup>3</sup>H<sub>2</sub>O/mg/hr, n=15, p<0.05). Conclusions: We conclude that astrocytes isolated from neonatal male vs. female cortex exhibit marked differences in response to oxygen-glucose deprivation, likely due to higher aromatase expression and estradiol formation in female cells. References: 1. Alkayed NJ, Harukuni I, Kimes AS, London ED, Traystman RJ, Hurn PD; Stroke. 1998;29:159-165. 2. McCullough LD, Blizzard K, Simpson ER, Oz OK, Hurn PD; J Neurosci. 2003; 23: 8701-8705. 3. Azcoitia I, Sierra A, Veiga S, Garcia-Segura LM. Ann N Y Acad Sci. 2003 Dec;1007:298-305.

**ISCHEMIC PRECONDITIONING PROTECTS THE HIPPOCAMPAL CA1 NEURONS BY INHIBITING SYNAPTIC ACTIVITY IN RAT****Thomas J. Sick, Ami P. Raval, Isabel Saul, Kunjan R. Dave, Raul Busto,****Miguel A. Pérez-Pinzón***Cerebral Vascular Disease Research Center, Department of Neurology and Neuroscience,  
University of Miami School of Medicine, Miami, FL, USA*

**Introduction:** Neurological disorders like global cerebral ischemia induce excitotoxicity, overactivation of NMDA receptors and high calcium influx leading to impaired synaptic function. Further, synaptic dysfunction is also accompanied subsequently by selective and delayed degeneration of pyramidal neurons in CA1 region of hippocampus. A previous report from our lab has shown that the ischemic preconditioning (IPC) improves neuronal survival in the CA1 region of hippocampus (1). Ischemic preconditioning (IPC) is an endogenous condition in which sublethal ischemic episodes render neurons resistant against subsequent lethal ischemic insults. The goal of present study was to determine whether IPC-induced neuroprotection also protected against synaptic dysfunction. **Methods:** In male Wistar (275 ± 10 g) rats, IPC was produced by bilateral carotid occlusions and systemic hypotension (50 mm Hg) for 2 minutes. 48 h following IPC, hippocampal slices of 400-µm thickness were sectioned, oxygenated with 95% O<sub>2</sub>-5% CO<sub>2</sub> in artificial cerebrospinal fluid, stored at 28 C for 1 h and transferred to the recording chamber. General population measurements of excitatory post-synaptic field potentials (fEPSP) were recorded from stratum radiatum of the CA1 hippocampal subfield, after electrical stimulation to the Schaffer collaterals (0.3 ms constant current pulses). After stable fEPSPs were recorded, input-output curves relating stimulus current intensity to fEPSP slope and amplitude were generated. To induce LTP tetanic stimulation (100 Hz) was applied for 1 s and test stimulation (1/30 sec) resumed for a period of 1 hr. To determine paired pulse facilitation/depression, paired stimulations at interval of 50 or 200 ms were applied through a constant-current stimulator with intensity sufficient to elicit 30% from maximum field potential. The initial negative-going slope of each fEPSP was measured as an index of synaptic strength and was expressed in mV/ms. **Results:** Our results demonstrated inhibition of LTP induction following IPC. In slices harvested from control animals, tetanic stimulation of 100 Hz to the Schaffer collaterals potentiated the fEPSP amplitude from pre-tetanus values of 4.39 ± 0.54 mV/msec to 6.73 ± 0.64 (n = 4) at 60 min post-tetanus (p<0.05). In contrast, fEPSP amplitudes of pre-tetanus and post-tetanus were 3.49 ± 0.41 mV/msec and 4.62 ± 0.63 mV/msec, respectively, in IPC group. To further understand the influence of IPC on short-term synaptic plasticity we measured paired-pulse modulation. Impaired pre-synaptic release following IPC was evident from significant inhibition in paired-pulse facilitation in hippocampal slices harvested 48 h after IPC when compared to controls. **Conclusion:** The present study clearly demonstrates inhibition of synaptic activity following IPC, which might be a possible mechanism for improved neuronal survival following lethal ischemic insult. Further, studies investigating the role of specific receptors or other cellular components will be essential to understand IPC mediated neuroprotection of synaptic function. **References:** [1] Dave KR, Saul I, Busto R, Ginsberg MD, Sick TJ, Perez-Pinzon MA. (2001) *J.Cereb.Blood.Flow Metab.*, 21(2):1401-10. **Grant support:** Supported by PHS grants NS34773, NS045676 and NS05820.

## ANALOGOUS NEUROPROTECTION INDUCED BY RESVERATROL AND ISCHEMIC PRECONDITIONING IN CA1 REGION OF HIPPOCAMPUS AFTER ISCHEMIA

Ami P. Raval, Kunjan R. Dave, Miguel A. Pérez-Pinzón

*Cerebral Vascular Disease Research Center, Department of Neurology and Neuroscience,  
University of Miami School of Medicine, Miami, FL, USA*

**Introduction:** Resveratrol, trans-3,5,4'-trihydroxystibene, is a naturally occurring phytoalexin produced by variety of plants in response to stress. Resveratrol is proven to have cardioprotective, anti-cancer, anti-aging and neuroprotective effects. Recent studies demonstrated either resveratrol treatment or caloric restriction in yeast activate Sir2 (Silent information regulator 2) [1]. Yeast Sir2 has homology to mammalian SIRT1- located in the nucleus, requires co-factor NAD and determines cell fate by deacetylating transcription factor-p53. Employing the organotypic hippocampal slice culture present study was carried out to investigate: (1) the efficacy of resveratrol pre-treatment (RT) for neuroprotection; and (2) similarities between the mechanisms of induction of neuroprotection by ischemic preconditioning (IPC) and RT. **Methods:** Hippocampal slices were obtained from 9-11 days old Sprague Dawley rats and cultured for 14-15 days. Slices were exposed to IPC (15 min of oxygen glucose deprivation (OGD)) or 1 h of RT (75,200  $\mu$ M) followed by 'test' ischemia (40 min of OGD) 48 h later. To characterize role of SIRT1, slices were exposed to sirtinol (10, 50, and 100  $\mu$ M) for 48 h of reperfusion after IPC/RT. Parameters like quantification of neuronal death in CA1 region of hippocampus and SIRT1 estimation were carried out. For SIRT1 assay slices were collected following IPC/RT/vehicle treatment-sham at 30 min / 48 h intervals. Propidium iodide (PI) fluorescence images were obtained using a SPOT CCD camera and were digitized using SPOT advanced software. Percentage of relative optical intensity was used as an index of cell death. Results are expressed, as mean  $\pm$  SD. Statistical significance was determined with an ANOVA and a Bonferroni's post-hoc test. **Results:** The RT (75  $\mu$ M) protected the CA1 neurons against subsequent lethal OGD ( $p < 0.001$ ) and mimics IPC. Higher dosage RT could not mimic IPC. Blocked of SIRT1 activation by sirtinol after IPC /RT abolished neuroprotection. PI fluorescence of RT (75  $\mu$ M), sirtinol treated (10  $\mu$ M), IPC and ischemic groups were  $38.04 \pm 8.81$  ( $n=7$ ),  $87.13 \pm 3.82$  ( $n=7$ ),  $34.13 \pm 19.25$  ( $n=20$ ) and  $63.5 \pm 8.96$  ( $n=5$ ), respectively. A proposed mechanism by which resveratrol protects cell survival is via the SIRT1. Thus, we measured SIRT1 activity in slices. The RT was able to stimulate SIRT1 activity by about 85 % ( $n=4$ ,  $P < 0.05$ ) at 30 min after treatment when compared with the sham ( $n=7$ ). However, RT ( $n=3$ ) induced activation in SIRT1 activity was abolished at 48 h. In contrast to RT, SIRT1 activity did not change in the IPC group at 30 min of reperfusion ( $n=4$ ) as compared to the sham. SIRT1 activity increased by 81 % ( $n=4$ ,  $p < 0.05$ ), as compared to sham, when measured 48 h after IPC. **Conclusion:** Resveratrol pre-treatment induce neuroprotection in CA1 hippocampal neurons to subsequent ischemia. Analogues neuroprotection induced by IPC/RT occur via activating novel SIRT1 pathway. IPC/RT and calorie restriction induced increase in life expectancy might share common pathway. **References:** [1] Howitz et al. Nature. 2003;425(6954):191 Grant support: PHS grants NS34773, NS05820, NS045676

## EFFECT OF $\epsilon$ PKC TRANSLOCATION ON RESPIRATION IN SYNAPTOSOMAL MITOCHONDRIA AFTER ISCHEMIC PRECONDITIONING

Gabriel Santamarina, Edilberto Alvarez, Kunjan R. Dave, Isabel Saul, Raul Busto, Miguel A. Perez-Pinzon

*Cerebral Vascular Disease Research Center, Department of Neurology, University of Miami School of Medicine, Miami, FL, USA*

Introduction: Recently we showed that protein kinase c epsilon ( $\epsilon$ PKC) played a key role in the signaling pathway of ischemic preconditioning (IPC) (1). In the same study we demonstrated that  $\epsilon$ PKC is translocated from cytosolic to the particulate compartment following IPC (1). However, the exact subcellular localization of the translocated  $\epsilon$ PKC after IPC has not been defined. The goals of the present study were to define the subcellular localization of translocated  $\epsilon$ PKC at different reperfusion periods after IPC and to define whether this translocation is accompanied by a physiological response. Since we showed that IPC protected brain against mitochondrial dysfunction (2), and other groups showed that activated  $\epsilon$ PKC exerts its anti-apoptotic effect by acting on mitochondria (3), we concentrated our studies on brain mitochondria after IPC. Method: IPC was produced by bilateral carotid occlusions and systemic hypotension (50mmHg) for 2min in the rat (2). The hippocampus was dissected out at different reperfusion times and subjected to the subcellular fractionation to separate synaptosomes, non-synaptic mitochondria, and cytosol. The level of  $\epsilon$ PKC was determined by Western blotting followed by densitometric analysis. The effect of  $\epsilon$ PKC activation on respiration of synaptosomal mitochondria was determined polarographically using  $\epsilon$ PKC specific peptide activator ( $\psi\epsilon$ RACK) (1,2). For respiration studies synaptosomes were permeabilized with 0.007 % digitonin. Results: We confirmed our previous findings that the amount of  $\epsilon$ PKC in soluble fraction of hippocampus was lower by 54% (n=3;p<0.05) and 57% (n=3;p<0.05) at 0.5h and 3h of reperfusion after IPC, respectively when compared with the corresponding sham group. Concomitantly, we found increases in levels of  $\epsilon$ PKC in non-synaptic mitochondrial fraction by 40% (n=3) only at 0.5h of reperfusion after IPC when compared with the sham group (n=2). Synaptosomal levels of  $\epsilon$ PKC increased by 32% (n=3), 76% (n=3), and 91% (n=3) at 0.5, 3, and 24h of reperfusion after IPC, respectively when compared with the corresponding sham group (0.5h,n=3; 1h,n=2; 3h,n=3). Since we found higher levels of  $\epsilon$ PKC in the synaptosomal fraction after IPC, in the next study we determined the effect of  $\epsilon$ PKC activation on mitochondrial functions in synaptosomes. The rate of oxygen consumption was higher by 39% (p<0.05) in  $\psi\epsilon$ RACK treated synaptosomes (n=8) compared to carrier peptide (Tat) treated synaptosomes (n=8), when succinate+glycerol-3-phosphate were used as the substrates. Similarly the rate of oxygen consumption was higher by 25% (p<0.05) in  $\psi\epsilon$ RACK treated synaptosomes (n=8) as compared to Tat treated synaptosomes (n=8), when ascorbate+TMPD were used as substrates. Conclusion: Increase in the level of synaptosomal  $\epsilon$ PKC after IPC and the effect of its activation on synaptosomal mitochondria suggest that higher levels of this anti-apoptotic PKC in synaptosomes may protect synaptosomal mitochondria from the excitotoxicity that results from cerebral ischemia. This suggests that a key mechanism by which  $\epsilon$ PKC is neuroprotective is by translocating to mitochondria. Grant support: Supported by PHS grants NS34773, NS045676 and NS05820. Reference: 1) Raval et al. (2003) J Neurosci. 23, 384-91. 2) Dave et al. (2001) J Cereb Blood Flow Metab. 21, 1401-10. 3) Baines et al. (2002) Circ Res. 90, 390-7.

## POSSIBLE ROLE OF CEREBELLAR FASTIGIAL NUCLEUS IN PRECONDITIONED NEUROPROTECTION

Shadon Rollins, Betty Chen, **Eugene Golanov**

*Department of Neurosurgery, University of Mississippi Medical Center, Jackson, MS, USA*

**Introduction:** In vivo or in vitro preexposure of brain cells to the sublethal stimuli increases their tolerance to the subsequent lethal insult suggesting existence of the endogenous neuroprotective mechanisms [1]. Exploration of the phenomenon of preconditioning also revealed the existence of indirect neuroprotection: increased tolerance to damaging insult of brain cells not directly affected by sublethal preconditioning stimulus [2]. Findings suggest the existence of system mechanisms of neuroprotection which activate in response to noxious stimuli and render brain cells tolerant to damaging insult. We demonstrated that tolerance to the damaging stimuli can be increased by stimulation of specific brain areas such as cerebellar fastigial nucleus (FN), subthalamic vasodilator area (SVA), or periaqueductal grey (PAG) [3]. This phenomenon was termed neurogenic neuroprotection. Cellular mechanisms, such as opening of ATP-sensitive potassium channels; increased mitochondrial tolerance to depolarization and apoptogenic stimuli, seem to be common for neurogenic neuroprotection and preconditioned neuroprotection [3]. These facts raise the possibility that FN participates in the mechanisms of ischemic preconditioning. We tested this hypothesis by analyzing the efficiency of global ischemic preconditioning in rats in which FN neurons were lesioned by excitotoxin. **Methods:** In anesthetized artificially ventilated Sprague Dawley rats (220-250g) global ischemia (GI) was triggered by four-vessel occlusion (5 min for preconditioning and 20 minutes for damaging insult). Blood gases and body temperature were maintained at normal levels. Arterial pressure, CBF and EEG were monitored. Seven days after the insult brains were histologically processed for quantitative evaluation of hippocampal CA1 neurons loss. FN or midline thalamic (control) neurons were lesioned three days before GI by microinjection of ibotenic acid with subsequent histological verification. **Results:** GI for 20 min decreased number of hippocampal neurons by  $34 \pm 1.2\%$  ( $n=6$ ,  $p<0.05$ ). Ischemic preconditioning (5 min GI) three days before the insult completely reversed GI-induced cell loss. Excitotoxic lesion of FN neurons three days before the preconditioning blocked salvaging effect of the latter: cell loss of  $36 \pm 0.13\%$  ( $n=5$ ,  $p<0.01$  compared to excitotoxic lesion of midline thalamus, which did not affect the salvaging effect of ischemic preconditioning). Lesion of FN neurons also aggravated cell loss induced by 20 min GI alone: cell loss of 59% ( $n=5$ ,  $p<0.01$ ). **Conclusions:** Neuroprotective effect of ischemic preconditioning can be reversed by lesion of FN neurons. Moreover, lesions of FN neurons aggravate hippocampal cells damage by global ischemia alone. Integrity of neurons of the cerebellar fastigial nucleus is necessary for the full expression of the neuroprotective effect of ischemic preconditioning. Findings suggest that FN may play physiological role in the mechanisms of ischemic preconditioning. FN may be a part of the intrinsic integrative neuroprotective mechanisms in the brain, which through activation of the cellular defensive mechanisms play an important role in the neuroprotection in vivo. These mechanisms may be involved in the indirect cross-neuroprotection phenomenon. [1]. Dirnagl, U., Simon, R. P., Hallenbeck, J. M. *Trends Neurosci.* 26, 248-254. 2003. [2]. Belayev, L., Ginsberg, M. D., Alonso, O.F. et al. *Neuroreport* 8, 55-59. 1996. [3]. Golanov, E. V., Zhou, P. *Cell. Mol. Neurobiol.* 23, 651-663. 2003.

## ISCHEMIC PRECONDITIONING PROMOTES NEUROPROTECTION VIA CYCLOOXYGENASE-2 INDUCTION IN VITRO

Eun Joo Kim, Ami P. Raval, Miguel A. Perez-Pinzon

*Cerebral Vascular Disease Research Center, Department of Neurology and Neuroscience,  
University of Miami, School of Medicine, Miami, FL, USA*

**Introduction:** Ischemic preconditioning (IPC) is a well established endogenous protective mechanism in which a brief, sublethal ischemic stimulus can reduce cell injury caused by subsequent lethal ischemic injury. Although numerous signaling pathways appear to be implicated for IPC in the brain, the effective protective mediators have not been fully characterized. Some studies demonstrated that upregulation of cyclooxygenase-2 (COX-2), prostaglandin synthase, is associated with IPC and that COX-2 derived prostaglandins (PGs) plays a role in the cardioprotective effects (1). It is also known that prostaglandins are neuroprotective in cerebral ischemia (2). However, the roles of COX-2 and COX-2 derived PGs during ischemic tolerance in brain remains undefined. In this study, we hypothesize that COX-2 play a key role in the protective mechanisms that ensue after IPC. **Methods and Results:** To determine the roles of COX-2 during the late phase of IPC, we used two different in vitro models: organotypic hippocampal slice cultures (OHSC) and mixed cortical neuronal cultures (MCN). OHSC and MCN are prepared from neonatal rat (9-11 days old) and rat embryo (18-19 days old), respectively. We examined whether COX-2 expression is induced after IPC in MCN. First, we determined that 1hr of IPC followed by 48 hr of reperfusion prior to 2 hr of a lethal ischemic insult (oxygen glucose deprivation- OGD) promoted significant neuroprotection in MCN (n=24, p<0.01). Next, we determined whether COX-2 was induced after IPC. MCN were preconditioned by 1 hr of OGD and then, cells were isolated at 8 hr, 15 hr and 24 hr of reperfusion. We found that COX-2 was induced at 15 hr and decreased at 24 hr following IPC. Previously, we have shown that a sublethal ischemic insult of 15 min, followed by 48 hr of reperfusion prior to 40 min of lethal ischemic insult induced neuroprotection in the CA1 region of hippocampus in OHSC (3). Based on this study, we administered NS 398 (COX-2 selective inhibitor, 10  $\mu$ M and 20  $\mu$ M) to OHSC for 48 hr of reperfusion after IPC. We found that inhibition of COX-2 activity (NS 398 20  $\mu$ M) following IPC abolished the IPC mediated neuroprotection in CA1 region of hippocampus (n=8, p<0.05). **Conclusions:** These results suggest that transient induction of COX-2 expression after IPC might activate the signal transduction pathway that leads to neuronal survival following subsequent lethal ischemic injury. (1) Shinmura K. et al., 2000. Proc. Natl. Acad. Sci. U.S.A. 97: 10197-10202 (2) McCullough L. et al., 2004. J. Neurosci. 24(1); 257-268. (3) Raval A. et al., 2003. J. Neurosci. 15; 384-391. Grant support: Supported by PHS grants NS34773, NS045676 and NS05820.

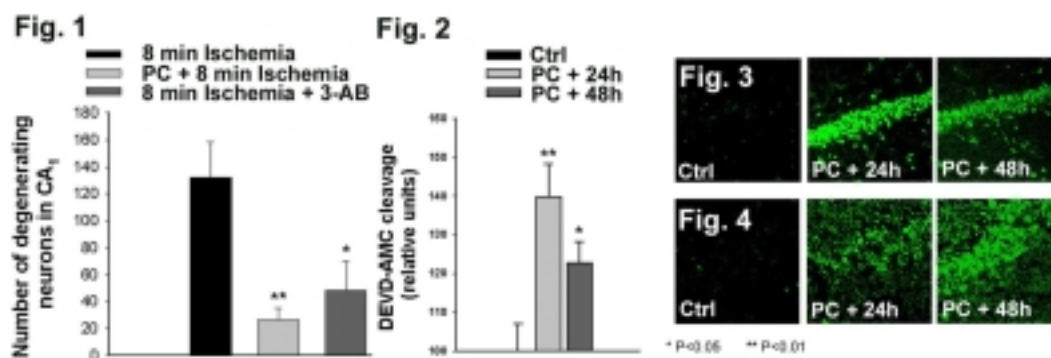
## IN VIVO ISCHEMIC PRECONDITIONING BY CASPASE-3 CLEAVAGE OF POLY(ADP-RIBOSE) POLYMERASE-1

Philippe E. Garnier<sup>1</sup>, San Won Suh<sup>2</sup>, Weihai Ying<sup>2</sup>, Raymond A. Swanson<sup>2</sup>

<sup>1</sup>Laboratoire de Pharmacodynamie et de Physiologie Pharmaceutique, Faculté de Pharmacie, Dijon, France

<sup>2</sup>Neurology Service, UCSF/VAMC, San Francisco, CA, USA

**Introduction:** Ischemic preconditioning has been correlated with numerous biochemical changes, but the actual effector mechanisms by which neurons gain resistance to ischemia remain uncertain. Emerging evidence now suggests that caspase-3 activation can occur in processes other than apoptotic cell death (1). Consistently, we recently showed using an in vitro model of preconditioning that PARP-1 cleavage by caspase-3 was in part responsible for the acquisition of neuronal ischemic tolerance (2). Here, we explored the possibility that such a mechanism could occur in an in vivo model of ischemic preconditioning in gerbils. **Methods:** Global ischemia was induced by a 8-min bilateral carotid artery occlusion. Ischemic preconditioning was performed by a 2-min artery occlusion 48h prior to the global ischemic episode. Neuronal death was quantified in the hippocampal CA1 subfield by Haematoxylin / Eosin staining 7 days after the global ischemia. PARP-1 inhibition was performed by i.p. injection of 3-aminobenzamide (30 mg/kg). Expression of the PARP-1 89 kDa cleavage product and the cleaved caspase-3 17 kDa active fragment were assessed by immunocytochemistry using a confocal microscope 24h and 48h after ischemic preconditioning. Caspase-3 activity was measured using the fluorogenic peptide DEVD-AMC. **Results:** Ischemic preconditioning affords a robust protection of CA1 neurons against a subsequent severe ischemic challenge (Fig 1). Because of the importance of PARP-1 activation in ischemic neuronal death, we tested the effect of the PARP-1 inhibitor 3-AB against the lethal ischemic episode. Neuronal death after global ischemia was reduced by i.p. injection of 3-AB (Fig 1). Since PARP-1 can be irreversibly inactivated by caspase-3 cleavage, we examined whether this process occurs in preconditioned animals. Ischemic preconditioning caused a significant increase in caspase-3 activity (Fig 2) and in the cleaved caspase-3 active fragment (Fig 3). This mechanism was associated with a significant expression of the PARP-1 89 kDa fragment (Fig 4) **Conclusion:** These findings suggest that caspase-3 inactivation of PARP-1 could be also an important effector mechanism in the acquisition of ischemic tolerance in vivo. The causative role for the observed PARP-1 cleavage in ischemic neuroprotection is currently being evaluated by blocking this cleavage with a caspase-3 inhibitor.



**MITOCHONDRIAL MECHANISM OF NEUROPROTECTION BY CART****Peizhong Mao, Rachel Jacks, Ardi Ardeshiri, Patricia D. Hurn, Nabil J. Alkayed***Department of Anesthesiology and POM, Oregon Health & Science University School of Medicine, Portland, OR, USA*

**BACKGROUND:** We previously demonstrated that cocaine and amphetamine regulated transcript (CART) reduces ischemic cell death induced in primary cultured cortical neurons by oxygen-glucose deprivation (OGD). However, the mechanism of protection by CART is unclear, in part due to lack of knowledge regarding its binding site or receptor. CART is a neuropeptide expressed in murine and human brain which has been implicated in a variety of brain functions, including energy metabolism, appetite control, drug addiction and neural responses to stress. **METHODS:** To identify CART interacting partners, we used a yeast two-hybrid system with CART's minimally functional carboxy-terminal region (CART 62-102) to screen a mouse brain cDNA library. We screened over 0.5 million yeast clones and selected clones positive for His3 and LacZ phenotypes. DNA sequence analysis of one positive clone revealed that the putative CART interacting protein was mouse succinate dehydrogenase (SDH), a mitochondrial enzyme that plays a crucial role in oxidative metabolism, energy production and electron transport. To determine if CART's binding to SDH alters its function and Complex II (CII) activity, we tested the effect of physiological concentrations of CART peptide (0.2-1 nM) on SDH and CII activities in mitochondrial extracts from primary cultured cortical neurons under baseline conditions and after OGD. SDH and CII activities were estimated by the reduction of 2,6-dichloroindiphenol (DCIP) and monitored spectrophotometrically after addition of SDH and CII substrates succinate and Coenzyme Q. **RESULTS:** CART increased SDH and CII activities by at least 2-fold in mitochondrial extracts from primary cultured cortical neurons (from  $6.0 \pm 1.6$  to  $14 \pm 2.2$  and from  $8.0 \pm 0.4$  to  $16.0 \pm 0.6$   $\mu\text{M}$  reduced DCIP /mg protein at 0.2 nM CART, respectively, mean  $\pm$  SE, n=3 each values). Twenty-four hours after OGD, SDH and CII activities were severely impaired ( $5.2 \pm 1.0$  and  $6.0 \pm 0.7$ , respectively, compared to  $14.5 \pm 1.1$  and  $17.5 \pm 1.0$   $\mu\text{M}$  reduced DCIP /mg protein in control cells, n=3). However, pretreatment with CART (0.2 nM 30 min before OGD) prevented the decline in SDH and Complex II activity after OGD in primary cultured cortical neurons ( $15.3 \pm 1.3$  and  $19.5 \pm 0.7$   $\mu\text{M}$  reduced DCIP /mg protein, respectively, n=3). **CONCLUSION:** We conclude that CART binds to and activates SDH, and that SDH activation by CART prevents the decline in mitochondrial function after ischemic injury and contributes to CART's neuroprotective action.

## UNIQUE PROPERTIES OF ISCHEMIC TOLERANCE FOLLOWING INTERMITTENT HYPOXIA

W. David Lust<sup>1</sup>, Jorge L. Gamboa<sup>1</sup>, Jose Valerio<sup>1</sup>, Michael Buczek<sup>1</sup>, Svetlana Pundik<sup>2</sup>,  
Warren R. Selman<sup>1</sup>

<sup>1</sup>Neurological Surgery, Case Western Reserve University, Cleveland, OH, USA

<sup>2</sup>Neurology, Case Western Reserve University, Cleveland, OH, USA

Introduction: We have previously shown that intermittent hypoxic (IH) preconditioning reduces infarct volume following focal ischemia concomitant with increases the EPO and VEGF expression. Here we characterized the consequences of IH, the optimum duration between IH and neuroprotection and the time threshold for conferring hypoxic preconditioning. Methods: Wistar rats were exposed to 2, 4 or 12 cycles of 10% hypoxia for 20 min plus normoxia for 40 min. Neuroprotection was assessed at 0, 1, or 3 days after the last IH exposure. The middle cerebral artery (MCA) was occluded by the monofilament technique for 2 h, rats sacrificed at 48 h of reperfusion and the infarct volume determined by TTC staining. Another set of hypoxic rats were anesthetised and perfused fixed with 4% paraformaldehyde at the end or 24 after last hypoxia or 2 days after MCA occlusion. Brains were post-fixed in 30% sucrose, sectioned at a thickness of 10 microns and stained immunocytochemically (IHC) using standard techniques. Results: Following 12 cycles of IH expression of caspase3 (C3) increased without evidence of TUNEL staining. The overexpression of C3 persisted following ischemia in normoxic (N) rats and there was an increase in TUNEL staining at 2 days. In the hypoxic ischemic group, the C3 staining remained elevated, but there was little TUNEL staining. Phosphorylated-AKT (p-AKT) staining was not evident in the N group after ischemia, but was pronounced in the preconditioned group. The optimal maturation time for neuroprotection after hypoxia was 1 and 3 days (group3- 4). The threshold for IH ischemic tolerance was significant after 2 and 12, but not 4 cycles of hypoxia (Group 5-7)(for details, see below). Conclusion: IH induced C3 expression in the absence of TUNEL staining following IH, resulted in an increase in pAKT, and produced ischemic tolerance at 2, but not 4 cycles of IH. These changes are compatible with an improved outcome following IH preconditioning. The short term ischemic tolerance may reflect the early classical preconditioning compared to delayed ischemic tolerance (1). The increased expression of VEGF and not EPO after 2 and 4 cycles distinguishes the IH from a single hypoxic episode. The importance of IH is that it may be better tolerated than a single episode and further results show that the IH neuroprotection may persist for longer periods of time. 1. Mergenthaler et al., *Metabolic Brain Disease*, 2004. Supported by Philip Morris External Research Program

GROUP	# HYPOXIC CYCLES	HYPOXIA HOURS	POST-HYPOXIC NORMOXIA (DAYS)	INFARCT VOLUMES (%) (x ± SD, n ≥ 9 rats.)	VEGF & EPO IHC
1	0	0	0	43 ± 3	-
2	12	4	0	41 ± 6.9	-
3	12	4	1	26 ± 7.5*	+
4	12	4	3	21 ± 12.4*	+
5	2	0.66	3	26 ± 9*	+VEGF - EPO
6	4	1.33	3	41 ± 5	+VEGF - EPO
7	12	4	3	30 ± 8*	+

Asterisks designate statistically different ( $p < 0.05$ ) from non-IHC groups. Staining was - reflecting no IHC or + indicating detectable IHC.

**REDUCED INFARCT VOLUMES FOLLOWING FOCAL ISCHEMIA IN DIET INDUCED KETOTIC RAT BRAIN**

Michelle Puchowicz<sup>1</sup>, Douglas Emancipator<sup>1</sup>, Jorge Gamboa<sup>2</sup>, Jose Valerio<sup>2</sup>, Kui Xu<sup>1</sup>,  
W.D. Lust<sup>2</sup>, Joseph C. LaManna<sup>1</sup>

<sup>1</sup>*Department of Anatomy, Case Western Reserve University, Cleveland, OH, USA*

<sup>2</sup>*Department of Neurological Surgery, Case Western Reserve University, Cleveland, OH, USA*

Introduction: Ketones, R-beta-hydroxybutyrate (BHB) and acetoacetate (AcAc) are known to be essential alternate energy substrates to glucose for most tissues, especially brain, under conditions of starvation, early development, fasting and heavy exercise, and a high fat diet. Clinicians and investigators have been interested in their use as alternate energy substrates to glucose, such as therapeutic agents for the treatment of hypoglycemia, seizure disorders, Alzheimer's and Parkinson's disease and as alternates to high lipid parenteral and enteral feedings (1). Treatment with ketone body precursors, such as 1,3-butanediol, has shown promising evidence towards ameliorating brain damage due to ischemia and/or reperfusion injury (2,3). The proposed biochemical mechanism is thought to be through ketosis. Therefore, we studied the effects of diet-induced ketosis on reperfusion injury in ketotic rat brain following reversible middle cerebral artery occlusion (MCAO). Methods: Male Wistar rats (n= 19), 28 days old (100g), were fasted 24h to deplete glycogen stores and initiate a state of ketosis. Rats were then divided into 3 groups fed either: standard lab-chow (control; n=5, STD), ketogenic (high fat, no carbohydrate; n=7, KG), or carbohydrate (high carbohydrate, low fat; n=7, CHO), or diet for three weeks. Rats were anesthetized with 2% halothane/O<sub>2</sub>/N<sub>2</sub>O and MCAO was performed using a monofilament model (4), occluded for 2h; rats were sacrificed at 24h of reperfusion and the infarct volumes determined by TTC staining. In another set of experiments, brain ketone uptake and regional blood flow were measured using a dual label unidirectional tracer method, which allows for quantitation of substrate (beta-hydroxybutyrate) at the endothelial boundary of the blood-brain barrier, as well as a simultaneous determination of blood flow (5). Results: The infarct volumes at 24h of reflow after 2h occlusions for each of the diet groups were 45.9 ± 21.5, 30.2 ± 5.1 and 14.4 ± 9.6 % (mean ± SD) of the ipsilateral hemisphere for STD, CHO, and KG, respectively. The magnitude of the decrease in KG diet was significantly different (p<0.05) from those of STD (68.7 ± 22.1 %) and CHO (52.4 ± 11.0 %). There was no difference in infarct volumes of the CHO relative to the STD diet group. Regional ketone uptake was significantly elevated (40 fold) in brain of the KG rats compared to STD and CHO; whereas, there were no differences in blood flow among each of the diet groups. Conclusion: Ketosis induced by KG diet reduced the infarct volume by 70% compared to STD diet and CHO groups. It appears that in brain, ketones may be neuroprotective against reperfusion injury that is not related to changes in blood flow. The precise mechanism remains to be determined, but may be hypothesized through restoration of energy status via regulation of glycolytic intermediates and/or mitochondrial function. References: [1] Veech RL. Prostaglandins Leukot Essent Fatty Acids. 70(3):309-19. Review (2004) [2] Lundy EF et al. Stroke.18(1):217-22(1987) [3] Sims NR, Heward SL. Brain Res.662(1-2):216-22 (1994) [4] Lust WD et al. Met.Br.D. 17(2): 113-21 (2002) [5] LaManna JC, Harik SI. Cereb Blood Flow Metab.6(6):717-23 (1986)

**REMOTE PRECONDITIONING PROTECTS THE RODENT BRAIN FROM FOCAL CEREBRAL ISCHEMIA**Samit Malhotra, Manjeet Singh, **Daniel M. Rosenbaum***Neurology, AECOM, New York, NY, USA*

Purpose: Brief periods of non lethal ischemia protects the brain from subsequent severe lethal ischemia. This phenomenon has been described as ischemia tolerance or preconditioning (PC). This phenomenon has also been described in other organs such as heart, muscle and retina. More recently PC has been shown not only to protect against the targeted organ itself but also other organs. This phenomenon has been referred to as remote preconditioning (RPC). The purpose of this study was to determine if ischemic preconditioning in the limb would protect the rodent brain from subsequent transient and permanent focal cerebral ischemia. Methods: Limb preconditioning was induced by infrarenal occlusion of the aorta (IOA). IOA was performed by three cycles of 10 minutes occlusion followed by 10 minutes of reperfusion in rats and mice. 24 hours later rats were subjected to 2 hours of middle cerebral artery occlusion (MCAo) by the intraluminal suture method whereas mice underwent permanent MCAo. Sham group of animals did not undergo IOA but were subjected to MCAo. Brain sections were stained with 2,3,5 triphenyl tetrazolium chloride (TTC) to assess infarct volume. Results: RPC resulted in significant reduction in infarct volume in both models. In the rat (transient focal ischemia) infarct volume was reduced by 40% at 24 hours following ischemia. In the mouse (permanent focal ischemia) infarct volume was reduced by 75% at 72 hours following ischemia. Conclusions: Remote ischemic preconditioning reduces the extent of cerebral infarction in the rodent. Transient limb ischemia is a simple preconditioning stimulus which may have important clinical application. This neuroprotective effect may be mediated via systemic factors capable of crossing the blood brain barrier.

## HYPOXIC PRECONDITIONING REDUCES EXPRESSION OF THE CYCLIN DEPENDENT KINASE 5 IN THE POST-ISCHEMIC NEURONS

Svetlana Pundik<sup>1</sup>, W. David Lust<sup>2</sup>, Jose Valerio<sup>2</sup>, Michael Buczek<sup>2</sup>, Randall D. York<sup>3</sup>,  
Karl Herrup<sup>3</sup>

<sup>1</sup>Neurology, Case Western Reserve University, Cleveland, OH, USA

<sup>2</sup>Neurosurgery, Case Western Reserve University, Cleveland, OH, USA

<sup>3</sup>Neuroscience, Case Western Reserve University, Cleveland, OH, USA

Background: Ischemic tolerance can be induced in the experimental animal models of focal cerebral ischemia by a transient exposure to various sublethal metabolic stresses prior to the onset of stroke. One such preconditioning technique, hypoxia, significantly improves the outcomes following occlusion of middle cerebral artery (MCAO) in rats, but the understanding of the processes involved in endogenous neuroprotection is lacking. We have previously shown that cell cycle processes are altered following focal ischemia as indicated by changes in expression, an increase in BrdU incorporation and up regulation of the cell cycle inhibitors, p16 and p21. These findings are supported by studies showing that cerebral ischemia simulates expression of certain cell cycle related processes and that their inhibition results in reduction of infarct volumes. Since cyclin dependent kinase 5 (CDK5) has been implicated in the pathogenesis of other neurodegenerative diseases, we examined the expression of the CDK5 in post-ischemic brain tissues of the animals with and without hypoxic preconditioning. Design/Methods: Adult male Wistar rats were exposed to either a continuous 2 hours or twelve 20 min/hour episodes of 10% normobaric hypoxia in computer software regulated hypoxic chamber. Control animals were also placed in the chamber without change in oxygen tension. Middle cerebral artery was occluded with monofilament technique for 2 hours and animals were sacrificed at 8, 24 or 48 hours of reperfusion. Volumes of infarction were determined either by TTC or cresyl violet at 24 hours of reperfusion following 2 hours of MCAO in animals with and without intermittent hypoxia. Coronal brain sections through the area supplied by middle cerebral artery were stained with antibodies to CDK5 and co-localized with neuronal marker NeuN. Results: Intermittent hypoxia reduced volumes of infarction by 35% when compared to the non-conditioned controls, which was not significantly different from the decrease of damage in the single exposure group. While CDK5 staining was increased following hypoxia only, its expression was also increased in postischemic neurons within all the regions in the territory of the occluded artery, including the penumbra and the ischemic core at 8, 24 and 48 hours of reflow. Both intermittent and continuous hypoxic preconditioning reduced the number of neurons that express CDK5 in the penumbra, but not the ischemic core. Conclusions: Our study demonstrates that intermittent hypoxia which might be better tolerated than a continuous hypoxic exposure induces a similar endogenous neuroprotective effect and increases CDK5 expression. CDK5 staining is increased at early and late times of ischemic reperfusion in the areas where neurons are destined to die, while hypoxic preconditioning reduced the appearance of CDK5 in the penumbra following ischemia. While CDK5 is essential for neuronal growth and development it obviously has pathological functions. One possible explanation is that the expression in CDK5 in both hypoxia and/or ischemia may be attributed to different activators (e.g. p35 vs p25) following the two events. Therefore, we postulate that CDK5 related processes might mediate both hypoxia induced ischemic tolerance and ischemic neuronal death.

**INCREASED SIRT1 FOLLOWING REPETITIVE HYPOXIC PRECONDITIONING: A MECHANISM FOR MEDIATING LONG-TERM TOLERANCE (LTT) TO FOCAL STROKE IN ADULT MOUSE BRAIN**

**Yolanda M. Rangel**, Angela B. Freie, Ronaldo S. Perez, Ernesto R. Gonzales, Tamer Altay, Allison Holt, Tae S. Park, Jeffrey M. Gidday

*Department of Neurosurgery, Washington University, St. Louis, MO, USA*

Acquisition of cerebral ischemic tolerance following preconditioning results from synergistic, multifactorial processes that promote cellular survival. However, to date, the endogenous neuroprotective window following preconditioning is transient and lasts only several days. We have recently developed new mouse models of induced tolerance, whereby neuroprotection against transient focal stroke, as well as reductions in cerebrovascular inflammation following TNF $\alpha$ , are extended to 4 weeks following the last of a series of repetitive hypoxic preconditioning (RHP) stimuli (1,2). The first objective of this study was to determine if such long-term tolerance (LTT) could also be achieved against permanent focal stroke. Male ND4/Swiss Webster mice were subjected to RHP (9 episodes of systemic hypoxia of varied duration [2 or 4 hours] and severity [11 or 8% O<sub>2</sub>] over a 15-day period), or to a single period of hypoxic preconditioning (SHP) (4h @ 8%), previously shown to be protective against permanent middle cerebral artery occlusion (MCAO) injury at 24h. Two weeks later, all animals were subjected to permanent MCAO by a craniotomy approach. RHP resulted in a statistically significant reduction (38%;  $p < 0.05$ ) in ischemic injury, whereas SHP showed no long-term neuroprotective effects. Thus, as with transient MCAO, LTT can protect against brain injury caused by permanent MCAO. Given that the window of neuroprotection with LTT coincides temporally with a reduced inflammatory response to TNF $\alpha$ , the second objective of this study was to identify specific proteins whose expression would be increased for a protracted period of time following RHP, and that had the capacity to modulate diverse neuronal survival and inflammation pathways. SIRT1 is a member of the Sir2 family of class III histone deacetylases, whose activity is associated with enhanced cell survival in models of aging (3, 4). Recent studies suggest that SIRT1 activation prevents axonal degeneration following injury (5), which may be mediated through the regulation of DNA damage responses (inhibition of p53 activity) and/or transcriptional silencing (for example inhibition of the pro-inflammatory transcription factor NF- $\kappa$ B) (6, 7). We subjected male ND4/Swiss Webster mice to RHP and immunoblotted for SIRT1 in whole cell lysates generated from cortical samples obtained at various times after RHP. We demonstrated a 2-fold increase in SIRT1 protein expression immediately after the last RHP stimulus, which remained elevated for at least 2 weeks. These studies indicate that RHP results in a sustained upregulation of SIRT1 protein coincident with the period of LTT. The modulation of postischemic inflammatory and apoptotic pathways by SIRT1 may contribute to the unprecedented protection associated with LTT. These novel signaling pathways triggered by RHP may serve as molecular targets for therapeutics designed to reduce brain injury in stroke. (1) Rangel Y. et al., Soc. Neurosci. Abstr. 457.6, 2004. (2) Altay T. et al., Soc. Neurosci. Abstr. 457.7, 2004. (3) Lin S. et al., Science 289:2126, 2000. (4) Cohen H. et al., Science 305:390, 2004. (5) Araki T. et al., Science 305:1010, 2004. (6) Vaziri H. et al., Cell 107:149, 2001. (7) Yeung F. et al., EMBO J 23:2369, 2004.

## ISCHEMIC PRECONDITIONING AND ERYTHROPOIETIN NEUROPROTECTION SHARE COMMON DOWNSTREAM PATHWAYS

Samit Malhotra, Lenore Ocave, Sean Savitz, Manjeet Singh, **Daniel M. Rosenbaum**

*Neurology, AECOM, New York, NY, USA*

**Purpose:** Ischemic preconditioning (IP) protects the brain by initiating both transcriptional and post-transcriptional mechanisms. A better understanding of the molecular underpinnings of IP may yield important therapeutic targets for stroke. One potential signaling pathway involves the activation of erythropoietin receptor (EPOR). Pretreatment with EPO leads to significant reduction in neuronal cell death caused by a variety of insults. The purpose of this study was to determine if IP and EPO share common downstream signaling pathways. **Methods:** Transient focal ischemia was induced by the intraluminal suture method in rats for 2 hours. IP consisted of three episodes of focal ischemia, each lasting 10 minutes and followed by 45 minutes of reperfusion. 72 hours later, animals were subjected to 2 hours of middle cerebral artery occlusion (MCAo). The soluble EPOR (1 µg/day ) or the PI-3 kinase inhibitor, Wortmannin (10 µmol/L in phosphate-buffered saline containing 2% dimethylsulfoxide) was given intraventricularly for five consecutive days starting 24 hours prior to IP and ending on the day of MCAo. In separate experiments without IP, animals were microinjected intraventricularly with Wortmannin (2 µL at 10 µmol/L concentration) or vehicle, for five consecutive days ending on the day of MCAo and also received intraperitoneal injection of EPO (2500 IU/kg) 24 hours prior to ischemia and at the time of MCAo. For all animals, twenty four hours after 2 hours of MCAo, the brains were removed and stained with 2,3,5 triphenyl tetrazolium chloride (TTC) to assess infarct volume. A graded neurological exam (GNE) was also performed at 24 hours following ischemia. **Results:** Animals pretreated with IP or EPO resulted in significant reductions in infarct volume and improvement in GNE as compared to sham IP or vehicle controls. The neuroprotective effect of IP and EPO was abolished by pretreatment with the soluble EPOR or the PI-3 kinase inhibitor, Wortmannin. **Conclusion:** These results suggest that the EPO/EPOR system may serve as an endogenous neuroprotective system and in part may underlie the neuroprotective effect of ischemic preconditioning. These results also demonstrate that both IP and EPO share common downstream signaling pathways involving PI-3 kinase.

## HYPOXIC PRECONDITIONING INCREASES EXPRESSION OF HIF PROLYL HYDROXYLASE 2 (EGLN1) IN NEONATAL RAT BRAIN

Nicole M. Jones, Philip M. Beart

*Brain Injury and Repair Group, Howard Florey Institute, Melbourne, Australia*

**Introduction:** Preconditioning with hypoxia can protect the brain against a subsequent hypoxic-ischaemic insult. Hypoxia alone is not sufficient to cause neuronal injury, however can induce changes in gene expression and intracellular signalling pathways. The expression of the hypoxia-inducible transcription factor (HIF-1) (1) and several HIF-1 target genes (2) are up-regulated after hypoxic preconditioning in neonatal rat brain. Recent evidence has demonstrated that a family of HIF prolyl hydroxylase enzymes (Egln1,2 &3) are important in regulating HIF-1 function. Under normoxic conditions, Hif-1 $\alpha$  protein is hydroxylated, allowing binding of von Hippel Lindau protein, making Hif-1 $\alpha$  a target for proteosomal degradation. Enzymatic activity of prolyl hydroxylases is oxygen-dependent, therefore under hypoxic conditions, degradation of Hif-1 $\alpha$  is prevented, allowing accumulation of Hif-1 $\alpha$  protein, dimerization with Hif-1 $\beta$  and the HIF-1 complex can bind to the hypoxia-responsive element of various HIF-1 target genes (VEGF, GLUT-1, EPO) (3). We have investigated whether hypoxic preconditioning can affect levels of Egln1 protein in neonatal rat brains.

**Methods:** Sprague Dawley rat pups (postnatal day 6) were exposed to preconditioning with hypoxia (3h, 8% oxygen) or normoxia (3h, room air). On postnatal day 7, pups were subjected to occlusion of the left common carotid artery, followed by a 2.5h hypoxic exposure. At 5 days after hypoxic-ischemic insult, pups were sacrificed and brains removed to examine neuroprotective effect of hypoxic preconditioning. A further group of pups were exposed to hypoxia preconditioning (p6) and at various times (0, 0.5h, 2, 4, 16 and 24h) after cortical tissue was obtained for Western blot analysis of Egln1 protein levels.

**Results:** Preconditioning with hypoxia afforded significant protective effect against hypoxic-ischemic insult in neonatal rat brain. Following exposure to hypoxia preconditioning, there was an increase in Egln1 protein compared with normoxic control tissue (80-120% increase, sustained from 0.5h-24h after reoxygenation;  $p < 0.05$ , ANOVA).

**Conclusions:** Modulation of HIF-1 function by prolyl hydroxylation is likely to be involved in the protective effect conferred by hypoxic preconditioning in neonatal rat brain. We have observed that Egln1 protein expression remains elevated up until 24 hours after hypoxic preconditioning – which could possibly be regulated by HIF-1 at the transcriptional level.

**References:** (1) Bergeron et al (2000) Role of hypoxia-inducible factor-1 in hypoxia-induced ischemic tolerance in neonatal rat brain. *Ann Neurol.* 48: 285-96. (2) Jones & Bergeron (2001) Hypoxic preconditioning induces changes in HIF-1 target genes in neonatal rat brain. *J Cereb Blood Flow Metab.* 21: 1105-14. (3) Sharp & Bernaudin (2004) HIF1 and oxygen sensing in the brain. *Nature Rev. Neurosci.* 5: 437-48.

**ANGIOTENSIN AT2 RECEPTOR PROTECTS AGAINST CEREBRAL ISCHEMIA-INDUCED NEURONAL INJURY**

**Jun Li**<sup>1</sup>, Juraj Culman<sup>3</sup>, Heide Hörtnagl<sup>1</sup>, Yi Zhao<sup>3</sup>, Nadezhda Gerova<sup>1</sup>, Melanie Timm<sup>1</sup>, Annegret Blume<sup>3</sup>, Mathias Zimmermann<sup>1</sup>, Kerstin Seidel<sup>1</sup>, Ulrich Dirnagl<sup>2</sup>, Thomas Unger<sup>1</sup>

<sup>1</sup>*Center for Cardiovascular Research (CCR), Institute of Pharmacology and Toxicology, Charité – University Medicine Berlin, Berlin, Germany*

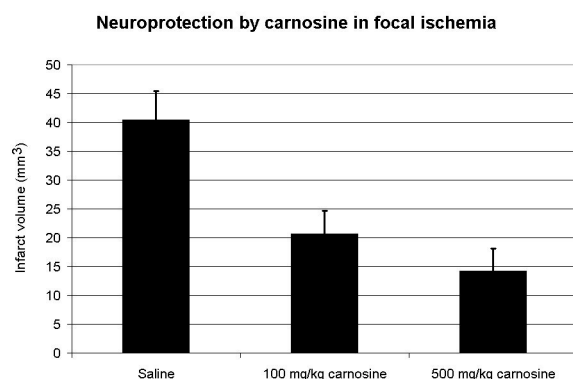
<sup>2</sup>*Department of Experimental Neurology, Charité – University Medicine Berlin, Berlin, Germany*

<sup>3</sup>*Institute of Pharmacology, University Hospital of Schleswig-Holstein, Campus Kiel, Christian-Albrechts-University of Kiel, Kiel, Germany*

Several lines of clinical and experimental evidence suggest an important role of the renin-angiotensin system in ischemic brain injury although the cellular regulation of the angiotensin AT1 and AT2 receptors and their potential relevance in this condition have not yet been clearly defined. We first assessed the regulation of brain AT1 and AT2 receptors in response to transient unilateral medial cerebral artery occlusion in rats by real-time RT-PCR, Western blot and immunofluorescence labelling. AT2 receptors in the peri-infarct zone were significantly upregulated 2 days following transient focal cerebral ischemia. Increased AT2 receptors, which were abundantly distributed in a large number of brain regions adjacent to the infarct area including cerebral frontal cortex, piriform cortex, striatum and hippocampus, were exclusively expressed in neurons. By contrast, AT1 receptors, which remained unaltered, were mainly expressed in astrocytes. In neurons of ischemic striatum, increased AT2 receptors were associated with intense neurite outgrowth. Blockade of central AT2 receptors with PD 123177 abolished the neuroprotective effects of central AT1 receptor blockade with irbesartan on infarct size and neurological outcome. In primary cortical neurons, stimulation of AT2 receptors supported neuronal survival and neurite outgrowth. Our data indicate that cerebral AT2 receptors exert neuroprotective actions in response to ischemia-induced neuronal injury, possibly by supporting neuronal survival and neurite outgrowth in peri-ischemic brain areas.

**CARNOSINE IS NEUROPROTECTIVE IN A MOUSE MODEL OF STROKE****Daniel Zemke, Rajanikant Krishnamurthy, Arshad Majid***Department of Neurology and Ophthalmology, Michigan State University, East Lansing, MI, USA*

Carnosine is a naturally occurring dipeptide found within glia and neurons of the brain that exhibits features characteristic of a neurotransmitter. Carnosine modulates the effect of zinc and copper released at synapses during neuronal activity, which have been linked to damage associated with Alzheimer's disease, stroke, and seizures. It also has antioxidant properties, and therefore may be useful for the prevention or treatment of oxidative damage in a number of neurological diseases including stroke. Stroke is one of the leading causes of death and disability in the United States. Carnosine has previously been shown to provide protection against ischemia in cultured cells and global ischemia in rats. The purpose of this study was to determine the effect of carnosine administration on the extent of brain damage in the mouse following experimentally induced focal ischemia, which better reproduces the conditions present in naturally occurring stroke. Carnosine (100 mg/kg or 500 mg/kg) was administered by intraperitoneal injection to male C57BL/6J mice 30 minutes prior to permanent occlusion of the middle cerebral artery. Damage to neural tissue was assessed after 24 hours by 2,3,5-triphenyl-tetrazolium chloride (TTC) staining. Infarct volumes were reduced by 49% and 65% in mice given 100 mg/kg and 500 mg/kg carnosine, respectively, versus saline-injected control mice. These results suggest that carnosine may be an important protective agent for the prevention of damage in stroke and other neurological diseases.

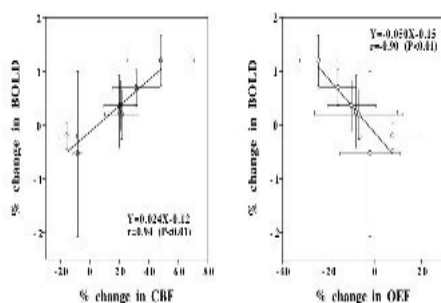


**CHANGES IN CEREBRAL BLOOD FLOW AND CEREBRAL OXYGEN METABOLISM DURING NEURAL ACTIVATION MEASURED BY POSITRON EMISSION TOMOGRAPHY: COMPARISON WITH CHANGES IN BLOOD OXYGENATION LEVEL-DEPENDENT CONTRAST MEASURED BY FUNCTIONAL MAGNETIC RESONANCE IMAGING**

Hiroshi Ito<sup>1</sup>, Masanobu Ibaraki<sup>2</sup>, Iwao Kanno<sup>2</sup>, Hiroshi Fukuda<sup>1</sup>, Shuichi Miura<sup>2</sup>

<sup>1</sup>*Department of Nuclear Medicine and Radiology, Institute of Development, Aging and Cancer, Tohoku University, Sendai,* <sup>2</sup>*Department of Radiology and Nuclear Medicine, Akita Research Institute of Brain and Blood Vessels, Akita, Japan*

Introduction: The discrepancy between the increases in cerebral blood flow (CBF) and cerebral metabolic rate of oxygen (CMRO<sub>2</sub>) during neural activation causes an increase in venous blood oxygenation and, therefore, a decrease in paramagnetic deoxyhemoglobin concentration in venous blood. This can be detected by functional magnetic resonance imaging (fMRI) as blood oxygenation level-dependent (BOLD) contrast. However, the relation between cerebral oxygen extraction fraction (OEF), that corresponds to the ratio of CMRO<sub>2</sub> to CBF, and BOLD contrast during neural activation has not been shown directly in human subjects. In the present study, changes in the OEF and in the BOLD signal during neural activation were measured by both positron emission tomography (PET) and fMRI in the same human subjects. Methods: C15O, 15O<sub>2</sub>, and H<sub>2</sub>15O PET studies were performed in each of seven healthy men (20-22 years, right-handed) at rest (baseline) and during performance of a right hand motor task. The motor task consisted of a finger tapping activity in which each finger of the right hand was sequentially touched to the thumb. fMRI studies were then performed to measure the BOLD signal under the two conditions. Z-score maps of the motor task condition measurement minus the baseline measurement and the baseline measurement minus the motor task condition measurement were created from CBF images using SPM99. Regions of interest (ROIs) were defined on all CBF, cerebral blood volume (CBV), OEF, CMRO<sub>2</sub>, and BOLD images for the statistically significant areas on the Z-score maps. Results: Significant relative hyperperfusion indicating neural activation during the motor task activity was observed in the left precentral gyrus, left superior frontal gyrus, right precentral gyrus, right cingulate gyrus, and right cerebellum. Significant relative hypoperfusion indicating neural deactivations during the motor task activity was observed in the left anterior part of cingulate gyrus and right occipital cuneus. A significant positive correlation was observed between changes in the CBF and the BOLD signal, and a significant negative correlation was observed between changes in the OEF and the BOLD signal for all ROIs. Conclusions: This supports the assumption on which BOLD contrast studies are based, that the discrepancy between increases in CBF and CMRO<sub>2</sub> during neural activation causes an increase in venous blood oxygenation.



## MECHANISMS OF DEEP BRAIN STIMULATION IN OBSESSIVE-COMPULSIVE DISORDER REVEALED BY 15O-H<sub>2</sub>O PET AND DIFFUSION TRACTOGRAPHY

J.C. Klein<sup>1,2</sup>, D. Lennartz<sup>3</sup>, J. Poggenborg<sup>4</sup>, K. Herholz<sup>1,2</sup>, K. Lackner<sup>4</sup>, V. Sturm<sup>3</sup>, W.D. Heiss<sup>1,2</sup>

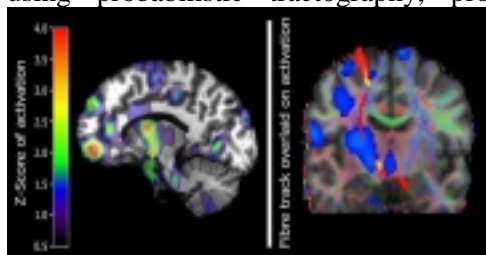
<sup>1</sup>Max-Planck-Institute for Neurological Research, Cologne, Germany

<sup>2</sup>Department of Neurology, University of Cologne, Cologne, Germany

<sup>3</sup>Department of Stereotactic Surgery, University of Cologne, Cologne, Germany

<sup>4</sup>Department of Radiology, University of Cologne, Cologne, Germany

**Introduction** Obsessive-compulsive disorder (OCD) is a disabling psychiatric disease, causing patients to repetitively perform actions or persevere thoughts whose futility is obvious to the patient, but refraining from these actions or thoughts instils overwhelming fear. In many cases, medication and behaviour therapy can ameliorate symptoms. In those who did not respond to conservative therapy, stereotactic implantation of electrodes into the right-sided nucleus accumbens and inhibitory deep brain stimulation (DBS) is a concept currently under evaluation at Cologne University's Department of Stereotactic Surgery. Advantages are a generally well-tolerated procedure and, in contrast to established lesional approaches, the ability to fully reverse it, should complications arise. **Methods** In one such patient, an electrode with 4 contact pads (Medtronic, Minneapolis, USA) was inserted into the shell region of the right sided nucleus accumbens using a Leibinger guidance system (Stryker Leibinger, Freiburg, D), the electrode was connected to a signal generator (Medtronic). Electrode trajectory was plotted into pre-surgical MR data using software developed at our lab. Before surgery, we obtained diffusion-weighted MR imaging on a 1.5T Gyroscan Intera system (Philips, Best, NL) using an 8 element phase-array head coil in SENSE mode. 32 isotropic diffusion encoding directions were applied to minimize directional uncertainty while maintaining tolerable scan times. The FSL software library (FMRIB, Oxford, UK) was used for probabilistic fibre tracking. One week after surgery, 15OH<sub>2</sub>O-PET (4 rest vs. 4 stimulation, unipolar, 3V, distal two electrodes) datasets were recorded on a Siemens/CTI ECAT HR scanner. As opposed to fMRI, this method is not hindered by the presence of the implants nor does it interfere with stimulation. Coregistration with anatomical MR and diffusion data was achieved using VINCI software. PET activation data was transformed to Z-scores using the AAT algorithm developed here. **Results** PET demonstrated significant stimulation-induced blood flow increase in right-sided pregenual, subgenual and orbitofrontal cortex as well as in striatal and frontolateral gray matter. Inhibition at the rostral edge of the electrode was detected, but Z-scores did not reach significance. Diffusion tractography depicted the anatomical pathways between disjoint cortical and subcortical stimulation foci, such as pallidal to frontolateral, pregenual to orbitofrontal, thus demonstrating the network responsible for remote effects of DBS. **Conclusion** For the first time, combined diffusion tractography and PET activation provide non-invasive in vivo insight into DBS's effects on cerebral activation along with its anatomical substrates. We demonstrated that DBS of the nucleus accumbens achieves increased activity in anterior cingulate and orbitofrontal cortex, areas that are part of the phylogenetically old limbic system and believed to play key roles in OCD symptom formation. Connectivity between deep brain and cortical activations was established using probabilistic tractography, proving that cortical activation is a remote effect of DBS.





**IMPACT OF SLEEP DEPRIVATION ON CEREBRAL A1 ADENOSINE RECEPTOR (A1AR) DENSITY: A PET STUDY****David Elmenhorst, Philipp T. Meyer, Andreas Matusch, Karl Zilles, Andreas Bauer***Institute of Medicine, Research Centre Juelich, Juelich, Germany*

There is evidence from animal experiments that adenosine is an important sleep propensity factor which exerts its function mainly via the A1 adenosine receptor (A1AR). Prolonged wakefulness causes a significant increase of extracellular adenosine in distinct brain regions promoting induction of sleep via A1ARs (1). Recently, in vivo investigation of cerebral A1ARs has become feasible by the selective ligand 18F-CPFPX and PET (2). This pilot study was intended to examine whether the A1AR binding of 18F-CPFPX is changed by prolonged wakefulness. Eleven healthy male volunteers participated in a dynamic 18F-CPFPX bolus/infusions-PET study with venous blood sampling (3). Seven subjects were scanned before and after 24 hours of sustained wakefulness and four subjects served as control group being measured twice on subsequent days after normal 8h night sleep. The realignment and co-registration of dynamic PET data according to the individual MRI and subsequent normalization to the MNI template were performed with SPM2. Regional distribution volume ratios (DVR) (cerebellum as input) using Logan's non invasive graphical analysis were determined. The apparent binding potential ( $BP_{app} = DVR - 1$ ) was calculated as outcome parameter. Comparing the  $BP_{app}$  values obtained before and after sleep deprivation revealed a tendency towards an increase of the  $BP_{app}$  at the second day (mean intraindividual relative change (day2-day1)/day1 in %  $\pm$  SD (paired t-test): frontal  $3.32 \pm 5.0\%$  ( $p=0.15$ ), parietal  $4.03 \pm 5.0\%$  ( $p=0.073$ ), occipital  $6.57 \pm 4.1\%$  ( $p=0.006$ ), striatal  $7.87 \pm 9.1\%$  ( $p=0.067$ )). In contrast there was no difference between both days in the control group (frontal  $1.36 \pm 6.6\%$  ( $p=0.96$ ), parietal  $0.02 \pm 2.0\%$  ( $p=0.86$ ), occipital  $0.63 \pm 2.0\%$  ( $p=0.64$ ), striatal  $-0.5 \pm 4.4\%$  ( $p=0.73$ )). These preliminary results show a tendency towards an increase of the  $BP_{app}$  of 18F-CPFPX after sleep deprivation. An increase of A1AR density would be in line with an upregulation of A1AR mRNA which was observed in animals under persistent sleep deprivation (1). To confirm these preliminary observations a larger number of subjects is currently under investigation. (1) Basheer R, Strecker RE, Thakkar MM et al. *Progress in Neurobiology* 73 (2004) 379-396. (2) Bauer A, Holschbach MH, Meyer PT et al. *Neuroimage*. 19 (2003) 1760-1769. (3) Meyer PT, Elmenhorst D, Bier D et al. *Neuroimage* (in press).

## **<sup>15</sup>O- PET SHOWS THAT CEREBRAL BLOOD VOLUME IS INCREASED IN HEAD INJURY, BUT MAY STILL NOT BE THE DOMINANT CAUSE OF INTRACRANIAL HYPERTENSION**

**David K. Menon**<sup>1,3</sup>, Jonathan P. Coles<sup>1,3</sup>, Tim D. Fryer<sup>3</sup>, Dot A. Chatfield<sup>1,3</sup>,  
Luzius A. Steiner<sup>1,2,3</sup>, Andrew J. Johnston<sup>1,3</sup>, Franklin I. Aigbirhio<sup>3</sup>, John C. Clark<sup>3</sup>,  
John D. Pickard<sup>2,3</sup>

<sup>1</sup>*Division of Anaesthesia, University of Cambridge, Cambridge, UK*

<sup>2</sup>*Department of Neurosurgery, University of Cambridge, Cambridge, UK*

<sup>3</sup>*Wolfson Brain Imaging Centre, University of Cambridge, Cambridge, UK*

Intracranial pressure (ICP) increases following traumatic brain injury (TBI) are multifactorial, and may be due to cytotoxic oedema, vasogenic oedema and/or vascular engorgement. We addressed the issue of the contribution of vascular engorgement to ICP elevation by directly measuring cerebral blood volume (CBV) with <sup>15</sup>O positron emission tomography (<sup>15</sup>O-PET) in well-characterised patients with head injury.

We undertook 61 <sup>15</sup>O-PET studies with measurement of CBF and CBV; ten in healthy volunteers and 51 in patients with TBI (15 within 24 hours, and 36 at 2 - 6 days post injury). The median (range) admission Glasgow Coma Score (GCS) in patients was 7(3-13), but, at the stage when imaging was undertaken, all patients required sedation and/or ventilatory support for ICP elevation or reductions in GCS to < 8. Patients received protocol driven therapy aimed at maintaining ICP < 20 mmHg, cerebral perfusion pressure (CPP) > 70 mmHg, and PaCO<sub>2</sub> at ~ 4.5 kPa.

PET studies were undertaken using steady-state techniques. Parametric maps of CBF, CBV, CMRO<sub>2</sub> and OEF were calculated using a blood-brain partition coefficient for H<sub>2</sub><sup>15</sup>O of 0.95 and a small to large vessel haematocrit ratio of 0.85. A standardised map with 12 regions of interest (ROI) was constructed for the supratentorial compartment, based on vascular territories and anatomical structures.

Patients had a mean (± SD) ICP of 17 ± 6 mmHg, a CPP of 74 ± 8 mmHg, and a significantly lower PaCO<sub>2</sub> than controls (4.5 ± 0.4 vs. 5.5 ± 0.4 kPa; p < 0.001). Despite these differences in PaCO<sub>2</sub>, when compared to controls, mean CBV in patient ROIs was significantly higher, both before and after 24 hours post injury (3.3 ± 0.8 ml/100ml vs. 3.8 ± 0.7 and 3.9 ± 0.7 ml/100ml, respectively; p < 0.01 at both time points). Differences between controls and patient groups were preserved when values were compared after averaging across all ROIs in individual patients (p < 0.05 and < 0.001, for early and late head injury, respectively). CBV was directly, rather than inversely, related to CBF at both time points (R: 0.56 and 0.48, respectively; p < 0.0001 for both). These findings suggest dysautoregulation or metabolically coupled changes in CBF, rather than autoregulatory vasodilatation in response to classical macrovascular ischaemia. CBV was inversely related to ICP (R: 0.39; p < 0.01), suggesting that vasodilatation was not the dominant cause of intracranial hypertension across the population of patients studied.

We show significant increases in CBV following TBI; both within and after 24 hours post TBI. While previous reports of low CBV in head injury may have been confounded by the indirect estimation of CBV,<sup>1</sup> our data support previous suggestions<sup>1</sup> that CBV increases may not be the dominant cause of intracranial hypertension in all subjects. Our findings are fully consistent with microvascular ischaemia, but the concordance of high CBF and CBV values suggests that CBV increases are mainly the consequence of abnormal vascular function, rather than macrovascular ischaemia.

**ASSESSMENT OF MICROGLIAL ACTIVATION IN PATIENTS WITH  
ALZHEIMER'S DISEASE USING [C-11]-(R)-PK11195 AND PET**

**Alie Schuitemaker<sup>1,2</sup>, Bart N.M. van Berckel<sup>2</sup>, Ronald Boellaard<sup>2</sup>, Marc A. Kropholler<sup>2</sup>,  
Cees Jonker<sup>1,3</sup>, Dick J. Veltman<sup>2,4</sup>, Philip Scheltens<sup>1</sup>, Adriaan A. Lammertsma<sup>2</sup>**

<sup>1</sup>*Department of Neurology, VU University Medical Centre, Amsterdam, The Netherlands*

<sup>2</sup>*Department of Nuclear Medicine and PET Research, Amsterdam, The Netherlands*

<sup>3</sup>*EMGO Institute, Amsterdam, The Netherlands*

<sup>4</sup>*Department of Psychiatry, Amsterdam, The Netherlands*

Background: [C-11]-(R)-PK11195 has been used to quantify microglial activation in neurodegenerative disorders. Two previous reports on [C-11]-(R)-PK11195 binding in Alzheimer's disease (AD) provided contradictory results (1,2) In the present study [C-11]-(R)-PK11195 binding was evaluated using both Statistical Parametric Mapping (SPM) and full kinetic analysis. For the latter both reference tissue and plasma input models were used. Methods: 13 AD patients (age 58 - 81 years), fulfilling the NINCDS-ADRDA criteria, and 17 age matched healthy controls (age 57 - 79 years) were included. Dynamic 3D PET scans, consisting of 22 frames over 60 minutes, were acquired following a bolus injection of ~370 MBq [C-11]-(R)-PK11195. Arterial whole blood concentration was monitored continuously using an online detection system. In addition, discrete samples were taken in order to derive a metabolite corrected plasma input curve. Finally, a T1-weighted structural MRI scan was acquired using a 1 Tesla scanner. Volume of distribution (Vd) images and binding potential (BP) images were generated using Logan (plasma input) and Ichise (cerebellum = reference tissue input) plots, respectively. Both sets of images were used in SPM analyses to assess differences in PK11195 binding between AD and controls. In addition, regions of interest (ROIs) were drawn on the individual co-registered MRI scans. ROI were defined bilaterally for posterior cingulate, medial temporal lobe, thalamus and cerebellum. The ROI were projected onto the dynamic [C11]-(R)-PK11195 scan to generate time-activity curves (TACs) for each region. TACs were fitted using (a) a simplified reference tissue model with cerebellum as reference tissue (3) and (b) a two tissue reversible plasma input model (K1/k2 ratio fixed to whole cortex)(4). Binding Potential (BP) was used as primary outcome measure of ROI analyses. Results: SPM analysis based on Vd images did not reveal any areas with statistically significant differences in [C-11]-(R)-PK11195 binding between both groups. SPM analysis based on BP images showed slightly increased PK11195 binding (p=0.05) in bilateral occipital and lateral temporal lobes of AD patients. ROI analysis using ANOVA with age as covariate revealed no statistically significant differences in BP between groups, although with the two tissue reversible plasma input model (K1/k2 ratio fixed to whole cortex) a general trend for increased BP was found in patients with AD. Conclusion: Overall, both SPM and ROI based analyses did not show increased [C-11]-(R)-PK11195 binding in AD, which is in accordance with the findings of Groom et al(2). The trend of increased binding in occipital and lateral temporal lobes in the SPM analysis based on BP images warrants further analysis. This requires precise delineation of these structures and a full kinetic analysis. References 1. Cagnin A et al. (2001) Lancet 358: 461-467 2. Groom GN et al. (1995) J Nucl Med 36: 2207-2210 3. Lammertsma AA and Hume SP (1996) Neuroimage 4: 153-158 4. Kropholler MA et al. (2004) Neuroimage 22, Suppl 2: T184

	Two tissue reversible model			Simplified reference tissue model		
	controls	Patients	P value	controls	Patients	P value
Postcingulate	1.39±0.29	1.71±0.86	0.18	0.038±0.040	0.053±0.048	0.41
MTL	1.62±0.33	1.85±0.78	0.27	0.083±0.044	0.073±0.070	0.57
Thalamus	1.46±0.41	1.69±0.63	0.27	0.024±0.053	0.020±0.036	0.62
Cerebellum	1.41±0.25	1.58±0.63	0.35			
Cerebrum	1.59±0.23	1.92±0.74	0.11	0.055±0.050	0.089±0.071	0.11

## EFFECTS OF EARLY REARING CONDITION ON THE CENTRAL SEROTONIN SYSTEM: [11C]DASB PET IMAGING OF SEROTONIN TRANSPORTERS IN ADOLESCENT PEER- AND MOTHER-REARED RHESUS MONKEYS

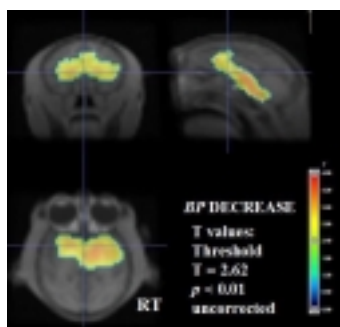
Masanori Ichise<sup>1</sup>, Douglass C. Vines<sup>1</sup>, Tami Gura<sup>2</sup>, Stephen J. Suomi<sup>3</sup>, J. Dee Higley<sup>2</sup>, Robert B. Innis<sup>1</sup>

<sup>1</sup>Molecular Imaging Branch, National Institute of Mental Health, Bethesda, MD, USA

<sup>2</sup>Laboratory of Clinical Studies-Primate Unit, DICBR, National Institute on Alcohol Abuse and Alcoholism, National Institutes of Health Animal Center, Poolesville, MD, USA

<sup>3</sup>Laboratory of Comparative Ethology, National Institute of Child and Human Development, National Institutes of Health Animal Center, Poolesville, MD, USA

**Introduction:** Peer-reared (PR) rhesus monkeys with early maternal separation later exhibit aggressiveness, impaired impulse control, and alcohol abuse; they also show low CSF 5-HIAA (a serotonin metabolite) and low basal plasma cortisol/ACTH with impaired response to acute stress (1, 2). Cortisol facilitates the gene expression of the serotonin transporter (SERT) via the stress axis. However, information on regional 5HT function in vivo in these animals is limited. The purpose was to compare regional brain SERT binding between PR and mother-reared (MR) monkeys with [11C]DASB, a SERT PET tracer. **Methods:** Two groups of mean age (3.4 y) and weight (5.7 kg) matched adolescent male rhesus monkeys (9 PR and 7 MR) were studied. PET data were acquired under isoflurane anesthesia (1.6%) for 2 h with a bolus injection of 4 mCi of [11C]DASB. Additionally, one monkey from each group underwent, on a different day, two 2 h [11C]DASB PET scans separated by 1 h, first with a bolus and infusion (B/I) of high specific activity (SA) (2000 mCi/ $\mu$ mol) and second with B/I of a low SA ( $\mu$  35 mCi/ $\mu$ mol). From the bolus PET data, parametric images of binding potential (BP=Bmax/KD', Bmax = transporter density, KD' = KD/f2, KD = dissociation constant and f2 = free tissue fraction) and relative blood flow (R1) were generated by the two-parameter multilinear reference tissue model using the cerebellum as reference tissue (3). The parametric images were normalized to a template MRI created from all 16 MRI scans. Group parameter differences were analyzed voxel-wise by a two-sample t test in SPM2. The magnitude of group parameter differences was evaluated by regions of interest (ROIs) analysis. The B/I PET data were used to estimate Bmax and KD' separately by a Scatchard analysis method. **Results:** In the PR, BP was decreased (T = 2.62, p < 0.01) by 15-20% in the raphe, thalamus, striatum, hippocampus/amygdala bilaterally and the remaining right temporal lobe; R1 was also decreased by 15-20% in similar regions more symmetrically except for thalamus where R1 were not different (Fig). The lower striatal BP (0.76) in the PR monkey than that (1.02) in the MR monkey was due to lower Bmax (40 pmol/mL) in the former than that (50 pmol/mL) in the latter with similar KD' values. **Conclusion:** These results agrees with the hypothesis that early maternal deprivation affects the development of the serotonin system and that decreased SERT binding in the critical brain regions may explain some of the behavioural and biochemical abnormalities in PR monkeys. **References:** [1] Higley JD, Suomi SJ, Linnoila M; Alcohol Clin Exp Res 20: 629-650 (1996) [2] Bastian ML, Sponberg AC, Sponberg AC, Suomi SJ, Higley JD; Dev Psychobiol 42:44-51 (2003) [3] Ichise M, Liow JS, Lu JQ, et al.; J Cereb Blood Flow Metab 23:11096-1112 (2003)





## RESOLUTION AND INVERSION TIME DEPENDENCE OF CBF MEASUREMENTS USING MRI: A POSSIBLE EXPLANATION FOR DISCREPANCY BETWEEN MRI AND PET

Manus J. Donahue<sup>1,2,3</sup>, Craig K. Jones<sup>1,3</sup>, Hanzhang Lu<sup>4</sup>, Peter C.M. van Zijl<sup>1,2,3</sup>

<sup>1</sup>Department of Radiology, Johns Hopkins University School of Medicine, Baltimore, MD, USA

<sup>2</sup>Department of Molecular Biophysics, Johns Hopkins University School of Medicine, Baltimore, MD, USA

<sup>3</sup>F.M. Kirby Research Center, Kennedy Krieger Institute, Baltimore, MD, USA

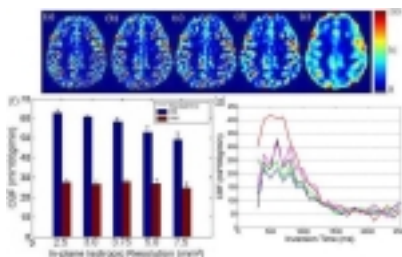
<sup>4</sup>Department of Radiology, New York University, New York, NY, USA

**INTRODUCTION** MRI-measured gray-matter (GM) cerebral blood flow (CBF) values are generally larger than PET values, with the underlying reason(s) remaining a topic of discussion [1]. PET literature commonly reports normal GM CBF values of 40–55 ml/100g/min, whereas MRI values as high as 100 ml/100g/min have been published [2]. We demonstrate two main causes of this discrepancy, one relating to GM CBF *overestimation* by the MRI approach of arterial spin labeling (ASL) and one relating to GM CBF *underestimation* by PET. First, ASL overestimates perfusion due to insufficient time for in-flowing labeled blood water to leave small arteries and enter tissue. Although this has been previously noticed [3], such short label inversion times (TI), remain in use at low magnetic field strength where the relaxation time T1 of arterial blood water is short (1350ms [4]). We evaluate TI influence on CBF measurements at 3T, where arterial T1 is much longer (1630ms [5]). Second, due to the low resolution at which PET measurements are acquired, partial volume effects between GM, white matter, and cerebrospinal fluid cause GM CBF to be underestimated. We evaluate these effects by analyzing ASL CBF maps as a function of resolution.

**METHODS** ASL studies were performed on 5 subjects at 3T using the transfer insensitive labeling technique (TILT [6]), a pulsed ASL technique that labels blood proximal to the imaging slice. Two sets of ASL experiments were performed: 1) To analyze partial volume effects, multiple-resolution studies were performed with FOV=240 mm, slice thickness=5 mm, and in-plane isotropic matrix sizes=96,80,64,48, and 32 (TR/TI = 2000/1500ms). Images were interpolated to identical in-plane resolution (128x128). 2) To analyze arterial flow contributions, CBF maps were generated varying TI between 100 ms and 2500 ms; these maps were overlaid on MR angiography (MRA) maps to isolate arterial flow regions.

**RESULTS** Multiple resolution CBF maps (in-plane resolution 2.5-7.5 mm<sup>2</sup>) in Figs. 1a-e illustrate how CBF varies with resolution, with 7.5 mm<sup>2</sup> roughly mimicking PET resolution. GM CBF decreases by approximately 20.5 % over this range (Fig.1f), thereby implicating partial volume effects at PET resolutions. CBF dependence on labeling delay is shown for five different regions of interest in Fig.1g. At TI<1500ms, CBF is greatly overestimated by MRI ASL due to arterial contributions, but CBF roughly plateaus at TI≥1500ms, once tagged arterial blood water has left the imaging slice and/or entered tissue. At 1.5T, the T1 of blood water is much shorter than at 3T, therefore perfusion imaging at TI≥1500 ms is difficult since most of the tag has decayed. These results largely reconcile the differences between PET and MRI CBF measurements and point toward a true measure of perfusion independent of imaging modality.

**REFERENCES** [1] Ye MRM. 2000;44:450. [2] Iida. JNM. 1998;39:1789. [3] Wong. NCNA. 1999;9:333. [4] Lu, MRM 2003;40:263, [5] Lu, MRM 2004;52:679 [6] Golay, JMRI. 1999;9:454.





**QUANTITATIVE ASSESSMENT OF THE CEREBRAL NICOTINIC  
ACETYLCHOLINE RECEPTORS (NACHR) IN PARKINSON'S DISEASE USING 2-  
[18F]F-A-85380-PET**

**Philipp Meyer**<sup>1</sup>, Kai Kendziorra<sup>1</sup>, Swen Hesse<sup>1</sup>, Henryk Barthel<sup>1</sup>, Georg Becker<sup>1</sup>, Dietlind Sorger<sup>1</sup>,  
Andreas Schildan<sup>1</sup>, Marianne Patt<sup>1</sup>, Anita Seese<sup>1</sup>, Gudrun Wagenknecht<sup>2</sup>, Donald Lobsien<sup>3</sup>,  
Florian Then Bergh<sup>4</sup>, Peter Brust<sup>5</sup>, Jörg Steinbach<sup>5</sup>, Claus Zimmer<sup>3</sup>, Johannes Schwarz<sup>4</sup>,  
Osama Sabri<sup>1</sup>

<sup>1</sup>*Department of Nuclear Medicine, University Hospital Leipzig, University of Leipzig, Leipzig, Germany*

<sup>2</sup>*Forschungszentrum Juelich, Institute for Medicine, Juelich, Germany*

<sup>3</sup>*Department of Radiology (Neuroradiology), University Hospital Leipzig, University of Leipzig, Leipzig, Germany*

<sup>4</sup>*Department of Neurology, University Hospital Leipzig, University of Leipzig, Leipzig, Germany*

<sup>5</sup>*Institute for Interdisciplinary Isotopic Research Leipzig, Leipzig, Germany*

**INTRODUCTION:** Epidemiological studies have demonstrated that tobacco smoking is associated with a lower incidence of Parkinson's disease (PD, Wirdefeldt K, 2005). As suggested by in vitro und in vivo animal studies nicotine seems to be a neuroprotective factor. The alpha4beta2-subunits of the nAChR, on which nicotine binds with its highest affinity seem to be involved. By using the radioligand 2-[18F]F-A-85380 and positron emission tomography (PET) we tested the hypothesis whether these receptors are altered in patients with PD (Pimlott SL, 2004). **METHODS:** Seven patients with PD (39-70 yrs), different clinical severity (UPDRS-III: 8-49, MMSE: 23-29), with symptomatic therapy and 5 age-matched normal subjects (37-64 yrs) were measured following a short-time infusion (90s) of the radioligand 2-[18F]F-A-85380 using PET (Siemens ECAT EXACT HR+, Germany) over a time period of 7 hours. Parametric images of the distribution volumes DV [mL/ccm] for 2-FA were calculated by Logan plot after correction of the arterial input function for plasma protein binding and radioactive metabolites. After co-registration with the individual MRI (Hermes Medical Solutions, Sweden), DVs in 23 ROIs (7 subcortical, 16 cortical) were analyzed. The binding potential BP=DV/DV corpus callosum -1 was calculated. In addition, the dopamine transporter (DAT)-availability in the basal ganglia was assessed using [123I]-FP-CIT-SPECT. **RESULTS:** In the patients with PD, 2-[18F]F-A-85380-BP decreases were found in the left caudate nucleus (-43.8%, p<0.05). There was a tendency for a decreased BP in the right caudate nucleus (-20.5%), in the left putamen (-13.2%), in pons (-5.9%) and in the cerebellum (-6.9%). There was a tendency for an increased BP in the thalamus, in the hippocampus and in the substantia nigra (+6.7%). **CONCLUSIONS:** This preliminary data strongly suggest an alteration of alpha4beta2 nAChRs availability in PD. This might be regional different (decreased in left caudate nucleus, in the basal ganglia, pons and cerebellum, increased in the thalamus, hippocampus and in the substantia nigra). Whereas the regional decrease of the alpha4beta2 nAChRs is in agreement with post mortem studies in PD, the increased availability of the alpha4beta2 nAChRs could represent a denervation supersensitivity. Further investigation in a larger group of patients is underway. **REFERENCES:** Pimlott SL, et al. Nicotinic acetylcholine receptor distribution in Alzheimer's disease, dementia with Lewy bodies, Parkinson's disease, and vascular dementia: in vitro binding study using 5-[125I]-A-85380, *Neuropsychopharmacology* 2004;29,108-116. Wirdefeldt K, et al. Risk and protective factors for Parkinson's disease: a study in Swedish twins, *Ann Neurol* 2005,57:27-33.

**MOOD CHANGES IN WOMEN WITH PREMENSTRUAL DYSPHORIA  
CORRELATE TO CHANGES IN BRAIN SEROTONIN PRECURSOR TRAPPING  
(11C-5-HYDROXY-L-TRYPTOPHAN)**

**Olle Eriksson<sup>1</sup>**, Anders Wall<sup>2</sup>, Ina Marteinsdottir<sup>3</sup>, Hans Ågren<sup>4</sup>, Per Hartvig<sup>5</sup>,  
Gunnar Blomqvist<sup>2</sup>, Bengt Långström<sup>2</sup>, Tord Naessén<sup>1</sup>

<sup>1</sup>*Department of Women's and Children's Health/Obstetrics and Gynaecology, University Hospital, Uppsala, Sweden*

<sup>2</sup>*Uppsala Imanet AB, University Hospital, Uppsala, Sweden*

<sup>3</sup>*Department of Neuroscience, Section of Psychiatry, University Hospital, Uppsala, Sweden*

<sup>4</sup>*Neurotec Department, Division of Psychiatry, Karolinska Institute, Stockholm, Sweden*

<sup>5</sup>*Hospital Pharmacy, University Hospital, Uppsala, Sweden*

Background: Premenstrual dysphoria is characterized by the cyclical occurrence of negative mood and physical symptoms during the luteal phase of the menstrual cycle. Cardinal symptoms are irritability, depression of mood, fatigue, affective lability, and impaired impulse control, all symptoms that can be alleviated by drugs increasing serotonergic signaling. Drugs inhibiting serotonin reuptake (the SSRIs) form the most effective pharmacological treatment known today. Thus, lowered serotonergic signaling during the luteal phase might be one symptom provoking factor in premenstrual dysphoria. The aim of the study was to test the serotonin hypothesis of this disorder i.e. of an association between premenstrual decline in brain serotonin function and concomitant worsening of self-rated cardinal mood symptoms. Method: Positron emission tomography was used to assess brain trapping of 11C-5-hydroxy-L-tryptophan, marked in the beta-position, in the follicular and premenstrual phases of the menstrual cycle in eight women with Premenstrual dysphoria. Brain trapping of this radiotracer is supposed to reflect presynaptic aromatic amino acid decarboxylase activity, the activity of the enzyme responsible for the conversion of 11C-5-hydroxy-L-tryptophan to 11C-serotonin. Region of interest analysis was performed in the following regions: dorso-lateral prefrontal cortex, medio-prefrontal cortex, the caudate nucleus, and the putamen, all on the left and right side, and in a single whole brain region of interest. Changes in mood and physical symptoms were assessed from daily VAS self-ratings. Results: Worsening of the cardinal mood symptoms irritability and depressed mood showed significant inverse associations to changes in brain 11C-5-hydroxy-L-tryptophan trapping whereas positive mood variables all showed positive associations and physical symptoms generally displayed weak or no associations. Conclusion: The results indicate strong inverse associations between worsening of cardinal mood symptoms of Premenstrual dysphoria and brain trapping of the serotonin precursor 11C-5-hydroxy-L-tryptophan. The results may in part support a role for serotonin in Premenstrual dysphoria and may provide a clue to the effectiveness of serotonin augmenting drugs in this disorder.

## PET IMAGING OF 5-HT<sub>1A</sub> RECEPTORS IN LATE-LIFE DEPRESSION: RELATIONSHIP TO TREATMENT RESPONSE

Carolyn C. Meltzer, Julie C. Price, Scott K. Ziolko, Chester A. Mathis, Lisa A. Weissfeld,  
Patricia R. Houck, Brian J. Lopresti, Benoit H. Mulsant, Charles F. Reynolds

*Departments of Radiology, Psychiatry, Neurology, and Biostatistics, University of Pittsburgh,  
Pittsburgh, PA, USA*

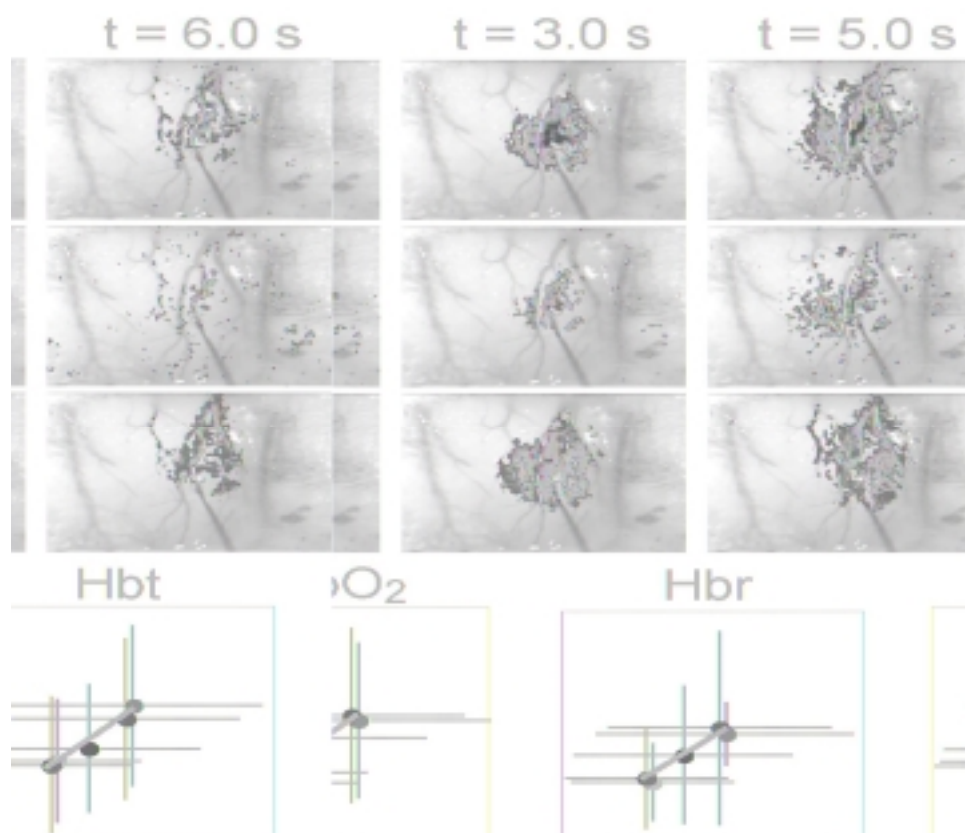
**Introduction.** Serotonergic dysfunction appears to be central to the development of depression, with increasing focus on the serotonin 1A (5-HT<sub>1A</sub>) receptor as a regulator of treatment response. The influence of age on the 5-HT system may also contribute to the unique challenges of depression treatment in the elderly. We recently demonstrated reduced [<sup>11</sup>C]WAY100635 binding in the midbrain region of the 5-HT<sub>1A</sub> autoreceptor (dorsal raphe nucleus; DRN) in untreated depressed elders, reflective of depression severity. The aim of the current study is to evaluate this finding in a larger cohort, and to determine whether [<sup>11</sup>C]WAY100635 binding is altered by and related to the success of antidepressant pharmacotherapy. **Methods.** [Carbonyl-<sup>11</sup>C]WAY 100635 PET was acquired prior to initiation of therapy in 21 patients with untreated (non-psychotic, non-bipolar) major depression (6M:15F; mean age:71.7±5.7), and 17 healthy control subjects (8M:9F; mean age:69.5 ± 6.7). Patients were subsequently treated with paroxetine as part of a clinical trial. PET imaging was repeated 6 weeks later in a subset of 8 patients (2M:6F; mean age:73.9 ± 3.9). Treatment response was reflected by a time to remission measure (i.e., time required to reach a Hamilton Depression Rating (HDR) score of 7 by weekly testing. Dynamic arterial blood sampling was performed over 60 min of emission scanning (ECAT HR+, 15 mCi; 90 min data was available in 7/8 pre/post treatment patients and 14 controls). Both compartmental (C) and Logan graphical (L) analyses (GLLS smoothing [1]) were used. Regional binding potential (BP) measures for DRN, mesial temporal cortex and prefrontal regions were determined by subtraction of the reference (cerebellum; CER) distribution volume (DV): BP=[DVROI - DVCER]. Data were corrected for cerebral atrophy using an MRI-based method. **Results.** Baseline [<sup>11</sup>C]WAY 100635 BP was significantly reduced in the DRN in depressed relative to control subjects for both analysis methods (C: patients 2.23 ± 0.83, controls 3.69 ± 1.56, p=0.001; L: patients 2.37 ± 1.00, controls 3.91 ± 1.42; p=0.0004). In patients, DRN BP demonstrated a significant inverse relationship with pre-treatment Hamilton Depression Rating scores (C: r = -0.62, p = 0.001; L: r=0.59, p=0.006), but not with time to remission. (C: r = -0.39, p =ns; L: r=0.23, p =ns). CER DV was lower in patients (0.56 ± 0.12) relative to controls (0.68 ± 0.22; p=0.04). There was no significant difference in regional BPs between pre- and post-treatment data in the 8 patients who underwent 2 scans. We observed no significant relationship between pre/post change in BP and time to remission, and post-treatment DRN BPs (C: 2.36 ± 1.26; L: 2.29 ± 0.81) remained reduced relative to controls (p<0.05). **Conclusion.** Our finding of decreased [<sup>11</sup>C]WAY100635 DRN binding in elderly depressed patients supports evidence of altered autoreceptor function in depression. These data, however, do not support a consistent influence of SSRI treatment on 5-HT<sub>1A</sub> receptor binding, or a relationship between PET measures of 5-HT<sub>1A</sub> binding and treatment response. (Supported by MH01210, MH59945, MH64625, MH43832, MH59769, MH01684, MH52247) [1] Logan J et al., J Cereb. Blood Flow Metab. 21: 307-320 (2001)

## SPATIOTEMPORAL EVOLUTION OF FUNCTIONAL HEMODYNAMIC CHANGES AND THEIR RELATIONSHIP TO NEURONAL ACTIVITY

Sameer Sheth, Michael Guiou, Arthur W. Toga

*Laboratory of Neuro Imaging, UCLA School of Medicine, Los Angeles, CA, USA*

Brain imaging techniques such as fMRI have provided important information about brain organization, but their ability to investigate fine-scale functional architecture is limited by the spatial specificity of hemodynamic responses. We investigated the spatiotemporal evolution of hemodynamic responses in rat somatosensory cortex. We combined the advantages of optical intrinsic signal imaging and spectroscopy to produce high-resolution two-dimensional maps of functional changes in tissue oxygenation and blood volume. CBF changes were measured with laser Doppler flowmetry, and simultaneously recorded field potentials allowed comparison between hemodynamic changes and underlying neuronal activity. For the first 2-3 seconds of activation, hemodynamic responses overlapped in a central parenchymal focus (Fig.1). Over time, CBV changes propagated retrograde into feeding arterioles, and oxygenation changes anterograde into draining veins. By 5-6 seconds, responses localized primarily in vascular structures distant from the central focus. The peak spatial extent of the hemodynamic response increased linearly with synaptic activity (Fig.2). This spatial spread may be due to lateral subthreshold activation or passive vascular overspill. These results imply early microvascular changes in volume and oxygenation localize to activated neural columns, and that spatial specificity will be optimal within a 2-3 second window following neuronal activation.



## CEREBRAL GABA DECREASE IN PATIENTS WITH SCHIZOPHRENIA MEASURED BY 1H MR CHEMICAL SHIFT IMAGING OF GABA

In-Young Choi<sup>1</sup>, Sang-Pil Lee<sup>1</sup>, Jun Shen<sup>2</sup>, Daniel C. Javitt<sup>3</sup>

<sup>1</sup>*Medical Physics, The Nathan Kline Institute, Orangeburg, NY, USA*

<sup>2</sup>*NIMH, NIH, Bethesda, MD, USA*

<sup>3</sup>*Cognitive Neuroscience and Schizophrenia, The Nathan Kline Institute, Orangeburg, NY, USA*

Introduction: GABA, the primary inhibitory neurotransmitter in the human brain, plays a pivotal role in normal brain function and energy metabolism [1]. Increasing evidence suggests that altered GABAergic function is involved in many neurological and psychiatric disorders, including schizophrenia. However, the regional alterations of cerebral GABA content in patients with schizophrenia, where the etiologic role of GABA has been proposed, have not been reported to date in the living human brain by in vivo GABA measurement using 1H GABA chemical shift imaging (CSI). Methods: Ten patients with a DSM-IV diagnosis of schizophrenia ( $32 \pm 10$  years old, mean  $\pm$  SD) and nine closely age-matched healthy control subjects ( $31 \pm 10$  years old) were studied on a 3 Tesla. All patients were without any antipsychotics or antiepileptic medication or mood stabilizers, and no lifetime history of substance dependence that can influence endogenous GABA contents in the brain. For in vivo studies, T1-weighted high-resolution MRI scans were acquired to select region of interest. The 1H GABA CSI sequence is based on a single shot selective MQ filtering method [2, 3]. The CSI slice was positioned across the prefrontal to parietal regions. The MR parameters for GABA CSI were FOV= 18 x 18 cm, Slice thickness= 3 cm, 6 x 6 PE steps, nt= 10 – 12. In vivo GABA concentration was estimated by the external reference method using a phantom with known concentration of GABA. Statistical analysis was performed using a t-test. Results: A preliminary quantitative analysis of the GABA distribution in parietal regions showed a significant decrease of GABA contents in patients with schizophrenia ( $0.5 \pm 0.2$   $\mu\text{mol/g}$ , n = 10) compared to that in controls ( $0.7 \pm 0.2$   $\mu\text{mol/g}$ , n = 9), 35% decrease ( $p < 0.02$ ). The importance of this study can be appreciated in the context of the large body of evidence implicating GABAergic dysfunction in the pathophysiology and etiology of schizophrenia. Currently, most studies of GABAergic function in schizophrenia have been performed on postmortem tissues, which have found a selective reduction of GABAergic neurons in the schizophrenic brains. Since GABA anabolism is known to produce abnormal GABA levels during ischemia, GABA concentrations measured postmortem are significantly distorted. The value of measuring GABA level in postmortem studies to assess GABAergic dysfunction is therefore quite limited. In this study, we found reduced GABA concentration in the parietal region, which may reflect the loss of GABAergic neurons in that region. Conclusion: The concentration of GABA reflects the viability of GABAergic function and GAD, the GABA-synthesizing enzyme. The total concentration of GABA has also been found to correlate with GABA release. The non-invasive MR study provides the possibility to assess the GABAergic function through the measurement of GABA levels in vivo. This non-invasive spectroscopy method will also allow longitudinal study of GABAergic response to treatment. References: [1] Robert E. *Biochem Pharmacol* 23: 2637 (1974). [2] Shen J, et al. *MRM* 41: 35 (1999). [3] Choi IY, et al. *MRM* 51: 1115 (2004). Grant support: NIH grants 8R01EB00315 and R03AG022193.

## RELATIVE CBF ESTIMATION FROM THE KINETICS OF HYPERPOLARIZED XE-129 NMR SPECTROSCOPY

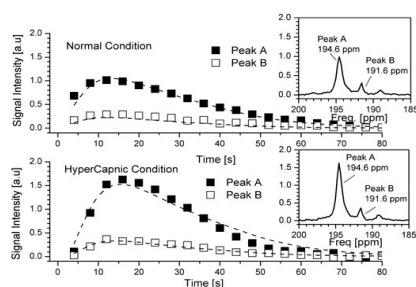
Kazuhiro Nakamura<sup>1,2</sup>, Jeff Kershaw<sup>1,2</sup>, Atsushi Wakai<sup>1,2</sup>, Yasushi Kondoh<sup>1</sup>, Hiroshi Sato<sup>3</sup>, Naoyuki Takei<sup>3</sup>, Iwao Kanno<sup>1</sup>

<sup>1</sup>Akita Research Institute of Brain and Blood Vessels, Akita, Japan

<sup>2</sup>Akita Industry Promotion Foundation, Akita, Japan

<sup>3</sup>GE Yokogawa Medical Systems, Hyogo, Japan

[Introduction] Hyperpolarized Xe-129 (HpXe) has the potential to be a new diffusible NMR tracer. Several uptake models have already been developed for estimating cerebral blood flow (CBF) from the kinetics of HpXe spectroscopy [1,2]. Nevertheless, a study during different CBF states has not been previously described. In this work, HpXe spectra were acquired from human volunteers while modulating the CBF with CO<sub>2</sub> inhalation. [Methods] Six healthy volunteers lay in a 1.5 T MR spectrometer. Each volunteer inhaled HpXe in both the normal and hypercapnic condition. Hypercapnia was induced by requiring the volunteer to inhale CO<sub>2</sub> gas (500 cc/min of pure CO<sub>2</sub>) mixed with room air for one minute prior to xenon inhalation. About 500 cc of HpXe supplied in a 1000cc Tedlar bag was connected to the inhalation mask with a 3-way cock for switching between HpXe and air. The volunteers turned the cock by themselves and quickly inhaled the HpXe, thereafter holding their breath for between 15 and 30 seconds. Spectra were acquired using a single hard-pulse acquisition sequence with a bandwidth of 8 kHz and the RF pulse centered at approximately 100 ppm from the gas peak. [Results] The figure shows the typical kinetics of two obvious peaks in HpXe spectra from a single volunteer. Each square denotes the acquired data and the dashed line is the fit calculated from an uptake model [2]. Two parameters, the longitudinal relaxation time within the alveoli (T<sub>1a</sub>) and the scaled magnitude (E<sub>f</sub>), were fitted to the data during the normal condition. Other parameters are fixed to values corresponding to the supposed origins of peaks A and B as gray and white matter, respectively. Since the gas polarization and inhaled volume were approximately the same for both experiments, the blood flow parameter is obtained by fitting the hypercapnic data using the same T<sub>1a</sub> and E<sub>f</sub> estimated from the normal condition. The estimated flow was 1.13 times larger than during the normal condition. The relative increase in the flow parameter during the hypercapnic condition was between 1.1 and 1.5 for all six volunteers. [Discussion] This is the first study to observe HpXe spectra from human brain after modulating CBF. The estimated relative increase in flow during the hypercapnic condition is comparable to values obtained in PET studies. The results strongly suggest that the CBF can be estimated from the kinetics of HpXe spectra. [Acknowledgments] This work was supported by the project of Japan Science and Technology Agency. [References] [1] Peled S., et al., Magn. Reson. Med., 36, 340-344, 1996 [2] Kilian W., et al., Magn. Reson. Med., 51, 843-847, 2004.



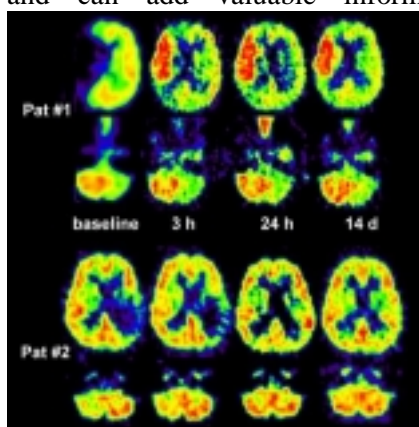
## CROSSED CEREBELLAR DIASCHISIS IN ACUTE HUMAN STROKE: A PET STUDY OF SERIAL CHANGES AND RESPONSE TO SUPRATENTORIAL REPERFUSION BY INTRAVENOUS THROMBOLYSIS

Jan Sobesky<sup>1,2</sup>, Alexander Thiel<sup>1,2</sup>, Karl Herholz<sup>1,2</sup>, Jobst Rudolf<sup>1</sup>, Wolf-Dieter Heiss<sup>1,2</sup>

<sup>1</sup>Department of Neurology, University Hospital of Cologne, Cologne, Germany

<sup>2</sup>Max-Planck-Institute for Neurologic Research, Cologne, Germany

**Background and Purpose:** Crossed cerebellar diaschisis (CCD) is well described in the subacute and chronic phase of stroke. However, there is few data about acute CCD and its serial changes after supratentorial reperfusion. Using positron emission tomography (PET) we (i) describe acute CCD in human MCA stroke; (ii) study time-dependent changes of CCD in relation to supratentorial reperfusion; (iii) describe its association to outcome parameters. **Methods:** Nineteen patients (8 female; mean age 67 years) with acute middle cerebral artery stroke received intravenous thrombolysis within 3 hours of symptom onset. Serial PET with 15O-water was performed before thrombolysis, 3 hours, 24 hours and 14 days later. CCD was defined as an asymmetry index. For supratentorial regions, the hypoperfusion volume (defined by the volume of CBF < 20 ml/100g/min) and the hypoperfusion asymmetry (defined by an asymmetry index) were assessed. Infarct volume at day 14 and NIHSS score at 3 months were used as outcome parameters. **Results:** Supratentorial hypoperfusion volume decreased from 25 ccm (median) before thrombolysis to 1.0 (3h), 0.2 (24h) and 0.1 (14 days). Baseline CCD was 13.4% and decreased continuously to 10.4% (3h), 9.9% (24h) and 6.1% (14 days). The NIHSS-score decreased from 11 (baseline) to 4 pts after 3 month. Final infarct volume was 1.1 ccm. CCD was not significantly associated to the severity of supratentorial hypoperfusion at any time point. CCD was significantly correlated to the volume of supratentorial hypoperfusion within the first hours after stroke (Spearman's rho,  $r=0.65$ ) but not later. Hypoperfusion volume was correlated to outcome parameters at the early stage only ( $r=0.68$ ). At later time points this association was lost since reperfusion was seen despite large final infarcts and poor outcome. In contrast, CCD correlated significantly to outcome values at all four measurements ( $r>0.7$ ). Patients with favourable outcome had lower CCD values and a marked decrease of CCD along the four measurements. Fig. 1 illustrates examples of successful reperfusion (Pat #2, no infarct) and non-nutritional reperfusion (Pat #1, 60 ccm infarct volume) **Conclusions:** These first PET data of serial CCD changes after intravenous thrombolysis within a three hour time window suggest that (i) CCD occurs as early as 3 h after stroke and recovers over time; (ii) in the first hours after stroke, CCD is closely related to the volume of supratentorial hypoperfusion. At later time points, however, CCD is partly disconnected from supratentorial perfusion and better associated to outcome parameters than the volume of supratentorial hypoperfusion itself; (iii) CCD is not susceptible to non-nutritional reperfusion and can add valuable information in order to interpret supratentorial reperfusion patterns.





## SIGNAL TO CONCENTRATION PROPORTIONALITY CONSTANTS FOR DYNAMIC CONTRAST T2\* MRI CEREBRAL BLOOD VOLUME MEASUREMENTS

George C. Newman<sup>1,2</sup>, Frank E. Hospod<sup>1</sup>, Howard A. Rowley<sup>2</sup>, Kari A. Pulfer<sup>2</sup>,

Sean B. Fain<sup>3</sup>

<sup>1</sup>*Department of Neurology, University of Wisconsin, Madison, WI, USA*

<sup>2</sup>*Department of Radiology, University of Wisconsin, Madison, WI, USA*

<sup>3</sup>*Department of Medical Physics, University of Wisconsin, Madison, WI, USA*

**Introduction:** Cerebral blood volume (CBV) measurements by T2\*-weighted dynamic contrast MRI requires an accurate determination of the ratio of gadolinium (Gd) in brain to that in blood. For example, the equation for calculating CBV after a Gd bolus includes the ratio of  $K(\text{tissue}) / K(\text{artery})$ , the proportionality constants relating signal change to Gd concentration in tissue and artery. Although, it is standard to assume that the ratio  $K(\text{tissue}) / K(\text{artery}) = 1$ , this may not be valid since  $K$  is dependent on Gd concentration and TE, as well as velocity and orientation. Fortunately, it is not necessary to know either constant but only their ratio. Because tissue and artery proportionality constants relating signal change to concentration for CT are independent of these factors, it can be shown that the ratio of CBV measurements made with identical kinetic paradigms by CT and MRI yields an experimental value for the ratio  $K(\text{tissue}) / K(\text{artery})$  needed for MRI. **Methods:** 10 volunteers completed MR and CT perfusion studies within two hours. MR studies (GE 1.5T Signa) used a bolus (70  $\mu\text{mol/kg}$  Omniscan®, TR1150/TE35, 12 slices, 5mm) and an infusion (180  $\mu\text{mol/kg}$  over 90 sec, 2500/35, same slices). CT studies (GE CTI ultra-fast 4-slice scanner) also used a bolus (50ml bolus Omnipaque® at 5ml/sec, 40 frames, 4 slices, 5 mm) and an infusion (50ml at 1 ml/sec, same slices, 1sec interscan delay). CBV was calculated for 3 cortical, 4 deep gray and 3 white matter bilateral ROIs on all scans using custom MATLAB software. Area under the curve (AUC) was calculated by both non-parametric (npAUC) and parametric (pAUC, after gamma variate fitting) methods. CT to MRI ratios were determined in each ROI of each subject prior to calculating means or variance. **Results:** The CT / MRI (and hence  $K(\text{tissue}) / K(\text{artery})$ ) ratios are not different from 1 for any method in deep gray or white matter but are significantly different for cortex. The Infusion method consistently produced the CT / MRI ratios closest to 1, the least variability and the highest gray matter to white matter ratios. **Discussion:** The assumption of unity for the proportionality constants is acceptable for deep gray and white matter but not in cortex where “blooming” of signal from leptomeningeal vessels into the parenchyma appears to exaggerate CBV considerably. Measurement of CBV by infusion yields more consistent values than measurement by contrast bolus.

$$CBV_{MRI} = \frac{h K_{tissue} \int -\ln(S_{tissue}(t) / S_{t,0}) dt}{\rho K_{artery} \int -\ln(S_{artery}(t) / S_{a,0}) dt}$$

	Cortex	Deep Gray	White
<b>CBV by CT</b>			
npAUC	2.3 ± 0.4	2.5 ± 0.5	2.0 ± 0.7
pAUC	2.5 ± 0.5	2.6 ± 0.5	2.2 ± 0.7
Infusion	2.8 ± 0.4	2.9 ± 0.4	2.2 ± 0.4
<b>CBV by MR</b>			
npAUC	3.7 ± 1.2	3.2 ± 1.1	2.7 ± 0.9
pAUC	4.3 ± 1.3	3.6 ± 1.2	2.9 ± 1.1
Infusion	3.8 ± 0.5	3.1 ± 0.4	2.3 ± 0.2
<b>Ratio of CT/MR</b>			
npAUC	0.71 ± 0.27	0.91 ± 0.44	0.93 ± 0.43
pAUC	0.67 ± 0.25	0.84 ± 0.37	0.95 ± 0.36
Infusion	0.80 ± 0.16	0.97 ± 0.20	1.05 ± 0.22

All values are means ± standard deviation. CBV values are in ml/100 gm

**MODULATION OF MOTOR MEMORY FORMATION BY LEVODOPA IN HEALTHY SUBJECTS AND IN CHRONIC STROKE PATIENTS: A STUDY WITH 11-C-RACLOPRIDE PET**

**Agnes Floel**<sup>1,2</sup>, Gaetan Garraux<sup>3</sup>, Peter Herscovitch<sup>4</sup>, Stefan Knecht<sup>2</sup>, Leonardo G. Cohen<sup>1</sup>

<sup>1</sup>*Human Cortical Physiology Section, National Institute of Neurological Disorders and Stroke, NIH, Bethesda, MD, USA*

<sup>2</sup>*Department of Neurology and IZKF Münster, University of Münster, Germany*

<sup>3</sup>*Human Motor Control Section, National Institute of Neurological Disorders and Stroke, NIH, Bethesda, MD, USA*

<sup>4</sup>*Positron Emission Tomography Imaging Section, Clinical Center, NIH, Bethesda, MD, USA*

Background: Motor memory formation (MMF), the cortical reorganization that accompanies motor training, may play a beneficial role in motor learning and in the functional recovery that follows injury to the central nervous system. However, MMF decreases with age. Dopaminergic activity, which contributes to motor learning and plasticity, experiences a similar decline with natural aging. The purpose of the present study was 1) to determine if pre-medication with levodopa restores MMF in the elderly to levels documented in younger individuals, 2) to evaluate if levodopa pre-medication leads to increased dopamine release in the dorsal striatum during training, as assessed by 11-C-raclopride PET (D2 receptor imaging), and 3) to compare patterns of dopamine release under levodopa pre-medication in normal volunteers and stroke patients. Methods: Transcranial magnetic stimulation (TMS) was employed to quantify MMF. Eight healthy elderly volunteers and 3 chronic stroke patients underwent two 11-C- raclopride PET sessions, following the administration of either levodopa or placebo. During each session, the subjects performed 30 minutes of motor training with their dominant hand (normal volunteers) or their paretic hand (stroke patients). Baseline and activation raclopride binding potentials (BPs) were assessed for ROIs in the striatum bilaterally for each session. Results: None of the elderly subjects showed significant MMF with training alone. Levodopa administration led to (a) an increase in training-dependent dopamine release in the contralateral striatum in healthy volunteers and in the ipsilateral striatum in the patient group and (b) an increase in the magnitude of MMF. Conclusions: 1) Motor training after levodopa pre-medication significantly increases dopamine release during training in the dorsal striatum, compared to the placebo condition. 2) Increased magnitude of MMF in healthy volunteers with levodopa pre-medication is associated with increased release of dopamine in the contralateral striatum during training, indicating that dopamine release may be a crucial factor in the development of MMF. 3) In stroke patients, motor training after levodopa-premedication also leads more striatal dopamine release. However, the increase in dopamine release is much larger in the ipsilateral (contralesional) dorsal striatum. This finding suggests recruitment of contralesional resources after stroke, possibly contributing to recovery of function. We are currently scanning additional subjects to substantiate these results.

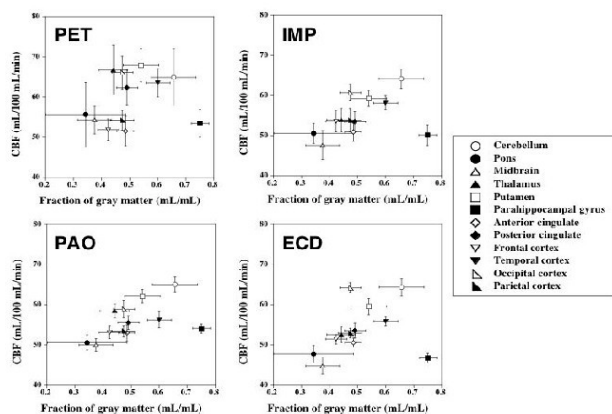
**NORMAL DATABASE OF CEREBRAL BLOOD FLOW MEASURED BY SPECT WITH I-123-IMP, TC-99M-HMPAO, AND TC-99M-ECD AND PET WITH O-15 LABELED WATER IN HUMANS: COMPARISON WITH VOXEL-BASED MORPHOMETRY**

Hiroshi Ito<sup>1</sup>, Kentaro Inoue<sup>1</sup>, Ryoji Goto<sup>1</sup>, Ken Okada<sup>1</sup>, Shigeo Kinomura<sup>1</sup>, Yasuyuki Taki<sup>1</sup>, Kazunori Sato<sup>1</sup>, Tachio Sato<sup>1</sup>, Iwao Kanno<sup>2</sup>, Hiroshi Fukuda<sup>1</sup>

<sup>1</sup>*Department of Nuclear Medicine and Radiology, Institute of Development, Aging and Cancer, Tohoku University, Sendai, Japan*

<sup>2</sup>*Department of Radiology and Nuclear Medicine, Akita Research Institute of Brain and Blood Vessels, Akita, Japan*

**Introduction:** Three accumulative tracers, I-123-IMP, Tc-99m-HMPAO, and Tc-99m-ECD were widely used to measure cerebral blood flow (CBF) in single-photon emission computed tomography (SPECT). In the present study, normal database of CBF measured by three SPECT tracers were built and compared with regional distribution of CBF measured by positron emission tomography (PET) with O-15 labeled water. The regional distribution of tissue fraction of gray matter determined from magnetic resonance (MR) images by using voxel-based morphometry (VBM) technique was also compared with CBF distributions. **Methods:** Total 59 healthy subjects were recruited (47-71 years of age). SPECT studies with I-123-IMP, Tc-99m-HMPAO, and Tc-99m-ECD were performed on 11, 20, and 17 subjects, respectively. PET studies were performed on 11 subjects. MR imaging studies for VBM were performed on 43 subjects who had SPECT study. All SPECT, PET, and MR images were transformed into the standard brain format using the SPM2 system. The radioactivities of each SPECT and PET image were globally normalized to 50 mL/100 mL/min. Gray matter, white matter, and cerebrospinal fluid images were segmented and extracted from all transformed MR images by VBM methods in the SPM2 system. **Results:** Differences in regional distribution of SPECT tracers as compared with O-15 labeled water were observed in the pons, mid brain, thalamus, putamen, parahippocampal gyrus, posterior part of cingulate gyrus, temporal cortex, and occipital cortex. No significant correlations were observed in all relations between tissue fraction of gray matter determined by VBM analysis and CBF values of PET or SPECT for all regions-of-interest. In particular, smallest CBF values per gray matter fraction were observed in hippocampal region. **Conclusions:** Differences in regional distribution of SPECT tracers were considered to be mainly caused by differences in the mechanism of retention of tracers in brain. Regional distribution of CBF was independent on regional distribution of gray matter, resulting in that the blood flow per gray matter volume were various for each brain region.



## TRANSFER RATE INDEX AS A NEW PARAMETER OF [<sup>201</sup>Tl]-SPECT IN BRAIN TUMORS

Yoshihiro Tohyama

*Department of Neurosurgery, Municipal 2nd Hospital of Otaru, Otaru, Japan*

Introduction 201Tl-SPECT has been useful for imaging of brain tumors, especially for malignant gliomas and metastatic brain tumors. It is known that 201Tl is taken up by tumor cells through Na-K ATPase and Na-K-2Cl-cotransport with the biologic behavior of 201Tl as a potassium analog. A new parameter of 201Tl-SPECT, transfer rate index, reflecting the unidirectional transfer into normal brain or tumor tissue is presented to evaluate intra tissue uptake of 201Tl. Patients and methods Twenty-one patients with intracranial lesions (10 malignant gliomas, 6 patients with 8 metastatic brain tumors, 2 meningiomas, 2 brain abscesses and 1 malignant lymphoma) received a dose of 111MBq of 201TlCl i.v. as a bolus. SPECT was initiated 10 min (early) and 3 h (delayed) after the injection using a three-head gamma camera (GCA-9300A/DI, TOSHIBA, Japan). The mean counts in ROIs placed over lesions (Ct), contralateral normal brain (Cn) and sagittal sinus (Ca) were measured from early and delayed SPECT images respectively. The Ct/Ca or Cn/Ca was assumed as the volume of distribution (DV) in lesions or normal brain. A time ( $\theta$ ) reflecting exposure time was calculated from Ca and median scanning time ( $t_1$ ; early,  $t_2$ ; delayed) of each SPECT. The slope of relationship between DV and  $\theta$  measured from the two points of early and delayed SPECT was defined as the transfer rate index in lesions (Kt) and normal brain (Kn). The transfer rate index ratio was applied as Kt/Kn. Retention index was also calculated as [Ct/Cn of early SPECT]/ [Ct/Cn of delayed SPECT] ratio. Results Transfer rate index in normal brain (Kn) was  $0.14 \pm 0.02$  (n=21) and tended to decrease with age. Transfer rate index in the lesions (Kt), transfer rate index ratio (Kt/Kn) and retention index in various lesions are shown in Table. Kt/Kn in benign lesion (meningioma and brain abscess) was under 1.0. Kt, Kt/Kn and retention index in malignant lesions (malignant gliomas, metastatic brain tumors and malignant lymphoma) were higher than those in benign lesion. Kt and Kt/Kn were highly sensitive especially in malignant gliomas. Comments The present study has provided a new parameter in 201Tl SPECT, transfer rate index, for evaluation of intra tissue uptake of 201Tl. The transfer rate index could be a good indicator for differentiating brain tumor and malignancy grading of the tumor. References 1) Taki S, Kakuda K, Kakuma K, et al., Nucl Med Commun. 20(7):637-45, 1999 2) Bradbury MW, Kleeman CR, Am J Physiol. 213(2):519-28, 1967 3) Patlak CS, Blasberg RG, Fenstermacher JD, J Cereb Blood Flow Metab. 3(1):1-7, 1983 4) Gehring PJ, Hammond PB, J Pharmacol Exp Ther. 155(1):187-201, 1967

Transfer rate index in the lesions (Kt), Transfer rate index ratio (Kt/Kn) and Retention index in various lesions

	Kt	Kt/Kn	Retention index
Malignant glioma(n=10)	0.39 ± 0.12	2.90 ± 1.00	0.81 ± 0.15
Metastasis(n=8)	0.17 ± 0.08	1.09 ± 0.49	0.60 ± 0.11
Meningioma(n=2)	0.13	0.95	0.48
	-0.67	-6.51	0.39
Asscess(n=2)	0.10	0.76	0.65
	0.02	0.18	0.36
Malignant lymphoma(n=1)	0.17	1.91	0.80

Mean ± S.D.

## CORRELATION OF FDG ACCUMULATION IN THE FRONTAL CORTEX WITH FRACTIONAL ANISOTROPY IN THE FRONTAL WHITE MATTER FIBER TRACTS

Kentaro Inoue<sup>1</sup>, Hiroshi Ito<sup>1</sup>, Shigeo Kinomura<sup>1</sup>, Ken Okada<sup>1</sup>, Masatoshi Ito<sup>2</sup>,  
Hiroshi Fukuda<sup>1</sup>

<sup>1</sup>*Department of Nuclear Medicine and Radiology, IDAC, Tohoku University, Sendai, Japan*

<sup>2</sup>*CYRIC, Tohoku University, Sendai, Japan*

**Introduction:** Activity in neural cells is coupled with glucose metabolism. Neural function of signaling are carried out by interconnection of neurons via neuronal fibers. Diffusion-tensor imaging (DTI) is recently becoming an established technique that allows in vivo visualization of white matter fiber tracts by measuring the anisotropy of water molecular diffusion. Several studies focusing on normal aging reported significant reduction in fractional anisotropy (FA) in the corpus callosum, deep and subcortical white matter. The purpose of this study was to examine whether degradation of microstructure of fiber tracts in the elderly was associated with change in the glucose metabolism in the cerebral cortex measured with 18F-FDG-PET. **Methods:** Sixteen healthy volunteers (male 11, female 5, age 73.3±2.3 yr) participated. A 10 min emission scan was performed with a SET2400W scanner from 45 min after the injection of 211±31 MBq of 18F-FDG. MRI measurement was performed using a Symphony 1.5T system. A volumetric T1-weighted image (T1WI) was acquired using a MPRAGE sequence. DTI was acquired using a single-shot diffusion-weighted echo planar imaging with six sets involving diffusion gradients placed along non-collinear directions ( $b = 1000$  seconds/mm<sup>2</sup>) and another set without diffusion weighting ( $b = 0$ ). A FA image was created using Dr. View/LINUX software. We placed regions of interest (ROI) using MRICro software on the splenium and genu of the corpus callosum, the deep white matter in the right (RFr) and left (LFr) frontal lobe on each FA image. Using SPM2 software, all PET images were anatomically normalized and globally normalized. Statistical analysis was performed using FA for each ROI as a covariate, and thresholded at  $P < 0.05$  (corrected). We also performed morphometric analysis of gray matter (GM), created by segmentation of the T1WI, to examine if there was GM atrophy that would explain correlation of 18F-FDG accumulation with FA. **Results:** FA for each ROI were; 0.70±0.056 in the splenium, 0.64±0.058 in the genu, 0.27±0.032 in the RFr, and 0.26±0.032 in the LFr, respectively. There was no statistically significant correlation of FA with age. We did not found statistically significant correlation of the GM concentration with FA, as well as with age. On the other hand, we found statistically significant positive correlation of 18F-FDG accumulation in the anterolateral frontal cortex bilaterally with FA of the genu of the corpus callosum, and in the posterior prefrontal cortex bilaterally, the right anterolateral prefrontal cortex and the left superior temporal cortex, with FA of the deep white matter of the right frontal lobe. There was no age effect in FDG accumulation. **Conclusion:** 18F-FDG accumulation in cortical areas was correlated with FA in the genu of the corpus callosum, and in the deep white matter of the right frontal lobe, without correlation with GM atrophy. The results suggest that neuronal activity in the cortex decreases with deterioration in microstructure of the fiber tracts, which could connect those cortical neurons with others, without causing significant GM atrophy.

## CHANGES IN THALAMIC BLOOD FLOW CAUSED BY SUBTHALAMIC DEEP BRAIN STIMULATION IN PARKINSON'S DISEASE

Kenichi Yamamoto, Atsushi Umemura, Kazuo Yamada

*Department of Neurosurgery and Restorative Neuroscience, Nagoya City University  
Graduate School of Medical Science, Nagoya, Japan*

Purpose: Recently, deep brain stimulation(DBS) of subthalamic nucleus(STN) has been highlighted as treatment of Parkinson's disease(PD). DBS produces a functional lesion in the brain and reduces activity of a focal area as well as ablative procedure. In PD, increased excitatory activity of the STN abnormally activates the internal portion of the globus pallidus(Gpi), which inhibits activity of several thalamic nuclei. The reduced thalamic activity is associated with the hypokinetic symptom of PD. Therefore, reducing the overactivity of STN by stimulation might have a considerable clinical effect in PD. In this study, we investigated the effect of STN DBS on thalamic blood flow in patients with PD. Methods: Six patients with intractable PD who underwent bilateral STN DBS were examined. Regional blood flow(rCBF) at rest was measured with perfusion SPECT in both states of stimulation-on and stimulation-off. The motor unified Parkinson's disease rating scale and Hohen and Yahr disability scale were used to evaluate the clinical condition in each state. Three-dimensional stereotactic surface projections(3D-SSP) was used to evaluate changes in thalamic blood flow by STN stimulation. The statistical difference was determined by two-sided paired t test(Stat 1tZ software). Difference with Z-score $\geq$ 1.64 was considered significant. Result: All patients showed significant improvement in motor function by STN stimulation. Bilateral STN stimulation significantly increased thalamic rCBF bilaterally in 2 patients and unilaterally in 3 patients. Conclusion: Increase of thalamic rCBF by STN DBS seems to be caused by disinhibition of thalamus, which may contribute to significant improvement of clinical symptoms in PD.

## DEPENDENCE OF THE HEMODYNAMIC RESPONSE TO FUNCTIONAL ACTIVATION ON THE CO<sub>2</sub>-INDUCED VASODILATION

Bojana Stefanovic, Jan M. Warnking, Karin M. Rylander, G. Bruce Pike

*McConnell Brain Imaging Centre, Montreal Neurological Institute, Montreal, QC, Canada*

Due to its potential to confound the interpretation of BOLD fMRI studies and its significance for the understanding of the biophysical mechanism of BOLD, the effect of the baseline on the activation-induced BOLD response has attracted renewed interest. For small perturbations from rest, published data have supported an additive BOLD signal model, with constant percent changes in BOLD signal irrespective of the resting CBF [1,2]. We investigated the effect of pronounced CO<sub>2</sub> induced dilation on both BOLD and CBF responses to functional activation. A 1x1x1mm<sup>3</sup> 3D T1-weighted GRE sequence (TR/TE of 22/10ms) was followed by interleaved 6-slice PASL and T2-weighted GRE sequences (4x4x5mm<sup>3</sup>; TR: 1.5s, TE: 22/50ms for CBF/BOLD) on a 1.5T Siemens Sonata. Twelve volunteers (7F, 5M; 27±1yrs) performed bilateral finger tapping at low (1.5Hz) or high (3Hz) frequency while presented with a radial yellow/blue checkerboard at low (50%) or high (100%) contrast alternating with rest and uniform grey baseline in 0.5/1.5/1min off/on/off blocks. Three levels of hypercapnia were induced by administering mixtures of CO<sub>2</sub> and air, with the inspired CO<sub>2</sub> of 5, 7.5 or 10% in 1/3/2min blocks. Two functional blocks (low/high in randomized order) preceded each hypercapnia block; with another “high” functional block applied during either first or second half of the hypercapnic period. A reference grey matter region (GRONI) not participating in either motor or visual processing was used to correct the activation induced changes during hypercapnia periods for temporal instability in the hypercapnia induced responses. A typical set of BOLD and CBF time courses, in MC ROI, VC ROI, and GRONI, is shown in Fig. 1a and b. When controlling for inter-subject variability, the effect of hypercapnia on the activation-induced response was significant for both BOLD ( $p < 10^{-6}$ ) and CBF ( $p < 10^{-4}$ ). The linear fits to activation-induced responses as a function of hypercapnia-induced changes are shown in Fig. 2. In view of the slope estimates ( $-0.32 \pm 0.01$  %/% for BOLD MC, VC;  $-0.18 \pm 0.02$  %/% for CBF MC and  $-0.13 \pm 0.01$  %/% for CBF VC), only the effect of hypercapnia on BOLD bears practical significance on this range of basal vasodilation. We observed a significant drop of activation-induced BOLD response magnitude with increasing basal flow levels, in accordance with the BOLD response models, whereby a significant drop in the basal deoxyhemoglobin concentration decreases its sensitivity to CBF increases. A very limited effect of the basal vasodilation on the relative CBF response is consistent with the existing literature [3] and testifies to the nature of CBF regulation following functional activation. These findings characterize the behavior of BOLD response for significantly elevated basal flow and describe the non-linear regime of the deoxyhemoglobin dilution model. [1] Corfield, NI, 13(6):1207-11, 2001. [2] Hoge, ISMRM, 1737, 1999. [3] Brown, JCBFM, 23:829-837, 2003.

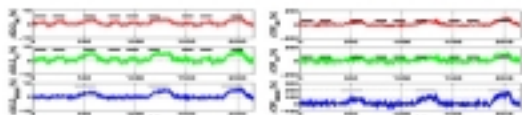


Fig. 1 Time courses of BOLD (MC) and CBF (VC) in MC (left) and VC (right) regions, and GRONI (blue).

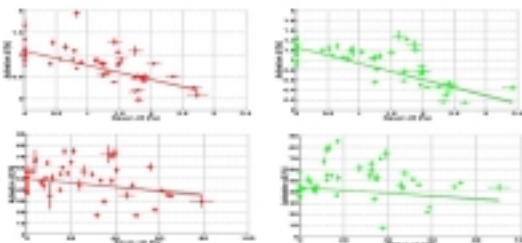


Fig. 2 The activation-induced responses (BOLD and CBF) in MC (left) and VC (right) regions vs. hypercapnia-induced signal changes for BOLD (top) and CBF (bottom).



## THE SPATIAL DEPENDENCE OF THE POST-STIMULUS UNDERSHOOT AS REVEALED BY HIGH RESOLUTION BOLD AND CBV WEIGHTED FMRI

Essa Yacoub, Kamil Ugurbil, Noam Harel

*University of Minnesota, Center for Magnetic Resonance Research, Minnesota MN, USA*

Increases in neural activity in the brain are followed by increases in cerebral blood flow (CBF), blood volume (CBV) and oxygen metabolism (CMRO<sub>2</sub>), which can be observed via the BOLD signal. It has been suggested that changes in CBV are slower both at the onset of the stimulus and the return to baseline once the stimulus is off. In addition, when the stimulus is off, there is an uncoupling between CBF and CBV, with the CBF returning to baseline quickly, resulting in the post-stimulus undershoot in the BOLD signal. A recent study showed evidence for sustained increases in CMRO<sub>2</sub> after the vascular response had fully recovered to baseline. These data suggest that the post-stimulus undershoot in the BOLD signal should be attributed to oxygen metabolism, and not delayed CBV changes, which were shown to return to baseline quickly. In our study, we investigated the spatial-temporal dynamics of CBV and the BOLD response, using a high spatial resolution cat model at 9.4 T. We used a visual stimulus consisting of binocular high-contrast square-wave moving gratings (0.15 cyc/deg, 2 cyc/s) and a coronal slice perpendicular to area 18 for the functional study. The GE BOLD response and GE CBV-weighted changes, following a bolus injection of MION (10mg Fe/kg), were both measured. The scan time for 1 image was 4 s and the spatial resolution was 150 x 150 x 2000  $\mu\text{m}^3$ . Following the MR session, a 3 mm cortical slab corresponding to the imaged plan was extracted and sectioned with a 15 $\mu\text{m}$  slice thickness with a cryostat and was stained with cresyl violet (Nissl) to determine the borders between layers. Functional time courses were generated by selecting ROIs in the tissue (layer IV) area as well as in the surface vessel areas and averaged over all cats. Figure 1 shows the temporal profiles of BOLD and CBV-weighted signals changes as a function of spatial location. The BOLD response showed the post-stimulus undershoot, similarly in both the tissue and large vessel areas, despite a larger positive BOLD signal in the vessel areas. In contrast, CBV temporal profiles were spatially dependent. In the tissue region, a sustained response is observed after the stimulus is off whereas the CBV response in the large vessel areas returns to baseline almost immediately after the stimulus is off. Our findings suggest that in the tissue, the BOLD post-stimulus undershoot must be in part explained by the sustained and elevated CBV response, however, there still may be contributions from elevated CMRO<sub>2</sub> levels. In the vessel areas the data suggests that the undershoot must come from either sustained CMRO<sub>2</sub> effects in the tissue which drain into the vessels, and/or decreases in CBF (without significant changes in CBV). Changes in CBV, CBF, and CMRO<sub>2</sub> may explain the post-stimulus undershoot; however, the contribution of each to the BOLD signal is spatially dependent.

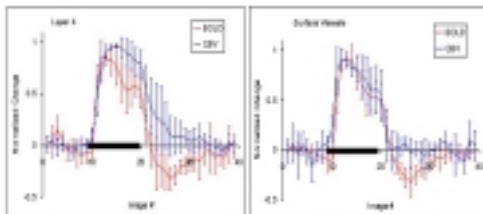


Fig 1 Average time courses of normalized change from 4 cats in layer 4 and surface vessel areas for both the BOLD and GE CBV-weighted signals. The black bar indicates stimulus.

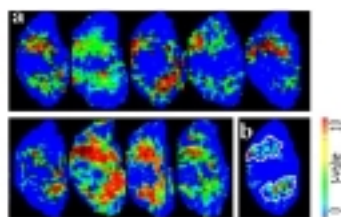
## THE INTRA AND INTER-SUBJECT REPRODUCIBILITY OF RODENT OLFACTORY BULB ACTIVITY MAPS MEASURED WITH fMRI

James R.A. Schafer<sup>1</sup>, Ikuhiro Kida<sup>2</sup>, Fuqiang Xu<sup>2</sup>, Douglas Rothman<sup>2</sup>, Fahmeed Hyder<sup>2</sup>

<sup>1</sup>*Department of Neuroscience, Yale School of Medicine, New Haven, CT, USA*

<sup>2</sup>*Department of Diagnostic Radiology, Yale School of Medicine, New Haven, CT, USA*

The first processing center in the mammalian olfactory system is the olfactory bulb (OB), a structure in which ~2000 neuropil spheroids called glomeruli encode the input from ~1000 types of olfactory receptor neurons, each specific for a particular chemical feature. Many imaging modalities have been used to simultaneously assess the activity of many of these channels and have provided insight into the way in which volatile odorants are represented in the OB. However, there has been little evaluation of the functional differences between animals or the extent to which given animal's response is conserved over multiple trials. Here we have used high-resolution fMRI to quantitatively evaluate the similarity of patterns produced by the same subject to a repeated stimulus and to compare the responses of different subjects to the same stimulus. Male Sprague-Dawley rats under urethane anesthesia were stimulated with iso-amyl acetate or carvone (-) in this study. All data were acquired on a modified 7T Bruker Biospec. Imaging experiments were performed using fast low-angle single-shot (FLASH) gradient-echo sequence. T1-weighted FLASH anatomical images have resolution of 110x110x250  $\mu\text{m}^3$ . Each fMRI experiment contained a series of 24 T2\*-weighted FLASH images (resolution = 220x220x250  $\mu\text{m}^3$ ). The mean image of the pre-stimulation "baseline" images was subtracted from the "stimulation" images on a pixel-by-pixel basis to generate student t-maps, which were overlaid onto the corresponding anatomical images to locate the activated region in the OB. Activity maps of the entire glomerular layer were constructed with an algorithm that integrates the glomerular data from multiple slices. OB activity maps from the same subject were highly conserved from trial to trial using the odorant carvone (-) at the same concentration and exposure duration. A quantitative comparison of the fraction of pixels activated by both trials for multiple odorants yielded values from 48 to 60%. In contrast, there was more substantial variability when a given odorant was tested in multiple subjects. Figure one shows the response of multiple animals to an equivalent exposure of iso-amyl acetate. While there is considerable variability in the fraction of the OB involved and the intensity of that involvement (1a), when the images are equivalently scaled and averaged it becomes clear that there are certain shared regions of activity (1b). This is consistent with genetic studies in which olfactory receptor neuron projections vary greatly between individuals but still localize to broadly defined regions. In conclusion, the consistency of intra-subject patterns and the variability of inter-subject patterns suggest that the primary causes for variations in the responses to identical stimuli are neuroanatomical. These findings help to validate the use of fMRI in the study of olfaction and recommend caution in comparing patterns from different animals. Figure One: The activity patterns of iso-amyl acetate in multiple animals. Concentration, 4 mM; duration, 2 minutes. (a) the equivalently scaled patterns from nine OBs (b) the average pattern from eighteen OBs – white boundaries indicate the most highly conserved regions.



## STANDARDIZED CBF-SPECT IMAGING ON EC-IC BYPASS SURGERY FOR HEMODYNAMIC CEREBRAL ISCHEMIA

Jyoji Nakagawara<sup>1</sup>, Hidehiro Iida<sup>2</sup>, Sunao Mizumura<sup>3</sup>, Toshiaki Osato<sup>1</sup>, Kenji Kamiyama<sup>1</sup>, Hidehiko Nakamura<sup>1</sup>

<sup>1</sup>*Department of Neurosurgery and Stroke Center, Nakamura Memorial Hospital, Sapporo, Japan*

<sup>2</sup>*Department of Radiological Science, National Cardiovascular Center, Sapporo, Japan*

<sup>3</sup>*Department of Radiology, School of Medicine, Nippon Medical University, Tokyo, Japan*

Background and purpose: Recent Japanese EC-IC Bypass Trial (JET Study) showed that the EC-IC Bypass was beneficial for stroke prevention in patients with Stage2 hemodynamic cerebral ischemia determined by quantified CBF-SPECT imaging (1). Stratification of hemodynamic cerebral ischemia was essential for patients' enrollment in this trial. However, standardization of quantified stratification of hemodynamic cerebral ischemia using CBF-SPECT imaging has not been established yet. In this paper, we evaluated newly developed two CBF-SPECT analysis as standardized techniques for improving measurement accuracy and judgment accuracy. Methods: Twenty patients with atherothrombotic stroke were involved in this study. Using quantified CBF-SPECT imaging such as IMP-ARG method(2), Stage2 hemodynamic cerebral ischemia was defined as CBF in the affected MCA territories less than 80% of mean CBF of normal subjects and vascular reserve (VR) [(acetazolamide-activated CBF - Resting CBF) / Resting CBF×100%] less than 10%. For improving measurement accuracy, Dual table ARG (DTARG) analysis was developed to provide same-day quantification of both resting CBF and acetazolamide-activated CBF using split dose of CBF tracer (IMP) and common arterial input function. For improving judgment accuracy, segmental extraction estimation (SEE) analysis (3) was introduced to present resting CBF, acetazolamide-activated CBF, VR, and stratification of hemodynamic cerebral ischemia unfolded pixel-by-pixel on the standardized brain surface images using 3-dimensional stereotactic surface projections (3D-SSP) technique (4). Results: Using DTARG method, both resting and acetazolamide-activated CBF-SPECT could be quantified pixel-by-pixel using dual table look-up method without an error of different input functions. Stage2 hemodynamic cerebral ischemia in symptomatic hemisphere was easily detected in comparison with two-day quantification of both resting CBF and acetazolamide-activated CBF in all patients. Using SEE analysis, severity of hemodynamic cerebral ischemia could be estimated from stereotactic and quantitative viewpoints based on standardized vascular territories without an arbitrary ROI analysis. Territories of Stage2 hemodynamic cerebral ischemia were displayed in 3D-SSP views in all patients. Conclusion: Standardization of quantified stratification of hemodynamic cerebral ischemia using CBF-SPECT imaging will be important issue in decision-making of indication of EC-IC Bypass surgery for cerebral ischemia. Both DTARG method and SEE analysis could be clinically applied as standardized techniques to improve measurement accuracy and judgment accuracy. References: (1) JET Study Group. Surg Cereb Stroke (Jpn) 30: 97-100, 2002 (2) Iida H, et al. J Nucl Med 35: 2019-2030, 1994 (3) Mizumura S, et al. Ann Nucl Med 18: 13-21, 2004 (4) Minoshima S, et al. J Nucl Med 36: 1238-1248, 1995

## VOXEL-BASED MORPHOMETRY (VBM) ANALYSIS IN ALZHEIMER'S DISEASE AN INSIGHT INTO HETEROGENEITY OF CEREBRAL ATROPHY

Akihiko Shiino<sup>1</sup>, Toshiyuki Watanabe<sup>3</sup>, Ichiro Akiguchi<sup>3</sup>, Shigehiro Morikawa<sup>2</sup>, Toshiro Inubushi<sup>2</sup>, Masayuki Matsuda<sup>1</sup>

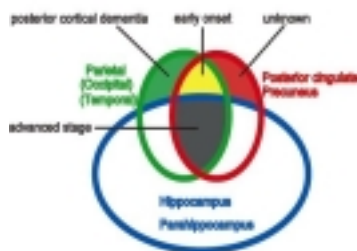
<sup>1</sup>Department of Neurosurgery, Shiga University of Medical Science, Ohtsu, Japan

<sup>2</sup>Molecular Neuroscience Research Center, Shiga University of Medical Science, Ohtsu, Japan

<sup>3</sup>Center of Neurological and Cerebrovascular Disease, Takeda Hospital, Kyoto, Japan

**Introduction:** Pathologic changes in Alzheimer's disease (AD) typically develop first in the transentorhinal regions of allocortex. The destructive process then spreads to the hippocampus, and eventually encroaches upon the neocortex. A recent study had shown that significant atrophy in the Pcing-Prec was observed in patients with early stage of AD and even in these with presymptomatic stage by using voxel-based morphometry (VBM) technique, which may raise a question as to whether pathological changes in these areas are involved in the early stage of AD. We studied to clarify this question, and have come to advocate a new hypothesis of subtype. **Subjects and Methods:** A total of 142 subjects was enrolled in this study. Twenty-six patients with AD and 12 patients with mild cognitive impairment (MCI) were recruited from specialized outpatient units. The diagnosis was based on thorough clinical, neuropsychological, and biological investigations, and all patients fulfilled the NINCDS-ADRDA criteria for probable AD. Since the criteria for amnesic MCI are not yet clearly established, we define MCI as the patients who have memory impairment beyond what is felt to be normal for their age but the MMSE score is over 24. Seventy-four healthy volunteers and 30 young volunteers were selected as control groups. The 3D T1-weighted MR images of the brain were obtained on a 1.5-T Signa Lx with a spoiled gradient-echo technique. For local-level analysis, we employed VBM methodology by SPM99 running on Medx software. We accepted a statistical threshold of  $p < 0.001$ . **Results:** Local decrease of gray matter volume with age was observed bilaterally in the operculum, insula, cingulate (mainly frontal cingulate), caudate nucleus, thalamus (anterior and medial parts), and hippocampus. When comparing the AD group to the age-matched control group, significant volume loss was observed in the parietal, hippocampal, internal orbitofrontal, and Pcing-Prec areas. We also studied the AD patients individually and classified into four groups according to the atrophic patterns; hippocampus, hippocampus plus parietal lobe, hippocampus plus Pcing-Prec area and Pcing-Prec area plus parietal lobe (Fig. 1). The onset age of the last group was significantly younger than the other three groups, but the MMS was not significantly different among these groups. The MCI group was composed of all subtypes except Pcing-Prec plus parietal type. **Discussion:** From our results we propose a hypothesis of "4 subtypes" in AD patients. Three of them basically conform to the Braak staging, that is, the initial pathological alterations develop in the transentorhinal and entorhinal regions. During progression of the disease, the affected areas would spread variously to the association cortices in these groups. On the other hand, the Pcing-Prec plus parietal type has distinctive features from the other. Patients in this group show significantly early onset and have relatively little volume loss in the medial temporal area. Atrophic process in the perisylvian and subcortical nuclei seemed to be basically influenced by aging.

A Concept Diagram of AD-subtype





## QUANTITATIVE TOMOGRAPHIC EVALUATION OF CEREBRAL PERFUSION WITH PERFUSION WEIGHTED MAGNETIC RESONANCE IMAGING IN THE PATIENT WITH MOYAMOYA DISEASE

Yoji Tanaka<sup>1,2</sup>, Tadashi Nariai<sup>2</sup>, Tsukasa Nagaoka<sup>3</sup>, Kiichi Ishiwata<sup>4</sup>, Michio Senda<sup>5</sup>, Kikuo Ohno<sup>2</sup>

<sup>1</sup>*Department of Neurosurgery, Soka City Hospital, Saitama, Japan*

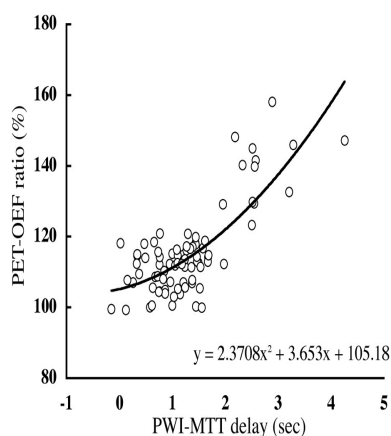
<sup>2</sup>*Department of Neurosurgery, Graduate School of Medicine, Tokyo Medical and Dental University, Tokyo, Japan*

<sup>3</sup>*Department of Physiology and Biophysics, Albert Einstein College of Medicine, New York, NY, USA*

<sup>4</sup>*Positron Medical Center, Tokyo Metropolitan Institute of Gerontology, Tokyo, Japan*

<sup>5</sup>*Department of Image Based Medicine, Institute of Biomedical Research and Innovation, Kobe, Japan*

**Background and purpose** Since various degrees of hemodynamic and metabolic abnormality and ischemic symptoms are observed in moyamoya disease patients, it is essential to identify the hemodynamic and metabolic status in these patients. In this study, we evaluated the accuracy of quantitative analysis and the ability for detecting misery perfusion by measuring perfusion weighted magnetic resonance imaging (PWI) in moyamoya disease patients. **Methods** Forty-one patients with angiographically defined moyamoya disease were studied with the use of PWI and positron emission tomography (PET) within a month interval of each other. The PWI data were calculated in two analytic methods, one was with deconvolution and the other was without deconvolution. Parametric tomographic axial images to express mean transit time (MTT), cerebral blood flow (CBF) and cerebral blood volume (CBV) was reconstructed. Data obtained on regions of interests (ROIs) among the anterior circulation was relatively expressed by using the data obtained from cerebellum as a control and compared with PET data respectively. The correlation between PWI-MTT and oxygen extraction fraction (OEF) by PET, or PWI-MTT and PET-CBV were also investigated. **Results** Parametric maps of PWI showed higher resolution than PET map, and indicated focal perfusion failure accurately. From the comparison with PET data, it was revealed that PWI data corresponded well with PET data (CBV, P value was <0.001 in each analytic method, MTT; P value <0.001). On the other hand, there were no significant correlation between PWI and PET data of CBF. From the comparison of PWI-MTT with PET-OEF, in the cerebral hemisphere, which MTT delay compared to cerebellum showed within around 2 seconds, the value of OEF ratio of did not exceed 120%. On the other hand, when MTT delay exceeded 2 seconds, OEF ratio accepted the tendency to begin to go up in proportion to the MTT delay. There was significant correlation between MTT delay and OEF ratio by PET ( $R=0.755$ ,  $r^2=0.606$ ,  $P<0.001$ ). This result may suggest that the existence and the grade of misery perfusion would be detectable by measuring PWI. **Conclusion** PWI measurement was sufficient to evaluate CBV and MTT quantitatively in patients with moyamoya disease. Of the various parameters, our results suggested that the degree of MTT delay could possibly be used to detect the existence and degree of misery perfusion.





## METHYLPHENIDATE-INDUCED CHANGES IN REGIONAL CEREBRAL BLOOD FLOW: A [15O]H<sub>2</sub>O PET STUDY IN HEALTHY VOLUNTEERS

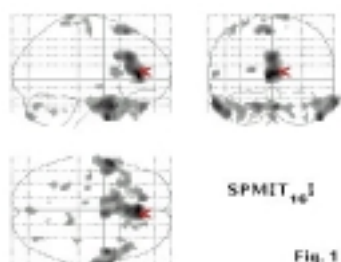
Joanna I. Udo de Haes<sup>1</sup>, Paul Maguire<sup>2</sup>, Anne M.J. Paans<sup>3</sup>, Piet L. Jager<sup>3</sup>, Johan A. den Boer<sup>1</sup>

<sup>1</sup>*Department of Biological Psychiatry, University of Groningen, Groningen, The Netherlands*

<sup>2</sup>*Department of Neurology, University Hospital Groningen, Groningen, The Netherlands*

<sup>3</sup>*PET Centre, University Hospital Groningen, Groningen, The Netherlands*

**Introduction** The dopaminergic system has been implicated in the pathogenesis and treatment of a variety of neuropsychiatric disorders, such as schizophrenia, depression and addiction. The (dys)function of the dopaminergic system may be studied by combining [15O]H<sub>2</sub>O PET with a dopaminergic drug challenge. With this approach, dopamine-induced changes in regional neural activity can be assessed in living subjects. In our study we were interested in the effect of methylphenidate (MP) induced increases in dopamine in healthy volunteers. In future studies, this method may be used to assess dopaminergic functional abnormalities in psychiatric patients. **Methods** Six healthy, right-handed, subjects participated in the study. On the day of the experiment, four [15O]H<sub>2</sub>O PET scans were made. The first two scans were made at 10 and 30 minutes after placebo injection and the following two scans at 10 and 30 minutes after MP (0.25 mg/kg i.v.) injection. The subjects were blind to the drug administered. During scanning, the behavioral condition of the subjects was standardized using a continuous performance task. Subjective ratings were obtained and blood samples were taken for growth hormone levels. The subjects were scanned using a Siemens ECAT Exact HR+ camera. Statistical Parametric Mapping (SPM99) was used for spatial transformation and statistical analysis. Contrasts were examined using paired t tests in a multiple-subjects design. The level of significance was set at  $p < 0.001$ , uncorrected for multiple comparisons. Clusters reaching a statistical threshold of  $p < 0.05$  (corrected for multiple comparisons) are presented. To investigate the prediction that the anterior cingulate (AC) was differentially activated in subjects with either high or low euphoria scores, we conducted a (multi-group) region of interest analysis using the marsbar toolbox (1). **Results** MP significantly elevated growth hormone levels. After receiving MP, the subjective experience varied from neutral to highly pleasurable. Ten minutes after MP administration, a significant increase in relative rCBF was found in the rostral AC, temporal poles, and the supplementary motor area (fig. 1). Significant reductions were seen in the superior temporal gyri, right medial frontal cortex and right inferior parietal cortex. At 30 minutes after MP administration, increases were seen in the AC, temporal pole and right cerebellum. No changes were observed in the striatum. The activation in the right rostral AC was significantly higher in the three subjects with the highest euphoria scores compared to the subjects with minimal MP-induced changes in euphoria. **Conclusion** The mood related increases in the rostral AC may be relevant with respect to previous studies that have shown the involvement of the (right) rostral AC in the pathogenesis of psychiatric disorders such as depression (2). We suggest that the combined MP challenge with functional imaging, as described in our study, may be a useful tool to study the functional integrity of the dopaminergic system in psychiatric disorders. 1. Brett M et al., *Neuroimage* 16: 497 (2002). 2. Mayberg HS et al., *Neuroreport*. 8(4):1057-61 (1997).





## CAUSE OF INCREASE IN SIGNAL INTENSITY IN T1-WEIGHTED IMAGES IN THE STRIATAL REGION AFTER GLOBAL ISCHEMIA

Yoshimasa Takeda, Hisami Aoe, Kiyoshi Morita

*Department of Anesthesiology, Okayama Univ. Med. School, Okayama City, Japan*

Introduction: Magnetic resonance (MR) imaging has been used to detect ischemic neuronal damage following cardiac arrest in the human brain. Although it has been reported that high signal intensity is observed in the striatum in vegetative patients on T1-weighted MR images at 1 – 2 weeks after ischemia insult, the cause of the increase in signal intensity in the striatal region after cardiac arrest has not been investigated. We hypothesized that phagocytic activity of microglia generates fatty degeneration in the striatum and that this results in an increase in the signal intensity in T1-weighted MR images. The present study was designed to determine the possible involvement of fatty degeneration of damaged neurons in the increase in signal intensity in the striatal region using global ischemia model in rats. Methods: Male Wistar rats were anesthetized with 1% halothane and were subjected to 20 minutes of 4-vessel occlusion. Five animals were used as sham controls. On day 1 (n=7), day 3 (n=7) or day 7 (n=7) after 4-vessel occlusion, rats were anesthetized with 1% halothane and were placed in a specially designed acrylic stereotaxic frame to obtain coronal T1-weighted MR images at the level of the striatum. T1-weighted imaging was performed using a 1.5 tesla unit with a 600-mm bore magnet equipped with an 85-mm (I.D.) detection coil. Images of 2 mm in section thickness were generated by a spin-echo sequence (repetition time of 500 msec and echo time of 15.0 msec). After obtaining MR images, each rat was immediately perfuse-fixed for histological evaluation. The frozen sections at the level of the striatum were double-stained with lectin and sudan black B for the detection of fatty degeneration and microglia, respectively. Results: On days 1 and 3, there were no apparent abnormalities in MR images or in histological findings in the striatal region. On day 7, however, T1-weighted MR images showed high signal intensity in the area corresponding to the striatum. T1 values in the striatal region were 480 ± 35, 483 ± 59, 492 ± 51 and 373 ± 32 msec in the sham control rats and in the rats on day 1, day 3 and day 7 after 4-vessel occlusion, respectively. In the same rats, histological observation revealed infiltration of microglia in which numerous fatty drops were observed in the cell body. There was a close relationship between the number of lectin-positive cells and the T1 value in the striatal region ( $R = 0.87$ ,  $p < 0.01$ ). Conclusions: The present study suggests that fatty degeneration of damaged neurons due to the phagocytosis of microglia plays an important role in the cause of the increase in signal intensity in T1-weighted MR images in the striatal region after global ischemia.

**CEREBROVASCULAR COLLATERALS AND MISERY PERFUSION IN PATIENTS WITH THE MIDDLE CEREBRAL ARTERY OCCLUSION: A COMBINED STUDY WITH PET AND ANGIOGRAPHY**

**Makiko Tanaka**<sup>1,2</sup>, Rishu Piao<sup>1,2</sup>, Naohiko Oku<sup>1</sup>, Yasuyuki Kimura<sup>1</sup>, Katsufumi Kajimoto<sup>1</sup>, Hiroki Kato<sup>1</sup>, Kazuo Kitagawa<sup>2</sup>, Masatsugu Hori<sup>2</sup>, Jun Hatazawa<sup>1</sup>

<sup>1</sup>*Division of Nuclear Medicine and Tracer Kinetics, Department of Diagnostic Medicine, Osaka University Graduate School of Medicine, Osaka, Japan*

<sup>2</sup>*Division of Stroke Research, Department of Internal Medicine and Therapeutics, Osaka University Graduate School of Medicine, Osaka, Japan*

**Background & Purpose:** Several longitudinal studies have demonstrated a significant association between increased oxygen extraction fraction (OEF) and a risk of subsequent stroke in symptomatic patients with occlusive cerebral artery disease [1, 2]. Elevated OEF and normal OEF were both observed in these patients. It is unclear which factors induce OEF change. We investigated an association between the collateral vasculature and elevation of OEF in patients with chronic middle cerebral artery (MCA) occlusion. **Methods:** We studied 13 patients with chronic ipsilateral MCA occlusion (9 symptomatic and 4 asymptomatic; 7 men and 6 women; mean age 57.6±11.3 years) who underwent a positron emission tomography (PET) study with O-15 steady-state inhalation method from April 2000 to December 2004. Collateral vasculature was evaluated by DSA (n=8) or MRA (n=5). The DSA or MRA was performed within 4 months before or after the PET study. We recorded (1) the side and the part of the MCA occlusion, (2) the occlusion or stenosis of the ipsilateral anterior cerebral artery (ACA) and the posterior cerebral artery (PCA), (3) the presence of the anterior and posterior communicating arteries (AcomA and PcomA, respectively), (4) the occlusion or stenosis of the contralateral major cerebral arteries, and (5) the occlusion or stenosis of the bilateral internal carotid arteries, the basilar artery, and the intracranial vertebral arteries, assessed by DSA or MRA. (6) The ipsilateral leptomeningeal collaterals were also evaluated in 8 patients by DSA. Since our normal population had OEF of 0.42±0.03, pathologically elevated OEF was defined as OEF 0.50 or more [3]. **Results:** The OEF of the ipsilateral MCA area was pathologically elevated in 4 patients and normal in 9 patients. All the patients with elevated OEF had a stenosis or occlusion in the collateral vasculature (ipsilateral ACA and PcomA). The MCA horizontal segment was not seen in the DSA. The patients with pathologically elevated OEF were all symptomatic. The patients with normal OEF (n=5) had well-developed leptomeningeal collaterals through ACA or PCA. The horizontal segment of occluded MCA was visualized retrogradely. **Conclusion:** The elevated OEF was specifically found in patients with MCA occlusion and co-existing multiple steno-occlusive lesions in the collateral vasculature. The vascular lesion other than occluded MCA may reduce cerebral perfusion pressure for collateral circulation. In patients with chronic MCA occlusion, the steno-occlusive lesion of collateral vasculature is one of the major factors to induce misery perfusion. **References:** [1] Grubb RL Jr., et al. JAMA 1998;280:1055-1060. [2] Yamauchi H, et al. J Neurol Neurosurg Psychiatry 1996;61:18-25. [3] Piao R, et al. Ann Nucl Med 2004;18:115-121.

**A COMPARISON OF FAIR AND CASL PERFUSION IMAGING IN MICE****Louise van der Weerd<sup>1</sup>, David L. Thomas<sup>2</sup>, Mark F. Lythgoe<sup>1</sup>, David G. Gadian<sup>1</sup>**<sup>1</sup>*RCS Unit of Biophysics, Institute of Child Health, London, UK*<sup>2</sup>*Medical Physics and Bioengineering, University College London, London, UK*

We present a quantitative comparison of continuous and pulsed spin labelling (CASL and FAIR respectively) in the mouse brain. The quantification of perfusion measurements is complicated by several physiological parameters such as the arterial transit time; also these parameters may change during abnormal conditions. The aim of this study is to compare the performance of the two sequences in mice, both for normal flow rates and during ischemia, when perfusion is low. Eight mice were anaesthetised and maintained on 1.3-1.7% isoflurane with 100% oxygen. The middle cerebral artery was occluded, and animals were scanned at 2 and 24 hours after occlusion. Coronal EPI images were obtained on a 2.35T SMIS MRI scanner. FAIR: Short repetition time FAIR sequence [1], non-selective inversion or a selective FOCI inversion pulse, delay time 1300 ms, TR 1.5 s, and 22 averages. CASL: transit time insensitive CASL [2], interleaved adiabatic inversion labelling and control measurements, post-labelling delay time 500 ms, TR 1 s, and 22 averages. T1sat and T1 were also measured. Data processing: 4 ROIs were selected in each animal for further analysis. FAIR: the ssIR data were used to fit M0, T1app and a. These values were then used to fit the magnetisation difference for CBF [1]. CASL: T1, T1sat and M0 were fitted using the IR data; subsequently these values were used to fit the magnetisation difference according to Alsop et al. [2] for CBF. FAIR was assumed to be transit time insensitive. For CASL: arterial transit time cortex 440 ms, basal ganglia 290 ms (previous results; data not shown). Transit time correction (see results): CASL: cortex 800 ms, basal ganglia 600 ms, based on previous rat studies [3]. FAIR: cortex 500 ms, basal ganglia 500 ms. For normal perfusion rates (>100 ml/100g/min) there was an excellent correlation between the CASL and FAIR data ( $r = 0.96$ ). The mean difference between the techniques was negligible, with a 95% confidence interval of -30 to +31 ml/100 g/min between the two methods for any given measurement. In the case of compromised CBF however, there was a marked discrepancy between the techniques, with FAIR showing little sensitivity to different flow rates, in agreement with earlier reports [1]. This is most likely due to increased arterial transit times during occlusion, which would render the assumption that the technique is transit-time insensitive invalid. A transit time correction in the FAIR and CASL calculations for the ROIs with low CBF improved the correspondence between the techniques, though there was still a difference, indicating that either the FAIR transit time during occlusion is even larger than estimated, or there are other confounding factors influencing the measurement. Further studies using transit-time insensitive sequences such as multi-TI FAIR or QUIPSS II [4] are needed to investigate this phenomenon. (1) Pell GS et al. (1999) *Magn. Reson. Med.* 41, 829-840. (2) Alsop DC, Detre JA. (1996) *J. Cereb. Blood Flow Metab.* 16, 1236-1249. (3) Thomas DL et al. (2003) *ISMRM*, 667. (4) Wong EC et al. (1998) *Magn. Reson. Med.* 39, 702-708.

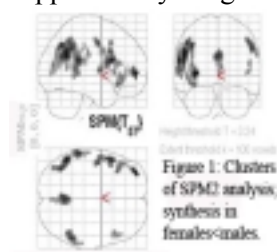
**SEROTONIN SYNTHESIS IS LOWER IN THE CORTICAL AREAS OF FEMALE THAN MALE HEALTHY PARTICIPANTS AS MEASURED WITH  $\alpha$ -[11C]METHYL-L-TRYPTOPHAN POSITRON EMISSION TOMOGRAPHY**

**Mirko Diksic<sup>1</sup>**, Yojiro Sakai<sup>1</sup>, Masami Nishikawa<sup>1</sup>, Marco Leyton<sup>2</sup>, Chawki Benkelfat<sup>2</sup>,  
Simon N. Young<sup>2</sup>

<sup>1</sup>*Montreal Neurological Institute, McGill University, Montreal, QC, Canada*

<sup>2</sup>*Department of Psychiatry, McGill University, Montreal, QC, Canada*

Dysregulation of the brain serotonergic system is a contributing factor to mood disorders. There are also reports suggesting a greater incidence of mood disorders in female patients. Serotonin (5-HT) synthesis is the first important step in serotonergic neurotransmission. The study of brain 5-HT synthesis was greatly improved by development of the  $\alpha$ -[11C]methyl-L-tryptophan ( $\alpha$ -MTrp) positron emission tomography (PET) imaging method. We reported before that 5-HT synthesis is reduced more in female than male subjects after tryptophan depletion, and that there are some region specific differences in 5-HT synthesis between male and female controls and patients with major depression. The objective of the present investigation was to compare 5-HT synthesis in male and female subjects using Statistical Parametric Mapping (SPM-2). Twenty-eight female (mean $\pm$ Standard Deviation (SD); 33.2 $\pm$ 17.2 years) and thirty-one male (29.8 $\pm$ 12.8 years) healthy volunteers were scanned for sixty minutes, and venous blood samples were taken at progressively increasing time intervals after injection of up to 10 mCi of tracer. The functional images of the brain trapping constant, which was shown in rats to correlate with 5-HT synthesis, were transferred to the standardized 3-D space and colocalized with each participant's MRI. The final functional images had a resolution of 8.2x9.5x10.5 mm. The voxel based comparison was done using clusters with 100 voxels and with the height  $p < 0.001$ . There was no cluster in which synthesis was greater in females than that in males, while there are seven clusters in which synthesis was lower in females than in males. The clusters showing difference are (see Figure 1): left frontal lobe middle and inferior frontal gyrus (BA 44), left and right parietal lobe supramarginal gyrus, left and right inferior parietal lobe (BA 40), left temporal lobe superior temporal gyrus, left limbic lobe cingulate gyrus and right posterior cingulate, right occipital lobe (precuneus; BA31), and left inferior frontal gyrus (BA 44 and BA 45). It is interesting to note that only cortical areas show significant differences between two genders. Because a relatively large cluster size was used in the comparisons smaller structures such as the amygdala and raphe nuclei would be missed. Some of the structures (e.g. cingulate, frontal lobe) showing a difference in synthesis between male and female subjects have been suggested to be involved in mood disorders. The lower 5-HT synthesis in female participants may be related to the higher incidence of affective disorders in that group. The research was supported by a grant from the Canadian Institutes of Health Research (MOP-42438).



**BRAIN METABOLIC FLUCTUATIONS IN ABSENCE OF STIMULI**Masaki Fukunaga, Silvina Horowitz, Peter van Gelderen, Jacco A. de Zwart, **Jozef H. Duyn***National Institutes of Health, Bethesda, MD, USA*

Mapping of brain function with blood oxygen level dependent (BOLD) magnetic resonance imaging (MRI) BOLD-MRI relies on the detection of focal changes in cerebral blood flow (CBF) in response to conditioned stimuli. However, in the absence of stimuli, the brain continues to show temporal fluctuations in blood flow as measured with BOLD and perfusion-based MRI (Biswal, *NMR.Biomed.* 1997). These fluctuations are substantially synchronized across functional regions that have an apparent functional relationship, and therefore might allow mapping and classification of the networks that underlie human brain function without the need for carefully conditioned stimuli. Despite their potential functional significance, the origin of the blood flow fluctuations has not been established. Potential sources include cognitive processes, fluctuations in vigilance and conscious awareness, and homeostatic (restorative) processes. Alternatively, the fluctuations might be caused by purely vascular events (e.g. vasomotor effect), without a substantial metabolic or neuronal component. In this study we used MRI methods to establish whether blood flow fluctuations in absence of stimuli subserved a metabolic process. For this purpose, we performed simultaneous BOLD and perfusion MRI at 3.0T on 7 normal volunteers during a visual task (5 min checkerboard-grey paradigm) and an extended (25min) rest period. The ratio between BOLD and perfusion changes was used as an indicator of metabolism (Hoge, *Proc.Nat.Acad.Sci.* 1999). As reference, a 10-minute breath-holding paradigm was inserted between the two conditions. The paradigm consisted of 5 stages of 40s breath-hold, 80s normal breathing. Physiologic monitoring included respiratory and cardiac cycles, as well as scalp potentials using a 64-channel EEG system. During rest conditions, we found substantial BOLD and perfusion signal fluctuations in most of neocortex, with strong correlations between functionally related regions. No significant correlations were found with cardiac and respiratory cycles. Frequency analysis of the fluctuations suggested that most energy was concentrated in the 0.01-0.1Hz band. The strongest fluctuations were observed during early (non-REM) sleep, as identified from EEG. Within visual cortex (VC), the amplitude of the fluctuations reached a level similar to that evoked with the task. BOLD and perfusion signals were highly correlated over most of cortex. The ratio of their fluctuation amplitude in VC averaged 1.66(0.41), 2.82(0.70), and 1.80(0.57) for task, breath holding paradigm, and rest (sleep) respectively. The difference between task and rest was insignificant ( $p=0.56$ ), while the ratios during task and rest were significantly ( $p=0.0003/0.017$ ) lower than during the breath-holding paradigm. The lower ratios are indicative of a relatively high oxygen extraction, suggesting involvement of a metabolic process during task and rest, and less so during breathholding. The findings indicate that spatially correlated fluctuations in CBF in absence of stimuli have a metabolic component and continue during early sleep. This has important implication for the design of brain mapping experiments and could shed light on the physiologic processes present during of rest and sleep. Further experiments are planned to investigate a potential role of processes facilitating synaptic plasticity (Huber, *Nature* 2004).

**REGIONAL REDUCTION IN N-ACETYL-ASPARTATE (NAA) LEVELS ARE CORRELATED WITH IMPAIRED OXIDATIVE BRAIN METABOLISM AND LONG-TERM BRAIN ATROPHY AFTER HUMAN TRAUMATIC BRAIN INJURY**

Paul Vespa<sup>1</sup>, Jeffrey Alger<sup>2</sup>, David McArthur<sup>1</sup>, H.S. Wu<sup>3</sup>, S.C. Huang<sup>3</sup>, Marvin Bergsneider<sup>1</sup>, Thomas Glenn<sup>1</sup>, Neil Martin<sup>1</sup>, David Hovda<sup>1</sup>

<sup>1</sup>Neurosurgery, UCLA, Los Angeles, CA, USA

<sup>2</sup>Radiology, UCLA, Los Angeles, CA, USA

<sup>3</sup>Nuclear Medicine, UCLA, Los Angeles, CA, USA

Introduction: Impairment in brain metabolism occurs after injury and may predict long term atrophy. Regional heterogeneity makes the assessment of metabolism difficult with a single focal monitor of metabolism, such as cerebral microdialysis (MD). Using MRI technology, specifically MRS NAA, regional heterogeneity can be studied and may shed light on the distribution and significance of changes in oxidative metabolism in humans. Elevation in lactate/pyruvate ratio as well as reduced MRS NAA are considered marker of metabolic distress and may indicate impaired oxidative capacity. Hypothesis: Brain regions of reduced NAA will demonstrate impaired oxidative capacity as indicated by reduced positron emission tomography (PET) rates of CMRO2 and elevated lactate/pyruvate ratio in MD. Methods: Patients with severe TBI underwent combined MD and multivoxel MRS within 96 hours of injury. Ninety-six voxels (1.5 cm<sup>3</sup>) per subject were studied, including voxels adjacent to the MD (VOI-MD) and near contusions. Regional maps of MRS analytes were made. Comparison of MRS NAA and microdialysis lactate/pyruvate were explored. Quantitative oxidative metabolic rates of CMRO2 were performed using PET. Volumetric MRI was performed within 1 week of injury and repeated at 6 months after injury to determine the degree of brain atrophy. Body of Results: Seventeen patients have undergone MRS imaging during the initial 96 hours after TBI. Mean NAA levels in normal appearing brain were 3.76 mM  $\pm$  3.66 compared with control subjects 9.3  $\pm$  1.2. Reduced NAA has been demonstrated regionally in areas adjacent to contusions (mean 1.98  $\pm$  1.77) compared with remote normal appearing brain (p < 0.001). On a voxel by voxel basis, 74.4% of voxels demonstrate reduced NAA. Post processing with NAA mapping has been completed and identification of the 1.5 cm<sup>3</sup> voxel of interest has been done. In the voxel adjacent to the microdialysis probe, NAA is highly negatively correlated with LPR (- 0.86, p < 0.001). In comparison with PET, anatomically co-registered regions of reduced NAA (< 2.0 mM) demonstrated lowest PET CMRO2 values (< 2.5 mg/100gm/min). Brain atrophy, defined as the net change in both grey and white matter in the entire brain and specifically the frontal lobe previously containing the microdialysis catheter were determined. There was a negative correlation (r = -0.86) between the early MRS NAA and the percentage of atrophy on 6 month MRI, with regions of NAA below 2.5 demonstrating a 45% relative increase in the amount of atrophy compared with regions in which NAA  $\geq$  4. Conclusion: Regions of low MRS NAA exhibit markers of impaired oxidative metabolism in cerebral microdialysis and PET studies. Reduced MRS NAA predicts the extent of long term brain atrophy after TBI.

## CHANGES IN BENZODIAZEPINE RECEPTOR BINDING IN DUTCH VETERANS WITH POSTTRAUMATIC STRESS DISORDER ASSESSED WITH [C-11]-FLUMAZENIL AND PET

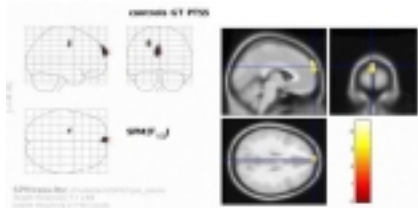
Elbert Geuze<sup>1,2</sup>, Bart N.M. van Berckel<sup>2,3</sup>, Ronald Boellaard<sup>3</sup>, Bert D. Windhorst<sup>3</sup>, Gert Luurtsema<sup>3</sup>, Herman G.M. Westenberg<sup>2</sup>, Adriaan A. Lammertsma<sup>3</sup>, Eric Vermetten<sup>1,2</sup>

<sup>1</sup>*Department of Military Psychiatry, Central Military Hospital, Utrecht, The Netherlands*

<sup>2</sup>*Department of Psychiatry, Rudolf Magnus Institute of Neuroscience, Utrecht, The Netherlands*

<sup>3</sup>*Department of Nuclear Medicine and PET Research, VU University Medical Centre, Amsterdam, The Netherlands*

**Introduction:** Benzodiazepine (Bz) receptors may play an important role in anxiety disorders such as posttraumatic stress disorder (PTSD). Indeed, SPECT imaging of Bz binding showed lower distribution volumes in the frontal cortex of patients with PTSD [1]. In addition, rats exposed to acute stress also showed reduced binding to Bz receptors in frontal cortex, hippocampus, and hypothalamus. The objective of the present study was to assess changes in Bz receptor binding in patients with PTSD versus healthy controls using [C-11]-Flumazenil and PET. **Methods:** Seven drug naïve veterans with PTSD and seven age matched control veterans with combat experience, but without PTSD, were recruited. Dynamic 3D scans (22 frames) with a total scan duration of 60 minutes were acquired after intravenous injection of ~370 MBq [C-11]-flumazenil. Arterial blood sampling was performed using both an online detection system and additional manual samples, generating a metabolite corrected arterial plasma input curve. Parametric volume of distribution (Vd) images were generated using Logan plot analysis using the dynamic data from 10 to 60 min p.i. Data were reconstructed using FBP Hanning 0.5, resulting in an image resolution of ~7 mm FWHM. Furthermore, prior to Logan plot analysis dynamic scans were smoothed using an additional 10mm FWHM Gaussian filter to reduce noise, thereby avoiding noise induced bias during Logan analysis. Next, these Logan plots were used in a voxel-based comparison between the two groups using Statistical Parametric Mapping (SPM). As images were already smoothed prior to Logan analysis, the usual smoothing within SPM was omitted. SPM was performed both with and without proportional scaling. Proportional scaling may be omitted because Logan plots are quantitatively accurate at the lower noise levels following smoothing. **Results:** SPM analysis, with and without proportional scaling, revealed no gross differences between patients and controls for most of the brain. However, both analyses, showed a discrete region in the (left) frontal cortex with statistically significantly ( $p < 0.01$ ) reduced [C-11]-Flumazenil binding in PTSD subjects (as indicated by the figure). **Conclusions:** The observed reduction of [C-11]-Flumazenil binding in the frontal cortex in PTSD subjects is consistent with findings based on SPECT imaging [1]. Other regions did not reveal this reduction, as might have been expected from small animal experiments. Although SPM analysis is useful in identifying regions with changes in ligand binding, full quantification of [C-11]-Flumazenil binding will require further kinetic analysis of the data. [1] Bremner et al. Am.J.Psychiatry, 2000



## NEUROPATHOLOGICAL FEATURES UNDERLYING DIFFERENT DEGREES OF MRI SIGNAL INTENSITY CHANGES DURING REPERFUSION AFTER TRANSIENT FOCAL ISCHEMIA IN THE RAT

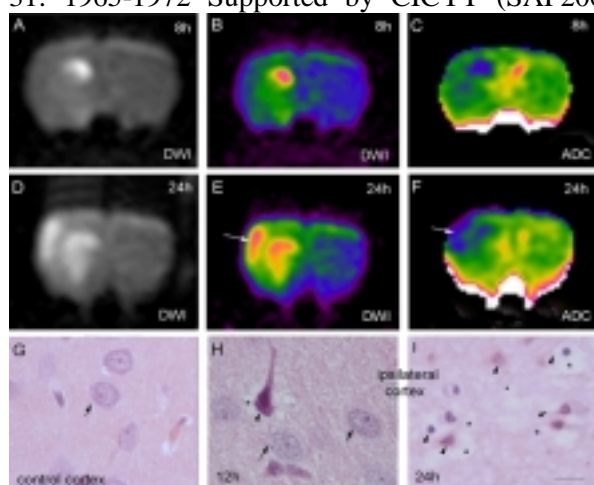
Anna M. Planas<sup>1</sup>, Abraham Martín<sup>1</sup>, Santiago Rojas<sup>1</sup>, Carles Falcón<sup>3</sup>, Noelia Montoya<sup>1</sup>, Núria Bargalló<sup>3</sup>, Angel Chamorro<sup>2</sup>

<sup>1</sup>Department of Pharmacology & Toxicology, IIBB-CSIC, IDIBAPS, Barcelona, Spain

<sup>2</sup>Stroke Unit, IMSN, Hospital Clínic, IDIBAPS, Barcelona, Spain

<sup>3</sup>Servei de Diagnostic Per la Imatge, Hospital Clínic, Barcelona, Spain

**Objectives:** Hyperintensity in diffusion-weighted imaging (DWI) and hypointensity in the apparent water diffusion coefficient (ADC) signals may occur in human stroke (1), and are seen in animals during MCA occlusion (2). Yet, these alterations return to baseline levels or partially recover at early reperfusion (3). Secondary ischemic damage becomes later apparent together with delayed recurrence of the DWI lesions (4). Here we sought to evaluate whether the degree of early MRI signal intensity changes predicted tissue damage, and to identify the underlying histopathological features. **Methods:** Sprague-Dawley rats (n=39) were subjected to transient (60 min) or permanent MCA occlusion and were killed at 8, 12, 15, 18 or 24h. One or two MRI studies (T2w, DWI) were performed on each rat between 1.5 and 24h. We evaluated the degree and volume of MRI changes in signal intensity, infarct volume (TTC), histopathology, and immunoreactivity to markers of cellular stress (Hsp72), astrocytes (GFAP), and microglia (OX42). **Results:** Subtle changes (<15%) in DWI and ADC signal intensity occurred from 90 min to 12h of reperfusion in the cortex (Fig. 1A-C), as compared with greater changes in the striatum, or in both regions after permanent ischemia. The volume of ADC changes at 12h was predictive of infarct volume at 24h. These mild changes were correlated with moderate and heterogeneous cell damage (Fig1H: arrowhead and asterisk; arrows point to normal in G,H). Afterwards, a shift in the degree of cortical MRI signal intensity (>30%) occurred (Fig.1D-F) concomitantly with overt manifestation of the TTC lesion, severe vacuolation of the neuropil (Fig1I, asterisks), and massive neural cell death (Fig. 1I, arrowheads). **Conclusions:** Transient ischemia induced a mild histological lesion in the cortex manifesting subtle MRI signal intensity changes up to 12h of reperfusion. This preceded a high increase in intracellular water content and neural cell death underlying a shift to overt DWI hyperintensity and ADC hypointensity. It is suggested that subtle and persistent MRI changes in the first 12h hours of reperfusion predict further delayed neuronal death. **References** 1. Warach S et al. (1995) *Ann Neurol* 37: 231-241 2. Hohen-Berlage M et al. (1995) *J Cereb Blood Flow Metab* 15: 1002-1011 3. Liu KF et al. (2001) *Stroke* 32:1897-1905 4. Neumann-Haefelin T et al. (2000) *Stroke* 31: 1965-1972 Supported by CICYT (SAF2002-01963) and FIS. S.R. has a fellowship from MEC.





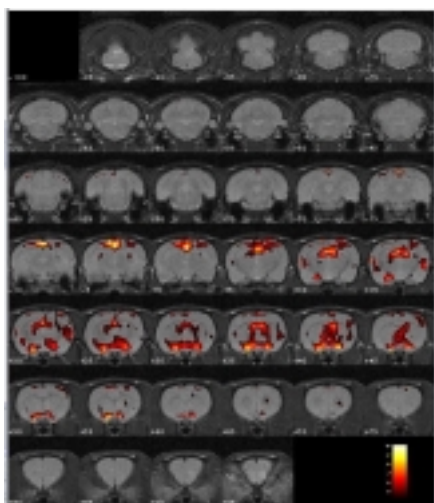
## ELUCIDATING THE FUNCTIONAL ACTIONS OF KETAMINE IN THE RAT BRAIN USING LOCOMOTOR, PHMRI AND MICRODIALYSIS TECHNIQUES

Clare L. Littlewood<sup>1</sup>, Nicholas Jones<sup>1</sup>, Stephen N. Mitchell<sup>2</sup>, Michael J. O'Neill<sup>2</sup>, Steven C.R. Williams<sup>1</sup>

<sup>1</sup>Neuroimaging Research Group, Institute of Psychiatry, London, UK

<sup>2</sup>Eli Lilly and Company, Windlesham, UK

**Introduction** The NMDA antagonist ketamine hydrochloride induces a psychotic-like state in man thought to be analogous to the positive, negative and disorganisation symptoms of schizophrenia (Andreasen et al., 1995 Arch Gen Psychiatry, 52, 341-51; Krystal et al., 1994 Arch Gen Psychiatry, 51, 199-214). To date, little research has been conducted into the neuroanatomical targets of subanaesthetic ketamine in rats (Burdett et al., 1995 Magn Reson Imaging, 13, 549-53; Duncan et al., 1999 Brain Res, 843, 171-83; Duncan et al., 1998 Brain Res, 787, 181-90). In our initial studies we evaluated the effects of ketamine (2.5, 10, 25 and 50mg/kg) on locomotor activity, measured by light beam interruptions, thus creating an appropriate pharmacodynamic input function for subsequent correlation with MRI (Roberts et al., in press). pHMRI was then utilised to elucidate the spatial and temporal alterations in brain activity following an acute dose of ketamine (25 mg/kg s.c.) via localised changes in Blood Oxygen Level Dependent (BOLD) MR signal. Microdialysis experiments using a separate group of rats examined temporal changes in dopamine concentrations in the nucleus accumbens (NAcc) following the same dose of ketamine. Results: 25 mg/kg ketamine produced a significant increase in locomotion and stereotypy in comparison to control animals. MRI analyses, revealed significant increases in BOLD signal following ketamine challenge, most notably in subcortical structures. Corresponding increases were seen in dopamine concentrations in the NAcc, an area known to be rich in dopaminergic fibres that are consistently activated by psychotomimetics (Kuczenski et al., 1991 JNeurosci, 11, 2703-12) **Conclusions:** 1. These results confirm previous observations that an acute dose of ketamine produces increases in locomotor behaviour and stereotypy in rats (Moghaddam et al., 1998 Science, 281, 1349-52) 2. The behavioural effects of ketamine may be mediated by its actions in discrete brain regions including subcortical regions that were observed using fMRI. 3. MRI technology appears sensitive to the neural effects of ketamine, with changes in BOLD contrast correlating to the pharmacodynamic and initial changes in the neurochemical profile of the drug 4. In the future we plan to investigate the potential interaction of antipsychotics on the ketamine-induced effects. The current data suggest that MRI may form a powerful tool for future research into schizophrenia and development of new antipsychotic medications. **Acknowledgements:** Funded by Eli Lilly and BBSRC studentship.





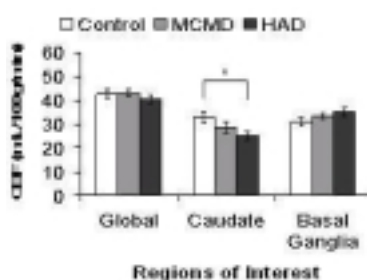
**REGIONAL BUT NOT GLOBAL CEREBRAL BASELINE BLOOD FLOW DIFFERENCES ARE PRESENT IN HIV ASSOCIATED DEMENTIA (HAD) USING CONTINUOUS ARTERIAL SPIN LABELING**

Beau M. Ances<sup>1</sup>, Anne C. Roc<sup>1</sup>, Dennis Kolson<sup>1</sup>, Joyce Okawa<sup>2</sup>, John Stern<sup>1</sup>, John A. Detre<sup>1</sup>

<sup>1</sup>Neurology, Hospital of the University of Pennsylvania, Philadelphia, PA, USA

<sup>2</sup>Infectious Disease, Hospital of the University of Pennsylvania, Philadelphia, PA, USA

**INTRODUCTION** The biological, medical, and social consequences of HIV infection in the brain include neurocognitive impairment, increased mortality, and decreased quality of life. Typically invasive tests such as lumbar puncture or time consuming neuropsychological performance tests are used to identify HIV patients as either asymptomatic, mild cognitive motor disorder (MCMD), or HIV associated dementia (HAD). We used non-invasive arterial spin labeling (ASL) MRI to obtain quantitative resting cerebral blood flow (CBF) measurements in global and regional areas typically affected by HIV. **METHODS** Forty-four HIV+ patients (31 males, 13 females,  $41 \pm 2$  yrs) and 10 seronegative controls (4 males, 6 females,  $47 \pm 2$  yrs) underwent standard physical, neurological and neuropsychological evaluation. The spectrum of HIV+ patients included: 15 asymptomatic, 19 MCMD, 10 HAD. The imaging protocol consisted of a localizer (TR/TE=20/5ms, 144x192, 3 slices, 9.6mm thick, 2 mins in duration), T1 weighted MPRAGE sequence (TR/TE=1620/3ms, 192x256, 160 slices, 1mm thick, 6 mins in duration), and ASL MRI sequence (TR/TE = 4000/17ms, 64x64, 12slices, 6mm thick, 6 mins in duration). Conversion to CBF values in ml/100g/min was performed using the general ASL perfusion model with subjects grouped into either controls, asymptomatic, MCMD, or HAD. ASL MRI images were normalized to Talairach space for region of interest (ROI) analysis. Since HIV is primarily a subcortical disease, ROIs known to be affected by HIV were included: caudate, globus pallidus. Brodmann's area 23 was also included as a control region. Multivariate analysis and paired t-tests were performed to determine significant differences in global CBF and ROI CBF between HIV+ patients and controls ( $p < 0.05$ ). **RESULTS** Global CBF was not significantly different in controls compared to other HIV subgroups (Figure 1). Within the caudate a decrease in CBF occurred with increasing dementia compared to controls ( $p < 0.05$ ). In contrast, within the globus pallidus a trend toward an increase in baseline flow was observed with increasing dementia (Figure 1). **DISCUSSION** HIV affects particular areas of the brain differently. These brain differences may be due to a relative destructive process that may occur within the caudate due to HIV. Cell loss may have lead to a reduction in baseline cerebral blood flow. In the basal ganglia a more inflammatory process is present with increased metabolism leading to an increase in baseline blood flow. The results suggest that measurements of CBF using ASL MRI may provide a surrogate marker of dementia and highlight the importance of a non-invasive easy method to classify subgroups of HIV patients. This method may also help determine who would benefit from earlier initiation of antiretroviral therapy.



## 2D CSI 1H MR SPECTROSCOPY OF CEREBRAL METABOLITES IN HIV ASSOCIATED DEMENTIA (HAD)

Beau M. Ances<sup>1</sup>, Anne C. Roc<sup>1</sup>, Sanjeev Chawla<sup>2</sup>, Harish Poptani<sup>2</sup>, John A. Detre<sup>1</sup>

<sup>1</sup>*Department of Neurology, Hospital of The University of Pennsylvania, Philadelphia, PA, USA*

<sup>2</sup>*Department of Radiology, Hospital of The University of Pennsylvania, Philadelphia, PA, USA*

**INTRODUCTION** HIV associated dementia (HAD) leads to cerebral metabolic changes in frontal white matter and subcortical grey matter [1-6]. Within these regions of interest (ROI), N-acetylaspartate (NAA), choline (Cho), and creatine (Cr) have typically been studied using single voxel 1H MR spectroscopy (MRS). 2D CSI 1H MRS provides greater localization with smaller voxel sizes of previously studied ratios as well additional metabolites such as lactate (LAC). We evaluated cerebral metabolite levels within the basal ganglia (BG), a subcortical grey matter region, and subcortical white matter (SWM) ROIs in HIV+ patients compared to controls using 2D CSI 1H MRS. **METHODS** Forty-four HIV+ patients (31 males, 13 females,  $41 \pm 2$  yrs) and 10 seronegative controls (4 males, 6 females,  $47 \pm 2$  yrs) underwent standard physical, neurological and neuropsychological evaluation. HIV+ patients were classified by the Memorial Sloan-Kettering system for HIV associated dementia complex (HAD) and grouped as asymptomatic (n=24) and symptomatic (n=21). MR apparatus was a 3T Siemens scanner equipped with the standard clinical quadrature head coil. Anatomical images were acquired by axial T1 weighted MPRAGE sequence (TR 1620ms, TE 3.87ms, 1mm slice thickness, FOV 25x25cm). Spectroscopy images were acquired with a SE with 2D phase encoding and outer volume saturation pulses for lipid suppression sequence (TR 2000ms, TE 135ms, n=3, 20mm slice thickness, FOV 20x20cm, voxel size 12.5 x 12.5 x 20). Voxels overlapping bilateral BG and SWM were analyzed. The area under the peak was measured for quantification of cerebral metabolites and calculated ratios of NAA/Cr and Cho/Cr were determined. Metabolic ratios between HIV+ groups were compared to controls by Student's t-test ( $p < 0.05$ ). LAC was considered present if an observed peak was greater than 1 standard deviation above noise. A paired t-test analysis was performed to determine significance across groups for the presence of LAC ( $p < 0.05$ ). **RESULTS** The percentage of visible lactate peaks in BG was significantly greater in HIV+ patients compared to controls ( $p < 0.05$ ). Although not significant in SWM, visible lactate peaks were more prominent in HIV+ groups. Within the SWM but not BG the NAA/Cr ratio was also significantly reduced in HIV+ patients compared to controls ( $p < 0.05$ ). In contrast, no consistent trend was observed for Cho/Cr ratio for either ROI. **DISCUSSION** Our results demonstrate that high field multi voxel 2D CSI 1H-MRS provides a more accurate understanding of cerebral metabolite changes in HIV+ patients. The reduction of NAA/Cr ratio seen in SWM may be due to neuronal loss from mitochondrial dysregulation. Gliosis, as measured by the Cho/Cr ratio, was not observed within HIV+ patients. The presence of LAC observed within BG in HIV+ patients compared to controls may reflect the presence of macrophages within the brain. These results support converging evidence that HIV is concentrated in certain areas of the brain with neuronal loss and inflammation leading to HAD. Furthermore, 2D CSI 1H-MRS, particularly in detecting LAC within BG, may serve as a biomarker in classifying HIV+ dementia.

**MISERY PERFUSION ACCELERATES SELECTIVE NEURONAL LOSS IN PATIENTS WITH STENO-OCCLUSIVE CEREBROVASCULAR DISEASES****Ekus Shimosegawa<sup>1</sup>, Masanobu Ibaraki<sup>1</sup>, Shigeki Sugawara<sup>1</sup>, Jun Hatazawa<sup>2</sup>,****Akifumi Suzuki<sup>1</sup>, Kazuhiro Takahashi<sup>1</sup>, Shuuichi Miura<sup>1</sup>**<sup>1</sup>*Research Institute of Brain and Blood Vessels, Akita, Japan*<sup>2</sup>*Osaka University Graduate School of Medicine, Osaka, Japan*

**Introduction:** Selective neuronal loss occurs after mild and/or short-duration brain ischemia. Since cerebral perfusion reserve (CPR) is one of the mechanism to maintain cerebral blood flow (CBF), its impairment may be a potential risk of selective neuronal loss. In order to clarify potential neuronal loss in the brain areas with impaired CPR, we investigated the relationship between cerebral vasoreactivity and central benzodiazepine receptor density in patients with steno-occlusive lesion of the major intracranial arteries. **Subjects and Methods:** The PET and I-123 iomazenil SPECT were performed in 8 patients with unilateral steno-occlusive lesion of the major intracranial arteries. The CPR was measured by means of the PET with O-15 labeled water during resting condition and after acetazolamide loading. The CPR was defined as (acetazolamide-loading CBF-resting CBF)/resting CBFX100(%). The oxygen extraction fraction (OEF), cerebral blood volume (CBV), and cerebral metabolic rate of oxygen (CMRO2) were also measured. Central benzodiazepine receptor density was measured by the SPECT with I-123 iomazenil. Early (30min post-injection) and delayed (3hours post-injection) scans of I-123 iomazenil SPECT were performed. The binding potential (BP) of central benzodiazepine receptor was estimated by creating the image of the distribution volume (Vd) based on the 2-compartment model. After image registration between the PET and Vd images, 11-12 circular regions of interests were located on the affected and unaffected cerebral cortices. The interval between the PET and SPECT study was within 1 week. Relative BP in the affected hemisphere was defined as a lesion-to-contralateral (L/C) ratio of Vd. Disturbed CPR lesion was defined as the areas with the resting CBF below 80% of the unaffected hemisphere with the CPR less than 10%, and relative BP in the lesion was analyzed in relation to the CPR, OEF, and CMRO2. **Results:** Mean CBF, CMRO2, OEF, and CPR in the lesion was 26.8±8.6ml/100ml/min, 2.07±0.43ml/100ml/min, 52±8%, and -4.5±6.7%, respectively. The mean OEF was significantly higher than that of unaffected cortices (42±4.1%, p<0.0001). The mean CMRO2 was significantly lower than that of the unaffected cerebral cortices (2.65±0.46ml/100ml/min, p<0.0001). The relative BP of this area (0.94±0.08) was significantly decreased when compared with unity (Wilcoxon t-test, p<0.0001). The relative BP in the areas with OEF more than 55% (0.90±0.07) was significantly lower than that with OEF less than 55% (0.93±0.07, p=0.041). **Discussion:** The present results demonstrated that the reduction of CBF and impaired CPR was associated with significant reduction of central benzodiazepine receptor density. Misery perfusion may facilitate loss of central benzodiazepine receptor. The metabolic reduction of the lesion may be due partly to the neuronal loss. **Conclusion:** Selective neuronal loss occurs in the areas with reduced CBF and impaired perfusion reserve and is accelerated by misery perfusion in patients with steno-occlusive cerebral artery disease.

## ASSESSMENT OF LITHIUM TREATMENT USING FMRI DURING STROKE RECOVERY IN RATS

Young R. Kim<sup>1,2</sup>, Maurits P.A. van Meer<sup>1,2,3</sup>, Emiri Tejima<sup>2</sup>, Joe B. Mandeville<sup>1</sup>, Teng-Yi Huang<sup>1</sup>, De M. Chuang<sup>4</sup>, Bruse R. Rosen<sup>1</sup>, Eng H. Lo<sup>2</sup>

<sup>1</sup>*MGH/MIT/HMS Athinoula A. Martinos Center for Biomedical Imaging, Charlestown, MA, USA*

<sup>2</sup>*Neuroprotection Laboratory/MGH, Charlestown, MA, USA*

<sup>3</sup>*Image Sciences Institute, University Medical Center, Utrecht, The Netherlands*

<sup>4</sup>*Molecular Neurobiology, Section National Institute of Mental Health, Bethesda, MD, USA*

An important function of lithium as a neuroprotective agent has been documented previously. Significant reduction in infarct size and DNA damages with the corresponding improvement of neurological scores were reported as results of post stroke lithium administration. In the current study, therapeutic efficacy of chronic lithium treatment was assessed by various MRI-derived parameters (i.e., apparent diffusion coefficient (ADC), fractional anisotropy (FA), and vessel size index (VSI)) and quantified with fMRI activity using electrical stimulation of rat forelimbs. The fMRI responses were examined by measuring the local hemodynamic MRI signal intensity based on blood oxygenation level dependence (BOLD) and cerebral blood volume weighted (CBVw) responses. The ipsilesional fMRI activations in the somatosensory (SS) cortex of lithium-treated (n=6) and saline-treated rats (n=6) two weeks after middle cerebral artery occlusion (MCAO) were compared. ADC and FA values of local brain tissues were significantly correlated with the magnitude of fMRI responses for the lithium-treated rats while no such correlations were seen in the saline controls. The ipsilesional/contralesional BOLD signal intensity response ratios of lithium-treated rats were larger than those of saline-treated control rats. In contrast, the CBVw response ratios were similar between two groups. These results demonstrated that the lithium-treatment of post-stroke animal models positively enhanced BOLD fMRI response in the lesion hemisphere. Overall activation volume and magnitude were larger for saline-treated rats than the lithium-treated group in both contra and ipsilesional somatosensory cortices. However, for both BOLD and CBVw responses, the mean activated volume ratio (ipsilesional/contralesional) was higher for lithium-treated rats than controls. The CBVw activation signal magnitude ratios (Figure 1 upper panel) were significantly higher than BOLD ratios for the control animals; however, similar for the lithium-treated rats. As shown in Figure 1 (bottom panel), functional status index (FSI) which represents the mean ratio between BOLD and CBVw ipsi/contralesional activation signal intensity ratio for the individual somatosensory cortex was significantly higher for lithium-treated rats than the control group. From the acquired ADC maps, ex vacuo dilation of the ipsilesional lateral ventricles was identified for most of rats while other structural damages (e.g., FA) were also evident at this late stage (2 weeks) of recovery. Among the acquired structural parameters, ADC and FA were significantly correlated with CBVw fMRI activation magnitude (i.e., area under the curve) for the lithium-treated rats while no such correlations were found for the saline controls. When compared to the contralesional values, the ipsilesional mean VSI ratio (ipsi/contra) was larger for the lithium-treated rats; however, the micro vascular volume (i.e., Delta-R2) ratio (ipsi/contra) was larger for control rats. These results imply that possible vascular transformation affects fMRI characteristics.

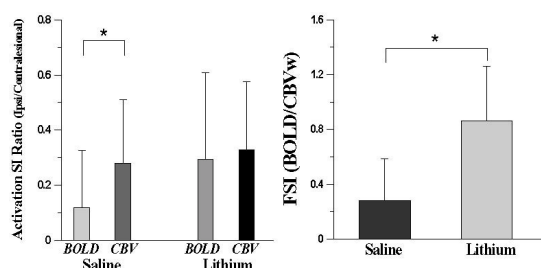


Figure 1. activation SI ratio and functional status index in somatosensory cortex.



## AGE DEPENDENCE OF 18F-FLUORODOPA UPTAKE RATE AND DOPAMINE TURNOVER PET MARKERS AND IMPLICATIONS FOR PARKINSON'S DISEASE PROGRESSION

Vesna Sossi<sup>1</sup>, James E. Holden<sup>2</sup>, Michael Schulzer<sup>1</sup>, Thomas J. Ruth<sup>3</sup>, A. Jonathan Stoessl<sup>1</sup>

<sup>1</sup>*University of British Columbia, Vancouver, BC, Canada*

<sup>2</sup>*University of Wisconsin, Madison, WI, USA*

<sup>3</sup>*TRIUMF, Vancouver, BC, Canada*

**Introduction.** 18F-fluorodopa (FD) is a widely used positron emission tomography (PET) marker to investigate the integrity of the dopaminergic system. The tissue and plasma input FD uptake rate constants (Kocc and Ki) (1-3) are used as measures of dopamine (DA) synthesis and storage. Recently, the DA effective distribution volume (EDV) was introduced as a measure of DA turnover (TO) ( $EDV = 1/TO$ ) (4). A relatively large increase in DA TO and a smaller decrease in DA uptake rate constant have been suggested as compensatory mechanisms in early Parkinson's disease (PD) (4-5). Here we investigated the age dependence of Ki, Kocc and EDV for caudate and putamen in healthy population and speculated on its implications on disease progression. **Methods.** Nine healthy volunteers (age  $58.1 \pm 11.8$  yrs, range 43-76) underwent a 4hrs long FD scan. Four 61 mm<sup>2</sup> circular regions of interest (ROIs) were placed on each striatum, and six 270 mm<sup>2</sup> circular ROIs were placed on the occipital cortex on five planes containing the striatal image on each frame of the dynamic sequence. Arterial blood samples were taken to obtain the plasma radioactivity time course with a subset analyzed for metabolites. Ki, Kocc and EDV values were calculated for the caudate and putamen separately with the left and right side averaged. **Results.** A significant negative correlation was found between putamen Ki and age ( $r^2 = 0.92$ ,  $p < 10^{-4}$ ) and between putamen EDV and age ( $r^2 = 0.48$ ,  $p = 0.039$ ). No significant age correlation was found for all other measures (caudate Ki:  $r^2 = 0.31$ ,  $p = 0.12$ , caudate EDV:  $r^2 = 0.12$ ,  $p = 0.36$ , Kocc putamen:  $r^2 = 0.35$ ,  $p = 0.09$  and Kocc cau:  $r^2 = 0.02$ ,  $p = 0.70$ ). **Discussion and conclusion.** Ki showed a robust age dependence in contrast to Kocc for the putamen, while no parameter showed age dependence for the caudate. The literature addressing Ki and Kocc age dependence in healthy humans has reported contradictory results (6-7 and others). Our results agree with work done in non-human primates (8) and suggest that Ki and Kocc have different sensitivities to age related degeneration of the dopaminergic function. EDV also shows an age related decline, implying an increase in DA TO in normal aging. Our findings imply that older individuals might have only limited ability to compensate for PD induced DA deficiency by increasing TO in contrast to younger ones. Likewise, a lower DA synthesis and storage rate in older individuals might lessen the system ability to maintain adequate DA levels in early PD. This might (i) permit a longer preclinical period in younger PD patients and (ii) explain a greater propensity for younger patients to develop motor complications. 1-2. Patlak et al., JCBF 3:1-7, 1983; JCBF 5:584-590, 1986 3. Martin et al., Ann Neurol 26: 535-542. 1989 4. Sossi et al., JCBF 24:869-876 2004 5. Lee et al., Ann Neurol 47:493-503 2000 6. Cordes et al., Ann Neurol 36(4) 667-670 1994 7. Eidelberg et al., JCBF 5:881-888 1993 8. Doudet et al., Psc Res 45:153-168, 1992.

## MULTIMODAL NAVIGATION SYSTEM WITH INTEGRATION OF PET DATA IN THE SURGICAL TREATMENT OF INTRINSIC BRAIN TUMORS

Toshio Sasajima<sup>1</sup>, Hiroyuki Kinouchi<sup>1</sup>, Masanobu Ibaraki<sup>2</sup>, Eku Shimosegawa<sup>2</sup>, Kazuhiro Takahashi<sup>2</sup>, Tohru Ohta<sup>1</sup>, Kennichi Shibata<sup>1</sup>, Akira Suzuki<sup>1</sup>, Jun Hatazawa<sup>2</sup>, Iwao Kanno<sup>2</sup>, Kazuo Mizoi<sup>1</sup>

<sup>1</sup>*Department of Neurosurgery, Akita University School of Medicine, Akita, Japan*

<sup>2</sup>*Department of Radiology and Nuclear Medicine, Research Institute of Brain and Blood Vessels, Akita, Japan*

**Introduction:** The present study aimed to explore whether the integration of PET data into a cranial neuronavigation system in combination with cortical functional mapping would enable neurosurgeons to optimize the tumor resection without postoperative neurological deterioration. **Methods:** Ten patients with intrinsic brain tumors including four oligodendrogliomas, two oligoastrocytomas, one pleomorphic xanthoastrocytoma, one glioblastoma, one gangliocytoma, and one fibrosarcoma were preoperatively examined with PET using C-11 methyl-L-methionine (Met) and F-18 fluorodeoxyglucose (FDG). Seven tumors located in the right frontal lobe or in the left parietal lobe, were close to motor or somatosensory cortex. The remaining three tumors were located in the temporal lobe. The tracer accumulation in the tumor was visually compared to the contralateral gray matter on PET images scanned 35 min and 50 min after intravenous injection of Met and FDG, respectively. The VectorVision<sup>2</sup> (BrainLAB AG, Munich, Germany) incorporated with thin-slice, contrast enhanced T1-weighted, and T2-weighted MRI scans was used as a navigation system. Met and FDG PET data were converted and fused with MR images by PatXfar5.2 and VectorVision Cranial Planning1.3 (BrainLAB AG, Munich, Germany) using an automatic image-fusion algorithm. PET images and somatosensory evoked magnetic fields of magnetoencephalography (MEG) were also superimposed on corresponding MR images. Silicon tubes were implanted as an anchoring marker for a resection to the margins of the resectable tumors that was demonstrated as the area of increased Met accumulation on co-registered images of PET and MRI in the navigation system. The tubes were inserted before dural incision to prevent from the dislocation due to brain shifts by the leakage of cerebrospinal fluid. The correct localization of the precentral gyrus was intraoperatively verified by cortical somatosensory evoked potential monitoring. **Results:** Met-PET clearly demonstrated tumor extent by increasing uptake of Met as a “hot” lesion in all patients. The areas of inhomogeneous FDG uptake in the tumors were completely surrounded by those of “hot” lesions on Met-PET images. The “hot” lesions on Met-PET were all larger in size than the Gd-enhancing lesions on MRI. The area of Met accumulation that is believed to be highly consistent with the distribution of tumor cells, extended sparsely over the T2-hyperintensity lesions. Postoperative MRI revealed that the tumors were totally resected in all eight patients, with silicon tubes implantation method. In contrast, the T2-hyperintensity lesions extending partly beyond the area of Met accumulation diminished on follow-up MRI. There was no additional morbidity caused by the surgical intervention in all patients. Follow-up MRI revealed no evidence of recurrent tumors in all patients 2 to 55 months (median, 31 months) after the tumor resection. **Conclusions:** The integration of the preoperative metabolic (PET), functional (MEG), and anatomic (MRI) images provides important information to optimize the tumor resection without an operative neurological morbidity. The silicon tube implantation method under the monitor of this navigation system is simple and accurate to determine the border of the intrinsic brain tumors to be resected. The complete resection of tumors defined as high-Met-uptake would be associated with improvement of the survival with better quality of life.

**INTERHEMISPHERIC NEURAL CONDUCTION VELOCITY ESTIMATED BY  
AUDITORY-EVOKED MAGNETIC FIELDS DECREASES CORRELATING WITH  
THE DEGREE OF DEPRESSIVE MOOD IN ELDERLY SUBJECTS**

**Hiroshi Oe<sup>1</sup>, Akihiko Kandori<sup>2</sup>, Tsuyoshi Miyashita<sup>2</sup>, Kuniomi Ogata<sup>2</sup>, Kotaro Miyashita<sup>1</sup>,  
Kuni Konaka<sup>2</sup>, Keiji Tsukada<sup>3</sup>, Hiroaki Naritomi<sup>1</sup>**

<sup>1</sup>*Department of Cerebrovascular Medicine, National Cardiovascular Center, Osaka, Japan*

<sup>2</sup>*Central Research Laboratory, Hitachi Ltd., Tokyo, Japan*

<sup>3</sup>*Department of Electronical and Electronic Engineering, Okayama University, Okayama,  
Japan*

Background: Magnetoencephalography studies have shown that the latency of auditory-evoked neuronal action waveforms (N100m and N50m peaks) detected at the temporal cortex ipsilateral to the auditory stimulation is delayed as compared with that detected at the contralateral side. Our recent auditory evoked magnetic fields (AEFs) study has indicated that auditory impulses originated from the unilateral ear first arrive at the contralateral temporal cortex and thereafter reach the ipsilateral temporal cortex through interhemispheric neural connections, thus, leading to the delay of ipsilateral N50m and N100m peak-latencies (1). Such a conduction pathway of auditory impulses makes it possible to measure interhemispheric neural conduction time from the difference of ipsilateral and contralateral N100m or N50m peaks. Elderly subjects with chronic dizziness often have depressive state and may later develop cognitive deterioration. In the present study, we measured interhemispheric neural conduction velocity (INCV, m/sec) from the distance between the ipsilateral and contralateral temporal cortices and the difference of ipsilateral and contralateral N50m peak latencies in elderly patients with chronic dizziness to elucidate whether the grade of INCV is related with depressive mood. Methods: 27 elderly patients ( $68 \pm 12$  years of age) complaining of dizzy sensation for more than 6 months were subjected to the study. The presence or absence of depressive mood was estimated with Zung's self-rating depression scale (SDS). The patients were classified into two groups, such as Group A with depressive mood (SDS >50) and Group B without depressive mood (SDS <50). AEFs study was performed using superconducting quantum interference device system (MC-6400, Hitachi Ltd.) with 64 co-axial gradiometer. INCV was calculated from the distance between the ipsilateral and contralateral temporal cortices and the difference of ipsilateral and contralateral N50m peak latencies. In Group A patients, AEFs study was repeated following antidepressive therapy with selective serotonin reuptake inhibitors (SSRI). Results: 10 patients (Group A) were depressive (SDS:  $58.2 \pm 7.6$ ) and the other 17 patients (Group B) were not depressive (SDS:  $38.0 \pm 5.3$ ). INCV was significantly smaller in Group A ( $10.3 \pm 9.0$  msec) than in Group B ( $23.7 \pm 11.3$  msec,  $p < 0.05$ ). When analyzed in the entire patients, INCV decreased significantly correlating with SDS scores ( $r = -0.57$ ,  $p < 0.001$ ). In Group A patients, following antidepressive treatment with SSRI, INCV increased significantly ( $12.2 \pm 8.9$  msec,  $p < 0.05$ ), and SDS scores decreased significantly ( $52.9 \pm 11.3$ ,  $p < 0.05$ ). Comments: The results of the present study suggest that the depressive mood is closely related with the reduction in INCV. The neural conduction velocity may play an important role in determining the mood condition in elderly subjects. Reference: (1) Oe H, Kandori A, Yamada N, et al: Interhemispheric connection of auditory neural pathways assessed by auditory evoked magnetic fields in patients with fronto-temporal lobe infarction. *Neuroscience Research* 44: 483-488, 2002

**MODELLING FOCAL BRAIN LESIONS: PERFUSION CHANGES INDUCED BY RTMS OVER LANGUAGE RELATED CORTEX**

Alexander Thiel<sup>1</sup>, Birgit Schumacher<sup>1</sup>, Karl Herholz<sup>1</sup>, Klaus Wienhard<sup>2</sup>, Walter F. Haupt<sup>1</sup>,  
Wolf-Dieter Heiss<sup>1,2</sup>

<sup>1</sup>*Department of Neurology, University of Cologne, Cologne, Germany*

<sup>2</sup>*Max-Planck-Institute for Neurological Research, Cologne, Germany*

**Introduction:** Rapid transcranial magnetic stimulation (rTMS) has been used to interfere with language function in normal subjects by inducing transient brain lesions with rapidly changing magnetic fields. The mechanism underlying this interference is unknown. We investigated the TMS-effect on rCBF in a PET study with normal subjects during language activation. Language activation studies in patients with real focal brain lesions of the dominant hemisphere have shown decreased rCBF in the area of the lesion and increased activation of homologous brain areas in the non-dominant hemisphere [1]. If rTMS is to be used as a model for focal brain lesions, the same effect should be expected from rTMS interference. **Methods:** 5 normal right handed male volunteers underwent repeated CBF measurements on an ECAT-EXACT PET scanner with O-15-water and PET during 4Hz rTMS at resting motor threshold over the triangular part of the left inferior frontal gyrus (ifg). Stimulation sites were localized on 3D reconstructions of the subject's brain and head from T1-weighted MR images [2]. CBF was measured three times under four conditions: rest with rTMS, overt verb generation with rTMS, rest with sham stimulation and verb generation with sham stimulation. PET images were coregistered to the MR-image, averaged within the four conditions and ratio-normalized for global CBF differences. Average PET-images were fused onto 3D reconstructions of the brain and the position of the TMS-coil over the target area was determined from the transmission scan. A cylindrical VOI of 20 mm diameter and 10 mm length (approximating the extent of the magnetic field) was positioned on the brain surface under the centre of the coil and mean rCBF within the VOI was measured [3]. The same measurement was done for a mirror region in the right hemisphere. TMS effect on rCBF was calculated as percent CBF-change within these VOIs for resting and verb generation conditions respectively. **Results:** During the resting condition TMS induced a median rCBF decrease of 6.3 % within the VOI under the centre of the coil relative to sham stimulation (signed rank test,  $p < 0.03$ ). In the homologous region of the right hemisphere a median decrease of 3.2% was observed which was not significant. During verb generation again an rCBF decrease of 1.7 % ( $p < 0.03$ ) was measured during TMS over the left ifg relative to sham stimulation. In the contralateral VOI over the right ifg however rCBF increased by 2% ( $p < 0.03$ ). **Conclusion:** Consistent with data from patients with real brain lesions, TMS induced a CBF decrease within the target region of the left inferior frontal gyrus during rest and verb generation. In the homologous area of the right hemisphere a TMS-induced increase of rCBF during verb generation was observed. These data indicate, that the effect of TMS induced transient brain lesions in normal subjects might be similar to the effect of real focal brain lesions. **References:** 1. Thiel et al. Ann. Neurol. 50, 620-629, 2001 2. Thiel et al. Ann. Neurol. 57, 128-131, 2005 3. Herholz et al. Neurosurgery 41, 1253-1260, 1997

## DIAGNOSIS OF MILD COGNITIVE IMPAIRMENT USING FRACTAL ANALYSIS IN CBF SPECT

Naohiko Oku<sup>1</sup>, Kenya Murase<sup>2</sup>, Kazuo Kitagawa<sup>3</sup>, Yasuyuki Kimura<sup>1</sup>, Katsufumi Kajimoto<sup>1</sup>,  
Ashik Bin Anser<sup>1</sup>, Makiko Tanaka<sup>3</sup>, Hiroki Katoh<sup>1</sup>, Masatsugu Hori<sup>3</sup>, Jun Hatazawa<sup>1</sup>

<sup>1</sup>*Department of Tracer Kinetics and Nuclear Medicine, Osaka University Graduate School of  
Medicine, Osaka, Japan*

<sup>2</sup>*Department of Allied Health Science, Osaka University Graduate School of Medicine,  
Osaka, Japan*

<sup>3</sup>*Department of Internal Medicine and Therapeutics, Osaka University Graduate School of  
Medicine, Osaka, Japan*

**Introduction:** Mild cognitive impairment (MCI) was described as a transitional phase from normal to Alzheimer's disease. Cerebral blood flow (CBF) measurement using single photon emission computed tomography (SPECT) in MCI patients is less sensitive than in Alzheimer's disease patients. and changes in CBF are small and patterns of CBF abnormality are not uniform in MCI patients. In this study, using fractal analysis we evaluated the distribution of CBF as measured by SPECT. The purpose of this study is to evaluate the clinical usefulness of fractal analysis in patients with MCI. **Subjects:** The subjects were 14 clinically diagnosed amnesic MCI patients (MCI group: mean age 70.6 years, mean MMSE score 25.8 +/- 1.6) and age matched 18 cognitively normal subjects (control group: mean age 66.9 years, mean MMSE score 28.5 +/- 1.3). **Methods:** The device we used was a high performance SPECT system (SPECT2000H, Hitachi Medico Co.Ltd., Tokyo, Japan). Subjects underwent CBF SPECT with Tc-99m HMPAO at resting condition. Reconstructed transaxial data (64 x 64 matrix, 44 slices, 4 x 4 x 4 mm voxel) were analyzed by a 3-dimensional fractal analysis. The analysis calculates the fractal dimension (FD) as the next equation.  $M(a) = ka^{-FD}$ , where  $a$  = percent threshold against peak voxel value in the whole brain,  $k$  = constant,  $M(a)$  = number of voxel which have values above corresponding threshold. High FD value indicates complexity of the voxel value distribution among data set (total voxels in the whole brain), in another word heterogeneity. **Results:** The mean FD value in MCI group (1.071 + 0.194 (mean +/- SD)) was significantly ( $p < 0.001$ ) higher than in control group (0.853 +/- 0.062). In MCI group, FD value correlated with neither MMSE score nor age. When cut off value was set at  $FD = 0.92$ , sensitivity and specificity to detect MCI by FD value were 78% and 83%, respectively. Out of 14 patients in MCI group, 4 had progressed dementia in the following 2 years. There was no difference in FD at initial SPECT between converters (1.05 +/- 0.11) and non-converters (1.08 +/- 0.22) in MCI group. **Conclusion:** Distribution of CBF in MCI patients was more heterogeneous than in normal subjects. Fractal analysis with CBF SPECT was a helpful tool to separate MCI patients from normal subjects. However, FD value alone seemed not predict the converter from MCI to dementia.

## FINGER FLEXION CONTRASTED TO EXTENSION ACTIVATES HIGHER-ORDER MOTOR CIRCUITRY

M.W. Stenekes<sup>1,3,5</sup>, J.M. Hoogduin<sup>1</sup>, Th. Mulder<sup>3</sup>, J.H.B. Geertzen<sup>5</sup>, K.L. Leenders<sup>2</sup>,  
J.-P.A. Nicolai<sup>4</sup>, **B.M. de Jong**<sup>2,1</sup>

<sup>1</sup>*BCN Neuro-Imaging Center, Groningen University, Groningen, The Netherlands*

<sup>2</sup>*Department of Neurology, University Hospital Groningen, Groningen, The Netherlands*

<sup>3</sup>*Department of Movement Sciences, Groningen University, Groningen, The Netherlands*

<sup>4</sup>*Department of Plastic Surgery, University Hospital Groningen, Groningen, The Netherlands*

<sup>5</sup>*Department of Revalidation, University Hospital Groningen, Groningen, The Netherlands*

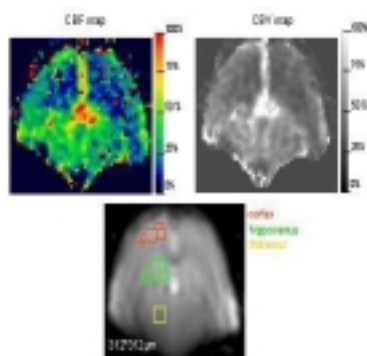
Purposeful movement such as grasping implies tuning of object shape and hand posture. This is organised by circuitry distributed over parietal and premotor regions. Within this circuitry, a sharp spatial segregation between the perceptual and motor representations does not exist. E.g., only observing objects to be grasped activates premotor cortex. Making hand postures, independent from target shape, is related to parietal activation. Moreover, the finding of mirror neurons shows that the observation of grasping by others, induces the activation of premotor regions mimicking one's own grasping. Even indirect stimuli such as the noise of hammering, elicits premotor activations reflecting the potential of using a hammer oneself. Finally, parieto-premotor circuitry is implicated in imagining task-related movements. In this study, we posed 2 questions. (1) Is simple finger flexion specifically associated with activation of higher-order motor circuitry, reflecting a connection like the above listed perceptual entrances? We hypothesised an intimate relation between such circuitry and finger flexion, because finger extension only provides an initial aperture, whereas subsequent flexion scales handmovement, enabling adequate grasping. (2) Over the motor cortex, the topographic representation of fingers is well documented. Here, we looked for segregation between flexion and extension movements of the same digits along the central sulcus, equivalent to the described proximal-distal representation of hand sensation. Cerebral BOLD responses were studied in twelve right-handed subjects (3T fMRI, Philips). Subjects listened by headphone to random beeps (20 per min). In the flexor movement condition, responses were made to each beep by 2 flexion movements with digits 2-5 (left hand). In the extensor condition, extension movements were similarly made. The control condition was listening to beeps. Data were acquired in four sessions, each constituted by four 30 s lasting motor-task blocks. Each motor block was preceded by a control block. The order of the two motor conditions was balanced. In each block, 11 brain volumes of 46 slices were obtained. Analysis was done by Statistical Parametric Mapping (SPM2, London). The 2 movement conditions were contrasted with control and with each other. Comparing left-hand finger flexion with extension showed activation of the left parietal cortex (x -32, y -60, z 56) and posterior parts of the insula, bilaterally (P<0.05, corrected whole brain volume; smoothing filter 10 mm). Parietal activation supported our hypothesis, and points at an association with praxis. Activation of the posterior insula is consistent with its supporting role in skeletomotor control. Compared to rest, the motor tasks showed overlapping activation along the contralateral central sulcus, at the hand representation. The centre of gravity for flexion was more superficial than for extension. Contrasted to each other (P<0.05, uncorrected; smoothing 4 mm), finger flexion activated a lateral part of the motor cortex (Brodmann's Area BA 4), extending over the surface of the precentral gyrus (BA 6). Extension movement was related to activation deep in the central sulcus. In conclusion, the relation between finger flexion and parieto-premotor circuitry, indicates that these simple movements may be regarded as building-stones for complex movements such as grasping.

## ASSESSMENT OF HEAMODYNAMIC PARAMETERS AND CEREBRAL BLOOD FLOW REACTIVITY USING IN VIVO BOLUS TRACKING AND ARTERIAL SPIN LABELING IN MICE

Greetje Vanhoutte, Marleen Verhoye, Annemie Van der Linden

*University of Antwerp, Biomedical Sciences, Bio-Imaging Laboratory, Antwerp, Belgium*

It is generally accepted that knowledge of the regional brain perfusion and assessment of the cerebrovascular reactivity is of great importance in the follow up of neurodegenerative diseases. In particular, since genetically engineered mouse models for neurodegeneration have proven to be of great value for studying the pathogenesis of a disorder at the molecular, cellular and behavioral levels, quantification of cerebral perfusion in these mice becomes extremely relevant. In order to improve in-vivo methods for evaluation of cerebral perfusion in mice, we implemented in-vivo echo planar imaging in control mouse brain and used it for application in bolus tracking (BT) experiments and arterial spin labeling (ASL) acquisitions to assess cerebral perfusion parameters. The BT-technique could quantitatively calculate cerebral blood volume (CBV) and cerebral blood flow (CBF) on a regional basis and ASL was used as a detection method of changing CBF upon a hypoxic challenge. In this way we could identify regional differences in CBV and CBF (Figure 1). The highest CBV values were found in the thalamus ( $7.59 \pm 0.41$  ml/100g). The hippocampus displayed a significant lower CBF at rest conditions as compared to the cortex ( $67.44 \pm 6.44$  ml/100g/min versus  $83.17 \pm 6.43$  ml/100g/min) and this seemed to be correlated with the observed reduction in the cerebrovascular response to hypoxia (relative CBF increase in cortex  $29.41 \pm 2.34\%$  versus  $15.13 \pm 2.29\%$  in the hippocampus) and a more pronounced hypoxia induced BOLD signal change. Our data provide clear evidence that it is possible to discern basal flow parameters in mouse brain and locate differences in spatial patterns of cerebrovascular reactivity in mice. BT-MRI and ASL were proven to provide complementary information on the perfusion status of the brain and this study shows for the first time the advantages of the combined use in mouse brain.



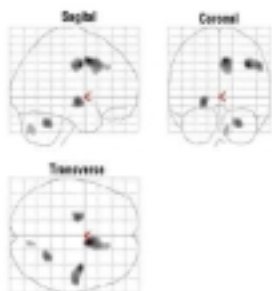
## TASK INTENSITY RELATED BRAIN ACTIVATION BY ERGOMETER EXERCISE MEASURED BY FDG-PET

Sabina Khondkar<sup>1</sup>, Keiichiro Yamaguchi<sup>1</sup>, Shoichi Watanuki<sup>1</sup>, Toshihiko Fujimoto<sup>2</sup>, Masatoshi Itoh<sup>1</sup>

<sup>1</sup>*Division of Cyclotron Nuclear Medicine, Tohoku University, Sendai, Japan*

<sup>2</sup>*Division of Medicine and Science In Sports and Exercise, Tohoku University, Sendai, Japan*

**Objectives:** The target of this study was to clarify absolute and relative changes in regional brain metabolism related with muscle exercise. Both subtraction and covariate analyses were carried out with task intensity as the main factor. Ergometer exercises at three different intensities were chosen as task loads. Serial whole-body FDG-PET measurements with heated venous radioactivity sampling were carried out. **Methods:** Three levels of exercise loads were designed at 40% (light), 70% (moderate) and 80% (heavy) VO<sub>2</sub>max, which corresponded to aerobic, intermediate and anaerobic conditions respectively. Seven healthy male volunteers performed the exercise three times with changing task loads on separate days. A total of 35 minute ergometer cycling was followed by emission and transmission scan with a 3D PET scanner. Correlations between the FDG uptake and task intensities were evaluated by voxel based covariate search using Statistical parametric mapping technique (SPM 2 software) at  $p < 0.001$  with an extended voxel numbers over 40. **Results and Discussions:** Absolute cerebral glucose metabolism was gradually decreased with increasing task intensity and significantly reduced at medium and high-level exercise. Subtraction analysis revealed significant increases in brain metabolism for ergometer cycling in frontal gyrus (BA 6, 9, 10, 11 and 44), precentral gyrus (BA 4 and 6), tempoparietal occipital cortex (BA 5, 18 and 40) and cingulate gyrus (BA 30). This study also identified a strong correlation in brain regions with respect to the task intensity (from light to heavy load) at four distinct regions (cingulate, precentral, pallidum and cerebellum) as shown in Figure 1. The cingulate and primary sensory motor area were highly correlated (survived after multiple comparison correction at  $p < 0.05$ , FDR corrected) mainly in the right side. The centroid associated with exercise intensity was located more lateral and lower to the leg somatotopy and corresponded in the face area. Similar activation pattern were observed in brain areas when heavy intensity group compared with the light load group. The face motor area related with intensity probably reflects clenching of jaws at extensive exercise. Leg motor area (M1) was not responding linearly in this study while previously reported to be positively related with movement rate. Non-linear response in M1 with increasing intensity during ergometer cycling suggest that these contradicting results may arise from differences in the nature and complexity of the motor task and intend that primary motor area may be related to other components of the task such as type of contractions, relaxation, feedback regulation, etc. The activation of globus pallidus with increasing intensity support the hypothesis that the basal ganglia motor circuit may be involved preferentially in controlling or monitoring the scale and/or dynamics of leg movements. This study confirmed several regions that responsible for elaboration and sensory association increases linearly with task intensity and also certain areas that do not. All findings are compatible with the idea that three motor controls mode is operative during aerobic or anaerobic level of exercise.



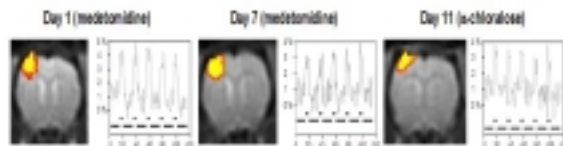


## A LONGITUDINAL AND TOTALLY NONINVASIVE fMRI PROTOCOL IN RATS

Ralph Weber, Pedro Ramos-Cabrer, Dirk Wiedermann, Mathias Hoehn

*In-Vivo-NMR-Laboratory, Max-Planck-Institute for Neurological Research, Cologne, Germany*

**Introduction:** Functional magnetic resonance imaging (fMRI) is a unique tool to study brain activity and plasticity changes. Most fMRI studies in rats have used  $\alpha$ -chloralose to anesthetize the animals. Because of the organ toxicity and need for blood vessel catheterization, longitudinal studies cannot be performed with  $\alpha$ -chloralose. Thus, we developed a totally noninvasive fMRI protocol, suitable to study recovery processes, using the  $\alpha$ 2-agonist medetomidine in combination with transcutaneous monitoring of blood gases, yielding robust patterns of functional brain activation at different time points, comparable with the results obtained under  $\alpha$ -chloralose. **Methods:** Wistar rats (n=4) were anesthetized at three different time points with halothane. After placement of a transcutaneous blood gas system (TCM4, Radiometer Copenhagen, Denmark) and forepaw stimulation electrodes, anesthesia was switched to a subcutaneous bolus (0.05 mg/kg) and continuous infusion (0.1 mg/kg/h) of medetomidine in the first two experiments, and intravenously applied  $\alpha$ -chloralose (36 mg/kg/h) in the third experiment. In 3 additional rats, only one fMRI experiment was performed under medetomidine. After each fMRI session, medetomidine was antagonized with an intraperitoneal injection of atipamezole. BOLD fMRI experiments were performed on a 7T animal scanner (Bruker BioSpin, Ettlingen, Germany). After pilot scans, multislice SE-EPI images were acquired using the following parameters: FOV: 2.56x2.56 cm<sup>2</sup>; 64x64 points; TR=3 s, TE = 30 ms. Both forepaws were stimulated alternately with rectangular pulses (2mA, 3Hz, 0.3ms). 115 EPI images were acquired using a paradigm in which ON vs. OFF stimulation periods were switched in a 60 s cycle (15 OFF + 5 ON), repeated 5 times, and ending with 15 OFF images. Brain activation maps were constructed using a t-test (p<0.01) in the program STIMULATE (University of Minnesota, USA). **Results:** All animals tolerated the non-invasive fMRI experiments very well and fully recovered within 2 minutes after injection of atipamezol. Identical and highly reproducible BOLD activation areas were observed in the contralateral primary somatosensory cortex during forepaw stimulation using both medetomidine and  $\alpha$ -chloralose (Fig. 1). The amplitudes of the BOLD signal were well comparable during stimulation under both anesthetics. Transcutaneous blood gas monitoring assured no significant changes in pCO<sub>2</sub> levels during experiments. **Discussion:** Using the  $\alpha$ 2-agonist medetomidine, we were able to perform repetitive and highly reproducible fMRI studies after forepaw stimulation in rats. Together with a continuous monitoring of transcutaneous pCO<sub>2</sub> values, our protocol can be used for totally noninvasive fMRI studies, allowing to perform longitudinal studies in the same animal to study functional recovery processes upon therapeutical treatment.



## DETECTION OF CHRONIC HEMOSIDERIN-LOADED MACROPHAGES ACCUMULATION AFTER STROKE IN THE RAT. INDICATOR OF LATE VASCULAR DEGRADATION?

Ralph Weber, Susanne Wegener, Pedro Ramos-Cabrer, Ulla Uhlenkueken, Mathias Hoehn

*In-Vivo-NMR Laboratory, Max-Planck-Institute for Neurological Research, Cologne, Germany*

**Introduction:** We studied the macrophage response in the chronic stage after 60 minutes of transient focal ischemia (MCAO) in rats using high-resolution 3D MR imaging. We detected hypointense areas on T2\*-weighted but not on T2-weighted MR imaging in the ischemic territory 10 weeks after the induction of ischemia, in all examined Wistar rats, and investigated these signals histologically. **Methods:** Two weeks after MCAO, T1- and T2-weighted and 3D-gradient echo T2\*-weighted images were acquired in 11 rats on a 7T experimental MR scanner. Three animals were sacrificed for histological analysis thereafter. In 8 animals a sham-implantation was conducted in the contralateral hemisphere and T1-, T2- and T2\*-weighted MR imaging was repeated after 8 weeks. HE-staining, Prussian blue iron-staining and immunostaining of ED-1 positive macrophages was performed after the end of the MRI observation period. **Results:** Areas with hypointense signals within the ischemic brain hemisphere were visible on T2\*-weighted MR images in all 8 rats at 10 weeks after MCAO, while they were present only in 5 of 8 rats after 2 weeks. Hypointense areas could be detected on T2-weighted MR images only in one animal with a massive subacute hemorrhagic transformation of the ischemic brain tissue. The T2\*-hypointense areas were mainly located in the dorsolateral striatum and corresponded to iron-loaded cells (fig. 1). Most of the iron-positive cells represented hemosiderin containing macrophages next to striatal blood vessels. **Discussion:** Hemosiderin containing macrophages accumulate next to blood vessels in the ischemic striatum in the chronic phase after transient MCAO and can be visualized in vivo by high resolution MR imaging, and histologically by a combination of Prussian blue staining and ED-1 immunostaining. Most likely, these hemosiderin containing macrophages are the result of microhemorrhages caused by an ongoing vascular degeneration. The accumulation and detection of endogenous iron-loaded cells has to be considered when implanting iron-loaded (stem) cells into the brain of rats subjected to transient focal ischemia.

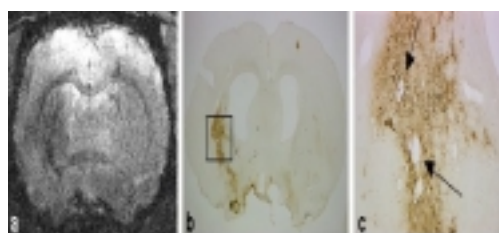


Fig. 1: The left ischemic striatum is hypointense compared with the contralateral hemisphere on T2\*-weighted MRI (a). Iron-loaded macrophages are found in the hypointense area on combined ED-1 immunostaining and iron staining (b). The box in panel b is shown at a higher magnification in panel c and shows the accumulation of iron-loaded macrophages around striatal blood vessels (arrows) (c).

## POSSIBLE CORTICO-SUBCORTICAL MOTOR CIRCUIT DISRUPTION IN PATIENTS WITH VASCULAR PARKINSONISM

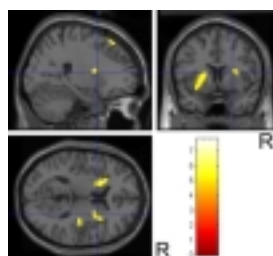
Masafumi Ihara<sup>1</sup>, Hidekazu Tomimoto<sup>1</sup>, Koichi Ishizu<sup>2</sup>, Hidefumi Yoshida<sup>3</sup>,  
Nobukatsu Sawamoto<sup>3</sup>, Kazuo Hashikawa<sup>3</sup>, Hidenao Fukuyama<sup>3</sup>

<sup>1</sup>Department of Neurology, Kyoto University Graduate School of Medicine, Kyoto, Japan

<sup>2</sup>Department of Nuclear Medicine and Diagnostic Radiology, Kyoto University Graduate School of Medicine, Kyoto, Japan

<sup>3</sup>Human Brain Research Center, Kyoto University Graduate School of Medicine, Kyoto, Japan

**Background:** [11C] flumazenil (FMZ), a ligand that selectively binds to the central benzodiazepine receptor in the neuronal membrane, is useful for evaluating neuronal viability in a PET scan. Using this ligand, we investigated whether there was a correlation between neuronal integrity in various brain structures and vascular parkinsonism (VaP) in patients with leukoaraiosis. **Methods:** Twelve patients whose T2-weighted MRI revealed confluent hyperintensities in the subcortical white matter (Schmidt scale score of 3) and several punctate high-intensity areas in the striatum and/or thalamus were studied using PET. Based on a two compartment, two parameter model using metabolite-corrected arterial input and PET-measured cerebral radioactivity, the distribution volume of FMZ (FMZ-Vd) was calculated in various regions of interest (ROIs) by non-linear curve fitting. Additionally, tracer kinetic analysis was applied for voxel-by-voxel quantification of FMZ-Vd and data analysis was performed using statistical parametric mapping (SPM). We also examined cerebral blood flow (CBF) and cerebral metabolic rate of oxygen metabolism (CMRO2) using the 15O gas steady-state method in these patients. **Results:** The subjects were divided into two groups based on their neurological signs i.e., patients with parkinsonism (group P; 3 men and 4 women; 73.7+/-4.6 yr) and those without parkinsonism (group NP; 1 man and 4 women; 77.0+/-3.2 yr). The mean+/-SD number of lacunae in the striatum was slightly but not significantly larger in group P (group P, 1.14+/-0.90; group NP, 0.60+/-0.55; p=0.26). ROI-based analysis demonstrated that FMZ-Vd tended to be lower in group P than in group NP. These reductions reached significance in the striatum (17.2%; p<0.01), although no significant difference was found in the other areas. CBF was also reduced in group P, although this reduction only reached significance in the striatum (25.4 %; p<0.05). CMRO2 also tended to be lower in group P. The largest reduction in CMRO2 was detected in the striatum (25.3%, p=0.076). SPM analysis showed that FMZ-Vd was significantly reduced in the bilateral striatum and the most rostral part of the right lateral premotor cortex (Puncorr<0.0005; figure). **Conclusions:** The premotor cortex, striatum, and the frontal white matter interconnecting them are essential components of the basal ganglia-thalamocortical 'motor' circuit. Given our findings that neuronal integrity is impaired in the striatum as well as the premotor cortex in VaP patients with WMLs, ischemic damage to the motor circuit may contribute to developing VaP.



**PREFRONTAL CORTICAL RESPONSE TO VERBAL-SPATIAL TWO-DIMENSIONAL TASK MEASURED BY FUNCTIONAL NIRS**Chenjun Li, Hui Gong, **Qingming Luo***The Key Laboratory of Biomedical Photonics of Ministry of Education, Huazhong University of Science and Technology, Wuhan, China*

Previous PET and functional MRI studies of working memory (WM) have suggested that prefrontal cortex (PFC) helps WM processes. However, there is controversy on the roles that different PFC regions play in information processes of different materials. Here, we reported a functional near-infrared spectroscopy (NIRS) study on the PFC activation caused by a two-dimensional (verbal versus spatial) n-back task. During the task being performed, concentration changes of oxy-Hb (HbO<sub>2</sub>), deoxy-Hb (Hb), and total-Hb (HbT) in subjects' prefrontal cortex, which being correlated with cerebral activation, were examined by a 24-channel functional NIRS imager. The behavioral performances (accuracy and response time) were recorded simultaneously. Results revealed that as memory load increased, subjects showed poorer behavioral performance as well as monotonously increasing magnitudes of the PFC activations. In addition, we found that when the subject performed the task as verbal material, the left ventrolateral PFC (VLPFC) and the bilateral dorsolateral PFC (DLPFC) were significantly activated, and when the subject performed the task as spatial material, the right VLPFC and the bilateral DLPFC were significantly activated. This result not only further substantiates previous view that cerebral information processing is lateralized to the left for verbal material and to the right for spatial material, not only provides an evidence that some collaboration mechanisms likely exist between bilateral hemispheres. **Keywords:** Near-infrared spectroscopy; Prefrontal cortex; Working memory; N-back task

**QUANTITATION OF KETAMINE INDUCED CHANGES OF rCBF****Hans R. Herzog<sup>1</sup>, Holger Holthusen<sup>2</sup>, Jan-Peter Nickel<sup>3</sup>, Lars Kemna<sup>1</sup>**<sup>1</sup>*Institute of Medicine, Research Center Juelich, Juelich, Germany*<sup>2</sup>*Department of Anesthesiology, Heinrich Heine University Duesseldorf, Duesseldorf, Germany*<sup>3</sup>*Department of Neurology, Heinrich Heine University Duesseldorf, Duesseldorf, Germany*

It has been reported that anesthetics influence the autoregulation of brain vessels differently. Ketamine, an NMDA receptor antagonist, is used for analgesia as well as general anesthesia and is known to effect rCBF. In this study PET-measurements using 15O-butanol were done to quantify regional cerebral blood flow (rCBF) in detail during three levels of ketamine anesthesia. Eight healthy male volunteers aged  $30 \pm 3$  yrs were examined. After bolus injections of 550 MBq of the freely diffusible rCBF tracer 15O-butanol each subject was scanned four times: during waking state (WS) and three different levels of ketamine application with dosages of 0.1, 0.38, and 1.5 mg S-ketamine per kg body weight. The three levels were antinociception (ANOC), analgesia (ANAL), and deep anesthesia (DA). 8Hz flicker light was applied as reference stimulus in all scans. PET-scanning was done with a Siemens scanner HR+ in 3D mode for 101 sec per condition and was accompanied by continuous arterial blood sampling. In addition, pCO<sub>2</sub>, pSaO<sub>2</sub>, systolic blood pressure (SBP), and heart rate (HR) were monitored. Time-radioactivity data of the reconstructed PET-images (all corrections done) were obtained for whole cerebrum (WC), frontal (FC), anterior cingulate (ACC), parietal (PC), and visual (VC) cortex, thalamus (TH), and cerebellum (CB). Applying the one-tissue compartment model of CBF and corrections for delay and dispersion of the blood data, rCBF was determined by non-linear curve fitting. pCO<sub>2</sub> did not decreased significantly from  $41.0 \pm 4.0$  mmHg for WS to  $37.9 \pm 4.3$  mmHg for DA. pSaO<sub>2</sub> remained unchanged, whereas SBP and HR became significantly greater by 10% and 41%, respectively. During WS global cerebral CBF was  $54.7 \pm 4.6$  ml/min/100g and increased slightly to  $59.1 \pm 8.9$  ml/min/100g at ANOC. When ANAL and DA were reached, cerebral CBF changed considerably by 49% and 88% to finally  $103 \pm 23.8$  ml/min/100g. Cerebellar rCBF increased much less by 30% and 55% at ANAL and DA, respectively. Whereas rCBF of the different cortical areas became greater by less than 24% from WS to ANOC, it increased by at least 39% at ANAL and 81% at DA - except for VC. During DA the activation in VC caused by the visual stimulation did not only disappear, but rCBF of VC became 30% lower than the global cerebral CBF. The greatest changes were observed in FC and ACC: from  $65.7 \pm 7.6$  to  $146.7 \pm 32.5$  ml/min/100g and from  $60.0 \pm 11.8$  to  $171.6 \pm 44.6$  ml/min/100g, respectively. rCBF of PC and TH during DA was only  $111.6 \pm 34.1$  and  $128.5 \pm 37.3$  ml/min/100g, respectively. This study reports detailed quantitative data on the effect of ketamine on rCBF which have not been available for humans until now. When the dosage of ketamine was increased to 0.37 mg/kg, so that the analgetic level was invoked, rCBF of all brain regions examined here except the visual cortex is significantly augmented with the greatest increases in the frontal and anterior cingulate cortex.

## VISUALIZING THE EFFECTS OF SCOPOLAMINE IN THE RAT BRAIN USING FUNCTIONAL MRI

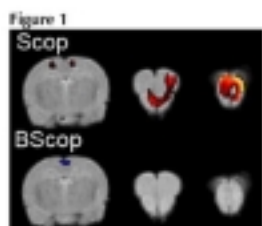
Diana Cash<sup>1</sup>, Toby J. Roberts<sup>1</sup>, Matthew D. Ireland<sup>1</sup>, Steve C.R. Williams<sup>1</sup>, Jacqueline A. Hunter<sup>2</sup>, Neil Upton<sup>2</sup>, David Virley<sup>2</sup>

<sup>1</sup>Neuroimaging Research Group, Institute of Psychiatry, London, <sup>2</sup>GlaxoSmithKline, Harlow, UK

**Introduction** – The cholinergic antagonist scopolamine mimics aspects of cognitive dysfunction that occur in dementias like Alzheimer’s disease. In particular, scopolamine-induced amnesia in rodents is frequently used to test putative cognition-enhancing therapies. Here, we have further characterised this model by monitoring the cerebral effects of scopolamine (and its analogue, butyl-scopolamine, which does not cross the blood brain barrier) in rats using functional MRI. **Methods** – 3 groups of 8 SD male rats (286±25g) received either scopolamine hydrobromide (0.8mg/kg), scopolamine-N-butyl bromide (0.8mg/kg) or vehicle saline i.p. one hour after commencement of fMRI. All rats were anaesthetised with iv  $\alpha$ -chloralose (65mg/kg bolus followed by 30mg/kg/h infusion). Mean arterial blood pressure, pulse and respiration were measured continuously in all animals, whilst blood glucose, pH and paCO<sub>2</sub> were measured at the start and end of scanning in over half the animals. MRI was performed using a 4.7T magnet and a conventional GE T2\*-sensitive sequence (effective TE 10ms, TR 0.94s, isotropic 0.125mm<sup>3</sup> voxels) producing a time-series of 130 whole brain scans over 2.5h. For group mapping, all images were movement corrected, normalised to standard space and smoothed using SPM’99 software, followed by noise filtering with MELODIC software (www.fmrib.ox.ac.uk). Data were scaled to the global brain signal and activation maps (SPM’99) were derived representing significant correlations with a pharmacokinetic input function. **Results** – There were no significant variations in any physiological parameters except for blood glucose, which was lowered by scopolamine (Table 1). Brain activation maps revealed significant increases in BOLD contrast after scopolamine injection in rostral regions including frontal (orbital) cortex and olfactory nuclei ( $p < 0.05$  corrected for multiple comparisons); in caudal regions BOLD increases were mostly localised to the retrosplenial cortex but extended to the CA1 hippocampal layer at a lower statistical threshold ( $p < 0.001$ , uncorrected). Such changes were absent from both saline and butyl-scopolamine treated rats. **Conclusions** – It is possible that the effects of scopolamine result from increased release of acetylcholine as their distribution encompasses areas innervated by cholinergic fibres from the basal forebrain. However, the increased regional BOLD contrast may also reflect a mismatch between CBF and glucose utilization, both of which are reportedly affected by scopolamine (1,2). The nature of these changes therefore requires further investigation using more direct techniques. In summary, this study demonstrates the utility of using fMRI with scopolamine challenge for in vivo investigation of the cholinergic basis of dementias. **References** – 1. Piercey et al. (1987) Brain Res. 424, 1-9; 2. Tsukada et al. (1997) Brain Res. 749(1), 10-17. **Figure 1.** Group statistical parametric maps showing statistically significant ( $p < 0.05$  corrected) signal increases (red) and decreases (blue) at app. –4.3mm, 4.2mm and 5.2mm from Bregma, left to right.

	Scop		B-Scop		Sal.	
	pre	post	pre	post	pre	post
MAP (mmHg)	80.6±5.3	79.8±5.8	75.8±5.9	77.4±7.7	78.6±8.2	78.6±5.9
Heart rate (beats/min)	382.3±28.5	395.5±41.7	375.3±41.9	388.5±61.5	386.2±34.3	386.5±113.3
Resp. rate (breaths/min)	74.6±6.2	74.4±13.3	77.5±8.2	73.5±9.3	76.5±5.5	71.3±6.6
Blood glucose (mmol/l)	4.4±1.7	3.6±0.9*	4.7±1.8	4.5±1.8	4.8±1.3	4.8±1.4
pH	7.37±0.04	7.35±0.04	7.38±0.02	7.36±0.06	7.40±0.04	7.36±0.03
paCO <sub>2</sub> (mmHg)	48.7±19.9	49.5±11.5	39.8±5.3	41.5±15.1	41.4±6.4	50.7±20.1

Mean±SD, n=8 per group. \*  $p < 0.05$  from pre. 2-way ANOVA.



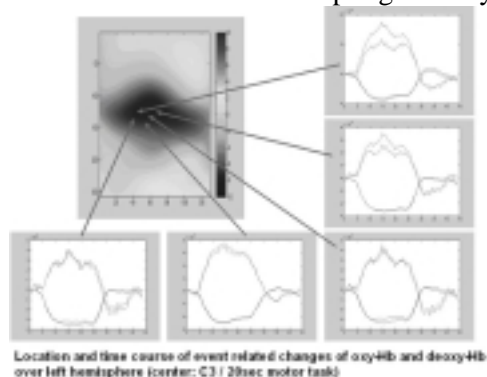


## SPATIOTEMPORAL CORRELATION OF NEURONAL ACTIVITY AND CEREBRAL BLOOD FLOW OF THE MOTOR CORTEX: NON-INVASIVE MEASUREMENT OF DC-EEG AND NEAR-INFRARED SPECTROSCOPY IN HUMANS DURING A MOTOR TASK

Christoph W. Drenckhahn<sup>1,2,3</sup>, Rainer Papsdorf<sup>1,2</sup>, Jens Steinbrink<sup>2</sup>, Hellmuth Obrig<sup>2</sup>, Stefanie Leistner<sup>3</sup>, Bruno M. Mackert<sup>3</sup>, Gabriel Curio<sup>3</sup>, Arno Villringer<sup>2,3</sup>, Ulrich Dirnagl<sup>1</sup>, Matthias Kohl-Bareis<sup>4</sup>, Jens P. Dreier<sup>1,2</sup>

<sup>1</sup>Department of Experimental Neurology, CCM, <sup>2</sup>Department of Neurology, CCM, <sup>3</sup>Department of Neurology, CBF, Charité Hospital, Universitätsmedizin Berlin, <sup>4</sup>RheinAhrCampus, University of Applied Sciences Koblenz, Remagen, Germany

**Aim:** To establish a bedside method to measure neurovascular coupling (NVC) during functional activation in healthy subjects as well as patients, in whom the NVC may be disturbed, e.g., due to stroke, head trauma or subarachnoid hemorrhage (SAH). **Methods:** We investigated the coupling of neuronal activation and cerebral blood flow (CBF) during voluntary hand movement in humans. For this purpose we non-invasively and simultaneously recorded alterations of slow-potential and oxy- and deoxy-hemoglobin (Hb) concentrations over the hand area of the primary motor cortex. Slow potentials were recorded with DC-EEG and oxy- and deoxy-Hb changes with near-infrared spectroscopy (NIRS). 20 female, strongly right handed volunteers underwent a simple motor task consisting of repetitive contraction of one fist for 20 s followed by movement of the other hand for 20 s. Movements were self paced (~1.5 Hz). Every 20 s a signal was applied (vibrating stimulus at the lower leg) to alternate between hands. We performed 46 stimulation blocks, 23 for each hand so that the whole trial took 15:20 minutes. 15 EEG Ag/AgCl sintered ring electrodes (impedance <2k $\Omega$ ), 8 light sources and 7 light detectors were positioned over the left primary motor cortex with C3 as central recording point. Data processing was performed using BrainAnalyser 1.05 (BrainProducts®) and BESA (MEGIS Software GmbH) for EEG and MatLab 6.5 software (The MathWorks, Inc.) for NIRS data. For spatial correlation, EEG source analysis was related to the point with the strongest decrease in deoxy-Hb. Distance and relation to C3 were determined using a 2D (NIRS) and a 3D (DC-EEG) mapping. Curves of slow potential and the indirect CBF parameters oxy- and deoxy-Hb were then temporally correlated. **Results:** According to the onset of right hand movement we detected a circumscribed negative shift of the DC potential over the left motor cortex accompanied by an increase in the concentration of oxy-Hb and a decrease in deoxy-Hb respectively in the same region. Deoxy-Hb started to decrease 1.2s after movement onset and reached its minimum within 6.6s (t[20%]=2.0s, t[50%]=3.6s, t[80%]=4.9s). Deoxy-Hb increased 2.8s after cessation of contralateral hand movement. Baseline was reached again within 7.0s (t[80%]=3.7s, t[50%]=5.1s, t[20%]=6.2s) and an overshoot for 1.6s was observed subsequently. **Conclusion:** We demonstrated that the combination of non-invasive DC-EEG and NIRS imaging is feasible to simultaneously detect changes in DC potential and indirectly in CBF in time and two spatial dimensions. The method is particularly useful to study NVC with a high temporal resolution. We will use the method to study conditions in which neurovascular coupling is likely to be disturbed as in the course of SAH.





**ACTIVATION OF THE VISUAL CORTEX IN INFANTS DURING NATURAL SLEEP USING MULTICHANNEL NEAR-INFRARED SPECTROSCOPY**

**Kusaka Takashi<sup>1</sup>**, Isobe Kenichi<sup>2</sup>, Okubo Kensuke<sup>1</sup>, Yasuda Saneyuki<sup>1</sup>, Kawada Kou<sup>1</sup>, Itoh Susumu<sup>1</sup>

<sup>1</sup>*Maternal and Perinatal Center, Faculty of Medicine, Kagawa University, Kagawa, Japan*

<sup>2</sup>*Department of Pediatrics, Faculty of Medicine, Kagawa University, Kagawa, Japan*

**Introduction:** During development, the brain undergoes sequential anatomical, functional, and organizational changes necessary to support the complex adaptive behavior of a mature normal individual. Delineation of developmental changes occurring in different regions of the brain would provide a means of relating various behavioral phenomena to maturation-specific brain structures, thereby enhancing our understanding of structure-function relationships in both normal and disease states. NIRS is a noninvasive method for detecting changes in the concentrations of oxyHb and deoxyHb at the bedside, and it has been used to study functional activation of various areas of the brain. In this study, we used to use NIRS to monitor the activities of the visual cortex as mirrored by hemodynamic responses in newborns subjected to photostimulation during natural sleep, and we compared them with normal adult response patterns. **Patients and Methods:** We examined five infants, aged 3 d to 2 wk, and five healthy adult volunteers using multichannel NIRS. Informed consent in writing was obtained from the parents of the infants and from the adult volunteers, and the protocol was approved by the local ethics committee. A probe consisting of 16 optical fibers, 8 for transmission and 8 for detection, was placed over the bilateral occipital region, with the center of probe at the level of the calcarine sulcus. The interoptode distance was 3 cm for adults and 2 cm for infants. Measurements in the infants were performed in the spine or prone position with the occipital region of the head touching the probe, and measurements were performed in the adults in a comfortable sitting position in a dark, quiet room. The subjects were exposed to stroboscopic white flashing light at 8 Hz projected on the eyelids during the stimulation period (15 seconds) and to non-flashing light during the rest period (45 seconds). The stimulation cycle was repeated 11 to 30 times. **Results:** In the adult subjects, as was shown previously, [oxyHb] and [totalHb] in the visual cortex increased with the photostimulation. In the neonates, on the other hand, [oxyHb] and [totalHb] in the visual cortex decreased and [deoxyHb] increased with photostimulation. There were no significant changes in any of these parameters in the no stimulation control group. The different response patterns to photostimulation in the visual cortices in neonates and adults might reflect developmental and behavioral differences. Its may reflect a different functional organization of the visual cortex in neonates or the on-going retinal development. **Conclusion:** We have reported NIRS measurement of functional hemodynamic responses in infants during natural sleep. The NIRS signal response patterns in neonates and adults are different. This difference may reflect differences in the behavioral or developmental state. **References:** Kusaka T, Kawada K, Okubo K, et al.; *Human Brain Mapping* 22:122-132, 2004. Kusaka T, Isobe K, Nagano K, et al.; *NeuroImage* 13: 944-952, 2001. Isobe K, Kusaka T, Nagano K, et al.; *Neurosci Lett* 299: 221-224, 2001.

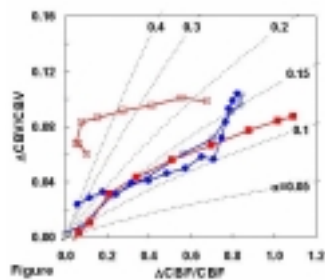
## DYNAMIC RELATIONSHIP BETWEEN CHANGES IN CBF AND CBV DURING SOMATOSENSORY STIMULATION: IMPLICATIONS FOR CALIBRATED FMRI

Ikunhiro Kida<sup>1,2</sup>, Fahmeed Hyder<sup>2</sup>

<sup>1</sup>Graduate School of Dental Medicine, Hokkaido University, Sapporo, Japan

<sup>2</sup>Magnetic Resonance Research Center, Yale University, New Haven, CT, USA

The relationship between dynamic changes in cerebral blood flow (CBF) and volume (CBV) are very important for calibrating fMRI so that changes in oxidative metabolism can be determined [1]. Although recent animal studies [2,3] have investigated dynamic changes in CBF and CBV ( $\Delta\text{CBF}/\text{CBF}$  and  $\Delta\text{CBV}/\text{CBV}$ ), the studies were limited by use of either non-quantitative methods or the CBF and CBV data had different spatial resolutions. Here towards the goal of calculating dynamic changes in cerebral metabolic rate for oxygen consumption (CMRo2) quantitatively, we demonstrate the combined method of the modified functional MRI for CBF [4] with contrast agent for CBV [5] to clarify the relationship between dynamic  $\Delta\text{CBF}/\text{CBF}$  and  $\Delta\text{CBV}/\text{CBV}$  of rat somatosensory cortex during forepaw stimulation with different stimulus duration (4,8,16,32 seconds). The figure shows the relationship between dynamic  $\Delta\text{CBF}/\text{CBF}$  and  $\Delta\text{CBV}/\text{CBV}$  for two stimulus duration (4 (blue) and 16 (red) seconds). The filled and opened symbols represent the period of transition from stimulus onset to peak and transition from stimulus offset to baseline, respectively. The dotted lines show the value of the parameter  $\alpha$  ranging from 0.05 to 0.4 in  $\text{CBV}=\text{CBF}^\alpha$ . The relationship between dynamic  $\Delta\text{CBF}/\text{CBF}$  and  $\Delta\text{CBV}/\text{CBV}$  was different throughout different stimulus durations and became complex as the stimulus duration became longer. The values of  $\alpha$  ranged from 0.05 to 0.15 during transition from stimulus onset to a peak, whereas the value ranged from 0.15 to 0.45 during transition to baseline after stimulus offset. Thus the Grubb's power exponent,  $\alpha=0.38$  [6], should be used with caution when being used for predicting changes in CMRo2 during transition [7] and even steady state [8] since the values of  $\alpha$  ranged from 0.10 to 0.25 under steady state throughout stimulus durations. This is the first study to directly investigate the relationship between the dynamic changes in CBF and CBV during transition periods (i.e. onset and offset of stimulation) using only MRI methods, which allow us to measure the transient changes with same spatial and temporal resolution in same subject. The modified fMRI method with contrast agent has a great potential to predict the dynamic changes in CMRo2 without any further perturbations or assumption. 1. Ogawa et al., *Biophys J* 64:803-12, 1993; 2. Mandeville et al., *Magn Reson Med* 3:615-24, 1998; 3. Jones et al., *Neuroimage* 15:474-87, 2002; 4. Kida et al., *JCBFM* 24:1369-81; 5. Kennan et al., *Magn Reson Med*, 37:953-6, 1997; 6. Grubb et al., *Stroke* 5:630-9, 1974; 7. Wu et al., *Magn Reson Med* 48:987-93, 2002; 8. Kim et al., *Magn Reson Med* 38:59-65, 1997 Supported by NIH (NS-037203, DC-003710, MH-067528) and NSF (DBI-0095173) grants.



## VISUALIZING ACTIVATED MICROGLIAS IN WERNICKE-KORSAKOFF SYNDROME BY [11C]PK11195 AND PET

Mihoko Tsukahara<sup>1,2</sup>, Kenji Ishii<sup>1</sup>, Yuichi Kimura<sup>1</sup>, Sachio Matsushita<sup>2</sup>, Susumu Higuchi<sup>2</sup>, Kiichi Ishiwata<sup>1</sup>

<sup>1</sup>Positron Medical Center, Tokyo Metropolitan Institute of Gerontology, Tokyo, Japan

<sup>2</sup>Department of Psychiatry, National Hospital Organization Kurihama Alcoholism Center, Kanagawa, Japan

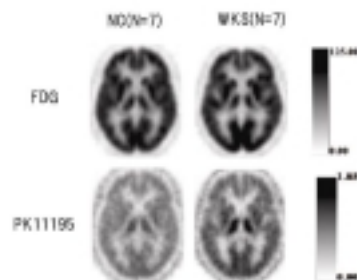
**Introduction** Wernicke's encephalopathy (WE), often seen in chronic alcoholics, results from thiamine deficiency and clinically develops ophthalmoplegia, ataxic gait, and confusion. It sometimes improves without any defect, but a part of WE subsequently progresses to Wernicke-Korsakoff syndrome (WKS) characterized by continuous amnesia. In chronic WKS, pathological changes are seen mainly in the periventricular regions of the third and fourth ventricles and aqueduct where the number of astrocytes is increased but neurons are relatively preserved. Severe neuronal loss occurs in thalamus and inferior olive. An experimental animal model of thiamine deficiency revealed that the reactive activated microglia appear in relatively early stage of WE and it might be a predictor for the prognosis. [11C]PK11195, specific radioligand for peripheral benzodiazepine binding site on activated microglia in the brain *in vivo*, has been used for imaging neuroinflammation by PET. The purpose of this study is to examine if the activated microglia in WKS can be visualized by [11C]PK11195 and PET as a marker of pathological process to assess status of the disease and prognosis.

**Subjects and Methods** We studied seven chronic WKS patients (ages 35-68) and seven healthy volunteers (ages 43-74) who were not habitual alcohol drinkers. All the subjects participated in two PET studies with [18F]FDG and [11C]PK11195. A 6-minute static scan was started at 45 minutes after the intravenous injection of 150MBq [18F]FDG. Regional cerebral glucose metabolism was evaluated semi-quantitatively by normalized regional activity in reference to the global activity. A dynamic PET scan was performed in a 3D mode for 60 minutes after the injection of 500MBq of [11C]PK11195 with serial arterial blood sampling and metabolite analysis. Parametric image of the distribution volume (DV) of [11C]PK11195 was created by Logan-plot method. Volumetric 3D MR images were obtained for anatomical reference. Two PET images were coregistered to individual MRI and regions of interest were placed on thalamus, anterior cingulate, caudate nucleus, and hippocampus.

**Results** The cerebral glucose metabolism was declined in WKS in thalamus, anterior cingulate, frontal and temporal cortex. The DV of [11C]PK11195 was elevated in most of regions in the brain, especially in pons and thalamus (Figure).

**Conclusions** Our preliminary results suggested that the activated microglia in WKS can be visualized by [11C]PK11195 and PET. This technique may be useful to monitor the pathological process in WKS and to predict the prognosis.

**Legend of Figure** Averaged images of FDG uptake and DV of PK11195 in normals (n = 4) and Wernicke-Korsakoff syndrome patients (n = 3). The elevation of DV in thalamus is shown in this slice.



**COUPLING BETWEEN EVOKED NEURAL AND HEMODYNAMIC RESPONSES IN THE SOMATOSENSORY CORTEX OF ISOFLURANE-ANESTHETIZED RATS****Kazuto Masamoto, Tae Kim, Mitsuhiro Fukuda, Ping Wang, Seong-Gi Kim***Department of Neurobiology, University of Pittsburgh, Pittsburgh, PA, USA*

**Aim:** Isoflurane anesthesia is commonly used for functional imaging studies in animals due to the ease of anesthetic induction and an ability to perform survival experiments. However, it was reported that functional-metabolic coupling in the rat somatosensory cortex induced by rectangular pulse stimulation (0.3-ms pulse duration and 5-Volt intensity at 3 Hz) was achieved only under alpha-chloralose anesthesia (Ueki et al. 1992). This observation can be due to either species variations (rats vs. other animals), and/or unoptimized somatosensory stimulus. In the present study, evoked neural and hemodynamic responses in the rat somatosensory cortex were characterized under isoflurane anesthesia. **Materials and methods:** Eight male Sprague-Dawley rats (350-450 g) were used for measurements of neural activity and hemodynamic responses induced by forepaw somatosensory stimulation, and two rats were used for functional MRI (fMRI) studies. End-tidal CO<sub>2</sub> and arterial blood pressure were continuously monitored and blood gases were maintained at a normal range. Isoflurane concentration was kept at 1.3-1.4% in a mixture of O<sub>2</sub> and air. The skull was thinned to measure 620-nm wavelength intrinsic optical imaging for the localization of the forelimb area. Local field potential (LFP) and cerebral blood flow (CBF) were simultaneously recorded at the activation focus induced by electrical forepaw stimulation using a tungsten microelectrode and laser-Doppler flowmetry, respectively. Parameters of forepaw somatosensory stimulus consisting of ten rectangular pulses were systematically varied by i) pulse width (0.1-5.0 ms) at fixed current (1.0 mA) and frequency (8 Hz), ii) current level (0.2-2.0 mA) at fixed pulse width (1.0 ms) and frequency (8 Hz), and iii) inter-pulse intervals (50-500 ms) at fixed pulse width (1.0 ms) and current (1.0 mA). Finally, blood oxygenation level-dependent (BOLD) fMRI (9.4T/31 cm, Varian System) was performed in isoflurane-anesthetized rats with optimized forepaw stimulation parameters as determined by LDF. **Results and discussion** Stimulus optimization: When pulse width and current level increased, the summation of LFP and the amplitude of CBF changes in the forelimb area were similarly augmented, and reached to plateau levels (90% of LFP and CBF plateau at 1.0 ms and 1.4 mA vs. 0.5 ms and 1.0 mA, respectively). On the other hand, the summation of LFP increased monotonically with an increase of inter-pulse intervals (90% of plateau: 250 ms), while the largest CBF change ( $70 \pm 30\%$ , Mean  $\pm$  SD) was found at stimulus frequency of 12 Hz (an inter-pulse intervals: 82.5 ms). These stimulus conditions did not change blood pressure. Our results indicate that coupling between evoked neural and hemodynamic response is not impaired under isoflurane-anesthetized rats, but that the optimum stimulus frequency is strongly influenced by the anesthesia used. **fMRI study:** Using BOLD fMRI in isoflurane-anesthetized rats, we detected the focal activation at the primary forelimb somatosensory area. This further indicates that the isoflurane-anesthetized rat model can be also used for hemodynamic-based functional imaging. Volatile isoflurane anesthetic can be used for rodent functional neuroimaging, allowing the repetition of survival studies over days and months for clinical and basic neuroscience research (e.g., development, learning, and plasticity).

**NON-STATIONARY GAUSSIAN SPATIO-TEMPORAL MODELING OF FMRI DATA****Jean-Michel Pignat**<sup>1</sup>, Oleksiy Koval<sup>2</sup>, Sviatoslav Voloshynoskiy<sup>2</sup>, Vicente Ibanez<sup>3</sup>,Thierry Pun<sup>2</sup><sup>1</sup>*Faculty of Medicine, University of Geneva, Geneva, Switzerland*<sup>2</sup>*Department of Informatics, Faculty of Sciences, University of Geneva, Geneva, Switzerland*<sup>3</sup>*Department of Psychiatry, University Hospital of Geneva, Geneva, Switzerland*

In functional magnetic resonance imaging (fMRI), modeling of the complex link between neuronal activity and its hemodynamic expression via the neurovascular coupling usually requires the use of elaborated models. To avoid linear assumptions and a priori modeling of this expected hemodynamic signal, Bayesian approaches have recently improved their accuracy in estimating and detecting brain activation. Recent studies, using Markov random field (MRF) to represent activated brain voxels and likelihoods to find the maximum a posteriori (MAP) estimation of model parameters, provided superior efficiency in comparison with the context-free and the statistical parametric mapping (SPM) approaches. We propose another approach for detecting brain activity by introducing non-Gaussian and non-stationary Gaussian image models that exploit local subband image statistics in the non-decimated wavelet domain. These statistical models, being very simple and tractable, have demonstrated state-of-the-art performance in a number of applications including lossy image compression, denoising and digital watermarking. Such an approach yields close form analytical solutions with low computational complexity that makes it very attractive in neuropsychological research allowing to obtain theoretical performance limits. These models in the scope of the Bayesian estimation framework are applied on synthetic fMRI data corrupted by an additive white Gaussian noise (AWGN) with varying variance and on real fMRI data obtained from a motor preparation task. Comparison of the results with those obtained using SPM maps demonstrates the high efficiency of the proposed method.

**CORRELATION OF CHANGES IN CORTICAL BOLD MR CONTRAST, NEAR-  
INFRARED SPECTROSCOPY AND LASER DOPPLER FLOW DURING BRAIN  
ACTIVATION AND TRANSIENT HYPERTENSION**

Ursula I. Tuor<sup>1,2</sup>, Min Qiao<sup>1</sup>, Rong Wang<sup>1,2</sup>, David Rushforth<sup>1</sup>, Tadeusz Foniok<sup>1</sup>,  
Susan Sea<sup>1</sup>, Boguslaw Tomanek<sup>1,2</sup>, R. Anthony Shaw<sup>3</sup>

<sup>1</sup>*MR Technology, Institute for Biodiagnostics (West), Calgary, AB, Canada*

<sup>2</sup>*Department of Clinical Neurosciences and Hotchkiss Brain Institute, University of Calgary,  
Calgary, AB, Canada*

<sup>3</sup>*Spectroscopy, Institute for Biodiagnostics, Winnipeg, Manitoba, Canada*

**Introduction:** Blood oxygenation-level dependent (BOLD) contrast used to detect brain activation using functional magnetic resonance imaging (MRI) is primarily a result of local decreases in deoxyhemoglobin (dHb) related to elevations in cerebral blood flow (CBF) produced by the coupling between changes in neural activity and local CBF. Transient hypertension producing hyperemia independent of alterations in the cerebral metabolic rate of oxygen consumption could also affect BOLD contrast. Presently, we compare the effect of transient hypertension and electrical forepaw stimulation on changes in: 1) BOLD contrast measured using functional MRI, 2) CBF measured with laser Doppler flowmetry and 3) cerebral oxygenation measured with near-infrared (IR) spectroscopy. **Material and Methods:** Functional MRI or near-IR experiments were performed in 19 chloralose anesthetized rats using identical preparations except that in the near-IR studies the skull was thinned and near-IR and Doppler probes were placed over the sensory motor cortex. In each animal, experiments investigated the 'activation' response to: 1) electrical stimulation of the forepaw, 2) increases in blood pressure (BP) or 3) a combination of an increase in BP and forepaw stimulation. For fMRI studies, experiments consisted of acquiring sets of 32 gradient echo T2\* images (TR/TE=70/10ms, flip angle=20°, matrix=128x128, slice thickness=1.5mm) using a 9.4T MRI system. Near-IR spectra were acquired every second during each paradigm of 320 seconds duration, and subsequently curve-fit (least squares) with the component absorptivity spectra of oxyHb, dHb, and water. MR images or spectra and flow data were collected with electrical stimulation of the forepaw either off or on, or during BP increases of 0, 30-45 or >60 mm Hg produced by the intravenous injection of norepinephrine (0.15-1.2µg/kg). For the fMRI experiments, a cross-correlation analysis (p<0.001) to either the stimulation paradigm or the time course of BP changes was used to identify voxels of activation in the sensory motor cortex from which their maximum MR signal intensity changes relative to initial baseline values was determined. **Results:** With electrical stimulation of the forepaw alone, activation was detected within the sensory motor cortex and the MR signal intensity increased by approx. 6%. Corresponding to these changes, forepaw stimulation resulted in increases in CBF and oxyHb and decreases in dHb. With increases in BP alone there were increases in CBF, MR signal intensity and oxyHb and decreases in dHb where the magnitude of these changes was dependent on the change in BP (e.g. MR signal intensity increased by 7+6%, p<0.05). When both forepaw stimulation and increases in BP were produced, the BOLD changes and CBF changes were enhanced compared with stimulation alone (e.g. MR signal intensity increased 15.4+ 4%, p<0.05 with >60 mm Hg changes in pressure). Such enhancement was less evident for the dHb and oxyHb changes. **Conclusions:** The response to either an increase in BP or electrical forepaw stimulation results in decreases in dHb and increases in flow, oxyHb and BOLD MR intensity. The BOLD and CBF changes produced by neuronal activation are enhanced by increases in BP. (Supported by Canadian Institutes of Health Research).

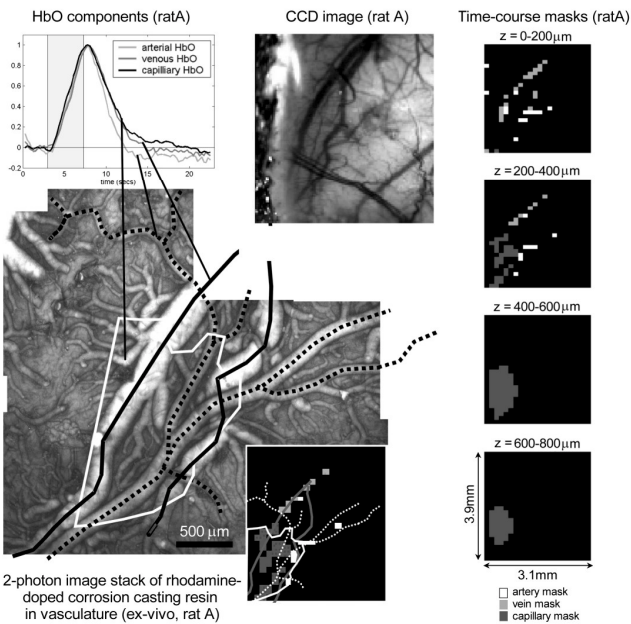
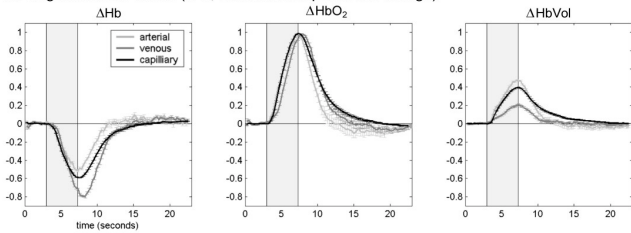
**THE USE OF DEPTH-RESOLVED OPTICAL IMAGING TO SEPARATE CORTICAL VASCULAR COMPARTMENTS DURING FUNCTIONAL ACTIVATION**

Elizabeth M.C. Hillman, Anna Devor, Anders M. Dale, Andrew K. Dunn, David A. Boas

*Athinoula A. Martinos Center for Biomedical Imaging, Massachusetts Gen Hospital, Charlestown, MA, USA*

Optical imaging of exposed cortex allows real-time observation of blood oxygenation and volume changes. These changes are most frequently visualized as 2D images, whose pixels represent superficially weighted sums of signals from deeper layers. We have developed a non-contact optical imaging system for visualizing cortical hemodynamics in 3D, to depths of >2mm, with 100-200 micron resolution (Hillman et al, Opt Lett 29(14), 2004). The new system has been used to image rat somatosensory cortex through thinned skull during forepaw stimulation. The ability to discriminate between hemoglobin changes in superficial and deeper layers, has enabled extraction of functional time-courses that correspond to three major vascular compartments; arterial, venous and capillary (Figure shows average trends for 5 rats). It has been found that, not only can these time-courses be reliably extracted from the 3D images, they can be used to isolate the spatial distributions of the three components (figure shows masks of voxels in 3D optical image corresponding to time-course characteristics). The good correspondence between the components' locations and the true vascular architecture (see figure) implies that the extracted functional time-courses indeed also represent the evolution of changes in the three compartments. Features include smaller volume changes, and significantly later onset times in veins, compared to arteries and capillaries. Arterial components show larger volume changes, and much earlier returns to baseline than capillary and venous compartments. These techniques and results will be discussed, along with their implications for fMRI, 2D optical imaging and quantification of the cerebral metabolic rate of oxygen consumption.

Average functional trends (n=5, normalized to peak HbO change)





**CEREBRAL CORRELATES OF CHRONIC ARTHRITIC PAIN IN COMPARISON WITH ACUTE EXPERIMENTAL PAIN USING 18 FDG POSITRON EMISSION TOMOGRAPHY (PET)**

**Bhavna Kulkarni<sup>1</sup>**, Emma Boger<sup>1</sup>, Peter Julyan<sup>2</sup>, Alison Watson<sup>1</sup>, Rebecca Elliott<sup>3</sup>,  
David Hastings<sup>2</sup>, Anthony K.P. Jones<sup>1</sup>

<sup>1</sup>*Human Pain Research Group, University of Manchester Rheumatic Diseases Centre, Clinical Sciences Building, Hope Hospital, Salford, UK*

<sup>2</sup>*North Western Medical Physics, Christie Hospital NHS Trust, Withington, UK*

<sup>3</sup>*Neuroscience and Psychiatry Unit, Stopford Building, University of Manchester, Manchester, UK*

Background: Using functional imaging techniques, mostly in healthy volunteers, it is now evident that pain is processed in a network of cortical and sub-cortical areas, termed the 'pain matrix'. Within this network a division of function has been proposed: i) Medial pain system (the medial thalamus, cingulate and insular cortices), that predominantly processes emotional aspects of pain and ii) Lateral pain system (the lateral thalamus and somatosensory cortices), that predominantly processes sensory-discriminative aspects of pain. At present the relevance of acute experimental pain studies is difficult to assess due to the small numbers of functional imaging studies performed in the chronic pain conditions. In order to address this, we have performed a study comparing chronic arthritic pain with acute experimental pain in the same patient group. Methods: 18 FDG PET was used to measure alterations in the regional cerebral glucose metabolism (rCMRGlucose) that indirectly correlated with neuronal activity. 12 patients with osteoarthritis predominantly affecting knee underwent PET scans during 3 randomised conditions: 1) Ongoing arthritic knee pain (chronic pain condition), 2) No / reduced pain (pain-free condition) and 3) Acute experimental pain (when free of arthritic pain). During the first condition, affected knee was maintained in a posture that aggravated pain during the experiment. In the second condition, pain-free state resulted from natural remission of pain and rest. In the third condition, acute experimental heat pain was induced using a thermode, when patients were free of their arthritic pain at rest. During the tracer uptake in all 3 conditions, patients were immobile and rated their perceived pain intensity and unpleasantness using 0 – 100 rating scale at 10 minute intervals. The intensity of the perceived pain was matched for both acute experimental pain and the arthritic pain. After scanning, patients gave an average retrospective pain rating. Data analysis was performed using Statistical Parametric Mapping (SPM2). Results: Across the group, significant differences (thresholded at  $p < 0.01$ ) were seen in the rCMRGlucose between the three conditions. i) Chronic arthritic pain Vs pain free condition increased rCMRGlucose in the bilateral perigenual cingulate, posterior cingulate, insula / SII, SI, MI, inferior parietal cortices, cerebellum, temporal cortices and left thalamus, caudate nucleus and amygdala. ii) Acute experimental pain Vs pain free condition increased rCMRGlucose in the bilateral insula / SII, SI, MI and inferior parietal cortices, left perigenual cingulate, thalamus and putamen. iii) Chronic arthritic pain Vs acute experimental pain increased rCMRGlucose in the bilateral anterior cingulate, posterior cingulate, orbitofrontal and prefrontal cortices, amygdalae, cerebellum and left sided caudate nucleus. Conclusions: This is the first functional imaging study to identify cerebral correlates of chronic musculoskeletal pain processing. We propose that in comparison with acute experimental pain, chronic pain is processed mainly in the medial pain system and is possibly driven by emotional aspects of pain. These results may open avenues for further physiological and pharmacological studies and improve upon the currently limited pain therapies.

**PURE ANARTHRIA DUE TO PRECENTRAL GYRUS INFARCTION : FMRI STUDY**

**Takanori Oikawa**, Reiko Fukatsu, Kinya Hisanaga, Masaaki Kato, Hiroshi Mochizuki,  
Hiroshi Saito

*Department of Neurology, Miyagi National Hospital, Miyagi, Japan*

Isolated pure anarthria (aphemia) due to precentral gyrus lesion is considered rare<sup>1,2,3</sup>. We describe five patients who presented with pure anarthria as their isolated or major symptom following a precentral gyrus infarction. Their speech were effortful, non fluent and dysprosodic. However, their language comprehension, repetition and naming abilities were normal. There were no buccofacial or pharyngeal muscle dysfunction. The demography and clinical characteristics of the patients are summarized in the table. The lesions were located on the left precentral gyrus in two (case 1 and 2) and on the right in three (case 3, 4, and 5) (figure). All patients were right handed. Four patients (case. 1, 2, 4 and 5) had atrial fibrillation and one (case 3) had patent foramen ovale with right to left shunt. The patients were studied using whole brain functional magnetic resonance imaging (fMRI) (Semens, 1.5T, echo planner imaging, bloodoxygenation-level dependent) with three tasks (naming, verb generation, categorization) to assess language dominant hemisphere<sup>4</sup>. fMRI showed left dominance of language in all patients. These results showed that pure anarthria was not related to language lateralization. Then, pure anarthria may not be aphasia but may be motor dysfunction or dysfunction of the lower system of language. 1. Tabuchi K, Odashima K, Fujii T, et al. The left central gyrus lesion and pure anarthria. *Rinshou Shinkeigaku* 2000;40:464-470 2. Tanji K, Suzuki K, Yamadori A, et al. Pure anarthria with predominantly sequencing errors in phoneme: a case report. *Cortex* 2001;37:671-678 3. RL Ruff, E Arbit. Aphemia resulting from a left hematoma. *Neurology* 1981;31:353-356 4. CA Cuenid, SY Biikheimer, L Hertz-Pannier et al. Functional MRI during word generation, using conventional equipment: A potential tool for language localization in the clinical environment. *Neurology* 1995;45:1821-1827

## 5-HT<sub>1A</sub> RECEPTOR DENSITY AND DEFENSIVE PERSONALITY - INTERACTION OF NEUROCHEMISTRY, PERSONALITY AND DEPRESSION EXPLORED WITH [11C]WAY 100635 PET

Eugenii A. Rabiner<sup>1,2</sup>, Andrew D. Lawrence<sup>3</sup>, Zubin Bhagwagar<sup>2,4</sup>, N. Venkatesha Murthy<sup>2</sup>, R. Alexander Bantick<sup>4</sup>, Philip J. Cowen<sup>4</sup>, Paul M. Grasby<sup>2</sup>

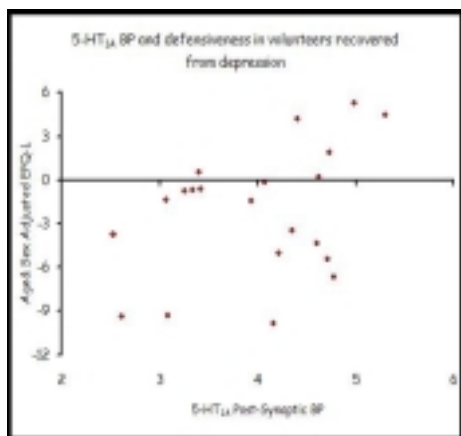
<sup>1</sup>*Translational Medicine and Technologies, GlaxoSmithKline, ACCI, Cambridge, UK*

<sup>2</sup>*MRC Clinical Sciences Centre, Imperial College, London, UK*

<sup>3</sup>*MRC Cognition and Brain Sciences Unit, Cambridge, UK*

<sup>4</sup>*Department of Psychiatry, University of Oxford, Oxford, UK*

**Background:** We previously demonstrated a negative correlation between post-synaptic 5-HT<sub>1A</sub> receptor density (measured with [11C]WAY-100635 PET) and defensive personality style (assessed as the Eysenck Personality Questionnaire Lie scale, EPQ-L), in 2 independent cohorts of healthy volunteers<sup>1,2</sup>. Both 5-HT<sub>1A</sub> receptor density and defensive personality have been linked to depressive illness. 5-HT<sub>1A</sub> receptor density decreases in subjects with a history of depression (whether currently depressed or not), raise the possibility of relative 5-HT<sub>1A</sub> receptor decrease being a pre-disposing factor for the development of depressive illness. The personality trait of defensiveness is linked to an inhibition of the perception of threat and an attenuated experience of negative affect. Subjects with high defensiveness scores have been shown to have a reduced lifetime rate of psychopathology. We therefore explored the relationship between 5-HT<sub>1A</sub> receptor density, defensiveness and depressive illness. **Methods:** 5-HT<sub>1A</sub> receptor density was assessed as previously described<sup>1</sup> using [11C]WAY 100635 on the ECAT 953B PET camera, and a basis function implementation of the simplified reference tissue model. Defensiveness was assessed as the score of the EPQ-L questionnaire. A group of 21 antidepressant free, euthymic patients (13M, 8F), with a past history of major depressive disorder, was examined and the results compared to our database of 65 healthy volunteers (61M, 4F) assessed previously<sup>1,2</sup>. As the EPQ-L correlates significantly with age all comparisons were controlled for age and sex. **Results:** We found a highly significant correlation between 5-HT<sub>1A</sub> receptor density and EPQ-L ( $r = 0.626$ ,  $DF = 17$ ,  $p = 0.004$ ). In healthy volunteers the equivalent correlation is also highly significant, but negative ( $r = -0.413$ ,  $DF = 61$ ,  $p = 0.001$ ). **Conclusions:** We demonstrated that the relationship between 5-HT<sub>1A</sub> receptor density and the personality trait of defensiveness, is modified by the presence of past depressive illness. Differences in neurochemical-cognitive-behavioural interaction between depressed patients and healthy volunteers, as well as the relationship of these findings to recently demonstrated links between 5-HT<sub>1A</sub> receptor system and religiosity<sup>3</sup>, will be discussed. 1 Rabiner et al, *Neuroimage*, 15(3): 620-632 (2002) 2 Rabiner et al, *Biol Psychiatry*, 53(8S): 214S (2003) 3 Borg et al, *Am J Psychiatry*, 160(11): 1965-1969 (2003).





**QUANTITATIVE PET DETERMINATION OF PERICONTUSIONAL TISSUE VIABILITY: CORRELATION WITH DIAGNOSTIC CT IMAGING AND IMPLICATIONS FOR SURGICAL REMOVAL FOLLOWING TRAUMATIC BRAIN INJURY**

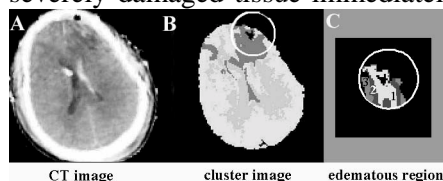
Hsiao-Ming Wu<sup>1</sup>, Sung-Cheng Huang<sup>1,2</sup>, Chin-Lung Yu<sup>1</sup>, Thomas, C Glenn<sup>3</sup>, Paul, M Vespa<sup>3</sup>, David, A Hovda<sup>1,3</sup>, Marvin Bergsneider<sup>3</sup>

<sup>1</sup>*Department of Molecular and Medical Pharmacology, David Geffen School of Medicine, UCLA, Los Angeles, CA, USA*

<sup>2</sup>*UCLA-DOE Institute for Molecular Medicine, David Geffen School of Medicine, UCLA, Los Angeles, CA, USA*

<sup>3</sup>*Division of Neurosurgery, David Geffen School of Medicine, UCLA, Los Angeles, CA, USA*

After traumatic brain injury (TBI), damaged brain tissue may demonstrate different degrees of hemorrhage, ischemia, or infarction. Surgical evacuation is often needed for lesions causing mass effect, but guidelines for the extent of tissue removal are unclear. In this study, we used positron emission tomography (PET) to study the tissue viability in pericontusional regions. Methods: Eight TBI patients (male; GCS 8-12) with intracerebral contusions were studied. In addition to routine CT scans, MR and PET scans, taken within four days after injury, were co-registered. Grey matter (GM) and white matter (WM) regions were separated using a MR-based segmentation technique. To analyze the pericontusion regions, we used a semi-automatic method to separate the contusional core and adjacent edema from the normal-appearing tissues using the conformal anatomical information derived from CT/MR images and cluster analysis. Metabolic changes occurring in contusions and surrounding tissues were comprehensively characterized using quantitative PET studies measuring regional cerebral blood flow (rCBF), oxygen extraction fraction (rOEF) and oxygen metabolism (rCMRO<sub>2</sub>). The coupling between flow and metabolism was evaluated by examining their correlations (voxel-wise rCBF vs. rOEF and rCBF vs. rCMRO<sub>2</sub>, respectively). Voxel values of rCMRO<sub>2</sub> in sixteen normal subjects were studied to determine a threshold value of living tissue for TBI data analysis. Results: The pericontusional region clustered into four distinct groups (e.g. Fig. A: CT image, B: cluster image). One cluster (in black; Fig. B) corresponded to the CT hyper-density contusional core and another (in dark gray) matched the surrounding CT hypo-density edematous tissue. PET data showed that the normal-appearing GM brain tissue adjacent to but 1 cm rim away from the hypo-density pericontusional region on CT had concurrent decreased flow/metabolism with a preserved ratio of rCBF to rCMRO<sub>2</sub>. The pericontusional region, however, had a variable flow/metabolism profile characterized by a nonviable core (i.e. CT hyper-density voxels) surrounded by damaged tissue (i.e. CT hypo-density voxels). The degree of flow/metabolic abnormalities centrifugally decreased with increasing distance from the core (e.g. labeled as group 1, 2 and 3, respectively, in Fig. C; the voxels correspond to the dark gray cluster within the circular area of Fig. B and were separated into three groups using two rCMRO<sub>2</sub> threshold values). Within the pericontusional CT hypo-density regions, 44 ± 19% (mean ± 1 s.d.; range 11-60%; n = 8) of the GM voxels had rCMRO<sub>2</sub> values less than the 5%ile of normal WM rCMRO<sub>2</sub> values (i.e. 0.46 ml/min/100g). In contrast, 22 ± 11 % (range 5-40%) of the GM voxels had rCMRO<sub>2</sub> values that were similar to (within 80% confidence interval) the corresponding TBI normal-appearing GM values. Conclusion: Our regional metabolic data suggest that the CT hyper-dense core and more than 10% of the adjacent hypo-dense area are severely damaged and likely nonviable (CMRO<sub>2</sub> values below 0.5 ml/min/100g). Surgical evacuation of severely damaged tissue immediately surrounding contusions is not expected to be harmful to the patient.





## DYNAMIC CEREBRAL RESPONSES TO PROLONGED HYPOGLYCAEMIA IN HEALTHY VOLUNTEERS MEASURED USING [15O]-H2O PET

Joel T. Dunn<sup>1</sup>, Laurence J. Reed<sup>2</sup>, Iain A. Cranston<sup>1</sup>, Paul K. Marsden<sup>3</sup>, Stephanie A. Amiel<sup>1</sup>

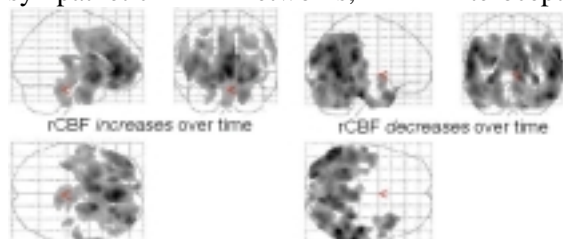
<sup>1</sup>*Department of Diabetes & Endocrinology, Guy's, King's and St Thomas' School of Medicine, King's College London, London, UK*

<sup>2</sup>*Department of Psychological Medicine, Guy's, King's and St Thomas' School of Medicine, King's College London, London, UK*

<sup>3</sup>*Clinical PET Centre, Guy's, King's and St Thomas' School of Medicine, King's College London, London, UK*

**Introduction:** Normal brain function is dependent on an adequate glucose supply that is maintained by a highly efficient homeostatic system keeping glucose levels within a well defined range. Acute hypoglycaemia in healthy subjects is associated with neuroendocrine and behavioural responses with distinct time-courses leading to awareness of the hypoglycaemic state. However, an important problem for sufferers of diabetes is 'hypoglycaemia unawareness' leading to potentially life threatening complications. Our aim was to investigate the regional brain responses to the onset and prolongation of acute hypoglycaemia in healthy volunteers using water positron emission tomography ([15O]-H2O PET), to determine the normal response prior to examining responses in diabetic subjects.

**Methods:** Seven healthy men underwent a hypoglycaemic insulin clamp to sustain a plasma glucose level of 2.6mmol/l over a 60 minute period. Subjects were scanned four times - at euglycaemia 30 minutes prior to reaching hypoglycaemic target and then at 30 minute intervals. **Results:** Adrenaline, noradrenaline, cortisol and growth hormone rose in all subjects with hypoglycaemia. Analysis of the PET data over time is shown in the figure, and revealed significant increases in regional cerebral blood flow (rCBF) ( $p < 0.05$ ) with hypoglycaemia in subgenual to rostral anterior cingulate, and contiguous regions spanning bilateral orbitomedial frontal cortices, amygdala and ventral striatum. Significant decreases in rCBF ( $p < 0.05$ ) over time were observed in retrosplenium, visual cortices, bilateral parietal and cerebellar vermis. Region of interest analysis revealed distinct time courses of responses, in particular early activation of orbitomedial frontal and amygdala, later engagement of anterior cingulate and disengagement of retrosplenium. **Discussion:** This is the first study to examine the evolution of neuronal responses to hypoglycaemia over time. The networks of regions involved are also known to be involved in the human response to primary stressors, e.g. pain, hunger, air hunger. Decreases in rCBF in the retrosplenial, visual and cerebellar cortices are consistent with the memory, visual and coordination disturbances associated with prolonged hypoglycaemia in diabetics. Considering hypoglycaemia as a dynamic state has also allowed us to identify pathways from correlates of neuroendocrine release with rCBF involving sympathetic networks, interoception and reward pathways.



## FRactal Correlation Structure in fMRI Data of Rat Brain

Peter Herman<sup>1,2</sup>, Ikuhiro Kida<sup>1,3</sup>, Basavaraju G. Sanganahalli<sup>1</sup>, Fahmeed Hyder<sup>1,4</sup>,  
Andras Eke<sup>2</sup>

<sup>1</sup>*Diagnostic Radiology, Yale University, New Haven, CT, USA*

<sup>2</sup>*Institute of Human Physiology and Clinical Experimental Research, Semmelweis University, Budapest, Hungary*

<sup>3</sup>*Oral Physiology, Hokkaido University, Sapporo, Japan*

<sup>4</sup>*Biomedical Engineering, Yale University, New Haven, CT, USA*

The raw fMRI data are normally analyzed by statistical methods (Student's t or non-parametric tests) to yield measures of physiological responses. This analysis assumes that successive events in the raw signal are independent (white noise) [1] and hence have a Gaussian distribution. Colored noise if present in the dynamic fMRI data can cause high rate of false positives [2]. Such positive correlations have been reported in human fMRI data [1,2] which are characterized by a spectrum with increasing power toward the low frequencies (1/f pattern). This 1/f pattern can be numerically characterized by a fractal parameter, the Hurst exponent, H. The fMRI experiments of the  $\alpha$ -chloralose (40 mg/kg/hr) anesthetized rats (n=12) were conducted on a 4.0T or 9.4T spectrometer using a 1H resonator/surface-coil radio-frequency probe [3] and echo-planar imaging (EPI). Gradient-echo EPI data were acquired with repetition time of 200 ms in matrices of 32×32 (4.0T) and 64×64 (9.4T). Data were collected in vivo and post mortem. Scaled windowed variance (SWV) method [4] was used to calculate the fractal parameter, H and the nearest neighbor correlation coefficient, r1 [5] from the fMRI time series. The length of the time series, 4096 scans (4.0T) and 8192 scans (9.4T), were adequate for a reliable estimation of H [6]. The fMRI data from the 4.0T magnet was dominated by white noise with H=0.53±0.014. All 9.4T fMRI time series showed fractional Gaussian noise (fGn) with H>0.5, different from white noise. The H of fGn within its lower and upper bounds of 0 and 1 characterizes the correlation structure itself: with H=0.5 the signal is random, H<0.5 indicates anti-correlation with negative r1, and H>0.5 indicates correlation with positive r1 [6]. Representative Hurst exponent maps obtained in vivo and post mortem were obtained for both 4.0T and 9.4T. In vivo cortical and subcortical gray matter regions exhibited much higher values of H (0.73±0.05) with r1=0.38 than white matter regions (H=0.57±0.01, r1=0.10). The post mortem results showed a significant (p<0.05) decrease in fractal structure obtained in both gray and white matter regions (H=0.61±0.03 and H=0.56±0.03, respectively) and the fractal or colored noise correlation structures were mainly broken in the gray matter regions (r1=0.17). High magnetic field fMRI data reveal fractal patterns across different brain regions. These findings should have implications in fMRI data processing: successive events of the fMRI signal are correlated hence statistical mapping should be used with prior treatment of data, such as creating surrogate time series, which destroys the correlation structure in a time series without the modification of actual values [7]. Supported by NIH (DC-003710, MH-067528), NSF (DBI-0095173), and OTKA (T34122) grants. [1] Purdon PL, Weisskoff RM (1998) *Human Brain Map* 6:239-249. [2] Aguirre GF et al (1998) *Magn Reson Med* 39:500-505. [3] Hyder F et al (2001) *NMR Biomed* 2001 14(7-8):413-31. [4] Cannon MJ et al (1997) *Physica A* 241:606-6. [5] van Beek J et al (1989) *Am J Physiol* 257:H1670-H1680. [6] Eke A et al (2002) *Physiol Meas* 23:R1-R38. [7] Teich MC et al (1997) *J Opt Soc Am A* 14(3):529-546.

## SIMULTANEOUS ACQUISITION OF FMRI AND EEG IN THE PICROTOXIN MODEL OF EPILEPSY

Michel B. Mesquita<sup>1,2</sup>, Michael J. Brammer<sup>1</sup>, Steven C. R. Williams<sup>1</sup>

<sup>1</sup>*Neuroimaging Research Group, Institute of Psychiatry, King's College London, London, UK*

<sup>2</sup>*Department of Physiology and Biophysics, Institute of Biological Sciences/Federal University of Minas Gerais, Belo Horizonte, Brazil*

(a)Background: One of the greatest challenges in epileptology is the identification and localisation of those brain areas responsible for eliciting and maintaining epileptiform activity. Furthermore, it is also important to ascertain whether there is any dynamic interaction between those different brain areas. Research has, to date, focused primarily on EEG. Although EEG has high temporal resolution, it lacks spatial resolution due to the inverse problem of dipole source localization. On the other hand, fMRI has great spatial resolution but a relatively poor temporal resolution due to the delayed haemodynamic response that we image, the so called BOLD (Blood Oxygenation Level Dependent) signal. To take advantage of the temporal resolution of EEG and spatial resolution of fMRI it would be desirable to combine both methods in a single technique. Even though several experiments have been reported in recent years using simultaneous acquisition of EEG and fMRI in humans, very few experiments have endeavoured to combine these techniques in animal studies. Here we describe our results using simultaneous acquisition of EEG and fMRI to study the picrotoxin model of epilepsy. (b)Methods: Male adult Wistar rats (330g) were anaesthetized with urethane (140mg/kg,i.p.) and carbon fibre EEG surface electrodes were placed over the skin of both cerebral hemispheres. The signals from the electrodes were amplified inside the bore of the fMRI scanner by a x2000 pre-amplifier, placed 25cm away from the head of the rat to decrease "magnetic gradient interference". The signals were then taken out of the magnet via optical fibre cables, reconverted into electrical signals, conditioned (CyberAmp380-Axon Instruments; amplification=200; high-pass filter=0.15Hz; low-pass filter=60Hz; Notch filter 50Hz) and then converted to digital data (MP100-Biopac Systems; sampling rate=500spl/s). Two raw signal channels were recorded and two digitally filtered channels were calculated in real time (low-pass filter at 60Hz with Q=1 + band-stop filters in 38, 76 and 114Hz). Physiological monitoring (respiration and temperature) was performed throughout the experiment. Dynamic MR images were acquired using a 4.7T imaging system (Varian; Gradient-echo; TR=1050ms; TE=10ms; 40 slices per volume affording one whole brain scan per minute for a total scan duration of 45mins.). Picrotoxin injection (8mg/kg,i.p.) was remotely performed after acquisition of the first 10 volumes, without interruption of imaging or EEG recording. (c)Results: we were able to acquire good quality EEG and fMRI data from all subjects. During the experiments all animals presented a typical evolution of the EEG morphology: electrodecremental response followed by isolated spikes, poli-spikes and spike-and-waves, culminating in status epilepticus. The MR images acquired showed a robust negative BOLD response (global minimum) in the caudate and nucleus accumbens and a positive response (global maxima) in the amygdale. (d)Conclusion: (1) The methodology described above is suitable for simultaneous acquisition of EEG and fMRI in anaesthetized animals. (2) The analysis of the images acquired during the electrodecremental response showed robust negative BOLD in the caudate and nucleus accumbens. (3) The negative BOLD signal change observed during the electrodecremental response suggests a correlation between amplitude variation of the EEG and the BOLD contrast.

**PET-FDG STUDY: REGIONAL ASSOCIATIONS WITHIN THE CORTICO-STRIATAL CIRCUITS IN OCD PATIENTS****Steven Haugbøl<sup>1</sup>, Gitte M. Knudsen<sup>1</sup>, Stefan Kemeny<sup>2</sup>, Li-Ching Lee<sup>3</sup>,****Steen G. Hasselbalch<sup>1</sup>, Elsebet S. Hansen<sup>4</sup>**<sup>1</sup>*Neurobiology Research Unit, Copenhagen University Hospital, Copenhagen, Denmark*<sup>2</sup>*Language and Speech Branch, National Institutes of Health, Bethesda, MD, USA*<sup>3</sup>*Department of Epidemiology, Johns Hopkins University, Baltimore, MD, USA*<sup>4</sup>*Department of Psychiatry, Copenhagen University Hospital, Copenhagen, Denmark*

**Introduction.** Obsessive-compulsive disorder (OCD) is characterized by recurrent, intrusive thoughts or stereotyped behaviour that interfere with daily living. Advanced structural and functional imaging tools have provided us with valuable information about the neuroanatomical pathophysiology in OCD patients. The objective of this study was to explore associations between regions within the orbitofrontal, dorsolateral, motor and limbic loop before treatment and after successful treatment with a selective serotonin reuptake inhibitor (SSRI). **Methods.** Twenty outpatients with OCD underwent two PET-FDG scans with an interval of 3-6 months. Regional cerebral glucose metabolism was quantitated using the autoradiographic method. The PET scans were preprocessed using SPM 99 and a region of interest (ROI)-based data extraction was done using in-house developed Matlab based software, 14 ROIs considered of relevance for OCD were included in the analysis. The 14 ROI's were segmented into four different cortico-striatal-thalamo-cortical-circuits. Regression analyses were done between ROI's in OCD patients before and after SSRI treatment. The Generalized Estimating Equation approach with an interaction term was applied to examine the associations between ROI's in OCD patients before and after SSRI treatment. **Results.** A significant negative association between the left caudate/ventral striatum and the left anterior cingulate was identified in OCD patients post treatment; however, there were no significant association before SSRI treatment. A negative association was found between right supplementary motor area and right putamen; and the association became weaker after treatment. **Conclusions.** Associations in glucose metabolism between brain circuits in patients with OCD are significantly altered upon successful pharmacological treatment. This finding may contribute to our understanding of OCD pathophysiology.

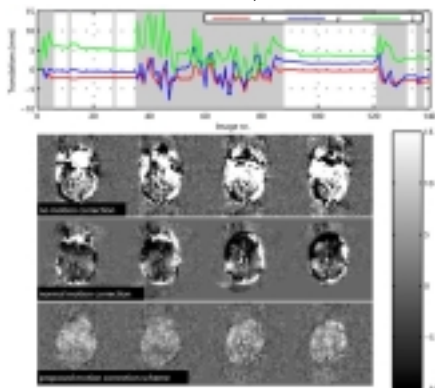
## ARTERIAL SPIN LABELING IN THE PRESENCE OF SEVERE MOTION

Karam Sidaros<sup>1</sup>, Kern Olofsson<sup>2</sup>, Maria J. Miranda<sup>1,2</sup>, Olaf B. Paulson<sup>1</sup>

<sup>1</sup>Danish Research Centre for Magnetic Resonance, Copenhagen University Hospital, Hvidovre, Denmark

<sup>2</sup>Department of Paediatrics, Copenhagen University Hospital, Hvidovre, Denmark

Perfusion measurements using Arterial Spin Labelling (ASL) are based on the subtraction of two MR images, one in which arterial blood is tagged (tag image) and one in which it isn't (control image). Due to low SNR, the measurement is averaged over 100-200 repetitions giving a total imaging time on the order of 5-10min. Motion artefacts can therefore be a problem when performing ASL measurements on certain patient groups, such as unsedated children and demented or psychiatric patients. Retrospective motion correction of the measured volumes reduces the motion artefacts, but is often insufficient to give usable perfusion images. We propose an automated scheme for overcoming motion artefacts in ASL measurements and demonstrate its ability to produce artefact-free images in unsedated neonates. The scheme is based on a two-step realignment. The acquired ASL images were realigned using the SPM2 ([www.fil.ion.ucl.ac.uk/spm/](http://www.fil.ion.ucl.ac.uk/spm/)) realignment tool [2]. Images from the periods with significant motion (absolute translations >2mm or rotations >1.5degrees between successive volumes) were discarded. The remaining volumes were realigned again and used for perfusion calculation. ASL measurements from 29 healthy, unsedated term neonates and preterm neonates scanned at term were analyzed using the proposed scheme. All images were acquired on a Siemens Magnetom Trio 3T scanner using a PICORE QUIPSS II sequence with the following imaging parameters: 16 slices, 5mm slice thickness, 0.5mm slice gaps, TI1/TI2/TR/TE=700/1500/2700/23ms, FOV=192mm, 64x64 matrix, GE-EPI readout, 140 repetitions with a total imaging time of 6:18min. The figure shows an example of the motion curves obtained by regular motion correction. The shaded areas are the periods with significant motion. The images are the mean perfusion-weighted images: without motion correction (upper row), after normal motion correction (middle row) and after motion correction with the proposed scheme (bottom row). It is clear that regular motion correction is insufficient. By discarding some of the images, it is possible to obtain artefact-free ASL images despite the severe motion. The average number of motion-free images for all infants was 92/140, and only 4/29 infants had less than 50 motion-free images and therefore had to be excluded due to insufficient SNR. In conclusion, we have demonstrated that acquiring non-invasive perfusion maps is possible despite motion. Using the proposed scheme, perfusion images of sufficient quality can be obtained at the cost of a reduced SNR compared to a motion-free scan, but without the need to repeat the scan.

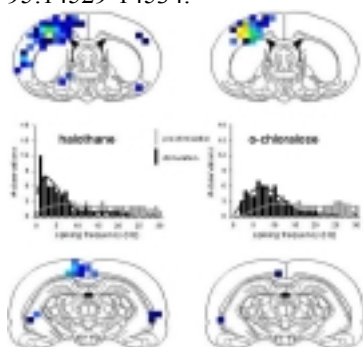


## NEURAL BASIS OF LOCALIZED AND DELOCALIZED fMRI PATTERNS

Natasja J.G. Maandag<sup>1,2</sup>, Arien J. Smith<sup>1,3</sup>, Hal Blumenfeld<sup>4</sup>, Robert G. Shulman<sup>1</sup>, **Fahmeed Hyder**<sup>1,5</sup>

<sup>1</sup>Diagnostic Radiology, Yale University, New Haven, CT, USA, <sup>2</sup>Intensive Care Medicine, University Medical Centre, Nijmegen, The Netherlands, <sup>3</sup>Neurosurgery, Mount Sinai Hospital, New York, NY, <sup>4</sup>Neurobiology, Yale University, New Haven, CT, <sup>5</sup>Biomedical Engineering, Yale University, New Haven, CT, USA

What connections can we draw between fMRI and neural firing patterns? The basic requirement of differencing in neuroimaging has limitations because subtraction of baseline activity removes an important part of the total activity [1]. Our prior studies have quantitatively revealed that most neurons in the ensemble (in a voxel) contribute differently before, during, and after the stimulation [2]. Since the ensemble activity of pyramidal neurons in layer 4 depends on sensory (or localized) input by the thalamus and global (or delocalized) input from other cortical regions, delocalized signals from a global workspace may affect localized stimulus-induced responses. To test the hypothesis that delocalized signals, which have been proposed to include subjective contributions [3], can modulate localized signals we conducted fMRI and electrophysiological studies in rats under varied conditions of anesthesia and forepaw stimulation. The fMRI experiments of  $\alpha$ -chloralose (40 mg/kg/hr) and halothane (0.7%) anesthetized rats were conducted on 7.0T or 9.4T systems using calibrated fMRI [1,2]. The electrical activity was measured by Tungsten microelectrodes. The extracellular signals were filtered to separate field and action potentials (FP, AP), where the AP data were binned for spiking frequency. While the fMRI data from both baselines (i.e., halothane and  $\alpha$ -chloralose) showed sensory-induced changes in the contralateral primary somatosensory and motor areas, there were increased delocalized activities observed with (light) halothane anesthesia. These regions were ipsilateral primary somatosensory, contralateral secondary somatosensory, as well as perirhinal and retrosplenial agranular areas. In contrast signals from delocalized regions were notably absent with (deep)  $\alpha$ -chloralose anesthesia. These results were supported by correlated changes in AP and FP time courses. The spiking frequency distributions measured from the most activated foci in the contralateral (and ipsilateral) primary somatosensory area(s). The contralateral distributions with (deep)  $\alpha$ -chloralose anesthesia showed a significant shift from low to high frequency values upon stimulation. The contralateral distribution shift was less noteworthy with (light) halothane anesthesia. The distributions for the baselines with halothane and  $\alpha$ -chloralose were significantly different, in which the degrees of global inputs assigned to higher frequencies dominated under (light) halothane anesthesia. The contralateral distributions upon stimulation with halothane and  $\alpha$ -chloralose were also significantly different, suggesting that under the (light) halothane anesthesia level the global inputs dominated whereas local changes were dominated under the (deep)  $\alpha$ -chloralose anesthesia. Since neuronal populations in different regions do not function as modules, the resultant fMRI or electrophysiological activity patterns arise from interactions of afferent and efferent connections – the latter of which was modulated by anesthesia in this study. These results provide the initial steps to explore the interactions of localized and delocalized underpinnings of the concept of the global workspace model [3]. Supported by NIH (DC-003710, MH-067528) and NSF (DBI-0095173) grants. [1] Hyder (2002) PNAS-USA 99:10771-10776. [2] Smith (2002) PNAS-USA 99:10765-10770. [3] Dehaene (1998) PNAS-USA 95:14529-14534.





## DOES GRAVITY AFFECT FUNCTIONAL CEREBRAL BLOOD FLOW RESPONSE?

Elizabeth R. Devine<sup>2</sup>, William P. Milberg<sup>3,4</sup>, **Jorge M. Serrador**<sup>1,2</sup>

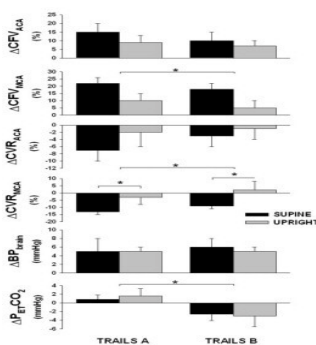
<sup>1</sup>*Division On Aging, Harvard Medical School, Boston, MA, USA*

<sup>2</sup>*Gerontology Division, Beth Israel Deaconess Medical Center, Boston, MA, USA*

<sup>3</sup>*VA Medical Research, New England GRECC-Boston Division, Boston, MA, USA*

<sup>4</sup>*Department of Psychiatry, Harvard Medical School, Boston, MA, USA*

Cerebral blood flow (CBF) is critical for proper neuronal function. Since flow is dependent on perfusion pressure, the cerebrovasculature dilates/constricts in response to driving pressure to maintain flow relatively constant. This process is termed autoregulation and essential to maintaining flow in the upright posture when the effect of gravity results in an ~20 mmHg reduction in perfusion pressure to the brain due to the hydrostatic gradient. Up regulation of CBF has been used extensively to localize cognitive activation, i.e. functional imaging. However, due to technical constraints the majority of this work has been done with subjects in the supine position. The recent development of transcranial Doppler (TCD) allows the continuous measurement of cerebral flow velocity (CFV) in the main cerebral arteries. By measuring flow velocity during cognitive tasks, we are able to perform functional TCD. To assess whether gravity had an effect on the functional response to a cognitive task (Trails A & B), we performed functional TCD on subjects in both the upright and supine positions. In addition to cerebral flow velocity in the anterior (ACA) and middle cerebral arteries (MCA) (TCD), we measured beat-by-beat blood pressure (Finapres) and breath-by-breath end tidal CO<sub>2</sub> (PETCO<sub>2</sub>) via nasal cannula (Datex-Ohmeda). Subjects were randomly assigned to either the supine or upright position, performed the task, and then moved to the other position, and performed the same task with different number and letter patterns. Upon going from the supine to upright position, subjects demonstrated a non-significant reduction in both ACA (-4±4%) and MCA (-3±2%) flow. In contrast mean arterial pressure increased (81±7 to 91±4 mmHg) although non-significant, while PETCO<sub>2</sub> did not change (40.8±1.3 vs 40.0±1.7 mmHg). During cognitive activation with either the Trails A or B there was a significant increase in flow associated with reductions in cerebrovascular resistance (CVR). Interestingly, this functional activation was attenuated in the upright posture (only significant in the MCA). Surprisingly, the functional activation was also reduced in Trails B compared to Trails A. This was likely the consequence of the hypocapnia that was only present during the Trails B assessment. These data highlight the possibility that functional response to cognitive activation may be affected by body position. Since our healthy control subjects demonstrate an attenuated response, one might postulate that patients with an impaired cerebrovasculature and already attenuated response in the supine position may be at even more risk when upright. Further work is necessary to determine what role perfusion pressure may play in functional cerebral blood flow response and how this attenuated response may impact on functional cognitive performance. This work supported by NASA, NIH NIDCD and Boston Veterans Administration.



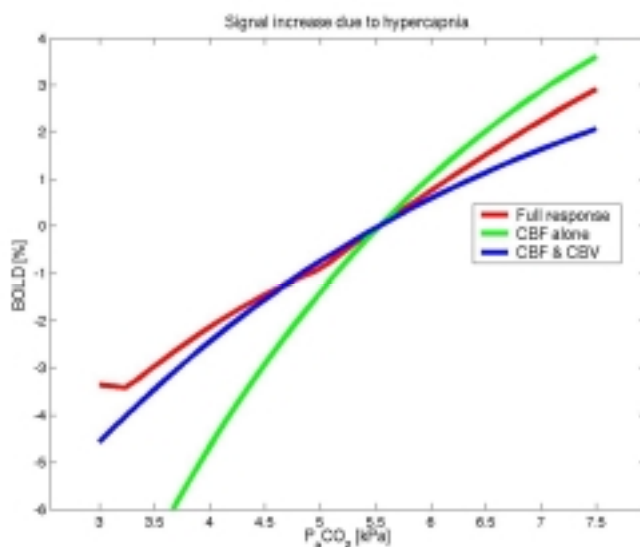


## MODELLING THE BOLD RESPONSE, A NUMERICAL APPROACH

Egill Rostrup, Olaf B. Paulson

*Danish Research Centre for Magnetic Resonance, Copenhagen University Hospital,  
Hvidovre, Denmark*

A comprehensive model of the BOLD response is presented, in which differential equations for cerebral O<sub>2</sub> and hemoglobin (Hgb) transport are solved numerically. Several features of cerebral O<sub>2</sub> transport can be investigated, and the consistency of current conceptions of BOLD responses tested. This study applies the model to the effects of arterial hematocrit, PaCO<sub>2</sub> and PaO<sub>2</sub>, in responses elicited by functional activation (fBOLD) and physiological perturbation (pBOLD). The model uses 4 major compartments: arterial, capillary and venous as well as an extravascular compartment. Within the intravascular compartment the distribution of O<sub>2</sub> between Hgb-bound and physically dissolved phases is updated for every time step,  $\delta t$ , as a function of local pH, PCO<sub>2</sub> and DPG. Total content of deoxy-Hgb is calculated as the sum of arterial, capillary and venous concentrations weighted by their respective volume fractions. The corresponding R<sub>2</sub>\*-contribution is calculated as proposed by Ogawa et al. (1993). Relationships between PaO<sub>2</sub>, PaCO<sub>2</sub> and CBF, as well as between CBF and CBV were taken from previous studies. The model predicted BOLD effects of the expected magnitude (1-3% at 1.5T), and confirmed an inverse relation between fBOLD and baseline CBF. A slight decrease in fBOLD response was seen with high baseline hematocrit and constant CBF, but an increase was seen when concomitant flow decreases were included (in agreement with empirical results). During hypercapnia the predicted pBOLD response was high when CBF changes alone were included (figure: green curve), but attenuated by the accompanying CBV change (blue curve). The response was elevated when all effects were included (red curve), mainly due to the effect of arterial hyperoxia (hyperventilation), less to pH changes. Several physiological effects thus were predicted in accordance with established results. The model suggests that known effects of hematocrit may be due to accompanying flow changes. During hypercapnia, arterial hyperoxia is an important factor which should be taken into account when used in calibration experiments for CMRO<sub>2</sub> determination. Numerical simulation seems helpful in interpreting BOLD effects caused by complex physiological responses.



## PET OEF REACTIVITY (OEFR) TO ACETAZOLAMIDE IN OCCLUSIVE VASCULAR DISEASE

Edwin M. Nemoto<sup>1</sup>, Howard Yonas<sup>1</sup>, Hiroto Kuwabara<sup>3</sup>, Ronda Pindzola<sup>1</sup>, Donald Sashin<sup>5</sup>, Yuefang Chang<sup>1</sup>, Tudor Jovin<sup>2</sup>, James Gebel<sup>4</sup>, Maxim Hammer<sup>2</sup>, Lawrence Wechsler<sup>2</sup>

<sup>1</sup>Department of Neurosurgery, University of Pittsburgh, Presbyterian University Hospital, Pittsburgh, PA, USA

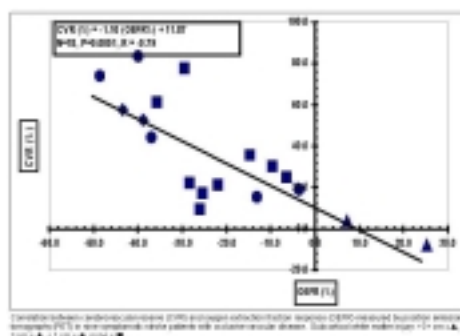
<sup>2</sup>Department of Neurology, University of Pittsburgh, Presbyterian University Hospital, Pittsburgh, PA, USA

<sup>3</sup>Department of Radiology, Johns Hopkins University, Baltimore, MD, USA

<sup>4</sup>Department of Neurology, Jewish Hospital, Louisville, KY, USA

<sup>5</sup>Department of Radiology, University of Pittsburgh, Presbyterian University Hospital, Pittsburgh, PA, USA

**Background and Purpose:** Cerebrovascular reserve (CVR) and oxygen extraction fraction (OEF) in symptomatic patients with carotid occlusive vascular disease (OVD) are proven independent predictors of increased stroke risk. However, a substantial number of patients identified by compromised CVR were normal by OEF and highly associated with subcortical white matter infarction. Our aim was to determine whether a vasodilatory challenge with acetazolamide could differentiate regions with normal OEF that are hemodynamically compromised by a positive OEF response (OEFR), i.e. increased OEF with cerebrovascular dilatation. **Methods:** Nine symptomatic patients with carotid OVD were studied by PET cerebral blood flow (CBF) and cerebral metabolic rate for oxygen (CMRO<sub>2</sub>) before and 15 min after acetazolamide. CVR and OEFR were calculated as the percent change in CBF and OEF from baseline. MCA territories were analyzed for PET variables by hemispheric average, separate axial 4-level analysis and parametric analysis. Subcortical white matter infarctions were graded from T2-weighted MRI. **Results:** The relationship between CVR-OEFR hemispheres was highly significant ( $P=0.0001$ ,  $R=-0.79$ )(see Fig). Positive OEFR values were correlated with the lowest CVR values and the most severe subcortical white matter infarction. Parametric analysis suggested increased CMRO<sub>2</sub> in acute and reduced CMRO<sub>2</sub> in chronic ischemic stress in these patients. **Conclusions:** Brain regions with normal OEF may be associated with a severely compromised hemodynamic state. A stress test with acetazolamide measures OEF reactivity (OEFR), which differentiates these regions. However, the stroke risk of the subgroup with normal OEF, elevated OEFR and compromised CVR remains to be determined.

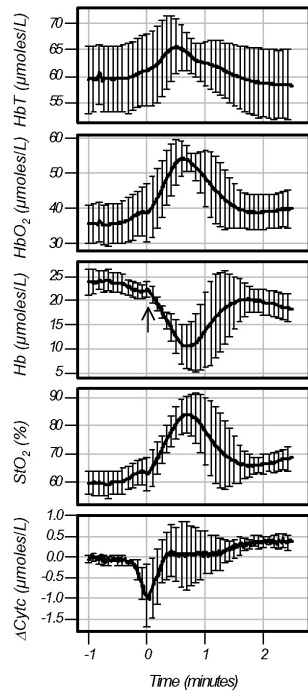


## AN "EARLY DIP" COINCIDES WITH MITOCHONDRIAL HYPOXIA DURING SPREADING DEPRESSION

Josephine H. Woodhams, Michelle A. Abajian, Roger J. Springett

*Department of Radiology, Dartmouth Medical School, Hanover, NH, USA*

**Introduction:** The early increase in deoxyhemoglobin (Hb), usually referred to as the early dip, is seen in many but not all functional activation studies. It is assumed to be the result of the increase in oxygen consumption (CMRO<sub>2</sub>) desaturating the capillary bed prior to the increase in blood flow (CBF). We have recently developed, and validated with cyanide, a visible spectroscopy algorithm that measures the oxidation state of mitochondrial cytochrome c (Cyt<sub>c</sub>) as well as the absolute hemoglobin concentration and saturation directly from the attenuation spectrum. Whereas the hemoglobin saturation (StO<sub>2</sub>) is sensitive to vascular oxygen tension (PvO<sub>2</sub>), Cyt<sub>c</sub> is sensitive to mitochondrial oxygen tension (PmO<sub>2</sub>). Spreading depression (SD) is a wave of depolarization followed by a hyperemia which propagates across the cortex. The combination of these measurements with an SD model in which there are large and dynamic increases in CMRO<sub>2</sub> and CBF is ideal for determining the role of oxygen gradients within the brain. **Methods:** Five Sprague Dawley rats were anaesthetised with isoflurane and ventilated. The scalp was removed and the skull over the parietal cortex was thinned to translucency with a burr. SD was induced by applying KCl to a small burr hole through the skull 3-4mm away from the optodes. **Results:** The figure shows total hemoglobin (HbT), oxyhemoglobin (HbO<sub>2</sub>), deoxyhemoglobin (Hb), StO<sub>2</sub> and changes in Cyt<sub>c</sub> during the passage of an SD wave. Maximum reduction of Cyt<sub>c</sub> during anoxia is typically 7-8 micromoles/L. A small rise in Hb is seen (arrow). Results are expressed as mean±SD. **Discussion:** The results show an increase in HbT and StO<sub>2</sub> as would be expected during an increase in CBF. However, prior to these increases, there is a small reduction in Cyt<sub>c</sub> that renormalizes during the onset of the hyperemia. The oxidation state of Cyt<sub>c</sub> should be independent of PmO<sub>2</sub> until PmO<sub>2</sub> falls below a critical level. The reduction in Cyt<sub>c</sub> is likely due to an increase in oxygen consumption that drives PmO<sub>2</sub> below the critical level. The increase in CBF then raises StO<sub>2</sub> and PvO<sub>2</sub> that subsequently increases the PmO<sub>2</sub> back above the critical level and Cyt<sub>c</sub> reoxidizes. A small increase in Hb is seen coincident with the reduction in Cyt<sub>c</sub> consistent with the increase in CMRO<sub>2</sub> partially desaturating the capillary bed.



**USING PHARMACOLOGICAL MRI TO MAP THE DOSE DEPENDENT ACTIONS OF THE AMPA POTENTIATOR LY451395 IN THE RAT BRAIN****Nicholas Jones<sup>1</sup>**, Michael J. O'Neill<sup>2</sup>, Mark Tricklebank<sup>2</sup>, Steve C.R. Williams<sup>1</sup><sup>1</sup>*Neuroimaging Research Group, Institute of Psychiatry, London, UK*<sup>2</sup>*Eli Lilly & Co. Ltd., Windlesham, UK*

Deficits in cognition are common in a range of psychiatric disorders including dementia, schizophrenia and depression. Evidence suggests that enhancement of glutamatergic, and more specifically  $\alpha$ -amino-3-hydroxy-5-methyl-4-isoxazolepropanoic acid (AMPA) receptor-mediated transmission may form a potential treatment strategy for these symptoms (Expert Opin Investig Drugs, 9, 765). Recently, a novel series of biarylsulfonamides, typified by LY451395 and LY404187, that are potent and centrally active AMPA receptor potentiators, have been described (CNS Drug Rev, 8, 255). These compounds act as positive allosteric modulators, increasing ion channel flux in the presence of agonist by suppressing desensitisation and/or deactivation of the receptors and are active in animal models of cognition (Curr Drug Targets CNS Neurol Disord, 3, 181). 2-deoxyglucose autoradiography and c-fos immunocytochemistry techniques show AMPA potentiators act at regions in the rat brain implicated with mnemonic processes such as the hippocampus and the frontal and anterior cingulate cortex (J Cereb Blood Flow Metab, 24, 1098). We have recently reported that the neural targets of a single dose of LY404187 can also be investigated using blood oxygenation level dependant (BOLD) pharmacological magnetic resonance imaging (phMRI [J Psychopharmacol 18 Suppl]). The current study aimed to further this work by investigating the effects of a range of doses of the AMPA potentiator LY451395 on BOLD contrast in the rat brain. Male Sprague Dawley rats were anaesthetised with isoflurane, secured in a stereotaxic frame and placed inside a 4.7 Tesla superconducting magnet. Using a continuous, three echo, gradient-echo (GE) sequence (TE = 5, 10, 15 msec; TR = 940msec; acquisition matrix = 64 x 64 x 24; FOV = 4cm<sup>2</sup>; yielding an isotropic voxel resolution of 0.5 x 0.5 x 0.5mm), whole brain volumes of 40 slices were acquired every minute for 180 minutes. 30 minutes into the scan subjects received an acute dose of 0.5 mg/kg, 1.5 mg/kg, 3.0 mg/kg LY451395 or vehicle (sc, n=7-9). Brain volumes were realigned, spatially normalised to a randomly chosen template and Gaussian smoothed. Post-processed images were analysed in SPM99 using a fixed-effects General Linear Model multi-subject covariates design. This created statistical parametric maps (SPMs) for each treatment group displaying statistically significant changes in BOLD contrast which correlated with the known pharmacokinetic profile of LY451395. No significant increases in BOLD contrast were observed in the vehicle or 0.5 mg/kg groups. The 1.5 mg/kg group displayed small increases in cortical BOLD contrast. An acute dose of 3.0 mg/kg LY451395 produced widespread bilateral increases in cortical BOLD signal, most notably in the visual and auditory cortices, the temporal association cortex and the ectorhinal cortex as well as a unilateral increase in the thalamus. These results demonstrate that phMRI can detect the dose-dependant actions of LY451395 in the rat brain and add to the accumulating evidence that the technique can be used for non-invasive in vivo investigations into the targets of CNS-active compounds.

## FUNCTIONAL STIMULATION DURING CEREBRAL ISCHEMIA

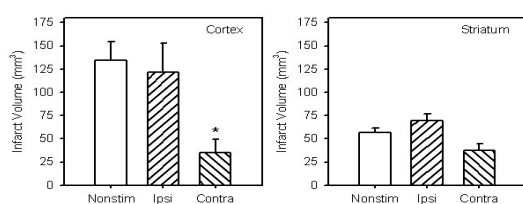
Mark G. Burnett<sup>2</sup>, Tomokazu Shimazu<sup>1</sup>, Tamas Szabados<sup>1</sup>, Hiromi Muramatsu<sup>2</sup>,

John A. Detre<sup>1</sup>, **Joel H. Greenberg<sup>1</sup>**

<sup>1</sup>*Department of Neurology, University of Pennsylvania, Philadelphia, PA, USA*

<sup>2</sup>*Department of Neurosurgery, University of Pennsylvania, Philadelphia, PA, USA*

**Introduction:** There are studies in the literature indicating that stimulation of the brain stem and spinal cord has potential for reducing ischemic damage, and that electromagnetic exposure can provide cytoprotection, although the mechanism of this neuroprotection has not been determined. Our laboratory has data showing that activation-flow coupling is preserved not only with pharmacological modification of cerebral blood flow but also during severe ischemia. This raises the question as to whether functional activation of ischemic tissue may provide neuroprotection, or alternatively, will worsen neuronal damage. **Methods:** Twenty-eight adult male Sprague-Dawley rats were anesthetized with halothane and prepared for temporary (90 min) occlusion of the right middle cerebral artery (MCA) using the filament model. Cerebral blood flow in the MCA territory was continuously monitored with a laser-Doppler flowmeter (LDF). Two subdermal needle electrodes were inserted into the dorsal forepaw and either the forepaw ipsilateral to the occlusion or contralateral to the occlusion was stimulated starting one minute into ischemia and continuing throughout the ischemic period (5 Hz, 2 mA, duty cycle = 4 sec on 3 sec off). A control group did not receive any forepaw stimulation. A neurological evaluation was undertaken following 24 hours of reperfusion and animals were then sacrificed and 1 mm thick slices stained with 2% 2,3,5-triphenyltetrazolium chloride (TTC). Cortical and striatal damage were measured separately. **Results:** The cortical infarct volume was significantly reduced in the contralateral stimulated group compared to both the ipsilateral stimulated group and the non-stimulated group ( $p < 0.05$ ) (figure). There was no significant difference between any of the groups for infarct volume in the striatum. Thus the neuroprotection was only obtained in the cortex, and only by stimulation of the forepaw contralateral to the stroke. The neurobehavioral score for the contralaterally stimulated group had a median of 6, smaller (less deficit) than that of the ipsilateral (median=9) and control (median=9) groups, but this decrease failed to achieve statistical significance. Considering that the striatal infarct volumes were somewhat similar in all the groups, this is not surprising. All of the animals exhibited a dramatic decrease of LDF upon occlusion of the MCA, with flow decreasing to approximately 26% of baseline in all the control groups. Fifteen minutes after occlusion, however, LDF in the ipsilateral and contralateral groups had increased to 34% of baseline, while LDF in the control group remained at 23-25%. Following removal of the filament, blood flow increased to 109-115% of baseline in all groups, with the control group decreasing to the control level within 10 minutes, whereas in the stimulated groups LDF decreased to 70-75% of the baseline level. **Conclusion:** Contrary to the expectation, functional activation of ischemic tissue may actually decrease tissue damage. The mechanism of this effect remains to be determined.



## DETECTION OF HAEMODYNAMIC CHANGES IN ZEBRA FINCH BRAIN BY OPTICAL AND FUNCTIONAL MAGNETIC RESONANCE IMAGING

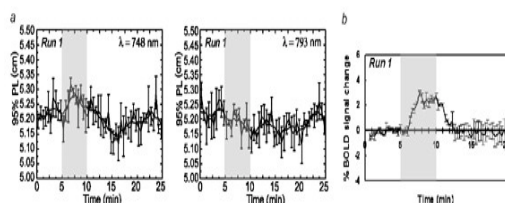
Tiny Boumans<sup>1</sup>, Clémentine Vignal<sup>2,3</sup>, Stéphane Ramstein<sup>2</sup>, Marleen Verhoye<sup>1</sup>, Johan Van Audekerke<sup>1</sup>, Stéphane Mottin<sup>2</sup>, Nicolas Mathevon<sup>3</sup>, Annemie Van der Linden<sup>1</sup>

<sup>1</sup>Bio-Imaging Lab, UA, Antwerp, Belgium

<sup>2</sup>LTSI CNRS UMR 5516, University Jean Monnet, St-Etienne, France

<sup>3</sup>NAMC CNRS UMR 8620, University Paris XI & LBA University Jean Monnet, Paris, France

Songbirds' vocal communication behaviour has been a favourite research domain for years. In order to study brain activation in response to acoustic stimuli, two different in-vivo methods that are able to assess neuronal activity based on detection of haemodynamic changes were compared within identical experimental settings. Optical imaging (non-invasive in-vivo broadband time-resolved spectroscopy) and functional magnetic resonance imaging (Blood Oxygenation Level Dependent MRI) were both performed in zebra finch brain upon a hypercapnic challenge known to induce a standard haemodynamic response. The use of these two methods offers the opportunity to compare their sensitivity and to correlate local variations in CBV and haemoglobin saturation level (obtained from optical data) with local BOLD signal variations (providing overall information on CBF, CBV and haemoglobin oxygenation). Both for optical imaging and fMRI, four adult female zebra finches (*Taeniopygia guttata*) were anaesthetized with 2% isoflurane while spontaneously breathing, and immobilized in a stereotactical device equipped with essential monitoring devices. Each bird underwent three runs of 5 minute hypercapnia (600 ml/min 7% CO<sub>2</sub>, 21% O<sub>2</sub>, 72% N<sub>2</sub>), interleaved by 20 minutes normocapnia (600 ml/min 21% O<sub>2</sub>, 79% N<sub>2</sub>). Optical imaging was performed with an ultrafast white laser and time-resolved spectrometer. With the 95% PL (i.e. mean path length of the light detected by the camera at 95% of the measured temporal profile) at 2 spectral windows centered at 748nm and 793nm, we quantify respectively the haemoglobin saturation level and CBV. MR imaging was performed at 300 MHz on a 7 Tesla in-vivo NMR microscope with horizontal bore and actively shielded gradient-insert (210 mT/m). The optical imaging data demonstrated that hypercapnia induced a significant increase of the hemoglobin saturation level in run1 ( $p=.01$ ) and run2 ( $p=.01$ ). No significant CBV changes were observed during run1 ( $p=.1$ ), run2 ( $p=.75$ ) and run3 ( $p=.5$ ). The fMRI data demonstrated the existence of significant BOLD signal changes for run1 ( $p<.001$ ), run2 ( $p<.001$ ) and run3 ( $p<.001$ ). No significant difference between the runs ( $p=.950$ ) was detected. As it was already shown that fMRI can be used to discern auditory induced activation in the songbird brain (Van Meir et al., NeuroImage, accepted), comparison of signal intensity changes upon a standard haemodynamic challenge provides a good indication whether optical imaging could be used as an alternative in-vivo method to probe acoustically induced brain activity in the songbird brain. Our data show that upon a 7% CO<sub>2</sub> challenge, fMRI is the most sensitive of the two displaying a 2.6% contrast increase as compared to the 1.2% contrast increase for optical imaging. Further optimization of the optical imaging protocol will be necessary in order to use it as a probe for in-vivo brain haemodynamic changes during acoustic recognition in small zebra finch brains. Figure: (a) Mean 95% PL changes (reflecting respectively haemoglobin saturation level and CBV) and (b) mean percent BOLD signal changes with standard errors for four birds during the first hypercapnia run (administration of 7% CO<sub>2</sub> is indicated by gray area).





**NO ASSOCIATION BETWEEN GENOTYPES OF THE 5-HT<sub>2A</sub> RECEPTOR GENE AND [18F]ALTANSERIN BINDING AS MEASURED WITH PET**

Steven Haugbøl<sup>1</sup>, Lars H. Pinborg<sup>1</sup>, Steen G. Hasselbalch<sup>1</sup>, Vibe G. Frøkjær<sup>1</sup>, Lis Hasholt<sup>2</sup>, Gitte M. Knudsen<sup>1</sup>

<sup>1</sup>*Neurobiology Research Unit, Copenhagen University Hospital, Copenhagen, Denmark*

<sup>2</sup>*Department of Medical Biochemistry and Genetics, University of Copenhagen, Copenhagen, Denmark*

**Background.** The serotonin 2A receptor has been suggested to play a role in a number of mental diseases including obsessive-compulsive, schizophrenia, affective disorders, Tourette's syndrome and migraine. To evaluate the genetic influence on the phenotypical expression of the 5-HT<sub>2A</sub> receptor binding in the human brain in vivo, we examined the allelic variations of single nucleotide polymorphism G-1438A and T102C and measured [18F]altanserin binding in the brain with PET. **Methods.** Sixty-eight controls were investigated with PET-[18F]altanserin using a bolus-infusion schedule to obtain steady-state of tracer in blood and tissue. Binding potential data for [18F]altanserin were measured in frontal cortex. A standard PCR procedure was used for genotyping. The comparison between groups was done by ANOVA, with age as a covariate. **Results.** The allelic frequencies in our sample were: G-1438A g/g: 41 %, g/a: 47 % and a/a: 11 %. T102C t/t: 42 %, t/c: 47 % and c/c: 11 %. 5-HT<sub>2A</sub> receptor binding did not differ significantly between subjects within the three genotypes for each polymorphism (mean ± SD): G-1438A: g/g (n = 28): 2.31 ± 0.96, g/a (n = 32): 2.61 ± 0.80, a/a (n = 8): 2.60 ± 1.31. T102C: t/t (n = 29): 2.36 ± 0.99, t/c (n = 32): 2.61 ± 0.80, c/c (n = 7): 2.41 ± 1.28. **Conclusion.** This study does not support the assumption that the genotypes G-1438A and T102C contribute directly to the regulation of the 5-HT<sub>2A</sub> receptors in the living human brain. That is, previous associations observed in obsessive-compulsive disorder and psychosis can not be substantiated through the phenotypic expression of 5-HT<sub>2A</sub> receptor binding.

**SEROTONIN RECEPTOR BINDING IN MILD COGNITIVE IMPAIRMENT  
STUDIED BY PET AND [18F]-ALTANSERIN**

**Steen G. Hasselbalch<sup>1,2</sup>, Karine Madsen<sup>1</sup>, Claus Svarer<sup>1</sup>, Lars Pinborg<sup>1</sup>, Jette Stokholm<sup>2</sup>,  
Søren Holm<sup>3</sup>, Olaf B. Paulson<sup>4</sup>, Gunhild Waldemar<sup>2</sup>, Gitte M. Knudsen<sup>1</sup>**

<sup>1</sup>*Neurobiology Research Unit, Rigshospitalet, Copenhagen, Denmark*

<sup>2</sup>*Memory Disorders Research Unit, Rigshospitalet, Copenhagen, Denmark*

<sup>3</sup>*PET and Cyclotron Unit, Rigshospitalet, Copenhagen, Denmark*

<sup>4</sup>*Danish Research Center for Magnetic Resonance, Hvidovre Hospital, Copenhagen,  
Denmark*

Background: In post mortem studies of patients with Alzheimer's disease (AD) reduced serotonin (5-HT) receptor density has been described. Using positron emission tomography (PET) in patients with AD with and without depression, reduced binding to the 5-HT<sub>2A</sub> receptor subtype in cortical areas was found in two studies (1;2). These reductions may reflect early and specific changes in the serotonergic transmitter system in AD. Aim: To evaluate possible changes in 5-HT<sub>2A</sub> receptor densities in cortical and mesial temporal lobe structures in patients with mild cognitive impairment (MCI). Methods: Fifteen patients with MCI of the amnesic type (considered to be prodromal AD) (8 females, 7 males, mean age 72, range 63-82, mean MMSE 26.3, range 23-30) and 15 age and sex matched control subjects were studied with PET and MRI. The distribution volumes of specific tracer binding (BP<sub>1</sub>) were calculated for 17 brain regions using cerebellum as a reference region and individual plasma-curves corrected for radiolabelled metabolites. Volumes of interest were applied by an automated MRI-based template approach (3). PET data was corrected for partial volume effects due to atrophy (2,4). Results: Significant reductions in BP<sub>1</sub> were found bilaterally in orbitofrontal cortex ( $p < 0.03$ , t-test) and in right entorhinal cortex ( $p < 0.05$ , t-test). Discussion: Reductions in 5-HT<sub>2A</sub> receptor binding were found in areas known to be affected early in the course of AD. It is likely that this reduction reflects a specific dysfunction of the serotonergic system in prodromal AD because atrophy could not explain the reduced tracer activity. Further, in a previous study of AD, applying atrophy correction did not change the finding of a reduction in 5-HT<sub>2A</sub> receptor binding in cortical areas, suggesting that a specific dysfunction of the serotonergic system can be demonstrated in vivo in AD (2). Reference List 1. Blin J., Baron J.C., Dubois B., Crouzel C., Fiorelli M., Attar-Levy D., Pillon B., Fournier D., Vidailhet M., and Agid Y. Loss of Brain 5-HT<sub>2</sub> Receptors in Alzheimer's Disease. In Vivo Assessment With Positron Emission Tomography and [18F]Setoperone. *Brain* 1993;116 ( Pt 3):497-510. 2. Meltzer C.C., Price J.C., Mathis C.A., Greer P.J., Cantwell M.N., Houck P.R., Mulsant B.H., Ben Eliezer D., Lopresti B., DeKosky S.T., and Reynolds C.F. III. PET Imaging of Serotonin Type 2A Receptors in Late-Life Neuropsychiatric Disorders. *Am.J Psychiatry* 1999;156(12):1871-8. 3. Svarer C., Madsen K., Hasselbalch S.G., Pinborg L., Haugbøl S., Frøkjær, V., Holm, S., Paulson O.B., Knudsen G.M. MR-based automatic delineation of volumes of interest in human brain PET images using probability maps. *Neuroimage* 2005 (in press). 4. Muller-Gartner H.W., Links J.M., Prince J.L., Bryan R.N., McVeigh E., Leal J.P., Davatzikos C., and Frost J.J. Measurement of radiotracer concentration in brain gray matter using positron emission tomography: MRI-based correction for partial volume effects. *J Cereb Blood Flow Metab.* 1992 Jul; 12(4):571-83.

## ASSESSMENT OF MICROGLIA ACTIVATION IN SCHIZOPHRENIA USING [11C](R)-PK11195 AND PET

**Bart N.M. van Berckel**<sup>1,2</sup>, Ronald Boellaard<sup>1</sup>, Marc A. Kropholler<sup>1</sup>, Esther Caspers<sup>2</sup>, Wiepke Cahn<sup>2</sup>, Adriaan A. Lammertsma<sup>1</sup>, René S. Kahn<sup>2</sup>

<sup>1</sup>*VU University Medical Centre, Department of Nuclear Medicine & PET Research,  
Amsterdam, The Netherlands*

<sup>2</sup>*Rudolf Magnus Institute for Neurosciences, Department of Psychiatry,  
Utrecht, The Netherlands*

Introduction Schizophrenia is a complex and chronic disease that affects different aspects of cognition and behaviour, including attention, perception, thought processes, emotion and volition. Schizophrenia is a brain disease that particularly involves decrements in grey matter, a finding that is supported by many imaging studies. The pathophysiology of these grey matter changes has not been clarified. Microglia activation is the consequence of virtually all conditions associated with neuronal injury. When activated following neuronal damage, microglia show a marked increase in the expression of peripheral type benzodiazepine binding sites, which are particularly abundant on cells of the mononuclear macrophage cell line. (R)-PK11195 ([1-(2-chlorophenyl)-N-methyl-N-1(1-methylpropyl)-3soquinolinecarboxamide) is a highly selective ligand for the peripheral benzodiazepine binding site. The purpose of the present study was to assess peripheral type benzodiazepine receptors expression, and thus microglia activation, in patients with schizophrenia using [11C](R)-PK11195 and PET. Methods In this ongoing protocol, 4 male patients with recent onset paranoid schizophrenia (DSM-IV criteria) and 5 age matched healthy male controls have been included to date. All patients were treated with atypical antipsychotics. PET scans were performed using an ECAT-EXACT HR+ scanner. A dynamic 3D scan, consisting of 22 frames over 60 minutes, was acquired following a bolus injection of ~370 MBq [11C](R)-PK11195. Arterial whole blood concentration was monitored continuously using an online detection system. In addition, discrete samples were taken in order to derive a metabolite corrected plasma input curve. Finally, for each subject a T1 weighted structural MRI scan was acquired using a Philips 1.5 Tesla scanner. For initial analysis, regions of interest (ROI) were defined on the co-registered MRI scan. ROI were defined for cerebellum, thalamus and whole brain. These ROI were projected onto the dynamic [11C](R)-PK11195 scans, thereby generating time activity curves for each region. A two-tissue reversible compartment model (K1/k2 fixed to values obtained from whole brain) was fitted to the data using the metabolite corrected plasma input curve as input function. Binding potential (BP) was used as primary outcome measure. Results and Discussion Statistical Analysis was performed using Student's t-test. The data suggest a slight, but non-significant global increase in [11C](R)-PK11195 binding in patients with schizophrenia. More subjects are needed, however, to increase statistical power. Insert table 1: A small but statistically significant increase in [11C](R)-PK11195 binding was noted in cerebellum, but not in thalamus in this small sample of patients with schizophrenia. Again, more patients need to be included for the detection of more subtle differences in [11C](R)-PK11195 binding. The results of this pilot study indicate that cerebellum might not be a suitable reference tissue for this patient group and even may be involved in the pathophysiology of schizophrenia.

Table 1: [11C](R)-PK11195 BP values (two tissue reversible model, K1/k2 ratio fixed)

	Controls (n=5)	Patients (n=4)	t value	p value
Thalamus	1.90 ± 0.27	2.17 ± 0.30	1.38	0.20
Cerebellum	1.86 ± 0.22	2.02 ± 0.24	2.31	0.06
Whole Brain	1.87 ± 0.23	2.26 ± 0.30	1.76	0.12

## IN VIVO MULTIMODAL (MRI, SPECT) IMAGING OF THE 6-OHDA RAT MODEL FOR PARKINSON'S DISEASE CORRELATED WITH BEHAVIOR AND HISTOLOGY

Nadja Van Camp<sup>1</sup>, Koen Van Laere<sup>2</sup>, Ruth Vreys<sup>1</sup>, Marleen Verhoye<sup>1</sup>, Erwin Lauwers<sup>3</sup>, Dirk Bequé<sup>2</sup>, Frederic Maes<sup>7</sup>, Alfons Verbruggen<sup>4</sup>, Zeger Debyzer<sup>5</sup>, Luc Mortelmans<sup>2</sup>, Jan Sijbers<sup>6</sup>, Johan Nuyts<sup>2</sup>, Veerle Baekelandt<sup>3</sup>, Annemie Van der Linden<sup>1</sup>

<sup>1</sup>*Bio-Imaging Lab, University of Antwerp, Antwerp, Belgium*

<sup>2</sup>*Division of Nuclear Medicine, University Hospital Gasthuisberg and KU Leuven, Leuven, Belgium*

<sup>3</sup>*Laboratory for Experimental Neurosurgery & NeuroAnatomy, KU Leuven, Leuven, Belgium*

<sup>4</sup>*Laboratory for Radiopharmaceutical Chemistry, KU Leuven, Leuven, Belgium*

<sup>5</sup>*Laboratory for Molecular Virology and Gene Therapy, KU Leuven, Leuven, Belgium*

<sup>6</sup>*Visielab, University of Antwerp, Antwerp, Belgium*

<sup>7</sup>*Department of Radiology/ESAT, University Hospital Gasthuisberg Leuven, Belgium*

**Introduction:** We present a multimodality imaging study characterizing the 6-hydroxydopamine lesion rat model for Parkinson's Disease on molecular, morphological, physiological and behavioral level. To that end we applied subsequently microSPECT and microMRI in the same animal. The co-registered microMRI, microSPECT data were spatially normalized to a microMRI rat brain template, specially designed for the application of multimodality studies. Except for high resolution anatomical imaging, MRI was used to investigate the sensitivity of MR relaxation, diffusion and perfusion parameters in detecting alterations within the affected striatum. The rats were tested behaviorally and finally sacrificed and assessed for histological correlations. **Materials & Methods:** **Animal model:** In six wistar rats unilateral lesions were performed by injection of 24 µg 6-hydroxydopamine (6-OHDA; Sigma, St.Quentin-Fallavier, France) within the substantia nigra. Six non-lesioned rats were included as control animals. **Behavior:** Amphetamine-induced asymmetric rotational behavior was investigated using an automated rotometer bowl. The analysis of amphetamine tests was based on net ipsilateral turns (defined as clockwise turning in case of a right-sided injection). **MicroSPECT:** Imaging was performed on a single-head Millenium GE SPECT gamma camera with a 3mm aperture single-pinhole collimator under Nembutal anaesthesia (60mg/kg). 300MBq of 123I-FP-CIT (123I-ioflupane) was applied to quantify dopamine transporter (DAT) bindingscapacity in the intact and affected striatum. Transporter binding indices were calculated as activity in the striatum divided by aspecific activity in the cerebellum minus 1, giving an indicator of DAT binding capacity. **MicroMRI:** MRI was performed on a 7 T (MRRS, UK) MR system under isoflurane anaesthesia administered in a 30-70% O<sub>2</sub>-N<sub>2</sub> mixture. Besides high resolution anatomical imaging T1, T2 and diffusion weighting imaging was performed as well as perfusion measurements. Co-registration was performed based on maximization of mutual information. Diffusion, T1, T2-and perfusion maps of basal ganglia were calculated in IDL. **Histology:** Three rats have been sacrificed to assess the extent of the lesion in the substantia nigra. To that end tyrosine hydroxylase specific staining was applied. **Results & Discussion:** Co-registration for all images allowed accurate delineation of the striatum on HR MRI for volume-based quantification of the microSPECT data. In a second phase, these data can be used for partial volume correction of the SPECT quantitative data. In all rats significant reduced binding capacity of DAT could be demonstrated, confirmed by histological and behavioral data demonstrating a near-complete lesion. The T2 relaxation parameter was significantly reduced in the affected striatum as compared to the contralateral intact striatum, suggestive for an increase of iron deposits within the striatum, which has been reported previously in PD patients and animal studies. The T1 relaxation time in the affected striatum was significantly increased as compared to the intact striatum and striatum of control animals. We suggest that the extracellular environment is reduced due to a loss of spines on the striatal target neurons. The apparent diffusion coefficient which reflects the extracellular space volume fraction was significantly reduced in the affected striatum. Also the resting state perfusion values were significantly decreased within the affected striatum, especially in regions corresponding to the globus pallidus.

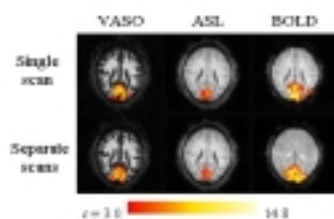


## SIMULTANEOUS MRI MEASUREMENT OF CEREBRAL BLOOD VOLUME, BLOOD FLOW AND BLOOD OXYGENATION IN HUMAN BRAIN

Yihong Yang, Hong Gu, Elliot A. Stein

*Neuroimaging Research Branch, National Institute on Drug Abuse, Baltimore, MD, USA*

Functional MRI (fMRI) techniques based on BOLD (blood oxygenation level-dependent) and CBF (cerebral blood flow) contrasts have been used extensively for mapping functional neuroanatomy. Recently, an fMRI technique based on cerebral blood volume (CBV) change or vascular space occupancy (VASO) contrast during brain activation was proposed. These MRI signals have different characteristics in terms of sensitivity and specificity in detecting brain activity. Simultaneous detection of multiple fMRI signals may have a number of advantages, including efficient acquisition of multiple functional images and minimal temporal variations between the images. Both arterial spin labeling (ASL) perfusion and VASO signals can be acquired utilizing an inversion recovery (IR) MRI pulse sequence. In the proposed method, an IR sequence with two excitation pulses were used, in which a VASO image was acquired at the blood nulling point (TI1), and an ASL perfusion image was collected at a later time (TI2) when labeled arterial spins had reached the capillary/tissue exchange sites. BOLD image was acquired with longer TE after the ASL image acquisition. MRI Experiments were performed on a 3T Siemens Allegra scanner. Echo-planar imaging (EPI) was used with TE of 6.6ms for VASO image, 7.6 ms for ASL image and 27ms for BOLD image with partial (75%) k-space acquisition, and TR of 2000ms. An adiabatic inversion pulse combined with a slab selection gradient was used for alternating slab-selective and non-selective inversion. TI1 was determined empirically on individual subjects and TI2 was 1200 ms. Functional MRI experiments were performed on 6 healthy volunteers using a block-designed visual stimulation paradigm (8 Hz flashing checkerboard). For comparison, individual VASO, ASL perfusion and BOLD images were acquired separately as well using conventional techniques, with the same stimulation paradigm and imaging parameters as close as possible. Simultaneously acquired (top) and sequentially acquired (bottom) VASO, ASL perfusion and BOLD activation maps are illustrated in the figure. As expected, while all three contrast mechanisms reflected neuronal activation within the primary visual cortex (V1), the highest contrast-to-noise ratio (CNR) was seen with BOLD, followed by VASO and then ASL. There was little qualitative difference between the combined single scan and the sequential scan acquisition methods for any of the three signals. Overall, since the proposed new technique took only 1/3 of the acquisition time but obtained similar activation maps compared to conventional techniques, a significant gain of CNR per unit time (approximately 1.73) was achieved with this new technique. This advantage is especially important for experiments with long stimulation paradigms, for which subject head motion and associated image artifacts are major concerns. The ability to collect multiple functional signals in a single scan is critical for functional brain studies involving transient and dynamic signal changes, such as in the study of drug-induced brain activation, in which conventional techniques requiring sequential acquisitions are not able to measure a single, nonreproducible event like a drug injection.



**DIFFERENTIATION OF LEWY BODY DEMENTIA FROM PARKINSON'S DISEASE  
WITH  
[C-<sup>11</sup>]DTBZ PET**

**Robert A. Koeppe<sup>1</sup>, Sid Gilman<sup>2</sup>, Larry Junck<sup>2</sup>, Mary Heumann<sup>2</sup>, Kris Wernette<sup>1,2</sup>,  
Kirk A. Frey<sup>1,2</sup>**

<sup>1</sup>*Department of Radiology, University of Michigan Medical School, Ann Arbor, MI, USA*

<sup>2</sup>*Department of Neurology, University of Michigan Medical School, Ann Arbor, MI, USA*

**Introduction:** Dementia with Lewy bodies (DLB) is a disorder characterized by parkinsonism (bradykinesia, rigidity, gait disorder) with dementia, fluctuating course, and hallucinations. DLB can begin with parkinsonism or with a dementia similar to that seen in Alzheimer's disease (AD). This study was designed to compare results from positron emission tomography (PET) imaging in patients with DLB, Parkinson's disease without dementia (PD), and AD to determine whether radionuclide imaging might help to identify both PD patients and patients with dementia presumed to be of the Alzheimer type who may later progress to develop DLB.

**Methods:** We performed PET scans using (+)-[<sup>11</sup>C]dihydrotetrabenazine ([<sup>11</sup>C]DTBZ) to examine vesicular monoaminergic binding site (VMAT2) density and cerebral cortical ligand transport ( $K_1$ ) in 25 patients with DLB, 30 with PD, 25 with AD, and 57 normal elderly controls (NC). Ten of the DLB patients developed parkinsonism one year or more before the onset of dementia (DLB-park) and 15 developed dementia before or up to one year after the onset of parkinsonism (DLB-cog). Ten to 18 mCi of [<sup>11</sup>C]DTBZ was administered to each subject, 55% as a bolus, followed by 45% as a continuous infusion over the remainder of the 60 min study. Equilibrium analysis of the PET data acquired 30-60 min post-injection was used to estimate the distribution volume ratio (DVR) relative to occipital cortex as an index of VMAT2 density. The first four minutes was used as an index of the blood-to-brain uptake rate ( $K_1$ ) of DTBZ.

**Results:** DTBZ binding was decreased significantly in the caudate nucleus, anterior putamen, and posterior putamen in the DLB and PD groups compared with both the AD and NC groups. The PD group had lower binding in the posterior putamen than the DLB-cog subgroup, and the DLB-park subgroup had lower binding than the DLB-cog subgroup in all three striatal structures. These patient groups showed an anterior-to-posterior binding gradient relative to NC; the deficit was smallest in the caudate nucleus and largest in the posterior putamen. The gradient was steeper in the PD group than in either DLB subgroup, but not different between the subgroups. These groups also showed significantly greater binding asymmetry than controls. The PD group had greater asymmetry than either DLB subgroup, while the asymmetry was nearly identical in DLB-park and DLB-cog.

Both DLB subgroups showed consistently larger transport deficits than the PD and NC groups, with the greatest differences in lateral temporal (-24% relative to NC), inferior temporoparietal (-24%), superior parietal (-30%), posterior cingulate (-26%), and occipital regions (-23%), in a pattern similar to that seen in the AD. The DLB-cog group showed lower  $K_1$  values in these structures than the DLB-park group, but differences did not reach significance. Cerebral cortical DTBZ  $K_1$  was decreased 4-8% in most regions in the PD group compared to the normal control group.

**Conclusion:** PET measurements of striatal binding and cerebral cortical transport with the VMAT2 ligand [<sup>11</sup>C]DTBZ can differentiate DLB both from PD based on transport measures and from AD based on binding measures.



## INTRACRANIAL VASCULAR TRANSFER FUNCTION IN ACUTE STROKE PATIENTS

Yang Wu<sup>1</sup>, Hongyu An<sup>2</sup>, Hamid Krim<sup>1</sup>, Katie Vo<sup>3</sup>, Jin-Moo Lee<sup>4</sup>, **Weili Lin**<sup>2</sup>

<sup>1</sup>*Department of Electrical Engineering, North Carolina State University, Raleigh, NC, USA*

<sup>2</sup>*Department of Radiology, University of North Carolina, Chapel Hill, NC, USA*

<sup>3</sup>*Department of Radiology, Washington University, St. Louis, MO, USA*

<sup>4</sup>*Department of Neurology, Washington University, St. Louis, MO, USA*

Vascular transfer function (VTF) could potentially provide highly relevant physiological information, particularly in patients with cerebrovascular diseases. In this study, we aim to investigate potential alterations of intracranial VTF in patients with acute stroke. The widely employed dynamic susceptibility contrast (DSC) MR approach was employed to acquire images and spatial independent component analysis (ICA) was used to determine local arterial function (LAF) ([1]), reflecting MR signal changes resulted in the passage of the injected contrast. Subsequently, pixel-by-pixel VTF was derived through the deconvolution of the LAFs with a global artery function (GAF) obtained from the middle cerebral artery (MCA) using singular value decomposition (SVD). The ability to non-invasively depict VTF may offer new insights into blood flow related alterations in acute stroke patients. Perfusion images (PWI) were acquired using DSC from three healthy volunteers at 3T and five acute stroke patients within 3-6 hrs from symptom onset at 1.5T using a single shot T2\*-weighted EPI sequence. In addition, diffusion-weighted (DWI) images were also acquired. GAF,  $C_{ga}(t)$ , was obtained through averaging contrast induced signal changes in the contralateral MCA with recirculation effects removed. The susceptibility related signal changes were converted to concentration curves. ICA analysis (ISP group, DTU, <http://isp.imm.dtu.dk/toolbox>) was applied to the concentration time curves throughout the entire brain [1]. LAFs,  $C_{la}(x,t)$ , were constructed based on both the spatial mappings and the temporal characteristics of the components, similar to that proposed in reference [1]. Finally, VTF ( $T(x,t)$ ) was obtained through SVD by deconvolving LAFs with GAF. In order to characterize how VTF differs between brain regions, DWI and PWI images were employed to define two region-of-interests (ROIs), namely, DWI-defined lesions and PWI/DWI mismatched regions while a normal ROI was defined in the contralateral hemisphere. In contrast, two ROIs were placed in the two hemispheres for the normal volunteers. Finally, the full-width-half-maximum (FWHM) and the power (EVTF) of the first harmonic of VTF were used to quantitatively determine the discrepancies between different ROIs. For comparison purposes, the EVTF obtained in stroke patients was normalized to that obtained from the normal volunteers. The FWHM obtained from normal volunteers is  $5.8 \pm 0.2$ s and  $6.0 \pm 0.02$ s, respectively, in the two ROIs. In contrast, for the stroke patients the DWI-defined lesions exhibit a much larger FWHM ( $9.0 \pm 8.8$ s) while a similar FWHM was obtained for both the PWI/DWI mismatched regions ( $5.5 \pm 1.7$ s) and the contralateral hemisphere ( $4.9 \pm 1.4$ s) when compared with that obtained in normal subjects. In addition, the normalized power of the first harmonic of the VTF demonstrates that the DWI-defined lesion, PWI/DWI mismatched regions, and the contralateral hemisphere is  $24.1 \pm 31.1\%$ ,  $43.5 \pm 35.4\%$ , and  $153.5 \pm 103.8\%$  with respect to that obtained in normal subjects, respectively. These findings suggest that the DWI-defined lesions exhibit the largest bolus dispersion and smallest power when compared with that obtained in the normal subjects as well as other brain regions in stroke patients. Although our study has a limited sample size, we have demonstrated a novel tool for obtaining VTF in acute stroke patients. [1] Calamante F et al, *Magn. Reson. Med.*, 52, 789-797, 2004.

## INFLUENCE OF VOLATILE INDUCTION AGENTS ON FMRI AND NEURAL ACTIVITY

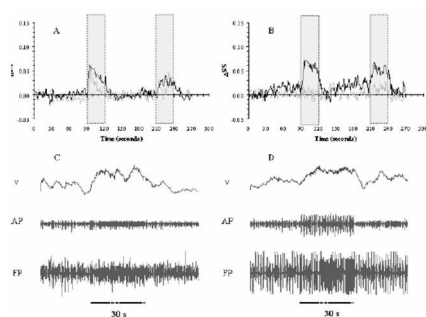
Basavaraju G. Sanganahalli<sup>1</sup>, Peter Herman<sup>1,2</sup>, Fahmeed Hyder<sup>1,3</sup>

<sup>1</sup>*Diagnostic Radiology, Yale University, New Haven, CT, USA*

<sup>2</sup>*Institute of Human Physiology and Clinical Experimental Research, Semmelweis University, Budapest, Hungary*

<sup>3</sup>*Biomedical Engineering, Yale University, New Haven, CT, USA*

Neuroimaging techniques are predominantly based on changes in CBF induced by alterations in neuronal activity and is generally carried out in animals under anesthesia, usually with  $\alpha$ -chloralose because of its minor effects on cardiovascular, respiratory, and reflex functions [1]. General anesthetics reduce neuronal activity in various regions of the mammalian CNS [2]. A considerable number of mechanisms have been suggested to mediate the depressant effects [3]. However it is still a matter of debate as to which molecular targets are truly relevant in producing the “true” anesthetic state [4]. Recent studies reported the relationship between the action of volatile anesthetics occurring on the molecular level and the corresponding effects on neuronal firing [5]. In this study we have used two volatile anesthetics (isoflurane, halothane) and studied the time-dependent induction effects for functional studies in  $\alpha$ -chloralose anaesthetized rats. During the animal preparation halothane (0.7%) / isoflurane (0.5%) were used for induction. The same forepaw stimulation protocol (30 s block design; 2 mA; 0.3 ms; 3 Hz) was used for both fMRI and extracellular recordings. All fMRI data (n=10) were obtained on a modified 9.4T Bruker horizontal-bore spectrometer (Billerica, MA) using a 1H resonator/surface coil RF probe. The images were acquired with gradient echo EPI sequence (TR/TE=1000/15 ms). Extracellular recordings (n=18) were first filtered to obtain action and field potentials (AP, FP) and then the AP data were binned to obtain spike rates (v). The changes in local CBF were measured with a laser-Doppler probe (Oxford Optronix, Oxford, UK). The purpose of this study was to examine the effects of isoflurane and halothane used for induction in  $\alpha$ -chloralose anaesthetized rats. The fMRI time courses after 3 hrs (gray) and 5 hrs (black) from isoflurane induction (A) showed generally moderate levels of intra-animal reproducibility, which was lacking with halothane (B). These fMRI responses were supported by similar CBF responses measured with laser-Doppler probes (data not shown). The electrophysiology results after 5 hrs (bottom) showed changes in neuronal activity, but the alterations were far less significant with isoflurane (C) than with halothane (D). These results together suggest that while isoflurane induction may result in a faster hemodynamic response, the changes in neuronal activity are slightly depressed. These results suggest caution for interpreting results from anesthetized rats where volatile agents are used for the induction phase. Supported by NIH (DC-003710, MH-067528) and NSF (DBI-0095173) grants. [1] Nakao et al., (2001) PNAS-USA 98:7593-7598 [2] Siesjo (1978) Brain Energy Metabolism (Wiley & Sons) [3] Richards (2002) Br J Anaesth 89:79-90 [4] Antognini et al., (2002) Br J Anaesth 89:156-166 [5] Rudolph et al., (2004) Nature Reviews 5:709-720





**ENDOTHELIN-1 AND TRANSCRANIAL DOPPLER IN MIGRAINE: FINDINGS IN INTERICTAL CONDITIONS AND DURING MIGRAINE ATTACK**

Hong Cha<sup>3</sup>, Xiangping Wang<sup>2</sup>, Lan Liang<sup>2</sup>, Jingpian Hou<sup>2</sup>, Zhimei Li<sup>2</sup>, Huawen Jin<sup>4</sup>, **Mei Wang<sup>1</sup>**

<sup>1</sup>Department of Anesthesiology, Columbia University, New York, NY, USA

<sup>2</sup>Department of Neurology, ChengDu Military Command, Kunming General Hospital, ChengDu, China

<sup>3</sup>Department of Nuclear Medicine, ChengDu Military Command, Kunming General Hospital, Kunming, China

<sup>4</sup>Kunming No 1. Hospital, Kunming, China

Introduction: The role of vascular phenomenon taking place during an attack of migraine is poorly understood. Our goal in this study was to measure systemic level of endothelin-1, which is the most potent vasoactive mediator known, and to assess vasomotor response through Transcranial Doppler ultrasound (TCD) monitoring in patients suffering from migraine with and without aura, both during the headache event and headache-free period. Material and Methods: Twenty healthy adult as controls and 63 patients with aura (n=27) and without aura (n=36) were enrolled in this study. To measure the mean flow velocity (MFV, cm/s) of cerebral arteries, TCD recording were performed according to conventional procedure. The insonation of anterior cerebral (ACA), middle cerebral (MCA) and posterior cerebral (PCA) arteries was done through acoustic windows in the temporal bone, just above zygomatic arch. The basilar artery (BA) and intracranial segments of the vertebral arteries (VA) were insonated through the foremen magnum. Endothelin-1 concentrations measured by immunoassay (RIA). The assay kit was provided by (People's Army General Hospital, East Asia Immunotechnology Institute). Results: Figure 1 show that Endothelin-1 content in both migraine periods and types are higher than in controls. There are no significant different in Endothelin-1 content in migraine patients with and without aura nor in attack or icterical periods. TCD shows that MFV in both migraine periods and types are higher than in controls. There are no significant different in MFV in migraine patients with and without aura nor in attack or icterical periods. There is positive relationship between MFV and Endothlin-1 content. MFV and endothelin-1 relationship in MCA in migraine patients with attack is  $r = 0.683$  ( $p < 0.01$ ); in interictal period  $r = 0.598$  ( $p < 0.01$ ): in migraine without aura patient,  $r = 0.622$  ( $p < 0.01$ ); in interictal peroid  $r = 0.514$  ( $p < 0.02$ ). Discussion and Conclusion: Endothelin-1 is most potent vasoconstrictor we known. In migraine patients, Endothelin-1 content is significantly higher than normal patients no matter of the migraine type and periods. MFV is significantly higher than normal patients no matter of the migraine type and periods. There is a positive correlation between the MFV and endothelin content. The migraine event might because of increasing production of endothelin or the higher levels of endothelin might be the consequence of hemodynamic shear stress in vasodilatory phase. Future study could be conducted in more well controled condition, such as Endothelin content in measure jugular blood sample during early event of migraine attack. It might be able to distinguish Endothelin increasing is the cause or the result of MFV perfusing.. All these could contribute to better understanding of pathphysiology of the migraine and future intervention.

Table 1. Comparison of Endothelin-1 in all groups

	Period	n	Plasma Endothelin-1 (pg/ml)
Migraine with aura	Attack	11	76.5 ± 19.1**
	Interictal	11	61.2 ± 19.9**
Migraine without aura	Attack	11	64.4 ± 23.0**
	Interictal	11	58.8 ± 18.8*
Control		20	48.2 ± 13.6

Note: All migraine compared to control \* $P < 0.05$ , \*\* $P < 0.01$ , Migraine attack compared to interictal period. \* $P < 0.05$ , \*\* $P < 0.01$ . Migraine with aura compared to without aura. \* $P < 0.05$ , \*\* $P < 0.01$ .

Table 2. Comparison of MFV (cm/s) in all groups

	Period	n	MCA	ACA	PCA	BA	VA
Migraine with aura	Attack	11	70.53 ± 11.4**	64.11 ± 11.4**	47.39 ± 11.4**	50.01 ± 11.4**	33.11 ± 11.4**
	Interictal	11	70.11 ± 11.4**	57.11 ± 11.4**	40.11 ± 11.4**	44.11 ± 11.4**	44.11 ± 11.4**
Migraine without aura	Attack	11	70.21 ± 11.4**	61.11 ± 11.4**	46.11 ± 11.4**	50.11 ± 11.4**	46.11 ± 11.4**
	Interictal	11	69.11 ± 11.4**	55.11 ± 11.4**	40.11 ± 11.4**	46.11 ± 11.4**	35.11 ± 11.4**
Control		20	42.11 ± 11.4	41.11 ± 11.4	30.11 ± 11.4	31.11 ± 11.4	31.11 ± 11.4

Note: All migraine compared to control \* $P < 0.05$ , \*\* $P < 0.01$ , Migraine attack compared to interictal period. \* $P < 0.05$ , \*\* $P < 0.01$ . Migraine with aura compared to without aura. \* $P < 0.05$ , \*\* $P < 0.01$ .



## A COMPARATIVE F-DOPA AND FDG PET STUDY OF PARKINSONIAN SUBJECTS WITHOUT EVIDENCE OF DOPAMINERGIC DYSFUNCTION

Vijay Dhawan, Andy Feigin, Yilong Ma, Dan Lewis, Chaorui Huang, David Eidelberg

*Center of Neurosciences, North Shore-LIJ Research Institute, Manhasset, NY, USA*

**Introduction:** Recent clinical trials in Parkinson's disease (PD) using dopaminergic imaging methods (DAT imaging with SPECT and F-dopa imaging with PET) have revealed that about 10-15% of parkinsonian patients have scans without evidence of dopaminergic deficit (SWEDD). Little is known about the neural mechanisms of the parkinsonism in these subjects. The objective of this study is to elucidate the neurophysiology underlying parkinsonian patients with SWEDD using PET imaging markers of metabolic and dopaminergic functions. **Methods:** We examined our collections of F-dopa scans from patients referred for the clinical diagnosis of parkinsonism. 29 patients (16 % of the total) were found to have normal striatal F-dopa uptake (not significantly different from the normal mean and within 2 standard deviations); 10 of them (6 women, 5 men; age  $38.8 \pm 10.8$  years) were also scanned with fluorodeoxyglucose (FDG) PET. We compared these FDG scans to those of an age-matched control group with SPM99 and assessed whether the SWEDD subjects express a previously identified PD-related covariance pattern (PDRP). Finally we performed a separate principal component (PC) analysis on the combined group of SWEDDs and controls to identify a pattern of abnormal brain metabolism specifically related to this condition. **Results:** SPM analysis showed no areas of significant metabolic difference between the SWEDD group and the controls. Brain network analysis revealed that PDRP was not expressed the SWEDD subjects. An additional network analysis on the combined SWEDD and control group identified a pattern (PC 1, accounting for 37% of variance) that distinguished the SWEDD group from the controls ( $p < 0.04$ ). This pattern was characterized by hypometabolism in bilateral prefrontal cortices and caudate, covarying with relative hypermetabolism in pons, midbrain, cerebellar vermis, and bilateral medial temporal cortex. **Conclusion:** Patients with SWEDD account for approximately 15% of subjects referred for diagnostic imaging for parkinsonism. In our cohort, these subjects tended to be young compared to typical parkinsonian patients. Although the regional metabolism appeared to be normal we found that these subjects express a specific abnormal brain network characterized by hypometablism in prefrontal cortex and caudate. This pattern suggests that some parkinsonian subjects with SWEDD may be characterized by abnormalities in striato-cortical connections in the setting of apparent normal dopaminergic function.

## EFFECTS OF ISOFLURANE INDUCTION ON INTER-ANIMAL REPRODUCIBILITY

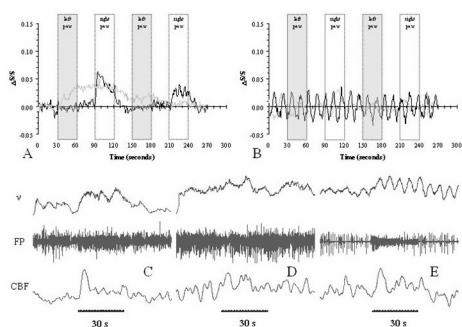
Basavaraju G. Sanganahalli<sup>1</sup>, Peter Herman<sup>1,2</sup>, Fahmeed Hyder<sup>1,3</sup>

<sup>1</sup>*Diagnostic Radiology, Yale University, New Haven, CT, USA*

<sup>2</sup>*Institute of Human Physiology and Clinical Experimental Research, Semmelweis University, Budapest, Hungary*

<sup>3</sup>*Biomedical Engineering, Yale University, New Haven, CT, USA*

While  $\alpha$ -chloralose has become the popular anesthetic of choice for functional studies in rodents, prior to the treatment of this drug a variety of volatile agents (e.g., halothane, isoflurane, enflurane) are used during the surgical preparation phase of the experiment [1,2,3]. Since these volatile induction agents themselves may have some residual effects on the final anesthesia level reached with  $\alpha$ -chloralose, it is important to know whether or not these effects modulate the functional response of the rodent to sensory stimuli. In this study we tested the inter-animal reproducibility efficacy of using isoflurane as an agent for induction in  $\alpha$ -chloralose anesthetized rats during forepaw stimulation. We combined fMRI, electrophysiology, and laser-Doppler flowmetry to measure the changes in BOLD, neuronal activity, and CBF from the somatosensory area. During the animal preparation halothane (0.7%) / isoflurane (0.5%) were used for induction in  $\alpha$ -chloralose anesthetized rats. The same forepaw stimulation protocol (30s block design; 2mA; 0.3ms; 3Hz) was used for both fMRI and extracellular recordings. All fMRI data were obtained on a modified 9.4T Bruker horizontal-bore spectrometer (Billerica, MA) using a 1H resonator/surface coil RF probe. The images were acquired with gradient echo EPI sequence (TR/TE=1000/15 ms). Extracellular recordings were first filtered to extract the action and field potentials (AP, FP) and then the AP data were binned for spike rates (v). The CBF was measured using a laser-Doppler probe (Oxford Optronix, Oxford, UK). In rats where the highly variable and oscillatory responses (0.03 to 0.15 Hz) were detected, even long experimental times did not produce the typical stimulus-induced response usually desired in functional experiments. The multi-modal results suggest caution in using isoflurane as the induction agent for functional studies (e.g., [1]), because of the high variability in the responses across the many rats as observed in this study (n=14). The figure shows data from several rats. The fMRI time courses (top) showed two trends: a typical hemodynamic response (dark trace in A), a lagged response (gray trace in A), and an oscillatory response (both traces in B). These fMRI data were supported by neuronal and CBF data (bottom) obtained by extracellular and laser-Doppler recordings. The multi-modal data showed the same trends as the fMRI data: a typical stimulation-induced response (C), a highly variable response (D), and an oscillatory response (E). The physiological status of all the rats shown in the figure was similar throughout the experiment. These results suggest caution when using isoflurane as an induction agent Supported by NIH (DC-003710, MH-067528) and NSF (DBI-0095173) grants. [1] Nakao et al., (2001) PNAS-USA 98:7593-7598 [2] Siesjo (1978) Brain Energy Metabolism (Wiley & Sons) [3] Richards (2002) Br J Anaesth 89:79-90 [4] Smith et al., (2002) PNAS-USA 99:10765-10770





## ACUTE INSULIN INDUCED HYPOGLYCEMIA: BLOOD FLOW AND METABOLISM IN HUMANS

Richard P Kennan<sup>1</sup>, Kan Takahashi<sup>2</sup>, Harry Shamoon<sup>1</sup>, **Jullie W. Pan<sup>2</sup>**

<sup>1</sup>*Department of Medicine, Albert Einstein College of Medicine, Bronx, NY, USA*

<sup>2</sup>*Department of Neurology, Albert Einstein College of Medicine, Bronx, NY, USA*

**Introduction:** How the human brain functions under conditions of acute hypoglycemia remains a complex question, by virtue of the potential simultaneous shifts in processes of perfusion, metabolism and changing demand. We examined this issue by measuring cerebral perfusion (CBF) and oxidative metabolism (CMRO<sub>2</sub>) in insulin induced hypoglycemia (HG) and euglycemia (EG) at rest and during sensorimotor activation in normal human subjects using magnetic resonance (MR). **Methods:** Experiments were performed with 12 subjects (9M, 3F; age 29.6±8.5). The protocol consisted of either insulin induced hypoglycemia (targeting a HG of 60mg/dl) followed by euglycemia (n=7), or in reverse order (n=7; two volunteers studied twice), each phase approximately 1.5hrs. EG was performed with the same insulin infusion rate to match the HG phase. All MR data were acquired at least 30min after stabilization of plasma glucose at either HG or EG levels. **MR:** All studies were performed with a Varian Inova whole body 4T human MR system. IR GE images were obtained to identify the plane of interest (motor cortex). Studies acquired were perfusion (FAIR-single shot EPI, activated and non-activated), gradient echo BOLD EPI and quantitative R<sub>2</sub>' (non-activated). All physiological studies were performed with FOV 192x192, 3mm isotropic resolution. Task activation was provoked with blocks of bilateral finger tapping. Quantitative R<sub>2</sub>' data were calculated from 16 field echoes prepared by either a 50 or 80msec spin echo.

Analysis of the BOLD data was done to identify regions of interest (105±15 pixels) in the motor and supplementary cortices. The flow and transverse relaxation data were incorporated into a model of deoxyhemoglobin concentration, oxygen extraction and consumption as described by numerous workers, . R<sub>2</sub>' is the blood susceptibility induced transverse relaxation rate, R<sub>2</sub>', fM the fractional change in oxygen consumption, fP fractional change in perfusion. **Results:** Stable plasma glucose levels were achieved, at 5.78±0.03mM, EG and 3.56±0.02mM, HG. Basal perfusion increased significantly from 56.4±13.6ml/100g/min (EG) to 64.3±7.6ml/100g/min (HG). Perfusion further increased significantly with activation in both EG and HG and were significantly different from each other, while the delta activated flows were not different. R<sub>2</sub>' remained the same between EG and HG. The finger tapping BOLD signal decreased from EG to HG (1.79±0.60% to 1.55±0.60% p<0.02). Modeling the R<sub>2</sub>' and perfusion data together demonstrated that in hypoglycemia, flow and metabolism remained well coupled. Similarly, evaluating the BOLD data with perfusion and R<sub>2</sub>' showed that fM/fP was remained coupled with a slope of 0.44±0.16 (R=+0.87) in EG, and 0.57±0.20 (R=+0.88) in HG. **Conclusions** Although the depth of hypoglycemia achieved in the present study was mild, we were able to detect a consistent increase in perfusion with hypoglycemia. The finger tapping task activation was not associated with any larger (delta) flow values. Metabolism appears to remain coupled with flow in mild HG. Thus although mild HG induces increases in basal perfusion and metabolism, a similar increase was not seen with the elementary activation. These data demonstrate that performance declines in mild to moderate hypoglycemia occurs with flow and metabolism staying coupled and both decreasing.

## ASSESSMENT OF ACUTE METABOLIC STRESS FOLLOWING TRAUMATIC BRAIN INJURY WITH 1H MAGNETIC RESONANCE SPECTROSCOPIC IMAGING IN HUMAN SUBJECTS

Paul M. Vespa<sup>1</sup>, David L. McArthur<sup>1</sup>, Maria Etchepare<sup>1</sup>, Jeffrey R. Alger<sup>2</sup>

<sup>1</sup>*Division of Neurosurgery, David Geffen School of Medicine at UCLA, Los Angeles, CA, USA*

<sup>2</sup>*Ahmanson-Lovelace Brain Mapping Center, David Geffen School of Medicine at UCLA, Los Angeles, CA, USA*

**Introduction:** Functional neuroimaging studies using positron emission tomography (PET) have demonstrated prolonged disturbance of oxidative metabolism following traumatic brain injury (TBI). Metabolic disturbance has been found in pericontusional brain areas, but may also extend well beyond the abnormal-appearing areas. Profoundly elevated interstitial lactate pyruvate ratio (LPR) measured in microdialysis studies on TBI patients also indicate the presence of oxidative metabolic disturbance within pericontusional and distant normal-appearing regions. We used 1H Magnetic Resonance Spectroscopic Imaging (1H-MRSI) and microdialysis in acute TBI cases to determine whether 1H-MRSI is sensitive to the disturbance of oxidative metabolism that occurs in TBI. **Methods:** We studied pericontusional versus normal N-acetylaspartate signal (NAA) and microdialysis versus NAA correlations in 15 and 6 (respectively) acute TBI subjects within 36 hours of injury by microdialysis and 1H-MRSI. 1H-MRSI was performed as part of a multiparametric 1.5 T MRI procedure with a Siemens Sonata MRI unit. 1H-MRSI acquisitions used the single slice (2-dimensional) chemical shift imaging pulse sequence as provided by the manufacturer with TR/TE = 1500/136 (msec). The spatial resolution was of 10 x 10 x 15 mm. Slice locations and volume excitation were adjusted to obtain spectra from regions within 10 mm of the microdialysis probe tip and pericontusional regions. 1H-MRSI acquisitions were performed at different brain locations, namely a supratentorial dorsal frontal-parietal region, and a middle fossa region incorporating the mesial temporal lobes and midbrain. Voxel spectra generated by the target regions (pericontusional, normal appearing white matter, and within 10 mm of the microdialysis probe) from the spectroscopic imaging arrays were selected for analysis. NAA levels were assessed using the manufacturer's software which performs non-linear curve fitting of the spectra. Absolute signal levels were determined by calibration against a phantom having known NAA concentrations. **Results:** Identification and quantification of lactate MRS signal was frequently complicated by the presence of large lipid signals that most often originated in the corners of the large selected volumes used in this study. Importantly, however, NAA signal was not affected by this localization artifact. NAA signal was reduced in pericontusional regions by 51% compared with normal appearing white matter ( $p = 0.0030$ ). An inverse logarithmic relationship was found between LPR and NAA level ( $p = 0.0027$ ,  $r^2 = 0.92$ ) and between LPR and NAA/CR ( $p = 0.0052$ ,  $r^2 = 0.88$ ) measured in the vicinity of the microdialysis probe. No statistically significant correlations between the other MRS metabolites (lactate, creatine, choline) and LPR were found, suggesting that the NAA findings are the result of a disturbance in NAA metabolism rather than overall cell loss. Further study is underway to establish whether the NAA signal losses are the result of metabolic dysfunction or tissue loss. **Conclusion:** The results suggest that NAA measures made by 1H-MRSI are sensitive to oxidative metabolic disturbance following TBI. 1H-MRSI may therefore provide a safer alternative to PET functional neuroimaging and microdialysis for the identification of oxidative stress in acute TBI.

## TEMPORAL EVOLUTION OF CEREBRAL METABOLIC RATE OF OXYGEN UTILIZATION USING MRI IN A MIDDLE CEREBRAL ARTERY OCCLUSION STROKE

Hongyu An<sup>1</sup>, Liansheng Chang<sup>1</sup>, Yang Wu<sup>2</sup>, Yasheng Chen<sup>1</sup>, Weili Lin<sup>1</sup>

<sup>1</sup>*Department of Radiology, University of North Carolina at Chapel Hill, Chapel Hill, NC, USA*

<sup>2</sup>*Department of Electrical Engineering, State University of North Carolina, Raleigh, NC, USA*

The balance between cerebral blood flow (CBF) and oxygen extraction fraction (OEF) is important in determining the status of tissue viability during acute cerebral ischemia (1, 2). After ischemic onset, CBF decreases, accompanied by an increase in OEF in order to maintain cerebral oxygen cerebral metabolic rate of oxygen utilization (CMRO<sub>2</sub>). A persisted or further reduced CBF results in a decline of CMRO<sub>2</sub>, leading to neural cell death. In this study, a T2\* (T2') approach (3) and a dynamic tracer method (4) are used to obtain OEF and CBF, respectively, which in turn allows the estimates of MR\_CMRO<sub>2</sub>, in a middle cerebral artery occlusion (MCAO) rat model. The temporal evolution of cerebral haemodynamic changes is examined. In total, three male Long Evans rats were studied. Cerebral ischemia was induced using the suture model inside the magnet bore with approved animal protocols. All images were acquired on a Siemens 3T Allegra scanner. A 2D multi-echo gradient echo/spin echo sequence (MEGESE) was utilized to obtain OEF (3). Apparent diffusion coefficient (ADC) maps was obtained from segmented EPI diffusion weighted images (DWI). MEGESE and DWI images were acquired prior to MCAO and continued up to three hours post MCAO. A tracer dynamic perfusion weighted imaging (PWI) was utilized to obtain CBF at the end of the entire study so as to avoid the contamination of contrast agent induced susceptibility for the oxygenation measurements. CBF is assumed to remain constant throughout the entire post MCAO period in a permanent MCAO. MR\_CMRO<sub>2</sub> was calculated by multiplying OEF and CBF. ROIs were defined in both ipsilateral and contralateral hemisphere to obtain ADC, OEF, CBF and CMRO<sub>2</sub> changes. Before MCA occlusion, ADC, OEF were not statistically different in the ipsilateral and contralateral hemisphere ROIs. Immediately after MCAO, ADC reduced, while OEF increased. As lesion progressed, the initially elevated OEF returned to or below the baseline, while the ADC might have little change. In addition, CMRO<sub>2</sub> showed a moderate decrease to 30-55% followed by a severe reduction to 9-20% of that of normal tissue. The time period of moderate reduction of CMRO<sub>2</sub> depends on the severity of CBF. In one rat, a 14% of CBF reduction corresponded to a 40 minutes moderate CMRO<sub>2</sub> reduction followed by severe CMRO<sub>2</sub> reduction. In another rat, a 21% CBF reduction allows a moderate CMRO<sub>2</sub> reduction for about 90 minutes. With a MCAO rat model, our results demonstrate the temporal biphasic behavior of OEF with an initial increase and followed by a returning baseline values. In addition, the temporal evolution of CMRO<sub>2</sub> agree with the reported results in the literature using PET (5). In conclusion, non-invasive methods to assess cerebral oxygenation status in vivo may provide us more insight into the ischemic tissue viability. References 1. Powers WJ, et al. *JCBFM*. 1985;5(4):600-8. 2. De Crespigny et al, *MRM* 27:391-397, 1992. 3. An H and Lin W, *JCBFM*, 20: 1225-1236, 2000. 4. Ostergaard et al, *MRM*, 36:715-725, 1996. 6. Heiss et al, *Cerebrovasc Brain Metab Rev* 5:235-263.

## VOLATILE INDUCTION AGENTS AFFECT ADAPTATION IN $\alpha$ -CHLORALOSE ANESTHETIZED RAT

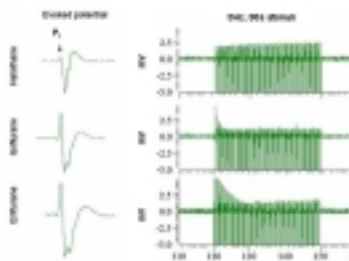
Basavaraju G. Sanganahalli<sup>1</sup>, Peter Herman<sup>1,2</sup>, Fahmeed Hyder<sup>1,3</sup>

<sup>1</sup>*Diagnostic Radiology, Yale University, New Haven, CT, USA*

<sup>2</sup>*Institute of Human Physiology and Clinical Experimental Research, Semmelweis University, Budapest, Hungary*

<sup>3</sup>*Biomedical Engineering, Yale University, New Haven, CT, USA*

In somatosensory stimulation experiments, non-volatile agents are generally used as the main anesthetic, whereas volatile agents are used for the initial induction phase [1]. This protocol is used because most non-volatile agents themselves do not provide sufficient depth of anesthesia rapidly, which is a specific requirement during the surgical procedure. For the initial surgical preparation volatile anesthetic agents like halothane, isoflurane and enflurane are generally used, because of they are fast acting and have reasonably short half-lifetimes [2]. In this study we examined the effects of these induction agents on artificially ventilated (70% N<sub>2</sub>O, 30% O<sub>2</sub>) Sprague-Dawley rats which were anesthetized with  $\alpha$ -chloralose (40 mg/kg/hr). We applied strong electrical stimuli at 3Hz frequency for 30s period to provoke somatosensory evoked potentials in the forepaw area of the brain approximately 4 hours after stopping exposure to the volatile induction agent. The extracellular recordings were conducted in layer 4 of the somatosensory cortex with Tungsten microelectrodes [3]. The electrical data with high bandwidth (20 kHz) were filtered to obtain field potentials (FP). Since the low pass filtering affects the time course of the electrical signals, we did not examine the latency of the different peaks in the evoked potential. Rather we examined the intensities of the different peaks of the evoked potential (P1, N1, N2, and P2) throughout the stimulation period, for every induction agent (figure left panel). The P1 peak of the evoked potential, which is generally associated with the thalamo-cortical pathway [4], decreased with time for isoflurane and enflurane induction (figure right panel). On the contrary P1 peak was very much depressed with halothane induction and it was not affected with time during stimulation. Assuming a simple exponential decay in the decrease of the P1 peak we calculated the time constant (where the amplitude decreased to the 1/e level). In the case of isoflurane the time-constant was  $7.89 \pm 1.04$ s (n=8), while the enflurane produced a more elongated decay with a time-constant of  $20.86 \pm 2.5$ s (n=6). The long time-constants with isoflurane and enflurane induction may be a consequence of these agents forming a negative feedback for the thalamo-cortical pathway such that the stimulus-induced evoked potentials adapted over prolonged stimulation [5]. In contrast halothane induction did not influence the adaptive mechanisms. Therefore halothane would seem to be a better choice for an induction agent in neurophysiology measurements (e.g., imaging with optical imaging and fMRI) studies because of the lack of adaptive tendencies in the measured signals during prolonged stimulation. Supported by NIH (DC-003710, MH-067528) and NSF (DBI-0095173) grants. [1] Nakao et al., (2001) PNAS-USA 98:7593-7598 [2] Richards (2002) Br J Anaesth 89:79-90 [3] Smith et al., (2002) PNAS-USA 99:10765-10770 [4] Tokuno et al., (1992) JCBFM 12:954-961 [5] Abbott et al., (2004) Nature 431:796:803



## TRANSIENT INCREASES IN BLOOD PRESSURE AFFECTS SENSORY-MOTOR ACTIVATION FOLLOWING STROKE USING FUNCTIONAL MR IMAGING IN THE RAT

Rong Wang<sup>1,2</sup>, Zhonghang Zhao<sup>3</sup>, David Rushforth<sup>1</sup>, Tadeusz Foniok<sup>1</sup>,  
Jaclyn I. Wamsteeker<sup>1</sup>, Alastair Buchan<sup>3</sup>, Boguslaw Tomanek<sup>1,3</sup>, Ursula I. Tuor<sup>1,2,3</sup>

<sup>1</sup>*IMR Technology, Institute for Biodiagnostics (West), Calgary, AB, Canada*

<sup>2</sup>*Experimental Imaging Center and Hotchkiss Brain Institute, University of Calgary,  
Calgary, AB, Canada*

<sup>3</sup>*Clinical Neuroscience, University of Calgary, Calgary, AB, Canada*

**Introduction:** Functional MR imaging (fMRI) detects neural activation through BOLD MR contrast as a result of alterations in cerebral hemodynamics accompanying a local change in brain function. However, in the case of stroke where autoregulation of cerebral blood flow to blood pressure (BP) changes may be impaired, a transient hypertension producing hyperemia that is not related to cerebral activation could also affect BOLD contrast. We hypothesized that a transient hypertension would produce an increase in the number of active voxels within T2\* images that is dependent on blood pressure and greater in infarcted tissues, thereby enhancing the cerebral activation response to simultaneous stimulation of the sensory-motor cortex. We investigated the effect of transient BP increases on the electrical stimulation induced activation in sensory-motor cortex (SMC) following stroke using functional MRI. **Method and Materials:** A sham procedure (n=5) or transient middle cerebral artery occlusion (MCAO, n=10) of 60 minutes duration was produced in anesthetized rats. Ischemic damage within the right SMC was confirmed using T2 imaging 2 days later. Seven days post MCAO, rats were prepared for functional MRI under alpha-chloralose anesthesia. For each scan a set of 32 gradient echo T2\* images were acquired under 3 different conditions: 1. two periods of electrical stimulation of the left or right forepaw, 2. arterial BP increases (norepinephrine, 0.15-1.2 ug/kg, I.V.), or 3. electrical stimulation with simultaneous BP increases. A regional 'activation response' was represented by the number of voxels with intensity changes identified using a cross correlation analysis (P<0.001) to either the stimulation time course or the BP time course. **Results:** One week after transient MCAO, the T2\* signal intensity within ischemic tissue was affected markedly by blood pressure changes. With BP increases alone, an 'activation response' correlating to the BP time course was detected in the injured but not the non-ischemic contralateral SMC. The number of active voxels correlating to the BP time course in the SMC increased from 0 with no pressure change to 45 at 31-45 mm Hg and 108 voxels at pressures >60 mmHg (P<0.001). In contrast, few voxels demonstrated an activation response to BP changes contralaterally. Despite no stimulation being applied, there was also an apparent 'activation response' of voxels correlating with the stimulation time course in the ischemically injured right SMC at BP >45 mm Hg (P<0.001). If stimulation was combined with BP increases, the number of active voxels in the right SMC increased from 10 to 84 for BP of 0 or >60 mmHg, respectively. In contrast, the number of active voxels in the uninjured cortex increased by only 19 voxels when right forepaw stimulation was accompanied by BP increases. **Conclusion:** Transient hypertension produces an increase in the number of active voxels detected by fMRI resulting in an enhanced detection of cerebral activation to simultaneous electrical stimulation of the SMC. This BP-dependent 'activation response' is greater in tissue injured by ischemia than in healthy tissue so that fMRI studies of diseased or damaged brain are more likely to be affected by arterial BP increases.

## EVALUATION OF SEROTONIN 1A RECEPTOR BINDING IN DIABETES AND DEPRESSION

**Julie C. Price**, David E. Kelley, Sigrid A. Hagg, Christopher M. Ryan, Scott K. Ziolko, Carolyn C. Meltzer, Dana Tudorascu, Lisa A. Weissfeld, Sati Mazumdar, Chester A. Mathis, Charles F. Reynolds

*Radiology, Medicine, Psychiatry, and Biostatistics, University of Pittsburgh, Pittsburgh, PA, USA*

**Introduction.** Research has shown a greater prevalence of depression in diabetes. It is estimated that 20% of diabetics will develop clinical depression during their lives, as compared to 5-10% of the general population. Animal models have shown hyperglycemia-induced alterations in the serotonin system, as well as structural and functional alterations in hippocampus. Positron emission tomography (PET) imaging studies have indicated altered serotonin-1A (5-HT<sub>1A</sub>) receptor binding in healthy depressed subjects relative to controls. The aim of the present study was to assess 5-HT<sub>1A</sub> receptor binding in Type 2 (NIDDM) diabetics, with and without depression. **Methods.** PET and [carbonyl-C-11]WAY 100635 were used to measure 5-HT<sub>1A</sub> receptor binding in non-depressed (NDD: n=15, 8M, 56±10 yrs) and depressed (DD: n=8, 3M, 63±11 yrs) Type 2 diabetics and medically healthy non-depressed controls (Cont: n=10, 3M, 66±11 yrs). The depressed diabetics were free of antidepressant medication at the time of the PET study. The Type 2 subjects were without major medical complications. PET and arterial blood data were acquired over 90 min (ECAT HR+, 15 mCi). The Logan graphical analysis (GLLS smoothing [1]) was used to determine regional binding potential (BP) measures that were based upon distribution volume (DV) ratios with the cerebellar DV as non-specific reference. Data were corrected for cerebral atrophy. **Results.** The dorsal raphe BP value was greatest for depressed diabetics (DRN BP: DD=5.0±0.7, NDD=4.1±1.4, Cont=3.8±0.7). Regression analysis, that controlled for body-mass index, indicated significantly greater DRN BP for depressed diabetics relative to non-depressed diabetics (p=0.01). The hippocampal BP was greatest for the non-depressed diabetics (HIP BP: NDD=11.3±3.6, DD=9.4±2.6, Cont=8.4±2.9) and different between NDD and control subjects (p<0.05). Trend level differences (p~0.1) were observed, between the diabetic groups, in lateral orbital frontal cortex and occipital. No group differences were evident for the cerebellar DV values (DD: 0.77±0.31, NDD: 0.81±0.34, Cont: 0.89±0.43). **Conclusion.** These findings suggest that depression in diabetes is not associated with widespread decreases in 5-HT<sub>1A</sub> receptor binding, relative to non-depressed diabetics. The results further suggest that alterations in serotonergic neurotransmission in diabetes and depression are consistent with reduced hippocampal neurotransmission via both lower hippocampal and greater DRN 5-HT<sub>1A</sub> receptor binding. This work was supported by K01 MH01976, MH01410, and P30 MH52247.

**DECREASING SYSTEMIC BLOOD PRESSURE IMPAIRS CEREBRAL VASCULAR RESERVES IN PATIENTS WITH STENO-OCCLUSIVE CEREBRAL VASCULAR DISEASES: A REPEATED I-123 SPLIT DOSE SPECT STUDY**

**Yasuyuki Kimura**<sup>1</sup>, Naohiko Oku<sup>1</sup>, Katsufumi Kajimoto<sup>1</sup>, Hiroki Kato<sup>1</sup>, Makiko Tanaka<sup>1</sup>, Ashik MD Ansar Bin<sup>1</sup>, Masakazu Kanai<sup>1</sup>, Kazuo Kitagawa<sup>2</sup>, Jun Hatazawa<sup>1</sup>

<sup>1</sup>*Department of Nuclear Medicine and Tracer Kinetics, Osaka University Graduate School of Medicine, Suita, Japan*

<sup>2</sup>*Department of Internal Medicine and Therapeutics, Osaka University Graduate School of Medicine, Suita, Japan*

**Introduction:** A recent randomized clinical trial showed that blood pressure lowering treatment reduced a stroke recurrence in patients with a prior stroke or transient ischemic attack(1). However, systemic blood pressure lowering may reduce cerebral perfusion pressure. In some patients with severe occlusive vascular lesions, blood pressure lowering may be harmful in stroke prevention. In this study, we tested our hypothesis that systemic blood pressure may affect the cerebral vascular reserves (CVR). **Methods:** We retrospectively investigated 52 consecutive patients who repeatedly underwent I-123 IMP SPECT with acetazolamide (ACZ) challenge test during 3 years (mean interval of the SPECT study was  $557 \pm 253$  days, male/female was 35/17, mean age was  $64.9 \pm 8.4$  years old). Before the SPECT study, each patient underwent neurological and neuroradiological evaluations (duplex carotid ultrasonography, MRI, and MR angiography). We measured systemic mean arterial blood pressure (MABP) at each examination time. The CVR was defined as follows;  $CVR (\%) = (\text{counts at ACZ loading SPECT} - \text{counts at resting SPECT}) / \text{counts at resting SPECT} * 100$ . The CVR was classified as follows; normal ( $CVR \geq 34.1\%$ ), mild impairment ( $25.3\% < CVR < 34.1\%$ ), or severe impairment ( $CVR \leq 25.3\%$ ). The above dividing CVR thresholds were determined as mean CVR - 1SD and mean CVR - 2SD of control group. We categorized the patients into 3 groups according to the longitudinal changes in the CVR classification as follows; the CVR classification was worsened or the CVR was impaired in both studies (Group 1), the CVR classification was improved (Group 2), or the CVR was both normal (Group 3). **Results:** 17 of 52 patients were classified as Group 1. In this group, their follow up MABP ( $93.3 \pm 12.3$  mmHg) was significantly lower than their initial MABP ( $99.2 \pm 9.9$  mmHg,  $p < 0.05$ ). 11 and 46 patients were classified as Group 2 and Group 3, respectively. In Group 2 and Group 3, their follow up MABP ( $97.6 \pm 9.2$  mmHg,  $99.2 \pm 12.3$  mmHg, respectively) was not significantly changed from their initial MABP ( $94.6 \pm 9.0$  mmHg,  $98.3 \pm 11.9$  mmHg, respectively). The frequency of arterial occlusion in Group 1 (11 of 17 patients; 65%) was significantly higher than that in Group 2 and 3 (4 of 11 patients; 36%, 8 of 24 patients; 33%). **Conclusion:** The present study demonstrated that systemic blood pressure reduction may impair cerebral vascular reserves. Patients who had vascular occlusion must be carefully treated in blood pressure lowering treatment. **References** (1)Randomised trial of a perindopril-based blood-pressure-lowering regimen among 6,105 individuals with previous stroke or transient ischaemic attack. *Lancet*. 2001;358:1033-1041

## COMPARISON OF BOLUS INJECTION AND CONTINUOUS INFUSION ARTERIAL INPUTS IN GD-DTPA CONTRAST-ENHANCED MRI

Tavarekere N. Nagaraja<sup>1</sup>, Vijaya Nagesh<sup>2</sup>, James R. Ewing<sup>3</sup>, Polly A. Whitton<sup>3</sup>, Joseph D. Fenstermacher<sup>1</sup>, Robert A. Knight<sup>3</sup>

<sup>1</sup>Anesthesiology, Henry Ford Health System, Detroit, MI, USA

<sup>2</sup>Radiation Oncology, University of Michigan, Ann Arbor, MI, USA

<sup>3</sup>Neurology, Henry Ford Health System, Detroit, MI, USA

**INTRODUCTION:** Magnetic resonance contrast agents (MRCA) can be intravenously (i. v.) administered by either bolus injection or continuous infusion. Two previous studies have employed these two input functions for comparison of resultant data, but came to different conclusions (1, 2). In this study, a rat model of transient cerebral ischemia was used and the differences in MRCA arterial inputs, contrast enhancement, estimates of gadolinium-diethylenetriaminepentaacetic acid (Gd-DTPA) influx constants (Ki) and Gd-DTPA affected-proton distribution volumes (Vp) between the two methods were evaluated. **METHODS:** Unilateral cerebral ischemia was induced in halothane anesthetized male Wistar rats (275-295 g; n=12) by suture occlusion of the right middle cerebral artery. After 3 hr of occlusion, the suture was withdrawn to initiate reperfusion. At ~2.5 hr post-reperfusion, Gd-DTPA-based contrast enhanced MR imaging was performed to localize extravascular enhancement and quantify Ki and Vp. For bolus injection, 0.02 mmol Gd-DTPA was injected through a femoral vein. For continuous infusion, a stepped-down procedure using a syringe pump was employed following published procedures (3) to quickly attain and maintain an elevated blood level of Gd-DTPA. Resultant arterial input functions from both were tracked with MRI using a T1-Look-Locker sequence by measuring changes in Gd-DTPA relaxation rates ( $\Delta R_1$ ;  $R_1=1/T_1$ ) in sagittal sinus as described previously (3). Offline image processing was performed to localize enhancing areas and calculate Ki and Vp using Patlak plots (3). **RESULTS:** The bolus injection produced a steep rise in Gd-DTPA levels in the sagittal sinus that decayed exponentially; the continuous infusion a steep rise that remained steady for the duration of the study (Figure). The continuous infusion schedule resulted in better visual enhancement and definition of the infarct than bolus injection (blinded observations), confirming a previous report (2). For bolus injection and for continuous infusion, the values (mean  $\pm$  SD) were  $0.004 \pm 0.001$  and  $0.006 \pm 0.005$  ml/g/min (Ki) and  $0.06 \pm 0.02$  and  $0.075 \pm 0.04$  ml/g (Vp), respectively ( $p>0.05$ ). **CONCLUSION:** Bolus injections may not result in complete resolution of the infarct because: 1) rapid diffusion into the tissue of smaller contrast agents such as Gd-DTPA may not define the infarct boundaries; and 2) backflux of the MRCA can underestimate blood-to-brain transfer kinetics. A continuous infusion schedule may help overcome these deficits by maintaining a steady blood level and a unidirectional driving force from vasculature to tissue. Therefore, despite its perceived shortcomings (1), a continuous infusion schedule may be applicable in identification of ischemic infarct and evaluating therapeutic effects (2). These data also confirm the usefulness of MR imaging of the sagittal sinus to non-invasively track arterial input functions. **References:** 1. Tofts PS, Berkowitz BA. *Magn Res Imaging* 12:81-91 (1994) 2. Merten CL, Knitelius HO, Assheuer J et al. *Neuroradiol* 41:242-248 (1999) 3. Ewing JR, Knight RA, Nagaraja TN et al. *Magn Res Med* 50:283-292 (2003) Grant support: Supported by RO1NS38540 and American Heart Association-Bugher Foundation Award (0270176N).

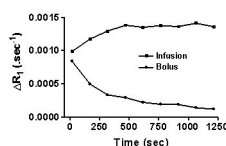


**Figure.** Representative sagittal sinus Gd-DTPA concentration over time after a bolus and constant infusion arterial input functions. Note the steep fall in levels in the former and the near steady state levels in the latter.

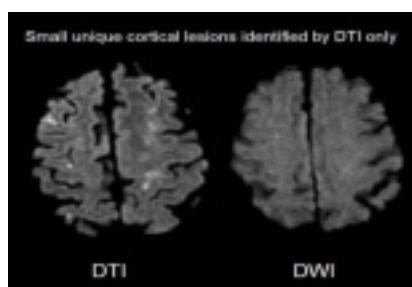


### HIGHER RATE OF CORTICAL INFARCTS SHOWN IN ACUTE STROKE PATIENTS USING HIGH RESOLUTION DIFFUSION WEIGHTED IMAGING.

Karima Benameur, Julie Bykowski, Marie Luby, Naomi Lewin, **Steven Warach**,  
Lawrence Latour

*National Institute of Neurological Disorders and Stroke-NIH, Bethesda, MD, USA*

Background and objective: Diffusion weighted imaging (DWI) has become a prominent method in the early detection of ischemic stroke, yet typical images are plagued by artifact, low spatial resolution, and low signal to noise ratio (SNR). We hypothesized that improving image quality by reducing voxel size and increasing SNR using a diffusion tensor (DTI) sequence would improve lesion conspicuity. Methods: 42 patients imaged between September 2003 and March 2004, diagnosed with ischemic acute stroke and imaged both with conventional DWI (3 direction, 7 mm thick, 28 sec) and DTI (19 direction, 3.5 mm thick, 256 sec) within 24 h of stroke onset were included in this study. Hyper-intense regions were segmented independently on co-registered trace-weighted images from both techniques by two readers blinded to patient identifiers then averaged between both readers. Discrete lesions were defined by a 3D morphometric analysis as contiguous hyper-intense voxels surrounded by non ischemic tissue. On a per patient basis, the volume and number of lesions were compared between both techniques using a Student T test and a Wilcoxon signed ranked test respectively. Results: The total lesion volume (sum across all lesions) per patient did not differ between techniques (7042 and 7052 mm<sup>3</sup> in DWI and DTI, respectively). Readers identified 253 lesions on DTI as compared to 129 lesions on DWI, for an average of 6.04 and 3.07 discrete lesions per patient respectively ( $p < 0.001$ ) and an average volume per lesion of 2866 mm<sup>3</sup> and 3643 mm<sup>3</sup> for DTI and DWI respectively ( $p < 0.001$ ). A total of 134 discrete lesions (53%) identified on DTI, having an average volume of 77 mm<sup>3</sup> per lesion, were not identified on DWI, while 7 lesions (0.05%) identified on DWI, having an average volume of 147 mm<sup>3</sup> per lesion, were not identified on DTI. Lesions found only on DTI tended to be located in cortical gray matter. Lesions identified only on DWI tended to be near regions of artifact. Moreover, single DWI lesions tended to appear as a geometrically complex, but contiguous lesion on DTI. Conclusions: Higher resolution DTI showed a higher number of discrete small cortical gray matter lesions than DWI. The clinical implications of those lesions is currently under investigation. Keywords: acute stroke, diffusion weighted imaging, diffusion tensor imaging, MRI, cortical small lesions.



**ABNORMAL COVARIANCE METABOLIC TOPOGRAPHY IN PATIENTS WITH PROGRESSIVE SUPRANUCLEAR PALSY: A FDG PET STUDY**

**Yilong Ma, Shivani Rachakonda, Thomas Eckert, Andy Feigin, Vijay Dhawan,  
David Eidelberg**

*Center of Neurosciences, North Shore-LIJ Research Institute, New York, NY, USA*

**Introduction:** It is often a challenge to diagnose Parkinson's disease (PD) and atypical Parkinsonian disorders solely on clinical criteria. Image analysis using statistical mapping can improve early differential diagnosis of PD from atypical syndromes such as progressive supranuclear palsy (PSP) and multiple system atrophy (MSA). Using brain network analysis and [18F]fluorodeoxyglucose (FDG) PET data, we have previously generated a PD-related covariance pattern (PDRP) to describe its unique abnormal metabolism. The expression of this network in individual patients is a sensitive imaging marker to assess the disease severity and progression, as well as to predict treatment outcome following medical and neurosurgical interventions. However we have found that PDRP is not expressed in patients with PSP, suggesting the existence of a specific metabolic topography of its own. In this study we sought to determine whether specific abnormal metabolic brain topography is associated with patients with PSP. **Methods:** We used FDG scans from 20 PSP patients whose diagnosis was clinically confirmed at follow-up (age =  $69 \pm 9$  years; disease duration =  $2.9 \pm 1.2$  years) and 22 age-matched normal controls (age =  $56 \pm 11$  years). Imaging studies were done on a GE Advance PET camera in 3D mode. All patients were scanned at least 12 hours off medications. Images of cerebral glucose metabolic rates were generated and transformed into a standard brain space. By examining spatial covariance based on principal component analysis, we performed calculations in the combined brain scans to identify principal components whose expressions can significantly separate PSP and control subjects. The specificity of this PSP network was then evaluated by computing prospectively its expression in PD and MSA patients with the same mean age and disease course. **Results:** Network analysis disclosed a significant PSP-related metabolic covariance pattern (PSP-RP) discriminating PSP patients from normal controls ( $p < 0.0001$ ). This characteristic pattern showed hypermetabolism in the thalamus, parietal, occipital, temporal, lateral frontal and motor cortices. Concurrently, hypometabolism was seen in the caudate and brainstem, as well as in the midline frontal cortex and insula. PSP-RP expressions in the PD and MSA cohorts were significantly lower than that in the PSP patients and did not differ from the normal group. **Conclusion:** This study reveals unique metabolic brain topography that is present in PSP but absent in PD and MSA patients. It can serve as a disease marker to help accurate diagnosis of PSP by clinicians. The quantification in single patient will be useful in differentiating PSP from early stage PD and MSA. It will be of interest to investigate whether PSP\_RP correlate with clinical symptoms and experimental therapies.

## STUDY OF TISSUE ATROPHY INVOLVEMENT IN SEMANTIC DEMENTIA USING ELASTIC MAPPING

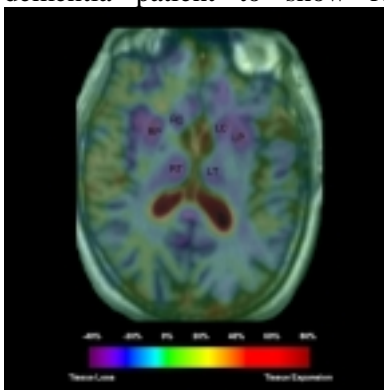
Alex Leow<sup>1</sup>, **Sung-Cheng Huang**<sup>2</sup>, James Becker<sup>3</sup>, Paul Thompson<sup>1</sup>

<sup>1</sup>Laboratory of Neuro Imaging, Department of Neurology, UCLA David Geffen School of Medicine, Los Angeles, CA, USA

<sup>2</sup>Department of Molecular and Medical Pharmacology and Department of Biomathematics, UCLA David Geffen School of Medicine, Los Angeles, CA, USA

<sup>3</sup>Department of Neurology, Psychiatry, & Psychology, University of Pittsburgh, Pittsburgh, PA, USA

**Introduction:** Elastic image mapping has been applied previously to MRI images to study brain development and various neurological disorders. In this study, elastic mapping is applied to serial MR images of a subject diagnosed with semantic dementia to examine regional brain atrophy associated with the dementia. **Methods:** Magnetic resonance imaging (MRI) scans of a 57 year-old male patient diagnosed with semantic dementia were obtained using gradient echo T1-weighted imaging (TR 25ms, TE 5ms, slice thickness 1.5mm, FOV 24x18cm, flip angle 40 degrees, no gaps). A total of four scans were obtained (baseline scan in 02/1993; follow-up scans in 10/1994, 02/1996, and 08/1999). Elastic mapping was then applied to deform later MRI scans (10/1994, 02/1996, and 08/1999) back to the first baseline MRI scan (02/1993). This temporal normalization allows the assessment of tissue expansion/loss in a voxel-by-voxel manner by looking at the determinant of the Jacobian operator (Jacobian map) applied to the resulting deformation field (values larger than 1 indicate tissue expansion; values less than 1 indicate atrophy or tissue loss). A region of interest (ROI) analysis using manual tracing was performed to compute average atrophic rates from the Jacobian maps in regions with observed atrophic changes. **Results:** The MRI scans showed existing left temporal lobe atrophy by visual inspection, although no active atrophy was detected in the Jacobian maps during the time period. By contrast, active atrophy was observed in the right temporal lobe. Closer inspection showed a posterior progression of the atrophy starting from the right temporal pole. Both the asymmetrical nature of temporal lobe atrophy and antero-posterior progression are consistent with previous studies. However, in this patient, we also noticed bilateral tissue loss in the caudate head, putamen, and thalamus (Figure). An annualized atrophic rate (as a percent change per year of the ROI values) showed more active tissue loss in the right middle and inferior temporal, and occipito-temporal lobe (-2.88%, -3.48%, and -2.88% per year, respectively), as well as bilateral putamen and thalamus (~-3% per year). Moreover, possible bilateral insula and cingulate gyrus involvement were also noted in the Jacobian maps. Our results showed more extensive brain tissue loss over time in this patient than previously reported by others in the literature. **Conclusion:** In addition to atrophy in left temporal lobe, semantic dementia also has progressive right temporal and basal ganglia involvement. Elastic image mapping allows quantitative analysis of serial brain MRI's of semantic dementia patient to show regional tissue loss associated with the progression of the disease.





**HIGH RESOLUTION MEASUREMENTS OF NEURONAL ACTIVITY, CEREBRAL BLOOD FLOW, AND FMRI DURING SPIKE-WAVE SEIZURES IN WAG/RIJ RATS**

**Hal Blumenfeld**<sup>1,2,3</sup>, Hrachya Nersesyan<sup>1</sup>, Manjula Khubchandani<sup>4</sup>, Ulrich Schridde<sup>1</sup>, Rachel Berman<sup>1</sup>, Douglas Rothman<sup>4</sup>, Fahmeed Hyder<sup>4</sup>

<sup>1</sup>*Department of Neurology, Yale University School of Medicine, New Haven, CT, USA*

<sup>2</sup>*Department of Neurobiology, Yale University School of Medicine, New Haven, CT, USA*

<sup>3</sup>*Department of Neurosurgery, Yale University School of Medicine, New Haven, CT, USA*

<sup>4</sup>*Department of Diagnostic Radiology, Yale University School of Medicine, New Haven, CT, USA*

**RATIONALE:** fMRI signals are normally related to cerebral blood flow (CBF) metabolism and neuronal activity. During absence seizures, patients experience brief episodes of staring, accompanied by spike-wave discharges (SWD) on electroencephalography (EEG). Neuroimaging studies of absence seizures have yielded contradictory results. Some have shown increased CBF or metabolism during SWD, while others have shown the opposite. Limited spatio-temporal resolution, and varying measurement conditions may be important causes of this variability. Therefore, the purpose of this study was to directly measure neuronal activity and neuroimaging signals at high spatio-temporal resolution during SWD through multi-modal recordings in WAG/Rij rats, an established animal model of human absence seizures. Establishing the relationship between neuronal activity and neuroimaging signals in SWD has significant practical applications for localizing and treating brain regions responsible for seizure generation. **METHODS:** fMRI measurements were performed in a 7T or 9.4T horizontal bore spectrometer in WAG/Rij rats under fentanyl/haloperidol anesthesia and neuromuscular blockade, during spontaneous SWDs. Simultaneous EEG recording was performed with carbon filament electrodes to determine the timing of seizures, and artifacts were removed. fMRI signals were then analyzed by comparing images acquired during seizures to baseline images. Results were superimposed on high-resolution anatomical images in the same coronal plane. We also measured physiological changes in brain regions identified to show fMRI signal changes during SWD, using a custom-built combination probe. The probe simultaneously recorded CBF using tissue laser Doppler flow (LDF), and extracellular multiunit activity at high time resolution from the same region during SWD and at baseline. **RESULTS:** Comparison of ictal and interictal epochs revealed focal bilateral increases in fMRI signal in both cortical and subcortical structures during SWD. We found that fMRI increases were localized mainly to primary somatosensory cortex and to specific thalamic and brainstem nuclei (n=12 WAG/Rij rats studied). The occipital cortex was spared. Electrophysiology mapping on 35 WAG/Rij rats, demonstrated strong correspondence between fMRI and electrophysiology for regions involved and spared during SWD. Combined LDF and electrophysiology studies were then performed, concentrating on the primary somatosensory (S1BF) and primary visual (V1M) cortex (respectively, involved and spared on fMRI). We found that in S1BF, each SWD produced a transient increase in the rate of neuronal firing, and with a delay of 2-3 seconds, a transient increase in CBF (n=12 WAG/Rij rats). V1M showed no significant changes in neuronal firing rate or CBF. **CONCLUSIONS:** Multi-modal high spatio-temporal measurements in the same system demonstrated that fMRI signals, CBF and neuronal firing all increased in regions intensely involved in SWD and did not change in regions spared by seizures. fMRI and CBF changes corresponded closely in space and time to changes in neuronal activity. These findings demonstrate that fMRI can be used to accurately map regional changes in brain function during seizures, which may help the development of improved therapies targeted at the involved regions.

## MAPPING THE FUNCTIONAL EFFECTS OF THE AMPA RECEPTOR POTENTIATORS LY450108 AND LY451395 WITH <sup>14</sup>C 2-DEOXYGLUCOSE AUTORADIOGRAPHY

Jill H. Fowler<sup>1</sup>, Michael J. O'Neill<sup>2</sup>, David Bleakman<sup>3</sup>, James McCulloch<sup>1</sup>

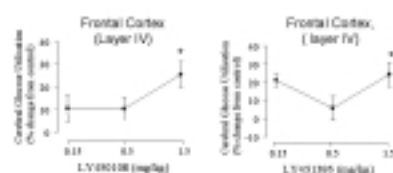
<sup>1</sup>*Division of Neuroscience, University of Edinburgh, Edinburgh, UK*

<sup>2</sup>*Eli Lilly and Co. Ltd., Surrey, UK*

<sup>3</sup>*Neuroscience Division, Lilly Corporate Centre, Indianapolis, IN, USA*

**Introduction:** AMPA receptor potentiators enhance AMPA receptor-mediated glutamatergic neurotransmission in the brain. The biarylpropylsulfonamides are a group of AMPA receptor potentiators with potential for treating a number of psychiatric (depression) and neurological (Alzheimer's and Parkinson's disease) disorders (O'Neill et al, 2004). The aim of the current study was to examine the effects of two of these AMPA receptor potentiators, LY450108 and LY451395, on cerebral glucose utilisation in the rat using <sup>14</sup>C-2-deoxyglucose (<sup>14</sup>C-2-DG) autoradiography, to compare and contrast the specific anatomical sites of action of these compounds. **Methods:** Male Sprague Dawley rats (417g±4g; n=35) received subcutaneous administration of LY450108 or LY451395 (0.15, 0.5 or 1.5mg/kg) or vehicle (5% DMSO, 24% βCD) 15 minutes prior to intravenous administration of 50μCi <sup>14</sup>C-2-DG. Cerebral glucose utilisation was quantified in 40 anatomical brain regions using a computer-based densitometer.

**Results:** LY450108 produced modest, dose dependent increases in glucose utilisation, with statistically significant increases observed in 14 anatomical areas following administration of the top dose (1.5mg/kg), notably the globus pallidus and substantia nigra. All doses of LY451395 also produced increases in glucose utilisation. Statistically significant increases were observed following administration of the high dose of LY451395 (1.5mg/kg), which effected increases in 11 anatomical brain regions, such as the hippocampus and nucleus accumbens. Both compounds increased glucose utilisation in the frontal and parietal cortex and dorsal raphe nucleus.



**Conclusion:** This study has revealed that both compounds have broadly similar effects on cerebral glucose utilisation, but with subtle differences. These data suggest that AMPA receptor potentiators enhance specific AMPA receptor-mediated processes in the cortex and limbic system.

Reference: O'Neill MJ, Bleakman D, Zimmerman DM, et al ; CNS Neurol Disord. 2004 (3):181-94 (2004)

## FUNCTIONAL MRI ANALYSIS USING VASCULAR MASKS

Elizabeth J. Yoder<sup>1</sup>, Wen-Chau Wu<sup>1</sup>, Yousef Mazaheri<sup>1</sup>, Eric C. Wong<sup>1,2</sup>, Richard B. Buxton<sup>1</sup>

<sup>1</sup>*Department of Radiology, UCSD Center for Functional MRI, La Jolla, CA, USA*

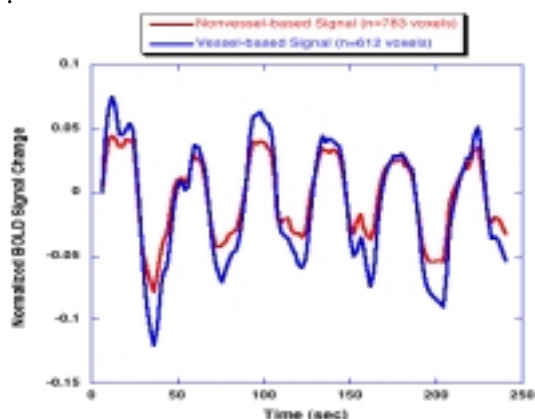
<sup>2</sup>*Department of Psychiatry, UCSD, La Jolla, CA, USA*

Functional magnetic resonance imaging (fMRI) using BOLD contrast is often used to map the locations of brain activity associated with sensation, motion, and cognition. Analysis of BOLD data typically identifies volumes of activation by mapping where BOLD signals are temporally correlated to task performance<sup>1</sup>. This procedure does not distinguish between volumes located near the origin of activation and those located in remote veins and sinuses. In order to separate BOLD signals in large veins and sinuses from BOLD signals in the parenchyma, we collected images of the brain's venous system and used these to create masks that were then applied to BOLD fMRI data analysis. MRI was performed on a General Electric 3.0 Tesla Signa EXCITE short bore system using a receive-only 8-channel head coil. Functional scans utilized a visual task (flickering checkerboard) in a block paradigm. Pulse sequences included a T2\*-weighted EPI sequence (120 reps, TR/TE = 2000/30.9ms, BW=62.5kHz, voxel dimension 1.5 mm<sup>3</sup>, 9 slices encompassing occipital cortex) and a 2D-MR Venogram (TOF/GR, TR/TE = 19/4.2ms, BW = 31.3kHz, voxel dimension 0.07x0.09x1.5 mm, Flip = 70°). Image processing was performed using AFNI (afni.nimh.nih.gov). Functional and vascular data sets were co-registered, and the brain portion of the images was extracted from the surrounding skull and used for subsequent analysis. BOLD signal correlations to a reference function were calculated for each voxel, and voxels with a correlation coefficient of 0.5 or greater were used to create an activation mask. A vascular mask was created from the 2.8% most intense brain voxels in the venogram, which approximates the amount of venous cerebral blood volume<sup>2,3</sup>. This voxel-selection method is independent of the absolute intensity values, which may vary with fluctuations in scanner gain. The higher spatial resolution of the vascular mask was resampled to match the lower spatial resolution of the functional data, and an inverse mask was created for nonvessel regions. Average time courses were generated for voxels contained in both the vessel and activation masks and in both the nonvessel and activation masks. As seen in the figure, response amplitude was higher for vessel-based signals than non vessel-based signals. Furthermore, the BOLD signal undershoot was more pronounced for vessel-based voxels than nonvessel-based voxels. In contrast, the response duration did not appear to differ between the two groups. These preliminary results suggest that vascular masks may be used to filter “downstream” vein and sinus signals from BOLD fMRI data in order to more precisely map, characterize, and quantify brain activations.

<sup>1</sup>Bandettini et al (1992) *Mag Reson Med* 25:390-397.

<sup>2</sup>Duong et al (2000) *Mag Reson Med* 43:393-402.

<sup>3</sup>An et al (2001) *Proc Intl Soc Mag Reson Med* 9:98.





## ESTIMATION OF THE TEMPORAL FEATURES OF CMRO<sub>2</sub> CHANGES FROM CBF AND BOLD FMRI DATA

Alberto L. Vazquez<sup>1</sup>, Vikas Gulani<sup>1,2</sup>, Gregory Lee<sup>1</sup>, Hernandez-Garcia Luis<sup>1</sup>, Douglas C. Noll<sup>1</sup>

<sup>1</sup>Functional MRI Laboratory, University of Michigan, Ann Arbor, MI, USA

<sup>2</sup>Department of Radiology, University of Michigan, Ann Arbor, MI, USA

### Introduction

Cerebral hemodynamics plays a very important role in the delivery of oxygen to brain tissue. The objective of this work is to estimate the dynamic changes in CMRO<sub>2</sub> that result from evoked changes in neuronal activity using CBF and BOLD fMRI data and also to determine how closely coupled are the changes in CMRO<sub>2</sub> to the changes in neuronal function.

### Methods

The model of the regional hemodynamics consisted of multiple parts that represent the various aspects of the hemodynamic response to a stimulus [1,2,3,4,5]. The coupling between the CMRO<sub>2</sub> and hemodynamic responses was examined by equating it as a first-order process from the neuronal response (akin to an intermediary process). A two-echo gradient-echo FAIR acquisition scheme was used to obtain simultaneous CBF and BOLD fMRI data with temporal resolution of 2s in a General Electric 3.0T MRI scanner [6]. Study participants were instructed to perform a visually cued finger tapping task with stimulation periods of 12s followed by 38s of rest.

### Results and Discussion

The CMRO<sub>2</sub> response was represented by a time constant ( $\tau$ ) and two scenarios were considered: (1) the CMRO<sub>2</sub> response is as fast as the neuronal response ( $\tau=0$ ), (2) the CMRO<sub>2</sub> response is slower than the neuronal response ( $\tau>0$ ). The results showed that a slower CMRO<sub>2</sub> response reduced the NMSE (normalized mean squared error) of the CBF and BOLD predictions versus a fast CMRO<sub>2</sub> response by 20% (Fig. 1). A fast CMRO<sub>2</sub> response produced larger NMSE estimates that included non-physiologic characteristics. These estimates suggest the CMRO<sub>2</sub> response is not as fast as the neuronal response, but moderately faster than the blood flow response (Fig. 1 right). These results are limited by the models and assumptions used and our current knowledge of the cerebral hemodynamics but these models can be used to increase our understanding of the hemodynamic mechanisms and exploit the information in the BOLD response under different physiological conditions.

### References:

- [1] Logothetis N, et al., Nature 412:150(2001);
- [2] Muller JR, et al., Science 285:1405(1999);
- [3] Valabregue R, et al., JCBFM 23:536(2003);
- [4] Buxton RB, et al., MRM 39:855(1998);
- [5] Davis TL, et al., PNAS 95:1834(1998);
- [6] Kim SG, et al., MRM 34:293(1995).

**OBSERVATION OF INTERHEMISPHERIC INTERACTIONS BETWEEN  
BILATERAL SOMATOSENSORY CORTICES THROUGH ACTIVITY-RELATED  
HEMODYNAMIC SIGNALS AND THEIR DEPENDENCE ON STIMULUS TIME LAG**

Masahito Nemoto<sup>1</sup>, Yoko Hoshi<sup>1</sup>, Eiji Kohno<sup>2</sup>, Chie Sato<sup>1</sup>, Toru Hirano<sup>2</sup>, Susumu Terakawa<sup>2</sup>

<sup>1</sup>*Department of Integrated Neuroscience, Tokyo Institute of Psychiatry, Tokyo, Japan*

<sup>2</sup>*Photon Medical Research Centre, Hamamatsu University School of Medicine, Hamamatsu, Japan*

[INTRODUCTION] Neural interactions between different cortical regions are critically dependent on cortico-cortical time lag of neuronal activities (Ogawa et al., 2000, PNAS). In somatosensory systems the time lag information is processed for integrating multiple stimulus inputs. Here we investigated interhemispheric interactions between bilateral somatosensory cortices through activity-related hemodynamic signals and their dependence on stimulus time lag. We measured optical intrinsic signals in rat somatosensory cortex evoked by electrical pulses to the contralateral hindpaw (test stimuli, TS) while delivering electrical pulses to the ipsilateral hindpaw or homotopic cortical regions of the contralateral hemisphere (conditioning stimuli, CS). [METHODS] Five Sprague-Dawley rats were studied. The parietal bone was thinned bilaterally. Cortical images were obtained from bilateral hemisphere with CCD and analyzed with MatLab programs. We used 586 and 610 nm optical signals to estimate cerebral blood volume and oxygenation, respectively. (1) TS (0.8-mA, 1-ms, 5-Hz, 10 pulses) or hindpaw CS (the same pulses) were delivered alone under  $\alpha$ -chloralose anesthesia. (2) TS were given after CS with varied stimulus time lags (80, 60, 40, 20 and 0 ms), or without CS. (3) The cortical CS (0.08-mA, 1-ms, 5-Hz, 10 pulses) were applied using double microelectrodes positioned near the center of the responses to the hindpaw CS at a depth around 500  $\mu$ m. The magnitude of signals was calculated as fractional changes in reflected light intensity relative to prestimulus baseline. The responses to CS-TS were then normalized by the responses to TS without CS on maximum-response circular ROI (1.5-mm diameter). [RESULTS] (1) 586 nm monophasic and 610 nm biphasic optical signals were observed not only in the cortical hemisphere contralateral to the stimulated hindpaw but in homotopic regions of the ipsilateral hemisphere with the magnitude of approximately 1/10 of contralateral responses. The ipsilateral 586 nm response regions slightly shifted to the midline compared with those of the response to contralateral hindpaw stimuli. The cortical CS elicited optical signals bilaterally in the same manner. (2) Normalized peak responses to the contralateral hindpaw TS with the ipsilateral hindpaw CS were  $92 \pm 12$ ,  $78 \pm 23$ ,  $56 \pm 27$ ,  $83 \pm 8$  and  $107 \pm 9$  (mean  $\pm$  SD) % at 80, 60, 40, 20 and 0 ms lag time, respectively. The optical responses were significantly suppressed at 40 ms and slightly augmented at 0 ms. The magnitudes of suppression and augmentation appeared larger when analyzed by the temporal or spatial summation method. (3) Normalized peak responses to contralateral hindpaw TS with cortical CS to the contralateral hemisphere showed the same patterns as with the ipsilateral hindpaw CS but the responses were highly suppressed at 20 ms and still suppressed at 0-ms lag time. [DISCUSSION] These results agreed with the hemodynamic responses observed through fMRI signals in the Ogawa's report. Probably all signals reflect the manner of interhemispheric neural interactions. The earlier suppression in the cortical CS-TS paradigm than in the hindpaw CS-TS paradigm may be explained by neural transmission time from the hindpaw to the contralateral cortex, suggesting interactions via interhemispheric callosal connections.

## DIFFUSE OPTICAL MEASUREMENT OF CEREBRAL METABOLIC RATE OF OXYGEN IN, ADULT BRAIN

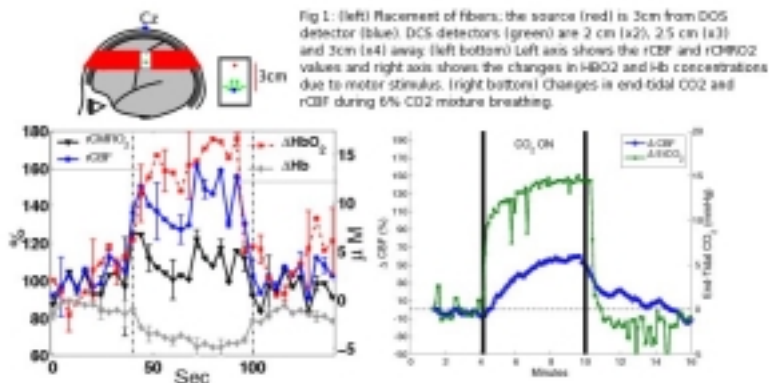
Turgut Durduran<sup>1</sup>, Guoqiang Yu<sup>1</sup>, Mark G. Burnett<sup>2</sup>, Chao Zhou<sup>1</sup>, Jiongjiong Wang<sup>3</sup>, John A. Detre<sup>3</sup>, Arjun G. Yodh<sup>1</sup>, Joel H. Greenberg<sup>3</sup>

<sup>1</sup>Department of Astronomy and Physics, University of Pennsylvania, Philadelphia, PA, USA

<sup>2</sup>Department of Neurosurgery, Hospital of University of Pennsylvania, Philadelphia, PA, USA

<sup>3</sup>Department of Neurology, University of Pennsylvania, Philadelphia, PA, USA

We combined diffuse optical (DOS) and correlation (DCS) spectroscopies to simultaneously measure the oxyhemoglobin (rHbO<sub>2</sub>), deoxyhemoglobin (rHb), total hemoglobin (rTHC) concentration and blood flow (rCBF) in adult human brain during a hypercapnic episode and sensorimotor stimulation. These measurements allowed calculation of the relative cerebral metabolic rate of oxygen (rCMRO<sub>2</sub>) in the human brain for the first time, to our knowledge, by use of all-optical methods. Briefly, ~3mW of light from three amplitude modulated lasers at 690, 785, and 830nm were fiber-coupled to the head. Photons transmitted were detected in reflection mode. Spectroscopic analysis was carried to calculate rHb, rHbO<sub>2</sub> and rTHC. A narrowband laser (5mW at 800nm), photon-counting, avalanche photo-diodes and a custom-build autocorrelator board was used for blood flow by fitting the obtained autocorrelation functions. The maximum penetration depth was about 2cm from the top of the scalp and we report averaged values from the probed tissue volume after a partial volume correction[1]. As a first step towards validation in human brain, measurements were made in five subjects at a resting cerebral pCO<sub>2</sub> and during 4-6 minute periods of increased pCO<sub>2</sub> induced by respiration of a 6% CO<sub>2</sub> gas mixture.. The end tidal CO<sub>2</sub>, heart rate, blood pressure and arterial oxygenation were monitored continuously. A typical response is shown in Figure 1 (right panel). Over the five subjects a sustained mean CBF increase of 35.4±9.6% corresponding to 14.7±4.7mmHg increase in pCO<sub>2</sub> was observed. This corresponds to a 2.4±0.4 %/mmHg rise in CBF, well within the values reported in the literature (2-3.6%/mmHg). Seven male volunteers participated in the sensorimotor cortical activation studies. One subject further participated in a 3-T fMRI study in which BOLD and arterial spin-labeled (ASL) perfusion data were obtained sequentially to compare to optical results from the same subject. Figure 1 (left panel) shows group averaged results which indicate mean changes for rCBF rHBO<sub>2</sub>, rHB, rTHC , rCMRO<sub>2</sub> of 39±10%, 12.5±2.8uM, -3.8±0.8uM, 8.3±2.3uM and 10.1±4.4% respectively in agreement with the literature. When the probe was placed away from the activation area, no significant, correlated changes were observed in the optical signals, demonstrating the local nature of the response. The feasibility of noninvasive optical measurement of blood flow and oxygen metabolism through the skull of the adult human is thus feasible, and the clinical potential of this hybrid, all-optical noninvasive, methodology is now being explored in patients suffering from severe head trauma. The optical technique offers a great deal of promise as a portable, non-invasive and relatively cheap modality, capable of doing longitudinal measurements of multiple important parameters. [1]T. Durduran, G. Yu, M. G. Burnett, J. A. Detre, J. H. Greenberg, J. Wang, C. Zhou, and A. G. Yodh, Opt. Lett., 29:1766-1768, 2004.





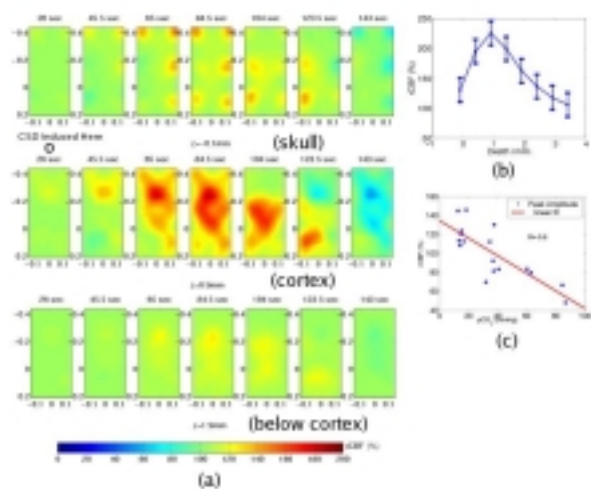
## DEVELOPMENT OF DIFFUSE CORRELATION TECHNIQUES FOR NON-INVASIVE MEASUREMENT OF CEREBRAL BLOOD FLOW AND OXYGEN METABOLISM IN RATS

Turgut Durduran<sup>1</sup>, Guoqiang Yu<sup>1</sup>, Chao Zhou<sup>1</sup>, Daisuke Furuya<sup>2</sup>, Joseph P. Culver<sup>1</sup>, Arjun G. Yodh<sup>1</sup>, Joel H. Greenberg<sup>2</sup>

<sup>1</sup>Department of Astronomy and Physics, University of Pennsylvania, Philadelphia, PA, USA

<sup>2</sup>Department of Neurology, University of Pennsylvania, Philadelphia, PA, USA

Our group has pioneered the development of diffuse correlation tomography (DCT) for measurement of cerebral blood flow (CBF) through the intact skull in animal models and finally in adult human brain. By combining DCT with simultaneous diffuse optical tomography (DOT) which images changes in oxyhemoglobin (rHbO<sub>2</sub>), deoxyhemoglobin (rHb) and total hemoglobin (rTHC) concentrations, and blood oxygen saturation (dYt), we can derive an image of the relative cerebral metabolic rate of oxygen (rCMRO<sub>2</sub>). Previously, we have obtained images in rat brain during hypercapnia [1] and focal transient ischemia [2], and now present data in cortical spreading depression (CSD). The development of this technique enables us to carry out longitudinal studies in small animals relatively noninvasively. After validating the combined DOT/DCT technique using a well characterized system (hypercapnia) [1], we then obtained data in a middle cerebral artery occlusion model in the rat [2]. In the penumbra, rCBF decreased to 42±4%, dYt decreased by 11±4% and rCMRO<sub>2</sub> decreased to 59±4%. These data are in reasonable agreement with values reported in the literature and were the first images of rCMRO<sub>2</sub> obtained by diffuse optical methods. Recently, we have induced cortical spreading depression (CSD) in twenty-six rats by applying KCl through a burr hole over the parietal cortex under hypocapnia, normocapnia, and hypercapnia. Figure 1a shows images of rCBF at selected time points and at different depths. A region of increased CBF progressed from the point where the KCl was applied, spreading throughout the cortex. The observed response was mainly constrained to the upper cortex, illustrating the depth selectivity of the imaging technique (Figure 1b). We observed significant correlations of the peak amplitude of rCBF and frequency of the CSD waves with alterations in pCO<sub>2</sub> (Figure 1c). Similar results were obtained in the oxygenation and CMRO<sub>2</sub> images. By imaging multiple parameters simultaneously we are able to characterize the CSD physiology more thoroughly than usual DOT. Overall these results have validated and demonstrated the utility of DCT methods in obtaining 3D dimensional, dynamic images of blood flow and hence enabling measurement of CMRO<sub>2</sub>. We discuss the extension of this technique to measurements in the adult human in an accompanying abstract. [1] C. Cheung, J. P. Culver, K. Takahashi, J. H. Greenberg, and A. G. Yodh, *Phys. Med. Biol.*, 46:2053-2065, 2001. [2] J. P. Culver, T. Durduran, T. Furuya, C. Cheung, J. H. Greenberg, and A. G. Yodh, *J. Cereb. Blood Flow Metab.* 23:911-924, 2003.





## NEURAL ACTIVATION IN HUMAN BRAIN DETECTED WITH HYPERPOLARIZED $^{129}\text{Xe}$ AND MRI

Yasushi Kondoh<sup>1</sup>, Kazuhiro Nakamura<sup>2,3</sup>, Jeff Kershaw<sup>2,3</sup>, Atsushi Wakai<sup>2,3</sup>, Naoyuki Takei<sup>4</sup>,  
Tetsuji Tsukamoto<sup>4</sup>, Iwao Kanno<sup>2</sup>

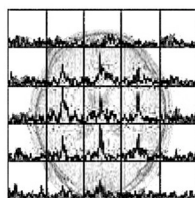
<sup>1</sup>Department of Neurology, Akita Research Institute of Brain and Blood Vessels, Akita, Japan

<sup>2</sup>Department of Radiology and Nuclear Medicine, Akita Research Institute of Brain and Blood  
Vessels, Akita, Japan

<sup>3</sup>Akita Industry Promotion Foundation, Akita, Japan

<sup>4</sup>GE Yokogawa Medical Systems, Hyogo, Japan

**INTRODUCTION:** Hyperpolarized  $^{129}\text{Xe}$  (HpXe) [1] has the potential to be an NMR tracer with a decay time of 10-25 s in blood and in tissue. In this study we apply it to detect neural activation in human. **METHOD:** Chemical shift imaging (CSI) was performed on a 1.5T MRI (GE Signa) with a birdcage coil tuned to the xenon resonance. Scans were performed with no slice selection. CSI spectra were obtained in either a 3x3 or 5x5 matrix, corresponding to voxel sizes of 6cm or 3.5 cm respectively. HpXe gas was produced by a commercial polarizing system (Toyoko-Kagaku Ltd, Tokyo). 500ml of HpXe gas (polarization ~8%) was supplied into a 1-L bag and the bag was connected to a manual inhalation unit. The subject inhaled HpXe from the bag and held their breath for 30 sec. The MRI scan started after the subject had indicated that they had inhaled all of the gas. Beginning 1 min before gas inhalation, the subject was instructed to watch a computer-generated pattern projected onto the backside of a translucent screen placed at the foot of the gantry bed. The screen was observed via a mirror attached to the birdcage coil. Measurements were carried out with an 8Hz-reversing checkerboard (CHK) and a fixed-point pattern used as a control (FIX). Five pairs of measurements (CHK and FIX) were carried out on three normal volunteers. **RESULTS:** Figure 1 shows CSI spectra superimposed on a proton T1-weighted image. All voxels revealed spectra of HpXe with multiple peaks. The main and second peaks are at 195 and 192 ppm with respect to the gas peak. We normalized the spectra by the height of main peak (195ppm) in the frontal cortex voxel and the CHK/FIX ratios at the visual cortex were then calculated. We found a relative increase of 1.37+/-0.17 for the main peak and 1.26+/-0.23 for the second peak. Assuming that the main and second peaks correspond to gray and white matter, respectively, and that the peak height mainly reflects increased delivery of HpXe due to an increase in blood flow, the relative increase in evoked CBF is approximately the same in both gray and white matter. **DISCUSSION:** This is the first study applying HpXe to the investigation of neural activation in humans. Fractional increases in CBF were found in both gray and white matter. An improvement in sensitivity to the HpXe signals promises to provide further useful information such as an excess production of lactate. **ACKNOWLEDGEMENT:** This work was supported by a project of the Japan Science and Technology Agency. References: [1] Albert M et al. Nature, 1995.



**PROBING METABOLIC AND VASCULAR CHANGES IN THE OLFACTORY GLOMERULI BY FUNCTIONAL OPTICAL AND RADIO-ISOTOPIC TECHNIQUES**

**Hirac Gurden**<sup>1,2,3</sup>, Frederic Pain<sup>1</sup>, Aurelie Desbree<sup>1</sup>, Roland Mastrrippolito<sup>1</sup>, Laurent Besret<sup>2</sup>, Gilles Bonvento<sup>2</sup>, Philippe Hantraye<sup>2</sup>, Zachary F. Mainen<sup>3</sup>, Philippe Laniece<sup>1</sup>

<sup>1</sup>*Groupe Interface Physique Biologie, Institut de Physique Nucleaire, CNRS UMR8608, Orsay, France*

<sup>2</sup>*CNRS-CEA, URA 2210, Service Hospitalier Frederic Joliot, Orsay, France*

<sup>3</sup>*Cold Spring Harbor Laboratory, Cold Spring Harbor, NY, USA*

Recording data related to brain metabolism and blood flow provides relevant signals for mapping brain activity including functional magnetic resonance imaging (fMRI), positron emission tomography (PET) and intrinsic optical signals imaging (IOSI). To further describe and understand these signals we present here recent data acquired through complementary functional techniques *in vivo* on a new promising model. This experimental model relies on the physiological activation of olfactory glomeruli by different odors in the rat. Olfactory glomeruli are the anatomically well-defined functional units of the olfactory bulb where the first step in the processing of olfactory information in the brain occurs. Interestingly, they present structural features such as dense population of astrocytes and specific capillary network to respond to high metabolic demands. To study the odor-evoked glomerular activation we used the following techniques: (i) IOSI: detection of changes in light reflectance arising from changes in blood oxygenation level, blood volume and light scattering, (ii) Laser Doppler Flowmetry (LDF): detection of red-light shift due to changes in the flow of blood cells in the local vascular network. (iii) Beta Microprobe: a new method developed in our lab to detect locally positrons emitted by 18-Fluoro-Deoxy-Glucose (FDG, Pain et al., 2002). Since the mechanisms triggering IOS in the brain tissue during neural activation are unknown, we first explored their cellular origin in the olfactory glomeruli. Using local pharmacology *in vivo* we showed that glomerular IOS are not triggered by the postsynaptic receptors but coupled to the presynaptic release and uptake of glutamate. Second, using LDF we were able to monitor stimulus-locked blood flow increases under odor stimulation. Third, using the Beta-Microprobe, we quantified kinetics of glucose metabolism in olfactory glomeruli *in vivo*. Compartmental modeling applied to our FDG data showed a significant change in the rate constants under odor stimulation compared to baseline with an overall increase of cerebral metabolic rate of glucose and an increase in the glycolytic activity at the hexokinase level. Taken together, these results show that olfactory glomeruli are a very attractive model for the study of brain metabolism and blood flow and their coupling to neural activity. Supported by CNRS-CEA, programme 'Imagerie du Petit Animal'.

**FOLLOW-UP STUDY OF AMYLOID DEPOSITION AND GLUCOSE METABOLISM  
IN PATIENTS WITH ALZHEIMER'S DISEASE**

**Anton Forsberg<sup>1</sup>**, Henry Engler<sup>2</sup>, Emma Larsson<sup>1</sup>, Gunnar Blomquist<sup>2</sup>, Anders Wall<sup>2</sup>,  
Bengt Långström<sup>2</sup>, Agneta Nordberg<sup>1</sup>

<sup>1</sup>*Karolinska University Hospital, Huddinge, Stockholm, Sweden*

<sup>2</sup>*Uppsala Imanet AB, Uppsala, Sweden*

Introduction: Presently, definitive diagnosis of AD requires histopathological demonstration of amyloid plaques and neurofibrillary tangles at autopsy. An in vivo amyloid-imaging technology that could contribute to accurate the diagnosis in early and perhaps pre-symptomatic stages of AD is under development (1; 2) Positron emission tomography (PET) is a useful tool, which can be used in diagnosis and to follow the progression of AD. Recently a new PET-tracer, PIB (11C-6-hydroxy-benzothiazol), was developed(3) revealing the presence of amyloid in AD patients. Aims: The aims of the follow-up study were: 1) To find changes in amyloid deposition in the AD patients after a period of 1.5 - 2.5 years. 2) To evaluate changes in the glucose cerebral metabolic rate (CMR<sub>glc</sub>) measured by FDG, and the relation with the amyloid deposition. Methods: 16 patients recruited from the dept. of geriatric medicine at Karolinska Univ. Hosp. Huddinge, Stockholm and previously examined in a Siemens HR+ PET camera at Uppsala Imanet, Sweden, were examined again after 1.5 - 2.5 years using the same protocol as before. Regions of interest (ROI:s) covering most of the cerebral cortex were selected and various kinetic models were used for the analysis (4) Results: A group of patients showed unchanged PIB uptake; another group, increased uptake and some patients showed lower PIB uptake at the second examination. The changes over time for the PIB uptake, revealed inter and intra-individual differences that might be coupled to differences in disease duration and progression, age, medication, or changes in the binding properties of the amyloid. Further analysis of the data and comparisons with changes in CMR<sub>glc</sub> are necessary. References: 1)H Engler, A Nordberg, G Blomquist et al. *Neurobiolog Aging* 23, 51:5249; 2002. 2)W Klunk ,H Engler, A Nordberg et al *Annals of Neurology*, 2004; 55:306-319. 3)Klunk WE, Wang Y, Huang G-F et al, *Life Sci* 2001; 69: 1471-1484 4) G Blomquist, H Engler, A Wall et al. Reference tissue methods in analyzing brain uptake of PIB with PET; *EJNM* 30: S215; 2003

## SEDATIVE PROFILES OF ANTIHISTAMINE DRUGS EVALUATED BY SUBJECTIVE SLEEPINESS, COGNITIVE TESTS, AND PET FOR MEASUREMENT OF CEREBRAL HISTAMINE H1 RECEPTOR OCCUPANCY

Manabu Tashiro<sup>1,2</sup>, Yumiko Sakurada<sup>1</sup>, Hideki Mochizuki<sup>1</sup>, Etsuo Horikawa<sup>3</sup>, Motohisa Kato<sup>1</sup>, Masatoshi Itoh<sup>2</sup>, Kazuhiko Yanai<sup>1</sup>

<sup>1</sup>*Department of Pharmacology, Tohoku University School of Medicine, Sendai, Japan*

<sup>2</sup>*Cyclotron and Radioisotope Centre, Tohoku University, Sendai, Japan*

<sup>3</sup>*Centre for Comprehensive Community Medicine, Saga University School of Medicine, Kyushi, Japan*

Histamine H1 receptor antagonists (antihistamines), used for the treatment of allergic disorders, often induce sedative side effects in patients. Such sedative side effects are potentially dangerous because they sometimes result in serious accidents among people who drive cars, operate aircrafts or heavy machinery. Recent drug development has produced various new generation antihistamines with potent anti-allergic effects but with limited sedation. It has become important to evaluate sedative properties of different antihistamines. In general, the limited sedative property results from limited permeability of blood-brain barrier. To measure the sedative property, various methods have been introduced such as measurement of subjective sleepiness, objective computer cognitive tests, actual car driving tests, measurement of cerebral histamine H1 receptor blockade with positron emission tomography (PET), etc. The present study compared sedative properties of a classical antihistamine (hydroxyzine), and of two different second-generation antihistamines, fexofenadine and cetirizine, in healthy Japanese volunteers, using the following measurements: (1) subjective sleepiness; (2) computer-based psychomotor tests; (3) brake reaction time (BRT) during actual car driving, with and without talking on a cellular phone; and (4) brain histamine H1R occupancy (H1RO) using PET with [<sup>11</sup>C]doxepin, a potent radioligand for histamine H1 receptors. Subjects were administered a single dose of fexofenadine 120 mg or cetirizine 20 mg in a double-blind, placebo-controlled, crossover design. Hydroxyzine 30 mg was included as a positive control. Subjective sleepiness, psychomotor performance (n=20) and H1RO with PET (n=12) were measured at baseline and 90 min post-dose. The car driving test (n=18) was conducted at baseline, and at 90 and 240 min post-dose. In results, fexofenadine was not significantly different from placebo for subjective sleepiness and computer-based psychomotor tests, and was significantly less impairing than cetirizine on some measurements (p<0.05). Fexofenadine and placebo were significantly less impairing than hydroxyzine on all measurements (p<0.005), but cetirizine was not. As for the results of car driving tests, subjects administered fexofenadine did not differ significantly from subjects receiving placebo in any test condition. In contrast, hydroxyzine-treated subjects were significantly more sedated and had slower BRTs compared with subjects given fexofenadine or placebo in all test conditions. In the driving test using cellular phones, fexofenadine was not significantly different from placebo and significantly less impairing than hydroxyzine (p<0.01). As for the H1RO measurement with PET, H1RO was negligible with fexofenadine (-0.1%), moderately high with cetirizine (26.0%) and high with hydroxyzine (>50%). In summary, the assessments had the following sensitivity to differentiate between the sedative profiles of antihistamines: H1RO with PET > psychomotor test > BRT with phone = sleepiness > BRT without phone. Fexofenadine 120 mg demonstrated a non-sedative profile and could be differentiated from cetirizine 20 mg. Drivers administered hydroxyzine were slower at recognizing hazards ahead and applying the brake compared with subjects given fexofenadine or placebo. Importantly, cellular phone operation was an additive factor, increasing BRTs in subjects given hydroxyzine. In contrast, fexofenadine did not impair CNS function in subjects involved in a divided attention task of driving and cellular phone operation.



**REGION-SPECIFIC, LONGITUDINAL ASSESSMENT OF FUNCTIONAL RECOVERY OF REPERFUSED BRAIN FOLLOWING TRANSIENT FOCAL ISCHEMIA IN MICE USING BICUCULLINE-INDUCED BRAIN ACTIVATION**

Téa Kekelidze<sup>1</sup>, Annett Spudich<sup>2</sup>, Martin Rausch<sup>3</sup>, Diana Kindler<sup>3</sup>, Claudio Bassetti<sup>2</sup>, Markus Rudin<sup>3</sup>, Ernst Martin<sup>1</sup>, Dirk Hermann<sup>2</sup>

<sup>1</sup>Neuroradiology & MR Center, Department of Diagnostic Imaging, University Children's Hospital Zurich, Zurich, Switzerland

<sup>2</sup>Department of Neurology, University Hospital Zurich, Zurich, Switzerland

<sup>3</sup>Discovery Technologies/Analytical Imaging Sciences, Novartis Institutes for Biomedical Research, Basel, Switzerland

**Introduction:** Structural integrity of the brain tissue during the acute phase following ischemic stroke does not necessarily imply recovery of function (NMR Biomed, 2000; 13:361-370). In fact, little is known about the region-specific relationship between structural and functional integrities after stroke. Functional magnetic resonance imaging (fMRI) using pharmacological stimulation paradigms inducing a global brain response is a sensitive method to study functional changes in the rodent brain in vivo (MRI, 2002; 20:447-454). **Methods:** We measured changes in local cerebral blood volume (CBV), induced by systemic infusion of the GABAA antagonist bicuculline in ischemic mice following 30 minutes of intraluminal middle cerebral artery (MCA) occlusion, using magnetite nanoparticles as an intravascular contrast agent. T2- and diffusion weighted (DW) images, as well as fMRI were acquired at different time-points after reperfusion (24 hr, 72 hr and 7 days). Changes in CBV were analyzed in various brain areas. **Results:** In response to bicuculline stimulation, region-specific increases in CBV were observed in the striatum, cortex and thalamus of control and sham-operated non-ischemic animals. In ischemic animals, on the other hand, functional response to bicuculline displayed a long-lasting reduction in the ischemic striatum and cortex, while structural integrity, as evidenced by T2 and DW signal hyperintensities, was compromised mainly in the striatum, but rarely in the cortex, even at three and seven days after lesioning (Fig. 1). **Conclusions:** a) bicuculline-induced global brain stimulation is a sensitive and informative method to characterize the functional recovery of post-ischemic mouse brain, b) as previously shown in rats, apparent anatomical integrity does not necessarily translate into functional integrity of certain brain structures in the mouse; on the other hand, an abnormal appearance of edematous tissue does not always imply compromised functional activity. The correlation of anatomical, metabolic and functional read-outs during different post-ischemic recovery periods can be further used to test various neuroprotective compounds for their ability to benefit the recovery of brain function.

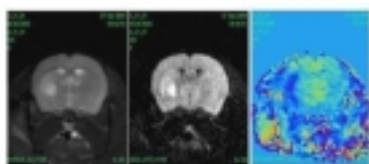


Figure 1. T2W, DWI and CBV maps acquired during 72 hr reperfusion period following 30 min MCAO.

## MAPPING OF CHOLINERGIC MUSCARINIC RECEPTOR ACTIVATION WITH PHARMACOLOGICAL MRI IN RAT BRAIN

Erik I. Hoff<sup>1,2</sup>, Robert J. van Oostenbrugge<sup>1</sup>, Ona Wu<sup>3</sup>, Jet P. van der Zijden<sup>3</sup>, Harry W. Steinbusch<sup>2</sup>,  
Rick M. Dijkhuizen<sup>3</sup>

<sup>1</sup>*Department of Neurology, University Hospital Maastricht, Maastricht, The Netherlands*

<sup>2</sup>*Department of Psychiatry & Neuropsychology, Division Cellular Neuroscience, European Graduate School of Neuroscience (EURON), Maastricht, The Netherlands*

<sup>3</sup>*Image Sciences Institute, University Medical Center Utrecht, Utrecht, The Netherlands*

**Introduction** - The central cholinergic system, and its chief neurotransmitter acetylcholine, modulate several cognitive functions of the brain. The cholinergic system has been implicated in various pathologies of the central nervous system, including stroke and vascular dementia. The aim of the present study was to assess the feasibility of pharmacological MRI (phMRI) in detecting muscarinic receptor activation *in vivo* in control and stroke rats.

**Materials and Methods** - Adult male rats (320-380g) were anesthetized and a lateral tail vein was cannulated for the administration of the muscarinic receptor agonist pilocarpine. Prior to MRI, peripheral muscarinic effects were blocked by injecting methyl-scopolamine (1 mg/kg, s.c.). We applied blood oxygenation level-dependent (BOLD) MRI to detect regional muscarinic activation patterns in response to pilocarpine injection (2.5 mg/kg, i.v.), in control rats (n = 5), as well as two weeks after 60-min intraluminal occlusion of the right middle cerebral artery (MCA) (n = 3). The data of control rats and MCA rats were separately coregistered and post-processed using MNI AutoReg software (Montreal Neurologic Institute, Canada). Activation maps were calculated by statistically comparing BOLD signal intensity before and after pilocarpine injection (Student's t-test; significance level:  $P < 0.01$  (Bonferroni-corrected)). BOLD signal intensity changes were calculated in different regions-of-interest (ROIs).

**Results** - Significant BOLD signal increases were found in basal forebrain, cerebral cortex, caudate putamen and thalamus of the control group. Transient 60-min MCA occlusion resulted in right-sided subcortical infarction at 2 weeks post-stroke. BOLD signal changes in control versus stroke animals, respectively, for the left (non-lesioned) hemisphere were as follows: basal forebrain ( $2.2 \pm 1.8\%$  vs.  $-0.4 \pm 0.1\%$ ), cerebral cortex ( $1.0 \pm 0.9\%$  vs.  $0.7 \pm 0.3\%$ ), caudate putamen ( $0.2 \pm 0.6\%$  vs.  $-1.0 \pm 0.3\%$ ) and thalamus ( $1.0 \pm 0.6\%$  vs.  $0.1 \pm 0.4\%$ ). BOLD signal changes in control versus stroke animals, respectively, for the right (lesioned) hemisphere were as follows: basal forebrain ( $2.2 \pm 2.0\%$  vs.  $-0.6 \pm 0.4\%$ ), cerebral cortex ( $1.0 \pm 0.6\%$  vs.  $0.3 \pm 0.2\%$ ), caudate putamen ( $1.1 \pm 0.9\%$  vs.  $-0.8 \pm 0.1\%$ ) and thalamus ( $1.1 \pm 1.1\%$  vs.  $-0.1 \pm 0.4\%$ ).

**Discussion** - We demonstrate that cholinergic projection fields can be detected *in vivo* by muscarinic receptor-stimulated phMRI in rat brain. Increased BOLD responses were detected in brain areas known to have a high density of muscarinic receptors. There was a tendency for diminished muscarinic receptor activation in rats with subcortical infarction, which may point toward stroke-induced disruption of the cholinergic system.

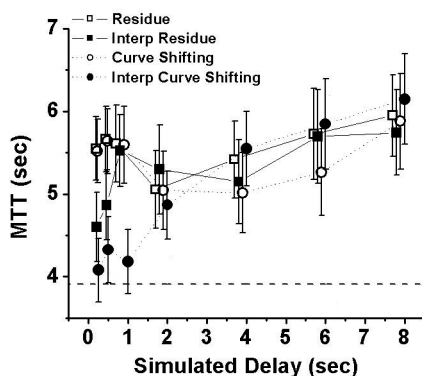
## IMPROVING MEAN TRANSIT TIME CALCULATIONS WITH BETTER ESTIMATES OF ARTERIAL DELAY

George C. Newman<sup>1,2</sup>, Frank Hospod<sup>1</sup>, Evan Delucia-Deranja<sup>1</sup>

<sup>1</sup>Department of Neurology, University of Wisconsin, Madison, WI, USA

<sup>2</sup>Department of Radiology, University of Wisconsin, Madison, WI, USA

**Introduction:** Non-parametric singular value decomposition deconvolution can produce a reliable estimate of mean transit time (MTT) from dynamic contrast imaging (1) but is sensitive to arterial delay and dispersion (2). In this study, we use computer simulations to compare methods of estimating arterial delay and test the hypothesis that a better estimate of delay will improve the estimate of MTT. **Methods:** Monte Carlo simulations were conducted using realistic models (3) of delayed and dispersed arterial input, recirculation, convolved tissue function and MR parameters at varying contrast to noise. Delay was estimated from 1) the time to peak of the deconvolved residue function, 2) a "curve shifting" method based on iterative convolution and deconvolution after gamma variate arterial curve fitting (4), 3) the time at which the arterial and tissue curves reached 3% of maximum, 4) and the time point at which the unfit curves exceeded 2 standard deviations of baseline. The residue and curve shifting methods were studied using the simulated TR and after five point interpolation of the data (eg - using a TR of 1.5 or interpolated data of 0.3 sec). MTT was calculated by the non-parametric SVD method after adjustment of the tissue data for the estimated delay. Errors in estimated delay and MTT were analyzed using non-linear multiple regression analysis and by visual analysis of graphs. **Results:** Estimates of delay based on curve shifting with interpolation consistently yielded the most accurate delay values, followed by the 3% method. Delay was severely overestimated from the residue function. Curve shifting underestimated delay with large arterial dispersions, but only if the delay exceeded 2 sec. MTT estimates at MTT of 4 sec with delays of less than 2 sec were significantly improved by the better estimates of delay from the interpolated curve shifting method (Figure). This method also improved MTT estimates at MTT of 10 or 16 sec, but only by about 0.5 sec. There was a consistent tendency for longer MTT to be underestimated with delays below 4 sec and overestimated above 4 sec. **Discussion:** Under the most commonly encountered conditions, with MTT values below 10 sec and mild or moderate delay and dispersion, estimates of delay by curve shifting of interpolated data improve estimates of MTT obtained by SVD deconvolution. With larger MTT, delay and dispersion, this method still produces the best estimates of delay but the gain for calculation of MTT are modest.



References: (1) Ostergaard L et al. Magn Reson Med;36:715-725;(1996) (2) Calamante F et al. Magn Reson Med;44:466-473; (2000) (3) Bassingthwaite JB et al. Circ Res;18:398-415;(1965) (4) Newman GC et al. Abst#67, Brain'03

## PREPARATION, CHARACTERIZATION AND APPLICATION OF AN ALBUMIN-LINKED, GADOLINIUM-BASED MAGNETIC RESONANCE CONTRAST AGENT

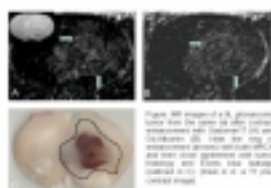
Tavarekere N. Nagaraja<sup>1</sup>, Richard L. Croxen<sup>1</sup>, Swayamprava Panda<sup>2</sup>, Jamie Churchman<sup>2</sup>, Polly A. Whitton<sup>2</sup>, Stephen L. Brown<sup>3</sup>, Joseph D. Fenstermacher<sup>1</sup>, James R. Ewing<sup>2</sup>

<sup>1</sup>Anesthesiology, Henry Ford Health System, Detroit, MI, USA

<sup>2</sup>Neurology, Henry Ford Health System, Detroit, MI, USA

<sup>3</sup>Radiation Oncology, Henry Ford Health System, Detroit, MI, USA

**INTRODUCTION:** Magnetic resonance imaging (MRI) of pathophysiological vascular events requires MR contrast agents (MRCA) linked to bioactive molecules. Here we describe a simple method to prepare a large MRCA by covalently linking albumin to the gadolinium-diethylenetriaminepentaacetic acid (Gd-DTPA), a commonly used MRCA. We employed a novel, Arsenazo III-based reaction to detect unbound gadolinium in the reaction mixture. The preparation was evaluated against a large, commercial MRCA, Gadomer17 (Schering AG, Germany) in a rat 9L gliosarcoma brain tumor. **METHODS:** The coupling of DTPA and gadolinium to bovine serum albumin (BSA) was performed using published procedures [1, 2]. To 15 ml of 10  $\mu$ mol BSA in HEPES buffer (pH 7.5), a suspension 0.714 g DTPA anhydride in DMSO was slowly added with constant stirring. The solution was maintained between pH 6-7 with the addition of 3 M NaOH. After stirring for 1 hr at room temperature, 0.742 g of gadolinium chloride dissolved in water was slowly added to the reaction mixture, until the very first indication of unchelated gadolinium was observed with 10  $\mu$ mol Arsenazo III in acetate buffer at pH 4.0 [3]. The mixture was stirred cold overnight, dialyzed x3 each v/s 0.1M citrate buffer (pH 6.5) and water and then lyophilized. This preparation and Gadomer17 were tested for contrast enhancement using the rat tumor model. After MRI, the rats were injected with the plasma albumin binding dye Evans blue for histological verification of leakiness of tumor vasculature. **RESULTS:** The product was free of unbound Gd when assayed [4]; molecular weight by electrophoresis was ~90 kDa, similar to other reported values [2]. The molar labeling ratio of Gd:BSA was about 30:1 [3]. During MRI it gave a similar, but not identical, pattern of enhancement as Gadomer17, which has a comparable molecular size (Figure, A & B). Most notable was the similarity in the ring of contrast enhancement of both and their close alignment to the highly vascular edge of the tumor (Figure, C). The image of Gd-Albumin resembled closely that of Evans blue leakage (Figure, B & C); the spread of Evans blue-albumin toward the midline and cortex was well matched by Gd-albumin contrast pattern. **CONCLUSION:** Arsenazo III reaction provides a simple, sensitive test for instantly detecting unbound Gd in MRCA. Excess Gd can precipitate the protein in the reaction mixture. Repetitive testing with Arsenazo III can prevent such negative outcomes during preparations. This method may also be applicable in preparation of Gd-chelates with other bioactive molecules. The tumor data suggests that Gd-albumin is useful for MR imaging of albumin distribution in experimental and human studies. **References:** [1] Hnatowich DJ et al. *Int. J. Appl. Radiat Isot* 33: 327-332 (1982) [2] Ogan MD et al. *Invest Radiol* 22: 665-671 (1987) [3] Hvattum E et al. *J Pharmaceut and Biomed Analysis* 13: 927-932 (1995) [4] Cassidy RM et al. *Anal Chem* 58: 1181-1186 (1986) Grant support: NIH-RO1HL70023



## REDUCTION IN CEREBRAL GLUCOSE METABOLISM IN DEPRESSED SUBJECTS FOLLOWING MEMANTINE ADMINISTRATION

**Dara M. Cannon**, Linda Mah, Carlos A. Zarate, Jaskaran Singh, Kirk D. Denicoff, Allison C. Nugent, Gerardo Solorio, Denise Sciallo, Hussein K. Manji, Wayne C. Drevets  
*Mood and Anxiety Disorders Program, National Institutes of Mental Health, NIH, DHHS, Bethesda, MD, USA*

Introduction: Glucose metabolism has been reported to be abnormally elevated in amygdala, ventrolateral prefrontal cortex (PFC) and orbital cortex and decreased in dorsoanterior, dorsomedial and subgenual regions of PFC in unmedicated depressed individuals using [18F]fluorodeoxyglucose (FDG) PET (1, 2). Because the glucose metabolism signal is dominated by the effects of glutamatergic signal, these abnormalities in depression may reflect corresponding alterations in glutamatergic activity (3). A recent pilot study reported mood elevating effects of a single administration of an NMDA receptor antagonist, ketamine (1). Similarly, MK-801 and AP-7, have demonstrated antidepressant effects in several animal models of depression. Memantine, an uncompetitive NMDA receptor antagonist with neuroprotective properties, putatively reduces glutamatergic output via open-channel block of the NMDA receptor-associated ion-channel. Thus, in this study we assessed glucose metabolism using [18F]FDG PET in subjects with Major Depressive Disorder (MDD) before and following chronic memantine administration. Methods: Twelve unmedicated depressed subjects meeting DSM-IV criteria for MDD were randomized to double-blind treatment: 5 received memantine (5-20mg/day; 3 female; mean age $\pm$ sd: 43 $\pm$ 10) and 7, placebo (3 female; 48 $\pm$ 10) for 8 weeks. Each participant underwent a baseline [18F]FDG PET scan and a second identical scan in their eighth week of treatment. Depression severity was rated using the Montgomery-Asberg Rating Scale for Depression (MADRS). Mann-Whitney U test was applied to assess the significance of changes in metabolism in the memantine group versus the placebo group. Results: MADRS scores following eight weeks of memantine (22 $\pm$ 9) or placebo (20 $\pm$ 11) were similar to each other as well as to baseline scores (30 $\pm$ 4 and 30 $\pm$ 3, respectively). Chronic memantine administration resulted in greater decreases in whole brain glucose metabolism compared to placebo administration ( $p=0.0177$ ). Cortical regions of interest, dorsolateral, dorsomedial and subgenual prefrontal cortices showed decreases in proportion to that detected for whole brain. Conclusion: Although memantine administration was not associated with clinical improvement, it did induce greater decreases in glucose metabolism compared to placebo in MDD subjects. Glucose metabolism in cortical regions was similarly decreased following 8 weeks of memantine compared to placebo administration. This reduction in cerebral glucose metabolism following memantine administration is compatible with a reduction in glutamatergic transmission due to NMDA receptor antagonism. References: 1.Drevets, WC, 1999. *Annals of the NY Acad Sci*, 614-637. 2.Berman RM, Cappiello A, Anand A, et al. *Biol Psychiatry*. 2000; 47:351-4. 3.Magistretti PJ and Pellerin L, 1999. *Phil. Transact. Royal Soc. London. Series B, Biol. Sci.* 354 (1387) 1155-63.

## MUSCARINIC CHOLINERGIC2 RECEPTOR BINDING IN BIPOLAR DISORDER: RELATION TO SALIENCY OF AFFECTIVE-WORDS

Dara M. Cannon<sup>1</sup>, Allison C. Nugent<sup>1</sup>, Kristine Erickson<sup>1</sup>, Rich E. Carson<sup>2</sup>,  
William C. Eckelman<sup>2</sup>, Dale O. Kieseewetter<sup>2</sup>, Earle E. Bain<sup>1</sup>, Shilpa K. Gandhi<sup>1</sup>,  
Gerardo Solorio<sup>1</sup>, Dennis Charney<sup>1</sup>, Wayne C. Drevets<sup>1</sup>

<sup>1</sup>*Mood and Anxiety Disorders Program, National Institutes of Mental Health, NIH, DHHS,  
Bethesda, MD, USA*

<sup>2</sup>*Clinical Center, NIH, Bethesda, MD, USA*

**Introduction.** The muscarinic-cholinergic system has been implicated in mood disorders by findings that, 1)cholinergic-agonist administration exacerbates depressive symptoms, 2)muscarinic-cholinergic agonists induce exaggerated effects on REM density and latency in depressives versus controls, 3)both manic and depressed bipolar disorder (BD) subjects show increased pupillary-sensitivity to the muscarinic-agonist pilocarpine, 4)a M2-receptor polymorphism was associated with increased risk for Major Depressive Disorder (MDD) in females. The current study investigated muscarinic-cholinergic receptor binding in mood disorders using PET and [18F]FP-TZTP, a muscarinic-agonist that is relatively selective for M2-receptors. In addition, because the cholinergic system plays major roles in learning the significance of emotional stimuli, the relationship between [18F]FP-TZTP binding and performance on an affective-word rating task was assessed. **Methods.** Central M2-receptor DV was measured in 27 currently-depressed subjects (12 BD, 15 MDD) and 20 controls (Mean+/-SD: Age HC:34+/-5; BD:33+/-6; MDD:36+/-8yrs). A 120-minute dynamic PET scan in 3D-mode was acquired using a GE-Advance scanner with arterial blood sampling. To provide an anatomical framework for image analysis and partial volume correction of the PET data, anatomical-MRI scans were obtained. Regional distribution volumes (DV) were obtained using a one-tissue compartment model. DV values were corrected for the plasma free-fraction (f1), and compared across groups using ANOVA. A subset of these subjects (8 BD, 13 MDD, 10 Controls) rated the valence and salience of emotional words. The relationship between affective-word rating and the [18F]FP-TZTP DV was assessed using Pearson correlation coefficient. **Results.** Whole brain [18F]FP-TZTP binding differed across subjects samples (ANOVA: F=3.49; p=0.039; n=47). This was accounted for by significantly lower binding in BD-subjects compared to healthy and MDD-subjects. MANOVA revealed decreased anterior cingulate (ACC) and occipital cortex binding in BD-subjects compared to healthy and MDD-subjects. Decreases ranged 16 to 21% across regions. In contrast, binding did not differ significantly between MDD-subjects and controls. Post-hoc voxel-by-voxel analysis of parametric images revealed significantly lower binding localized to anterior, dorsal and posterior cingulate cortices in BD-subjects compared to healthy or MDD-subjects.

As hypothesized, depression severity correlated negatively with whole brain [18F]FP-TZTP binding ( $r=-0.33$ ;  $p=0.026$ ). The saliency score for affective-word ratings was negatively correlated with whole brain [18F]FP-TZTP DV for the BD-subjects ( $r=-0.80$ ;  $p=0.017$ ). **Conclusion.** ACC [18F]FP-TZTP DV was significantly lower in depressed BD-subjects versus controls and MDD-subjects. Because [18F]FP-TZTP binding is sensitive to endogenous ACh concentrations, this reduction in [18F]FP-TZTP DV in BD-subjects may reflect either:1)increased baseline levels of ACh or 2)decreased M2-receptor density and/or increased affinity (Kd). These data are potentially consistent with the exaggerated responses observed in BD-subjects to cholinomimetic agents. The inverse relationship between depression severity and [18F]FP-TZTP DV is consistent with findings that physostigmine exacerbates depressive sx's in BD. In contrast, while equally depressed, MDD-subjects, appeared to have similar M2-receptor binding to controls. Finally, the inverse correlation between [18F]FP-TZTP DV and the salience of affective-words is noteworthy given the role of the cholinergic system in assigning the saliency of experiential stimuli.

**ABSOLUTE VERSUS RELATIVE 'DEACTIVATION': A COMPARISON OF SEVEN COGNITIVE TASKS USING QUANTITATIVE XE-133 SPECT****Georg Deutsch, Beverly Corbitt, Omur Sen, Hong-Gang Liu, Janis O'Malley***Division of Nuclear Medicine, Department of Radiology, University of Alabama at Birmingham, Birmingham, AL, USA*

Most analysis of activation data in PET and fMRI involves relative changes in rCBF distribution between conditions. This is in part due to the prevailing assumption that pattern changes and not fluctuations in absolute rCBF represent the important data regarding brain activity-cognition relationships. Normalized redistribution analysis invariably shows "deactivation" as well as activation. We present data showing that "deactivation" can represent either true reduction in cerebral activity or be an artifact of normalization that misses important global changes. These changes appear to reflect the extent of novelty versus routinization of task and control conditions. Methods: 27 subjects participated in three protocols involving 7 tasks and baseline scans during quantitative rCBF studies: 1) Passive visual stimulation involving multiple images, followed by a forced choice recognition task, 2) 3-dimensional mental rotation and speech sound discrimination, 3) Linguistic Components - phonetic ("br") and semantic ("living") target tasks and continuous recognition memory of a word series. Whole brain scans were performed every 10 seconds using a modified Picker triple-head tomograph. rCBF was calculated from reconstructed Xe-133 clearance data (24 scans); final images were generated representing rCBF in ml/100g/min. Data analysis was performed to determine the pattern of redistribution of rCBF and the absolute rCBF changes associated with significant activation or "deactivation" findings via: 1) an ROI method using ANOVA on a multi-region profile of mean absolute rCBF, 2) SPM2, 3) inspection of quantitative mean rCBF images created using spatially normalized Xe SPECT scans. Results: All tasks except passive visual stimulation and the semantic target task resulted in absolute increases in all cortical ROI. Only in these two conditions did SPM and absolute rCBF analysis concur regarding "deactivated" regions. Visual stimulation resulted in decreased rCBF in frontal ROI along with increase in occipital cortex. SPM identified activation and "deactivation" consistent with these absolute rCBF changes. There was concordance between SPM "deactivation" and absolute rCBF reduction in right temporal-parietal regions during the semantic task. In all other conditions there was agreement in activated regions, but significant "de-activation" on SPM was seen only as a less-than-average increase in absolute rCBF compared to other regions. This occurred in parietal-temporal areas during the phonetic task and in frontal cortex during auditory memory and mental rotation. Conclusion: Redistribution of rCBF without change in mean cortical rCBF seems to occur in cases of passive sensory stimulation and in task conditions involving fairly routine or well mastered operations, such as our semantic task in which rCBF was lower compared to other linguistic operations and resting baseline. In such situations there is concordance between deactivation seen on SPM and absolute rCBF analysis. Global increases occur in situations involving more novel cognitive operations, and may include control conditions designed to isolate "lower" stages of processing but which may be less familiar in isolation and thus more contrived. Our data indicate that although regional reductions in absolute activity do occur, at least part of the "deactivation" seen on non-quantitative imaging and typical SPM analysis does not represent physiological reduction because systematic global changes are ignored.

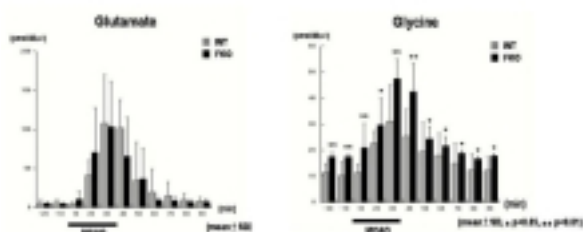
## ROLE OF GLYCINE IN ISCHEMIC NEURONAL INJURY -THE STUDY USING FUNCTIONAL KNOCKOUT MICE OF GLYCINE CLEAVEGE ENZYME

Masaya Oda<sup>1</sup>, Hiroyuki Kinouchi<sup>1</sup>, Shigeo Kure<sup>2</sup>, Taku Sugawara<sup>1</sup>, Suguru Yamaguchi<sup>1</sup>, Kenichi Sato<sup>2</sup>, Yoichi Matsubara<sup>2</sup>, Tomoya Omae<sup>1</sup>, Kazuo Mizoi<sup>1</sup>

<sup>1</sup>*Division of Neurosurgery, Department of Neuro and Locomotor Science, Akita University School of Medicine, Akita, Japan*

<sup>2</sup>*Department of Medical Genetics, Tohoku University School of Medicine, Sendai, Japan*

**Introduction:** Although glycine is an inhibitory neurotransmitter in the brain stem and the spinal cord, it acts as a coagonist in excitatory neurotransmission at the N-methyl-D-aspartate (NMDA) subtype of glutamate receptors. Activation of the NMDA receptors is known to mediate neuronal injury after cerebral ischemia, however, the role of glycine in ischemic injury has not been clarified. In this study we investigated the extracellular glycine concentrations in the functional knockout (FKO) mice of glycine cleavage enzyme following cerebral ischemia and the effect of extracellular glycine concentration on the ischemic neuronal injury. **Methods:** FKO mice were generated by overexpressing a dominant-negative mutant glycine decarboxylase. The total glycine concentrations of the brain in FKO mice are 1.4 times higher than those of C57BL/6 wild-type (WT) mice. Cerebral ischemia was produced by the transient occlusion of middle cerebral artery (MCA) for 30 min, with the intraluminal suture method. CBF of the ipsilateral MCA cortex was measured by the laser doppler flowmetry. The mice with a CBF reduction to less than 10 % of the preischemic control level were only adopted in this study. The extracellular levels of amino acids (alanine, glutamate, glycine, taurine) in the dialysate were determined by high-performance liquid chromatography with electrochemical detector in both mice before and 2h after transient MCA occlusion. The mice were sacrificed 24h after reperfusion and coronal brain slices were incubated in 2% solution of 2,3,5-triphenyltetrazolium chloride for measurement of the cerebral infarct volume. **Results:** The extracellular glycine concentration of FKO mice significantly increased compared to Wt mice after the onset of MCA occlusion (FKO; preischemia  $18.4 \pm 3.4$ , postischemia  $48.4 \pm 30.4$ , Wt; preischemia  $12.9 \pm 2.0$ , postischemia  $31.1 \pm 13.9$  pmol/20 $\mu$ l, mean $\pm$ SD, n=5). The increase of extracellular glycine concentration was sustained in both groups following reperfusion and the sustained increase lasted longer in the FKO mice. On the other hand, extracellular concentrations of other amino acids including glutamate increased during ischemia as reported previously, and there were no significant differences between them. The infarct volume in Tg mice was 52.6% larger than that of the Wt mice (Tg;  $95.03 \pm 15.6$ , Wt;  $62.2 \pm 8.6$  mm<sup>3</sup>, mean $\pm$ SD) **Comments:** FKO of glycine cleavage enzyme causes the increase of both intracellular and extracellular glycine concentrations of the brain. The extracellular glycine concentrations of the brain in FKO mice were more significant than those in Wt mice after cerebral ischemia. FKO mice with high extracellular glycine concentration showed the significantly large infarct volume. These results suggest that extracellular glycine affect the sensitivity of NMDA receptors to glutamate and that glycine may play a key role in excitatory neuronal damage through NMDA receptors after cerebral ischemia.





**NORMOBARIC HYPEROXIA THERAPY EXERTS ITS NEUROPROTECTIVE EFFECT THROUGH AN INCREASE IN TISSUE PO<sub>2</sub> AND A DECREASE IN FREE RADICAL GENERATION, CASPASES AND MMP EXPRESSION IN THE ISCHEMIC PENUMBRA**

Shimin Liu<sup>1</sup>, Wenlan Liu<sup>1</sup>, Wei Ding<sup>1</sup>, Honglian Shi<sup>1</sup>, Gary A. Rosenberg<sup>2</sup>, **Ke J. Liu<sup>1</sup>**

<sup>1</sup>*College of Pharmacy, University of New Mexico Health Sciences Center, Albuquerque, NM, USA*

<sup>2</sup>*Department of Neurology, University of New Mexico Health Sciences Center, Albuquerque, NM, USA*

Stroke is a leading cause of death and disability. However, current treatments are ineffective. Oxygen therapy aimed at increasing tissue pO<sub>2</sub> has been used as a potential treatment modality. Unfortunately, most experiments with oxygen therapy were conducted without monitoring the actual interstitial pO<sub>2</sub> level that is essential for penumbral tissue to survive, and also a critical parameter for evaluation of the efficiency of oxygen therapy. Using the unique capability of in vivo electron paramagnetic resonance (EPR) oximetry to measure localized interstitial pO<sub>2</sub>, we have conducted EPR-guided oxygen therapy by monitoring penumbral pO<sub>2</sub> in a rat model of 90-min transient ischemia while normobaric hyperoxia is administered. Our results reveal that penumbral pO<sub>2</sub> level can be modulated by changing the percentage of oxygen content in the breathing gas, and that 95% O<sub>2</sub> given to rats is capable of raising penumbral interstitial pO<sub>2</sub> close to the physiological (pre-ischemic) value during ischemia. However, 95% O<sub>2</sub> also caused an increase in penumbra pO<sub>2</sub> to a level that was twice as high as the pre-ischemic level when given during reperfusion. Oxygen therapy with 95% O<sub>2</sub>, begun immediately after ischemia and continued for 90-min significantly reduced infarction volume by 40% and improved neurological function. Oxygen therapy given upon reperfusion also reduced infarction volume by 15%, but it was not statistically significant. In order to investigate the possible molecular mechanism for the observed neuroprotective effect of hyperoxia treatment, we have studied the effects of oxygen therapy in the ischemic penumbra. We focused specifically on the generation of free radicals and the activation of matrix metalloproteinase (MMP) and caspase, two well characterized mechanisms leading to cerebral injury that are regulated through free radical generation. Our results demonstrate that 95% O<sub>2</sub> treatment administered during the 90-min ischemia decreased the formation of 8-hydroxy-2'-deoxyguanine, a biomarker of oxidative DNA damage. Furthermore, 90-min ischemia dramatically increased the MMP-2 and 9 expression at 24 hrs post reperfusion, while hyperoxia treatment decreased penumbral MMP-9 expression by 50%. Interestingly, there was no difference in MMP-2 expression between the oxygen treated and non-treated groups. Similarly, 90-min cerebral ischemia induced approximately a 100% increase in 22 kD cleaved caspase-8 and a 25% increase in 43 kD cleaved caspase-8 in the penumbra, as compared to the contralateral side during normoxia. Hyperoxia treatment significantly decreased caspase activation in the penumbra. These results establish for the first time that normobaric hyperoxia oxygen therapy exerts its neuroprotective effect during ischemia through the increase of penumbral tissue pO<sub>2</sub>, which leads to a reduction in free radical generation, and consequently, caspases and MMPs expression.

**EP1 RECEPTORS ARE RESPONSIBLE FOR COX-2 MEDIATED NEUROTOXICITY**

**Josef Anrather**, Ping Zhou, Takayuki Kawano, Liping Qian, Camile Gooden,  
Costantino Iadecola

*Weill Medical College of Cornell University, Division of Neurobiology, Department of  
Neurology and Neuroscience, New York, NY, USA*

There is increasing evidence that cyclooxygenase-2 (COX-2), a rate-limiting enzyme for prostanoid synthesis, is involved in the mechanism of ischemic brain injury. However, the reaction products responsible for COX-2-mediated neurotoxicity have not been defined. Prostaglandin E2 (PGE2) is the major COX-2 derived prostanoid produced following brain injury and is involved in the mechanisms of glutamate excitotoxicity (Ann. Neurol. 55, 668). PGE2 acts on four receptor subtypes (EP1-4). While activation of EP2 receptors is neuroprotective (J. Neurosci. 24, 257), EP1 receptors mediate injury in other organs (Hypertension 42, 1183). Therefore, in this study we tested the hypothesis that EP1 receptors mediate the neurotoxicity exerted by COX-2. Methods: Brain lesions were produced by injecting NMDA into the parietal cortex of wild-type mice or mice lacking EP1 receptors (EP1<sup>-/-</sup>). Lesion volumes were determined 24 hours later in thionine-stained sections. The COX-2 inhibitor NS398 (NS) (20mg/kg) or the EP1 antagonist SC51089 (SC) (10µg/kg) was administered systemically. Organotypic hippocampal slices from newborn mice were used after 2 weeks in culture. Slices were exposed to oxygen-glucose deprivation (OGD) for 1 hour and assayed for cell death 24 hours later. Intracellular free Ca<sup>++</sup> was determined in cortical mixed cultures by ratiometric fluorography using Fura-2 as an indicator. Results: The COX-2 inhibitor NS and the EP1 receptor antagonist SC produced comparable reductions in NMDA-induced lesions (figure A). Co-administration of NS and SC did not produce added protection (figure A). However, the free radical scavenger SOD (100mU) reduced lesion volume further (figure A), indicating that the injury was not maximally reduced. EP1<sup>-/-</sup> mice showed a reduction in lesion volume similar to SC-treated wild-type mice. OGD-induced cell death in hippocampal slices was reduced by 32.9±2.4% by NS and by 29.2±2.1% by SC (p<0.05 from vehicle; n=15/group). Co-treatment with NS and SC did not confer added protection (p>0.05 from NS or SC alone; n=15/group). To gain insight into the mechanism by which EP1 receptors promote neuronal cell death, we monitored intracellular free Ca<sup>++</sup> in cultures exposed to NMDA (100µM) in the presence or absence of NS or SC. NS or SC significantly attenuated NMDA-induced rise in intracellular free Ca<sup>++</sup> (figure B). Conclusions: EP1 receptors contribute to the neurotoxicity exerted by activation of NMDA receptors or OGD. The observation that the protection conferred by COX-2 or EP1 receptor inhibition are not additive is consistent with the hypothesis that they exert their deleterious effects through the same cell death pathway and support the idea that EP1 receptors mediate the deleterious effects of COX-2. EP1 receptors may promote cell death by facilitating the Ca<sup>++</sup> overload produced by excitotoxicity.

## NEGATIVE NEUROVASCULAR COUPLING DURING ANOXIC DEPOLARIZATION AND PERI-INFARCT SPREADING DEPRESSIONS IN ACUTE FOCAL CEREBRAL ISCHEMIA IN MICE

Cenk Ayata<sup>1,2</sup>, Hwa Kyoung Shin<sup>1</sup>, Phillip Jones<sup>3</sup>, Andrew K. Dunn<sup>3</sup>, David A. Boas<sup>3</sup>,  
Michael A. Moskowitz<sup>1</sup>

<sup>1</sup>*Stroke and Neurovascular Regulation Lab, Department of Radiology, Massachusetts  
General Hospital, Harvard Medical School, Charlestown, MA, USA*

<sup>2</sup>*Stroke and Neurointensive Care Unit, Department of Neurology, Massachusetts General  
Hospital, Harvard Medical School, Charlestown, MA, USA*

<sup>3</sup>*Martinos Center for Biomedical Imaging, Department of Radiology, Massachusetts General  
Hospital, Harvard Medical School, Charlestown, MA, USA*

Background: Peri-infarct spreading depressions (PISDs) have previously been linked to worsening focal ischemic damage, and this effect has been attributed to the additional metabolic burden imposed on the ischemic brain. Here we propose an additional hypothesis based on the vascular consequences of ischemic depolarization. Our overall hypothesis states that ischemic neuroglial depolarization and elevated extracellular K<sup>+</sup> adversely impact tissue perfusion within the depolarized tissue by, for example, causing vasoconstriction. This secondary reduction in CBF in turn worsens tissue ischemia creating a cycle that expands the infarct during acute stroke and ultimately results in tissue necrosis. Methods: We tested this hypothesis by measuring CBF using laser speckle-flowmetry with high spatial and temporal resolution, to investigate the impact of anoxic depolarization (AD) and PISDs on CBF within the core and penumbra during distal middle cerebral artery occlusion (dMCAO) in mice. To assess the impact of neuroprotectants on the progression of CBF in ischemia, one of the following were administered i.p. 1h prior to dMCAO: vehicle (n=15), MK-801 (5 mg/kg, n=7), 7-chlorokynurenic acid (100 mg/kg, n=4), dextromethorphan (10 mg/kg, n=4), NBQX (60 mg/kg, n=4). Results: In all animals, dMCAO abruptly reduced CBF to 20-30% of baseline in the center of ischemic cortex. Within 1-2 min after dMCAO, AD caused a further reduction in CBF (15-20% of baseline). Spontaneous waves of PISDs (2.9±0.5/h; ±SEM) caused waves of hypoperfusion in both the core and the penumbra. During each PISD, the area comprising the ischemic core (defined as <20% residual CBF) grew by 12±4%, whereas during the time between PISDs, this area did not increase (-5±3%, p<0.01). Hence, AD and PISDs exacerbated the CBF deficit, and expanded the severely ischemic cortex in a stepwise fashion. The expansion of CBF deficit was attenuated by the NMDA receptor-channel blocker MK-801 and NMDA receptor glycine site antagonist 7-chlorokynurenic acid. When measured 60 minutes after dMCAO, the area of severely ischemic cortex was 40% and 45% smaller in MK-801 (p<0.01) and 7-chlorokynurenic acid treated mice, respectively, compared to vehicle controls. Sigma-one receptor agonist dextromethorphan also reduced the area of severe CBF deficit by 55% (p<0.05), whereas the AMPA/kainate receptor blocker NBQX did not. In summary, we showed that AD and PISDs worsen focal ischemic damage in penumbra and the core by a negative neurovascular coupling. Neuroprotective agents MK-801, 7-chlorokynurenic acid and dextromethorphan (drugs that are known to inhibit spreading depression) improve the CBF deficit, perhaps by stabilizing the neuroglial membranes, and therefore, interfering with the adverse vasoconstrictive effects of tissue depolarization. NBQX, which does not inhibit spreading depression, does not improve CBF. Such a secondary CBF-dependent benefit may be a critical determinant of concentric reduction of cerebral infarcts by neuroprotective drugs primarily inhibiting ischemic neuroglial depolarization.

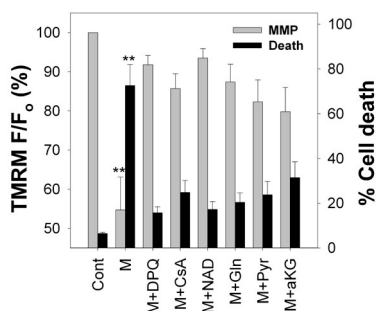
## METABOLIC SUBSTRATES PREVENT PARP1-MEDIATED MITOCHONDRIAL DYSFUNCTION AND CELL DEATH

Conrad C. Alano<sup>1,2</sup>, Weihai Ying<sup>1,2</sup>, Raymond A. Swanson<sup>1,2</sup>

<sup>1</sup>Department of Neurology, University of California at San Francisco, San Francisco, CA, USA

<sup>2</sup>Department of Neurology, Veterans Affairs Medical Center, San Francisco, CA, USA

**INTRODUCTION:** Poly(ADP-Ribose) Polymerase-1 (PARP1) participates in DNA repair, and consumes NAD<sup>+</sup> to form PAR polymers on acceptor proteins [1]. PARP1 hyperactivation occurs in ischemic stroke and excitotoxicity, and promotes cell death by mechanisms that remain poorly understood. Induction of the mitochondrial permeability transition (MPT) is a causative factor in both apoptotic and necrotic cell death in excitotoxicity and ischemia [2]. We previously showed that MPT induction is necessary for PARP1-mediated cytotoxicity, and that NAD<sup>+</sup> repletion is protective [3]. Here we show that i) NAD<sup>+</sup> protection against PARP1 hyperactivation requires glucose, and ii) tricarboxylic acid (TCA) substrates prevent PARP1-induced mitochondrial dysfunction and cell death. We hypothesize that PARP1 hyperactivation leads to glycolytic blockade through NAD<sup>+</sup> depletion, and provide further evidence of NAD<sup>+</sup> as a link between PARP1 activation, mitochondrial dysfunction, and cellular demise. **METHODS:** Mouse cortical astrocytes and neurons were prepared as previously described [3]. DNA damage was performed with the DNA alkylating agent, MNNG (M; 100µM) for 30min. Pharmacological compounds: PARP inhibitor DPQ (D; 25µM); MPT inhibitor CsA (C; 200nM); NAD<sup>+</sup> (2-5mM). Cell death was assayed after 24h by LDH release (astrocytes) and PI-staining (neurons). Mitochondrial membrane potential (MMP) was assayed with the potentiometric indicator TMRM (1nM), and fluorescence (F) was normalized to baseline (Fo). MPT induction was assayed using calcein/mitotracker. Values expressed as mean ± SE (n=3; \*\*p<0.001 compared to control). **RESULTS:** MNNG activated PARP1 by inducing DNA damage. PARP1 hyperactivation led to NAD<sup>+</sup> depletion, and also promoted MMP depolarization (gray bars), MPT induction, and cell death (black bars). These were prevented in PARP1 deficient cells, by PARP1 inhibition (DPQ), or MPT inhibition (CsA). Restoration of intracellular NAD<sup>+</sup> after PARP1 hyperactivation prevented collapse of MMP, MPT induction, and cell death. NAD<sup>+</sup> protection against PARP1-mediated MMP depolarization and cell death was dependent on glucose. NAD<sup>+</sup> did not inhibit PARP1 activation. Treatment with TCA cycle substrates (glutamine (Gln), pyruvate (Pyr), or alpha-ketoglutarate (aKG)) to bypass glycolysis and directly provide substrate to mitochondria, also prevented MMP depolarization and cell death, further suggesting glycolytic failure with PARP1 hyperactivation. **CONCLUSION:** These results indicate that PARP1 hyperactivation leads to glycolytic inhibition, presumably through NAD<sup>+</sup> depletion. This leads to a decrease in substrate availability to mitochondria, which promotes mitochondrial dysfunction and subsequent cell death cascade. Therefore, cellular NAD<sup>+</sup> serves as a key molecular signal for MPT induction and subsequent cell death. **REFERENCES:** [1] Virag and Szabo; *Pharmacol Rev.* 54(3):375-429 (2002) [2] Friberg and Wieloch; *Biochimie* 84(2-3):241-50 (2002) [3] Alano et al, *J Biol Chem*;279(18):18895-902 (2004) (CCA) Supported by VA Merit Grant





## DETECTION OF CORTICAL SPREADING DEPRESSION AND PERI-INFARCT DEPOLARISATIONS IN THE INJURED HUMAN BRAIN

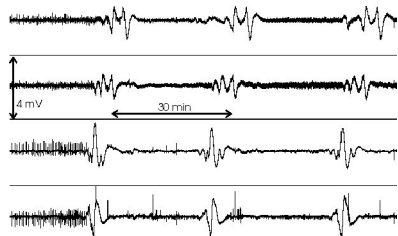
Martin Fabricius<sup>1</sup>, Susanne Fuhr<sup>1</sup>, Robin Bhatia<sup>2</sup>, Martyn Boutelle<sup>3</sup>, Parastoo Hashemi<sup>3</sup>, Anthony J. Strong<sup>2</sup>, Martin Lauritzen<sup>1</sup>

<sup>1</sup>*Glostrup Hospital, University of Copenhagen, Dept. of Clinical Neurophysiology, Glostrup, Denmark*

<sup>2</sup>*Department of Neurosurgery, Kings College, London, UK*

<sup>3</sup>*Department of Chemistry, Kings College, London, UK*

**Introduction:** In animal studies waves of peri-infarct depolarisations (PIDs) propagate from the penumbra region around focal brain lesions into intact brain regions, where they show the characteristics of cortical spreading depression (CSD) {1}. Recurrent PIDs are associated with increases in final infarct volume {2}. Clinical neuroprotection studies using NMDA-receptor antagonists that block CSD and PID have been disappointing. To select patients that may benefit from this treatment, it seems important to detect CSDs and PIDs reliably in man. We reported transient depressions of electrocorticographic activity (ECoG) spreading with a speed similar to experimental CSD, in 5/14 brain injured patients {3}. We have now improved the technique to enable detection of cortical depolarisations: The COSBID study ( [www.cosbid.org](http://www.cosbid.org) ). **Methods:** ECoG was recorded for up to 120 hours from twelve acutely brain-injured human patients by six platinum electrodes placed near foci of damaged cortical tissue. The ECoG was high pass filtered at 0.02 Hz to enable recording of slow potential changes (SPC) of 2-3 minute duration to prove that ECoG depressions were identical to CSD, and to be able to record PIDs in otherwise electrically silent cortical tissue. **Results:** Six patients displayed a total of 49 spontaneous episodes of spreading depression of the ECoG. ECoG depressions were invariably accompanied by stereotyped SPCs (Figure), and spread across the cortex at 3,3 (1,0-10) mm/min (median (range)). The amplitude of the SPCs was 0,1-4,0 mV. In 5/6 patients the ECoG recovered spontaneously. In one patient we recorded recurrent SPCs, but without recovery of the initial ECoG activity (Figure). This may represent the first direct recording of PIDs in acute human brain injury. CSD was recorded in 4/5 patients with traumatic brain injury, and in 2/7 patients with spontaneous cerebral haemorrhages or SAH. **Conclusion:** The spreading ECoG depressions recorded in patients are identical to CSDs recorded in animal experiments. We furthermore provide direct electrophysiological evidence for the existence of PIDs and hence a penumbra in the human brain. We hypothesise that CSDs and PIDs might contribute to the tissue damage in acute brain disorders. **References:** 1. Nilsson et al. *J. Cereb. Blood Flow Metab.* 13:183-192, 1993. 2. Mies et al, *Neuroreport* 4: 709-711, 1993. 3. Strong et al. *Stroke* 33: 2739-2744, 2002.



## CYTOPLASMIC, MITOCHONDRIAL OR ER STRESS RESPONSE AFTER TRANSIENT CEREBRAL ISCHEMIA

Chunli Liu<sup>1</sup>, Jessie Truttner<sup>2</sup>, Shaoyi Chen<sup>1</sup>, Dalton Dietrich<sup>2</sup>, Helen Bramlett<sup>2</sup>, **Bingren Hu**<sup>1</sup>

<sup>1</sup>*Department of Neurology, University of Miami School of Medicine, Miami, FL, USA*

<sup>2</sup>*Department of Neurosurgery, University of Miami School of Medicine, Miami, FL, USA*

Background: Cellular proteins in non-native states, i.e., newly synthesized, misfolded, denatured, or damaged, expose their sticky hydrophobic surfaces, and are highly prone to toxic aggregation. There are several cellular defense systems to cope toxic aggregation of non-native proteins in normal cells. Molecular chaperones can shield hydrophobic surfaces, thereby blocking their toxic aggregation. Irreparably damaged proteins must be quickly eliminated from cells, mostly by the ubiquitin-proteasomal system. Brain ischemia disables ATP-dependent molecular chaperone-assisted folding and ubiquitin-proteasome-mediated degradation, resulting in accumulation of non-native proteins during the postischemic phase. Non-native proteins activate cell defense systems, i.e., cellular stress responses, to induce expression of molecular chaperones, folding enzymes and components of the ubiquitin-proteasomal system during the postischemic phase. There are different signal pathways regulating expression of molecular chaperones residing in the cytoplasm, ER or mitochondria, respectively. This study investigated induction of major chaperones of different cellular compartments in order to figure out in which cellular compartments non-native proteins may be overproduced after brain ischemia. Methods: Fifteen min of transient cerebral ischemia followed by 30 min, 4, 24 h of reperfusion in rats was utilized to investigate induction of major cytoplasmic, ER-luminal, and mitochondrial chaperones, respectively, by in situ hybridization, confocal microscopy and western blot analysis. Results: Major ER luminal chaperones Herp, GRP78, GRP94, calnexin and PDI, major mitochondrial chaperone HSP60, and major cytoplasmic chaperone HSP70 were studied. The most dramatically induced chaperone was HSP70 in the cytoplasm. Mitochondrial chaperone HSP60 was relatively less induced, whereas the ER-luminal stress genes Herp, GRP78 and GRP94 were least induced after ischemia. In addition, induction of cytoplasmic HSP70 was started as early as 30 min of reperfusion, peaked at 4 h and declined thereafter in ischemic surviving neurons, but induction was continuously increased in ischemic vulnerable neurons until the onset of delayed neuronal death after ischemia. Induction of mitochondrial and ER-luminal chaperones was started late, at 4 h of reperfusion, and was seen only in ischemic vulnerable neurons after ischemia. Western blot analysis and confocal microscopy further confirmed that different signaling pathways regulate induction of chaperones in different neuronal compartments after ischemia. Discussion: Induction of molecular chaperones is a common endogenous cellular defense response to stress conditions that lead to cellular overproduction of non-native proteins. Overproduced non-native proteins in the cytoplasm activate cytoplasmic heat-shock transcription factors, thus promoting expression of cytoplasmic stress genes such as HSP70. Whereas overproduced non-native proteins in the ER lumen trigger the ER-stress response via activation of ER membrane-associated transcription factors ATF-6 and Ire-1, thus inducing expression of ER stress genes Herp, GRP78, GRP94, calnexin and PDI. Therefore, activation of either cytoplasmic stress gene or the ER stress gene signaling pathway reflects in which cellular compartments non-native proteins are overproduced. This study suggests that non-native proteins are predominantly overproduced in the cytoplasm, and to a much lesser degree, in the mitochondria and the ER lumen after ischemia. These results support the notion that cytoplasmic non-native proteins may play an important role in delayed neuronal death after brain ischemia. Supported by: NS040407.

**NADPH-DIAPHORASE ACTIVITY AND CB-28KD IMMUNOREACTIVITY IN SPINAL NEURONS OF NEONATAL RATS AFTER A PERIPHERAL NERVE LESION**

**Zahra Fallah**

*Histology Department, Medical School of Artesh University, Tehran, Iran*

Our previous studies have shown that median and ulnar nerve lesion induced calbindin (CB) immunoreactivity in some injured motoneurons in developing rats. Motoneuron death induced by sciatic nerve transection in neonatal rats has been related to induction of neuronal isoform of nitric oxide synthase (nNOS). The present study investigated whether expression of CB and NADPH-d activity, a marker for nNOS is related to the death or survival of forelimb motoneurons in response to axotomy. After median and ulnar nerve transection at either P2 or P7, NADPH-diaphorase histochemistry was performed on cervical spinal cord sections to analyze the induction of nNOS in motoneurons retrogradely labeled with fast blue and immunostained for CB. NADPH-diaphorase reactivity was not detectable in fast blue (FB) labeled motoneurons up to 2 weeks after nerve lesion at P2. However, following nerve lesion at P7, some FB labeled motoneurons showed NADPH-d activity 2 weeks after nerve lesion. These NADPH-d positive motoneurons were not CB immunoreactive. These results are discussed the possible role of nitric oxide and CB in neuroprotection or neurodegeneration. Key words: axotomy, motoneuron, NADPH-diaphorase, calbindin

## SUPEROXIDE CAUSES ENDOPLASMIC RETICULUM DAMAGE AND ACTIVATES APOPTOTIC MACHINERY IN ISCHEMIC NEURONS

Takeshi Hayashi<sup>1</sup>, Pak H. Chan<sup>2</sup>, Guang Jin<sup>1</sup>, Kentaro Deguchi<sup>1</sup>, Shoko Nagotani<sup>1</sup>, Yoshihide Sehara<sup>1</sup>, Hanzhe Zhang<sup>1</sup>, Xiquan Wang<sup>1</sup>, Isao Nagano<sup>1</sup>, Mikio Shoji<sup>1</sup>, Koji Abe<sup>1</sup>

<sup>1</sup>Department of Neurology, Okayama University Graduate School of Medicine and Dentistry, Okayama, Japan

<sup>2</sup>Neurosurgical Laboratories, Stanford University School of Medicine, Stanford, CA, USA

<Background> The endoplasmic reticulum (ER), which plays active roles in apoptosis, is susceptible to oxidative stress. Because superoxide is massively produced in the brain after ischemia, oxidative injury to ER may be implicated in ischemic neuronal cell death. When the ER stress is not so severe, protein synthesis is inhibited, which are attempts to prevent cellular catastrophe. When ER stress is very severe, however, the cells activate the apoptotic machinery. Induction of activating transcription factor-4 (ATF-4) and C/EBP-homologous protein (CHOP) are the features of ER stress-induced cell death. We investigated changes in ATF-4 and CHOP expression after brain ischemia, and compared the results between wild-type (Wt) and superoxide dismutase-1 (SOD1) transgenic (Tg) animals. <Methods> We used two different in vivo ischemia models. We first investigated the effect of Tg SOD1 overexpression on ATF-4 and CHOP expression using a rat global ischemia model, with which ample evidence of ER's active role in neuronal cell death has been obtained. The relationship between superoxide production and ATF-4 induction, as well as ER lipid peroxidation, was confirmed also with this mode. We next used a mouse focal ischemia model, because this model is more akin to human stroke. Using Wt and SOD1 Tg mice, we investigated the ATF-4 and CHOP induction after ischemic injury. <Results> In Wt rat brains after transient global ischemia, ATF-4 and CHOP were increased in the hippocampal CA1 neurons that would undergo apoptosis later. The Tg rats had only a mild increase of these molecules (Fig.1) and minimal neuronal degeneration. Mouse brains after focal ischemia also revealed that SOD1 overexpression reduced ATF-4 and CHOP induction. When superoxide was visualized with ethidium, signals for ATF-4 and superoxide overlapped, which further supported the active role of superoxide in the ER stress. ER lipids were robustly peroxidated in Wt animals but were attenuated in Tg ones (Fig. 2), which indicated that superoxide actually damaged ER membrane. <Conclusion> Our results strongly suggest that oxidative ER damage is implicated in ischemic neuronal cell death, both in the global and focal ischemia models.

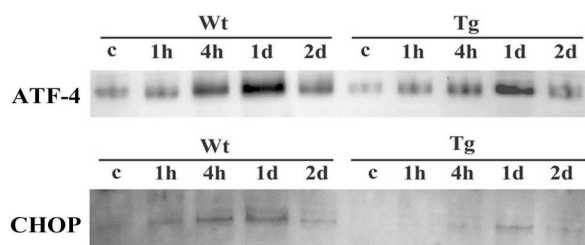


**Fig. 1**  
Western blotting showed that transgenic SOD1 overexpression attenuated ATF-4 and CHOP induction.

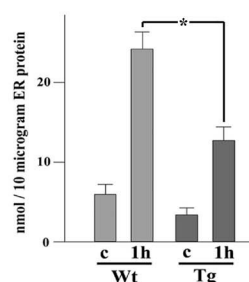


**Fig. 2**  
Change of thiobarbituric acid reactive substances which represent lipid peroxidation. (\*p<.01)

**DIABETES MELLITUS CAUSES ASTROCYTE DAMAGE AFTER ISCHEMIA AND REPERFUSION INJURY**

**Pingan Li**, Chaonan Ding, Marianna Muranyi, Qingping He, Yanling Lin

*Department of Cell Molecular Biology, University of Hawaii, Honolulu, USA*

Diabetes or hyperglycemia exacerbates brain damage induced by ischemia and reperfusion. One factor responsible for this increased damage is enhanced acidosis during ischemia. It has been reported that astrocytes are vulnerable to hypoxia under acidic condition; therefore, astrocytes may also be targets of hyperglycemia. The objectives of the present study are to determine whether hyperglycemia recruits astrocytes during the damage process and whether astrocytes morphological or functional alterations will lead to increased production of inducible NO synthases (iNOS) and NO metabolite, peroxynitrate (ONOO<sup>-</sup>). Streptozotocin-induced 4 weeks diabetic rats subjected to 5 min of forebrain ischemia and followed by 30 min, 6 hrs, 1-, and 3- days of recovery. Astrocyte morphology was studied using GFP immunofluorescent staining and electron microscopy. Productions of iNOS and peroxynitrate were measured by immunohistochemistry and western blot analysis. GFAP immunocytochemistry showed that ischemia activated astrocytes in the cortex and hippocampus as reflected by increased numbers of GFAP positive cells, increased numbers of processes and enlarged cell bodies. The astrocyte activation was observed after 30 min of reperfusion, peaked at 3 days and remained elevated after 7 days reflow. In contrast, with the preexisting diabetic condition, astrocytes were activated after 30 min of reperfusion, however, number of GFAP positive cells significantly reduced after 3 days. Ultrastructural studies revealed that diabetic hyperglycemia caused astrocytic chromatin condensation, nuclear shrinkage and mitochondrial swelling after 1day reperfusion. Western blot analysis demonstrated that while iNOS increased after 6h-3d reperfusion in both diabetic and non-diabetic animals, ONOO<sup>-</sup> increased only in diabetic rats after 3d reperfusion. Because ONOO<sup>-</sup> is produced when NO reacts with superoxide, this results suggest that diabetic hyperglycemia may increase ONOO<sup>-</sup> production by enhancing the formation of superoxide. To test whether was the case, we injected hydroethidine, a marker for in vivo production of superoxide, into the rats before inducing ischemia. After 3 days of recirculation, the animals were sacrificed and brains were sectioned and examined using a confocal laser-scanning microscope at the excitation of 480 nm and emission of 567 nm. The results demonstrated that diabetes enhanced production of superoxide in vivo after ischemia and reperfusion episode. Collectively, these data suggest that astrocytes are targets of hyperglycemic ischemia. Increased production of ONOO<sup>-</sup> and superoxide may play a major role in mediating the detrimental effects of hyperglycemia on cerebral ischemia

**SUBUNIT-SPECIFIC EFFECTS OF NMDA RECEPTOR SIGNALING:  
IMPLICATIONS FOR STROKE**

Yitao Liu<sup>1</sup>, Tak Pan Wong<sup>1</sup>, Michelle Aarts<sup>2</sup>, Lidong Liu<sup>1</sup>, Dongchuan Wu<sup>1</sup>, Jie Lu<sup>1</sup>,  
Michael Tymianski<sup>2</sup>, Yu-Tian Wang<sup>1</sup>

<sup>1</sup>*Brain Research Center, University of British Columbia, Vancouver, BC, Canada*

<sup>2</sup>*Toronto Western Hospital Research Institute, Toronto, ON, Canada*

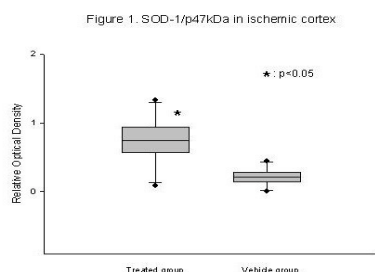
Ischemic brain damage is largely due to excitotoxicity triggered by over-activation of N-methyl-D-aspartate receptors (NMDARs). However, to date none of the NMDAR antagonists have shown therapeutic benefit in clinical trials for stroke. The reasons for this failure are not fully understood. We show here that, in stroke models in vitro and in vivo, blockade of the NR2A-containing NMDARs does not confer neuroprotection, and instead, it results in exacerbation of neuronal death. In contrast, selectively blocking the NR2B-containing NMDAR subtype still attenuates ischemic brain injury. To unravel the mechanisms underlying these opposing effects, we examined the individual role of these two NMDAR subtypes in neuronal fate in mature cortical cultures and found that the NR2A-containing NMDARs mediate neuronal survival while the NR2B-containing counterparts are coupled to neuronal apoptosis. We also showed that NR2A- and NR2B-containing NMDARs co-localize at synaptic (2A:2B~2:1) and extrasynaptic (2A:2B~1:3) sites. The effects of these two NMDAR subtypes on neuronal fate are dependent on the subunit composition rather than the subcellular location. These findings not only provide a molecular basis for why NMDAR antagonists were inefficacious in treating stroke, but suggest that the conventional conception about treatment of ischemic brain damage with NMDAR antagonists may have to be renovated. We propose that a promising strategy for stroke treatment should combine functional enhancement of the NR2A-containing NMDARs with selective suppression of the NR2B-containing counterparts.

## ELECTROCORTICOGRAPHIC EVIDENCE OF DETERIORATING PENUMBRA CONDITIONS ASSOCIATED WITH DELAYED PERI-INFARCT DEPOLARIZATIONS FOLLOWING REPERFUSION IN RAT FOCAL CEREBRAL ISCHEMIA

Jed A. Hartings, Michael L. Rolli, Frank C. Tortella

*Division of Psychiatry and Neuroscience, Walter Reed Army Institute of Research, Silver Spring, MD, USA*

Changes in electroencephalographic (EEG) activity following focal cerebral ischemia include focal slowing, voltage attenuation, and the waxing and waning of stereotyped activities including PLEDs, seizures, and interictal discharges. However, spreading depolarizations (SD), in the form of cortical spreading depression or peri-infarct depolarizations, are the dominant electrophysiologic events after middle cerebral artery occlusion (MCAo), occurring not only during ischemia but also in a 'secondary phase' throughout the period of infarct maturation 8-24 h post-ischemia. Here we study manifestations of SDs in electrocorticographic (ECoG) patterns to investigate ECoG diagnostics of depolarization events and characterize effects of secondary phase, post-reperfusion depolarizations. Monopolar ECoG signals were recorded continuously from epidural, non-polarizable electrodes during 2 h of MCAo and 22 h reperfusion in freely behaving rats. Recordings were made frontal and parietal electrodes adjacent to the presumed 'penumbra'. Signals were amplified for recording of DC potential and traditional AC-coupled ECoG (0.5-50 Hz band pass). During 2 h MCAo, ECoG amplitude was suppressed relative to baseline. Brief (mean: 72 sec) seizures and SDs (mean: 14 events) recurred frequently but without temporal relationship to each other. During SD, ECoG amplitude remained constant, indicating penumbral conditions (Figure, top). Following reperfusion, seizures and SDs ceased, ECoG amplitude recovered, and over the next several hours pathologic delta waves (polymorphic delta activity and PLEDs) dominated the ECoG with progressively increasing amplitude. After a variable period (4-12 h), the ECoG amplitude decreased dramatically in association with the onset of a prolonged repetitive series of depolarizations (mean: 58 events). Initial depolarizations in this phase produced transient depressions of the high amplitude ECoG signal (Figure, middle). After several repetitive depolarizations, however, the ECoG became permanently depressed, with no further transient depressions during subsequent depolarizations (Figure, bottom). These results were confirmed with bipolar ECoG recordings from penumbral regions. Finally we show that depolarizations could be detected in baseline shifts of the AC-ECoG signal with a low (0.03 Hz) high-pass cutoff setting. Baseline shifts signalled the derivative of the DC potential. The progressive decrement and then permanent depression of the ECoG caused by secondary phase SDs evidences deleterious effects of post-reperfusion depolarizations, and likely the progressive recruitment of penumbral and/or core-infarcted tissue. Furthermore, the lack of transient ECoG depression during SD in this period demonstrates penumbral conditions and suggests that depolarizations can be manifested as 'peri-infarct depolarizations' even following reperfusion.





**ACUTE AMYLOID-BETA, CEREBRAL PENETRATING ARTERIOLES AND OXYGEN RADICAL****Hans H. Dietrich***Department of Neurosurgery, Washington University, St.Louis, MO, USA*

Amyloid-beta (Ab) is the hallmark peptide deposited in amyloid plaques found in Alzheimer's disease. Ab is primarily and continuously produced by astroglia with nano-molar concentrations in the cerebro-spinal fluid (CSF). However, after head trauma, an Ab increase in the CSF into the micro-molar range was observed. The effect of such increased concentrations of Ab on the cerebral micro-vasculature is not known. Methods: Rat cerebral penetrating arterioles were cannulated, pressurized to 60 mmHg and observed at 37C in vitro. After development of spontaneous tone and viability testing, freshly dissolved amyloid-beta40 (Ab40) was added (1 nM to 1uM) and the vessel diameter change measured. Dose response to Adenosine tri-phosphate (ATP, 1pM to 10 uM) before and after Ab40 (100 nM) was observed. In cell cultures of rat cerebral microvascular endothelial (RCMEC) and smooth muscle cells (RCMSMC), we measured oxygen radical production with MitoTracker red. Results: Ab40 dose-dependently constricted penetrating arterioles by ~25%, decreased dilation to low concentrations of ATP and enhanced transient ATP-induced constriction. Ab40 dose dependently increased fluorescence in RCMEC and RCMSMC, which was dose-dependently inhibited by MnTBAP (O<sub>2</sub>- and peroxynitrite scavenger), but not by superoxide dismutase or catalase. Conclusion: Acute Ab40 directly affects cerebral arterioles. Increased Ab40 after head trauma may lead to arteriolar constriction and reduced dilatory response to ATP, contributing to local hypoperfusion. Production of oxygen radical, O<sub>2</sub>- and/or peroxynitrite, may be one mechanism involved in the Ab40 effects observed. Supported by NIH RO1 NS30555, NIH P50 AG05681 and ADRC Washington University.

**DOES TISSUE PLASMINOGEN ACTIVATOR MEDIATE NEUROGENENERATION  
IN THE 1-METHYL-4-PHENYL-1, 2, 3, 6- TETRAHYDROPYRIDINE (MPTP)  
MOUSE MODEL OF PARKINSON'S DISEASE?**

**Gabriel T. Liberatore**<sup>1,2</sup>, Swee Jin Mok<sup>2</sup>, Kate Sidon<sup>2</sup>, David W. Howells<sup>1,2</sup>

<sup>1</sup>*National Stroke Research Institute, Heidelberg, Victoria, Australia*

<sup>2</sup>*Department of Medicine, University of Melbourne, Austin Health, Heidelberg, Victoria, Australia*

Introduction: Microglial activation is implicated as a mediator of dopaminergic degeneration in the substantia nigra. In other systems, tissue plasminogen activator (t-PA) may play a central role in mediating microglial induced neuronal degeneration possibly by damaging the extra-cellular matrix or activation of glutamatergic excitotoxicity by cleavage of the NR1 subunit of the NMDA receptor. Importantly, t-PA is produced at high levels in the substantia nigra pars compacta of wild-type mice. Our aim was to examine whether transgenic mice lacking t-PA were protected against the effects of the dopaminergic neurotoxin 1-methyl-1,2,3,6-tetrahydropyridine (MPTP). Methods: Cohorts of 9 male C57Black/6J mice and t-PA<sup>-/-</sup> mice (25-30g) received four 20mg/kg i.p. injections of MPTP at 2-hour interval. Control mice and t-PA<sup>-/-</sup> mice received injections of saline alone. One week after the animals were sacrificed under pentobarbital anaesthesia by perfusion-fixation and sections through the substantia nigra collected for counting of total and dopaminergic neuron numbers, microglia and astrocytes. The density of dopaminergic innervation of the striatum was determined by tyrosine hydroxylase immunohistochemistry. Results: The t-PA<sup>-/-</sup> mice started with 30% ( $p < 0.001$ ) fewer dopaminergic neurons than wild-type controls however dopaminergic innervation of the striatum was maintained. In wild type animals, MPTP caused a 42% ( $p < 0.001$ ) loss of dopaminergic neurons and marked terminal loss in the striatum (52%,  $p < 0.01$ ). The nigral dopaminergic neurons of t-PA<sup>-/-</sup> mice were not killed in significant numbers by MPTP but despite this insensitivity, striatal terminal loss was marked (63%,  $p < 0.001$ ). MPTP-treated wild-type mice showed a marked astrogliosis (9 fold,  $p < 0.001$ ) that was not seen in the MPTP treated t-PA<sup>-/-</sup> mice. The nigras of t-PA<sup>-/-</sup> mice contained only ~3% ( $p < 0.001$ ) of the microglial population seen in wilt-type mice. Conclusions: t-PA<sup>-/-</sup> mice exhibit a developmental loss of dopaminergic neurons and these cells are relatively insensitive to the effects of MPTP. Microglial numbers were reduced and the normal astroglial response to MPTP was greatly attenuated.

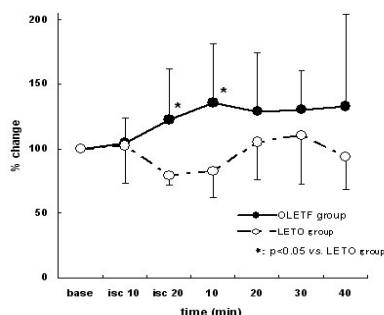
## PRODUCTION OF NITRIC OXIDE IN A DIABETIC ANIMAL MODEL (OLETF) DURING FOREBRAIN ISCHEMIA AND REPERFUSION

Tomokazu Shimazu, Nobuo Araki, Tsuyoshi Ohkubo, Yoshio Asano, Masahiko Sawada, Daisuke Furuya, Harumitsu Nagoya, Masamizu Yamazato, Yasuo Ito, Yuji Kato, Kunio Shimazu

*Department of Neurology, Saitama Medical School, Saitama, Japan*

**Introduction:** Hyperglycemia during acute cerebral ischemia is associated with poor prognosis. As we had already clarified the change in nitric oxide (NO) production during cerebral ischemia and reperfusion, we investigated the cerebral NO production in Otsuka Long Evans Tokushima Fatty (OLETF) rats, an animal model of obesity and type 2 diabetes. **Methods:** Male OLETF rats (n=4), 500-580g in weight and male Long-Evans Tokushima Otsuka (LETO) rats (control group, n=6), 490-530g in weight, were anesthetized by intraperitoneal injection of pentobarbital sodium. NO production was continuously monitored by in vivo microdialysis. Microdialysis probes were inserted into the left striatum and hippocampus and were perfused with Ringer's solution at a constant rate 2 $\mu$ l/min. Laser Doppler probes were also inserted into the right striatum and hippocampus. Blood pressure, blood gases and temperature were monitored and maintained within normal ranges throughout the procedure. After 2 hours equilibrium period, fractions were collected every 10 minutes. Forebrain cerebral ischemia was produced by occlusion of both common carotid arteries, and systemic hypotension (MABP < 50mmHg) was induced by hemorrhage. After 20 minutes, the loops around both common carotid arteries were released and the blood was re-infused. Levels of NO metabolites, nitrite (NO<sub>2</sub><sup>-</sup>) and nitrate (NO<sub>3</sub><sup>-</sup>), in the dialysate were determined using the Griess reaction. **Results:** (1) Blood Pressure: There was no significant difference between OLETF group and LETO group. (2) Cerebral Blood Flow (CBF): The OLETF and LETO animals with forebrain ischemia did not differ significantly in CBF during cerebral ischemia and reperfusion. (3) Nitric oxide: Baseline, the OLETF animals had a total nitric oxide level of 1.55  $\pm$  0.39  $\mu$ mol/l (mean  $\pm$  SD) in hippocampus, which was significantly lower than that in hippocampus of the LETO animals (2.30  $\pm$  0.61  $\mu$ mol/l) (P < 0.05). During cerebral ischemia and 10 minutes after the start of reperfusion, the NO<sub>2</sub><sup>-</sup> level showed significantly higher in hippocampus in OLETF rats (124.7  $\pm$  44.0 % and 130.3  $\pm$  57.2 %) than that of control LETO rats (77.5  $\pm$  13.0 % and 71.1  $\pm$  19.5 %). During cerebral ischemia and after reperfusion, the level of total NO in hippocampus of OLETF rats (122.4  $\pm$  39.5 % and 135.5  $\pm$  45.7 %), was significantly higher than that of control LETO rats (79.3  $\pm$  7.4 % and 82.6  $\pm$  20.4 %) (Fig.1). While, in striatum there was no significant difference in either NO<sub>2</sub><sup>-</sup> or NO<sub>3</sub><sup>-</sup> or total NO between the OLETF and LETO groups. **Conclusion:** These data suggest that the hippocampal baseline of the NO production in OLETF rats as type 2 diabetic animal model is lower than that of non-diabetic animals. These in vivo data also suggest that hyperglycemia influences on the NO production in hippocampus, and the activity of brain NO synthase may be more enhanced in diabetic rats following cerebral ischemia.

Figure. 1 The Level of total NO in Hippocampus





**SEIZURE-INDUCED NEURONAL NECROSIS WITH INTERNUCLEOSOMAL DNA CLEAVAGE IS CASPASE-INDEPENDENT****Denson G. Fujikawa<sup>1,2,3</sup>, Rosen B. Trinidad<sup>1</sup>, Xingrao Ke<sup>4</sup>**<sup>1</sup>*VA Greater Los Angeles Healthcare System, North Hills, CA, USA*<sup>2</sup>*Department of Neurology, UCLA Geffen School of Medicine, Los Angeles, CA, USA*<sup>3</sup>*Brain Res. Institute, UCLA, Los Angeles, CA, USA*<sup>4</sup>*Department of Pediatrics, University of Utah School of Medicine, Salt Lake City, UT, USA*

**Objective:** Our objective was to determine if either caspase-9 or caspase-8, upstream cysteine proteases in the intrinsic mitochondrial and Fas death receptor extrinsic caspase-dependent pathways respectively, is activated following lithium-pilocarpine-induced status epilepticus (LPCSE). **Background:** Seizure-induced neuronal death is morphologically necrotic, but involves programmed processes such as internucleosomal DNA cleavage (DNA laddering). It is controversial whether caspase-dependent pathways are activated following SE. We have shown that caspase-3, the central downstream executioner caspase in both pathways, is not activated by LPCSE, but the lack of downstream activation of caspase-3 does not rule out initial activation of either pathway. **Methods:** Adult male Wistar rats were given lithium chloride, 3 mEq/kg i.p. The next day they received either pilocarpine, 30-60 mg/kg i.p., or saline i.p. After 3 h of LPCSE, diazepam (10 mg/kg) and phenobarbital (25 mg/kg) were given i.p. to control rats or to stop the seizures. Rats recovered for 6 or 24 h, after which they were killed with pentobarbital, and their brains were removed and dissected into the six brain regions we have shown exhibit necrotic neurons and DNA laddering: dorsal and ventral hippocampus, amygdala and piriform cortex, entorhinal cortex and neocortex. The thymuses of rats given saline or methamphetamine (MAP) were used as negative and positive controls for caspase-8 and -9 activation, by IETD-AFC and LEHD-AFC cleavage assays for enzyme activity respectively (n=3 in each group), and by assessing immunoreactivity for active caspase-9 and caspase-8. Enzyme activity assays and immunohistochemistry were also performed on the six brain regions (pooled from 4 brains) of control and SE rats with 6 h and 24 h recovery periods. The enzyme activity data was analyzed with 3-factor, repeated-measures ANOVA and post-hoc t-tests. **Results:** The thymuses of rats given MAP 8 h previously showed an 8-fold elevation of LEHD-AFC (caspase-9) activity compared to saline-treated control thymuses (0.0248 0.0183 vs. 0.194 0.0418 units/g protein, mean SEM, p<0.05), but no increase in IETD-AFC (caspase-8) activity (0.0979 0.00814 vs. 0.159 0.0264 units/g protein, p=0.09). There was no difference between the control and SE groups in either LEHD-AFC or IETD-AFC activity in the six brain regions at either 6 h or 24 h following SE (0.0138 0.00925 vs. 0.00502 0.00226 units/g protein for LEHD-AFC activity in amygdala-piriform cortex, e.g., at 24 h [p=0.99]). Thymus tissue showed active caspase-9 immunoreactivity but no caspase-8 immunoreactivity. None of the six brain regions in control and SE groups showed active caspase-9 or caspase-8 immunoreactivity 6 h or 24 h after SE. **Conclusions:** Neither caspase-8 or caspase-9 is activated following LPCSE, further evidence that seizure-induced neuronal necrosis with DNA laddering is a caspase-independent programmed process.

## EXPRESSION OF GLUTATHIOLATED PROTEIN FOLLOWING TRAUMATIC BRAIN INJURY IN RATS

Hiroshi Nawashiro<sup>1</sup>, Hidetoshi Ooigawa<sup>1</sup>, Akiko Yano<sup>1</sup>, Namiko Nomura<sup>1</sup>,  
Hirotaka Matsuo<sup>2</sup>, Katsuji Shima<sup>1</sup>, Koji Uchida<sup>3</sup>

<sup>1</sup>*Department of Neurosurgery, National Defense Medical College, Tokorozawa, Japan*

<sup>2</sup>*Department of Physiology, National Defense Medical College, Tokorozawa, Japan*

<sup>3</sup>*Graduate School of Bioagricultural Sciences and Institute for Advanced Research, Nagoya University, Nagoya, Japan*

**Introduction:** Reactive oxygen species are thought to play an important role in traumatic brain injury (TBI). The transient incorporation of glutathione into cellular proteins is an established response to oxidant stress and could provide a mechanism for reversible covalent modification in response to reactive oxygen species. This is the first report concerning the expression of glutathiolated protein (GP) following TBI in rats. The aim of the present study is to elucidate the distribution of GP in the normal rat brain, and after TBI induced by lateral fluid percussion. **Materials and methods:** Adult male Sprague-Dawley rats (300-400 g) were subjected to lateral fluid percussion injury of moderate severity (3.5-4.0 atm) using the Dragonfly device model. Dr. K. Uchida generated the antibody against GP. The details of antibody will be provided (manuscript in preparation). Topographic distribution of immunoreactivity for GP was examined using immunohistochemistry. GP levels were also quantified using Western blot analysis. Double immunostaining using anti-GFAP or anti-rBAT antibody with GP was performed. **Results:** In the normal rat brain, GP immunoreactivity was observed in neuronal cell bodies and neuropil, whereas nuclei of the neurons were faintly stained. Astrocytes were moderately immunoreactive for GP. Perivascular staining was also noted. Increased GP immunoreactivity 3 days after TBI was observed especially in astrocytes. The reduced glutathione molecule consists of three amino acids - glutamic acid, glycine and cysteine. rBAT (related to b(0,+)-amino acid transporter) is the heavy chain of the cysteine transporters in the brain. Following TBI, numerous cells immunopositive for GP also presented rBAT immunoreactivity. **Conclusion:** These results indicate that GP might play some role after traumatic brain injury. The up regulation of rBAT might correlate with increased GP immunoreactivity in astrocytes after traumatic brain injury.

**ENDOPLASMIC RETICULUM STRESS INDUCED BY SPINAL CORD ISCHEMIA IN RABBITS: INDUCTION OF GRP78 AND CASPASE12 IN MOTOR NEURONS****Masahiro Sakurai<sup>1</sup>, Koji Abe<sup>2</sup>, Yasuto Itoyama<sup>3</sup>, Koichi Tabayashi<sup>4</sup>**<sup>1</sup>*Department of Cardiovascular Surgery, National Hospital Organization Sendai Medical Center, Sendai, Japan*<sup>2</sup>*Department of Neurology, Okayama University Graduate School of Medicine, Okayama, Japan*<sup>3</sup>*Department of Neurology, Tohoku University Graduate School of Medicine, Sendai, Japan*<sup>4</sup>*Department of Cardiovascular Surgery, Tohoku University Graduate School of Medicine, Sendai, Japan*

Objective: The mechanism of spinal cord injury has been thought to be related to the vulnerability of spinal motor neuron cells against ischemia. However, the mechanisms of such vulnerability are not fully understood. Because we previously reported that spinal motor neurons were lost probably by programmed cell death, and it has been appreciated that several cell death-inducing pathways are set in motion subsequent to the cellular stress that affects ER, collectively known as ER stress. Therefore, we investigated a possible mechanism of neuronal death by immunohistochemical analysis for Grp78 and caspase12. Methods: We used a rabbit spinal cord ischemia model with use of a balloon catheter. The spinal cord was removed at 8 hours, 1, 2, or 7 days after 15 min of transient ischemia (n = 5, each time point), and histological changes were studied with hematoxylin-eosin staining. Western blot analysis for Grp78 and caspase12, temporal profiles of Grp78 and caspase12 immunoreactivity, and double-label fluorescence immunocytochemical studies were performed. Results: The majority of motor neurons were preserved until 2 days, but were selectively lost (about 70%) at 7 days of reperfusion. Western blot analysis revealed scarce immunoreactivity for Grp78 and caspase12 in the sham-operated spinal cords. However, they became apparent at 8 hours after transient ischemia (p < 0.0001), which returned to the baseline level at 1 day (p < 0.0001). Double-label fluorescence immunocytochemical study revealed that both Grp78 and caspase12 were positive at 8 hours of reperfusion in the same motor neurons which eventually die. Conclusion: This study demonstrated that immunoreactivities for both Grp78 and caspase12 were induced in the same motor neuron which eventually die. These results suggest that endoplasmic reticulum stress were induced in motor neurons by transient spinal cord ischemia in rabbits.

## References:

1. Sakurai M, Nagata T, Abe K, Horinouchi T, Itoyama Y, Tabayashi K. Survival- and death promoting events after transient spinal cord ischemia in rabbits: induction of Akt and caspase3 in motor neurons. *J. Thorac. Cardiovasc. Surg.* 2003; 125: 370-377.
2. Shibata M, Hattori H, Sasaki T, Gotoh J, Hamada J, Fukuuchi Y. Activation of caspase-12 by endoplasmic reticulum stress induced by transient middle cerebral artery occlusion in mice. *Neuroscience.* 2003; 118: 491-9.
3. DeGarcia DJ, Kumar R, Owen CR, Krause GS, White BC. Molecular pathway of protein synthesis inhibition during brain reperfusion: implication for neuronal survival or death *J Cereb. Blood Flow Metab.* 2002; 22: 127-141.

**SPREADING DEPRESSION (SD) WAVES IN THE BRAINSTEM CAN BE ELICITED AFTER BLOCKADE OF POTASSIUM CHANNELS – EVIDENCE FOR THE ROLE OF EXTRACELLULAR POTASSIUM IONS AS A DRIVING FORCE?****Frank Richter<sup>1</sup>, Alfred Lehmenkühler<sup>2</sup>, Hans-Georg Schaible<sup>1</sup>**<sup>1</sup>*Friedrich Schiller University, Institute of Physiology/Neurophysiology, Jena, Germany*<sup>2</sup>*Center for Pain Therapy, St. Vincent Hospital, Duesseldorf, Germany*

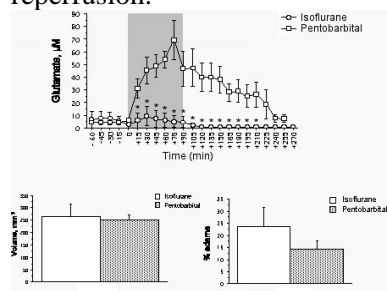
SD waves can be elicited by KCl but not by pricking in the brainstem of rats younger than 13 days after acetate conditioning whereas this protocol failed to elicit SDs in the brainstem of older or adult rats (J. Neurophysiol. 90, 2003, 2163-70). In the past, we have shown that the blockade of neither N-, nor L- and T-, nor P/Q-type calcium channels interfered with the occurrence of brainstem SD waves. Even after blockade of NMDA receptors SD waves could still be elicited in the immature brainstem. These findings raised the issue whether potassium ions ( $[K^+]_e$ ) according to Grafsteins hypothesis could ignite and propagate SDs in the brainstem irrespectively from the above-mentioned channels and receptors. To test this we recorded SD-related DC deflections and changes in  $[K^+]_e$  with ion-selective microelectrodes based on valinomycin (FLUKA 60031) in the brainstem of urethane-anesthetized rats (1.5 g/kg, i.p.) aged 11-14 days, and in the brainstem of sodium-thiopental (100 mg/kg, i.p.) anesthetized adult rats. Two pipettes were glued together spanning horizontally over 400  $\mu\text{m}$  to observe propagation of SDs across the brainstem and were inserted into a region close to the trigeminal nucleus. For acetate conditioning the brainstem was superfused with warmed, carbogen-equilibrated artificial cerebrospinal fluid (ACSF) in which 75 % of the chloride was replaced by sodium acetate.  $K^+$ -channels were either blocked by 10 mM tetraethylammonium chloride (TEA) or by 1 mM barium chloride ( $\text{BaCl}_2$ ). After testing for SD by applying a KCl crystal to the surface of the non-conditioned brainstem, the brainstem was superfused for a period of 20 min with acetate-ACSF containing the  $K^+$ -channel blocker. Then KCl was applied again to elicit SD, and after either a waiting time of 5 min or after a SD wave superfusion with the blocking solution was continued for another 20 min. In immature rats usually 3 sequences of acetate-ACSF containing TEA or  $\text{BaCl}_2$  were given, in adult rats up to 6 sequences.  $\text{BaCl}_2$  did not interfere with brainstem SDs in 11 to 12-day old rats. They were unchanged in amplitudes and shape (DC deflections up to 15 mV, increases in  $[K^+]_e$  up to 55 mM). TEA was also without immediate effect, but after 20 min superfusion a continuously increasing negative deflection of the DC potential was observed that was in some rats accompanied by spontaneously and repetitively occurring SDs. The concomitant elevations in  $[K^+]_e$  did not differ from those of SDs without TEA, but the  $[K^+]_e$  remained elevated after the SD (2-4 mM compared to previous values per 20 min superfusion) and did not return to initial values. Interestingly, we were able to elicit SD even in the brainstem of 14-day-old or adult rats with the same TEA-acetate preparation. We conclude that i) blockade of potassium channels allows KCl-induced SD to occur in the brainstem even in adult animals probably via increased neuronal excitability due to an reduced resting potential. ii) Since KCl was still able to induce SDs after blockade of potassium channels,  $K^+$  ions could drive those SDs by moving through non-specific cation-channels.

## EFFECTS OF ISOFLURANE ON THE ISCHEMIA-INDUCED RELEASE OF EXCITATORY AMINO ACIDS, BRAIN SWELLING AND INJURY IN A MODEL OF TRANSIENT ISCHEMIA IN RATS

Marie-Françoise Ritz, Petra Schmidt, Aminadav Mendelowitsch

*Department of Research University Hospital Basel, Basel, Switzerland*

**Introduction:** The volatile anesthetic agent isoflurane was thought to provide neuroprotection against ischemic damage, however, this effect remains controversial. **Material and Methods:** In this study, we compared the efflux of several excitatory amino acids such as glutamate and taurine, brain tissue injury and brain swelling in male rats subjected to 90 minutes ischemia followed by 24 hours of reperfusion. These rats were anesthetized either with pentobarbital (50 mg/kg, ip), or with isoflurane (1.5% in a mixture of 70% N<sub>2</sub> - 30% O<sub>2</sub> via a nose mask). Using the middle cerebral artery transient occlusion (MCAO) model, combined with intracerebral microdialysis, we monitored the variations of glutamate and taurine concentrations in the extracellular space before occluding the MCA, during the occlusion period and during the first 3 hours of reperfusion. At the end of the reperfusion period, the ischemic damage and brain water content were evaluated by immunohistological staining of the brains using anti-MAP-2 antibodies. **Results:** Isoflurane completely prevented the dramatic efflux of glutamate observed during occlusion in rats anesthetized with pentobarbital, and slightly reduced the ischemia-induced release of taurine. However, no difference in the size of the brain lesion was observed between both anesthetics, but isoflurane induced the formation of a bigger brain edema. **Conclusions:** These results suggest that, although isoflurane inhibits the release of the majorexcitotoxic neurotransmitter glutamate during ischemia, this agent does not efficiently protect the brain against ischemic damage. Moreover, it may exaggerate ischemia-induced brain swelling, by decreasing taurine release during ischemia. Blocking the excitotoxic pathway during ischemia may be necessary but does not seem to be sufficient to efficiently improve brain outcome after ischemia-reperfusion.



**CONCENTRATION DEPENDENT EFFECTS OF ESTROGEN AND PROGESTINS  
ON CELL DEATH IN CORTICAL CULTURES****Doug Lobner, Julie Hjelmhaug, Abed K. Salous***Department of Biomedical Sciences, Marquette University, Milwaukee, WI, USA*

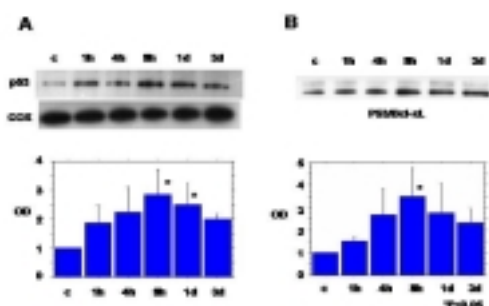
Estrogen has been shown to be neuroprotective both in vitro and in vivo. However, the concentration of estrogen used has often been non-physiological. Therefore, we characterized the effects of a wide range of estrogen (17 $\beta$ -estradiol) concentrations (from 1 nM to 10  $\mu$ M) on neuronal death in cortical cultures. The effects of estrogen were tested on apoptotic death induced by exposure to serum deprivation or nifedipine, and on necrotic death induced by exposure to iron, buthionine sulfoximine (BSO), NMDA, or kainate. Estrogen was protective at  $\mu$ M concentrations against iron, BSO, and kainate toxicity. At these concentrations estrogen acted as a free radical scavenger as measured by inhibition of BSO induced oxidative stress assayed by dichlorofluorescein (DCF) fluorescence. The only effect observed at a physiological concentration of estrogen (10 nM) was potentiation of NMDA toxicity. This effect of estrogen was associated with increased NMDA stimulated calcium influx. The potentiation of cell death and increased calcium influx were both blocked by the estrogen receptor antagonist, ICI 182,780. The protective effects of high concentration estrogen were not blocked by ICI 182,780, in fact, ICI 182,780 enhanced the protection, suggesting that a damaging effect of estrogen receptor activation was masked by a protective non-receptor effect. These results indicate a lack of protective effects by physiological concentrations of estrogen, and raise the concern that physiological concentrations of estrogen may potentiate neuronal injury. In contrast to the effects of estrogen, progesterone was protective against NMDA toxicity at a physiological concentration (10 nM). However, the synthetic progestin, medroxyprogesterone, commonly used for hormone replacement therapy, was only protective at a high concentration (10  $\mu$ M). Since hormone replacement therapy typically involves the use of both an estrogen and a progestin further study of various estrogens and progestins, both alone, and in combination, are necessary.

## MITOCHONDRIAL TRANSLOCATION OF P53 FOLLOWING TRANSIENT GLOBAL ISCHEMIA IN RATS

Hidenori Endo, Hiroshi Kamada, Chikako Nito, Tatsuro Nishi, Pak H. Chan

*Department of Neurosurgery, Department of Neurology and Neurological Sciences, and Program in Neurosciences, Stanford University School of Medicine, Stanford, CA, USA*

**Introduction:** The mechanism of p53-mediated apoptosis after cellular stress remains unclear. p53 can mediate apoptosis by transcriptional activation of proapoptotic genes like the BH3-only proteins Noxa and Puma, Bax, p53 AIP1, Apaf-1, and PERP. In addition, evidence for transcription-independent p53-mediated apoptosis has been accumulating. Release of cytochrome c from mitochondria to the cytosol is a critical step in apoptotic cell death. Recent studies have shown that the p53 protein can directly induce permeabilization of the outer mitochondrial membrane by forming a complex with the protective Bcl-xL protein, resulting in cytochrome c release. However, the mitochondrial p53 pathway remains unclear in the death of vulnerable hippocampal CA1 neurons after transient cerebral ischemia. **Materials and methods:** To examine the p53 mitochondrial pathway following ischemia-reperfusion injury, we used a transient global cerebral ischemia (tGCI) model in rats (1, 2). After 1, 4, 8, 24, and 72h of reperfusion, samples were taken from the hippocampal CA1 subregion to extract protein from the mitochondrial fraction, and used for Western blot and immunoprecipitation analysis. To examine the effects of p53, an inhibitor, 2-(2-lmino-4, 5, 6, 7-tetrahydrobenzothiazol-3-yl)-1-p-tolyethanone hydrobromide (pifithrin  $\alpha$ ), was administered intravenously. **Results:** Western blot analysis of the mitochondrial fraction showed p53 gradually increased in a time-dependent manner after tGCI, which means ischemia-reperfusion injury induces translocation of p53 to mitochondria (Fig. A). Pifithrin  $\alpha$  had no effect on p53 mitochondrial translocation after ischemia. We did a coimmunoprecipitation study to investigate the change in p53 binding with Bcl-xL or Bcl-2. This analysis for p53 immunoreactivity precipitated by Bcl-xL or Bcl-2 in the mitochondrial fraction revealed that p53/Bcl-xL binding, but not p53/Bcl-2 binding, gradually increased in a time-dependent manner after the tGCI (Fig. B), indicating that p53 bound to Bcl-xL in mitochondria in hippocampal CA1 neurons that were subsequently destined to die 3 days later. **Conclusions:** In this study, we demonstrated that p53 translocates to mitochondria and binds to Bcl-xL after tGCI. Mitochondrial translocation of p53 and protein interaction between p53 and Bcl-xL might induce release of cytochrome c from mitochondria to the cytosol, resulting in delayed hippocampal CA1 neuronal cell death. We suggest that this is a novel mechanism underlying the convergence of cell death pathways involving both p53 and antiapoptotic proteins in promoting neuronal apoptosis in vulnerable CA1 neurons after cerebral ischemia. **References:** (1) Sugawara T et al.; J Neurosci 22(1):209-17, 2002 (2) Sugawara T et al.; J Neurosci 19(22):RC39 (1-6), 1999 **Grant Support:** Supported by National Institutes of Health grants p50 NS14543, RO1 NS25372, RO1 NS36147, and RO1 NS 38653, and an American Heart Association Bugher Foundation award.





## INCREASED OXIDATIVE BIOMARKER IN PLASMA REFLECTS THE CEREBRAL OXIDATIVE DAMAGE IN RATS

Keiko T. Kitazato<sup>1</sup>, Hao Liu<sup>1</sup>, Masaaki Uno<sup>1</sup>, Atsuhiko Suzue<sup>1</sup>, Kyoko Nishi<sup>1</sup>, Shinji Manabe<sup>1</sup>, Hiroyuki Yamasaki<sup>1</sup>, Yuichi Takahashi<sup>1</sup>, Hiroyuki Itabe<sup>2</sup>, Shinji Nagahiro<sup>1</sup>

<sup>1</sup>*Department of Neurosurgery Institute of Health Biosciences, The University of Tokushima Graduate School, Tokushima, Japan*

<sup>2</sup>*Department of Biological Chemistry, School of Pharmaceutical Sciences, Showa University, Tokyo, Japan*

**Background and Purpose-** Oxidative stress contributes to post-ischemic brain damage. There is a time lag between the oxidative brain damage and the neuronal cell death and the part of the oxidative damaged cells have been considered to be salvageable. If we can predict the oxidative brain damage using plasma biomarkers, it would be useful to detect patients with the salvageable cells. Previously, we first demonstrated that plasma oxidized low-density lipoprotein (OxLDL) increased in the patients with acute cerebral infarction. However, whether plasma biomarker reflects the cerebral oxidative damage remains unclear. In this study, we assessed the correlation between plasma 8-hydroxy-2'-deoxyguanosine (8-OHdG), as a marker of oxidative DNA damage and progressive brain damage in rats subjected to transient and permanent ischemia. Furthermore, we monitored the change of the plasma 8-OHdG and OxLDL in patients with hypothermia. **Methods-** Male wistar rats were subjected to permanent-, 0.5-, 1-, 2-h MCAO. At various times thereafter, the infarct volume, 8-OHdG levels in plasma and brain tissue, DNA fragmentation, and immunohistochemical observations on their brains were recorded and compared. Plasma OxLDL levels were determined by ELISA using DLH3, anti-oxidized phosphatidylcholine antibody. **Results-** At 12 h after 2-h MCAO-reperfusion, the infarct volume was increased; it peaked at 24-72 h. 8-OHdG-containing cells in the cortical infarct border zone and penumbra were observed at 12 h, the number of 8-OHdG-positive cells was highest at 24 h and they co-localized with DNA single-strand breaks (SSB) indicating apoptosis cells only within infarct border. SSB positive cells were expansively observed from the caudate putamen into the cortical region at 6-12 h and highest in the cortical region at 72 h; it was consistent with DNA degradation. Plasma 8-OHdG significantly increased at 12 h, and peaked at 24 h after reperfusion ( $1.1 \pm 0.7$  ng/mL (mean  $\pm$  SD); controls  $0.3 \pm 0.1$ ;  $p < 0.01$ ); this increase was in step with increased cortical infarct volume, and reflected immunohistochemical findings in the cortical region but not the caudate putamen. These findings indicate that the increased plasma 8-OHdG in acute phase after MCAO-reperfusion reflects the cortical oxidative damage and precedes the cortical neuronal cell death. In the permanent MCAO model, plasma 8-OHdG levels were associated with the brain contents of 8-OHdG. Plasma 8-OHdG was lower in the 0.5- and 1-h than 2-h MCAO model in consistent with the cortical infarct volume size, suggesting that it corresponds to the severity of the oxidative cortical damage. During hypothermia, patients with cortical infarction had the decreased OxLDL and 8-OHdG levels in their plasma. However, in step with rewarming both markers transiently increased. This finding suggests that the oxidative markers could be served the monitoring of the treatment of acute cerebral infarction. **Conclusions-** Our findings indicate that oxidative markers in plasma may be an indicator of oxidative brain damage in acute cerebral infarction and increased plasma marker predict the presence of the penumbra as well as the cortical infarct.

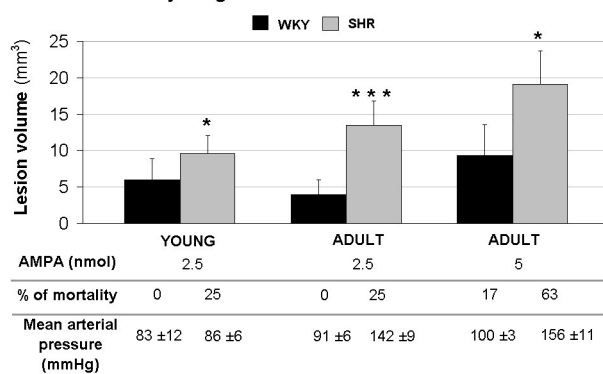
## AMPA BUT NOT NMDA RECEPTORS STIMULATION INDUCES AN EXACERBATED BRAIN LESION IN SPONTANEOUSLY HYPERTENSIVE RATS

Clotilde Leblond, Julien Chuquet, Eric T. MacKenzie, Omar Touzani

UMR CNRS 6185, Université de Caen, Centre Cyceron, France

**Introduction:** It is well known that chronic arterial hypertension is not only a major risk factor for cerebral ischemia, but also a preeminent factor of exacerbation of the resulting infarct. The definitive mechanisms underlying arterial hypertension-induced increase in ischemic brain damage are not well understood. Our hypothesis is that in spontaneously hypertensive rats (SHR), beside the effects of arterial hypertension on the cerebral vasculature, the vulnerability to cerebral ischemia could be attributed to direct effects of hypertension on the neuroglia compartment and/or to genetic mechanisms unrelated to hypertension. Here we studied the potential implication of glutamatergic receptors (NMDA and AMPA), that are highly involved in neuronal death occurring during cerebral ischemia. **Materials and Methods:** In the present studies, the effects of cerebral ischemia and those of intrastriatal injections of NMDA and AMPA on the lesion size were examined in young SHR (7 weeks), in which hypertension is not yet developed, adult SHR (14 weeks), and in age-matched normotensive rats (WKY). Under sevoflurane anesthesia, the rats underwent transient (90 min) intraluminal middle cerebral artery occlusion (MCAO), and cerebral blood flow (CBF) was monitored using laser Doppler flowmetry. The infarct volume was quantified 24 h later. Excitotoxic lesion were induced by intrastriatal administration of NMDA (75nmoles) or AMPA (2.5 and 5 nmoles). The data are expressed as mean  $\pm$  SD, statistics were performed by ANOVA. **Results:** Despite the same degree of reduction in cortical CBF in all the four groups of animals studied, both young and adult SHR displayed exacerbated brain ischemic lesions ( $244.6 \pm 31.6$  (n=7) and  $312.3 \pm 129.5$ mm<sup>3</sup> (n=7) respectively) compared to age-matched WKY rats ( $131.2 \pm 76.2$  (n=8) and  $92.0 \pm 56.5$ mm<sup>3</sup> (n=8)). No significant difference in NMDA-induced lesion between adult WKY and SHR was observed ( $21.0 \pm 8.9$  (n=9) and  $16.3 \pm 3.8$  (n=7)). In contrast, AMPA administration resulted in a dramatic increase in the size of the lesion and the rate of mortality in both young and adult SHR compared to WKY rats (see figure). **Conclusions:** These results show that, in spontaneously hypertensive rats, the exacerbation of both ischemic and AMPA-induced brain lesion is not totally dependent on the level of blood pressure. The fact that NMDA-induced brain lesion was similar in SHR and WKY, argues for a major role of AMPA receptors in the vulnerability of SHR to cerebral ischemia.

AMPA-induced striatal lesion in young and adult WKY and SHR



## OXYGEN TREATMENT AFTER PERINATAL HYPOXIA-ISCHEMIA REDUCES NEURONAL DAMAGE AT SHORT SURVIVAL TIMES, BUT WORSENS INJURY WITH LONG-TERM SURVIVAL

Kristin M Noppens<sup>1</sup>, J. Regino Perez-Polo<sup>2</sup>, David K. Rassin<sup>3</sup>, Karin N. Westlund<sup>4</sup>, Roderic Fabian<sup>5</sup>, Thomas A. Kent<sup>5</sup>, Marjorie R. Grafe<sup>1</sup>

<sup>1</sup>*Department of Pathology, Oregon Health and Science University, Portland, OR, USA*

<sup>2</sup>*Department of Human Biol Chem. & Genetics, University of Texas Medical Branch, Galveston, TX, USA*

<sup>3</sup>*Department of Pediatrics, University of Texas Medical Branch, Galveston, TX, USA*

<sup>4</sup>*Department of Neurosciences & Cell Biology, University of Texas Medical Branch, Galveston, TX, USA*

<sup>5</sup>*Department of Neurology, Baylor College of Medicine, Houston, TX, USA*

Brain injury resulting from hypoxic-ischemic (H/I) damage during the perinatal period is an important cause of neonatal morbidity and mortality. Infants with hypoxia are commonly treated with 100% oxygen, which may further exacerbate injury via free radical formation and DNA damage. PARP-1 is activated in response to DNA damage, but its role in H/I cell death remains uncertain. PARP-1 knock-out is neuroprotective in male, but not female perinatal mice (Hagberg et al., *J Neurochem* 90:1068, 2004). It is unknown if there are sex differences in the response to H/I in outbred animals. Dated, pregnant Wistar rats were purchased from Charles River. HI was induced on day P7 by irreversible common carotid artery ligation and subsequent hypoxia. Pups were anesthetized with halothane and the left common carotid artery was electrocauterized. After recovery from anesthesia and surgery, pups returned to their mother for 2-4 hours. Sham-operated animals were anesthetized, and the carotid artery exposed, but not ligated. Pups were then exposed to hypoxia (8% oxygen/balance nitrogen) in a humidified Plexiglas box at 37 C for 2 hours. Hypoxia only (H) pups were returned to room air, while hypoxia/hyperoxia (HH) pups were exposed to 100% O<sub>2</sub> for another 2 hours. Pups were returned to their mother until euthanasia at survival times of 2, 6, 12, 48 and 96 hours, and 6 weeks after hypoxia (n=8 each sex per group per treatment). Brains were perfusion fixed with 4% paraformaldehyde and stained with H&E. The degree of injury was graded on a scale of 0-4. Statistical analysis was performed using Kruskal-Wallis analysis of variance, with post-hoc Mann-Whitney Rank Sum tests. When males and females were combined, H and HH groups at all survival times except 6 weeks H had significantly greater histologic injury scores compared to the corresponding sham groups. At 12 hr survival, the H group had more cortical injury than the HH group (1.94 +/- 1.3 vs 0.94 +/- 0.85, p = 0.02). At 6 weeks, however, the HH group had greater injury scores than the H group for both cortex (2.56 +/- 1.79 vs 1.0 +/- 1.46, p = 0.013), and hippocampus (2.47 +/- 1.9 vs 1.0 +/- 1.46). At other survival times the differences were not significant due to high intragroup variability. When groups were broken down by sex, at 12 hours only females had significant differences (H=2.63 +/- 1.41, HH=0.75 +/- 1.04, p=0.021). The female H group had greater injury than the male H group (2.63 +/- 1.41 vs 1.33 +/- 0.87, p=0.036). At 6 weeks, both HH females and HH males had more cortical injury than the corresponding H groups, but not statistically significant due to high variability within groups (fHH=2.67 +/- 1.73 vs fH=0.89 +/- 1.45, mHH=2.44 +/- 1.94 vs mH= 1.13 +/- 1.55). There were no differences in cortical or hippocampal injury between males and females at 6 weeks. These results indicate that while treatment with 100% oxygen may improve short-term outcome, it worsens brain injury at 6 weeks survival.

## DIFFERENTIAL ROLE OF SYNAPTIC AND EXTRASYNAPTIC NMDA RECEPTORS IN GLUTAMATE MEDIATED NEURONAL INJURY

Frédéric Léveillé, Olivier Nicole, Eric MacKenzie, Alain Buisson

*UMR 6185, CNRS Université de Caen, Cycleron, France*

It has been known for 30 years that high concentrations of glutamate induce cell death in vitro and that similar extracellular concentrations are present in the rodent brain during ischaemia. It was subsequently shown that NMDA receptors mediate most of the glutamate-induced cell death in vitro and in vivo. Taken together, these data suggested that administration of NMDA antagonists in human beings could prevent cell death and confer neuroprotection after stroke. However, discouraging news started to accumulate as the clinical trials were terminated. Despite these developments, the theory of glutamate-induced excitotoxicity, the major power that forced NMDA receptor antagonists into human trials, has not been questioned. So it is possible that a fundamental misunderstanding of the pathophysiological roles of NMDA receptors may have been at the origin of absence of efficacy of glutamate antagonists in the treatment of stroke in Man. In the present study, we investigate the influence of NMDA receptors cellular locations on excitotoxicity. Materials and methods : All experiments were performed on murine primary cortical cultures containing both neurons and astrocytes prepared from foetal swiss mice at 14-16 days gestation. Cultures were used after 14 days in vitro. Neuronal death was quantified by the measurement of lactate dehydrogenase (LDH) release from damaged cells into the bathing medium. Intracellular free Ca<sup>2+</sup> measurement were performed by using videomicroscopy, confocal microscopy and calcium sensitive fluorescent probes Fura-2 and Fluo-3. Results: By blocking GABA<sub>A</sub> receptor function (with bicuculline at 50µM + 4-AP at 2.5 mM), cortical neurons fire burst of action potential which resulted in calcium plateaus visualized by videomicroscopy. This increase in intracellular calcium concentration is fully blocked by the co-application of TTX (at 0.5 µM), a compound known to inhibit electrical activity and by the co-application of AP-5, a selective NMDA receptor antagonist. These results demonstrate the pivotal role of synaptic NMDA receptors in the calcium plateaus induced by bicuculline treatment. Next we exposed primary cortical neurons for 24h to an intense activation of synaptic NMDA receptors by treatments with increasing doses of bicuculline. This treatment did not induce any neurotoxicity. In order to investigate the role of extrasynaptic NMDA receptors in glutamate neurotoxicity, we selectively inactivated synaptic NMDA receptors by exposing neurons to a NMDA receptor open-channel blocker (MK801 at 10µM) under bicuculline treatment and we performed bath application of increasing concentration of NMDA. In these conditions, we measured a dose dependant increase in intracellular calcium concentration mediated by the selective activation of extrasynaptic NMDA receptors. When applied for 24h, this conditions induced a dose dependant neurotoxicity. In conclusion, these results demonstrate that synaptic NMDA receptors activation promotes important intracellular calcium concentration increase that do not lead to excitotoxicity. While the activation of extrasynaptic NMDA receptors are directly involved in the neurotoxic effect of glutamate. Therefore a selective targeting of extrasynaptic glutamate receptors may improve the beneficial effect of NMDA antagonists for the treatment of stroke. This work was supported by the Institut Paul Hamel.

**FURTHER EVIDENCES FOR THE ROLE OF INOSITOL TRISPHOSPHATE AS AN EXCITOTOXIC DEATH SIGNAL IN HIPPOCAMPAL NEURONS**

S. Yamamoto, K. Ibaraki, T. Tsuboi, T. Sakurai, S. Terakawa

*Photon Medical Research Center, Hamamatsu University School of Medicine, Hamamatsu, Japan*

**INTRODUCTION:** We previously observed, under the video enhanced contrast-differential interference contrast (VEC-DIC) microscope, that the intact cultured neurons showed large nuclei containing an amorphous nucleoplasm, and that glutamate produced granulation inside the nucleus within 20 minutes (1). This nuclear change corresponds to DNA fragmentation (2). During this process, glutamate stimulates inositol trisphosphate (IP<sub>3</sub>) pathway, increases nucleoplasmic Ca<sup>2+</sup> concentration ([Ca<sup>2+</sup>]<sub>n</sub>). N-methyl-D-aspartate receptor activation also stimulates IP<sub>3</sub> pathway, and aggravates the process during glutamate excitotoxicity (2). On the other hand, mounting evidences revealed that mitochondrial dysfunction plays important roles during excitotoxic neuronal death. In this study, we examined whether mitochondrial toxin induces the nuclear change; and if so, we sought to determine the mechanism underlying the morphological changes. **METHODS:** Hippocampal neurons were obtained from one-day-old rats, and morphological changes were observed under a VEC-DIC microscope. Using a confocal laser microscope, mitochondrial membrane potential was measured with JC-1, a fluorescence indicator for mitochondrial membrane potential, changes in [Ca<sup>2+</sup>]<sub>n</sub> were assessed with fluo-3, a Ca<sup>2+</sup>-sensitive dye, and IP<sub>3</sub> signal was detected with green fluorescent protein fused to the PH domain which translocates from the plasma membrane to the cytoplasm when IP<sub>3</sub> increases. **RESULTS:** Within 20 min, carbonyl cyanide-4-(trifluoromethoxy)phenylhydrazone (FCCP; 1-10 μM), a potent mitochondrial uncoupler, dose-dependently decreased mitochondrial membrane potential and induced granulation inside the nucleus under the VEC-DIC microscope, which was identical to the findings induced by glutamate (100 μM – 1 mM). Toxic dosage of FCCP increased [Ca<sup>2+</sup>]<sub>n</sub> before inducing the nuclear changes. A removal of Ca<sup>2+</sup> from the medium did not affect the time course of both [Ca<sup>2+</sup>]<sub>n</sub> increase and the nuclear changes. Toxic dosage of FCCP increased intracellular IP<sub>3</sub> concentration before inducing nuclear changes. When the neurons were permeabilized with β-escin (1 μM), an application of IP<sub>3</sub> (1-10 μM) with EGTA (5 mM), a Ca<sup>2+</sup> chelating agent, dose-dependently increased [Ca<sup>2+</sup>]<sub>n</sub> and induced rapid granular changes in the nucleus, which were inhibited by coadministration of heparin (5 U/ml), an IP<sub>3</sub> receptor inhibitor, indicating that IP<sub>3</sub> directly increased [Ca<sup>2+</sup>]<sub>n</sub> without extranuclear Ca<sup>2+</sup>. **COMMENTS:** Glutamate stimulates IP<sub>3</sub> pathway, increases [Ca<sup>2+</sup>]<sub>n</sub>, and induces DNA fragmentation during the early phase of necrosis in the hippocampal neurons. Associated mitochondrial dysfunction also stimulates IP<sub>3</sub> pathway, and aggravates the process of acute DNA fragmentation during glutamate excitotoxicity. Since the nucleus itself is a Ca<sup>2+</sup> store and has IP<sub>3</sub> receptors, IP<sub>3</sub> can directly increase [Ca<sup>2+</sup>]<sub>n</sub>. This nuclear calcium signal controls a variety of nuclear functions, including gene transcription, DNA synthesis, and DNA repair. Probably, the increase in [Ca<sup>2+</sup>]<sub>n</sub> persisting above the physiological level results in the damage of nuclear DNA. **REFERENCES** 1) Ikeda J et al. (1996) Nuclear disintegration as a leading step of glutamate excitotoxicity in brain neurons. *J Neurosci Res* 43: 613-622. 2) Yamamoto S et al. (2003) Excitotoxic signal rapidly induces random DNA fragmentation through inositol trisphosphate pathway. *J Cereb Blood Flow Metab* 23 (Suppl): 338. Supported by the grants from the Japan Society for the Promotion of Science: #14571306 and #16390407.

## POLY-ADP-RIBOSYLATION IS A PREVALENT POST-TRANSLATIONAL MODIFICATION OF MITOCHONDRIAL PROTEINS IN THE BRAIN

Yi-Chen Lai<sup>1,4</sup>, Yamming Chen<sup>4</sup>, Xiaopeng Zhang<sup>4</sup>, Paula D. Nathaniel<sup>4</sup>, Fengli Guo<sup>5</sup>, Larry W Jenkins<sup>3,4</sup>, Simon C. Watkins<sup>5</sup>, Patrick M. Kochanek<sup>1,2,4</sup>, Csaba Szabo<sup>6</sup>, Robert S.B. Clark<sup>1,2,4</sup>

<sup>1</sup>Department of Critical Care Medicine, Children's Hospital of Pittsburgh, Pittsburgh, PA, USA

<sup>2</sup>Department of Pediatrics, Children's Hospital of Pittsburgh, Pittsburgh, PA, USA

<sup>3</sup>Department of Neurological Surgery, Children's Hospital of Pittsburgh, Pittsburgh, PA, USA

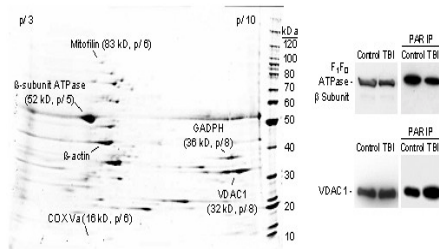
<sup>4</sup>Safar Center for Resuscitation Research, University of Pittsburgh, Pittsburgh, PA, USA

<sup>5</sup>Center for Biologic Imaging, University of Pittsburgh, Pittsburgh, PA, USA

<sup>6</sup>Inotek Corp., Beverly, MA, USA

**Introduction:** Poly-ADP-ribosylation is an important post-translational modification of proteins involved in DNA repair, maintenance of genomic integrity and transcriptional regulation. The addition of poly-ADP-ribose polymers (PADPR) is an energy requiring process utilizing NAD; and is mediated through poly-ADP-ribose polymerases (PARP). Although PARP plays an important role in cell homeostasis, over-activation under conditions of extensive DNA damage can lead to energy failure, and cell death via the release and nuclear translocation of mitochondrial apoptosis-inducing factor (AIF). We have previously demonstrated the presence of PARP and PADPR in the mitochondria. However, the specific mitochondrial targets of poly-ADP-ribosylation remain undefined. **Hypothesis:** Target proteins of poly-ADP-ribosylation in the mitochondria include those involved in energetics and apoptosis. **Methods:** We first verified the presence of PARP and PADPR in isolated rat brain mitochondria and in mitochondria of injured brain after experimental controlled cortical impact (CCI) by immuno-electronmicroscopy. To identify potential substrates of poly-ADP-ribosylation, immunoprecipitation using an antibody against PADPR was performed in isolated brain mitochondria after nitrosative stress with peroxynitrite and in mitochondrial-enriched fractions of injured brain after CCI, followed by small format 2-D gel electrophoresis. Peptides of interests were analyzed by matrix assisted laser desorption/ionization mass spectroscopy (MALDI-MS). Identified proteins of interest were then confirmed by standard Western Blot. **Results:** Immuno-electronmicroscopy demonstrated the presence of PARP-1 and PADPR both in isolated mitochondria *ex vivo* and in mitochondria of injured brain *in vivo*. 2-D gel electrophoresis detected multiple poly-ADP-ribosylated mitochondrial proteins. Several potentially important proteins were identified as PARP substrates, including (see figure): the  $\beta$  subunit of F<sub>1</sub>F<sub>0</sub> ATPase (complex V), voltage-dependent anion channel-1 (a key component of the mitochondrial permeability transition pore), cytochrome oxidase subunit Va, glyceraldehyde-3-phosphate dehydrogenase and mitofilin (mitochondrial inner membrane protein). **Conclusions:** These data show that poly-ADP-ribosylation is a prevalent post-translational modification of mitochondrial proteins. The finding that components of the electron transport chain, glycolysis and mitochondria membrane permeability transition pore are substrates of poly-ADP-ribosylation points to additional mechanisms by which PARP may regulate mitochondrial energetics and contribute to the release of apoptogenic factors after brain injury. *Support:* NS38620/NS30318/HD40686

Poly-ADP-Ribosylated Mitochondrial Proteins after TBI





**PERI-INFARCT DEPOLARISATIONS ARE A CAUSE AS WELL AS AN EFFECT OF  
CORTICAL ISCHAEMIA IN THE GYRENCEPHALIC BRAIN**

**Anthony J. Strong<sup>1</sup>**, Peter J. B. Anderson<sup>1</sup>, Helena R. Watts<sup>1</sup>, David J. Virley<sup>2</sup>,  
Andrew P. Lloyd<sup>3</sup>, Toshiaki Nagafuji<sup>4</sup>, Mitsuyoshi Ninomiya<sup>5</sup>

<sup>1</sup>*Department of Clinical Neurosciences (Neurosurgery), Kings College Hospital, London, UK*

<sup>2</sup>*Neurosciences CEDD, GlaxoSmithKline, Harlow, UK*

<sup>3</sup>*Statistical Sciences, GlaxoSmithKline, Harlow, UK*

<sup>4</sup>*Strategic Development Department, Shionogi & Co. Ltd., Osaka, Japan*

<sup>5</sup>*Discovery Research Laboratories, Shionogi & Co., Ltd., Osaka, Japan*

Introduction Laser speckle flowmetry allows detailed examination of evolution of focal cortical ischaemia. Using this method, we assessed the contribution of secondary deterioration in perfusion to the evolution of the ischaemic process in the gyrencephalic brain, with special reference to the role of peri-infarct depolarisations. Methods In 11 cats anaesthetised with chloralose (60 mg/kg), the cortical territory of the right middle cerebral artery (MCA) was exposed under oil, and the vessel occluded for four hours. Perfusion in the superficial cerebral cortex was imaged at ~13-sec intervals with laser speckle flowmetry, yielding a signal related to perfusion{1}. Mean grey levels representing perfusion in the core (ectosylvian, EG), intermediate (suprasylvian, SG) and outer penumbral (marginal, MG) gyri were extracted at 15-minute intervals. Entire image sets were reviewed as time lapse videos for evidence of propagating changes in perfusion. Results In 7 experiments there was a substantial area of ischaemia after 4 hours (Group 1, Table), whereas in the remaining 4 (Group 2) perfusion was close to baseline, having recovered to that level on core and penumbral gyri within 10 minutes of occlusion. Immediate postocclusion perfusion was similar in the 2 groups, but in 5 of Group 1 there was a substantial secondary deterioration in perfusion between 10 and 240 minutes (the remaining 2 achieved little collateral perfusion). One or more spontaneous, sudden reductions in perfusion occurred on SG in all of these 5 experiments, and propagated in 1,2 or 3 gyri, with a rate characteristic of spreading depression or of peri-infarct depolarisation (PID). In 4 of the 5 studies, they were associated with sustained reductions in perfusion and enlargement of the area of ischaemia. On lateral MG (MCA), changes were transient and often biphasic (reduction, then increase). Discussion The incidence of experiments with minimal or no ischaemia (Group 2) at 4 hours (despite an initial effect of occlusion comparable with the lesion group) resembles earlier results in this species{2}. SG and EG were better collateralised at 10 minutes in Group 2, and remained so at 240 min (Table). Perfusion fell secondarily in Group 1, especially in EG. These experiments indicate graphically that PIDs are associated with marked, secondary reductions in perfusion in the ischaemic, gyrencephalic brain, in addition to their known adverse metabolic effects. They also show that PIDs are not the only cause of delayed loss of perfusion. References 1. Dunn AK et al, J Cereb Blood Flow Metab 21: 195-201 2. Strong AJ et al, J Cereb Blood Flow Metab 3: 86-96 Acknowledgement This work was carried out in collaboration with the sponsors, Shionogi-GlaxoSmithKline Pharmaceuticals LLC. We thank Andrew Dunn for the speckle imaging software.

Group	After occlusion			10 min.			240 min.		
	MG	SG	EG	MG	SG	EG	MG	SG	EG
1: mean (n=7): SD	65.8 (11.7)	47.4 (12.3)	48.8 (9.1)	93.8 (10.1)	76.3 (15.5)	66.4 (18.7)	106.0 (25.0)	60.4 (16.8)	34.3 (12.5)
2 (n=4)	76.4 (17.5)	53.2 (20.8)	53.3 (11.7)	114.9 (15.2)	107.4 (21.7)	97.8 (16.2)	102.7 (9.2)	113.0 (23.9)	104.4 (15.4)

**EFFECTS OF NATURAL ANTHRAQUINONES ON NEURONAL SURVIVAL IN RAT BRAIN NEURON**Hsin-Hsueh Lee<sup>1</sup>, Yi-Hsuan Lee<sup>2</sup>, **Ling-Ling Yang**<sup>1</sup><sup>1</sup>*Department of Pharmacognosy, Graduate Institute of Pharmaceutical Science, School of Pharmacy, Taipei Medical University, Taipei, Taiwan*<sup>2</sup>*Department of Physiology, School of Medicine, Taipei Medical University, Taipei, Taiwan*

Recently the herbal medicine was widely used to treat the neurodegenerative diseases. Neuroinflammation is a characteristic of pathologically affected tissue in several neurodegenerative disorders. These changes are particularly observed in affected brain areas of Alzheimer's disease (AD) and neuronal injury. In the central nervous system, ischemic insult-induced neuronal injury is believed to result from glutamate toxicity and glucose deprivation. Rhubarb—the root of *Rheum officinale* is one of the famous Chinese herbs as astringent bitters in gastric constipation and in diarrhea. It is used to treat blood stasis and cathartic by traditional medicine. Rhubarb has a very broad spectrum of biological activities and pharmacological functions, such as laxative, antiphlogistic, and homeostatic in the treatment of constipation, diarrhea, jaundice, and gastro-intestinal hemorrhage, etc. In this study, five natural anthraquinones of *R. officinale* were investigated the neuroprotective effects against glutamate/NMDA (Glu/NMDA) stimulation in primary cultured rat brain cortical neurons. Cell death was accessed by lactate dehydrogenase (LDH) release assay for necrosis, and mitochondrial activity was accessed by 3-(4,5-dimethylthiazol-2-yl)-2,5-diphenyl tetrazolium bromide (MTT) reduction activity assay. Among the five anthraquinones tested, it was found aloin, emodin and aloe-emodin decreased MTT reduction activity, whereas sennoside A and B significantly reduced Glu/NMDA-increased LDH release in cultured neurons. These results suggest that Rhubarb extract contain both neuroprotective and neurotoxic anthraquinones

## **SURVIVAL OF NEWBORN NEURONS IN THE ADULT HIPPOCAMPUS IS ENHANCED BY BCL2 OVEREXPRESSION IN THE NORMAL AND ISCHEMIA**

**Tsutomu Sasaki**, Kazuo Kitagawa, Yoshiki Yagita, Emi Omura-Matsuoka, Shiro Sugiura, Kenichi Todo, Kohji Matsushita, Masatsugu Hori

*Division of Strokeology, Department of Internal Medicine and Therapeutics, Osaka University Graduate School of Medicine, Osaka, Japan*

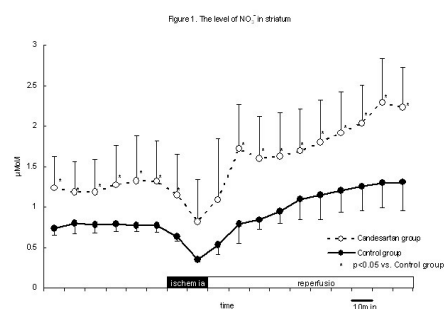
**Background:** Neural progenitors in the adult hippocampus continually proliferate and differentiate to the neuronal lineage, and ischemic insult promotes neural progenitors proliferation. However, newborn neurons show a progressive reduction in numbers during the initial few weeks, and the basic mechanisms that control survival of the remaining neurons are not well elucidated. Bcl-2, an anti-apoptotic gene, is a crucial regulator of programmed cell death in CNS development and in apoptotic and necrotic cell death following various stress stimuli, including ischemia. However, the effect of Bcl-2 on adult neurogenesis has been presently unknown. Thus, we tested whether Bcl-2 overexpression enhances newborn neurons survival in the adult hippocampus *in vivo* and *in vitro*. **Subjects and Methods:** 1) Newborn cells profiles: BrdU was used to label proliferating cells. Mice were killed at 1, 7, 14, 21, and 30 days after BrdU administration, transcardially perfused with 4% PFA and immunohistochemistry was performed. 2) Bcl-2 overexpression: To examine the effect of Bcl-2 on new neurons survival, transgenic mice overexpressing human bcl-2 under a NSE promoter (Bcl-2 Tg) were used. Expression of the human-bcl-2 transgene was evaluated, and then the proliferation, differentiation, and survival in the mice were determined. 3) Transient forebrain ischemia: Both common carotid arteries were occluded for 12 min. Thereafter experimental protocol was same as above. 4) Hippocampal primary culture: Hippocampal neuronal cultures with BrdU labeling were prepared from P0 Bcl-2 Tg and their littermates. At 7, 14 and 30 days after seeding, the survivals of newborn neurons were compared between the two groups. **Results:** Newly generated neurons in the hippocampal dentate gyrus showed a progressive reduction and became stable after 4 weeks. TUNEL-positive cells were detected in the subgranular zone (SGZ) and inner layer of the granule layer (GCL). The expression of human-bcl-2 gene can be detected both in immature and mature neurons. Bcl-2 Tg showed a significant increase in the number of BrdU-positive cells in the SGZ and GCL 30 days after BrdU injections compared with the littermates, both in the normal and ischemia. No difference in proliferation and differentiation were observed. Hippocampal culture also showed the enhanced survival of nascent BrdU-positive neurons in Bcl-2 Tg at 30 days after seeding. **Conclusion:** Bcl-2 promotes newborn neurons survival in the hippocampal dentate gyrus under normal and ischemic conditions. These results indicate that modulation of Bcl-2 levels in combination with neurotrophins may have implications for therapeutic intervention to enhance neurogenesis for functional restoration, particularly after ischemia.

## EFFECTS OF CANDESARTAN ON NO PRODUCTION IN AGED SPONTANEOUS HYPERTENSIVE RAT DURING GLOBAL CEREBRAL ISCHEMIA AND REPERFUSION

Harumitsu Nagoya, Nobuo Araki, Tsuyoshi Ohkubo, Yoshio Asano, Masahiko Sawada, Daisuke Furuya, Kimihiko Hattori, Tomokazu Shimazu, Masamizu Yamazato, Yasuo Ito, Yuji Kato, Mikiko Ninomiya, Kunio Shimazu

*Neurology, Saitama Medical School, Saitama, Japan*

**Introduction:** It is suggested that angiotensin II type Ia receptor blocker (ARB) reduces the infarction volume in experimental cerebral ischemia. The relationship between renin-angiotensin system and nitric oxide (NO) is well known. The purpose of this study is to investigate the effect of ARB on the cerebral NO production during cerebral ischemia and reperfusion in aged spontaneous hypertensive rat (SHR). **Methods:** Twelve male SHR were used; control group (n=6) [350-420g in weight ; 12 months old] and candesartan group (n=6) [treated with candesartan 10mg/kg/day for two weeks. 325-410g in weight; 18 months old]. They were anesthetized by intraperitoneal injection of pentobarbital sodium. NO production was continuously monitored by in vivo microdialysis. Microdialysis probes were inserted into the left striatum and hippocampus and were perfused with Ringer's solution at a constant rate 2 $\mu$ l/min. Laser Doppler probes were also inserted into the right striatum and hippocampus. After 2 hours equilibrium period, fractions were collected every 10 minutes. Forebrain cerebral ischemia was produced by occlusion of both common carotid arteries, and systemic hypotension (MABP < 50 mmHg) induced by hemorrhage. After 20 minutes, the loops around both common carotid arteries were released and the blood was re-infused. Levels of NO metabolites, nitrite (NO<sub>2</sub><sup>-</sup>) and nitrate (NO<sub>3</sub><sup>-</sup>), in the dialysate were determined using the Griess reaction. **Results:** (1) Blood Pressure; Mean BP for 40 minutes before ischemia in the candesartan group [109  $\pm$  11 mmHg (mean  $\pm$  SD)] showed significantly lower than that of the control group [158  $\pm$  26] (p<0.05). (2) Cerebral Blood Flow (CBF) in hippocampus and striatum; No differences in both groups were shown. (3) Nitric oxide; The levels of NO<sub>2</sub><sup>-</sup> in striatum of the candesartan group were significantly lower than those of the control group (p<0.05) in 20, 30, 60, 90, 100 minutes after the start of reperfusion. The levels of NO<sub>2</sub><sup>-</sup> in hippocampus of the candesartan group were significantly lower than those of control group (p<0.05) in 10 minutes of ischemia and 70 minutes after reperfusion. The levels of NO<sub>3</sub><sup>-</sup> in striatum of the candesartan group were significantly higher than those of the control group (p<0.05) before ischemia and during reperfusion. (Fig.1) The levels of NO<sub>3</sub><sup>-</sup> in hippocampus of the candesartan group were significantly higher than those of the control group (p<0.05) after the start of reperfusion. **Conclusion:** These data suggest that NO production in striatum in aged SHR was enhanced by candesartan. It is concluded that candesartan recovered the NO production in aged SHR, as we have already reported that NO production in aged SHR decreased compared to the young one.



**EFFECTS OF HBO WITH REDUCTION OF INOS AND HIF -1 $\alpha$  IN MOTOR NEURONS AFTER TRANSIENT SPINAL CORD ISCHEMIA IN RABBITS**

Noritaka Murakami<sup>1</sup>, Masahiro Sakurai<sup>2</sup>, Takashi Horinouchi<sup>1</sup>, Jun Ito<sup>1</sup>, Shin Kurosawa<sup>1</sup>, Masato Kato<sup>1</sup>

<sup>1</sup>*Department of Anesthesiology, Tohoku University Graduate School of Medicine, Sendai, Japan*

<sup>2</sup>*Department of Cardiovascular Surgery, National Hospital Organization Sendai Medical Center, Sendai, Japan*

**INTRODUCTION.** The purpose of this study is to investigate how ischemia-induced immunoreactivity of hypoxia-inducible factor (HIF) -1 $\alpha$  and inducible nitric oxide synthase (iNOS) were modified under hyperbaric oxygenation (HBO) in a rabbit transient spinal cord ischemia model. HIF-1 is a transcription factor that functions as a master regulator of oxygen homeostasis and its overexpression is regarded as harmful to hypoxic lesions. HIF-1 regulates its downstream pathways, including NOS pathways, which are related to hypoxia-induced injuries. We hypothesize that HBO, when applied at an early stage of ischemia, may provide enough oxygen to the ischemic lesions to reduce the accumulation of HIF-1 $\alpha$ . Thus, we examined the effects of HBO on these factors with our reproducible rabbit spinal ischemia model. **METHODS.** Thirty three Japanese white rabbits weighing 2 to 3 kg were involved in this study. A spinal cord ischemia model of infrarenal aortic occlusion for 15 min was employed. A balloon-tipped catheter was placed in the abdominal aorta without inflation of the balloon in three out of 33 rabbits as sham control. The other rabbits, randomized into two groups, underwent ischemic insults with the balloon inflation for 15 minutes. One hour HBO at 3 atmospheres absolute with 100 % oxygen at 30 minutes after reperfusion were employed in the rabbits in group A (n=15) and no treatment in group B (n=15). All rabbits were sacrificed at 4, 8, 12, 24, and 48 h after reperfusion and we performed immunohistochemical studies of iNOS and HIF-1 $\alpha$  induction. **RESULTS.** Spinal motor neurons in ventral gray matter in group B was decreased significantly compared with those in group A. Motor neurons in group B were strongly labeled for iNOS at 12 and 24h after reperfusion, while its immunoreactivity of the motor neurons in group A was no more than those in sham group. Motor neurons in group B were strongly labeled for HIF-1 $\alpha$  at 8 and 12h after reperfusion, whereas motor neurons in group A were barely labeled. **CONCLUSION.** We conclude that HBO therapy given at 30 minutes after ischemic insult exerted protective effects against ischemic spinal cell damage. HBO reduced the degree of induction of HIF-1 $\alpha$  and iNOS immunoreactivity after transient spinal cord ischemia. According to our results, it may be speculated that HBO, if applied at an early stage after ischemia, has beneficial effect on spinal cord ischemia. **REFERENCES** 1. Matrone C, Pignataro G, Molinaro P, et al: HIF-1 $\alpha$  reveals a binding activity to the promoter of iNOS gene after permanent middle cerebral artery occlusion. *J Neurochem* 2004; 90: 368-378 2. Murakami N, Horinouchi T, Sakurai M, et al: Hyperbaric oxygen therapy given 30 minutes after spinal cord ischemia attenuates selective motor neuron death in rabbits. *Crit Care Med* 2001; 29: 814-818

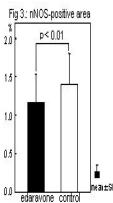
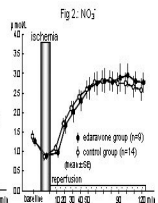
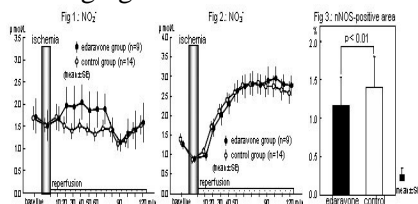
## EFFECT OF EDARAVONE, A NOVEL FREE RADICAL SCAVENGER, ON NITRIC OXIDE PRODUCTION AND nNOS ACTIVITY DURING CEREBRAL ISCHEMIA AND REPERFUSION IN MICE

Takeshi Ohkubo<sup>1</sup>, Nobuo Araki<sup>1</sup>, Yoshio Asano<sup>1</sup>, Masahiko Sawada<sup>1</sup>, Daisuke Furuya<sup>1</sup>,  
Tomokazu Shimazu<sup>1</sup>, Harumitsu Nagoya<sup>1</sup>, Masamizu Yamazato<sup>1</sup>, Yasuo Ito<sup>1</sup>, Yuji Kato<sup>1</sup>,  
Mikiko Ninomiya<sup>1</sup>, Keisuke Ishizawa<sup>2</sup>, Takanori Hirose<sup>2</sup>, Kunio Shimazu<sup>1</sup>

<sup>1</sup>*Department of Neurology, Saitama Medical School, Saitama, Japan*

<sup>2</sup>*Department of Pathology, Saitama Medical School, Saitama, Japan*

**Introduction:** Nitric oxide (NO) plays an important role in the pathogenesis of neuronal injury during cerebral ischemia. Edaravone has scavenging effect toward free radicals such as hydroxyl radicals and inhibiting action to lipid peroxidation, but its direct action for NO production is not clarified. We investigated the effects of edaravone on NO production and on nNOS activity during cerebral ischemia and reperfusion. **Methods:** Twenty three C57BL/6 mice were used in the study. Edaravone (3mg/kg) was intravenously infused just before each brain ischemia in 9 mice (edaravone group), and the drug was not administered in the remaining 14 mice (control group). The animals were anesthetized with 2% halothane and maintained with 0.5-1% halothane. NO production was continuously monitored by in vivo microdialysis. A microdialysis probe was inserted into the left striatum and perfused with Ringer's solution at a constant rate of 2  $\mu$ l/min. After 2 hours equilibrium period, fractions were collected every 10 minutes. A laser Doppler probe was placed on the right skull surface. Global ischemia was produced by clipping both common carotid arteries using Zen clips for 10 minutes. The levels of nitrite (NO<sub>2</sub><sup>-</sup>) and nitrate (NO<sub>3</sub><sup>-</sup>) in the dialysate samples were measured by the Griess reaction. After euthanasia, the brains were immunostained with an anti-nNOS antibody. To determine the fractional area density of nNOS-immunoreactive pixels to total pixels in the whole field, the captured images were analyzed with image analysis software. Mann-Whitney's U test was used for the group comparisons. **Results:** (1) Blood Pressure: No significant difference was observed between edaravone group and control group. (2) Cerebral Blood Flow (CBF): CBF decreased to 3.7 $\pm$ 0.7(mean $\pm$ SE)% in edaravone group and 4.4 $\pm$ 0.7 in control group during ischemia. After reperfusion, CBF transiently returned to baseline values and then gradually decreased significantly in both group. There was no significant difference between the two groups. (3) NO Metabolites (Fig1, Fig2): In edaravone group, the level of NO<sub>2</sub><sup>-</sup> increased significantly at 20 minutes (2.0 $\pm$ 0.4  $\mu$ mol/L) and 40 minutes (2.0 $\pm$ 0.4) ( $p$ <0.05) after reperfusion compared with baseline value (1.7 $\pm$ 0.4), but no significant differences were obtained in comparison to control groups. NO<sub>3</sub><sup>-</sup> levels in edaravone group decreased significantly during ischemia (0.9 $\pm$ 0.1) ( $p$ <0.005) and then increased significantly at from 20 (1.7 $\pm$ 0.2) ( $p$ <0.05) to 120 minutes (2.8 $\pm$ 0.2) ( $p$ <0.001) after reperfusion in comparison to baseline value (1.3 $\pm$ 0.2). But no significant differences were observed between the two groups. (4) nNOS-positive area (Fig3): nNOS-positive area in edaravone group (1.17 $\pm$ 0.05%) was significantly lower than that of control (1.40 $\pm$ 0.07) ( $p$ <0.01). **Conclusion:** The above data indicate that edaravone does not affect the whole NO production but inhibits nNOS activity. It has been reported that nNOS might exacerbate acute ischemic injury. These data suggest the possibility that edaravone exerts the brain protective effect not only through scavenging action toward free radicals but also through the influence on NO metabolism.





**NADH IS A NOVEL CYTOPROTECTIVE AGENT AGAINST PARP-1-MEDIATED NEURONAL AND ASTROCYTE DEATH****Weihai Ying, Keqing Zhu, Tiina Kauppinen***Department of Neurology, UCSF and VA Medical Center, San Francisco, CA, USA*

Poly(ADP-ribose) polymerase-1 (PARP-1) plays a key role in oxidative cell death. Excessive PARP-1 activation is also one of the important mediators of neuronal death in cerebral ischemia. Our recent studies have provided direct evidence supporting the hypothesis that NAD depletion mediates PARP-1 cytotoxicity: extracellular NAD can enter into astrocytes to restore intracellular NAD in cells with PARP-1 activation, which can prevent PARP-1-induced cell death even when added 3-4 hrs after PARP-1 activation. In this current study we tested our hypothesis that NADH, the reduced form of NAD, may also be used to decrease PARP-1-induced cell death by using murine neuronal and astrocyte cultures. The DNA damaging agent MNNG, a widely used PARP activator, was used to induce significant neuronal and astrocyte death in this study. We found that incubation with 0.1 - 1 mM NADH dose-dependently decreased PARP-1-induced neuronal death, even when NADH was added at 2 hrs after washout of the PARP activator. PARP-1-mediated astrocyte death was also dose-dependently decreased by NADH added immediately after MNNG washout. To elucidate the mechanisms underlying the protective effects of NADH, we assessed the effects of NADH treatment on intracellular NADH and NAD. We found that PARP-1 activation significantly decreased intracellular NADH levels in astrocytes, which was restored by treatment with NADH for 1 hr after MNNG washout. NADH treatment also significantly increased intracellular NAD levels in the cells. Since both NADH and NAD mediate energy metabolism, mitochondrial permeability transition and intracellular signaling, our study suggests that NADH may decrease PARP-1 toxicity by restoring intracellular NAD and NADH. Collectively, our study provides the first evidence suggesting that NADH is a novel cytoprotective agent, and that NADH can enter into cells to increase intracellular NAD and NADH. NADH might be used as a new drug for decreasing ischemic brain injury and cell damage in other PARP-1-associated diseases. (Supported by grants from the American Heart Association and the Dept. of Veterans Affairs (WY)).

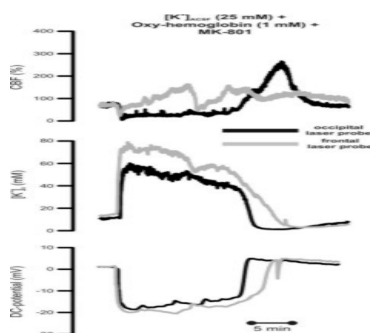
## THE N-METHYL-D-ASPARTATE RECEPTOR (NMDAR) ANTAGONIST MK-801 DOES NOT BLOCK SPREADING ISCHEMIA IN THE RAT

Jens P. Dreier<sup>1,2</sup>, Olaf Windmüller<sup>1,2</sup>, Gabor C. Petzold<sup>1,2</sup>, Karl M. Einhäupl<sup>1,2</sup>, Ute Lindauer<sup>1,2</sup>, Uwe Heinemann<sup>1,2</sup>, Ulrich Dirnagl<sup>1,2</sup>

<sup>1</sup>Department of Experimental Neurology, Charité University Medicine Berlin, Berlin, Germany

<sup>2</sup>Institute of Neurophysiology, Humboldt University, Berlin, Germany

**Introduction:** Spreading depression (SD) is associated with increased cerebral blood flow (CBF). This coupling between neuronal activation and CBF during SD is inverted by combined subarachnoid application of the NO-scavenger oxy-hemoglobin (Hb) and elevated K<sup>+</sup> so that the neuroglial depolarization wave is accompanied by an ischemic flow change (= spreading ischemia [SI]). Based on the induction of SI by red blood cell products, it has been hypothesized that SI could be the pathophysiological correlate of the widespread cortical infarcts representing the predominant lesion pattern in patients after subarachnoid hemorrhage. NMDAR antagonists reliably block SD under normal conditions. Therefore, we tested here whether NMDAR antagonists would also block SI. **Methods:** A cranial window was implanted in rats under thiopental anesthesia. Artificial cerebrospinal fluid (ACSF) was brain topically superfused. CBF was measured with laser-Doppler flowmetry. Intracortical DC-potential and extracellular K<sup>+</sup>-concentration were measured with two K<sup>+</sup>-sensitive microelectrodes (measuring depth 300  $\mu$ m). In group 1 (n=6), we tested the effect of intravenous (i.v.) MK-801 (5mg/kg) on SI generated by increasing K<sup>+</sup> concentration in the ACSF ([K<sup>+</sup>]ACSF) stepwise (3, 25, 35mM) at 60min intervals during continuous application of Hb. In group 2 (n=5), we increased [K<sup>+</sup>]ACSF to 130mM at the cranial window until SDs were detected. Subsequently, the cortex was superfused with physiological ACSF again, followed by MK-801 i.v. To determine whether SD could still be elicited under this condition, [K<sup>+</sup>]ACSF was again raised to 130mM for 60min. In group 3 (n=5), two cranial windows were implanted over the ipsilateral hemisphere. The same protocol as in group 2 was followed for the caudal window, while the rostral window was superfused with physiological ACSF throughout the experiment. **Results:** Despite NMDAR blockade, SI occurred under [K<sup>+</sup>]ACSF at 35mM and Hb in all experiments similarly as reported previously without MK-801 (Figure). [K<sup>+</sup>]o gradually increased before SI occurred (8.6 $\pm$ 2.8mM caudally, 12.6 $\pm$ 1.9mM rostrally) and showed a transient peak during SI. In group 2, in response to 130mM [K<sup>+</sup>]ACSF, [K<sup>+</sup>]o only increased to 7.7 $\pm$ 6.8mM (caudally) and 5.7 $\pm$ 5.8mM (rostrally). SD occurred in all animals. Compared to SI, DC-shift duration as well as extent and duration of the hypoperfusion were significantly smaller (P<0.001, t-test). Following MK-801, [K<sup>+</sup>]ACSF at 130mM again induced recurrent episodes of SD in all animals. In group 3, raising [K<sup>+</sup>]ACSF at the caudal window caused a gradual rise in [K<sup>+</sup>]o (6.7 $\pm$ 3.7mM), whereas it remained constant at the rostral window. During 60min superfusion with high [K<sup>+</sup>]ACSF, 5 $\pm$ 4 SD occurred at the caudal window. 3 $\pm$ 1 of these SD propagated into the rostral window. Following MK-801, SD still occurred caudally (8 $\pm$ 2/h). However, SD propagation was completely blocked. **Conclusion:** If SI is the pathophysiological correlate of the cortical lesions after SAH, it is unlikely that NMDAR antagonists alone are sufficient to protect the brain. Elevated baseline [K<sup>+</sup>]o reduces the efficacy of NMDAR antagonists to block SD.





## NEUROPROTECTIVE ACTIVITY OF NEUROSERPIN AGAINST NMDA RECEPTOR-MEDIATED EXCITOTOXICITY

Nathalie Lebeurrier<sup>1</sup>, Géraldine Liot<sup>1</sup>, Jose-Pascual Lopez-Atalaya<sup>1</sup>,  
Monica Fernandez-Monreal<sup>1</sup>, Peter Sonderegger<sup>2</sup>, Denis Vivien<sup>1</sup>, Carine Ali<sup>1</sup>

<sup>1</sup>*INSERM- Avenir 'T-PA in The Working Brain', Caen, France*

<sup>2</sup>*Institute of Biochemistry, Zürich, Switzerland*

Stroke results from the occlusion of a cerebral artery by a fibrin clot. Currently, the only approved treatment for stroke is the use of tPA (tissue-type Plasminogen Activator) as a thrombolytic agent (1). Although tPA is beneficial in the vascular compartment, tPA is deleterious in the cerebral parenchyma by modifying properties of the NMDA receptor. Indeed, tPA cleaves the NR1 subunit of the NMDA receptor leading to a potentiation of the NMDA-induced calcium influx (2). Based on these observations, we have investigated whether neuroserpin (NS), a brain-derived tPA inhibitor (3), could prevent this deleterious pro-excitotoxic activity of tPA. By using cultured cortical neurons, we have tested whether recombinant NS could influence excitotoxicity induced by NMDA or AMPA, two glutamatergic agonists. Although NS failed to alter AMPA-induced necrosis, it displayed a dose-dependent neuroprotective activity (up to 50%) against NMDA receptor-mediated neuronal death. By using calcium videomicroscopy imaging, we evidenced that NS decreases NMDA-induced calcium influx in neurons. Moreover, preliminary results show that NS reduces the lesion induced by the striatal injection of NMDA. These data suggest that promoting NS expression in the brain of stroke patients could prevent the deleterious effect of tPA in the brain parenchyma (potentiation of excitotoxic neuronal death) without affecting the beneficial thrombolytic activity of tPA in the vascular compartment. To address this question, we are investigating the regulation of NS expression by using luciferase gene reporter, real time PCR and immunoblotting to identify new ways to control the production of endogenous NS. References: 1) NINDS (1995) *N Engl J Med.* 333:1581-7. 2) Nicole et al. (2001) *Nat Med.* 7:59-64. 3) Krueger et al. (1997) *J Neurosci.* 17:8984-96.

## GLUTAMATE RECEPTOR SUBUNIT 2 (GLUR2) EXPRESSION MEDIATES PROTECTION CONFERRED TO CA1 NEURONS FROM ISCHEMIC DAMAGE BY PRIOR FIMBRIA-FORNIX DEAFFERENTATION

Jaspreet Kaur<sup>1</sup>, Zonghang Zhao<sup>1</sup>, Rose M. Geransar<sup>2</sup>, Ping Sun<sup>1</sup>, Alastair M. Buchan<sup>1,3</sup>

<sup>1</sup>*Hotchkiss Brain Institute and Calgary Stroke Program, Department of Clinical Neurosciences, University of Calgary, Calgary, AB, Canada*

<sup>2</sup>*Department of Biochemistry, University of Calgary, Calgary, AB, Canada*

<sup>3</sup>*University of Oxford, Oxford, UK*

**Introduction:** In animal models of stroke there are two forms of ischemic insults; focal infarction (representative of thromboembolic stroke) and global cerebral ischemia with widespread but selective neuronal death (representative of cardiac arrest). Transient global ischemia causes delayed but specific CA1 pyramidal neuronal death. Fimbria-fornix pathway is an important modulator of hippocampal function and sends afferents to the CA1 pyramidal neurons and prior deafferentation (FF lesion) of this pathway confers neuroprotection after ischemic insult. Such vulnerability may in part be due to changes in expression of calcium impermeable AMPA (GluR2 containing) receptors in CA1 neurons. We hypothesized that maintenance of GluR2 receptors in neurons may be one of the underlying molecular mechanisms for this protection. **Methods:** Adult male Wistar rats were exposed to 10 min of ischemia by 4 vessel occlusion (4VO) 13 days after deafferentation and sacrificed 7 days post ischemia. Coronal sections were taken for H&E staining. Immunofluorescent labeling for GluR2 and neuronal nuclear protein (NeuN) was done on adjacent sections. CA1 region of the dorsal hippocampus was divided into various sectors for cell counts. The optical intensity of GluR2 protein was quantified in these corresponding sectors using ImagePro Plus software. In another group, protein extracts of CA1 region were used to run SDS-PAGE. Subsequently, the protein was transferred onto nitrocellulose membrane and probed with anti-GluR2 and anti-actin immunoglobulins. Protein bands were visualized using enhanced chemiluminescence under FlourS-Max Imager (BioRad, Hercules, CA, USA). Densitometric data determined using QuantityOne software are presented as ratio of GluR2 normalized to densitometric values for actin. Quantitative RT-PCR experiments using the comparative Ct method for determining relative expression of GluR2 are underway. Student's t-test was used to determine the statistical significance between groups. **Results:** On the ipsilateral lesioned ischemic side, the CA1 showed 70% surviving neurons compared to 27% on the contralateral. This protection was observed to be long term. Fluorescent intensity of GluR2 protein was higher on the ipsilateral than on contralateral CA1 (755±205 vs. 416±136; p<0.01). Densitometric measurements of GluR2 protein bands in western blots also showed higher values on the ipsilateral CA1 (0.233±0.07 vs. 0.119±0.01; p<0.02). Quantitative RT-PCR experiments using the comparative Ct method for determining relative expression of GluR2 gene to confirm immunofluorescent data are ongoing. **Conclusions:** Profound neuroprotection following lesioning was observed in the ipsilateral medial CA1 region at 7 days following similar periods of ischemia, which would ordinarily induce complete cell death. There was no sparing of injury on the contralateral side. Regional GluR2 upregulation following FF deafferentation provides a protective effect on CA1 pyramidal neurons after transient forebrain ischemic insult.

## CHARACTERIZING THE EVOLUTION OF THE ISCHEMIC PENUMBRA USING PH WEIGHTED IMAGING

Phillip Z. Sun<sup>1,2</sup>, Jinyuan Zhou<sup>1,2</sup>, Weiyun Weiyun<sup>3</sup>, Judy Huang<sup>3</sup>, Peter C.M. van Zijl<sup>1,2</sup>

<sup>1</sup>Department of Radiology, Johns Hopkins University School of Medicine, Baltimore, MD, USA

<sup>2</sup>F.M. Kirby Research Center, Kennedy Krieger Institute, Baltimore, MD, USA

<sup>3</sup>Department of Neurosurgery, Johns Hopkins University School of Medicine, Baltimore, MD, USA

**INTRODUCTION:** The decision to use thrombolytic agents for ischemic stroke treatment hinges on characterization of the ischemic penumbra, the still viable tissue under risk of progression to infarction. The diffusion-perfusion mismatch approach in MRI<sup>1,2</sup> identifies tissue that has not experienced cell depolarization but is at risk of infarction. However, areas of hypoperfusion may sometimes only reflect benign oligemia. Recently, the possibility to perform pH-weighted (pHw) imaging with MRI was developed.<sup>3</sup> Because reduced tissue pH directly reflects impairment of oxidative metabolism, we hypothesized that diffusion-pH mismatch may better define the fraction of the ischemic flow penumbra at risk of infarction. Here, pHw imaging was combined with diffusion, perfusion and relaxation imaging to characterize evolution of acute ischemia in a rat model of permanent middle cerebral artery occlusion (MCAO). **METHODS.** Adult male Wister rats (280-320grams, n=15). Anesthesia: isoflurane(2.5%). Permanent MCAO preparation (suture). All images (4.7 T) acquired using single-shot EPI, facilitating co-registration. In-plane resolution: 0.5x0.5mm<sup>2</sup>, slice-thickness 2mm. Evolution was followed until 3.5hrs post-occlusion with 24hr follow up to assess T2-hyperintensity, known to agree with infarction as assessed by histology. **RESULTS/DISCUSSION.** In all animals, the maximal MCA area was hypoperfused, but no T1 and T2 changes were found during the first 3.5 hrs of imaging. Rats showed heterogeneous temporal evolution of the pHw and diffusion deficits. Based on data, we could assign three groups: 1) perfusion-deficit = pH-deficit = diffusion-deficit (n=5); 2) perfusion-deficit = pH-deficit > diffusion-deficit (n=6); 3) perfusion deficit > pH-deficit diffusion deficit (n=4). In groups 1 and 2, all animals evolved to full infarction over the initial area of perfusion-deficit. In group 3, in some animals the area of pH-deficit evolved to almost the area of perfusion-deficit (e.g. see first row in figure). Even though the pH-deficit area was larger than the diffusion area at 3.5 hrs, the animal evolved to full infarction over the remaining period to follow-up, in agreement with our hypothesis. In the second animal in the figure, the pH-diffusion mismatch remained small during the first 3.5 hrs. The 24 hr follow-up showed an infarcted region in reasonable agreement with the pH deficit at 3.5 hrs and much smaller than the perfusion deficit, again in line with our hypothesis. **CONCLUSIONS:** These initial data show that pHw imaging may have the potential to be a useful addition to the acute stroke exam by providing an opportunity to subdivide the area of perfusion deficit into regions of benign oligemia and impaired oxygen metabolism, with the latter having more predictive power for ultimate progression to infarction. Follow-up studies with models of reversible ischemia are needed to further confirm the hypothesis that a pHw-diffusion mismatch may be a better predictor of treatment risk assessment. **REFERENCES:** 1. Warach et al. JCBFM 1996;16:53, 2. Schaefer et al, AJNR 2002;23,1785. 3. Zhou et al. Nature Med. 2003; 9:1085. Research support: NIH/NIBIB 8R01EB002634

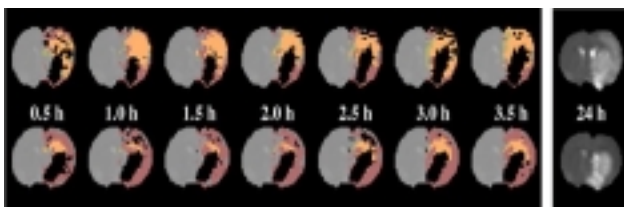


Fig. 1: Evolution of pHw-deficit (orange) and Diffusion deficit (black) with respect to perfusion deficit (purple) as a function of time post-MCAO occlusion. Hyperintensity in the T2 image at 24 hrs shows final infarction area.



**CENTRAL ROLE OF NEURONAL IKAPPABALPHA KINASE (IKK) IN CEREBRAL ISCHEMIA**

**Oliver Herrmann**<sup>1,5</sup>, Rossanna de Lorenzi<sup>2,5</sup>, Sajjad Muhammad<sup>1</sup>, Wen Zhang<sup>1</sup>, Martin Koehrmann<sup>1</sup>, Ioana Potrovita<sup>1</sup>, Ira Maegele<sup>1</sup>, Cordian Beyer<sup>3</sup>, James R. Burke<sup>4</sup>, Thomas Wirth<sup>3</sup>, Manolis Pasparakis<sup>2</sup>, Bernd Baumann<sup>3,5</sup>, Markus Schwaninger<sup>1,5</sup>

These Authors Contributed Equally

<sup>1</sup>*Department of Neurology, University of Heidelberg, Heidelberg, Germany*

<sup>2</sup>*Mouse Biology Programme, European Molecular Biology Laboratory, Monterotondo, Italy*

<sup>3</sup>*Department of Physiological Chemistry, University of Ulm, Ulm, Germany*

<sup>4</sup>*Bristol-Myers Squibb Pharmaceutical Research Institute, Princeton, NJ, USA*

The transcription factor NF-kappaB is activated in cerebral ischemia and promotes ischemic neurodegeneration with inflammatory and apoptotic effects. Activation of NF-kappaB is triggered by IkappaB-kinase (IKK) but may also occur independent of IKK. To find out if IKK is critical for damage in cerebral ischemia, we used both genetic and pharmacological approaches to reduce IKK activity. Mice with floxed IKK-2 alleles were crossed with a nestin-Cre line resulting in selective deficiency of IKK-2 in neural cells or with a CaMKII-Cre line resulting in selective deficiency in neurons. Western-blot-analysis of brain tissue was performed to prove the deficiency of IKK-2 protein. Furthermore, we expressed a dominant-negative mutant of IKK-2 in neurons, which inhibits both subunits of IKK. As a pharmacological approach, we injected BMS-345541, a selective inhibitor of IKK, or NaCl 0.9% as control icv at different time points. All mice underwent an occlusion of the distal branches of the middle cerebral artery (MCAO) by coagulation as a model of permanent cerebral ischemia. IKK was rapidly activated after MCAO followed by decrease of total IkappaB $\alpha$  protein. These processes were reduced in mice with genetic inhibition of IKK. We found a significant reduction of infarct size 48 hours after MCAO in all genetically altered mouse lines. Equally, BMS-345541 in different doses reduced the infarct size up to 60% when injected as late as 4.5 hours after MCAO. The neuroprotective effect of BMS-345541 was confirmed when infarct size was measured 2 weeks after MCAO. TUNEL staining evaluated by laser scanning cytometry showed a reduction of apoptotic signs after treatment with BMS-345541. In summary these data clarify the central role of IKK in ischemic brain damage as shown consistently by different genetic and pharmacological approaches. Above all our experiments suggest that IKK is a worthwhile drug target in stroke therapy with a promising therapeutic time frame.

**INHIBITION OF NITRIC OXIDE SYNTHASE DOES NOT PREVENT  
PHOSPHORYLATION OF THE ALPHA SUBUNIT OF EUKARYOTIC INITIATION  
FACTOR TWO FOLLOWING BRAIN ISCHEMIA AND REPERFUSION**

**Heather L. Montie, Donald J. DeGracia**

*Department of Physiology, Wayne State University, Detroit, MI, USA*

Purpose: Overproduction of nitric oxide (NO) following brain ischemia and reperfusion (I/R) contributes to the pathophysiology of I/R injury. However, the scope of NO's actions during brain I/R are not completely understood. In cell culture, NO has been shown to induce endoplasmic reticulum (ER) stress and activate components of the unfolded protein response (UPR). The UPR is an ER stress response that inhibits protein synthesis to stop the further accumulation of misfolded proteins within the ER lumen, and increases transcription of ER-related genes to repair the ER. Translation arrest following the UPR is due to phosphorylation of the alpha subunit of eukaryotic initiation factor 2 (eIF2 alpha) by the ER transmembrane eIF2 alpha kinase PERK. Brain I/R causes ER stress and activates PERK. Because NO has been shown to induce the UPR in cell culture, we here evaluated the role of NO on eIF2 alpha phosphorylation and PERK activation following cardiac arrest and resuscitation in several brain regions and several peripheral organs. Methods: Transient global brain ischemia was induced by cardiac arrest, and reperfusion was by critical care cardiopulmonary resuscitation with all animals maintained normothermic throughout. Experimental groups (n=3 per group) were conducted in the presence and absence of 200 mg/kg of the nonspecific nitric oxide synthase (NOS) inhibitor L-NAME: nonischemic controls (NIC), 10 min ischemia plus 10 min (10R), 10R + L-NAME (10RN), 90 min (90R) reperfusion and 90R + L-NAME (90RN). PERK activation and eIF2 alpha phosphorylation were determined by Western blot in brain regions, heart, kidney, liver, lung, pancreas and skeletal muscle. Brain regions included: brainstem, midbrain, cerebellum, thalamus, hippocampus and cerebral cortex. The effect of the NO donor S-nitroso-N-acetyl-penicillamine (SNAP) on PERK activation and eIF2 alpha phosphorylation in cultured neuroblastoma cells was also studied. Results: Brain regions generally showed large increases in eIF2 alpha phosphorylation and PERK activation. We report here for the first time that I/R induce PERK activation and eIF2 alpha phosphorylation in kidney and liver. Heart showed evidence of eIF2 alpha phosphorylation. Pancreas, lung and skeletal muscle showed no change in eIF2 alpha phosphorylation with ischemia and reperfusion. Although SNAP activated PERK in cultured neuroblastoma cells, administration of L-NAME had no effect on levels of eIF2 alpha phosphorylation in all brain regions and responsive peripheral organs. Discussion: Although NO activated PERK in cultured cells, activation of the UPR following I/R in brain and responsive peripheral organs appeared to occur independent of NO formation. Thus, it is likely that NO production is not proximal to PERK activation in the setting of ischemia and reperfusion injury. Further, our results showing that the UPR is active in kidney and liver, and to a small extent in heart, clarify peripheral contributions to the cellular pathophysiology of resuscitation from cardiac arrest. Work supported by NIH grant NS044100 (D.J.D.).

**IN VIVO PPAR $\alpha$  ACTIVATION ATTENUATES CEREBROVASCULAR  
ENDOTHELIAL DYSFUNCTION VIA IMPEDING NADPH OXIDASE-DERIVED  
SUPEROXIDE AND AUGMENTING TETRAHYDROBIOPTERIN IN  
MINERALOCORTICOID HYPERTENSION**

Lixin Li<sup>1</sup>, Song-Jie Liao<sup>1,2</sup>, Li Lin<sup>1</sup>, Jin-Sheng Zeng<sup>2</sup>, Alex F. Chen<sup>1</sup>

<sup>1</sup>*Departments of Pharmacology, Neurology and Neuroscience, Michigan State University,  
East Lansing, WI, USA*

<sup>2</sup>*Department of Neurology and Stroke Center, The First Affiliated Hospital, Sun Yat-Sen  
University, Guangzhou, China*

**Introduction:** Hypertension is an independent risk factor for stroke. Peroxisome proliferator-activated receptors (PPARs) are a family of nuclear receptor-dependent transcription factors. PPAR $\alpha$  agonist fenofibrate has been shown to abrogate increased arterial prepro-endothelin-1 (preproET-1) and superoxide levels in deoxycorticosterone acetate (DOCA)-salt hypertension with unknown mechanism(s). We have reported that ET-1 induces endothelial dysfunction in the carotid arteries via NADPH oxidase-derived superoxide in this low renin hypertension model. Therefore, the present study tested the hypothesis that chronic PPAR $\alpha$  activation in vivo reduces blood pressure and endothelial dysfunction via impeding cerebrovascular NADPH oxidase/superoxide and augmenting eNOS cofactor tetrahydrobiopterin (BH4) in DOCA-salt rats. **Methods:** DOCA-salt or sham-operated adult male rats were treated with fenofibrate (150 mg/kg/day) for 4 weeks beginning with DOCA-salt regimen. Oxidative stress markers and endothelial function were determined in the carotid arteries afterwards. **Results:** Average systolic blood pressure was significantly increased in DOCA-salt rats (186 $\pm$ 8 vs. 122 $\pm$ 3 mmHg, DOCA vs. sham), which was blunted by fenofibrate (186 $\pm$ 8 vs. 139 $\pm$ 6 mmHg, DOCA vs. DOCA+PPAR $\alpha$ , all n=11-16, p<0.01). Concomitantly, treatment with fenofibrate significantly reduced arterial NADPH oxidase activity (44.2 $\pm$ 4.2 vs. 21.6 $\pm$ 1.7 nmol/min/mg tissue DOCA vs. DOCA+PPAR $\alpha$ ), superoxide level (0.62 $\pm$ 0.04 vs. 0.37 $\pm$ 0.04 nmol/min/mg protein), VCAM-1 expression (0.46 $\pm$ 0.07 vs. 0.28 $\pm$ 0.04, VCAM-1/actin ratio, all n=5-10, p<0.05) and serum lipid peroxidation (TBAR 1.92 $\pm$ 0.08 vs. 5.18 $\pm$ 1.9 mol/L, n=10, p<0.01). Furthermore, treatment with fenofibrate significantly augmented arterial BH4 level (1.23 $\pm$ 0.21 vs. 3.21 $\pm$ 0.88 pmol/mg protein, n=7-8, p<0.05) and endogenous eNOS activity (6.00 $\pm$ 0.40 vs. 12.96 $\pm$ 1.61 nmol/mg protein, DOCA vs. DOCA+PPAR $\alpha$ , n=8-9, p<0.05), resulting in improved endothelium-dependent NO-mediated relaxation in response to acetylcholine (39.73 $\pm$ 2.98 vs. 78.31 $\pm$ 3.83%, DOCA vs. DOCA+PPAR $\alpha$ , n=9-10, p<0.05). **Conclusion:** These findings indicate that in vivo PPAR $\alpha$  activation prevents progression of hypertension and reduces cerebrovascular endothelial dysfunction via impeding arterial NADPH oxidase-derived superoxide and augmenting eNOS essential cofactor BH4 in low renin mineralocorticoid hypertension. (Supported by American Heart Association grants #0130537Z and #0455594Z (to AFC), China Medical Board (CMB) grant #00730 and the National Natural Sciences Foundation of China grants #39940012 and #30271485 (to JSZ).

## ENDOCYTOSIS AND AUTOPHAGY IN CEREBRAL ISCHEMIA AND EXCITOTOXICITY

Anne Vaslin, Julien Puyal, Vanessa Waechter, Tiziana Borsello, **Peter G.H. Clarke**

*DBCM, University of Lausanne, Lausanne, Switzerland*

Endocytosis and autophagy are known to be enhanced in some cases of neuronal death, and there is evidence that they can be directly involved in the death mechanism. We here report that both these trafficking events are enhanced by cerebral ischemia in neonatal (P12) rats, in which the main (cortical) branch of the middle cerebral artery was occluded by cauterization in association with clamping of the common carotid artery on the same side for 1.5 h. We also analyze the endocytic phenomenon pharmacologically in dissociated neuronal cultures exposed to NMDA. The enhanced endocytosis was shown in rats that received an intracerebroventricular injection of 4.4 kD FITC-dextran at the time of carotid unclamping, and were sacrificed 24 h later. There was strong neuronal endocytosis restricted to the ischemic zone, which was specifically labelled by immunocytochemistry for early endosomal antigen 1 (EEA1). In dissociated neuronal cultures a similar NMDA-induced endocytosis of FITC-dextran was observed; it increased with the dose of NMDA and the duration of NMDA treatment, and with a toxic dose the strongest endocytosis was observed microscopically to be in neurons stained with propidium iodide (a marker for dying or dead cells). However, to study specifically the endocytotic mechanism without the complication of cell death, we determined a combination of NMDA concentration and timing that enhanced endocytosis but with minimal cell death, as judged by LDH release, and measured the endocytosis in cellular extracts by fluorescence spectrometry. This revealed two components of dextran internalisation: they were both confirmed to be endocytic by the fact that they did not occur at 4°C, but they had completely different pharmacological profiles. One occurred constitutively (even in the absence of NMDA) and was blocked by inhibitors of classical fluid-phase dynamin-independent endocytosis (e.g. by wortmannin). The other component was induced by NMDA, insensitive to fluid-phase inhibitors, but sensitive to inhibitors of dynamin-mediated endocytosis such as 0.4M sucrose and also to the JNK pathway inhibitor D-JNKI1, a powerful neuroprotectant. The latter inhibitors had little effect on the constitutive component of endocytosis. Although most dynamin-mediated endocytosis is receptor-mediated, competition experiments showed that the NMDA-induced endocytosis did not depend on a receptor specific for dextran. Enhanced lysosomal activity, presumably autophagy, was shown in neurones within the ischemic region (again at 24 h after carotid unclamping) by acid phosphatase histochemistry and by immunohistochemistry for lysosome-associated membrane protein (LAMP)-1. Cathepsin D was also increased in the ischemic region, but appeared to be in glia, not in neurons. The importance of these results is twofold. 1) They suggest that a specific JNK-dependent endocytic pathway and an autophagic pathway may be targets for neuroprotection in cerebral ischemia and neonatal asphyxia. 2) The induced endocytosis may provide a means for delivering neuroprotective agents specifically into the cells that need them.

## APPLICATION OF IN VIVO ESR SPECTROSCOPY TO MEASUREMENT OF CEREBROVASCULAR ROS GENERATION IN STROKE

Mayumi Yamato, Toshiaki Watanabe, **Hideo Utsumi**

*Graduate School of Pharmaceutical Sciences, Kyushu University, Fukuoka, Japan*

Reactive oxygen species (ROS) are believed to be very important in ischemic nerve cell death. Nitroxyl radicals react with  $O_2^-$  in the presence of reducing agents and with  $\bullet OH$ , and hence suppress lipid peroxidation. These reactions were reported to reduce the electron spin resonance (ESR) signals for the nitroxyl radical, and we proposed the utilization of nitroxyl radicals as spin probes for in vivo ESR spectroscopy to determine ROS generation in vivo. This study used an in vivo ESR spectroscopy / spin probe technique to measure directly the generation of reactive oxygen species (ROS) in the brain after cerebral ischemia-reperfusion. Transient middle cerebral artery occlusion (MCAO) was induced in rats by inserting a nylon thread into the internal carotid artery for 1 h. The in vivo generation of ROS and its location in the brain were analyzed from the enhanced ESR signal decay data of three intra-arterially injected spin probes with different membrane permeabilities. The ESR signal decay of carbamoyl-PROXYL having intermediate permeability was significantly enhanced 30 min after reperfusion following MCAO, while no enhancement was observed with the other probes or in the control group. The enhanced in vivo signal decay was significantly suppressed by superoxide dismutase (SOD). Neither catalase nor 100 mM DMTU ( $\bullet OH$  scavenger) suppressed the enhanced signal decay rate. None of the inhibitors had any effect on the signal decay rate in the sham-operated group. The results of this study suggest that the enhanced signal decay observed in MCAO rats is caused, not by the Fenton reaction but through a reaction that involves SOD. Nitroxyl radicals are known to act as antioxidants that reduce oxidative damage. Therefore, the presence of carbamoyl-PROXYL should reduce the degree of transient MCAO damage, assuming that the enhanced signal decay of carbamoyl-PROXYL, which was used to confirm in vivo ROS generation, is related pathologically to the transient MCAO injuries. Brain damage was barely discernible until 3 h of reperfusion, and was clearly suppressed with the probe of intermediate permeability. The antioxidant MCI-186 (edaravon) completely suppressed the enhanced in vivo signal decay following transient MCAO. These results clearly demonstrate that ROS are generated at the interface of the cerebrovascular cell membrane when reperfusion follows MCAO in rats, and that the ROS generated during the initial stages of transient MCAO cause brain injury.

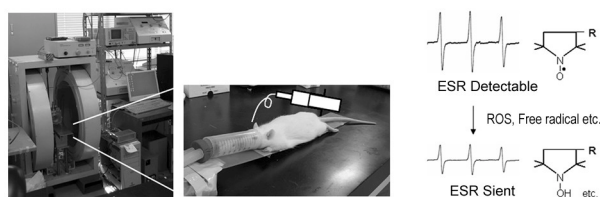


Figure 1 *in vivo* ESR spectroscopy and spin probe ESR spectra

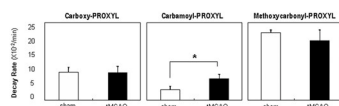


Figure 2 Signal decay rates of the three PROXYLs

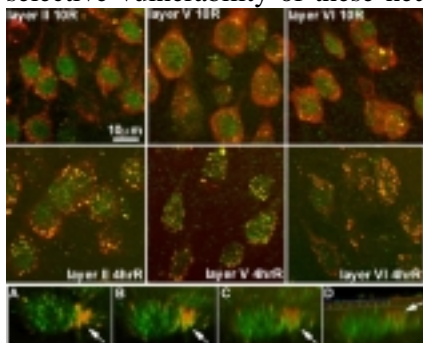
## ASSESSMENT OF STRESS GRANULES IN MOTOR CORTEX FOLLOWING GLOBAL BRAIN ISCHEMIA AND REPERFUSION

Foaz Kayali<sup>1</sup>, Heather L. Montie<sup>1</sup>, Jose A. Rafols<sup>2</sup>, Donald J. DeGracia<sup>1</sup>

<sup>1</sup>*Department of Physiology, Wayne State University, Detroit, MI, USA*

<sup>2</sup>*Department of Anatomy and Cell Biology, Wayne State University, Detroit, MI, USA*

**Purpose:** Brain ischemia and reperfusion (I/R) cause phosphorylation of the alpha subunit of eukaryotic initiation factor 2 (eIF2 alpha), a reversible event associated with neuronal protein synthesis inhibition. However, irreversible translation arrest correlates with cell death. eIF2 alpha phosphorylation leads to formation of stress granules (SGs), cytoplasmic foci containing 48S preinitiation complexes and the mRNA binding protein TIA-1. SGs are sites of translationally inactive protein synthesis machinery, and their persistence may distinguish ischemic vulnerable brain regions. As cortical layers V and VI show ischemic vulnerability, we evaluated SG formation in layers II, V and VI neurons of motor cortex following global brain I/R. **Methods:** SGs were evaluated by double-labeling immunofluorescence for two SG components: small ribosomal subunit protein S6 and TIA-1. 40X images were acquired in a Zeiss Apotome system. S6 was also evaluated by Western blot. Transient global brain ischemia was induced by cardiac arrest, and reperfusion was by critical care cardiopulmonary resuscitation with all animals maintained normothermic throughout. Experimental groups (n=3 per group) were: nonischemic controls (NIC), 10 min ischemia plus 10 min (10R), 90 min (90R) and 4 hr reperfusion (4hrR). **Results:** S6 staining (red) was cytoplasmic, and TIA-1 (green) was mainly nuclear. Colocalization of S6 and TIA-1 as yellow cytoplasmic foci defined SGs. Representative samples at 10R and 4hrR are shown in the Figure for layers II, V and VI of motor cortex, as indicated. SGs were present at 10R in all three layers. SGs quantitatively increased in layers V and VI, but not II. By 4hrR, SGs coalesced into larger structures (Figure, middle panels). There was a noticeable loss of ribosomal protein S6 at 4hrR that was most pronounced in layer 5, although there was cell to cell heterogeneity of S6 staining. By Western blot, S6 decreased 50% by 4hrR in unfractionated cortical homogenates. 3D reconstruction of a layer 5 pyramidal neuron showed SG localization mainly at the base of the apical dendrite, forming “trichromatic” columnar structures (rotation of 3D image shown in panels A-D, arrow points to SGs at base of apical dendrite. A is top view of neuron, D is side view). **Discussion:** All three cortical layers showed evidence of SGs. By 4 hrR, SGs had become larger, and free S6 protein had decreased. Cells containing more S6 protein (a marker of the 40S ribosomal subunit) not confined to SGs will have a greater capacity for protein synthesis. That some layer 5 neurons showed large decreases in S6 protein may relate to the selective vulnerability of these neurons. Work supported by NIH grant NS044100 (D.J.D.).



## EVOLUTION OF FOCAL CEREBRAL ISCHAEMIA IN RATS OBSERVED BY OPTICAL INTRINSIC SIGNALS IMAGING

Shangbin Chen, Zhe Feng, Pengcheng Li, Shaoqun Zeng, **Qingming Luo**

*The Key Laboratory of Biomedical Photonics of Ministry of Education, Huazhong University of Science and Technology, Wuhan, China*

Male Sprague-Dawley rats (n=8, 300~350 g) were subjected to focal cerebral ischaemia by inserting a nylon thread (0.2 mm diameter) into the lumen of the left internal carotid artery (ICA) and occluding the origin of the middle cerebral artery (MCA). Optical intrinsic signals imaging (OISI) at 550 nm light wavelength through thinned parietal bone was used to monitor the underneath cortex (an area about 6 x 8 mm). During the following 4 h, a series of spontaneous spreading waves of depolarization was detected. The early waves (during the early 2 h) usually invaded the whole parietal cortex, but the optical signals were varied regionally. In medial cortical region, the signals were quite similar to that observed during normoxic spreading depression (SD). In lateral region, time course of the signals showed a higher increase of reflectance intensity ( $5.3\pm 0.6\%$ ) followed by milder decrease of reflectance ( $-5.6\pm 0.5\%$ ) for limited perfusion reserve. The late waves (during the late 2 h) propagated only through the medial cortical region, the corresponding optical signals characterized as conspicuous spreading reflectance decrease ( $14.2\pm 1.4\%$ ). The source points of those waves were dynamically located in the left hemisphere cortex, sometimes out of the observed area, and sometimes inside. The general trend was toward to medial cortex. In the imaged cortex, the size of the area that the spreading waves could propagate decreased with the increase of waves number, which indicated that the focal ischemic lesion was developing and the infarct size was expanding. At the end of 4 h, significant morphologic change of the lateral cortex was observed: the region showed distinguished higher reflectance intensity, and the capillary network turned to blurry. After optical imaging, the brain was removed from the cranium, immersed in 2% 2,3,5-triphenyltetrazolium chloride (TTC) and incubated for 30 minutes at 37°C. The stained brain showed infarct cortex accounting about 70% of the left hemisphere cortex, and the part of parietal cortex that had been infarct was consistent with the lateral region we mentioned above. The results implied: (1) the functional impairment of penumbral could be revealed by optical intrinsic signals (OIS), (2) the infarct size increased with the spontaneous waves of depolarization, (3) the penumbral become infarction in <4 h, (4) the infarct region of parietal cortex located in the lateral. The optical imaging provided an indirect but reliable method to investigate the evolution of focal cerebral ischaemia with high spatial resolution. **Keywords:** Focal cerebral ischaemia, Middle cerebral artery occlusion, Optical intrinsic signals imaging, Spreading depression

## CONTRIBUTION OF HEMODYNAMICS AND LIGHT SCATTERING TO THE CHANGES IN OPTICAL INTRINSIC SIGNAL DURING CORTICAL SPREADING DEPRESSION IN RATS

Pengcheng Li, Yuanyaun Yang, **Qingming Luo**

*The Key Laboratory of Biomedical Photonics, Huazhong University of Science and Technology, Wuhan, China*

Optical intrinsic signals (OIS) imaging has been shown a powerful method for characterizing the spatial and temporal pattern of the propagation of cortical spreading depression (CSD) with high resolution. However, the possible physiological mechanisms underlying these OIS during CSD still remain incompletely understood. In this study, spectroscopic recording of the changes in OIS during pinprick induced CSD were performed at the exposed cortex of  $\alpha$ -chloralose/urethane anesthetized Sprague-Dawley rats (male, n=12) using a fiber optic reflectance spectrometer (PC-1000, Ocean Optics Inc.) to estimate the contribution of hemodynamics and light scattering to the changes in OIS. The fiber probe (source-detector fiber separation: 0.2 mm) was placed at cortical parenchyma site avoiding large blood vessels. For each animal, five CSDs were elicited with an interval of half an hour. On each CSD induction, the spectra data was collected over a 400 seconds period at the rate of 2 Hz. The changes in the concentration of HbO<sub>2</sub> and Hb, and changes in light scattering was estimated by fitting the experimental reflectance spectra data to a modified Beer-Lambert equation using a linear least squares fitting procedure, for a spectral range of 460~630 nm. The fit was good with a residual error less than 5% in most experiments. In this experiment, four-phasic changes in OIS were observed at 460 nm ~ 570 nm, but triphasic changes were observed at longer wavelength. The fitting results showed that the CSD induced an initial increase in concentration of HbO<sub>2</sub> (amplitude:  $9.0\pm 3.7\%$ ), which was  $26.2\pm 18.6$  s earlier than the onset of increase of Hb concentration. The increase in concentration of Hb reached its maximum value  $47.2\pm 5.9$  s earlier than that of HbO<sub>2</sub>. Whereas the concentration of HbO<sub>2</sub> showed a four-phasic change, the light scattering showed a triphasic change and the concentration of Hb only showed a biphasic change. The timing relationship between OIS and concentration of HbO<sub>2</sub> and Hb indicated that the initial phase of the decreased IOS at 550 nm was only caused by the concentration increase of oxygenated hemoglobin at cortical parenchyma sites. But during the second phase of the increased optical reflectance at 550 nm, more complicated physiological mechanisms may be involved, not only the changes in concentration of HbO<sub>2</sub>, Hb and Hbt, but also the changes in light scattering contributed significantly to the increase of optical reflectance. When the concentration of HbO<sub>2</sub> shows a small decrease ( $7.8\pm 4.5\%$ ), the concentration of Hb increased  $24.5\pm 10.8\%$ , simultaneously with a significant increase of light scattering. Interestingly, in our previous studies, a slight constriction of the pial arteries was observed during this phase of OIS. The constriction of the pial artery and the increase of concentration of total hemoglobin at cortical parenchyma site suggest that the regulations of the pial artery and capillary during this phase may be controlled by different mechanisms. During the followed third phase of light decrease at 550 nm, an increase of blood volume (concentration of total hemoglobin), an increase of oxygenation and decrease of scattering all contributed to the change of intrinsic optical signal.

**Keywords:** Cortical spreading depression, Light scattering, Hemodynamics, Spectroscopic, Optical intrinsic signal

**APOPTOSIS INDUCING FACTOR (AIF) IS ESSENTIAL FOR NEURONAL CELL DEATH FOLLOWING TRANSIENT FOCAL CEREBRAL ISCHEMIA**

Carsten Culmsee<sup>1</sup>, Changlian Zhu<sup>2</sup>, Miriam Höhn<sup>1</sup>, Stefan Landshamer<sup>1</sup>, Uta Mamrak<sup>3</sup>, Klas Blomgren<sup>2</sup>, **Nikolaus Plesnila**<sup>3</sup>

<sup>1</sup>*Biotechnology, Department of Pharmacy, University of Munich, Munich, Germany*

<sup>2</sup>*Perinatal Center, Department of Physiology, Goeteborg University, Goeteborg, Sweden*

<sup>3</sup>*Laboratory of Experimental Neurosurgery, Institute for Surgical Research, University of Munich, Munich, Germany*

Introduction: Delayed neuronal cell death is a major hallmark of ischemic stroke and a primary target for neuroprotective strategies. Apoptosis-inducing factor (AIF) promotes caspase-independent apoptosis upon translocation to the nucleus. Methods & Results: Here we show that AIF translocates to the nucleus and is associated with apoptotic DNA damage in primary neurons and immortalized HT22 hippocampal neurons after oxygen-glucose-deprivation or exposure to glutamate. In order to provide evidence for the essential role of AIF in glutamate-induced neuronal cell death we employed AIF targeted small interfering RNA (siRNA) to downregulate the protein. Both, mRNA levels and protein levels were reduced to less than 20 % in primary neurons or HT22 cells after AIF-siRNA treatment for 48 h. Moreover, RNA interference (RNAi)-mediated downregulation of AIF provided profound protection against excitotoxic cell death in primary neurons and HT22 cells. In a mouse model of reversible middle cerebral artery occlusion, rapid AIF translocation to the nucleus was associated with apoptotic nuclear morphology and DNA damage, and occurred prior to cytochrom c release in ischemic neurons. Furthermore, mutant mice expressing AIF at low levels exhibited significant decreases in infarct volume and delayed neuronal cell death after transient cerebral ischemia. Conclusion: These results provide compelling evidence for the primary involvement of AIF in neuronal cell death in models of neuronal apoptosis related to cerebral ischemia and suggest that therapies targeting caspase-independent cell death signaling may provide protection in cerebrovascular disease or other pathological conditions where programmed cell death is prominent.

**ALTERED PARVOALBUMIN EXPRESSION IN METHADONE TOLERANT RATS****Andres A. Quintero**, Mauricio Palacios*Seccion de Farmacologia, Universidad Del Valle, Cali, Colombia*

Opioids are pharmacological agents frequently used in different clinical applications including severe pain management and prevention of focal or global ischemia consequences during neurosurgical procedures. However, this group of substances is characterized by a quick onset of tolerance. By using immunohistochemical techniques we evaluated the expression of the calcium binding protein parvoalbumin, (an intracellular calcium homeostasis marker) in normal subjects and in methadone- tolerant rats. Methods: adult male Wistar rats were separated in two groups (n=7 each). The first group received an oral dose of 9mg/kg/day of methadone. The second group was used as control. To asses tolerance, a hot plate test was used. Results. An increased expression of parvoalbumin was documented in clinically methadone- tolerant rats when compared with control subjects. Parvoalbumin is a cytosolic calcium-binding protein that may act as a calcium buffer, and an augmented expression is an indicative of increased intracellular calcium. It has been suggested that this increased calcium influx may be a consequence of NMDA upregulation during tolerance. Therefore, even though opioids may attenuate the effect of brain ischemia in surgical patients, opioid tolerance could deteriorate the subject's condition.

**ROS GENERATION IS AMELIORATED BY ISCHEMIC PRECONDITIONING IN ORGANOTYPIC HIPPOCAMPAL SLICE CULTURES****Robert Dugger, Ami P. Raval, Miguel A. Pérez-Pinzón***Cerebral Vascular Disease Research Center, Department of Neurology and Neuroscience,  
University of Miami School of Medicine, Miami, FL, USA*

**Introduction:** Ischemic preconditioning (IPC) is an endogenous mechanism for neuroprotection against ischemia/reperfusion injury. Our earlier findings suggest that IPC protects the integrity of mitochondrial oxidative phosphorylation after cerebral ischemia [1]. Studies in heart suggest that mitochondria generate reactive oxygen species (ROS) via the mitochondrial ATP sensitive potassium channel, which then activate downstream kinases. Employing organotypic hippocampal slice cultures, we aimed to investigate whether (1) IPC reduced ROS generation during a subsequent lethal ischemic event, and whether (2) reactive oxygen species (ROS) generated in the mitochondrial respiratory chain act as a trigger of IPC.

**Methods:** Hippocampal slices were obtained from 9-11 days old Sprague Dawley rats. Slices were cultured for 14-15 days before experiments. Slices were divided in 4 groups, viz. sham, ischemia (40 min of oxygen-glucose deprivation (OGD)), IPC-1 (48 h prior to ischemia, slices were exposed to IPC-15 min of OGD) and IPC-2 (represents only 15 min of OGD without subsequent ischemic insult). Individual slices were incubated with the cell-permeant dihydorhodamine 123 (DHR) (5  $\mu$ M, 30 min), washed and transfer to an interface chamber mounted on a fluorescence microscope, where they were exposed to OGD (40/15 min). In the chamber slices were superfused with warmed (35-36 degree C) ACSF at a rate of 1 ml/min, and oxygenated with humidified 95% O<sub>2</sub>, 5% CO<sub>2</sub>. OGD of either 40/15 min was achieved by changing ACSF to aglycemic ACSF for 5 min followed by switching the gas composition from 95/5% O<sub>2</sub>/CO<sub>2</sub> to 95/5% N<sub>2</sub>/CO<sub>2</sub> for 35/10 min, respectively. The rhodamine fluorescence images were obtained every 5 min using a SPOT CCD camera and digitized using SPOT advanced software. Quantification of neuronal death in CA1 region was carried out using propidium iodide (PI) staining technique. Percentage of relative optical intensity of rhodamine /PI fluorescence was used as an index of ROS generation/cell death, respectively. Statistical significance was determined with an ANOVA test followed by a Bonferroni's post-hoc test.

**Results:** Slices exposed to ischemia followed by 1 h of reperfusion injury showed significant increase in ROS production. Quantification of rhodamine fluorescence demonstrated 51 % (% of baseline) (n = 5) increase after ischemia as compare with 7 % (n = 6) in control slices (p < 0.05). IPC to slices reduced ROS production during subsequent ischemic episode to 21% (n = 5) as compared with ischemic group (p<0.01). IPC to organotypic slices itself showed 20% (n = 3) increase in ROS, although not at the levels of the ischemic tissue. In correspondence to above mentioned results quantification of PI fluorescence in ischemic and IPC groups were 55.39  $\pm$  4.05 % (Mean  $\pm$  SD) (n = 17) and 22.65  $\pm$  1.61 % (n = 12), respectively (p < 0.05).

**Conclusion:** Our study demonstrate that mild increases in ROS will be neuroprotective, whereas larger increases in ROS may induced cell death CA1 region of hippocampus in organotypic slice cultures.

**References:** [1] Dave KR, Saul I, Busto R, Ginsberg MD, Sick TJ, Perez-Pinzon MA. (2001) *J.Cereb.Blood.Flow Metab.*, 21(2):1401-10. Grant support: PHS grants NS34773, NS05820, NS045676

## SIGMA RECEPTORS MEDIATE POTENT NEUROPROTECTION IN VIVO AND INHIBIT NEURONAL DEPOLARISATION AND SWELLING IN RAT BRAIN SLICES

Jennifer K. Callaway<sup>1</sup>, Christine Molnar<sup>2</sup>, Song T. Yao<sup>1</sup>, Bevyn Jarrott<sup>1</sup>, R. David Andrew<sup>2</sup>

<sup>1</sup>*Brain Injury and Repair Team, Howard Florey Institute, University of Melbourne, Parkville, Australia*

<sup>2</sup>*Department of Anatomy and Cell Biology, Queen's University, Kingston, ON, Canada*

Excessive release of glutamate has traditionally been accepted to be the first detrimental event leading to brain damage at the onset of stroke. However, within 2 min of stroke onset, neurons and glia in the ischemic core undergo a profound loss of membrane potential caused by failure of the Na<sup>+</sup>/K<sup>+</sup> ATPase pump. This 'ischemic' or 'anoxic' depolarisation (AD) results in cellular swelling and acute neuronal injury which is not inhibited by NMDA receptor antagonists or ion channel blockers although a 'soup' of both may block it in slices(1,2,3). While this result complements current thinking that a cocktail of drugs may be needed to treat stroke(4), Anderson and colleagues(5) found that sigma-1-receptor ligands display a remarkable ability to inhibit AD suggesting that currently unknown mechanisms are involved in AD and the ensuing brain damage. The present study compared the effects of the novel compound AM-36, an antioxidant, Na<sup>+</sup> channel blocker and a sigma-1-receptor ligand, carbetapentane (CP, a sigma -1-receptor ligand) and dibucaine (a Na<sup>+</sup> channel blocker) upon AD onset. AD was imaged using intrinsic optical signalling(5) (IOS) in submerged neocortical slices as a focal increase in light transmittance that then propagated at 2 mm/min across gray matter. Slices (400µm) from Sprague Dawley rats (21-30 d) were equilibrated in aCSF bubbled with 95%O<sub>2</sub>/5%CO<sub>2</sub> and superfused with aCSF at 3ml/min. Slices were incubated with or without drugs at 31°C for 45min prior to imaging and exposure to oxygen-glucose deprivation (1mM glucose aCSF bubbled with 95% N<sub>2</sub>/5%CO<sub>2</sub>) at 35°C. AD onset was blocked or delayed vs vehicle controls (6.2±0.2 min) by 50 µM AM-36 (8.2±0.5 min), 10µM dibucaine (7.8±0.3 min) or 50µM CP (7.4±0.0 min). In separate experiments, neocortical field potentials were evoked from slices incubated with 10µM dibucaine or 50µM AM-36. Dibucaine reduced field potentials by 88% while AM-36 and CP did not alter the response. Thus AD suppression appears mediated by sigma-receptor activation and not Na<sup>+</sup> channel blockade. Competition binding studies in progress confirm µM affinity of AM-36 and dibucaine for sigma-1-receptors. In vivo, both AM-36 (6 mg/kg ip), and the sigma-1-receptor ligand 4-PPBP (10 µmol/kg ip) potently reduced neuronal damage following endothelin-1-induced focal ischemia in conscious rats(6). These effects were mediated at least in part via inhibition of neuronal and inducible nitric oxide synthase (NOS) upregulation after stroke. In brain slices, preliminary studies showed no effect of pre-incubation with the specific neuronal NOS inhibitor 7-nitroindazole on AD (control: 6.6±0.7 vs 7-NI: 7.2±0.5 min, P>0.05). The present studies have found potent inhibition of neuronal damage in vivo and in brain slices by drugs acting on sigma-1-receptors. The mechanism of action of sigma ligands is yet to be determined, but may involve inhibition of NOS in vivo. (1)Obeidat, AS et al (2000) *J Cereb Blood Flow Metab* 20: 412; (2)Obrenovitch, TP. (2001) In: *Neuroprotection: Basic and Clinical aspects*. (Lo EH and Marweh J, eds), Prominent Press; (3)Rossi, DJ et al (2000) *Nature* 403:316; (4)Callaway, JK (2004) *Current Neuropharmacol.*, 2:277; (5)Anderson, TR et al (in press) *J. Neurophysiol*; (6)Callaway, JK et al (1999) *Stroke* 30:2704.

## MUTANT UBIQUITIN ACCUMULATE IN CA1 PYRAMIDAL CELLS AFTER TRANSIENT GLOBAL ISCHEMIA IN GERBIL

Kazuo Yamashiro, Takao Urabe, Nobutaka Hattori, Yoshikuni Mizuno

*Neurology, Juntendo University, Tokyo, Japan*

**Objective:** Proteasomal dysfunction in the hippocampus CA1 region after transient global ischemia in gerbil was reported previously. Recently the accumulation of ubiquitin-B (UBB) +1 protein was observed in the neurons of patients with tauopathy that proteasome activity also impaired. UBB+1 is an aberrant protein that was generated by a transcriptional dinucleotide deletion. UBB+1 has a novel COOH-terminus and lacks the functional carboxyl-terminal residue. UBB+1 lose the ability of ubiquitination and blocks the proteasome function. We investigate the contribution of UBB+1 in delayed neuronal death after transient global ischemia. **Methods and materials:** Male Mongolian Gerbils weighing 60 to 80g were anesthetized with 1.5% isoflurane in a mixture of 30% O<sub>2</sub> and 70% N<sub>2</sub>O via a face mask with spontaneous breathing. The bilateral common carotid arteries were transiently occluded using aneurysm clips for 5 minutes. Then the clips were removed to restore the cerebral blood flow. Gerbils were sacrificed under deep anesthesia at 1, 2, 3, 4 days after ischemia (n=6 at each time points) and brains were removed. The hippocampus CA1 region, CA3 and dentate gyrus were separately dissected under microscope and RT-PCR was performed to analyze UBB+1 mRNA in each region of hippocampus. For immunohistochemistry, the brains were perfusion-fixed with 4% paraformaldehyde in PBS and frozen in dry ice. Coronal sections were prepared using a cryostat. Immunostaining of UBB+1 protein by the avidin-biotin-peroxidase complex (ABC) method and double immunofluorescence staining with UBB+1 and TUNEL were performed. **Results:** UBB+1 mRNA was detected in every region of hippocampus at every time point after ischemia and also in the non-ischemic control animals. No UBB+1 protein immunoreactivity was observed in every region of hippocampus at 1 day after ischemia and non-ischemic control. In CA1 region, UBB+1 immunoreactivity appeared in the cytoplasm of pyramidal cells at 2 days after ischemia. The cytoplasmic immunoreactivity increased from 2days to 4 days after ischemia. At 4 days after ischemia, double immunofluorescence staining revealed that UBB+1 immunoreactive CA1 pyramidal neurons co-localized with TUNEL-positive cells. In contrast, UBB+1 protein was transiently detected at 2 days after ischemia in CA3 and dentate gyrus, however, UBB+1 immunoreactive cells disappeared at 3 and 4 days after ischemia. No TUNEL-positive cells were observed in CA3 and dentate gyrus. **Discussion:** In human brain, UBB+1 mRNA is generated in both neurodegenerative disease and nondemented control, while, the accumulation of UBB+1 protein is only observed in tauopathy that caused by impaired protein degradation via the ubiquitin-proteasome system. In this study, UBB+1 mRNA was present not only in the dying cells of CA1 but also in the surviving cells of CA3 and Dentate gyrus. In contrast to UBB+1 mRNA, UBB+1 protein only accumulated in CA1 region. We concluded that mutant ubiquitin may be a key mediator of the ubiquitin-proteasome dysfunction-induced neuronal signaling pathway and may have an important role in modifying delayed neuronal death.

**INCREASED EXTRACELLULAR POTASSIUM CONCENTRATION REDUCES THE EFFICACY OF N-METHYL-D-ASPARTATE RECEPTOR ANTAGONISTS TO BLOCK SPREADING DEPRESSION IN HUMAN AND RAT BRAIN SLICES**

**Gabor C. Petzold**<sup>1,2</sup>, Stephan Haack<sup>1</sup>, Dirk Megow<sup>1</sup>, Katharina Buchheim<sup>2</sup>, Uwe Heinemann<sup>3</sup>, Ulrich Dirnagl<sup>1,2</sup>, Jens P. Dreier<sup>1,2</sup>

<sup>1</sup>*Department of Experimental Neurology, Charité - University Medicine Berlin, Berlin, Germany*

<sup>2</sup>*Department of Neurology, Charité - University Medicine Berlin, Berlin, Germany*

<sup>3</sup>*Department of Neurophysiology, Charité - University Medicine Berlin, Berlin, Germany*

**Introduction:** Spreading depression (SD)-like depolarizations may augment neuronal damage in neurovascular disorders such as stroke, traumatic brain injury, and subarachnoid hemorrhage. Under physiological conditions, SDs are blocked by N-methyl-D-aspartate receptor (NMDAR) antagonists. However, under pathological conditions, SD-like depolarizations occur in presence of an increased extracellular potassium concentration ( $[K^+]_o$ ). We here tested whether this increase in baseline  $[K^+]_o$  would reduce the efficacy of NMDAR antagonists to block SD-like depolarizations in human and rat brain slices. **Methods:** We prepared acute neocortical slices from rats and from patients undergoing surgery for pharmacoresistant epilepsy. SD was recorded by two  $K^+$ -sensitive/reference microelectrodes and by measuring intrinsic optical signals. To investigate SD under high  $[K^+]_o$ , the extracellular  $K^+$  concentration in the artificial cerebrospinal fluid ( $[K^+]_{ACSF}$ ) was increased in a stepwise manner until SD occurred spontaneously. To study SD under physiological  $[K^+]_o$ , SD was evoked by a local neocortical microinjection of 3 M KCl using a glass capillary. The effects of the competitive NMDAR antagonist D-2-amino-5-phosphonovaleric acid (2-APV, 30  $\mu$ M) and the non-competitive NMDAR antagonist dizocilpine (MK-801, 20  $\mu$ M) were investigated. **Results:** In slices perfused with 2-APV in which  $[K^+]_{ACSF}$  was increased in a stepwise manner ( $n = 6$ ), SD occurred when  $[K^+]_o$  had reached  $12.3 \pm 1.7$  mM. Following post-SD recovery, slices were perfused with 2-APV under continuously elevated  $[K^+]_{ACSF}$ . No SD occurred under this condition, whereas SDs were detected at the same  $[K^+]_{ACSF}$  in control slices of the contralateral hemisphere. Subsequently,  $[K^+]_{ACSF}$  was further raised by 5 mM during continuous perfusion with 2-APV, inducing SD in all slices. The same protocol was followed in another group ( $n = 6$ ), but MK-801 was applied instead. The first SD occurred when  $[K^+]_o$  had reached  $11.6 \pm 3.1$  mM. No further SD was detected during perfusion with MK-801 at this  $[K^+]_{ACSF}$ , contrarily to control slices. When  $[K^+]_{ACSF}$  was further increased by 5 mM, SD occurred in all slices perfused with MK-801. In human slices in which  $[K^+]_{ACSF}$  was increased in a stepwise manner ( $n = 5$ ), SD occurred when  $[K^+]_o$  reached  $23.9 \pm 3.6$  mM. Subsequently, MK-801 was perfused at the elevated  $[K^+]_{ACSF}$ . No further SD occurred during that period, whereas SDs were seen in neighboring slices that served as controls. Subsequently,  $[K^+]_{ACSF}$  was further raised by 5 mM during continuous perfusion with MK-801, inducing SD in all slices. In slices perfused with physiological  $[K^+]_{ACSF}$ , in which SD was triggered by a local KCl microinjection, SD was completely blocked by either MK-801 or 2-APV, whereas repetitive SDs were inducible in control slices. **Discussion:** The efficacy of NMDAR antagonists to block SD was significantly reduced by high  $[K^+]_{ACSF}$  in rat and human brain slices. Our data suggest that a pathological rise in baseline  $[K^+]_o$  may critically reduce the efficacy of NMDAR inhibitors on SD-like depolarizations in cortical areas moderately affected by energy depletion, e.g., in the ischemic penumbra.

## HYPOTHERMIA DECREASES THE PROTEIN LEVELS OF TNF FAMILY MEMBERS AND THEIR SIGNALING INTERMEDIATES AFTER TRAUMATIC BRAIN INJURY

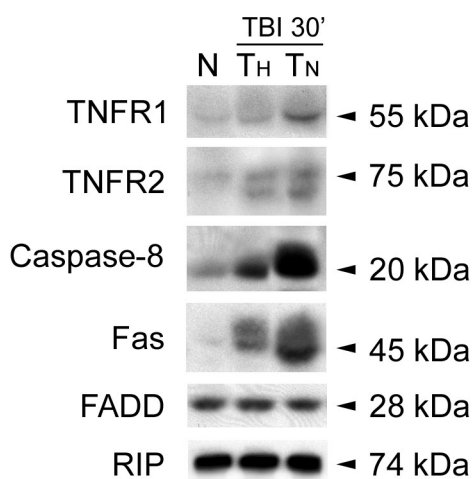
George Lotocki<sup>1,3</sup>, Robert W. Keane<sup>2,3</sup>, Ofelia F. Alonso<sup>1,3</sup>, **W. Dalton Dietrich**<sup>1,3</sup>

<sup>1</sup>*Department of Neurological Surgery, University of Miami Miller School of Medicine, Miami, FL, USA*

<sup>2</sup>*Department of Physiology and Biophysics, University of Miami Miller School of Medicine, Miami, FL, USA*

<sup>3</sup>*The Miami Project to Cure Paralysis, University of Miami Miller School of Medicine, Miami, FL, USA*

**Introduction:** Activation of tumor necrosis factor (TNF) and Fas receptor signaling cascades has been implicated in various pathologies of central nervous system. Our previous work has shown that moderate traumatic brain injury (TBI) upregulates TNF- $\alpha$  mRNA and protein, increases the protein levels of TNF receptor 1 (TNFR1), its signaling intermediates, and increases recruitment of TNFR1 into plasma membrane specialized microdomains, lipid rafts (1). Redistribution of TNFR1 in the plasma membrane altered association of TNFR1 with downstream intermediates that may signal death. Recent data have shown that therapeutic hypothermia significantly reduces TNF  $\alpha$  mRNA expression in rat hippocampus (2). Multiple studies indicate that hypothermia is protective, however, it is not known whether hypothermia alters the expression and protein levels of TNF receptor family members and their signaling intermediates. **Methods:** We performed immunoblot analysis of brain cortical lysates of adult male Sprague Dawley naïve (N) rats (N=3), rats subjected to normothermic (TN) (37 C) moderate (1.8 – 2.2 atm) fluid-percussion TBI with 30 min survival (N=3). Another group was subjected to moderate TBI with 30 min of pre- and post-traumatic hypothermia (TH) (33 C) (N=3). **Results:** TBI resulted in the increased levels of TNFR1, caspase-8 and Fas as previously observed (1). In contrast, mild hypothermia decreased protein levels of TNFR1, TNFR2, Fas, and an upstream, activated caspase-8, compared to normothermic levels. Protein levels of TNFR signaling intermediates including FADD and RIP did not appear to be significantly altered by hypothermia at this study period. **Conclusions:** These data provide evidence that hypothermia affects not only TNF but also Fas signaling in the rat cortices early after TBI. Therapeutic hypothermia may improve histopathological and behavioral outcomes after TBI by targeting death signaling cascades. **References:** (1) Lotocki G. et al., *J Neuroscience* 24(49):11010-11016, 2004. (2) Vitarbo EA et al., *Neurosurgery* 55:416-425, 2004. Supported by NIH grants NS42133 and NS30291.





**PI-3/AKT KINASE PATHWAY CONTRIBUTES TO NEUROPROTECTIVE EFFECT OF HYPOTHERMIA AGAINST CEREBRAL ISCHEMIA IN RATS**

Heng Zhao<sup>1,2</sup>, Takayoshi Shimohata<sup>1</sup>, Jade Q. Wang<sup>2</sup>, Guohua Sun<sup>1</sup>, David W. Schaal<sup>1</sup>, Robert M. Sapolsky<sup>1,2,3</sup>, Gary K. Steinberg<sup>1,3</sup>

<sup>1</sup>*Neurosurgery, Stanford University, Stanford, CA, USA*

<sup>2</sup>*Biological Sciences, Stanford University, Stanford, CA, USA*

<sup>3</sup>*Neurology and Neurological Sciences, Stanford University, Stanford, CA, USA*

Purpose and background: Mild hypothermia may reduce apoptosis after stroke, and the PI3/AKT kinase pathway may be involved in ischemic apoptosis, but the effects of hypothermia on the AKT pathway in ischemia is not known. AKT kinase may block apoptosis by phosphorylating the substrates FKHR and GSK3 $\beta$ , and AKT is activated by growth factors via a pathway that requires the kinases PI3 Kinase and PDK1. PTEN, a lipid phosphatase, downregulates PI3K activity. We studied the effect of moderate hypothermia on phosphorylation (P) of PTEN (Ser380), PDK1 (Ser241), AKT(Ser473), FKHR(Ser256), and GSK3 $\beta$ (Ser9) in a model of focal ischemia. AKT activity in vitro was analyzed, and we tested whether inhibition of the AKT pathway reverses the protective effect of hypothermia. Methods: Focal ischemia was induced by occluding the left MCA permanently and both CCAs for 1 h in rats maintained at 37°C or 30°C for 1h. For another two groups, 10  $\mu$ l of a specific PI3 kinase inhibitor, LY 294002, dissolved in DMSO and ethanol to 10 mM, or its vehicle, was injected intraventricularly 1 h before and 24 h after hypothermic ischemia onset. Infarct size was measured 2 days later. Other groups were sacrificed at 30 min after MCA occlusion and 30 min, 4, 8, 24 and 48 h after reperfusion. Whole cell homogenates from the penumbra of the ischemic cortex were prepared for Western blots. An AKT kinase assay was performed for tissues harvested at 4 and 24 h. Behavior was assessed up to 2 months. Results: Hypothermia reduced infarct size by 84% ( $P < 0.001$ ) and improved neurological function ( $P < 0.05$ ). At 37°C P-AKT decreased during ischemia, increased at 30 min and 4 h ( $n = 3-5$ /group;  $P < 0.05$ ) after reperfusion, and decreased after 8 h. AKT kinase assay indicated that AKT activity decreased at 4 h, so phosphorylation levels of P-AKT may not represent AKT activity. P-FKHR, P-GSK3 $\beta$  and P-PDK1 decreased after ischemia at all time points ( $P < 0.001$ ). P-PTEN decreased from 30 min after occlusion to 8 h post-reperfusion, then recovered from 24 to 48 h. Hypothermia did not increase P-AKT at 30 min or 4 h after reperfusion compared to sham, but attenuated its decrease during ischemia and 8 h after reperfusion. Nevertheless, AKT kinase assay showed that AKT activity at 4 and 24 h was maintained by hypothermia. Although P-PDK1 decreased at 4 and 8 h after reperfusion in hypothermic animals, decreases in overall levels of P-PDK1 were smaller compared to normothermia ( $P < 0.05$ ). P-FKHR transiently increased at 30 min after reperfusion and then decreased in hypothermic rats. The most striking effect of hypothermia was to block the decrease in P-PTEN at all time points ( $P < 0.05$ ). Surprisingly, hypothermia did not attenuate dephosphorylation of P-GSK3 $\beta$ , suggesting that dephosphorylation of GSK3 $\beta$  may not contribute to brain damage. In hypothermic animals the PI3 kinase inhibitor worsened infarct size by 53% ( $n = 5$ ) compared to vehicle ( $n = 6$ ) ( $p < 0.05$ ). Conclusion: The AKT pathway plays a critical role in preventing ischemic damage. Hypothermia protects in part by preserving AKT activity and attenuating the apoptotic effects of PTEN, PDK1 and FKHR.

**ALTERATIONS OF INTRACRANIAL PRESSURE MAY LEAD TO SECONDARY  
DETERIORATION BY INDUCING PERI-INFARCT DEPOLARIZATIONS**

Masao Umegaki, Yannic Waerzeggers, Yasuhiro Sanada, Gerhard Rosner,  
Christian Dohmen, Wolf-Dieter Heiss, Rudolf Graf

*MPI for Neurological Research, Cologne, Germany*

Introduction Peri-infarct depolarizations may progressively injure the ischemic penumbra (1). Other factors known to worsen conditions in the subacute stage of focal brain ischemia include brain swelling and rise of intracranial pressure (ICP), which potentially results in a malignant course of infarction (2). We intended to investigate the relevance of steady and transitory ICP elevations in focal ischemia for the induction of peri-infarct depolarizations in subcortical regions of ischemic territories. Methods In 11 anesthetized cats, the left middle cerebral artery (MCA) was prepared transorbitally. Micropipette calomel electrodes inserted into the medial and lateral portion of the left caudate nucleus measured the direct current (DC) potential and the spontaneous electrical activity (EEG). Laser Doppler probes measured cortical blood flow (LDF) extradurally on ectosylvian gyrus ipsilateral to MCAO. A strain-gauge MicroSensor and a thermocouple measured subdurally intracranial pressure (ICP) and brain temperature, respectively, on the contralateral marginal gyrus. All parameters were continuously recorded before and for 24 hours following permanent MCA occlusion. Results In all animals, severe focal ischemia was conformed by LDF. Different types of peri-infarct depolarizations (negative DC shifts  $>10$  mV) included terminal depolarizations (TD: without repolarization), long depolarizations (LD: repolarization after  $65\pm 48$  min) and spreading depression-like depolarizations (SD:  $5\pm 1$  min). In 4/11 cats, these depolarizations ( $n=23$ ; 14 SDs, 4 LDs and 5 TDs) were either associated with a) gradual, long-lasting or b) with rather steep, temporary ICP elevations. Analysis of the temporal relationship between ICP and DC alterations revealed that in 22/23 cases, the starting points of ICP rises preceded those of depolarizations, although the time spans between starting points differed considerably (mean  $14.9\pm 21.4$  min). Gradual, long-lasting ICP elevations were severe ( $542\pm 282$  % of control) and resulted always in TD or LD. In 4 cases of TD, malignant infarction with transtentorial herniation developed finally. Steep, temporary ICP elevations ( $60\pm 54$  % of control) led in all instances to the induction of SDs Conclusion Our study reveals a close relationship between temporary and permanent elevations of ICP and the induction of different types of tissue depolarization including peri-infarct spreading depression and characterizes therefore a relevant process of progressively worsening conditions in the subacute stage of focal ischemia. Literature 1. Ohta et al. (2001) *Stroke* 32:535-543 2. Toyota et al. (2002) *Stroke* 33:1383-1391

## CONDITIONS OF PROTECTION BY HYPOTHERMIA AND EFFECTS ON APOPTOTIC PATHWAYS IN A MODEL OF PERMANENT MIDDLE CEREBRAL ARTERY OCCLUSION

Heng Zhao<sup>1,2</sup>, Jade Q. Wang<sup>2</sup>, Guohua Sun<sup>1</sup>, Midori A. Yenari<sup>4</sup>, Robert M. Sapolsky<sup>1,2,3</sup>, Gary K. Steinberg<sup>1,3</sup>

<sup>1</sup>*Neurosurgery, Stanford University, Stanford, CA, USA*

<sup>2</sup>*Biological Sciences, Stanford University, Stanford, CA, USA*

<sup>3</sup>*Neurology and Neurological Sciences, Stanford University, Stanford, CA, USA*

<sup>4</sup>*Neurology, University of California, San Francisco, CA, USA*

**Purpose and Background:** Hypothermia is protective in stroke models, but findings from permanent occlusion models are conflicting. To determine whether hypothermia is effective in such cases, we induced focal ischemia in rats by permanent distal middle cerebral artery (MCA) occlusion, which models a scenario in which the MCA remains occluded but partial reperfusion occurs through collaterals. **Methods:** The left MCA was occluded permanently and the CCAs were reopened after 2 h, leading to partial reperfusion, in 6 groups of rats (Table 1) maintained at 37°C, 33°C (mild hypothermia), or 30°C (moderate hypothermia) during and after occlusion. Two days later rats were sacrificed for infarct size measurement. Immunofluorescence staining was used to detect cytochrome c and AIF translocation. **Results:** Infarct size did not differ from normothermic control (group 1) when hypothermia was mild and relatively brief (groups 2-3; see Table 1). Infarct size in rats exposed to mild hypothermia both during and post-ischemia (group 4) was reduced about 22% relative to group 1. When temperature was decreased to 30°C (group 5) robust protection was observed; an additional 2 h hypothermia during reperfusion in group 6 did not further reduce infarct size. Subcellular translocation of cytochrome c and AIF in the ischemic margin was not blocked by mild hypothermia in groups 2 or 3, but was attenuated in group 4 and blocked in groups 5 and 6. **Conclusion:** Mild hypothermia is protective in a model of permanent MCA occlusion if it is extended an additional 2h. Short durations of hypothermia are protective if temperature is lowered to 30°C. The protection might be achieved by blocking AIF and cytochrome c mediated apoptosis.

Table 1. Experimental groups

Group	Temp during first 2h	Temp during second 2h	Infarct Size (Mean±SEM) (%)	Reduction in infarct size (%)	P value (vs group 1)	n
1	37	37	63±3	0		7
2	33	37	65±4	-2	0.988	5
3	37	33	61±4	3	0.710	7
4	33	33	49±3	22	0.004	6
5	30	37	36±5	43	<0.001	7
6	30	30	36±4	43	<0.001	4

## SIGNIFICANCE OF PROTEIN HISTIDINE PHOSPHATASE FOR NEURONAL VIABILITY

Susanne Klumpp<sup>1</sup>, Anette Mäurer<sup>1</sup>, Daniela Faber<sup>2</sup>, Martina Lehmann<sup>2</sup>, Gunther Bechmann<sup>1</sup>, Thomas Wieland<sup>3</sup>, Susanne Lutz<sup>3</sup>, Thomas Gudermann<sup>2</sup>, Olaf Pinkenburg<sup>2</sup>, Josef Krieglstein<sup>2</sup>

<sup>1</sup>*Institut für Pharmazeutische und Medizinische Chemie, Westfälische Wilhelms-Universität Münster, Münster, Germany*

<sup>2</sup>*Institut für Pharmakologie und Toxikologie, Philipps-Universität Marburg, Marburg, Germany*

<sup>3</sup>*Institut für Pharmakologie und Toxikologie, Ruprecht-Karls-Universität Heidelberg, Mannheim, Germany*

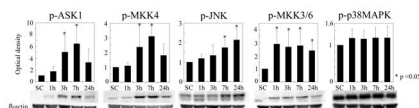
Introduction: During the last two decades many proteins regulating neuronal death and survival have been described. The activity of these proteins is influenced by reversible phosphorylation. Thus, protein kinases and protein phosphatases are major regulators of cell viability. We have recently detected a protein histidine phosphatase (PHP) in eukaryotes [1] and have identified ATP citrate lyase (ACL) [2] and the  $\beta$ -subunit of heterotrimeric G-proteins as substrates of PHP. Since PHP is markedly expressed in brain tissue we attempted to unravel the physiological role of PHP in neuronal function. Methods: PHP was expressed in E.coli. ACL was purified from rat brain and its activity determined by a 2-step enzyme assay. Localization of PHP and ACL was studied by western blot analysis and immunocytochemistry in brain, in primary cultures of neuronal cells (E18 and P1) and in neuronal and cholinergic cell lines. SH-SY5Y and SN56 cells were also used for overexpression (adenoviral vector) and knockdown (antisense and RNAi) of PHP. Cell viability was characterized by means of cell morphology and staining with Hoechst 33258. Results: PHP was found in the cytosol of cells and co-localized with ACL. After in vitro phosphorylation of ACL at his-760 (autophosphorylation or phosphorylation by nucleoside diphosphate kinases), dephosphorylation of ACL by PHP reduced ACL enzyme activity. Addition of PHP-antisense to cells yielded a neuroprotective effect on staurosporine-induced cell death. On the other hand, the increase in PHP protein detected upon overexpression of PHP was in parallel to an increasing rate of damaged and dying cells. Discussion: Our results provide evidence that PHP is involved in the regulation of cell viability. This might be attributed, at least in part, to its action on ACL, the enzyme producing acetyl-CoA thus providing the basis for lipid- and ACh synthesis. Cell viability depends on enzymatically active ACL, which is phosphorylated at his-760. It can be dephosphorylated, hence inactivated, by PHP. Accordingly, a PHP inhibitor might be a powerful neuroprotectant, particularly for cholinergic cells, because in these cells the inhibitor could improve lipid and acetylcholine synthesis. References: [1] S. Klumpp, J. Hermesmeier, D. Selke, R. Baumeister, R. Kellner and J. Krieglstein: Protein histidine phosphatase: A novel enzyme with potency for neuronal signaling. *J. Cereb. Blood Flow & Metab.* 22, 1420-1424 (2002) [2] S. Klumpp, G. Bechmann, A. Mäurer, D. Selke and J. Krieglstein: ATP-citrate lyase as a substrate of protein histidine phosphatase in vertebrates. *Biochem. Biophys. Res. Commun.* 306, 110-115 (2003)

## ACTIVATION OF AN EARLY AND NOVEL ASK1-MKK4-JNK SIGNALING PATHWAY AFTER FOCAL CEREBRAL ISCHEMIA IN RATS

Hiroshi Kamada, Chikako Nito, Hidenori Endo, Tatsuro Nishi, Pak H. Chan

*Department of Neurosurgery, Department of Neurology and Neurological Sciences, and Program in Neurosciences, Stanford University School of Medicine, Stanford, CA, USA*

**Introduction:** Apoptosis signal-regulating kinase 1 (ASK1), a member of the mitogen-activated protein kinase (MAPK) kinase kinase family, activates the MAPK kinase (MKK) 4/7-c-Jun N-terminal kinase (JNK) and MKK3/6-p38 MAPK pathways. ASK1 is strongly activated in response to diverse stress and apoptotic stimuli. However, whether ASK1 is activated after transient focal cerebral ischemia and leads to JNK or p38 MAPK activation remains to be fully understood. We examined the activation of the MAPK cascade, including ASK1, after transient middle cerebral artery occlusion (MCAO) in rats. **Methods:** Adult male Sprague-Dawley rats (body weight 250-280g) were used. Under anesthesia with 1.5% isoflurane, the left MCA was occluded by insertion of a 3-0 nylon suture. After 90 min of MCAO, blood flow was restored by withdrawal of the nylon suture. For Western blotting studies, the entire MCA territory on the ischemic side was quickly removed 1, 3, 7, and 24h after reperfusion (n=4 at each time point, including a sham-operated group). We performed Western blotting analysis for phospho-ASK1, phospho-MKK4, phospho-JNK, phospho-MKK3/6, and phospho-p38 MAPK. **Results:** Expression of phospho-ASK1 increased at 3h, reached a peak at 7h, and kept increasing to 24h after transient MCAO. Expression of phospho-MKK4 increased 3, 7, and 24h after transient MCAO. The maximal increase in phospho-MKK4 expression was observed 7h after transient MCAO. phospho-JNK expression initially increased at 3-7h and reached a peak 24h after transient MCAO. The increase in phospho-ASK1 expression was accompanied by the increase in phospho-MKK4 expression, followed by the increase in phospho-JNK expression. In contrast, phospho-MKK3/6 expression increased significantly 1h after transient MCAO, before expression of phospho-ASK1 increased, and kept increasing to 24h after transient MCAO. phospho-p38 MAPK expression slightly increased from 1h to 24h, but not significantly. The temporal pattern of phospho-ASK1 expression was different compared with phospho-MKK3/6 or phospho-p38 MAPK. **Conclusions:** Our results demonstrate that brain damage after transient brain ischemia triggers activation of the MAPK cascade, including early expression and phosphorylation of ASK1, and suggest that ASK1 might play a pivotal role in activation of the MKK4-JNK pathway, which is involved in neuronal apoptosis after transient focal cerebral ischemia, as previously reported (Okuno et al., 2004). **References:** (1) Okuno S, Saito A, Hayashi T, Chan PH; *J Neurosci* 24:7879-7887, 2004 **Grant support:** NIH grants P50NS14543, RO1 NS25372, RO1 NS36147, and RO1 NS38653, and the AHA Bugher Foundation.

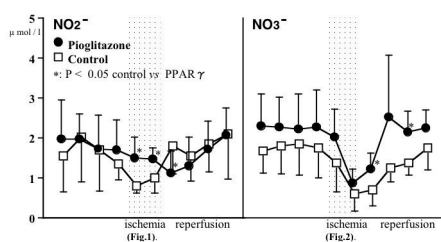


## EFFECT OF PPAR GAMMA AGONIST ON CEREBRAL NITRIC OXIDE PRODUCTION DURING CEREBRAL ISCHEMIA AND REPERFUSION

M. Yamazato, N. Araki, T. Ohkubo, Y. Asano, M. Sawada, D. Furuya, K. Hattori, T. Shimazu, H. Nagoya, Y. Ito, Y. Kato, M. Ninomiya, K. Shimazu

*Department of Neurology, Saitama Medical School, Saitama, Japan*

**Introduction:** We have reported that peroxisome proliferator-activated receptor (PPAR gamma) agonist, pioglitazone, protects against cerebral injury by anti-oxidant mechanisms.[1] The neuroprotective effect of pioglitazone induces SOD-1, suggesting that PPAR gamma activation is involved as a mechanism of the protection against cerebral injury. It is suggested that nitric oxide synthase is closely related to PPAR especially in inflammatory change. The purpose of this study is to investigate the effect of pioglitazone on the nitric oxide production in brain during ischemia and reperfusion. **Methods:** Seventeen male Wistar rats were used. We gave pioglitazone 20 mg/kg/day in 10 rats for 4 days (pioglitazone group), and 7 rats were used as control group. Microdialysis probes were inserted into the left striatum and hippocampus. The probes were perfused with Ringer's solution at a constant rate of 2  $\mu$ l/min. After 2 hours equilibrium period, the fractions were collected every 10 minutes. Laser Doppler probes were also inserted into right striatum and hippocampus. Cerebral ischemia was produced by bilateral occlusion of common carotid arteries and induced hypotension (mean blood pressure was less than 50 mmHg) by exsanguination of the blood for 20 minutes. After 20 minutes ischemia, bilateral common carotid arteries were reopened and blood was reperfused. The levels of nitrite (NO<sub>2</sub><sup>-</sup>) and nitrate (NO<sub>3</sub><sup>-</sup>) in the dialysate samples were measured by the Griess reaction. **Results:** 1) Blood Pressure There were no significant differences between the two groups. 2) Cerebral Blood Flow (CBF) (1) Striatum: No significant differences were observed between the two groups. (2) Hippocampus: CBF in pioglitazone group ( $215.7 \pm 62.5\%$ , mean  $\pm$  SD) showed significantly higher than that of control group ( $149.9 \pm 39.1\%$ ) in 10 minutes after reperfusion. 3) Nitric oxide (1) Striatum: The level of NO<sub>2</sub><sup>-</sup> in pioglitazone group ( $1.5 \pm 0.5$ ,  $1.5 \pm 0.3$   $\mu$ mol/l) showed significantly higher than that of control group ( $0.8 \pm 0.2$ ,  $1.0 \pm 0.4$ ) during ischemia. The level of NO<sub>2</sub><sup>-</sup> in pioglitazone group ( $1.1 \pm 0.6$ ) showed significantly lower than that of control group ( $1.8 \pm 0.7$ ) 10 minutes after the start of reperfusion (Fig.1). The level of NO<sub>3</sub><sup>-</sup> in pioglitazone group ( $1.2 \pm 0.4$ ,  $2.2 \pm 0.5$ ) showed significantly higher than that of control group ( $0.7 \pm 0.4$ ,  $1.4 \pm 0.3$ ) at 10 and 30 minutes after reperfusion (Fig.2). The level of total NO (NO<sub>2</sub><sup>-</sup> + NO<sub>3</sub><sup>-</sup>) in pioglitazone group ( $3.5 \pm 1.2$ ,  $2.4 \pm 0.4$ ) was significantly higher than that of control group ( $2.2 \pm 0.8$ ,  $1.6 \pm 0.6$ ) during ischemia. (2) Hippocampus: There were no significant differences between the two groups. **Conclusion:** These data suggest that pioglitazone activate nitric oxide synthase in the striatum during cerebral ischemia. **Reference;** (1) Shimazu et al. Stroke.2005; 36 (in press)



## CHOLINERGIC THALAMIC EXCITATION RESULTS IN REMOTE CASPASE-INDEPENDENT CELL DAMAGE AND SEIZURES

Angelique Regnier<sup>1,2</sup>, Jasleen Shant<sup>1</sup>, Sima Mraovitch<sup>2</sup>, Betty Chen<sup>1</sup>, Eric Vicaut<sup>2</sup>,  
Eugene Golanov<sup>1</sup>

<sup>1</sup>*Department of Neurosurgery, University of Mississippi Medical Center, Jackson, TN, USA*

<sup>2</sup>*Laboratoire D'Etude de la Microcirculation, Faculté de Médecine Université Paris VII, Paris, France*

**Introduction:** The nature of the brain lesions in temporal lobe epilepsy remains largely unknown. Unilateral administration of carbachol (CCh) in the lateral thalamus of Wistar rats triggers secondary generalized convulsive seizures (GCS) associated with bilateral hippocampal cell loss and ipsilateral damage of the piriform/entorhinal cortices and amygdala [1,2] comparable to human mesial temporal lobe sclerosis. The objectives of the study was to establish (1) whether phenomenon of thalamic-evoked lesion-accompanied GCS is strain and species independent; (2) whether regional cerebral blood flow (rCBF) in the piriform cortex is affected by thalamic CCh microinjections and (3) whether apoptotic neuronal death pathway is involved in remote thalamic-evoked brain lesions. **Methods:** Experiments were performed in Sprague Dawley (SD) rats and C56B7 mice. Animals were anesthetized and CCh (100nmol/100nl in PBS) was stereotaxically injected into thalamic ventroposterolateral/reticular nuclei (VPL/nRT). Animals were allowed to recover and were observed for 2 hours for seizures. 24-72 hours later animals were euthanized; brains were removed and processed for DNA fragmentation (dUTP nick end-labeling, TUNEL); for caspase-3 activation; for changes in levels of major histocompatibility complex 1 (MHC1); and histology. Piriform cortex rCBF (laser Doppler flowmetry) and EEG (monopolar) were recorded before and 4 hours after CCh microinjection in anesthetized rats. **Results:** In accord with earlier observations in Wistar rats [2] microinjections of CCh in VPL/nRT triggered multiple ( $4.6\pm 1.5$ ) episodes of GCS in SD rats ( $n=4$ ) and mice ( $n=5$ ) accompanied in 24-72 hours by lesions in hippocampus, piriform/entorhinal cortices, and amygdala as revealed by thionin staining. rCBF in piriform cortex increased by  $128.30\pm 90.7\%$  ( $p>0.05$ ,  $n=2$ ) within 2 minutes after ipsilateral thalamic CCh microinjections and gradually returned to the baseline in  $45\pm 31.8$  minutes. rCBF remained at the baseline level during the rest of observation period (4h) while EEG demonstrated multiple episodes ( $6.5\pm 4.5$ , duration  $33.7\pm 23$  sec) of spike-wave activity. In mice unilateral intrathalamic CCh administration ( $n=5$ ) also initiated GCS comparable to those observed in rats. Subsequent histological analysis revealed TUNEL positive staining bilaterally in the ventromedial thalamus, hypothalamus and hippocampus, amygdaloid complex and piriform cortex. TUNEL positivity in the ipsilateral piriform cortex and amygdala was accompanied by lesions, while no lesions were observed in thalamic or hypothalamic areas. Only low levels of caspase-3 activation were seen in the TUNEL positive regions. In the presence of lesions MHC1 immunolabeling increased in ipsilateral piriform/entorhinal cortices, amygdala and bilaterally in the hippocampus. However no changes of MHC1 immunoreactivity were observed in animals presenting only GCS. **Conclusions:** We conclude that (1) induction of GCS and temporal lobe damages after thalamic stimulation is strain and species independent; (2) brain damages in the piriform/entorhinal cortices and amygdala are not associated with a decrease in rCBF; (3) early TUNEL positivity is not necessarily associated with brain lesions within 72 hours; (4) thalamic-evoked brain lesions seem independent of caspase-3 activation; (4) immune mechanisms may be involved in the thalamic-evoked brain lesions. [1] Mraovitch S, Calando Y.; Neuroreport 3 519-23 (1995). [2] Mraovitch S et al.; Neurobiol. Disease, submitted (2005).

**LIPID RAFTS MEDIATE FAS APOPTOTIC SIGNALING AFTER SPINAL CORD INJURY**

Angela R. Davis<sup>1</sup>, Jessie S. Truettner<sup>2</sup>, Alex E. Marcillo<sup>2</sup>, W. Dalton Dietrich<sup>2</sup>,  
**Robert W. Keane<sup>1</sup>**

<sup>1</sup>*Department of Physiology and Biophysics, University of Miami Miller School of Medicine, Miami, FL, USA*

<sup>2</sup>*Department of Neurological Surgery and Miami Project to Cure Paralysis, Miami, FL, USA*

Fas and FasL are elevated in the spinal cord after traumatic injury, but the role of the Fas/FasL system in apoptotic signaling pathway after spinal cord injury (SCI) remains unclear. Female Fischer rats were subjected to moderate cervical (C5) SCI using the Electromagnetic SCI Device (ESCID). Immunoblot analysis of spinal cord lysates was performed to determine the time course of FasL/Fas expression after SCI. Within 15 min after SCI, increased levels of Fas were present in lysates, whereas little or no change in the levels of FasL was observed. In order to investigate the involvement of lipid rafts in Fas signaling, detergent-resistant microdomains were isolated from spinal cord lysates by discontinuous sucrose density gradient fractionation. In sham-operated animals, a small proportion of FasL, but not Fas was present in lipid rafts. SCI induced two phases of Fas recruitment to lipid raft microdomains. The first phase was rapid occurring within 15 min after SCI and the second phase was initiated after 24 hours. Subsequently, Fas-associated death domain (FADD) and caspase-8 were recruited to lipid rafts. To determine if FasL neutralizing antibody alters Fas and FasL association with lipid raft fractions, rats were injected i.p. with FasL-specific antibody immediately after injury. FasL neutralization did not change the association of FasL in lipid rafts, but significantly blocked the association of Fas with lipid rafts. Lastly, we performed targeted gene knockdown of FasL in vivo using sequence specific inhibition of FasL mRNA by siRNA. RT-PCR analysis revealed that siRNA treatment decreased levels of Fas mRNA by 30%. These studies show that the dynamic composition of the raft and nonraft regions of the plasma membrane of CNS cells may play an important role in specifying responses induced by Fas and offer new approaches to the therapeutic treatment of acute SCI, as well as clarify mechanisms by which these agents provide their neuroprotective effects. Supported by NIH-NINDS PO1NS3866 NS38665.

## CASPASE-DEPENDENT MECHANISMS ARE INVOLVED IN DELAYED CELL DEATH IN A RAT MODEL WITH CRITICALLY REDUCED CEREBRAL BLOOD FLOW

Axel Heimann, Sylvia Hartmann, Beat Alessandri, Oliver Kempfski

*Institute for Neurosurgical Pathophysiology, Johannes Gutenberg-University, Mainz, Germany*

Background: Neuronal damage occurs in the ischemic core but also in 'the ischemic penumbra'. The core grows rapidly at the expense of the penumbra and thus, neuropathological investigations of the cell death proves to be complicated in arterial occlusion models. In our model we perform a critical reduction of regional cerebral blood flow, mimicking the metabolic conditions in the penumbra in order to study the temporal course of cell death and potential apoptotic mechanism involved. Material and Methods: Male Wistar rats were anaesthetized, intubated and ventilated throughout the entire experiment. The left carotid artery was cannulized for blood pressure monitoring and blood gaze control. Local cerebral blood flow (lCBF) was bilaterally assessed by laser Doppler. Tissue impedance as a parameter for cell swelling was measured in the ipsilateral (penumbra) hemisphere. After stable baseline (30 min) penumbra conditions were provoked by hypobaric hypotension causing a critical CBF reduction in the ipsilateral hemisphere for 30 minutes. In addition cortical spreading depression (SD) was elicited four times during 'penumbra-period' by intracortical injection of 150 mM KCl as metabolic challenge. To study the time course of cell death rats were allowed to survive for either one (n=3;Gr-A), two (n=6;Gr-B) or seven days (n=6;Gr-C) before histological evaluation. In order to investigate whether apoptosis-related mechanisms are involved animals received an intracerebroventricular injection of a pan-caspase-inhibitor (zVADfmk 160 ng, n=6;Gr-D) or placebo (0.2% DMSO, n=6;Gr-E) 20 minutes after end of hypotension. These animals survived 7 days for histological evaluation. Results: Hypobaric hypotension induced a significant 53% lCBF reduction in the ipsilateral hemisphere in groups A, B, C. Accordingly, cerebral perfusion declined by 55% in the caspase-inhibitor experiment (Gr-D and Gr-E). After induced cortical spreading depression during hypotension the tissue impedance increased by 51% indicating massive cell swelling triggered by SD. Cell swelling recovered only after normalization of blood pressure. The histological evaluation showed a late cell loss in the ipsilateral hemisphere (364.2±74 /mm<sup>2</sup>, Gr-A; 262.0±69 /mm<sup>2</sup>, Gr-B; 217.0±69 /mm<sup>2</sup>, Gr-C). Compared to native brains (mean density 369.0±71 /mm<sup>2</sup>), a significant cell deficit was in group C. That delayed cell death was prevented by a zVADfmk bolus (Gr-D: 376.4±58 neurons/mm<sup>2</sup>) as compared to the placebo group (Gr-E: 264.21±84.59 /mm<sup>2</sup>). There were no differences in neuron density in the contralateral hemispheres neither of the 'time-course'-groups (413.8±63/mm<sup>2</sup>, Gr-A; 335.2±74 /mm<sup>2</sup>, Gr-B; 319.7±37 /mm<sup>2</sup>, Gr-C) nor of the placebo (385.9±61 /mm<sup>2</sup>) and zVADfmk (398.9±62 /mm<sup>2</sup>) group. Conclusion: zVADfmk reduces neuronal damage and thus, caspase-dependent mechanisms are involved in the delayed neuronal cell death occurring in tissue with critically reduced CBF.

## ERYTHROPOIETIN INDUCES NEUROPROTECTION IN EXPERIMENTAL INTRACEREBRAL HEMORRHAGE VIA ENOS UPREGULATION AND STAT3 ACTIVATION

Soon-Tae Lee<sup>1</sup>, Kon Chu<sup>1,2</sup>, Manho Kim<sup>1</sup>, **Jae-kyu Roh<sup>1</sup>**

<sup>1</sup>*Stroke & Neural Stem Cell Laboratory In Clinical Research Institute, Department of Neurology, Seoul National University Hospital, Seoul National University, Seoul, Korea*  
<sup>2</sup>*Center for Alcohol and Drug Addiction Research, Seoul National Hospital, Seoul, Korea*

Erythropoietin (EPO) is tissue-protective in preclinical models of ischemic, traumatic, toxic, and inflammatory injuries. Both EPO and its receptor are expressed throughout the brain in glial cells, neurons and endothelial cells. In this study, we investigated whether EPO treatment reduces cerebral inflammation, edema and perihematomal cell death after experimental intracerebral hemorrhage (ICH), and whether functional recovery is enhanced. ICH was induced using stereotaxic infusion of collagenase into the left basal ganglia of adult rats. EPO (5,000 IU/kg) or PBS was administered intraperitoneally at 20 minutes after ICH induction and daily afterwards for 3 or 14 days. Seventy-two hours after ICH induction, we checked hematoma volume using spectrometric methods and water content in both hemispheres separately. TUNEL, activated caspase-3 staining and caspase-3 activity assay were done for the perihematomal cell death, and myeloperoxidase (MPO) activity was analyzed for inflammation. Expression of eNOS, pSTAT3, STAT3, and pSTAT5 was measured by western blotting. Behavioral tests were performed weekly up to 35 days after ICH. The volume of hemorrhage was decreased in EPO-treated group by 25% at 3 days after ICH ( $p < 0.05$ ). EPO reduced the brain water content in the lesioned hemisphere compared with ICH-only group ( $p < 0.01$ ). In EPO-treated group, the numbers of TUNEL+, MPO+, and OX42+ cells, activated caspase-3+ cells were decreased in the periphery of hematoma ( $p < 0.01$ ). Western blotting showed significant upregulation of eNOS and pSTAT3 expression in EPO-treated group compared with the ICH-only group, while protein expression of STAT3, STAT5 and pSTAT5 has not been changed. EPO-treated rats recovered better at 14 days after ICH throughout 35 days in both rotarod and limb placing tests ( $p < 0.01$ ), and the degree of functional improvement in EPO-treatment group was faster and better than that of ICH-only group. In this study, we provide evidences that EPO has therapeutic effects in ICH. EPO treatment enhances the functional recovery, and induces the pleiotropic neuroprotection including the reduction of hematoma volume and edema, and the inhibition of apoptosis and neuroinflammation. Both eNOS upregulation and enhanced STAT3 phosphorylation may be involved in this action of EPO.

**THE PROTECTIVE EFFECT OF LIPOPHILIC IRON CHELATOR 2, 2'-DIPYRIDYL AFTER FOCAL CEREBRAL ISCHEMIA CLOSELY CORRELATES WITH LIMITATION OF APOPTOTIC CELL DEATH**

Michaël C. Van Hoecke, Anne Prigent-Tessier, Philippe E. Garnier, Christine Marie,  
|Alain Beley

*Laboratoire de Pharmacodynamie et Physiologie Pharmaceutique (L3P), Faculté de Pharmacie, Dijon, France*

**INTRODUCTION** : Two different forms of cell death have been distinguished morphologically following ischemia: necrotic and apoptotic cell death. Necrosis has been traditionally referred to brain infarction. However, more recent reports have suggested that apoptosis may become of greater importance than previously thought in focal ischemic injury, by participating to the extension of the lesion. The aim of the present study was (i) to carefully depict the temporal and spatial cell death progression during the enlargement of the lesion, with particular attention to apoptosis and (ii) to evaluate the effects of the lipophilic antioxidant iron chelator 2,2'-dipyridyl (DP). **METHODS** : Cortical ischemia was performed by chemical photothrombosis. Histological measurements (conventional histology, immunohistofluorescence for the cleaved caspase-3) were followed over a period of 24h after the onset of ischemia. Biochemical measurements (DNA fragmentation, immunoblot analysis of cleaved caspase-9 and 3, and cleaved PARP-1, a major substrate caspase-3 substrate) were followed in parallel in three punched tissue regions, distincts in term of neuronal survey : (i) the lesion core that definitively underwent infarction, (ii) surrounding tissue that could be rescued by systemic administration of DP, (iii) tissue, outside this latter region. **RESULTS** : The lesion volume remained stable for at least 4h after photothrombosis, thus representing the initial core of the infarct. Two separate waves of neuronal cell death could be distinguished. In the first wave, shrunken dark neurons were massively present as early as 2h following the onset of ischemia. From this initial neuronal abnormal population, progressive and time-dependent changes of both necrotic and apoptotic cell death were observed leading to ghost neurons and apoptotic bodies after 24 h. The extension of the lesion coincided with a second wave of cell death. After 12 h, the lesion volume had markedly increased. Massive and rapid neuronal loss occurred at the infarct border which appeared as a sharply demarcated pale region with abundant ghost neurons and apoptotic bodies. Procaspase and poly(ADP-ribose) polymerase-1 (PARP-1) cleavages were also detected in the infarct core and surrounding damaged tissue. DP treatment completely blocked the enlargement of the lesion, the infarct border being rescued from the infarction. Furthermore, neuronal density was increased in the infarct core. Finally a large decrease of apoptotic bodies was associated with a significant drop of caspase and PARP-1 cleavages suggesting that the protective effect of DP closely correlated with limitation of apoptotic cell death. **CONCLUSION** : Overall results indicate that (i) neuronal apoptotic and necrotic death initially evolve in concert in the infarct core from an initial population of damaged neurons, probably depending locally on the vulnerability and environment of each cell and that (ii) surrounding tissue leads massively to death in a second wave. These results also favour the view that apoptosis contributes to the expansion of the lesion following photothrombosis and point out the possibility that, at least in some circumstances, neurons in the ischemic core can be salvaged.

**MECHANISMS OF VASCULAR REACTIVITY DURING CORTICAL SPREADING DEPRESSION (CSD) AND CORTICAL SPREADING ISCHEMIA (CSI)**

Ute Lindauer, Ulrich Dirnagl, Jens P. Dreier

*Department of Experimental Neurology, Charité Hospital, Berlin, Germany*

Introduction: The cerebral blood flow response to CSD in vivo in the rat can be inverted to severe vasoconstriction (CSI) by nitric oxide synthase (NOS) inhibition and elevated potassium concentration (1). In addition we have recently shown that CSI in vivo can be modelled in vitro in the isolated middle cerebral artery (MCA) by application of combined extraluminal ion changes according to changes of the extracellular milieu during CSI (2). The aim of this study was to further evaluate the role of endothelial and neuronal NOS and the vascular endothelium for vasodilation and vasoconstriction during CSD/CSI induced ion changes, respectively. Methods: Rats were anesthetized, decapitated, and the brain was rapidly removed. The MCA was carefully dissected from the brain, cannulated and pressurized. Vascular reactivity to CSD/CSI induced ion changes (mmol/l: Na<sup>+</sup> 60; K<sup>+</sup> 50; Ca<sup>2+</sup> 0.1; Mg<sup>2+</sup> 0.7; Cl<sup>-</sup> 110; glucose 5.0; pH 6.90; osmolarity ~224) was investigated under baseline conditions and following NOS inhibition, cytochrome P450-epoxygenase inhibition or endothelium removal, respectively. Results: In response to CSD/CSI ion cocktail the arteries significantly dilated from  $107 \pm 8 \mu\text{m}$  to  $146 \pm 15 \mu\text{m}$ . In presence of the unspecific NOS inhibitor L-NNA we found vasoconstriction from  $85 \pm 5 \mu\text{m}$  to  $73 \pm 10 \mu\text{m}$ . In contrast, in presence of the n-NOS specific inhibitor 7-NI vasodilation was only prevented. During unspecific as well as n-NOS specific NOS inhibition, application of the L-type calcium channel antagonist nimodipine not only reestablished but significantly augmented vasodilation to CSD/CSI ion-cocktail. CYP450-epoxygenase inhibition with miconazole did not change vasodilation to CSD/CSI induced ion changes. Following removal of the endothelium by transient air application a slight vasodilation was observed at baseline conditions (diameter before and after air application:  $116 \pm 10 \mu\text{m}$  and  $136 \pm 7 \mu\text{m}$ , respectively). Starting from this new baseline, CSD/CSI ion-cocktail induced a significant vasoconstriction to  $98 \pm 8 \mu\text{m}$ . Conclusion: Application of CSD/CSI ion-cocktail caused vasodilation of the MCA in absence and vasoconstriction in presence of unspecific NOS inhibition or following removal of the endothelium. Specific n-NOS inhibition only prevented vasodilation. These results indicate that mediators released from the endothelium play an important role for vasodilation during CSD/CSI induced ion changes, preventing vasoconstriction during enhanced potassium concentrations. The exact nature of these mediators have to be revealed in further experiments, but it seems likely that endothelial NO plays a predominant role. References: [1] Dreier JP, Körner K, Ebert N, et al.; *J Cereb Blood Flow Metab* 18, 978-990 (1998) [2] Dreier JP, Windmüller O, Foddiss M, et al.; *Abstract Viewer/Itinerary Planner*. Washington, DC: Society for Neuroscience Programm No 22.9 (2004) Supported by DFG and Hermann and Lilly Schilling Foundation

**NULL MUTATION OF P53 ATTENUATES HIPPOCAMPAL NEURONAL DEATH IN VIVO FOLLOWING GLOBAL ISCHEMIA IN MICE**Ichiro Yonekura<sup>1,3</sup>, **Nobutaka Kawahara**<sup>1,3</sup>, Akio Asai<sup>2,3</sup>, Takaaki Kirino<sup>1,3</sup><sup>1</sup>*Department of Neurosurgery, Graduate School of Medicine, The University of Tokyo, Tokyo, Japan*<sup>2</sup>*Department of Neurosurgery, Saitama Medical Center, Saitama, Japan*<sup>3</sup>*Solution Oriented Research for Science and Technology (SORST), Japan and Science Technology Corporation (JST), Saitama, Japan*

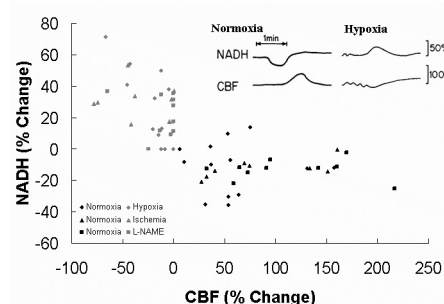
Tumor suppressor gene p53 controls cell death after various stresses. However, the role of p53 in neuronal death after brain ischemia has been poorly understood. Here, we evaluated a direct causal link of p53 with neuronal death following global cerebral ischemia using p53 deficient mice. We used p53 mutant mice backcrossed for twelve generations to avoid bias in the genetic background. These mutants, as well as wild-type mice, were subjected to transient global ischemia by 3-vessel occlusion method, in which no difference in severity of ischemia was noted as evidenced by anoxic depolarization and cortical blood flow. The resulting neuronal death in the hippocampal CA1 sector was extensive in p53 wild-type mice: the surviving neuronal count was  $9.3 \pm 3.0$  % of the normal control. However in mutant mice homozygous for p53, marked and significant attenuation of ischemic injury was observed, in which the neuronal count amounted to  $61.3 \pm 34.0$  % ( $p < 0.0037$ ). In wild-type mice, intense p53-like immunoreactivity was observed in hippocampal CA1 neurons at 12 hours after ischemia, and mRNA for Bax, a direct downstream target of p53, was also increased. These results indicated that p53 plays a crucial role in ischemic neuronal death in vivo, and suggest that this molecule could be a therapeutic target in neuronal death following cerebral ischemia.

## THE EFFECT OF OXYGEN SUPPLY ON OXYGEN BALANCE DURING CORTICAL SPREADING DEPRESSION IN THE RAT BRAIN

Judith Sonn, Avraham Mayevsky

*Faculty of Life Sciences, The Leslie & Susan Gonda Multidisciplinary Brain Research Center, Bar-Ilan University, Ramat-Gan, Israel*

Background: Cortical spreading depression (CSD) was shown to be an important pathophysiological event in various experimental and clinical situations. The phenomenon is known as a multifactorial event causing an increase in oxygen consumption (1). It occurs spontaneously during pathological conditions (such as: ischemia, hypoxia, head injury) contributing additional neuronal damage. Objective: The aim of the present study was to determine the interrelation between O<sub>2</sub> supply (cerebral blood flow-CBF) and O<sub>2</sub> balance (mitochondrial NADH redox state) simultaneously, during the passage of CSD waves across the cerebral cortex under a decrease in tissue oxygenation: hypoxia, ischemia and inhibition of NO synthesis. Methods: A special multiprobe assembly (MPA) enabled us to monitor continuously the CSD wave from its front line until complete recovery, simultaneously by various surface probes used (2). Hypoxia was induced by inhaling the animals with a gas mixture (87% N<sub>2</sub> + 12% O<sub>2</sub> + 1% CO<sub>2</sub>). Partial ischemia was induced by permanent bilateral carotid artery occlusion, 24 hours before the experiment was performed. Inhibition of NO synthesis was achieved by IP injection of 50mg/kg L-NAME. CSD waves were induced by diluted KCl solution. Peak amplitude values (% changes at maximum and minimum) were calculated for CBF and NADH during the initial phase of CSD. The CBF vs NADH peak values were sited on a graph and slopes were calculated. Results: During normoxia, CSD showed a characteristic increase in CBF and oxidation cycles in NADH whereas, after lowering oxygen supply a reduction cycle in NADH and a decrease in CBF were found. A representative analog illustration of CSD during normoxia and hypoxia is shown in the presented figure (upper right). The figure shows a clear separation and different slopes (4 times higher during low tissue oxygenation) in CBF vs NADH amplitudes during CSD under normoxia (-0.145, dark signs) as compared to hypoxia, partial ischemia and after L-NAME administration (-0.567, gray signs). Covariance analysis showed a significant higher interaction ( $F=26.55$ ,  $df=2, 59$ ,  $p<0.0001$ ) between CBF and NADH during CSD under hypoxia, partial ischemia and after L-NAME administration as compared to normoxia. This increase in interaction between CBF vs NADH may indicate a closer coupling between these two parameters under low tissue oxygenation during CSD. Conclusions: 1. The lack in oxygen, under hypoxia, partial ischemia and after inhibition of NO synthesis, became more severe during CSD propagation. The severity level was detected by the additional decrease in oxygen supply and oxygen balance. 2. CSD under different oxygen balance conditions can lead to changes in the interaction between O<sub>2</sub> supply and O<sub>2</sub> balance in brain tissue. References: (1) Lauritzen M. (1987). *Acta Neurol. Scand.* 76:1-40 (2) Sonn J. and Mayevsky A. (2000). *Brain Res.* 882:212-216.



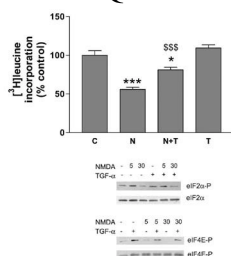
## NMDA MODULATES THE PHOSPHORYLATION OF SEVERAL TRANSLATION FACTORS AND INHIBITS PROTEIN SYNTHESIS IN NEURAL CULTURES

Valerie Petegnief<sup>1</sup>, M. Elena Martin<sup>2</sup>, Matilde Salinas<sup>2</sup>, Anna M. Planas<sup>1</sup>

<sup>1</sup>Department of Pharmacology and Toxicology, IIBB-IDIBAPS, Barcelona, <sup>2</sup>Servicio de Bioquímica-Investigación/Hospital Ramon Y Cajal, Madrid, Spain

**Introduction:** Persistent inhibition of protein synthesis dooms neurons to death after cerebral ischemia<sup>1</sup>. Excitotoxicity is also well-known to inhibit translation but the underlying mechanisms are not fully understood<sup>2,3</sup>. Translation is regulated by the phosphorylation state of some eukaryotic initiation and elongation factors (eIFs and eEFs). Phosphorylation of eIF2 $\alpha$ <sup>Ser51</sup> and eEF2<sup>Thr56</sup> are associated with protein synthesis inhibition. Here, we studied protein synthesis and the phosphorylation of the Akt and Erk1/2 upstream kinases and/or the function of several translation factors during N-methyl-D-aspartate (NMDA) lesion in neuron/glia cultures. In addition, we studied how insulin and transforming growth factor- $\alpha$  (TGF- $\alpha$ ), that stimulate Akt and Erk1/2 respectively, affected protein synthesis. Finally, since many deleterious effects of NMDA are attributable to NO<sup>4</sup>, we also tested whether neuronal NOS (nNOS) inhibition reverted the NMDA effect. **Methods:** Primary rat neuron/glia cortical cultures were exposed for 5 or 30 min to 35  $\mu$ M NMDA<sup>3</sup>. Thereafter, cells were collected and processed for phospho-eIF2 $\alpha$ , -eIF4E, -eIF4E-BP-1, -eEF2, -Akt, -Erk1/2 western blots. Protein synthesis was measured by incorporation of [<sup>3</sup>H]leucine into proteins after exposure to NMDA for 15 or 30 min. Phosphatases, eIF2B and eIF4F activities were measured after 30 min, as described<sup>5,6</sup>. Cultures were treated with TGF- $\alpha$  (100ng/ml), insulin (1 $\mu$ g/ml) or 7-nitroindazole (7-NI) (100 $\mu$ M). **Results:** We found that NMDA induced 21% and 42% inhibition of protein synthesis (ANOVA, P<0.01, n $\ge$ 8) after 15 and 30 min, respectively. A 5-min exposure to NMDA caused eIF2 $\alpha$  phosphorylation, which decreased below control after 30 min. This later effect was concomitant with dephosphorylation of Akt, eIF4E and eIF4E-BP-1, while phospho-eEF2 was not modified and phospho-Erk1/2 was increased compared to control. In spite of these dephosphorylations, NMDA did not alter PP2A and total phosphatase activities. NMDA affected neither eIF4F nor eIF2B activities. The NMDA-induced translation inhibition was not affected by insulin but it was partly prevented by TGF- $\alpha$  (ANOVA, P<0.05, n=11), which phosphorylated eIF4E and decreased by 50% PP2A activity (ANOVA, P<0.01, n $\ge$ 9). 7-NI, an inhibitor of nNOS, did not revert the inhibition of protein synthesis induced by NMDA. **Conclusions:** NMDA induced a strong decrease in translation in mixed neuron/glia cultures that may be related to a transient phosphorylation of eIF2 $\alpha$ . This inhibition is not mediated by reduction of eIF2B and eIF4F activities, by phosphorylation of eEF2 or by nNOS activation. TGF- $\alpha$ , but not insulin, was able to partially prevent this NMDA effect; the underlying mechanism is currently under investigation.

**References** (1) DeGracia et al. 2002, J. Cereb.Blood Flow Metab 22:127 (2) Marin et al. 1997, J. Neurosci. 17: 3445 (3) Petegnief et al., 2003, J. Biol. Chem 278: 29552 (4) Sattler et al, 1999, Science 284: 1845 (5) Quevedo et al, 2003. J. Biol. Chem. 19: 16579 (6) artín de la Vega et al, 2001. Biochem. J. 357: 819





### MILD HYPOTHERMIA INHIBITS FAS EXPRESSION AND CASPASE-8 ACTIVATION FOLLOWING EXPERIMENTAL STROKE

Jong Youl Kim<sup>2</sup>, Liping Liu<sup>1</sup>, Danye Cheng<sup>3</sup>, Maya Koike<sup>1</sup>, Francis Blankenberg<sup>3</sup>,  
Jong Eun Lee<sup>2</sup>, Midori A Yenari<sup>1</sup>

<sup>1</sup>Neurology, University of California, San Francisco & San Francisco VAMC, San Francisco, CA, USA

<sup>2</sup>Anatomy & BK21 Project for Medical Science Institute of Bioscience and Biotechnology, Yonsei University, Seoul, Korea

<sup>3</sup>Radiology, Stanford University Medical Center, Stanford, CA, USA

**Introduction:** Mild hypothermia is protective, and is associated with less apoptosis. Prior work has established that this protective effect is associated with better mitochondrial preservation and thus, suppress of the intrinsic apoptotic pathway as evidenced by reduced cytosolic cytochrome c redistribution (3), decreased caspase-3 processing (5), and, in some reports, increased Bcl-2 (2, 4) and decreased Bax (1) expression. Only recently has it become recognized that brain tissue may undergo apoptotic death via the extrinsic, or receptor mediated pathways. One of the most studied of these pathways is that triggered by Fas/FasL, leading to caspase-8 activation. **Methods:** Male Sprague Dawley rats were subjected to 2 h middle cerebral artery occlusion (MCAO) with 2 h intraischemic mild hypothermia (brain temperature=33C). Brain tissue was collected 2 (n=9), 6 (n=8) and 24 h (n=18) for histology, immunostaining and Western blot analysis in a manner previously published by our group (3), and assessed for Fas, FasL and caspase-8 expression. Double immunofluorescent labeling was also performed to identify Fas and caspase-8 levels in neurons (NeuN), astrocytes (GFAP) and phagocytes (ED1). To more directly assess the significance of the Fas/FasL pathway in ischemic stroke, 11 rats were treated with 400 mg of anti-FasL antibody (Pharmingen) (or vehicle) i.p. immediately upon reperfusion and 3 days later, then assessed at 7 d. **Results:** Mild hypothermia significantly reduced infarct size and reduced numbers of TUNEL positive cells (P<0.05). Double immunofluorescent labeling at 24 h indicated that Fas was expressed largely in neurons and phagocytes as well as some astrocytes. Interestingly, caspase-8 was observed in phagocytes, rare astrocytes but no neurons. There was no significant change in the staining pattern among hypothermic animals. Mild hypothermia significantly reduced expression of Fas (P<0.05) and processed (but not pro-) caspase-8 (P<0.05). Interestingly, FasL levels were increased by mild hypothermia. Among rats treated FasL antibody, infarct size was significantly reduced by 87% compared to vehicle treatment (P<0.01). Similarly, numbers of TUNEL positive cells were also reduced in FasL antibody treated brains (P<0.05). **Conclusions:** The Fas/FasL apoptotic pathway is involved in cell death following experimental stroke, as FasL antibody treatment is neuroprotective. Mild hypothermia is associated with reduced Fas expression and caspase-8 activation. Even though mild hypothermia increases FasL expression, the reduction in Fas receptor may explain the reduction in apoptosis by this pathway. Alternatively, some reports have proposed that proteases such as the matrix metalloproteinases (MMPs) trigger the Fas pathway by cleaving FasL, liberating it to stimulate its receptors. Since mild hypothermia also reduces MMPs (6,7), it is possible that mild hypothermia may prevent FasL cleavage and thus inhibit Fas-mediated apoptosis by inhibiting upstream MMPs. **References:** 1: Eberspacher E et al. J Neurosurg Anesthesiol. 2003 15(3):200-8. 2: Inamasu J et al. Acta Neurochir Suppl. 2000;76:525-7. 3: Yenari MA et al. J Cereb Blood Flow Metab. 2002 22(1):29-38. 4: Zhang Z et al. Mol Brain Res. 2001 95(1-2):75-85. 5: Phanithi PB et al. Neuropathology. 2000 20(4):273-82. 6: Hamann GF et al. Stroke. 2004 35(3):764-9. 7: Wagner S et al. Brain Res. 2003 984(1-2):63-75.

**NEUROPROTECTION AGAINST ISCHEMIC CA1 NEURODEGENERATION BY PITUITARY ADENYLATE CYCLASE ACTIVATING POLYPEPTIDE VIA CAMP-RESPONSE-ELEMENT-BINDING PROTEIN-MEDIATED ENHANCEMENT OF ENDOGENOUS DNA REPAIR**

Wenjin Li<sup>1</sup>, Yumin Luo<sup>1</sup>, Masanori Iwai<sup>1</sup>, Yanqin Gao<sup>2</sup>, Guodong Cao<sup>1</sup>, **Jun Chen**<sup>1,3</sup>

<sup>1</sup>*Neurology, University of Pittsburgh, Pittsburgh, PA, USA*

<sup>2</sup>*National Key Laboratory of Neurobiology, Fudan University, Shanghai, China*

<sup>3</sup>*Geriatric Research, Educational and Clinical Center, Pittsburgh VA Health Care System, Pittsburgh, PA, USA*

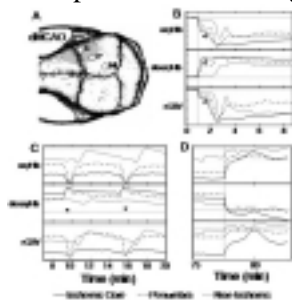
Emerging evidence suggests that accumulation of oxidative DNA damage in nuclear genome is an important contributing factor in neuronal cell death after cerebral ischemia. It has been shown in various models of cerebral ischemia/reperfusion that there is accumulation of oxidative DNA base damage and apurinic/apyridinic abasic site (AP site) in injured neurons, which could mediate neuronal degeneration by triggering various pro-apoptotic molecules. In the brain most types of oxidative DNA damage are repaired via the base-excision repair (BER) pathway that is highly inducible in response to various sublethal stimuli. Thus, interventions that enhance the activity of the BER pathway may be a potential therapeutic strategy against ischemic cell death. In the present study, we have examined the neuroprotective effect of the neuropeptide pituitary adenylate cyclase activating polypeptide (PACAP) in the rat model of transient global cerebral ischemia. Further, we have investigated the role of BER regulation as a potential mechanism underlying the effect of PACAP. PACAP, when infused intracerebroventricularly in the rat, potently protected against CA1 neuronal cell death after global cerebral ischemia produced by 12 minutes of 4-vessel occlusion. Associated with this neuroprotection, PACAP treatment reduced the accumulation of oxidative DNA lesions, especially AP site, and subsequently attenuated the activation of pro-apoptotic molecules p53 and PUMA in the CA1 sector, suggesting that the effect of PACAP may involve the acceleration of the repair process of endogenous oxidative DNA damage. To investigate the underlying mechanism, cellular BER activity and the expression of BER enzymes were measured in the hippocampal extracts. The results revealed that PACAP markedly enhanced the hippocampal expression (at both mRNA and protein levels) and activities of the essential BER enzymes AP endonuclease (APE) and DNA polymerase-beta. Furthermore, based on the results of inhibition studies, the inducible effect of PACAP on the BER pathway was found to be dependent on the phosphorylation and nuclear translocation of cAMP-response-element-binding protein (CREB), which mediated the enhanced transcription of both APE and DNA polymerase-beta. Finally, the effect of PACAP on BER and neuroprotection was mimicked by the administration of a cAMP/protein kinase A (PKA) agonist. The results of the present study demonstrate the neuroprotective effect of PACAP in hippocampal CA1 neurons after transient global cerebral ischemia. The effect of PACAP is dependent on the activation and nuclear translocation of CREB, and involves CREB-mediated activation of BER pathway for endogenous DNA repair. The results suggest that enhancement of neuronal DNA repair capacity by PACAP or other means may be a novel potential therapeutic approach to limit ischemic neuronal loss. (This project was supported by NIH grants NS36736, NS38560, NS 43802, and NS45048)

## SIMULTANEOUS MULTIMODAL OPTICAL IMAGING OF CEREBRAL BLOOD FLOW AND OXYGENATION IN FOCAL ISCHEMIC CORE AND PENUMBRA IN MICE

Hwa Kyoung Shin<sup>1</sup>, Phillip Jones<sup>2</sup>, Andrew K. Dunn<sup>2</sup>, David A. Boas<sup>2</sup>, Michael A. Moskowitz<sup>1</sup>,  
Cenk Ayata<sup>1,3</sup>

<sup>1</sup>Stroke and Neurovascular Regulation Lab, Department of Radiology, <sup>2</sup>Martinos Center for Biomedical Imaging, Department of Radiology, <sup>3</sup>Stroke Service and Neurointensive Care Unit, Department of Neurology, Massachusetts General Hospital, Harvard Medical School, Boston, MA, USA

**Background:** Anoxic depolarization (AD) and periinfarct spreading depressions (PISDs) perturb membrane ionic balances and impose additional metabolic burden on ischemic brain. We developed a multimodal optical imaging system to investigate the effects of AD and PISDs on oxygen delivery and utilization in the core and penumbra with high spatial and temporal resolution. **Methods:** We performed real-time 2D multispectral reflectance imaging and laser speckle flowmetry through intact skull, to simultaneously image changes in oxyhemoglobin (oxyHb), deoxyhemoglobin (deoxyHb), total hemoglobin (rCBV), and rCBF in focal cerebral ischemia and reperfusion. Ischemia was induced by distal middle cerebral artery occlusion (dMCAO) for 60-90 minutes through a temporal craniotomy, in intubated and ventilated mice under full physiological monitoring. **Results:** dMCAO reduced rCBF to 20-30% of baseline in the core, while rCBV initially remained unchanged (B, vertical line). Within 1-2 minutes after dMCAO AD developed (B, arrowhead) and caused a large reduction in rCBV, suggesting active vasoconstriction or passive vascular collapse. This was accompanied by a further drop in rCBF in the core (15-20% of baseline). DeoxyHb abruptly increased in the core upon dMCAO, and did not significantly change during AD, whereas changes in oxyHb closely followed those of rCBV and rCBF. PISDs (2-3/h) caused further reductions in rCBV, rCBF and oxyHb both in the core and the penumbra (C, \*). DeoxyHb was increased by PISDs both in the core and the penumbra, suggesting that oxygen consumption continues in these ischemic territories. A ring of relative increase in rCBV invariably surrounded the infarct rim. Upon reperfusion (D, vertical dashed line), rCBF, rCBV and oxyHb increased and deoxyHb decreased towards baseline levels; in about 30% of experiments deoxyHb decreased below pre-ischemic levels, suggesting that oxygen utilization in the severely ischemic core failed to recover completely upon reperfusion. **Conclusion:** These data suggest that AD and PISDs increase oxygen consumption and reduce oxygen delivery in both the core and the penumbra. Multispectral reflectance imaging simultaneously with LSF provides better understanding of the dynamic changes in rCBF and tissue oxygenation during acute focal cerebral ischemia, and may identify irreversible metabolic injury in focal ischemia and reperfusion. **Figure:** (A) Regions of interest used to quantify the changes in oxyHb, deoxyHb and total Hb. C: core, P: penumbra, NI: non-ischemic cortex. (B) Changes at the onset of dMCAO (vertical dashed line) and after AD (arrowhead). (C) Effects of PISDs (\*). (D) Changes upon reperfusion (vertical dashed line). Horizontal lines indicate pre-ischemic baseline. Vertical axis shows changes in oxyHb, deoxyHb and total Hb (rCBV) in arbitrary units. Horizontal axis shows time after dMCAO. (B), (C), and (D) are representative tracings from separate experiments.





**FREE RADICAL GENERATION IS INVOLVED IN HYPOGLYCEMIA-INDUCED NEURONAL DEATH**Sang Won Suh, Koji Aoyama, Elizabeth Gum, **Raymond A. Swanson***Department of Neurology, University of California, San Francisco and Veterans Affairs Medical Center, San Francisco, CA, USA*

It is now recognized that neuronal death after hypoglycemia is not a simple result of energy failure resulting from hypoglycemia, but is instead the result of a cell death program that is initiated by hypoglycemia. It will be important to fully understand the sequence of events in this cell death pathway in order to identify late, downstream points at which intervention can be made. A rat model of insulin-induced hypoglycemia was used to assess vesicular zinc release, superoxide production, and the therapeutic potential of a superoxide dismutase (SOD) mimetic, 4-hydroxy-2,2,6,6-tetramethylpiperidine-1-oxyl (TEMPOL). Hypoglycemia was induced by 15 U / kg insulin injection and terminated by glucose infusion after 30 minutes of isoelectric EEG. Vesicular zinc staining with N (6 methoxy 8 quinolyl) para toluenesulfonamide (TSQ) showed that glucose reperfusion potentiated vesicular zinc release from the hippocampus, and that this release is prevented by the neuronal nitric oxide synthase (NOS) inhibitor, 7-nitroindazole (7NI). Dihydroethidine (dHEt) detection of superoxide showed superoxide production to be only minimally increased during hypoglycemia, but markedly increased by re-infusion of glucose. This superoxide production was attenuated by intraventricular injection of a zinc chelator, disodium calcium ethylene-diamine tetraacetic acid (CaEDTA), suggesting that zinc release is upstream event of superoxide production. Treatment with TEMPOL before the glucose reperfusion blocked production of superoxide and reduced neuronal death by more than 60% in hippocampus and cortex when evaluated 1 week after the hypoglycemia. These results suggest that glucose reperfusion-induced vesicular zinc release and subsequent superoxide production are major factors mediating hypoglycemic neuronal death, and that superoxide mimetics can rescue neurons that would otherwise die after severe hypoglycemia. Juvenile Diabetes Research Foundation (SWS, JDRF3-2004-298), Department of Veterans Affairs, and NIH (RAS, NS41421, NS051855-01).

**APOPTOSIS IS MAINLY INDUCED IN ASTROCYTE BUT NOT MEDIATED VIA ANGIOTENSIN AT1 RECEPTOR AFTER CEREBRAL ISCHEMIA**

**Jun Li**, Christa Thöne-Reineke, Nadezhda Gerova, Melanie Timm, Mathias Zimmermann, Maxim Krikov, Thomas Unger

*Center for Cardiovascular Research (CCR), Institute of Pharmacology and Toxicology, Charité - University Medicine Berlin, Berlin, Germany*

Our recent findings suggest that angiotensin AT2 receptor-mediated neuroprotection is required for the beneficial actions of angiotensin AT1 receptor antagonist in rat models of brain ischemia. It is unknown whether a direct inhibition of cerebral AT1 receptor-mediated actions (i.e. apoptosis) is also contribute to these cerebroprotections of AT1 receptor antagonists. The present study was designed to examine the in vivo role of AT1 receptors in cerebral ischemia-induced apoptosis. We first assessed apoptosis induction in the brain in response to transient unilateral medial cerebral artery occlusion in rats by Western blot analysis and immunofluorescence staining. Forty-eight hours after ischemia, Western blot analysis showed an upregulation of p53 in the peri-infarct zone when compared to sham operated controls. Immunofluorescence staining further revealed that cerebral ischemia induced the expression of cleaved caspase-3 in the peri-infarct zone when compared to contralateral side or sham operated controls. By double immunofluorescence staining, we could confirm that both AT1 receptor and increased cleaved caspase-3 were mainly located in GFAP+ astrocytes. To clarify the in vivo role of AT1 receptor in astrocyte apoptosis, an AT1 receptor antagonist (candesartan, 0,1 mg/kg) was injected subcutaneously over a period of 5 days before cerebral ischemia. Candesartan significantly improved neurological outcome and reduced the infarct size forty-eight hours after cerebral ischemia. However, the upregulated p53 and cleaved caspase-3 remained unaltered after candesartan treatment. Thus, brain AT1 receptors do not seem to be involved in astrocyte apoptosis following cerebral ischemia. These findings indicate that a direct inhibition of apoptosis in the brain may not play a role in the neuroprotective effects of the AT1 receptor antagonist after cerebral ischemia.

**REDISTRIBUTION OF APOPTOSIS PROMOTERS: XAF1, SMAC/DIABLO AND HTRA2 DURING TRANSIENT FOREBRAIN ISCHEMIA/REPERFUSION****Abdelhaq Rami, Markus David Siegelin***Dr Senckenbergische Anatomy - Department of Anatomy III, University Clinic, Frankfurt, Germany*

The neuropathology following brain injury after cerebral ischemia includes both, selective neuronal necrosis and apoptosis. Caspases are key regulators of apoptosis and are essential for the execution of cell death. Caspase activity is controlled through a wide range of regulatory mechanisms, including a family of genes encoding for inhibitors of apoptosis proteins (IAPs). Convincing anti-apoptotic activity has been shown for a subset of mammalian IAPs. XIAP, cIAP1, cIAP2. XIAP (X-linked inhibitor of apoptosis protein) is the best characterized mammalian IAP and is also the most potent and versatile regulator of cell death. Regulation of XIAP involves at least three recently discovered proteins: XAF-1 (XIAP-associated factor 1), Smac/Diablo (Second mitochondrial activator of caspase/direct IAP-binding protein with low pI) and HtrA2/Omi (high-temperature requirement serine protease A2 or Omi). XAF-1 is ubiquitously expressed in normal tissues and inhibits XIAP and localized in the nucleus. When co-expressed in cell lines, XAF-1 retains normally cytosolic localized XIAP in the nucleus. To investigate whether IAPs and their inhibitors XAF1, Smac/DIABLO, HtrA2 may play a role in the apoptotic machinery after ischemia, we analyzed dynamics in their expression pattern and in their localisation. Ischemia was performed in Wistar rats by clamping both common carotid arteries and reducing blood pressure to 40 mmHg for 10 min. Animals were decapitated at different times post-ischemia and processed for histology, immunohistochemistry and immunoblotting by using antibodies directed against XIAP-BIR2, Smac/DIABLO, HtrA2 and cleaved caspase-3 (P17). XAF-1 staining and colocalization with XIAP was seen in the selectively vulnerable CA1-subfield of the hippocampus. In damaged neurons, we found that XAF-1 colocalized with XIAP in the nuclei, suggesting that it sequestered XIAP, allowing the pathological apoptosis to proceed. Smac/Diablo is a mitochondrial protein, which binds to XIAP, antagonizing its anti-apoptotic activity. This role of XIAP is supported by our findings, as it colocalized after ischemia very well with Smac, and as these double-labelled cells presented signs of damage. HtrA2 is another mitochondrial protein released upon apoptotic stimuli that binds to XIAP and promotes cell death. The strong HtrA2 immunoreactivity around the nuclei of damaged neurons, that stained also for XIAP and Smac, supports a concerted action of these proteins after ischemia. Increased intensity of Smac and HtrA2 stainings presumably indicates release from mitochondria. Here presented data report to our knowledge for the first time an involvement of XAF-1 and HtrA2 in the apoptotic dynamics following global cerebral ischemia in rats.

**SPREADING DEPOLARIZATIONS IN HUMAN TRAUMATIC BRAIN INJURY****Jed A. Hartings<sup>1</sup>**, Anna T. Mazzeo<sup>3</sup>, Martin Fabricius<sup>2</sup>, Frank C. Tortella<sup>1</sup>, M. Ross Bullock<sup>3</sup><sup>1</sup>*Division of Psychiatry and Neuroscience, Walter Reed Army Institute of Research, Silver Spring, MD, USA*<sup>2</sup>*Department of Clinical Neurophysiology, Glostrup Hospital, Copenhagen, Denmark*<sup>3</sup>*Department of Neurosurgery, Virginia Commonwealth University, Richmond, VA, USA*

In experimental stroke, recurrent peri-infarct depolarizations (PIDs) are known to mediate the progressive deterioration of penumbral border zones into core infarction. PIDs are similar to cortical spreading depression (CSD), except that the hyperemia accompanying CSD is replaced by transient or permanent decrease in cerebral blood flow, exacerbating ischemic conditions. In rats and humans, CSD-like spreading depolarizations (SD) also occur following traumatic brain injury (TBI), although the hemodynamic correlates (i.e. CSD vs. PID) have not yet been determined. Nonetheless, Strong et al. have shown that SDs occurring over the initial days post-injury are associated with development of low brain glucose, suggesting a detrimental PID-like effect. Here we investigate clinically the correlates and incidence of SD in TBI. Patients requiring craniotomy for lesion/hematoma evacuation and/or decompression were enrolled in the Co-Operative Study on Brain Injury Depolarizations ([www.cosbid.org](http://www.cosbid.org)) after obtaining research consent. Sub-dural linear electrode strips with six contacts were implanted near the contused region during the craniotomy procedure and four-channel recordings, AC amplified with a 0.02 Hz high pass cutoff, were then made in a sequential bipolar recording configuration. A microdialysis catheter was implanted intraparenchymally near the strip to monitor neurochemistry. Patients were ventilated, paralyzed, and sedated with morphine. Recordings were terminated immediately prior to withdrawal from sedation. SDs were identified by analyzing the amplitude of the electrocorticogram (ECoG) and shifts in the ECoG baseline potential which reflect the DC potential negativity caused by depolarization. Criteria for identification of SDs were an abrupt, >50% decrement of ECoG amplitude on at least one channel, followed by gradual recovery, and sequential baseline shifts on at least two channels. Six male patients aged 18-67 were enrolled with GCS 4-9 upon admission. ECoG strips were placed in either the left temporal (n=3) or right frontal lobe (n=3). Recordings were initiated from 0.6 to 5 days post-injury and recording durations thereafter ranged from 2.0 to 5.7 days, with a median of 5.0. Three of six patients (50%) experienced recurrent SDs numbering 4, 6, and 14. All SDs occurred between days 3-8 post-injury, but the majority of events (14/24; 58%) occurred on day six. In two patients, several (4 and 7) SDs recurred regularly at short intervals not exceeding 4 h and 2.5 h, respectively. During these periods, mean body temperatures were 38.5°C and 38.8°C, respectively, and always exceeded 37.8°C and 38.0°C. These results confirm the common occurrence of CSD-like depolarizations in the human brain as a sequela of TBI. Previously Strong et al. found, with similar recordings of a mean 36 h duration, that 4/11 (36%) patients with traumatic intracranial hemorrhages exhibited CSD-like events. The present results suggest that CSD-like events may have an even higher incidence and a delayed or prolonged time course. Results further suggest that episodes of fever may create a permissive environment for the initiation/propagation of depolarizations, consistent with the effectiveness of hypothermia to suppress PIDs in experimental stroke. Other factors influencing the occurrence of SD as well as effects on neurochemistry, hemodynamics, and outcome are under investigation by COSBID.

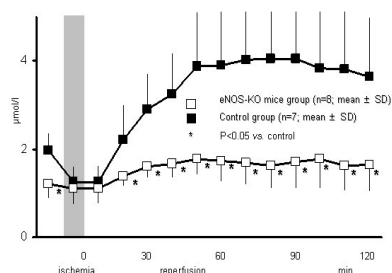
## NITRIC OXIDE PRODUCTION DURING CEREBRAL ISCHEMIA AND REPERFUSION IN ENDOTHELIAL NITRIC OXIDE SYNTHASE KNOCKOUT MICE

Yasuo Ito, Nobuo Araki, Takeshi Ohkubo, Yosio Asano, Masahiko Sawada, Daisuke Furuya, Kimihiko Hattori, Tomokazu Shimazu, Harumitsu Nagoya, Masakiyo Yamazato, Yuji Kato, Mikiko Ninomiya, Kunio Shimizu

*Neurology, Saitama Medical School, Saitama, Japan*

**Introduction:** It is suggested that endothelial nitric oxide synthase (eNOS) is closely related to cerebral autoregulation because cerebral autoregulation is impaired in eNOS knockout mice [1]. It is also suggested that eNOS may protect brain tissue during cerebral ischemia. The purpose of this study is to investigate the cerebral blood flow and the kinetics of cerebral production of NO during cerebral ischemia and reperfusion and the activity of nNOS in mice deficient in eNOS. **Methods:** (1) Male eNOS knockout mice [n=8] and control mice (C57BL/6 mice [n=7]) were anesthetized by halothane. NO production was continuously monitored by in vivo microdialysis. Microdialysis probes were inserted into the left striatum and perfused with Ringer's solution at a constant rate 2  $\mu$ l/min. Laser Doppler probes were also inserted into the right striatum. Fractions were collected every 10 minutes. Forebrain cerebral ischemia was produced by occlusion of both common carotid arteries for 10 minutes. Levels of nitric oxide metabolites, nitrite (NO<sub>2</sub><sup>-</sup>) and nitrate (NO<sub>3</sub><sup>-</sup>), in the dialysate were determined using the Griess reaction. (2) Brain sections were immunostained with an anti-nNOS antibody. To determine the fractional area density of nNOS-immunoreactive pixels to total pixels of the whole field, the captured images were analyzed. Mann-Whitney U test was used for group comparisons. **Results:** 1) Blood Pressure: eNOS knockout group (85.0  $\pm$  18.4 mmHg) showed significantly higher blood pressure than that of the control group (68.6  $\pm$  10.9), before ischemia, and 10, 60, 80 minutes after the start of reperfusion. 2) Cerebral Blood Flow (CBF): No significant differences were obtained between the two groups. 3) Nitric oxide metabolites: (1) NO<sub>2</sub><sup>-</sup>: There were no significant differences between the two groups. (2) NO<sub>3</sub><sup>-</sup>: eNOS knockout group (1.20  $\pm$  0.33  $\mu$ mol/L) showed significantly lower than that of control group (1.97  $\pm$  0.49) before ischemia, and 20~120 minutes after the start of reperfusion. (Fig.1) (3) total NO (NO<sub>2</sub><sup>-</sup>+ NO<sub>3</sub><sup>-</sup>): eNOS knockout group (3.04  $\pm$  0.37  $\mu$ mol/L) showed significantly lower than that of the control group (4.35  $\pm$  1.01  $\mu$ mol/L) at 10 minutes before ischemia, and 30~120 minutes after the start of reperfusion. (4) nNOS activity: There were no significant differences in the percentage of nNOS-immunoreactive pixels to whole area between eNOS knockout group (0.57  $\pm$  0.61%) and the control group (0.60  $\pm$  0.68%). **Conclusion:** The above data suggested that high blood pressure in the eNOS knockout mice may be due to lack of NO production by eNOS, and that NO production in striatum during ischemia and reperfusion is closely related to both activity of nNOS and eNOS. **References:** [1] Huang Z et al: Enlarged infarct in endothelial nitric oxide synthase knockout mice are attenuated by nitro-L-arginine. *J Cereb Blood Flow Metab* 16:981-987, 1996.

Figure 1. The level of the NO<sub>3</sub><sup>-</sup>

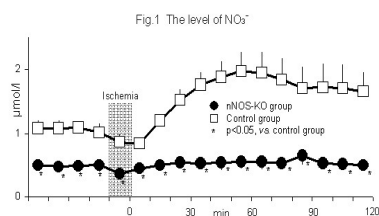


## NITRIC OXIDE PRODUCTION DURING CEREBRAL ISCHEMIA AND REPERFUSION IN NEURONAL NITRIC OXIDE SYNTHASE KNOCKOUT MICE

Y. Kato, N. Araki, T. Ohkubo, Y. Asano, M. Sawada, D. Furuya, K. Hattori, T. Shimazu,  
M. Yamazato, H. Nagoya, Y. Ito, M. Ninomiya, K. Shimazu

*Department of Neurology, Saitama Medical School, Saitama, Japan*

**Introduction:** Nitric oxide (NO) plays an important role in the pathogenesis of neuronal injury during cerebral ischemia. [1] It was reported that infarct volumes in nNOS knockout mice decreased significantly 24 hours after middle cerebral artery occlusion and was suggested that nNOS exacerbated acute ischemic injury. Therefore, we investigated the dynamics of cerebral NO production in nNOS knockout mice during cerebral ischemia and reperfusion. **Methods:** Male nNOS knockout mice (n = 6) and littermate mice (control group) (n = 7) were anesthetized by halothane. NO production was continuously monitored by in vivo microdialysis. Microdialysis probes were inserted into the left striatum and perfused with Ringer's solution at a constant rate 2  $\mu$ l/min. Laser Doppler probes were also inserted into the right striatum. After 2 hours equilibrium period, fractions were collected every 10 minutes. Forebrain cerebral ischemia was produced by occlusion of both common carotid arteries for 10 minutes. Levels of nitric oxide metabolites, nitrite (NO<sub>2</sub><sup>-</sup>) and nitrate (NO<sub>3</sub><sup>-</sup>), in the dialysate were determined using the Griess reaction. Brain sections were immunostained with an anti-nNOS antibody (polyclonal, 1:400, Zymed). To determine the fractional area density of nNOS-immunoreactive pixels to total pixels of the whole field, the captured images were analyzed. Mann-Whitney U test was used for group comparison analysis. **Results:** (1) Blood Pressure: There were no significant difference between nNOS knockout mice (78.9  $\pm$  6.9 mmHg; mean  $\pm$  SD) and control group (66.5  $\pm$  8.0). Only in 120 minutes after reperfusion, nNOS knockout mice (77.5  $\pm$  15.4) showed significantly higher blood pressure than those of control group (57.9  $\pm$  14.7) in 120 minutes after reperfusion. (2) Cerebral Blood Flow (CBF): During cerebral ischemia, no significant differences in CBF were observed between the two groups. CBF in nNOS knockout mice (61.1  $\pm$  19.5 % of the baseline level) was significantly higher than that of control group (42.1  $\pm$  9.5 %) in 70, 90~120 minutes after the start of reperfusion. (3) Nitric oxide: a) NO<sub>2</sub><sup>-</sup>: No significant differences were seen in the two groups. b) NO<sub>3</sub><sup>-</sup>: The levels of NO<sub>3</sub><sup>-</sup> in nNOS knockout mice were significantly lower than those of control group before and during ischemia, and during reperfusion (Fig.1). (4) nNOS activity : The percentage of nNOS-immunoreactive pixels to whole area in nNOS knockout mice (0.06  $\pm$  0.12%) was significantly lower than that of the control group (0.62  $\pm$  0.57 %). **Conclusion:** The above data suggest that nNOS leads to neurotoxicity by producing NO during cerebral ischemia and reperfusion. **Reference:** [1] Huang Z et al: Effects of cerebral ischemia in mice deficient in neuronal nitric oxide synthase, *Science* 265: 1883-1885, 1994.



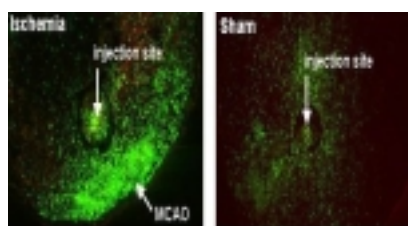
**MIGRATION AND MORPHOLOGY CHANGES OF BONE MARROW CELLS IN ISCHEMIC AND PERI-ISCHEMIC AREAS OF THE MOUSE BRAIN DEMONSTRATED BY CHRONIC IN VIVO IMAGING**

Alexy Tran Dinh<sup>1</sup>, Nathalie Kubis<sup>1</sup>, Yutaka Tomita<sup>1</sup>, Bartosz Karaszewski<sup>1</sup>, Yolande Calando<sup>2</sup>, Karim Oudina<sup>2</sup>, Hervé Petite<sup>2</sup>, Jacques Seylaz<sup>1</sup>, Elisabeth Pinard<sup>1</sup>

<sup>1</sup>INSERM U 689, Université Paris 7, Paris, France

<sup>2</sup>CNRS UMR 7052, Université Paris 7, Paris, France

**Introduction:** Many experimental approaches of cell therapy in cerebral ischemia are based on bone marrow grafts. These approaches generally need to sample the mouse brain, making any longitudinal analysis on each animal impossible. Here, we describe the fate of bone marrow cells (BMC) at the neocortical surface during several weeks of ischemic conditions, and report the complementary immunostaining study. **Methods:** A closed cranial window was chronically implanted over the left parietal cortex in C57/BL6 mice, the left MCA was occluded either proximally (n=4) or distally (n=5) across the window, as recently described<sup>1</sup>. Sham-operated mice were also studied (n=5). Fresh BMC overexpressing the green fluorescent protein (GFP) were injected (3x10<sup>5</sup> cells in 0.5µl) at 1-mm depth through the window 24h after ischemia or sham-operation. BMC were repeatedly analyzed in vivo through the window using confocal microscopy for 15 or 30 days. At the end of the in vivo investigation period, fixed brains were processed for immunocytochemistry. **Results:** In all mice, many green fluorescent round cells were present under the window just after injection. One day later, numerous elongated fluorescent cells were grouped toward the injured area in ischemic mice, whereas cells were scattered around the injection site in sham mice. On following days, the number of fluorescent cells under the window increased markedly (maximum at 15 days) and their localization beside the occlusion point was conspicuous in ischemic mice (fig.1), whereas cells disappeared or remained scattered in sham mice. Fluorescent cells appeared ramified, reminiscent of microglia. Histologically, migration of GFP-expressing cells toward the injured area was clearcut. Some individual fluorescent cells were along the corpus callosum, most cells were grouped in the peri-ischemic area, while some cells were within the lesion. Nearly all green fluorescent cells localized in the periphery of the lesion and exhibiting morphology changes expressed the Iba1 antigen, a microglial protein. These cells were often apposed on the wall of CD31-labeled microvessels. No other immunostaining (NeuN, GFAP, vimentin, actin, NG2) revealed any co-localization. **Figure 1:** Confocal images of fluorescent BMC under a cranial window 7 days after their local injection in an MCA-occluded mouse (left) and in a sham mouse (right). Note the high density of cells and their grouping toward the ischemic area, as opposed to the lower density and scattering of cells around the window in sham mice. **Conclusion:** The time-course of fluorescent BMC migration and phenotype changes was followed in vivo by confocal microscopy over 1 month. The use of 2 different occlusion points revealed that migration was specifically directed toward the lesioned area. Histology confirmed that BMC were attracted by the lesion and acquired a microglial phenotype. These data strongly support the use of BMC to target potential therapeutic factors to ischemic areas. **References:** 1- Tomita Y, Kubis N, Calando Y, et al (2005) J Cereb Blood Flow Metab In press



## NESTIN-EXPRESSING CELLS DIVIDE AND ADOPT A COMPLEX ELECTROPHYSIOLOGICAL PHENOTYPE AFTER TRANSIENT BRAIN ISCHEMIA

Golo D. Kronenberg<sup>1,2,4</sup>, Wang Li Ping<sup>3</sup>, Michael Synowitz<sup>3</sup>, Karen Gertz<sup>1</sup>, Juri Katchanov<sup>1</sup>, Rainer Glass<sup>3</sup>, Christoph Harms<sup>1</sup>, Gerd Kempermann<sup>4</sup>, Helmut Kettenmann<sup>3</sup>, Matthias Endres<sup>1</sup>

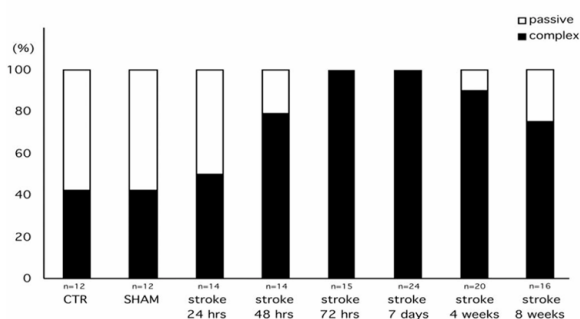
<sup>1</sup>Experimental Neurology, Charite, Berlin, Germany

<sup>2</sup>Department of Psychiatry, Charite, Berlin, Germany

<sup>3</sup>Cellular Neurosciences, Max-Delbrück-Center for Molecular Medicine, Berlin, Germany

<sup>4</sup>Neuronal Stem Cells, Max-Delbrück Center for Molecular Medicine, Berlin, Germany

The intermediate filament protein nestin is upregulated in response to cerebral ischemia; the significance of this, however, is incompletely understood. Here, we used transgenic mice that express green fluorescent protein (GFP) under control of the nestin promoter to characterize the fate of nestin-expressing cells up to 8 weeks following occlusion of the middle cerebral artery (MCAo) and reperfusion. The population of nestin-GFP+ cells increased in the ischemic lesion rim and core within 4 days, did not become TUNEL-positive and was detectable up to 8 weeks in the lesion scar. Nestin-GFP+ cells proliferated in situ and underwent approximately one round of cell division. They were not recruited in large numbers from the subventricular zone (SVZ) as indicated by absence of co-labeling with intracerebroventricularly injected dye DiI in the majority of nestin-GFP+ cells. Nestin-GFP+ cells expressed the chondroitin sulfate proteoglycan NG2 and nestin protein, but typically lacked mature astrocytic markers, i.e. glial fibrillary acidic protein (GFAP) or S100b. Vice versa, the majority of GFAP+ cells lacked nestin expression and surrounded the ischemic lesion by 4 days. The electrophysiological properties of nestin-GFP+ cells were analyzed in acute brain slices at different time points after MCAo/ reperfusion. Based on the membrane currents, two populations of nestin-GFP+ cells were identified. (1) A 'complex' current pattern was characterized by outwardly rectifying currents activated by depolarization and inward rectifying, inactivation currents induced with hyperpolarization. (2) The current profile of the second subpopulation was characterized by time and voltage-independent 'passive' currents. Recordings in acute slices from controls and sham-operated animals demonstrated that only about half of nestin-GFP+ cells displayed complex membrane properties and expressed AMPA receptors but lacked glutamate transporters similar to progenitor cells. In contrast, by 4 days after the insult all nestin-GFP+ cells expressed these properties (Figure 1). The absence of TUNEL-reaction in nestin-GFP+ cells and the fact that 24 hours following MCAo/ reperfusion, nestin-GFP+ cells were still detectable suggest that passive nestin-GFP+ cells had not undergone apoptosis or selective necrosis. We infer from our data that in response to the ischemic injury nestin-GFP+ cells with passive membrane properties transform into complex cells. We hypothesize that the change in physiological properties induced by the ischemic insult is directed toward a specific network function of nestin-expressing cells.



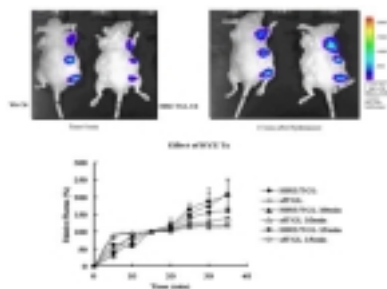


## MULTI-MODAL IMAGING OF ACUTE AND CHRONIC UP-REGULATION OF HYPOXIA-INDUCIBLE FACTOR-1 (HIF-1) IN GLIOMAS

Tadashi Miyagawa, Inna Serganova, Vladimir Ponomarev, Ronald Blasberg

*Department of Neurology, Memorial Sloan-Kettering Cancer Center, New York, NY, USA*

**Objective:** Detection and assessment of tumor hypoxia, blood flow dependent hypoxia (acute) and oxygen diffusion dependent hypoxia (chronic), are important to understand tumor biology. This study addresses whether in vivo multi-modal imaging systems can be used for assessment of acute and chronic up-regulation of hypoxia-inducible factor-1 (HIF-1) in astrocytic tumors. **Methods:** A multimodality reporter gene system for radionuclide, fluorescence, and bioluminescence (BLI) imaging was developed [1] and placed under the control hypoxia responsive elements (HRE/TGL), and transduced to C6 and RG2 cells. After selection using flow cytometry, HRE/TGL-RG2 and -C6 cells were implanted subcutaneously in mice. Constitutively expressing TGL and wild-type tumor cells were also implanted in the same animals as positive and negative controls, respectively. Acute tumor hypoxia was induced by i.p. injection of Hydralazine (HYZ). To investigate the feasibility of BLI to image acute up-regulation of HIF-1, sequential BLI was performed with or without HYZ treatment. Thereafter, autoradiographic imaging was performed following [18F]-FDG, [3H]-Xanthine and [14C]-FIAU administration to investigate the quantitative and spatial relationship between glucose metabolism, tumor blood flow and HIF-1 expression, respectively [2]. **Results:** HYZ treatment significantly increased BLI photon emission intensity in the HRE/TGL tumors, but not in positive and negative control tumors. Radiotracer evaluations revealed that HYZ reduced tumor blood flow from 0.36 to 0.10 (ml/min/g), suggesting that HYZ can induce acute tumor hypoxia by decreasing blood flow. Autoradiographic images showed a good spatial relationship between FDG and FIAU uptake in viable, non-necrotic portions of the tumors, indicating enhanced glucose metabolism in the same tumor regions with up-regulation of HIF-1 expression. Microscopic observation showed that GFP and immunostaining with pimonidazole were consistent with the FDG and FIAU autoradiograms. **Conclusion:** The multimodality HRE/TGL reporter system can be used to visualize hypoxic conditions by fluorescence, BLI and radiotracer imaging. BLI appears to be very sensitive to changes induced by acute hypotension, and to chronic hypoxic conditions in large tumors. HIF-1 expression in tumors, as assessed by FIAU uptake, occurred in a blood flow-dependent manner. 1. V. Ponomarev, et al. A novel triple-modality reporter gene for whole-body fluorescent, bioluminescent, and nuclear noninvasive imaging. *Eur J Nucl Med Mol Imaging*. 31(5): 740 (2004) 2. T Miyagawa, RG Blasberg. Quantitative Measurement of Local Cerebral Blood Flow in Mice :A comparative study for [14C]-Iodoantipyrine, [3H]-Antipyrine, [3H]-Nicotine and [3H]-Xanthine. *J Cereb Blood Flow Met* 23: s125 (2003).



**CEREBRAL ISCHEMIA INDUCES DIFFERENT REGULATION EVENTS IN THE HIPPOCAMPAL SUBFIELDS CA1 AND CA3 – A CELL-TYPE SPECIFIC EXPRESSION PROFILING STUDY**

**Oliver Sorgenfrei**<sup>1</sup>, Christine Böhm<sup>1</sup>, Dieter Newrzella<sup>1</sup>, Payam Pahlavan<sup>2</sup>, Wolfgang Kuschinsky<sup>2</sup>, Holger Hiemisch<sup>1</sup>, Armin Schneider<sup>1</sup>

<sup>1</sup>*Axaron Bioscience AG, Heidelberg, Germany*

<sup>2</sup>*Institute for Physiology and Pathophysiology, University of Heidelberg, Heidelberg, Germany*

**INTRODUCTION:** Different areas of the brain display different susceptibilities to ischemic insults. Most likely, the reason for this lies in differences in the expressed genome under normoxic conditions and/or differential regulation of gene expression after ischemia. One prominent and well-documented example of differential vulnerability to ischemia of similar cell-types are the hippocampal subfields CA1 and CA3. While several groups have put forward observations of individual genes differentially expressed in these neurons, we are the first to systematically study gene expression on the whole genome level in these regions by a novel technique that links laser microdissection to DNA-array analysis (“Axaminer™”). The identification of genes that confer ischemic resistance could provide novel pharmacological targets for cerebral ischemia. **MATERIALS:** Male C57/bl6 mice were subjected to combined unilateral occlusion of the CCA and subsequent generalized hypoxia as described<sup>1</sup>. 24 h after induction of ischemia, brains were rapidly removed and frozen. Expression profiles of the CA1 and CA3 regions were obtained with the Axaminer™ technology. I. e. laser microdissection was used to dissect the CA1 and CA3 regions from cryosections, RNA was extracted and amplified using a proprietary protocol, and hybridized to 21k DNA-arrays. Gene regulation in CA1 vs. CA3 regions from sham-treated and ischemic animals (N=4 each) was analyzed. **RESULTS:** Gene expression profiling of CA1 vs. CA3 neurons under normoxic conditions already detected about 500 differentially expressed genes. The analysis of each region under normoxic compared to hypoxic conditions revealed more than 2,000 regulated genes for each of the regions. The cell-type specific expression profiling approach making use of Axaminer™ enabled the investigation of the difference in adaptation of CA1 and CA3 neurons to ischemic conditions. The comparison of the regulation factors obtained for each region yielded a group of about 100 genes that exhibit differential regulation upon induction of ischemia. Among these were genes known to be involved in neuroprotection like inhibin beta-a and b, metallothioneins and genes that were hitherto not associated with neuroprotection opening new avenues for further research towards neuroprotective drugs. **CONCLUSION:** By using the novel Axaminer™ technique we could identify the differential functional genome under normoxic and hypoxic conditions in the two hippocampal subfields likely forming the basis of differing ischemic vulnerability. This knowledge can now be exploited for the development of new drugs for the treatment of cerebral ischemia. **References:** 1. Vannucci, S. J. et al. *J Cereb Blood Flow Metab* 21, 52-60 (2001). HH: present address: Office of Technology, Schering AG, 13342 Berlin, Germany

## THE CONSEQUENCES OF HERPES SIMPLEX VIRUS (HSV) VECTOR DELIVERY OF GADD34 ON FOCAL ISCHAEMIA IN THE MOUSE

F. White<sup>1</sup>, C. McCabe<sup>1</sup>, S.M. Brown<sup>2</sup>, J. Harland<sup>1</sup>, I.M. Macrae<sup>1</sup>

<sup>1</sup>*Division of Clinical Neuroscience, University of Glasgow, Glasgow, UK*

<sup>2</sup>*Crusade Laboratories Ltd., Glasgow, UK*

Growth arrest and DNA damage 34 (GADD34) is one of a family of proteins induced by endoplasmic reticulum stress, cell cycle arrest and DNA damage. GADD34 facilitates recovery of inhibited protein synthesis through the unfolded protein response (UPR). Protein synthesis inhibition is a critical event and a serious consequence of brain ischaemia. Originally, protein synthesis inhibition was thought to be protective, limiting the toxicity of misfolded proteins. However in the long-term it becomes maladaptive and detrimental to cell survival. We recently reported that GADD34 is upregulated in the peri-infarct zone following focal ischaemia in rodent and human brain. The aim of this investigation was to assess if overexpression of GADD34 (or its fragments) influenced ischaemic damage. The complete GADD34 gene (or amino or conserved carboxy terminal fragments) was cloned into a shuttle vector (RL1iresGFP) and recombinant HSV produced that expresses the novel gene in place of the gene coding ICP34.5. Novel GADD34 expression was confirmed by Western blot. The recombinant viruses were injected stereotaxically (10 to the 6 p.f.u) into the mouse striatum (n=8 per group). Control groups received medium or control ICP34.5 null mutant virus (1716). Twenty-four hours later, ischaemia was induced by a stereotaxic injection of the vasoconstrictor peptide, endothelin 1 (400pmol) at the same site. Mice were then killed by perfusion fixation 72 hours later. Ischaemic damage was assessed in histologically stained sections. Administration of full length GADD34 virus resulted in significantly increased infarct volume compared to control (from  $1 \pm 0.1$  to  $1.5 \pm 0.1$  mm<sup>3</sup>) ( $p < 0.05$ , ANOVA, unpaired Student's t-test) (Fig 1). The other constructs did not influence infarct volume significantly. HSV immunohistochemistry confirmed virus distribution. GADD34 shares sequence homology with the HSV protein ICP34.5, a specific determinant of virulence. Growth curves in SKNSH human neuroblastoma cells confirmed that the full length GADD34 gene compensated for lack of ICP34.5 and restored virulence (Fig 2). Protein synthesis profiles show that GADD34 precludes protein synthesis shutdown in specific cell types in vitro. These results indicate that GADD34 can modulate cellular protein synthesis. Infarct volume was significantly greater in the presence of virus expressing the full length GADD34 gene. Other methods of GADD34 delivery are currently under investigation as the protein is developed further as a therapeutic target.

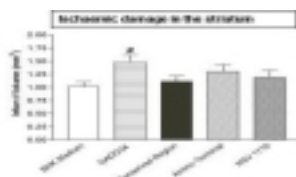


Fig 1

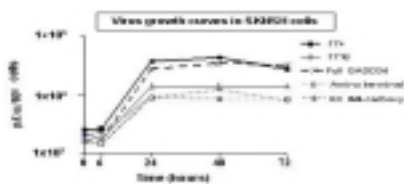


Fig 2

**ASSESSING THE EFFECTS OF A CONTRAST AGENT ON THE ABILITY OF NEURAL STEM CELL GRAFTS TO RECOVER BEHAVIOURAL IMPAIRMENTS IN A RAT MODEL OF STROKE: A 1 YEAR SERIAL MRI STUDY**

**Michel Modo<sup>1</sup>**, Cori Smee<sup>1,4</sup>, John S. Beech<sup>2</sup>, Maria Ashioti<sup>1</sup>, Thomas J. Meade<sup>3</sup>, Jack Price<sup>4</sup>, Steve C.R. Williams<sup>1</sup>

<sup>1</sup>*Neuroimaging Research Group - Neurology, Institute of Psychiatry, London, UK*

<sup>2</sup>*Department of Medicine, University of Cambridge, Cambridge, UK*

<sup>3</sup>*Department of Chemistry, Northwestern University, Evanston, IL, USA*

<sup>4</sup>*Department of Neurosciences, Institute of Psychiatry, London, UK*

Transplantation of neural stem cells in ischemia-damaged brains is an attractive novel therapeutic strategy. Still, at present it is unclear how these cells promote behavioral recovery. The dynamic nature of the processes involved in lesion evolution and graft-induced recovery necessitate a repeated assessment of an individual subject over time. The use of contrast agent-loaded cells followed serially over time with MRI provides the opportunity to assess the relevance of the site of these cells to behavior. We here report the use of serial MRI over 1 year with concomitant behavior to evaluate for how long contrast agent-loaded cells were visible on MRI scans and if the presence of the bimodal contrast agent GRID inside transplanted cells affected their ability to promote behavioral improvements after a stroke. Methods: Sprague-Dawley rats underwent 60 minutes of right intraluminal thread middle cerebral artery occlusion 2 weeks prior to transplantation of 100 000 neural stem cells from the MHP36 stem cell line into the contralateral hemisphere. MHP36 cells were either labeled with the bimodal contrast agent GRID or with the non-MRI enhancing fluorescent dye PKH26 prior to grafting. Animals were assessed on the bilateral asymmetry test concomitant to MRI examinations 1 week prior to transplantation and 1, 4, 12, 26, 39, and 52 weeks post-implantation. MRI examinations were conducted on a 4.7T Varian system affording a spatial resolution of 128  $\mu\text{m}$  in plane with a thickness of 600  $\mu\text{m}$ . Results: GRID-labeled cells were clearly visible on the MRI scans and by 1 week already appeared to have crossed the corpus callosum into the damaged hemisphere. At 4 weeks following transplantation, GRID-labeled transplants indicate that MHP36 delineate the area around the lesion and potentially participate in processes of recovery. No behavioral recovery, however, was observed at this time point, but previous studies suggest that between 4 and 6 weeks a definite change in behavior can be observed in these animals. Behavioural recovery therefore appears to lag behind the arrival of transplanted cells in the peri-infarct area. By 3 months following implantation, only cells in the injection tract were still visible on MRI scans suggesting that either the label inside the cells was degraded or that cells have died. Although no behavioral improvement in the removal of 'sticky tape' from the animals' forepaw was observed in animals with GRID-labeled transplants, a definite improvement of animals with PKH26-labeled transplants was observed. Conclusion: These results suggest that loading of cells with contrast agents to assess their in vivo survival provides invaluable information about their migration and location over extended time periods, but will need further investigations to allow contrast-agent labeled cells to fulfill their full potential for brain repair.

**STABILIZATION OF HYPOXIA-INDUCIBLE FACTOR 1 $\alpha$  IN NEURAL STEM CELLS WITH PROLYL HYDROXYLASE INHIBITION INDUCES DELAYED TOLERANCE AGAINST FOCAL CEREBRAL ISCHEMIA****Kon Chu**<sup>1,2</sup>, Soon-Tae Lee<sup>1</sup>, Keun-Hwa Jung<sup>1</sup>, Seung U. Kim<sup>3,4</sup>, Manho Kim<sup>1</sup>, Jae-Kyu Roh<sup>1</sup><sup>1</sup>*Stroke & Neural Stem Cell Lab, Department of Neurology, Seoul National University Hospital, Seoul, Korea*<sup>2</sup>*Center for Alcohol and Drug Addiction Research, Seoul National Hospital, Seoul, Korea*<sup>3</sup>*Division of Neurology, Department of Medicine, UBC Hospital, University of British Columbia, Vancouver, BC, Canada*<sup>4</sup>*Brain Disease Center, Ajou University, Suwon, Korea*

Cytoprotective strategies using pharmacological agents have yielded limited success in the prevention of cerebral ischemic injury. Tolerance to cerebral ischemia can be induced experimentally by a number of physical or pharmacologic strategies. Recent data indicate that Hypoxia-inducible factor 1 $\alpha$  (HIF-1 $\alpha$ ) plays major roles in the prevention of myocardial and cerebral ischemia. Inhibitors of HIF-1 prolyl hydroxylases (e.g. Deferrioxamine, DFX) stabilize the transcriptional activator HIF-1 $\alpha$  and activate target genes involved in compensation for ischemia, such as erythropoietin and VEGF. In this study, we are to investigate whether HIF-1 $\alpha$  may be stabilized in human neural stem cells (NSCs) by inhibition of prolyl hydroxylase, and stabilization of HIF-1 $\alpha$  in NSCs may induce prolonged ischemic tolerance. DFX (0.4mM) was added to the cultures of human NSCs (F3), and mRNA or protein levels of HIF-1 $\alpha$  were analyzed. In DFX-treated NSCs, protein level of HIF-1 $\alpha$  was increased about 100 folds time-dependently, up to 24 hours (0-72 hrs), while mRNA expression was unchanged. Unlike the DFX-treated NSCs, no changes in protein expression were observed in the hypoxia (1% O<sub>2</sub>)-treated NSCs. Subsequent transcriptional activation (VEGF, Glut-1, CXCR4) of HIF-1 $\alpha$  was also observed. To test an ability to induce ischemic tolerance in vivo, DFX-treated NSCs (100,000 cells) and naïve NSCs (100,000 cells) were transplanted in the left striatum of adult rats (n=12 respectively). 7 days following the transplantation, 90 minutes-focal cerebral ischemia with reperfusion (MCAO) was performed and rats were sacrificed at 24 hours. Infarct volumes were reduced in both NSCs groups, compared with MCAO-only with PBS injection group (Corrected lesion volume%: DFX-treated NSCs group: 8-12%; naïve NSCs group: 18-23%; MCAO-only group: 38-45%; p<0.01) by examining TTC staining, and NeuN- or Map-2ab immunohistochemistry. Striatal infarcts were further reduced in DFX-treated NSCs group. Histologic examination showed less TUNEL-positive cells and less GFAP-positive astrogliosis were found in both NSCs groups, and further decrease in DFX-treated NSCs group (p<0.001). These findings provide evidence that HIF-1 $\alpha$  stabilization in human NSCs can be achieved effectively by inhibition of prolyl hydroxylase, and HIF-1 $\alpha$ -stabilized NSCs may induce delayed ischemic tolerance.

**AGGRAVATION OF ISCHEMIC BRAIN INJURY BY PRION PROTEIN DEFICIENCY, BUT LACK OF NEUROPROTECTION BY ELEVATED PRION PROTEIN LEVELS: ROLE OF TYROSINE KINASES**

Annett Spudich<sup>1</sup>, Rico Frigg<sup>2</sup>, Ertugrul Kilic<sup>1</sup>, Ülkan Kilic<sup>1</sup>, Bruno Oesch<sup>2</sup>, Alex Raeber<sup>2</sup>, Claudio L. Bassetti<sup>1</sup>, **Dirk M. Hermann**<sup>1</sup>

<sup>1</sup>*Department of Neurology, University Hospital Zurich, Zurich, Switzerland*

<sup>2</sup>*Prionics AG, Schlieren, Switzerland*

**Purpose:** The physiological role of the cellular isoform of prion protein, PrP<sup>c</sup>, is largely unknown. It has recently been suggested that PrP<sup>c</sup> may confer neuroprotection in the brain, possibly via anti-oxidative actions. The aim of this study was to define the role of PrP<sup>c</sup> in the pathophysiology of ischemic stroke. **Methods:** PrP<sup>c</sup> knockout (Prnp0/0), wild-type and PrP<sup>c</sup>-transgenic (tga20) mice were subjected to 30 minutes of intraluminal middle cerebral artery (MCA) occlusion. Brain injury and cell signalling were assessed at 24 and 72 hours of reperfusion. **Results:** In immunohistochemical experiments we show that PrP<sup>c</sup> expression is absent in the brains of Prnp0/0 mice, detectable in wild-type controls and elevated in tga20 mice. We provide evidence that PrP<sup>c</sup> deficiency increases infarct size by ~200%, while transgenic PrP<sup>c</sup> restores tissue viability, albeit not above levels in wild-type animals. To elucidate the mechanisms underlying Prnp0/0-induced injury, we performed Western blots, which revealed increased activities of STAT-1, ERK-1/-2, JNK-1/-2 and caspase-3 in ischemic brains of Prnp0/0 mice, but no differences between wild-type and tga20 animals. **Conclusions:** Whereas Prnp0/0 massively increases ischemic brain injury, the elevated PrP<sup>c</sup> expression in transgenic tga20 mice does not confer additional neuroprotection, when compared with wild-type animals. Elevated levels of STAT-1, ERK-1/-2, JNK-1/-2 and caspase-3 activities in PrP<sup>c</sup> deficient mice suggest a role of tyrosine kinases in Prnp0/0-induced cell death.

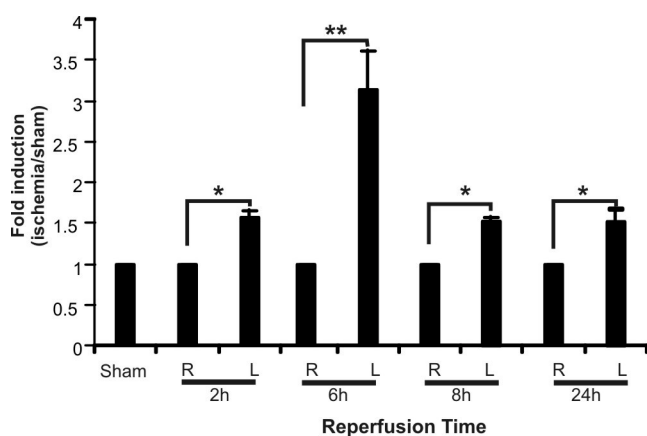
## NEUROPILIN-1 IS A MOLECULAR TARGET OF THE TRANSCRIPTION FACTOR E2F1 AND IS INVOLVED IN CEREBRAL ISCHEMIA-INDUCED NEURONAL DEATH

Sheng T. Hou<sup>1,2</sup>, Susan X. Jiang<sup>1</sup>, Melissa Sheldrick<sup>1,2</sup>, Angele Desbois<sup>1</sup>

<sup>1</sup>*Experimental Therapeutics Laboratory, NRC Institute for Biological Sciences, National Research Council Canada, Ottawa, ON, Canada*

<sup>2</sup>*Department of Biochemistry, Microbiology and Immunology, University of Ottawa, Ottawa ON, Canada*

After cerebral ischemia, neurons must integrate a multitude of both inhibitory and stimulatory molecular cues, generated as a result of cortical damage, into a functional response. More often than not the response is one of growth cone collapse, axonal retraction and cell death. The mechanisms through which a repelled axon may transduce a death signal to the soma and through which the soma may signal axonal retraction/collapse remain largely unknown, however the neuropilin family of receptors for the repellent semaphorins has been implicated in such responses. Our previous studies have shown that the nuclear transcription factor E2F1 pathway plays an important role in modulating neuronal death in response to a wide range of insults such as glutamate toxicity and cerebral ischemia. Using a high density DNA microarray, we identified that the expression of an axonal guidance molecule, neuropilin-1, is regulated by the transcription factor E2F1. Bioinformatics analysis allowed the identification of a putative E2F1 binding site in the promoter region of neuropilin-1. Subsequent electrophoretic mobility gel shift analysis provided evidence to demonstrate that E2F1 protein is indeed physically capable of binding with specificity to the NRP-1 promoter sequence. Moreover, such binding by E2F1 to the promoter sequence increased in mouse brains subjected to focal cerebral ischemia (Fig 1). The increased occupation of E2F1 at the neuropilin-1 promoter sequence correlated with the temporal induction profile of the mRNA level of neuropilin-1, suggesting that E2F1 transcriptionally up-regulated neuropilin-1 during neuronal death following cerebral ischemia. Taken together, these findings support a model in that nuclear death factors contribute to processes which determine the fate of the damaged distal axons by increasing the amounts of receptors expression to axonal repellent guidance cues that may ultimately lead to cell death and failure to regenerate. Blocking this detrimental signal transduction pathway may have potential therapeutic values. Supported by the Heart and Stroke Foundation of Canada grant-in-aid (NA5393) to STH. MS is supported by a Graduate Student's Scholarship from the Heart and Stroke Foundation of Ontario.



**EFFECT OF BONE MARROW TRANSPLANTATION OF CYTOSOLIC  
PHOSPHOLIPASE A2 DEFICIENT MICE IN FOCAL CEREBRAL  
ISCHEMIA/REPERFUSION INJURY**

**Sadaharu Tabuchi<sup>1</sup>**, Yasutaka Yamamoto<sup>2</sup>, Takashi Watanabe<sup>1</sup>, Naonori Uozumi<sup>3</sup>,  
Takao Shimizu<sup>3</sup>

<sup>1</sup>*Department of Neurosurgery, Institute of Neurological Sciences, Tottori University School of  
Medicine, Yonago, Japan*

<sup>2</sup>*Division of Regenerative Medicine and Therapeutics, Tottori University School of Medicine,  
Yonago, Japan*

<sup>3</sup>*Department of Biochemistry and Molecular Biology, University of Tokyo, Faculty of  
Medicine, Tokyo, Japan*

As we reported previously (Acta Neurochir Suppl., 2003), disruption of cytosolic phospholipase A2 (cPLA2) resulted in significant reduction of infarct area and neurological deficit severity in the MCA occlusion model using cPLA2 deficient mice. But the exact mechanism of protection and main target of cPLA2 disruption in CNS have been still unknown. After a cerebral infarction, there is an acute inflammatory response with entry of neutrophils, macrophages, and other blood elements into the ischemic zone. The current study was to investigate the contribution of bone marrow-derived cells in the mechanism. We transplanted bone marrow from male cPLA2 deficient mice into female C57BL/6J mice. Achievement of transplantation was confirmed by existence of Y chromosome. Approximately 4 month after transplantation, the recipient mice underwent suture occlusion of middle cerebral artery (MCA) and reperfusion. Quantification of cerebral infarction was determined by TTC staining followed by volumetric analysis of digitized image. Neurological deficit was evaluated according to modified 4-point scale as described previously. The infarction volume of recipient mice transplanted with cPLA2 deficient mice tend to be smaller than the mice transplanted with wild type mice but not statistically significant. The neurological deficit score also revealed no significant difference. There are some underlying problems for the evaluation of results. We report the preliminary results and discuss those problems.

## GENETIC DISSECTION OF CEREBRAL FAMILIAL ARTERIOVENOUS MALFORMATION

Katsunobu Takenaka<sup>1</sup>, Takatsugu Murakawa<sup>1</sup>, Toru Iwama<sup>2</sup>, Hiroyasu Yamakawa<sup>3</sup>, Toshifumi Kamiryo<sup>4</sup>, Jafar J. Jafar<sup>4</sup>, Roman Herzig<sup>5</sup>, Masamitsu Abe<sup>6</sup>, Kazuo Tabuchi<sup>6</sup>, Kayoko Inoue<sup>7</sup>, Akio Koizumi<sup>7</sup>

<sup>1</sup>Dept. of Neurosurgery, Takayama Red Cross Hospital, Takayama, Japan, <sup>2</sup>Dept. of Neurosurgery, Gifu University Graduate School of Medicine, Gifu, Japan, <sup>3</sup>Dept. of Neurosurgery, Gifu Prefectural Gero Hot Spring Hospital, Gifu Japan, <sup>4</sup>Dept. of Neurosurgery, New York University Medical Center, New York, NY, USA, <sup>5</sup>Stroke Centre, Clinic of Neurology, Faculty Hospital, Olomouc, Czech Republic, <sup>6</sup>Dept. of Neurosurgery, Faculty of Medicine, Saga University, Saga, Japan, <sup>7</sup>Dept. of Health and Environmental Sciences, Kyoto University Graduate School of Medicine, Kyoto, Japan

**Introduction:** While syndromic cerebral arteriovenous malformations (AVMs) with hereditary hemorrhagic telangiectasia (HHT) or, Sturge-Weber or von Hippel-Lindau disease often occur within families, familial nonsyndromic AVM are rare. There are, however, several familial AVM cases, suggesting a genetic background for nonsyndromic AVMs. Familial AVMs have been reported only 16 cases in the English literature. The authors report on two patients with AVM in one family and the genetic analysis of five families, as well as reviewing literature. **Case reports:** Case 1; This 51-year-old man presented in November, 1975 with a seizure and became unconscious. Neurological and general examination was normal. A right carotid angiography revealed a large AVM fed by the right anterior cerebral artery in the frontal lobe. The AVM was subtotally removed without neurological complication. Case 2; This 58-year-old woman presented in September, 2001 with difficulty in speaking and right hemiparesis. Examination disclosed motor aphasia. CT demonstrated a hematoma located in the left frontoparietal lobes. Left carotid angiography revealed an AVM mainly fed the left middle cerebral artery and mainly draining into the superior sagittal sinus through the cortical vein. Right carotid angiography revealed an unruptured saccular aneurysm in anterior cerebral artery. After surgery to remove the hematoma and AVM nidus, the aphasia and hemiparesis much improved. **Subjects and methods for the linkage analysis:** Five families with AVM participated from all over the world. Two families (#1 and #2) are from a central part of Japan and one family (#3) from Kyushu, Japan. One family (#4) is from the central Europe and another (#5) from the USA. Genome-wide linkage analysis was conducted with 382 microsatellite markers with a mean resolution of 10 cM. Since there are uncertainties about the penetrance and mode of inheritance, a nonparametric allele sharing method was chosen using a linkage software "Merlin". **Results:** The familial cases summarized in Table 1 consisted of 25 males and 23 females. The mean age of 45 familial patients of 22 families was 28.6 years (the age was not reported in three cases). The presenting signs or symptoms were mainly intracranial hemorrhage (20 cases) and seizures (10 cases). Five chromosomal regions (6q24-6q27, 7p22-7p15, 13q21-13q31, 16p11.2-16p11.1, and 20q12-20q13.1) were potentially interesting (nominal  $p < 0.05$ ) in Table 2. Sequence analysis was conducted for the Ephrin B2 gene, which was a potential candidate gene on Chromosome 13. Sequencing of the entire coding exons 1 to 5 revealed only SNPs. **Conclusion:** Genetic determinants are definitively involved in familial AVM. There are five candidate chromosomal regions for familial AVM, of which regions on Chromosome 6 and 7 are the most probable regions.

Table 1 Characteristics of all familial cases

Criteria		Number of cases
Family relationship	Parent-child	3
	Mother-son	1
	Father-son	2
	Father-daughter	1
	Grandparent-parent-child	1
Siblings	Grandfather-mother-daughter	1
	Sister-sister	5
Cousins	Brother-brother	5
	Sister-brother	3
Uncle-niece		2
		1

Table 2 Summary of the linkage analysis

Chromosome	cM from the top	Flanking markers	Syntenosomal localization
6*	137.156	D2S308-D2S294	6q24-q27
7*	1.414	D7S51-D7S07	7p22-7p15
13	79.75	D13D065-D13S158	13q21-13q31
16	39.36	D16S304-D16S308	16p11.2-16p11.1
20	55.60	D20S107-D20S119	20q12-20q13.1

\*most likely linked regions



## **INFLUENCE OF GROWTH FACTORS ON PROLIFERATION AND DCX DOUBLESTAINING AFTER TRANSIENT FOCAL CEREBRAL ISCHEMIA**

**Kathrin Baldauf, Petra Henrich-Noack, Klaus G. Reymann**

*Leibniz Institute for Neurobiology, Neuropharmacology, Magdeburg, Germany*

**Introduction:** Neurogenesis occurs in the adult mammalian brain in two specialized germinal zones: the subventricular zone (produces new neurons destined for the olfactory bulb) and the granular cell layer of the dentate gyrus of the hippocampus. Stroke leads to a marked increase of cell proliferation in the subventricular zone [1]. Moreover, the fate of BrdU positive cells is influenced by growth factors like epidermal growth factor (EGF), directing cells into the glial lineage and fibroblast growth factor (FGF), directing cells into the neural lineage [2]. However it is unclear whether this proliferation can be induced by growth factors in a model of mild ischemia and whether these factors can promote the neural lineage in this model. Therefore this study aimed at verifying the occurrence of post-stroke nerve cell division and influence of growth factors in a transient, endothelin-1- induced middle cerebral artery occlusion model (e-MCAO), and the number of cells, directing to the neural lineage in different areas of the post ischemic brain. **Materials:** Male Sprague Dawley rats were subjected unilaterally to eMCAO by application of endothelin-1. After ischaemia a miniosmotic pump was implanted and the thymidine analogon bromodeoxyuridine (BrdU; 1 mg/ml), a marker of DNA synthesis that labels dividing cells and their terminal progeny, and BrdU + EGF/FGF was infused directly into the ventricle. After 12 days pumps were removed and after 14 days brains were perfusion-fixed and sections were processed for histochemistry for evaluation of the infarct area or immunofluorescence. Primary antibodies used were the specific markers anti-BrdU for newly generated cells and doublecortin for migrating cells. For detection and quantification we used confocal laser scanning microscopy. **Results:** 2 weeks after eMCAO we found BrdU-positive cells in the striatum, ventricle wall and the dentate gyrus of the hippocampus. EGF/FGF-2 had a promotional effect on the number of BrdU-positive and DCX-positive cells in the lateral ventricle, whereas ischemia itself had no effects on the BrdU-positive cells in the lateral ventricle, but in the striatum. Partly these cells are doublelabeled. Interestingly, the growth factor effect was inversed in the dentate gyrus. **Conclusions:** Our results suggests: that EGF/FGF post-stroke treatment has a promotional effect on the number of BrdU-positive and DCX-positive cells in the ventricle wall and the striatum, whereas doublelabelling was only altered in the ipsilateral striatum. In the non-damaged hippocampus, the effect of growth factors attenuated cell proliferation and doublelabelling. **References:** [1] Arvidson A., Collin T., Kirik D., Kokaia Z., Lindvall O., *Natur Medicine* 2002, 8(9): 963-970 [2] Kuhn HG, Winkler J, Kempermann G, Thal LJ, Gage FH. *J Neurosci* 1997, 17: 5820-5829

## SERIAL AND SIMULTANEOUS PET MEASUREMENT OF FETAL NIGRAL TRANSPLANTATION IN HEMI-PARKINSON MODEL RATS WITH [11C]PE2I AND [11C]RACLOPRIDE

Motoki Inaji<sup>1,2</sup>, Takahito Yoshizaki<sup>3</sup>, Kiyoshi Ando<sup>2</sup>, Jun Maeda<sup>2</sup>, Takashi Okauchi<sup>2</sup>, Shigeru Obayashi<sup>2</sup>, Tetsuya Suhara<sup>2</sup>, Hideyuki Okano<sup>3</sup>, **Tadashi Nariai**<sup>1</sup>, Kikuo Ohno<sup>1</sup>

<sup>1</sup>*Department of Neurosurgery, Tokyo Medical and Dental University, Tokyo, Japan*

<sup>2</sup>*Brain Imaging Project, National Institute of Radiological Science, Chiba, Japan*

<sup>3</sup>*Department of Physiology, Keio University, Tokyo, Japan*

**Purpose:** We applied the in vivo measurement of pre- and post-synaptic dopaminergic function with Positron Emission Tomography (PET) to assess the alteration of neural transmission after fetal nigral transplantation to hemi-Parkinson model rats. **Method:** We transplanted  $4.0 \times 10^5$  fetal mesencephalic cells in the damaged striatum of unilaterally 6-OHDA lesioned rats. We performed PET scans with [11C]PE2I (PET tracer of dopamine transporter) and [11C]raclopride (that of D2 receptor) to evaluate the pre- and post-synaptic dopaminergic function before, and 2 and 4 weeks after transplantation in the same individual. PET scan was performed in 2-dimensional acquisition mode with a high-resolution PET camera, SHR7700 (Hamamatsu Photonics). Rats were fixated by ear bar and incision bar under isoflurane anesthesia. After 20 min transmission scan for attenuation correction, 90 min dynamic emission scan started immediately after a tracer injection (ca. 37 MBq/ 300ml) via tail-vein. The acquired images were reconstructed with a 4-mm of Hanning filter. The regions of interest were placed over the bilateral striatum and cerebellum. Regional binding potential (BP;  $k_3/k_4$ ) of dopamine transporter and D2 receptor were calculated using a simplified reference tissue model, and cerebellum was used as reference region. Rotational behavior test with apomorphine and methamphetamine, in vitro autoradiography with [11C]PE2I and [11C]raclopride, and measurement of dopamine contents by HPLC were simultaneously performed. **Results:** In the PET studies, binding potential of [11C]PE2I in the transplanted striatum increased significantly four weeks after the transplantation. Then the binding potential of [11C]raclopride, which was up-regulated in all experimental period in sham rats, decreased significantly 4 weeks after transplantations. In vitro autoradiographic studies corresponded with the results of PET studies. Number of rotations induced by methamphetamine and apomorphine injection significantly decreased after transplantation. Dopamine contents in the striatum significantly increased. **Discussion:** The increase in the binding of [11C]PE2I in the transplanted striatum was detected with PET and it indicated not only survival, but maturation and function of the transplanted cells. Although the recovery of pre-synaptic function was incomplete, complete recovery of the rotational behavior test was observed 4 weeks after transplantation. These results strongly suggest the contribution of up-regulated post-synaptic D2 receptors to the recovery of the dopaminergic function. We considered that the serial and simultaneous PET measurement of pre- and post-synaptic dopaminergic function is inevitable to investigate the functional recovery of dopaminergic function by the neural transplantation therapy.

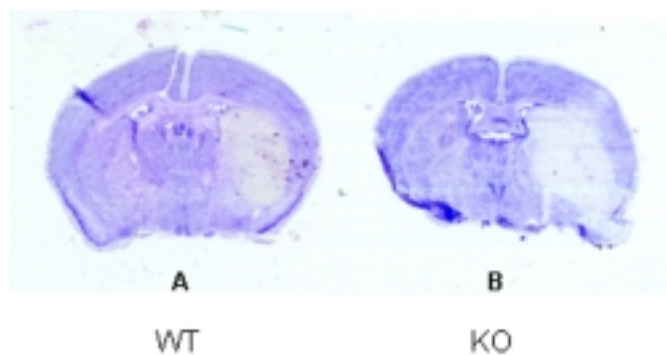
**DEFICIENCY OF PAR-2 GENE INCREASES ACUTE FOCAL ISCHEMIC BRAIN INJURY**

**Guang Jin**<sup>1</sup>, Takeshi Hayashi<sup>1</sup>, Junichi Kawagoe<sup>2</sup>, Toshiaki Takizawa<sup>2</sup>, Tetsuya Nagata<sup>1</sup>, Isao Nagano<sup>1</sup>, Mikio Shoji<sup>1</sup>, Koji Abe<sup>1</sup>

<sup>1</sup>*Department of Neurology, Graduate School of Medicine and Dentistry, Okayama University, Okayama, Japan*

<sup>2</sup>*Tokyo New Drug Research Laboratories II, Pharmaceutical Division, Kowa Co., Ltd., Tokyo, Japan*

**Purpose:** Proteinase-activated receptor 2 (PAR-2) is involved in many cellular functions, but its roles in the cerebral ischemia were unclear yet. We investigated the effect of PAR-2 in cerebral ischemia by using PAR-2 knockout mice. Furthermore, we studied how PAR-2 affects the intracellular signaling and astrocytes function. **Method:** One hour of tMCAO was induced in male PAR-2 knockout and wild type mice, and the brains were removed at 5 min, 8, and 24 hr after reperfusion. The infarction was evaluated by cresyl violet staining at 24 hr after reperfusion. PAR-2 and p-ERK expression were detected by immunostaining and western blotting. The activation of astroglia was evaluated by GFAP staining; TUNEL staining was used as markers of apoptosis. **Results:** PAR-2 was normally distributed mainly in neurons, and strongly up-regulated at 8 to 24 hours after tMCAO. Deficiency of PAR-2 gene significantly increased the infarct volume and the number of TUNEL positive cells at 24 hour of reperfusion. The strong neuronal expression of p-ERK was induced with a peak at 5 min, which was significantly reduced in PAR-2 KO mice. Astroglial activation was also greatly inhibited at 24 hours after tMCAO in PAR-2 KO mice. **Conclusion:** These results demonstrate that the deficiency of PAR-2 gene increases the acute ischemic cerebral injury, associating with suppression of neuronal ERK activation and reactive astroglial activation.



**NEUROPROTECTIVE EFFECT OF ANTISENSE OLIGODEOXYNUCLEOTIDES IN EXPERIMENTAL INTRACEREBRAL HEMORRHAGE IN RATS****Huijin Yan**<sup>1</sup>, Mengzhou Xue<sup>2</sup>, Christopher Power<sup>3</sup>, Marc R Del-Bigio<sup>2</sup>, James Peeling<sup>1,4</sup><sup>1</sup>*Department of Radiology, University of Manitoba, Winnipeg, Manitoba, Canada*<sup>2</sup>*Department of Pathology, University of Manitoba, Winnipeg, Manitoba, Canada*<sup>3</sup>*Clinical Neurosciences, University of Calgary, Calgary, AB, Canada*<sup>4</sup>*Department of Pharmacology and Therapeutics, University of Manitoba, Winnipeg, Manitoba, Canada*

Using a collagenase-induced rat model of intracerebral hemorrhage (ICH), we showed that ICH is characterized by parenchymal hematoma formation with surrounding inflammation and tissue destruction. Our continuous works on the role of inflammation and free radicals in the pathogenesis of neurological deficit and tissue damaging in ICH showed that treatment with fucoidan (anti-inflammatory), or immunosuppressant FK-506, or free radical trap NXY-059, or Minocycline (matrix metalloproteinase down-regulating) could reduce brain damage and improve behavioral outcome in rats following ICH. We further demonstrated that intracerebral injection of antisense oligodeoxynucleotides (ORF4-PE) to target pro-inflammatory cytokine significantly reduced tumor necrosis factor (TNF- $\alpha$ ) mRNA and protein expression in striatum and cortex in rats after ICH, and that this was also accompanied by reduced neuronal loss and decreased neurological deficits (STROKE 2001:32:240-248). The present study tested whether administration of ORF4-PE via the ipsilateral internal carotid artery (ICA) is also effective in the same animal model. Briefly, 26 SD rats were pentobarbital anesthetized and ICH was induced by intrastriatum collagenase injection. The ipsilateral external carotid artery was cannulated near the carotid bifurcation for injection of ORF4-PE into the ICA one hour after ICH procedure. Rats received ORF4-PE 20, 200, 2000  $\mu$ g in 200 ml saline given over 30 minutes, or only 200 ml saline as control. Neurological deficits (postural reflex, circling, beam walking) were assessed at 24 and 48 hours after ICH. Neutrophil level around the hematoma was determined by histo-pathological examination at 24 and 48 hours. There was a dose-dependant improvement in both neurological deficit score and neutrophil infiltration in ORF4-PE treated group vs control group. In particular, the differences were highly significant ( $p < 0.001$ ) in the group treated with 2000  $\mu$ g ORF4-PE. ICA administration might be an effective and practical means of delivery of ORF4-PE to the brain following ICH in rats. (Supported by The Heart and Stroke Foundation of Manitoba).

## PEROXISOME PROLIFERATOR-ACTIVATED RECEPTOR-Y ACTIVATION AS A MECHANISM OF PREVENTIVE NEUROPROTECTION INDUCED BY PIOGLITAZONE TREATMENT

Kimihiko Hattori<sup>1</sup>, Tomokazu Shimazu<sup>1</sup>, Ikuo Inoue<sup>2</sup>, Nobuo Araki<sup>1</sup>, Shigehiro Katayama<sup>2</sup>, Kunio Shimazu<sup>1</sup>, Joel H. Greenberg<sup>3</sup>

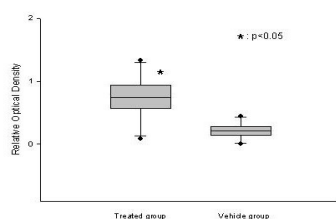
<sup>1</sup>Department of Neurology, Saitama Medical School, Saitama, Japan

<sup>2</sup>Department of Internal Medicine, Saitama Medical School, Saitama, Japan

<sup>3</sup>Department of Neurology, University of Pennsylvania, Pennsylvania, PA, USA

**Introduction:** We have previously reported that a peroxisome proliferator-activated receptor (PPAR-Y) agonist protects against cerebral injury by anti-oxidant mechanisms<sup>1</sup>. The neuroprotective effect of a PPAR-Y agonist, pioglitazone induced SOD-1, suggesting that PPAR-Y activation was involved as a mechanism of the protection against cerebral injury. PPAR-Y agonists also have the ability to decrease reactive oxygen species generation. Here, we investigate the effects of pioglitazone on the expression of the superoxide generating enzyme nicotinamide adenine dinucleotide phosphate (NADPH) oxidase in cerebral tissue. **Methods:** Twelve male Sprague-Dawley rats were treated with pioglitazone (20 mg/kg per day, n=6) or vehicle (n=6) for 4 days at which time they, underwent 90-minutes of MCAO. The brain was removed 2 hours into reperfusion, and tissue was obtained from the cortex of the ischemic hemisphere and examined for CuZn-SOD (SOD 1) and 22-kDa, 47-kDa (NADPH subunits) and nNOS levels by Western blot. Briefly, small brain tissue samples (40 mg) were added to PBS buffer and homogenized. After centrifugation at 500g for 3 minutes, the supernatant was removed. The amount of protein, which was loaded for Western blotting, was 15 µg. To correct for loading, we used the expression of GAPDH as the housekeeping protein. Antibodies against SOD 1 and 22-kDa, 47-kDa and nNOS were used for Western blotting. After protein blotting, membranes were incubated with horseradish peroxidase-conjugated anti-goat monoclonal antibody. Antigen detection was performed with a chemiluminescence detection system. Results were obtained by calculating a ratio of the SOD 1 protein levels to 22-kDa, 47-kDa and nNOS protein levels and reported as relative optical density. Significant differences between groups were determined with the Mann-Whitney test. **Results:** The level of CuZn-SOD was increased in the cortex in treated animals ( $42.7 \pm 22.2$  vs.  $12.5 \pm 10.4$ ; treated group vs. vehicle group, mean  $\pm$  SD) ( $P < 0.05$ ). The ratio of the SOD 1 protein level to the 47-kDa subunit protein level of NADPH oxidase in the ischemic cortex 2 hours after transient MCAO was significantly increased by treatment with pioglitazone ( $0.74 \pm 0.41$  vs.  $0.22 \pm 0.15$ ) ( $P < 0.05$ ) (figure 1.). Additionally, the ratio of the SOD 1 protein level to the nNOS in the ischemic cortex, also significantly increased by treatment with pioglitazone ( $2.87 \pm 1.59$  vs.  $0.51 \pm 0.44$ ) ( $P < 0.05$ ). **Conclusions:** These data, which show that a PPAR-Y agonist increased the ratio of the SOD 1 (as a free radical scavenger) protein levels to the 47-kDa subunit protein level of NADPH oxidase (as a production of free radical) suggest that the role of PPAR-Y is specific to events occurring during reperfusion. Our data point to free radical scavenging as the mediator of this neuroprotection. [Reference] 1. Shimazu et al. A Peroxisome Proliferator-Activated Receptor-Y Agonist Reduces Infarct Size in Transient but not in Permanent Ischemia. *Stroke*.2005; 36.

Figure 1. SOD-1/p47kDa in ischemic cortex





## POST-ISCHEMIC GENE TRANSFER OF IL-10 PROTECTS AGAINST GLOBAL BRAIN ISCHEMIA

Takashi Shichita, **Hiroaki Ooboshi**, Yasuhiro Kumai, Masahiro Kumai, Junichi Takada, Takanari Kitazono, Setsuro Ibayashi, Mitsuo Iida

*Department of Medicine & Clinical Science, Kyushu University, Fukuoka, Japan*

**Background and Purpose:** Gene therapy may be a promising approach for treatment of brain ischemia [1,2] although studies that revealed protective effects of gene therapy initiated after ischemia are limited. Our goal in this study was to examine the effect of gene transfer of interleukin-10 (IL-10), an anti-inflammatory cytokine, after induction of global brain ischemia.

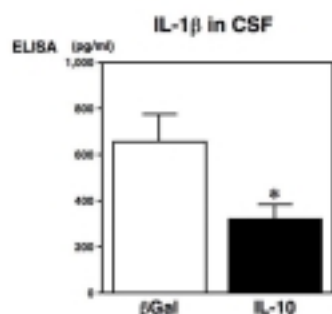
**Methods:** Global brain ischemia was produced by bilateral carotid occlusion of aged spontaneously hypertensive rats (aged 15 to 22 months old, n=14) [3]. Cerebral blood flow (CBF) during ischemia was measured by laser Doppler flowmetry. Sixty minutes after ischemia, adenoviral vectors encoding human IL-10 (AdIL10, n=7) or vectors encoding  $\beta$ -galactosidase (Ad $\beta$ gal, n=7) were injected into the lateral ventricle. Five days after brain ischemia, cerebrospinal fluid (CSF) was withdrawn for measurement of interleukin-1 $\beta$  (IL-1 $\beta$ ) and tissue necrosis factor- $\alpha$  (TNF $\alpha$ ), and hippocampal neuronal damages were determined by hematoxyline-eosin staining and the terminal deoxynucleotidyl transferase-mediated dUTP-biotin in situ nick end labeling (TUNEL) staining.

**Results:** Physiological parameters were not different between both treatment. CBF reduction during bilateral carotid occlusion ( $13.2\pm 2.6\%$ , mean $\pm$ SEM, of the resting value for Ad $\beta$ gal and  $12.5\pm 1.8\%$  for AdIL10) and the recovery after recirculation were not different between both groups. IL-10 gene transfer significantly ( $p<0.05$ ) reduced the amount of IL-1 $\beta$  in CSF by 41% (Figure) and significantly ( $p<0.01$ ) augmented that of TNF $\alpha$  by 49%. Furthermore, the IL-10 gene transfer after global ischemia significantly preserved hippocampal CA1 neurons (intact neurons:  $95\pm 18/\text{mm}$  for Ad $\beta$ gal,  $174\pm 20/\text{mm}$  for AdIL10,  $p<0.02$ ) and significantly diminished TUNEL positive cells ( $128\pm 27/\text{mm}$  for Ad $\beta$ gal,  $61\pm 12/\text{mm}$  for AdIL10,  $p<0.05$ ).

**Conclusions:** Adenovirus-mediated gene transfer of IL-10 into the lateral ventricle initiated after global brain ischemia modulated production of cytokines and attenuated hippocampal neuronal damages. Therefore, gene transfer of IL-10 to the ischemic brain may be a promising approach for treatment of brain ischemia.

### References:

1. Heistad DD, Faraci FM. Gene therapy for cerebral vascular disease. *Stroke*. 1996;27:1688-1693.
2. Ooboshi H, Ibayashi S, Takada J, Yao H, Kitazono T, Fujishima M. Adenovirus-mediated gene transfer to ischemic brain. Ischemic flow threshold for transgene expression. *Stroke*. 2001; 32:1043-1047.
3. Yao H, Sadoshima S, Ooboshi H, Sato Y, Uchimura H, Fujishima M. Age-related vulnerability to cerebral ischemia in spontaneously hypertensive rats. *Stroke*. 1991;22:1414-1418.





## HEAT SHOCK PROTEIN OVEREXPRESSION - EFFECT ON EXPERIMENTAL STROKE

Louise van der Weerd<sup>1,2</sup>, Mark F. Lythgoe<sup>1</sup>, Romina Aron Badin<sup>1,2</sup>, Jackie de Belleruche<sup>4</sup>, David L. Latchman<sup>2</sup>, David G. Gadian<sup>1</sup>

<sup>1</sup>RCS Unit of Biophysics, Institute of Child Health, London, UK

<sup>2</sup>Medical Molecular Biology Unit, Institute of Child Health, London, UK

<sup>3</sup>Department of Medical Physics and Bioengineering, University College London, UK

<sup>4</sup>Department of Neuromuscular Diseases, Division of Neuroscience and Psychological Medicine, Imperial College London, London, UK

Heat shock proteins (HSPs) have been reported to increase cell survival in response to a wide range of cellular challenges. In order to investigate the effect of these proteins *in vivo*, transgenic (tg) mice overexpressing HSP27 or HSP70 have been compared to wild-type (WT) mice in a middle cerebral artery occlusion (MCAO) model of permanent cerebral ischaemia. To assess the protective effect of HSPs following permanent ischaemia, the lesion size was estimated after 24 hours of ischaemia using a multi-slice T2-weighted MRI scan. 4 groups of mice were used: 1. HSP27 tg (n=5), 2. HSP27 WT (n=6), 3. HSP70 tg (n=5) and 4. HSP70 WT (n=6). The MCA was permanently occluded by advancing a 180- $\mu$ m-diameter filament into the internal carotid artery past the MCA junction. Multi-slice coronal images were obtained 24 hours after the onset of stroke. A 2.35T horizontal bore SMIS MR scanner was used with the following imaging parameters: T2-weighted SE sequence with FOV 20 mm, 1 mm slice thickness, 9 slices and 128  $\times$  64 pixels. The relative infarcted area per slice was defined as the ratio of the lesion area to the whole brain size. All data are presented as mean  $\pm$  SD. The relative infarcted area was larger in the WT mice than in the HSP27-overexpressing animals for every slice ( $P < 0.05$  using degrees of freedom adjusted repeated measures ANOVA). The same is true for HSP70-overexpressing mice. Overall, the lesion is  $30 \pm 3\%$  and  $27 \pm 4\%$  of the whole brain volume in the HSP27 WT and HSP70 WT mice respectively, compared to  $20 \pm 7\%$  and  $19 \pm 6\%$  in the HSP27tg and HSP70tg animals. In-situ hybridisation showed high expression levels of HSP27 and HSP70 throughout the brain in HSP27tg and HSP70tg mice respectively. With this particular model, the lesion is significantly smaller for both HSP27 and HSP70 overexpressing mice compared to WT animals. Interestingly, similar work using HSP27 or HSP70 gene delivery via a viral vector in a rat model of transient MCAO showed protection for HSP27, but not for HSP70 [1]. The difference between these experiments is probably partly due to the amounts of HSP overexpression and their spatial distribution, which are not the same in the transgenic mouse model and the viral delivery rat model. Furthermore, the different MCAO models (permanent versus transient) are known to influence the amount of apoptosis expected in infarcted tissue, and thus the differences between the two models may reflect the different inhibitory actions of HSP27 and HSP70 in the apoptotic cascade. References Aron-Badin et al. Neuroprotective effect of virally delivered HSPs in experimental stroke, submitted. Acknowledgments We thank the BBSRC and Wellcome Trust for financial support.

## GENE THERAPY FOR STROKE USING VIRAL DELIVERY OF HEAT SHOCK PROTEINS

Romina Aron Badin<sup>1,2</sup>, Mark F. Lythgoe<sup>1</sup>, Louise van der Weerd<sup>1,2</sup>, David L. Thomas<sup>3</sup>,  
David L. Latchman<sup>2</sup>, David G. Gadian<sup>1</sup>

<sup>1</sup>*RCS Unit of Biophysics, Institute of Child Health, London, UK*

<sup>2</sup>*Medical Molecular Biology Unit, Institute of Child Health, London, UK*

<sup>3</sup>*Department of Medical Physics and Bioengineering, University College London, London, UK*

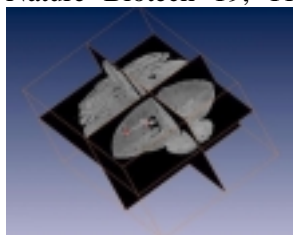
Heat shock proteins (HSPs) are molecular chaperones with essential roles in cellular function such as modulation of the proteolytic machinery and acceleration of cell repair. This study uses MRI to assess the effects of pre-ischaemic viral delivery of HSPs on lesion size in a rat middle cerebral artery (MCA) occlusion model of reversible focal ischaemia. Perfusion maps of a 2-mm brain slice within the MCA territory were acquired to measure cerebral blood flow (CBF) and multislice T2-weighted scans were used to determine lesion volume 24 hours after ischaemia. Male rats were anaesthetised with 2% isoflurane in 100% O<sub>2</sub>. Viral suspensions (2.5 µl of 2x10<sup>6</sup> pfu) of herpes simplex virus carrying HSP27 (n=6), HSP70 (n=6), or LacZ (n=6) as a control, were stereotactically injected into rat striatum. Three days post-injection, rats were re-anaesthetised for middle cerebral artery occlusion (MCAO) by intraluminal insertion of a 290-µm-suture past the MCA junction. After 30 minutes the suture was completely withdrawn to reperfuse the tissue and rats were allowed to recover for 24 hours before scanning. Coronal images were obtained approximately 0.5 mm from bregma on a 2.35 Tesla horizontal bore SMIS magnet with 40x20 mm FOV, 2 mm slice thickness and 128x64 pixels. T1 and CASL (continuous arterial spin labelling) EPI sequences were run for quantitative CBF mapping (3) and multislice T2-weighted SE images (1mm slice thickness, 9 slices, TE=120 ms, TR=1500 ms) were acquired for lesion definition. All animals were imaged under general anaesthetic (halothane 2% in a 70:30 N<sub>2</sub>O:O<sub>2</sub> mix) with physiological monitoring (ECG, rectal temperature). Three days later, the brains were extracted and immunohistochemistry and Western blots were carried out in order to verify expression levels of virally delivered HSPs in the brain. Total lesion volume was reduced by 44.8% (p=0.02) in HSP27 treated animals compared to controls whereas no significant differences were found between HSP70 treated and control animals (p=0.88). CASL maps indicated that there was no significant difference in relative CBF 24 hours after reperfusion in normal and ischaemic hemispheres between the groups that could account for differences in lesion size. Histological analysis of brain sections showed widespread staining for HSPs in basal ganglia and cortex. Western blots performed 72 hours after MCAO revealed that levels of HSP expression in HSP injected hemispheres were 4 times higher than in LacZ injected controls. In conclusion, we show that non-invasive MRI techniques can detect a significant reduction in lesion size after HSP27 gene delivery in a rat model of reversible focal cerebral ischaemia. (1) Richter-Landsberg C, Goldbaum O (2003) *Cell Mol. Life Sci.* 60, 337-349. (2) Kelly S, Yenari M (2002) *Curr. Med. Res. Op.* 18, 55-60. (3) Alsop DC, Detre JA (1996) *J Cereb. Blood Flow Metab.* 16, 1236-1249.

## MR CELLULAR IMAGING OF MAGNETICALLY LABELED NEURAL STEM CELLS IN A DYSMYELINATED MOUSE BRAIN MODEL

Piotr Walczak, Dorota Kedziorek, Assaf A. Gilad, **Jeff W.M. Bulte**

*Department of Radiology, Johns Hopkins University School of Medicine, Baltimore, MD, USA*

**Introduction** Dysmyelination, caused by defective genes encoding for myelin components is rare in humans (Pelizaeus-Merzbacher disease). Several dysmyelinated animal models have served as a framework to study the potential of cell therapy, in particular as related to the myelinating properties of transplanted neural stem cells, which has also relevance to CNS repair in multiple sclerosis. **In vivo** magnetic resonance (MR) cell tracking of magnetically labeled cells has been successfully applied to non-invasively visualize the biodistribution and migration of transplanted stem cells and progenitors in two rat models of dysmyelination, the myelin-deficient rat [1] and the shaker rat [2]. In this study, we report on the applicability of serial MRI cell tracking in the dysmyelinated shiverer (shi) mouse brain at high field strength (11.7 T). **Materials and Methods** The LacZ-transfected neural stem cell line C17.2 was magnetically labeled with Feridex and poly-L-lysine [3]. C17.2 cells (80,000 in 2  $\mu$ l) (n=9 mice) or an equal volume of saline (n=2 mice) were injected into the right ventricle of neonatal (P1-3) shi mice. **In vivo** MR imaging was performed at 1, 3, and 5 weeks after cell transplantation using a Bruker 11.7T Avance spectrometer. Brains were then removed and imaged **ex vivo** at high-resolution (65  $\mu$ m isotropic). Cell distribution was verified by staining for myelin, LacZ, dextran, and iron. **Results** Serial **in vivo** MR imaging at the different time points revealed that cells appeared to remain within the ventricles for prolonged times. The **ex vivo** imaging showed migration of hypointense, labeled cells into the brain parenchyma including the corpus callosum, striatum and cortex (Fig. 1). The hypointense signal dots, each representing single cells, closely matched the cell biodistribution as detected by X-gal histochemistry and iron staining. The shaker phenotype of the transplanted shiverer mice, apparent at P12, was not altered throughout the course of 60 days as compared to non-transplanted controls. Consistently, new myelination could not be observed. **Conclusion** These results demonstrate that magnetically labeled neural stem cells migrate long distances from the transplantation site and can be accurately tracked by MR imaging. However, new myelination and rescue of the shiverer phenotype could not be observed. Thus, further optimization of cell therapy will be needed in which MRI cell tracking may become a useful guiding tool. **References** 1) JW Bulte et al., PNAS 96, 15256-61 (2004); 2) JW Bulte et al., Nature Biotech 19, 1141-7, 2001; 3.) JA Frank, et al., Radiology 228, 480-7, 2003.



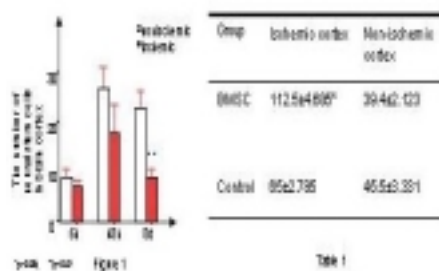
## THERAPEUTIC BENEFIT OF BONE MARROW STROMAL CELLS AFTER CEREBRAL ISCHEMIA IN RABBIT

Xiaoping Wang<sup>1</sup>, Fengcai Tang<sup>2</sup>

<sup>1</sup>*Division of Neonatal-Perinatal Medicine, Emory University, Atlanta, GA, USA*

<sup>2</sup>*Harbin Medical University, Department of Neurobiology, Harbin, China*

**Introduction:** Bone marrow stromal cells (BMSCs) are capable of differentiating into various cell types, including astrocytes and neurons (1); therefore, they were used for cell and gene therapy. In this study, we investigated the therapeutic benefit of transplantation of BMSCs for cerebral insult in rabbits. **Method:** Fresh bone marrow was harvested aseptically, and BMSCs were dissociated and cultured. Then the BMSCs marked with PKH67 were induced to differentiate into neuron-like cells *in vivo* and *in vitro*. *In vitro*, BMSCs and neurons from the fetus brain were co-cultured. At 5 days after culture, BMSCs were observed by inverted fluorescence microscope and identified by immunofluorescence method. *In vivo*, focal cerebral ischemia (FCI) was induced in New Zealand white rabbits by inserting a nylon monofilament suture embolus into the right external carotid artery to cause the middle cerebral artery occlusion. At 24 h after FCI, intracerebral transplantation of BMSCs (n=8) was performed [1]. From 6h after transplantation, BMSCs were observed and identified by immunofluorescence method. **Results:** The BMSCs engrafted in the brain migrated and survived. The number of PKH67 positive cells in the ischemic brain significantly increased compared to the control brain without transplantation of BMSCs (Table 1). Some BMSCs expressed neuron-specific onolase(NSE), indicating differentiation of neuron-like cells. Additionally, the number of neural stem cells (NSC) was significantly increased in the ischemic hemisphere after 8 days of FCI compared to nonischemic hemisphere (p<0.05) (Fig. 1). *In vitro*, immunohistochemistry revealed that 32.72±2.561% BMSCs express NSE when co-cultured with neural cells. In contrast, no NSE-positive BMSCs were observed in control culture. **Conclusion:** BMSCs appear to selectively migrate to the ischemic hemisphere and differentiate into neuron-like cells expressing NSE. **References:** 1. Goto S, Yamada K, Yoshikawa M, Okmura A, Ushio Y. GABA receptor agonist promotes reformation of the striatonigral pathway by transplant derived from fetal striatal primordia in the lesioned striatum. *Exp Neurol* 1997; 147(2): 503-9



**TRAFFICKING OF HUMAN NEURAL STEM CELLS IS REGULATED BY STROMAL CELL-DERIVED FACTOR-1 $\alpha$  / CXCR4- CHEMOKINE RECEPTOR 4 SIGNALING**

**Kon Chu**<sup>1,2</sup>, Soon-Tae Lee<sup>1</sup>, Keun-Hwa Jung<sup>1</sup>, Seung U. Kim<sup>3,4</sup>, Manho Kim<sup>1</sup>, Jae-Kyu Roh<sup>1</sup>

<sup>1</sup>*Stroke & Neural Stem Cell Lab, Department of Neurology, Seoul National University Hospital, Seoul, Korea*

<sup>2</sup>*Center for Alcohol and Drug Addiction Research, Seoul National Hospital, Seoul, Korea*

<sup>3</sup>*Division of Neurology, Department of Medicine, UBC Hospital, University of British Columbia, Vancouver, BC, Canada*

<sup>4</sup>*Brain Disease Center, Ajou University, Suwon, Korea*

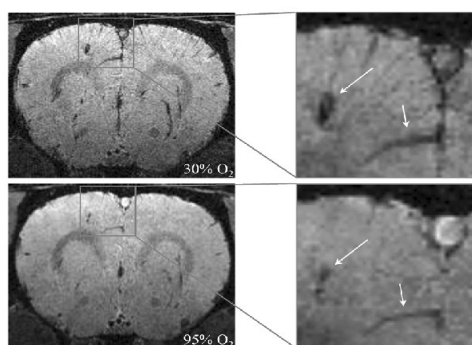
Stimulation of endogenous neural stem cells (NSCs) or NSCs transplantation via systemic or intraparenchymal injection has been reported as potentially powerful new therapeutic strategies for various neurological disorders. However, the trafficking of NSCs to areas of tissue damage is poorly understood. Stromal cell-derived factor-1 (SDF-1) and the chemokine receptor CXCR4 are highly expressed in the central nervous system, and are essential to homing of circulating hematopoietic stem cells (HSCs), mesenchymal stem cells (MSCs) and cancer cells to bone marrow and liver. In the ischemic brains, expression of SDF-1 and CXCR4 is upregulated in the penumbral area. To extend these observations, we used human NSCs (F3) line to investigate CXCR4 and SDF-1 expression with FACS analysis to determine the intracellular distribution of CXCR4 receptors. To verify the effect of SDF-1 on human NSCs, transwell assay toward SDF-1 gradient was performed. Protective effects of SDF-1 were evaluated by spontaneous apoptosis with serum /growth factor withdrawal, cell cycle analysis with FACS, and BrdU / Ki-67 labeling index. Human NSCs express SDF-1 $\alpha$  and CXCR4. FACS analysis showed most human NSCs had intracellular form of CXCR4 (98-99%), while 0.5-4% of them express in the membrane surface. CXCR4 protein was present in two forms, 49 kDa and 82 kDa (N-glycosylated form), similar to the patterns in MSCs (dimeric, 66/130 kDa) but different from those of HSCs or cancer cells. SDF-1 $\alpha$  (5 ng/ml) inhibited 54 % of spontaneous apoptosis induced by serum / growth factor deprivation, and increased the S phase by FACS analysis with enhanced BrdU / Ki-67 labeling index. Transwell assay showed the migration of NSCs toward SDF-1 $\alpha$  (500 ng/ml) gradient by 30% increase when compared to the control. Pre-incubation of neutralizing anti-CXCR4 antibody blocked the effects of SDF-1 $\alpha$  on human NSCs. In this study, we confirmed the expression of CXCR4 in human NSCs, which mediate the migration of NSCs according to the SDF-1 $\alpha$  gradient. Strategies to modulate the SDF-1/CXCR4 signaling may improve homing and engraftment of NSCs to brain.

## STEM CELL VISUALIZATION IN THE RAT BRAIN BY AN IMPROVED MRI PROTOCOL

Uwe Himmelreich, Pedro Ramos-Cabrer, Ralph Weber, Susanne Wegener, Mathias Hoehn

*In-Vivo NMR Laboratory, Max-Planck-Institute for Neurological Research, Cologne, Germany*

**Introduction** Three-dimensional Magnetic Resonance Imaging (MRI) can achieve microscopic resolution to monitor cellular dynamical processes. In order to discriminate implanted cells from host tissue, they must be labelled. Iron oxide nanoparticles (USPIO) function as such label and generate pronounced contrast in T2\*-weighted images. This approach is now well established [1, 2]. However, intrinsic T2 and T2\* effects caused by paramagnetic deoxyhemoglobin in red blood cells of blood vessels may complicate the data analysis. Changes in the deoxyhemoglobin level were the basis of MRI studies that have addressed the effect of blood oxygenation level-dependent (BOLD) contrast [3]. We have utilized the BOLD effect for the suppression of intrinsic T2 and T2\* effects and improved stem cell detectability by modification of the inhalation gas in an animal model. **Methods** Experiments were performed in accordance with NIH animal protection guidelines and approved by governmental authorities. Male Wistar rats (n=10, 250-550g) were anesthetized with 1% halothane. Three animals were part of a study where USPIO labeled embryonic stem cells were implanted in a stroke model (see [2]). The gas mixture for anesthesia was varied between: (A) 30-35% oxygen (O<sub>2</sub>) and 65-70% N<sub>2</sub>O and (B) 95% O<sub>2</sub> and 5% CO<sub>2</sub>. The gas mixture was changed from mixture (A) to (B) after completion of the MRI experiments with mixture (A), without repositioning the animal. MRI experiments were performed on an experimental animal scanner at 4.7 Tesla or 7 Tesla (Bruker BioSpec) equipped with actively shielded gradient sets 200 mT m<sup>-1</sup>. For rf irradiation and signal detection custom-built coils were used. A 12-cm-diameter Helmholtz coil arrangement served for rf excitation, whereas signal detection was achieved with a 2.3 cm (4.7T)/ 3.0 cm (7T) surface coil. **Results** Rats tolerated the 4 hours procedure very well. Two animals were imaged multiple times (up to four times). Images with gas mixture B (95% O<sub>2</sub>, 5% CO<sub>2</sub>) resulted in substantial reduction of intrinsic T2 and T2\* effects by blood vessels compared to the usually used gas mixture A (30-35% O<sub>2</sub>, 65-70% N<sub>2</sub>O). Small blood vessels were not visible and major blood vessels were reduced in size by up to 80%. The hypointense signal of USPIO labelled embryonic stem cells was not affected. **Figure 1:** Suppression of intrinsic T2\* effects by modification of the anesthesia gas. **Conclusion** The increased amount of oxygen in the anesthesia gas and the resulting BOLD effect enables a clear distinction between hypointensity effects caused by labelled cells and intrinsic hypointensity caused by paramagnetic oxyhemoglobin in blood vessels. This improves the unambiguous monitoring of cell migration substantially. **References:** 1. Bulte et al.; Nat. Biotechnol. 19, 1141 (2001). 2. Hoehn et al.; PNAS 99, 16267 (2002). 3. Ogawa et al; PNAS 87, 9868 (1990).



**ONO-5046 ATTENUATES DELAYED MOTOR NEURON DEATH AND AFFECTS THE INDUCTION OF BDNF, P-ERK AND CASPASE3 AFTER SPINAL CORD ISCHEMIA IN RABBITS**

**Takashi Yamauchi**<sup>1</sup>, Masahiro Sakurai<sup>2</sup>, Yoshiaki Sawa<sup>1</sup>, Koji Abe<sup>3</sup>, Hikaru Matsuda<sup>1</sup>

<sup>1</sup>*Department of Cardiovascular Surgery, Osaka University Graduate School of Medicine, Osaka, Japan*

<sup>2</sup>*Departments of Cardiovascular Surgery, National Hospital Organization Sendai Medical Center, Sendai, Japan*

<sup>3</sup>*Department of Neurology, Okayama University Graduate School of Medicine, Okayama, Japan*

**Objective:** The mechanism of delayed ischemic spinal cord injury during thoracoabdominal vascular surgery is speculated to be triggered by the apoptosis of spinal motor neuron cells. Recently, it has been shown that activated neutrophil play a central role in ischemia-reperfusion injury of the central nerve system. Moreover, neutrophil elastase might be one of the deteriorating factors of neutrophil caused injury. Therefore, we tested the hypothesis that ONO-5046, which is specific inhibitor of neutrophil elastase, can prevent the delayed ischemic spinal cord injury possibly through apoptosis related signal transduction. **Methods:** Rabbit spinal cord ischemia model with a balloon catheter was used in this study. Spinal cord was removed 8 hour, 1, 2, and 7 days after 15 minutes of transient spinal ischemia with or without ONO-5046 administration. Cell damage was analyzed by counting the number of motor neurons. The temporal profile of immunoreactivity of CPP32 (caspase3), brain-derived neurotrophic factor (BDNF) and phosphorylated extracellular signal-regulated kinase (p-ERK) were also investigated. **Results:** In the control group, lower limb function and most motor neurons were preserved until 2 days but were lost at 7 days after reperfusion. In the ONO-5046 treated group, the functional deficits were attenuated and motor neurons were more preserved histologically at 7 days. The induction of caspase3 was significantly reduced by ONO-5046 treatment. Furthermore, the expression of BDNF and p-ERK was prolonged. **Conclusions:** The results indicate that ONO-5046 may protect motor neurons from ischemic injury by reducing caspase3 and prolonging the expression of BDNF and p-ERK. ONO-5046 may be a strong candidate for use as a therapeutic agent in the treatment of ischemic spinal cord injury. Reference 1, Sakurai M, Hayashi T, Abe K, et al. Induction of glial cell line-derived neurotrophic factor and c-ret proto-oncogene-like immunoreactivity in rabbit spinal cord after transient ischemia. *Neurosci Lett* 1999; 276: 123-6. 2, Shimakura A, Kamanaka Y, Ikeda Y, Kondo K, Suzuki Y, Umemura K. Neutrophil elastase inhibition reduces cerebral ischemic damage in the middle cerebral artery occlusion. *Brain Res* 2000; 858: 55-60.

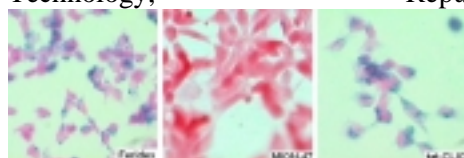
## COMPARATIVE EVALUATION OF THREE SUPERPARAMAGNETIC IRON OXIDE NANOPARTICLES, FERIDEX, MION-47, AND TAT-CLIO, TO LABEL HUMAN NEURAL STEM CELLS

Miyeoun Song<sup>1</sup>, Yunhee Kim<sup>1</sup>, Woo Kyung Moon<sup>2</sup>, **Byung-Woo Yoon<sup>1</sup>**

<sup>1</sup>*Department of Neurology, Clinical Research Institute, Seoul National University Hospital, Seoul, Korea*

<sup>2</sup>*Department of Diagnostic Radiology, Seoul National University Hospital, Seoul, Korea*

**Introduction:** Superparamagnetic iron oxides nanoparticles (SPION) are useful tracking markers of stem cell and used for numerous in vivo applications such as magnetic resonance imaging contrast enhancement. In the present study, we compared three different SPION such as standard superparamagnetic iron oxides (feridex), monocrySTALLine iron oxide nanoparticles (MION-47), and crosslinked iron oxides with tat peptide (tat-CLIO) in terms of their capacity to label human neural stem cells (hNSCs). **Methods:** hNSCs were incubated in cell culture media containing each SPION with which concentrations and incubation times have been modified from previous studies. Cell labeling with iron was assessed by Prussian blue stain and iron contents of the cell were analyzed by atomic absorption furnace spectrophotometer (AAS). Proliferation and vitality of hNSCs after SPION labeling were also evaluated using an investigation of long-term cell proliferation ability to continue and trypan blue dye exclusion test, respectively. The localization of iron oxides in hNSCs was investigated by Prussian blue stain and transmission electron microscopy. Furthermore, the retention of SPION in the cells were evaluated at different incubation time points of 6, 24 and 30 hr. **Results:** Incorporation of the each SPION appeared not to affect cell proliferation and vitality as compared with these of the nonlabeled cells. Within the cytoplasm iron oxide nanoparticles were presented. Cellular iron was detected in almost all hNSCs that were incubated with feridex or with tat-CLIO, but not with MION-47 as determined by Prussian blue stain. In addition, assessment using AAS revealed that tat-CLIO-labeled cells had more iron contents by two times and ten times when compared with cells labeled with feridex and MION-47, respectively. Moreover, labeling of cells with tat-CLIO revealed the longest retention of SPION in hNSCs up to 30 hr. **Conclusion:** Taken together, our study suggests that magnetic labeling of hNSCs using tat-CLIO is a useful tool for tracking and probably magnetic resonance imaging in future stem cell studies. **Grant support:** supported by a grant (SC13161) from Stem Cell Research Center of the 21st Century Frontier Research Program funded by the Ministry of Science and Technology, Republic of Korea.



**TIME-DEPENDENT SYSTEMATIC MIGRATION OF INTRAVENOUSLY TRANSPLANTED HUMAN NEURAL STEM CELLS IN ISCHEMIC RATS**Miyoun Song, Sun Ryu, Youngju Kim, Yunhee Kim, **Byung-Woo Yoon***Department of Neurology, Clinical Research Institute, Seoul National University Hospital, Seoul, Korea*

**Introduction:** The migration of intravenously transplanted human neural stem cells (hNSCs) in ischemic rats was investigated. **Methods:** hNSCs were colabeled with Endorem and BrdU, and then the hNSCs ( $4 \times 10^6$  cells) were intravenously injected in ischemic rats. After injection, rats were sacrificed at different time points (3hr, 6hr, 1d, 3d, 5d, 7d, 14d and 21d) and each rat brain and six organs (liver, lung, heart, intestine, kidney, spleen) were isolated, followed by histological analysis. **Results:** On 3d after transplation, hNSCs were detected in the focal ischemia lesion of rat brain and remained for 21d whereas they were not observed in any other organs that were tested. However, hNSCs were detected in the spleen at entire time points. **Conclusion:** Our study demonstrates that the intravenously transplanted hNSCs migrated specifically into ischemia lesion with the exception of the spleen.

**Grant support:** This study was supported by a grant of the Korea Health 21 R & D Project, Ministry of Health & Welfare, Republic of Korea. (Project No. : 0405-B002-0205-0001)

## FOCAL CEREBRAL ISCHEMIA INCREASES TYPE 2 IODOTHYRONINE DEIODINASE

Koji Seki<sup>1</sup>, Hideaki Imai<sup>2</sup>, Tatsuya Shimizu<sup>2</sup>, Katsuhiko Tsunekawa<sup>1</sup>, Takayuki Kasahara<sup>1</sup>,  
Takayuki Ogiwara<sup>1</sup>, Nobuhito Saito<sup>2</sup>, Masami Murakami<sup>1</sup>

<sup>1</sup>Department of Clinical Laboratory Medicine, Gunma University Graduate School of Medicine, Maebashi, Japan

<sup>2</sup>Department of Neurosurgery, Gunma University Graduate School of Medicine, Maebashi, Japan

**Background and Purpose:** Thyroid hormones play important roles in normal brain maturation and normal brain function. T<sub>4</sub>, which is a major secretory product of the thyroid gland, needs to be converted to T<sub>3</sub> by iodothyronine deiodinase to exert its biological activity. Type 1 iodothyronine deiodinase (D1) activity is present in thyroid gland, liver, and kidney, whereas type 2 iodothyronine deiodinase (D2) activity is present in brain, anterior pituitary, brown fat, and pineal gland. While D1 activity is known to decrease in the hypothyroid state and mainly contributes to the circulating T<sub>3</sub> level, D2 activity increases in the hypothyroid state and plays a pivotal role in providing local intracellular T<sub>3</sub>. D2, therefore, plays an important role to maintain local intracellular T<sub>3</sub> concentration in brain. Although D2 is inactivated by ubiquitin-proteasome system at posttranslational level, it is not known whether D2 expression is altered after cerebral ischemia that is known to affect ubiquitin-proteasome system. In the present study, we have evaluated the effect of focal cerebral ischemia on D2 mRNA and D2 activity in the rat. **Methods:** Permanent middle cerebral artery occlusion was employed in halothane anesthetized adult Sprague Dawley rats (Tamura model). Rats (n=30) were decapitated at 24 hours, 3 days and 7 days after ischemia. Sections of 20 μm thickness were cut on a cryostat and were stained with hematoxylin and eosin, and examined by a light microscope. These sections were examined by in situ hybridization of D2 mRNA using digoxigenin-labeled antisense cRNA probe for rat D2. D2 activity was measured by the release of I- from 2nM [<sup>125</sup>I] T<sub>4</sub> in the presence of 20 mM DTT and 1 mM PTU in dissected tissues such as ipsilateral remote cortex and contralateral cortex. **Results:** D2 mRNA was ubiquitously expressed in the brain, and was expressed in neurons and astrocytes, confirmed by immunostaining with the neuronal marker and astrocytic marker, NeuN and GFAP, respectively. Although D2 mRNA expression was markedly decreased in ischemic core cortex, D2 mRNA expression did not altered neither in remote cortex of ipsilateral cortex nor contralateral cortex at 24 hours, 3 days and 7 days after MCA occlusion. In contrast, D2 activity in ipsilateral cortex was significantly increased compared with contralateral cortex at 3 days after MCA occlusion (p<0.05), but not at 24 hours and 7 days after ischemia (Figure). **Conclusions:** The present results demonstrated that D2 activity, but not D2 mRNA, in ipsilateral cortex was significantly increased after focal cerebral ischemia. It is suggested that focal cerebral ischemia may affect D2 degradation by modulating ubiquitin-proteasome system at posttranslational level. The present study suggests that local intracellular T<sub>3</sub> production by D2 may be involved in the pathophysiology of focal cerebral ischemia.

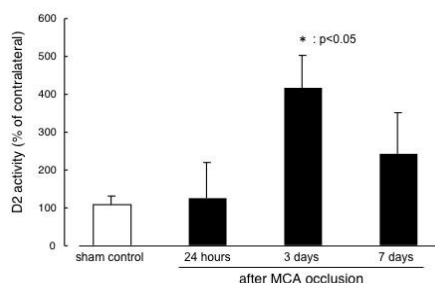


Fig. D2 activity in ipsilateral cortex was compared with contralateral.



## TRANSPLANTED STEM CELLS UNDERGO CELLULAR FUSION IN EXPERIMENTAL , BRAIN TRAUMA

Zsombor Lacza<sup>1,2</sup>, Eszter M. Horváth<sup>1,2</sup>, Attila Csordás<sup>2</sup>, Márk Kollai<sup>2</sup>, Csaba Szabó<sup>2</sup>,  
David W. Busija<sup>1</sup>

<sup>1</sup>Wake Forest University Health Sciences, Department of Physiology and Pharmacology,  
Winston-Salem, NC, USA

<sup>2</sup>Semmelweis University, Institute of Human Physiology and Clinical Experimental Research,  
Budapest, Hungary

Recent *in vitro* studies showed that stem cells might undergo cell fusion (1), however, there is no *in vivo* evidence for this phenomenon in the brain. Our goal was to investigate the possibility of cell fusion in a model of traumatic brain injury followed by grafting of embryonic cortical cells.

Cold lesion was applied to induce brain trauma in halothane anesthetized adult male Wistar rats as described (2). Six days later, BrdU-labelled (50 mg/kg ip 24 hours before harvesting) E14 embryonic brain cell suspension was grafted into the penumbra in 3 deposits (3 µl each; 50 000 cells/µl). Six days later the brain was removed for immunohistochemical processing. Characterization of the grafted cell suspension was performed on methanol-fixed smears, a BrdU antibody was applied to evaluate the effectiveness of labeling and an anti-Nestin antibody was used to calculate the proportion of stem cells. Investigation of the grafted cells was achieved by confocal fluorescent microscopy in triple-labeled sections. Lineage specific markers were labeled with red fluorescence [glial fibrillary acidic protein (GFAP) for astrocytes, myelin basic protein (MBP) for oligodendrocytes and neurofilament 68 (NF68) for neurons]. The BrdU antibody was labeled with a green fluorescent tag and the nuclei were counterstained with the far-red fluorescent To-Pro. Nine sequential sections covering the center of the lesion were evaluated to allow for quantitation.

Nuclear labeling with BrdU was detected in 26% of the donor cell suspension, while the stem cell marker nestin labeled 34% of the cells. Six days after grafting, the surviving labeled cells were distributed on the surface of the lesion and in the penumbra. The majority of these cells did not show any morphological signs of differentiation and did not express cell-line specific markers. A small percentage of surviving BrdU positive cells (0.5%) had two distinct nuclei, one was unlabelled and one was BrdU positive, which is a sign of cell fusion. These cells were similar in appearance and size to the astrocytes in the vicinity and expressed the astrocytic marker GFAP. None of the double-nuclei positive cells were MBP or NF68 positive.

We conclude that spontaneous fusion involving grafted embryonic cells can occur in the regenerating brain tissue following traumatic injury. This is the first *in vivo* report that shows possible cellular fusion involving transplanted embryonic cells in the brain.

Supported by the NIH (HL30260, HL46558, HL50587); the Hungarian OTKA (D-45933, T-029169, T-037885, T-037386) and ETT (248/2003, 249/2003)

1. Ying, Q. L., Nichols, J., Evans, E. P. and Smith, A. G. (2002) *Nature* 416, 545-548
2. Lacza, Z., Horvath, E. and Busija, D. W. (2003) *Brain Res Brain Res Protoc* 11, 145-154

## CHRONIC SURVIVAL AND FUNCTION OF ADULT STEM CELLS FROM ADIPOSE TISSUE IN THE ISCHEMIC MOUSE BRAIN

Nathalie Kubis<sup>1</sup>, Yutaka Tomita<sup>1</sup>, Valérie Planat<sup>2</sup>, Alexy Tran Dinh<sup>1</sup>, Yolande Calando<sup>1</sup>, Monique André<sup>2</sup>, Ludovic Waekel<sup>1</sup>, Bartosz Karaszewski<sup>1</sup>, Luc Pénicaud<sup>2</sup>, Bernard I. Lévy<sup>1</sup>, Jean-Sébastien Silvestre<sup>1</sup>, Louis Casteilla<sup>2</sup>, Jacques Seylaz<sup>1</sup>, **Elisabeth Pinard**<sup>1</sup>

<sup>1</sup>INSERM U 689 Cardiovascular Research Center Lariboisière, Université Paris 7, Paris, France

<sup>2</sup>CNRS UMR 5018, Laboratoire de Neurobiologie, Plasticité Tissulaire et Métabolisme Énergétique, Université Paul Sabatier, Toulouse, France

**Introduction:** Similar to bone marrow, the stromal vascular fraction (SVF) of white adipose tissue contains pluripotent cells such as hematopoietic progenitors and mesodermal stem cells<sup>1,2</sup>. Particularly, SVF has been shown to have a proangiogenic potential in the mouse ischemic hindlimb model<sup>3</sup>. The present study aims at evaluating a possible interest of SVF for therapeutical approaches in cerebral ischemia.

**Methods:** A closed cranial window was chronically implanted over the left parietal cortex of C57/BL6 mice (n=16) without reflecting the dura<sup>4</sup>. The left MCA was occluded either proximally or distally across the cranial window. Green fluorescent protein-expressing (GFP<sup>+</sup>) SVF cells (5x10<sup>4</sup> cells in 0.5 µl), cultured as previously described<sup>3</sup>, were intracerebrally and ipsilaterally injected 24h after ischemia. Fluorescent cells were observed *in vivo* through the window using confocal microscopy at different time points for up to 15 days. At prescribed times, brains were processed for immunocytochemistry using various antibodies linked to Alexa 594 fluorophore, to identify endothelial, smooth muscle, microglial and glial cells.

**Results:** In ischemic mice, the number of GFP<sup>+</sup> cells visible through the cranial window increased throughout the study (Fig.A) Many cells slightly migrated toward the ischemic area. In contrast, few GFP<sup>+</sup> cells were scattered over the region tested in sham mice, and their number decreased over time. Histology revealed high plasticity of SVF cells, characterized by elongation, tubular shapes, and encircling vessels (Fig.B). Some GFP<sup>+</sup> cells infiltrated the ischemic tissue. GFP<sup>+</sup> cells occasionally co-localized with CD31 or α-actin, while they often surrounded CD31 labeling or were surrounded by α-actin labeling. No co-localization with Vimentin or Iba1 was observed. There were no major differences between the two ischemia models tested.

**Conclusion:** This study demonstrates that adipose-lineage cells can survive at least 15 days in the ischemic brain, adapting to brain architecture, and having close relationships with vessels in the peri-ischemic area. Consequently, these cells could be used as carriers to deliver various factors helpful for brain tissue repair.

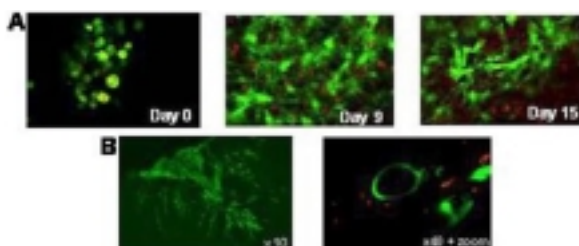
### References:

Cousin B, Andre M, Arnaud E, et al. (2003) *Biochem Biophys Res Commun.* 301: 1016-22.

Zuk PA, Zhu M, Mizuno H, et al. (2001) *Tissue Eng.* 7: 211-28.

Planat-Bernard V, Silvestre JS, Cousin B, et al. (2004) *Circulation* 109: 23-30

4- Tomita Y, Kubis N, Calando Y, et al (2005) *J Cereb Blood Flow Metab* In press





**TRAUMATIC BRAIN INJURY COUPLED WITH SECONDARY HYPOXIA LEADS TO A MILD ENDOPLASMIC RETICULUM STRESS RESPONSE IN THE RAT**

Jessie S. Truettner<sup>1</sup>, Bingren Hu<sup>2</sup>, Ofelia F. Alonso<sup>1</sup>, Helen M. Bramlett<sup>1</sup>,  
W. Dalton Dietrich<sup>1</sup>

<sup>1</sup>*Department of Neurological Surgery, Neurotrauma Research Center, and The Miami Project to Cure Paralysis, University of Miami Miller School of Medicine, Miami, FL, USA*

<sup>2</sup>*Department of Neurology, University of Miami Miller School of Medicine, Miami, FL, USA*

**Introduction:** Traumatic brain injury (TBI) initiates a series of secondary injury cascades that participate in the pathogenesis of traumatic cell injury. These include electrophysiological, biochemical, and molecular events associated with excitotoxicity, inflammation and apoptosis. An immediate reaction by vulnerable and nonvulnerable brain regions to trauma is a cellular stress response. Genes involved in producing a variety of stress response proteins, including cytosolic, mitochondrial, and endoplasmic reticulum (ER) associated, may be rapidly induced or upregulated after injury. These genetic responses may also be exacerbated by secondary hypoxia, which represents a common secondary insult in TBI patients. In this study, specific stress genes were assessed by in situ hybridization after TBI both with and without a 30 min secondary hypoxic insult. **Methods:** Male Sprague-Dawley rats were traumatized by moderate (1.8-2.2 atm) fluid-percussion brain injury. Experimental groups included sham and moderate TBI, with or without secondary hypoxia. Four and 24 hour survival times were assessed. Brains were removed, cryosectioned, and hybridized to 35S labeled riboprobes for the following genes: HSP70, HSP60, GRP78, calnexin, and PDI. **Results:** The cytosolic chaperone HSP70 was strongly induced by TBI in the ipsilateral cerebral cortex at 4 hours. Secondary hypoxia increased this expression to include areas of the ipsilateral hippocampus and thalamus, and the bilateral striatum. The mitochondrial membrane bound chaperone HSP60 was induced by TBI at a lower level in the ipsilateral outer cortical layers at 4-24 hours and was not affected by secondary hypoxia. GRP78, an endoplasmic reticulum stress response gene, was induced by TBI in the ipsilateral outer cortical layers, as well as in the dentate gyrus. Secondary hypoxia did not alter this expression. Calnexin and PDI, both constitutive ER protein folding mediators, were unaffected by TBI or hypoxia. Hypoxia alone failed to induce any of these stress genes in sham operated control rats. **Conclusions:** The cytosolic response to stress caused by TBI is very strong and is augmented with the addition of secondary hypoxia. In contrast, the ER and mitochondrial stress response to TBI, even in the presence of secondary hypoxia, is comparatively mild. These findings indicate that distinct parts of the cell may respond to metabolic stresses and cerebral insults in unique ways and possibly by different mechanisms. Induction of either cytoplasmic stress genes or ER luminal stress genes reflects in which cellular compartments non-native proteins may be overproduced. This study suggests non-native proteins are overproduced mainly in the cytoplasm, and to a lesser degree, in the mitochondria and ER lumen after TBI. These new findings may help to clarify therapeutic targets to reduce the detrimental consequences of secondary insults after TBI. Supported by NIH grants NS42133 and NS30291

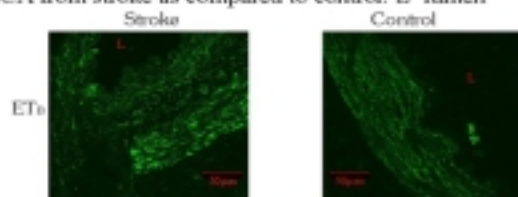
## GENE EXPRESSION IN HUMAN CEREBRAL ARTERIES

Petter Vikman, Lars Edvinsson

*Department of Medicine, Experimental Vascular Research, Lund University, Lund, Sweden*

Background and purpose: Experimental animal studies of cerebral ischemia reveals an upregulation of receptors in the middle cerebral artery (MCA) leading to the ischemic area. Our hypothesis is that these changes cause increased brain damage because of an increased vessel contractility. To further investigate this hypothesis and to see if it is true in man we have investigated the gene expression in human MCA after a stroke and compared with the expression in MCA of patients deceased due to an extracerebral cause. Methods: The samples were obtained post-mortem. The gene expression was analysed with real-time PCR and microarray. Results: We investigated the expression of genes previously shown to be important in animal models with real-time PCR (e.g. ETA, ETB, AT1, AT2 and 5-HT<sub>2A/1B/1D</sub>). The expression of ETA, ETB and 5-HT<sub>1B</sub> was significantly upregulated in the stroke samples in comparison to control (n=3-8, Students t-test,  $p \leq 0,05$  was considered significant) while the expression of AT1, AT2 and 5-HT<sub>1A/2D</sub> had a tendency towards upregulation albeit not significantly. Hence these findings was consistent with previous findings in experimental stroke. The expression of ETB was also confirmed on protein level with immunohisto-chemistry where stroke affected vessels showed a higher expression of ETB in comparison to control. (Figure 1). To broaden our knowledge of the expression profile in cerebral vessels after a stroke, microarray investigations were done. Several new genes were found to be significantly upregulated in the MCA of stroke patients and of those seven were chosen for further investigation with real-time PCR; ELK3, LY64, Metallothionin IG and POU3F4 were upregulated while Actin alpha<sub>2</sub>, RhoA and smoothelin were downregulated. Six of these were regulated the same way when examined with real-time PCR. Conclusion: The gene expression in the human samples indicates that the gene expression in the human MCA after a stroke is similar to that seen in the MCA after experimental occlusion in rats. With microarray we found several new genes that were related to smooth muscle function which supports the dynamic changes that occur in the MCA distributing to the stroke region in the ischemic hemisphere.

Figure 1. Comparison of the amount of ET<sub>B</sub> receptor protein as shown with immunohistochemistry. There is a stronger ET<sub>B</sub> signal in MCA from stroke as compared to control. L=lumen



**IDENTIFICATION OF GENES RELATED TO PI3-K/AKT SURVIVAL SIGNALING PATHWAYS IN CEREBRAL CORTEX AFTER FOCAL ISCHEMIA IN RATS****Shizuo Hatashita<sup>1</sup>, Ikuko Ogino<sup>2</sup>, Takashi Mitsuhashi<sup>3</sup>**<sup>1</sup>*Neurosurgery, Juntendo University Urayasu Hospital, Urayasu, Japan*<sup>2</sup>*Neurosurgery, Juntendo University, Tokyo, Japan*<sup>3</sup>*Neurosurgery, Tokyo Metropolitan Hiroo General Hospital, Tokyo, Japan*

**Introduction:** Cerebral ischemia leads to induction and suppression of various genes whose interplay promotes the ischemic neuronal death. The serine-threonine kinase, Akt, plays a central role in survival signaling and translational control, and its activation is mediated by phosphatidylinositol 3-kinase (PI3-K). The present study is designed to evaluate differently expressed genes associated with PI3-K/Akt survival signaling pathways in the cortical tissue of induced ischemia using oligonucleotide microarrays. We also analyze the expression of several genes encoding enzymes and molecules with immunohistochemistry. **Methods:** Sprague-Dawley rats were anesthetized with ketamine (40mg/kg) and xylazine (10mg/kg). Focal ischemia was induced by occlusion of the left middle cerebral artery (MCA) for 1 and 3 hours in 10 rats. Five sham-operated rats served as controls. After animals were sacrificed, total RNA was isolated from ischemic cortex. Double-stranded cDNA was synthesized from total RNA. Biotin-labelled cRNA was synthesized from cDNA and hybridized to the U34A Genechip (Affymetrix). The cross-comparisons were made between MCA occlusion and sham operation. The average change in expression was greater than 2.0 fold over sham. Additionally, expression of enzymes and molecules related to PI3-K/Akt pathways was examined with immunohistochemistry. Fluorescence double-immunostaining was used to elucidate the cellular localization. **Results:** The different regulation of genes that are related to PI3-K/Akt pathways was induced with focal ischemia. The expression of Akt 2 gene was up-regulated at 1 hour after MCA occlusion, then down-regulated at 3 hours. PI3-K gene was up-regulated to 2.81-fold at 1 hour. Gene expression of insulin-like growth factor 1(IGF-1) and insulin receptor substrate-1, relating to the upstream signaling for underlying PI3-K activation, was up-regulated at 1 hour after MCA occlusion (>5.0 fold). In addition, genes for IGF-binding protein 3 and IGF-binding protein 5 were up-regulated at 3 hours. Gene expression of Akt downstream targets, including NFκB, Caspase9, Forkhead box transcription factors and BAD, did not change after MCA occlusion. In contrast, expression of cAMP responsive-element modulator (CREM) and cAMP responsive-element-binding protein alpha (CREB) genes was up-regulated at 1 and 3 hours after MCA occlusion, respectively. Several genes for intracellular signal transduction, including growth hormone receptor, interleukin 3 receptor, growth factor receptor-bound protein 2 and integrin beta 1, were not affected by focal cerebral ischemia. The phospho-Akt and PI3-K immunoreactivities were evident in the neuron of the ischemic core and penumbra both 1 and 3 hours after MCA occlusion, but the relative number of positive cells was low. Double staining for Akt showed colocalization with several PI3-K positive neurons. No colocalization was observed in the neuron with the cellular damage. At 3 hours after MCAO, immunoreactivity of phospho-Akt was diminished, compared with that at 1 hour. **Conclusion:** These findings indicate that PI3-K and Akt are activated with insulin-like growth factor-1 in the ischemic cortical neurons, depending on the degree of cellular damage. This PI3-K/Akt pathway can promote cell survival and prevent apoptosis by activating target transcription factor, cAMP responsive-element modulator. The PI3-K/Akt signaling pathway mediated by insulin-like growth factor is a possible role in the protection of ischemic neuronal death.

## NEURAL STEM CELLS DECREASE NEURONAL LOSS INDUCED BY ISCHEMIA/REPERFUSION IN MICE

**Carmen Capone**<sup>1</sup>, Simona Frigerio<sup>2</sup>, Alessia Cafici<sup>1</sup>, Chiara Carlesso<sup>1</sup>, Simone Pizzimenti<sup>1</sup>, Maurizio Gelati<sup>2</sup>, Giulio Alessandri<sup>2</sup>, Eugenio Parati<sup>2</sup>, MariaGrazia De Simoni<sup>1</sup>

<sup>1</sup>*Laboratory of Inflammation and Nervous System Diseases, Mario Negri Institute, Milan, Italy*

<sup>2</sup>*Laboratory of Neurobiology and Neuroregenerative Therapies, Carlo Besta Neurological Institute, Milan, Italy*

We investigated the effect of neural stem cell (NSC) infusion on brain ischemia/reperfusion injury. Ischemia was achieved by middle cerebral artery occlusion in C57/Bl6 mice. A 6-0 monofilament nylon suture, blunted at the tip by heat and coated in poly-L-lysine was introduced into the common carotid artery and advanced so as to block middle cerebral artery. The filament was advanced until a > 70% reduction of blood flow compared to preischemic baseline was observed. At the end of a 30 min ischemic period, blood flow was restored by removing the filament. To confirm the adequacy of the vascular occlusion, blood flow was measured by Laser Doppler flowmetry. Selected stem cells, isolated from newborn C57BL/6 mice, expressing b-galattosidase gene, were injected intracerebroventricularly in mice (5x10<sup>5</sup>/5ml) at the end of ischemia. The distribution and migration of stem cells in ischemic and non-ischemic brains were evaluated by X-Gal staining at different time points. Two hours after ischemia, stem cells could be observed near the injection site, attached to the ependyma and beginning to move inside the brain parenchyma. At 24h stem cells were still present in the brain parenchyma, but many of them could be found inside the vessels, both in the ipsi- and in the contralateral side. At day 5 and day 14 the majority of b-gal positive cells could be found inside the vessels, both in the ipsi- and in the contralateral side. At these two time-points in sham-operated mice no positive cell could be found in brain parenchyma or in vessels, indicating that if there was no lesion, cells were washed out. Fourteen days after ischemia neuronal loss was evaluated by cresyl violet staining. Neurons in the striatal region were counted by an image analysis software (AnalySIS). For each brain, three 20mm sections, including the anterior, medial and posterior striatum, were analysed and on each section six fields were examined at 40 $\times$  magnification. The number of neurons was estimated as percentage of neurons in the ipsilateral side versus those in the contralateral side. Mice receiving NSC showed a significant reduction of neuronal loss compared to those receiving saline (NCS: 4.9 $\pm$  3.5% saline: 26.2 $\pm$  7.1%) These data indicate that NSC are recruited by ischemic injury and that they are able to reduce the neuronal damage induced by ischemia/reperfusion.

## POTASSIUM CHANNELS IN ISCHEMIC CORTICAL TISSUE AFTER MIDDLE CEREBRAL ARTERY OCCLUSION OF RATS

Shizuo Hatashita<sup>1</sup>, Takashi Mitsuhashi<sup>2</sup>, Ikuko Ogino<sup>3</sup>

<sup>1</sup>Neurosurgery, Juntendo University Urayasu Hospital, Urayasu, Japan

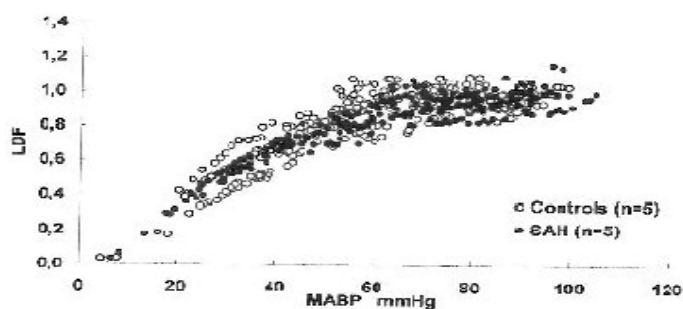
<sup>2</sup>Neurosurgery, Metropolitan Hiroo General Hospital, Tokyo, Japan

<sup>3</sup>Neurosurgery, Juntendo University, Tokyo, Japan

**Introduction:** The activity of potassium channels plays an important role in the cell volume regulatory mechanism of ischemic cell death. More than 70 potassium channels have been identified primarily with the different genes encoding for K<sup>+</sup> channel principal and accessory subunits and their genealogical relationships. The present study is designed to evaluate differently expressed genes encoding for potassium channel principal subunits in the cortical tissue after focal cerebral ischemia by oligonucleotide microarrays. We also use immunohistochemistry to clarify the cellular localization of several potassium channels on ischemic cortical tissue. **Methods:** Sprague-Dawley rats were anesthetized with ketamine (40mg/kg) and xylazine (10mg/kg). Focal ischemia was induced by occlusion of the left middle cerebral artery (MCA) for 1 and 3 hours in 10 rats. Five sham-operated rats served as controls. After animals were sacrificed, total RNA was isolated from ischemic cortex. Double-stranded cDNA was synthesized from total RNA. Biotin-labelled cRNA was synthesized from cDNA and hybridized to the U34A Genechip (Affymetrix). The cross-comparisons were made between MCA occlusion and sham operation. The average change in expression was greater than 2.0 fold over sham. In addition, expression of several genes encoding for potassium channel principal subunits was examined with immunohistochemistry. Fluorescence double-immunostaining with mouse anti-neuronal nuclei antibody or anti-microtubule-associated protein 2 antibody was also used to elucidate the cellular localization. Cells were imaged under a fluorescence microscope. **Results:** Several genes of voltage-gated (Kv) K<sup>+</sup> channels and inward rectifier (Kir) K<sup>+</sup> channel were differently regulated in cortical tissue by focal ischemia. Expression of shaker-related subfamily member 4 (Kv1.4) and shaw-related subfamily member 2 (Kv3.2) genes were up-regulated at 3 hours after MCA occlusion. Neuronal potassium channel alpha subunit (Kv8.1) gene was also up-regulated while shab-related subfamily member 1 (Kv2.1) gene was down-regulated. At 1 hour after MCA occlusion, in contrast, gene expression of inward rectifier 11 (Kir2.3) was only up-regulated. The gene expression of other K<sup>+</sup> channels, Ca<sup>2+</sup>-activated K<sup>+</sup> channels and "Leak" K<sup>+</sup> channels, was not affected with focal cerebral ischemia. Genes for auxiliary subunits of potassium channel principal subunits did not also change in ischemic cortical tissue. The intensity of Kir 2.3 immunoreactivity was increased in the ischemic tissue at 1 hour after MCA occlusion. Expression of Kir 2.3 was mainly seen in the cytoplasm within swollen neurons, particularly around the nucleus. At 3 hours after MCA occlusion, Kv1.4 immunoreactive staining had a patchy appearance within the ischemic core. The distribution of Kv1.4 immunoreactivity was intensely observed in neurons with cellular shrinkage and axons. In contrast, Kv2.1 immunoreactivity was greatly decreased in neuronal cell bodies and processes, particularly membrane of cells, compared with that of the non-occluded hemisphere. **Conclusion:** These findings indicate that several principal subunits of voltage-gated K<sup>+</sup> channels and inward rectifying K<sup>+</sup> channel are induced in the ischemic neurons of cortical tissue. The voltage-gated K<sup>+</sup> channels, Kv1.4, Kv2.1, Kv3.2 and Kv8.1, are related to cell volume regulation under ischemic neuronal death. In particular, the inward rectifier 11 K<sup>+</sup> channel may mediate immediately ischemic change in intracellular ion homeostasis.

**EXPRESSION PROFILING IN THE PHOTOTHROMBOTIC RAT MODEL:  
IDENTIFICATION OF GENES POTENTIALLY INVOLVED IN PLASTICITY****Wolf-R. Schäbitz<sup>1</sup>, Carola Krüger<sup>2</sup>, Domus Cira<sup>1,2</sup>, Clemens Sommer<sup>3</sup>, Armin Schneider<sup>2</sup>**<sup>1</sup>*Department of Neurology, University of Münster, Münster, Germany*<sup>2</sup>*Axaron Bioscience AG, Heidelberg, Germany*<sup>3</sup>*Department of Neuropathology, University of Ulm, Ulm, Germany*

**Introduction:** Gene expression changes with potential effects on cortical plasticity have not been studied in great detail. We postulated that genes that are implied in plasticity or recovery are characterized by 1.) their persistent regulation over long time intervals after ischemia, or their induction in a delayed mode after ischemia, and / or 2.) their regulation in the periinfarct area, or in the contralateral homotopic cortex. In order to study these events we chose the photothrombotic model of cortical ischemia, as the infarct is small and defined, does not interfere with survival of the animals, and animals are known to recuperate from the lesion, implying active recovery mechanisms. We applied a sensitive fragment display technique, restriction-mediated differential display (RMDD) to systematically study gene expression changes following the lesion at 6 h, 2 days, and 3 weeks to observe long-term changes. **Material and Methods:** Photothrombotic ischemia was induced using an i.v. infusion of the photosensitive dye rose bengal, and illumination of the sensory-motor cortex with a light source. Using coronal sections, periinfarct areas were dissected by punch biopsies, and processed for RNA extraction. The RMDD protocol was performed as described 1. Quantitative PCR was done using the Lightcycler system (Roche Diagnostics). Immunohistochemistry was performed on 2 µm paraffin sections. **Results:** We were able to identify over 50 genes that were regulated at each time point examined, a surprisingly high number of which were regulated in the contralateral homotopic cortex. Quantitative PCR was used to confirm the regulation of selected genes, and immunohistochemistry was used to demonstrate the pattern and cellular origin. Several candidates for involvement in cortical plasticity processes could be identified that follow the requirements outlined above. Further work is needed to indeed prove the contribution of these genes to plasticity. **Conclusion:** The extent of differential gene regulation even at late intervals after cortical ischemia was unexpected and indicates strong plastic reactions 3 weeks after ischemia in the ipsilateral infarct-adjacent cortex, and in the homotopic contralateral context. Two groups of genes that appear particularly interesting are those related to neurogenic events (e.g. nestin and stathmin), and synaptic events (e.g. synaptotagmin 4). Our data have potential implications for strategies to enhance post-stroke rehabilitation. **References:** 1. Schneider, A., Fischer, A., Weber, D., von Ahsen, O., Scheek, S., Krüger, C., Rossner, M., Klausner, B., Faucheron, N., Kammandel, B., et al. 2004. Restriction-mediated differential display (RMDD) identifies pip92 as a pro-apoptotic gene product induced during focal cerebral ischemia. *J Cereb Blood Flow Metab* 24:224-236.



	$^{133}\text{Xe}$	LDF
I.I. (control)	---	$58 \pm 1.8$ (n=5)
LL(NA)	$119 \pm 11.2$	$57 \pm 4.9$ (n=5)
I.I.(SAH)	---	$63 \pm 1.7$ (n=5)
LL(SAH+NA)	$105 \pm 5.9$	$75 \pm 4.4$ (n=6)

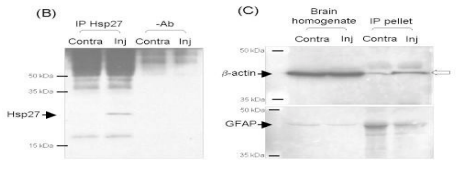
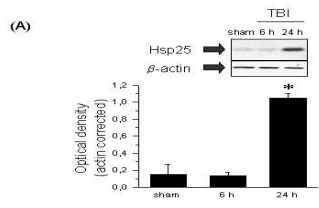
582

### SPATIO-TEMPORAL PROFILE OF SMALL HEAT-SHOCK PROTEIN HSP27 INDUCTION IN RAT BRAIN FOLLOWING FLUID-PERCUSSION INJURY TO THE LATERAL PARIETOTEMPORAL CEREBRAL CORTEX; INVOLVEMENT WITH BETA ACTIN

Jae-Hyuk Yi, Raquel Herrero, Chun-lei Wang, Alan Stewart Hazell

*Department of Medicine, CHUM, St-Luc Hospital, Montreal, QC, Canada*

Heat shock protein 27 (Hsp27) belongs to a group of small Hsps that perform a variety of functions including molecular chaperoning, regulation of actin dynamics and antioxidative activity, and inhibition of apoptosis. In adult rat brain, constitutive neuronal expression of Hsp27 is present in neurons and occasionally non-neuronal cells including astrocytes, ependymal cells and the choroid plexus. Since little is currently known of the involvement of Hsp27 in cerebral trauma, we have examined the effects of moderate fluid-percussion injury (FPI) on the spatio-temporal patterns of Hsp27 induction and potential interaction of Hsp27 with other structural proteins in rat brain. In the ipsilateral parieto-temporal cortex, Hsp27 protein levels were increased over 7-fold at 24 h following the insult compared to sham controls by immunoblotting (Figure, A), and which persisted for up to 7 days post-trauma. Immunohistochemical assessment revealed a mainly astroglial pattern of staining for Hsp27 in the cortex, hippocampus, and thalamic nuclei ipsilateral to the injury with some immunoreactivity also extending into contralateral hippocampal structures. Immunoprecipitation studies using both injured and contralateral cortical brain tissue of 24 h post-injured rats showed that Hsp27 immunoprecipitated only from the injured, but not contralateral, cortex at 24 h post-injury (Figure, B). In addition, Hsp27 immunoprecipitate from 24 h post-injured ipsilateral cortex coimmunoprecipitated with beta actin, and not GFAP (Figure, C). Our results suggest that FPI produces a large, predominantly astroglial-specific induction of Hsp27 that is widespread in the injured hemisphere. Given its previously identified role as a chaperone protein, interaction of Hsp27 with actin may indicate an important function for this gene in stabilization of actin filaments in astroglia, a potentially valuable contributing factor to the known resistance of these cells to trauma-induced stress. Supported by CIHR, Canada.





## VASCULOGENESIS, ANGIOGENESIS AND LOCAL BLOOD FLOW RECOVERY AFTER EMBRYONIC STEM CELLS TRANSPLANTATION IN THE ISCHEMIC BRAIN

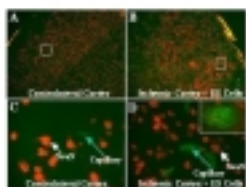
Ling Wei<sup>1,3</sup>, Jianan Wang<sup>2</sup>, Michelle Hedrick<sup>1</sup>, Chang-ling Li<sup>1,2</sup>, Christine L Keogh<sup>1</sup>, David I Gottlieb<sup>3</sup>, Shan Ping Yu<sup>1</sup>

<sup>1</sup>*Departments of Pathology and Pharmaceutical Sciences, Medical University of South Carolina, Charleston, SC, USA*

<sup>2</sup>*Department of Cardiology, Sir Run Run Shaw Hospital, University, Hang Zhou, China*

<sup>3</sup>*Department of Neurology, Washington University, St. Louis, MO, USA*

Stroke is a vascular disease in which brain cell death is initiated by a great reduction in blood flow. Only a few minutes of markedly lowered local blood flow (focal ischemia) may injure neurons and non-neuronal cells (e.g., endothelial cells and astrocytes) and lead to their death. Vasculogenesis is a process in which angioblasts differentiated into endothelial cells to form a primitive capillary network; whereas angiogenesis is the sprouting of capillaries from pre-existing blood vessels. Both mechanisms may contribute to neovascularization during embryogenesis and repair of damaged tissues in adults. The multi-potent embryonic stem (ES) cells can differentiate into neural cells and endothelial cells in vitro and in vivo. The multi-potentiality of ES cells provides a potential strategy for repairing the damaged brain after ischemic stroke. To examine the feasibility of ES cell transplantation in the ischemic brain and functional benefits of neovascularization, this study explored differentiations of transplanted ES cells in a rodent focal ischemia model. Transient focal cerebral ischemia was induced in adult male animals by 30-min occlusion of middle cerebral artery. Mouse ES cells were differentiated down neural lineages using the retinoic acid “4-/4+” protocol. To be able to identify ES cells after transplantation, ES cells were genetically marked with green fluorescent protein GFP or pre-labeled with BrdU and Hoechst. ES cell transplantation was performed 7 days after ischemia. Differentiation of ES cells was demonstrated by specific antibodies including MAP2, neurofilament, NeuN for neuron-like cells, GFAP for astrocytes, NG-2 for oligodendrocytes, Glut-1 and CD-31 for endothelial cells. Transplanted ES cells survived, differentiated and form functional structure in the ischemic core and penumbra regions. ES cell-derived endothelial cells formed new vesicular structures 7 – 14 days after transplantation. Local blood flow measured by Laser Doppler restored in the former ischemic region. Stroke animals received ES cell transplantation showed improved neurological and behavioral function 20-30 days after the transplantation. Our study demonstrates potential strategy of using ES cell transplantation to repair damaged brain tissues for reconstruction of neurovascular networks. The restoration of local blood supply and neuronal activities supports long-term functional benefits of ES cell transplantation after stroke. Supported by NIH NS37373, NS45155, and AHA-Bugher Award 0170063N and 0170064N.





## CHOLESTEROL, ABC TRANSPORTERS, AND BETA-AMYLOID PRODUCTION IN BRAIN CELLS

Aimee Jones<sup>1</sup>, Yeung Yam<sup>1,2</sup>, Ke Pei<sup>1,3</sup>, **Wandong Zhang**<sup>1,2</sup>

<sup>1</sup>*Institute for Biological Sciences, National Research Council of Canada, Ottawa, ON, Canada*

<sup>2</sup>*Faculty of Medicine, University of Ottawa, Ottawa, ON, Canada*

<sup>3</sup>*The Hospital Affiliated to the Shandong University of Traditional Chinese Medicine, Shandong, China*

**Introduction:** Amyloid precursor protein (APP) processing and production of beta-amyloid peptides (AB) has been recently linked to altered cholesterol metabolism in Alzheimer's disease (AD). Hypercholesterolemia is an early risk factor for AD and decreased prevalence of AD is observed with use of cholesterol-lowering drugs. It is hypothesized that altered levels of cholesterol and ratio of cholesterol to phospholipid in brain cell membrane affect APP processing and AB production. A group of ATP-binding cassette (ABC) transporters (ABCA1, ABCG1 and ABCG4) is known to specifically mediate cellular cholesterol/phospholipid transport to HDL. It was reported that overexpression of ABCA1 in neuroblastoma N2a cells affects APP processing and AB production. We have shown here that the levels of ABCG1 and ABCG4 expression are higher than that of ABCA1 in human brain, and up-regulation of ABCG1 and ABCG4 expression induced by a LXR agonist and cholesterol depletion affect AB production in N2a cells. **Methods:** Membrane cholesterol in N2a cells was depleted using cyclodextran (2.5~5mM) or N2a cells were treated with a nuclear receptor LXR agonist TO901317 (1~2.5 uM). Culture media and RNA were harvested at 2, 4, 6, 8, 12, and 24hr for these experiments. RNA samples were isolated from N2a cells and human brain tissues by Trizol. The expression of ABC transporters and beta-actin was determined by RT-PCR. AB1-40 secretion in the media was analyzed by ELISA. **Results:** RT-PCR analyses of six brain tissues showed that the levels of ABC transporter expression are ABCG4>ABCG1>ABCA1. Cholesterol depletion in N2a cells decreased AB1-40 secretion initially at 2 and 4hr as compared with controls, and AB1-40 secretion was then significantly increased at 8, 12 and 24hr (Fig. 1). RT-PCR showed that the expression of ABCA1, ABCG1, and ABCG4 in cholesterol-depleted cells was not affected. However, RT-PCR revealed that TO901317 strongly stimulated expression of ABCG4, ABCA1 and ABCG1 in N2a cells (ABCG4>ABCA1>ABCG1). ELISA showed that AB1-40 secretion from TO901317-treated cells was at the same level as the controls at early time points, but significantly increased at 8, 12 and 24hr (Fig. 2). **Conclusion:** Cholesterol transporters ABCG4 and ABCG1, like ABCA1, are highly expressed in human brain. Cholesterol depletion affects AB production in N2a cells. Fukumoto et al (1) reported that treatment of N2a cells with TO901317 increased AB secretion, and ABCA1-siRNA decreased AB secretion. Other reports (2,3) showed that treatment of N2a cells with LXR agonists induced ABCA1 expression and decreased AB secretion. Our results appear to be in agreement with Fukumoto et al's finding and show that ABCG1 and ABCG4 are regulated by nuclear receptor LXR and LXR-regulated expression of ABCG4 and ABCG1 affects APP processing and increases AB secretion. Our work suggests that cholesterol and ABC transporter-mediated cholesterol transport may be important factors affecting APP processing/AB production in brain cells. **References:** 1. Fukumoto H, et al (2002) J Biol Chem. 277(50):48508-48513. 2. Koldamova RP, et al (2003) J Biol Chem. 278(15):13244-13256. 3. Sun Y, et al (2003) J Biol Chem. 278(30):27688-27694.

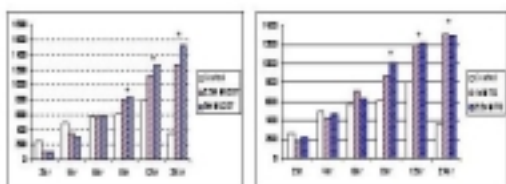


Fig. 1 Cholesterol depletion with cyclodextran (CD) and AB<sub>1-40</sub> secretion from N2a cells (n=6/2C)

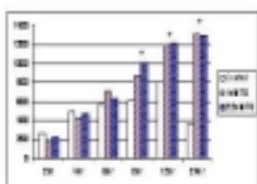


Fig. 2 LXR agonist TO901317 treatment and AB1-40 secretion from N2a cells (n=6/3C)



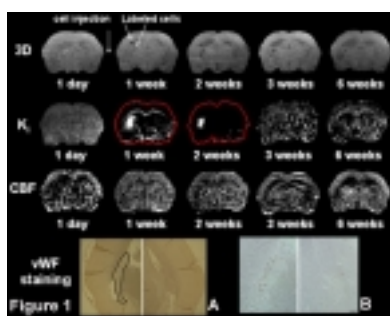
## MRI INVESTIGATION OF ANGIOGENESIS AFTER NEURONAL PROGENITOR CELL THERAPY OF STROKE

Quan Jiang<sup>1,2,3</sup>, Zheng Gang Zhang<sup>1,3</sup>, Guang Liang Ding<sup>1</sup>, Li Zhang<sup>1</sup>, Lian Li<sup>1</sup>, Rui Lan Zhang<sup>1</sup>, Lei Wang<sup>1</sup>, He Meng<sup>1</sup>, James R. Ewing<sup>1,2,3</sup>, Qing Jiang Li<sup>1</sup>, Robert A. Knight<sup>1,2,3</sup>, Michael Chopp<sup>1,2,3</sup>

<sup>1</sup>Department of Neurology, Henry Ford Health System, Detroit, <sup>2</sup>Department of Physics, Oakland University, Rochester, <sup>3</sup>Departments of Neurology, Wayne State University, Detroit, MI, USA

**INTRODUCTION:** Cell therapy improves functional recovery in experimental stroke<sup>1</sup>, which may be related to cell therapy induced angiogenesis<sup>2</sup>. In this study, we report for the first time that quantitative MRI can dynamically monitor cell mediated induction of angiogenesis. **MATERIALS AND METHODS:** Neural progenitor cells were labeled by superparamagnetic particles using a biolistic device “gene gun”<sup>1</sup>. Eight male Wistar rats were placed in a stereotaxic frame.  $1 \times 10^5$  superparamagnetic labeled cells were injected into the cisterna magna 48 h after stroke. MRI measurements were performed from one day before to 6 weeks after cell transplantation. Three dimensional MRI,  $T_{1sat}$  ( $T_1$  in the presence of an off-resonance irradiation of the macromolecules of brain),  $T_1$ ,  $T_2$ , cerebral blood flow (CBF), cerebral blood volume (CBV), and blood-to-brain transfer constant ( $K_i$ ) of Gd-DTPA were used to measure migration and localization of labeled cells and to characterize biophysical changes of angiogenesis after cell therapy. To detect superparamagnetic labeled cells in the host brain and angiogenesis, brain sections were stained for iron using Prussian blue reaction, and for angiogenesis using vWF immunostaining. **RESULTS:** The labeled cells selectively migrated towards ischemic boundary regions as detected by MRI from 1 to 6 weeks after cell transplantation (Fig 1, 3D). Different temporal changes in biophysical parameters were detected between ischemic regions with and without angiogenesis. MRI revealed an increase in  $K_i$  in the angiogenic region (Fig1,  $K_i$ ), which maximized at 2 weeks and returned to normal at 6 weeks. The vWF immunoreactive images showed an increase in numbers of vWF immunoreactive vessels (Fig 1). The angiogenic region exhibited increased ( $p < 0.01$ ) CBF and CBV compared to that in the non-angiogenic ischemic region at 6 weeks after cell therapy. The relative  $T_{1sat}$  and  $T_2$  values in angiogenic region were also significantly lower ( $T_{1sat}$ ,  $p < 0.05$  at 1 to 6 weeks and  $T_1$ ,  $p < 0.05$  at 6 weeks,  $T_2$ ,  $p < 0.05$  at 3 to 6 weeks) than that in the non-angiogenic ischemic region after cell therapy. Of these methods,  $K_i$ , CBF, and CBV appear most useful measurements to identify and predict angiogenic location and areas.  $T_{1sat}$ ,  $T_1$ , and  $T_2$  provide complimentary information to characterize ischemic tissue with and without angiogenesis. **DISCUSSION:** These studies show that MRI can dynamically monitor labeled cell migration, distribution and angiogenic impact on ischemic tissue. Angiogenesis after cell therapy in ischemic brain colocalizes with the distribution of implanted cells. These cells may promote angiogenesis by expressing or inducing the expression of angiogenic factors like VEGF in parenchymal tissue<sup>2</sup>. Our data also suggest that  $K_i$ , CBF, and CBV are important methodologies for potential application to the cell therapy of stroke patients.

Chen J et al. *Circ Res.* 2003;92:692-9. 1. Zhang RL et al. *Neuroscience.* 2003;116:373-82. 2. REFERENCES: Grant support: Supported by NINDS grants PO1 NS23393 and NS42345, RO1 NS38292, NS48349, NS43324, and HL64766.





## MAGNETIC LABELING OF HUMAN NEURAL PROGENITOR CELLS FOR IN VIVO MRI MIGRATION ANALYSIS FOLLOWING TRANSPLANTATION IN STROKE

Raphael Guzman<sup>1</sup>, Bliss Tonya<sup>1</sup>, Uchida Nobuko<sup>4</sup>, Greve Joan<sup>3</sup>, Sun Guo Hua<sup>1</sup>, Palmer Theo<sup>1</sup>,  
Moseley Mike<sup>2</sup>, Steinberg Gary<sup>1</sup>

<sup>1</sup>Department of Neurosurgery, Stanford University, Stanford, CA, USA

<sup>2</sup>Department of Radiology, Stanford University, Stanford, CA, USA

<sup>3</sup>Department of Bioengineering, Stanford University, Stanford, CA, USA

<sup>4</sup>Stem Cells Inc., Palo Alto, CA, USA

**Introduction:** Stroke remains the leading cause of serious long-term adult disability in western countries. Recent attention has focused on restoring brain function through neural stem cell transplantation. Neural stem cells transplanted into the brain have been shown to undergo long-range, targeted migration towards lesion sites. The ability to non-invasively monitor stem cell migration is of great importance for future transplantation studies. Here we demonstrate that human neurosphere cells derived from CNS stem cells (hCNS-SC) can safely be labeled with FDA-approved paramagnetic iron oxide particles (SPIO) and that their migration following stroke can be analyzed using magnetic resonance imaging (MRI).

**Methods:** Human hCNS-SC-derived neurosphere cells were incubated overnight with SPIO (5 $\mu$ g/ml) (Feridex, Advanced Magnetics, USA) complexed to Protamine Sulfate (2.5 $\mu$ g/ml). Cell viability after transfection was assessed by Trypan blue dye exclusion assay. Male SD rats (300  $\pm$  10 g, n=7) were subjected to permanent distal middle cerebral artery occlusion (dMCAo) with carotid artery occlusion for 1 hr. One week later the iron-labelled human neurosphere cells (1 x 10<sup>5</sup> cells/ $\mu$ l) were injected into 3 peri-infarct sites (1  $\mu$ l/site) ventromedially on the A-P axis. All rats received daily intraperitoneal injection of cyclosporine A (10 mg/kg). MRI (4.7T) was performed before and several times after transplantation for up to 5 weeks. Histochemistry for iron (Prussian blue) and immunohistochemistry with a human-specific nuclear antibody was done thereafter.

**Results:** Mean cell viability was 93.6% ( $\pm$  3.5 SD). Pre-transplantation MRI showed the stroked area on T2-weighted images and served as a reference image for post-transplantation comparison. At 1 week post-transplantation grafts were identified on T2\*- and T2-weighted MR images as hypointense areas adjacent to the stroke without clear evidence of migration (Figure A). Subsequent MR images revealed progressive loss of infarcted cortex and migration of iron labeled human cells towards the lesioned area (Figure B). Targeted migration of NPC was confirmed by immunohistochemistry (Figure C). The hypointense signal as seen on MRI was correlated with Prussian blue stained coronal brain sections.



**MORPHOLOGICAL VERIFICATION OF HEMORRHAGIC STROKE MODEL****Mykola M. Danylov<sup>1</sup>, Sergiy V. Kyrychenko<sup>2</sup>, Sergiy P. Khalimonchuk<sup>2</sup>**<sup>1</sup>*Institute of Pharmacology and Toxicology, Department of Pathomorphology, Kiev, Ukraine*<sup>2</sup>*Institute of Pharmacology and Toxicology, Department of Pharmacokinetics, Kiev, Ukraine*

Among the methods of hemorrhagic stroke modelling there are ones which connected with autogenic blood infusion into certain cerebral regions of experimental animals. Several methods of such approach are proposed, in particular by Mirzoyan R.S. et al. (2000), Makarenko A.N. et al. (2002), Hua Y. et al. (2002), Kitaoka T. et al. (2002) etc. The aim of this work was morphological verification of severity-standardized experimental intracerebral hemorrhage model which was previously approved in our laboratories (Yarosh O.K. et al., 2004). Materials and methods. All experiments were conducted according to the guidelines issued by the Institutional Animal Care Committee. Thirty six pubescent male Wistar rats (250.0±30.0 g) had been used. For reproduction of mild, moderate, and severe hemorrhagic stroke animals were divided into 3 groups (12 animals in each group). Under thiopental anesthesia (40 mg/kg intraperitoneally) and stereotaxic procedure heparinized autogenic blood from lateral caudal vein was infused in capsula interna (CI) area with the rate of 5-10 µl/min. Mild, moderate, and severe stroke was reproduced by infusion of 10 µl, 20 µl, and 30 µl of autogenic blood on 100 g of animal weight, respectively (or 25, 50, and 75 µl, respectively, considering that average rat weight was 250 g). Three animals from each experimental group were killed after 1, 5, 10, and 14 days of stroke. Brains were removed, fixed in 96% ethanol and imbedded with paraffin. Histological slices were stained with hematoxylin-eosin and cresylviolet for further light microscopy. Results. In group with mild stroke lethal outcome was observed only in 1 animal (9%) on the 7th day of experiment. In group with moderate and severe stroke mortality made up 18% (throughout 1 day) and 78% (throughout 2 days), respectively. Macroscopically there were hematomas with clear outline. Blood inrush into cerebral ventricles was not noticed. Microscopically hematoma size diminished progressively in each group according to increase in stroke duration. Large amount of macrophages and hemosiderin deposits were observed just after the 1st day of stroke irrespective of hematoma size. Outside hematoma there were rarity of cerebral tissue, cribrures (especially in hippocampus), average and large solitary cysts in cortical and subcortical areas. Status lacunaris was observed in homolateral and heterolateral hemispheres with glial reaction and lacuna size growth according to increase in stroke severity and duration. Conclusions. Morphological data indicate good representative potential of hemorrhagic stroke stages, and duration of each stage development is much less as compared with well-known human stroke manifestations. Thus such improved model of hemorrhagic stroke can be applied in further neuropathological research.

**CBF IMAGING AND GLOBAL CBF QUANTIFICATION IN NORMAL RATS USING DEDICATED PINHOLE SPECT SYSTEM**

Philippe Choquet<sup>1</sup>, Vincent Israel-Jost<sup>1</sup>, **Izzie J. Namer**<sup>1</sup>, Pascal Bilbault<sup>2</sup>,  
François Schneider<sup>2</sup>, André Constantinesco<sup>1</sup>

<sup>1</sup>*Service de Biophysique et Médecine Nucléaire, Hôpitaux Universitaires de Strasbourg, CHU  
Hautepierre, Strasbourg, France*

<sup>2</sup>*Service de Réanimation Médicale, Hôpitaux Universitaires de Strasbourg, CHU  
Hautepierre, Strasbourg, France*

This work is intended to evaluate [99mTc]-radiolabeled pharmaceuticals for brain perfusion measurements in rats using pinhole SPECT. Our experiments aim to obtain quantitative data in normal animals. A dedicated Anger type rotating gamma camera (field of view 170 mm x 170 mm, 25 photomultipliers) was used with 1.5 mm hole diameter's pinhole collimator (Gaede Medizinsysteme GmbH, Freiburg, Germany). 15 to 20 mCi of [99mTc]-hexamethyl propylamine oxime (Amersham Health, Little Chalfont, UK), was administered to 10 Wistar adult rats under general gaseous anesthesia (isoflurane 2%), through intravenous femoral catheter. During tracer administration, 120 planar images of 0.5s were recorded. Ten minutes after, 48 projections of 1 min were acquired over a 180 dorsal arc. A specific cone beam algebraic reconstruction algorithm, taking into account distortion of projection through pinhole, was employed leading to reconstructed voxel's sizes of 0.34 mm<sup>3</sup>. Micro-CT (eXplore LOCUS, General Electric Medical Systems, London, Canada) images of the same animal were fused with SPECT data for anatomical registration. Using the Patlak formalism, modified by Matsuda, we calculate global CBF values for each cerebral hemisphere. Images' contrast reflects normal tracer's uptake in the different cerebral territories. Signal to noise ratios in human and rat brain perfusion's images are comparable. Calculation leads to a gCBF of 110.1 ml/100g/min  $\pm$  11.4 value in the range of reference data. This technique could be used to assess CBF in pathological conditions in rats.

**EFFECT OF EDARAVONE ON HYPER-ACCUMULATION AROUND THE LESION BY 18F-FDG PET IN PRIMATE THROMBOEMBOLIC STROKE**

Tetsuya Yoshikawa<sup>1</sup>, Teruo Susumu<sup>1</sup>, Yuki Akiyoshi<sup>1</sup>, Koichiro Fukuzaki<sup>1</sup>, Ryoichi Nagata<sup>1</sup>, Yasukatsu Izumi<sup>2</sup>, Yasuhiro Wada<sup>3</sup>, Yasuyoshi Watanabe<sup>3</sup>, Hiroshi Iwao<sup>2</sup>, Go Kito<sup>1</sup>

<sup>1</sup>*Shin Nippon Biomedical Lab (SNBL), Kagoshima, Japan*

<sup>2</sup>*Department of Pharmacology, Osaka City University Medical School, Osaka, Japan*

<sup>3</sup>*Department of Physiology, Osaka City University Medical School, Osaka, Japan*

**Background:** In cerebral thromboembolic stroke, decreased cerebral blood flow leads to a critical disturbance of energy supply. Although pathophysiologic changes have been observed in focal cerebral ischemia models in which the middle cerebral artery was occluded with artificial materials, few studies of the cerebral metabolic rate of glucose (CMR<sub>glc</sub>) in the ultra-acute stage of thromboembolic stroke models have been published. Free radicals are involved in various processes of damage in ischemic brain tissue, and edaravone is a widely known free radical scavenger, which is licensed in Japan and used for therapy in the acute phase of human stroke. Therefore, the aim of this study was to investigate whether elevated glucose uptake after thromboembolic stroke correlates with the process of brain tissue damage, and to determine whether edaravone affects elevated glucose uptake. **Methods and Results:** Thromboembolic stroke was produced in male cynomolgus monkeys (n=8). Permanent obstruction of the left middle cerebral artery was achieved by injecting an autologous blood clot via the left internal carotid artery. PET studies were performed using microPET Primate 4 (Concorde Microsystems Inc., Knoxville, TN). 2-[18F]fluoro-2-deoxy-D-glucose (18F-FDG) was administered intravenously at 2 mCi/kg and CMR<sub>glc</sub> was measured before embolization, and at 6 and 24 hours after embolization. Edaravone was injected at a rate of 1 mg/kg/hr for 3 h from 1 h after embolization. At 6 hours after stroke, increased 18F-FDG accumulation (1.4 times) was noted in the parietal and temporal cortices in all cases, while CMR<sub>glc</sub> in the insular cortex and basal ganglia, regarded as the ischemic core region, decreased to < 70% of the pre-values. However, regions in which hyper-accumulation of 18F-FDG is observed, changed to loss of FDG hot spot after 24 hours of embolization. In histological analysis, these regions of changed FDG accumulation were almost completely infarcted area by 24 hours after embolization. Conversely, in the edaravone-treated group, increased 18F-FDG accumulation was maintained at > 90% of the pre-values in the parietal and temporal cortexes and thalamus, but not in the putamen or insular cortex, at 24 hours after embolization. **Conclusion:** The results of the present study demonstrate that increased 18F-FDG accumulation around lesions in the ultra-acute stage of cerebral ischemic stroke is closely associated with infarct volume in the late stage. However, edaravone has a beneficial effect on decreased 18F-FDG uptake in the area around the ischemic core. Consequently, it may be postulated that this mechanism is involved in free radical generation resulting from ischemia.

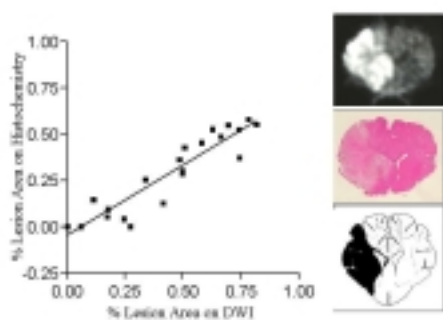
## NEW MODEL OF FOCAL CEREBRAL ISCHEMIA IN THE MINIATURE PIG

Hideaki Imai<sup>1</sup>, Kenjiro Konno<sup>2</sup>, Mitsunobu Nakamura<sup>1</sup>, Tatsuya Shimizu<sup>1</sup>, Chisato Kubota<sup>1</sup>, Koji Seki<sup>1</sup>, Fumiaki Honda<sup>1</sup>, Shinichiro Tomizawa<sup>1</sup>, Yukitaka Tanaka<sup>1</sup>, Hidekazu Hata<sup>2</sup>, Nobuhito Saito<sup>1</sup>

<sup>1</sup>Department of Neurosurgery, Gunma University Graduate School of Medicine, Maebashi, Japan

<sup>2</sup>Institute of Experimental Animal Research Gunma University Graduate School of Medicine, Maebashi, Japan

**Background and Objectives:** Animal models relevant to man are indispensable in investigating the efficacy of new therapeutic modalities. The importance of both white matter and grey matter damage, in experimental stroke research is also being increasingly recognized. In accordance with the demands for experimental stroke models to include species with gyrencephalic brains, we have focused on the miniature pig. This paper provides information on both the surgical technique for middle cerebral artery occlusion (MCAO) and the methods of quantitation of ischemic damage to both grey and white matter using line diagrams of the miniature pig brain. **Methods:** Sixteen miniature pigs weighing 14-24 kg were randomly divided into three groups: permanent MCAO (n=5), permanent internal carotid artery occlusion (ICAO) (n=6) and a sham operated group (n=5). The operation was performed under general anesthesia via a frontotemporal approach. MCAO and ICAO was induced by electrocoagulation of the MCA from a point proximal to the origin of the lenticulostriate artery to a distal point where it crosses the olfactory tract and the ICA at a point proximal to the posterior communicating artery, respectively. At 24 hours after surgery the volume of ischemic damage was evaluated by MRI and then the animal was sacrificed, a coronal brain sections stained with haematoxylin and eosin (grey matter damage) or amyloid precursor protein (APP) immunohistochemistry (white matter damage). Quantitative histopathology was used to map the infarct onto 16 pre-selected line diagrams. **Results:** Histological examination and MRI findings demonstrated no areas of ischemia in the cerebral hemispheres of any of the sham-operated animals. By contrast, in the MCAO group, all animals had ischemic damage in basal ganglia and frontal cortex. The volume of the infarct in the MCAO and the ICAO measured directly from MRI scans was  $16.2 \pm 1.1$  and  $1.5 \pm 0.5$  cm<sup>3</sup> (mean  $\pm$  SD), respectively. There was a good correlation between the histopathological and MRI findings ( $r^2 = 0.86$ ,  $p < 0.0001$ ) (Figure) although the infarct volume measured by quantitative histopathology was smaller than that measured by MRI, since mapping onto line diagrams reduces the impact of cerebral edema and brain swelling on measurement of infarct volume. For quantification of axonal damage immunohistochemical study using APP antibody was used and provided total APP score of  $43.8 \pm 3.5$  (mean  $\pm$  SD) in the MCAO. **Conclusions:** This paper describes a simple and reproducible method for the induction of white and grey matter damage in focal cerebral ischemia with minimum invasiveness. This miniature pig stroke model has utility for studying the pathophysiology of ischemia in gyrencephalic brain and for the assessing the therapeutic efficacy of drugs prior to initiating human clinical trials.





## A SIMPLE AND STANDARDIZED MOUSE MODEL OF CEREBRAL ISCHEMIA-HYPOXIA

Faisal Adhami<sup>1</sup>, Guanghong Liao<sup>1</sup>, Aryn Schloemer<sup>1</sup>, Frank Sharp<sup>2</sup>, Chia-Yi Kuan<sup>1</sup>

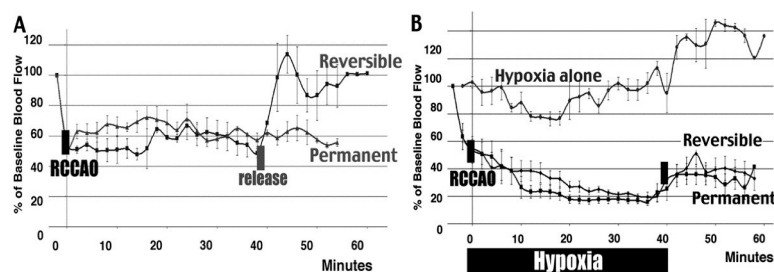
<sup>1</sup>*Department of Pediatrics, Cincinnati Children's Hospital Medical Center, Cincinnati, OH, USA*

<sup>2</sup>*MIND Institute and Department of Neurology, University of California at Davis, Sacramento, CA, USA*

**Introduction:** The ischemia penumbra area, the prime target for neuroprotective therapy, is characterized by moderate reduction of both blood flow and oxygenation. The Levine/Vannucci model (unilateral common carotid artery occlusion plus hypoxic challenge inside a chamber) mimics the combination of ischemia and hypoxia, but only produces inconsistent brain damage in adult mice. The poor reproducibility of brain damage is likely to the inability to control the body temperature of mice inside the hypoxic chamber. We tested whether tight control of the core temperature can improve the consistency of brain injury in adult mice.

**Methods:** The right common carotid artery (CCA) of 8-10 week-old male C57Bl/6 mice is permanently ligated under anesthesia with isoflurane. After closing the wound, 7.5% oxygen with 0.5-1% isoflurane is delivered to the mouse through a nose cone on the surgical table. The spontaneous respiration of the mouse is maintained at 100-110 breaths per minute by adjust the concentration of isoflurane. The core temperature is monitored by a rectal probe and maintained at 36.5-37.5°C with a heating pad. After 40 minutes of hypoxia challenge, mice are re-oxygenated with room air and sacrificed at different times for analysis.

**Results:** Neurological and histological analysis shows a high degree consistency of brain injury in 90% of the challenged mice. Magnetic Resonance Imaging (MRI) shows the brain injury covers the stratum, cortex, and thalamus unilaterally. This paradigm triggers acute IL-1 $\beta$  induction, myelin destruction, and cytotoxic edema within 6 hours, and causes delayed IL-6 production and vasogenic edema at later time. This paradigm activates initial apoptotic events including the mitochondrial release of Cytochrome c and AIF and the activation of Caspase-9 and -8, and induces cytoprotective HSP70, ERK, and AKT signaling in the same brain region, similar to the situation of the penumbra. Physiological studies show the combination of unilateral CCA occlusion and hypoxia increases the cerebrovascular resistance and reduces the cerebral blood flow (CBF) to 20% of the normal value during hypoxia. There is also a “no-reflow” phenomenon after re-oxygenation and release of the CCA occlusion (Fig.1A Rebound of CBF after the release of CCA occlusion; Fig.1B No-reflow after ischemia-hypoxia).



**Conclusion:** These results establish a simple and reproducible mouse model of cerebral ischemia-hypoxia that resembles the penumbra area. This standardized model of stroke is suitable for large-scale mouse studies of neuroprotective therapy.

**ENDOVASCULAR DILATION OF RAT CAROTID ARTERY BY ULTRAVIOLET LASER LIGHT TRANSMITTED BY MICROCATHETERIZED OPTICAL FIBER****Brant D. Watson<sup>1</sup>, Ricardo Prado<sup>1</sup>, Adelfa Morales<sup>1</sup>, John Rose<sup>2</sup>**<sup>1</sup>*Department of Neurology, University of Miami, Miami, FL, USA*<sup>2</sup>*VasCon LLC, Miami, FL, USA*

**Introduction:** Mechanically-based treatments for stenosis and vasospasm of cerebral arteries are undergoing avid development, but perforation and embolus formation can still occur as complications (1). We describe a clinical prototype device for inducing arterial dilation, apparently via nitric oxide production in smooth muscle cells (2), by means of endovascular irradiation with ultraviolet (UV) laser light. **Methods:** Male Sprague-Dawley rats (500–750g) were anesthetized with isoflurane and mechanically ventilated. A custom microcatheter (O.D. 940  $\mu$ m, I.D. 760  $\mu$ m) with a lubricious coating and smooth bullet-shaped head (VasCon LLC) was introduced transfemorally by means of a 360  $\mu$ m guidewire under X-ray fluoroscopy, and positioned inside the left common carotid artery (CCA) at the C2-C3 level. A “baseline” CCA diameter was obtained by injecting contrast medium (Visipaque 320 mg/ml) at the CCA blood flow rate (15% of cardiac output assuming a cardiac index of 250 ml/min/kg) for 5 sec, followed by a 2 min “saline flush” at 1 ml/min. The beam from a Coherent 90-6 argon ion laser configured for 351 nm UV light was focused (Optics for Research) into a fused silica optical fiber (Ocean Optics). The output end of the fiber (100  $\mu$ m core diameter, 3 M length) featured a conical end (apex angle 35 degrees), which in aqueous media converted the input beam into an expanding ring-shaped beam. The fiber was inserted until just distal to the catheter end, and there was centered axially by a spiral fixture. The inner CCA wall was irradiated 1 min with the UV ring beam (20 watts/cm<sup>2</sup> initial intensity) during saline infusion (1 ml/min). The fiber was removed and the CCA response monitored with Visipaque at the “saline flush” and then “baseline” rate. **Results:** Baseline CCA diameter was  $1.15 \pm 0.20$  mm and the saline flush diameter (resulting from CCA compression owing to lower saline injection rate) was  $0.53 \pm 0.03$  mm. Following UV irradiation, the saline flush diameter became  $0.77 \pm 0.11$  mm, while the “baseline” CCA diameter expanded to  $1.40 \pm 0.22$  mm (n = 4). The percentages of dilation with respect to the respective initial diameters thus averaged 45% at the saline infusion rate (p < 0.05) and trended toward 22% at the normal blood flow rate (n.s.) The dilations persisted for at least 15 min (3). **Conclusions:** Endovascular UV laser irradiation induces arterial dilation while avoiding the traumatic complications (1) of mechanical methods. The UV laser method can induce dilation without damaging smooth muscle cells (3). This is notable because UV-facilitated arterial dilation can be induced in the presence of severe endothelial damage (3) - a primary cause of vasospasm (4). Finally, this UV procedure appears to lie within the range of skills known to interventionalists. **References:** (1) HC Schumacher et al, *J Vasc Interv Radiol* 15:S123-S132, 2004; (2) KL Andrews et al, *Heart Failure Rev* 7:423-445, 2002; (3) BD Watson et al, *Stroke* 33: 428-434, 2002; (4) BA Iuliano et al, *J Neurosurg* 100:287-294, 2004. Grant support provided by 5 R21 NS048297 from NINDS.

**CONSIDERATIONS IN THE SELECTION OF BEHAVIOURAL TESTS TO GAUGE RECOVERY AFTER INTRACEREBRAL HEMORRHAGIC STROKE IN RATS**

Crystal MacLellan<sup>1</sup>, Angela Auriat<sup>1</sup>, Steven McGie<sup>1</sup>, Reginia Yan<sup>2</sup>, Maxine DeButte<sup>1</sup>,  
**Frederick Colbourne<sup>1,2</sup>**

<sup>1</sup>*Psychology, University of Alberta, Edmonton, AB, Canada*

<sup>2</sup>*Centre for Neuroscience, University of Alberta, Edmonton, AB, Canada*

Cerebral ischemia and hemorrhage (stroke) are leading causes of death and disability. The goal of experimental cytoprotectants (neuroprotection) for stroke is to reduce cell death and thereby improve functional outcome. Rodents (rat, gerbil, mouse) are most commonly used to model ischemic and hemorrhagic insults. Despite the fact that behavioral recovery is the clinical endpoint of greater concern, many cytoprotection studies rely solely upon histopathological endpoints (e.g., infarct volume) to gauge treatment efficacy (DeBow et al., 2003; *Can. J. Neurol. Sci.*). Furthermore, those studies that assess recovery often use only a neurological deficit score (NDS; e.g., paw placement, spontaneous rotation) and do not use more demanding / informative tests (e.g., skilled reaching). Successful translation of putative cytoprotectants from rodent models to human will depend upon how well treatments are initially assessed. Many functional tests are available in the rat and have been used in focal ischemia studies. Presently, we used a battery of functional tests, which are sensitive to sensory and motor system dysfunction, to gauge outcome after an intracerebral hemorrhagic stroke (ICH) largely targeting the striatum. Sixty adult male Sprague Dawley rats (N = 15 per group) were stereotaxically infused with 1  $\mu$ L of sterile saline containing 0 (SHAM), 0.06 (MILD lesion), 0.12 (MODERATE lesion), or 0.18 U (SEVERE lesion) of bacterial collagenase. Testing began one day following ICH and was repeated over 30 days. Tests included the horizontal ladder and beam walking tests, swimming, limb-use asymmetry (cylinder) test, a NDS, an adhesive tape removal test of sensory neglect, and the staircase and single pellet tests of skilled reaching. At present, the NDS, staircase, neglect and single-pellet tests have been analyzed. Overall, these tests revealed significant impairments (vs. SHAM) that improved over time (e.g., deficits on the NDS were greatest on days 1 and 2). However, despite significant differences in lesion size, we were often unable to statistically distinguish between MILD and MODERATE or MODERATE and SEVERE groups (e.g., neglect test). As for skilled reaching, the staircase test revealed significant contralateral forelimb impairments in the three ICH groups and was often able to distinguish among ICH groups. The SEVERE group also had significant ipsilateral impairments. Skilled reaching impairments were also found with the single-pellet test in the ICH groups. However, it was not possible to compare success among ICH groups because many rats in the MODERATE and SEVERE groups completely switched limb preference. Indeed, a detailed analysis of the entire reaching sequence with the contralateral limb was only possible in the SHAM and MILD groups. In conclusion, multiple behavioral tests are needed to comprehensively evaluate functional recovery after ICH. However, some tests (e.g., neglect test) are either not recommended for this model owing to the time required to test animals, variability, and the insensitivity to lesion size, or are of limited use (e.g., for small lesions). Finally, our results show that modest neuroprotection (e.g., reducing lesion size from SEVERE to MODERATE) may not consistently improve functional recovery, thereby necessitating the use of several tests.

## HYPERACTIVE AND ANXIOUS PHENOTYPE FOLLOWING BRIEF ISCHEMIC EPISODES IN MICE

Benjamin Winter<sup>1</sup>, Georg Juckel<sup>2</sup>, Mustafa Balkaya<sup>1</sup>, Heide Hörtnagl<sup>3</sup>, **Matthias Endres**<sup>1</sup>

<sup>1</sup>*Department of Neurology, Charite Berlin, Berlin, Germany*

<sup>2</sup>*Department of Psychiatry, Charite Berlin, Berlin, Germany*

<sup>3</sup>*Institute Pharmacology and Toxicology, Charite Berlin, Berlin, Germany*

Post-stroke emotional and behavioural abnormalities include a wide range of emotional and cognitive disturbances and have significant impact on long-term outcome. In animals models of stroke however there is little evidence of possible behavioural correlates of such post-stroke neuropsychiatric conditions. Here, we tested whether mild focal brain ischemia induces long-term behavioural changes and neuropsychiatric outcome in mice. 129/SV wild-type mice were anesthetized with isoflurane and subjected to 30 min filamentous occlusion of the left or right middle cerebral artery (MCAo) followed by reperfusion or sham operation (n = 10 animals per group). Eight weeks after MCAo, animals were consecutively subjected to three behavioural tests, i.e. (1) spontaneous locomotor activity testing (day 56), (2) the elevated plus-maze (day 63 and (3) the modified Porsolt forced swim test (on day 70). We present evidence that mild cerebral ischemia is associated with increased spontaneous locomotor activity (right MCAo > left MCAo > sham) and with post-stroke anxiety (left MCA > right MCAo > sham), but we obtained no evidence of a post-stroke depressive phenotype. Noradrenaline levels were significantly increased by 30 – 45 % in the ischemic striatum and significantly correlated with locomotor activity ( $r = 0.48$ ) while the levels of dopamine and homovanillic acid were decreased compared to sham operated animals. The ischemic lesion was confined to the ipsilateral striatum and scattered neuronal death was observed in a number of remote brain regions. In conclusion, brief ischemic episodes induce an hyperactive, anxious but not depressive phenotype in mice, that may relate to left versus right hemispheric lesion location, specific alterations in brain monoamine levels and selective neurodegeneration.

## CHARACTERISATION OF THE NEOCORTICAL CLIP MODEL OF FOCAL CEREBRAL ISCHAEMIA BY MRI, NEUROLOGICAL ASSESSMENT, BEHAVIOUR AND IMMUNOHISTOCHEMISTRY

Maria Ashioti<sup>1</sup>, John S. Beech<sup>2</sup>, Andrew S. Lowe<sup>1</sup>, Mike Modo<sup>1</sup>, Mayke Hesselink<sup>3</sup>, Steve C.R. Williams<sup>1</sup>

<sup>1</sup>*Institute of Psychiatry, Neuroimaging Research Group, London, UK*

<sup>2</sup>*University of Cambridge, Department of Medicine, Addenbrooke's Hospital, Cambridge, UK*

<sup>3</sup>*Solvay Pharmaceuticals, Weesp, The Netherlands*

**Introduction** The development of therapeutic agents for the treatment of ischaemic stroke crucially depends on their efficacy in pre-clinical animal models. The neocortical clip model of focal cerebral ischaemia in the rat involves the occlusion of the middle cerebral artery (MCA) at a point distal to the lenticulostriate perforators which produces a lesion confined to the cortex only. This model provides a more defined and potentially reproducible ischaemic lesion and it has been successfully used in novel neuroprotection studies (1). In an attempt to further improve its translational qualities we have characterised the neocortical clip model of cerebral ischaemia using serial in vivo Magnetic Resonance Imaging (MRI), behavioural and neurological assessment, and immunohistochemistry in order to evaluate the structural and functional properties of this lesion. **Methods** The MCA was occluded in spontaneously hypertensive rats for 0 (n=10), 60 (n=8) and 120 (n=5) minutes. MRI was performed 2 days pre surgery and 1, 3 and 7 days post-surgery. Behavioural assessment was performed 2 days pre-surgery and 3 and 7 days post-surgery whilst neurological deficits were monitored daily. After scanning was completed the animals were perfused with 4% paraformaldehyde to allow immunohistochemistry for neuronal loss (NeuN), astrocytosis (GFAP) and macrophage (ED1) infiltration. **Results** MRI analyses showed that occlusion of the MCA for 0 minutes (sham-controls) did not produce a lesion whereas occlusion for 60 minutes produced a lesion that remained relatively stable over time (1 day  $60 \pm 67$  mm<sup>3</sup>, 7 days  $66 \pm 59$  mm<sup>3</sup>). 120 minute occlusion caused a severe cortical infarct 1 day post surgery ( $285 \pm 77$  mm<sup>3</sup>) which decreased by 7 days ( $174 \pm 65$  mm<sup>3</sup>,  $p < 0.05$ ). Lesion volume was significantly larger with 120 minute occlusion than that of 60 minutes at all time points (1 and 3 days  $p < 0.001$ , 7 days  $p < 0.05$ ). Behavioural assessment and neurological deficit scoring correlated with each other ( $r = 0.626$ ,  $p < 0.05$ ) and with respect to lesion volume ( $r = 0.648$ ,  $p < 0.01$  and  $r = 0.781$ ,  $p < 0.01$ ) and demonstrated that functional capacity is reflected in the size of the lesion. The success rate of cerebral infarction was 65% which was possibly due to the subtle but observed inconsistency of the MCA tree within individual animals. Ex vivo histology of the MR defined lesion demonstrated a loss of NeuN positive cells and around the border an upregulation of GFAP positive astrocytes, both indicative of tissue damage. Histology also indicated a large inflammatory response with the presence of macrophages in the lesion territory. **Conclusion** The neocortical clip model has produced ischaemic lesions when present, that are reliably restricted to the cortical territories of the MCA. The duration of occlusion also appears to dictate lesion severity and evolution which may prove to be useful for probing therapeutic interventions at different stages of stroke progression.

## SELECTIVE AND REVERSIBLE OCCLUSION OF THE MIDDLE CEREBRAL ARTERY IN RATS BY AN INTRALUMINAL APPROACH

Jianya Ma, Thaddeus S. Nowak, Jr.

*Department of Neurology, University of Tennessee, Memphis, TN, USA*

**Introduction.** Intraluminal filaments are widely used to produce focal ischemia in rodents [1,2]. These result in significant CBF deficits outside the middle cerebral artery (MCA) territory [3], and in rats can lead to confounding hyperthermia during occlusion. The presented studies optimized the design and use of an occluding filament to permit selective and reversible MCA occlusions in rats, avoiding these complications. **Methods.** Silicone cylinders (diameter 0.30 mm, length 0.7-0.8 mm) were molded onto 6-0 suture. These were introduced into the cerebral vasculature of adult male Wistar rats (250-300 g, n=107) under halothane anesthesia, using established surgical procedures [1,2]. The final procedure included prior heparinization of the device as well as subcutaneous dosing of the animal (100 IU/kg). All rats were fitted with telemetry probes (Mini Mitter Co., Sun River, OR, USA). Infarct volumes were assessed at 3 days by triphenyltetrazolium chloride staining. **Results.** Optimized filaments entered the MCA in 85% of animals (Fig. 1), with failures attributable to anatomical variation at its origin. Heparin prevented spontaneous hyperthermia that otherwise occurred in 30% of animals (Fig. 2). Infarct volume at 3 days increased with occlusion duration and reached a maximum after 3 h (Fig. 3), with a distribution restricted to the MCA territory. **Conclusions.** Selective filament occlusion of the MCA is feasible in rats. The device is simply made and required surgery uses standard approaches. Heparin prevents incidental hypothalamic ischemia and hyperthermia secondary to clot formation along the suture. Failures can be excluded by postmortem inspection of the vascular anatomy. Such anatomical considerations must be addressed in extending the approach to other rat strains. With adjustment in scale the device should also be applicable to mice. [1] Koizumi et al., *Jpn. J. Stroke* 8:1-8 (1986) [2] Zea Longa et al., *Stroke* 20:84-91 (1989) [3] Kanemitsu et al., *J. Cereb. Blood Flow Metab.* 22:1196-1204 (2002) Supported by USPHS grant NS42267

**Fig. 1**

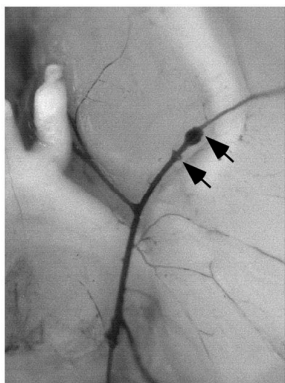


**Fig. 2**

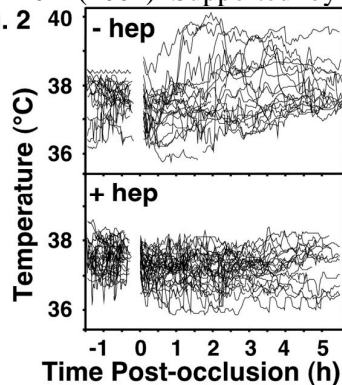
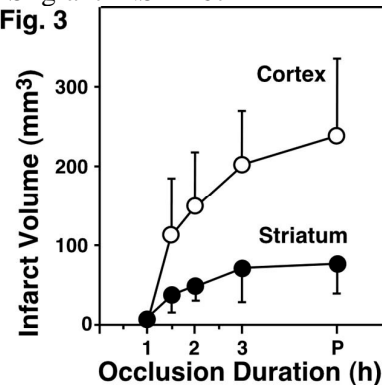


**Fig. 3**



**ALTERED CEREBROVASCULAR CONTROL IN RESPONSE TO HYPERTENSION  
IN A NOVEL TRANSGENIC RAT MODEL OF MALIGNANT HYPERTENSION**Paul A.T. Kelly<sup>1</sup>, Linda Ferrington<sup>1</sup>, John J. Mullins<sup>2</sup><sup>1</sup>*Division of Neuroscience, University of Edinburgh, Edinburgh, UK*<sup>2</sup>*Centre for Cardiovascular Science, University of Edinburgh, Edinburgh, UK*

Background and Purpose: Animal models which have been generated to investigate the pathophysiology of hypertensive vascular injury generally require surgical or pharmacological intervention or depend upon the constitutive expression of endogenous genes. A novel inbred rat model with inducible hypertension has recently been generated using a renin transgene under the transcriptional control of the cytochrome P450, Cyp1a1 promoter (1). The transgene is expressed primarily in the liver and is rendered inducible by xenobiotics such as indole-3 carbinol (I3C). The purpose of this study was to examine the effects of a temporally regulated period of inducible hypertension upon neocortical perfusion in this transgenic model, and to compare the effects with hypertension induced by chronic nitric oxide synthase (NOS) inhibition. Methods: Adult rats from the established transgenic line TGR(Cyp1a1Ren2) on a Fischer F344 background, were taken at random and fed for 14 days with either standard powdered food (n=10) or food supplemented with I3C (n=10) as described previously (1). Two groups of non-transgenic Fischer rats were injected (i.p.) with L-NAME (75mg.kg<sup>-1</sup>; n=10) or saline (n=10) once daily for 14 consecutive days. On the day of the experiment (day 15) neocortical cerebral blood flow (LCBF) and glucose utilization (LCMRglu) were measured in equal numbers from each treatment group, using [14C]-iodoantipyrine and [14C]-2-deoxyglucose quantitative autoradiography respectively. Mean arterial blood pressure (MABP) and blood gases were measured in each animal. Data (mean ± s.e.m.) were analysed using t-test with Bonferroni correction (p<0.05) and region-specific LCBF/ LCMRglu ratios were analysed using Mann-Whitney U-test (p<0.05). Results: With the exception of MABP, there were no significant differences in physiological parameters between any of the groups. MABP in transgenic rats fed with I3C (175 ± 3mmHg) was significantly increased from control levels (136 ± 3mmHg) and similar significant increases were found following chronic L-NAME (135 ± 2 to 181 ± 5mmHg). Neither LCMRglu nor LCBF were significantly different from control in L-NAME treated rats. In contrast, whilst there were no significant changes LCMRglu in I3C-fed transgenic rats, LCBF was significantly increased in all 6 cortical areas examined. The largest increase (80%) was in frontal cortex (from 101 ± 2 to 181 ± 7ml.100g<sup>-1</sup>.min<sup>-1</sup>) and the smallest (18%) in cingulate cortex (from 141 ± 3 to 167 ± 6ml.100g<sup>-1</sup>.min<sup>-1</sup>). These increases in LCBF in the absence of any change in LCMRglu resulted in a significant increase in cortical flow metabolism ratios (P< 0.004, Mann-Whitney), indicating a relative hyperaemia. Conclusions: Although both models were found to induce similar levels of hypertension, evidence of cerebrovascular dysfunction was found only in the inducible transgenic model. This model will facilitate studies of the cellular and genetic mechanisms underlying hypertension-induced vascular injury and repair, and may provide a basis for the identification of novel therapeutic targets for vascular disease. 1. Kantachuvesiri S et al. (2001) J Biol Chem 276; 36727-36733.

## CEREBROVASCULAR PRESSURE TRANSMISSION: CHANGES IN HIGHEST MODAL FREQUENCY INDUCED BY VASODILATION

Michael L. Daley<sup>1</sup>, Massroor Pourcyrus<sup>2</sup>, Shelly D. Timmons<sup>3</sup>, Charles W. Leffler<sup>4</sup>

<sup>1</sup>*Department of Electrical and Computer Engineering, The University of Memphis, Memphis, TN, USA*

<sup>2</sup>*Departments of Pediatrics, Obstetrics/Gynecology, University of Tennessee Health Science Center, Memphis, TN, USA*

<sup>3</sup>*Department of Neurosurgery, University of Tennessee Health Science Center, Memphis, TN, USA*

<sup>4</sup>*Departments of Physiology and Pediatrics, University of Tennessee Health Science Center, Memphis, TN, USA*

Introduction: The ultimate goal of this work is to continuously assess cerebrovascular autoregulation of patients with brain injury to permit improved intensive care management and therapy. To accomplish this goal we have been exploring system identification modeling techniques that could be applied to arterial blood pressure (ABP) and intracranial pressure (ICP) recordings typically available in intensive care settings. Our numerical modeling approach has been to use a Windkessel model to define the mathematical structure of cerebrovascular pressure transmission of ABP to ICP. Given this mathematical structure an analytical description of cerebrovascular pressure transmission is constructed for the segment of time defined by each recording interval. Just as the modal frequencies, critical vibration modes, of a tuning fork reflect its structural properties; the modal frequencies of cerebrovascular pressure transmission reflect the structural and functional properties of the cerebrovascular bed. To quantify changes in cerebrovascular pressure transmission, we chose to evaluate changes in the highest modal frequency (HMF) which represents the highest critical vibration frequency of transmission. Vasodilation and vasoconstriction change the structural and functional properties of the vessels within the arterial-arteriolar bed and result in a change of cerebrovascular pressure transmission. The purpose of this experimental study is to examine changes in HMF and pial arterial diameter (PAD), before, during, and following vasodilatory challenge induced by brief hypercapnia. Methods: ABP and ICP recordings sampled at 250 Hz, cerebral perfusion pressure (CPP), HMF, PAD obtained by video micrometry, partial pressure of arterial blood gases, and pH, before, during, and following induction of a brief five min hypercapnic challenge were evaluated in six piglets equipped with a cranial window. Results: Group mean measurements of HMF, CPP, PAD, PCO<sub>2</sub>, PO<sub>2</sub>, and pH taken at baseline, during challenge, and post-challenge conditions and statistical comparison are given (see Table 1). Conclusions: Significant increases of mean HMF and mean PAD occur during vasodilation induced by brief hypercapnia. Such a result suggests that high values of HMF associated with high values of CPP are indicative of inappropriate vasodilation and loss of pressure regulation.

Table 1: Summary of Means ( $\pm$  S.D.) of HMF, CPP, PAD, PCO<sub>2</sub>, PO<sub>2</sub>, and pH

	N	HMF (Hz)	CPP (mmHg)	PAD ( $\mu$ m)	PCO <sub>2</sub> (mmHg)	PO <sub>2</sub> (mmHg)	pH
Baseline	6	21.3 ( $\pm$ 12.3) <sup>4</sup>	65.1 ( $\pm$ 13.2)	92.3 ( $\pm$ 10.2) <sup>2</sup>	30.0 ( $\pm$ 2.6) <sup>1</sup>	90.2 ( $\pm$ 22.1)	7.34 ( $\pm$ 0.11) <sup>1</sup>
Challenge	6	58.5 ( $\pm$ 42.9) <sup>4</sup>	54.9 ( $\pm$ 17.5)	124.3 ( $\pm$ 19.) <sup>2</sup>	68.3 ( $\pm$ 7.7) <sup>1</sup>	74.8 ( $\pm$ 10.1)	7.06 ( $\pm$ 0.06) <sup>1</sup>
Post-Challeng	6	29.9 ( $\pm$ 15.2)	63.7 ( $\pm$ 20.7)	95.9 ( $\pm$ 8.5) <sup>3</sup>	33.0 ( $\pm$ 5.2) <sup>1</sup>	88.2 ( $\pm$ 18.4)	7.3 ( $\pm$ .06)

<sup>1</sup> Significant difference between mean values at  $p < 0.005$ . <sup>2</sup> Significant difference between mean values at  $p < 0.01$ . <sup>3</sup> Significant difference between mean values at  $p < 0.025$ . <sup>4</sup> Significant difference between mean values at  $p < 0.05$ . <sup>5</sup> N is the number of piglets with 10 minute pressure recordings sampled at 250 Hz with value of HMF determined on each 8 s segment. Entries in table represent grand mean values across all piglets



## SPATIO-TEMPORAL DYNAMICS OF INFARCT EVOLUTION USING MR-BASED PREDICTION ALGORITHMS

Ona Wu<sup>1,2</sup>, Toshihisa Sumii<sup>3</sup>, Masao Sasamata<sup>4</sup>, Bruce R. Rosen<sup>5</sup>, Eng H. Lo<sup>3</sup>, Rick M. Dijkhuizen<sup>1,5</sup>

<sup>1</sup>Image Sciences Institute, University Medical Center Utrecht, Utrecht, The Netherlands

<sup>2</sup>Center for Functionally Integrative Neuroscience, Århus Univeristy Hospital, Aarhus, Denmark

<sup>3</sup>Neuroprotection Research Laboratory, Massachusetts General Hospital, Boston, MA, USA

<sup>4</sup>Institute for Drug Discovery Research, Yamanouchi Pharmaceutical Co., Ltd., Tsukuba, Japan

<sup>5</sup>MGH/MIT/HMS Athinoula A. Martinos Center for Biomedical Imaging, Boston, MA, USA

**Introduction:** In recent intravenous thrombolysis trials [1], some benefit was noted for stroke patients treated between 3-6 h, though caution was advised for its administration beyond the recommended 3 h therapeutic time window [2]. It has been speculated that diffusion-weighted (DWI) and perfusion-weighted (PWI) MRI, may provide an objective guideline for identifying patients most likely to benefit. Multiparametric algorithms combining these modalities have been shown to accurately predict tissue infarction [3]. However, duration of ischemia has not been explicitly incorporated in such algorithms. This study investigates the spatio-temporal dynamics of infarction risk as a function of occlusion duration using a rat embolic stroke model. **Methods:** Unilateral stroke was induced by embolic occlusion of the middle cerebral artery (n=8). DWI and PWI experiments were performed at 44±10, 76±5, 139±6, 259±6, 318±5 min post-occlusion. Apparent diffusion coefficient (ADC), CBF, CBV and mean transit time (MTT) maps were calculated, normalized with respect to contralateral values and used along with occlusion duration as covariates in predictive algorithms which outputs the probability of infarction on a voxel-wise basis [3]. Lesions were defined as tissue with ADC < 2 SD from contralateral values at the final MRI. Predicted lesion volumes consisted of tissue exhibiting > 50% risk. **Results:** Figure 1 demonstrates the spatiotemporal evolution of infarction risk as a function of occlusion duration calculated using MR data acquired at the initial time point for one rat. The predicted risk of infarction was found to significantly increases with occlusion time for all animals (79±5%, 80±5%, 81±5%, 84±5%, 85±5%) (p<.05). Also evident is the spatial heterogeneity of infarction risk within the lesion. Predicted lesion volumes were significantly correlated to measured hemispheric lesion volume assuming different occlusion times (p<.05). **Discussion:** This study shows infarction risk increases with occlusion time, consistent with clinical and experimental experience. Importantly, these time-dependence findings were determined algorithmically without prior assumptions. This supports the concept that infarction likelihood depends on both depth and duration of ischemic injury. In addition, the changing spatial heterogeneity of infarction risk exhibited over time may reflect the transition of potentially salvageable to irreversibly damaged tissue. Further studies with histological validation are needed to fully explore this aspect. **In conclusion,** this study demonstrates the potential of statistical algorithms for improved characterization of ischemic injury as well as for identifying salvageable tissue after stroke. **References:** 1. Hacke W, et al. Lancet. 2004; 363, 768-74. 2. The National Institute of Neurological Disorders and Stroke rt-PA Stroke Study Group. NEJM. 1995; 333, 1581-7. 3. Wu O, et al. Stroke. 2001; 32, 933-42.

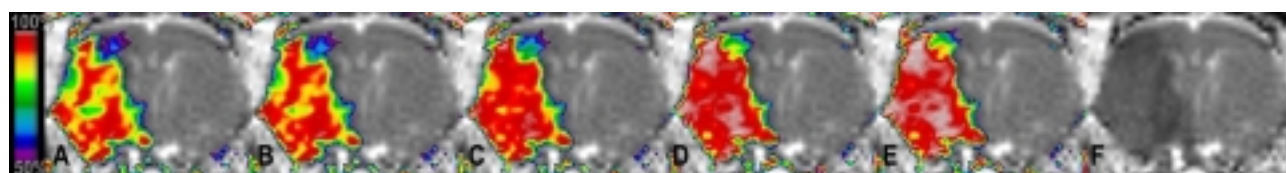


Fig 1 Predicted risk of infarction assuming occlusion of (A) 52, (B) 85, (C) 150, (D) 273, (E) 329 min & (F) ADC values at 329 min.



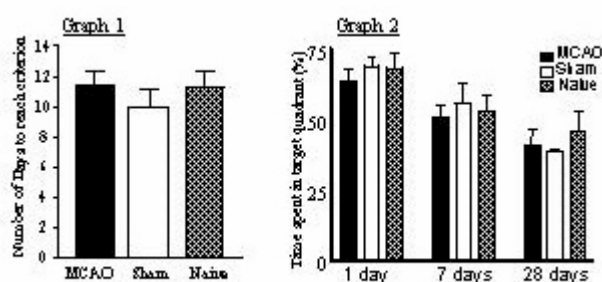
## UNILATERAL PROXIMAL OCCLUSION OF THE MIDDLE CEREBRAL ARTERY HAS NO EFFECT ON ACQUISITION OR RETENTION OF SPATIAL MEMORY

Deborah Bingham<sup>1</sup>, Stephen J. Martin<sup>2</sup>, I. Mhairi Macrae<sup>1</sup>, Richard G.M. Morris<sup>2</sup>, Hilary V.O. Carswell<sup>1</sup>

<sup>1</sup>Wellcome Surgical Institute, Division of Clinical Neuroscience, University of Glasgow, Glasgow, UK

<sup>2</sup>Laboratory for Cognitive Neuroscience, Division of Neuroscience, University of Edinburgh, Edinburgh, UK

Stroke is the third most common cause of death and the primary cause of morbidity in the United Kingdom. It can be associated with deterioration in both sensorimotor and cognitive skills. Proximal occlusion of the middle cerebral artery (MCAO) in rodents is a widely used model of experimental cerebral ischaemia, which has been used to investigate the effect of stroke on cognition in spatial learning, such as the watermaze. However, findings to-date have been varied, depending on when testing was started after MCAO and the duration of training and testing, raising doubts about the utility of MCAO in rodents to study memory deficits. The present study was designed to discriminate between sensorimotor and spatial memory to establish whether MCAO has a significant influence on both the acquisition and retention of spatial memory. Female Lister Hooded rats (n=10) underwent MCAO. The artery was electrocoagulated from the origin of the lenticulostriate arteries to the inferior cerebral vein and then transected to ensure complete occlusion. Sham animals (n=9) underwent the same procedure except the artery was not occluded or transected and a group of naïve, unoperated animals (n=8) was included. Training in the watermaze commenced 10 days after MCAO with 3 days of training to a visible escape platform of varying positions from different start positions. The animals were then trained to find a hidden escape platform at a fixed location (spatial reference memory). The start position was varied and the first trial every day was a probe trial where no platform was present for the first 60 seconds. For acquisition, animals were trained until they spent at least 50% of the probe trial in the quadrant where the platform was normally placed (target quadrant) for 3 consecutive days. The retention of memory was tested 1, 7 and 28 days after this criterion was reached. MCAO induced a consistent infarct involving both cortex and caudate which by 28 days was represented by ipsilateral tissue loss of  $32.1 \pm 2.8$  % of the contralateral hemisphere (mean  $\pm$  S.E.M). The watermaze results revealed no deficit in acquisition or retention of memory in MCAO animals compared to sham and naïve animals. There was no difference in the average number of days to reach acquisition criterion (Graph 1), and no difference in the proportion of time spent in the target quadrant during the retention tests (Graph 2). Data are presented as mean  $\pm$  S.E.M. In conclusion, this study, designed to differentiate between spatial memory and sensorimotor deficits, revealed no evidence for deficits in memory acquisition or retention following MCAO. *DB was supported by: University of Glasgow Scholarship and the William Ramsey Henderson Trust Travel award.*





## CORRELATION OF INFARCT VOLUME WITH FUNCTIONAL OUTCOME IN AN EMBOLIC MCA OCCLUSION MODEL IN RATS

Max Nedelmann<sup>1</sup>, Thomas Wilhelm-Schwenkmezger<sup>1</sup>, Beat Alessandri<sup>2</sup>, Axel Heimann<sup>2</sup>, Felicitas Schneider<sup>1</sup>, B. Martin Eicke<sup>1</sup>, Marianne Dieterich<sup>1</sup>, Oliver Kempfski<sup>2</sup>

<sup>1</sup>*Department of Neurology, Johannes Gutenberg University, Mainz, Germany*

<sup>2</sup>*Institute for Neurosurgical Pathophysiology, Johannes Gutenberg University, Mainz, Germany*

**Background:** The embolic MCA occlusion model in rats is used to study recanalisation mechanisms in acute stroke. Next to the determination of morphological lesion size as an outcome parameter, the assessment of functional outcome may improve the value of this animal model. A comprehensive functional testing should allow a discrimination between the degrees of ischemic brain damage. Aim of this study was therefore, to evaluate a neurological score consisting of different sensorimotor tests and a parallel bar crossing test for their correlation with the infarct sizes after embolic MCA occlusion. **Methods:** Male Wistar rats were submitted to MCA clot embolism (n=14) or sham surgery (n=7). The emboli were placed by means of a polyethylene catheter (OD 0,28-0,3mm), that was transiently advanced into the right distal internal carotid artery. In order to achieve a larger variety of lesion size, subgroups were subjected to differently sized emboli (30 and 40 mm in 7 animals, respectively). Animals were followed up every day for 6 days. Outcome assessment consisted of a parallel bar crossing test and a neurological score with ten different items (including different motor, coordinative and sensory functions). Functional impairment was scored from 0 (no impairment) to 100 (no reaction to any stimuli). Animals were perfusion-fixed (4% paraformaldehyde) on postoperative day 7, brains were removed and 3µm-thick sections were Hematoxylin-eosin stained for quantification of infarct volume (blinded examination). **Results:** The infarct volume depended on the initial length of the applied blood clot (clot length 40mm: 53.22±/43.15mm<sup>3</sup>, p=0.002 compared to sham; clot length 30mm: 19.86±/18.77mm<sup>3</sup>, p=0.009). For both subgroups, there was a significant impairment on the neurological score, with only partial improvement during the follow up period and significant impairment on day 6 (clot length 40mm: 41.4±/13.1, p=0.001 compared to sham; clot length 30mm: 25.7±/16.2, p=0.003). On follow up day 6, there was a highly significant correlation between the determined infarct volume and the functional outcome (R=0.80, p=0.0006). There were statistically significant functional deficits for both subgroups on the parallel bar crossing test (traversing time and number of foot faults) during the complete follow-up period. The correlation with infarct volume was significant up to day 4 (traversing time: R=0.55, p=0.01; foot faults: R=0.60, p=0.004), but failed significance on day 6 (traversing time: R=0.25, p=0.38; foot faults: R=0.38, p=0.18). **Conclusions:** In this embolic MCA occlusion model, application of emboli with a clot length of 40mm is superior to 30mm with regard to reliability and extent of lesion size and with regard to the degree and persistence of the functional impairment during the evaluated follow-up period. We present outcome tests that provide quantitative and objective tools to test functional impairment in rats following embolic stroke. Best results are achieved with a neurological deficit score which is easy to perform and correlates significantly with infarct volume. We conclude that functional outcome testing may serve as a complementary evaluation tool in recanalisation studies of embolic stroke in rats.

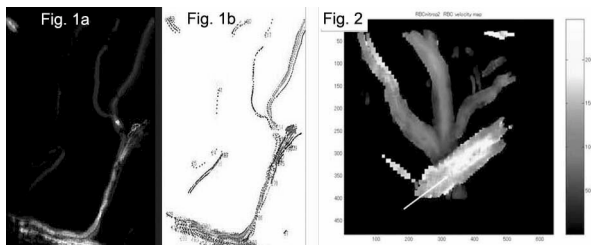
## SOFTWARE (KEIO-IS2) FOR AUTOMATICALLY TRACKING RED BLOOD CELLS (RBCS) WITH CALCULATION OF INDIVIDUAL RBC VELOCITIES IN SINGLE CAPILLARIES OF RAT BRAIN

Istvan Schiszler<sup>1</sup>, Hidetaka Takeda<sup>1</sup>, Minoru Tomita<sup>1</sup>, Yutaka Tomita<sup>2</sup>, Takashi Osada<sup>1</sup>, Miyuki Unekawa<sup>1</sup>, Norio Tanahashi<sup>1</sup>, Norihiro Suzuki<sup>1</sup>

<sup>1</sup>Department of Neurology, School of Medicine, Keio University, Tokyo, Japan

<sup>2</sup>Laboratoire de Biologie et Physiologie Moléculaire du Vaisseau INSERM U 541, Paris, France

Confocal fluorescence microscopy offers the potential to visualize cells at high resolution in living animals. However, studies of tissue microcirculation *in vivo* are limited by inability to follow individual red blood cells (RBCs) moving heterogeneously in space and time. Here we present our software (KEIO-IS2), which, in combination with high-speed (125-1000 sec<sup>-1</sup> shutter speed) confocal fluorescent microscopy, can quantitatively treat RBC flow in single capillaries. Urethane-anesthetized Wistar rats (n=26) received intravenous injection of FITC-RBCs so that bright particles were observable flowing on a dark background with the confocal microscope (Seylaz et al. JCBFM 19:863,1999). Images were recorded directly to computer in uncompressed AVI file format. The dimensions of the measurement region were 250 micron x 300 micron, with a layer thickness of ca. 20 micron, and the cortex could be scanned vertically down to 100 micron in depth. The recording period was usually 10 sec at a frame rate of 1/250 sec. The recorded movies were analyzed with MATLAB® and KEIO-IS2 software, which can track individual, rapidly moving RBCs on the acquired confocal images. The program exploits the light intensity difference between the dark background and the light RBCs in the visual field of the microscope to detect the RBCs automatically. It is possible to specify several parameters, such as the scale, the minimal RBC size and flow velocity, and the intensity threshold value, to customize the software. The algorithm for RBC tracking is as follows. First a gray level thresholding is applied to each frame to differentiate RBCs from background brightness, then all particles having at least 8 connected pixels are recognized as RBCs. Displacement of the particles in subsequent frames is analyzed, and the software builds up the tracks of the moving RBCs frame-by-frame and calculates the velocities of individual RBCs (displacement over frame interval). The results can be exported for further statistical analysis. Some results of RBC tracking through single capillaries are shown in Fig. 1a (RBC velocities ranging from 0.3-7.0 mm/s) and 1b (RBC trackings, see also M. Tomita et al. (Brain 05)). Fig. 2 shows an RBC shower in an artery of 100 micron sliced at 20 micron thickness longitudinally at its center. We could calculate intravascular velocity profiles and wall shear rates. This software would also be applicable to labeled platelets and white blood cells, providing a powerful tool for hemorrheological studies in the brain microvasculature.



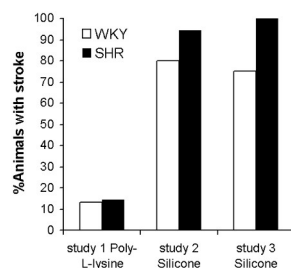
## AN IMPROVED TECHNIQUE FOR SILICONE-COATING THE SUTURE USED IN RAT MCA OCCLUSION INCREASES STROKE INDUCTION RATE, REDUCES MORTALITY, AND IS EFFECTIVE ACROSS A WIDE WEIGHT AND AGE RANGE

Neil J. Spratt<sup>1,2</sup>, **John A. C. Fernandez**<sup>1,2</sup>, Michelle Chen<sup>1,2</sup>, Sarah S. J. Rewell<sup>1,2</sup>, Susan F. Cox<sup>1,2</sup>, Leena van Raay<sup>1,2</sup>, Lisa Hogan<sup>1,2</sup>, David W. Howells<sup>1,2</sup>

<sup>1</sup>Department of Medicine, University of Melbourne, Austin Health, Melbourne, Australia

<sup>2</sup>National Stroke Research Institute, Austin Health, Melbourne, Australia

**Introduction:** Thread occlusion of the rat middle cerebral artery (MCA) is widely used to model stroke, but has previously been reported to be ineffective in aged animals, in which hyperostosis of the carotid canal may hinder insertion of rigid sutures. Study of aged animals and those with co-morbidities is recommended to more closely mimic human stroke. However, despite previous success and consistency in inducing strokes in young rats using non silicone-coated sutures (albeit with some mortality), we also observed a low rate of successful stroke induction in aged rats using the same technique. Therefore we aimed to modify the MCA thread-occlusion method to improve stroke induction across a wide weight and age range. **Methods:** A new method was developed for coating the distal 5mm of monofilament sutures with silicone, creating a highly consistent tip diameter. Various tip diameters were tested for effectiveness of stroke induction in rats of varying weight and age. Stroke induction rate in aged rats was compared with that obtained using heat-treated poly-L-lysine sutures (Fig. 1). Mortality rates were compared between suture types for different operators, in: young, aged and different strains of rat, and in hypertensive and diabetic animals (n = 296). **Results:** A diameter of 0.36 mm appeared optimal for induction of stroke in rats of varying age, weight and strain. The rate of successful stroke induction in aged rats increased from 14% to 80% when these sutures were used. Mortality was reduced from 25-30% to 7% or less in young or old rats with or without co-morbidities (diabetes and hypertension). **Conclusions:** This technique produced sutures with an extremely uniform, adherent silicone-coated tip, which was soft, smooth and malleable. These sutures reliably produced stroke across a wide range of ages and weights, with low mortality even in aged rats with co-morbidities. This technique enhances the ability to more closely model human ischaemic stroke. **Figure 1:** Histogram showing the proportion of aged (16 months) WKY and SHR rats with evidence of stroke 24 hours post MCA-occlusion using different occluding sutures. Study 1 (n=15 WKY, 14 SHR) used poly-L-lysine coated sutures, studies 2 (n=15 WKY, 18 SHR) and 3 (n=8 WKY, 14 SHR) used silicone coated sutures. A single experienced operator performed all surgery.



## A NEW TECHNIQUE FOR THE MAPPING OF OXYGEN TENSION ON THE BRAIN SURFACE

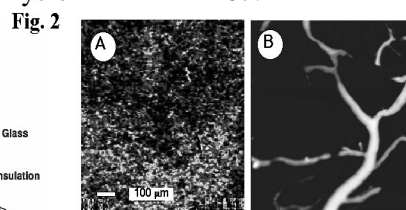
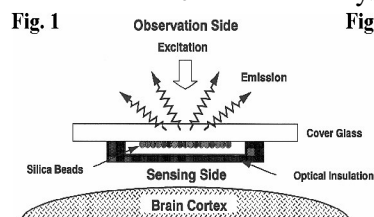
Satoshi Kimura<sup>1</sup>, Keigo Matsumoto<sup>2</sup>, Yoshio Imahori<sup>1</sup>, Katsuyoshi Mineura<sup>1</sup>,  
Toshiyuki Itoh<sup>3</sup>

<sup>1</sup>*Department of Neurosurgery, Kyoto Prefectural University of Medicine, Kyoto, Japan*

<sup>2</sup>*Department of Neurosurgery, Kobe Social Insurance Hospital, Kobe, Japan*

<sup>3</sup>*Department of Physiology, Kyoto Prefectural University of Medicine, Kyoto, Japan*

**Introduction:** The measurement of oxygen tension (PO<sub>2</sub>) in the brain is quite important in the study of ischemic diseases. To date, most PO<sub>2</sub> measurements have been performed using oxygen microelectrodes. However, the microelectrode is not always a suitable tool for studying brain oxygenation because insertion of the electrode into the brain per se causes hemorrhage and hence leads to erroneous PO<sub>2</sub> measurement. Furthermore, microelectrodes only measure PO<sub>2</sub> at specific points within the tissue. To overcome these difficulties, we visualized the spatial distribution of PO<sub>2</sub> in the brain surface as epifluorescent microscopic patterns, using the oxygen-sensitive fluorescent membrane technique (1) with proper modifications. **Methods:** An oxygen-quenching fluorescence dye, tris (1,10-phenanthroline) ruthenium (II) chloride hexahydrate, was immobilized in silica-gel beads 3 μm in diameter and the dyed beads were embedded in a highly gas-permeable (~20 μm thick), opaque silicone-rubber film formed on a microscope coverslip. Unlike the original method, intended for transparent mesenteric tissue (1), the opaque silicone elastomer was adopted to minimize the effect of the redox state of the brain tissue on the optical measurement of PO<sub>2</sub>. The feasibility of this technique for use in brain microcirculatory studies was assessed using Pulsinelli's four-vessel occlusion rat. Under pentobarbital anesthesia (35 mg/Kg, i.p.), male Wistar rats (300-350g, n=8) underwent bilateral electrocauterization of the vertebral arteries. After 24 hours recovery, two cranial windows were made in the skull under anesthesia (15% urethane, 10 ml/Kg, s.c.) and the oxygen-sensitive membrane was placed on the brain, with the PO<sub>2</sub>-sensing side in very gentle contact with the brain surface through one cranial window (Fig. 1). Under artificial ventilation, the animals were subjected to occlusion of the common carotid arteries, which resulted in reversible brain ischemia as monitored by a Laser-Doppler flowmeter through the other window. During the ischemia/reperfusion periods, the fluorescence pattern on the oxygen-sensitive membrane was video-recorded continuously and subjected to subsequent playback analysis and conversion to PO<sub>2</sub> values. **Results:** The present method enabled us to visualize the PO<sub>2</sub> gradient on the rat brain surface without causing cortical injury. Figure 2 shows a typical example of PO<sub>2</sub> gradient at control state (A), and the microvasculature in the corresponding area (B). High-PO<sub>2</sub> areas appear bright and low-PO<sub>2</sub> areas are dark. In ischemia/reperfusion protocol, heterogeneity in the PO<sub>2</sub> distribution on the brain surface was detected, in particular between the periarteriolar region and other regions, and this heterogeneity was increased in association with ischemia. **Conclusion:** This visualization technique was considered to be a new potent tool for the study of oxygen transport and metabolism in the brain. **References:** [1] Itoh T, Yaeagashi K, Kosaka T et al.; Am J Physiol 267: H2068-H2078 (1994).



**BRAIN VENOUS HYPERTENSION INDUCES ANGIOGENESIS THROUGH OVEREXPRESSION OF HYPOXIA-INDUCIBLE FACTOR-1 (HIF-1)**Yiqian Zhu<sup>1</sup>, Fanxia Shen<sup>1</sup>, Yongmei Chen<sup>1</sup>, William L. Young<sup>1,2,3</sup>, **Guo-Yuan Yang**<sup>1,2</sup><sup>1</sup>*The Center for Cerebrovascular Research, Departments of Anesthesia and Perioperative Care, University of California, San Francisco, CA, USA*<sup>2</sup>*Department of Neurological Surgery, University of California, San Francisco, CA, USA*<sup>3</sup>*Department of Neurology, University of California, San Francisco, CA, USA*

**Introduction:** Brain venous hypertension is present in many cerebrovascular diseases such as arteriovenous malformation. However, how venous hypertension worsens vascular abnormality is unclear. Hypoxia-inducible factor 1 (HIF-1) is an upstream activator of many adaptive responses to tissue. Although decreased O<sub>2</sub> delivery is the well-known stimulus, recent evidence points to a direct mechanical effect to activate HIF-1. This effect has been recently described in chondrocytes, subject to joint motion. Inflammatory cytokines, such as the interleukins (IL), induce angiogenic factors such as vascular endothelial growth factor (VEGF) and function as tumor and endothelial cell growth factors. Current study was to investigate the modest non-ischemia degree of venous hypertension affects the expression of HIF-1 $\alpha$  and the changes parallels to the levels of IL-6. **Methods:** To establish a non-ischemic venous hypertension model mimicking the hemodynamic changes in human AVM, we have recently implemented the rat model described by Lawton et al (Ref). Four groups (n=6 per group) of adult Spring-Dowley rat weighting 300 to 350 underwent 1) common carotid artery (CCA) occlusion alone; 2) CCA and external jugular vein (EJV) anastomosis alone; 3) CCA and EJV anastomosis plus transverse sinus and sagittal sinus (TS/SS) occlusion (Fistula+Sinus Occlusion); and 4) sham group. Mean arterial pressure (MAP), sagittal sinus pressure (SSP), surface cerebral blood flow (using a laser Doppler flowmetry, LDF sCBF), and the diameter of CCA and EJV were examined before and after surgery procedure. **Results:** There were no differences in mean blood pressure and sCBF before and after surgery among the four groups. Western blot analysis showed that expression of HIF-1 $\alpha$  was increased in the brain venous hypertension rats compared to the other three groups (1.8 $\pm$ 0.3 vs. 1.1 $\pm$ 0.2, 1.2 $\pm$ 0.2, and 1 $\pm$ 0.1; respectively, p<0.05). Immunohistochemistry shows that HIF-1 positive staining was mainly observed in microvessels located parasagittally, in rat brain cortex and sub-cortex. Under higher magnification, HIF-1 $\alpha$  positive staining appeared localized to the cell nuclei. Further study verified that interleukin-6 (IL-6) was also increased in the brain venous hypertension rats, which paralleled to the HIF-1 expression (IL-6: 149 $\pm$ 17 pg/ml vs. 112 $\pm$ 10, 118 $\pm$ 22, and 122 $\pm$ 10 pg/ml; respectively, p<0.05). **Conclusion:** Non-ischemic venous hypertension induced HIF-1 $\alpha$  and the presumably downstream signal, IL-6, both of which may play an important role in pathological angiogenesis. Brain venous hypertension has an intrinsic pro-angiogenic character, which may be independent of its potential to induce tissue ischemia.

**Reference:**

[1] Lawton MT, et al. Redefined role of angiogenesis in the pathogenesis of dural arteriovenous malformations. *J Neurosurg* 1997;87:267-274

Supported by NIH grants: PO1 NS and RO1 NS27713 (WLY) and R21 NS45123 (GYG)

## WHITE MATTER INJURY IN KAOLIN-INDUCED NEONATAL RAT HYDROCEPHALUS

Osaama H. Khan<sup>1,2</sup>, Marc R. Del Bigio<sup>1,2</sup>

<sup>1</sup>*Department of Pathology, University of Manitoba, Winnipeg, Manitoba, Canada*

<sup>2</sup>*Manitoba Institute of Child Health, Winnipeg, Manitoba, Canada*

Hydrocephalus is a common neurological condition characterized by obstruction of cerebrospinal fluid (CSF) flow leading to enlargement of CSF-containing ventricular cavities in the brain. The primary target of injury is axons in the periventricular white matter. The stretching of axons leads to dysfunction and ultimately axotomy. Many experiments in mature animals systems indicate that white matter blood flow is decreased. A decrease in oxygen saturation should lead to production of oxygen free radicals and activation of the transcription factor hypoxia inducible factor 1 alpha (HIF). HIF further activates a cascade of cellular responses, notably, vascular endothelial growth factor (VEGF). The main effect of VEGF is to cause production of new blood vessels. Its expression can have an influence on vascular permeability and could play a role in water dysregulation in the hydrocephalic brain. Our first goal was to characterize the structural changes of a neonatal model of kaolin-induced hydrocephalus in rat. Our second goal was to investigate the molecular sequence of events resulting from ischemia. Sprague-Dawley rats underwent kaolin injection into the cisterna magna at postnatal day 1. They had enlarged ventricles by 7 days and severe dilatation by 21 days as assessed by magnetic resonance imaging (MRI) and histology. Periventricular white matter, including corpus callosum and internal capsule, was edematous at 7 days and severely atrophic at 21 days. ELISA and Western blots revealed decreased expression of myelin associated proteins including myelin basic protein (MBP). Pimonidazole hydrochloride (2-nitroimidazole) specifically binds to thiol groups of proteins, peptides and amino acids in a hypoxic environment. Following subcutaneous administration, immunohistochemistry demonstrated hypoxia-associated adducts in periventricular glial cells. Nitrotyrosine, an oxidative stress marker, could be detected by immunohistochemistry extensively in white matter and around some blood vessels. Weak labeling was also seen around large neurons in cerebral cortex. HIF and 4-Hydroxy-2-nonenal (HNE) for endogenous lipid peroxidation are currently under investigation. VEGF immunohistochemistry in normal rats revealed positive cortical neurons in 7-day old rats; this diminished at 21 days. The pattern of expression shifted to white matter glial cells in hydrocephalic rats. VEGF expression determined by ELISA supports those findings. In this model of neonatal kaolin induced hydrocephalus, hypoxia in white matter might contribute to the destructive changes.

**ISOMETRIC FORCE MEASUREMENT IN MOUSE CEREBRAL ARTERIES:  
ESTABLISHING REFERENCE VALUES AND CHARACTERIZING FUNCTIONAL  
CONSEQUENCES OF ENDOTHELIAL NITRIC OXIDE SYNTHASE KNOCK-OUT  
IN THE BASILAR ARTERY**

Armin Hilpert<sup>1</sup>, Zoltan Benyo<sup>2</sup>, Lothar Schilling<sup>1</sup>

<sup>1</sup>*Division of Neurosurgical Research, Department of Neurosurgery, University Hospital  
Mannheim, University of Heidelberg, Heidelberg, Germany*

<sup>2</sup>*Department of Pharmacology, University of Heidelberg, Heidelberg, Germany*

Genetically modified mice are increasingly important tools in biomedical research. The increasing number of transgenic mouse strains available has raised the need to develop adequate tools for characterizing the functional consequences of overexpressing, knocking out, or inserting a gene. We have, therefore, adapted the methodology of isometric force measurement to study the vasoreactivity of mouse cerebral arteries *in vitro*. Ring segments (approximately 1 mm in length) of the basilar artery (BA) were obtained from NMRI, C57/black6 (C57B6), endothelial nitric oxide synthetase knock-out (eNOS<sup>-/-</sup>) mice and the corresponding wild-type line (eNOS<sup>+/+</sup>). The segments were transferred into organ bathes filled with a modified Krebs-Henseleit solution maintained at 37 C, and continuously gassed with a mixture of 77%/17.5%/5.5% N<sub>2</sub>/O<sub>2</sub>/CO<sub>2</sub>. Contractile responses were elicited by membrane depolarisation (equimolar substitution of NaCl by KCl), or cumulative application of U46619 (a thromboxane A<sub>2</sub>-analogue) or endothelin-1 (ET-1). Relaxation was induced by applying increasing concentrations of Na-nitroprusside (SNP) or 8-bromo dibutryl-cyclic GMP (8br-cGMP) on top of stable precontraction with U46619 (1E-7 M). Contraction is given in absolute terms (mN force). Relaxation is calculated in % decrease of precontraction. Values are given as mean±SD. In NMRI mice, different levels of resting tension (RT) upon membrane depolarisation (by increasing the K<sup>+</sup> concentration)-induced contraction were studied. In segments with a RT >1.75 mN (2.0±0.2 mN), depolarisation-induced contraction was 1.9±0.6, somewhat bigger than with lower RT (1.4±0.2 mN; contraction, 1.7±0.4 mN). Thus, RT was set to 2 mN in further experiments. Contraction induced by high K<sup>+</sup> Krebs solution was 2.3±0.6 in NMRI, 2.3±0.6 in C57B6, 2.6±0.8 in eNOS<sup>+/+</sup>, and in eNOS<sup>-/-</sup> 3.3±1.0 (p<0.05 vs all other strains). Additional results are listed in the table below with † p<0.1 and \*p<0.05 vs. eNOS<sup>+/+</sup>. The study presents for the first time data on vascular reactivity of mouse cerebral arteries employing the isometric force measurement technique. The results indicate pronounced differences in depolarisation- and receptor-induced contraction in different mouse strains. Furthermore, SNP enhanced relaxation in eNOS<sup>-/-</sup> mice significantly, probably indicating a hypersensitivity of the sGC due to the lack of NO release from the endothelial cells. Thus, this technique allows a powerful method to study in great detail the functional consequences of a given type of genetic engineering in mouse cerebral arteries.

		NMRI	C57B6	eNOS <sup>+/+</sup>	eNOS <sup>-/-</sup>
U46619	pD <sub>2</sub>	7.144±0.35	7.274±0.39	7.144±0.28	7.044±0.28
	E <sub>max</sub>	3.84±1.3	2.54±1.3	2.64±0.7	2.54±1.2
ET-1	pD <sub>2</sub>	9.624±0.39	not tested	9.044±0.40	8.784±0.51
	E <sub>max</sub>	3.04±1.2	not tested	1.764±0.64	2.14±1.3
SNP	pD <sub>2</sub>	5.184±0.96	4.564±0.39	4.564±0.24	5.094±0.63†
	E <sub>max</sub>	40.54±11.8	67.04±13.3	60.14±11.4	83.34±11.1*
cGMP	pD <sub>2</sub>	4.784±0.38	4.534±0.20	4.524±0.14	4.434±0.17
	E <sub>max</sub>	66.24±15.1	73.94±13.1	77.54±7.0	77.44±16.0

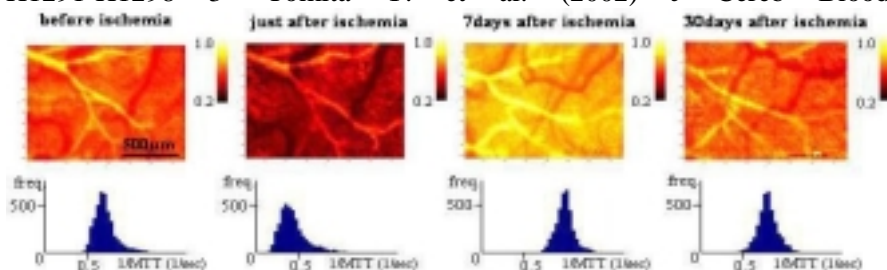
## CORTICAL MICROFLOW QUANTITATIVE MEASUREMENTS WITH HIGH SPATIAL AND TEMPORAL RESOLUTION OVER 1 MONTH AFTER FOCAL CEREBRAL ISCHEMIA IN MICE

Yutaka Tomita<sup>1</sup>, Alexy Tran Dinh<sup>1</sup>, Istvan Schiszler<sup>2</sup>, Minoru Tomita<sup>2</sup>, Norihiro Suzuki<sup>2</sup>, Nathalie Kubis<sup>1</sup>, Elisabeth Pinard<sup>1</sup>, Jacques Seylaz<sup>1</sup>

<sup>1</sup>Cardiovascular Research Center Lariboisière, INSERM U 689, Université Paris 7, Paris, France

<sup>2</sup>Department of Neurology, Keio University School of Medicine, Tokyo, Japan

**Introduction:** A new model of murine focal cerebral ischemia whose pathophysiological microcirculatory processes can be chronically and directly investigated in vivo was reported recently<sup>1</sup>). The present study examines the feasibility and interest of the long-term use of a high-spatial-resolution optical method for 2-D CBF measurements. The method is derived from that of Schiszler et al.<sup>2</sup>) and was initially developed for acute quantitative measurements in rats<sup>3</sup>). In this presentation, infarct-evolution and/or recovery processes up to 30 days in the same mouse, at the same location were measured repeatedly in vivo using laser-scanning confocal fluorescence dynamic microscopy<sup>1</sup>). **Methods:** A closed cranial window was chronically implanted over the left parietal cortex of C57/BL6 mice. Focal ischemia was induced in 8 mice by topical thermocoagulation of two MCA branches through the window<sup>1</sup>), while 5 sham mice were not subjected to ischemia. Rhodamin B isothiocyanate-dextran (MW=71200, 20mg/ml) was repeatedly injected (<0.01ml as a bolus) into the tail vein to fluorescently label plasma for each measurement. Rhodamine-dilution images of microvessels in a ROI (1.3mm x 0.9mm) at the surface of the ischemic cortex were digitally video-recorded in real-time (25 frames/sec). Images of the same ROI in the same mouse were obtained before, just after, and at 7 and 30 days after arterial occlusion. Sequential frames of Rhodamin-dilution curves over less than 5 sec were analyzed off-line with Matlab software (KEIO-IS) to obtain blood distribution (H) and mean transit time (MTT)<sup>2</sup>), affording a 2-D microflow (1/MTT) map consisting of 2500 flow values (50x50 matrices, spatial resolution = 26µm x 18µm) and a histogram of the flow values with 1st, 2nd, 3rd, and 4th moments. **Results:** Just after arterial occlusion, mean microflow values decreased from 0.59±0.09 to 0.47±0.08 (1/sec, p<0.01). At 7 and 30 days after ischemia, the mean values were not significantly different from baseline. The index of heterogeneity was increased from 0.45±0.04 to 0.58±0.12 (p<0.01) by arterial occlusion and then gradually turned to homogeneity (Figure 1). Functional anastomoses and vascular remodeling were evidenced. There were no significant changes of flow velocity in sham mice. **Conclusion:** The present data show for the first time that quantitative repeated measurements of 2-D microflow in mice can be performed in the long term with high spatial and temporal resolution, through a chronic cranial window, using in vivo confocal dynamic microscopy. Such an approach represents a powerful tool to investigate long-term pathophysiological microcirculatory changes, or to compare microflow changes during cortical activations in the same mouse. **Figure 1:** Example of 2-D flow maps during 4 phases. The scale indicates the degree of flow velocity in each matrix. Histograms of each corresponding period are placed below. **References:** 1- Tomita Y. et al. (2005) J Cereb Blood Flow Metab, in press. 2- Schiszler I. et al. (2000) Am J Physiol 279: H1291-H1298 3- Tomita Y. et al. (2002) J Cereb Blood Flow Metab 22: 663-669



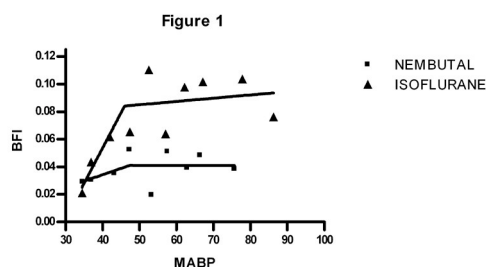


## APPLICATION OF NIRS IN MICE: ASSESSING CEREBRAL BLOOD FLOW AND CEREBRAL AUTOREGULATION

Helga Blockx, Geoffrey De Visscher, Willem Flameng

*C.E.H.A. Katholieke Universiteit Leuven, Leuven, Belgium*

The introduction of transgenic mice models in neuroscience is associated with the need for miniaturisation of measuring systems such as multi-wavelength near infrared spectroscopy (NIRS). Our NIRS-system, developed at the University College London, can be used for the assessment of oxyhemoglobin ([Hb]), deoxyhemoglobin ([HbO<sub>2</sub>]), and oxidised cytochrome oxidase (CuA) in the brain in toto and has already been validated for rats<sup>1</sup> and mice<sup>2</sup>. We examined the possibilities of this technique in mice, the main research animal in transgenic models. Indocyanine green (ICG) is a tracer to measure blood flow index (BFI), an indication for cerebral blood flow<sup>2,3</sup>. In a first study we determined the optimal ICG dose providing a sufficiently large signal in the brain of mice and estimate the effect of the tracer injection upon the other NIRS variables. We subsequently injected 0.5, 1, 2.5, 5 and 10 $\mu$ l ICG in mice (n = 12) through the external jugular vein. Due to significant changes in optical path length after large ICG boli, back-calculation of NIRS variables was incorrect. It is therefore not possible to simultaneously measure CBF and [Hb], [HbO<sub>2</sub>] and CuA. The disturbance caused by ICG rose with larger ICG bolus, demonstrating the need to minimise bolus volume. On the contrary, while investigating variability by dividing BFI by the injection volume, we found that small injection volumes result in a large variability, indicating the need to increase the injected bolus. Therefore, at present the optimal bolus to measure CBF in mice is 2.5 $\mu$ l ICG. Further attempts to increase reproducibility of the 1 $\mu$ l bolus injection is under development. In a second study we compare the cerebral autoregulation curves (BFI vs mean arterial blood pressure (MABP)) in mice anaesthetised with Isoflurane (n = 9) and Nembutal (n = 4). The cerebral autoregulation curve, for which MABP was lowered in steps of approximately 10 mmHg by blood withdrawal, was estimated by calculating the mean BFI per MABP and fitting a 'two lines with a breakpoint' model (fig 1). Isoflurane anaesthetised mice had an increased CBF when compared to Nembutal mice. This is in accordance with the findings of Hendrich and colleagues<sup>4</sup> who found, using MRI, that cerebral blood flow values are lower during anesthesia with pentobarbital as compared to Isoflurane. In conclusion, we find the optimal ICG bolus to measure cerebral blood flow in mice to be 2.5 $\mu$ l and demonstrate that near infrared spectroscopy can be used to investigate cerebral autoregulation in mice. 1. De Visscher, doctoral thesis, 2002 2. De Visscher et al., *Adv. Exp. Med. Biol.* in press 3. De Visscher et al., *Comp. Biochem. Physiol.* 132(1): 87-95, 2002 4. Hendrich et al., *Magn. Reson. Med.* 46: 202-6, 2001



## FK506 EXTENDED THERAPEUTIC TIME WINDOWS OF THROMBOLYSIS WITHOUT INCREASING RISK OF HEMORRHAGIC TRANSFORMATION ON EMBOLIC RAT

Seiji Okubo<sup>1</sup>, Hironaka Igarashi<sup>2</sup>, Tomoyuki Kanamatsu<sup>3</sup>, Yasuo Katayama<sup>2</sup>

<sup>1</sup>*Department of Neurology, Tokyo Metropolitan Tama Geriatric Hospital, Tokyo, Japan*

<sup>2</sup>*The Second Department of Internal Medicine, Nippon Medical School, Tokyo, Japan*

<sup>3</sup>*Department of Environmental Engineering for Symbiosis, Faculty of Engineering, Soka University, Tokyo, Japan*

**Introduction:** Thrombolysis by recombinant tissue plasminogen activator(rt-PA) is effective for acute cerebral ischemia. Because of short therapeutic time window and risk for hemorrhagic transformation(HT) which is most harmful side effect of thrombolysis, rt-PA has been used only limited number of patients. There are clinical demands for neuroprotective agents that can extend the therapeutic time window or reduce hemorrhage. On the other hand, FK-506 is reported to damage vascular endothelial cell and increase BBB permeability in animal experiment, and brings about cerebral vasculitis or cerebral hemorrhage in clinical cases. These results evoke us the concern with the adverse interaction of rt-PA and FK506 to increase the risk of hemorrhagic transformation. From these points of view, we evaluated therapeutic efficacy and influence against HT of combined therapy with rt-PA and FK506 for embolic model in rats. **Material and Methods:** 18pieces of 1mm length from the fibrin rich portion in clots were gently infused via ICA of Sprague-Dawley rats(n=66). Intravenously, 0.3mg/kg of FK506 was administered after 60minutes from embolization. 10% of total 10mg/kg of Alteplase was injected as a bolus and remainder was infused continuously for 30minutes at 60, 90 and 120minutes after embolization. Eight groups(n=6 respectively); control(saline only), namely FK506, Alteplase-60min, Alteplase90min, Alteplase120min, FK506+Alteplase60min, FK506+Alteplase90min and FK506+Alteplase120min, were compared by relative regional(rr) CBF using laser-doppler flowmetry, final infarct volume from TTC stain and HT using spectrophotometric assay of extraction. and lesion measurement of ADC and CBV map using MRI was undergone on other set of Alteplase90min, FK506+Alteplase90min, and control(n=6 respectively). **Results:** After embolization, rrCBF decreased to about 20% in all groups. Control and FK506 group shows persistent rrCBF decline for at least six hours. Administration of rt-PA partially restored rrCBF to about 70% of pre-ischemic level. Combined treatment of FK506 did not alter the restoration of rrCBF. In the groups rt-PA alone at 60 minutes after embolization, infarct volume were significantly smaller than control group, however group of 90 and 120 minutes after embolization did not ameliorate the infarction. In the group of combined FK506+rt-PA at 60 and 90 minutes, infarct volume were significantly smaller than control group, however group of 120 minutes did not ameliorate the infarction. FK506 alone did not diminish the infarct volume compared with control. FK-506 did not affect the hemorrhagic volume on each pair of the group with identical rt-PA administration schedules. In MRI study, both ADC and rCBV lesion volumes before rt-PA administration did not differ among three groups. In rt-PA alone group, final infarct volume, which revealed by TTC stain, was significantly smaller than rCBV lesion volume, but not ADC lesion volume. Final infarct volume of combined therapy group was significantly smaller than both ADC and rCBV lesion volume. Final infarct volume of combined therapy was significantly smaller than that of control. **Conclusions:** FK506 extend therapeutic time windows of thrombolysis without increasing risk of hemorrhagic transformation. FK506 did not ameliorated ADC revealed ischemic lesion during ischemia, however salvaged part of ADC revealed lesion which was destined to infarct in rt-PA alone treated rat.

**RHEOENCEPHALOGRAPHIC EVIDENCE OF COMPLEMENT ACTIVATION-RELATED CEREBROVASCULAR CHANGES IN PIGS**

**Michael Bodo**<sup>1</sup>, Janos Szebeni<sup>1</sup>, Lajos Baranyi<sup>1</sup>, Sandor Savay<sup>1</sup>, Frederick Pearce<sup>1</sup>, Carl Alving<sup>1</sup>, Rolf Bunger<sup>2</sup>

<sup>1</sup>*Walter Reed Army Institute of Research, Silver Spring, MD, USA*

<sup>2</sup>*Department of Anatomy, Physiology and Genetics, Uniformed Services University of the Health Sciences, Bethesda, MD, USA*

Intravenous administration of Doxil and other liposomes in pigs can cause severe cardiopulmonary and hemodynamic abnormalities, including pulmonary hypertension, systemic hypotension, falling cardiac output and tachy- or bradycardia with arrhythmia, ventricular fibrillation and cardiac arrest. The phenomenon, which is due to complement activation by the liposome membranes, suggests a model for acute hypersensitivity reactions (manifested in hyper- or hypotensive episodes, chest pain, dyspnea) caused by liposomal drugs in patients. However, some other manifestations (e.g., anxiety, confusion, headache) could not be readily explained by changes in systemic circulation, pointing to possible direct effects of complement activation on the cerebrovascular system. The goal of the present study was to explore liposome-induced changes and changes related to complement activation in cerebral blood flow (CBF) using rheoencephalography (REG), the measurement of changes of electrical impedance in the skull. REG measurements were performed on anesthetized pigs (n = 24 pigs, 57 liposome injections, 19 types of liposomes). Systemic (SAP) and pulmonary arterial pressure, cardiac output, EKG, REG were recorded on a PC. Data were processed off-line. Following liposome infusion, pig SAP decreased robustly, and the changes described above were again observed (massive pulmonary hypertension, systemic hypotension and severe cardiac abnormalities, including falling cardiac output and tachy- or bradycardia with arrhythmia). A significant, transient decrease in REG pulse amplitudes occurred in 40 of 51 cases. A 78.43% decrease in REG amplitude was observed, which lasted only a few seconds. This transient decrease preceded the actual onset of circulatory shock, before changes in pulmonary and systemic arterial pressures, and also preceded a decrease of CO<sub>2</sub> levels in exhaled air. In about half of the animals (51.9%), REG pulse amplitude first decreased then increased, an indication of transient cerebral vasoconstriction and vasodilatation, which occurred while SAP was low or falling. In 48.1% of the animals, REG amplitude remained depressed or decreased further. In 26.3 % of the animals, both types of CBF response to cardiovascular shock induced by liposomes were observed. Different liposomes produced no qualitative differences in cardiovascular reactions; increased doses of all liposomes elicited severe reactions. In the Doxil subgroup (n=12), the decrease in REG pulse amplitude was statistically significant (P = 0.003) after Doxil administration; average amplitude decrease was 42.5 ± 16.5 %, and the CBF response was autoregulatory in 91.6 % (11 out of 12). This study gives direct evidence of cerebrovascular changes caused by liposome administration. The fact that the CBF decrease preceded the CO<sub>2</sub> decrease during the reaction supports our hypothesis that liposome infusion has a direct impact on cerebrovascular reactivity.

**REAL TIME MONITORING DURING HYPOXIA-ISCHEMIA IN THE NEWBORN RAT BRAIN SHOWS BILATERAL CHANGE IN MITOCHONDRIAL NADH LEVELS**Mark S. Wainwright<sup>1</sup>, Efrat Michaely<sup>2</sup>, Avraham Mayevsky<sup>2</sup><sup>1</sup>*Division of Pediatric Neurology, Northwestern University Medical School, Chicago, IL, USA*<sup>2</sup>*Leslie and Susan Gonda Brain Research Center, Faculty of Life Sciences, Bar Ilan University, Ramat Gan, Israel*

Background: Compromise of mitochondrial function is acknowledged as a pivotal step in the cellular response to acute brain injury including hypoxia-ischemia (HI) in the developing brain. Studies of changes in mitochondrial function in vivo in response to cerebral ischemia have been limited. The availability of such data would enhance our understanding of the mechanisms by which mitochondria contribute to cell injury during ischemia and would facilitate development of methods to monitor cellular injury in clinical practice. Objective: We used a well-established model of perinatal HI (unilateral carotid ligation combined with hypoxia) to determine the mitochondrial response to cerebral ischemic injury in vivo in real-time. We used multiparametric monitoring to determine changes in NADH fluorescence, cerebral blood flow (CBF) and hemoglobin (Hb) oxygenation during HI. Methods: Postnatal day (P)7 rats were anesthetized and temperature stabilized ( $36.5 \pm 0.2^\circ\text{C}$ ) under 100% oxygen. A suture was placed around the right common carotid without interrupting blood flow. Fiber optic probes were secured on the skull over the left and right hemisphere. NADH fluorescence, CBF, Hb oxygenation and temperature recording was initiated. After a 5 minute period of physiologic stabilization, rats were subject to permanent right carotid ligation by tightening the suture around the right carotid. Ligation was confirmed by a reduction in ipsilateral CBF. After a 5 minute ligation period, rats were exposed to hypoxia (10% oxygen/balance nitrogen) delivered via facemask. Two durations of hypoxia were compared, brief (15) and prolonged (40 minutes). At the conclusion of hypoxia, rats were either resuscitated using 100% oxygen or sacrificed by nitrogen anoxia. Results: In the brief hypoxia group, in the right (ischemic hemisphere) NADH (values expressed as % baseline  $\pm$  SEM; n = at least 6 for all groups) showed no significant increase ( $98.5 \pm 15$ ) during ischemia. With the addition of hypoxia, NADH increased significantly ( $118 \pm 6$ ). CBF decreased during ischemia ( $39 \pm 5$ ) and further during HI ( $7.6 \pm 3$ ). In the non-ischemic (left) hemisphere, NADH did not increase during ischemia ( $4 \pm 5$ ) or but was increased during HI ( $11 \pm 2$ ). However, CBF changes in the left hemisphere were  $88 \pm 4$  during ischemia and  $60 \pm 14$  during HI. To determine the effects of more severe insult on mitochondrial function we exposed the rats to prolonged (40 min) hypoxia after right carotid ligation. NADH increased ( $8 \pm 4$ ) during ischemia. With the addition of hypoxia, NADH increased significantly ( $20 \pm 3$ ). CBF decreased during ischemia ( $24 \pm 9$ ) and further during HI ( $5 \pm 2$ ). Recovery of CBF and NADH during resuscitation in 100% oxygen was significantly impaired in the prolonged HI group compared to brief HI. Conclusions: Mitochondrial injury can be detected in vivo in real time during HI using multiparametric monitoring. Increases in NADH are associated with a fall in CBF in both hemispheres in this unilateral HI model. This approach permits direct measurement of mitochondrial function during brain injury and in the longer-term may serve a comparable role in clinical practice for the early detection of tissue injury.

**USE OF RHEOENCEPHALOGRAPHY FOR PRIMARY STROKE PREVENTION**

**Michael Bodo**<sup>1</sup>, Gyorgy Thuroczy<sup>1</sup>, Mike Bodo, Jr.<sup>1</sup>, Tamas Nebella<sup>1</sup>, Gyula Panczel<sup>2</sup>,  
Kornel Sipos<sup>1</sup>, Peter Bonoczk<sup>1</sup>, Zoltan Nagy<sup>2</sup>, Andras Javor<sup>3</sup>

<sup>1</sup>*Kalman Santha Foundation, Budapest, Hungary*

<sup>2</sup>*National Stroke Center, Budapest, Hungary*

<sup>3</sup>*Semmelweis University Medical School, Budapest, Hungary*

Stroke is the third leading cause of death worldwide and the most frequent cause of brain damage in adults. Screening for arteriosclerosis at an early stage of disease could detect high-risk individuals and populations before the onset of stroke. Doppler ultrasound, the traditional method to detect carotid disease, is expensive and difficult to administer on a large scale. The aim of this study was to test the applicability of a computerized screening system utilizing rheoencephalography (REG) to identify individuals at high-risk for stroke. REG estimates cerebrovascular alteration caused by arteriosclerosis, expressed as the elongated rise time of the REG pulse wave. Methodology was previously published (1,2). Data were collected in a rural area (Hungary) using the computerized screening system to record risk factors for arteriosclerosis, including a history of transient ischemic attack. Carotid flow (CF) data measured by Doppler ultrasound were also collected for comparison. A cross-sectional survey was conducted for 546 people (REG, N=390; CF, N=252). Subjects' blood chemistry data and EKG were also assessed. In evaluating elasticity of brain arteries, the REG standard originally established by Jenkner was modified. A REG peak time of 180 ms or above (CF: mean velocity above 40 cm/sec) was considered a cerebrovascular alteration (3). REG and Doppler (CF) data: sclerotic brain arteries estimated by REG were 52.78% (m) and 55.8% (f). Pathologic CF was 29.41% (m) and 39.08% (f). The regression lines of age versus REG rise time and CF in male and female groups were similar, but the slope of REG was about ten times steeper than that of CF (1, 4). Brain vessel responses (CBF autoregulation) have been found to be size dependent. Previous results support the hypothesis that REG reflects CBF autoregulation (arteriolar functioning). Animal studies have shown that REG may reflect CBF autoregulation more accurately than Doppler. These results are consistent with REG literature indicating that an increase in REG rise time indicates decreased arteriolar elasticity. REG rise time may be the earliest sign of cerebrovascular sclerosis, indicating the presence of disease at an earlier stage than Doppler. The computerized system utilizing REG is simple to administer, non-invasive, cheap, and has potential as a tool for mass screenings of target populations. References 1. Bodo et al: A complex cerebrovascular screening system (Cerberus). *Medical Progress through Technology*, 21(2):53-66, 1995. 2. Kornhauser SH. Cerebrovascular diagnostic system. *American Journal of Electromedicine*, 69-71, June 1997. 3. Jenkner FL. Rheoencephalographic differentiation of vascular headaches of various causes. In: Markovich SE, (ed). *International conference on bioelectrical impedance. Annals of the New York Academy of Sciences*, 170/2: 661-65, 1970. 4. Bodo et al. Cerebrovascular aging assessment by Cerberus. In: Klatz R, Goldman R (eds): *Anti-aging medical therapeutics*, vol. II. Health Quest, Marina Del Ray, CA, 86-95, 1998.

## IMAGE ANALYSIS OF IMMUNOHISTOPATHOLOGY FROM MICRO- TO MACRO-SCALE: APPLICATION TO ISCHEMIC BRAIN TISSUE

Chunyan Wu<sup>1,2</sup>, **Weizhao Zhao**<sup>1,2</sup>, Baowan Lin<sup>1</sup>, Myron Ginsberg<sup>1</sup>

<sup>1</sup>*Department of Neurology, University of Miami School of Medicine, Miami, FL, USA*

<sup>2</sup>*Department of Biomedical Engineering, University of Miami, Coral Gable, FL, USA*

**Introduction:** Immunochemical staining techniques are commonly used to assess neuronal, astrocytic and microglial alterations in stroke research. Conventional methods of analyzing immunohistology are based on image classification techniques applied to a specific anatomic location at high magnification. Such micro-scale (x10 or above) localized image analysis limits one for further correlative studies with other imaging modalities on whole brain sections. Direct feature extraction in macro-scale (x1 or x2.5) is not feasible. This report presents a semi-automated image analysis method that performs convolution-based image classification on x4 magnification images, extracts numerical data representing positive immunoreactivity, and creates a corresponding quantitative macro-scale image. **Materials and Experimental Description:** Following 2 h middle cerebral artery occlusion (MCAo) by intraluminal suture model, rats were perfusion-fixed under halothane anesthesia following a 3-day survival period. Brain sections of 10 $\mu$ m thickness were stained by EBA, lectin, GFAP or other methods to investigate cellular alterations, and viewed by a Nikon microscope equipped with a Sony 3CCD camera. The camera was interfaced to an image analysis system, MCID-M2. Each x4 magnification view was digitized and tiled by a motor stage controlled by the MCID-M2 software in a mosaic manner to form a TIFF format file for image analysis. **Methods:** Image analysis for high magnification view is usually successful. For x4 magnification images, however, immunopositive pixels cannot be identified straightforwardly. We used several image-processing techniques to cope with variances in intensity distribution, as well as artifacts caused by light scattering or heterogeneity of antigen expression. Image classification was obtained by convolving the K-means clustering kernel over the tiled images. We then performed a morphological noise removal process (for single pixels or small area), called image closing. Following this process, another morphological filtering process, called image opening, was performed to filter unwanted target (large objects). In the last step of process, quantitative information was extracted and converted to a macro-scale image. Quantitative information includes the number of positively stained cells, number of positively stained vessels, or percentage area occupied by positively stained objects. This process is different from the "zoom out" function, which shows only averaged optical density of the corresponding pixel array in the micro-scale image, because it converts immunopositive objects within the corresponding window into numerical data; thus, the pixel intensity indeed represents a particular feature quantitatively. **Results:** We applied the convolution-based K-means clustering method to the x4 images. The result was compared with that obtained from the x10 images by the conventional methods. For five areas covering the injured hemisphere, the conventional method estimated 1.37 $\pm$ 0.22% immunopositive area in the corresponding hemisphere, and the designed method estimated 1.44 $\pm$ 0.17%, both under anti-EBA staining; there was no significant difference between the two methods ( $p < 0.05$  ANOVA). **Conclusion:** The result confirms that the convolution-based K-means clustering approach can be reliably applied to relatively low magnification images with considerable improvement in computational efficiency (compared to x10 images, 6.25-times processing time saved by using x4). The resultant quantitative macro-scale images can be correlated to other imaging modalities. Grant support: NIH NS05820 (M.D.G.) and NSF DUE-0127290 (W.Z.)

**ALTERATION OF OXYGEN METABOLISM IN MCA OCCULSION RAT MODEL BY POSITRON EMISSION TOMOGRAPHY WITH INJECTABLE O-15-OXYGEN**

Yasuhiro Magata<sup>1</sup>, Takashi Temma<sup>2</sup>, Mikako Ogawa<sup>1</sup>, Takahiro Mukai<sup>3</sup>,  
Hidekazu Kawashima<sup>3</sup>, Yuji Kuge<sup>2</sup>, Hiroshi Watabe<sup>4</sup>, Hidehiro Iida<sup>4</sup>, Hideo Saji<sup>2</sup>

<sup>1</sup>*Laboratory of Genome Bio-Photonics, Photon Medical Research Center, Hamamatsu University School of Medicine, Hamamatsu, Japan*

<sup>2</sup>*Department of Patho-Functional Bioanalysis, Graduate School of Pharmaceutical Sciences, Kyoto University, Kyoto, Japan*

<sup>3</sup>*Department of Nuclear Medicine and Diagnostic Imaging, Graduate School of Medicine, Kyoto University, Kyoto, Japan*

<sup>4</sup>*Department of Investigative Radiology, National Cardiovascular Center Research Institute, Suita, Japan*

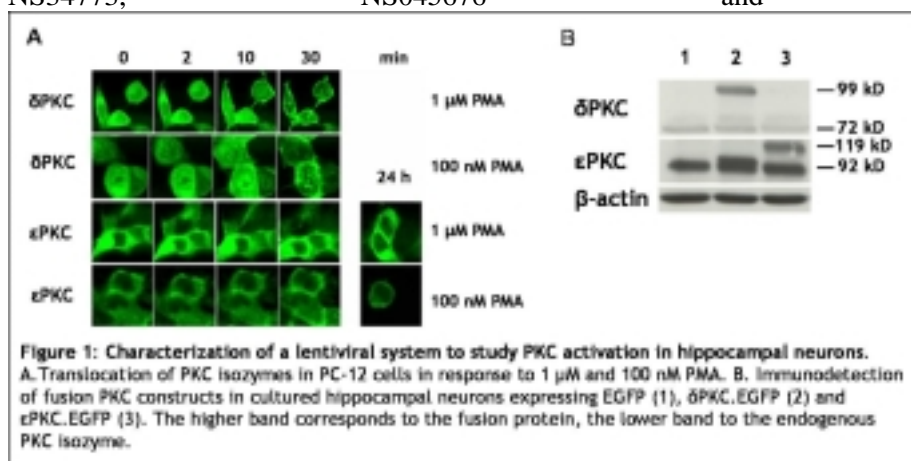
**Background and Purpose:** Stroke is one of major cause of death all over the world. Recently, local fibrinolytic treatment of brain embolism with t-PA is effective during a few hours after the onset with the infarction tissue alive. Although the threshold of cerebral blood flow (CBF) for tissue viability which closely related to treatment efficiency is reported to be 35 % in comparison with the normal CBF value, the parameters related to oxygen metabolism can directly define the pathological condition of the lesion in vivo. Furthermore, experiments using small animal models are valuable to explore pathological alterations of the lesion and estimate novel therapeutic methods. A permanent ischemia rat model is usually applied for this purpose although the alteration of oxygen metabolism after the onset is not clear. We have previously reported a new imaging tool, injectable O-15-oxygen, to estimate oxygen metabolism in a small animals. On these bases, alteration of oxygen metabolism after the onset of brain infarction was evaluated using injectable O-15-oxygen to characterize the MCA occlusion rat model in this paper. **Methods:** Male Sprague-Dawley rats (250 to 310 g) were used for this study. The right middle cerebral artery (MCA) was occluded intraluminally using a nylon monofilament under the anesthesia. Rats were divided into two groups; 1 hour or 24 hours after the operation, two serial PET scans (SHR-7700L, Hamamatsu Photonics, Hamamatsu, Japan) were performed using O-15-water (for estimation of CBF) and radiolabelled O-15-oxygen blood (injectable O-15-oxygen)1). Each PET scan consisted of 12 x 10 second with arterial blood sampling. Each parameter was calculated on each hemisphere of successive four slices. **Results:** At 1 hour in the right hemisphere, CBF decrease (ratio of right to left hemisphere:  $0.65 \pm 0.17$ ) and compensatory increase of oxygen extraction fraction (OEF) ( $1.17 \pm 0.22$ ) were observed, leading to light decrease of cerebral metabolic rate for oxygen (CMRO2) ( $0.74 \pm 0.15$ ). At 24 hours, marked CBF decrease ( $0.53 \pm 0.17$ ) and loss of compensatory OEF mechanism resulted in serious decrease of CMRO2 ( $0.48 \pm 0.17$ ). **Conclusion:** Compensatory mechanism of oxygen metabolism was observed 1 hour after the onset of MCA occlusion while lost at 24 hours. It meant the progression of the pathological condition during 24 hours and these changes in small animals could be detected using injectable O-15-oxygen and PET. Therefore, injectable O-15-oxygen can be used for the evaluation of new therapeutic methods to improve the brain infarction in the functional point of view. **References:** 1. Y. Magata et al. J Cereb Blood Flow Metab 2003; 23:671.

## A LENTIVIRUS-BASED MODEL TO STUDY THE SELECTIVE ACTIVATION OF DELTA AND EPSILON PKC DURING ISCHEMIA AND ISCHEMIC PRECONDITIONING

Jesus Purroy, Ami Raval, Eun Joo Kim, Miguel A. Perez-Pinzon

*Cerebral Vascular Disease Research Center, Department of Neurology and Neuroscience,  
University of Miami Miller School of Medicine, Miami, FL, USA*

Ischemic preconditioning (IPC) is a phenomenon by which a tissue suffering a sublethal ischemic episode develops tolerance against a subsequent ischemic event. A number of signaling pathways have been demonstrated in ischemic preconditioning, including protein kinase C epsilon (ePKC), Erk 1/2 and NFkB. In contrast, PKC delta (dPKC) promotes apoptosis after cerebral ischemia. The goal of the present study was to develop a lentiviral-based model to study selective activation of either dPKC or ePKC under conditions similar to IPC or ischemia. Methods: To study how ePKC promotes ischemic tolerance and how dPKC promotes cell death, we have developed a lentivirus-based model. Rat dPKC and ePKC cDNA was cloned in frame with EGFP in a three plasmid lentiviral system developed by Naldini (Science, 272:263, 1996). PC-12 cells and hippocampal neurons were superfused with viral solution (MOI ~100). Slices were injected with 10,000 transducing units of lentivirus using a picospritzer (General Valve). One week later fluorescence was determined by using a two-photon laser scanning microscope (Olympus BX51WI) analyzed with LaserSharp2000 (BioRad). Results: We report here that we were able to express rat dPKC and ePKC tagged with EGFP in rat cultured hippocampal neurons and organotypic hippocampal slices using a lentiviral vector. Significant fluorescence can be observed in infected neurons. Significant translocation of dPKC and ePKC was achieved with the general PKC activator phorbol myristate acetate (PMA) in PC-12 cells. 1  $\mu$ M PMA induced translocation of dPKC to the plasma membrane within 10-30 minutes, but not of ePKC even after 24 h (Figure 1A). At low PMA concentrations (100 nM) ePKC translocates to the membrane after 24 h. We detected both the native and the fusion isozymes by Western blot on protein extracted from cultured hippocampal neurons (Figure 1B). Conclusions: These findings suggest a difference in substrate affinities between both PKC isozymes and may explain why one translocates after IPC (ePKC) and the other after ischemia (dPKC). Grant support: Supported by PHS grants NS34773, NS045676 and NS05820.



## CHANGES IN CEREBRAL BLOOD FLOW MODALITIES DURING HEMORRHAGE IN RATS

Michael Bodo<sup>1</sup>, Frederick Pearce<sup>1</sup>, Lajos Baranyi<sup>1</sup>, Rocco Armonda<sup>2</sup>

<sup>1</sup>*Department of Resuscitative Medicine, Department of Membrane Biochemistry, Reed Army Institute of Research, Silver Spring, MD, USA*

<sup>2</sup>*Division of Neurosurgery, National Capital Consortium, Section of Cerebrovascular Surgery and Interventional Neuroradiology, Walter Reed Army Medical Center, Washington D.C., USA*

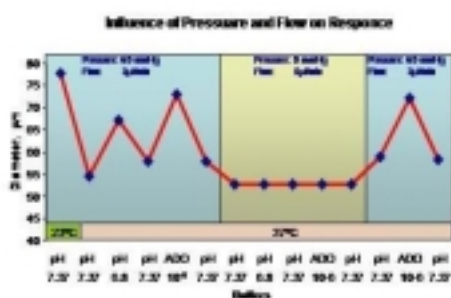
The optimal life sign monitor in the practice of emergency medicine would be a technique to detect the earliest pathological change. Since the brain is the most sensitive organ in response to hypoxia/ischemia, "cardio-pulmonary resuscitation should be brain-oriented" (Peter Safar, 1998). Nevertheless, monitoring of cerebral blood flow (CBF) is not performed in the practice of emergency medicine in either civilian or military environments. CBF reactivity monitoring is an appropriate primary parameter to evaluate cerebral resuscitation due to a systemic or regional cerebral injury leading to possible irreversible brain injury. Unlike CBF monitoring this technique of CBF reactivity is being proposed as a non-invasive, mobile, and non-operator dependant means of evaluating an unconscious patient. The ideal life sign monitor would be one that reflects CBF non-invasively, continuously and globally. Because the most common cause of death following serious military and civilian injuries is hemorrhage, the goal of this study was to describe CBF changes during hemorrhage and to compare various CBF modalities in order to identify the optimal CBF vital sign monitor. A computer controlled rat hemorrhage model was introduced for resuscitation purposes. In anesthetized rats blood was removed at a rate required to achieve a mean arterial blood pressure (MABP) of 40 mmHg over 15 min. Shed blood was measured and used as an indicator of compensation/decompensation phase. Continuous recording was taken during 30 minutes of compensatory phase with intracranial rheoencephalogram – (iREG; n = 14), laser Doppler flowmetry (LDF; n = 3), and carotid flow by ultrasound (n = 11). Data were stored and processed off-line. During the initial phase of hemorrhage, when MABP was close to 40 mmHg, intracranial REG amplitude transiently increased (81 %), while LDF (78 %) and carotid flow (52 %) decreased and changed with systemic arterial pressure. Intracranial REG amplitude change suggests classical CBF autoregulation, indicating its close relationship to arteriolar changes (1). The studies indicated that 1) iREG may reflect cerebrovascular responses more accurately than changes in local CBF measured by LDF and carotid flow; CBF autoregulation was present at the beginning of SAP 40 mmHg. The physiological background or resolution of this virtual conflict is: "Flow through large arteries may be constant despite changes of regional flow in tissue" (2) REG may indicate promise as a continuous, non-invasive life sign monitoring tool with potential advantages over EKG, ultrasound, and other measurement techniques normally applied in clinical practice. Additional quantitative studies are in progress; the following studies are needed: 1) to test CBF autoregulation during the entire period of hemorrhage (with CO<sub>2</sub> inhalation); 2) to estimate REG during graded increases in intracranial pressure; 3) to estimate REG during graded decreases in SAP; and 4) to test various data processing methods of the REG signal. Reference (1) Kontos H A et al 1978 Responses of cerebral arteries and arterioles to acute hypotension and hypertension. *Am. J. Physiol. Heart Circ. Physiol.* 34 H371-83 (2) Reivich M, Waltz A G 1980 Circulation and metabolic factors in cerebrovascular disease. In: *Cerebrovascular survey report*, NIH, Bethesda, MD.

## REACTIVITY OF NON-PRESSURIZED, NON -PERFUSED CEREBRAL ARTERIOLES

Leonid Groysman, Greg Miekisiak, Alexander Beylin, David Kung, **H. Richard Winn**

*Neurosurgery, Mount Sinai Medical Center, New York, NY, USA*

**OBJECTIVE:** There has been a series of recent publications using in vitro hippocampal and cortical slices which document changes in cerebral arterioles during neuronal activation. These in vitro vessels studied in slices are non-pressurized and non-perfused. Thus, the appropriateness of extrapolation to the in vivo vascular responses is unclear. The vascular response of isolated pressurized, perfused in vitro cerebral arterioles have been well characterized. In contrast, the responses in non-pressurized, non perfused cerebral arterioles remains to be determined. Consequently, the goal of the following experiments was to study the arteriolar response in non-pressurized, non-perfused cerebral vessels. **METHODS:** Penetrating intracerebral arterioles from adult male Sprague-Dawley rats were dissected at 4°C and transferred to a temperature controlled bath mounted on inverted microscope. The bath temperature was raised to 37°C and maintained at a constant flow of buffered saline 1 ml per minute. The vessel reactivity was assessed by applying adenosine (ADO) extraluminally at concentration 10E-6 M in buffered saline and by changing the pH of the buffered saline from pH 6.8 and 7.6. For comparison, we also determined the responses in pressurized, perfused penetrating arterioles. **RESULTS:** We observed minimum or inconsistent reactivity in non-pressurized vessels. There was no significant changes in vessel diameter with warming the bath (from 22°C to 37°C), after application of adenosine at concentration 10E-6M or in response to pH changes. In contrast, in pressurized (60 mm Hg), perfused (2-4 uL) arterioles, we observed vasoconstriction after increase in bath temperature from 22 C to 37 C, vasodilatation in response to adenosine application, and appropriate response to change of the pH of the bath: constriction with raising the pH from 7.37 to 7.6. and vasodilatation from 7.37 to 6.8. **CONCLUSIONS:** These results signify the importance of intraluminal pressure and flow for preservation of physiological reactivity of penetrating cerebral arterioles. We therefore urge caution in extrapolating physiologic significance of responses observed in non-pressurized, non-perfused arterioles in hippocampal and cortical slices.



## ADIABATIC $T_{1\rho}$ CONTRAST GENERATED IN HUMAN BRAIN 4T IMAGES

Shalom Michaeli<sup>1</sup>, Dennis Sorce<sup>1</sup>, Charles Springer<sup>2</sup>, Kamil Ugurbil<sup>1</sup>, Michael Garwood<sup>1</sup>

<sup>1</sup>CMRR and Department of Radiology, University of Minnesota Medical School, Minneapolis, MN, USA

<sup>2</sup>Advanced Imaging Research Center, Oregon Health & Science University, Portland, OR, USA

**Synopsis** Dipolar interaction is the dominant relaxation mechanism affecting  $T_{1\rho}$  in tissue during a train of adiabatic full passage pulses placed prior to the excitation pulse. We demonstrate that  $T_{1\rho}$  relaxation depends significantly on the modulation functions for the adiabatic pulses. This dependence leads to a novel MRI  $^1\text{H}_2\text{O}$  contrast in human brain images.

**Introduction** Here we investigate adiabatic  $T_{1\rho}$  contrast, which is generated by placing a train of AFP pulses prior to the AHP excitation pulse with no interpulse intervals. We show that exchange-induced  $T_{1\rho}(T_{1\rho\text{ex}})$  and the contribution of dipolar interactions depend on the adiabatic pulse modulation functions used. This was utilized to modulate  $^1\text{H}_2\text{O}$   $T_{1\rho}$  contrast in images of the human occipital lobe at 4T. It was shown that the dynamic averaging (DA), e.g., equilibrium chemical exchange (CE) and diffusion in locally different magnetic susceptibilities, contribution to the  $^1\text{H}_2\text{O}$   $R_{1\rho}$  relaxation rate constants in human brain tissue is small. Adiabatic  $T_{1\rho}$  contrast provides a possibility to directly assess self-relaxations and cross-relaxations in living tissue and to estimate the order parameter of the interactions.

**Methods** Imaging studies were conducted with a 4T whole body MRI/MRS system. AFP pulses of the hyperbolic secant family, HS1 and HS4, were inserted prior to the AHP of the sequence.  $T_{1\rho}$  images were acquired incrementing the number of AFP pulses (pulse length 3 ms,  $\omega_1^{\text{max}}=2.5$  kHz). Spiral readout ( $0.7 \times 0.7$  mm<sup>2</sup> in-plane resolution, FOV = 18 cm, 256-matrix and 8 segments, at = 35 ms, thickness 3 mm) was used for the acquisition.

**Results and discussion**  $^1\text{H}_2\text{O}$  NMR relaxation in tissue arises from complicated molecular mechanisms that include equilibrium water exchange and magnetic interactions between the protons of different molecular constituents in several tissue compartments. To simulate this, we use a simple, two-site model that represents two water populations. These two reservoirs are coupled by the two-site exchange (2SX) mechanism. In our interpretation three major issues are considered: 1) the orientational order of  $^1\text{H}$  dipolar interactions and its contribution to the relaxation dispersion; 2) the effect of dipolar relaxations of water protons and macromolecular protons; 3) 2SX between two water populations.  $T_{1\rho}$  relaxation is significantly affected by the adiabatic pulse modulation functions used. In this study, the ratio  $T_{1\rho}(\text{HS1})_{m-90^\circ} / T_{1\rho}(\text{HS4})_{m-90^\circ} \approx 2$  was obtained (5 individuals). Our analysis suggested that the contribution to  $T_{1\rho}$  relaxation due to CE in human brain is small. This in turn implies that dipolar relaxations dominate under these experimental conditions. In this work, the formalism for the three-spin system dipolar relaxations was implemented for the HS1 and HS4 pulses, and the auto-relaxation and cross-relaxation relaxation pathways were investigated [3].

**References** [1] Michaeli S, Sorce DJ, Idiyatullin D, Ugurbil K, Garwood M. *J Magn Reson* 169:293-299 (2004); [2] Michaeli S, Grohn H, Grohn O, Sorce DJ, Kauppinen R, Springer C, Ugurbil K, Garwood M. accepted for *Magn Reson Med* (2004); [3] Burghardt I, Konrat R, Bodenhausen G *Mol Phys*, 75, 467-486 (1992).

**Acknowledgment** This work was supported by NIH grants CA92004, RR08079, NS40801, and EB00422, the Keck Foundation, and the Mind Institute.

## LOSS OF DISTENSIBILITY IN CEREBRAL ARTERIES WITH CHRONIC HYPERTENSION AND VASOSPASM AFTER SUBARACHNOID HEMORRHAGE

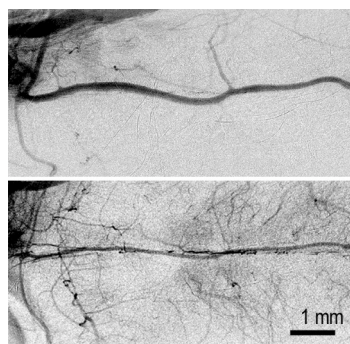
Takeshi Kondoh<sup>1</sup>, Seiji Nakajima<sup>1</sup>, Akitsugu Morishita<sup>1</sup>, Haruo Yamashita<sup>1</sup>, Eiji Kohmura<sup>1</sup>, Takashi Sakurai<sup>2</sup>, Kohichi Yokono<sup>2</sup>, Keiji Umetani<sup>3</sup>

<sup>1</sup>*Department of Neurosurgery, Graduate School of Medicine, Kobe University Department of Neurosurgery and Internal and Geriatric Medicine, Graduate School of Medicine, Kobe University, Kobe, Japan*

<sup>2</sup>*Department of Internal and Geriatric Medicine, Graduate School of Medicine, Kobe University, Kobe, Japan*

<sup>3</sup>*Japan Synchrotron Radiation Research Institute, Hyogo, Japan*

**Introduction:** Rat subarachnoid hemorrhage (SAH) model has been widely used recently but its angiographical assessment is difficult due to small size of the animals to maintain physiological parameters and due to the small size of arterial lumen for angiographic measurement. We developed a microangiography system using monochromatic synchrotron radiation X-rays at SPring-8, a third generation synchrotron radiation facility. In Brain03 meeting we have reported autoregulatory changed of small arteries under hypercapnia and hypotension. In this study, we assessed the distensibility of major trunk arteries after subarachnoid hemorrhage in normotensive and hypertensive rats. **Methods:** Twenty adult Wistar Kyoto rats (WKY) and 13 stroke prone spontaneously hypertensive rats (SHR-SP) were prepared SAH by double hemorrhage injection method into cisterna magna or sham operation as control. Microrangiography was performed on day 7 by retrograde injection of 0.2 ml contrast media via external carotid artery for imaging of internal carotid artery and 0.4 ml for basilar artery. Angiography was repeated 4 times in each rat before and after loading of hypercapnia at 100-120 mmHg of PaCO<sub>2</sub>. The diameters of major trunk vessels were assessed. Histological observation of artery lumen and wall were also performed. **Results:** Angiographical vasospasm was demonstrated in basilar artery in WKY with 68 % of diameter of control. In ICA and other major trunk in WKY and all the arteries in SHR-SP did not demonstrate vasospasm. Hypercapnia induced loss of distensibility in BA of WKY. In SHR-SP, this distensibility was impaired regardless hemorrhage. Histological study demonstrated basilar artery in WKY thickened at 179 % after SAH and became similar to non-hemorrhagic SHR-SP. ICA in WKY and both BA and ICA in SHR-SP were unchanged in wall thickness before and after SAH. **Conclusions:** High quality angiography demonstrated deteriorated distensibility of spastic artery only in basilar artery of normotensive rats, which was well-correlated to histological change of arterial wall. Preexisting pathological deterioration in artery of SHR-SP might lead less affected spastic change after SAH. **Figure** Spastic basilar artery in SHR-SP with SAH before (upper) and after (lower) hypercapnia. **Reference** [1]Kondoh T, Sakurai T, Ikeda M, et al.; J Cereb Blood Flow Metab 23(suppl): 185 (2003)



## SYNCHROTRON RADIATION X-RAYS DEMONSTRATE SMALL CEREBRAL VESSELS IN NORMAL MOUSE AND VARIATIONS UNDER ISCHEMIA IN RAT

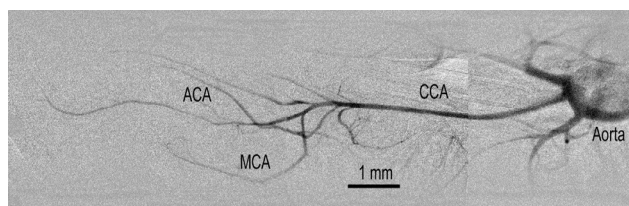
Masahiro Tamaki<sup>1</sup>, **Takashi Mizobe**<sup>1</sup>, Keiji Kidoguchi<sup>1</sup>, Junnji Koyama<sup>1</sup>, Takeshi Kondoh<sup>1</sup>, Haruo Yamashita<sup>1</sup>, Takashi Sakurai<sup>2</sup>, Kohichi Yokono<sup>2</sup>, Keiji Umetani<sup>3</sup>

<sup>1</sup>*Department of Neurosurgery, Graduate School of Medicine, Kobe University Department of Neurosurgery and Internal and Geriatric Medicine, Graduate School of Medicine, Kobe University, Kobe, Japan*

<sup>2</sup>*Department of Internal and Geriatric Medicine, Graduate School of Medicine, Kobe University, Kobe, Japan*

<sup>3</sup>*Japan Synchrotron Radiation Research Institute, Hyogo, Japan*

**Introduction** Cerebral ischemic rodent models in mouse and rat are widely used in experimental study but their anatomy of arteries before and after ischemic event are rarely demonstrated. With a microangiography system using monochromatic synchrotron radiation X-rays at SPring-8, a third generation synchrotron radiation facility, we studied two experimental ischemic models; MCA occlusion model rat (permanent focal ischemia) and bilateral ICA occlusion model (chronic forebrain ischemia). We also studied cerebral angiography in mouse in which only the high-spatial-resolution imaging with SPring-8 can demonstrate small vessels. **Methods** Microangiography was performed by retrograde injection of 0.2 ml contrast media via external carotid artery for imaging of internal carotid artery and 0.4 ml for basilar artery. In MCA occlusion model, microclip was applied on MCA by craniectomy and angiography was performed 3 hours after initiation of ischemia (acute), 24, 48 and 72 hours after ischemia induction (n=5). Angiography was repeated in each animal after induction of hypercapnia with arterial blood CO<sub>2</sub> at 110-120 mmHg. The diameters of major trunk vessels were then assessed. In forebrain ischemic model, one month after bilateral ICA ligation, angiography of vertebral artery and basilar artery was performed (n=12) and compared with acute occlusion (n=3). In normal mouse, microtube was placed in neck ECA and various volume of contrast medium was injected into ICA. **Results** In MCA occlusion model, occlusion points were identified in all rats but variation of development of MCA branches and collateral vessels were demonstrated. Under hypercapnia, distension of ICA was observed in acute and 72 hours after ischemia but distensibility was low in 24 and 48 hours. In bilateral ICA occlusion, dilated ACA and MCA were observed in which contrast medium was filled via well-developed Pcom. In acute ICA occlusion, supratentorial arteries were not demonstrated. In normal mouse, 50ul of 50 % diluted contrast medium was found to be the best condition to demonstrated ICA, MCA and ACA. The diameter of these major trunks were less than 100 um. **Conclusions** Experimental ischemic model in rats had different distensibility depending on the time after the onset of ischemia that was associated with development collateral vessels. To study acute therapeutic approach such as thrombolysis by tPA using rat experimental model, angiographical evaluation should be considered to reveal the exact mechanism and effective time point of the agents. We also showed feasibility of cerebral angiography in mouse. Using synchrotron radiation X-rays, repeat examination can be achieved and this allows us to study further of cerebral vessels using transgenic mouse.



**A NOVEL IN VITRO MODEL TO STUDY THE EARLY STAGES OF TRANSIENT MCA ISCHEMIA/REPERFUSION: THE ISOLATED GUINEA PIG BRAIN**

**Marco de Curtis**, Pastori Chiara, Librizzi Laura, Regondi Cristina, Bruzzone Maria Grazia

*Department of Experimental Neurophysiology, Istituto Nazionale Neurologico, Milan, Italy*

The events that characterize the early phases of focal cerebral ischemia are difficult to analyze because of the experimental restrictions imposed by the available animal models. We developed a new model of transient ischemia and reperfusion in the isolated guinea pig brain maintained in vitro by arterial perfusion. In this preparation the neuronal and the vascular compartments are structurally and functionally preserved and interact in a close-to-in vivo condition (de Curtis et al, 1991 *Hippocampus* 1; 341; Muhlethaler, de Curtis et al, 1993 *Eur J Neurosci* 5:915; de Curtis et al, 1998 *Brain Res Protoc* 3:221). The isolated guinea pig brain preparation is maintained in vitro with the ventral surface exposed and is perfused through the arterial system via the basilar artery in an open incubation chamber. The Willis circle in this preparation is under direct visual control with a stereomicroscope. To analyze the early events during transient ischemia, we ligated for 30 minutes the medial cerebral artery (MCA) with a silk string. The MCA territory was re-perfused for 3-4 hours after transient occlusion. Before, during and after MCA ligation, field potential electrophysiological recordings were performed in different cortical areas involved and spared by the ischemia. The changes in amplitude of the responses and the presence of spreading depression events were evaluated during occlusion and reperfusion. At the end of the experiment, that lasted 5-6 hours in vitro, brains were fixed with 4% paraaldehyde to evaluate the ischemic area. Magnetic resonance scans were performed in the isolated brains to evidence the ischemic lesion. Brain was then cut in coronal 50  $\mu\text{m}$  section and immunohistochemistry with antibodies against the neuronal cytoskeletal protein MAP-2 was performed. A good correlation between the MR images and the area identified by immunohistochemistry was observed. The present report describes a new model of transient ischemia and reperfusion developed in the isolated guinea pig brain preparation, that could be utilized to study the early-stage events that occur during the ischemic process.

## TOWARDS A ROUTINE ANALYSIS OF ANATOMICAL AND FUNCTIONAL POST MORTEM SLICES IN 3 DIMENSIONS

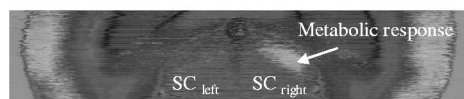
Julien Dauguet<sup>1,2</sup>, Albertine Dubois<sup>1</sup>, Anne-Sophie Hérard<sup>3</sup>, Laurent Besret<sup>3</sup>,  
Gilles Bonvento<sup>3</sup>, Philippe Hantraye<sup>1,3</sup>, **Thierry Delzescaux**<sup>1</sup>

<sup>1</sup>*Service Hospitalier Frédéric Joliot, CEA, Orsay, France*

<sup>2</sup>*Epidaure Project, INRIA Sophia Antipolis, France*

<sup>3</sup>*URA CEA-CNRS 2210, Orsay, France*

Purposes: Post mortem imaging provides both anatomical and functional information at microscopic resolution and can be considered as a gold standard for macroscopic *in vivo* studies. We propose a generic, robust and automated protocol integrated in a graphic interface to digitalize, reconstruct and analyze functional volumes of rodent brain based on coronal post mortem slices. The first application of this work concerns the 3D analysis of an activation study on a group of rats to investigate the metabolic response to visual stimulation in superior colliculus (SC). Methods: After injection of [14C]2-deoxyglucose, adult Long Evans rats (n=5) were visually stimulated during 45 minutes with a moving checkerboard displayed on a computer screen with left eye opened (activated SC<sub>right</sub>) and right eye masked (non activated SC<sub>left</sub>). After sacrifice, cryostat sections (20  $\mu$ m thickness) were obtained in coronal incidence for the whole SC (about 150 sections), exposed to generate autoradiographic information and converted to Cerebral Metabolic Rate of Glucose (CMRGlu). The same sections were then stained with histological dye. An optimized digitalization (600 dpi resolution) was proposed by simultaneously acquiring group of slices at the same time. The individualization of each slice from these global scans was then realized using a dedicated method. A slice to slice registration based on the block-matching method was then performed for the anatomical series leading to a consistent 3D anatomical volume. The autoradiographic volume was then reconstructed by directly matching 2D functional slices with their corresponding registered anatomical slices. A manual segmentation of SC was realized and used to calculate the mean activity  $m$  and the standard deviation  $s$  in non activated SC<sub>left</sub>. The maximal CMRGlu sub-region was automatically outlined in the SC<sub>right</sub> using  $m+2s$  threshold. An automated symmetrization of this sub-region in the SC<sub>left</sub> was computed and an increased metabolic percentage was calculated for each rat. Results: The part of the rat brain including the whole SC was automatically reconstructed for anatomical and functional data of all rats. Mean volumes calculated were respectively  $3.71 \pm 0.34 \text{ mm}^3$  for SC<sub>right</sub>,  $3.61 \pm 0.35 \text{ mm}^3$  for SC<sub>left</sub> and  $0.38 \pm 0.18 \text{ mm}^3$  for the sub-region of maximal metabolic response (about 10% of SC<sub>right</sub> volume). The location of the activity in SC<sub>right</sub> was consistent for the five rats. Increased metabolic response was estimated to  $26 \pm 6\%$ . Conclusion: 3D morphological and functional parameters of interest (location, volume, CMRGlu) have been derived from histological slices. This study demonstrated 1) the feasibility of this automated procedure to analyze group of animals and 2) the possibility to perform 3D quantitation with a high reproducibility. In the future, this method will allow merging post mortem and *in vivo* (microPET) information.



Fusion of anatomical and functional reconstructed volumes in axial incidence



Axial 3D view of SC: 1) sub-region of maximal CMRGlu automatically extracted, 2) symmetrized sub-region

### VARIABILITY OF SF-36 SCORES WITHIN GOSE CATEGORIES

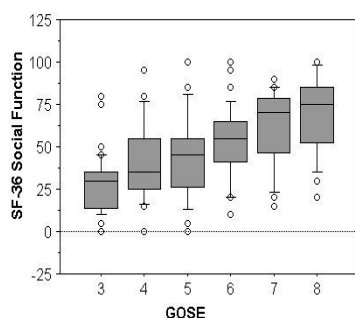
Joanne G. Outtrim<sup>1</sup>, Doris A. Chatfield<sup>1</sup>, Christine Conway-Smith<sup>2</sup>, Edna Shephard<sup>2</sup>,  
 Laura Moore<sup>2</sup>, Peter J. Hutchinson<sup>3</sup>, John D. Pickard<sup>3</sup>, David K. Menon<sup>1</sup>

<sup>1</sup>*Department of Anaesthesia, Addenbrooke's Hospital, Cambridge, UK*

<sup>2</sup>*Neurosciences Critical Care Unit, Addenbrooke's Hospital, Cambridge, UK*

<sup>3</sup>*Department of Neurosurgery, Addenbrooke's Hospital, Cambridge, UK*

Measuring the outcomes of patients following head injury is important for research studies<sup>1</sup>, clinical audit<sup>2</sup> and assessing rehabilitation requirements in individual patients. The tools that are used to quantify such outcome must be appropriate for the intended purpose. The Glasgow Outcome Score (GOS)<sup>3</sup> and, more recently, the extended Glasgow Outcome Score (GOSE)<sup>4</sup> have been used in clinical trials and audit studies to define outcomes in patient groups. However, these scores are sometimes used to characterise outcomes in individual patients. This is inappropriate, since functional outcomes in individual patients may be poorly described by these scoring tools. We have sought to address this issue by comparing GOS and GOSE against the Short Form-36 health survey (SF-36)<sup>5</sup>, a patient-reported score of health-related quality of life in a large cohort of patients surviving head injury. Outcome measurements were collected on 227 patients with head injury admitted to the regional neurosurgical intensive care unit. Participants were aged between 16 and 86 (median 31) with median (range) post resuscitation GCS of 7 (3-15). Twenty-two patients had mild, 53 moderate, and 152 severe head injury. Data obtained included the GOS, GOSE and the UK version of the SF-36. Forms were sent by post approximately 6 months post injury, and were completed by the patients (with the help of a family member or partner, if required). SF-36 scores in different measurement domains were plotted against the GOSE and relationships assessed using non-parametric statistical methods. We found a highly significant correlation between the GOSE and scores in individual SF-36 domains ( $p < 0.0001$  for all comparisons), with Spearman Rank rho values between 0.47 and 0.68. However, we found large variations in the spread of SF-36 values within each GOSE category, with the largest interquartile ranges observed in the domains of Emotional Role and Social Function (Fig). The GOS and GOSE are extremely useful measures of outcome in groups of patients following head injury, and have proved valuable in the conduct of clinical trials and audit of clinical outcomes as a means of quality assurance. However, our data underline the pitfalls of using these scoring systems as descriptors of functional outcome and quality of life in individual subjects. A better understanding of the causes of intra-category variability in SF-36 scores might provide one means of devising new outcome scoring systems that improve on the GOSE. The failure of experimentally successful neuroprotective interventions in clinical trials has, in some part, been attributed to the lack of sensitivity of outcome assessment.<sup>6</sup> Such improved scoring systems may go some way towards addressing this issue. 1. Clifton GL et al. *J Neurotrauma* 2002;19:293-301 2. Patel et al. *Intensive Care Med* 2002; 28:547-53. 3. Jennett B, Bond M. *Lancet* 1975; 1:480-4. 4. Wilson et al. *J Neurotrauma* 1998; 15: 573-85. 5. Jenkinson C, Wright L. *Auditorium* 1993; 2: 7-12. 6. Narayan et al. *J Neurotrauma* 2002; 19: 503-57.



## THE RELATIONSHIP BETWEEN BRAIN TISSUE OXYGEN PARTIAL PRESSURE THRESHOLDS AND MICRODIALYSIS MARKERS OF ISCHAEMIA IN TRAUMATIC BRAIN INJURY

Jurgens Nortje<sup>1,3,4</sup>, Peter J. Hutchinson<sup>2,3,4</sup>, David A. Zygun<sup>1,4</sup>, Pippa G. Al-Rawi<sup>2,3</sup>, Mark T. O'Connell<sup>2,3</sup>, David K. Menon<sup>1,3,4</sup>, Arun K. Gupta<sup>1,4</sup>

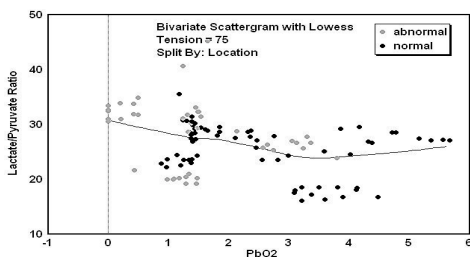
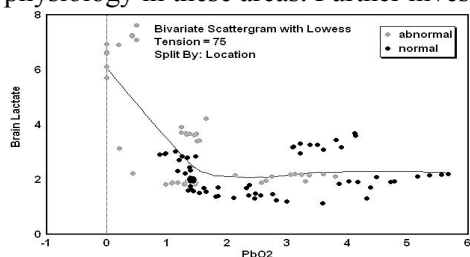
<sup>1</sup>Department of Anaesthesia, University of Cambridge, Addenbrooke's Hospital, Cambridge, UK

<sup>2</sup>Department of Neurosurgery, University of Cambridge, Addenbrookes Hospital, Cambridge, UK

<sup>3</sup>Wolfson Brain Imaging Centre, University of Cambridge, Addenbrookes Hospital, Cambridge, UK

<sup>4</sup>Neurosciences Critical Care Unit, Addenbrookes Hospital, Cambridge, UK

While cerebral ischaemia contributes significantly to secondary brain injury following trauma, there are no data on critical thresholds of brain tissue pO<sub>2</sub> (PbO<sub>2</sub>) for metabolic compromise. The aim of this study was to identify ischaemic thresholds for changes in brain tissue lactate concentrations and lactate/pyruvate ratio. Eleven patients with severe traumatic brain injury, with brain tissue oxygen tension (Neurotrend™) and microdialysis monitoring in place, were studied within the first 4 days following injury, over 4 hour epochs during which physiology was carefully monitored and stabilised as part of a protocol involving transfusion of red cells. All patients were managed according to the Addenbrooke's Hospital Neuro-critical Care Unit head injury algorithm. Data for brain PbO<sub>2</sub>, and microdialysate glucose, lactate and pyruvate were measured over 20-minute intervals. Relationships between PbO<sub>2</sub> and brain lactate level as well as lactate/pyruvate ratio were examined, and the significance of relationships assessed using non-parametric statistical methods. The eleven patients had a mean age of 34 years (range: 17 – 64), a median post-resuscitation GCS of 9 (range: 4 – 13) and 55% were female. Seven patients had the monitors placed in structurally normal-appearing tissue on CT scan, while in four patients the monitors were in abnormal tissue. Pooled mean ( $\pm$  standard deviation) PbO<sub>2</sub> was  $2.15 \pm 1.3$  kPa, lactate  $2.77 \pm 1.58$  mmol/l, pyruvate  $105 \pm 52$   $\mu$ mol/l, and L/P ratio  $26.6 \pm 5.4$ . There were no significant differences between normal and abnormal tissue, but PbO<sub>2</sub> was less than 1 kPa only in abnormal tissue. Fitting with a Lowess function appeared to show an inflection point for increases in lactate at PbO<sub>2</sub> below  $\sim 1.5$  kPa (Fig; Spearman-Rank  $\rho$ : - 0.347,  $p < 0.001$ ). While the relationship between PbO<sub>2</sub> and L/P ratio was also statistically significant (Spearman-Rank  $\rho$ : - 0.358,  $p < 0.001$ ), clear PbO<sub>2</sub> threshold levels were less well defined. Brain tissue oxygen displays a threshold at about 1.5 kPa below which brain lactate increases in abnormal tissue. The absence of clear increases in L/P ratio below this threshold raises the possibility that brain lactate elevation in these areas may not entirely be due to tissue hypoxia. As PbO<sub>2</sub> in normal tissue did not drop below 1 kPa, our data may be less representative of physiology in these areas. Further investigation is required in patients with low PbO<sub>2</sub>.





## CAN CEREBRAL AUTOREGULATION BE ASSESSED WITHOUT MEASURING CEREBRAL BLOOD FLOW?

Marek Czosnyka<sup>1</sup>, Ajay Kumar<sup>1</sup>, Luzius Steiner<sup>2</sup>, Eric A. Schmidt<sup>3</sup>, John D. Pickard<sup>1</sup>

<sup>1</sup>*Academic Neurosurgery, Addenbroke's Hospital, Cambridge, UK*

<sup>2</sup>*Department of Anesthesiology, University Hospital, Basel, Switzerland*

<sup>3</sup>*Department of Neurosurgery, Hopital Purpan, Toulouse, France*

Cerebral autoregulation is becoming more popular as a useful parameter in clinical practice. It has been demonstrated that dynamic autoregulation assessed using transcranial Doppler ultrasonography is associated with outcome following severe head injury, worsens with impairment of cerebral blood inflow in patients with carotid artery stenotic disease and when vasospasm arises in patients after subarachnoid haemorrhage, etc (1). Although current techniques for calculation of dynamic autoregulation do not require pharmacological changes in arterial pressure, the measurement in clinical practice is still difficult and depends on continuous insonation of the Middle Cerebral Artery- subject to artifacts mainly caused by the minor displacement of the ultrasound probes. We introduced Pressure Reactivity Index (PRx) derived from continuous monitoring of arterial pressure (AP) and intracranial pressure (ICP) to clinical practice in 1990s. Previously PRx has been positively correlated with outcome (1), PET-CBF derived autoregulation (2) and cerebral metabolism rate for oxygen (3). Our objective was to correlate PRx with Transcranial Doppler dynamic autoregulation index (Mx) and outcome in a large group of head injured patients. Data from intermittent bedside monitoring of ICP, AP, cerebral perfusion pressure (CPP=ABP-ICP) and of transcranial Doppler middle cerebral artery blood flow velocity (FV) in 237 patients were analysed retrospectively. Indices describing cerebral autoregulation and pressure reactivity were calculated as correlation coefficients between 'slow waves' of mean FV and CPP (Mx) and ABP and ICP (PRx) over moving three minute periods. Data were averaged over multiple recordings made in the same patients and compared to clinical outcome at 6 months after head injury. All patients were sedated, paralysed and ventilated during the period when brain variables were monitored. Both PRx and Mx were well correlated with each other ( $R=0.58; p<0.00001$ ). The absolute difference between Mx and PRx increased with greater ICP ( $R=0.27; p<0.0001$ ) and with worse outcome ( $R=0.21; p<0.003$ ). Both indices correlated positively with rising ICP and negatively with decreasing CPP, but the associations were stronger for PRx than Mx. Both indices were significantly correlated with outcome and were able to differentiate between fatal and non-fatal outcome with comparable power. However, where multiple regression was applied to outcome prediction, only mean ICP, age and PRx were retained as independent outcome predictors ( $R=0.35; p<0.00001$ ). Although significantly inter-correlated in a group analysis, pressure-reactivity may be, in individual case, different from dynamic autoregulation. Pressure-reactivity seems to be more robust in head injured patients when continuous ICP monitoring is required. REFERENCES 1.Czosnyka M, Smielewski P, Piechnik S, Pickard JD. Clinical significance of cerebral autoregulation. *Acta Neurochir Suppl.* 2002;81:117-9 2. Steiner LA, Coles JP, Johnston AJ, Chatfield DA, Smielewski P, Fryer TD, Aigbirhio FI, Clark JC, Pickard JD, Menon DK, Czosnyka M. Assessment of cerebrovascular autoregulation in head-injured patients: a validation study. *Stroke.* 2003 Oct;34(10):2404-9. 3. Steiner LA, Coles JP, Czosnyka M, Minhas PS, Fryer TD, Aigbirhio FI, Clark JC, Smielewski P, Chatfield DA, Donovan T, Pickard JD, Menon DK. Cerebrovascular pressure reactivity is related to global cerebral oxygen metabolism after head injury. *J Neurol Neurosurg Psychiatry.* 2003;74(6):765-70.

## ASYMMETRY OF CEREBRAL CIRCULATION IN INJURED BRAIN

Marek Czosnyka<sup>1</sup>, Piotr Smielewski<sup>1</sup>, Ajay Kumar<sup>1</sup>, Eric A. Schmidt<sup>2</sup>, Magdalena Hiler<sup>1</sup>,  
Basil F. Matta<sup>3</sup>, John D. Pickard<sup>1</sup>

<sup>1</sup>*Academic Neurosurgery, Addenbrooke's Hospital, Cambridge, UK*

<sup>2</sup>*Department of Neurosurgery, Hopital Purpan, Toulouse, France*

<sup>3</sup>*Department of Anaesthesiology, Addenbrooke's Hospital, Cambridge, UK*

**Objective:** We previously demonstrated that in injured brain the level of asymmetry of CBF autoregulation between injured and uninjured hemispheres correlates with intracranial pressure, size of contusion, midline shift and larger asymmetry associates with worse outcome (1). We extended our investigation on other indices describing cerebral haemodynamics, aiming Transcranial Doppler-derived Critical Closing Pressure (CCP). CCP is the arterial pressure below which the vessels theoretically collapse. Hypothetically it is the sum of intracranial pressure and vessels' wall tension in the cerebral circulation. Therefore, CCP has been postulated to be used as an 'estimator' of intracranial pressure. Other scientists also hypothesized that the measure of brain cerebral perfusion pressure would be more appropriate if it is expressed as a difference between arterial blood pressure and CCP rather than the difference between arterial and intracranial pressure (2). We attempted to investigate these questions in clinical practice, studying trans-hemispherical asymmetry of CCP and its correlation with radiological findings on CT scans in head injury patients and comparing absolute values of CCP with various, directly monitored brain variables. **Method:** Intracranial pressure (ICP), arterial blood pressure and middle cerebral artery blood flow velocity were recorded daily in 119 ventilated patients after head trauma. Waveforms were processed to calculate CCP. CT scans were analysed according to a system based on the Marshall classification. Outcome was assessed according to Glasgow Outcome Score at 6 time after injury. **Results:** Left-right differences in CCP correlated with midline shift on the CT scan ( $r=0.48$ ;  $p<0.02$ ) showing lower CCP at the side of brain expansion. Asymmetry of CCP also corresponded with the side of the head lesion ( $p<0.007$ ) and the side of the craniotomy where it was performed ( $p<0.012$ ). In both cases CCP was lower at the affected side of the brain than on contralateral side. Absolute CCP weakly correlated with brain swelling ( $r=-0.23$ ;  $p<0.03$ ) and arterial pressure ( $r=0.21$ ;  $p<0.02$ ) but did not correlate with ICP. Correlation between CCP and cerebrovascular resistance (calculated as cerebral perfusion pressure and blood flow velocity) was excellent ( $R=0.5$ ;  $p<0.001$ ). Cerebral perfusion pressure calculated as the difference between mean arterial pressure and CCP did not correlate with outcome, while 'traditional' cerebral perfusion pressure (mean arterial pressure minus intracranial pressure) did. **Conclusions:** Critical closing pressure is disturbed by localised brain lesions. Its asymmetry corresponds to asymmetrical findings on CT scans. CCP seems to describe vascular resistance better than to approximate intracranial pressure. Our data suggest that on side of brain contusion, brain expansion leading to the midline shift, or craniotomy vessels are more dilated than on contra lateral side, rendering cerebrovascular resistance to decrease. **REFERENCES** 1. Schmidt EA, Czosnyka M, Steiner LA, Balesteri M, Piechnik SK, Matta, BF, Pickard JD. Asymmetry of pressure autoregulation after traumatic brain injury. *J Neurosurg.* 99(6): 991-8, 2003 2. Weyland A, Buhre W, Grand S, Ludwig H, Kazmaier S, Weyland W, Sonntag H. Cerebrovascular tone rather than intracranial pressure determines the effective downstream pressure of the cerebral circulation in the absence of intracranial hypertension. *J Neurosurg Anesthesiol.* 2000 Jul; 12(3): 210-6.

## INCREASED PENTOSE PHOSPHATE CYCLE FLUX FOLLOWING SEVERE TRAUMATIC BRAIN INJURY: A <sup>13</sup>C-LABELING STUDY

Joshua R. Dusick<sup>1</sup>, Thomas C. Glenn<sup>1</sup>, Yung C. Lee<sup>2</sup>, W.N. Paul Lee<sup>2</sup>, Paul M. Vespa<sup>1</sup>, Sara Bassilian<sup>2</sup>, Soyoun J. Lee<sup>2</sup>, Stefan M. Lee<sup>1</sup>, Neil A. Martin<sup>1</sup>

<sup>1</sup>*UCLA Division of Neurosurgery and Brain Injury Research Center, Los Angeles, CA, USA*

<sup>2</sup>*Harbor-UCLA Medical Center and Los Angeles Biomedical Research Institute, Torrance, CA, USA*

### Introduction:

Patients with traumatic brain injury (TBI) routinely exhibit cerebral glucose uptake in excess of that expected by the low levels of oxygen consumption and lactate production, bringing into question the metabolic fate of glucose metabolized by the brain. Utilizing <sup>13</sup>C-glucose labeling, prior studies have demonstrated increased flux through the pentose phosphate cycle (PPC) during times of cellular stress, such as hypothermia and cellular transformation. The PPC supplies substrates for macromolecular synthesis, DNA repair, and free radical scavenging. This study assessed the PPC following TBI utilizing <sup>13</sup>C-labeling techniques.

### Methods:

<sup>13</sup>C-glucose (Cambridge Isotope Laboratories; Andover, MA) was infused for 60 min in 7 consented, severe-TBI patients (GCS ≤ 9; 6 males and 1 female) and 6 normal subjects (3 males and 3 females), mean ages 43.8 and 36.8, respectively (p = 0.54). Arterial and jugular bulb blood sampled during infusion was analyzed for <sup>13</sup>C-labeled isotopomers of lactate by gas chromatography coupled to mass spectroscopy. Lactate produced by the action of glycolysis can result in m0 or m2 lactate (lactate with zero or two carbon-13 atoms, respectively). One carbon-13 is lost as CO<sub>2</sub> in the PPC, resulting in m1 lactate (only one carbon-13 atom). The product of lactate concentration and fractional abundance of these isotopomers determines blood levels. Arterial-venous differences determine cerebral PPC contribution. Finally, a previously derived formula (PPC = [m1/m2]/[3+{m1/m2}]) for PPC based on the ratio of m1 to m2 lactate yields the flux of glucose through the PPC relative to glycolysis.

### Results:

There was good enrichment of labeled glucose in arterial-venous blood (mean TBI 17.3% and normal 28.7%; p<0.0001) and incorporation into lactate, demonstrating metabolism of labeled substrate. The PPC was increased in TBI patients relative to normal subjects (23.58% vs. 8.04%, respectively; p=0.002). In the TBI patients there were trends towards correlation of the PPC with CMRO<sub>2</sub> (r=0.77, p=0.1) and jugular lactate (r=0.9, p=0.08). There was no correlation with enrichment of labeled glucose for either TBI (r=0.4, p=0.5) or normal subjects (r=-0.37, p=0.5).

### Conclusion:

<sup>13</sup>C-labeling techniques allow detection and quantification of altered metabolic fluxes. Glucose consumed by the brain after TBI appears to be redirected towards alternate metabolic pathways. In particular, flux through the PPC is increased after TBI relative to normal. Whether this increased flux represents metabolic dysfunction or, alternatively, a physiologic response to injury is unclear. However, increased flux through the PPC supplies many substrates that may be critically important for minimizing secondary injury and initiating recovery. Foremost among these are reducing equivalents for prevention of oxidative injury and for lipid biosynthesis, and ribose for DNA repair, replication and transcription, and thus protein synthesis indirectly as well. Elucidating this altered metabolic milieu in the brain following TBI may open doors for novel metabolic support to prevent secondary injury and improve outcomes. In the future, the labeling technology utilized in this study could be used with <sup>13</sup>C MR spectroscopy, which would allow more direct monitoring of brain metabolism *in vivo* and also add regional and anatomic detail to the findings.

## THE APPLICATION OF RAPID-SAMPLING, ON-LINE MICRODIALYSIS TO INTRAOPERATIVE BRAIN MONITORING DURING ANEURYSM SURGERY

Robin Bhatia<sup>1</sup>, Parastoo Hashemi<sup>2</sup>, Emma Perpinan-Corcoles<sup>2</sup>, Mark C. Parkin<sup>3</sup>, Sarah E. Hopwod<sup>4</sup>, Martyn G. Boutelle<sup>2</sup>, Anthony J. Strong<sup>1</sup>

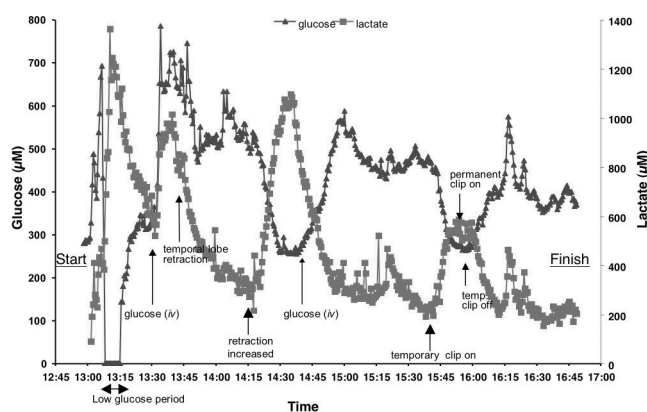
<sup>1</sup>Department of Clinical Neurosciences, Kings College London, London, UK

<sup>2</sup>Department of Bioengineering, Imperial College London, London, UK

<sup>3</sup>Department of Chemistry, University of Michigan, Detroit, MI, USA

<sup>4</sup>Department of Physiology, Imperial College London, London, UK

**INTRODUCTION:** Brain microdialysis during aneurysm surgery was introduced by Landolt et al (1) and has been described more recently by Kett-White et al (2). Both studies concluded that intraoperative monitoring could detect focal ischaemia *in vivo*; however, availability of metabolic information about disturbed homeostasis was delayed by least 30 minutes, because of sampling and analysis times. We therefore believe that for results of intraoperative microdialysis to influence patient management and hence outcome, we require: (i) rapid online analysis of metabolites in a continuous flow of dialysate. (ii) a shortened 'event-to-detection' time. **METHODS:** We conducted a prospective study, LREC-approved, on patients requiring surgery for ruptured middle cerebral artery (MCA, n=7) or posterior communicating aneurysms (n=1). Microdialysis catheters (CMA 70) were inserted into cortex at risk of ischaemia after opening the dura. The dialysate fed continuously (via 1m of fine tubing) into a flow-injection assay for glucose and lactate, each sampled at 30-sec intervals (3). Outcome was ranked at discharge. **RESULTS:** The figure shown is an example of a procedure to clip a left MCA aneurysm, with arrowed annotated events. Note that this patient experienced a period of low dialysate glucose (<150µM) for 12 minutes, and was given 2 boluses of iv glucose during the course of the procedure, resulting in rapid but non-sustainable rises. Time between events and detection: range 8 - 20min (mode value 9 min). Temporal lobe retraction (n=7): lactate +71 %, glucose -25%. Glucose bolus infusion (n=4): +587% (peak at 16min). Temporary proximal clip (n=6): mean clip time: 8.1min; lactate + 72%; glucose change -24%. Periods of low glucose: 7 under 150µM, 3 undetectable. In 6 patients outcome quality correlated inversely with duration of glycopaenia (dialysate glucose <150µM, Spearman's Ranked: r<sub>2</sub>=0.94, p < 0.05). **CONCLUSIONS:** The method robustly detects changes after 9 minutes (limited by surgical site-to-sensor transit), and thereby the ischaemic events associated with temporary clipping and lobe retraction. This enables the possibility of real-time feed-back and prompt changes in management (surgical or anaesthetic). The adverse effect of intraoperative glucose depletion on outcome after aneurysm surgery resembles findings in head injury (4). **REFERENCES:** 1. Landolt H et al. (1996) *Neurol Res* 18(4) 370-376 2. Kett-White R et al. (2002) *J Neurosurg* 96 1013-1019. 3. Parkin MC et al. (2005) *J. Cereb. Blood Flow Metab.* (In press) 4. Vespa, P.M. et al. (2003) *J. Cereb. Blood Flow Metab.* 23, 865-877.





## THE LACTATE:PYRUVATE RATIO AFFECTS HYPEREMIA IN HUMANS FOLLOWING TRAUMATIC BRAIN INJURY

Daniel Hirt, Thomas C. Glenn, Paul M. Vespa, Jane S.Y. Lee, Neil A. Martin

*Division of Neurosurgery, David Geffen School of Medicine at University of California at Los Angeles, Los Angeles, CA, USA*

Introduction: We have recently shown in rat middle cerebral arteries that the lactate:pyruvate (L:P) ratio, a modulator of the cellular NADH:NAD<sup>+</sup> (redox potential), is a regulator of vascular function. Additionally, Ido et al. (2) reported that cerebral blood flow (CBF) in activated rat brain is modified by changes in the L:P ratio: CBF was augmented when the ratio was raised and attenuated when the ratio was lowered. To further investigate this phenomenon, the relationship of cerebral parenchymal L:P ratio to cerebral perfusion after traumatic brain injury (TBI) was determined. Methods: Thirty-five consented TBI patients (age 36 +/- 16, admission GCS 6.8 +/- 2.5, 74% male) were prospectively studied with cerebral microdialysis (CMA/Microdialysis, Stockholm, Sweden) and continuous jugular venous oxygenation (SjVO<sub>2</sub>), which was used as an indicator of cerebral perfusion status. 133Xenon cerebral blood flow studies (Ceretroneix, Randers, Denmark) were conducted daily to verify the perfusion results of the SjVO<sub>2</sub> measurements. Results: A time dependent relationship between the L:P ratio and the first two phases of cerebral perfusion was observed. During the initial phase (<24 hours post injury) the mean hourly SjVO<sub>2</sub> was 70+/-9.0% while during the second phase (24-48 hours), the SjVO<sub>2</sub> rose significantly (p=0.0001) to 75+/-8.2%, indicative of increased cerebral perfusion. The L:P ratio did not correlate with SjVO<sub>2</sub> during the initial phase (r=0.05, p=0.683) but was significantly positively correlated with SjVO<sub>2</sub> during the next 24 hours (r=0.38, p=0.0001). No significant correlation between L:P ratio and SjVO<sub>2</sub> was seen after 48 hours. Discussion: This study showed that L:P ratio was a potent modulator of cerebral perfusion during the hyperemic phase following injury, thus suggesting an important contribution of the redox potential to vascular function. The effects of L:P ratio on cerebral perfusion are consistent both with (I) the need for higher flows to increase reoxidation of free NADH by LDH, and (II) the evidence that increased flows appear to exceed the need for oxygen and glucose to support increased energy metabolism. (1, 2) Additionally, this study demonstrated the temporally variable nature of post-traumatic cerebral perfusion.

Supported by NINDS 30308 and the UC Neurotrauma Initiative.

1. Cholet, N., Seylaz, J., Lacombe, P. & Bonvento, G. (1997) *J. Cereb. Blood Flow Metab.* 17, 1191-1201.
2. Ido, Y., Chang, K., Woolsey, T.A. & Williamson, J.R. (2001) *FASEB J.* 15, 1419-1421.

## CEREBRAL LACTATE EXTRACTION FRACTION AND OUTCOME FOLLOWING HUMAN TRAUMATIC BRAIN INJURY

Thomas C. Glenn, W. John Boscardin, Paul M. Vespa, David A. Hovda, Daniel F. Kelly, Neil A. Martin

*Neurosurgery, UCLA, Los Angeles, CA, USA*

**Introduction:** Previous studies in traumatic brain injury (TBI) patients have shown that during the acute period after injury, that the brain may take up lactate from the blood (Glenn, et al., 2003). The fate of this lactate, be it for cerebral metabolism or accumulation in the extracellular fluid has not been determined. In an effort to better determine the kinetics of cerebral lactate uptake, utilization, or accumulation, we investigated the degree of lactate uptake as a function of arterial lactate concentration (Lactate Extraction Fraction, LEF). Additionally, the LEF was compared between patient outcome groups. **Methods:** Fifty-seven consented TBI patients and 34 consented normal volunteers were enrolled in the study. The mean patient age was  $36 \pm 17$  years (range 16-81 years) and 17 (28.8%) were female, whereas the volunteer group's mean age was  $33 \pm 9$  (range 21-55) and 32% were female. The median post-resuscitation GCS score was 6 with a range of 3 to 15; 86% of patients had an initial  $GCS \leq 8$ . Arterial and jugular venous blood samples were collected twice daily for 6 days and analyzed for lactate, glucose, and oxygen. Cerebral metabolic rates were calculated by multiplying the arterial venous difference (AVD) by the cerebral blood flow as determined by the  $^{133}\text{Xenon}$  clearance technique. The LEF was calculated when the AVD for lactate was greater than zero:  $LEF = (CMR_{lac} \text{ (umol/g/min)} / \text{Arterial Lactate (umol/ml)}) * 100$ . Statistical analyses included mixed effects models controlled for intra-subject correlation. **Results:** Cerebral lactate uptake showed a time dependent pattern, as shown by percent studies with uptake: Day 0, 65.2%; Day 1, 58.1%; Day 2, 39.0%; Day 3, 40.5%; Day 4 43.9%; and Day 5 20.0%. Arterial lactate correlated positively with  $CMR_{lac}$  ( $r=0.39$ ,  $p=0.0001$ ). Four normal volunteers also exhibited lactate uptake and had an LEF of  $1.27 \pm 2.34$ . LEF varied as a function outcome at 12 months. For patients with a good Glasgow Outcome Score (GOS) of 4 or 5, their mean LEF was  $2.25 \pm 2.36$  whereas patients with a poor outcome, GOS 1-3 had a mean LEF of  $1.40 \pm 1.13$ . This difference was statistically significant,  $p=0.03$ . **Summary and Conclusions:** This study investigated cerebral lactate uptake as a function of arterial lactate concentration. Cerebral lactate uptake is a frequent occurrence in the acute phase after TBI in humans. Patients with a good recovery at 12 months exhibited a higher LEF than patients with a poor outcome. This finding suggests that patients with a good outcome may utilize mechanisms that increase lactate uptake and/or utilization. Future studies are needed to determine the fate of lactate uptake by the brain following TBI. Supported by NINDS 30308 and the UC Neurotrauma Initiative Glenn TC, Kelly DF, Boscardin WJ, McArthur DL, Vespa PM, Oertel MF, Hovda DA, Bergsneider M, Hillered L, Martin N. Energy dysfunction as a predictor of outcome after moderate or severe head injury: indices of oxygen, glucose and lactate metabolism. *J Cereb Blood Flow Metab* Oct;23(10):1239-50, 2003

## DETECTING BRAINSTEM INJURY WITH ACUTE MRI FOLLOWING SEVERE HEAD TRAUMA

Richard J. Mannion<sup>1,2</sup>, David Menon<sup>1,3</sup>, Justin Cross<sup>1,4</sup>, Peter Bradbury<sup>1,3</sup>, Jonathan Coles<sup>1,3</sup>

Dot Chatfield<sup>1,3</sup>, John D. Pickard<sup>1,2</sup>, Peter J.A. Hutchinson<sup>1,2</sup>

<sup>1</sup>Wolfson Brain Imaging Centre, <sup>2</sup>Department of Neurosurgery, <sup>3</sup>Department of Anaesthesia, <sup>4</sup>Department of Radiology, Cambridge, UK

Traumatic brain injury (TBI) is the most common cause of death and major disability in young people. Outcome is often difficult to predict from factors such as mechanism of injury, initial Glasgow Coma Score and imaging. Currently, CT is the imaging modality of choice and has led to the introduction of complex CT-based classification systems of head injury. CT is satisfactory for the detection of haematomas and contusions in the cerebral hemispheres but is much less effective at documenting diffuse injury and posterior fossa lesions. There are, therefore, a significant number of patients in whom outcome is much worse than would be predicted from their presenting CT scan. This aim of this study is to look at the role of acute MRI (T2, FLAIR, gradient echo) in detecting the presence of brainstem injury in patients following TBI and to correlate the findings with outcome at 6 months (Glasgow Outcome Score). Twenty-nine patients (mean age 37 years, range 18-70, 79% male) admitted to the neuro-critical care unit with TBI requiring ventilation underwent CT and MRI within 3 days of injury. Brainstem lesions were detected in 7 patients on MRI scan but none were diagnosed by CT. The types of brainstem injury varied widely and an assessment was made as to whether injury type had any relationship with the nature of supratentorial injury. All 7 patients with brainstem injury had an unfavorable outcome (death, vegetative state or severe disability). Of the 22 patients without brainstem lesions, 10 had a poor outcome. The relationship between brainstem lesions and outcome was highly significant. ( $p < 0.005$ , Chi Squared Test). This study suggests that early MRI detects a significant number of brainstem lesions that are not seen on CT and offers the potential to increase our understanding of the nature of supratentorial injury following head trauma.

## **'ICM+': VERSATILE SOFTWARE FOR ANALYSIS OF CEREBROVASCULAR DYNAMICS IN CLINICAL PRACTICE**

**Peter Smielewski<sup>1,2</sup>, Marek Czosnyka<sup>1</sup>, Philip Lewis<sup>1</sup>, John D. Pickard<sup>1,2</sup>**

<sup>1</sup>*Neurosurgery Unit, University of Cambridge, Cambridge, UK*

<sup>2</sup>*Wolfson Brain Imaging Centre, University of Cambridge, Cambridge, UK*

**Introduction:** Contemporary brain monitoring in clinical practice includes multiple global and local modalities such as ABP, ICP, Transcranial Doppler, Laser Doppler Flowmetry, brain tissue oxygenation, jugular bulb oxygen saturation, Near Infrared Spectroscopy, etc. Measured variables require time- and/or frequency-domain on-line analysis to derive further information from spontaneous waves present in those signals (e.g. cardiac related, respiratory and slow waves). Analysis of cross-correlation between signals such as blood flow velocity, laser Doppler-flux or tissue oxygenation helps in the assessment of mechanisms related to cerebral blood flow regulation. **Methods:** ICM+ software has been developed in house, borrowing from our 10 years experience in data monitoring and analysis in the neuro critical care unit in Addenbrookes Hospital, Cambridge. Previous versions of the software have allowed us to collect multimodal data from nearly 600 severely head injured patients, along with secondary indices calculated online describing cerebral autoregulation and pressure-volume compensation. ICM+ includes a calculation engine that allows easy configuration and real-time trending of complex parameters. The program records raw signals, and calculates time trends of summary parameters. Configuration of analyses utilises arithmetic expressions of statistical and signal processing functions (moving average, correlation, power spectrum, coherence etc). The software allows configuration of several levels of analysis with the output of each one providing input to the next. The final data are displayed in a variety of ways including simple time trends, as well as time window based histograms, cross histograms, correlations etc, to facilitate data browsing and mining. The post-processing tools also support the calculation of indices of cerebrovascular reactivity from recordings made during interventions like transient hyperaemic response, rapid leg-cuff deflation and CO<sub>2</sub> reactivity tests. The ICM+ package facilitates the modification of existing methods of analysis of cerebral haemodynamics and the development of new algorithms. In addition to on-line trends of calculated values and indices, the software also saves raw data from bed side monitors, which enables building up a library of signals for post-processing. These saved raw signals can subsequently be processed using the on-line analysis engine, thus providing a means of testing novel indices and methods of on-line data processing. Tools for manual marking of, and automatic detection of artefacts in the input signals and resulting time trends are provided to ensure high quality of the analysis results. **Results:** To verify the usefulness of ICM+ for assessment of cerebrovascular dynamics 187 patients with severe head injury were analysed. In total, 563 recordings of ICP, ABP and TCD FV from 187 patients were processed using a variety of different analysis configurations. Results showed strong correlations between autoregulation indices Mx, Prx and Outcome, and allowed detailed investigation of these relationships. Detailed discussion of those results is presented elsewhere. **Conclusion:** ICM+ is a universal tool for clinical and academic purposes. Its flexibility and advanced signal processing features are specialized for the needs of multidisciplinary brain monitoring, and it is particularly well suited for investigations into cerebral haemodynamics.

**EFFECTS OF SUBDURAL HEMORRHAGE, MASS LESION AND CONTROLLED CORTICAL IMPACT ON MULTI-PARAMETRIC NEUROMONITORING IN PIGS****Beat Alessandri**, Ralph Timaru-Kast, Anke Meissner, Oliver Kempfski, Axel Heimann*Institute for Neurosurgical Pathophysiology, Johannes Gutenberg-University, Mainz, Germany*

A common problem in traumatic brain injury (TBI) is the effect of acute subdural hemorrhage (ASDH), especially if accompanied by contusion, leading to a high mortality rate. Little is known about the acute pathophysiological mechanisms of such an injury type and the role of blood constituents or shear volume. Therefore, the goals of this study were to establish a porcine model of acute subdural hematoma (ASDH), to study the effect of ASDH as secondary injury after controlled cortical impact (CCI) and to distinguish the effects of blood from sole mass effects (paraffin oil). 43 pigs were used, and intravenously anaesthetised by alpha-chloralose. After cannulation of femoral artery and vein animals were fixed in a stereotaxic frame for drilling a large craniectomy (20mm) for application of TBI and small burr holes for oxygen (Licox), temperature and microdialysis probes (CMA/70). A SEP (somatosensory evoked potential) electrode and an intraventricular ICP sensor were also applied [Alessandri et al., *J. Neurotrauma* 20(12), 2003]. Measurements were made at least every 15 minutes throughout the experiment. After a baseline period (60min), TBI was initiated by: (a) CCI at 2.5m/s, 9mm injury depth; (b) subdural infusion of 2mL, 5mL or 9mL venous blood (0.5mL/min); (c) 5mL paraffin oil and (d) a combined CCI and ASDH trauma (2mL, starting 10min after CCI). Sham pigs received all interventions, but no TBI. Twelve (12) hours after TBI, brains were removed and analysed histologically. Subdural infusion of 9mL blood elevated ICP to  $34.7 \pm 3$  mmHg (peak:  $46 \pm 3$  mmHg at 20min) during the first post-TBI hour and remained close to 30mmHg throughout the study, whereas ICP after 2mL and 5mL blood recovered quickly from peak  $22.3 \pm 4$  and  $29.4 \pm 5$  mmHg. Ipsilateral tissue oxygen decreased acutely to 40-60% of baseline ( $23.3 \pm 1.1$  mmHg) after ASDH, but except for 9mL, oxygen recovered within several hours. Glutamate was long-lasting increased only in the 9mL group, adding to the large histological damage. The assessed contusion index [Adams, 1985] did not differ between the 2- and 5mL-group. A 2mL ASDH as secondary injury affected neuromonitoring parameters as well as histology only slightly when compared to CCI trauma. Peak ICP was  $13.7 \pm 2$  (CCI) and  $17 \pm 3.4$  mmHg (CCI+2mL blood) and ptiO<sub>2</sub> decreased to 70% of baseline in both cases. In both CCI-groups, but not the 2mL ASDH group SEP amplitude declined below 50% (CCI 37.8%, CCI+2mL: 36.9%, 2mL: 80.3% at 120min post-TBI) throughout the entire experiment. Comparison of 5mL subdural blood and paraffin oil infusion revealed no differences in neuromonitoring and contusion index. A porcine model of ASDH could be established with a threshold blood volume for long lasting neuromonitoring effects between 5 and 9mL (7-13% of brain volume). A volume of 2mL blood was insufficient to potentiate the effects of brain contusion. Furthermore, the similar effects of 5mL blood or paraffin indicate that the acute increase of ICP determines processes leading to a 'subacute' histological damage found after 12 hours, and that additional effects due to blood contact with brain tissue (e.g. inflammation) may be detected only at later time-points.

## INVESTIGATION OF THE CEREBRAL HAEMOGLOBIN AND CYTOCHROME SIGNALS USING NEAR INFRARED SPECTROSCOPY DURING HEAD UP TILT IN PATIENTS WITH ORTHOSTATIC HYPOTENSION

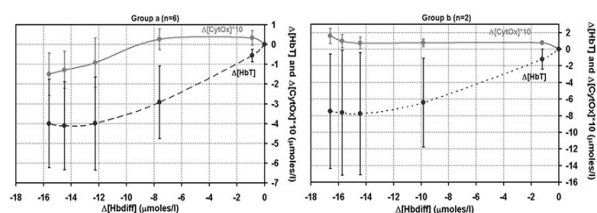
Martin Tisdall<sup>2</sup>, Ilias Tachtsidis<sup>1</sup>, Katharine Bleasdale-Barr<sup>3</sup>, Chris J. Mathias<sup>3</sup>, Dave T. Delpy<sup>1</sup>, Clare E. Elwell<sup>1</sup>, Martin Smith<sup>2</sup>

<sup>1</sup>Medical Physics and Bioengineering, University College London, London, UK

<sup>2</sup>Department of Neuroanaesthesia & Neurocritical Care, The National Hospital for Neurology and Neurosurgery, London, UK

<sup>3</sup>Autonomic Unit, The National Hospital for Neurology and Neurosurgery, London, UK

**Introduction:** The cardiovascular and cerebrovascular responses to head up postural change are severely compromised in primary autonomic failure (AF) because of sympathetic denervation. AF patients therefore exhibit hypotension and show signs of cerebral hypoperfusion during a head-up tilt. In this study we employed near infrared spectroscopy (NIRS) to investigate changes in haemoglobin and cytochrome oxidase redox state ([CytOx]) during periods of severe cerebral hypoperfusion defined as a drop in cerebral haemoglobin difference ( $[Hbdiff]=[oxyhaemoglobin]-[deoxyhaemoglobin]$ ) of at least  $10\mu\text{mol/l}$  [1]. **Methods:** 12 patients were studied and data were recorded (i) when supine and (ii) during passive head up tilt to 60 degrees. A continuous wave four wavelength NIRS system (NIRO 300, Hamamatsu Photonics KK) measured changes in cerebral tissue oxyhaemoglobin ([HbO<sub>2</sub>]) and deoxyhaemoglobin ([HHb]) and  $[HbT]=[HbO_2]+[HHb]$  and [CytOx] using an age corrected differential pathlength factor [2]. Beat-to-beat blood pressure (BP) was measured non-invasively using a Portapres® system. Using the [Hbdiff] signal we identified the start of the head up tilt and the maximum drop and acquired 5 sequences of 10sec mean values from the start to the maximum of the drop. **Results:** 8 patients demonstrated a maximum drop in the [Hbdiff] signal of at least  $10\mu\text{mol/l}$ , 6 patients (group a) demonstrated a reduction in [CytOx] and 2 patients (group b) exhibited no change, which was unrelated to the drop in the other signals. These mean changes ( $\pm$ SD) are shown in the figure. **Conclusions:** We have shown that in some AF patients postural hypotension is associated with a reduction in [Hbdiff] accompanied by a fall in [CytOx], possibly indicating severe cerebral cellular dysoxia. The pattern of [CytOx] change shown in Group a, has previously been demonstrated using NIRS [3]. In 2 patients there is no response in the [CytOx] signal. It has been reported that large changes in chromophore concentrations, can lead to artifacts in the observed changes in low concentration chromophores, such as [CytOx] [4], in the data presented here there is no evidence of crosstalk between the haemoglobin and [CytOx] signals. However individual differences in the anatomy of the different layers of the adult head (scalp/skull and brain) could introduce ‘contamination’ to the [CytOx] signal [5]. Measurement of [CytOx] might be a useful adjunct during monitoring of cerebral ischaemia. **References** [1] Tachtsidis I, Cooper CE, McGown A.D, Makker H, Delpy DT, and Elwell CE; Biomedical Topical Meetings OSA WF6 (2004) [2] Duncan A, Meek JH, Clemence M, Elwell CE, Tyszczuk L, Cope M, and Delpy DT; Phys. Med Biol 40, 295-304 (1995) [3] Cooper CE, Delpy DT, Nemoto EM; Biochem. J 332 ( Pt 3), 627-632 (1998) [4] Uludag K, Kohl M, Steinbrink J, Obrig H, and Villringer A; J Biomed. Opt 7, 51-59 (2002) [5] Choi J, Wolf M, Toronov V, Wolf U, Polzonetti C, Hueber D, Safonova LP, Gupta R, Michalos A, Mantulin W, and Gratton E; J Biomed. Opt 9, 221-229 (2004).





**CARBON DIOXIDE PROVIDES NEUROPROTECTION IN FLUID PERCUSSION INJURED RATS**

**Michael L. Rolli**<sup>1</sup>, Eleanor Lee<sup>2</sup>, Anthony J. Williams<sup>1</sup>, Geoffrey S.F. Ling<sup>2</sup>,  
Frank C. Tortella<sup>1</sup>

<sup>1</sup>*Division of Psychiatry and Neuroscience, Walter Reed Army Institute of Research, Silver Spring, MD, USA*

<sup>2</sup>*Uniformed Services, University of Health Sciences, Bethesda, MD, USA*

**Introduction:** Traumatic brain injury is a leading cause of death and disability among young adults (18-45 years old) and a leading combat casualty. This project examines the effects of hypercarbia on brain injury following fluid percussion injury in the rat. **Methods:** Anaesthetized rats underwent tracheostomy, arterial cannulation, and moderate cerebral fluid percussion injury (2.75-3.00 atm). For one hour following fluid percussion injury the animal's PaCO<sub>2</sub> was altered by adjusting minute ventilation, and maintained at a predetermined level for one hour. Each group was controlled for temperature and pO<sub>2</sub>. The rats were euthanized and perfused at 72 hours and their brains harvested for histopathology (H&E). Brain injury areas were demarcated and total volumes interpolated. **Results:** Mean injury volumes ( $\pm$  SD) were 42.39 $\pm$ 12.17 mm<sup>3</sup>, 25.27  $\pm$ 12.62 mm<sup>3</sup>, 24.45 $\pm$ 8.32 mm<sup>3</sup>, 16.46 $\pm$ 21.73 mm<sup>3</sup>, in animals with mean pCO<sub>2</sub> values of <40 (normal controls), 45, 55, and 60 mmHg, respectively. Statistical analysis revealed significant differences (P <0.05) in comparing brain injury volume of hypercarbic animals to normocarbic controls. **Discussion:** In conclusion, rats sustaining a moderate fluid percussion injury have a significant decrease in injury volume when treated with one-hour of post-traumatic hypercarbia in the setting of normal oxygenation compared to rats with normal pCO<sub>2</sub> values. These findings warrant further investigation into the mechanisms behind the neuroprotective effects of post-traumatic hypercarbia and the pathophysiological sequelae of its use in the setting of traumatic brain injury. Ongoing experiments are examining the effects of hypercarbia following penetrating brain injury measuring brain tissue O<sub>2</sub>, brain temperature, intracranial pressures (ICP), laser Doppler cerebral blood flow, DC/EGG, and 72h histopathology.

## CAN WE ASSESS CEREBROVASCULAR AUTOREGULATION AFTER HEAD INJURY USING BRAIN TISSUE OXYGEN PRESSURE REACTIVITY?

Matthias Jaeger<sup>1</sup>, Martin Soehle<sup>2</sup>, Martin U. Schuhmann<sup>1</sup>, Jürgen Meixensberger<sup>1</sup>

<sup>1</sup>*Department of Neurosurgery, University of Leipzig, Leipzig, Germany*

<sup>2</sup>*Department of Anaesthesiology and Intensive Care Medicine, Rheinische-Friedrich-Wilhelms University, Bonn, Germany*

Background: The aim of this study was to investigate whether two newly developed indices of brain tissue oxygen (PtiO<sub>2</sub>) pressure reactivity, named OR<sub>x</sub> and bPtiO<sub>2</sub>, allow an estimation of the status of cerebrovascular autoregulation after head injury? This was accomplished by validating these new indices against an established parameter for the assessment of autoregulation, the cerebrovascular pressure reactivity index (PR<sub>x</sub>). Methods: In 27 patients after severe head injury continuous monitoring of mean arterial blood pressure (MAP), intracranial pressure (ICP), cerebral perfusion pressure (CPP), and partial pressure of brain tissue oxygen (PtiO<sub>2</sub>) was performed for an average period of 6.5 days. OR<sub>x</sub> was calculated as a moving correlation coefficient between values of CPP and PtiO<sub>2</sub>. The bPtiO<sub>2</sub> was calculated as a moving value of the slope of the linear regression function between CPP and PtiO<sub>2</sub>. PR<sub>x</sub> was calculated as described by Czosnyka et al. as a moving correlation coefficient between values of ICP and MAP. Outcome was assessed at six months after trauma (Glasgow Outcome Scale). Results: OR<sub>x</sub> and bPtiO<sub>2</sub> correlated significantly with PR<sub>x</sub> ( $r = 0.55$  for OR<sub>x</sub>,  $r = 0.53$  for bPtiO<sub>2</sub>,  $p < 0.01$ ). PR<sub>x</sub> and OR<sub>x</sub> showed a significantly negative correlation to the monitored PtiO<sub>2</sub> values ( $r = -0.42$  for PR<sub>x</sub>,  $r = -0.41$  for OR<sub>x</sub>,  $p < 0.05$ ) and patient outcome ( $r = -0.52$  for PR<sub>x</sub>,  $r = -0.62$  for OR<sub>x</sub>,  $p < 0.01$ ), whereas bPtiO<sub>2</sub> did not. ICP and CPP showed no correlation to outcome. Conclusion: The results of this study suggest, that the newly developed indices OR<sub>x</sub> and bPtiO<sub>2</sub>, which describe the relationship between changes of CPP and PtiO<sub>2</sub>, might provide additional information on the status of cerebrovascular autoregulation after TBI, as both correlated well with PR<sub>x</sub>. The data furthermore indicate that patients with impaired autoregulation are at increased risk for secondary cerebral hypoxia and poor outcome. In contrast, patients with better reactivities presented with better outcome.

**RADIOGRAPHIC VALIDITY OF TRANSCRANIAL DOPPLER CEREBRAL BLOOD FLOW VELOCITY MEASUREMENT**

**Michael J. Souter**<sup>1,2</sup>, Gavin W. Britz<sup>2,3</sup>, Michael S. Kincaid<sup>1</sup>, Basavaraj Ghodke<sup>3</sup>,  
Arthur M. Lam<sup>1,2</sup>

<sup>1</sup>*Anesthesiology, University of Washington, Seattle, WA, USA*

<sup>2</sup>*Neurosurgery, University of Washington, Seattle, WA, USA*

<sup>3</sup>*Radiology, University of Washington, Seattle, WA, USA*

The validity of Transcranial Doppler cerebral blood flow velocity (TCD) as an index of cerebral blood flow hinges on the assumption that the insonated cerebral vessel diameters do not change (outside the circumstances of vasospasm). This assumption has been challenged (1) particularly when considering the sensitivity and specificity of TCD to pathological and anesthesia induced changes in CBF. Accordingly we examined changes in both TCD flow velocities and angiographically derived cerebral artery diameters, in patients undergoing elective cerebral artery aneurysmal coiling, with crossover from a vasoconstrictor to a vasodilator anesthetic. Methods: Four patients were initially examined. Patients received a standard induction technique with propofol, paralytics and narcotics, and were stabilized on propofol infusion thereafter to control blood pressure within 20% of preanesthesia values. They were endotracheally intubated, with invasive arterial pressure monitoring, end-tidal and arterial CO<sub>2</sub> (PaCO<sub>2</sub>) measurement. Baseline measurements of middle cerebral artery (MCA) and internal carotid artery (ICA) flow velocities were made, along with radiographic measurements of cerebral arterial diameters at A1, M1, M2 and M3 segments. The anesthetic agent was changed to 2% isoflurane (end-tidal concentration) and measurements repeated. Blood pressure and arterial CO<sub>2</sub> was held constant with changes in ventilation and the use of phenylephrine as required. Results: The mean change in mean arterial pressure (MAP) was 0.5% (SD 9.2) with PaCO<sub>2</sub> of 0.25% (SD 2.1). The MCA and ICA experienced mean changes of 3% (SD 9.6) and 19.1% (SD 15.9), while the A1, M1, M2 and M3 diameters changed by 5.4% (SD 8.7), 1.7% (SD 2.4), 7.9% (SD 2.7) and 3.6% (SD 5.1) respectively. Conclusions: 1. Minimal changes in arterial diameter were seen accompanying similar changes in intracranial TCD flow velocities under conditions of controlled pCO<sub>2</sub> and MAP. 2. TCD blood flow velocity would appear to be a reasonable index of cerebral blood flow. Further data will be presented. References: 1. Dahl A, Russell D et al. Simultaneous assessment of vasoreactivity using transcranial Doppler ultrasound and cerebral blood flow in healthy subjects. *J Cereb Blood Flow Metab.* 1994;14:974-81

**ANALYSIS OF DYNAMIC TESTING OF CEREBRAL PRESSURE  
AUTOREGULATION ASSESSED BY THE CUFF DEFLATION METHOD****Roman Hlatky<sup>1,2</sup>, Alex B. Valadka<sup>1</sup>, Claudia S. Robertson<sup>1</sup>**<sup>1</sup>*Department of Neurosurgery, Baylor College of Medicine, Houston, TX, USA*<sup>2</sup>*Center for Neurosurgical Sciences, University of Texas Health Science Center, San Antonio, TX, USA*

The cuff deflation technique for studying dynamic cerebral pressure autoregulation (PA) was introduced by Aaslid et al. (Aaslid, Stroke, 1989) based on findings that the cerebral blood flow response to sudden changes in mean arterial blood pressure (MAP) has a characteristic latency. Dynamic methods for testing cerebral PA are more practical than static method, but have not been well-validated in critically ill patients. The process of cuff deflation is innocuous in the normal subject, but the systemic and cerebral effects of cuff deflation in the patient with a severe traumatic brain injury have not been studied systematically. The purpose of this study was to examine the physiological effects of cuff deflation, and to study the consequences of these physiological effects on the calculation of autoregulatory index (ARI). 381 individual cuff deflations in 24 patients with severe head injury were examined. The physiological parameters were recorded in each patient before, during, and after a step drop in blood pressure. The thigh cuff technique as described by Aaslid et al. was used to induce the drop in blood pressure. PA was graded by generating an ARI value from 0 to 9 by the method proposed by Tiecks et al. (Tiecks, Stroke, 1995). The pattern of changes in most of the physiological variables consisted of an initial decrease, followed after a short time by recovery back to baseline or even to an elevated level. MAP decreased by an average value of  $19 \pm 5$  mmHg following the cuff deflation. MAP rapidly dropped during the first 2-3 seconds after the cuff deflation, but the nadir MAP was not reached until  $8 \pm 7$  seconds after the cuff deflation. This drop in MAP resulted in a similar transient decrease in FV of  $19 \pm 8$  cm/sec, decrease in SjvO<sub>2</sub> of  $5.5 \pm 3.0\%$ , and in PbtO<sub>2</sub> of  $2.0 \pm 1.2$  mmHg. The changes in physiological variables during the different phases following cuff deflation were highly correlated. The tracings for MAP and CPP were nearly identical during the first few seconds after the cuff deflation. After 30 seconds, the ICP increased variably among individual patients causing some differences between the MAP and CPP curves. ARI was calculated twice for each set of cuff deflation data by using first the MAP and then the CPP as the input function for the modeled FV curves. The difference between the two ARI values was zero for 70% and within one for 93% of the cuff deflations on the left, and the difference was zero for 73% and within one for 95% of the cuff deflations on the right. The results of this studies show only transient and relatively minor perturbations in systemic physiology induced by the cuff deflation method for dynamic testing of cerebral pressure autoregulation. Furthermore, this study provides additional evidence supporting a methodological question regarding the need to use of CPP rather than MAP as the input function for the determination of ARI.

**FAILURE OF PENTOBARBITAL TO REDUCE CEREBRAL OXYGEN  
CONSUMPTION IN RATS AFTER NON-HAEMORRHAGIC CLOSED HEAD  
INJURY**

**Geoffrey De Visscher<sup>1</sup>, Servan Rooker<sup>3</sup>, Helga Blockx<sup>1</sup>, Phillippe Jorens<sup>4</sup>, Jan Verlooy<sup>3</sup>,  
Marcel Borgers<sup>2</sup>, Robert S, Reneman<sup>2</sup>, Koen van Rossem<sup>5</sup>, Willem Flameng<sup>1</sup>**

<sup>1</sup>*Laboratory for Cardiovascular Research, CEHA, Catholic University of Leuven, Leuven,  
Belgium*

<sup>2</sup>*Department of Molecular Cell Biology, CARIM, University of Maastricht, Maastricht,  
The Netherlands*

<sup>3</sup>*Department of Neurosurgery, University Hospital Antwerp, Antwerp, Belgium*

<sup>4</sup>*Department of Intensive Care Medicine, University Hospital Antwerp, Antwerp, Belgium*

<sup>5</sup>*Barrier Therapeutics, Geel, Belgium*

Different studies have advocated the use of barbiturates (Miller et al., 1981; Eisenberg et al., 1988) in neurotrauma while others have presented contradictory data (Schwartz et al., 1984; Ward et al., 1985). The recent meta-analysis published by Roberts (2000) shows a dramatic lack of effect with 68% of unresponsive patients and a 25% chance of inducing a blood pressure drop. Via a currently not completely understood mechanism, barbiturates depress cerebral oxygen consumption and cause a secondary decrease in cerebral blood flow. This vasoconstrictive action results in a decreased cerebral blood volume in the arterial compartment which consequently decreases ICP (Hoff et al., 1977; Smith 1977; Kassell et al., 1980; Pappas and Mironovich 1981). Since it is unknown whether barbiturates suppress cerebral oxygen metabolism early after cerebral trauma, we evaluated the influence of pentobarbital on cerebral oxygen handling of normal rats and rats subjected to non-haemorrhagic closed head injury (CHI). Our multi-wavelength near infrared spectroscopy (NIRS)-system, developed at the University College London, can be used for the assessment of concentrations of oxyhaemoglobin, deoxyhaemoglobin and oxidised cytochrome oxidase in the brain in toto. Oxygen delivery was assessed by measuring cerebral perfusion and oxygen extraction, enabling the calculation of cerebral metabolic rate of oxygen (CMRO<sub>2</sub>). Mitochondrial function was assessed by studying changes in the oxidised cytochrome oxidase concentration. CHI causes changes in both systemic and cerebral haemodynamics. Cerebral blood flow was reduced to 66% of the control value but the cerebral metabolic rate of oxygen remained unchanged. Pentobarbital administration induced a significant lowering of the cerebral oxygen consumption in normal rats associated with a secondary decrease in cerebral perfusion. In rats subjected to CHI, pentobarbital was unable to lower the cerebral metabolic demand and did not cause a decrease in perfusion. Pentobarbital was unable to significantly modulate mitochondrial function, as assessed by the change in oxidised cytochrome oxidase signal, in traumatised rats whereas it exerted this effect in all control animals. The oxidised cytochrome oxidase signal, although unaltered when considering the whole group, clearly shows that we have 4 irresponsive animals and 2 responsive animals. Only 2 of 6 animals show the "hyperoxidation" of cytochrome oxidase after administration of the pentobarbital, a feature found in every pentobarbital treated control. This proportion, although a crude estimate, is in accordance with the findings mentioned above. We therefore conclude that pentobarbital is unable to perform its beneficial effects on the cerebral metabolic in 2 out of 6 rats subjected to CHI. Eisenberg et al., *J. Neurosurg.* 69:15-23, 1988 Hoff et al., *Acta Neurol. Scand. Suppl* 64:158-9, 1977 Kassell et al., *Neurosurgery* 7:593-7, 1980 Miller et al., *J. Neurosurg.* 54:289-99, 1981 Pappas and Mironovich, *Am. J. Hosp. Pharm.* 38:494-498, 1981 Roberts, *Cochrane Database. Syst. Rev.* CD000033, 2000 Schwarz et al., *Can. J. Neurol. Sci.* 11:434-40, 1984 Smith, *Anesthesiology* 47:285-93, 1977 Ward et al., *J. Neurosurg.* 62:383-8, 1985

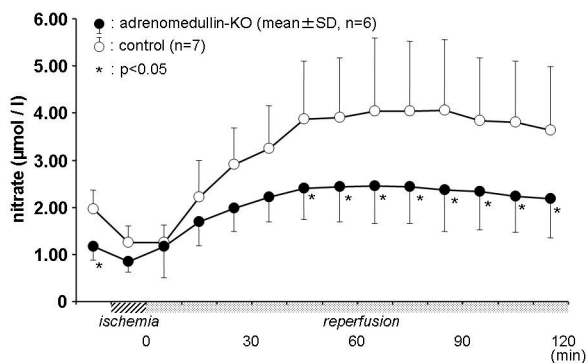
## EFFECTS OF ADRENOMEDULLIN ON NITRIC-OXIDE PRODUCTION DURING FOREBRAIN ISCHEMIA AND REPERFUSION IN MICE

Daisuke Furuya, Nobuo Araki, Takeshi Okubo, Yoshio Asano, Masahiko Sawada, Tomokazu Shimazu, Harumitsu Nagoya, Masamizu Yamazato, Yasuo Ito, Yuji Kato, Mikiko Ninomiya, Kunio Shimazu

*Department of Neurology, Saitama Medical School, Moroyama, Japan*

[Introduction] We have reported that rostral ventrolateral medulla (RVLM) might modify the CBF autoregulation 1). Xu et al 2) have shown that injections of adrenomedullin into RVLM increase blood pressure, which is mediated by nitric oxide (NO). The purpose of this study is to investigate the effects of adrenomedullin on NO production during forebrain ischemia and reperfusion. [Methods] Adrenomedullin-knockout (AM-KO) mice (n=6, 26-40g) and C57 BL / 6J (control, n=7, 22-27g) were anesthetized by intraperitoneal injection of pentobarbital sodium. NO production was continuously monitored by in vivo microdialysis. The probes were inserted into the left striatum and perfused with Ringer's solution at a constant rate of 2 $\mu$ l / min. A laser Doppler probe was fixed on the right scalp to measure CBF continuously. Blood pressure (BP), blood gases and body temperature were monitored and maintained physiologically. After 2 hours equilibrium period, fractions were collected every 10 minutes. Forebrain cerebral ischemia was produced by occlusion of both common carotid arteries. After 10 minutes, the loops around both common carotid arteries were released. Levels of NO metabolites, nitrite (NO<sub>2</sub><sup>-</sup>) and nitrate (NO<sub>3</sub><sup>-</sup>), in the dialysate were determined using the Griess reaction. [Results] 1) BP: There was no significant difference between AM-KO and control group. 2) CBF: Each group did not differ significantly in CBF during cerebral ischemia and reperfusion. 3) NO metabolites: (a) NO<sub>2</sub><sup>-</sup>; Baseline, the AM-KO animals had a nitrite level of 1.63  $\pm$  0.52  $\mu$ mol / l (mean  $\pm$  SD) in striatum, which was lower (p<0.05) than that of control animals (2.84  $\pm$  0.66  $\mu$ mol / l). The levels in AM-KO group showed significantly lower than that of control group at 70 and 80 minutes after reperfusion. (b) NO<sub>3</sub><sup>-</sup>; The AM-KO animals had a nitrate level of 1.45  $\pm$  0.38  $\mu$ mol / l, which was lower (p<0.05) than control group (1.99  $\pm$  0.41  $\mu$ mol / l). The levels in AM-KO group showed lower (p<0.05) than control group between 50 and 120 minutes after the start of reperfusion (Figure). [Conclusion] These data suggest that the adrenomedullin might mediate neuronal NO synthase in the brain during ischemia and reperfusion. [References] 1) K. Hattori et al: J CBF Metabol 15 (suppl 1): s494, 1995, 2) Y. Xu, T. L. Krukoff: Am J Physiol Integr Comp Physiol 287: R729-R734, 2004

Change of Nitrate : Comparison between Adrenomedullin-KO and Control.



**SIMULTANEOUS MEASUREMENT OF DOPAMINE TRANSPORTERS AND D2/D3 RECEPTORS IN DRUG NAÏVE SCHIZOPHRENIA****Yuan-Hwa Chou<sup>1</sup>, Tung-Ping Su<sup>1</sup>, Wen-Sheng Huang<sup>2</sup>, Ying-Kai Fu<sup>3</sup>**<sup>1</sup>*Department of Psychiatry, Taipei Veterans General Hospital & National Yang Ming University, Taipei, Taiwan*<sup>2</sup>*Department of Nuclear Medicine, Tri-Service General Hospital & National Defense Medical Center, Taipei, Taiwan*<sup>3</sup>*Institute of Nuclear Energy Research, Lung-Tan, Taoyuan, Taiwan*

**Introduction** The dopamine transporters (DATs) and dopamine D2/D3 receptors are implicated in a variety of neuropsychiatric disorders. Both sites are also targets for drug treatment. Previous single photon emission computed tomography (SPECT) studies have demonstrated that co-injection of radioligand [99mTc]TRODAT for DAT and 123I-labeled iodobenzamide (123IBZM) for D2/D3 receptors image can assess both pre- (DATs) and postsynaptic sites (D2/D3 receptors) of the dopaminergic system simultaneously. The aim of this study was to measure both pre and post markers of dopaminergic system in drug naïve schizophrenia. **Methods** Seven drug naïve schizophrenia and eleven age-matched healthy controls were recruited. Each subject received one SPECT examination after intravenous administration of 740 MBq (20 mCi) [99mTc]-TRODAT and 185 MBq (5 mCi) [123IBZM]. SPECT data were acquired by a dual head gamma camera equipped with ultra-high resolution fan beam collimators. An equilibrium ratio model was used for data analysis. Two sets of SPECT data were obtained using energy windows of 15% centered on 140 keV for 99mTc and 10% asymmetric with a lower bound at 159 keV for 123I. Region of interest (ROI) analysis method was performed using predefined templates from magnetic resonance image (MRI). Cerebellum was used as a reference region. **Results** The major findings including (1) DATs binding had no significant changes between controls and schizophrenia ( $3.17 \pm 0.73$  vs.  $2.65 \pm 0.27$ ,  $p=0.052$ ). However, D2/D3 receptors binding was significantly lower in drug naïve schizophrenia than those in controls ( $3.90 \pm 0.58$  vs.  $2.79 \pm 0.54$ ,  $p=0.001$ ). (2) There was a well correlation of left to right binding for both DATs and D2/D3 receptors in controls (Pearson's correlation coefficient (pcc)=0.80,  $p=0.003$  for DATs, 0.96,  $p=0.000$  for D2/D3 receptors) but the left to right correlation was disappeared in schizophrenia (pcc=0.54,  $p=0.20$  for DATs, 0.70,  $p=0.08$  for D2/D3 receptors). (3) The asymmetric indices of post to pre binding were  $0.15 \pm 0.12$  in controls ( $p=0.002$ , one sample t-test) and  $0.02 \pm 0.12$  in schizophrenia ( $p=0.67$ , one sample t-test). **Conclusion** This study clearly demonstrates the feasibility of simultaneous imaging of both pre- and postsynaptic binding sites of the dopaminergic system in drug naïve schizophrenia with dual-isotope SPECT technique. The abnormalities of D2/D3 receptor binding support the dopamine hypothesis and further elucidate that schizophrenia might be a disease with postsynaptic but not presynaptic disturbance.

**DESMOTEPLASE (DSPA) DOES NOT INTERACT WITH OR CLEAVE THE NMDA RECEPTOR NR1 SUBUNIT: POSSIBLE MOLECULAR BASIS FOR IMPROVED TOLERABILITY IN TREATMENT OF ACUTE ISCHEMIC STROKE**

José Lopez Atalaya<sup>1</sup>, Karim Benchenane<sup>1</sup>, Hervé Castel<sup>1</sup>, Carine Ali<sup>1</sup>, Karl-Uwe Petersen<sup>2</sup>, Denis Vivien<sup>1</sup>

<sup>1</sup>*INSERM-Avenir GIP Cyceron, University of Caen, Caen, France*

<sup>2</sup>*PAION Deutschland, Aachen, Germany*

Over the last decade, tissue type plasminogen activator (tPA) has been implicated in a variety of brain functions. It is secreted from growth cones or extending neurites, modulates neurite outgrowth and promotes neuronal migration in vitro. tPA has also been involved in glutamatergic-dependent processes such as synaptic plasticity and long term potentiation. For example, tPA deficient mice display alterations in learning paradigms and memory processes. Similarly, tPA has been shown to play an important role in the pathogenesis of seizures, multiple sclerosis, trauma and ischemic brain injury 1. Thrombolysis by tissue type plasminogen activator (tt-PA) is currently the only approved treatment in acute ischemic stroke (NINDS, 1995)2. However, experimental models suggest that rt-PA could have deleterious effects by potentiating ischemic neuronal death. We have previously demonstrated that rt-PA promotes excitotoxic neuronal death by interacting with and cleaving the N-terminus of the NMDA receptor NR1 subunit, at arginine 260, thereby augmenting NMDA receptor-signalling 3-4. DSPA is a related plasminogen activator derived from bat saliva and lacks the Kringle2 domain. More recently, DSPA administered 3 to 9 hours after acute ischemic stroke in man, has been shown to produce high reperfusion rates and an improved clinical outcome with a favorably low bleeding risk 5. In this study, we demonstrate that DSPA, unlike rt-PA, neither interacts with nor cleaves the NR1 subunit. These data are consistent with the observation that, in contrast to rt-PA, DSPA does not potentiate NMDA-induced neuronal death in murine models 6. They provide a molecular basis that possibly explains why DSPA has a more favorable profile compared to rt-PA in the treatment of acute ischemic stroke.

**PHYSIOLOGICAL AND PATHOLOGICAL IMPLICATIONS OF THE tPA/NR1 INTERACTION : AN IMMUNIZATION-BASED INVESTIGATION**

**Hervé Castel**<sup>1</sup>, Karim Benchenane<sup>1</sup>, Monica Fernandez-Monreal<sup>4</sup>, José Lopez-Atalaya<sup>1</sup>, Rose-Marie Bluthé<sup>2</sup>, Michel Boulouard<sup>3</sup>, François Dauphin<sup>3</sup>, Eric T. MacKenzie<sup>4</sup>, Robert Dantzer<sup>2</sup>, Omar Touzani<sup>4</sup>, Carine Ali<sup>1</sup>, Denis Vivien<sup>1</sup>

<sup>1</sup>*INSERM-Avenir, Université de Caen, Caen, France*

<sup>2</sup>*Neurobiologie Intégrative, INRA, CNRS, Institut François Magendie, Université Bordeaux 2, Bordeaux, France*

<sup>3</sup>*UPRES EA 2126, Centre D'Etudes et de Recherches sur le Médicament de Normandie, Caen, France*

<sup>4</sup>*CNRS UMR 6185, Université de Caen, Caen, France*

Tissue-type plasminogen activator (tPA) is thought to be involved in several brain functions and dysfunctions. Its vascular thrombolytic activity led to its use for ischemic stroke treatment. However, increasing evidence suggests that tPA potentiates excitotoxic neuronal death. Accordingly, we have recently shown that tPA can directly modulate N-methyl-D-aspartate (NMDA) receptor signalling by cleaving the arginine 260 within the amino-terminal domain of the NR1 subunit (ATD-NR1). The deleterious effects of tPA during excitotoxic neuronal death suggests that blocking its effect on NMDA-signalling might improve stroke treatment without hindering its beneficial fibrinolytic action. To validate this postulate, and to investigate the relevance of tPA-mediated control of NMDA receptor signalling in vivo, we developed a protocol of immunization in mice against ATD-NR1 including the interaction domain with tPA. Complete Freund's adjuvant (CFA) or recombinant ATD-NR1 (amino acids 19-371) dissolved in CFA were injected intraperitoneally once a week during four weeks. By immunoblotting, we show that sera harvested from immunized mice recognized recombinant ATD-NR1, while sera from control mice (CFA only) did not. We then postulated that the antibodies produced in the immune response might have a therapeutic value by physically preventing the interaction between tPA and NR1. We have thus performed excitotoxic lesions by injecting NMDA into the striatum of control and immunized mice, with or without intravenous injection of tPA (1 mg/kg). In CFA-injected animals, while NMDA alone led to an excitotoxic lesion of around 13 mm<sup>3</sup>, tPA, when injected intravenously, potentiated twice the lesions (29.5 mm<sup>3</sup>). In contrast, intravenous tPA was unable to potentiate NMDA-induced excitotoxic injury in ATD-NR1-vaccinated mice. No difference was observed between NMDA-induced lesion in naïve, CFA-, or ATD-NR1- vaccinated mice. We then addressed the relevance of this tPA/NMDA receptor interaction in brain physiology. Since tPA is thought to modulate some cognitive functions, we tested the immunized mice in a hippocampal-dependent spatial memory task (Y maze) that does not require previous learning. Locomotor activity was not different between naïve, CFA-injected and ATD-NR1-immunized mice. However, spatial memory was clearly impaired in ATD-NR1-immunized mice as compared to control or CFA-injected mice. This deficit was transient, since it disappeared 5 weeks after the last injection. Mice were also tested in an amygdala-dependent social discrimination task. Social memory was also impaired in immunized mice as compared to control or CFA-injected mice. The binding of endogenous tPA to NR1 is thus physiologically relevant, suggesting that the proteolytic activity of tPA is critical for some normal functions of NMDA receptors in the adult brain. In conclusion, this is the first in vivo demonstration that the ability of tPA to potentiate NMDA receptor signalling is critical, both during physiological and pathological brain conditions. Moreover, the immunization protocol developed here opens therapeutic and fundamental scientific interesting perspectives.

**CEREBRAL NICOTINIC ACETYLCHOLINE RECEPTORS IN PATIENTS WITH ALZHEIMER'S DISEASE OR VASCULAR DEMENTIA - EVALUATION WITH 2-[18F]F-A85380 AND POSITRON EMISSION TOMOGRAPHY (PET)**

**Kai Kendziorra**<sup>1</sup>, Philipp Meyer<sup>1</sup>, Henryk Barthel<sup>1</sup>, Georg Becker<sup>1</sup>, Dietlind Sorger<sup>1</sup>, Andreas Schildan<sup>1</sup>, Swen Hesse<sup>1</sup>, Marianne Patt<sup>1</sup>, Anita Seese<sup>1</sup>, Kristina Richter<sup>2</sup>, Eva Hammerstein<sup>2</sup>, Claus Zimmer<sup>3</sup>, Hermann Josef Gertz<sup>2</sup>, Osama Sabri<sup>1</sup>

<sup>1</sup>*Clinic of Nuclear Medicine, University Leipzig, Leipzig, Germany*

<sup>2</sup>*Clinic of Psychiatry, University Leipzig, Leipzig, Germany*

<sup>3</sup>*Department of Neuroradiology, Clinic of Radiology, University Leipzig, Leipzig, Germany*

**Objectives:** Although Alzheimer's disease (AD) has been recognized as a distinct clinical entity for nearly one hundred years now, its pathogenesis still remains unknown to a large extent. However, there is evidence in the literature for cholinergic mechanisms playing a crucial role in memory processes. Further, deterioration of memory and other cognitive functions in dementia, especially in AD, is known to be associated with a deficiency of nicotinic acetylcholine receptors (nAChR). Initial reports indicate that cholinergic drugs, known to be effective in AD, may bring a similar benefit to patients with vascular dementia (VaD). The mechanism of this cholinergic response in VaD remains poorly understood. The new radioligand 2-[18F]fluoro-3-(2(S)-azetidylmethoxy)pyridine (2-[18F]F-A85380) binds specifically to the  $\alpha 4\beta 2$  subtype of the nAChR. This PET study was initiated to investigate the state of the nAChR in different types of dementia. **Methods:** Thirteen patients with dementia of different aetiology and severity (6 with AD, 5 with VaD and 2 with mild cognitive impairment (MCI); Mini Mental State Examination (MMSE) = 6 to 27 points) underwent 2-[18F]F-A85380-PET (370 MBq; ECAT Exact HR+ scanner, Siemens/CTI, USA). In addition, five non-smoking healthy subjects were scanned as control group. Parametric images of the nAChR distribution volume (DV) were calculated using the Logan Plot. For this purpose, the radioactivity of the parent compound fraction obtained from arterial blood sampling and corrected for decay, plasma protein binding and radiolabelled metabolites, was used as input function. The DV data images were co-registered to a individual anatomical MRI using the mutual information algorithm implemented in BRASS (Hermes Medical Solutions, Sweden). Thus, the anatomical information was used to draw 22 individual sets of cortical or subcortical regions of interest. The corpus callosum was applied as a reference region to calculate the binding potential (BP). **Results:** In comparison to the control group, all patients with AD and four out of the five patients with VaD showed a significant reduction of the nAChR BP in different cortical and subcortical regions (thalami, both caudate heads, white matter bilateral, frontal cortex, brainstem, left occipital cortex;  $p=0.001-0.049$ ). In contrast, the two patients with MCI revealed no pathologic findings. For all patients, a positive correlation between the MMSE and the nAChR BP was observed in different cortical regions (right caudate head, brainstem, left temporal cortex;  $r=0.58$  to  $0.61$ ;  $p=0.005$  to  $0.009$ ). **Conclusions:** From these preliminary data in a small patient group it is concluded that 2-[18F]F-A85380-PET seems to be suitable to in vivo characterize the nAChR state in humans. Of interest, in our patients, nAChR availability was found to be a measure of dementia severity. The nAChR deficits detected in both AD and VaD provide evidence for an overlap between both entities with respect to cholinergic neurotransmission. The ongoing studies will serve to substantiate these preliminary findings with results from larger patient cohorts.

**DIRECT CEREBROVASCULAR EFFECTS OF CB1 RECEPTOR ACTIVATION BY THE SYNTHETIC ENDOCANNABINOID HU-210 IN VIVO**Marion A. Simpson<sup>1</sup>, J. Leanne Leith<sup>2</sup>, Linda Ferrington<sup>2</sup>, **Paul A.T. Kelly<sup>2</sup>**<sup>1</sup>*Division of Clinical Neuroscience, University of Edinburgh, Edinburgh, UK*<sup>2</sup>*Division of Neuroscience, University of Edinburgh, Edinburgh, UK*

**Background and Purpose:** In addition to their presence on central neuronal processes, cannabinoid (CB1) receptors, mediating vasodilatation, have also been identified on cerebral blood vessels (1). To investigate the possible role of CB1 receptors in cerebrovascular regulation in vivo, we examined the effects of the synthetic endocannabinoid HU-210 on local cerebral blood flow (LCBF) and glucose use (LCMRglu) in parallel groups of rats. **Methods:** Adult male Dark Agouti rats were injected with either 100mg/kg i.v. HU-210 (n=12) or saline with 5% propylene glycol and 2% Tween 80 (n=12). Measurement of LCBF (with [14C]-iodoantipyrine) or LCMRglu (with [14C]-2-deoxyglucose) was initiated at 30 and 20 minutes post-treatment respectively (2) in equal numbers from either treatment group. Tissue samples were dissected post mortem from hippocampus, striatum, and three neocortical brain areas for assessment of tracer concentrations (2). Mean arterial blood pressure (MABP) and heart rate (HR) were monitored constantly, and blood gases at intervals with the final measurement immediately before the start of blood flow measurements. Data (mean±SEM) were analysed by t-test, and LCBF/ LCMRglu ratios by Mann-Whitney U-test (P<0.05). **Results:** HU-210 significantly decreased MABP (from 142±1 to 105±6mmHg) and HR (from 484±6 to 232±18 beats.min<sup>-1</sup>), and significantly increased PaCO<sub>2</sub> (from 32.0±0.7 to 45.7±1.6 mmHg). These effects were established by 5 minutes and persisted relatively unchanged throughout the rest of the experimental period. HU-210 induced significant decreases in LCMRglu in all five brain regions examined, ranging from -19% in frontal cortex (from 69±1 to 55±3µmol.100g<sup>-1</sup>.min<sup>-1</sup>) to -31% in occipital cortex (from 60±1 to 41±2µmol.100g<sup>-1</sup>.min<sup>-1</sup>). In contrast, there was a tendency for LCBF to be increased in all regions following HU-210, although significant increases were found only in striatum (+19%; from 122±4 to 145±6ml.100g<sup>-1</sup>.min<sup>-1</sup>) and hippocampus (+16%; from 94±2 to 110±3ml.100g<sup>-1</sup>.min<sup>-1</sup>). However, the hypercapnia associated with HU-210 treatment could in itself result in cerebrovascular dilatation and increased cerebral blood flow. With a conservative correction factor introduced to allow for hypercapnia (3ml.mmHg<sup>-1</sup> rise in PaCO<sub>2</sub> from control mean), corrected LCBF values were found to be similar to control with no significant increases or decreases, despite the decreases in metabolism. Thus, even with a correction factor introduced for hypercapnia, HU-210 administration was associated with a change in the fundamental relationship that normally links cerebral perfusion to metabolic demand, and the ratios of flow to metabolism across the brain areas as a whole were significantly increased. The effect was most marked in parietal and occipital cortices where ratios increased from 2.25 and 2.03, to 2.83 and 2.61 respectively. **Conclusions:** The consistent increase in LCBF/ LCMRglu ratios throughout the brain suggests that, as well as its depressant effects on neuronal activity, HU-210 may also interact with cerebrovascular CB1 receptors to produce dilatatory effects which are independent of metabolic drive. This hyperaemia, relative to metabolic demand, could provide a contributory mechanism to the neuroprotective properties that have been reported for cannabinoids. 1. Gebremedhin D et al. (1999) *Am J Physiol* 276; H2085-2093. 2. Kelly PAT et al. (1994) *Brain Res* 665; 315-318.

**LOCAL CEREBRAL METABOLIC RESPONSE TO 8-OH-DPAT IN DARK AGOUTI RATS IS ALTERED BY PRIOR EXPOSURE TO 3,4,- METHYLENEDIOXYMETHAMPHETAMINE (MDMA)**

Linda Ferrington<sup>1</sup>, J. Lianne Leith<sup>1</sup>, Douglas E. McBean<sup>2</sup>, Henry J. Olverman<sup>1</sup>, Paul A.T. Kelly<sup>1</sup>

<sup>1</sup>*Division of Neuroscience, University of Edinburgh, Edinburgh, UK*

<sup>2</sup>*School of Health Sciences, Queen Margaret University College, Edinburgh, UK*

Introduction: A single exposure to 3,4,-methylenedioxyamphetamine (MDMA) induces serotonergic terminal depletion in Dark Agouti (DA) rats (1), although by six weeks post-MDMA cerebral function is normalised (2). The compensatory mechanisms that follow initial MDMA-induced effects on cerebral glucose use (LCMRglu) are unclear, although alterations in serotonergic receptors may be involved. In this study we examined the effects of the selective 5-HT<sub>1A</sub> agonist, 8-OH-DPAT upon LCMRglu in DA rats exposed to MDMA six weeks previously. Methods: DA rats were injected i.p. with MDMA (15mg.kg<sup>-1</sup>) or saline (both n=10). 6 weeks later equal numbers from each group were injected i.v. with 8-OH-DPAT (1mg.kg<sup>-1</sup>) or saline 1 minute prior to the measurement of LCMRglu using [14C]-2-deoxyglucose quantitative autoradiography. Data (mean±sem) from 62 brain areas were analysed using t-test with Bonferroni correction (p<0.05). Results: There were no significant differences between pre-treatment groups in either physiological variables or LCMRglu following acute saline. In both pre-treatment groups 8-OH-DPAT produced significant decreases in MABP (137±3 to 119±4mmHg in saline and 138±2 to 121±3 mmHg in MDMA), temperature and heart rate. In saline pre-treated rats, 8-OH-DPAT produced widespread reductions in LCMRglu significantly different from control in 28 of the 62 brain areas analysed. Most marked significant decreases were observed in motor areas (entopeduncular nucleus, from 58±9 to 33±3 mmol.100g.min<sup>-1</sup>) limbic areas (medial amygdala, 58±7 to 30±4) neocortex (entorhinal cortex, 70±3 to 49±3) and raphé nuclei (median raphé, 87±3 to 66±4; paramedian raphé, 82±3 to 61±4). Significant increases in LCMRglu were observed in just 3 brain areas (frontal cortex layer IV, 109±5 to 140±9; layer VI 90±4 to 107±5). In keeping with previous work (Quate et al, 2004), MDMA pre-treatment produced a statistically significant 33% reduction in 5-HT receptor binding (p<0.05). With the exception of hippocampus, in the MDMA group 8-OH-DPAT-induced reductions in LCMRglu were both less widespread and less marked (range -4 to -45%), in comparison with responses observed in the saline group (-16% to -60%) while 8-OH-DPAT-induced increases in LCMRglu observed in saline animals were potentiated. Significant reductions in LCMRglu were observed in 7 brain areas most markedly in limbic areas (medial amygdala from 61±4 to 33±4 mmol.100g.min<sup>-1</sup>; ventral CA1, 62±2 to 41±4). Significant increases in LCMRglu were observed in 11 brain regions predominantly in neocortex (frontal layer IV, 97±3 to 164±6; layer VI, 84±3 to 126±7; sensorimotor layer IV, 105±4 to 162±11; layer VI, 89±3 to 133±7) although significant increases were also observed in motor and limbic areas. In hippocampus 8-OH-DPAT produced similar significant reductions in LCMRglu in both groups. (e.g. dorsal CA1, saline: 57±2 to 41±3; MDMA: 55±2 to 45±3). Conclusions: These results suggest that MDMA-induced serotonergic depletion is followed by changes in 5-HT<sub>1A</sub> receptor function. However, the effects of these changes are not uniform throughout the brain and may reflect the relative importance of 5-HT<sub>1A</sub> autoreceptors and postsynaptic 5-HT<sub>1A</sub> receptors, particularly in hippocampus. References: Quate L., et al (2002) BJP, 137: 127P Quate, L., et al. (2004) FENS Abstr. 2, A219.9. This study was funded by EC Grant No. QLG3-CT-2002-00809

## SEROTONIN 2A RECEPTOR BINDING IN HEALTHY TWINS GENETICALLY PREDISPOSED TO MAJOR DEPRESSION IN COMPARISON WITH UNDISPOSED CONTROLS

Vibe G. Frokjaer<sup>1</sup>, Maj V. Christensen<sup>2</sup>, Kirstine A. Bojsen-Moller<sup>1</sup>, Erik L. Mortensen<sup>3</sup>, William Baare<sup>4</sup>, Claus Svarer<sup>1</sup>, Jakob Madsen<sup>5</sup>, Lars V. Kessing<sup>2</sup>, Gitte M. Knudsen<sup>1</sup>

<sup>1</sup>Neurobiology Research Unit, Copenhagen University Hospital Rigshospitalet, Copenhagen, Denmark

<sup>2</sup>Department of Psychiatry, Copenhagen University Hospital Rigshospitalet, Copenhagen, Denmark

<sup>3</sup>Institute of Public Health, University of Copenhagen, Copenhagen, Denmark

<sup>4</sup>Danish Magnetic Resonance Center, Hvidovre University Hospital, Hvidovre, Denmark

<sup>5</sup>PET and Cyclotron Unit, Copenhagen University Hospital Rigshospitalet, Copenhagen, Denmark

**Introduction.** Disturbances in serotonergic transmission is involved in the pathophysiology of depression. Previous PET studies have been inconsistent with regard to the direction and regional distribution of the 5-HT<sub>2A</sub> alterations in major depression. Genetic factors play an ethiological role in both major depression and personality profiles. In particular a high neuroticism score is known to be associated with an increased risk of developing major depression. We tested whether the regional cerebral 5-HT<sub>2A</sub> receptor binding differed between a group of genetically predisposed twins and a group of undisposed controls. Further, we tested if differences in personality traits of the neuroticism dimension, within the predisposed group, correlated to the regional 5-HT<sub>2A</sub> receptor binding. **Materials and methods.** Twelve healthy twins (median age 44 (22-61)) genetically predisposed to depression and 12 healthy and undisposed volunteers (median age 46 (22-63)) were investigated with MRI and [18F]-altanserin PET. Female:male ratio was 9:3 in both groups reflecting the profile in depression. The steady-state binding potential (BP<sub>1</sub>) was determined in 19 brain regions using cerebellum as a reference region and metabolite corrected plasma concentration. All subjects completed the NEO-PI-R personality questionnaire, which evaluates the broad personality dimensions of neuroticism, extraversion, openness, agreeableness, and conscientiousness each based on 6 personality traits. Group comparisons between regional 5-HT<sub>2A</sub> receptor binding were performed using the Mann-Whitney test. In a multiple linear regression analysis of data from the predisposed group, the personality trait scores of the neuroticism dimension were compared to the regional 5-HT<sub>2A</sub> receptor binding with adjustment for age and gender. **Results.** The regional 5-HT<sub>2A</sub> receptor binding did not differ between the subjects genetically predisposed to depression and the undisposed controls. In the predisposed group, we found a trend towards a positive correlation between the cortical 5-HT<sub>2A</sub> receptor binding and the personality trait depression, a component of neuroticism. The trend ( $p < 0.10$ ) was found in the following limbic regions: 1. left anterior cingulate ( $r = 0.66$ ,  $p = 0.051$ ), 2. right entorhinal cortex ( $r = 0.60$ ,  $p = 0.082$ ), and 3. left entorhinal cortex ( $r = 0.62$ ,  $p = 0.070$ ). In addition, a positive correlation between 5-HT<sub>2A</sub> receptor binding and the anxiety component of neuroticism was found in the right entorhinal cortex ( $r = 0.72$ ,  $p = 0.027$ ). **Conclusion.** Our preliminary data did not show any significant difference between the subjects genetically predisposed to depression and the undisposed controls. In the predisposed group, a positive correlation between 5-HT<sub>2A</sub> receptor binding and the anxiety component of neuroticism was found in the right entorhinal cortex. Furthermore, a trend towards a positive correlation between the personality trait depression and the 5-HT<sub>2A</sub> receptor binding was present in limbic regions. If reproduced in the larger sample, this suggests that in subjects at risk for major depression limbic 5-HT<sub>2A</sub> receptor binding may serve as a trait marker for major depression.

**NICOTINIC ACETYLCHOLINE RECEPTORS IN PATIENTS WITH PARKINSON'S DISEASE AND ALZHEIMER'S DISEASE: SPECIFIC BINDING OF 2-[18F]F-A-85380 IN THE CEREBRAL WHITE MATTER AS DEMONSTRATED BY PET AND COMPARISON WITH DIFFUSION TENSOR MRI (DTI)**

**Philipp Meyer**<sup>1</sup>, Donald Lobsien<sup>2</sup>, Kai Kendziorra<sup>1</sup>, Henryk Barthel<sup>1</sup>, Swen Hesse<sup>1</sup>, Georg Becker<sup>1</sup>, Andreas Schildan<sup>1</sup>, Marianne Patt<sup>1</sup>, Dietlind Sorger<sup>1</sup>, Anita Seese<sup>1</sup>, Annette Foerschler<sup>2</sup>, Florian Then Bergh<sup>3</sup>, Peter Brust<sup>4</sup>, Jörg Steinbach<sup>4</sup>, Hermann-Josef Gertz<sup>5</sup>, Johannes Schwarz<sup>3</sup>, Claus Zimmer<sup>2</sup>, Osama Sabri<sup>1</sup>

<sup>1</sup>*Department of Nuclear Medicine, University Hospital, University of Leipzig, Leipzig, Germany*

<sup>2</sup>*Department of Radiology (Neuroradiology), University Hospital, University of Leipzig, Leipzig, Germany*

<sup>3</sup>*Department of Neurology, University Hospital, University of Leipzig, Leipzig, Germany*

<sup>4</sup>*Institute for Interdisciplinary Isotopic Research, Leipzig, Germany*

<sup>5</sup>*Department of Psychiatry, University Hospital, University of Leipzig, Leipzig, Germany*

**INTRODUCTION:** In post mortem studies, alterations of the alpha4beta2 subunits of the nicotinic acetylcholine receptors (alpha4beta2 nAChR) were found in the cortex and in the subcortical nuclei of patients with Parkinson's disease (PD) and Alzheimer's disease (AD) (Pimlott SL, 2004). The availability of alpha4beta2 nAChRs on subcortical projection fibers in the cerebral white matter (WM) in vivo has neither been demonstrated nor quantified in PD or AD. The aims of this study were: (i) to test the hypothesis that the availability of the nAChR in the WM can be assessed quantitatively by using positron emission tomography (PET) and the radioligand 2-[18F]F-A-85380 (2-FA), which binds on alpha4beta2 nAChR with high affinity and selectivity, (ii) to evaluate whether the availability of the nAChR is altered in the WM of patients with PD and AD and (iii) to investigate whether there are systematic differences between PD and AD with regard to axonal damage as studied with diffusion tensor MRI (DTI). **METHODS:** Seven patients with PD (39-70 yrs; UPDRS-III: 8-49), 4 patients with AD (71-81 yrs; MMSE: 6-22) and 5 normal subjects (37-64 yrs) were studied over a time period of 7 hours using 2-FA PET. In addition, 4 subjects were studied with 2-FA PET before and after smoking of one cigarette (approx. 0.9mg nicotine; 7-8 hours p.i.). DTI: The fractional anisotropy (FA), which is a measure of the axonal degeneration, was assessed. The results were normalized (reference region: corpus callosum) and expressed as relative FA (rel-FA). 2-FA PET: Distribution volumes were calculated using the Logan plot after correction of the arterial input function for plasma protein binding and radioactive metabolites. After co-registration with the individual MRI (DTI), the binding potential (BP) in 10 ROIs was assessed. **RESULTS:** Smoking of one cigarette resulted in a displacement of the radioactivity from thalamus (44.5%), brain stem (29.3%) and periventricular white matter (31.8%). In comparison with normal subjects, increased 2-FA-BP were found in PD and AD in the right capsula interna (PD +58.2% [p<0.05], AD +32.0%), left capsula interna (+14.1%, +5.8%) and periventricular (+48.5%, +32.9%). Rel-FA (DTI) in PD: capsula interna (PD +10.0%; AD +2.0%), periventricular (PD -4%; AD +32%). In patients with PD, a negative correlation between 2-FA-BP in the periventricular white matter and MMSE (Rho=-0,88; p<0.05) was demonstrated. **CONCLUSIONS:** Smoking of one cigarette results in a relevant displacement of 2-FA all brain regions including the cerebral white matter. This indicates that 2-FA binds specifically on subcortical cholinergic projection fibers. The increased 2-FA-BP in the white matter in patients with PD and AD may be a result of a denervation supersensitivity and / or hyperexpression of nAChRs as a result of neuroinflammation, which may coincide with PD and AD, respectively. The number of patients which have been studied is relatively small. However, our initial results suggest that 2-FA-PET combined with diffusion tensor MRI bears the potential to assess in vivo axonal neurodegeneration and its functional consequences on cholinergic neurotransmission. **REFERENCES:** Pimlott SL, et al. Neuropsychopharmacology 2004; 29, 108-116



**NEUROSTEROIDS SENSITIZE FEMALE MICE TO STRESS**

Althea S. Hayden<sup>2,3</sup>, Veronique Devignot<sup>2,3</sup>, John P. Adelman<sup>2</sup>, James Maylie<sup>3</sup>,  
**Paco S. Herson<sup>1</sup>**

<sup>1</sup>*Department of Anesthesiology & Peri-Operative Medicine, OHSU, Portland, OR, USA*

<sup>2</sup>*Vollum Institute, OHSU, Portland, OR, USA*

<sup>3</sup>*OB/GYN, OHSU, Portland, OR, USA*

**Introduction:** Episodic Ataxia type-1 (EA1) is a hereditary human neurological disorder that causes stress-induced loss of motor coordination. In EA1 mice, as in their human counterparts, stress results in ataxia and loss of motor coordination [1]. At the cellular level EA1 mice have altered GABA synaptic activity in cerebellar Purkinje neurons that may underlie the behavioral phenotype [1]. Our EA1 mice have revealed a striking gender bias, with females being much more sensitive to stress. Therefore, we tested the hypothesis that females are more sensitive to stress due to the presence of ovarian hormones that affect the GABAergic system. **Methods:** Behavior: The duration the mice are able to run before falling off the accelerating rotarod (latency) was used to assess motor coordination. On the day of experimentation mice were given five baseline trials followed by our stress paradigm consisting of i.p. injection of 10 mg/kg isoproterenol (ISO) and 20 min. forced exercise, followed by 3 final rotarod trials. Electrophysiology: Sagittal cerebellar slices (400  $\mu$ M thick) were prepared from WT and EA1 littermates (8-12 weeks old). Whole-cell voltage clamp experiments were made from Purkinje cells visualized with infrared DIC on a Leica DMLFS upright microscope. Spontaneous Purkinje cell GABA currents (sIPSCs) were recorded at  $-60$  mV using a standard CsCl based internal solution. **Results:** We have found that only female EA1 mice experience impaired motor coordination in response to stress as measured by the accelerating rotarod, reducing their latency from  $56.1 \pm 3.8$ s to  $37.6 \pm 4.9$ s ( $n=15$ ; ANOVA  $p < 0.05$ ). Pre-treatment of wild-type mice with 1 mg/kg ALLO (a progesterone metabolite that is a potent positive modulator of GABAA receptors [2,3]) also resulted in a gender specific effect following stress, altering the latency of female mice from  $61.6 \pm 4.1$ s to  $30.6 \pm 3.8$ s ( $n=8$ ; ANOVA  $p < 0.05$ ), while having a significantly smaller effect on male mice ( $n=8$ ). Injection of picrotoxin (GABAA antagonist) prior to treatment with ALLO prevented the sensitizing effects of ALLO in female mice ( $n=7$ ), indicating that ALLO caused its behavioral effects by enhancing GABAergic transmission. In addition, ovariectomy abolished the increased sensitivity observed in female mice ( $n=7$ ). Consistent with our behavioral data, GABAA receptor currents recorded in female Purkinje cells are 10-fold more sensitive to potentiation by ALLO than GABAA receptor currents recorded from male Purkinje cells. **Conclusion:** Increased GABA activity onto Purkinje cells increases sensitivity to stress-induced loss of motor coordination [1]. The progesterone metabolite ALLO, a positive modulator of GABAA receptor activity, sensitizes female mice to stress to a greater degree than male mice. The presence of ovarian sex steroids is required to maintain the gender difference in sensitivity to ALLO. Behavior and electrophysiology data indicate that female GABA activity is more sensitive to ALLO than male GABA activity in the cerebellum. **References:** 1. Herson PS et al. (2003) *Nature Neuroscience* 6(4):378-383 2. Majewska MD et al. (1986) *Science* 232(4753):1004-1007 3. Paul SM & Purdy RH (1992) *FASEB J* 6(6):2311-2322

**EFFECT OF RIVASTIGMINE ON BRAIN BUTYRYLCHOLINESTERASE  
ACTIVITY IN PATIENTS WITH ALZHEIMER'S DISEASE**

**Juha O. Rinne**<sup>1</sup>, Jere Virta<sup>1</sup>, Kjell Nagren<sup>1</sup>, Tarja Jarvenpaa<sup>1</sup>, Anne Roivainen<sup>1</sup>,  
Vesa Oikonen<sup>1</sup>, Timo Kurki<sup>2</sup>

<sup>1</sup>*Turku PET Centre, Turku, Finland*

<sup>2</sup>*Department of Radiology, Turku University Hospital, Turku, Finland*

**Objective.** First to assess brain butyrylcholinesterase (BuChE) activity and to characterize the distribution of cerebral BuChE activity in healthy volunteers. Second to evaluate the effect of rivastigmine (an inhibitor of both acetylcholinesterase and BuChE) on brain BuChE activity in patients with Alzheimer's disease (AD). **Methods:** A specific BuChE tracer, N-[11C]methyl-4-piperidyl n-butyrate ([11C]MP4B), and 3D PET imaging with MRI co-registration for anatomical reference were used for in vivo assessments of BuChE activity using GE Advance PET scanner. The rate constant (k<sub>3</sub>) for hydrolysis of [11C]MP4B reflecting BuChE activity was calculated using metabolite purified plasma as an input function. Average left and right hemisphere values were used for the analyses. **Results.** In healthy controls (n=7) k<sub>3</sub> values were highest in the cerebellum followed by pons, striatal structures and thalamus, while lower k<sub>3</sub> values was seen in the cortical areas. AD patients treated with rivastigmine (n=5) showed around 50% inhibition of BuChE activity, compared with control values. **Conclusions.** BuChE distribution in healthy volunteers was in accordance with that previously reported in post mortem studies of human brain, indicating that [11C]MP4B PET is a valid indicator of cerebral BuChE activity in humans in vivo. This is further supported by rivastigmine-induced inhibition of brain BuChE activity in patients with AD. Further studies his may have important clinical implications, since BuChE may represent a large part of cholinesterase activity as AD progresses, and because of its apparent association with amyloid plaques and neurofibrillary tangles.

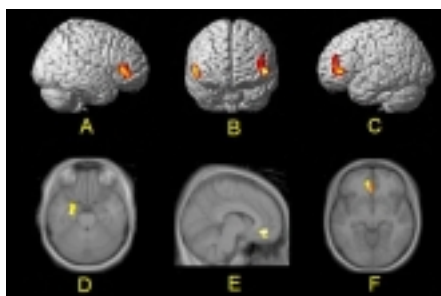
## CORTICAL DOPAMINE RELEASE DURING WORKING MEMORY AND ATTENTION IN HUMANS

Sargo Aalto<sup>1</sup>, Anna Bruck<sup>2</sup>, Matti Laine<sup>1</sup>, Kjell Nagren<sup>2</sup>, **Juha O. Rinne<sup>2</sup>**

<sup>1</sup>*Abo Akademi University, Turku, Finland*

<sup>2</sup>*Turku PET Centre, Turku, Finland*

High-affinity dopamine D2 receptor tracer, [11C]FLB 457 competes in binding with endogenous dopamine, and according to the binding competition principle, the decrease in the binding potential indirectly indicates dopamine release. We explored the cortical dopaminergic correlates of cognition in vivo in humans using [11C]FLB 457 and a within-subject counter-balanced displacement paradigm. The design included a baseline resting state and two cognitive tasks, working memory (2-back) and vigilance (0-back). Twelve healthy male volunteers were studied with a GE Advance PET scanner in 3D mode. Each subject was scanned three times (rest, 0-back, 2-back) using a 69 min [11C]FLB 457 scanning period. The n-back tasks continued throughout the duration of the scan. ROI analysis showed that BP of [11C]FLB 457 decreased in the ventrolateral frontal cortex (VLFC), the medial temporal lobe (MT) and the ventral anterior cingulate (AC), indicating task-related increases in dopamine concentration. We found an average decrease of 11.3 % (left 9.4%; right 13.2%) of BP in the VLFC bilaterally ( $F_{1,6}=14.50$ ,  $p=0.008$ ) and a 14 % decrease in the left MT ( $F_{1,6}=14.28$ ,  $p=0.009$ ) during the working memory task compared to the vigilance task. In the left ventral AC, the vigilance task induced an 11 % decrease in BP compared to the baseline condition ( $F_{1,6}=16.88$ ,  $p=0.006$ ), whereas the working memory task induced an 8.5 % decrease in BP from the baseline level ( $F_{1,6}=13.49$ ,  $p=0.01$ ). The main effect of the condition was not significant in the inferior parietal cortex ( $F_{2,12}=1.01$ ,  $p=0.39$ ) or in the dorsolateral frontal cortex ( $F_{2,12}=0.63$ ,  $p=0.55$ ). An independent SPM analysis confirmed the results of the ROI analysis (Figure). The reaction times showed that the participants performed well throughout the lengthy cognitive tasks. Our results reveal regional dopamine release during vigilance and working memory tasks in vivo in man and demonstrates a novel approach, where PET imaging enables non-invasive examination of the involvement of the cortical dopamine systems in cognitive functions in healthy humans. Further methodological development could enable to detect also short duration dopaminergic effects during various behavioural tasks. Figure legend: Visualization of SPM analysis. In comparison to the vigilance task, the binding potential (BP) of [11C]FLB 457 decreased during the working memory task bilaterally in the VLFC (panels A – C) and in the left medial temporal cortex (panel D). Compared to the resting baseline, both the vigilance task (panel E) and the working memory task (panel F) induced a decrease in the BP of [11C]FLB 457 in the left ventral AC. Reference: Aalto S, Brück A, Laine M, Nägren K, Rinne J.O. Frontal and temporal dopamine release during working memory and attention tasks in healthy humans – a PET study using high-affinity dopamine D2 receptor ligand [11C]FLB 457. in press, Journal of Neuroscience.



## NICOTINIC ACETYLCHOLINE RECEPTORS IN THE PATIENTS WITH PARKINSON'S DISEASE: 5IA-SPECT

**Kazuo Hashikawa**<sup>1</sup>, Hidefumi Yoshida<sup>1</sup>, Nobukatsu Sawamoto<sup>1</sup>, Shigetoshi Takaya<sup>1</sup>, Chihiro Namiki<sup>1</sup>, Hiroko Nishi<sup>1</sup>, Tomohiko Asada<sup>1</sup>, Kenichi Oishi<sup>1</sup>, Kenji Aso<sup>1</sup>, Kazumi Iseki<sup>1</sup>, Hidekazu Kawashima<sup>2</sup>, Koichi Ishizu<sup>2</sup>, Hideo Saji<sup>3</sup>, Hidenao Fukuyama<sup>1</sup>

<sup>1</sup>*Human Brain Research Center, Kyoto University Graduate School of Medicine, Kyoto, Japan*

<sup>2</sup>*Department of Nuclear Medicine and Diagnostic Imaging, Kyoto University Graduate School of Medicine, Kyoto, Japan*

<sup>3</sup>*Department of Patho-Function Bioanalysis, Kyoto University Graduate School of Pharmaceutical Science, Kyoto, Japan*

**Introduction:** In the post mortum examinations, the loss of the nicotinic acetylcholine receptors (nAChRs) was reported in the patients with Parkinson's disease. So the dysfunction of nicotinic nerve system might have some roles in their symptoms, both motor dysfunction and cognitive impairments. In this study, we investigate the densities of nAChRs in the patients with Parkinson's disease without cognitive deficits. **Methods:** We selected two groups of patients by their symptoms, tremor dominant and akinesia dominant. A group of tremor dominant (Group T: mean age = 67.2±7.8 y.o.) was consisted of 5 patients whose chief complaint is tremor and had no apparent akinesia. A group of akinesia dominant (Group A: mean age = 69.4±7.8) was consisted of 5 patients, who had akinesia but no apparent tremor. Five healthy volunteers with no history of smoking (Group C: age = 54.2±11.1) were also studied for control. Ninety-minute dynamic SPECT acquisition was performed just after an intravenous injection of approximately 167 MBq of 123I 5-iodo-A-85380 (5IA), a specific radioligand for the  $\alpha 2\beta 4$  subtype of nAChRs[1]. Additional 20 min dynamic SPECT images around 2 hours, 3 hours and 4 hours after the injection were performed. Using filtered back projection with Butterworth filter for pre-filter and Chang method for attenuation correction, total 75 frame dynamic transaxial images were obtained. Simultaneously, twenty-seven arterial samples were withdrawn from the cubital artery. The pure 5IA concentrations were obtained by the metabolite correction by TLC-plate for each subject and used as the input function in following kinetic analyses. Regions of interests were settled on the cortices, the thalamus, the pons, the cerebellum and the basal ganglia. The distribution volumes (DV) were calculated by using 2-compartment model. **Results:** In the visual analysis of the images at 4 hours after the injection, the highest uptakes were observed in the thalamus and the brain stem, moderate uptakes in the cerebellum and basal ganglia and the lowest in the cortices in all groups. Among cortices, the uptakes in the occipital lobes were lower than those in other cortices. The DV values of Group A, Group T and Group C were 10.1±12.4, 12.4±2.1 and 13.8±2.5 at the frontal cortices, 10.6±1.8, 12.7±2.3 and 14.6±3.0 at the parietal cortices, 11.0±2.0, 13.3±2.6 and 14.3±2.7 at the temporal cortices, 9.8±1.9, 12.3±2.6 and 13.5±2.8 at the occipital cortices, 13.9±3.4, 17.3±4.3 and 18.2±4.3 at the cerebellum, 18.6±4.1, 22.0±3.9 and 25.5±5.8 at the thalamus, 14.5±2.3, 17.3±3.9 and 20.1±3.9 at the pons, 13.1±2.5, 15.1±2.8 and 16.4±3.2 at the basal ganglia, respectively. In all regions, the mean values of DV are the lowest in Group A, the middle in Group T and the highest in Group C. The mean values of DV of Group A were significantly lower than those of Group C at the frontal, parietal, occipital cortices, thalamus and pons ( $p < 0.05$ ). **Conclusion:** This result suggests that nicotinic nerve function might be related to akinesia in Parkinson's disease.

**References:** [1] Saji H, et al; *Ann Nucl Med* 16:189-200, 2002.

[2] Mamede H, et al., *J Nucl Med* 45: 1458-70, 2004.



## THE INFLUENCE OF PROLONGED HYPOKINESIA ON THE LEVELS OF GABA, GLUTAMATE AND GLYCINE IN WHITE RAT BRAIN CORTEX

Vilen P. Hakobyan, Oleg P. Sotckiy, Lusine G. Zhamharyan, Varduhi H. Karapetyan,  
Irena Z. Loryan

*Yerevan State Medical University after M. Heratsi, Department of Pharmacology, Yerevan,  
Armenia*

**INTRODUCTION:** It has been established recently restricted movement activity or hypokinesia (HK) is a peculiar chronic stress and it is the most significant risk factor in the development of cardio- and cerebrovascular, metabolic diseases, neurological and behavioral disorders etc. During last years a considerable attention has been given to the metabolism of neuroactive amino acids (GABA, Glutamate and Glycine) with the connection of their adaptive role in stress situations. The specific aim of this study is determination of the influence of hypokinesia (15, 30 and 45 days) on GABA, Glutamate and Glycine levels in the rats' brain cortex. **DESIGN AND METHODS:** White male rats (n=36) were killed by decapitation after anesthetizing with Nembutal 40mg/kg IP. HK was achieved by placing rats in the individual narrow Plexiglas cages during 15, 30 and 45 days. Isocratic separation of GABA, Glutamate and Glycine derivatives (derivatized by O-phthalaldehyde) obtained using a reverse-phase HPLC-system with electrochemical detection, which comprised 150x4.6mm "Nucleosil" 100-5 C18 column. The mobile phase comprised phosphate buffer at pH5.6 containing 5% methanol. Statistical data manipulation was performed by software SPSS11.0. Statistical significance of the data was computed by two-way analysis of variance followed by Student's *t* test. **RESULTS:** The analysis of GABA and Glutamate contents in the brain cortex has shown decrease in the all studied periods which is more expressed on the 45<sup>th</sup> day of HK. So, the content of GABA on the 45<sup>th</sup> day of HK valid decreased by 49,28% (p=0.0005) compared to the control (258.3±52.8mcg/g – in control group and 131±21.2mcg/g – after 45-day HK). The decrease in Glutamate level was statistically valid compared to the control during the all studied periods (2.9±0.58mg/g – in control group; 2.07±0.29mg/g – after 15-day HK (p=0.02); 2.04±0.15mg/g – after 30-day HK (p=0.001); 1.5±0.1mg/g – after 45-day HK (p=0.005)). The analysis of Glycine level has shown statistically valid increased by 74% (p=0.03) on the 30<sup>th</sup> day of HK compared to the control (72.1±17.2mcg/g – in control group and 125.6±40.3mcg/g – after 30-day HK). The changes in Glycine level on the 45<sup>th</sup>-day of HK were analogous to GABA and Glutamate, but decrease comparison with control was statistically invalid. **CONCLUSION:** Earlier, we showed decrease of brain's energetic metabolism under the conditions of HK. By comparison of energy metabolism changes with GABA and Glutamate contents we can suppose the participation of these neuroactive amino acids in Robertson's GABA-shunt. Taking into consideration the reducing of Glycine's level on the 45<sup>th</sup>-day of HK we attempt to explain by means of Glycine deamination into pyruvate and its subsequent oxidation into TCA-cycle. Thus, we can conclude that neuroactive amino acids form their adaptive ability not only by neurotransmission but also by participation in energy metabolism.

**IN VIVO IMAGING OF BETA-AMYLOID LOAD IN TRANSGENIC RODENTS  
WITH [F-18]FDDNP MICROPET**

Vladimir Kepe<sup>1</sup>, Gregory M. Cole<sup>2</sup>, Jie Liu<sup>1</sup>, Dorothy G. Flood<sup>3</sup>, Stephen P. Trusko<sup>3</sup>,  
Nagichettiar Satyamurthy<sup>1</sup>, Sung-Chen Huang<sup>1</sup>, Gary W. Small<sup>1</sup>, Andrej Petric<sup>4</sup>,  
Michael E. Phelps<sup>1</sup>, **Jorge R. Barrio**<sup>1</sup>

<sup>1</sup>*UCLA David Geffen School of Medicine, Los Angeles, CA, USA*

<sup>2</sup>*VA Medical Center, Sepulveda, CA, USA*

<sup>3</sup>*Cephalon Inc., West Chester, PA, USA*

<sup>4</sup>*University of Ljubljana, Ljubljana, Slovenia*

**Introduction:** The availability of various animal models of Alzheimer's disease (AD) gives us a unique opportunity to study in detail the neuropathological processes characteristic for this disease. The triple transgenic rat model of beta-amyloid deposition, recently developed by Cephalon Inc. and Xenogen Biosciences, expressing high levels of beta-amyloid deposits in aged animals, is an excellent target for the microPET imaging due to the much larger brain size compared with mice. In our work we applied microPET with [F-18]FDDNP, a beta-amyloid binding molecular probe, to visualize the beta-amyloid deposits and to quantitate the beta-amyloid load in the living brains of these animals with the purpose of beta-amyloid load monitoring. **Methods:** All animal scans were performed with a Concorde Focus microPET camera and the scan duration was 60 min after the tracer injection. The animal population consisted of 3 triple transgenic rats aged 15 months and of 2 control rats (Sprague-Dawley) aged 9 months. The data analysis was performed on the dynamic images which were reconstructed using filtered backprojection reconstruction. The dynamic images were also used to perform Logan plot graphical analysis with cerebellum as reference region and to generate the distribution volume (DV) parametric images. Regions of interest were drawn on several cortical regions and on hippocampus and were used to extract the time-activity curves from the dynamic images and DV values from the parametric images for all ROIs. **Results:** We have observed the elevated levels of [F-18]FDDNP binding (compared to cerebellum) in several cortical regions but not in the subcortical regions or white matter regions (DV: frontal  $1.32 \pm 0.04$ ,  $p < 0.0005$ ; hippocampus  $1.23 \pm 0.05$ ,  $p = 0.001$ ). This pattern of cortical signal distribution correlates well with the known distribution of beta-amyloid deposits in the brains of these rats where cortical regions have dense deposits of plaques but the subcortical areas and cerebellum either have very low level of the deposits or are free of them. As expected, the results of the experiments performed on controls animals do not show any significant signal above the cerebellar level neither in cortical nor in subcortical regions (DV: frontal  $1.04 \pm 0.01$ ; hippocampus  $0.99 \pm 0.04$ ). **Conclusions:** [F-18]FDDNP microPET is the first successful method for in vivo visualization of the beta-amyloid load in any rodent transgenic model of Alzheimer's disease which for the first time opens the possibility of temporal monitoring of the beta-amyloid load changes in these animals. It also opens the possibility of monitoring the beta-amyloid load changes which may result from the therapeutic interventions.

## BP-2

### SIMPLIFIED QUANTIFICATION OF PIB AMYLOID IMAGING PET STUDIES

Brian J. Lopresti<sup>1</sup>, William E. Klunk, Chester A. Mathis, Jessica A. Hoge, Scott K. Ziolkowski, Xueling Lu, Carolyn C. Meltzer, Steven T. DeKosky, Julie C. Price

<sup>1</sup>Radiology, Psychiatry, and Neurology, University of Pittsburgh, Pittsburgh, PA, USA

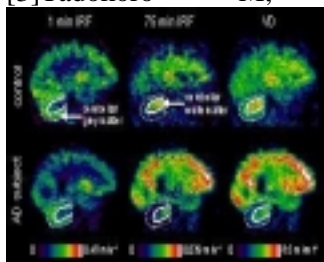
**Introduction.** We recently reported the first positron emission tomography (PET) studies of the [C-11]-labeled amyloid-binding radiotracer, Pittsburgh Compound-B (or PIB), performed in Uppsala, Sweden. These semi-quantitative studies showed greater PIB retention in Alzheimer's disease (AD) patients, relative to healthy control subjects (parietal;  $p=0.0002$ ) that was consistent with amyloid deposition in AD. Quantitative PIB studies have been performed in Pittsburgh in three groups: AD, mild cognitive impairment (MCI), and healthy controls. The present study compares arterial and reference tissue measures of PIB retention. **Methods.** PET studies were performed over 90 min (ECAT HR+, 14±2 mCi) in 16 patients (6 mild-moderate AD: 67±10yrs; 10 MCI: 72±9 yrs) and 8 controls (65±16 yrs). Arterial blood was collected and metabolite-corrected input functions were determined. Magnetic resonance images were acquired for region-of-interest definition and atrophy correction of the PET data. Regional PIB distribution volume (DV) values were determined using the Logan analysis with either arterial (ART90) or cerebellar (CER90) data as input. PIB retention was assessed using the distribution volume ratio (DVR: regional DV measure normalized to the cerebellar reference DV). For a subset of subjects (5 AD, 5 MCI, 5 controls), analyses also were performed using carotid ROI data (CAR90) as input with arterial metabolite correction or the simplified reference tissue method (SRTM:  $DVR=BP+1$ , where BP is binding potential). Results were compared to the Logan ART90 DVR values. **Results.** Greatest PIB retention was observed in AD posterior cingulate (PCG DVR: AD=2.62±0.34, Cont=1.25±0.20). Heterogeneous PIB retention was observed in MCI subjects, which ranged from control to AD levels. Similar PIB retention was noted in cerebellum (n=24, CER DV=3.67±0.5). For the subset of 15 subjects, all methods yielded the same regional rank order of average PIB retention in AD subjects (see Table). The CAR90 DVRs agreed best with the ART90 DVRs (PCG:  $r^2=0.98$ , slope = 0.95), with more bias observed in the CER90 DVR (PCG:  $r^2=0.97$ , slope = 0.85). The SRTM DVR was most biased but strongly correlated with the ART90 values (PCG:  $r^2=0.92$ , slope = 0.78). For a given region, the rank order of individual subject DVR values was maintained across the various Logan analyses, while deviation of this rank order was sometimes observed in the SRTM DVRs. **Conclusion.** These results support the validity of image-based methods for the quantification of PIB retention in control, MCI, and mild to moderate AD subjects. The carotid method provided excellent results but its usefulness will require validation of radiolabeled metabolites from venous samples. Of the reference tissue methods, the Logan CER90 was less biased than SRTM. The performance of these methods in severe AD subjects and in longitudinal studies remains to be investigated. This work was supported by MH070729, NIA, Alzheimer's Association, GE Health Care.

Group	Region	Logan DVR ART90	Logan DVR CAR90	Logan DVR CER90	SRTM BP+1
CONTROL	Posterior Cingulate	1.24 ± 0.22	1.30 ± 0.27	1.22 ± 0.17	1.42 ± 0.26
	Parietal	1.29 ± 0.26	1.30 ± 0.26	1.26 ± 0.20	1.33 ± 0.25
	Lateral Temporal Cortex	1.19 ± 0.18	1.16 ± 0.19	1.18 ± 0.13	1.13 ± 0.12
	Cerebellum	3.38 ± 0.34 (DV)	7.53 ± 0.71 (DV)	--	--
AD	Posterior Cingulate	2.63 ± 0.38	2.61 ± 0.35	2.39 ± 0.26	2.51 ± 0.25
	Parietal	2.55 ± 0.46	2.55 ± 0.42	2.34 ± 0.39	2.31 ± 0.09
	Lateral Temporal Cortex	2.37 ± 0.44	2.37 ± 0.42	2.17 ± 0.31	2.27 ± 0.22
	Cerebellum	3.79 ± 0.55 (DV)	7.63 ± 0.85 (DV)	--	--

## PARAMETRIC IMAGING OF [11C]PIB STUDIES USING SPECTRAL ANALYSIS

Rainer Hinz<sup>1</sup>, Gunnar Blomquist<sup>2</sup>, Paul Edison<sup>3</sup>, David J. Brooks<sup>1,3</sup><sup>1</sup>Hammersmith Imanet Ltd., London, UK<sup>2</sup>Uppsala Imanet AB, Uppsala, Sweden<sup>3</sup>MRC Clinical Sciences Centre, London, UK

Introduction: The novel positron emission tomography (PET) tracer [11C]PIB has previously been shown to be a marker of amyloid deposits in brain of Alzheimer's disease (AD) patients [1]. For differential diagnosis of early dementia with imaging techniques, a PET study design which is able to reliably distinguish between amyloid load in normal elderly and in AD is required. Because of the scattered occurrence of focal amyloid deposits in AD, exploratory interrogation of parametric images with statistical parametric mapping (SPM) may be more appropriate than an a priori defined region-of-interest based analysis. Here, we report the use of spectral analysis [2] to generate parametric images of [11C]PIB binding. Methods: After bolus administration of 370 MBq [11C]PIB, 3D PET data were acquired on the ECAT EXACT HR+ scanner. The metabolite corrected arterial plasma input function was generated using an on-line blood detector and 10 discrete arterial samples which were analyzed on an HPLC system. 100 logarithmically spaced basis functions between 0.0008 1/s and 0.1 1/s were used as the functional base. Parametric images of the total volume of distribution (VD) as well as of the impulse response function (IRF) at various time points were generated [3]. Results: The figure shows sagittal views of parametric images from a control (top row) and an AD subject (bottom row). The IRF image at 1 minute shows predominantly grey matter areas with high values. The AD subject, however, shows globally lower values with association cortical areas in particular being targeted. The IRF image at 75 minutes in the control marks white matter regions with high values, and shows very little retention in the grey matter. In the AD subject, very high IRF 75 min values are obtained throughout the cortex in particular targeting frontal and occipital areas. Cerebellar grey matter showed similar [11C]PIB binding in AD and controls. The VD images resemble those of the 75 min IRF. However, when normalised to cerebellar grey matter, the contrast of the 75 min IRF image is superior to that of the VD image. In the AD subject the ratios of the frontal over the cerebellar values are 2.3 for the VD and 4.3 for the 75 min IRF, respectively. In the control subject the frontal/cerebellum ratio is 1.1 with either analysis. Conclusion: Spectral analysis is a powerful tool for the generation of parametric images from [11C]PIB studies. It separates the tissue response function into the early, blood flow dependent signal component and the later signal component indicative of [11C]PIB retention to amyloid plaques. Imaging the IRF at late time produces a higher contrast than the VD image. The use of spectral analysis does, however, require the measurement of the plasma input function. References: [1]Klunk WE, et al.; Ann Neurol 55,303–319(2004). [2]Cunningham VJ, et al.; in: Quantification of brain function: tracer kinetics and image analysis in brain PET; Uemura K et al. (editors); 101–108(1993). [3]Tadokoro M, et al.; as in [2]; 289–294(1993).



## BP-4

### **CORRELATION OF REGIONAL CEREBRAL AMYLOID LOAD IN ALZHEIMER'S DISEASE, MEASURED WITH [11C]-PIB PET USING SPECTRAL ANALYSIS AND TISSUE UPTAKE RATIOS, WITH PERFORMANCE ON RECOGNITION MEMORY TESTS**

**Paul Edison**<sup>1</sup>, Hilary Archer<sup>2</sup>, Rainer Hinz<sup>3</sup>, Alexander Hammers<sup>1</sup>, Alexander Gerhard<sup>1</sup>, Nicola Pavese<sup>1</sup>, Yen Tai<sup>1</sup>, Gary Hotton<sup>1</sup>, Dawn Cuttler<sup>2</sup>, Nick Fox<sup>1</sup>, Martin Rossor<sup>1,2</sup>, David J. Brooks<sup>1,3</sup>

<sup>1</sup>*MRC Clinical Sciences Centre Hammersmith Hospital, Imperial College London, UK*

<sup>2</sup>*University College London, London, UK*

<sup>3</sup>*Hammersmith Imanet, London, UK*

Background: [11C]-PIB is a novel PET tracer which binds to amyloid plaques in Alzheimer's disease (AD). Using Spectral analysis or Logan analysis with arterial input functions it has been reported that [11C]-PIB PET can distinguish AD patients from healthy controls. For the wider use of PIB PET as a diagnostic marker a non invasive method of analysis is essential. Pathological studies have shown that PIB binds to fibrillar but not to amorphous amyloid. The cerebellum is devoid of fibrillar amyloid in AD and so should provide a reference brain area. Objective: 1. To determine whether measurement of regional cerebral [11C]-PIB binding using "target to cerebellar ratios" (RATIO) gives comparable findings to spectral analysis (SA) - dependent on an arterial plasma input function) in AD. 2. To correlate regional cortical [11C]-PIB uptake obtained with these methods with performance on recognition memory tests in AD patients and to assess test retest variability. Methods: 12 early AD patients (MMSE scores 15-26) and 9 healthy age-matched control subjects underwent [11C]-PIB PET. All subjects had online arterial sampling and parametric images of the Impulse response function at 75 minutes were generated using spectral analysis. All subjects were then analysed using a RATIO method where cerebellar grey matter was defined as the tissue reference and ratio images were generated from 60-90 minutes. Object maps were created by segmenting individual MRIs and spatially transforming the grey matter images into standard stereotaxic MNI space on which a probabilistic atlas was superimposed. [11C]-PIB uptake was correlated with memory tests using ANOVA. 5 AD patients underwent repeat [11C]-PIB PET within 6 weeks of their first scan. Results: Using spectral analysis, the AD patients showed significantly raised [11C]-PIB binding in frontal (2.3x), temporal (2.1x), and parietal association (2.4x) cortex along with cingulate (2.5x) and occipital cortex (1.8x). Amyloid binding was also detected in striatum (2.4x) but not in thalamus or cerebellum. Using the "RATIO" method there were similar increases in [11C]-PIB binding in frontal (2.1x), temporal (1.9x), and parietal association (2.1x) cortex, cingulate (2.3x) and occipital (1.8x) cortex, and striatum (2.1x) compared to cerebellum. All these regional binding increases were statistically significant,  $p < 0.001$ . There was no significant increase in regional cerebral [11C]-PIB binding in controls compared to AD or normal cerebellum. The test-retest variability was 6-8% across cortical regions for the RATIO method and 8-10% for spectral analysis. MMSE scores showed a trend towards correlation with cortical amyloid load ( $p = .08$  RATIO;  $.09$  SA) with both approaches. Performances on the short Warrington Recognition Memory Test for Faces (RMTF) and Words (RMTW) were both significantly correlated ( $p < 0.001$ ) with 11C-PIB binding in cortical association areas using both analytical approaches. Conclusion: Our findings demonstrate that "Target to cerebellum" 60-90' ratios provide a robust and non invasive method for analyzing r[11C]-PIB retention in AD patients and give comparable results to the more invasive spectral analysis. Test-retest variability is slightly better with "Target to cerebellum" ratio method and both methods demonstrate that amyloid load correlates with memory performance in Alzheimer's disease.

**BP-5**

**VALIDATION OF [11C]MP4A AND [11C]MP4P AS TRACERS FOR QUANTIFYING BRAIN AChE ACTIVITY WITH PET BASED ON IN VIVO AND IN VITRO HUMAN STUDIES**

Noriko Tanaka<sup>1</sup>, Hajime Matsuura<sup>2</sup>, Hitoshi Shinotoh<sup>1</sup>, Sigeki Hirano<sup>1</sup>, Yasukazu Sato<sup>1</sup>, Tetsuya Shiraishi<sup>1</sup>, Shuichi Sendoda<sup>3</sup>, Hiroki Namba<sup>4</sup>, Shuichi Tanada<sup>1</sup>, Toshiaki Irie<sup>1</sup>

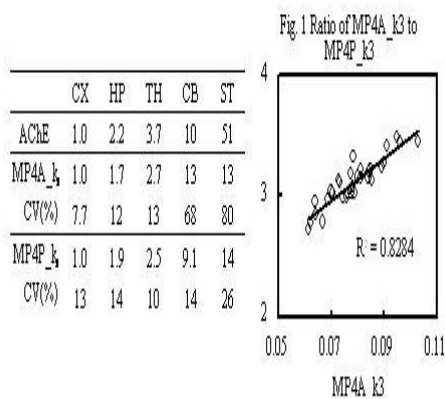
<sup>1</sup>Department of Medical Imaging, National Institute of Radiological Sciences, Chiba, Japan

<sup>2</sup>Siemens Asahi Medics Co Ltd., Tokyo, Japan

<sup>3</sup>Toshiba Information System Co Ltd., Tokyo, Japan

<sup>4</sup>Department of Neurosurgery, Hamamatsu School of Medicine, Hamamatsu, Japan

Background: N-[11C]methylpiperidin-4-yl acetate ([11C]MP4A) and propionate ([11C]MP4P) have been used for quantification of AChE activity in living humans with PET. Reactivity of [11C]MP4A with AChE is known to be 4-5 times higher than that of [11C]MP4P. On the other hand, distribution of AChE within the brain is not uniform (Table), low in cortex (CX), moderate in hippocampus (HP) and thalamus (TH), high in cerebellum (CB) and striatum (ST). In this study, to make a better choice between the two tracers for each brain region of above, precisions and biases of regional k3 values (AChE index) were compared. Methods: Twenty normal subjects for [11C]MP4A and 15 for [11C]MP4P were participated in PET study. Dynamic PET scans were performed over 40 min/14 frames for [11C]MP4A and 60/16 frames for [11C]MP4P with arterial blood sampling for input function measurement. After anatomical normalization of the PET images, dynamic data were obtained from 31 cortical ROIs and 17 non-cortical ROIs, and k3 values (AChE index) were estimated by standard non-linear least squares analysis. Using post-mortem brain tissues, regional AChE activity was measured by Ellman's method. Results: Except striatum with very high AChE activity, good correlations were obtained between AChE activity and k3 values for [11C]MP4A (R>0.98) and [11C]MP4P (R>0.99). While [11C]MP4P gave precise k3 in all regions, with 10-26% of coefficient of variation (CV), [11C]MP4A gave acceptable k3 CV only in regions with low to moderate AChE activity (Table). However, across 31 cortical ROIs, [11C]MP4A gave significantly lower k3 CV (7.7±0.9%) compared with [11C]MP4P (13.4±2.1%). Sensitivity of [11C]MP4A was about twice that of [11C]MP4P. Interestingly, k3 ratio of [11C]MP4A to [11C]MP4P depended on AChE activity across cortical regions (Fig.1), suggesting that AChE-specificity of [11C]MP4P may be insufficient in cortical regions. Conclusion: For whole brain AChE mapping, [11C]MP4P with lower AChE-reactivity is more suitable because of lower k3 CV compared with [11C]MP4A. However, in cortex, [11C]MP4A may be better choice because of lower k3 CV and is expected to have higher sensitivity in detecting cortical AChE reduction in such diseases as Alzheimer's disease and dementia with Lewy bodies.



**COMPARISON OF KINETIC MODELLING STRATEGIES OF N-[11C]-METHYLPIPERIDIN-4-YL-PROPRIONATE ([11C]-PMP) IN NORMALS AND PATIENTS WITH MILD COGNITIVE IMPAIRMENT (MCI)**

**Virginie Kinnard<sup>1</sup>, Patrick Dupont<sup>1</sup>, Mathieu Vandebulcke<sup>2</sup>, Koen Van Laere<sup>1</sup>, Guy Bormans<sup>3</sup>, Tjibbe de Groot<sup>3</sup>, Alfons Verbruggen<sup>3</sup>, Rik Vandenberghe<sup>2</sup>**

<sup>1</sup>*Department of Nuclear Medicine, KU Leuven - UZ Gasthuisberg, Leuven, Belgium*

<sup>2</sup>*Department of Neurology, KU Leuven - UZ Gasthuisberg, Leuven, Belgium*

<sup>3</sup>*Labo Radiopharmaceutical Chemistry, KU Leuven, Leuven, Belgium*

Introduction: To investigate the rate of acetylcholinesterase (AChE) in Alzheimer's disease, N-[11C]-Methylpiperidin-4-yl-Propionate and Positron Emission Tomography are used. In a clinical environment, it is important to simplify the acquisition as much as possible by avoiding arterial blood sampling and/or to have fast methods available. Methods: In 18 subjects (10 normals and 8 MCI patients; mean age: 67 yr in both groups), data were acquired dynamically for one hour (4 x 15s, 4 x 60s, 2 x 150s, 10 x 300s) on a HR+ after the injection of 300 MBq [11C]-PMP. Arterial blood samples were drawn to measure the plasma input function and to determine the metabolite fraction. Dynamic images were reconstructed using 3D-FBP with randoms, scatter and attenuation correction. An adjustment for small movements was applied between all the time frames and the data were coregistered to the subject's T1 weighted MRI. Segmentation of the MRI was done according to the optimized VBM approach and the dynamic data were transformed into the same MNI space. A partial volume correction was then applied to each frame, according to the method of Müller-Gartner (Müller-Gartner et al. 1992). Kinetic modelling was performed using three different approaches: (1) a "standard" irreversible two-tissue compartment model with non-linear fitting of the parameters, (2) a fast linearized model (Blomqvist 1984) and (3) a 'non-invasive' model which does not require arterial blood sampling (Zündorf et al., 2001) with the cerebellum, characterized by a high AChE uptake, as reference region. A correlation analysis between the three models was performed taking model (1) a priori as the most accurate model. Correlation coefficients were calculated in the cerebellum, the cortical (temporal, frontal, parietal and occipital) and subcortical regions. Results: Comparison of the linearized model with model (1) showed a good agreement (median correlation value 0.95) in all cortical regions (range over all subjects: 0.86 to 0.99) except for one MCI patient in which the correlation in the parietal region was very low ( $r = 0.13$ ). Lower correlations were found in the subcortical regions and the cerebellum (range over all subjects: 0.74 to 0.94 respectively 0.64 to 0.89), except for another MCI patient with a correlation of  $r = 0.13$  in the subcortical regions. Comparing the non-invasive model with model (1) showed a similar behaviour: good correlation in the cortical regions (median correlation in the temporal lobe: 0.92, occipital lobe: 0.98, parietal lobe: 0.94 and frontal lobe: 0.78) but low correlations were seen in the subcortical regions and the cerebellum. Overall, a systemic underestimation of AChE was found for the non-invasive model in cortex. The correlation between the models did not differ between normals and MCI patients. Conclusion: A simplified tissue reference model and the (fast) linearized model can be used to study AChE in cortical regions but not in subcortical or cerebellar regions. References: Müller-Gartner et al. 1992, JCBFM 12, 571 Blomqvist 1984, JCBFM 4, 629 Zündorf, G., et al., 2002. In: Senda, M., et al. (Eds.), Brain Imaging Using PET. Academic Press, San Diego, CA, pp. 41– 46.

## EVALUATION OF [<sup>11</sup>C]-(+)-PHNO AS AN AGONIST RADIOTRACER FOR IMAGING HIGH-AFFINITY DOPAMINE D<sub>2</sub> RECEPTORS

Alan A. Wilson<sup>1</sup>, Nathalie Ginovart<sup>1</sup>, Patrick McCormick<sup>1</sup>, Doug Hussey<sup>1</sup>, Ken Singh<sup>1</sup>, Armando Garcia<sup>1</sup>, Sylvain Houle<sup>1</sup>, Philip Seean<sup>2</sup>, Suzi Vanderspeck<sup>1</sup>, Shitij Kapur<sup>1</sup>

<sup>1</sup>Vivian M Rakoff PET Imaging Centre, Centre for Addiction and Mental Health, Department of Psychiatry, Toronto, ON, Canada

<sup>2</sup>Department of Pharmacology, University of Toronto, Toronto, ON, Canada

In vivo imaging of dopamine D<sub>2</sub> receptors with agonists, as opposed to the more commonly employed antagonist, radiotracers, could provide important information on the high affinity (functional) state of the D<sub>2</sub> receptor in illnesses such as Schizophrenia or Movement Disorders. We report here our evaluation of the potent dopamine D<sub>2</sub> agonist, [<sup>11</sup>C]-(+)-PHNO, as a potential radiotracer for imaging the high affinity state of D<sub>2</sub> receptors with positron emission tomography (PET). Ex vivo biodistribution studies in rat brain demonstrated that [<sup>11</sup>C]-(+)-PHNO crossed the blood-brain barrier readily and had an appropriate regional brain distribution for a radiotracer which maps dopamine D<sub>2</sub> receptors. [<sup>11</sup>C]-(+)-PHNO binding was saturable and demonstrated excellent signal to noise as measured by its striatum to cerebellum ratio of 5.4 at 60 min post-injection (Fig. 1). D<sub>2</sub> binding was highly stereospecific; the inactive enantiomer [<sup>11</sup>C]-(-)-PHNO displayed no preferential regional uptake. Blocking and displacement studies were consistent with reversible, selective, and specific binding to the dopamine D<sub>2</sub> receptors. Pre-administration of haloperidol or raclopride (0.5 mg/kg i.v. or s.c.) reduced specific binding by >90% while the D<sub>1</sub> selective antagonist, SCH 23390, had no effect.  $\beta$ -Microprobe experiments with [<sup>11</sup>C]-(+)-PHNO also demonstrated high specific binding of [<sup>11</sup>C]-(+)-PHNO in rat striatum in vivo and allowed the determination of a binding potential for [<sup>11</sup>C]-(+)-PHNO in the striatum of 2.4 (Fig. 2). Physico-chemical measurements (e.g. Log D of 2.14±0.02; n=12) and brain radioactive metabolite measurements were in full accord with the desired properties of a neuroreceptor imaging agent for PET. All of the above, coupled with the documented full D<sub>2</sub> agonistic properties of (+)-PHNO, strongly indicate that [<sup>11</sup>C]-(+)-PHNO is a leading candidate radiotracer for the imaging of the dopamine D<sub>2</sub> high affinity state using PET.

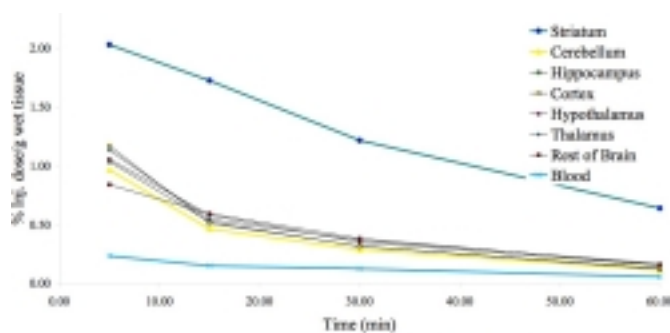


Figure 1. Distribution of [<sup>11</sup>C]-(+)-PHNO in Rat Brain: Ex Vivo

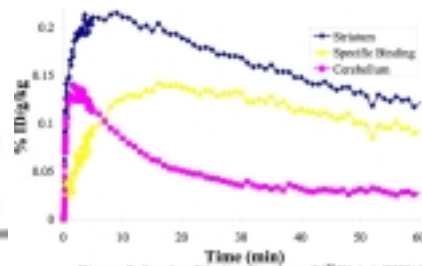


Figure 2. In vivo Biodistribution of [<sup>11</sup>C]-(+)-PHNO in Rat Brain ( $\beta$ -microprobe)

## IN VIVO EVALUATION OF [11C]CNS-5161 AS A USE-DEPENDENT LIGAND FOR THE NMDA GLUTAMATE RECEPTOR CHANNEL

Wynne K. Schiffer<sup>1</sup>, Deborah Pareto-Onghena<sup>2</sup>, HaiTao Wu<sup>1</sup>, Kuo-Shyan Lin<sup>1</sup>, Andrew R. Gibbs<sup>3</sup>, Joanna S. Fowler<sup>1</sup>, Jean Logan<sup>1</sup>, David L. Alexoff<sup>1</sup>, Stephen L. Dewey<sup>1</sup>, Anat R. Biegon<sup>2</sup>

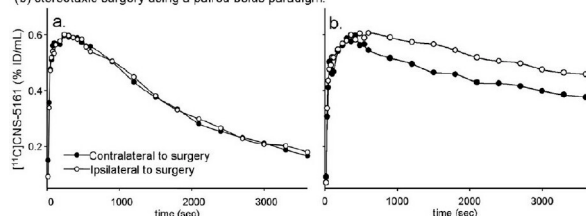
<sup>1</sup>Chemistry Department, Brookhaven National Laboratory, Upton, NY, USA

<sup>2</sup>Medical Department, Brookhaven National Laboratory, Upton, NY, USA

<sup>3</sup>Department of Functional Imaging, Lawrence Berkeley National Laboratory, Berkeley, CA, USA

**Introduction:** Traumatic and ischemic brain injury (TBI) is accompanied by excessive glutamate efflux which results in increased opening of and ion flux through NMDA receptors (NMDAR). Because this may cause excitotoxicity, the activation status of NMDAR and its change over time have important clinical implications. We have labeled the compound CNS-5161 with tritium and carbon-11 (1) and studied its sensitivity to changes in NMDAR activation by binding, autoradiography and microPET. Our hypothesis was that NMDAR activation by glutamate, NMDA or brain injury would increase [11C]CNS-5161 affinity, an event followed by NMDAR hypofunction and metabolic depression (2). **Methods:** [3H]CNS-5161 (0.5mCi/Kg, N=3) was injected in the tail vein of rats 5min after NMDA (40mg/Kg SC) or saline and brains removed 20 or 60 min later for autoradiography. Serial microPET experiments in rats (n=6) were performed using [11C]CNS-5161 (0.5-1.9 mCi/animal; specific activity 2.2-6.3 Ci/ $\mu$ mole) at 3 times: either prior to, minutes or hours after surgical brain injury consisting of microdialysis probe insertion (stereotaxic surgery) targeting the right striatum. ROI analysis was performed using PMOD software to co-register images and apply an atlas template. **Results:** [3H]CNS-5161 binding affinity to brain membranes was increased in presence of glutamate and glycine ( $K_d=2.3\pm 0.08$  Vs.  $5.6\pm 0.4$ nM in the absence of glutamate). In intact controls, the frontal cortex/cerebellum ratio was  $1.2\pm 0.15$ , blocking with MK801 gave  $0.9\pm 0.1$  and NMDA pretreatment to open channels gave  $1.7\pm 0.2$ . [3H]CNS-5161 data provided evidence that injury-induced glutamate release increases radiotracer affinity for the open channel and suggested that the changing slope of the washout would appropriately reflect radiotracer affinity. Consistently, there was a significant increase in [11C]CNS-5161 affinity immediately following the trauma (inversely proportional to a 72 and 95% decrease in the rate of dissociation in the left and right cortex, respectively) that receded by 2 hours after the surgery. There was no significant change in [11C]CNS-5161 affinity in the cerebellum at any point, consistent with in vitro data (13.6 and 6.7% change in the left and right washout,  $p<0.05$ ). **Discussion:** These results suggest CNS-5161 is a radiotracer with in vivo sensitivity to the activated state of NMDAR, whose affinity depends on glutamate-induced activation of the ion channel complex. Injured animals demonstrated more sustained uptake in cortex, hippocampus and striatum but not in the cerebellum, which was undistinguishable from controls. Future PET studies using [11C]CNS-5161 in stroke or TBI victims may help determine the functional status of the receptors in individual subjects and the potential efficacy of NMDAR inhibition or stimulation. 1 Luthra, S. et al. (2004) NeuroReceptor Mapping pp. P-55 2 Biegon, A. et al. (2004) Proc Natl Acad Sci U S A 101, 5117-5122

Figure 1. Time activity of [11C]CNS-5161 in the frontal/parietal cortex before (a) and 7 min after (b) stereotaxic surgery using a paired bolus paradigm.





## EVALUATION OF [C-11]R116301 AS A TRACER FOR THE IN VIVO MEASUREMENT OF NK1 RECEPTORS IN HUMAN SUBJECTS

Saskia P. A. Wolfensberger<sup>1,3</sup>, Anu J. Araikainen<sup>1</sup>, Bart N.M van Berckel<sup>1</sup>, Ronald Boellaard<sup>1</sup>, William D.H. Carey<sup>2</sup>, Wieb Reddingius<sup>2</sup>, Dick J. Veltman<sup>1,3</sup>, Bert D. Windhorst<sup>1</sup>, Josée E. Leysen<sup>1</sup>, Adriaan A. Lammertsma<sup>1</sup>

<sup>1</sup>*Department of Nuclear Medicine & PET Research, VU University Medical Centre, Amsterdam, The Netherlands*

<sup>2</sup>*Johnson & Johnson Pharmaceutical Research & Development, Beerse, Belgium*

<sup>3</sup>*Department of Psychiatry, VU University Medical Centre, Amsterdam, The Netherlands*

Background: R116301 is an orally active, potent and selective non-peptide NK1 receptor antagonist with a  $K_i$  of 0.45 nM against human NK1 receptors. The binding affinity of R116301 for human NK2 and NK3 receptors is 1600 and 230 fold lower, respectively. R116301 suppresses various aspects of substance P (SP) induced behaviour in vivo and behaves as a full antagonist in vitro. SP mediates fear responses and anxiety, and probably has a role in sensation of visceral pain. Objective: The objective of this pilot study was to evaluate [C-11]R116301 as a potential PET ligand for investigating NK1 receptors in vivo. Methods: PET studies were performed in 3 normal controls. Each PET session consisted of 2 [C-11]R116301 scans, 5 hours apart. Exactly 3.5 hours before the second scan, a single oral (blocking) dose of 125 mg aprepitant was given. Individual scan sessions consisted of a transmission scan and a dynamic emission scan following intravenous administration of ~370 MBq [C-11]R116301. The 3D emission scan consisted of 23 frames with progressive increase in frame duration and a total scan duration of 90 minutes. In addition, using on-line detection and discrete manual samples, a metabolite corrected arterial plasma input function was derived. For each subject, both pre- and post-aprepitant scans were co-registered to the corresponding individual MRI. Regions of interest (ROI) were defined on the MRI scans and projected onto both co-registered PET scans to generate tissue time-activity curves (TAC). Whole striatum was used as the structure with the highest density of NK1 receptors, and cerebellum as reference tissue. Scan data were analysed using arterial input compartment models, reference tissue models and simple striatum to cerebellum ratios. Results: In figure 1 pre-aprepitant TAC are shown for striatum and cerebellum. Equilibrium was reached relatively early after injection, and striatum to cerebellum ratios were almost identical for the intervals 20-90 and 60-90 minutes. Following aprepitant administration these ratios decreased 63, 51 and 20% relative to the corresponding baseline data. Pre- and post-aprepitant scans for one subject are shown in figure 2. Compartmental analysis was not possible as arterial input curves were distorted due to significant sticking of [C-11]R116301 to the wall of the PTFE tubing. Reference tissue models showed a major reduction in binding potential (BP) due to aprepitant administration, but standard errors of baseline BP were too high for reliable quantification. Conclusion: These preliminary results indicate that [C-11]R116301 has potential as a radioligand for in vivo assessment of NK1 receptors in the human brain. Further studies are required for developing a reliable quantitative method.

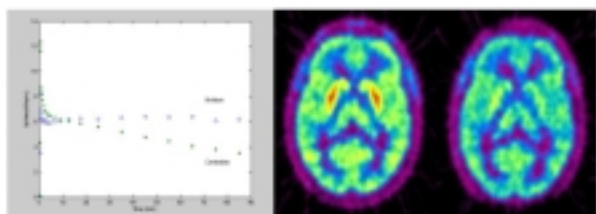


Figure 1: (Left) Pre-aprepitant TAC of striatum (s) and cerebellum (\*). (Middle & right) Pre and post injection images of subject 1.



**SYNTHESIS, IN VIVO EVALUATION AND DIRECT COMPARISON WITH [18F]FPS OF A NOVEL SIGMA-1 RECEPTOR RADIOTRACER [18F]2-FLUOROETHYL-[(4-CYANOPHENOXY)METHYL]PIPERIDINE ([18F]WLS1.002)****Rikki N. Waterhouse, Jun Zhao, Raymond C. Chang, Patty Carambot***Department of Psychiatry, Columbia University, New York, NY, USA*

Introduction: Sigma-1 receptors are expressed throughout the CNS and are implicated in schizophrenia and depression. We have evaluated recently the high affinity ( $K_D = 0.5 \pm 0.2$  nM,  $\log P = 2.8$ ) sigma-1 receptor radiotracer [18F]2-Fluoropropyl-[(4-cyanophenoxy)methyl]piperidine ([18F]FPS) in rodents, baboons and performed the first brain imaging study and safety evaluation of this tracer in healthy humans. In contrast to suitable kinetics in the baboon brain (equilibrium was reached by 60-80 min), in the human CNS [18F]FPS does not reach equilibrium by 4 hr, supporting the development of a lower affinity tracer. Studies in rats also indicated very slow clearance of [18F]FPS from the brain, suggesting that the awake rat may be a better model than baboons for predicting the regional brain kinetics of these sigma-1 receptor tracers in humans. We describe here the synthesis and in vivo evaluation in rats of [18F]WLS1.002 ( $K_i = 5$  nM,  $\log P = 2.42$ ), a structurally similar, lower affinity sigma-1 receptor tracer compared to [18F]FPS. A comparison is made between the brain uptake and clearance of [18F]WLS1.002 and [18F]FPS. Methods: [18F]WLS1.002 was synthesized by heating the corresponding N-ethylmesylate precursor in anhydrous [18F]fluoride/K222/acetonitrile for 15 min. Purification was accomplished by reversed phase HPLC, and solutions of [18F]WLS1.002 were formulated in sterile saline. Regional brain biodistribution (5–90 min; eight regions), metabolism and pharmacologic blocking studies of [18F]WLS1.002 (25  $\mu$ Ci, 100  $\mu$ l saline, iv) were carried out in awake adult male rats. The drugs used in blocking studies included WLS1.002, FPS, BD1008, and SM-21. All were administered (1mg/kg, 100  $\mu$ l saline, iv) 5 min prior to tracer injection. The data obtained from these studies were compared to that collected previously for [18F]FPS. Results: [18F]WLS1.002 was synthesized ( $n = 6$ ) in good yield ( $58 \pm 8\%$  EOB), and high specific activity ( $2.89 \pm 0.80$  Ci/ $\mu$ mol EOS) and radiochemical purity ( $98.3 \pm 2.1\%$ ). Whole brain activity ( $n = 4$ ) for [18F]WLS1.002 was  $1.41 \pm 0.06$  %ID/g at 5 min and was reduced by 33% to  $0.96 \pm 0.30$  %ID/g by 90 min, whereas for [18F]FPS no significant reduction was noted over this same time period. Examination of regional brain distribution revealed a localization for [18F]WLS1.002 like that of [18F]FPS. At 15 min, highest %ID/g of [18F]WLS1.002 was in occipital cortex ( $1.86 \pm 0.06$  %ID/g), Frontal Cortex ( $1.76 \pm 0.38$  %ID/g), Striatum ( $1.44 \pm 0.25$  %ID/g), and lowest in the hippocampus ( $1.01 \pm 0.02$  %ID/g). In all regions examined, peak uptake occurred by 5 min, followed by clearance of [18F]WLS1.002 that was significantly faster than [18F]FPS. Blood activity from 15–90 min was low ( $< 0.07$  %ID/g). Metabolite analysis (1 hr) revealed that [18F]WLS1.002 remained highly intact in the brain. Blocking studies (1 hr) showed a  $>90\%$  reduction in [18F]WLS1.002 brain uptake by sigma-1 binding drugs but not by the sigma-2 selective compound SM-21. Conclusion: [18F]WLS1.002 exhibits excellent characteristics in vivo and may provide a superior brain imaging radiotracer for human PET studies due to its lower sigma-1 receptor affinity and faster CNS clearance compared to [18F]FPS.

## BP-11

### RADIOLABELLING AND IN VIVO EVALUATION OF [11C]GSK215083 AS POTENTIAL PET RADIOLIGAND FOR THE 5-HT<sub>6</sub> RECEPTOR IN THE PORCINE BRAIN

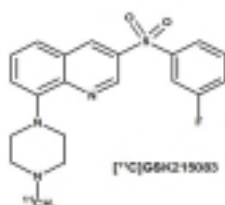
Laurent Martarello<sup>1</sup>, Vincent J. Cunningham<sup>1</sup>, Julian C. Matthews<sup>1</sup>, Eugenii Rabiner<sup>1</sup>, Steen Jakobsen<sup>2</sup>, Antony D. Gee<sup>1</sup>

<sup>1</sup>GlaxoSmithKline, ACCI Addenbrooke's Hospital, Cambridge, UK  
<sup>2</sup>Aarhus PET Centre, Aarhus University Hospital, Aarhus, Denmark

The 5-hydroxytryptamine-6 (5-HT<sub>6</sub>) receptor is one of 14 distinct mammalian 5-HT (serotonin) receptors expressed in the central nervous system through which 5-HT is involved in regulating a number of diverse biological processes (1). Binding studies with [125I]SB258585, have localised 5-HT<sub>6</sub> receptors almost exclusively in the CNS (2). In these reports, SB258585 showed a high level of binding in rat, and pig striatal tissues and low in the cerebellum. In man SB258585 binding pattern is similar to rat and pig, being strongest in caudate, putamen, moderates in cerebral cortex and low in the cerebellum (3). Despite its good in vitro profile, the development of SB258585 as an in vivo imaging tool was hampered due to its poor brain penetration properties and to date no successful 5-HT<sub>6</sub> ligand has been reported for use in PET. We present here the radiolabelling and preclinical evaluation of [11C]GSK215083 a novel tool to probe the 5-HT<sub>6</sub> receptors in vivo. [11C]GSK215083, [11C-N-methyl]3-[(3-fluorophenyl)sulfonyl]-8-(4-methyl-1-piperazinyl) quinoline, was prepared by N-methylation of the corresponding desmethyl precursor with [11C]MeOTf in methanol:acetonitrile in presence of 2,2,6,6-tetramethylpiperidine, followed by HPLC purification. In a pilot study [11C]GSK215083 was evaluated in anesthetized Yorkshire pigs (40kg). [11C]GSK215083 readily enters the brain reaching peak regional tissue concentrations at approximately 20min post injection followed by a slow washout from brain regions known to be rich in 5-HT<sub>6</sub> receptors with highest uptake and retention observed in striatum. The observed rank order of regional brain concentrations was striatum>cortical regions>cerebellum, consistent with reported 5-HT<sub>6</sub> receptor densities and localisation determined by tissue section autoradiography in animals and man. Upon injection of [11C]GSK215083, striatum to cerebellum and cortex to cerebellum ratios of 2 to 1 and 1.5 to 1, respectively were reached at 60 min post injection. Co-administration of [11C]GSK215083 with escalating dose of authentic GSK215083 (0.005, 0.05 and 0.5mg/kg) have located a saturable and dose dependent signal in the striatum and cortical regions. Treatment of pigs with the 5-HT<sub>6</sub> binding drug, clozapine (6.25mg/kg), significantly reduced the specific binding in striatum as compared to cerebellum. No significant effect on [11C]GSK215083 signal in striatum was observed following treatment with ketanserin (0.3mg/kg), a selective 5-HT<sub>2a</sub> receptor antagonist, in contrast the same treatment reduced >90% specific binding in frontal cortex. Radio-HPLC analysis revealed that [11C]GSK215083 is rapidly metabolised in arterial plasma, representing approximately 60% of the total radioactivity 30min post injection. [11C]GSK215083 shows properties suitable for studies probing 5HT<sub>6</sub> receptor in man with PET.

#### References

- (1) Wooley, ML et al. Current Drug Targets-CNS & Neurological Disorders, 2004, 3, 59-79
- (2) Hirst, WD, et al. Brit. J. Pharmacol, 2000, 130, 1597-1605
- (3) East, SZ, et al. Synapse, 2002, 45, 191-199





**CHARACTERIZATION OF DOSE DEPENDENT NOREPINEPHRINE  
TRANSPORTER BLOCKADE BY ATOMOXETINE IN HUMAN BRAIN USING 11C  
MENER PET**

Dean F. Wong<sup>1</sup>, Hiroto Kuwabara<sup>1</sup>, P. David Mozley<sup>2</sup>, Robert F. Dannals<sup>1</sup>, Anil Kumar<sup>1</sup>,  
Weiguo Ye<sup>1</sup>, James R. Brasic<sup>1</sup>, Mohab Alexander<sup>1</sup>, William Mathews<sup>1</sup>, Daniel Holt<sup>1</sup>,  
Francois Vandenhende<sup>2</sup>, Albert Gjedde<sup>3</sup>

<sup>1</sup>Radiology, Johns Hopkins Medical Institutions, Baltimore, MD, USA

<sup>2</sup>Lilly Research Laboratories, Indianapolis, IN, USA

<sup>3</sup>Aarhus University, Aarhus, Denmark

Atomoxetine (Strattera) is a highly selective norepinephrine transporter (NET) antagonist that is indicated for the treatment of attention deficit disorders. The purpose of this study was to establish the NET occupancy-plasma atomoxetine relationships for healthy adults and identify minimal doses that produce the maximal occupancy. Methods: Ten volunteers (33 ± 3 years; 9M, 1F) participated with Group 1 (n=3) receiving 40 to 160 mg daily. PET scans were acquired at baseline and 12 hours after the last dose on days 11, 18, and 19. Group 2 (n=7) was treated with 20 to 160 mg daily with scans at baseline and at 3 time-points after the last dose on day 10. Each 90-minute PET utilized high specific activity (19 ± 2 Ci/micromole) 11C MeNER with average activity (19 ± 0.2 mCi) and mass (0.5 ± 0.04 micrograms). Subjects had radial arterial input (first two scans-group 1, all scans-group 2). Volumes of interest (VOIs) were defined for the thalamus, putamen, caudate nucleus, pons, and cerebellum on SPGR MRI. Binding potential (BP) was estimated with four approaches: Linear version of simplified reference tissue method using (1) white matter (LSRTM-WM) and (2) the caudate (LSRTM-CN), (3) one-tissue compartmental models with arterial input (1C-art) and (4) arterial input hyperplot (art-HP), with the latter two techniques using an inhibition plot method to estimate distribution volume [1, 2] The percent occupancy was obtained by calculating the reduction in BP during the on-drug conditions. The Michaelis Menten equation (NET-OCC=Omax• [atomox] p/ (k+ [atomox] p)) where Omax is the maximal occupancy and [atomox] p is the plasma atomoxetine. Results: The kinetics of the radiotracer was found to be relatively slow peaking at about 70 to 90 minutes after injection. The brain injected dose peaked at slightly more than 2%. Plasma atomoxetine ranged from 0.25 to 1329 ng/ml. The Omax for the thalamus, a typical region, were 34% (LSRTM-WM), 59.7% (LSRTM-CN), 61.5 (1C-art), and 48.0% (Art-HP) Eighty percent of Omax was achieved in all subjects who had a daily 80 mg dose for 10 days. Plasma atomoxetine decreased sharply after the last dose in post-discontinuation scans, consistent with its known plasma half-life. Conclusions: The results illustrate the feasibility of measuring NET blockade with MeNER. However, its slow kinetics, relatively low target-to-background levels, and the apparent absence of an ideal reference region in humans, create uncertainty about the absolute occupancy. The inability to show complete saturation at supra-therapeutic doses might reflect non-competitive inhibition between the radiotracer and the inhibitor. However, the dose occupancy curves were similar with all 4 methods, confirm the apparent saturation at multiple plasma levels, and demonstrate the principle of NET occupancy as an aid for future NET drug development.

[1] Gjedde, A. (2003) Molecular Nuclear Medicine, Springer-Verlag.

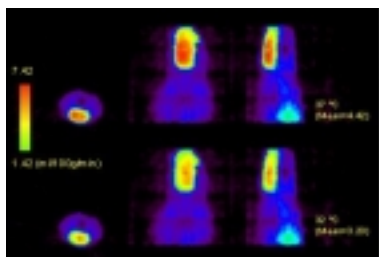
[2] Wong, D., Nestadt, G., Cumming, P., Yokoi, F., & Gjedde, A. (2001), Physiological Imaging of the Brain with PET, Academic Press.

## NONINVASIVE MEASUREMENTS OF CBF AND CMRO2 IN THE RAT BRAIN USING MICROPET IMAGING

Seong-Hwan Yee, Peter T. Fox

*Research Imaging Center, University of Texas Health Science Center At San Antonio, San Antonio, Texas, USA*

**Introduction:** Despite decades of research, the mechanism of regulating blood flow and oxygen metabolism associated with neural activation still remains unclear. To study that issue, reliable measurement of cerebral oxygen metabolic rate (CMRO<sub>2</sub>), as well as cerebral blood flow (CBF), is essential. Of the imaging tools, the blood oxygenation level dependent MRI technique based on the hypercapnia calibration (1) has been extensively used, although it estimates only the relative changes. However, the PET-based absolute quantification technique has been hardly applied for small animals due to technical difficulties. Here, we report novel methods overcoming existing difficulties for absolute quantification of CBF and CMRO<sub>2</sub> in rats using a high-resolution dedicated animal PET (microPET). No arterial blood sampling procedure for the determination of an arterial input function (AIF) was performed. **Methods:** Rats were imaged using the O-15 labeled tracers. An intravenous bolus injection of H<sub>2</sub>15O (2) and a bolus inhalation of O<sub>15</sub>O (3) were used for CBF and CMRO<sub>2</sub> measurements, respectively. The AIF required for absolute quantification was obtained using a time-activity curve over the heart after necessary corrections. We have validated our method in two ways. The first was to validate our intravenous injection (H<sub>2</sub>15O) technique based on non-invasive AIF determination against the intracarotid injection technique which does not require AIF measurement. The second was to validate overall CBF and CMRO<sub>2</sub> techniques using a hypothermia challenge to see hypothermic suppression effect on both measurements. For each rat, the right external carotid artery and a femoral vein were catheterized for injecting O-15 water for CBF measurements and a tracheotomy was performed for administering O-15 oxygen for CMRO<sub>2</sub> measurement. During imaging procedure, alpha-chloralose (30 mg/kg/hr, intravenous infusion) was used for anesthetic. CBF and CMRO<sub>2</sub> measurements were done in hypothermia (rectal temperature: 32 °C) and normothermia (37 °C) successively for each rat. **Results:** Our data for 10 rats shows that the CBF (ml/100g/min) values obtained using the intravenous injection based on non-invasive AIF determination (normothermia: 54.62±5.08, hypothermia: 45.23±6.05) agreed well with the reference values obtained using the intracarotid injection (normothermia: 54.37±4.60, hypothermia: 47.41±8.64). In addition, the CMRO<sub>2</sub> (ml/100g/min) was reduced by 26.7% by the hypothermia (normothermia: 5.00±0.36, hypothermia: 3.66±0.58), as expected. A CMRO<sub>2</sub> comparison map between hypothermia and normothermia obtained for a rat is shown in Fig. 1: Axial, coronal and sagittal slices from the left. Hypothermic suppression effect on the CMRO<sub>2</sub> is clearly shown. **Discussion and conclusion:** Quantitative CBF and CMRO<sub>2</sub> measurement techniques using microPET without requiring arterial blood sampling for small animals were proposed and validated for the first time. Our technique would be of great use for any CBF/CMRO<sub>2</sub> measurement study using small animals (e.g. brain activation studies) as well as for validating other techniques (e.g. MRI-based techniques). **References:** 1. Davis et al., PNAS 1998; 95:1834-1839; 2. Raichle et al., J Nucl Med 1983; 24:790-798; 3. Ohta et al., J Cereb Blood Flow Metab 1992; 12:179-192



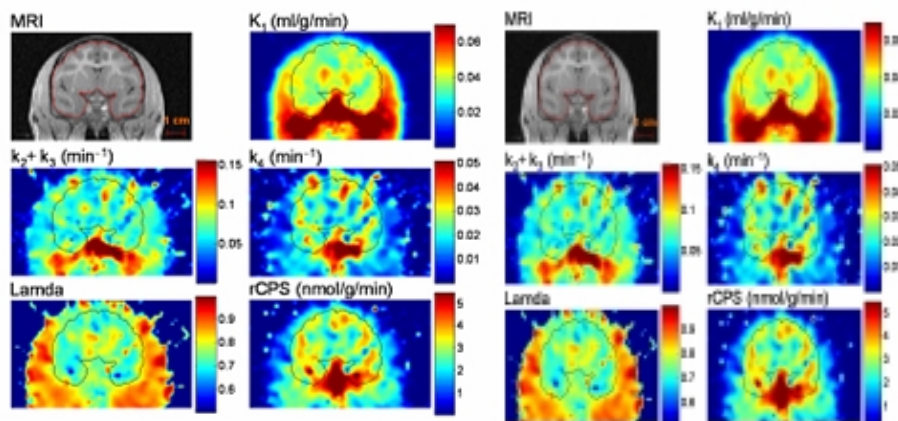


**MEASUREMENT OF REGIONAL RATES OF CEREBRAL PROTEIN SYNTHESIS WITH L-[1-<sup>11</sup>C]LEUCINE AND PET WITH CORRECTION FOR RECYCLING OF TISSUE AMINO ACIDS: COMPARISON OF REGION OF INTEREST AND VOXEL-BASED ANALYSES**

Kathleen C. Schmidt, Carolyn Beebe Smith

*Unit of Neuroadaptation and Protein Metabolism, NIMH, Bethesda, MD, USA*

Introduction: We have validated in monkeys a method for quantitative determination of regional rates of cerebral protein synthesis (rCPS) with L-[1-<sup>11</sup>C]leucine and PET (1). The method uses a kinetic modeling approach to estimate  $\lambda$ , the fraction of the precursor pool for protein synthesis derived from arterial plasma (2). The present study was undertaken to examine the feasibility of performing voxel-wise kinetic modeling analyses and to compare results with region of interest (ROI) analyses. Methods: Anesthetized monkeys were dynamically scanned for 60 min following injection of L-[1-<sup>11</sup>C]leucine. A total of 9 studies were performed. ROIs were placed on MR images and transferred to co-registered PET images to construct tissue time activity curves. For ROI-based analyses, kinetic model rate constants and  $\lambda$  were estimated for whole brain and several gray and white matter regions. rCPS was computed as  $rCPS = [(K_1 k_4) / (k_2 + k_3 + k_4)] (C_p / \lambda)$  where  $C_p$  is the arterial plasma leucine concentration.  $K_1$ - $k_4$  are rate constants for transport of leucine from plasma to brain, from brain to plasma, for catabolism of leucine, and for incorporation of leucine into protein, respectively. For voxel-based analyses, rate constants,  $\lambda$ , and rCPS were estimated for each voxel and averaged. Because estimates of  $k_2 + k_3$  and  $k_4$  in kinetically heterogeneous tissues are expected to decline with time (3), estimations were performed for both analysis methods over 0-30 and 0-60 min intervals. Results: In whole brain 98.5% of voxels yielded valid parameters over 0-60 min (Fig). Regionally  $K_1$ ,  $k_2 + k_3$ , and  $k_4$  were 12-15%, 22-36%, and 30-40% lower, respectively, estimated using voxel-based compared to ROI-based methods. rCPS and  $\lambda$  estimates were in closer agreement: rCPS was 1-9% lower and  $\lambda$  1-5% higher when computed by voxel-based methods. Rate constant estimates decreased with increasing fitting interval, but declines were sharper with voxel-based analyses.  $\lambda$  and rCPS were more stable with increasing fitting interval:  $\lambda$  decreased 0-7% with voxel-based and increased 0-2% with ROI-based analyses; rCPS varied  $\pm 11\%$  with voxel-based and 0-13% with ROI-based analyses. Conclusions: Decreases in rate constant estimates with increasing fitting interval are consistent with tissue heterogeneity, even in voxel-based analyses. Lower estimates of individual rate constants with voxel-based analyses are consistent with negative biases observed at high noise levels in simulation studies (2). Voxel-based analyses, therefore, do not avoid the problem of tissue heterogeneity and may yield negatively biased rate constants.  $\lambda$  and rCPS were robustly estimated by both methods. References: (1) SmithCB, SchmidtKC, QinM, et al, JCBFM 2005 (In press) (2) SchmidtKC, CookM, QinM, et al, JCBFM 2005 (In press) (3) SchmidtK, MiesG, SokoloffL, JCBFM 11:10-24, 1991





**DEVELOPMENT OF LONGITUDINAL PET STUDIES FOR EXPERIMENTAL ANIMAL MODELS**

**Lia C. Liefwaard**<sup>1</sup>, Bart A. Ploeger<sup>1,2</sup>, Carla F.M. Molthoff<sup>3</sup>, Ronald Boellaard<sup>3</sup>, Hugo W.A.M. de Jong<sup>3</sup>, Adriaan A. Lammertsma<sup>3</sup>, Meindert Danhof<sup>1,2</sup>, Rob A. Voskuyl<sup>1,4</sup>

<sup>1</sup>*Division of Pharmacology, LACDR, Leiden University, Leiden, The Netherlands*

<sup>2</sup>*LAP & P Consultants BV, Leiden, The Netherlands*

<sup>3</sup>*Department of Nuclear Medicine & PET Research, VU University Medical Centre, Amsterdam, The Netherlands*

<sup>4</sup>*Epilepsy Institute of The Netherlands, Heemstede, The Netherlands*

**Introduction** The GABAA-receptor plays an important role in epileptogenesis. A key question is to what extent down regulation or changes in properties of the GABAA-receptor can explain pharmacoresistance to antiepileptic drugs. Several methods for assessing GABAA-receptor properties using [<sup>11</sup>C]flumazenil (FMZ) and PET have been described. These methods usually provide quantitative measures of either the total volume of distribution in tissue or the binding potential (BP). The BP is defined as the ratio of Bmax and KD. To derive Bmax and KD separately, multiple scans need to be performed. In the present study a full saturation approach was developed, in which the whole range of receptor occupancies, obtained in a single experiment, was used to calculate Bmax and KD. **Methods** After injection of an excess amount of FMZ, fully saturating the receptors, the concentration time curves of FMZ in brain (using a single LSO layer HRRT PET scanner) and arterial blood (using HPLC-UV) were measured. From these data, Bmax and KD were estimated using population pharmacokinetic (PK) modelling. A 4-compartment PK model was used, comprising 1 blood, 1 tissue (body) and 2 brain (free + non-specific binding and specific binding) compartments. Population PK modelling allows for simultaneous analysis of the data from all animals, whilst still taking inter-individual parameter variability into account. **Results** 24 rats were scanned, injecting either 2000 ug (n=2), 1000 ug (n=1), 500 ug (n=7), 100 ug (n=3), 50 ug (n=3), 25 ug (n=2), or 1 ug (n=6) FMZ. Following a dose of 1 ug FMZ no blood concentrations could be measured, because of the detection limit of the HPLC-UV method. Population PK-modelling, however, permits analysis of incomplete individual datasets. Using this approach, it was possible to derive separate (population) values for Bmax (14.5 +/- 3.7 ng/ml) and KD (4.7 +/- 1.5 ng/ml) with a satisfactory degree of precision. **Conclusions** A novel full saturation approach is reported, which allows for simultaneous estimation of both Bmax and KD in a single experiment per individual animal. This method is now available for analysis of an ongoing study in an experimental animal model for epilepsy (amygdala kindling). Moreover, this approach can also be used in human studies.

## IMAGING POST-ISCHAEMIC CELLULAR CHANGES USING <sup>11</sup>C-FLUMAZENIL & MICROPET FOLLOWING TEMPORARY DISTAL MCA OCCLUSION IN THE SPONTANEOUS HYPERTENSIVE RAT (SHR)

Jessica L. Hughes<sup>1</sup>, John S. Beech<sup>2</sup>, Tim D. Fryer<sup>3</sup>, Rob Smith<sup>3</sup>, Oksana Golovko<sup>3</sup>, Marcel Cleij<sup>3</sup>, Franklin I. Aigbirhio<sup>3,4</sup>, David K. Menon<sup>2</sup>, John C. Clark<sup>3</sup>, Jean-Claude Baron<sup>4</sup>

<sup>1</sup>Centre for Brain Repair, <sup>2</sup>Division of Anaesthesia, <sup>3</sup>Wolfson Brain Imaging Centre, <sup>4</sup>Neurology Unit, University of Cambridge Clinical School, Addenbrooke's Hospital, Cambridge, UK

**Introduction.** Previous PET studies have suggested that [<sup>11</sup>C]flumazenil (FMZ) is adequate to map neuronal death in vivo<sup>1,2</sup>. Thus, FMZ may be useful for in vivo sequential investigation of neuronal loss following stroke, both acutely in the infarcted tissue and subsequently in the structurally surviving penumbra. To investigate this possibility a small-animal PET scanner (microPET P4) has been used to image central benzodiazepine receptors in the transiently ischaemic rat cortex using FMZ. Six male SHRs have been imaged in a longitudinal study design and FMZ distribution volume (DV) maps have been compared to immunohistology. **Methods.** On Day 1 each SHR was subjected to 45min distal MCAo to maximise cortical ischaemia<sup>3</sup>. Following 60mins of reperfusion FMZ was injected and image data was acquired for 75mins. The images were reconstructed using 3D filtered backprojection, with corrections applied for normalisation, randoms, dead time, attenuation, decay and sensitivity. DV maps were calculated from image and input function data using the pmod kinetic modelling package. Further imaging was conducted at 48hrs and 14dys. After the final scan the experiment was terminated by transcardial perfusion fixation. Brains were processed immunohistochemically. **Results.** FMZ binding is significantly lower ( $p=0.02$ ) in ipsilateral cortex (IC) compared to contralateral cortex (CC) 1hr after reperfusion. At 48hrs, subjects with more ischaemic damage (shown immunohistologically) demonstrate higher FMZ binding in IC versus CC. DV values also show a transient global increase in FMZ binding at Day 2. By Day 14, DV maps show lower FMZ binding in IC compared to CC; this effect varied between subjects, depending on the extent of inflammation and neuronal loss observed via immunohistology. **Conclusions.** The results indicate bi-phasic changes in FMZ binding in the occluded cortex and globally after temporary brain ischaemia. Final interpretation of the focal FMZ changes will benefit from further histopathological categorisation into infarcted, selective neuronal loss or normal tissue, and from more detailed image analysis. However, other factors, over and above neuronal loss, such as blood brain barrier disruption, endoepine release, and GABAA receptor modulation may be contributing to the observed changes.

1. Heiss, W.D., Kracht, L.W., Thiel, A., Grond, M. & Pawlik, G. *Brain* 124, 20-9 (2001).
2. Sette, G. et al. *Stroke* 24, 2046-2057 (1993).
3. Buchan, A.M., Xue, D. & Slivka, A. *Stroke* 23, 273-279 (1992).

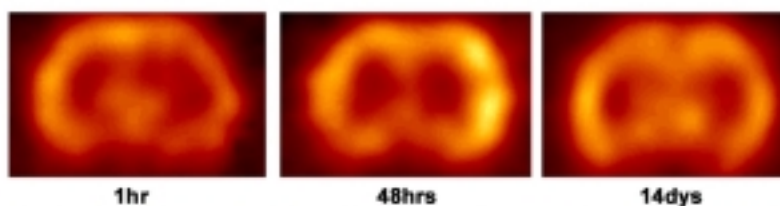


Figure 1. Example subject's DV maps at three time points post MCA reperfusion. Coronal slices are shown, the ipsilateral hemisphere is displayed on the right.

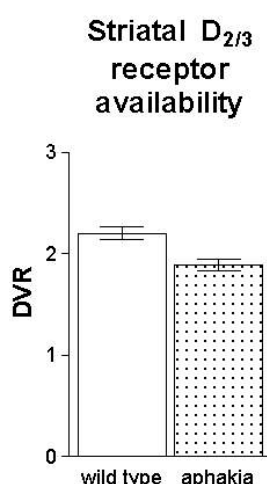
### DOPAMINE D<sub>2/3</sub> RECEPTOR BINDING IN APHAKIA MICE MEASURED BY MICROPET

Pedro Rosa-Neto, Andrew L. Goertzen, Mirko Diksic, Alain Dagher, Shadrek Mzengeza, Jean-Paul Soucy, Kelvin C. Luk, Vladimir Rymar, Abbas F. Sadikot, Alan C. Evans

*Montreal Neurological Institute, Montreal, QC, Canada*

**Rationale:** Several PET studies performed in the early phase of Parkinson's disease show an enhanced availability of striatal D<sub>2/3</sub> receptors compared to a control population. In rodent striatum increases of D<sub>2/3</sub> receptors density follows 6-OH lesions. This finding suggests an up-regulation of D<sub>2/3</sub> receptors secondary to the progressive degeneration of dopamine afferent fibers. The aphakia mouse harbors a mutation on the Pitx3 gene which, similarly to Parkinson's, causes degeneration of dopamine cells that innervates the dorsal striatum. However, unlike Parkinson's disease, dopamine deficits are already present in the neonatal life. We used the aphakia mouse to test the hypothesis that the up-regulation of D<sub>2/3</sub> receptors occurs independently of the age at which the dopaminergic deficit takes place. **Methods:** Baseline [<sup>11</sup>C]raclopride PET scans were performed in three male aphakia (N=3, 23±2g) and two C57 control mice (N=2, 38±2 g) using a CTI Concorde Microsystems microPET R4 scanner. PET data were obtained in animals anesthetized with isoflurane 2% administered by a nose cone. Each subject had a sixty-minute dynamic acquisition, which started concomitantly with bolus administration of [<sup>11</sup>C]raclopride (14-31 MBq) radioligand in the tail vein. Subsequently, data were reconstructed using Fourier rebinning followed by 2D filtered back projection, and time activity curves were obtained using regions of interest in both striatum (target region) and cerebellum (reference region). The output measure, distribution volume ratio (DVR), was calculated by the Logan reference tissue graphical method for irreversible ligands. **Results:** Preliminary analysis shows DVR of 1.89±0.2 for aphakia and 2.20±0.09 for C57 controls. Results are summarized in Figure 1. **Conclusion:** These preliminary results support the use of microPET to evaluate the impact of genetically induced changes of dopamine neurotransmission in D<sub>2/3</sub> receptor availability. **Figure 1.** [<sup>11</sup>C]raclopride DVRs obtained from aphakia (N=3) and control mice (N=2).

#### References:



Alexoff DL et al. Reproducibility of <sup>11</sup>C-raclopride binding in the rat brain measured with the microPET R4: effects of scatter correction and tracer specific activity. J Nucl Med 44(5):815-822.

This work was founded by the Canadian Institute of Health Research (CIHR).

**THE IMPACT OF ANESTHETIC DRUGS ON D1 RADIOLIGAND [3H]SCH 23390 BINDING IN VIVO**Ningning Guo<sup>1,2</sup>, Nosirudeen Quadri<sup>1,2</sup>, Zhihong Zhu<sup>1,2</sup>, Marc Laruelle<sup>1,2</sup><sup>1</sup>*Department of Psychiatry, Columbia University, New York, NY, USA*<sup>2</sup>*Division of Functional Brain Mapping, New York State Psychiatric Institute, New York, NY, USA*

Recent findings suggested that D1 and NMDA receptors display complex interactions in the brain, and that NMDA receptors regulate D1 receptor trafficking [1]. Our previous results have shown that NMDA blockade-induced D1 receptor internalization in the striatum can be examined by the D1 radioligand [3H]SCH 23390 in vivo in rodent models [2]. Application of anesthesia with the combination of ketamine plus isoflurane masked the effect of NMDA blockade on [3H]SCH 23390 binding in vivo in baboons and rats, while urethane anesthesia did not affect [3H]SCH 23390 binding [2]. However, the carcinogenic effect of urethane has limited the application of this drug mostly to nonsurvival studies in nonhuman primates. In search of anesthesia suitable to image the effect of NMDA blockade on D1 receptor binding in vivo in baboons, several anesthetic drugs including ketamine, isoflurane, chloral hydrate, propofol, and the induction agents acepromazine and telazol, were tested in the present studies in rodent models.

Male Sprague-Dawley rats were treated with ketamine (25 mg/kg, i.p.), isoflurane (2.0 - 3.0%), chloral hydrate (400 mg/kg, i.p.), propofol (10 mg/ml/injection, i.p.), acepromazine (10 mg/kg, i.v.), and telazol (40 and 100 mg/kg, i.p.) 30 min prior to radiotracer injection, and kept anesthetized during the experiments. The effect of MK 801 (1 mg/kg, i.p.) on D1 receptor binding was also examined under anesthesia with chloral hydrate or propofol. The drug-treated and control animals received the radiotracer [3H]SCH 23390 (< 8 mCi, mass < 32 ng/rat) through the tail veins and were sacrificed 1 hr after the tracer injection. The brain regions were dissected and counted with a gamma counter. The specific binding index was measured as V3', the ratio of region of interest (ROI) to cerebellum minus one. The differences between control and drug treated animals in [3H]SCH 23390 binding in vivo were analyzed with a Student's t-test. Ketamine, isoflurane, and chloral hydrate induced significant increases in [3H]SCH 23390 V3' in different brain regions in anesthetized rats. Propofol, acepromazine, acepromazine plus propofol, or telazol (100 mg/kg) anesthesia decreased [3H]SCH 23390 striatal V3' (20-30%) in the brain, a similar effect as urethane anesthesia [2]. Like anesthesia with ketamine plus isoflurane, chloral hydrate anesthesia masked the effect of MK 801 induced increase in [3H]SCH 23390 striatal V3'. Compared to propofol alone, MK 801 produced 30% increase in the striatal V3' in rats anesthetized with propofol. In conclusion, the present study indicates that ketamine, isoflurane or chloral hydrate administration resulted in significant increase in [3H]SCH 23390 in vivo binding in rats, that they would mask the effect of NMDA blockade on D1 receptor trafficking. However, anesthetic drug propofol, and induction agents acepromazine and telazol did not increase [3H]SCH 23390 binding in vivo. These drugs are therefore promising anesthetic agents for imaging studies in both primates and rodents concerning the interaction of NMDA and D1 receptors. Reference: 1. Scott, L. et al. Proc Natl Acad Sci U S A 99, 1661-4 (2002); Pei L. et al, J Neuroscience, 24, 1149-1158 (2004). 2. Guo, N. et al. Neuropsychopharmacology 28, 1703-11 (2003).

**QUANTIFICATION OF PET STUDIES WITH THE HIGH AFFINITY D2/D3 RECEPTOR LIGAND [C-11]FLB-457: RE-EVALUATION OF THE VALIDITY OF USING A CEREBELLAR REFERENCE REGION**

Marie-Claude Asselin<sup>1</sup>, Andrew J. Montgomery<sup>2</sup>, Susan P. Hume<sup>1</sup>, Paul M. Grasby<sup>2</sup>

<sup>1</sup>*Hammersmith Imanet, Hammersmith Hospital, London, UK*

<sup>2</sup>*MRC Clinical Sciences Centre, Hammersmith Hospital, London, UK*

Introduction: The PET radioligand [C-11]FLB-457 was developed in order to study extrastriatal tissues where the D2/D3 receptor densities are 1-2 orders of magnitude lower than in the striatum. Most PET/[C-11]FLB-457 studies have been quantified using the simplified reference tissue model (SRTM), assuming that the D2/D3 receptor density in the cerebellum is negligible. The present study investigated the effects of specific binding in the reference region on estimates of radioligand affinity (KD), regional binding potential (BP) and receptor occupancy. Methods: Ex vivo saturation studies were conducted in 17 Sprague-Dawley rats by either varying the dose of [C-11]FLB-457 injected or pre-dosing with stable ligand. The in vivo affinity was estimated from the single-site binding model that included a parameter for non-specific uptake (Bns), and from Scatchard analyses using either Bns or cerebellar uptake as an estimate of free ligand concentration. Ten male volunteers underwent a 90-min dynamic PET study in the ECAT/EXACT3D tomograph after a bolus injection of [C-11]FLB-457. The volume of distribution (VD) was estimated from ROI-derived time-activity curves (thalamus, hippocampus, frontal cortex, cerebellum) using a two-tissue compartment four-rate constant model with a metabolite-corrected plasma input function. BP was calculated as VD ratio minus 1, assuming that the cerebellum is a suitable reference region. The apparent BP and occupancy (relative reduction in BP) were estimated using equations derived to account for the presence of specific binding in the reference region and compared to values estimated without specific binding. Results: In rat brain, radioligand binding decreased with increasing dose of stable ligand in all tissues, including the cerebellum. From the single-site binding model parameters, the cerebellar BP(=Bmax/Bns) is estimated to be ~1.5. The in vivo KD is overestimated by a factor of ~5, if the cerebellum is used as an estimate of non-specific uptake. Using D2/D3 receptor density (Bmax) measurements in postmortem human brains, the striatal BP is underestimated by ~5% for the low affinity radioligand [C-11]raclopride (KD~1nM) compared to ~50% for the high affinity radioligand [C-11]FLB-457 (KD~0.02nM). The cortical BP is underestimated by >50% for both radioligands, indicating that the D2/D3 receptor density in the cerebellum is too high relative to that in cortical regions for use as a reference region, regardless of the affinity of the radioligand. As the cerebellar BP is simulated to increase from 0.1 to 3, the occupancy is increasingly underestimated, but uniformly across regions of different receptor densities. However, if the occupancy is lower in the reference than in the target regions, low density regions appear to have a higher occupancy than high density regions. Conclusion: Specific binding was estimated to account for more than half of the cerebellar uptake of [C-11]FLB-457, invalidating its use as an estimate of non-specific binding. The in vivo affinity of [C-11]FLB-457 may be even higher than previously estimated, thereby increasing the specific activity required in order to avoid the mass effect of co-injected stable FLB-457. Measurements of regional receptor occupancies using radioligands of different affinities may obscure or create differential occupancies between regions of different receptor densities.

## FORMATION OF BINDING POTENTIAL MAPS OF ADENOSINE A1 AND A2A RECEPTORS USING INDEPENDENT COMPONENT ANALYSIS WITHOUT ARTERIAL BLOOD SAMPLING

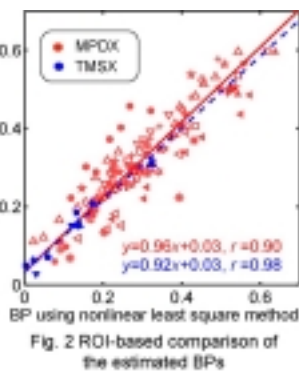
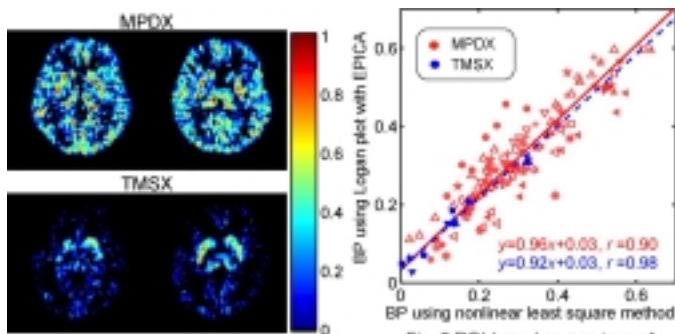
Mika Naganawa<sup>1</sup>, Yuichi Kimura<sup>2</sup>, Tadashi Nariai<sup>3</sup>, Kenji Ishii<sup>2</sup>, Keiichi Oda<sup>2</sup>, Yoshitsugu Manabe<sup>1</sup>, Kunihiro Chihara<sup>1</sup>, Kiichi Ishiwata<sup>2</sup>

<sup>1</sup>Graduate School of Information Science, Nara Institute of Science and Technology, Nara, Japan

<sup>2</sup>Positron Medical Center, Tokyo Metropolitan Institute of Gerontology, Tokyo, Japan

<sup>3</sup>Department of Neurosurgery, Tokyo Medical and Dental University, Tokyo, Japan

**Introduction:** The adenosine A1 and A2A receptors in the human brain can be visualized by PET with [11C]MPDX [1] and [11C]TMSX [2], respectively. Previously we proposed a method for extracting a plasma time-activity curve (pTAC) using independent component analysis (EPICA) from dynamic PET images [3] to omit serial arterial blood sampling in kinetic analysis. EPICA is a pTAC extraction method assuming that spatial distributions of the brain tissue and the blood vessels are statistically independent. In this study, EPICA was applied to dynamic PET images with two adenosine receptor ligands, and parametric images on distribution volumes (DVs) and binding potentials (BPs) were estimated by Logan plot using the estimated pTAC. **Methods:** Dynamic PET scans were performed on 18 subjects (including 11 normal volunteers and 7 patients with epilepsy or other disorders) with [11C]MPDX, and 5 normal volunteers with [11C]TMSX. The DVs were calculated in each voxel by Logan plot using the EPICA-estimated pTAC. The candidate for reference region was manually drawn on the cerebellum. Voxels beyond 80 percentile of DV image were excluded to refine the reference region. BP maps were calculated using the DV images and the reference regions. Several ROIs ([11C]MPDX: 7, [11C]TMSX: 2) were placed on each subject's image, and nonlinear least square method was applied for ROI-based comparison. **Results:** The examples of the estimated BP maps were shown in Fig. 1. BP maps of [11C]MPDX show relatively high values across the brain, while BP maps of [11C]TMSX show extremely high values in striatum and thalamus, as compared with other areas. ROI-based comparison was shown in Fig. 2. There was close agreement between both calculated results. **Conclusion:** We conclude that EPICA allows BP parametric imaging of adenosine A1 and A2A receptors without arterial blood sampling. **Reference:** [1] K. Ishiwata, et al., *Ann Nucl Med*, Vol. 16, 377-382, 2002. [2] K. Ishiwata, et al., *Ann Nucl Med*, Vol. 17, 457-462, 2003. [3] M. Naganawa, et al., *IEEE Trans Biomed Eng*, Vol. 52, No. 2, 2005.





## BOLUS-PLUS-INFUSION TRANSFORMATION (BPIT) OF BOLUS-ONLY PET EXPERIMENTS: APPLICATIONS TO DOPAMINE RECEPTOR AND TRANSPORTER LIGANDS

Hiroto Kuwabara, Anil Kumar, Weiguo Ye, Dean F. Wong

*Radiology, Johns Hopkins University, Baltimore, MD, USA*

Objectives: We reported the BPIT plot whose independent variable was time as a novel variation of the graphical analysis (NeuroImage 22: T81). In this study, we compared BPIT with a linear version of the simplified reference tissue method (SRTM; Ichise et al., 2003) and reference tissue graphical analysis (RTGA; Logan et al. 1996) in dopamine-related ligands of varying dissociation levels. Methods: Healthy control subjects were studied with PET following a bolus injection of [11C]raclopride, a DA D2/D3 receptor ligand (n=21), [11C]methylphenidate (n=21), a DA membrane transporter ligands, or [11C]DTBZ, a VMAT-2 ligand (n=15). Radioactivity time-profiles were obtained for anterior (ant-) and posterior (post-) putamen (Pu) and caudate nucleus (CN), ventral striatum (VS), and cerebellum (Cb). BPIT utilized the plateau portion (t0-90 min) of the following plot:  $w_1 \cdot A(T) + w_2 \cdot \int_{t_0}^T A(t)dt$  where  $w_1$  and  $w_2$  are constants and  $A(T)$  represents the radioactivity in a region. The time  $t_0$  was determined on each ligand as the first frame after the slowest peak among all striatal regions across all subjects. The ligand-specific  $t_0$  values were used in variations of SRTM and RTGA where the reference region terms were excluded from respective operational equations (SRTM-R and RTGA-R). In variations including the reference region terms (SRTM+R and RTGA+R), reported circulation times were used while the brain-to-blood clearance rate constant of the reference regions ( $k_2R$ ) was estimated per subject (SRTM+R) or set to reported values (RTGA+R). The differences between BP estimates of two approaches were expressed by percent deviation:  $(BP_1 - BP_2)/(BP_1 + BP_2) \cdot 100$ , where subscripts 1 and 2 denote BP estimates of two approaches to compare. Results: Estimates of  $t_0$  were 30, 50, and 40 min for [11C]rac, [11C]MP, and [11C]DTBZ, respectively. Using ligand-specific  $t_0$ , a no slope model described the BPIT plot better than a linear model in more than 96% regions (i.e., the BPIT plot reached a plateau). Percent deviations between the approaches are listed in the Table. BPIT, STRM, and RTGA yielded essentially identical estimates of regional BP for [11C]rac scans. The three methods yielded identical regional BP using -R variations for [11C]MP scans, while slight deviations were observed between +R and -R variations. We found relatively large SD for [11C]DTBZ although deviations remained minimal. Conclusions: This study indicated that the BPIT plot reached a plateau at ligand-specific  $t_0$ . After  $t_0$ , BPIT yielded essentially identical estimates of BP as variations of SRTM and RTGA without the reference region terms. Therefore, we conclude that BPIT is an alternative approach for the ligands examined in this study. Further investigation may be due regarding whether including or excluding the reference tissue term in SRTM and RTGA for [11C]MP.

Table Percent deviation of BP estimates between methods (mean  $\pm$  standard deviation)

Approaches	[11C]Raclopride	[11C]Methylphenidate	[11C]DTBZ
SRTM-R vs. BPIT	0.26 $\pm$ 0.22	0.52 $\pm$ 0.75	-0.28 $\pm$ 14.3
RTGA-R vs. BPIT	0.14 $\pm$ 0.25	0.12 $\pm$ 0.71	-0.94 $\pm$ 8.8
SRTM-R vs. SRTM+R	-0.19 $\pm$ 0.53	2.6 $\pm$ 1.4	0.63 $\pm$ 18.5
RTGA-R vs. RTGA+R	0.03 $\pm$ 0.28	-3.2 $\pm$ 1.8	1.9 $\pm$ 9.1

## DEVELOPMENT OF A TRACER KINETIC MODEL FOR THE ANALYSIS OF (R)-[11C]VERAPAMIL DATA

Mark Lubberink<sup>1</sup>, Gert Luurtsema<sup>1</sup>, Bart N.M. van Berckel<sup>1</sup>, Ronald Boellaard<sup>1</sup>, Rolf Toornvliet<sup>2</sup>,  
Eric J.F. Franssen<sup>2,3</sup>, Adriaan A. Lammertsma<sup>1</sup>

<sup>1</sup>*Department of Nuclear Medicine and PET Research, VU University Medical Centre, Amsterdam, The Netherlands*

<sup>2</sup>*Department of Pharmacy, VU University Medical Centre, Amsterdam, The Netherlands*

<sup>3</sup>*Department of Pharmacy, OLVG, Amsterdam, The Netherlands*

Introduction: P-glycoprotein (P-gp) mediated transport across the blood-brain barrier (BBB) may play an important role in several neurological disorders. Although racemic [11C]verapamil has been used for assessing P-gp function [1], potential difference in kinetics between both isomers dictates the use of an optically pure tracer for quantitative studies. Verapamil can be metabolised through N-demethylation and N-dealkylation, with labelled metabolites amounting to ~70% of total plasma activity one hour p.i. in rats [2]. N-dealkylated metabolites, which have high lipophilicity and are similar to verapamil itself, probably undergo rapid brain uptake and, unlike N-demethylated metabolites, probably also show affinity for P-gp. The aim of the present work was to study the kinetics of (R)-[11C]verapamil in humans and to develop a pharmacokinetic model for the analysis of P-gp mediated transport of (R)-[11C]verapamil, incorporating the contribution of its radioactive metabolites. Methods: Dynamic PET scans (60 minutes) were acquired in ten healthy volunteers (mean age 43, range 21-68) following intravenous injection of ~370 MBq (R)-[11C]verapamil. Six volunteers were scanned twice on the same day for test-retest analysis. During the scan arterial blood was monitored continuously and additional samples were taken for metabolite analysis. Total plasma, parent verapamil, HPLC (N-dealkylation) metabolite and polar (N-demethylation) metabolite input curves were determined. PET images were segmented based on co-registered MRI data. Whole brain grey matter data were analysed with various reversible one or two tissue compartment models, with separate metabolite compartments, assuming that either only verapamil or verapamil and any combination of metabolites cross the BBB, and using Logan analysis with a single input function either corrected or not corrected for one or both of the metabolites. Results: Metabolites due to N-dealkylation and N-demethylation each represented 20 to 30% of total plasma radioactivity at 1 h p.i. Fit results are given in the table. Most models fitted the data well and the Akaike criterion did not point to a definite 'best' model, with differences in optimal model between subjects. The lowest mean test-retest variability (2.9 %) was found for a single tissue model without any metabolite correction. There was good agreement between the results of the Logan analysis and those of the corresponding compartment models. Conclusion: Based on rat data, metabolites of (R)-[11C]verapamil are likely to cross the BBB. However, a compartment model including separate metabolite compartments leads to high test-retest variability. This is probably due to the statistical uncertainty of the parent fraction and HPLC metabolite data, as well as the increased number of model parameters. Assuming similar kinetics for (R)-[11C] verapamil and HPLC metabolites, a one input, one tissue model with correction for polar metabolites only leads to a good compromise between fit quality and test-retest variability. Further studies into the kinetics of the radioactive metabolites of (R)-[11C]verapamil are necessary to define the biologically most correct model. [1] Bart J et al, Neuroimage 20:1775-82, 2003 [2] Luurtsema G et al, Nucl Med Biol, in press

	Akaike weight mean (SD)	T/R variability (%)	V <sub>d</sub> mean (SD)
V 2T	0.15 (0.08)	22	1.20 (0.32)
V+M1 2T	0.12 (0.08)	14	0.77 (0.15)
V 1T, M2 1T	0.12 (0.08)	8	0.51 (0.08)
V+M1+M2 1T	0.10 (0.11)	3	0.60 (0.09)
V 1T, M1+M2 1T	0.10 (0.04)	5	0.53 (0.08)
V+M1 1T	0.09 (0.11)	4	0.69 (0.11)
V+M1 1T, M2 1T	0.07 (0.03)	8	0.53 (0.09)
V+M1+M2 2T	0.07 (0.06)	7	0.63 (0.09)
V 1T, M1 1T, M2 1T	0.02 (0.01)	8	0.50 (0.08)

V = verapamil

M1 = N-dealkylation metabolites (HPLC)

M2 = N-demethylation metabolites (polar fraction)

xT = number of tissue compartments



**A RAPID CBF/CMRO<sub>2</sub> MEASUREMENT WITH A SINGLE PET SCAN WITH DUAL-TRACER/INTEGRATION TECHNIQUE IN HUMAN**

**Takuya Hayashi**, Nobuyuki Kudomi, Hiroshi Watabe, Hisashi Oka, Kohei Hayashida,  
Yoshinori Miyake, Hidehiro Iida

*National Cardiovascular Center, Research Institute, Osaka, Japan*

CBF/CMRO<sub>2</sub> may be quantified using PET with <sup>15</sup>O-tracers, but the conventional three-step technique (3S) requires a long study period, attributed to need for separate acquisition for three radioactive tracers for CBF (H<sub>2</sub><sup>15</sup>O or C<sup>15</sup>O<sub>2</sub>), CMRO<sub>2</sub> (<sup>15</sup>O<sub>2</sub>), and CBV (C<sup>15</sup>O). Simultaneous determination of CBF, CMRO<sub>2</sub> and CBV from a single dynamic <sup>15</sup>O<sub>2</sub> scan is known to suffer from statistical uncertainty. We recently developed a rapid technique that allows sequential administration of two of three tracers (for CBF and CMRO<sub>2</sub>) in a single PET scan, and generates quantitative CBF/CMRO<sub>2</sub> images with a dual-tracer integration method (DTI). This study asked whether this technique is feasible in normal human subjects and how accurate quantitative values it provides in comparison with the 3S and non-linear fitting method (NLM). Eight normal subjects (24.2 ± 2.6 y.o) participated in this study. The protocol of the study was approved by the local ethical committee. All subjects received three emission scans, i.e., a 4-min scan after short bolus administration of C<sup>15</sup>O, a 9.5-min scan with dual administration of C<sup>15</sup>O<sub>2</sub> followed by <sup>15</sup>O<sub>2</sub>, and a 9-min scan with <sup>15</sup>O<sub>2</sub> followed by H<sub>2</sub><sup>15</sup>O. With correction for blood volume using the first C<sup>15</sup>O scan data, CBF/CMRO<sub>2</sub> images were generated by 3S using the first part of the second (CO<sub>2</sub>) and the third scan (O<sub>2</sub>), whereas those by DTI method were calculated using both part of PET data in each of the second or the third scan. The calculation used a mathematical formula derived from a single-tissue compartment model including a correction for blood volume and an assumed partition coefficient for water. Regional quantitative values of CBF/CMRO<sub>2</sub> in the DTI was compared with those by 3S and NLM. We also compared by voxel-by-voxel CBF or CMRO<sub>2</sub> images between the second and the third DTI scan to test the regional difference. Global CBF or CMRO<sub>2</sub> values for the DTI did not differ from those by the 3S, and between the second and third DTI scans. The cortical regional values of the DTI neither differed significantly from those of 3S and NLM. In contrast, CMRO<sub>2</sub> values of the white matter region in both 3S and DTI differed significantly from NLM, as was predicted from a simulation study for the error in the assumed partition coefficient. Voxel-based comparison of CBF images between the second and the third DTI scan showed significant difference at brain regions around nasal cavity, and at the somatosensory areas that may come from the difference in methodology (inhalation or venous-injection of CBF tracer) and physiology (sensation of intravenous injection), respectively. These were also seen when compared CMRO<sub>2</sub> images, but at a lower height threshold. These results suggest that this DTI technique generates CBF/CMRO<sub>2</sub> images with a considerably shortened scan period, which are comparable to those by 3S, in terms of quantitative accuracy and image quality. The technique may be of use for clinical studies in patients particularly with acute stroke, and also for investigation of metabolic coupling during neuronal activation or pharmacological challenges in human.

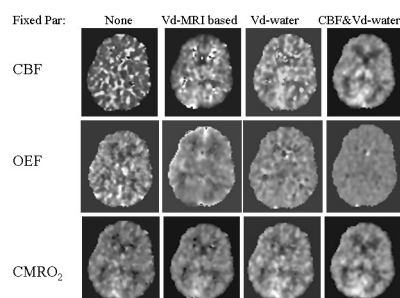
## ACCURACY AND QUALITY OF PARAMETRIC CBF, OEF AND CMRO<sub>2</sub> IMAGES: EFFECTS OF FIXING PARAMETERS

Ronald Boellaard<sup>1</sup>, Abraham Rijbroek<sup>2</sup>, Adriaan A. Lammertsma<sup>1</sup>

<sup>1</sup>Department of Nuclear Medicine and PET Research, VUmc, Amsterdam, The Netherlands

<sup>2</sup>Department of Surgery, VUmc, Amsterdam, The Netherlands

Introduction: Parametric CBF, OEF and CMRO<sub>2</sub> images can be derived from oxygen-15 labelled H<sub>2</sub>O, O<sub>2</sub> and CO scans. Traditionally, this is performed using a steady state approach. With some cyclotrons, such as the RDS 112, however, these tracers can only be administered as a bolus or short inhalation. Therefore, a basis function method was developed for generating parametric images based on bolus/short inhalation administration and dynamic PET scans [1]. In the present study, several variations of this basis function method were implemented and the effects on parametric image quality assessed. Methods: The basis function method [1] is based on a modified version of the kinetic model as described by Mintun et al. [2]. In this study various implementations of this basis function method were developed. These methods differed in the number of parameters derived from the water scan that were subsequently fixed in fitting the oxygen data: dispersion, volume of distribution of water (Vd) and CBF. An additional implementation used fixed values of Vd derived from a co-registered and segmented MRI scan. Note that CBF images were generated from the oxygen scan alone, except when CBF was reused from the water scan. First, simulations were performed to assess the effects of fixing none, one or more parameters on the accuracy and precision of CBF (from oxygen scan alone), OEF and CMRO<sub>2</sub> as function of noise (0.5, ..., 25%). Next, using each implementation, parametric CBF, OEF and CMRO<sub>2</sub> images were calculated for 10 clinical studies. Results: Both simulations and clinical images showed that bias (>25%) and poor reproducibility (>100%) of CBF and OEF were substantial when no parameter was fixed. Bias and precision improved to acceptable levels (<10 and 25%, respectively) when Vd was fixed from the water scan. Reusing Vd from the water scan provided slightly poorer precision for all parameters than when using fixed Vd values for grey and white matter (based on MRI scan), but may be more accurate in clinical practice. Bias and precision of CMRO<sub>2</sub> was almost independent of specific model implementation. The quality of clinical parametric images, as shown in figure 1, was consistent with the findings of the simulation study, indicating that primarily the quality of CBF and OEF images depend on the number of parameters reused. Conclusions: Accuracy and precision of CBF and OEF and, the quality of parametric CBF and OEF images depend on the specific basis function method implementation, i.e. 'better' results are obtained by fixing or reusing more parameters from the water data within the analysis of the oxygen scan. However, CMRO<sub>2</sub> data with sufficient image quality can be obtained without reusing or fixing any parameters.



**THE D2-AGONIST RADIOTRACER [11C]-(+)-PHNO SHOWS A MARKED INCREASE IN SENSITIVITY TO AMPHETAMINE CHALLENGES WHEN COMPARED TO [11C]RACLOPRIDE IN THE CAT BRAIN**

**Nathalie Ginovart**<sup>1,2</sup>, Alan A. Wilson<sup>1,2</sup>, Matthaeus Willeit<sup>1</sup>, Ken Singh<sup>1</sup>, Douglas Hussey<sup>1</sup>, Armando Garcia<sup>1</sup>, Sylvain Houle<sup>1,2</sup>, Shitij Kapur<sup>1,2</sup>

<sup>1</sup>*PET Centre, Centre for Addiction and Mental Health, Toronto, ON, Canada*

<sup>2</sup>*Department of Psychiatry, University of Toronto, Toronto, ON, Canada*

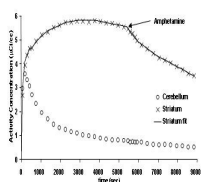
Imaging the high affinity state of the D2-receptor using agonist radioligands has aroused considerable interest recently as it could allow for measurements of the functional state of the receptor rather than the total receptor population as measured by antagonist radioligands. Here we report on the evaluation of [11C]-(+)-PHNO as a potential radioligand for in vivo study of the high affinity state D2-receptor using positron emission tomography (PET) in the cat brain. Five cats were anesthetized with isoflurane and scanned using the high resolution PET camera system CPS-HRRT. At baseline conditions, high levels of radioactivity were observed in the striatum whereas low levels of radioactivity were observed in cerebellum. Radioactivity in cerebellum peaked within two minutes post-injection and decreased rapidly thereafter. Radioactivity in striatum peaked at 8-10 minutes post-injection, demonstrating that [11C]-(+)-PHNO binding in this structure is reversible and reaches equilibrium within the time frame of a PET experiment. The striatal binding potential (BP) approximated using the ratio of specific/non-specific (specific = striatum – cerebellum, non-specific = cerebellum) between 31 and 60 minutes post-injection was  $3.75 \pm 0.51$  (n=5). Pretreatment with raclopride (1mg/kg; i.v.) or haloperidol (0.5mg/kg; i.v.) reduced [11C]-(+)-PHNO striatal BP by 85% and 94%, respectively, indicating that the majority of radioligand binding in striatum represents specific binding to D2-receptors. Pretreatment with SCH23390 had no effect on [11C]-(+)-PHNO binding. A direct comparison of [11C]-(+)-PHNO and [11C]NPA binding in the same cat showed that [11C]-(+)-PHNO displayed a higher striatal BP than [11C]NPA (3.41 versus 1.59), suggesting that [11C]-(+)-PHNO may be more sensitive than [11C]NPA for in vivo imaging of the high-affinity D2-receptors. Comparison of the dose-effect of amphetamine (0.1, 0.5 and 2 mg/kg i.v.) on both [11C]-(+)-PHNO and [11C]raclopride binding in striatum showed that [11C]-(+)-PHNO was more sensitive to the dopamine releasing effect of the drug. The highest dose of amphetamine induced a 83-88% inhibition of [11C]-(+)-PHNO binding (n=3) and a 60-63% inhibition of [11C]raclopride binding (n=2). Preliminary data showed that the ED50 of amphetamine for inhibiting [11C]-(+)-PHNO and [11C]raclopride striatal bindings were 0.25 mg/kg and 0.63 mg/kg, respectively. Interestingly, the hyperbolic function used to fit the dose-effect data and derive ED50 values best fitted the experimental data when the maximal occupancy value was set at 100% for [11C]-(+)-PHNO and when it was set at only 80% for [11C]raclopride. These results suggest that, in contrast to what is observed with the antagonist radioligand, amphetamine-released dopamine had access to the entire population of D2-receptors recognized by [11C]-(+)-PHNO. Preliminary human PET scans with [11C]-(+)-PHNO are underway. Initial results obtained in 2 healthy volunteers show high striatal uptake with a BP of 2.66 and 2.86, respectively, as approximated using the simplified reference tissue model. These data indicate that [11C]-(+)-PHNO binding in striatum is specific for D2-receptors. The high penetration of [11C]-(+)-PHNO in brain, its high signal to noise ratio, its favourable in vivo kinetics as well as its high sensitivity to amphetamine shows that [11C]-(+)-PHNO has highly suitable characteristics for probing the high-affinity state of D2-receptors with PET.

## METHODOLOGICAL DEVELOPMENT OF DYNAMIC DOPAMINE RELEASE USING [18F]DESMETHOXYFALLYPRIDE

Todd E. Barnhart<sup>1</sup>, Alexander K. Converse<sup>2</sup>, Terrence R. Oakes<sup>2</sup>, Jonathan A. Nye<sup>3</sup>, David W. Dick<sup>3</sup>, Dhanabalan Murali<sup>3</sup>, Fabio Ferrarelli<sup>4</sup>, Marchello Massimini<sup>4</sup>, Guilio Tononi<sup>4</sup>, Mary L. Schneider<sup>5,6,7</sup>, Julie A. Larsen<sup>6,7</sup>, Jogeshwar Mukherjee<sup>8</sup>, Charles K. Stone<sup>9</sup>, Onofre T. DeJesus<sup>3</sup>, Robert J. Nickles<sup>3</sup>, Andrew D. Roberts<sup>1</sup>

<sup>1</sup>Wolfson Molecular Imaging Centre, University of Manchester, UK, <sup>2</sup>Keck Laboratory for Functional Brain Imaging, <sup>3</sup>Dept. of Medical Physics, <sup>4</sup>Dept. of Psychiatry, <sup>5</sup>Department of Psychology, <sup>6</sup>Dept. of Kinesiology, <sup>7</sup>Harlow Center for Biological Psychology, Univ of Wisconsin-Madison, WI, <sup>8</sup>Dept. of Psychiatry & Human Behavior, Univ of California-Irvine, Irvine, CA, <sup>9</sup>School of Medicine, Univ of Wisconsin-Madison, WI, USA

**Introduction:** There is a need for an appropriate longer lived ligand for use in dopamine release experiments which would allow for a single bolus injection, a single dynamic scan, and include both baseline and activation conditions. To this end, dopamine release experiments using the dopamine D2-type receptor antagonist [18F]desmethoxyfallypride were performed for the purpose of methodological development of a single bolus and scan technique. The dopamine release was the response to an injection of d-amphetamine (rhesus) or to transcranial magnetic stimulation (TMS) (human), which has been shown to non-invasively release dopamine (Strafella, 2001). [18F]Desmethoxyfallypride, like [11C]raclopride, is susceptible to competition from endogenous dopamine (Mukherjee, 1996), whereby dopamine released reduces available binding sites for the tracer. The observed reduction in tracer binding therefore indicates increased synaptic dopamine concentration. New implementation of the simplified reference region method (SRRM) (Lammertsma, 1996) provided the quantization of changes in binding potentials (BP). **Methods:** The dopamine release experiment using [18F]desmethoxyfallypride/d-amphetamine was performed on a rhesus monkey. An injection of [18F]desmethoxyfallypride (5 mCi) was given at the beginning of the 150-minute scan. At 90 minutes, d-amphetamine was injected (0.4mg/kg). The dopamine release experiment using [18F]desmethoxyfallypride/TMS used an injection of [18F]-desmethoxyfallypride (5 mCi) given at the beginning of the 150-minute scan. The left dorsolateral prefrontal cortex was stimulated with 1 Hz TMS, 90 minutes into the session at 120% of motor threshold. TMS pulses were delivered for 90 seconds followed by 90 seconds or rest and repeated for a total of 360 pulses. Modeling was based upon the SRRM, divided into three time periods, (baseline, activation, and post-activation), solving for R1, k2, and multiple BPs, one for each period, making a dynamic reference region model (DRRM). The constants were then solved for by recursively filling the array and using the IDL amoeba function minimizing the cost function. **Results:** The figure shows TACs for the [18F]desmethoxyfallypride/amphetamine ROI data in the cerebellum and the striatum versus the DRRM fit. BP decreased by 30% for the amphetamine and 12% for TMS between baseline and post-activation. **Conclusion:** The most important result of this work demonstrates [18F]desmethoxyfallypride's ability to measure activation corresponding to dopamine release in a single scanning session, made possible by the 18F 110 minute half-life. Modeling techniques such as DRRM are easily applied to these activation protocols providing binding potentials for both baseline and activation conditions. [18F]Desmethoxyfallypride provides an improved PET tracer and methodology for dopamine release experiments and studies of the time course of the dopaminergic response. Mukherjee et al,(1996)Life Sciences 59:669-678. Lammertsma and Hume,(1996)Neuroimage 4:153-158. Strafella et al.,(2001)Journal of Neuroscience 21:1-4.





## ESTIMATION OF RECEPTOR OCCUPANCY AND SYNAPTIC DOPAMINE AFTER AMPHETAMINE CHALLENGE: A COMPETITION MODEL APPROACH

Hiroto Kuwabara, Anil Kumar, James Brasic, Ayon Nandi, Dean F. Wong

*Radiology, Johns Hopkins University, Baltimore, MD, USA*

**Objectives:** Recently changes in receptor density (Bmax) and dissociation constant (KD) were reported to explain all of the observed decreases in binding potential (BP) after amphetamine challenge. In this report, we estimated the occupancy (O-amph) and synaptic concentration (C-amph) of amphetamine-derived DA assuming no changes in Bmax and KD (a competition model) to speculate whether the BP changes were in fact explained by occupancy changes. **Methods:** Eight healthy subjects (age:  $25 \pm 6$ ) were studied with PET for 90 min following a bolus injection of [11C]raclopride. Each subject underwent one high specific activity scan under a baseline (HSA-B), one HSA scan following i.v. amphetamine (0.3mg/kg; HSA-A), and one low specific activity baseline scan (LSA-B). Radioactivity time-profiles were obtained for anterior (ant-) and posterior (post-) putamen (Pu) and caudate nucleus (CN), ventral striatum (VS), and cerebellum (Cb). Regional estimates of BP were obtained by the bolus-plus-infusion transformation (BPIT) approach (NeuroImage 22: T81 & T117) using Cb as a reference region, together with bound raclopride (B-rac in pmol/ml) in HSA-B and LSA-B scans. Regional Bmax and KD were obtained by the Eadie-Hofstee plot:  $B = -BP \cdot KD + B_{max}$  where B is the sum of bound baseline DA (B-base, assumed a 10% occupancy) and B-rac. The total bound of the HSA-A scan (B) was obtained by inserting observed BP to the plot. Then, bound amphetamine-derived DA (B-amph) was obtained by subtracting B-base and B-rac from B. The occupancy by amphetamine-derived DA was obtained by dividing B-amph by Bmax. Finally the synaptic concentrations of baseline and amphetamine-derived DA (C-base and C-amph) were obtained using the following equation after a modification:  $O = C / (KD + C)$ . Separately amphetamine induced DA release (DAR) was calculated as follows:  $(BP_{base} - BP_{amph}) / BP_{base} \cdot 100$  (%). **Results:** Regional estimates of Bmax, KD, occupancy by amphetamine-derived DA, intra-synaptic concentrations of baseline and amphetamine-derived DA are listed in the Table. Amphetamine induced increases in intra-synaptic DA ranged from 61% (ant-CN) to 159% (post-Pu). **Conclusions:** This study indicated that synaptic DA increased modestly (<200%) following amphetamine challenge when a 10% baseline DA occupancy was assumed. The magnitudes were consistent with the several fold-increase in extracellular DA reported in microdialysis studies in non-human primates. Thus, we conclude that a competition model may be able to describe changes in DA kinetics without assuming changes in Bmax and KD in acute amphetamine challenge.

Table: Regional values of the competition model (Assuming a 10% baseline DA occupancy)

Variables (unit)	Ant-Pu	Post-Pu	Ant-CN	Post-CN	VS
B <sub>max</sub> (pmol/ml)	37.6450	36.4442	29.7452	17.6628	27.8143
K <sub>D</sub> (pmol/ml)	11.5118	10.9114	10.6427	9.4812	11.5816
C <sub>base</sub> (%)	8.8036	14.5942	6.0011	6.4461	9.5028
C <sub>amph</sub> (pmol/ml)	1.3602	1.2602	1.2602	1.1401	1.3602
C <sub>total</sub> (pmol/ml)	1.1405	1.2608	0.7605	0.7607	1.3604
DAR (%)	9.6460	15.9446	6.4635	6.9667	10.4332

**EFFECT OF ACUTE SYSTEMIC BACLOFEN ON AMPHETAMINE STIMULATED STRIATAL DOPAMINE RELEASE AS MEASURED IN RATS WITH [3H]RACLOPRIDE****Rikki N. Waterhouse, Raymond C. Chang, Patty Carambot, Harold A. Sackeim***Department of Psychiatry, Columbia University, New York, NY, USA*

Introduction: Recent reports demonstrate that the GABA-B receptor agonist baclofen attenuates the reinforcing effects of cocaine and amphetamine in rats. Baclofen also appears to be an effective treatment in patients addicted to cocaine. With respect to mechanism of action, microdialysis studies have revealed that baclofen attenuates psychostimulant induced increases in dopamine efflux in the rat nucleus accumbens. We provide here a first assessment of the effect of baclofen on D-amphetamine (amph) stimulated striatal dopamine release using radiotracer methods. Methods: Indirect measurement of striatal dopamine concentration changes were made through regional brain biodistribution analyses using the dopamine D2/3 antagonist radiotracer [3H]raclopride. Drugs or carrier were administered to awake male rats (220-265 g) 5-30 min prior to [3H]raclopride injection (12  $\mu$ Ci, 100  $\mu$ l saline), including saline (100  $\mu$ l, iv), amphetamine (1, 5, 8 and 10 mg/kg, iv), baclofen (0.25, 1.0 and 2.5 mg/kg ip), and the GABA-B antagonist CPG 54626 (2.5 mg/kg, ip). Regional %ID/g values were determined 45 min after tracer administration, and striatum to cerebellum (ST/CB) ratios calculated. Results: A dose dependent amphetamine induced reduction of [3H]raclopride ST/CB ratios was observed, with lower ST/CB ratios occurring with higher amphetamine dose [saline ST/CB:  $8.49 \pm 1.12$ , n = 8; 1 mg/kg amph:  $8.27 \pm 1.55$ , p = 0.50, n = 4; 5 mg/kg amph:  $6.51 \pm 0.32$ , p < 0.001, n = 4; 8 mg/kg amph ST/CB:  $4.67 \pm 0.49$ , n = 14, p < 0.001; 10 mg/kg:  $4.63 \pm 0.91$ , p < 0.001, n = 14]. Increased hyperactivity and other known amphetamine-associated behaviors were observed for all doses. Since 8 mg/kg amphetamine induced a maximal reduction in ST/CB ratios, we chose to first study baclofen effects using at this dose. Compared to saline, 8 mg/kg amphetamine caused a significant reduction of [3H]raclopride ST/CB ratios (saline ST/CB:  $8.49 \pm 1.12$ , n = 8; amph ST/CB:  $4.67 \pm 0.49$ , n = 14, p < 0.001). Baclofen alone did not alter [3H]raclopride binding (ST/CB:  $8.79 \pm 0.86$ , n = 4, p = 0.65). However, baclofen (2.5 mg/kg) significantly blunted amphetamine stimulated dopamine release as measured with [3H]raclopride (ST/CB ratio:  $6.53 \pm 1.15$ , n = 11, p < 0.0017 compared to the amph group). The effect of baclofen on amphetamine stimulated dopamine release was maximum at 2.5 mg/kg and was partially prevented by CPG 54626 ( $5.85 \pm 0.59$ , n = 4, p = 0.24). Conclusions: These data support that GABA-B receptor activation by baclofen attenuates amphetamine stimulated striatal dopamine release, and that this subsequently impacts occupancy of dopamine at D2/3 receptors. In addition, the data reveal that [11C]raclopride or other dopamine receptor PET tracers may be used to follow the effects of GABA-B agonists on psychostimulant drug induced dopamine release in animal models and humans. In addition to drug addiction research, these findings may be relevant to the study of schizophrenia, where the reported loss of GABA-B receptors in the CNS may be at least partly responsible for the well-documented sensitivity to amphetamine in these patients.

**ADENOVIRUS-INDUCED OVEREXPRESSION OF D2 RECEPTORS ALTERS THE RESPONSIVITY OF STRIATAL DOPAMINE**

Wynne K. Schiffer<sup>1,2</sup>, David L. Alexoff<sup>1</sup>, Hubert H.M. Van Tol<sup>3</sup>, Vinal Patel<sup>1</sup>,  
Stephen L. Dewey<sup>1,2</sup>

<sup>1</sup>*Chemistry Department, Brookhaven National Laboratory, Upton, NY, USA*

<sup>2</sup>*Graduate Program In Neuroscience, Department of Neurobiology & Behavior, Stony Brook University, Stony Brook, NY, USA*

<sup>3</sup>*Department of Pharmacology, Faculty of Medicine, University of Toronto, Toronto, ON, Canada*

Introduction: Regulating dopamine (DA) D2 receptor (D2R) expression is a natural mechanism to adjust DA transmission in response to physiological demands. Because changes in receptor expression may cause significant alterations in neurochemical transmission, we (1) examined basal DA following acute, genetically-induced changes in D2R and (2) determined the extent to which this modifies the DA response to amphetamine with combined microPET/microdialysis experiments. Methods: Microdialysis cannula were surgically implanted in both striata of adult rats (250g, N=21). Of the animals that were inoculated (n=11), D2R expression was modified in one striatum using a recombinant vector (AdRSVD2; "ipsilateral") while the contralateral striatum received an inactive vector (AdRSVNull; "contralateral"). microPET/microdialysis procedures are described in (1). Paired-bolus sessions consisted of a baseline scan (dynamic scan 1, DY1) followed by amphetamine (AMPH; 5.0 mg/kg i.v.) and second scan (DY2). Adenovirus was infused into each striatum after these scans. Two days later, more scans were performed followed by scans 8 and 15d later. After each session, 30–50 $\mu$ Ci [11C]rac was infused through probes during a 20min acquisition to locate the adenovirus. ROI analysis used PMOD software to co-register images and apply an atlas template. Binding potential (BP) was assessed graphically and the AMPH-induced change in specific binding was calculated as  $100 \cdot (DY2 - DY1) / DY1$ . Results: Basal DA and [11C]rac BP were not significantly different prior to adenovirus. Consistent with autoradiographic data, AdRSVD2 increased striatal [11C]rac binding and decreased DA. Control adenovirus in the contralateral striatum did not alter DA or [11C]rac binding. The ipsilateral (AdRSVD2) [11C]rac BP progressively increased relative to the contralateral (AdRSVNull) striatum, with a peak at 24% on Day 15. DA, however, declined to 44.5% of the AdRSVNull striatum at 2 days, and this decrease peaked at 65% of control at 8 days and began to rebound by 15 days. No behavioral effects were observed. When these animals were challenged with systemic AMPH, the DA response and the change in [11C]rac BP were exacerbated in the hemisphere ipsilateral to the AdRSVD2 infusion. For every one percent decrease in BP in the control (AdRSVNull) striatum, there was a 12% increase in ECF DA regardless of the time after inoculation. In the presence of altered D2R density, a one percent decrease in BP was related to a 50% increase in DA 2 d later, 20% increase at 8 days and 7% increase at 15 days. In contrast, absolute concentrations of DA did not reflect this exacerbated responsiveness due to the extent of basal decline. Discussion: Increasing D2 receptor density in the striatum increases [11C]rac binding and decreases DA. In this situation, AMPH-stimulated DA release is proportionally exacerbated relative to the contralateral striatum. This is consistent with observations in schizophrenic populations of increased D2R and responsiveness to AMPH. However, our data caution that a reduction in basal pools of DA can produce a similar observation and should be considered in the interpretation of clinical imaging experiments. References: 1 Schiffer, W.K. et al. (2005) J Neurosci Methods (in press)

## THE EFFECT OF IONIC ENVIRONMENTS ON THE AFFINITY OF D2-DOPAMINE RECEPTOR RADIOLIGANDS

Christine A. Parker, Julian C. Matthews, John Brown, Antony D. Gee, Eugenii A. Rabiner

*GlaxoSmithKline, ACCI, Addenbrooke's Hospital, Cambridge, UK*

Introduction: Interpretation of changes in PET radioligand binding to G-protein coupled receptors (GPCRs) usually assumes a single receptor population. The affinity of ligands for GPCRs such as the D2-dopamine receptor (D2-DA) depends on the coupling of the receptor to the G-protein as well as the ionic environment. In vivo, the ionic environments will vary significantly from extracellular to cytoplasmic to endosomal receptor localisation. The affinity of PET radioligands for GPCRs will therefore depend on the coupling state and the cellular location of the receptor, effectively creating several receptor populations to consider. Understanding the interaction of ionic environment and G-Protein coupling on GPCR affinity for a radioligand is essential for the accurate interpretation of PET data. We investigated the effect of extracellular and early endosomal ionic environments, and the interaction of these with the coupling states of the D2-DA receptors on the in vitro binding properties of three commonly used PET radioligands, [3H]raclopride, [3H]FLB-457 and [3H]spiperone in rat striatal membranes. Methods: Rat striata (150 µg/ml protein) were incubated with either extracellular buffer (50 mM Tris HCl, 140 mM Na<sup>+</sup>, 5 mM K<sup>+</sup>, 1.5 mM Mg<sup>2+</sup>, 1.5 mM Ca<sup>2+</sup>, 110 mM Cl<sup>-</sup>, pH 7.4, 30 oC) or early endosomal buffer (20 mM MES, 10 mM Na<sup>+</sup>, 140 mM K<sup>+</sup>, 0.5 mM Mg<sup>2+</sup>, 0.003 mM Ca<sup>2+</sup>, 10 mM Cl<sup>-</sup>, pH 6.0, 30 oC), in the absence or presence of GTP (100 µM) for 30 minutes (30 oC). Subsequently the assays were incubated with one of the three radioligands, [3H]raclopride (400 pM - 60 nM), [3H]FLB-457 (5 pM - 1.5 nM) or [3H]spiperone (10 pM - 3 nM) for 60 minutes (30 oC). The specific binding component was defined by addition of haloperidol (1 µM). Assays were terminated by filtration through Whatman GF/B filters, and bound radioactivity counted on a liquid scintillation counter. Results: Equilibrium dissociation constant data (K<sub>d</sub>) for the radioligands in the absence and presence of GTP in the two ionic environments are given (Table 1). Extracellular buffer: GTP altered the affinity of the butyrophenone antagonist, [3H]spiperone, for the D2-DA receptors, but did not alter the affinity of the benzamide antagonists, [3H]raclopride and [3H]FLB-457 for the D2-DA receptors. Early endosomal buffer: For both benzamide radioligands, 8 to 34 fold lower K<sub>d</sub> values were exhibited for the D2-DA receptors. Spiperone exhibited 1.4 to 2.3 fold lower K<sub>d</sub> values for the D2-DA receptors compared to the extracellular conditions. Conclusion: All D2-DA radioligands examined exhibited lower K<sub>d</sub> values for the D2-DA receptors in the early endosomal buffer compared with the extracellular buffer. As one might expect, the benzamide radioligands exhibited the greatest degree of change. In extracellular buffer, GTP altered the affinity of [3H]spiperone for the D2-DA receptors demonstrating the sensitivity of [3H]spiperone for the affinity state of the D2-DA receptor.

	[ <sup>3</sup> H]Raclopride	[ <sup>3</sup> H]FLB-457	[ <sup>3</sup> H]Spiperone
<i>Extracellular</i>			
dH <sub>2</sub> O	1.839 ± 0.339	0.098 ± 0.021	0.322 ± 0.029
GTP	3.137 ± 1.108	0.096 ± 0.014	0.256 ± 0.013
<i>Early endosomal</i>			
dH <sub>2</sub> O	14.047 ± 5.404	3.324 ± 1.78	0.451 ± 0.036
GTP	28.265 ± 3.013	2.006 ± 0.688	0.594 ± 0.063

Table 1: K<sub>d</sub> values (nM; mean ± sem, n=4) for each radioligand in both buffers ± GTP (100 µM)

**IMAGING RETROGRADE TRANSPORT AND EXPRESSION OF D2 RECEPTORS AFTER STRIATAL GENE TRANSFER**

Wynne K. Schiffer<sup>1,2</sup>, Anat R. Biegon<sup>3</sup>, Hubert H.M. Van Tol<sup>4</sup>, Joanna S. Fowler<sup>1</sup>, Vinal Patel<sup>1</sup>, Jean Logan<sup>1</sup>, Stephen L. Dewey<sup>1</sup>

<sup>1</sup>*Chemistry Department, Brookhaven National Laboratory, Upton, NY, USA*

<sup>2</sup>*Graduate Program In Neuroscience, Department of Neurobiology & Behavior, Stony Brook University, Stony Brook, NY, USA*

<sup>3</sup>*Medical Department, Brookhaven National Laboratory, Upton, NY, USA*

<sup>4</sup>*Department of Pharmacology, Faculty of Medicine, University of Toronto, ON, Canada*

Introduction: Recombinant adenoviral vectors efficiently enter neurons and deliver their modified genetic cargo to the host cell nucleus, which is often remote from the site of inoculation. Because it is not known whether receptor proteins are also expressed remotely, we (1) examined extrastriatal changes in D2R expression following striatal inoculation and (2) determined the consequence of these effects on extracellular (ECF) DA. To do so, we used a simultaneous small animal positron emission tomography (microPET)/microdialysis approach to measure D2R expression and DA transmission in the same animals over time. Methods: Microdialysis cannula were implanted in both striata of adult rats (250-300g, n=15). D2R expression was modified with a recombinant adenoviral vector (AdRSVD2) while the contralateral striatum received an inactive vector (AdRSVNull). microPET/microdialysis procedures can be found in (1). Immediately after the first [<sup>11</sup>C]raclopride ([<sup>11</sup>C]rac) scan, AdRSVD2 or AdRSVNull were infused into each striatum. Two, eight and 15d later, another scan was performed. Autoradiography on a subset of animals (n=4) has been described and quantitated in (2). [<sup>3</sup>H]NMSP for D2R, [<sup>3</sup>H]PK11195 for activated microglia and cresyl violet staining of Nissl bodies were used on alternating 20 µm brain slices. microPET data was reconstructed using maximum a posteriori (MAP) algorithm with a pixel size of 0.4X0.4X1.2mm (x,y,z). ROI analysis was performed using PMOD software to co-register images and apply an atlas template which included the striatum, globus pallidus (GP) and VTA/substantia nigra (VTA/SNig). Binding potential (BP) was assessed graphically for all regions using cerebellar input for reference. Results: Basal ECF DA levels and [<sup>11</sup>C]rac BP were not significantly different prior to adenovirus. Two days after inoculation, autoradiography indicated a 15.2±3.3% increase in D2R in the AdRSVD2 striatum and [<sup>11</sup>C]rac BP was also higher than the control striatum (15.2±4.5%). Basal ECF DA was 24.5±2.1% lower than the contralateral hemisphere, which was unaltered by AdRSVNull. Eight days after AdRSVD2, [<sup>3</sup>H]NMSP and [<sup>11</sup>C]rac binding in STR were higher than at 2d. Four animals had visible evidence of retrograde transport to VTA/SNig in the [<sup>11</sup>C]rac radioactivity distribution, substantiated by [<sup>3</sup>H]NMSP autoradiography which showed additional activity in GP. A significant increase in the specific binding of [<sup>3</sup>H]PK11195 was observed in STR, GP and VTA/SNig. At this time, basal ECF DA decreased to 51±19% of control values. While various measures of D2R density decreased by 15d, ECF DA remained at 50% of control levels. Discussion: Eight days following striatal insertion of AdRSVD2, D2R were expressed in GP and VTA/SNig. There was no temporal correlation with this remote expression and the change in basal ECF DA. Activated microglia began to appear in distant regions at 2d and [<sup>3</sup>H]PK11195 binding peaked at 8d. This supports the notion that immune responses may be remotely transported from the site of inoculation and this is regionally uncoupled from retrograde D2R expression. 1 Schiffer, W.K. et al. (2005) J Neurosci Methods (in press) 2 Biegon, A. et al. (2004) Proc Natl Acad Sci USA 101, 5117-5122

## FIRST PERFORMANCE MEASUREMENTS WITH THE CLEARPET NEURO SCANNER

Karl Ziemons<sup>1,4</sup>, Andreas Bauer<sup>2</sup>, Uwe Heinrichs<sup>1,4</sup>, Hans Herzog<sup>2</sup>, Markus Holschbach<sup>3</sup>,  
Uwe Pietrzyk<sup>2,4</sup>, Matthias Streun<sup>1,4</sup>, Simone Weber<sup>1,4</sup>, H.H. Coenen<sup>3</sup>, Horst Halling<sup>1</sup>,  
Paul Lecoq<sup>4</sup>, Christian Morel<sup>4</sup>, Stefaan Tavernier<sup>4</sup>, Karl Zilles<sup>2</sup>

<sup>1</sup>Central Institute for Electronics, Forschungszentrum Juelich, Juelich, Germany

<sup>2</sup>Institute of Medicine, Forschungszentrum Juelich, Juelich, Germany

<sup>3</sup>Institute of Chemistry, Forschungszentrum Juelich, Juelich, Germany

<sup>4</sup>Crystal Clear Collaboration

The ClearPET project is proposed by working groups of the Research Center Jülich (FZJ). The aim of this project is to apply the non-invasive PET technique to in vivo investigations of signal transduction in non-human primates under physiological conditions. While in recently developed dedicated small animal PET systems a high spatial resolution of about ~1.5mm was the main research interest, it has become clear that it is equally important not to sacrifice the sensitivity of the scanners since the specific activity of the radiotracers used may be limited. In collaboration with the Crystal Clear network (CCC) we have developed a dedicated 2nd generation high performance PET scanner, called ClearPET Neuro. High sensitivity and high spatial resolution for the ClearPET camera is achieved by using a phoswich arrangement combining two types of lutetium-based scintillator materials: LSO and LuYAP:Ce. The dual layer created by 8x8 crystals of 2x2x10mm<sup>3</sup> are coupled to multi-channel photomultiplier tubes (PMT). A unit of four PMTs arranged in-line in axial direction represents one of 20 sectors of the ring design. The opening diameter of the ring is variable between 130mm and 300mm, the axial detector length is 110mm. The PMT pulses are digitized by free-running ADCs which allows the determination of the gamma energy, the phoswich layer and even the exact pulse starting time for coincidence detection. The gantry allows rotation of the detector ring as well as tilting up to 90 degrees to measure non-human primates in an upright sitting position. A small animal bed or a monkey seat can be mounted in a fixed position to the rotatable gantry. The intrinsic measurements are done with a ClearPET prototype and have shown a spatial resolution with a mean of 1.48mm FWHM and a typical energy resolution of (24,3±0.4)% for the LuYAP layer and (23,2±0.3)% for the LSO layer. First tomographic measurements with the ClearPET Neuro scanner are being performed with a full-equipped gantry and will be presented.

## GLUCOSE METABOLISM IN DISTINCT HUMAN MIDBRAIN NUCLEI AND CORRELATIONS WITH OTHER BRAIN REGIONS

**Karl Herholz**, Klaus Wienhard, Jiri Cizek, Alexander Thiel, Stefan Vollmar, Johannes Klein,  
Wolf-Dieter Heiss

*Department of Neurology, MPI & University, Cologne, Germany*

Introduction Midbrain nuclei have many projections to other brain regions and pivotal influence on basic brain functions, such as attention and consciousness. They are often affected in neurodegenerative disease causing severe clinical symptoms. Improvement of spatial resolution with latest generation of PET brain scanners allows measurement of their functional activity. Methods Resting cerebral glucose metabolism (with eyes closed) was measured in seven young male normal volunteers (age  $31.7 \pm 5.0$  yrs) on the high-resolution research tomography (HRRT; CTI, Knoxville; FWHM 2.2 mm) (1). Data used for reconstruction were recorded from 30 to 60 min after i.v. injection of 370 MBq FDG. Reconstruction using OSEM-3D (span 3, 3 iterations) with correction for attenuation, scatter, and decay yielded data sets of 256x256x207 isotropic voxels (1.22 mm size). They were registered to the ICBM brain template (2) using a new hierarchical free-form block matching algorithm for adjustment of individual anatomical variation. The ICBM volumes of interest (VOI) template was modified to distinguish the midbrain regions listed in the table. Quality of VOI matching was checked by visual inspection of coregistered MRI and metabolic homogeneity of VOIs. For each VOI, significance of correlation was accepted at Results Glucose metabolism differed significantly among midbrain regions ( $p < 0.001$ , see table) without significant asymmetry. All midbrain regions (except left inferior colliculus) showed significant positive bilateral correlations with cerebellum, other midbrain regions, globus pallidum, lateral geniculate body, pons, and some significant negative correlations with basal and lateral occipital cortex. Positive correlations with hippocampal and parahippocampal structures were closest and most extensive in dorsal midbrain, possibly mediated by reticular formation activity. Correlations with other cortical structures and basal ganglia were generally absent or negative. Conclusion This study demonstrates that functional analysis of major human midbrain nuclei is possible with HRRT PET. Their glucose metabolism in resting waking state is positively correlated with cerebellum and pons but only with few forebrain regions (pallidum, geniculate body, and hippocampal structures). Reference List 1) Heiss WD, Habedank B et al. J Nucl Med 2004; 45(11):1811-1815. 2) Mazziotta J, Toga A et al. Philos Trans R Soc Lond B Biol Sci 2001; 356(1412):1293-1322.

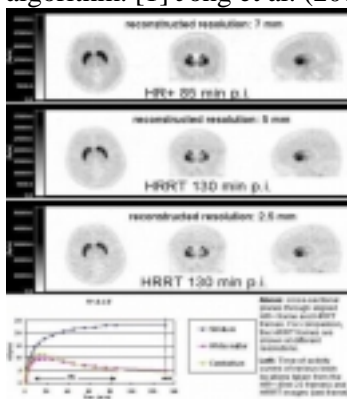
Table: Glucose metabolism (relative to global brain average)		
Structure	mean	S.D.
N. ruber	1.044	0.085
Dorsal midbrain (reticular formation)	0.993	0.081
Anterior midbrain (subst. nigra)	0.911	0.08
White matter (cerebral peduncles)	0.638	0.05
Inferior colliculi	1.14	0.108

## QUANTITATIVE ACCURACY OF THE HIGH RESOLUTION RESEARCH TOMOGRAPH: EXPERIMENTAL AND CLINICAL EVALUATION

Hugo W.A.M. de Jong<sup>1</sup>, Ronald Boellaard<sup>1</sup>, Bart N.M. van Berckel<sup>1</sup>, Mirthe M. Ponsen<sup>2</sup>,  
Adriaan A. Lammertsma<sup>1</sup>

<sup>1</sup>Department of Nuclear Medicine and PET Research, <sup>2</sup>Department of Neurology, VU University Medical Center, Amsterdam, The Netherlands

**Introduction:** The High Resolution Research Tomograph (HRRT) is a new, dedicated brain PET scanner, designed for a resolution of <3 mm combined with high sensitivity. Although PET is a quantitative imaging technique, many corrections are needed to achieve sufficient accuracy for in vivo applications. Although basic performance characteristics have been investigated [1], the applicability of this scanner for neuro-imaging, in particular neuroreceptor, applications still needs to be fully assessed. The purpose of this study was to evaluate the accuracy of dead-time, attenuation and scatter corrections, to assess image uniformity and the effect of outside field-of-view (FOV) activity on quantification. To this end, both phantom experiments and a clinical evaluation were performed. **Methods:** For the experimental study, a 20 cm diameter cylindrical phantom, filled with an 18-F solution with activity concentrations ranging from 1 to 15 kBq/cc, was used. Contrast was created by inserting two cylinders of 5 cm diameter, filled with 1/3 and 2/3 of the background activity concentration. The phantom was measured both with and without a 20 cm cylinder, containing 25 MBq 68-Ge, placed just outside the FOV. Quantitative accuracy was assessed by ROI analysis of the (3D OSEM) reconstructed images. Clinical evaluation included four [18F]-FP-β-CIT studies. A dynamic 90 minutes scan was acquired on an ECAT EXACT HR+ scanner. After this scan the patient was transferred to the HRRT scanner and an additional scan of 15 minutes was acquired, starting approximately 120 minutes p.i. Time activity curves were generated after alignment of HRRT with HR+ images. **Results:** Dead-time and decay corrections were accurate within 1.0%. Out of FOV activity increased only the randoms rate slightly. Reconstructed activity concentrations in the background and two inserts were within 8% of the expected values, whilst observed contrasts were accurate within 2%. Inter- and intraplane uniformities were 4.3 and 8.3%, respectively. Quantification, uniformity and linearity were not affected by outside FOV activity. Clinical evaluation showed that ROI values of several regions in the HRRT PET images were within 8% of the values extrapolated from HR+ time-activity curves (see figure). Furthermore, visual inspection revealed that HRRT images similar to HR+ images, but with superior resolution. **Conclusion:** Linearity, dead time and attenuation corrections of the HRRT were sufficiently accurate for clinical applications. Effects of outside FOV activity were minimal, thereby obviating the need for additional shielding. Inter-plane and intra-plane uniformity were, however, suboptimal. Improvements can be expected from new scatter correction methods. Clinical results showed a deviation of less than 8% from HR+ data and images had comparable image quality, but higher resolution. It is concluded that the HRRT is suitable for quantitative neuro-imaging applications, but that it would benefit from refinement of the scatter correction algorithm. [1] Jong et al. (2004) Proceedings IEEE Medical Imaging Conference, Rome



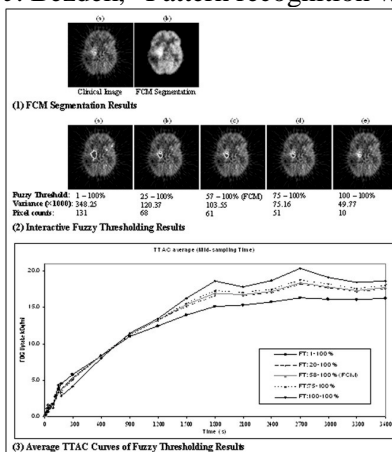


## INTERACTIVE FUZZY TEMPORAL THRESHOLDING FOR THE SEGMENTATION OF DYNAMIC BRAIN PET IMAGES

Jinman Kim<sup>1,2</sup>, Weidong Cai<sup>1</sup>, Dagan Feng<sup>1,2</sup>, Stefan Eberl<sup>1,3</sup>

<sup>1</sup>Biomedical and Multimedia Information Technology (BMIT) Group, School of Information Technologies, The University of Sydney, Australia, <sup>2</sup>Center for Multimedia Signal Processing (CMSP), Dept. of Electronic and Information Engineering, Hong Kong Polytechnic University, Hong Kong, <sup>3</sup>Department of PET and Nuclear Medicine, Royal Prince Alfred Hospital (RPAH), Sydney, Australia

**Introduction:** Fully automated segmentation of PET images is very challenging due to the limited spatial resolution and signal to noise ratio in the PET images. It also does not easily accommodate optimization of parameters to extract out particular features or structures of interest to the physician in a given patient. In this study, we propose an interactive fuzzy thresholding method which can be used to interactively control the automatic segmentation results of dynamic PET images. Our approach permits the physician to weight the relative importance of the threshold while exploring the segmentation result. **Methods:** The dynamic images are automatically segmented into similar temporal kinetic features based on iterative fuzzy-c-means cluster analysis (FCM) into predefined number of clusters [1]. In this approach, a fuzzy logic algorithm assigns probabilistic membership function (weighting) to every pixel representing the likelihood that the pixel is a member of a particular cluster. Upon convergence of cluster analysis, pixels are assigned to a cluster for which it has the highest membership. The proposed fuzzy thresholding works by controlling the fuzzy membership threshold of a selected cluster. By lowering the threshold, additional pixels with weaker membership can be assigned to a cluster. On the other hand, by increasing the threshold, fewer pixels of only the highest membership are likely to be clustered. We demonstrate the effectiveness of our method based on dynamic [18F]2-fluoro-deoxy-glucose (FDG) PET clinical human brain images. **Results:** The first row of the figure shows a single slice from the last temporal frame of a patient study with a cerebral tumor and the corresponding FCM automatic segmentation result which partitioned the image into clusters with similar temporal features. In the second row, the interactive fuzzy threshold results for the cluster representing tumor uptake are presented, where (c) is the result from the automatic FCM. Note that by adjusting the fuzzy threshold from (c), only the pixels with similar temporal features are affected, rather than all pixels with similar intensity value as in intensity-based thresholding. Accordingly, variance and pixel counts are lowered when the threshold is increased, where lower variance indicates better similarity among the pixels in the cluster. The average TTAC curves plotted in the third row shows that the results of fuzzy threshold maintains consistency and only adjusts pixels that are similar in temporal behavior. **Conclusion:** The proposed fuzzy thresholding could be useful for physicians to interactively correct the automatic segmentation results, and therefore, potentially ease the performance requirements of automatic segmentation methods. **References:** [1] J. Bezdek, "Pattern recognition with fuzzy objective function algorithm", New York: Plenum, 1981.





**COMPARISON OF TWO METHODS FOR CORRECTION OF PARTIAL VOLUME EFFECTS IN PET****Elena Rota Kops<sup>1</sup>, Anthonin Reilhac<sup>2</sup>**<sup>1</sup>*Institute of Medicine, Research Center Juelich, Juelich, Germany*<sup>2</sup>*McConnell Brain Imaging Centre, Montréal Neurological Institute, McGill University, Montreal, QC, Canada*

The low spatial resolution of PET scanners results in partial volume (PV) effects which limit the accurate quantification in anatomical structures such as the cerebral cortex and subcortical regions. Several correction methods have been proposed to deal with these effects. In a first study [1], using simulated data, we compared the PV correction of some cortical regions, obtained with i) the correction algorithm implemented at the Research Center Juelich (PVC-J) and ii) the one implemented at the Brain Imaging Centre of Montréal (PVC-M). Here, still using simulated data, the impact of mis-registration between the PET and the anatomical data on accuracy of the correction, as well as the correction of real dynamic PET data are presented. The PVC-J algorithm - based on the work of Müller-Gärtner - has a fully 3D implementation. The resulting corrected grey matter (GM) activity images are obtained by dividing voxel-wise the uncorrected GM images (without white matter contribution) by the GM probability map, derived from the convolution of the corresponding MR segmented image by a 3D spatially variant gaussian function, which reproduces the actual PET image resolution. The PVC-M algorithm - based on the work of Rousset - accounts for the mutual PV effects between any possible tissue structure. After tissue classification of the high resolution MR data, cerebral structures of interest are chosen. Each structure is convolved with a spatially invariant 3D gaussian kernel yielding a set of 3D probability maps, from which recovery and cross-contamination factors are computed. Measured time-activity curves are finally corrected using the correction factor set. A PET dynamic acquisition of an adenosin receptor study was first corrected by both methods and furthermore used to build simulated dynamic data [1] which were translated and rotated by 1 & 2 mm and 1 & 2 degrees, respectively, with respect to the simulated MR image. In case of real data, the mean recovery factor over the dynamic data (6-90 min) of GM is  $1.36 \pm 0.05$  for PVC-M and  $1.41 \pm 0.01$  for PVC-J, while in the thalamus region it is  $1.17 \pm 0.03$  for PVC-M and  $1.22 \pm 0.02$  for PVC-J. For the mismatched data, the relative difference between the corrected activity values, obtained with the two correction algorithms, and the references was compared. In all but the rotation about the z-axis case, the results are highly consistent. For the rotations about the z axis, the values given by PVC-M and PVC-J show a difference up to about 2.0%. Furthermore, some curves show an instability in the values during the last 30 minutes of the dynamic series, independent from region, mismatch, and method. In this time period the receptor data are affected by lower statistics and low signal-to-contrast ratio. As in the first comparison study, the presented data show an overall high consistency of the results obtained from the two different methods concerning the adenosine receptor. Some of the observed discrepancies could result from the ways the time activity curves are computed with both correction algorithms. [1] E.Rota Kops, A.Reilhac. Conference Record of IEEE MIC 2004, Rome

**MOTION CORRECTION ELIMINATES DISCONTINUITIES IN PARAMETRIC PET IMAGES OF NEURORECEPTOR BINDING**

**Hans R. Herzog<sup>1</sup>**, Lutz Tellmann<sup>1</sup>, Roger Fulton<sup>2</sup>, Isabelle Stangier<sup>1</sup>, Elena Rota Kops<sup>1</sup>, Kay Bente<sup>1</sup>, Uwe Pietrzyk<sup>1</sup>

<sup>1</sup>*Institute of Medicine, Research Center Juelich, Juelich, Germany*

<sup>2</sup>*Department of PET & Nuclear Medicine, Royal Prince Alfred Hospital, Sydney, Australia*

Head movements during PET studies of cerebral neuroreceptors with positron emission tomography (PET), which are often recorded as dynamic studies over periods ranging from one to two hours, do not only lead to blurred images, but, by distorting pixel time-activity curves, may also seriously disturb the kinetic analysis. Here we report on the effect of head motion on parametric images of the distribution volume ratio (DVR) as well as on the elimination of artefacts, if the dynamic PET data are corrected for head movements. For this purpose we utilized six PET studies done with the 5HT<sub>2A</sub>-receptor ligand [18F]-altanserin. Prior to the tracer injection a transmission scan of 10 min was recorded for measured attenuation correction. During the PET scan, which was acquired in listmode for 1 h, the position of the head was monitored by a Polaris infrared motion tracking system. The listmode data were sorted into 42 time frames between 10 s and 2 min in duration. A time frame consists of 63 images of 128 x 128 voxels with a voxel size of 2 mm x 2 mm x 2.43 mm. The motion correction used the multiple acquisition frame (MAF) approach, which calculates individual attenuation files for each emission frame and its corresponding head position to avoid a misalignment between transmission and emission data. After reconstruction of attenuation corrected emission frames each image frame was realigned to match the head position of the first emission frame. Both the motion corrected and not corrected dynamic images were evaluated by the non-invasive Logan plot method to obtain parametric images of DVR. In addition, a dynamic [18F]-altanserin PET scan was simulated and affected by similar movements as seen in the human studies. In this way data without statistical noise could be analysed. DVR images of motion-affected [18F]-altanserin scans showed artefacts whose extent was dependent on the amount of movement. The artefacts were mainly located at the border of the cortical tissue, especially at the interior edge towards white matter. The artefacts exhibited as discontinuities and small spots, whose values exceeded the expected DVR values or were even negative. The discontinuities were found with movements of 4 mm and greater. Isolated spots were present even with movements of only 2 mm. The artefacts disappeared when the MAF based motion correction was applied. The observations obtained in human data could be confirmed in the simulated noise free [18F]-altanserin images confirming that the artefacts are due to motion and not to statistical noise. Whereas the native PET images look just blurred, if the patient has moved during the PET scan, parametric images of the Logan DVR, which are calculated by pixel-wise linear regression, contain severe discontinuities primarily at the cortical edge. At this location, the data used in the DVR calculation change between grey and white matter data because of the head motion. The MAF based head motion correction is able to avoid the described errors.

**BP-38**

**FRAME-TO-FRAME MOTION CORRECTION IMPROVES TEST-RETEST VARIABILITY OF [18]F-DOPA UPTAKE MEASUREMENTS AND THE DETECTION OF INCREASES FOLLOWING GDNF INFUSIONS**

**Gary Hotton, Ignasi Vendrell, Brooks David**

*Division of Neuroscience and MRC Clinical Sciences Centre, Imperial College, London, UK*

Glial cell line-derived neurotrophic factor (GDNF) exerts potent neurotrophic effects on dopaminergic neurons in-vitro and in animal models of Parkinson's disease (PD). We have investigated the effect of GDNF on [18]F-dopa uptake in the putamen of five patients with advanced PD and examined the validity of using frame-to-frame motion correction to improve image quality in this data set. Methodology: Paired [18]F-dopa PET scans were acquired on eleven healthy normal subjects (mean age 66.5 years). Parametric images of [18]F-dopa influx constants ( $K_i$ ) were generated before and after frame-to-frame motion correction and the test retest variability examined with and without frame-to-frame motion correction using a region of interest (ROI) approach. Chronic intraputamenal infusions of GDNF were undertaken in five patients with advanced PD (mean age 54 yrs, disease duration 19 yrs). [18]F-dopa PET scans were performed on the five patients at baseline and at six monthly intervals for the first 2 years of GDNF infusion. Parametric images of [18]F-dopa uptake constants ( $K_i$ ) were generated before and after frame-to-frame motion correction and sampled using an ROI approach. Results: Frame-to-frame motion correction reduced the test retest variability of putamen [18]F-dopa uptake in normal subjects from 12.37% to 5.61%. The chronic infusion of GDNF resulted in a 23% ( $p < 0.05$ ) increase in the whole putamen  $K_i$  ( $p < 0.01$ ) and a 60% increase in posterior putamen  $K_i$  ( $p < 0.001$ ) over the course of the 2 years. Significant lesser increases in posterior putamen  $K_i$  were also observed at the 6, 12, and 18 month time points but only following motion correction. Conclusion: Frame-to-frame head motion correction is an effective means of reducing head motion induced image degradation. It improves [18]F-dopa test retest reproducibility and enhances the detection of focal increases in [18]F-dopa uptake in PD patients chronically treated with IPU GDNF

**ACTIVE CONTOUR BASED EFFICIENT REGISTRATION FOR BIOMEDICAL BRAIN IMAGES****Xiuying Wang<sup>1</sup>**, David D. Feng<sup>1,2</sup><sup>1</sup>*School of Information Technologies, The University of Sydney, Sydney, Australia*<sup>2</sup>*Department of Electronic and Information Engineering, The Hong Kong Polytechnic University, Hong Kong*

**INTRODUCTION:** Since information from multiple medical imaging modalities is usually of complementary nature, proper extraction and registration of the embedded information and knowledge is essential to improve quality and safety of healthcare. Biomedical image registration enables the analysis and visualization of multimodality datasets simultaneously, and facilitates the integration and smart use of relevant anatomical and functional information. Because of its important role in clinical decision-making, operation planning, and image-guided surgery, brain image registration has been extensively studied, and numerous rigid algorithms and great progresses have been achieved. However, efficient elastic brain image registration is challenging and highly demanded for clinical applications, e.g., cranial image-guided surgery. We propose an innovative elastic and automatic registration method to improve the computational efficiency. **METHODS:** The approach consists of two steps. However, preprocessing step is required for multimodal brain image registration, for example, in the registration of MRI and PET images, morphological operations and Canny edge extraction algorithm need to be carried out to extract cerebral tissues from MRI images. Step 1 (efficient non-iterative affine registration): by using affine-invariant moment-based features, centroids, and major axes, affine parameters are directly derived by minimizing mean squared error (MSE) and time-consuming iterative optimization procedure is avoided. Step 2 (elastic registration based on active contour): active contours are energy-minimizing splines which can detect the closest contour of an object. The shape deformation of an active contour is driven by both internal energy and external energy. Firstly, contour is automatically extracted from study image as initial contour estimation of reference image. Because affine deformations have been corrected in step 1, this estimation can speed up the elastic registration convergence. and then, by iteratively applying external forces derived from reference image, the deformation field can be obtained, and elastic registration can be achieved. **RESULTS:** The approach has been validated by experiments on registering PET-MRI brain images and PET-PET images. By using IBM personal computer (Pentium 4, 3.0GHz), the average computation time for 2-D images of 256\*256 is about 68 seconds, mainly spent on elastic registration procedure. The initial contour estimation plays an important role in computational efficiency of elastic registration procedure. Different active contours influence registration performance and efficiency as well. Traditional expansion (ballooning) approach cannot result in high registration performance when initial contour estimation is much bigger than the real one. By using gradient vector flow (GVF) active contour, problem of concavity can be overcome and better registration performance can be achieved. **CONCLUSION:** An efficient method is provided for elastic registration of biomedical brain images. Its clinical applications may include neurosurgery, minimally invasive procedure, disease monitoring, and treatment assessment.

## PREDICTING DRUG CONCENTRATIONS IN BRAIN USING POSITRON EMISSION TOMOGRAPHY AND VENOUS INPUT: MODELING OF ARTERIAL-VENOUS CONCENTRATION DIFFERENCES

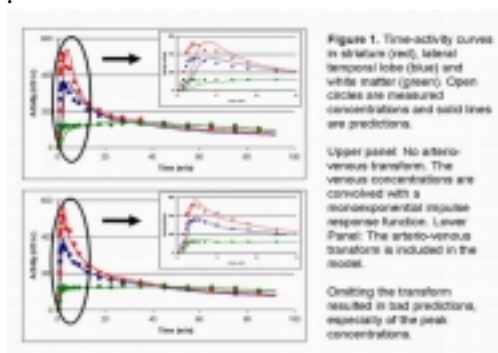
Stina Syvänen<sup>1,2</sup>, Gunnar Blomquist<sup>1</sup>, Lieuwe Appel<sup>1</sup>, Margareta Hammarlund-Udenaes<sup>2</sup>, Bengt Långström<sup>1,3</sup>, Mats Bergström<sup>1,2</sup>

<sup>1</sup>Uppsala Imanet, Uppsala, Sweden

<sup>2</sup>Department of Pharmaceutical Biosciences, Uppsala University, Uppsala, Sweden

<sup>3</sup>Department of Organic Chemistry, Uppsala University, Uppsala, Sweden

**Introduction:** The concentrations in arterial and venous plasma are different for all compounds. The differences are usually largest during the first minutes after administration. It is therefore not possible to use venous time-activity data instead of arterial time-activity data as input function when modeling transport from blood to different organs in a positron emission tomography (PET) study. However, arterial sampling is more complicated and involves larger risks for the patient than venous sampling. In addition, venous sampling is standard in pharmacokinetic studies. The purpose of the study was to investigate the possibility to construct an input function from venous time-activity data using an arterio-venous transform. If a model between venous and brain concentrations (including an arterio-venous transform) could be established, it would be possible to use such a model for the prediction of brain kinetics based on an arbitrary administration mode by applying this model on venous plasma PK. **Methods:** This concept was tested with data from a clinical PET study in which both arterial and venous plasma sampling was done in parallel to PET measurement of brain drug kinetics. The labeled study drug was a cyclooxygenase-2 (COX2) inhibitor and was administered at tracer doses (<10 ug). The main feature of the method is the inclusion of an arterio-venous transform in the kinetic model. We have studied three different arterio-venous transforms (Tav); a monoexponential function, a biexponential function and a monoexponential function combined with a delta impulse term. Assuming time invariance and linearity, the venous-arterial relationship can be described as  $C_{ve} = C_{ar} * T$  and  $C_{ar} = C_{ve} * T_{av-1}$ , where  $C_{ve}$  and  $C_{ar}$  are concentration in venous and arterial plasma, respectively, \* indicates convolution,  $T_{av}$  is the arterio-venous transform and  $T_{av-1}$  is the inverse of the transform. We then extend the model to include the transport into the brain by adding a second convolution step, i.e.  $C_{br} = C_{ve} * T_{av-1} * T_{br}$ , where  $T_{br}$  is a monoexponential or a biexponential impulse response function describing the brain kinetics and  $C_{br}$  is concentration in brain. **Results and discussion:** The model was evaluated according to two different criteria; the difference between the area under the measured curve and the predicted curve (AUCdif) and a run test for randomness of the residuals between predictions and measurements. AUCdif was considerably smaller when the transform was used in combination with a venous input compared to a model based on venous input without transform and comparable to a model based on arterial input. The run test indicated random residuals for the majority of the subjects. It was also shown that three different brain regions with different shaped time-activity curves could be modeled with a common arterio-venous transform together with an individual brain distribution model





**GENERALIZATION OF A PHYSIOLOGICAL MODEL OF INPUT FUNCTION FOR PET DATA ANALYSIS****Koon-Pong Wong<sup>1</sup>**, David D. Feng<sup>1,2</sup><sup>1</sup>*Department of Electronic and Information Engineering, The Hong Kong Polytechnic University, Hong Kong*<sup>2</sup>*School of Information Technologies, The University of Sydney, Sydney, Australia*

Introduction: Tracer kinetic modeling has been widely used to analyze and/or interpret tissue time-series data obtained with dynamic PET studies quantitatively in terms of physiological or pharmacological parameters. Estimation of these parameters requires a mathematical model (which describes the kinetics of radiotracer in the tissue) and an input function (IF) to the model (usually obtained through frequent peripheral blood sampling or by imaging blood pool). However, measurement noise in tissue and in plasma or blood (the IF) can hamper reliable estimation of parameters. Considerable work has been done on PET imaging to improve the accuracy of tissue data. Correction of errors associated with IF, however, received much less attention. Direct use of measured (noisy) IF in kinetic modeling can lead to statistical uncertainties in the estimated parameters. Fitting blood data by mathematical functions has been found useful in reducing statistical fluctuations but abrupt changes in the input function and differed in administration protocols can cause ill-conditioned fitting. A physiologically reasonable model should be more appropriate for this task. The focus of this work is to generalize an IF model of single-bolus injection of radiotracer so that the case of constant tracer infusion of a finite duration can also be accommodated. Methods: A 4-compartment model, parameterized by a sum of 4-exponentials (with a pair of repeated eigenvalues), which consists of 7 parameters (6 for the model plus a time delay) can reasonably describe the kinetics of blood circulatory system upon a single-bolus injection [Int J Biomed Comput 1993;32:95-110]. For constant tracer infusion over a finite duration T, the above parameterization is found inadequate to fit the blood data. In this study, a generalization is proposed in which the constant tracer infusion is modeled as a unit rectangular pulse (with a duration equals T) convolved with the response function of the single-bolus IF model. Since numerical calculation of convolution integral in the generalized IF model can introduce computation errors, we make use of the superposition and time-shift properties of linear systems for which a simple subtraction of the analytically-integrated model response function from its delayed (for time T) version can be computed instead. When T=0, the generalized model is reduced to the single-bolus IF model. Results: Dynamic FDG-PET studies were performed on 12 patients few months after surgical removal of the brain tumor. FDG was administered using an automated infusion pump which delivers the tracer at a flow rate of 100mL/hr over 3 min. Dynamic images and blood data were acquired continuously over 60 min. Assuming counting statistics noise, blood data was fitted to the 8-parameter generalized IF model. For comparisons, data was also fitted to a sum of n-exponentials (n=1,2,3). It was found that the generalized IF model provided reliable and reproducible fits to the blood data, whereas fitting by sum of exponentials failed in majority cases. Conclusions: The model presented here provides an efficient means to reduce noise and interpolation of blood data. Its application to PET data analysis is warranted. Supported by HKPolyU Grant (G-YX13) and RGC-HK Grant (PolyU-5192/03E).

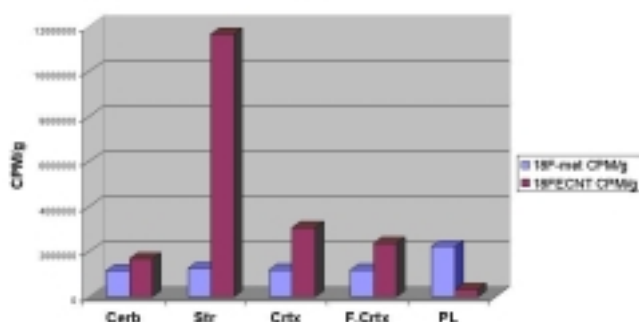
## A RADIOACTIVE METABOLITE OF THE DOPAMINE TRANSPORTER PROBE, [<sup>18</sup>F]FECNT, ENTERS RODENT AND PRIMATE BRAINS

Sami S. Zoghbi, Umesha Shetty, Masanori Ichise, Masahiro Fujita, Douglass M. Vines, Masao Imaizumi, Jieih-San Liow, Jay Shah, John L. Musachio, Victor W. Pike, **Robert B. Innis**

*Molecular Imaging Branch, NIMH, Bethesda, MD, USA*

**Objective:** The net effect of an accumulating radioactive metabolite of [<sup>18</sup>F]FECNT in rat brain was a time-dependent increase in distribution volume ( $V_d$ ). The purpose of this study was to identify this radioactive metabolite in the rat and to examine whether a similar accumulation of radioactivity occurred in primate brain. **Methods:** Two rats (av. wt., 278 g) were infused with [<sup>18</sup>F]FECNT, one with 0.85 mCi/h at 1.5 mL/h (no-carrier-added) and another with 1.45 mCi/h (plus 120  $\mu$ g carrier FECNT) for 1.0 h, at which time rats were sacrificed. Plasma and various brain sections (St, Crtx, fCrtx and Cereb) were resected from the first animal. These and the whole brain from the second animal were counted in a gamma counter and analyzed by RP-HPLC. Guided by the radiochromatogram, various HPLC fractions from the carrier-added experiment were collected, quantified for radioactivity and further analyzed by LC-MS-MS for various metabolite remnants. The stability of [<sup>18</sup>F]FECNT was measured *in vitro* in rat brain homogenates. Two human subjects (wt.: 93.10 and 99.2 kg) were injected with [<sup>18</sup>F]FECNT (9.71 and 10.7 mCi, respectively) and scanned kinetically for 260 min, while 3 rhesus monkeys (wt.:  $12 \pm 2$  kg) were injected with [<sup>18</sup>F]FECNT ( $3.1 \pm 0.6$  mCi) and scanned kinetically under isoflurane anesthesia (1.6 %) for 300 min. In every case an arterial input function was determined.  $V_d$  was determined by the ratio of the concentration of brain radioactivity to that of the parent radioligand in plasma. **Results:** [<sup>18</sup>F]FECNT represented 90.2, 71.8, 66.7, 59.3 and 13.2% of the radioactivity in St, Crtx; fCrtx, Cereb and plasma at 60 min, respectively. The same data adjusted for tissue weight and total radioactivity demonstrated that the radioactive metabolite distributed at equal concentrations to all the tissues, while the [<sup>18</sup>F]FECNT accumulated about six more times in Str than in other tissues. LC-MS-MS identified *N*-dealkylated FECNT as a metabolite in the rat brain while radio-HPLC detected a radioactive metabolite eluting with the void volume, which is presumed to be [<sup>18</sup>F]fluoroacetaldehyde or its oxidation product [<sup>18</sup>F]fluoroacetic acid. [<sup>18</sup>F]FECNT was stable in brain homogenates *in vitro* for 24 h. **Conclusions:** Strong evidence indicates that a [<sup>18</sup>F]fluoroalkyl compound is the radioactive metabolite of [<sup>18</sup>F]FECNT in rat and that this originates in the periphery and distributes non-specifically in rat brain. Consistent with this rodent data,  $V_d$  for cerebellum (a receptor-free region) increased about 1.74 times between 60 and 300 min after injection in human and 1.97 times between 50 and 240 min after injection into a non-human primate. This radioactive metabolite exacerbates the difficulty of quantification of dopamine transporters with this radioligand.

Bio Dist Of [<sup>18</sup>F]FECNT and [<sup>18</sup>F]-Metabolite (Polar) in Plasma and Various Rat Brain Tissues  
1-Hour Post IV Constant Infusion of [<sup>18</sup>F]FECNT as Characterized by RP-HPLC





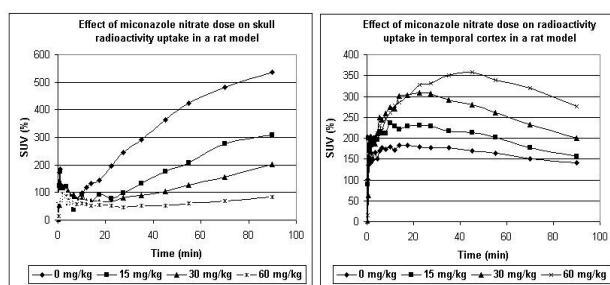
### INHIBITION OF IN VIVO DEFLUORINATION OF [18F]FCWAY IN RAT

Dnyanesh N. Tipre<sup>1</sup>, Sami S. Zoghbi<sup>1</sup>, Jehi-San Liow<sup>1</sup>, Michael V. Green<sup>2</sup>, Jurgen Seidel<sup>2</sup>, Masanori Ichise<sup>1</sup>, Victor W. Pike<sup>1</sup>, **Robert B. Innis<sup>1</sup>**

<sup>1</sup>*Molecular Imaging Branch, NIMH, Bethesda, MD, USA*

<sup>2</sup>*Nuclear Medicine, NIH, Bethesda, MD, USA*

**Objectives:** [18F]FCWAY is used in human subjects as a radioligand for PET imaging of brain 5-HT<sub>1A</sub> receptors, but suffers from significant defluorination and troublesome skull uptake of radioactivity. Our aim was to inhibit defluorination of [18F]FCWAY in a rat model. **METHODS:** Defluorination was examined by means of radio-TLC in i) phosphate buffer (0.1M; pH 7.4), ii) rat whole blood and iii) rat liver microsomes with and without NADPH. Inhibitors of cytochrome P450 2E1 enzymes (cimetidine, diclofenac and miconazole) were tested for their ability to inhibit defluorination in rat liver microsomes. The effects of miconazole dose on skull radioactivity uptake and spillover, metabolism of radioligand, brain radioactivity uptake and image contrast after i.v. [18F]FCWAY administration to rat were studied with PET. **RESULTS:** Defluorination of [18F]FCWAY occurred in rat liver microsomes only in the presence of NADPH, and not in phosphate buffer or rat whole blood. Defluorination of [18F]FCWAY in rat liver microsomes alone or in the presence of cimetidine, diclofenac, or miconazole, each for 30 min, was 13, 13, 5 and 2% respectively. After pretreatment of rats with 0, 15, 30 or 60 mg/kg miconazole nitrate, PET indicated that the skull uptake of radioactivity at 90 min after i.v. [18F]FCWAY administration was 540, 300, 180 and 82% SUV, while brain radioactivity was 137, 75, 68 and 89% SUV, respectively. The respective ex vivo measures of brain radioactivity were 41, 47, 52 and 74% SUV. Peak radioactivity in temporal cortex in vivo was 221, 236, 277 and 358% SUV, and at 35 min temporal cortex to cerebellum radioactivity ratios were 4, 6, 7 and 14, respectively. The biological half-life of radioligand was 11.2 and 19.5 min after pretreatment of rats with 0 and 30 mg/kg miconazole nitrate, respectively. **CONCLUSION:** Miconazole effectively suppresses defluorination of [18F]FCWAY in rat in vivo, possibly by competitive inhibition of cytochrome P450 enzymes. This reduces the impact of the partial volume effect. Miconazole also reduces radioligand metabolism, thereby increasing plasma radioligand level and brain uptake of radioactivity. Consequently, overall PET image contrast is improved.



**PERFORMANCE OF MAP-BAYESIAN METHODS FOR MANAGING LOSS OF METABOLITE SAMPLES IN PET LIGAND STUDIES**

Mary E. Spilker<sup>1</sup>, Gjermund Henriksen<sup>2</sup>, Till Sprenger<sup>3</sup>, Michael Valet<sup>3</sup>, Isabelle Stangier<sup>2</sup>, Hans-J. Wester<sup>2</sup>, Thomas R. Toelle<sup>3</sup>, Henning Boecker<sup>2</sup>

<sup>1</sup>*Visualization and Computer Vision Lab, GE Global Research Center, Niskayuna, NY, USA*

<sup>2</sup>*Nuklearmedizinische Klinik, Klinikum Rechts Der Isar - TUM, Munich, Germany*

<sup>3</sup>*Neurologische Klinik, Klinikum Rechts Der Isar - TUM, Munich, Germany*

**INTRODUCTION:** Invasive PET experiments provide valuable tracer kinetic information, but also contain several sources of error and uncertainty. Potential errors in metabolite measurements are often overlooked but can degrade the accuracy of the final quantification of distribution volume and binding potential. Improper or insufficient quantification of the amount of intact tracer can occur for several reasons, including loss of blood samples and insufficient sample volume. Moreover, HPLC-analysis requires isolation of protein-reduced plasma from the samples. Accidental losses during these work-up procedures may occur and the quantification of HPLC data can be noisy due to insufficient separation of intact tracer from metabolites. Finally, increased uncertainties in the quantification are encountered for the samples drawn at later time points of the study due to low count rates. To manage situations where lost or inaccurate (noisy) metabolite samples occur, we hypothesized that the inclusion of population information via model parameter priors and MAP-Bayesian statistics could be used to stabilize the quantification of metabolite kinetics. To evaluate whether this method is applicable to PET metabolite data, we have undertaken a study simulating loss of data using [18F]FDPN data as an example. **METHODS:** Thirteen healthy male volunteers ( $39.1 \pm 9.5$  years) participating in ongoing clinical research studies with [18F]FDPN were included here. Details of the data acquisition are similar to those reported elsewhere (Spilker et al., Neuroimage 2004). Samples for metabolite quantification were taken at 5, 15, 30, 60 and 90 minutes p.i.. To simulate loss of metabolite samples, single or multiple points were eliminated from the sequence and either a bi- or mono- exponential function was fit to the data under three conditions: 1) using only available data; 2) using available data and parameter priors with MAP-Bayesian statistics; 3) using an average curve from the population. To generate the parameter priors, the bi-exponential model ( $A \cdot \exp(-at) + B \cdot \exp(-bt)$ ) was fit to each individual's full dataset and subsequently each parameter's mean and standard deviation (SD) were calculated. Prior information (mean and SD) was imposed on only the two exponents of the function; not on the coefficients in front of the exponentials. **RESULTS:** The results indicated that the inclusion of prior information via Bayesian statistics performed best when there was a severe loss of data. In these situations, the loss of data required a model order reduction from a bi-exponential function to a mono-exponential function under condition 1, while condition 2 was able to maintain the bi-exponential form and better approximated the true data. When only a single data point was lost, conditions 1 and 2 performed similarly; while in all cases condition 2 resulted in a better approximation of the true metabolite kinetics compared to condition 3. **CONCLUSION:** Parameter priors and Bayesian statistics can be useful in modeling noisy and sparse datasets. This method may help stabilize analysis procedures in these situations, thereby increasing our confidence in the final outcome parameters such as distribution volume and binding potential in ligand PET experiments.

**GENDER DEPENDENT RATE OF METABOLISM OF THE OPIOID RECEPTOR-  
PET LIGAND F-18-FLUOROETHYL-DIPRENORPHINE**

**Gjermund Henriksen**<sup>1,2</sup>, Mary E. Spilker<sup>1</sup>, Till Sprenger<sup>3</sup>, Stefan Platzer<sup>3</sup>, Achim Berthele<sup>3</sup>,  
Thomas R. Toelle<sup>3</sup>, Henning Boecker<sup>1</sup>, Markus Schwaiger<sup>1</sup>, Hans-Juergen Wester<sup>1</sup>

<sup>1</sup>*Department of Nuclear Medicine, Klinikum Rechts Der Isar, Technische Universität  
München, München, Germany*

<sup>2</sup>*Department of Chemistry, University of Oslo, Oslo, Norway*

<sup>3</sup>*Department of Neurology, Klinikum Rechts Der Isar, Technische Universität München,  
München, Germany*

**Aim:** To address the question of whether gender related differences exist in the metabolism rate of (F-18)FDPN and comment on its potential implications for design and analysis of future PET studies. **Methods:** 6-O-(2-F-18-fluoroethyl)-6-O-desmethyldiprenorphine ((F-18)FDPN) is a non-selective opioid receptor ligand frequently used in positron emission tomography (PET). Experimental studies show that there are sex dependent differences in opioid analgesia which may be, at least in part, due to gender differences in the activity of the enzymes responsible for metabolizing opioids. In order to investigate potential gender dependent differences in the metabolism rate of (F-18)FDPN, 19 healthy volunteers were included in this study (9 females and 10 males; mean age of 42 +/- 12 years). The fraction of intact (F-18)FDPN present in plasma was determined by reverse-phase HPLC. A corrected plasma input function was generated on the basis of these HPLC data which in advance were corrected for recovery of radioactivity from plasma. The rate of metabolism of (F-18)FDPN was mathematically quantified by using a bi-exponential function ( $A \exp(-a \times t) + B \exp(-b \times t)$ ) to the individual dynamic metabolite data. **Results:** Statistically significant gender differences in the input function were not found for age, weight, body-mass-index, and dose. However, significant differences ( $p < 0.01$ ) in two of the four kinetic parameters (A, B, a, b) describing the rate of metabolism were found between the two groups, with female subjects metabolizing (F-18)FDPN faster than males. These differences were found in the contribution of the fast and slow kinetic components (A and B) of the model describing the distribution of radioactive species in plasma, indicating a higher rate of enzyme-dependent degradation of (F-18)FDPN in females than in males. **Conclusion:** Gender dependent classification of subjects included in PET studies with (F-18)FDPN might influence data analysis and experimental protocols. Our findings reinforce the need for individualized metabolite correction during (F-18)FDPN scans. In certain cases, where grouping of subjects is used to generate a normalized reference plasma input function, only gender specific grouping will give valid estimates

## MULTI-INPUT SPECTRAL ANALYSIS FOR EVALUATION OF THE CONTRIBUTION OF RADIOACTIVE METABOLITES IN (R)-[11C]VERAPAMIL PET DATA

Mark Lubberink, Gert Luurtsema, Ronald Boellaard, Adriaan A. Lammertsma

*Dept. of Nuclear Medicine and PET Research, VU University Medical Centre, Amsterdam, The Netherlands*

Introduction: (R)-[11C] verapamil has been proposed as a PET ligand for measuring P-glycoprotein (P-gp) function in humans [1]. Verapamil can be metabolised through N-demethylation and N-dealkylation. Part of the metabolites probably undergo rapid brain uptake and N-dealkylation metabolites probably also show affinity for P-gp. Compartmental tracer kinetic analysis did not resolve whether the contribution of radioactive metabolites of (R)-[11C] verapamil should be included in the analysis of (R)-[11C] verapamil data. Spectral analysis could reveal the number of compartments contained in the data as well as the limitations to the number of compartments that can be resolved due to the noise in the data. The aim of the present study was to evaluate the contribution of radioactive metabolites to the (R)-[11C]verapamil signal using a multi-input spectral analysis method. Methods: (R)-[11C]verapamil PET data from ten healthy volunteers was used. An essentially noise-free typical (R)-[11C]verapamil blood curve and time-activity curve (TAC) were calculated based on the mean arterial blood curve, metabolite data and whole brain grey matter TAC of all subjects. Then, 1000 verapamil, N-dealkylation metabolite and N-demethylation metabolite input function sets were simulated with noise based on estimated measurement uncertainty. Simulations were repeated using a mean TAC noise level of 5% as well. These simulated data were used as input for spectral analysis assuming that either only verapamil or verapamil and any combination of metabolites cross the blood-brain barrier. Spectral analysis was applied to both measured and simulated data using 30 basis functions for each input function, with decay constants of the impulse responses varying between 0 and 5 min<sup>-1</sup> where 0 min<sup>-1</sup> describes irreversible uptake of the tracer. Results: Figure 1 shows the basis function spectrum for noise-free data and histograms of the selected basis functions for simulated and patient data, as described in the figure caption. Conclusion: Although radioactive metabolites may have different kinetics than the parent compound, the different compartments cannot be resolved when metabolite data are included. The uncertainty in parent and N-dealkylation metabolite fractions (as both determined by HPLC) is probably too large to treat these fractions separately, and the similar shape of both metabolite fractions makes them also difficult to separate. Omission of metabolite compartments tends to lead to the selection of an irreversible compartment by spectral analysis. A simplified model assuming that parent and N-dealkylated metabolites have identical kinetics and that uptake of N-demethylation metabolites can be neglected leads to separable compartments even for noisy data. [1] Bart J et al, Neuroimage 20:1775-82, 2003

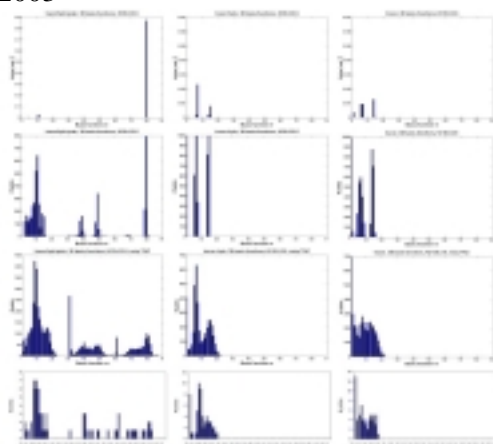


Figure 1 - Spectral analysis results with three separate parent, APLC and APLC input functions (left), a summed parent+APLC input function, and only parent input (right). Top to bottom: spectrum of noise-free data, simulated noisy TAC with noisy metabolite data, simulated noisy TAC with noisy metabolite data, and data measured in healthy volunteers. The selected 30 basis functions are based on input 1, the central 30 on input 2 and the rightmost 30 on input 3.



**IMPACT OF UNMETABOLIZED TRACER FUNCTION MODELING ON QUANTIFICATION OF [CARBONYL-11C]WAY-100635 PET IMAGES**

Valentina Bovo, Alessandra Bertoldo, Claudio Cobelli

*Department of Information Engineering, University of Padova, Padova, Italy*

**INTRODUCTION** Although many models can be used to describe the unmetabolized tracer function (UF), usually, [carbonyl-11C]WAY-100635 UF is modeled in two different ways: with a linear interpolation or with an exponential model (one exponential plus a constant or a sum of two exponentials). Our goal was to understand if and how much a different UF modeling could affect the quantification of [carbonyl-11C]WAY-100635 images.

**MATERIALS & METHODS** We considered [carbonyl-11C]WAY-100635 studies coming from 4 young healthy women and, first, modeled UF data with a linear interpolation (Lin) and calculated the relative metabolite-corrected plasma activity curve (Cp\_Lin). Then, we modeled the same UF data with an exponential model (Exp), obtaining the relative metabolite-corrected plasma activity curve (Cp\_Exp). Successively, we applied spectral analysis [1,2] to characterize the reversible and irreversible components of the system. SA was implemented by using the metabolite-corrected plasma activity curves as input function and considering the following ROIs: Anc (anterior cingulate cortex), Cer (cerebellum), Hip (hippocampus), Lof (lateral orbital frontal cortex), Mtc (mesial temporal cortex), and Occ (occipital cortex).

**RESULTS** The two UF models produce two different metabolite-corrected plasma activity curves. In particular, an important difference between Cp\_Lin and Cp\_Exp was point out in all the subjects during the first 5 minutes of the experiment while was undetectable afterwards. In spite of this, SA indicates that a difference (evaluated as 5min AUC difference in percent) between Cp\_Lin and Cp\_Exp  $\leq 30\%$  does not have any relevant impact on the quantification of the ROIs. In particular, using Cp\_lin or Cp\_Exp, SA indicates the presence of the same three components (same amplitudes at the same frequencies) in the intermediate frequency range that corresponds to the presence of three reversible compartments. But, when the difference between Cp\_Lin and Cp\_Exp is  $> 30\%$ , SA returns two different spectra. In particular, when Cp\_lin is used as input function, SA indicates the presence of three distinct components in the intermediate frequencies in all the ROIs. Differently, when Cp\_Exp is employed and Anc, Cer and Occ are analyzed, SA still shows the presence of three distinct components in the intermediate frequencies but having amplitudes and frequency position different from those obtained using Cp\_Lin. When Cp\_Exp is employed and Hip, Lof and Mtc are considered, SA detects only two distinct components in the intermediate frequencies.

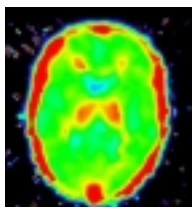
**CONCLUSION** The model chosen to obtain [carbonyl-11C]WAY-100635 metabolite-corrected plasma activity curves has an impact on the quantification of the spectrum components if the difference between Cp\_lin and Cp\_Exp is greater than 30%. In particular, the use of Cp\_lin or Cp\_Exp resolves in a different spectrum in terms of number of components and/or their amplitudes and position in the frequency range. When the difference between Cp\_lin and Cp\_Exp is  $\leq 30\%$ , SA gives the same results. We conclude that UF modeling is critical since it may affect the selection of the compartmental model to quantify [carbonyl-11C]WAY-100635 images. 1) J Cereb Blood Flow Metab, 13:15-23, 1993. 2) IEEE Trans Biomed Eng.; 45:1429-1448, 1998.

**GENERATING PARAMETRIC BINDING POTENTIAL AND VOLUME OF DISTRIBUTION IMAGES USING A NOVEL 2D BASIS FUNCTION METHOD AND THE TWO TISSUE COMPARTMENT PLASMA INPUT MODEL**

**Ronald Boellaard**, Marc A. Kropholler, Bart N.M. van Berckel, Adriaan A. Lammertsma

*Department of Nuclear Medicine and PET Research, VUmc, Amsterdam, The Netherlands*

Introduction: Basis function methods (BFM) have been developed for generating images of binding potential and perfusion [1,2,3]. These methods are based on a one-dimensional (1D) series of basis functions. In the present study a 2D BFM was developed for generating binding potential (BP) and volume of distribution (Vd) images based on a two tissue compartment plasma input model. Methods: The time activity curve of a two tissue compartment model can be described by convolution of the plasma input with 2 exponentials. The 2D BFM is based on pre-computing both convolutions for a series of discrete exponential values, i.e. 2 sets of basis functions are generated. For each combination of basis functions, the optimal set of fit parameters and the corresponding value of the cost function can be obtained by simple linear regression. The combination of basis functions and fit parameters, which provides the lowest value of the cost function, can then be used to calculate BP and Vd. A simulation study was performed to study the effects of noise on accuracy and precision of BP and Vd obtained with this 2D BFM procedure. In addition, the shape of the 2D landscape of cost function values was determined for all simulations to study depth and location of local and global minima. Simulations were performed using a typical whole blood and plasma input curve, micro parameter values based on [11C]-(R)-PK11195 studies, and 0, 5, 7.5 and 10% noise levels. Results: Cost function landscapes revealed that, in general, global minima were located near 'typical' curves within this landscape. Occasionally, however, the global minimum was found at large distances from 'typical' curves, resulting in unrealistic BP or Vd. From these results a constraint on combinations of basis function was derived (valley of desire) to avoid trapping in global minima outside the physiological realistic range, which could not be achieved by simple tuning the basis function range. Next BP and Vd were calculated using the 2D BFM with and without this constraint. The latter calculations showed that use of this additional constraint reduced BP and Vd bias from 1.27 and 1.12 to 1.20 and 1.05, respectively, at a noise level of 10%. In addition, BP and Vd precision (COV) improved from 78 and 62% to 46 and 15%, respectively. An example of a Vd image showing increased [11C]-(R)-PK11195 binding in the thalamus is given below. Conclusion: A novel 2D BFM method was developed for generating parametric images of BP and Vd. To avoid large bias and poor precision at noise levels typical for parametric applications, the method needs to be constrained to specific combinations of basis functions, which can be derived from a typical shape of 2D cost function landscape. Accuracy and precision of this constrained version seems sufficient for calculating parametric Vd images. [1] Gunn et al, NeuroImage 1997 [2] Lodge et al, JNM 2000 [3]Boellaard et al. NeuroImage2004



## CLUSTERING APPROACH FOR VOXEL-BASED LOGAN PLOT TO IMPROVE NOISE REDUCTION CAPABILITY

Yuichi Kimura<sup>1</sup>, Jyunnichi Yano<sup>2</sup>, Mihoko Tsukahara<sup>3</sup>, Mika Naganawa<sup>4</sup>, Kenji Ishii<sup>1</sup>,  
Kiichi Ishiwata<sup>1</sup>

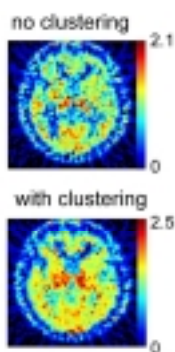
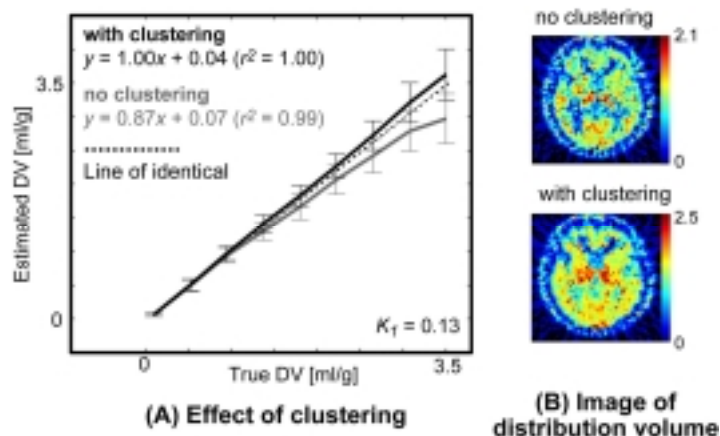
<sup>1</sup>*PET Center, Tokyo Metropolitan Institute of Gerontology, Tokyo, Japan*

<sup>2</sup>*School of Science and Engineering, Waseda University, Tokyo, Japan*

<sup>3</sup>*KURIHAMA Alcoholism Center, National Hospital Organization, Kanagawa, Japan*

<sup>4</sup>*Graduate School of Information Science, Nara Institute of Science and Technology, Nara, Japan*

[Introduction] The aim of this study is to develop noise reduction capability for Logan plot using a clustering approach. Logan plot is widely used algorithm because of its portability and model independent property. However, a distribution volume (DV) tends to be underestimated with existence of noise in a tissue time activity curve (tTAC). This is sometimes serious in case of voxel-by-voxel Logan plot to form images of receptor-radioligand kinetics. [Method] First, voxel-based tTACs are clustered based on radioligand kinetics. The ratio of a tTAC and tTAC multiplied by time is related to  $k_2$  (Y Kimura, NeuroImage 9:554), and the clustering is performed based on the ratio. Then, gathered tTACs are averaged in a cluster to improve their noise statistics. Logan plot is applied to the averaged tTACs. [Results and Comment] We applied the proposed method to simulation data and clinical image of <sup>11</sup>C-PK11195. The simulation result is shown in Fig-A where the true DV and the estimates are plotted on x- and y-axis. The gray solid line derived from Logan plot without clustering shows around 15% underestimation, meanwhile the clustering approach can compensate the noise in tTAC (the black solid line). Fig-B demonstrates parametric images of DV with/without clustering. The contrast around the thalamus is improved. We conclude that the clustering approach is useful for voxel-based Logan plot.



**KINETIC PARAMETRIC ANALYSIS FOR FEATURE EXTRACTION IN FDOPA-PET STUDY**

**Ren-Shyan Liu<sup>1,2</sup>, Hong-Dun Lin<sup>3</sup>, Kang-Ping Lin<sup>3</sup>**

<sup>1</sup>*Department of Nuclear Medicine, National Yang-Ming University Medical School, Taipei, Taiwan*

<sup>2</sup>*National PET/Cyclotron Center, Taipei Veterans General Hospital, Taipei, Taiwan*

<sup>3</sup>*Department of Electrical Engineering, Chung-Yuan University, Taiwan*

Background and Purpose: Nowadays dynamic FDOPA-PET imaging is routinely performed for quantitative analysis of physiological activities of brain tissues for Parkinson’s disease; however, the significant tissue region boundary is suffered from high noise problem. Thus, a novel feature extraction method based on analyzing kinetic parametric information that obtained from a series of time ranges is presented to exactly extract brain structures from the parametric images. Method: In this study, physiological information, including tissue time-activity curves (TACs) and derived “kinetic parametric curves (KPCs)”, are incorporated to segment desired brain tissues, such as striatum, gray and white matters, from dynamic FDOPA-PET studies. The Patlak graphic method is used to generate kinetic parametric images by integral from different time ranges (0 to 20, 40, 60, 80, 100 and 120 min), respectively. The obtained tissue kinetic factors are estimated based on compartmental modeling analysis, and the plasma curve from human PET study is used as the input function. To classify the brain tissues, the KPCs and TACs data sets of dynamic PET images were clustered using minimum difference (distance) and vector (trend) to clustering centers defined previously by iterative procedure to classify the tissue regions corresponding to similar biochemical behavior in this study. The algorithm can be defined as Eq. (1). where  $K_i$  and  $T_i$  are the pixel level data, and the  $V_{K_i}$  and  $V_{T_i}$  are the vectors of KPCs and TACs, respectively. The subscript “c” added to each notation is denoted as cth clustering center. When the minimum difference and maximum similarity of KPCs and TACs to clustering centers occur simultaneously, the class “C” was determined. Results: As a result, 10 sets of dynamic FDOPA-PET studies were used to validate the performance of the segmentation method provided in this paper. To estimate the kinetic parametric data by using Patlak graphic method in different time ranges (0 to 20, 40, 60, 80, 100 and 120 min), the data sets of three clustering centers were shown in Fig 1. By clustering the whole image data sets by Eq. 1, and the original image and segmentation results were shown in Fig 2. Conclusion: In this study, the method can effectively extract brain tissues, including striatum, GM and WM in dynamic FDOPA-PET images. Moreover, the segmentation result reveals more complete brain structures extracted from functional images, and the method can also be used as preprocess that is much helpful for structural/ functional image registration.

$$C = \min_{i,j} \sum_{k=1}^n |K_i - K_c| + |T_i - T_c| \quad (1)$$

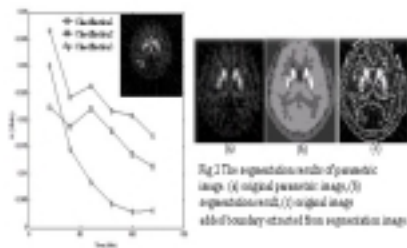


Fig 1 The kinetic parametric factors estimated in different time ranges (0 to 20, 40, 60, 80, 100 and 120 min).

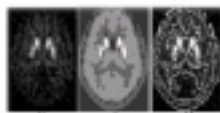


Fig 2 The segmentation results of parametric image: (a) original parametric image, (b) segmentation result, (c) original image with boundary extracted from segmentation image.

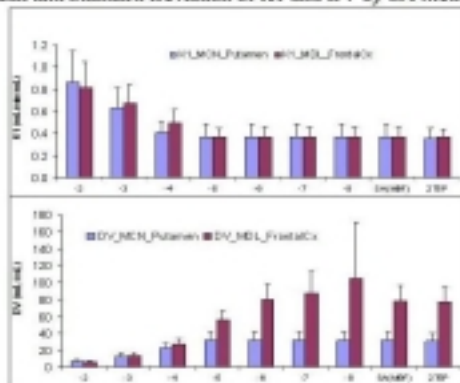
## SPECTRAL ANALYSIS WITH A MINIMAL BASIS FUNCTIONS APPROACH FOR QUANTIFICATION OF LIGAND-RECEPTOR DYNAMIC PET STUDY

Yun Zhou, Weiguo Ye, James R. Brasic, Mohab Alexander, John Hilton, Dean F. Wong

*Department of Radiology, Johns Hopkins University School of Medicine, Baltimore, MD, USA*

Spectral analysis (SA) (Cunningham and Jones, 1993, *J. Cereb. Blood Flow Metab*, 13: 15-23) has been used to evaluate tracer kinetics in ligand-receptor dynamic PET study. SA is a modeling independent approach that assumes that the impulsive response function for tissue tracer kinetics measured by PET can be expressed as a sum of exponentials of  $\alpha \exp(-\beta t)$ , where  $\alpha$  and  $\beta$  are nonnegative values that can be estimated by basis functions approach with Lawson and Hanson nonnegative least squares (NNLS) algorithm. The basis functions set  $\{\exp(-\beta t)\}$  is commonly determined by equally sampling  $\log(\beta)$  in a predefined range (Turkheimer et al., 2003, *Phys Med Biol*. 48(23):3819-41). The objective of this study is to develop and evaluate an automatic basis functions selection algorithm for SA. Methods: SA with a minimal basis functions and NNLS algorithm are used for parameter estimation (SAMBF). SAMBF is implemented as below: Starting with a initial basis functions set  $\{\exp(-\beta t)\}$  by sampling  $\log(\beta)$  from 0 to -1 with a given step size  $\Delta < 0$  (-0.02 is used in the study), a forward iteration to expand basis functions set with step size  $\Delta$  is stopped until a criterion of minimizing the residual sum of squares of fitting is satisfied. To evaluate the effects of fixed range of  $\beta$  on estimates, SA with  $\log(\beta)$  fixed at -2, -3, ... -8 is also implemented. For comparison, a 2-tissue 5-parameter (2T5P) ( $K_1, k_2, k_3, k_4, V_p$ ) ( $BP = k_3/k_4$ ) compartmental model with the constraint of  $K_1/k_2 = DV(\text{reference tissue})$  is used for target tissue modeling. Eight  $[^{11}\text{C}]\text{MDL } 100,907$  ( $[^{11}\text{C}]\text{MDL}$ ) and  $[^{11}\text{C}]\text{McN5652}$  ( $[^{11}\text{C}]\text{MCN}$ ) human dynamic PET studies are used for evaluation. Each PET scan is performed on a GE Advance scanner with 90 min 3D data acquisition. Regions of interest of cerebellum, cingulate, occipital, orbital frontal, parietal, pre-frontal, superior frontal, and temporal cortices are drawn on the co-registered MRI images, and then applied to dynamic PET images to obtain time activity curves (TACs) for kinetic analysis. Metabolite-corrected plasma TACs is used as input function. Results: In the following Fig., the  $\log(\beta)$  (mean  $\pm$  standard deviation) determined by SAMBF is  $-4.6 \pm 0.26$ , for putamen in  $[^{11}\text{C}]\text{MCN}$  study, and  $-5.5 \pm 0.11$  for superior frontal cortex in  $[^{11}\text{C}]\text{MDL}$  study. As  $\log(\beta)$  decreases from -2 to -8, the  $K_1$  estimates from conventional SA tend to  $K_1(\text{SAMBF})$ . However, following figure also demonstrates that the  $DV$  estimates from SA increases as  $\log(\beta)$  decreases for tissue of slow kinetics. SAMBF and 2T5P provide comparable estimates of  $K_1$  and  $DV$  for all tissues in both  $[^{11}\text{C}]\text{MCN}$  and  $[^{11}\text{C}]\text{MDL}$  PET studies. In conclusion, spectral analysis with a minimal basis functions approach is simple, robust, and reliable for quantification of ligand-receptor dynamic PET. NIH grants AA12839 DA00412 NS38927.

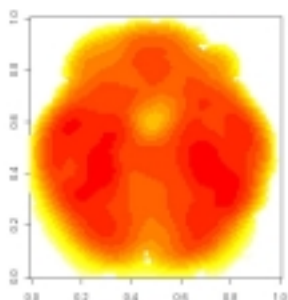
Mean and Standard Deviation of  $K_1$  and  $DV$  by SA Methods





**FUNCTIONAL LOGISTIC REGRESSION WITH PET IMAGING DATA: A VOXEL-LEVEL CLINICAL DIAGNOSTIC TOOL**Philip T. Reiss<sup>1,3</sup>, **R. Todd Ogden**<sup>1,2,3</sup>, J. John Mann<sup>2,3</sup>, Ramin V. Parsey<sup>2,3</sup><sup>1</sup>*Department of Biostatistics, Columbia University, New York, NY, USA*<sup>2</sup>*Department of Psychiatry, Columbia University, New York, NY, USA*<sup>3</sup>*Department of Neuroscience, New York State Psychiatric Institute, New York, NY, USA*

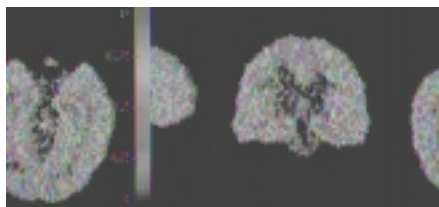
In statistical analysis of brain imaging data comparing groups, one approach is to regard each voxel of an image as a response variable, with diagnostic group and other covariates used as predictors. Alternatively, one could use a within-subject design to examine effects of treatment or changes in clinical state. Commonly, a test statistic is computed for each voxel, and analysis focuses on determining which subset of voxels is “significant”. An alternative approach is to regard two- or three-dimensional images as predictors of binary variables such as treatment response status, suicide attempter status, etc. This functional logistic regression model is an example of “functional data analysis,” which extends more traditional methodology to allow for curves (or, in higher dimensions, images) as either predictors or response variables. We describe an approach to predict any binary response using voxel-based images of outcome measures or estimates of binding. In classical logistic regression, the log-odds of the response variable are modeled as a linear combination of a set of covariates, and its coefficients are estimated. Further inference involves determining which covariates are most important for predicting the outcome. By contrast, in functional logistic regression with an image as a predictor, the log-odds for a subject are modeled as the integrated product of the subject’s image and a coefficient image which must be estimated from the data. This image can be interpreted analogously to the coefficient vector in classical logistic regression: Locations at which the image is far from zero indicate the corresponding brain region is important in predicting the response. Since the dimension of the image is much higher than the number of subjects, the coefficient image must be constrained to be smooth in order to fit the model. We accomplish this by first projecting the coefficient image onto a 2-D or 3-D radial B-spline basis, and then applying a functional version of principal components regression to further reduce the dimensionality of the estimated coefficient function. Adequate smoothness of the coefficient image is ensured by imposing a roughness penalty whose magnitude is determined by generalized cross validation. It is straightforward to further extending this general methodology to allow for the addition of a vector of covariates (including relevant genotypes) or a second image. The example coefficient image in Figure 1 was computed for predicting diagnosis using one 2-D slice of BP’ (f1Bmax/KD) in a [11C]McN5652 study of depression. Peaks and valleys in the image indicate brain areas that are particularly useful in prediction of diagnosis. This general procedure has many potential applications in neuroreceptor imaging, including identifying at-risk individuals, treatment planning, and predicting suicide attempts. Once a model has been fit, the probability of the binary outcome may be estimated for any new subjects by applying the model to his/her image.





**MIXTURE MODELING FOR PET NEURORECEPTOR STUDIES**Huiping Jiang<sup>1</sup>, **R. Todd Ogden**<sup>2,3</sup>, J. John Mann<sup>2,3</sup>, Ramin V. Parsey<sup>2,3</sup><sup>1</sup>*Division of Biostatistics, New York State Psychiatric Institute, New York, NY, USA*<sup>2</sup>*Department of Psychiatry, Columbia University, New York, NY, USA*<sup>3</sup>*Department of Neuroscience, New York State Psychiatric Institute, New York, NY, USA*

Standard compartmental kinetic modeling is commonly used for quantifying PET neuroreceptor binding. Drawbacks with this approach are its reliance on the choice of model and that the nonlinear least squares (NLLS) algorithm used for fitting such models requires substantial computational expense. One alternative to kinetic modeling is the graphical analysis of Logan, et al., (1990) (and its variants), which allows estimation of distribution volume without requiring a specific compartmental model. Another alternative is the method of Gunn, et al. (2002), in which each voxel time-activity curve (TAC) is expressed as a weighted sum of basis functions. We offer another alternative, building on the general mixture modeling framework described by O'Sullivan (1994). In our construction, an approximation to the full unconstrained kinetic model, each voxel TAC is modeled as a sum of exponentials, each convolved with a plasma input function, with the time constant for each term constrained to be the same across all voxels. Thus, each voxel's TAC is modeled as a mixture of sub-TACs, which can roughly be regarded as curves expressing a variety of binding levels. Fitting a mixture model with  $K$  components involves computing  $K$  coefficients for each voxel and a total of  $K$  time constants. For a given choice of time constants, all coefficients can be computed efficiently by applying a nonnegative linear least squares algorithm. With this as a nested step, estimation of time constants may be accomplished using a standard NLLS algorithm. The choice of model order  $K$  may be made using standard model selection criteria, such as AIC. By constraining the time constants to be the same for all voxels, this method "borrows strength" across voxels and thus allows both for the ability to fit approximations to higher order compartmental systems than could not be modeled using one-voxel-at-a-time methods and also for greater stability of estimation of the shared parameters. In addition, this framework allows for the creation of maps of the contributions of each component separately. The computational expense involved in fitting our mixture model is no greater than that required for competing methods and is considerably less than usual kinetic modeling. Through simulation, we demonstrate that the mixture model has good agreement with standard kinetic modeling when estimating binding outcome measures even for general kinetic structure (i.e., no shared time constants in the simulated data). Figure 1 displays a sample VT map from a WAY study using  $K=4$  components. References: Gunn, et al. (2002). *J Cereb Blood Flow Metab* 22: 1425-39. Logan, et al. (1990). *J Cereb Blood Flow Metab* 10: 740-7. O'Sullivan (1994). *Stat Methods Med Res* 3: 87-101.



**MODELING OF DYNAMIC PET DATA USING LINEAR VOLTERRA EQUATIONS****Koon-Pong Wong<sup>1</sup>**, David D. Feng<sup>1,2</sup><sup>1</sup>*Department of Electronic and Information Engineering, The Hong Kong Polytechnic University, Hong Kong*<sup>2</sup>*School of Information Technologies, The University of Sydney, Sydney, Australia*

**Introduction:** Positron emission tomography (PET), with a wide variety of radiopharmaceuticals, provides measurements of tissue physiology of various organ systems in vivo. Common to all quantitative PET studies is the use of tracer kinetic modeling to extract the physiological information from the tissue time-series data and interpret those information in terms of physiologically meaningful parameters of a 'workable' mathematical model that describes the exchange of labeled compounds between plasma and tissue. Conventionally, linear compartmental approach is employed for model formulation with the use of implicit models, in which the relation between the system response and input is modeled by linear ordinary differential equations. Model parameters can be estimated by fitting the tissue time-activity curves (TACs) to the analytical but nonlinear solution of the differential equations or by means of linearization approaches such as multiple-time graphical techniques or generalized linear least squares (GLLS) methods. An alternative strategy to implicit modeling is investigated in this study, where explicit models (in which the relation of system response and input is modeled by convolution integrals) are applied to kinetic modeling and parameter estimation based on the theory of Volterra integral equations.

**Methods:** An integral equation is an equation in which the unknown function of one or more variables, occurs under the integral sign. If a physical (nonlinear) system is time invariant with certain restrictions, then the relation between the input and the output can be represented by a Volterra functional series, which is a sum of integral equations with increasing order of kernels. For a linear time invariant system, Volterra functional series is simply a convolution integral of the input function and the first-order Volterra kernel, which is the impulse response of the system. It can also be shown that linear Volterra integral equations can be converted into ordinary differential equations with prescribed initial values, or vice versa, under certain conditions. Therefore, for a specific radiopharmaceutical used in quantitative PET studies, one can construct an explicit model in terms of Volterra integral equations, whose representation is equivalent to that of compartmental model represented by differential equations and their auxiliary conditions. Volterra integral equation approach also introduces an efficient parameter estimation method. Instead of using nonlinear least squares fitting to the analytic nonlinear solution of the implicit model, parameter estimation can be achieved by linear algebraic techniques.

**Results:** Computer simulations were performed using tracer FDG as an example. Noisy tissue TACs were generated with realistic Gaussian noise added on the curves. Parameter estimates derived from the Volterra integral equation approach were compared with those obtained from nonlinear least-squares fitting to the analytical solution of the differential equations. Good agreement (slope~1; intercept~0;  $r>0.97$ ;  $p<0.001$ ) between the parameter estimates was found and the Volterra approach requires much less computation time.

**Conclusions:** The method presented here provides an alternative and efficient means to kinetic modeling and parameter estimation in quantitative PET study of various radiopharmaceuticals upon appropriate correction of any labeled compounds present in tissue and in plasma. Supported by research grants from HKPolyU (G-YX13) and RGC-HK (PolyU-5192/03E).

## A FRAMEWORK OF INCORPORATING VARIANCE ESTIMATES INTO WAVELET ANALYSIS IN PET METABOLISM AND RECEPTOR STUDIES

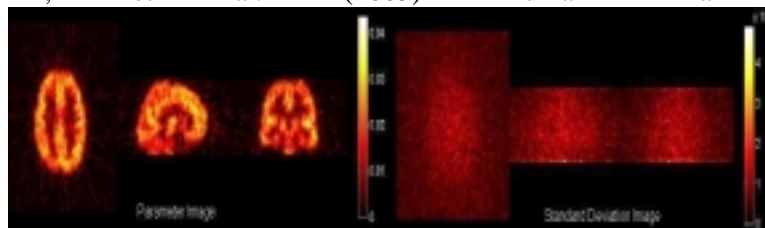
John A.D. Aston<sup>1</sup>, Hong-Ren Su<sup>1</sup>, Roger N. Gunn<sup>2</sup>, Federico E. Turkheimer<sup>3</sup>

<sup>1</sup>*Institute of Statistical Science, Academia Sinica, Taipei, Taiwan*

<sup>2</sup>*GlaxoSmithKline, Greenford, London, UK*

<sup>3</sup>*Imperial College, London, UK*

Recently, methods have been developed to estimate the variance of parameter estimates derived using wavelet methods [1]. Previous methods of analysis in the wavelet domain [2-4] had only yielded estimates of the parameters after transformation back into the image domain. The development of methods which return the additional variance information present the opportunity for further analyses which incorporate the attractive properties of wavelet based methods. The underlying principle of the method of variance estimation is that whilst the variance parameters from wavelet space cannot be easily transformed back into image space, as they are a matrix (2nd order) as opposed to the intrinsic vector (first order) of the parameter estimates, there do exist first order estimates associated with the variance which can easily be transformed, namely the residuals. Thus by transforming back the residuals subject to the equivalent shrinkage of that of the parameter estimates, it is possible to determine the variance of the parameter estimates in the image domain. These methods have been derived and validated on linear models, and linearly transformed data. The figure shows one such PET FDG study and its error variance after thresholding in the wavelet domain. The ability to use these methods with common non-linear PET compartmental models will be discussed further in the abstract by Su, HR et al. In neuropsychology, simple association has been considered the lowest level of evidence for functional segregation, the higher levels being respectively dissociation and double dissociation. The determination of dissociation requires the within-brain comparison of task related effects between two or more locations. Jernigan et al [5] suggested the use of t-statistics for point-wise comparisons between brain locations to assess dissociation. However, statistical maps are characterized by high noise levels and require regularization to allow a detailed assessment of regional variability. Wavelet methods are natural candidates for the regularization task. They provide a parsimonious multiresolution characterization of the signal and efficiently whiten the correlated noise processes of functional images. With the introduction of the error estimates for wavelet methods, dissociation investigation now becomes possible. The error variances allow surrogates for t-value maps to be derived. However, not only is it of importance to know the error variances but it is also of interest to characterise the underlying distribution with a view to integration of the methodology into the hypothesis testing framework. The error estimates are the first step in a characterisation of these distributions which can in turn be used to perform hypothesis testing. References [1] Aston JAD, et al. (2005) Neuroimage, in press. [2] Ruttimann UE, et al. (1998) IEEE TMI 17:142-154. [3] Turkheimer FE, et al. (2003) IEEE TMI 22:289-301. [4] Turkheimer FE, et al. (2000). JCBFM 20(11): 1610-1618. [5] Jernigan TL, et al. (2003) Human Brain Mapping 19:90-95.



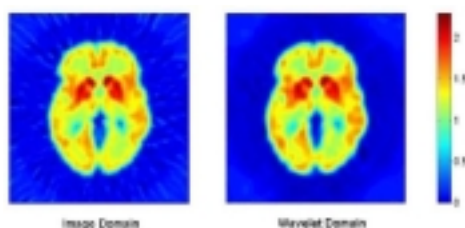
**INTEGRATION OF PET COMPARTMENTAL MODELS AND WAVELET  
ANALYSIS TECHNIQUES: A FEASIBILITY STUDY**

**Hong-Ren Su<sup>1</sup>, John A.D. Aston<sup>1</sup>, Michelle Liou<sup>1</sup>, Philip E. Cheng<sup>1</sup>, Federico E. Turkheimer<sup>2</sup>**

<sup>1</sup>*Institute of Statistical Science, Academia Sinica, Taipei, Taiwan*

<sup>2</sup>*Imperial College, London, UK*

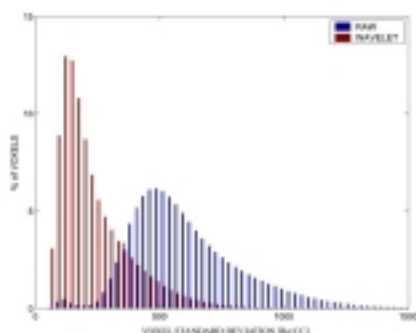
Wavelet analysis has become routinely used in neuroimaging, especially in PET image analysis. Techniques have been developed which combine spatial wavelet transforms and linear temporal models [1,2]. However, in PET, often the temporal model can be well described using a compartmental model [3]. Compartmental models are non-linear models and as such some of the assumptions made when wavelet analysis is used are no longer justified. The advantage of wavelet analysis is that spatially correlated data can be analyzed easily and the resulting estimates will have better mean squared error properties. Here, we investigate the feasibility of combining PET compartmental models with wavelet spatial models, in order to integrate the advantages of both underlying techniques. We have investigated using the Simplified Reference Tissue Model (SRTM) [4] both in the image domain and in the wavelet domain, where the data had been transformed using Battle-Lemarie wavelets. A simulation based on several blocks in a small artificial image was considered, where each block had a time activity curve (TAC) associated with it. These TACs were generated from the underlying true model using parameter values based on real data. In addition a simulated PET image was generated using a PET simulator and analyzed. In the wavelet domain, in both studies, the data was analyzed firstly without any shrinkage being performed, and subsequently using three different shrinkage operators; hard shrinkage, soft shrinkage and linear shrinkage. The variances used in the shrinkage were estimated in two different ways, block by block using the parameter values themselves, and point-by-point using the time series data [5]. The results of our simulation studies suggest that it is indeed possible to combine the two techniques of PET compartmental modeling and spatial wavelet analysis. The small block simulation showed that in the presence of spatially correlated noise, the wavelet analysis results have better power signal to noise ratio (pSNR) properties than the corresponding image domain results. While there was a small improvement in the overall image, a greater improvement was seen in the regions containing true signal (as opposed to the background). It was also found that linear shrinkage with point-by-point variance estimation gave the greatest improvement in pSNR. As can be seen in the figure, the result of the wavelet shrinkage analysis of the PET simulator data is much smoother than the image domain result, and does not contain spurious pixels of large intensity. This work demonstrates, through simulation, that the integration of PET compartmental models and wavelet analysis techniques is feasible, certainly for the SRTM. It would be of interest to examine other compartmental models, and of course, apply this method to real data sets. [1] Ruttimann UE, et al. (1998) IEEE TMI 17:142-154 [2] Turkheimer FE, et al. (2003) IEEE TMI 22:289-301 [3] Gunn RN, et al. (2001) JCBFM 21:635-652 [4] Gunn RN, et al. (1997) Neuroimage 6:279-287 [5] Aston JAD, et al (2000) Neuroimage, 12:245-256



## OPTIMIZATION OF WAVELET PROCESSING OF DYNAMIC PET DATA

Nathaniel M. Alpert<sup>1</sup>, Anthonin Reihlac<sup>2</sup>, Tat T. Chio<sup>3</sup>, Ivan Selesnick<sup>3</sup><sup>1</sup>*Division of Nuclear Medicine, Massachusetts General Hospital, Boston, MA, USA*<sup>2</sup>*McConnell Brain Imaging Centre, Montreal Neurological Institute, Montreal, QC, Canada*<sup>3</sup>*Department of Electrical & Computer Engineering, Polytechnic University, Brooklyn, NY, USA*

Several groups have reported that wavelet denoising can be used to increase the signal-to-noise (SNR) of dynamic PET studies (4D PET). But wavelet denoising can be applied in different ways and the process involves the arbitrary choice of “strength” parameters. Too much denoising results in a loss of resolution and biased concentration histories. The goal of this work is to study how to optimize wavelet denoising for neuroreceptor studies. Event by event Monte Carlo simulation was used to create an ensemble of 50 dynamic data sets. The simulation incorporates the geometry, electronic and detector characteristics of a commercial PET scanner (ECAT HR+) as well as the nuclear interactions necessary to describe the coincidence, random and scatter events. Temporal and spatial distribution of radioactivity was defined using a digital brain phantom and measured kinetic parameters. Sinograms for 70 minutes of data were computed to be similar to the noise level of <sup>11</sup>C-raclopride in the human brain and then reconstructed using filtered back projection. 3D-wavelet denoising was applied to the ensemble of simulations. We studied denoising schemes that used either a fixed threshold for all wavelet coefficients or alternatives in which we varied thresholds for each sub-band. The wavelet transform of the mean of 50 fifty simulations was taken as the expected value. The RMS difference between the mean and noisy simulations was minimized by varying the thresholds. Noise was measured as the voxel-wise sample standard deviation for both conventional and denoised data sets. We also computed binding potential (BP) for the raw and processed data, with voxel-wise mean and standard deviation as end points. Bias was computed for both concentration and BP as the difference in means for the raw and denoised data set. Three-dimensional wavelet denoising with a single threshold yielded increased SNR, but only at the expense of significant bias. Optimization of sub-band thresholds yielded a 2x improvement in SNR for the 4D concentration data (See Fig.) and a 1.5x improvement for PB. More than 84% of voxels had bias less 3%. We conclude that optimized wavelet denoising can increase SNR in dynamic PET with low bias and minimal loss of resolution.



**IMPROVING ACCURACY AND PRECISION OF PET PHARMACOKINETIC ANALYSIS USING WAVELET BASED DENOISING OF TIME ACTIVITY CURVES**

**Maqsood Yaqub**, Ronald Boellaard, Marc Kropholler, Mark Lubberink,  
Adriaan Lammertsma

*Department of Nuclear Medicine & PET Research, VU University Medical Center,  
Amsterdam, The Netherlands*

**INTRODUCTION** Kinetic analysis of PET data suffers from bias and poor precision due to high noise levels in tissue time activity curves (TACs), especially at the voxel level. The purpose of the present study was to investigate several wavelet based denoising strategies with respect to their capacity to improve accuracy and precision of pharmacokinetic parameters derived from these TACs. **METHODS** The wavelet method used in this study was designed for denoising TACs and was implemented as follows. First, each TAC was temporarily extended by adding 4 zero's in front of the TAC and, using multi-exponential extrapolation, 4 points at the end. The resulting TAC was resampled at 64 time points (requirement for the dyadic wavelet, DPWT [1]). Next, peaks (0-5 min) and tails (5-60 min) of the TACs were calibrated separately to find the best filter combination in terms of type of wavelet function (Daubechies 4-16, Symmlet 4-6, Coiflet 1-3 [2]), the number of times of downscaling and the type of thresholding (VISU or SURE [3]). After filtering, denoised TACs were obtained by inverse transformation, down scaling and removal of temporary points. Simulations were performed to evaluate the effects of these wavelet-denoising methods on accuracy and precision of pharmacokinetic analyses. Wavelet denoising was applied to simulated noisy TACs based on [11C]-PK11195 data. Time dependent variance was simulated at 4 different noise levels (COV = 2.5, 5, 7.5 and 10%). For each noise level 300 TACS were generated. These noisy TACs were used both with and without wavelet filtering to estimate volume of distribution (Vd) and binding potential (BP) using nonlinear regression analysis. **RESULTS** Daubechies-8 and Symmlet-4 wavelet functions yielded good results for the peak, and Coiflet (2 and 3) for the tail. In all cases SOFT SURE thresholding yielded 'better' TACs than VISU soft filtering after downscaling to level 3 (tail) and 5 (peak). Using this optimal set of wavelet parameters, about ~75 and 100% of filtered TACs showed closer agreement with noiseless TACs than corresponding unfiltered TACs for peak and tail, respectively. Furthermore, use of wavelet filtering resulted in Vd and BP values with less bias and better precision than those without filtering. For example, BP bias reduced from 15 to 7% at a simulated noise level of 7.5%. Although there was only a slight decrease in bias at very high noise levels (>10 %), use of wavelet filtering resulted in a significant reduction of outliers from 15 to 4%. **CONCLUSION** After careful calibration of wavelet filters, bias and precision of pharmacokinetic parameters, especially BP, can be improved significantly. Furthermore, wavelet denoising seems to be most effective at higher noise levels (5 to 10%), thereby making it a promising tool for improving the quality of parametric images. **REFERENCES** 1. N. Getz, Electronics Research Laboratory, U.C. Berkeley, 1992 2. I. Daubechies, Comm. Pure App Math, 41:909-996, 1988 3. D. Donoho, IEEE Trans Inform Theory, 41:613-627, 1995

**BINDING POTENTIAL UNDERESTIMATION WITH REFERENCE TISSUE  
MODELS: INSIGHT FROM [CARBONYL-11C]WAY-100635 SIMULATION STUDIES**

Valentina Bovo, Alessandra Bertoldo, Claudio Cobelli

*Department of Information Engineering, University of Padova, Padova, Italy*

INTRODUCTION Reference tissue (RT) and simplified reference tissue (SRT) models used in conjunction with [carbonyl-11C]WAY-100635 data underestimate the binding potential (BP) when compared to values obtained using kinetic modeling with arterial input function. This underestimation is due to violation of the assumptions underlying RT and SRT. The purpose of this study was to quantify by simulation the extent of BP bias in presence of one or more RT and SRT assumption violations. MATERIALS & METHODS Healthy brain time activities were simulated using a representative plasma input function for [carbonyl-11C]WAY-100635 and a two-tissue model (2TM) to obtain typical lateral orbital frontal cortex (Lof) and hippocampus (Hip) ROI, or one-tissue model (1TM) to obtain typical cerebellum (Cer - reference) ROIs. Since RT and SRT assume a negligible ROI blood volume ( $V_b=0$ ) and equal distribution volumes of not specifically bound tracer between reference and ROI ( $V_f+ns(ROI)=V_f+ns(Cer)$ ), to test the effect of these assumptions, Lof, Cer, and Hip activities were generated assuming  $V_b=0\%$ ,  $5\%$  or  $10\%$  and  $V_f+ns(ROI)=V_f+ns(Cer)$  or  $V_f+ns(ROI)\neq V_f+ns(Cer)$ :  $\pm 20\%$ ,  $35\%$ , &  $45\%$ . We also tested the assumption that the reference region is modeled with a 1TM, therefore a typical Cer activity was also generated by using a 2TM. RESULTS The mean results are: if Cer is modeled with a 1TM model,  $V_f+ns(ROI)=V_f+ns(Cer)$ , and  $V_b=0\%$  parameters  $R1$  and BP are not biased, while the other parameters ( $k_2$ ,  $k_3$ ,  $k_4$  for the RT and  $k_2$  for the SRT) are either under- or over-estimated. As soon as one of RT and SRT assumptions fails, BP is biased. For example, with Cer described by 1TM,  $V_f+ns(ROI)=V_f+ns(Cer)$  and  $V_b=5\%$ , BP bias is  $\sim 25\text{-}30\%$  and  $BP_{RT}\neq BP_{SRT}$ . If Cer is modeled by 2TM,  $V_f+ns(ROI)=V_f+ns(Cer)$  and  $V_b=5\%$ , BP underestimation reaches  $40\%$  and  $BP_{RT}=BP_{SRT}$ . If  $V_b=0\%$ , and Cer is modeled by 1TM, but  $V_f+ns(ROI)<V_f+ns(Cer)$ , BP underestimation is of  $25\%$  when the difference between  $V_f+ns$  is  $20\%$ ; underestimation increases when this difference is larger. If  $V_b=0\%$ , and  $V_f+ns$  are equal but Cer is modeled by 2TM, there is a  $20\%$  BP underestimation. When all the three assumptions are violated, eg  $V_b=5\%$ ,  $V_f+ns(ROI)<0.35\cdot V_f+ns(Cer)$  and Cer described by 2TM, BP is underestimated of about  $60\%$ . Of note is that simulations always give  $BP_{RT}=BP_{SRT}$  whenever Cer is not modeled as postulated by RT and SRT model, i.e. by 1TM. CONCLUSION Simulations indicate that a correct estimation of BP with RT and SRT is possible if all the assumptions underlying these models are verified. As soon as one of them fails, BP is underestimated (at least  $25\%$ ) and the other RT and SRT parameters are also biased. In addition, only if Cer is modeled with a 1TM then  $BP_{RT}\neq BP_{SRT}$ . Since our previous RT and SRT analysis on real [carbonyl-11C]WAY-100635 data [1] showed  $BP_{RT}=BP_{SRT}$ , our findings support that Cer has a more than 1TM structure and that BP is heavily underestimated ( $\sim 50\%$  by assuming a  $V_b=5\%$ ). 1) Neuroimage, vol 22 (Suppl.2), T65, 2004

## EVALUATION OF REFERENCE TISSUE MODELS FOR ANALYSING [11C](R)-PK11195 STUDIES

Marc A. Kropholler<sup>1</sup>, Bart N.M. van Berckel<sup>1</sup>, Alie Schuitemaker<sup>1,2</sup>, Hedy Folkersma<sup>3</sup>, Gert Luurtsema<sup>1</sup>, Albert D. Windhorst<sup>1</sup>, Ronald Boellaard<sup>1</sup>, Adriaan A. Lammertsma<sup>1</sup>

<sup>1</sup>*Department of Nuclear Medicine & PET Research, VU University Medical Centre, Amsterdam, The Netherlands*

<sup>2</sup>*Department of Neurology, VU University Medical Centre, Amsterdam, The Netherlands*

<sup>3</sup>*Department of Neurosurgery, VU University Medical Centre, Amsterdam, The Netherlands*

Introduction [11C](R)-PK11195 is a tracer of microglia activation in the brain. Most studies used a reference tissue model (RTM) for measuring activation [1], but these models have not been validated against a plasma input model. The purpose of this study was to validate several RTMs against a previously described two tissue compartment plasma input model with fixed  $K_1/k_2$  (PIM) [2]. Methods Five RTMs were evaluated: A. Two target and one reference tissue (full RTM) [3]; B. One target and one reference tissue (simplified RTM) [4]; C. Two target and two reference tissues; D. Model C with  $k_4 = k_4'$ ; E. Three target and two reference tissues with  $k_5 = k_5'$  and  $k_6 = k_6'$ . Two methods were evaluated that obtained BPsp indirectly through Vd: F. Two target and one reference tissues; G. Two target and two reference tissues. One combined method was evaluated: H. BPsp from method B, corrected for BPns by multiplying with  $1+BP'$ ns calculated using PIM. Simulations were performed to assess accuracy and precision of BPsp using clinically relevant parameter values, and varying BPsp, BPns and Vb. 500 runs per parameter set were performed. Noise was varied between 0 and 10% COV. Using clinical data, results from RTMs were compared with those from PIM. Results For standard parameter values (7.5% noise), simulations showed biases of -58%, -15% and -5% and variabilities (COV) of 26%, 35% and 22% for methods B, D and H, respectively. Varying noise (0 - 10%) resulted in changing bias from -61 to -58% (method B), from 2.5 to 18% (method D) and from 0 to 8% (method H), and in reducing precision from 0 to 30%, 50% and 28% for methods B, D and H, respectively. Other methods provided poor accuracy and/or precision. Increasing BPns increased bias for methods B and D, but did almost not effect accuracy of method H. For small BPsp method D became unstable, whilst methods B and H still provided reasonable estimates. Clinical evaluation showed that methods A and B provided nearly identical results (R-squared = 0.94), but method B had better precision. Results from methods B, D and H correlated reasonably well with PIM (R-squared = 0.74, 0.65 and 0.84, respectively). Other methods resulted in very low correlations (R-squared <0.06), consistent with simulation results. Discussion Both simulations and clinical data showed that only methods B, D and H correlate with PIM. Apart from the best correlation, method H also showed the lowest bias at various simulated BPns, BPsp and Vb values. COV for both methods B and H were much lower than for method D. Method H allows for accurate and precise estimations of both BPsp and BPns. Method B is recommended when a plasma input is not available. 1. Cagnin, A. et al. (2001) Lancet 358:461-467 2. Kropholler, M. A. et al. (2005) J Cereb Blood Flow Metab, in print 3. Lammertsma, A. A.; Hume, S. P. (1996) Neuroimage 4:153-158 4. Hume, S. P. et al (1992) Synapse 12:47-54

**EFFECTS OF REFERENCE TISSUE VERSUS PLASMA INPUT PARAMETRIC KINETIC MODELLING ON STATISTICAL PARAMETRIC ANALYSIS OF [11C](R)-PK11195 BINDING IN ALZHEIMER'S DISEASE (AD) AND YOUNG AND OLD SUBJECTS**

**Alie Schuitemaker**<sup>1,2</sup>, Bart N.M. van Berckel<sup>2</sup>, Marc A. Kropholler<sup>2</sup>, Philip Scheltens<sup>1</sup>, Cees Jonker<sup>1,4</sup>, Dick J. Veltman<sup>2,3</sup>, Adriaan A. Lammertsma<sup>2</sup>, Ronald Boellaard<sup>2</sup>

<sup>1</sup>*Department of Neurology, VU University Medical Center, Amsterdam, The Netherlands*

<sup>2</sup>*Department of Nuclear Medicine and PET Research, Amsterdam, The Netherlands*

<sup>3</sup>*Department of Psychiatry, Amsterdam, The Netherlands*

<sup>4</sup>*EMGO Institute, Amsterdam, The Netherlands*

Introduction: [11C](R)-PK11195 is a tracer of microglial activation in the brain. In previous studies PK11195 binding was analysed using reference tissue models<sup>1</sup>, showing increased binding in the thalamus with age<sup>2</sup>. Up to date PK11195 binding amongst young, old and AD subjects has not yet been analysed using statistical parametric mapping (SPM). Therefore, a study was performed to evaluate SPM analysis of PK11195 binding in AD versus old and young subjects. SPM analysis was based on: (1) binding potential (BP) images obtained with a reference tissue input (Ichise multilinear regression) and (2) volume of distribution (Vd) images obtained with plasma input (Logan plots). Methods: Thirty [11C](R)-PK11195 studies with on-line arterial sampling were included (8 young (< 40 y) and 12 old controls (>60 y) , and 10 AD patients). Using the on-line whole blood curve and a number of manual arterial samples, a metabolite corrected plasma input curve was derived. A reference tissue input curve was obtained from a region of interest over cerebellum. PET scans were reconstructed using FBP Hanning 0.5. Additional smoothing with a 10 mm FWHM Gaussian filter was performed to reduce noise to acceptable levels, thereby avoiding noise induced bias<sup>3</sup> during Ichise and Logan plot analysis. Subsequently, SPM analysis of both Ichise and Logan images was performed without further smoothing, i.e. the standard smoothing in SPM was omitted. Because Vd images represent total distribution volume, including free and non-specific binding, SPM analysis of Vd data was performed with and without proportional scaling. Results: SPM analysis without proportional scaling based on Vd images did not show any regions with differences in PK11195 binding amongst all groups. When proportional scaling was applied, only a trend (p<0.1) of increased PK11195 binding was observed in both thalami. When SPM analysis was performed using BP images, significantly (P<0.001) increased PK11195 binding in the thalamus was observed in both older and AD subjects, compared with young controls. Furthermore, SPM of BP images showed additional areas (e.g. occipital, lateral temporal areas and subcortical structures (presumably nucleus subthalamicus)) with increased binding in elderly and AD subjects. Discussion: Logan plots provide Vd values, which depend on the sum of free, specifically and non-specifically bound ligand. As non-specific binding of PK11195 is relatively high, SPM analysis of Vd images without proportional scaling may be confounded by intersubject variability in non-specific binding. To some extent this may be compensated by proportional scaling, explaining the observed trend of increased uptake in the thalamus after such scaling. SPM analysis of BP images was found to be most powerful. As BP images only represent increased (specific) binding, it does not suffer from the large contribution and variability of non-specific binding. In addition, reference tissue input models may provide better precision than plasma input models, because they do not need (noisy) metabolite corrections. References: 1.Lammertsma AA and Hume SP (1996) *NeuroImage* 4: 153-158 2. Cagnin A, Brooks DJ et al. (2001) *The Lancet* 358: 461- 467 3. Slifstein M and Laruelle M (2000) *J Nucl Med* 41: 2083-2088

**MONTE CARLO SIMULATION FOR REFERENCE TISSUE-BASED LINEAR ANALYSIS OF [11C]MP4A AND [11C]MP4P: ASSESSMENT OF OPTIMAL REGIONS AND OPTIMIZATION FOR PRECISE MEASUREMENT OF BRAIN AChE ACTIVITY**

Koichi Sato<sup>1,2</sup>, Kiyoshi Fukushi<sup>1</sup>, Hitoshi Shinotoh<sup>1</sup>, Shin-ichiro Nagatsuka<sup>1</sup>, Noriko Tanaka<sup>1</sup>, Tsuneyoshi Ota<sup>1</sup>, Tetsuya Shiraishi<sup>1,2</sup>, Shigeki Hirano<sup>1</sup>, Shuji Tanada<sup>1</sup>, Hiroki Namba<sup>1</sup>, Masaomi Iyo<sup>2</sup>, **Toshiaki Irie<sup>1</sup>**

<sup>1</sup>*Department of Medical Imaging, National Institute of Radiological Sciences, Chiba, Japan*

<sup>2</sup>*Department of Psychiatry, Graduate School of Medicine, Chiba University, Chiba, Japan*

**Background:** We have proposed reference tissue-based linear analysis without arterial blood sampling for measurement of brain AChE activity using N-[11C]methylpiperidin-4-yl acetate ([11C]MP4A), where cerebellum or striatum that have high AChE activity was used as a reference [1]. The striatal reference analysis was also applicable for N-[11C]methylpiperidin-4-yl propionate ([11C]MP4P) [2]. In this study, characterization and optimization of this method, including assessment of regions where precise  $k_3$  (an index of AChE activity) would be measurable, were performed by computer simulation. **Methods:** Monte Carlo simulations were performed to assess precision and bias of  $k_3$  estimates obtained from cerebellar or striatal reference analysis of [11C]MP4A and striatal reference analysis of [11C]MP4P. The time-radioactivity curves were derived based on full compartment model with fixed input function and fixed kinetic parameter except  $k_3$  for each tracer. The target  $k_3$  values were varied so as to include regions with low (cerebral cortex) and moderate (thalamus) AChE activity. The reference  $k_3$  was estimated from reported in vitro AChE activity ratio across temporal cortex/cerebellum/striatum and normal temporal  $k_3$  value. PET data error was estimated as described previously [3], where a region-of-interest volume of 1 to 5 mL was used, and 100 data sets were generated for each target  $k_3$  condition. **Results:** The COV (coefficient of variation) of  $k_3$  in each linear analysis was less than 20% across the  $k_3$  range tested for each tracer (corresponded to regions with low-to-moderate AChE activity), although gradually increased with increasing  $k_3$ . The  $k_3$  bias in striatal reference analysis of [11C]MP4A remained within  $\pm 5\%$  across the  $k_3$  range tested. The cerebellar reference analysis of [11C]MP4A gave a minus-bias that gradually increased (absolute value) with increasing  $k_3$ , reaching about -15% in the thalamus. In the case of [11C]MP4P, the striatal reference analysis gave small minus-biases (within 5%) to  $k_3$  in the cerebral cortex and thalamus. When the PET data error was added to reference time-radioactivity data as well as target data, the COV of  $k_3$  was slightly increased. The error-added reference curve was also fitted by biexponential function; the COV was improved without significant change in bias. The nonlinear calculation in the reference tissue-based analysis, using another operational equation derived without linear transformation, was also available; the  $k_3$  estimates were also subjected. **Conclusions:** The cerebellar or striatal reference analysis of [11C]MP4A and striatal reference analysis of [11C]MP4P gave acceptable bias and COV to  $k_3$  in the regions with low-to-moderate AChE activity. Since the  $k_3$  value of [11C]MP4P is relatively small compared to the value of [11C]MP4A, more precise  $k_3$  estimation was expected in the thalamus by using [11C]MP4P. The use of fitted reference data did not affect the bias but improved COV. The fitting procedure would be useful, though the raw reference data was used in the original protocol [1]. [1] Nagatsuka et al. (2001) J Cereb Blood Flow Metab 21: 1354-1366 [2] Sato et al. (2004) J Cereb Blood Flow Metab 24: 600-611 [3] Tanaka et al. (2001) J Cereb Blood Flow Metab 21: 295-306

## A GENERALIZED REFERENCE TISSUE MODEL FOR QUANTIFICATION OF DYNAMIC PET WITH BOLUS PLUS CONTINUOUS INFUSION TRACER ADMINISTRATION AND PHARMACOLOGICAL CHALLENGE

Yun Zhou<sup>1</sup>, Weiguo Ye<sup>1</sup>, Mingkai Chen<sup>2</sup>, Anil Kumar<sup>1</sup>, Mohab Alexander<sup>1</sup>, Christopher J. Endres<sup>1</sup>,  
Tomas R. Guilarte<sup>2</sup>, Dean F. Wong<sup>1</sup>

<sup>1</sup>*The Russell H. Morgan Department of Radiology and Radiological Science, Johns Hopkins University  
School of Medicine, Baltimore, MD, USA*

<sup>2</sup>*Department of Environmental Health Sciences, Bloomberg School of Public Health, Baltimore, MD, USA*

Bolus followed by constant infusion for tracer administration (B/I) has been used for ligand-receptor dynamic PET study to measure changes of tracer binding due to neurological or pharmacological stimulation. Concentration ratio (CR) method is commonly used to quantify the stimulus-induced binding changes. CR method is based on the assumption that all tissue concentrations are at steady state within a given time period. The objective of this study is to develop and evaluate a full modeling approach to measure the amphetamine-induced binding potential (BP) changes in B/I dynamic PET study. Methods: A 4-parameter generalized reference tissue model (GRTM), ( $R_1$ ,  $k_2$ ,  $BP_0$ ,  $BP_1$ ) is derived from a 3-parameter ( $R_1$ ,  $k_2$ ,  $BP$ ) simplified reference tissue model (SRTM) by assuming  $R_1$ , and  $k_2$  are constants, and  $BP$  is a step function that varies from  $BP_0$  in pre-phase to  $BP_1$  at post-amphetamine phase, where  $R_1$  is the ratio of transport rate from blood to brain tissue, and  $k_2$  is the efflux rate constant from free and nonspecific binding compartment to blood. A 4-parameter GRTM with only 2-parameter ( $k_2$  and  $BP_1$ ) SRTM for post phase is also derived from the assumption that reference tissue tracer concentration is constant in post phase (GRTM2). GRTM and GRTM2 were applied to 11 monkey [<sup>11</sup>C]raclopride (RAC). At each PET study, about 25 mCi high specific activity RAC was delivered by B/I with a 75:1 bolus to infusion ratio. Amphetamine was injected at 40 min post tracer bolus injection with a dose level of 2 mg/kg. Each Dynamic PET scan was performed on a GE Advance scanner with acquisition protocol of total 90 min. Images were reconstructed using filtered back projection with a ramp filter which resulted in a spatial resolution of about 4.5 mm FWHM at the center of the field of view. Irregular ROIs of cerebellum (reference tissue) and striatum were defined on the first 45 min integrated PET images. For comparison, two CR methods to estimated  $BP_0$  and  $BP_1$  are calculated as: CR1:  $BP_0 = C_{str}(30-40)/C_{ref}(30-40)-1$ ,  $BP_1 = C_{str}(60-90)/C_{ref}(60-90)-1$ ; CR2:  $BP_0 = C_{str\_SRTM}(60-90)/C_{ref}(60-90)-1$ ,  $BP_1 = C_{str}(60-90)/C_{ref}(60-90)-1$ , where  $C_{str\_SRTM}$  is extrapolated by SRTM with parameters determined by model fitting at pre-phase only. The amphetamine-induced dopamine release (DAR) is estimated by BP as  $DAR = (BP_0 - BP_1)/BP_0$ . GRTM and CR methods were also evaluated by computer simulation. A cerebellum time activity curve from a typical study and wide range of parameters were used to simulate striatum of different kinetics and DAR levels. Results: In monkey study, the mean and standard deviation (mean(STD)) of estimates are listed in the following table. GRTM and GRTM2 provide almost same estimates. The DAR estimates from CR methods are significantly lower than those obtained by GRTM method ( $p < 0.0001$ ). Computer simulation shows that the DAR calculated by CR1 and CR2 are significantly underestimated in 71% and 30% from true values, respectively. A paired T-Test demonstrate that there is no significant difference in AIC values between GRTM and GRTM2 model fitting. In conclusion, GRTM is a robust and reliable kinetic modeling approach to quantify the B/I dynamic PET with pharmacological challenge.

**Mean and Standard (n=11) Deviation (mean(STD)) of Estimates**

Methods	$R_1$	$k_2$	$BP_0$	$BP_1$	DAR
GRTM	0.88 (0.08)	0.13 (0.02)	2.99 (0.29)	2.09 (0.39)	0.30 (0.11)
GRTM2	0.90 (0.08)	0.13 (0.02)	3.05 (0.32)	2.04 (0.36)	0.33 (0.09)
CR1			2.59 (0.31)	2.34 (0.39)	0.09 (0.19)
CR2			3.01 (0.29)	2.34 (0.39)	0.23 (0.09)



**EFFECT OF AMPHETAMINE ON DOPAMINE D2 RECEPTOR BINDING IN THE PRIMATE BRAIN WITH THE AGONIST LIGAND [11C]MNPA**

Nicholas Seneca<sup>1,2</sup>, Sjoerd Finnema<sup>1</sup>, Masanori Ichise<sup>2</sup>, Balazs Gulyas<sup>1</sup>, Håkan Wikstrom<sup>3</sup>, Robert B. Innis<sup>2</sup>, Lars Farde<sup>1</sup>, Christer Halldin<sup>1</sup>

<sup>1</sup>*Karolinska Institute, Department of Clinical Neuroscience, Psychiatry Section, Stockholm, Sweden*

<sup>2</sup>*National Institute of Mental Health, Molecular Imaging Branch, Bethesda, MD, USA*

<sup>3</sup>*University of Groningen, Department of Medicinal Chemistry, Groningen, The Netherlands*

**Introduction:** We have previously reported the development of a new high affinity dopamine D2 agonist, [11C]MNPA [1]. (R)-2-CH3O-N-n-propylnorapomorphine (MNPA) is a highly selective D2 agonist with an IC50 of 1.0 nM compared to NPA with 4.8 nM. Recently, PET imaging with D2 agonist radioligands supports preferential labeling of D2 receptors in the high affinity state [2,3]. The aim of the present study was to assess the vulnerability of the in vivo binding of [11C]MNPA to pharmacological manipulation in synaptic DA assessed with PET in cynomolgus monkey and compared to that of the D2 receptor antagonist radiotracer [11C]raclopride. **Methods:** A total of 32 PET measurements were performed using i.v. bolus injection of [11C]MNPA (n = 24) and [11C]raclopride (n = 8) in four cynomolgus monkeys. In each monkey a baseline measurement was followed by a pretreatment measurement in which amphetamine (AMPH at 0.1, 0.2, 0.5, and 1.0 mg/kg) was injected i.v. approximately 20 min prior to the radioligand. For each dose of AMPH, the same monkey was used in the comparison between the two radioligands. For [11C]MNPA, the mean injected radioactivity was  $55 \pm 7$  MBq at baseline and  $56 \pm 5$  MBq for AMPH pretreatment. The total mass injected for [11C]MNPA was  $0.55 \pm 0.68$   $\mu$ g at baseline and  $0.42 \pm 0.46$   $\mu$ g during AMPH pretreatment. Data were analyzed with the multilinear reference tissue model (MRTM2) [4]. **Results:** AMPH caused a dose-dependent reduction in [11C]MNPA binding potential of  $10 \pm 9\%$  at 0.1 mg/kg,  $23 \pm 6\%$  at 0.2 mg/kg,  $26 \pm 2\%$  at 0.5 mg/kg and  $39 \pm 17\%$  at 1.0 mg/kg. [11C]Raclopride binding was unchanged at 0.1 mg/kg but was decreased by 23% at 0.2 mg/kg, 17% at 0.5 mg/kg and 26% at 1.0 mg/kg. AMPH reduced [11C]MNPA binding to D2 receptors more profoundly than did [11C]raclopride to D2 binding at both high and low doses of amphetamine, indicating that the agonist radioligand is more sensitive to changes in endogenous dopamine concentration. Based on these results, the percentage of D2 receptors in high affinity state was calculated to be 63%. **Conclusions:** These results show that the agonist radioligand [11C]MNPA is more sensitive than the antagonist radioligand [11C]raclopride to displacement by endogenous dopamine. For this reason, an agonist radioligand may contribute more to understanding dysfunction in the dopamine system in illnesses such as schizophrenia and Parkinson's disease. **References:** 1. Finnema et al., NeuroImage 22 Suppl. 2 (2004); P24. 2. Narendran et al., Synapse (2004); 53(3) 188-208. 3. Mukherjee et al., Synapse (2004); 54(2) 83-91. 4. Ichise et al., J Cereb Blood Flow Metab (2003); 23(9) 1096-112.

### [11C]RACLOPRIDE IMAGING OF DOPAMINE RELEASE IN RHESUS MONKEYS

Alexander K. Converse<sup>1</sup>, Todd E. Barnhart<sup>2</sup>, Corinne B. Dallas<sup>3</sup>, Salma Jivan<sup>4</sup>, Julie A. Larson<sup>5</sup>, Terrence R. Oakes<sup>1</sup>, Andrew D. Roberts<sup>2</sup>, Thomas J. Ruth<sup>4</sup>, Nicholas T. Vandehey<sup>3</sup>, Mary L. Schneider<sup>5</sup>

<sup>1</sup>Waisman Laboratory for Functional Brain Imaging, University of Wisconsin, Madison, WI, USA

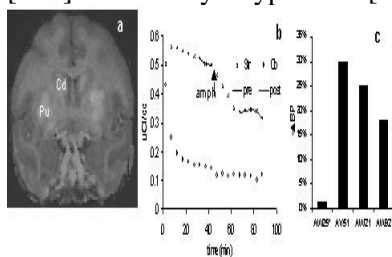
<sup>2</sup>Manchester Molecular Imaging Centre, Manchester, UK

<sup>3</sup>Department of Medical Physics, University of Wisconsin, Madison, WI, USA

<sup>4</sup>TRIUMF, University of British Columbia, Vancouver, BC, Canada

<sup>5</sup>Department of Kinesiology, University of Wisconsin, Madison, WI, USA

**GOAL:** For a variety of purposes we have begun implementation of a PET method for studying dopamine release. We used the dopamine D2-type receptor antagonist [11C]raclopride to study dopamine function in the rhesus monkey brain in response to an amphetamine challenge. [11C]raclopride is susceptible to competition from endogenous dopamine, whereby dopamine released into extracellular space reduces the number of binding sites available for the tracer. **METHODS:** Dopamine release induced by d-amphetamine was imaged using [11C]raclopride in 3 rhesus monkeys with the UW microPET. After a transmission scan using a 68Ge point source, a 90 minute emission scan began with injection of a bolus of [11C]raclopride (1.0 mCi in 5 mL in 10 s, SA = 170 mCi/umol). The bolus was immediately followed by an infusion of [11C]raclopride (1.5 mCi in 45 mL over 90 min at 0.5 mL/min). D-amphetamine sulfate (0.4 mg/kg) was injected (i.v.) 45 minutes after initial injection of [11C]raclopride. Emission data were binned into sinograms (18 x 5 min) with corrections for dead time and random coincidences. Images were reconstructed with FBP with attenuation correction. ROIs were drawn on coregistered MRIs and TACs were generated. The binding potential prior to amphetamine injection at 45 minutes was determined by  $BP_0 = DVR_0 - 1 = Str_0/Cb_0 - 1$  and after injection by  $BP_{amph} = DVR_{amph} - 1 = Str_{amph}/Cb_{amph} - 1$ , where  $Str_0$  and  $Cb_0$  are the average striatal and cerebellar tracer concentrations from 30-45 min and  $Str_{amph}$  and  $Cb_{amph}$  are the averages from 65-90 min. The binding change is expressed as the fraction  $DBP = (BP_{amph} - BP_0)/BP_0$ , and this is a measure of the fractional reduction in D2 receptor occupancy due to release of endogenous dopamine. **RESULTS:** As a test of the method, we performed a scan and analysis without amphetamine on one monkey (AW25) and obtained a change in binding of  $DBP = -1.2\%$ . Three other monkeys were given amphetamine, and the average measured reduction in [11C]raclopride binding was  $DBP = -24\% \pm 6\%$  (SD, n=3). The figure shows the following: (a) microPET image of [11C]raclopride (0-45 min) overlaid on MRI for AV51 at anterior commissure showing binding in caudate (Cd) and putamen (Pu). (b) Time-activity curves for striatum (Str) and cerebellum (Cb) for AW92. Arrow indicates time of amphetamine injection (0.4 mg/kg). (c) Reduction in striatal [11C]raclopride binding (-DBP) for four subjects. \*AW25 received no amphetamine as a test of the method. **CONCLUSIONS:** This result agrees with the observed 21%  $\pm$  11% (SD, n=4) decrease in binding with the same amphetamine dose reported earlier (A. Breier et al. PNAS 94:2569-2574, 1997). We intend to apply this method for a variety of purposes including studies of monkeys exposed to moderate alcohol levels in utero, human dopamine response to tasks, and simultaneous imaging of dopamine release and blood flow alteration. As alternatives to [11C]raclopride, we are also considering the use of [18F]desmethoxyfallypride or [18F]fallypride.





## DISPLACEMENT DETECTABILITY OF [18F]MPPF FROM 5-HT1A RECEPTORS BY ENDOGENOUS SEROTONIN: A MONTE CARLO SIMULATION STUDY

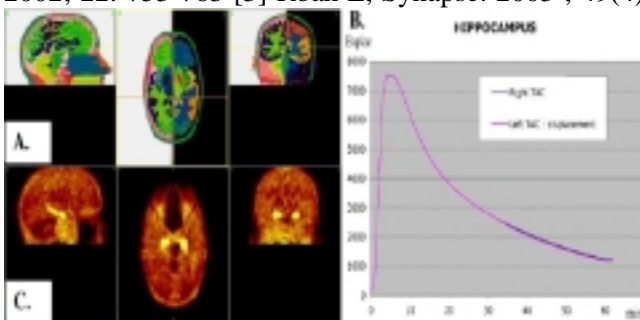
Nicolas Costes<sup>1</sup>, Anthonin Reilhac<sup>1,3</sup>, Axel Martinez<sup>1</sup>, Isabelle Merlet<sup>2</sup>

<sup>1</sup>CERMEP- Imagerie du Vivant, PET Centre, Lyon, France

<sup>2</sup>EA1880, Federative Institute of Neurosciences, Claude Bernard University, Lyon, France

<sup>3</sup>Mc Connell Brain Imaging Centre, Montreal Neurological Institut, Mc Gill University, Montreal, QC, Canada

**Introduction:** 5-HT1A receptors are largely involved in psychiatric and neurological disorders such as depression, schizophrenia, dementia, or epilepsy. The MPPF fluorine 18 labeled tracer, competitor to endogenous serotonin binding on 5-HT1A receptors [1], has been quantified and validated for clinical investigations [2]. Studies in rat [3] have shown that variations in serotonin concentration can be detected with MPPF, which would be of particular interest for human in vivo examination. Although theoretically, the discrimination of a displacement in non-noisy modeled kinetic is obvious, it may be undetectable in noisy real conditions of measure with PET. **Objective:** The aim of this study was to evaluate the detectability of a displacement of MPPF binding consecutive to a serotonin release on a Monte-Carlo simulated PET data set. **Methods:** Six MPPF PET dynamic data sets were simulated with the SORTEO Monte-Carlo simulator [4] reproducing the physical disintegration process, the photon transport and the detection by CTI Exact HR+ camera. Emission volumes came from segmented MRI brain images classified in labeled cortical and subcortical brain structures (Fig A.). In regions rich in 5-HT1A receptor, emission kinetics were analytically simulated from the compartmental model. Regions from the right hemisphere had a standard kinetics resulting from a single bolus injection of [18F]-MPPF tracer dose, whereas homologous regions of the left hemisphere resulted from a more complex model including an endogenous compartment from which a release of serotonin was simulated 20 minutes post-injection (Fig B). In regions poor in 5-HT1A receptors and in background, kinetics were extracted from actual PET data obtained from a normative database acquired with our HR+ camera. After the simulation of PET acquisition processes (Fig C), regional time-activity curves were extracted from dynamic PET data to compute MPPF binding parameters with an adequate model. Parametric images were also computed. A statistical analysis of normal regions versus regions with displacement was performed to detect serotonin concentration modifications, both in ROI level and in a voxel based level with SPM. Simulated data were compared with actual data to evaluate realism of the simulations and detectability of displacement. **Results:** Comparisons between left and right mean ROI values revealed a significant difference induced by the serotonin release. The individual SPM analysis did not reveal significant differences with normal subjects, whereas in the SPM group analysis, significant differences were found in some clusters located in regions with displacement. In conclusion, the sensitivity for detecting a displacement depended on the availability of 5-HT1A receptor, the number of subjects, and the size of cortical structures. [1] Zimmer L, et al., JNeurochem 2002; 80: 278-86 [2] Costes N, et al. JCBF 2002; 22: 753-763 [3] Rbahl L, Synapse. 2003 ; 49(4):239-45 [4] Reilhac, et al. IEEE TNS 2004; 51: 46-52





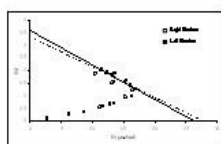
**QUANTIFYING IN VIVO DOPAMINERGIC D2-RECEPTORS BMAX AND KDVR WITH MICROPET® FOCUS AFTER A SINGLE INJECTION OF [11C]RACLOPRIDE**

Laurent Besret<sup>1</sup>, Jean-Dominique Gallezot<sup>2</sup>, Frédéric Dollé<sup>2</sup>, Philippe Hantraye<sup>1,2</sup>,  
Marie-Claude Grégoire<sup>1</sup>

<sup>1</sup>URA CEA-CNRS 2210, Service Hospitalier Frédéric Joliot, Orsay, France

<sup>2</sup>CEA-UIIBP, Service Hospitalier Frédéric Joliot, Orsay, France

**Background and Purpose:** Dopaminergic D2-receptors quantification in vivo provides important information in the study of cerebral diseases, especially for degeneration or neural repair follow-up. [11C]raclopride binding in rat striata has been recently fully characterised and all model parameters were identified with a multi-injection approach and a beta-microprobe (Mauger et al., submitted data). Simulations derived from these results showed that a simpler protocol could be used in a PET imaging framework. This study aims at validating a single injection protocol, without any blood sampling, which allows the simultaneous estimation of Bmax and KdVr. This will be performed by estimating Bmax and KdVr on a population of living rats, and correlate these quantities with ex vivo Bmax and Kd obtained on the very same striata. **Method:** Each rat (male Sprague-Dawley anesthetized with isoflurane) was placed in a stereotactic frame and underwent 3 to 4 PET scans (microPET® Focus™ 220, Concorde Microsystem) performed on separate days. The protocol is based on a partial saturation method (Delforge et al., 1990). All scans, except one, were performed after an intra-veinous injection of [11C]raclopride (74 to 111 MBq) that aimed at occupying 70% of the receptors. The last scan (pre-saturation) was performed after pre-treatment with a large amount of raclopride (1mg/kg, i.v.). The animals were pre-treated with cimetidine (150 mg/kg, i.p.) 50 minutes prior to each PET scan, and the acquisition lasted for 60 minutes. In vivo Bmax and KdVr were estimated on late data, showing a “dynamic equilibrium” where the Scatchard equations are still valid (due to [11C]raclopride characteristics). Based on pre-saturation data, cerebellum was used as a reference region, and B/F (bound/free) was plotted against B (bound). A few days after the last scan, rats were sacrificed. Their brain was quickly removed and striata were dissected and frozen for subsequent [3H]raclopride binding. Binding was performed in duplicate, after incubation of 2 hours at room temperature [3], on each structure separately, providing an ex vivo estimate of Bmax and Kd. Figure 1 shows a typical Scatchard plot, for left and right striata. Bmax and KdVr values are consistent with those obtained in the former study. Mean values were 22.7 pmol/ml and 8.5 nM, with a relative SD of 16 and 15%, respectively. Preliminary results show that a minimum of 70% of receptor occupation has to be reached in order to achieve a good accuracy of the estimators. Ex vivo binding is currently being carried out. **Conclusion:** A non-invasive simple protocol that allows simultaneous quantitation of D2-receptor density and affinity with [11C]raclopride is presented and validated. This will provide a very useful tool for assessing neuro-transmission variations in animal models of neurodegenerative disease. [1] Mauger G. et al., J. Cereb. Blood Flow Metab., submitted. [2] Delforge J. et al., J. Nucl. Med. 1996, 37(1): 5-11. [3] Seeman et al., Eur. J. Pharmacol., 1992, 227: 139-146.



**MEASURING THE INTEGRITY OF THE DOPAMINE SYSTEM IN RATS WITH  
[11C]DIHYDROTETRABENAZINE: MICROPET VS PHOSPHOR IMAGING  
AUTORADIOGRAPHY**

Elissa M. Strome, Ivan L. Cepeda, **Doris J. Doudet**

*University of British Columbia, Pacific Parkinson Research Centre, Vancouver, BC, Canada*

Positron emission tomography (PET) is a powerful tool for in vivo imaging of brain function in human and non-human primates and more recently in small animals such as rodents. As in human subjects, in vivo microPET can be used to evaluate longitudinally the extent of lesions or the effects of pharmacological challenges or potential therapies in animal models of diseases. It is however important to validate and correlate the in vivo data against currently used methods, either behavioural or post mortem assessments. Using the 6-OHDA model of Parkinson's Disease and [11C](±)dihydro-tetrabenazine (DTBZ), a tracer of the striatal dopaminergic (DA) terminals not sensitive to regulation as an index of lesion severity, we compared, in the same animals, in vivo data from a Concord microPET R4 scanner to in vitro autoradiography with the same tracer and to in vivo behavioral evaluation with a test known to be sensitive to moderate to severe nigro-striatal lesions and not requiring pharmacological challenges, the tapered ledged beam walking test (TLBWT). Adult male Sprague-Dawley rats with a wide range of 6-OHDA-induced DA nigro-striatal lesions were tested in the TLBWT test, scanned with DTBZ (100 mCi/100 gr body weight; SA>500 Ci/mmol) under ketamine anesthesia, before being sacrificed for phosphor imaging autoradiography. For microPET imaging, the ratio of striatal/cerebellar activity was calculated between 30 and 60 min post tracer injection. In vitro binding was performed by incubating 20 µm coronal sections in 5 nM DTBZ. Specific binding was calculated as (total binding)-(non-specific binding). The data were converted in pmol/cc tissue using standard curves and the specific activity at incubation [1]. The number of hindlimb errors in the narrow beam of TLBWT was used as the behavioral measure of interest. The in vivo and in vitro DTBZ binding were significantly correlated ( $r = 0.71$ ). Neither in vivo nor in vitro DTBZ binding correlated significantly with the behavioral scores, likely because behavioral deficits were detected in only the most severely lesioned animals. In summary, although microPET DTBZ binding was more sensitive to mild lesions than the behavioral scores, the mildest lesions were more easily identified with in vitro DTBZ binding. In addition, as expected due to its greater spatial resolution, autoradiography allowed better structure (caudate vs putamen vs accumbens for example) identification than microPET. However, the good correlation between in vivo and in vitro binding data suggests that DTBZ/microPET imaging is an excellent tool to assess in vivo the severity of lesions of the DA system in animal models of PD and associated disorders. It also suggests that post-mortem evaluation remains a needed confirmation when actual extent and location of the lesions are important parameters of a study [1] Strome E.M., Jivan S., Doudet D.J. "Quantitative in vitro phosphor imaging using [3H] and [18F] radioligands: effects of chronic desipramine treatment on serotonin 5HT2 receptors" J. Neurosci.Methods 141:143-154 (2005) Supported by: CIHR and NSERC

**EVALUATION OF THE SEROTONIN TRANSPORTER LIGAND [123I]ADAM FOR SPECT STUDIES IN HUMANS**

**Vibe G. Frokjaer<sup>1</sup>, Lars H. Pinborg<sup>1</sup>, Jacob Madsen<sup>2</sup>, Gitte M. Knudsen<sup>1</sup>**

<sup>1</sup>*Neurobiology Research Unit, Copenhagen University Hospital Rigshospitalet, Copenhagen, Denmark*

<sup>2</sup>*PET and Cyclotron Unit, Copenhagen University Hospital Rigshospitalet, Copenhagen, Denmark*

**Aim:** The radiotracer, [123I]ADAM, is a new tool for SPECT-imaging of in-vivo serotonin transporters (SERTs). So far, no study describing the kinetics of [123I]ADAM, its metabolites, or the selectivity of the ligand in humans has been published. The aims of this study were to evaluate quantification of [123I]ADAM with simplified models against full kinetic modeling, to investigate [123I]ADAM metabolites, and to validate the selectivity of [123I]ADAM binding through a SSRI blocking experiment. **Material and methods:** Six healthy volunteers, 3 men and 3 women, with a median age of 31 years (range 24-43) were included. After IV bolus injection of [123I]ADAM (median dose 260 MBq, range 206-329) dynamic SPECT scanning was conducted over 5.5 hours. Arterial plasma samples were taken and fractions of parent compound and labelled metabolites were determined by high performance liquid chromatography (HPLC) after solid phase extraction. Starting at 4 hours from injection, five of the subjects received intravenous injection of citalopram (0.25mg/kg) in order to block specific SERT binding. Due to unacceptable side effects three subjects received a reduced dosage (0.05, 0.07 and 0.11 mg/kg). The side effects were reversed within a few minutes allowing continuation of data acquisition. **Results:** Preliminary data analysis in three subjects including 4 brain regions, showed a significant correlation between results from the simplified tissue reference model (STRM) and full kinetic modelling using arterial input: Two-tissue compartment model (2T)/STRM:  $r=0.92$ , graphical analysis/STRM  $r=0.93$ . Also, the ratio method correlated well with 2T ( $r=0.94$ ), and graphical analysis ( $r=0.89$ ). Time activity curves of the brain uptake of tracer before and after SSRI blocking showed displacement of tracer in all midbrain regions but not in cerebellum, justifying that cerebellum represents non-specific binding. The time course of fractional unchanged [123I]ADAM varied from subject to subject typically being around 50% at 20 minutes, decreasing to 5-12 % 3-4 hours after injection. A labelled lipophilic compound was found in two subjects. The fraction of this lipophilic compound peaked around 2 hours after injection where it constituted about 13%. The concentration of [123I]ADAM increased following blocking with citalopram whereas the concentration of the lipophilic metabolite remained constant suggesting that this metabolite does not bind to SERTs. **Conclusion:** Quantification of SERT with [123I]ADAM is feasible with the simplified models which yields proportional measures to those from full kinetic modeling. Cerebellar activity represents nonspecific binding only and can serve as a reference region. [123I]ADAM metabolism is highly variable and in some subjects labelled lipophilic metabolites can be detected. Based on our data, however, it does not seem that the labelled metabolite binds to SERT. More subjects will be included for the evaluation of quantification models. Further, the stability of [123I]ADAM in full blood as well as in samples prepared for HPLC analysis will be evaluated in order to test whether the lipophilic compound observed truly represents a metabolite.

**BP-70**

**USE OF AN [18F] SETOPERONE BOLUS + INFUSION PROTOCOL TO DELINEATE AGE RELATED REDUCTION IN 5HT2A RECEPTOR BINDING POTENTIAL IN FEMALE RHEBUS MONKEYS**

Wai-Si Eng, **Stephen Krause**, Christine Ryan, Holly Sleph, Maria Michener, Marie Holahan, Eric Hostetler, Liza Gantert, Marie-Jose Belanger, Daniel Rubins, Sandra Sanabria, Richard Hargreaves, Jacquelynn Cook, H. Donald Burns

*Imaging Research, Merck Research Labs, West Point, PA, USA*

The physiologic process of aging is known to have an effect on the brain concentration of some monoaminergic receptors. In addition, studies have suggested a causal link between sex hormones and these receptor changes. Accordingly, we were interested to see in our colony of geriatric rhesus monkeys if we could demonstrate an age- and sex-related difference in 5HT2A receptor concentration in the brain using the PET tracer [18F] Setoperone. This tracer has a 10-50x greater affinity for the 5-HT2A receptor than the D2 receptor, but provides a specific signal for both receptors in vivo. Since D2 receptor density is low in cortical regions and 5HT2A is high, while the opposite is true in striatum, [18F] Setoperone can be used to evaluate both receptors. "Chase" studies with risperidone, a non-selective antagonist of both 5-HT2A and D2 demonstrated significant displacement of the tracer from both 5-HT2A and D2 receptors. Studies were conducted in propofol anesthetized, older (n=5, 26-29 yrs) female Rhesus monkeys and young female (n=2, 8 yrs) and male Rhesus monkeys (n=2, 8 and 10 yrs) as controls in an ECAT HR+ PET camera. At the time of the scans, estradiol levels were  $95 \pm 11$  pg/ml in the young female monkeys compared to  $35.3 \pm 6.5$  pg/ml in the older monkeys. [18F] Setoperone was administered as a bolus followed by a matched constant-rate infusion for 200 minutes, adjusted to compensate for tracer elimination in the bolus, to achieve steady-state brain uptake. Tracer uptake reached a steady state in the brain after 120 min (reflected by constant target-to-cerebellum ratio). Indices of 5HT2A and D2 receptor binding were calculated from the occipital cortex/cerebellum and striatum/cerebellum ratios between 140 and 200 minutes, respectively. The cerebellum was used as a reference region since it is essentially devoid of both 5-HT2A and D2 receptors. The uptake ratios of occipital cortex/cerebellum binding (an index of the 5-HT2A receptor binding potential) and striatum/cerebellum (an index of the D2 receptor binding potential) were calculated. The test-retest reproducibility of this protocol was found to be < 10 % in male Rhesus monkeys. Results indicated an 15% and 24% reduction in binding potential for D2 and 5HT2A receptors respectively in the older females compared to the young females. As expected, the binding potential for 5HT2A receptor in young males was comparable to that in the young females. These studies suggest [18F] Setoperone may be used in a convenient protocol to show age related reductions in 5HT2A and D2 receptor binding in post-menopausal woman. An advantage of using such a protocol with [18F] setoperone is that both 5-HT2A and D2 receptors can be evaluated in the same study.

**BP-71**

**TEST-RETEST MEASUREMENTS OF 5-HT<sub>2A</sub> RECEPTORS WITH  
[18F]ALTANSERIN PET**

**Steven Haugbøl**, Gitte M. Knudsen, Vibe G. Frøkjær, Steen G. Hasselbalch, Lars H. Pinborg

*Neurobiology Research Unit, Copenhagen University Hospital, Copenhagen, Denmark*

Background. The role of serotonin in many neuropsychiatric diseases necessitates the development of reliable measures of serotonin receptor binding in humans. In this study we assessed the reproducibility of [18F]altanserin for measurement of 5-HT<sub>2A</sub> receptors in humans. Methods. Six healthy men aged from 33 to 67 years were investigated with PET-[18F]altanserin using a bolus-infusion schedule to obtain steady state of tracer in blood and tissue. Each person was PET scanned twice with an interval of 2-14 days. Binding potential (BP) data were obtained for [18F]altanserin in three automatically defined brain regions: Frontal cortex, cingulate and striatum. Two different outcome measures were evaluated: BP1 ( $C_{voi} - C_{ref} / C_{plasma}$ ) and BP2 ( $(C_{voi} - C_{ref}) / C_{ref}$ ). Results. Both BP1 and BP2 showed higher reproducibility in brain areas with high 5-HT<sub>2A</sub> receptor binding. For the BP1 measurements the mean variability of the difference ( $100 \times ABS(\text{test} - \text{retest}) / (\text{mean test and retest})$ ) was: Frontal cortex (5.4%), cingulate (6.1%) and striatum (17%). For BP2 the variability was: Frontal cortex (7.6%), cingulum (10.2%) and striatum (19.7%). Intraclass correlation between test and retest for same regions was for BP1: 0.85, 0.69, and 0.04 and for BP2 0.91, 0.87, and 0.63. Conclusion. These data suggest that PET imaging with [18F]altanserin permits calculation of reproducible measures of 5-HT<sub>2A</sub> receptor in areas with high tracer binding and supports feasibility of continuing using [18F]altanserin in evaluation of mental diseases.

**SYNTHESIS OF N-METHYL-2-(2-AMINO-4-[18F]FLUOROPHENYLTHIO)BENZYLAMINE AS SEROTONIN TRANSPORTERS IMAGING AGENT**

Grace G. Shiue<sup>1</sup>, Joel H. Greenberg<sup>2</sup>, **Chyng-Yann Shiue**<sup>1</sup>

<sup>1</sup>*Department of Radiology, University of Pennsylvania, Philadelphia, PA, USA*

<sup>2</sup>*Department of Neurology, University of Pennsylvania, Philadelphia, PA, USA*

Introduction: There has been considerable interest in the development of PET radioligands that are useful for imaging serotonin transporters (SERT) in the living human brain. Recently, N,N-dimethyl-2-(arythio)benzylamines have been labelled with 11C and 18F as promising SERT PET radioligands [1-7]. One of them is 4-[18F]-ADAM (1) [2] and the other is N,N-dimethyl-2-(2-amino-4-trifluoromethylphenylthio)benzylamine [7]. The N-methyl-2-(2-amino-4-trifluoromethylphenylthio)benzylamine has been shown to be less lipophilic, but has higher brain uptake in rat than its N,N-dimethyl counterpart [7]. The purpose of this study was to synthesize N-methyl-2-(2-amino-4-[18F]fluorophenylthio)benzylamine (3) and compare it with compound 1 as a SERT imaging agent. Methods: N-methyl-2-(2-amino-4-[18F]fluorophenylthio)benzylamine (3) was synthesized by nucleophilic substitution of the multi-step synthesized N-methyl-2-(2,4-dinitrophenylthio)benzylamine (2) with K[18F]/Kryptofix 2.2.2 in DMSO at 130 degree C for 25 minutes followed by reduction with NaBH<sub>4</sub>-Cu(OAc)<sub>2</sub> in EtOH at 78 degree C for 20 minutes and purification with HPLC (10 x 250 mm, Phenomenex Luna 2; CH<sub>3</sub>CN:0.1 M HCO<sub>2</sub>NH<sub>4</sub> (30:70) containing 0.3 v% of acetic acid; 5 ml/min). Results: N-methyl-2-(2-amino-4-[18F]fluorophenylthio)benzylamine (3) was synthesized in ~ 5-10% yield with a synthesis time of 150 minutes from EOB. The radiochemical purity was > 97%, and the specific activity was 0.5-1 Ci/μmol. The radiochemical yield of compound 3 was similar to that of compound 1. Conclusion: N-methyl-2-(2-amino-4-[18F]fluorophenylthio)benzylamine (3) has been synthesized in moderate yield with high radiochemical yield and specific activity. The pharmacological profile of this agent is under investigation. References: [1] Ginovart N, Wilson AA, Meyer JH et al., J Cereb Blood Flow Metab 21:1342-1353 (2001) [2] Shiue GG, Choi S-R, Fang P et al., J Nucl Med 44:1890-1897 (2003) [3] Fang P, Shiue GG, Shimazu T et al., Appl Radiat Isot 61:1247-1254 (2004) [4] Huang Y, Hwang D-R, Bae S-A et al., Nucl Med Biol 31:543-556 (2004) [5] Huang Y, Narendran R et al., Nucl Med Biol 31:727-738 (2004) [6] Zhu Z, Guo N, Narendran R et al., Nucl Med Biol 31:983-994 (2004) [7] Wilson A and Houle S J Labeled Compd Radiopharm 42:1277-1288 (1999)

**[123I]TPCNE: A NOVEL SPET TRACER FOR THE SIGMA-1 RECEPTOR BINDS IRREVERSIBLY IN HUMANS IN VIVO**

**James M. Stone**<sup>1</sup>, Erik Arstad<sup>2</sup>, Kjell Erlandsson<sup>2</sup>, Rikki N. Waterhouse<sup>3</sup>, Peter J. Ell<sup>2</sup>,  
Lyn S. Pilowsky<sup>1,2</sup>

<sup>1</sup>*Institute of Psychiatry, Kings College London, London, UK*

<sup>2</sup>*Institute of Nuclear Medicine, University College London, London, UK*

<sup>3</sup>*Department of Psychiatry, New York State Psychiatric Institute and Columbia University,  
New York, NY, USA*

Background: The sigma-1 receptor is of increasing relevance to neuropsychiatric function and illness (Leonard 2004). [123I]TPCNE (1(trans-[123I]iodopropen-2-yl)-4-[(4-cyanophenoxy)methyl]piperidine;  $K_i = 0.67$  nM;  $\log P = 3.36$ ) is a novel SPET ligand for the sigma-1 receptor which has demonstrated high selectivity and potency for the receptor in pre-clinical studies (Waterhouse et al 1997). Here we report kinetics and characteristics of this tracer in four healthy volunteers, including one individual scanned at time points up to 30 hours after injection. Method: Four healthy volunteers were recruited (1 female, 3 male, mean age=32). All subjects received a bolus dose of approximately 185MBq [123I]TPCNE. Dynamic data acquisition with a brain dedicated Picker Prism 3000XP and arterial sampling began simultaneously. Scanning continued at time points up to 3.5 hours in three subjects. In one subject scanning continued at time points up to 5.5 hours on the first day and then continued on the following day up to 30 hours after injection. Data were metabolite-corrected and analysed by compartmental modelling with both reversible and irreversible models. Results: Blood and plasma curves showed a rapid clearance after peaking between 45 and 60 s p.i., with <1% of the peak value left in plasma at 30 min p.i. The parent fraction was high throughout the scan, going from ~97% at 10 min p.i. to ~78% at 60 min p.i.. Brain uptake was rapid with a widespread distribution, reaching a maximum between 30 and 90 min p.i., with no significant clearance during the time of the scan. The maximum total brain uptake was ~8.7% of injected activity. The rank order of tracer uptake in different brain regions was posterior cingulate > cerebellum > thalamus > striatum > cortex > white matter. The two-day scan (n-1) showed that there was practically no clearance of tracer up to 30 hours after injection. Conclusions: [123I]TPCNE is a promising SPET ligand for the sigma-1 receptor that shows exceptionally high, irreversible brain uptake with highest binding in posterior cingulate. References: Leonard BE. Sigma receptors and sigma ligands: background to a pharmacological enigma. *Pharmacopsychiatry*. 2004 Nov;37 Suppl 3:S166-70. Waterhouse RN, Mardon K, Giles KM, Collier TL, O'Brien JC. Halogenated 4-(phenoxy)methylpiperidines as potential radiolabeled probes for sigma-1 receptors: in vivo evaluation of [123I]-1-(iodopropen-2-yl)-4-[(4-cyanophenoxy)methyl]piperidine. *J Med Chem*. 1997 May 23;40(11):1657-67.

**[123I]TPCNE: A NOVEL SPET TRACER FOR THE SIGMA-1 RECEPTOR IS DISPLACEABLE IN HUMANS IN VIVO WITH LOW DOSE ORAL HALOPERIDOL**

**James M. Stone**<sup>1</sup>, Kjell Erlandsson<sup>2</sup>, Erik Arstad<sup>2</sup>, Rikki N. Waterhouse<sup>3</sup>, Peter J. Ell<sup>2</sup>,  
Lyn S. Pilowsky<sup>1,2</sup>

<sup>1</sup>*Institute of Psychiatry, Kings College London, London, UK*

<sup>2</sup>*Institute of Nuclear Medicine, University College London, London, UK*

<sup>3</sup>*Department of Psychiatry, New York State Psychiatric Institute and Columbia University,  
New York, NY, USA*

Background: The sigma-1 receptor is of increasing relevance to neuropsychiatric function and illness (Leonard 2004). [123I]TPCNE (1(trans-[123I]iodopropen-2-yl)-4-[(4-cyanophenoxy)methyl]piperidine;  $K_i = 0.67$  nM;  $\log P = 3.36$ ) is a novel SPET ligand for the sigma-1 receptor which has demonstrated high selectivity and potency for the receptor in pre-clinical studies (Waterhouse et al 1997). Haloperidol is an antipsychotic drug known to be a potent antagonist of the sigma-1 receptor. Here we have used a pre-dose haloperidol challenge to validate the specific binding of [123I]TPCNE binding in healthy volunteers. Method: Seven healthy volunteer subjects were recruited (2 female, 5 male, mean age=31, range=20-52). Three of the subjects (1 female, 2 male, mean age=30 range=22-40) received an oral dose of haloperidol (2.5mg) approximately 1 hour prior to the commencement of the scan. All subjects were given a bolus dose of approximately 185MBq [123I]TPCNE. Dynamic data acquisition with a brain dedicated Picker Prism 3000XP and arterial sampling began simultaneously. In two of the haloperidol treated subjects, arterial sampling was not possible, but venous samples were taken to generate time activity blood data for future analyses. Scanning continued at time points up to 3.5 hours. Data were metabolite-corrected and analysed by compartmental modelling with both reversible and irreversible models. The outcome measure was total volume of distribution (VT) in the case of the reversible models, and effective uptake rate ( $K_i$ ) for the irreversible models. Results: Time activity curves from all three haloperidol treated subjects indicated clear displacement in all brain regions. The haloperidol treated subject with full arterial sampling had lower measures of binding in all regions regardless of the kinetic modelling method used than any of the control subjects. The mean estimated occupancy by haloperidol varied depending on region from 42% in the cerebellum to 73% in the thalamus. Conclusions: [123I]TPCNE is a selective and specific ligand for the sigma-1 receptor that is displaceable in humans in vivo with haloperidol. As expected based on the widespread expression of the sigma-1 receptor in the primate CNS, we failed to identify a non-displaceable reference region in the brain for this radioligand. References: Leonard BE. Sigma receptors and sigma ligands: background to a pharmacological enigma. *Pharmacopsychiatry*. 2004 Nov;37 Suppl 3:S166-70. Waterhouse RN, Mardon K, Giles KM, Collier TL, O'Brien JC. Halogenated 4-(phenoxy)methylpiperidines as potential radiolabeled probes for sigma-1 receptors: in vivo evaluation of [123I]-1-(iodopropen-2-yl)-4-[(4-cyanophenoxy)methyl]piperidine. *J Med Chem*. 1997 May 23;40(11):1657-67.

## EVALUATION OF [<sup>11</sup>C](-)-*o*-METHYLVESAMICOL AS A PET LIGAND FOR MAPPING VESICULAR ACETYLCHOLINE TRANSPORTERS

Kiichi Ishiwata<sup>1</sup>, Kazunori Kawamura<sup>1</sup>, Hideo Tsukada<sup>2</sup>, Shingo Nishiyama<sup>2</sup>, Yuichi Kimura<sup>1</sup>, Kazuhiro Shiba<sup>3</sup>

<sup>1</sup>Positron Medical Center, Tokyo Metropolitan Institute of Gerontology, Tokyo, Japan

<sup>2</sup>Central Research Laboratory, Hamamatsu Photonics K.K., Hamakita, Japan

<sup>3</sup>Advanced Science Research Center, Kanazawa University, Kanazawa, Japan

Introduction: Presynaptic cholinergic markers could be used for estimating the integrity of the cholinergic systems in the human brain with neurological diseases such as Alzheimer's disease. Several radiolabeled vesamicol derivatives have been proposed as the probes to detect vesicular acetylcholine transporter (VACHT) by PET and SPECT. Substituted positions and optical isomerization of the derivatives altered their affinities for VACHT and sigma receptors (1). Here we prepared [<sup>11</sup>C](-)-*o*-methylvesamicol ([<sup>11</sup>C](-)-OMV) and evaluated in vivo its properties as a PET radioligand for mapping VACHT. Methods: The affinities of vesamicol derivatives for VACHT were investigated by membrane binding assay. [<sup>11</sup>C](-)-OMV and [<sup>11</sup>C](+)-*p*-methylvesamicol ([<sup>11</sup>C](+)-PMV) were prepared by the reaction of the corresponding trimethylstanylvesamicol and [<sup>11</sup>C]CH<sub>3</sub>I in the presence of Pd<sub>2</sub>(dba)<sub>3</sub>, (*o*-tol)3P, CuCl and K<sub>2</sub>CO<sub>3</sub>. Biodistribution of [<sup>11</sup>C]OMV was investigated in male Wistar rats by tissue dissection and ex vivo autoradiography. VACHT-specific uptake of [<sup>11</sup>C](-)-OMV in the rat brain was evaluated in blocking studies with cold (-)-OMV, (-)-vesamicol, (+)-pentazocine and SA4503 (500 nmol/kg co-injection). A conscious male rhesus monkey underwent 91-min PET scan with [<sup>11</sup>C](-)-OMV using a model SHR-7700 (Hamamatsu Photonics K.K., Hamamatsu, Japan). Results: (-)-OMV exhibited in vitro a high affinity for VACHT and low affinity for sigma<sub>1</sub> receptor (Table 1). In rats the brain uptake of [<sup>11</sup>C](-)-OMV was 1.1 %ID/g at 5 min postinjection, and retained a high level for 60 min. The brain uptake was significantly inhibited by co-injection of cold (-)-OMV, (-)-vesamicol and SA4503 (60-70% reduction), but not of (+)-pentazocine. Ex vivo autoradiography showed different regional brain distribution patterns between [<sup>11</sup>C](-)-OMV and [<sup>11</sup>C](+)-PMV. In the monkey brain (Fig. 1), the binding of [<sup>11</sup>C](-)-OMV was reversible and an apparent equilibrium state was found at 20-40 min. Conclusion: These findings show that [<sup>11</sup>C](-)-OMV is a potential VACHT radioligand that exhibited appropriate brain kinetics during the time frame of <sup>11</sup>C-labeled tracers.

### Reference:

- Shiba K, Yano T, Sato W, et al; Life Sci 71:1591-1598 (2002).

Table 1. Affinities of vesamicol derivatives for VACHT and sigma receptors.

	K <sub>i</sub> (nM)		
	VACHT	Sigma <sub>1</sub>	Sigma <sub>2</sub>
(-)-Vesamicol	4.4 ± 0.6	73.8 ± 11.2	367 ± 68
(-)-OMV	6.7 ± 1.6	33.7 ± 5.9	282 ± 30
(+)-OMV	22.5 ± 2.0	10.7 ± 2.0	231 ± 21
(-)-PMV	22.9 ± 0.4	8.1 ± 2.0	42.7 ± 6.3
(+)-PMV	199 ± 32	3.0 ± 0.2	40.7 ± 2.9
SA4503	50.2 ± 7.2	4.4 ± 1.0	242 ± 17
(+)-Pentazocine	315 ± 121	5.5 ± 2.0	2470 ± 150

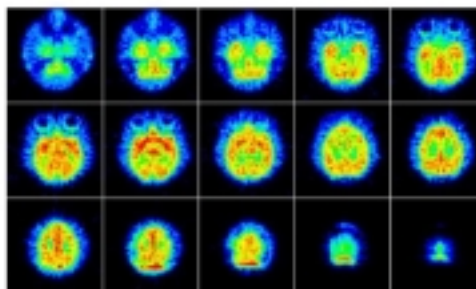


Figure 1. PET image of [<sup>11</sup>C](-)-OMV in the monkey brain.

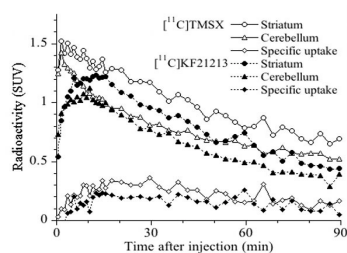


## IN VIVO EVALUATION OF [11C]TMSX AND [11C]KF21213 FOR MAPPING ADENOSINE A2A RECEPTORS: BRAIN KINETICS IN THE CONSCIOUS MONKEY AND P-GLYCOPROTEIN MODULATION IN THE MOUSE BRAIN

Kiichi Ishiwata<sup>1</sup>, Hideo Tsukada<sup>2</sup>, Yuichi Kimura<sup>1</sup>, Kazunori Kawamura<sup>1</sup>, Norihiro Harada<sup>2</sup>,  
Harry H Hendrikse<sup>3</sup>

<sup>1</sup>Positron Medical Center, Tokyo Metropolitan Institute of Gerontology, Tokyo, Japan, <sup>2</sup>Central Research Laboratory, Hamamatsu Photonics K.K., Hamakita, Japan, <sup>3</sup>PET Center, Groningen University Hospital, Groningen, The Netherlands

Introduction: Adenosine is an endogenous modulator of several physiological functions in the central nervous system and in peripheral organs. The effects are mediated by four adenosine receptor subtypes: A1, A2A, A2B and A3. Recently we successfully visualized the A1 and A2A receptors (A1R and A2AR) in the human brain by PET with [11C]MPDX ([1-methyl-11C]8dicyclopropylmethyl-1-methyl-3-propylxanthine) and [11C]TMSX ([7-methyl-11C](E)8(3,4,5-trimethoxystyryl)-1,3,7-trimethylxanthine), respectively (1, 2). As for A2AR ligands, we previously found that [11C]KF21213 ([7-methyl-11C] (E)8(2,3-dimethyl-4-methoxystyryl)-1,3,7-trimethylxanthine) exhibited much more superior properties in rodents than [11C]TMSX (3). The A2AR-affinity and selectivity for TMSX vs KF21213 were  $K_i = 5.9 \text{ nM}$  vs  $3.0 \text{ nM}$  and  $A1R/A2AR = 290$  vs  $>3300$ . The striatum-to-cerebellum uptake ratio (signal-to-noise ratio) of [11C]KF21213 was three-fold that of [11C]TMSX. Here we compared the brain kinetics of [11C]TMSX and [11C]KF21213 in the monkey brain. We also investigated whether penetration of [11C]TMSX across the blood-brain barrier were modulated by P-glycoprotein in mice. Methods: A conscious male rhesus monkey successively underwent two 91-min PET scans with [11C]TMSX and [11C]KF21213 using a model SHR-7700 (Hamamatsu Photonics K.K., Hamamatsu, Japan). For evaluating P-glycoprotein modulation in mice, the brain uptake of [11C]TMSX was measured following i.v. treatment with cyclosporine A (50 mg/kg) or verapamil (1 mg/kg) 30 min prior tracer injection and the brain uptake of [11C]verapamil was measured 10 min after i.v. injection of cold TMSX (0.5 mg/kg) Results: As shown in a figure, the brain uptake of [11C]KF21213 was lower than that of [11C]TMSX. The striatum uptake of [11C]KF21213 reached in nearly equilibrium state at 15 min, while that of [11C]TMSX gradually decreased with time. The specific uptake (A2AR-rich striatum – A2AR-poor cerebellum) of [11C]KF21213 was lower than that of [11C]TMSX. Treatment with cyclosporine A significantly enhanced the [11C]TMSX uptake in the striatum, cerebral cortex and cerebellum (about 170% of control,  $p < 0.001$ ). Cold verapamil did not block the brain uptake of [11C]TMSX, whereas cold TMSX slightly reduced the brain uptake of [11C]verapamil (16%,  $p < 0.05$ ). Comments: Previous studies with rodents showed that [11C]KF21213 had more suitable properties for mapping A2AR than [11C]TMSX and other radioligands (3), however, in the primate brain [11C]TMSX exhibited a larger signal-to-noise ratio (difference uptake between striatum and cerebellum) than [11C]KF21213, suggesting that [11C]TMSX was the most suitable tracer for mapping A2ARs by PET among the xanthine-type tracers proposed to date. We also confirmed that brain uptake of [11C]TMSX was modulated in vivo by P-glycoproteins. References: 1. Fukumitsu N, Ishii K, Kimura Y, et al; *Ann Nucl Med* 17:511–515 (2003). 2. Ishiwata K, Mishina M, Kimura Y, et al; *Synapse* 55:133–136 (2004). 3. Wang WF, Ishiwata K, Nonaka H et al; *Nucl Med Biol* 27:541–567 (2000).





**DISTRIBUTION OF ADENOSINE A2A RECEPTORS IN HUMAN BRAIN USING [C-11]TMSX PET**

**Masahiro Mishina**<sup>1,2,3</sup>, Kiichi Ishiwata<sup>2</sup>, Kenji Ishii<sup>2</sup>, Yuichi Kimura<sup>2</sup>, Kazunori Kawamura<sup>2</sup>, Keiichi Oda<sup>2</sup>, Toru Sasaki<sup>2</sup>, Shiro Kobayashi<sup>1</sup>, Yasuo Katayama<sup>3</sup>

<sup>1</sup>*Neurological Institute, Nippon Medical School Chiba-Hokusoh Hospital, Chiba, Japan*

<sup>2</sup>*Positron Medical Center, Tokyo Metropolitan Institute of Gerontology, Tokyo, Japan*

<sup>3</sup>*The Second Department of Internal Medicine, Nippon Medical School, Tokyo, Japan*

**Introduction** Adenosine plays a role as an endogenous modulator of synaptic functions in the central nervous system. Adenosine A2A receptors are known to stimulate adenylyl cyclase. Selective adenosine A2A receptor has attracted attention as the treatment of Parkinson's disease without worsening dyskinesia (1). We developed a PET ligand, [7-methyl-C-11]-(E)-8-(3,4,5-trimethoxystyryl)-1,3,7-trimethylxanthine ([C-11]TMSX), for mapping the adenosine A2A receptors (2). This study is the first report for distribution of adenosine A2A receptors in the human brain using the [C-11]TMSX PET. **Methods** We recruited six normal male subjects, without history of neurological disease or any abnormalities on physical or neurological examinations (mean age  $\pm$  SD, 27.7  $\pm$  11.8). Magnetic resonance imaging (MRI) were also obtained with the spoiled gradient-recalled echo in steady state technique for any organic abnormalities in the subjects' brain. A dynamic series of decay-corrected PET scans was performed for 60 minutes, and the arterial blood was sampled during the scan to measure radioactivity and labeled metabolites. Parametric images of distribution volume (DV) for [C-11]TMSX were generated using a graphical analysis (3). We also generated an early image by adding up frames of the dynamic scan from 0 to 10 minutes for each subject (4). The MRI was 3-dimensionally registered to the early image of each subject, and was used as a reference for placing regions of interest (ROIs) on PET image (5). Circular ROIs of 10-mm diameter were placed in the parametric images over cerebellum, brainstem, thalamus, head of caudate nucleus, putamen, frontal lobe, temporal lobe, parietal lobe and occipital lobe for each subject. Values for DV in these regions were calculated as mean of pixel value in the circular ROIs. **Results** The DV was large in the putamen and head of caudate nucleus, and was small in the cerebral cortex, especially frontal lobe. **Conclusion** Past studies proved a functional interaction between adenosine A2A and dopamine D2 receptors. [C-11]TMSX PET demonstrated that adenosine A2A receptors were enriched in the striatum, as well as postmortem studies reported.

**References**

1. W. Bara-Jimenez et al., *Neurology* 61, 293 (2003).
2. K. Ishiwata et al., *J Nucl Med* 41, 345 (2000).
3. J. Logan, *Nucl Med Biol* 30, 833 (2003).
4. M. Mishina et al., *Ann Nucl Med* 14, 193 (2000).
5. B. A. Ardekani et al., *J Comput Assist Tomogr* 19, 615 (1995).



**COMPARISON OF VARIOUS MODELS FOR ANALYSING [11C]FLUMAZENIL STUDIES**

**Ursula M.H. Klumpers**<sup>1,2</sup>, Dick J. Veltman<sup>1,2</sup>, Emile F.I. Comans<sup>2</sup>, Marc A. Kropholler<sup>2</sup>,  
Ronald Boellaard<sup>2</sup>, Witte J.G. Hoogendijk<sup>1</sup>, Adriaan A. Lammertsma<sup>2</sup>

<sup>1</sup>*Department of Psychiatry, VU University Medical Centre, Amsterdam, The Netherlands*

<sup>2</sup>*Department of Nuclear Medicine & PET Research, VU University Medical Centre,  
Amsterdam, The Netherlands*

Background: Flumazenil (FMZ) is a specific, reversibly bound high-affinity neutral antagonist of the benzodiazepine site at the  $\beta$ -aminobutyric acid (GABA)-A receptor. In general, a single tissue compartment model with plasma input is used for analysis. For clinical studies, however, reference tissue models have also been used. Objective: To determine the relation between different plasma input and reference tissue models and to define the optimal model for analysis of clinical FMZ studies. Methods: Eleven drug free patients (4 male; age range 22-54, average  $37.5 \pm 10.8$  years) with a major depressive episode (DSM IV) and nine healthy controls (6 male; age range 22-43, average  $32.4 \pm 7.4$  years) were included. A dynamic 3D scan with a duration of 60 minutes was acquired following bolus injection of  $\sim 370$  MBq FMZ. During the scan, arterial whole blood was monitored continuously using an on-line detection system and, at set times, discrete samples were taken in order to derive the metabolite corrected plasma curve. In addition, for each subject a T1-weighted structural MRI scan was acquired, using a 1.5 Tesla MRI scanner. The MRI scans were co-registered with summed FMZ images. Regions of interest (ROI) were defined on these co-registered MRI scans for the following structures: anterior, ventrolateral, dorsolateral and orbitomedial prefrontal cortex, anterior and posterior cingulate, medial and lateral temporal lobe and insular area, parietal and occipital area, cerebellum, hippocampus, putamen, thalamus, pons and white matter. ROIs were projected onto the dynamic FMZ scans, generating time activity curves for each region. Data were analysed using both single tissue (1T) and reversible two tissue (2T) compartment models with plasma input, providing values of the volume of distribution (Vd) of FMZ. In addition, both full (FRTM; 4 parameters) and simplified (SRTM; 3 parameters) reference tissue models were investigated, resulting in measures of binding potential (BP). In the latter analysis, both pons and white matter were investigated as reference tissue. Results: Due to technical problems, 1 control and 2 patient scans could not be analysed. According to Akaike and Schwarz criteria, for most patients the 1T model was selected for pons, white matter and the basal structures putamen and thalamus and the 2T model for the other structures. Across all structures and patients, the 2T model was selected in 61% of the fits. For these cases, Vd values obtained with the 2T model were, on average,  $6 \pm 4\%$  higher than those obtained with the 1T model. Across all structures and patients, the SRTM model was selected in 82 and 73% of the fits when pons and white matter were used as reference tissue, respectively. Pearson Correlation between BP from SRTM and Vd from the 2T model was 0.997 and 0.988 using pons and white matter as reference tissue, respectively. Conclusion: In contrast to previous studies, for cortical structures, a 2T model provides slightly better fits in the majority of cases. Use of a 1T model may result in a slight ( $\sim 6\%$ ) underestimation of Vd. Use of SRTM with pons as reference tissue is a good alternative for clinical studies.

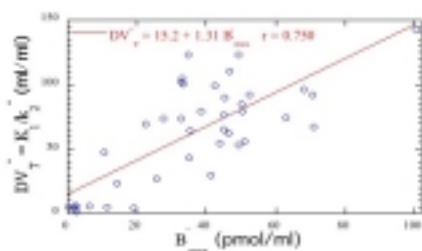
**SPECT QUANTIFICATION OF BENZODIAZEPINE RECEPTOR  
CONCENTRATION AND LIGAND AFFINITY USING A DUAL-LIGAND  
APPROACH**

**Philippe Millet<sup>1</sup>**, Marcelle Moulin-Sallanon<sup>1,2</sup>, Vicente Ibáñez<sup>1</sup>

*Unité de Neuroimagerie Psychiatrique, Hôpitaux Universitaires de Genève, Genève,  
Switzerland*

<sup>2</sup>*Unité E340, INSERM, Grenoble, France*

Introduction: The benzodiazepine receptor concentration is currently measured with the PET-[11C]flumazenil (FMZ) and the SPECT-[123I]iomazenil (IMZ) (1, 2). However, while PET is used for quantitative studies, SPECT is restricted to the use of semi-quantitative approaches which only estimates a receptor density index. Here, benzodiazepine receptors – [123I]iomazenil interactions are studied with SPECT using a dual-ligand approach to estimate all binding parameters. Methods: SPECT studies were carried out on nine normal volunteers using the following protocol: tracer injection (T0); displacement with unlabelled FMZ injection (T0 + 70 min); co-injection of [123I]IMZ and unlabelled FMZ (T0 + 110 min). At the scan start time, an injection of about 2 mCi of [123I]IMZ was given intravenously. The displacement procedure consisted of 0.02 mg/kg of FMZ, and the co-injection procedure was a mixture of [123I]IMZ (2 mCi) and FMZ (0.02 mg/kg). The three compartment model developed in this study, involves two parts to simulate [123I]IMZ and FMZ kinetics, with distinct K1, k2, kon and koff parameters for each part, and a common parameter: the receptor density, B'max. Because of the large number of parameters, the model was simplified using fixed relations between IMZ and FMZ parameters and a coupled identification procedure. Therefore, only five parameters were identified (B'max, K1, k2, kon/VR, koff) from which the total distribution volume (DVT) was calculated ( $DVT = K1/k2(1 + B'max/KdVR)$ ). With the first 70 min of the SPECT data, and using a one tissue-compartment model, we estimated K1 and k'2 parameters and calculated an index of receptor density, the total distribution volume ( $DV''T = K1/k''2$ ). Five regions were used to quantify model parameters (pons, cerebellum, temporal, frontal and occipital cortex). Results: From the nine volunteers, the mean values of receptor density across regions ranged from 7 to 69 pmol/ml and the mean values of ligand affinity from 2.3 to 3.7 pmol/ml. There was a linear relationship between DVT and DV''T values with a correlation coefficient close to unity. Figure shows a comparison of DV''T values with the corresponding B'max values. In spite of a large variability, there is a high correlation between both parameters. Conclusion: Using SPECT and the dual-ligand approach all parameters of the model can be quantified with correct standard errors. Despite of the complexity of such approach, it may be use to estimate reference values of biological parameters. References: 1. Abi-Dargham et al. (1994) J Nucl Med 35, 228-38. 2. Millet, P., et al. (2000) J Cereb Blood Flow Metab 20, 1587-603. Grant support: Swiss National Science Foundation N 31-64020.00 and 3100A0-104185



**QUANTIFICATION OF BRAIN PHOSPHODIESTERASE 4 IN RATS USING [11C]ROLIPRAM PET AFTER ANTIDEPRESSANT TREATMENT**

Masahiro Fujita<sup>1</sup>, Masao Imaizumi<sup>1</sup>, Sami S. Zoghbi<sup>1</sup>, Matthew S. Crescenzo<sup>1</sup>, Jinsoo Hong<sup>1</sup>, John L. Musachio<sup>1</sup>, Jian Q. Lu<sup>1</sup>, Vanessa L. Cropley<sup>1</sup>, Jehi S. Liow<sup>1</sup>, Antony D. Gee<sup>2</sup>, Jurgen Seidel<sup>3</sup>, Michael V. Green<sup>3</sup>, Victor W. Pike<sup>1</sup>, Ronald S. Duman<sup>4</sup>, Robert B. Innis<sup>1</sup>

<sup>1</sup>Molecular Imaging Branch, National Institute of Mental Health, Bethesda, MD, USA

<sup>2</sup>Translational Medicine and Technology, PET Division, GlaxoSmithKline, Cambridge, UK

<sup>3</sup>National Institute of Biomedical Imaging and Bioengineering, National Institutes of Health, Bethesda, MD, USA, <sup>4</sup>Psychiatry & Pharmacology, Yale University School of Medicine, New Haven, CT, USA

Objective: Phosphodiesterase 4 (PDE4) catabolizes the second messenger cyclic adenosine monophosphate and plays critical roles in brain diseases such as mood disorders and drug addiction. The objectives of this study were to measure PDE4 in living rats using positron emission tomography (PET) and also to apply the established method of quantification to antidepressant treated rats. Methods: To establish a method of quantification, high (n=6) and low specific activity (SA) (n=2) active (R-[11C]rolipram) and high SA less active (S-[11C]rolipram) (n=2) enantiomers were intravenously administered to image non-treated Sprague Dawley rats using the ATLAS PET Scanner. Frequent arterial samples were taken to measure unmetabolized [11C]rolipram using radio-HPLC. Total distribution volumes (VT') were calculated using 1- (1C) and unconstrained 2-compartment (2C) models. Additional groups of rats were treated with Imipramine (IMI; 15-17 mg/kg/day) (n=5) or saline (SAL; n=5) for 20-27 days. On the last day of the administration, these rats were imaged with high SA R-[11C]rolipram. VT' was measured using an arterial input function of free plus protein bound (total) high SA R-[11C]rolipram and the 2C model. After PET scan, each animal was euthanized, and frontal cortex and hippocampus were sampled. Using the membrane fraction of each of these samples, Bmax and Kd were measured with homogenate binding assay using [3H]rolipram. Results: In non-treated rats, in all regions, high SA R studies showed later and greater brain uptake, and slower washout than low SA R and S studies. In all regions and in all studies, the 2C model gave significantly better fitting than the 1C model. The poor fitting by the latter caused underestimation of VT' by 19-31%. The 2C model identified VT' reasonably well with coefficient of variation less than 10%. VT' values by this model were 16.4-29.2 mL/cm<sup>3</sup> in high SA R, 2.9-3.5 in low SA R, and 3.1-3.7 in S studies. IMI and SAL-treated groups showed similar plasma free fraction of high SA R-[11C]rolipram (IMI: 30±3%, SAL: 31±2%), which justified PET quantification using total high SA R-[11C]rolipram as the input function. While the homogenate binding assay showed a significant decrease of Bmax/Kd in hippocampus in IMI-treated rats, PET measurement showed only a weak trend of decrease. Conclusions: Specific binding of R-[11C]rolipram was accurately measured in living rats. In high SA R- studies, 86% of VT' was specific binding. Distribution and Bmax/Kd of PDE4 in animal models can now be studied by measuring VT' of high SA R-[11C]rolipram. The difference between in vivo and in vitro measurement in IMI and SAL-treated rats may have been caused by different phosphorylation state of PDE4, which affects the affinity of rolipram, or partial volume effects in the PET measurement.

## INVESTIGATION OF ACUTE MODULATION OF cAMP IN VIVO WITH PET USING [<sup>11</sup>C]ROLIPRAM

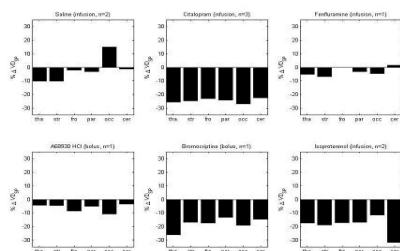
Christine A. Parker<sup>1</sup>, Julian C. Matthews<sup>1</sup>, Roger N. Gunn<sup>1</sup>, Laurent Martarello<sup>1</sup>, Vincent J. Cunningham<sup>1</sup>,  
Dirk Bender<sup>2</sup>, Steen Jakobsen<sup>2</sup>, Svend B. Jensen<sup>2</sup>, Stephen T. Knibb<sup>1</sup>, Antony D. Gee<sup>1</sup>

<sup>1</sup>GlaxoSmithKline, ACCI, Addenbrooke's Hospital, Cambridge, UK

<sup>2</sup>PET Centre, Bygning, Aarhus, Denmark

**Introduction:** There is a desire to develop PET probes for *in vivo* imaging of second-messenger systems. Cyclic-AMP (cAMP) is a continuously produced nucleotide which is catabolised by phosphodiesterase-4 (PDE4) enzymes. PDE4 expression and conformation is altered by cAMP concentrations, and therefore PDE4 measures are an indirect measure of cAMP function. Using the selective PDE4 inhibitor, [<sup>11</sup>C]rolipram(1), it is possible to image the distribution of PDE4 enzymes with PET(2). Rolipram exists as two enantiomers, with *S*(+)-rolipram having approximately 10-fold lower affinity for PDE4 than *R*(-)-rolipram *in vitro* and *in vivo*(3). cAMP levels may be altered acutely or chronically. The aim of this study was to investigate whether acute agonism of cAMP-coupled receptors induces regional changes in the [<sup>11</sup>C]rolipram PET signal consistent with the known receptor pharmacology. **Methods:** In all studies, Yorkshire/Landrace porcines (40Kg, n=10) were anaesthetised by induction with ketamine and midazolam, and maintained with isoflurane. Baseline [<sup>11</sup>C]R(-)- and [<sup>11</sup>C]S(+)-rolipram scans were performed followed by a pharmacological challenge and further [<sup>11</sup>C]R(-)- and [<sup>11</sup>C]S(+)-rolipram scans in each subject. The pharmacological agents were administered at least 30 minutes prior to the subsequent [<sup>11</sup>C]rolipram scans; citalopram (SSRI, 20mg/hr), fenfluramine (serotonin-transporter blocker, 50mg/hr), A68930 HCl (D<sub>1</sub>-dopamine receptor agonist, 0.075mg/Kg), bromocriptine (D<sub>2</sub>-dopamine receptor agonist, 1.25mg/Kg) and isoproterenol (β<sub>2</sub>-adrenoceptor agonist, 7.5μg/Kg) and saline as a control (n=2). Dynamic data were collected over the brain for 90 minutes (EXACT HR scanner-3D) and frequent arterial samples were taken to assay concentrations of parent radioactivity. Six regions of interest (ROI; thalamus(tha), striatum(str), frontal cortex(fro), parietal cortex(par), occipital cortex(occ) and cerebellum(cer)) were defined on each baseline [<sup>11</sup>C]R(-)-rolipram scan and applied to all scans in that subject to generate time activity curves (TACs). Logan analyses (plasma input) were applied to all TACs to estimate total tissue volumes of distribution ( $V_D$ ) and two outcome measures were calculated; (i)  $V_D^{R-}$  and (ii)  $V_D^{Sp} = V_D^{R-} - V_D^{S+}$ . **Results and Discussion:** The changes between baseline and challenge conditions were similar for both outcome measures ( $V_D^{R-}$  and  $V_D^{Sp}$ ). The percentage changes for  $V_D^{Sp}$  post challenge are given (figure). For challenges with multiple studies the mean is presented for each region. A68930 and (+)fenfluramine did not produce changes in the rolipram signal above that observed with saline. Challenges with citalopram, bromocriptine and isoproterenol exhibited, at best, small global changes in rolipram binding with no apparent regional differentiation. cAMP turnover is generally rapid in response to an acute challenge, leading to a transient signal that may not be detectable in the time frame of a PET study. To conclude, these data suggest acute agonism of cAMP-coupled receptors may be difficult to image using PET. Further studies are planned to assess the effect of chronic modulation of cAMP on PDE4 expression, as measured by PET.

1. Nemoz G et al 1985 Biochem Pharmacol 34(16) 2997-3000 2. DaSilva J et al 2002 Eur J Nuc Med 29 1680-1683. 3. Parker C et al 2004 Synapse, in press





**CHARACTERIZING THE OPTIMAL ACQUISITION DURATION OF  
[18F]FLUOROETHYL-DIPRENORPHINE PET STUDIES**

**Henning Boecker**<sup>1</sup>, Till Sprenger<sup>2</sup>, Germund Henriksen<sup>1</sup>, Isabelle Stangier<sup>1</sup>, Hans J. Wester<sup>1</sup>,  
Thomas R. Toelle<sup>2</sup>, Mary E. Spilker<sup>1</sup>

*Nuklearmedizinische Klinik, Munich, Germany*

*<sup>2</sup>Neurologische Klinik, Munich, Germany*

Introduction: Compared to the PET tracer [11C]DPN, the F-18-labelled homologue 6-O-(2-[18F]fluoroethyl)-6-O-desmethyldiprenorphine ([18F]FDPN) has a longer half-life while maintaining similar pharmacologic properties. Thus, [18F]FDPN allows for more experimental flexibility and applications at centers without an on-site cyclotron. Here, we wished to determine the ideal duration of [18F]FDPN dynamic PET studies. Methods: [18F]FDPN PET scans were acquired in eight healthy male volunteers (mean age 36.8 years, range 33 – 40 years) using a Siemens/CTI ECAT EXACT HR+ scanner (Knoxville, TN, USA) in 3D mode. Images were acquired over 120 minutes with arterial blood and metabolite sampling. Each subject's dynamic dataset was realigned and normalized to a ligand-specific template in SPM2 (Wellcome Dept. of Cognitive Neurology, London, UK). Binding kinetics were quantified under protocols of different lengths in different VOIs defined using the MARSBAR toolbox (marsbar.sourceforge.net). We analyzed amygdala, caudate, putamen, thalamus, cingulate, frontal, and occipital VOIs. VOI extraction and kinetic analyses were performed in PMOD Medical Imaging Program, version 2.5 (PMOD Group, Zurich Switzerland). To evaluate the quantification of [18F]FDPN binding kinetics under protocols of different lengths (40, 60, 80, 90, 100, and 120 minutes), a 1 tissue or 2 tissue compartment model was fit to the VOI data with a measurement error variance defined to be equal to the average VOI concentration divided by the frame length. Results: The VOI data in the group of eight volunteers indicate that compared to the full 120 minute acquisition, DV values can be estimated within a 10% error range when reducing the acquisition time to 90 minutes. While larger VOIs show around a 10% bias at 60 minutes, smaller VOIs show enhanced bias of up to approximately 18 %. The correlation analyses of the DV estimates between the full and the shortened acquisition protocols indicate that a good replication of DV values, both at low and high binding, is attained with shortened schedules of 100 and 90 minutes. At 80 minutes the correlation is characterized by more variability and a trend towards increased deviation in high binding regions compared with low binding regions. This trend is further augmented in the 60 and 40 minute protocols, which results in a substantial underestimation of the DV in the 40 minute protocol. Conclusions: The evaluation of [18F]FDPN distribution volumes under protocols of different lengths shows that a 90 minute protocol results in less than 10 % bias compared to the full length protocol in all regions analyzed. This acquisition time represents a reasonable cut-off between enhanced parameter precision with longer sampling and increased noise and uncertainty with shorter sampling. However, if an experimentalist is interested in adopting an even shorter protocol, the increased bias in DV must be weighted against the benefits of a shorter protocol.

**TOWARDS IMPROVED TEST-RETEST RELIABILITY IN QUANTITATIVE  
LIGAND PET: [11C] DIPRENORPHINE AS AN EXAMPLE**

**Alexander Hammers**<sup>1,2</sup>, Marie-Claude Asselin<sup>3</sup>, Safiye Osman<sup>3</sup>, Rainer Hinz<sup>3</sup>,  
Federico Turkheimer<sup>1</sup>, Gary Hotton<sup>1</sup>, David J Brooks<sup>1</sup>, John S Duncan<sup>2</sup>, Matthias J Koeppe<sup>1,2</sup>

<sup>1</sup>*MRC Clinical Sciences Centre and Division of Neuroscience, Faculty of Medicine, Imperial  
College, Hammersmith Hospital, London, UK*

<sup>2</sup>*Department of Clinical and Experimental Epilepsy, Institute of Neurology, UCL, London,  
and National Society for Epilepsy MRI Unit, Chalfont St Peter, UK*

<sup>3</sup>*Hammersmith Imanet, Hammersmith Hospital, London, UK*

Background: [11C]Diprenorphine (DPN) PET images all subtypes of opioid receptors. Various methods of data acquisition and analysis are used. We describe our revisited methodology for acquiring high quality DPN brain PET studies and compare the influence of various combinations of movement correction, different amounts of injected activity and derivation of input function on test-retest data. Methods: Ten healthy controls were studied twice. Five each were injected with ~135 MBq and ~185 MBq of [11C]DPN. All had high resolution MRI and quantitative 95' listmode [11C]DPN PET, rebinned into 32 time frames, on a Siemens/CTI ECAT HR++ scanner. Movement was assessed on decay-corrected time-activity curves derived from ROIs drawn on summed activity (ADD) images. Movement correction was performed by wavelet denoising the dynamic time frames, coregistering them to the first 120 second frame with a mutual information method, and reslicing the original time series (MVCORR images). Online blood collection was 90' (~135MBq group) and shortened to 15' for the ~185MBq group. Both groups had discrete blood samples throughout the length of the scan for calibration and metabolite analysis. Metabolite-corrected arterial plasma input functions were derived using only the first 15' of online blood collection for both groups; and using all 90' of data for the ~135MBq group ("CONTINUOUS\_IF"). Spectral analysis was used to produce parametric images of DPN volume-of-distribution (VD). In addition, 28 minutes to 58 minutes ADD images were created from the MVCORR images for the ~185MBq group. This led to four sets of VD images (~135MBq group and ~185MBq group, both MVCORR and Non-MVCORR), one set of ~185MBq MVCORR ADD images, and one set of ~135MBq MVCORR CONTINUOUS\_IF images. For image sampling, our probabilistic brain atlas was warped onto each individual's MRI scan using the deformations toolbox in the Statistical Parametric Mapping software (SPM2) and these were then coregistered onto each individual PET. We assessed hippocampus, thalamus, cerebellum and inferior frontal gyrus. Test-retest bias (order effect) and significance of differences in test-retest reliability were assessed using MANOVA. Test-retest reliability was calculated using intraclass correlation coefficients (ICC). Results: There was a small but significant order effect, with the second scan showing a VD on average 1.8% lower. The rank order of ICCs was ~185MBq Non-MVCORR (0.949) > ~185MBq MVCORR (0.944) > ~185MBq MVCORR ADD (0.934) > ~135MBq Non-MVCORR (0.876) > ~135MBq MVCORR CONTINUOUS\_IF (0.863) > ~135MBq MVCORR (0.782). The higher noise level of the ~135MBq images was captured by MANOVA with borderline significance (p<0.069); there was a significant improvement for the ~185MBq group in the inferior frontal gyrus, right thalamus and right cerebellum. There was no overall effect of MVCORR. However, in one subject with significant movement, correction vastly improved test-retest reliability, approximately halving the difference between first and second datapoint. Summary and Conclusions: Overall, injecting the higher dose of ~185MBq markedly improved test-retest reliability, with % T-RT variation decreasing by ~20-50%. MVCORR slightly worsened test-retest reliability in the ~135MBq group. It had no overall effect in the ~185MBq group but appears indicated in those subjects in whom movement is detected.

## DIFFERENT PATTERNS OF PIB UPTAKE IN AD PATIENTS

Gunnar Blomquist<sup>1</sup>, Rainer Hinze<sup>2</sup>, Henry Engler<sup>1</sup>, Agneta Nordberg<sup>3</sup>, Bengt Långström<sup>1</sup><sup>1</sup>Uppsala Imanet AB, Akademiska Sjukhuset, Uppsala, Sweden<sup>2</sup>Hammersmith Imanet Ltd., London, UK<sup>3</sup>Neurotec Department, Karolinska University Hospital Huddinge, Stockholm, Sweden

**Introduction:** Recently the <sup>11</sup>C labelled compound PIB has been demonstrated to image brain  $\beta$ -amyloid in Alzheimer's disease (AD) <sup>(1)</sup>. Here we report the use of net accumulation and unidirectional influx of PIB for inter-subject differentiation of patients with clinical AD diagnosis.

**Methods:** Uptake data were acquired on an ECAT EXACT HR+ camera during 60 min following bolus administration of approximately 300 MBq of PIB. The time course of radioactivity in arterial plasma corrected for labelled metabolites was determined and used as input function. Four healthy controls (HC) and four AD patients were examined. Parametric maps were constructed using a linear algorithm <sup>(2)</sup>.

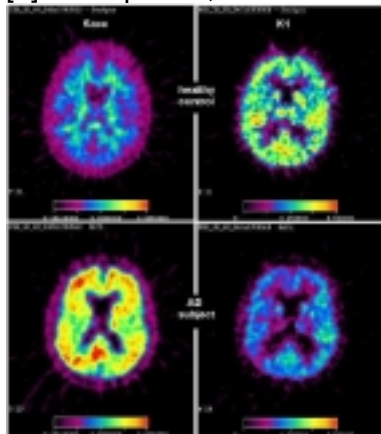
**Results:** The data distributions in Gjedde-Patlak plots followed asymptotically straight lines after 30 min, characteristic for irreversible kinetics. The tracer is thus far from equilibrium during the first hour after administration, and consequently models with irreversible kinetics are appropriate. The simple model with one reversible and one irreversible tissue compartment and three rate constants was applied. The unidirectional influx rate constant  $K_1$  (right part of figure) was found to be of the order of 0.2-0.3 min<sup>-1</sup> (whole brain), corresponding to relatively high extraction (40-60%) and indicating that  $K_1$  might be a quite good index of CBF. The accumulation of PIB in frontal and parietal cortex measured with the macro parameter (net accumulation rate constant)  $K_{acc} = K_1 k_3 / (k_2 + k_3)$  was found to give a good discrimination between the AD-patients and the HC subjects (left part of figure), except for two AD patients where PIB net accumulation was close to the low values found in the HC subjects (cf. upper left in the figure). These two patients had lower  $K_1$  than the HC subjects in many cortical areas, close to the values found for the other two patients with high net accumulation of PIB (cf. lower right in the figure). The MMSE scores for the former patients were close to normal, in the range 28-29.

**Conclusion:** A group of patients with clinical diagnosis AD but with very low PIB accumulation could not be discriminated from the HC subjects with only PIB net accumulation as measure. Also in this AD group we found comparatively low cortical  $K_1$  values, suggesting that their symptoms can be related to a vascular deficit rather than  $\beta$ -amyloid deposition.

**References:**

[1] Klunk WE, Engler H, et al.; Ann Neurol 55, 303-319, 2004

[2] Blomquist G; J Cereb Blood Flow Metab 4, 629-632, 1984





**QUANTIFICATION IN VIVO OF NICOTINIC ACETYLCHOLINE RECEPTORS DENSITY AND AFFINITY IN THE BABOON BRAIN USING 2-[18F]FLUORO-A-85380 AND A MULTI-INJECTION APPROACH**

**Jean-Dominique Gallezot**<sup>1</sup>, Marie-Claude Grégoire<sup>2</sup>, Michel Bottlaender<sup>1</sup>, Dollé Frédéric<sup>1</sup>, Saba Wadad<sup>1</sup>, Christine Coulon<sup>1</sup>, Michèle Ottaviani<sup>1</sup>, Jacques Delforge<sup>1</sup>, André Syrota<sup>1</sup>, Héric Valette<sup>1</sup>

<sup>1</sup>*DSV/DRM/SHFJ, CEA, Orsay, France*

<sup>2</sup>*URA 2210, CNRS, Orsay, France*

Introduction: Quantifying brain nicotinic acetylcholine receptors in vivo could be very useful in neurodegenerative diseases, such as Parkinson and Alzheimer diseases, and in tobacco addiction. 2-[18F]fluoro-A-85380 is a high affinity alpha4beta2 nicotinic receptor radioligand (1). Volume of distribution has already been quantified in healthy humans (2). The aim of this study was to quantify the receptor site density B'max and the equilibrium dissociation constant KdVR, and characterize all compartmental kinetics. Methods: The two experimental protocols were based on the multi-injection approach (3). They consisted of three injections of labeled and/or unlabeled ligand. The first one aimed to estimating B'max and KdVR. and was composed of a tracer injection, followed by a partial saturation injection and then a displacement (TPSD protocol). The second protocol was designed to estimate the dissociation rate constant koff more precisely. It consisted of a tracer injection followed by a displacement and finally a second injection of labeled ligand (TDI protocol). Two baboons were scanned with a CPS HR+ positron tomograph. Each baboon underwent one TDI and two TPSD experiments. Eight regions of interest were delineated (thalamus, putamen, caudate, cortices, cerebellum). The model structure was composed of three compartments (plasma, free, and specifically bound ligand) and 6 parameters. The relative standard error on the parameter estimates (RSD) was evaluated with a sensitivity analysis and the covariance matrix. The arterial plasma concentration, after correcting for metabolites, was used as the input function. Results: In all regions, B'max and KdVR could be estimated from a single TPSD experiment. However, kon/VR and koff were highly correlated, and could not be identified separately. The TDI experiments allowed to estimate koff with good accuracy in the thalamus. The estimated values (0.35 and 0.36 min<sup>-1</sup>) were in good accordance with the value found in vitro in rats at 37 C (0.3 min<sup>-1</sup>). In the extra-thalamic regions, koff could not be estimated and was therefore assumed to be equal to the one found in the thalamus. The use of this koff value in the TPSD experiment analyses allowed to estimate kon/VR in all regions. The other parameters RSD were slightly improved without any significant change of the estimates. B'max estimates ranged from 3.0±0.4 pmol/mL in thalamus, 1.2±0.4 pmol/mL in putamen, 0.82±0.08 pmol/mL in cerebellum, 0.65±0.06 pmol/mL in frontal cortex, to 0.24±0.01 pmol/mL in occipital cortex. B'max RSD were 5%, 12%, 19% and 27% in thalamus, frontal cortex, putamen and occipital cortex, respectively. kon/VR estimates were 0.5±0.2 mL/min/pmol, 0.3±0.1 mL/min/pmol and 0.1±0.1 mL/min/pmol in the occipital cortex, thalamus and putamen, respectively. Conclusion: This study shows that a three injection experiment, using the TPSD protocol can provide estimates of the B'max and KdVR values in baboon brain. An additional experiment is required to identify kon/VR and koff and to characterize all compartmental kinetics. References: (1) Valette, et al. J Nucl Med 1999;40:1374-1380 (2) Gallezot, et al. J Nucl Med 2005, in press (3) Delforge J, et al. Circulation 1990;82:1494-504

## INHIBITION OF METABOLIC STEPS IN SEROTONIN BIOSYNTHESIS: PET STUDIES WITH [11C]-5-HYDROXY-L-TRYPTOPHAN

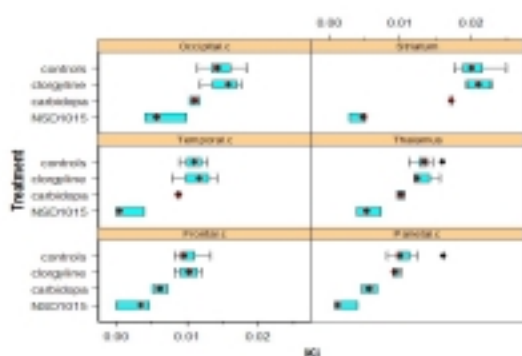
Pinelopi Lundquist<sup>1,3</sup>, Gunnar Blomquist<sup>2</sup>, Per Hartvig<sup>3</sup>, Bengt Långström<sup>2</sup>

<sup>1</sup>Division of Pharmacokinetics and Drug Therapy, Dept. of Pharmaceutical Biosciences, Uppsala University, Uppsala, Sweden

<sup>2</sup>Uppsala Imanet, Uppsala, Sweden

<sup>3</sup>Hospital Pharmacy, University Hospital, Uppsala, Sweden

Background [11C]-5-Hydroxy-L-tryptophan, [11C]-HTP, is apart from the radiolabel identical to the endogenous compound that will undergo both conversion to serotonin by the enzyme aromatic L-amino acid decarboxylase (AADC) and further catabolism by monoamine oxidase to hydroxyindole acetic acid (5-HIAA). It was suggested that the rate constant of tracer trapping reflects the conversion rate constant from 5-HTP to serotonin by AADC, independent of tracer transport<sup>1</sup>. Rhesus monkey PET studies were performed to further examine [11C]-HTP as a PET tracer for serotonin synthesis. The effect of irreversible transfer in the reference region was also addressed. Methods Cerebral [11C]-HTP kinetics was investigated after inhibition of monoamine oxidase A with clorgyline (2 mg/kg), or with one of the AADC inhibitors carbidopa (5 mg/kg, not entering the brain) and NSD1015 (10 mg/kg). A reference tissue model with irreversible transfer both in the target ( $k_3$ ) and in the reference region ( $l_3$ ) was used to fit data. The macro-parameter  $K_i = k_2k_3/(k_2+k_3)$  represents an index for the transfer rate ( $\text{min}^{-1}$ ) of 5-HTP to serotonin<sup>2</sup>.  $k_2$  is the rate constant for transport out of the target region.  $l_3$  was obtained from experiments where blood samples were taken (7 of 17 controls, 1 of 2-4 treatment scans), using the corresponding model with a plasma input function to fit the reference region (cerebellum) time-activity data. Results The mean  $l_3$  in control monkeys was  $0.0182 \text{ min}^{-1}$  ( $\pm 0.0055$ ). Binding was altered after treatment and  $l_3$  in each group (clorgyline  $0.0161 \text{ min}^{-1}$ , carbidopa  $0.0133 \text{ min}^{-1}$ , NSD1015  $0.0076 \text{ min}^{-1}$ ) was used when fitting the reference tissue model to the data. In the figure, box plots of regional  $K_i$  values are presented. Pretreatment with clorgyline did not change  $K_i$ , which suggested that although 5-HIAA was formed, the majority of radiolabelled compounds were trapped in the tissue. After pretreatment with carbidopa a slight decrease in  $K_i$  was seen. Carbidopa inhibits peripheral metabolism of 5-HTP and cause more tracer to reach the brain, but this increase does not change  $K_i$  appreciably as AADC operates far from saturation. Both peripheral and central blockade of AADC with NSD1015 resulted in a decrease in  $K_i$ , as expected, as the decarboxylation process in the brain was blocked. Conclusion The results illustrate that the applied model for [11C]-HTP with irreversible transfer in the reference region provides an index for the transfer rate,  $K_i$ , which gives good discrimination between regions. Treatment effects in these small monkey groups could be considered as support for the suggested process being studied with this tracer. 1. Hagberg et al., J Cereb Blood Flow Metab 2002;22(11):1352-1366 2. Blomquist et al., EJNM 2001;28(8):1106-7





## VISUALIZATION OF CORRELATED NEURAL AND METABOLIC FUNCTIONS IN TEMPORAL LOBE EPILEPSY BY A CORRELATION ANALYSIS WITH MULTIPLE PET STUDIES

Ikuma Takahashi<sup>1</sup>, Tadashi Nariai<sup>2</sup>, Koji Uemura<sup>3</sup>, Taketoshi Maehara<sup>2</sup>, Kenji Ishii<sup>4</sup>, Akihiko Uchiyama<sup>1</sup>, Hinako Toyama<sup>5</sup>

<sup>1</sup>Department of Integrative Bioscience and Biomedical Engineering, Waseda University, Tokyo, <sup>2</sup>Department of Neurosurgery, Tokyo Medical and Dental University, <sup>3</sup>Medical Information Processing Office, Research Center for Charged Particle Therapy, National Institute of Radiological Sciences, Chiba, <sup>4</sup>Positron Medical Center, Tokyo Metropolitan Institute of Gerontology, Tokyo, <sup>5</sup>Department of Health Service Management, International University of Health and Welfare, Tochigi, Japan

**Introduction** Positron emission tomography (PET) is a powerful tool to examine the functional changes of brain using various radiopharmaceuticals by measuring brain metabolism and neuroreceptors. Nonetheless, there have not been suitable image analysis methods to analyze the interaction of multiple parameters of brain other than the classical analysis by placing regions of interests. We developed an objective voxel based image analysis method to depict the areas showing significant correlation with the reference areas among the multiple PET images. We expected to detect the functional correlation of diseased brain which cannot be detected by single tracer analysis. **Materials & Methods** Scan data were obtained from nine patients with intractable temporal lobe epilepsy aged  $28.8 \pm 11.2$  years, 3 men and 6 women after obtaining their written informed consent. 9 patients underwent PET examination with 3 tracers; 18F fluorodeoxyglucose (18F-FDG) to measure cerebral glucose metabolism, 11C-Flumazenil (11C-FMZ) to measure central benzodiazepine receptors (cBDZ-Rs), and [1-methyl-11C]8-dicyclopropylmethyl-1-methyl-3-propylxanthine (11C-MPDX) to measure the adenosine A1 receptor (A1-R). Dynamic PET scans were conducted in 2D mode on Headtome V (Shimadzu Inc. JAPAN) and T1-weighted MR images of the brain were obtained by Magnetom VISION (Siemens, Germany), 1.5 Tesla from all the patients. All PET images were coregistered to patient's own MR images and each MR images were spatially transformed to the template MR image by SPM99. Next, the mesial temporal structure including hippocampus on the focus side was detected from the each MR image as a reference area and a correlation coefficient ( $R_{kxy}$ ) between the reference area and each voxel of whole the brain was calculated by equation (1):  $R_{kxy} = S_{xy} / (S_{xx} * S_{yy})^{1/2} \dots (1)$  where,  $R_{kxy}$  is the Pearson's correlation coefficient at voxel k in the brain.  $S_{xy}$ ,  $S_{xx}$  and  $S_{yy}$  represent the covariance value between the mean value intensity in the reference area ( $x_i$ ) and the intensity of voxel k of coregistered PET images ( $y_{ki}$ ), and the variance value of  $x_i$  and the  $y_{ki}$ , respectively. We made nine maps showing correlations between FDG PET image and fluctuation in FDG at reference area, FMZ and FDG, MPDX and FDG, FDG and FMZ and so on. The regions statically high correlated with the reference area and of volumes over 200 voxels are detected automatically from the images, and overlaid to MR images to identify anatomical localization. **Results** FDG and MPDX at the focus, FDG and FMZ at contra-lateral to focus, and FDG at lateral temporal lobe positively correlated with FMZ at reference; MPDX at cerebral cortex negatively correlated (Fig). In the Figure, Orange clusters show positive correlation and blue is negative. **Discussion** This method was useful in making a synthetic interpretation of multiple PET parameters in relation to epileptic condition. Such objective manipulation of multiple PET parameters may provide new analysis method to investigate the pathophysiology of cerebral disorders.

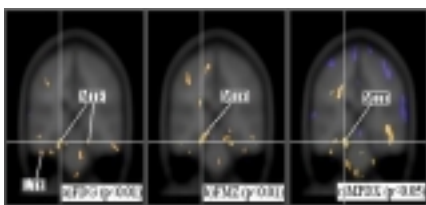


Fig Correlation map with PET. ME: mesial temporal lobe LATE: lateral temporal lobe



**DIRECT DETERMINATION OF THE LUMPED CONSTANT FOR  
FLUORODEOXYGLUCOSE (FDG) IN AWAKE RATS**

Laura Ravasi<sup>1,3</sup>, Joji Tokugawa<sup>1</sup>, Toshi Takayama<sup>2</sup>, William C. Eckelman<sup>1</sup>, Lou Sokoloff<sup>2</sup>,  
**Kathleen C. Schmidt<sup>2</sup>**

<sup>1</sup>*PET Department, Clinical Center, NIH, Bethesda, MD, USA*

<sup>2</sup>*LCM, NIMH, NIH, Bethesda, MD, USA*

<sup>3</sup>*Institute of Radiology Sciences, Universita' Degli Studi di Milano, Milan, Italy*

Quantitative determination of regional cerebral glucose utilization (rCMRglc) with PET and 2 [18F]fluoro-2-deoxy-D-glucose (18FDG) requires a so-called lumped constant (LC) to convert rates of FDG phosphorylation into rCMRglc. The LC for FDG in rats has not yet been directly determined. We have now determined it by the model-independent, steady-state method of Sokoloff et al. (1977) in normoglycemic awake rats with [U 14C]FDG. Arterial blood and plasma were sampled from femoral arteries; infusions were administered via femoral veins; and representative cerebral venous blood was obtained via a cannula in the confluence of sinuses. The catheters and cannula were inserted under halothane anesthesia, and LC determinations were made 3 hours after recovery from the anesthesia. The time courses of arterial and cerebral venous blood and plasma concentrations of [14C]FDG and glucose were measured from 25 to 45 minutes following onset of a programmed infusion designed to maintain constant arterial plasma concentrations of [14C]FDG. This period was selected to ensure achievement of steady states of cerebral uptakes of [14C]FDG and glucose manifested by constancy of arterial-cerebral venous blood differences for both. Determinations were limited to studies in which plasma and blood glucose and [14C]FDG levels remained constant within 10% (Fig. 1). The mean value  $\pm$  SD for LC obtained in four animals was  $0.43 \pm 0.09$ , a value approximately 12% below the LC value for 2-deoxyglucose in rats.

**QUANTITATIVE MEASUREMENT OF CEREBRAL METABOLIC RATE OF GLUCOSE BY MEANS OF DUAL-HEAD COINCIDENCE GAMMA CAMERA AND 2-DEOXY-2- [18F] FLUORO-D-GLUCOSE**

**Katsufumi Kajimoto<sup>1</sup>**, Naohiko Oku<sup>1</sup>, Yasuyuki Kimura<sup>1</sup>, Makiko Tanaka<sup>2</sup>, Hiroki Kato<sup>2</sup>, Kazuo Kitagawa<sup>2</sup>, Masatsugu Hori<sup>2</sup>, Jun Hatazawa<sup>1</sup>

<sup>1</sup>*Division of Tracer Kinetics, Osaka University Graduate School of Medicine, Osaka, Japan*

<sup>2</sup>*Department of Internal Medicine and Therapeutics, Osaka University Graduate School of Medicine, Osaka, Japan*

Introduction: Recently, dual-head coincidence gamma camera (DHC) has been developed. This system has sodium-iodine detectors and a coincidence detection mode. Although the DHC system has been used for the qualitative assessment of 2-deoxy-2-[18F]fluoro-D-glucose (FDG) whole body distribution in nuclear oncology, to the best of our knowledge, there have been no studies on the quantitative measurement of regional cerebral metabolic rate of glucose (CMR<sub>glc</sub>). The purpose of this study was to measure regional CMR<sub>glc</sub> by using the DHC. Methods: We studied seven healthy male volunteers who showed no clinical evidences of cognitive and neurological deficits. Their mean age was 30.2±5.8 years (range:25-39 years). Data acquisition was performed by use of VERTEX Plus MCD (ADAC Laboratories, Milpitas, CA). This system has in-plane spatial resolution of 10 mm (FWHM) and a sensitivity of 3.0 cps/Bq/ml. The brain scanning was started 30 or 70 min after injection of 185 or 111 MBq of FDG. The emission data were collected for 30 min. Sixty four projections of coincidence detection were obtained at 50 seconds per projections every 5.6 for 360 (180 ×2), in a 128×128 matrix. Frame-by-frame decay correction was performed before image reconstruction using a Butterworth filter (cut-off frequency 1.20 cycles/cm, order 10). The Chang's postreconstruction attenuation correction was applied to the slices by fitting an ellipse to the scalp contour for the entire brain with an attenuation coefficient of 0.08 cm<sup>-1</sup>. The final reconstructed axial image was generated from 4.0 mm-thick slices with ordered subset expectation maximization algorithm (subset: 8, iteration: 4). Serial arterial blood samplings were done from a catheter placed in the radial artery to measure plasma radioactivity and glucose. Regional CMR<sub>glc</sub> was calculated according to the autoradiographic method (1) originally developed by Sokoloff et al (2). The incorporated metabolic rate constants were K<sub>1</sub>=0.102, k<sub>2</sub>=0.130, and k<sub>3</sub> =0.062, and the lumped constant was 0.42. Results: The mean value of regional CMR<sub>glc</sub> for the frontal, temporal, parietal, occipital cortexes, thalamus and cerebellum was 4.5±0.8, 4.7±0.8, 4.5±0.8, 4.3±0.8, 3.7±0.6 and 4.8±0.8, respectively. The mean CMR<sub>glc</sub> for global cerebral cortexes was 4.5±0.7mg/100g/min. These values were slightly lower than the published values of the CMR<sub>glc</sub> on normal volunteers measured by positron emission tomography. Conclusion: By taking influences of attenuation correction, dead time correction and scatter fraction into account, the quantitative measurement of brain glucose metabolism is possible by the DHC. Reference: 1.Phelps ME, Huang SC, Hoffman EJ, et al. *Ann Neurol* ; 6 : 371-388, 1979. 2.Sokoloff L, Reivich M, Kennedy C, et al. *J Neurochem*; 28: 897-916, 1977.

**FEASIBILITY OF DERIVING CBF, OEF AND CMRO2 FROM A SINGLE DYNAMIC PET SCAN USING A SHORT INHALATION OF OXYGEN-15 LABELLED MOLECULAR OXYGEN**

**Ronald Boellaard<sup>1</sup>**, Abraham Rijbroek<sup>2</sup>, Gert Luurtsema<sup>1</sup>, Henri N.J.M. Greuter<sup>1</sup>,  
Adriaan A. Lammertsma<sup>1</sup>

<sup>1</sup>*Department of Nuclear Medicine and PET Research, VUmc, Amsterdam, The Netherlands*

<sup>2</sup>*Department of Surgery, VUmc, Amsterdam, The Netherlands*

Introduction: Traditionally, CBF, OEF and CMRO2 are obtained using the oxygen-15 steady state technique and PET. This technique requires 3 scans (H2O, CO and O2) during continuous administration of tracers. The purpose of the present study was to investigate the feasibility of deriving accurate CBF, OEF and CMRO2 data from a single dynamic PET scan using a short bolus inhalation of O2. Methods: Previously, a simulation study was performed showing that accurate CBF, OEF and CMRO2 values could be obtained from a single (bolus inhalation) O2 scan, but only by fixing the volume of distribution of water (Vd) parameter [1]. Therefore, these simulations were extended to investigate the effects of using incorrect values of Vd on the accuracy and precision of CBF, OEF and CMRO2. Moreover, this approach was validated using ten clinical studies with dynamic H2O, CO and O2 scans and continuous arterial blood sampling. Clinical data were analysed in two ways. First, CBF, OEF and CMRO were calculated using data from all three scans, i.e. OEF and CMRO2 were derived from the oxygen scan by reusing CBV, CBF and Vd from the CO and H2O scans. Secondly, data from the O2 scan alone were used in combination with a co-registered and segmented MRI scan. The MRI scan was used to assign Vd values to grey and white matter voxels. To this end, a whole brain time activity curve of the O2 scan was fitted without any fixed parameter, thereby estimating global Vd per patient. This global value was subsequently used to scale the gray and white matter Vd values based on the MRI data. Results: Simulations showed that errors of ~10% in Vd value may lead to a bias of ~20% in CBF and OEF (but only ~3% in CMRO2), indicating that using an average (population) Vd may not be feasible in clinical practice and that individual patient values should be assigned. Clinical evaluation revealed reasonable correlations between CBF, OEF and CMRO2 using both methods. Linear regression showed average ( $\pm$ SD) slopes of  $1.07\pm 0.07$ ,  $1.04\pm 0.10$  and  $1.02\pm 0.05$  and average correlation coefficients of 0.88, 0.64 and 0.99 for CBF, OEF and CMRO2, respectively, after discarding outliers. However, large bias (>50%) and/or outliers were obtained in case of poor oxygen gas delivery and/or small amounts of C-11 contamination of the oxygen gas (~0.5% or more), which occurred in 50% of the studies. Conclusions: Calculation of CBF, OEF and CMRO2 from a single dynamic O2 scan in combination with a co-registered and segmented MRI scan is feasible. This method is, however, very sensitive to poor gas delivery and to small amounts of C-11 contamination of the oxygen-15 tracers. Therefore, it should only be used when online assessment of the quality of the acquired data is available. Moreover, both simulations (data not shown) and clinical data suggest that CBF, OEF and CMRO2 derived from a single O2 scan show somewhat poorer reproducibility than those derived by reusing CBF and Vd from an H2O scan. [1] Boellaard et al. IEEE MIC proceedings, 2004, Rome

## RAPID CBF/CMRO<sub>2</sub> MEASUREMENT IN A SINGLE PET SCAN WITH DUAL TRACER ADMINISTRATION

Nobuyuki Kudomi, Takuya Hayashi, Hiroshi Watabe, Hidehiro Iida

Department of Investigative Radiology, Advanced Medical-Engineering Center, National Cardiovascular Center-Research Institute, Osaka, Japan

**Introduction:** CBF/CMRO<sub>2</sub> may be quantified using PET with <sup>15</sup>O-tracers, but the conventional three-step technique (3S) requires a relatively long study period, attributed to need for separate acquisition for <sup>15</sup>O<sub>2</sub>, H<sub>2</sub><sup>15</sup>O, and C<sup>15</sup>O tracers. Simultaneous fitting of dynamic Single-<sup>15</sup>O<sub>2</sub> time activity curve to CBF/CMRO<sub>2</sub> in addition to V<sub>0</sub> suffers from statistical uncertainty. In this study, we present a novel technique that provides a pixel-by-pixel calculation of CBF/CMRO<sub>2</sub> from a single dynamic PET acquisition with a sequential administration of <sup>15</sup>O<sub>2</sub> and H<sub>2</sub><sup>15</sup>O, which may be of use for rapid and accurate assessment in pharmacological and/or cognitive studies. **Methods:** A mathematical formula was derived based on a single-tissue compartment model [1] and treating a vascular component as V<sub>0</sub>, i.e., tissue radioactivity (CPET(t)) can be expressed as  $CPET(t) = E \int A_o \cdot \exp(-ft/p) + f A_w \cdot \exp(-ft/p) + V_0 A_o$ , where A<sub>o</sub> and A<sub>w</sub> denote oxygen and water input functions, f is CBF, E is OEF, and p(=0.8mL/g) is partition coefficient for water. Quantitative images of CBF/CMRO<sub>2</sub> were calculated using basis function method (BFM) [2], in which parameters can be estimated using linear least squares by dealing with non-linear terms by choosing a discrete spectrum for f and forming the corresponding basis function. Experiments were carried out to validate this technique on anaesthetized monkeys (n=6) by comparing the global values of OEF (gOEF) varied by changing PaCO<sub>2</sub> to those obtained by simultaneous arterio-sinus blood sampling (gOEFA-V), and on normal young human subjects at rest (n=6) by comparing CBF/CMRO<sub>2</sub> values with those by non-linear least square method (NLM). We also performed a simulation study to estimate sensitivities to various error sources. **Results:** gOEF agreed with gOEFA-V ( $y=0.94x+0.04$ ,  $P<0.001$ ) in monkey. The regional CBF, OEF and CMRO<sub>2</sub> values in cortical regions by the present method were  $0.75 \pm 0.20$  mL/min/g,  $0.39 \pm 0.03$  and  $0.053 \pm 0.012$  mL/min/g and, those from NLM were  $0.73 \pm 0.19$  mL/min/g,  $0.40 \pm 0.03$  and  $0.053 \pm 0.015$  mL/min/g, respectively. No significant difference was found between the two methods. The obtained image quality for CBF, OEF and CMRO<sub>2</sub> was reasonably comparable to that of 3S (Fig.1). The simulation study showed error sensitivity of the present technique to delay or dispersion of the input function, and the error in the partition coefficient was equivalent to that observed for 3S. **Conclusion:** These results show that this rapid technique has ability for accurate assessment of CBF/CMRO<sub>2</sub> for clinical and research purpose. **References:** [1] Mintun MA, Raichle ME, Martin WR, Herscovitch P (1984) J Nuc, Med 25:177 [2] Gunn RN, Lammertsma AA, Hume SP, Cunningham VJ (1997) Neuroimage 6:279 Grant support: The present work was supported by the Program for Promotion of Fundamental Studies in Health Science of the Organization for Pharmaceuticals.

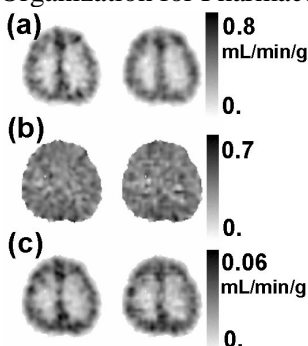


Fig. 1: Functional images of (a)CBF (b)OEF and (c)CMRO<sub>2</sub> by 3S(left) and the present method (right).



ESTIMATION OF 150 PET IN HEALTHY VOLUNTEERS WITH AUTOMATED ROI ANALYSIS BY FINESRT

Ryo Takeuchi<sup>1</sup>, Keiichi Matsumoto<sup>2</sup>, Setsu Sakamoto<sup>2</sup>, Yuhji Nakamoto<sup>2</sup>, Michio Senda<sup>2</sup>

<sup>1</sup>Radiology, Kobe City General Hospital, Kobe, Japan

<sup>2</sup>Image-Based Medicine, Institute of Biomedical Research and Innovation, Kobe, Japan

Introduction; Under the conditions of major cerebral arterial stenosis, increased OEF is reported to play an important role as a major risk factor for cerebral infarction and return to normal after revascularization therapy. Consequently, measurement of OEF and CMRO2 is useful for determination of indication for revascularization therapy. However, anatomical constitution of the OEF images, which were generated by the calculation using CBF images, was not so clear as those of the CBF images, which were directly generated by kinetic analysis of dynamic PET data and arterial input functions. Therefore, the results of the conventional ROI (region of interest)analysis of the OEF and CMRO2 images had serious problems in the objectivity and reproducibility. We already established the automated constant ROI analysis software for the cerebral gray matter named "FineSRT". In this study we tried to estimate OEF and CMRO2 images of the normal volunteers using FineSRT. Materials and methods; Nine healthy volunteers (age range 44-58 years, mean 51.8 years, 9 men) were enrolled. The parametric images of CBF, OEF and CMRO2 were calculated according to the method of autoradiography. Using FineSRT, the OEF and CMRO2 images of each subject were anatomically standardized first with the same moving parameters determined by the CBF image and CBF PET template image under SPM99 algorithm. The standardized images were consequently analyzed using the constant ROI template, which was composed of 1394 ROIs grouped into 41 areas corresponding to respective cerebral convolutions as shown in the Table, and area-weighted mean value for each of the 41 areas based on the PET count in each ROI were calculated. The mean and standard deviation (SD) of the respective area-weighted mean OEF, CMRO2 and CBF values of all subjects' 41 areas were calculated and compared. Results; Significant correlation was expectedly not shown between OEF and CBF values (Fig. 1;  $r=0.038$ ,  $R^2=0.001$ ) but between CMRO2 and CBF (Fig. 2;  $r=0.908$ ,  $R^2=0.825$ ). As shown in the Table, the mean and SD of 41 OEF values were  $42.56 \pm 3.27$  mL/100gr/min (range 31.64-46.68), and OEF values of the caudate tail (31.64), the hippocampus (35.75), the amygdaloid body (34.82) and the thalamus (37.34) were conspicuously lower than those of the other areas. Conclusion; FineSRT enables objective quantification of each cerebral gyrus of PET images. The normal OEF values of almost all gyri were observed around 42.56 irrespective of their CBF values, but lower threshold was needed for the evaluation of caudate tail, hippocampus, amygdaloid body and thalamus.

Table. Mean and SD of the nine volunteers' area-weighted average of OEF, CMRO2 and CBF

	SuperiorFrontal	MedialFrontal	PancaentralLobe	AnteriorCingulate	Subcallosal	Orbital	Rectal	MiddleFrontal	InferiorFrontal	Precentral	Postcentral
OEF	42.76 ± 3.95	42.66 ± 3.43	43.34 ± 3.65	39.39 ± 2.94	41.63 ± 3.52	46.30 ± 3.41	43.81 ± 2.76	43.71 ± 3.24	42.84 ± 3.44	42.93 ± 4.24	43.51 ± 3.64
CMRO2	2.62 ± 0.48	3.20 ± 0.53	3.37 ± 0.97	3.07 ± 0.38	3.71 ± 0.56	3.86 ± 0.63	4.05 ± 0.55	3.01 ± 0.44	3.09 ± 0.35	2.82 ± 0.50	2.83 ± 0.46
CBF	37.74 ± 4.63	45.98 ± 6.06	46.78 ± 11.89	47.85 ± 5.02	53.57 ± 6.43	49.30 ± 5.85	54.64 ± 5.71	41.73 ± 4.62	43.96 ± 4.27	40.46 ± 6.23	39.92 ± 5.64

	Insula	SuperiorParietal	InferiorParietal	Supramarginal	Angular	SuperiorTemporal	MiddleTemporal	InferiorTemporal	TransverseTemporal	SuperiorOccipital	MiddleOccipital
OEF	42.20 ± 2.87	45.35 ± 3.90	44.38 ± 3.01	44.25 ± 2.42	45.89 ± 3.08	41.52 ± 3.34	44.22 ± 3.00	45.05 ± 3.13	40.38 ± 3.18	46.11 ± 3.36	46.42 ± 2.89
CMRO2	3.41 ± 0.44	2.77 ± 0.56	3.00 ± 0.47	3.01 ± 0.39	3.38 ± 0.44	3.08 ± 0.33	2.98 ± 0.35	2.82 ± 0.35	3.86 ± 0.64	3.09 ± 0.40	2.96 ± 0.45
CBF	48.73 ± 5.86	37.56 ± 6.12	41.40 ± 4.98	41.60 ± 4.89	44.45 ± 5.40	45.21 ± 4.79	41.25 ± 4.42	38.64 ± 4.47	56.72 ± 8.89	40.77 ± 4.62	38.82 ± 4.88

	InferiorOccipital	PrecuneusLower	Cuneus	Hippocampus	Fusiform	Lingual	Panahippocampal	AmygdaloidBody	Thalamus	Putamen	GlobusPallidus
OEF	46.68 ± 3.56	44.93 ± 3.09	44.66 ± 3.31	35.75 ± 2.71	45.23 ± 3.16	44.18 ± 3.03	39.71 ± 2.52	34.82 ± 3.46	37.34 ± 2.79	45.05 ± 3.20	44.29 ± 2.97
CMRO2	3.40 ± 0.51	4.41 ± 0.76	3.86 ± 0.61	2.41 ± 0.25	3.45 ± 0.49	4.04 ± 0.60	2.66 ± 0.41	2.63 ± 0.56	2.76 ± 0.41	3.57 ± 0.60	3.08 ± 0.47
CBF	43.89 ± 6.91	56.86 ± 6.92	50.91 ± 6.09	42.38 ± 4.80	46.01 ± 5.93	53.84 ± 6.69	41.30 ± 5.17	46.50 ± 7.75	44.72 ± 4.55	47.22 ± 6.71	42.92 ± 5.55

	CaudateHead	CaudateTail	PrecuneusUpper	Cingulate	PosteriorCingulate	Vermis	AnteriorLobe	PosteriorLobe	Average
OEF	45.48 ± 4.29	31.64 ± 4.96	44.37 ± 3.04	41.03 ± 3.91	42.38 ± 3.22	39.95 ± 2.97	39.46 ± 3.30	41.28 ± 3.21	42.56 ± 3.27
CMRO2	2.08 ± 0.44	1.46 ± 0.30	3.19 ± 0.93	3.35 ± 0.55	4.07 ± 0.75	3.62 ± 0.55	3.19 ± 0.54	4.50 ± 0.82	3.22 ± 0.60
CBF	30.00 ± 3.87	30.45 ± 4.02	46.89 ± 8.33	49.12 ± 6.63	54.27 ± 5.48	54.26 ± 9.71	48.65 ± 6.78	63.43 ± 10.48	45.65 ± 6.90

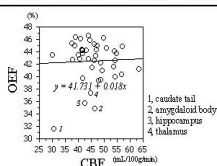


Fig. 1. Scatter plot of CBF as measured by OEF

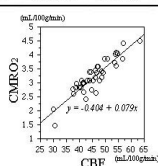


Fig. 2. Scatter plot of CBF as measured by CMRO2

**BP-93**

**DEVELOPMENT OF SINOGRAM-BASED ESTIMATION METHOD OF DELAY TIME OF ARTERIAL INPUT FUNCTION WITH O-15 TRACER AND PET STUDY**

**Hiroshi Watabe, Nobuyuki Kudomi, Takuya Hayashi, Hidehiro Iida**

*Department of Investigative Radiology, National Cardiovascular Center Research Institute, Suita, Japan*

Delay time of arterial input function measured by an external radiation detector must be estimated correctly in order to accurately measure rCBF or CMRO<sub>2</sub> with O-15 tracer and PET by autoradiographic method. Conventionally, in order to estimate the delay time, the measured arterial input curve is compared with tissue time activity curve (TTAC) from reconstructed image and the delay time is determined by the fitting procedure. Instead of getting TTAC from the reconstructed image (image based method), Shidahara et al[1] proposed a method to get TTAC from the sinogram data (sinogram based method), which enables more rapid estimation of the delay time. CO<sub>2</sub> or O<sub>2</sub> gas is usually supplied by a mask and a subject inhales the radioactive gas through the mask. During PET acquisition, radioactive gas in mask and nasal cavity contributes large artifact on the sinogram data and it is difficult to estimate delay time from the sinogram data. We proposed a new method to estimate the delay time using the sinogram data and the attenuation map (attenuation weighted sinogram method). In the present method, the attenuation map was used to eliminate the effect of the gas outside the brain region from the sinogram data. For the validation of the present method, PET data with CO<sub>2</sub> (n=10) were analyzed. Three methods, namely the image base method, the sinogram base method and the attenuation weighted sinogram method were used to estimate the delay time. The estimated delay times and calculated rCBF images by three methods were compared. Due to the radioactivity outside of the brain, the sinogram method significantly overestimated the delay time and thus underestimated the rCBF value compared with the image base method. On the other hand, there were good agreements between the delay times estimated by the attenuation weighted sinogram method and the image base method. The present method can eliminate the effect of the radioactivity outside of the brain on the sinogram data and estimate the delay time accurately and fast enough for clinical use. Reference [1] Shidahara et al Ann Nucl Med 2002 16(5):317-27

**SOURCES OF VARIABILITY IN OXYGEN-15 PET STUDIES IN ACUTE BRAIN INJURY – IMPACT ON SAMPLE SIZE ESTIMATION**

**Jonathan P. Coles**<sup>1,2</sup>, Tim D. Fryer<sup>2</sup>, Peter G. Bradley<sup>1,2</sup>, Jurgens Nortje<sup>1,2</sup>, Peter Smielewski<sup>2,3</sup>, Kenneth Rice<sup>4</sup>, John C. Clark<sup>2</sup>, John D. Pickard<sup>2,3</sup>, David K. Menon<sup>1,2</sup>

<sup>1</sup>*Division of Anaesthesia, University of Cambridge, Cambridge, UK*

<sup>2</sup>*Wolfson Brain Imaging Centre, University of Cambridge, Cambridge, UK*

<sup>3</sup>*Department of Neurosurgery, University of Cambridge, Cambridge, UK*

<sup>4</sup>*Medical Research Council Biostatistics Unit, Institute of Public Health, Cambridge, UK*

The potential of Oxygen-15 positron emission tomography (PET) to investigate acute brain injury and the effect of therapeutic interventions is limited by inter- and intra-subject variability. We have tried to quantify these limitations when steady state PET is used to measure cerebral blood (CBF), cerebral blood volume (CBV), oxygen metabolism (CMRO2) and oxygen extraction fraction (OEF). We obtained PET images from 10 healthy volunteers and 24 patients within 10 days of head injury with a median (range) Glasgow Coma Score of 7 (3 – 13). Using a region of interest map comprising 15 regions covering the whole brain we calculated inter-subject variability in both groups, while the intra-subject variability was calculated from two consecutive PET studies in a cohort of six patients (test-retest reproducibility). The acquisition of PET data in two frames provided the opportunity of using individual frames to calculate two independent sets of metabolic images, which could be used to assess reproducibility within the context of a single pre-intervention baseline PET study (within-session reproducibility). In this way we obtained repeated measurements of CBF, CMRO2 and OEF, but not CBV, within the same study session in controls and patients under unchanged physiological conditions. We compared assessments of reproducibility obtained using these two approaches: the test-retest reproducibility (two independent studies) and the within-session reproducibility (two independent frames within a single study). Inter-subject coefficients of variation (CoV) for CBF, CBV, CMRO2 and OEF in patients (32.9 +/- 2.2, 15.2 +/- 2.1, 23.2 +/- 2.0 and 22.5 +/- 3.4 %) were generally larger than in controls (13.5 +/- 1.4, 22.5 +/- 2.8, 12.8 +/- 1.1 and 7.3 +/- 1.2 %). The CoV for the test-retest reproducibility measurements in patients were 2.1 +/- 1.5, 3.8 +/- 3.0, 3.7 +/- 3.0 and 4.6 +/- 3.5 %, respectively. The within-session reproducibility CoV for CBF, CMRO2 and OEF in patients (4.2 +/- 4.6, 2.2 +/- 2.0 and 4.8 +/- 4.7 %) were smaller than in controls (8.4 +/- 7.6, 5.3 +/- 3.9, 5.7 +/- 4.4 %). Although large inter-subject variability creates difficulties with studies of small patient groups, estimated sample sizes are moderated by the fact that the changes in cerebrovascular physiology in disease are often dramatic. These figures are irrelevant to the design of interventional studies, where the subject is his or her own control, and the relevant parameter is intra-subject variability or reproducibility. The CoV figures for reproducibility are substantially smaller and provide important reference data. In addition, the within-session and test-retest reproducibility measurements are comparable. This implies that within-session reproducibility measurements can be used to assess the significance of any change in physiology following a therapeutic intervention. These data provide guidance for designing interventional studies, and suggest it should be possible to detect differences of approximately 10 – 15% in controls, and 5 – 10% in head injured patients where systemic physiology is tightly controlled. While each centre should develop its own bank of such data, the figures provided will allow initial generic approximations of sample size for such studies.

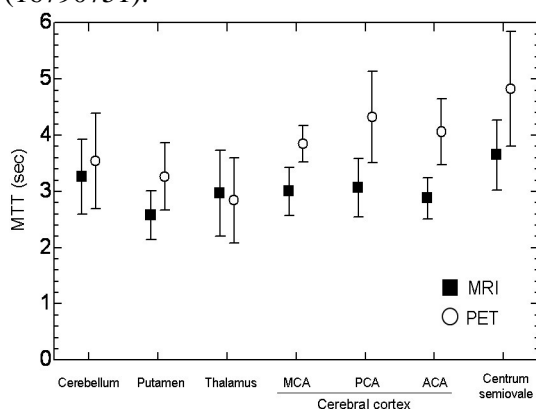
## CEREBRAL VASCULAR MEAN TRANSIT TIME DETERMINED BY PET AND DSC-MRI

Masanobu Ibaraki<sup>1</sup>, Hiroshi Ito<sup>2</sup>, Eku Shimosegawa<sup>1</sup>, Hideto Toyoshima<sup>1</sup>, Keiichi Ishigame<sup>1</sup>,  
Kazuhiro Takahashi<sup>1</sup>, Syuichi Miura<sup>1</sup>, Iwao Kanno<sup>1</sup>

<sup>1</sup>Department of Radiology and Nuclear Medicine, Akita Research Institute of Brain and Blood Vessels,  
Akita, Japan

<sup>2</sup>Department of Nuclear Medicine and Radiology, Institute of Development, Aging and Cancer, Tohoku  
University, Sendai, Japan

**Introduction:** Cerebral vascular mean transit time (MTT), calculated as the ratio of cerebral blood volume (CBV) to cerebral blood flow (CBF), is expected to be inversely proportional to cerebral perfusion pressure. Dynamic susceptibility contrast-enhanced magnetic resonance imaging (DSC-MRI) with a Gd-based contrast agent is being applied increasingly for cerebral perfusion study, although positron emission tomography (PET) measurement has been regarded as the gold standard for quantification of CBF. The objective of this study was to examine the difference between MTT determined by PET (PET-MTT) and that determined by DSC-MRI (MRI-MTT). **Materials and Methods:** Subjects were seven healthy volunteers, 20-21 years of age. In the PET study, the CBV image was derived from scanning after [15-O]-CO inhalation. CBF was calculated by least-squares fitting of the dynamic data obtained with [15-O]-H<sub>2</sub>O bolus injection and continuous arterial sampling. In the DSC-MRI study with bolus injection of Gd-based contrast agent, dynamic data were obtained with a 1.5T scanner at 1-second intervals using a gradient-echo EPI. CBV was calculated by integrating the time-concentration curve. CBF was determined with the use of singular value decomposition deconvolution [1] incorporated with correction for the effect of tracer delay [2]. **Regions of interest** 10 mm in diameter were drawn on the PET and DSC-MRI images. **Results and Discussion:** Average MTTs are shown in Figure 1. The PET data were consistent with previously reported PET data in terms of regional distribution of MTT [3]. The MRI-MTT differed regionally, as did the PET-MTT. However, MRI-MTTs were systematically shorter than PET-MTTs except in the thalamus. A possible explanation for this difference is the sensitivity of each imaging modality to vascular components: PET measurements for CBV are obtained with the use of [15-O]-CO and are equally sensitive to all vascular components, whereas DSC-MRI signals originate from the microvasculature in vicinity to the brain parenchyma. Thus, MTT obtained via DSC-MRI should be shorter than MTT obtained via PET imaging. Therefore, the two sets of data appeared consistent, although potential sources of error in the two methods should be carefully considered. **References:** [1] Ostergaard L et al.; Magn. Reson. Med. 36, 715-725 (1996). [2] Ibaraki M et al.; J Cereb Blood Flow Metab. in press. [3] Ito H et al.; Neuroimage. 19, 1163-1169 (2003). This research was supported in part by a Ministry of Education, Science, Sports and Culture Grant-in-Aid for Young Scientists (16790751).





**ORDERED SUBSET EXPECTATION MAXIMIZATION ALGORITHM FOR IMAGE RECONSTRUCTION AFFECTS THE SPM ANALYSIS IN PATIENTS WITH MILD ALZHEIMER'S DISEASE**

Yasuhiro Katsura, Ryohei Matsuura, Yasuhiro Akazawa, Piao Rishu, Ansar M.D. Ashik, Yasuyuki Kimura, Katsufumi Kajimoto, Naohiko Oku, Shinji Hasegawa, **Jun Hatazawa**

*Department of Nuclear Medicine and Tracer Kinetics, Osaka, Japan*

Background: Recently, the ordered subset expectation maximization (OSEM) algorithm was developed to reconstruct the PET and SPECT images. This iterative algorithm allowed incorporation of realistic modeling of the data acquisition process and statistical noise, which refined estimates of the activity distribution. Since the statistical image analyses such as the Statistical Parametric (SPM) or three dimensional stereotactic surface display (3D-SSP) methods rely on the accurate measurement of activity distribution in the brain, the results may be affected by the use of the OSEM. In this study, we show that the image reconstruction algorithm employed affects the result of the statistical image analysis in mild Alzheimer's disease. Materials and Methods: Sixteen patients with probable Alzheimer's disease (8 men and 8 women; age range, 56-78 y; mean age, 70.6 years) and 6 normal controls (1 men and 5 women; age range, 48-69; mean age, 62.8 years) were studied. Their diagnosis was based on the criteria of the National Institute of Neurological and Communicative Disorders and Strokes and the Alzheimer's Diseases and Related Disorders association (NINCDS-ADRDA). All patients underwent neuropsychological testing that revealed quantified, objective evidence of memory impairment with no apparent loss in general cognitive, behavioral, or functional status at the study. The score was greater than 20 on the mini-mental State Examination (MMSE). Cerebral blood flow was measured by means of Tc-99m HMPAO and a high-performance, 4-head rotating gamma camera equipped with a low-energy, general-purpose, parallel-hole collimator with a spatial resolution of 13.0-mm full width at half-maximum (Gamma View SPECT 2000H, Hitachi Medical Co). The transaxial images were reconstructed with the Filtered Back Projection algorithm (FBP) and the OSEM (iteration 4; subset 8) in each patient. The SPM99 and 3D-SSP were used for the statistical image analysis. All reconstructed images were smoothed using a Gaussian filter with a full-width half maximum of 12 mm in the SPM analysis. The gray matter threshold was set to be 0.8. Results: In the SMP analysis, the cluster of significant CBF reduction was found in the lateral temporal cortices and posterior cingulated gyrus ( $p < 0.01$ ) when the FBP was employed. When the OSEM was used, it was found in the posterior cingulated gyrus ( $p < 0.01$ ). In the 3D-SSP analysis, posterior cingulated gyrus hypoperfusion was detected by both reconstruction algorithms. Discussion: We demonstrated that the result of the SPM analysis is affected by the choice of image reconstruction algorithm. We visually inspected images reconstructed with the OSEM and the FBP. We found that the contrast between the posterior cingulated gyrus and surrounding structures were less in the OSEM than in the FBP. This may be due to the dependence of convergence time on the spatial frequencies in the OSEM procedure. Conclusion: Although the OSEM algorithm is now the most widely used iterative reconstruction method, it may affect the SPM analysis when mild AD patients are studied.

**ORDERED SUBSET EXPECTATION MAXIMIZATION ALGORITHM FOR IMAGE RECONSTRUCTION APPLIED TO ZERO-FLOW OR LOW-FLOW MIMICKING BRAIN PHANTOM**

Yasuhiro Akazawa, Yasuhiro Katsura, Ryohei Matsuura, Piao Rishu, Ansar M.D. Ashik, Yasuyuki Kimura, Katsufumi Kajimoto, Naohiko Oku, Shinji Hasegawa, **Jun Hatazawa**

*Department of Nuclear Medicine and Tracer Kinetics, Osaka University Graduate School of Medicine, Osaka, Japan*

Background: The measurement of cerebral blood flow (CBF) by means of single photon emission computed tomography (SPECT) is a complimentary method to diagnose a brain death. It is difficult to prove a zero-flow state of the brain in the tomographic image because of an image reconstruction noise. We aimed to improve a reliability of the SPECT CBF measurement in a brain death state by utilizing the ordered subset expectation maximization (OSEM) algorithm for image reconstruction. Materials and Methods: Brain phantom consisting of the skull part and intracranial part (cylindrical or Hoffman phantom) was employed. First, the skull part was filled with 12.7% solution of copper sulfate dissolving  $2.58 \times 10^{-1}$  MBq/ml  $^{99m}\text{Tc-O4}$ . The cylindrical intracranial part was filled with physiological saline (Phantom 1 mimicking intracranial zero-flow state). Second, the cylindrical intracranial part was replaced by Hoffman phantom filled with  $1.12 \times 10^{-2}$  MBq/ml  $^{99m}\text{Tc-O4}$  for gray matter compartment and  $5.59 \times 10^{-3}$  MBq/ml  $^{99m}\text{Tc-O4}$  for white matter compartment (Phantom 2 mimicking 5% CBF or 2.5% CBF compared with that of skull). Third, the 16cm-diameter cylindrical phantom was filled with saline solution dissolving  $4.26 \times 10^{-2}$  MBq/ml sodium pertechnetate ( $^{99m}\text{Tc-O4}$ ). (Phantom 3 to test the system sensitivity). The Gamma View SPECT 2000H system (Hitachi Medical Co, Tokyo) was used for the scanning. The acquisition parameters were as follows; 20% symmetrical window (centered on  $^{99m}\text{Tc}$  140 keV photopeak), high resolution collimator, 128 8seconds-acquisition, 64x64 image matrix, Butterworth filter (order 10, cutoff frequency 0.50cycle/cm) and the Chang's method with attenuation coefficient of 0.08  $\text{cm}^{-1}$ . The scan data were reconstructed by means of the filtered back projection (FBP) algorithm or the ordered subset expectation maximization (OSEM) algorithm. The 10cm-diameter oval region of interest (ROI) was placed on the intracranial part of the phantom image for count reading. Result: In the Phantom 1, mean count and standard deviation was  $0.367 \pm 1.04$  and  $0.00867 \pm 0.165$  for the FBP and the OSEM (iteration 4; subset 8), respectively, indicating the OSEM value was much close to zero. In the Phantom 2, we were able to visually detect phantom brain structures such as cortical and central gray matter only when the OSEM was employed. In the Phantom 3, mean count/pixel was  $239 \pm 33$  and  $144 \pm 15$  for the FBP and OSEM algorithm, respectively. Discussion: The present study demonstrated that zero-flow state or low-flow state of the brain could be more reliably visualized by means of the OSEM algorithm. Although the system sensitivity of the FBP appeared higher than that of the OSEM, this may be due to the inclusion of more noise in the FBP method. Since the OSEM algorithm allowed incorporation of effects of attenuation and scatter, modeling of statistical noise, and non-negative count assumption, it refined an accuracy of the tomographic activity distribution. For the evaluation of brain death state using a brain perfusion SPECT, the OSEM algorithm should be utilized for image reconstruction.

**STRATEGY OF SPECT RECONSTRUCTION FOR ABSOLUTE QUANTITATION OF CEREBRAL FUNCTION IMAGE****Kyeong Min Kim<sup>1,3</sup>, Hidehiro Iida<sup>1,3</sup>, Mayumi Nakazawa<sup>2,3</sup>, Kinuko Abe<sup>2,3</sup>**<sup>1</sup>*Department of Investigative Radiology, National Cardiovascular Center Research Institute, Osaka, Japan*<sup>2</sup>*Nihon Medi-Physics, Hyogo, Japan*<sup>3</sup>*QSPECT & Dual Table ARG Group, Japan*

Introduction: Recent advance in SPECT could incorporate accurate corrections for attenuation and scatter. Despite various equipment conditions of SPECT, such as different collimator design and/or energy window settings, a novel SPECT reconstruction package (QSPECT) may provide quantitative images of in vivo distribution of radio-tracers in clinical studies. In this work, we have evaluated accuracy and reproducibility of reconstructed images among different scanners from different manufacturers installed in different institutions. Methods: Six institutions were involved in this study using one of the following 4 SPECT cameras, namely E.CAM dual-headed from Toshiba-Siemens (n=1), PRISM IRIX triple-headed from Shimazu (n=1), MillenniumVG dual-headed from GE (n=1), and GCA-9300A triple-headed from Toshiba (n=3). Absolute sensitivity (Becquerel per mL in reconstructed images, or Becquerel Calibration Factor (BCF)) was calibrated using a syringe of I-123 solution supplied from a radio-pharmaceutical company (Nihon-Medi Physics, Tokyo, Japan). Uniform cylindrical phantom of known radioactivity concentration and multiple rod phantoms were scanned in each institution. Images were reconstructed using a software package, QSPECT, with a scatter correction by means of the transmission-dependent convolution subtraction technique, and OSEM procedures including the attenuation correction process. Cross calibration factor (CCF) that illustrates the relative sensitivity between external well-counter and SPECT, was estimated. Accuracy and the inter-institutional reproducibility were then evaluated for those reconstructed images. CBF study was performed with split-injection of I-123 IMP, on patients with cerebrovascular disease, and cerebral function was evaluated using the image obtained by this approach. Results: BCF values were dependent on to collimator design and the number of detector. The three institutions that had the same SPECT camera (GCA-9300A) demonstrated a good agreement of the BCF value (COV of 2.6%). The pixel values in the reconstructed images, which should represent the absolute radioactivity concentration in units of Bq/mL, were in a good agreement with the true radioactivity concentration for the uniform cylindrical phantom, i.e. the difference was  $10.5 \pm 1.7\%$  for all 6 institutions. CCF values that represent the sensitivity of well-counter and should be less than 1, were in a narrow range (from 0.5 to 0.8), which supported the robustness of this approach in radioactivity measurement. The pixel values of reconstructed IMP image showed about 8% of injected dose on the normal region, which was consistent with previous reports of IMP uptake in brain tissue. Conclusion: The presented SPECT reconstruction could provide quantitative images that represent regional radioactivity concentration in units of Bq/mL. These quantitative values appeared to be consistent and reproducible among different hardware setup supplied from different manufacturers, which resulted in the improved evaluation of cerebral function. Selection of adequate methodologies for the accurate scatter and attenuation correction procedures was essential to appropriate measurement of radioactivity. Thus, this approach can be feasible for quantitation of physiological functions, as has been done only by PET, and may be useful in multi-center trials. Acknowledgement: Supported by the Program for Promotion of Fundamental Studies in Health Science of the Organization for Pharmaceutical Safety and Research (of Japan).

**DEFINING PARAMETERS FOR AN ADAPTATIVE 3D WIENER FILTER IN IMAGE RESTORATION OF SPECT CEREBRAL BLOOD FLOW STUDIES: A NOVEL APPROACH****Jean-Paul Soucy<sup>1</sup>, Wei Li<sup>2</sup>, Jean Meunier<sup>2</sup>**<sup>1</sup>*CHUM/MNI, Montréal, QC, Canada*<sup>2</sup>*DIRO, U. de Montréal, Montréal, QC, Canada*

Multiple factors (attenuation, scattering, scanner response, etc) significantly degrade SPECT images. and multiple techniques have been proposed to correct for those and therefore yield more quantitatively exact SPECT studies, with the aim of improving clinical classification of patients as well as results from research using this technique. Application of a Wiener filter during reconstruction, which minimizes the mean square error between the original object and its estimate (the image), is a well-validated and relatively simple approach to this problem. Optimal use of this technique requires a priori information such as the point spread function (PSF) of the imaging system and the power spectrum ratio of the original object to image noise, but this information is not generally available. We have applied a new adaptation of this approach to cerebral blood flow studies obtained in SPECT with <sup>99m</sup>Tc labeled agents. Here, we start with a Gaussian function to model the PSF of the SPECT system, and a constant to replace the noise-to-signal power spectrum ratio [1]. The PSF width and power-spectrum ratio are then iteratively optimized to improve image contrast between white and gray matter while keeping image mottle (or variance) within each region at a tolerable level (as defined in [2,3]). To track precisely the contrast and mottle, the white and gray matter regions are identified from an anatomical MRI of the same patient previously co-registered to the SPECT study [4]. Simulation results with a realistic brain model (digital Hoffman phantom [5], "degraded" with 3D Gaussian noise (at such count levels, Poisson noise would yield comparable results) and then blurred with a 3D Gaussian function to simulate an actual SPECT study) show marked contrast improvement while maintaining the mottle at an acceptable level: with object contrast between white and gray matter (as defined in [2]) set at 0.427 and degraded to 0.074 post blurring, filtering increased contrast to 0.378, with the mottle (proportionally averaged for gray and white matter) actually decreasing (0.224 to 0.182). Tests conducted with actual clinical SPECT cases exhibit similar contrast improvement (0.045 to 0.104) with a limited (and still acceptable [2]) mottle increase (0.198 to 0.276). We believe that this technique for defining the parameters of a 3D adaptive Wiener filter will be useful in clinical practice, where significant data degradation limits detection of anomalies with SPECT, because it automatically generates the best combination of those parameters, leading to significantly improved contrast quantification with little noise amplification. [1] R. C. Gonzalez, P. Wintz, *Digital Image Processing*, Addison-Wesley, Reading MA, 1977, pp. 215 [2] S. Webb, A. P. Long, R. J. Ott, M. O. Leach, M. A. Flower *Med. Phys.*, 1985, vol. 12, pp. 53-58 [3] M. Mignotte, and J. Meunier, *IEEE Trans. Biomedical Engineering*, 2000, vol. 47, pp. 274-280 [4] R. P. Woods, J. C. Mazziotta, S. R. Cherry, *J. Comput. Assist. Tomogr.*, vol. 17, pp. 536-546, 1993. [5] E. J. Hoffman, P. D. Culter, W. M. Digby, J. C. Mazziotta, *IEEE Trans. Nucl. Sci.*, vol. 37, pp. 616-620, 1990.

## Course I: Imaging of brain activity: Basic methods and underlying physiology

### General information

Brain Imaging based on vascular signals: fMRI, PET, and optical imaging

This course gives an introduction to non-invasive brain imaging methods based on vascular signals such as fMRI, optical imaging, and PET. For each method, basic technical aspects of data acquisition, data analysis, and stimulus design are described in detail. Special emphasis is laid on the physiological basis of the respective signal and the applicability of the methods in disease models and in the clinical setting. In a final talk, a role of each method in the “concert of functional brain imaging methods” is defined.

### Program details

**Tuesday, June 7**

Course I 'Imaging of brain activity: basic methods and underlying physiology' <i>Part 1 Basics of Brain Activation Studies (PET, fMRI)</i> Chair: Arno Villringer, Universitätsklinikum Charité, Berlin, Germany		Auditorium
09:00-09:45	<b>Introduction, Signals of vascular neuroimaging methods (fMRI ; PET, Optics)</b> A. Villringer	
09:45-10:30	<b>Basic physics, technical aspects of fMRI</b> B. Savoy	
10:30-11:15	<b>New Signals in fMRI: DWI, neuronal currents</b> P. Bandettini	
11:15-12:00	<b>Experimental Design and Basic Statistics of functional neuroimaging</b> R. Göbel	
12:00-12:45	<b>New Approaches to fMRI data analysis</b> E. Bullmore	
12:45-13:15	lunch break (exhibition & poster area)	
13:15-14:00	<b>Connectivity Studies based on Vascular Brain Imaging</b> C. Büchel	
14:00-14:45	<b>TMS and vascular brain imaging</b> T. Paus	
14:45-15:00	<b>General Discussion</b>	

## Course II: In vivo modeling of stroke

### General information

The proper experimental investigation of cerebral ischemia necessitates the use of physiologically regulated, reproducible animal models. The objective of this course is to provide a comprehensive exposition of animal models of cerebral ischemia. Major emphasis will be placed upon practical laboratory aspects, enabling the participants to develop and apply these models in their own laboratories. The rationale for the use of these models will be explored in detail, and their pitfalls and shortcomings will be presented. Expert speakers will cover both rodent models of focal ischemia (comprising mechanical, suture-occlusion, and photochemical models), as well as global-ischemia and larger-animal models. Other speakers will explore the neuropathology of ischemia, the importance of brain temperature regulation, experimental image-analysis, and the application of PET, MRI, and fMRI to these models. Taken together, the course should provide a solid basis for the use of in vivo models of cerebral ischemia.

### Program details

#### Tuesday, June 7

Course II 'In vivo modeling of stroke'		KC-07
Chairs: Myron D. Ginsberg, University of Miami, USA		
09:00-09:05	<b>Introduction</b> Myron Ginsberg (Miami)	
09:05-09:20	<b>Vascular anatomy in rodents</b> Kazuo Kitagawa (Osaka) <i>Mechanical models of focal cerebral ischemia:</i>	
09:20-09:35	<b>1. in normotensive rats</b> I.M. Macrae (Glasgow)	
09:35-09:50	<b>2. in spontaneously hypertensive rats</b> Hiroshi Yao (Fukuoka)	
09:50-10:05	<b>Intraluminal MCA suture-occlusion in rat and mouse</b> Ludmila Belayev (Miami)	
10:05-10:20	<b>Photochemical methods of vascular occlusion / reperfusion</b> Brant Watson (Miami)	
10:20-10:30	<b>Discussion</b>	

## Course II: In vivo modeling of stroke

### General information

The proper experimental investigation of cerebral ischemia necessitates the use of physiologically regulated, reproducible animal models. The objective of this course is to provide a comprehensive exposition of animal models of cerebral ischemia. Major emphasis will be placed upon practical laboratory aspects, enabling the participants to develop and apply these models in their own laboratories. The rationale for the use of these models will be explored in detail, and their pitfalls and shortcomings will be presented. Expert speakers will cover both rodent models of focal ischemia (comprising mechanical, suture-occlusion, and photochemical models), as well as global-ischemia and larger-animal models. Other speakers will explore the neuropathology of ischemia, the importance of brain temperature regulation, experimental image-analysis, and the application of PET, MRI, and fMRI to these models. Taken together, the course should provide a solid basis for the use of in vivo models of cerebral ischemia.

### Program details

#### Tuesday, June 7

Course II 'In vivo modeling of stroke'		KC-07
Chairs: Myron D. Ginsberg, University of Miami, USA & Akira Tamura, Tokyo, Japan		
11:00-11:15	<b>Focal cerebral ischemia in the cat</b> Raymond Koehler (Baltimore)	
11:15-11:30	<b>Focal cerebral ischemia in primates</b> Gregory Del Zoppo (LaJolla)	
11:30-11:45	<b>Brain temperature monitoring and regulation</b> Frederick Colbourne (Edmonton)	
11:45-12:00	<b>Global ischemia models in rat and mouse</b> Nobutaka Kawahara (Tokyo)	
12:00-12:15	<b>Neuropathology of ischemia: necrosis, apoptosis, other</b> Roland Auer (Calgary)	
12:15-12:30	<b>Discussion</b>	

## Course II: In vivo modeling of stroke

### General information

The proper experimental investigation of cerebral ischemia necessitates the use of physiologically regulated, reproducible animal models. The objective of this course is to provide a comprehensive exposition of animal models of cerebral ischemia. Major emphasis will be placed upon practical laboratory aspects, enabling the participants to develop and apply these models in their own laboratories. The rationale for the use of these models will be explored in detail, and their pitfalls and shortcomings will be presented. Expert speakers will cover both rodent models of focal ischemia (comprising mechanical, suture-occlusion, and photochemical models), as well as global-ischemia and larger-animal models. Other speakers will explore the neuropathology of ischemia, the importance of brain temperature regulation, experimental image-analysis, and the application of PET, MRI, and fMRI to these models. Taken together, the course should provide a solid basis for the use of in vivo models of cerebral ischemia.

### Program details

#### Tuesday, June 7

Course II 'In vivo modeling of stroke'		KC-07
Chairs: Myron D. Ginsberg, University of Miami, USA & Akira Tamura, Tokyo, Japan		
13:30-13:45	<b>Image-analysis of experimental ischemic neuropathology</b> Weizhao Zhao (Miami)	
13:45-14:00	<b>Brain imaging in animal ischemia: promises and pitfalls:</b> <b>1. PET</b> W.D. Heiss (Cologne)	
14:00-14:15	<b>2. MRI</b> Matthias Hoehn (Cologne)	
14:15-14:30	<b>3. Functional MRI</b> Rick Dijkhuizen (Utrecht)	
14:30-15:00	<b>Summary and General Discussion</b> Myron Ginsberg (Miami)	

## Course I: Imaging of brain activity: Basic methods and underlying physiology

### General information

Brain Imaging based on vascular signals: fMRI, PET, and optical imaging

This course gives an introduction to non-invasive brain imaging methods based on vascular signals such as fMRI, optical imaging, and PET. For each method, basic technical aspects of data acquisition, data analysis, and stimulus design are described in detail. Special emphasis is laid on the physiological basis of the respective signal and the applicability of the methods in disease models and in the clinical setting. In a final talk, a role of each method in the “concert of functional brain imaging methods” is defined.

### Program details

**Tuesday, June 7**

Course I 'Imaging of brain activity: basic methods and underlying physiology' <i>Part 1 Basics of Brain Activation Studies (PET, fMRI)</i> Chair: Arno Villringer, Universitätsklinikum Charité, Berlin, Germany		Auditorium
09:00-09:45	<b>Introduction, Signals of vascular neuroimaging methods (fMRI ; PET, Optics)</b> A. Villringer	
09:45-10:30	<b>Basic physics, technical aspects of fMRI</b> B. Savoy	
10:30-11:15	<b>New Signals in fMRI: DWI, neuronal currents</b> P. Bandettini	
11:15-12:00	<b>Experimental Design and Basic Statistics of functional neuroimaging</b> R. Göbel	
12:00-12:45	<b>New Approaches to fMRI data analysis</b> E. Bullmore	
12:45-13:15	lunch break (exhibition & poster area)	
13:15-14:00	<b>Connectivity Studies based on Vascular Brain Imaging</b> C. Büchel	
14:00-14:45	<b>TMS and vascular brain imaging</b> T. Paus	
14:45-15:00	<b>General Discussion</b>	

## Course II: In vivo modeling of stroke

### General information

The proper experimental investigation of cerebral ischemia necessitates the use of physiologically regulated, reproducible animal models. The objective of this course is to provide a comprehensive exposition of animal models of cerebral ischemia. Major emphasis will be placed upon practical laboratory aspects, enabling the participants to develop and apply these models in their own laboratories. The rationale for the use of these models will be explored in detail, and their pitfalls and shortcomings will be presented. Expert speakers will cover both rodent models of focal ischemia (comprising mechanical, suture-occlusion, and photochemical models), as well as global-ischemia and larger-animal models. Other speakers will explore the neuropathology of ischemia, the importance of brain temperature regulation, experimental image-analysis, and the application of PET, MRI, and fMRI to these models. Taken together, the course should provide a solid basis for the use of in vivo models of cerebral ischemia.

### Program details

#### Tuesday, June 7

Course II 'In vivo modeling of stroke'		KC-07
Chairs: Myron D. Ginsberg, University of Miami, USA		
11:00-11:15	<b>Focal cerebral ischemia in the cat</b> Raymond Koehler (Baltimore)	
11:15-11:30	<b>Focal cerebral ischemia in primates</b> Gregory Del Zoppo (LaJolla)	
11:30-11:45	<b>Brain temperature monitoring and regulation</b> Frederick Colbourne (Edmonton)	
11:45-12:00	<b>Global ischemia models in rat and mouse</b> Nobutaka Kawahara (Tokyo)	
12:00-12:15	<b>Neuropathology of ischemia: necrosis, apoptosis, other</b> Roland Auer (Calgary)	
12:15-12:30	<b>Discussion</b>	

## Course I: Imaging of brain activity: Basic methods and underlying physiology

### General information

Brain Imaging based on vascular signals: fMRI, PET, and optical imaging

This course gives an introduction to non-invasive brain imaging methods based on vascular signals such as fMRI, optical imaging, and PET. For each method, basic technical aspects of data acquisition, data analysis, and stimulus design are described in detail. Special emphasis is laid on the physiological basis of the respective signal and the applicability of the methods in disease models and in the clinical setting. In a final talk, a role of each method in the “concert of functional brain imaging methods” is defined.

### Program details

**Tuesday, June 7**

Course I 'Imaging of brain activity: basic methods and underlying physiology' <i>Part 1 Basics of Brain Activation Studies (PET, fMRI)</i> Chair: Arno Villringer, Universitätsklinikum Charité, Berlin, Germany		Auditorium
09:00-09:45	<b>Introduction, Signals of vascular neuroimaging methods (fMRI ; PET, Optics)</b> A. Villringer	
09:45-10:30	<b>Basic physics, technical aspects of fMRI</b> B. Savoy	
10:30-11:15	<b>New Signals in fMRI: DWI, neuronal currents</b> P. Bandettini	
11:15-12:00	<b>Experimental Design and Basic Statistics of functional neuroimaging</b> R. Göbel	
12:00-12:45	<b>New Approaches to fMRI data analysis</b> E. Bullmore	
12:45-13:15	lunch break (exhibition & poster area)	
13:15-14:00	<b>Connectivity Studies based on Vascular Brain Imaging</b> C. Büchel	
14:00-14:45	<b>TMS and vascular brain imaging</b> T. Paus	
14:45-15:00	<b>General Discussion</b>	

## Course II: In vivo modeling of stroke

### General information

The proper experimental investigation of cerebral ischemia necessitates the use of physiologically regulated, reproducible animal models. The objective of this course is to provide a comprehensive exposition of animal models of cerebral ischemia. Major emphasis will be placed upon practical laboratory aspects, enabling the participants to develop and apply these models in their own laboratories. The rationale for the use of these models will be explored in detail, and their pitfalls and shortcomings will be presented. Expert speakers will cover both rodent models of focal ischemia (comprising mechanical, suture-occlusion, and photochemical models), as well as global-ischemia and larger-animal models. Other speakers will explore the neuropathology of ischemia, the importance of brain temperature regulation, experimental image-analysis, and the application of PET, MRI, and fMRI to these models. Taken together, the course should provide a solid basis for the use of in vivo models of cerebral ischemia.

### Program details

#### Tuesday, June 7

Course II 'In vivo modeling of stroke'		KC-07
Chairs: Myron D. Ginsberg, University of Miami, USA		
13:30-13:45	<b>Image-analysis of experimental ischemic neuropathology</b> Weizhao Zhao (Miami)	
13:45-14:00	<b>Brain imaging in animal ischemia: promises and pitfalls:</b> <b>1. PET</b> W.D. Heiss (Cologne)	
14:00-14:15	<b>2. MRI</b> Matthias Hoehn (Cologne)	
14:15-14:30	<b>3. Functional MRI</b> Rick Dijkhuizen (Utrecht)	
14:30-15:00	<b>Summary and General Discussion</b> Myron Ginsberg (Miami)	

# Course I: Imaging of brain activity: Basic methods and underlying physiology

## General information

Brain Imaging based on vascular signals: fMRI, PET, and optical imaging

This course gives an introduction to non-invasive brain imaging methods based on vascular signals such as fMRI, optical imaging, and PET. For each method, basic technical aspects of data acquisition, data analysis, and stimulus design are described in detail. Special emphasis is laid on the physiological basis of the respective signal and the applicability of the methods in disease models and in the clinical setting. In a final talk, a role of each method in the "concert of functional brain imaging methods" is defined.

## Program details

### Wednesday, June 8

<b>Course I 'Imaging of brain activity: basic methods and underlying physiology'</b> <b>Part 2 Optical Brain Imaging</b> Chair: Arno Villringer, Universitätsklinikum Charité, Berlin, Germany		Auditorium
17:00-17:45	<b>Optical Imaging: From Animal to Man</b> D. Boas	
17:45-18:30	<b>Optical Imaging of Brain Activity</b> H. Obrig	

## Course III Impact of anesthesia on CNS research

### Program details

Wednesday, June 8

<b>Course III 'Impact of anesthesia on CNS research'</b> Chair: Richard J. Traystman, Oregon Health & Sciences University, Portland, OR, USA		KC-07
17:00-17:30	<b>Mechanisms of Anesthetics on Brain</b> Oliver Kempfski, Johannes Gutenberg-University, Mainz, Germany	
17:30-18:00	<b>Anesthetics protect Brain from Ischemie</b> David Warner, Duke University, Durham, NC, USA	
10:30-11:15	<b>Anesthetics do not Protect Brain from Ischemie</b> Richard J. Traystman, Oregon Health & Sciences University, Portland, OR, USA	

# Course I: Imaging of brain activity: Basic methods and underlying physiology

## General information

Brain Imaging based on vascular signals: fMRI, PET, and optical imaging

This course gives an introduction to non-invasive brain imaging methods based on vascular signals such as fMRI, optical imaging, and PET. For each method, basic technical aspects of data acquisition, data analysis, and stimulus design are described in detail. Special emphasis is laid on the physiological basis of the respective signal and the applicability of the methods in disease models and in the clinical setting. In a final talk, a role of each method in the "concert of functional brain imaging methods" is defined.

## Program details

**Thursday, June 9**

<b>Course I 'Imaging of brain activity: basic methods and underlying physiology'</b> <b>Part 3 Functional Brain imaging: An integrative View</b> Chair: Arno Villringer, Universitätsklinikum Charité, Berlin, Germany		Auditorium
17:00-17:45	<b>Functional brain mapping: What do blood flow, glucose and oxygen consumption, BOLD, bolus tracking, ASL, and MEG have in common, if anything? Or: On the foundations of nephrology."</b> A. Gjedde	
17:45-18:30	<b>Beyond vascular brain imaging</b> A. Villringer	

## Course IV Stem Cells

### General information

The raise of neural stem cell biology has changed our views on what might be therapeutically possible in neurological and psychiatric disorders. Can lost neuronal populations be replaced from endogenous or transplanted sources? Regenerative adult neurogenesis in animal models of stroke and recruitment of endogenous and implanted precursor cells into ischemic lesions suggest that cellular plasticity could be used as a means to restore structure and function after damage. However, the found regeneration is minute and many fundamental questions are open. This short course gives an introduction to neural stem cell biology and adult neurogenesis and aims at conveying a realistic image of what neural stem cell biology might do for stroke research.

### Program details

**Thursday, June 9**

<b>Course IV 'Stem Cells'</b> Chair: Gerd Kempermann, Charité University Hospital and Max Delbrück Center for Molecular Medicine (MDC), Berlin, Germany		KC-07
17:00 – 18:30	The course is seminar-style and has three parts with ample time for discussion: <ol style="list-style-type: none"><li>1. <b>An introduction to neural stem cell biology</b></li><li>2. <b>An introduction to adult neurogenesis</b></li><li>3. <b>Neural stem cells and adult neurogenesis in stroke</b></li></ol>	

**COMPARTMENT-RESOLVED IMAGING OF ACTIVITY DEPENDENT DYNAMICS OF  
CORTICAL BLOOD VOLUME AND OXIMETRY****Amiram Grinvald, Rina Hildesheim, Ivo Vanzetta***Neurobiology, Weizmann Institute Rehovot, Rehovot, Israel*

Optical imaging, PET and fMRI all rely on vascular responses to image neuronal activity. Although these imaging techniques are successfully used for functional brain mapping, the detailed spatio-temporal dynamics of hemodynamic events in the various microvascular compartments have remained unknown. Here, we used high-resolution optical imaging in area 18 of anesthetized cats to explore sensory-evoked blood-volume (CBV) changes in the various cortical microvascular compartments, selectively. To avoid the confounding effects of hematocrit and oximetry changes, we developed and used a new fluorescent blood plasma tracer and combined these measurements with optical imaging of intrinsic signals at a near-isosbestic wavelength for hemoglobin (565nm). The vascular response began at the arteriolar level, rapidly spreading towards capillaries and venules. Larger veins lagged behind. Capillaries exhibited clear blood-volume changes. Arterioles and arteries had the largest response, whereas the venous response was smallest. Information about compartment-specific oxygen consumption dynamics was obtained in imaging sessions using 605nm illumination, a wavelength known to reflect primarily oximetric changes, thus being more directly related to electrical activity than CBV changes. Those images were radically different: the response began at the parenchyma level, followed only later by the other microvascular compartments. These results have implications for the modeling of fMRI responses and suggest that the Balloon Model in its original formulation needs to be modified. Furthermore, functional maps obtained by imaging the capillary CBV response were similar but not identical to those obtained using the early oximetric signal, suggesting the presence of different regulatory mechanisms underlying these two hemodynamic processes.



## NEURONAL BASIS OF NEUROIMAGING IN MOTOR NETWORKS

Mark Hallett

*Human Motor Control Section, NINDS, Bethesda MD, USA*

In attempting to understand the physiology of the brain, it is most helpful to combine a number of imaging and physiological techniques. A multimodality approach with fMRI, EEG and transcranial magnetic stimulation (TMS) allows a comprehensive non-invasive approach. There needs to be particular caution using the BOLD technique for fMRI since it is so far removed from neuronal events. Recent demonstrations are reassuring that show perfusion technique results to be similar to BOLD results.[1] The main executor of movement in the cortex is the contralateral primary motor cortex (M1) and generally it shows the largest BOLD signal in fMRI experiments. The timing of M1 activity can be seen with the latter part of the movement-related cortical potential (MRCP) with EEG measurements. M1 activity is greater with more frequent movements, movements with greater amplitude and with greater force. In no-go trials of go/no-go experiments, there is no fMRI activity in M1 suggesting that nothing is happening.[2] However, there is similar EEG activity compared with go trials, and TMS studies show active inhibition,[3] suggesting that there is inhibitory activity in M1, but that this does not reveal itself with fMRI. The failure of fMRI to show change in this circumstance has been interpreted as due to the fact that inhibition does not take as much metabolic energy as excitation. On the other hand, prolonged suppression of a motor action does show a negative BOLD response (as well as TMS inhibition), suggesting that with inhibition over a longer time, the activity in the network is diminished.[4] Some fMRI studies show an increased activity in the ipsilateral motor cortex while others show a decrease. EEG shows similar activity contralaterally and ipsilaterally in the early part of the MRCP and less activity ipsilaterally in the latter part of the MRCP. TMS can show excitation or inhibition depending on the motor task. Detailed analysis of the fMRI signal shows that increases likely derive from premotor cortex and decreases from M1.[5] Hence, ipsilateral M1 may be inhibited and ipsilateral premotor cortex excited. 1. Garraux, G., M. Hallett, and S.L. Talagala, CASL fMRI of subcortico-cortical perfusion changes during memory-guided finger sequences. *Neuroimage*, 2005;25:122-32. 2. Waldvogel, D., et al., The relative metabolic demand of inhibition and excitation. *Nature*, 2000;406:995-8. 3. Sohn, Y.H., K. Wiltz, and M. Hallett, Effect of volitional inhibition on cortical inhibitory mechanisms. *J Neurophysiol*, 2002;88:333-8. 4. Hummel, F., et al., To act or not to act. Neural correlates of executive control of learned motor behavior. *Neuroimage*, 2004;23:1391-401. 5. Hanakawa, T., et al., Finger and face representations in the ipsilateral precentral motor areas in humans. *J Neurophysiol*, 2005 (in press)



## NEURONAL BASIS OF OPTICAL IMAGING SIGNALS IN SENSORY CORTEX

Anna Devor<sup>1,2</sup>, Istvan Ulbert<sup>1,4</sup>, Andrew K. Dunn<sup>1</sup>, Suresh N. Narayanan<sup>1</sup>, Stephanie R. Jones<sup>1</sup>,  
Mark L. Andermann<sup>1</sup>, David A. Boas<sup>1</sup>, Anders M. Dale<sup>2,3</sup>

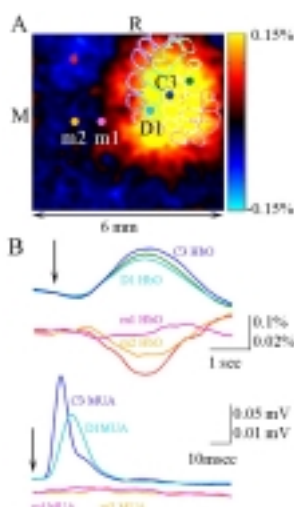
<sup>1</sup>MGH, Harvard Medical School, Charlestown, USA

<sup>2</sup>Department of Neurosciences, UCSD, San Diego, USA

<sup>3</sup>Department of Radiology, UCSD, San Diego, USA

<sup>4</sup>Institute for Psychology of the Hungarian Academy of Sciences, Budapest, Hungary

The advent of non-invasive imaging methods such as functional magnetic resonance imaging (fMRI) has made it possible to obtain spatial maps of hemodynamic 'activation' in the human brain under a variety of conditions. However, the indirect and poorly understood nature of the coupling between these hemodynamic signals and the underlying neuronal activity has greatly limited the interpretability of neuroimaging results. In our laboratory, we address the question of coupling between pre- and post-synaptic neuronal activity, and the hemodynamic response in rodent somatosensory cortex in response to a localized tactile stimulus. We use full-field multiple-wavelength (spectroscopic) optical imaging of the intrinsic signals that enables simultaneous measurements of oxyhemoglobin (HbO), deoxyhemoglobin (Hb) and total hemoglobin (HbT) and simultaneous electrophysiological recordings of spiking and synaptic activity. Our results show that (1) the hemodynamic response within one cortical column as a function of the stimulus intensity increases beyond saturation of local spiking and synaptic activity. Therefore, a "point" hemodynamic response is a non-linear function of neuronal activity. (2) This disproportional increase in the local hemodynamic response cannot be explained by increasing per-synaptic activity, because inputs from the thalamus (VPM and POm) show saturation with an increase in the stimulus intensity similar to the one demonstrated by the local activity in the cortex. (3) The non-linearity can be explained at least in part by the fact that a point hemodynamic measure is influenced by neuronal activity across multiple cortical columns. (4) HbO and HbT hemodynamic responses can be well approximated by space-time separable functions with an antagonistic center-surround spatial pattern extending over several millimeters. The surround "negative" hemodynamic activity does not correspond to observable changes in neuronal activity (see figure). Thus, the hemodynamic response is not just a temporal convolution of the neuronal activation, but is also a spatial convolution. Consequently, attempts at characterizing the neurovascular relationship based on point measurements of electrophysiology and hemodynamics may yield inconsistent results, depending on the spatial extent of neuronal activation. The complex spatial integration of the hemodynamic response should be considered when interpreting fMRI data in terms of neuronal activity.



A. A ratio image of HbO at the peak of the response. Electrophysiological recordings were performed at the locations of D1 and D2 barrels inside Barrel field and m1 and m2 outside Barrel field. B. Timecourses of HbO (top) and spiking activity (bottom) from the locations shown in A. The locations are color coded. The vertical scale for the locations outside Barrel field is magnified  $\times 5$ . Arrows denote stimulus delivery. M=medial, R=rostral, MUA= multiple unit activity.



**INV04**

**READING VASCULAR CHANGES IN BRAIN IMAGING: IS DENDRITIC CALCIUM  
THE KEY?**

**Martin J. Lauritzen**

*University of Copenhagen, Copenhagen, Denmark*

A key goal in functional neuroimaging is to track the neuronal correlates of mental activity based on signals related to local changes in metabolism and blood flow. Recent findings indicate that the dendritic processing of excitatory synaptic inputs correlates more closely than the generation of spikes with the brain imaging signals. The correlation is often non-linear and context-sensitive, and cannot be generalized for every condition or brain region. The vascular signals are mainly produced by rises in intracellular calcium in neurons and possibly astrocytes, which activate key enzymes that produce vasodilators to generate increments in flow and, in turn, the positive BOLD (blood-oxygen-level-dependent) signal. Our new knowledge of the cellular mechanisms of functional brain imaging signals place constraints on the interpretation of the data.



**INTRODUCTION TO THE NEUROVASCULAR UNIT****Thomas P. Jacobs***Neural Environment Cluster, Ninds/nih, Bethesda MD, USA*

For many years, a neurocentric view toward mechanisms of ischemic brain injury and repair has significantly contributed to our knowledge of the molecular pathways of excitotoxicity, oxidative stress and apoptosis. However, translation of these laboratory results into clinically effective stroke treatments remains a major challenge. To address this issue and the prediction that strokes will increase in our aging population, the U.S. Congress requested the National Institute of Neurological Disorders and Stroke (NINDS) to develop a stroke research action plan through the Stroke Progress Review Group (SPRG). The SPRG identified research on the cellular and functional interactions among the capillaries, glia, and neurons of the brain, termed the 'neurovascular unit' (NVU), as a top priority. The NVU strategy looks beyond the single cell for a more integrative answer to ischemic brain damage which may be closer to modeling the clinical reality. The NVU construct is intended to facilitate a better understanding of the integration of cerebrovascular and neurobiological mechanisms in the development of the healthy brain, in the maintenance of function in the aging brain, and in neurological disorders and stroke. A major goal is to improve our knowledge of cell-cell communication within the NVU and how vascular function may contribute to the initiation and/or progression of neurological diseases over the lifespan. The NVU concept focuses attention on the interactions among cells of the brain and blood vessels and includes the endothelium, extracellular matrix, glia, pericytes and neurons. After ischemia, perturbations in neurovascular functional integrity initiate several cascades of injury. Neuronal cell death ultimately underlies ischemic brain injury and the NVU concept suggests that proximal triggers in endothelium play an important upstream role. For example, signals such as oxidative stress, together with neutrophil and/or platelet interactions with activated endothelium, upregulate matrix metalloproteinases, plasminogen activators and other proteases, which degrade matrix and lead to blood-brain barrier leakage. Disruption of cell-matrix homeostasis might also trigger cell death pathways in both vascular and parenchymal compartments. Refocusing research on how endothelial injury affects brain tissue damage applies not only to stroke, but may also contribute to understanding neurodegenerative disorders, like vascular dementia, Alzheimer's disease, MS and ALS, in which vascular changes are observed. Thrombolysis trials firmly establish the idea that timely reperfusion can salvage the ischemic brain. The efficacy of hypothermia so far confirms that multiple molecular cascades are indeed operational in human brain and that neuroprotection is an achievable goal. Ultimately, new approaches for targeting the NVU, based on biological considerations, could be developed to improve potential combination or multi-targeted treatments for stroke and other neurological disorders.

**INV-06**

**tPA AS AN EFFECTOR OF MICROGLIAL ACTIVATION**

Jian Wang, Iordanis Gravanis, John Sheehan, **Stella Tsirka**

*University Medical Center at Stony Brook, Stony Brook NY, USA*

Tissue Plasminogen Activator (tPA) is currently the only FDA approved treatment of thrombotic stroke. It is expressed at high levels in the murine brain parenchyma by neurons and microglia, and is thought to regulate physiological processes that include tissue remodeling, plasticity and neurite outgrowth. Such functions have been attributed to its ability to initiate proteolytic cascades that lead to the processing or degradation of extracellular matrix proteins and possibly other substrates. Other roles of tPA involve non-proteolytic events, such as protein-protein interactions, in functions like microglial activation, interaction with zinc, seizures from ethanol withdrawal. However, it has also been implicated in brain pathologies, that proceed via an excitotoxic mechanism, thus raising concern about its use as a safe therapeutic agent. Understanding the role(s) of tPA, both proteolytic and non-proteolytic, as well as the function of activated microglia would allow to elucidate aspects of physiologic and pathologic brain function and could potentially improve the available therapies of neurological disease.

**TPA AS AN 'INTERFACE' BETWEEN BLOOD AND BRAIN**

**Denis Vivien**

*INSERM-Avenir, Université De Caen, GIP CYCERON, Caen, France*

Over the last decade, tPA has been implicated in a variety of brain functions. It is secreted from growth cones or extending neurites, it modulates neurite outgrowth and promotes neuronal migration. tPA has also been involved in physiological glutamatergic-dependent processes such as synaptic plasticity and long term potentiation. In addition, t-PA has been shown to play an important role in the pathogenesis of seizure, multiple sclerosis, trauma and ischemic brain injury. In a previous study, we have shown that the proteolytic activity of t-PA enhances the N-methyl-D-aspartate (NMDA) receptor-mediated signalling (Nicole et al., 2001). Here, we provide evidences that tPA is able to cross the intact blood brain barrier both in vitro and in vivo and that this mechanism is independent of its proteolytic activity and mediated by an interaction with a LDL-related receptor, LRP. Overall, these data suggest that blood-derived tPA could influence neuronal functioning. Accordingly, intravenous injection of tPA potentiates the NMDA-induced brain lesion in rats even in the absence of blood brain barrier leakage. As a model demonstrating that preventing the NMDA-dependent effect of tPA could improve the efficiency of thrombolysis in the treatment of stroke, we evidence that the blood-derived tPA failed to enhance NMDA-dependent signalling in a model of mice previously vaccinated with the amino-terminal domain (ATD) of NR1 subunit of the NMDA receptor. Thus, we propose a new concept suggesting that tPA is one of the key element of the interface between the blood and the brain parenchyma.



**PLASMINOGEN ACTIVATORS AND SYNAPTIC PLASTICITY****Nicholas W. Seeds***Neuroscience, University of Colorado HSC, Denver CO, USA*

In addition to its role in the vascular system, plasminogen activator (PA) is involved in neural development, excitotoxic cell death, and has been implicated in aspects of cerebral synaptic remodeling associated with cerebellar motor learning, visual cortex ocular dominance columns, and hippocampal & corticostriatal LTP. During a complex motor task cerebellar granule neurons show a rapid and transient induction of mRNA for the extracellular protease tissue plasminogen activator (tPA). This induction of tPA is cerebellar specific, and is not seen in the cerebella of exercised or stressed mice, and is distinct from simple performance phenomena. Knock-out mice lacking the tPA gene show a significant reduction in both rate and extent of learning the complex motor task. Furthermore, blocking tPA activity by infusion of PAI-1 or tPA-STOP during training dramatically impairs motor learning. Thus, tPA plays an important role in motor learning, in which tPA may facilitate synaptic plasticity. We have explored the possibility that PA may also play a role in synaptic plasticity in the spinal cord. The crossed phrenic phenomenon (CPP) describes respiratory functional plasticity that arises following spinal cord injury; whereby, phrenic motoneuron drive to the diaphragm is restored following activation of “functionally ineffective” medullary respiratory neuron synapses on phrenic motoneurons (PMN). Synaptic remodeling is thought to occur during the characteristic delay period following spinal cord injury before the CPP becomes functional. The mechanisms underlying this synaptic plasticity are not well-defined. Our ultimate aim is to understand the underlying molecular mechanisms of this functional recovery using a mouse model amenable to a molecular genetic approach, and ours is the first report of CPP in mice. Using electromyographic (EMG) recordings from the diaphragm, we examined the inter-operative delay time between spinal cord hemisection and contralateral phrenicotomy required for diaphragm response, as compared to animal death from asphyxia at zero time. For each animal, a spinal cord hemisection was performed on the left side at C2. A contralateral phrenicotomy was performed the next day (overnight animals), 6-8 hours, 4-5 hours, or 1-2 hours post-hemisection. As the inter-operative delay was reduced, the proportion of mice displaying the CPP decreased from 100% for overnight animals, 94% in 6-8h, 82% in 4-5h, to 76% for 1-2 h mice. A critical 1-2hr window is required for this synaptic plasticity. In situ hybridization shows that uPA and tPA mRNAs are rapidly induced in C4-5 ventral spinal cord neurons in the ipsilateral phrenic nucleus compared to the contralateral PMN and sham controls, with markedly elevated tPA protein at 1hr. post-hemisection. This specific and concomitant induction of PA suggests a role in CPP spinal cord plasticity, which may ultimately lead to therapeutic uses for PA in spinal cord injury.



**THROMBOLYSIS - WHERE WE ARE**

**W. Hacke**

*Department of Neurology With Policlinic, UniversitätsKlinikum Heidelberg, Heidelberg, Germany*

After approval of thrombolytic therapy in the USA, Canada Europe and many parts of Asia, decisions for wider approval of i.v. t-PA in a three hour time window are still pending. While the individual study basis for i.v. rt-PA is in public domain for quiet a while, there are new aspect of intravenous thrombolysis, on which this presentation will focus. They include 1. results from combined analysis of 6 rt-PA trials (ATLANTIS A and A, ECASS I and II and NINDS part I and II) 2. the usefulness of MRI assisted patient selection 3. new developments to enhance the efficacy of thrombolytic therapy with focus on new devices and combination therapies 4. Results from recent trials such as DIAS and AbESTT



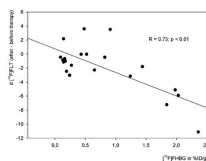
## IMAGING-GUIDED GENE THERAPY OF GLIOMAS

Andreas H. Jacobs<sup>1,2,3</sup>, Maria A. Rueger<sup>1,2</sup>, Alexandra Winkeler<sup>1,3</sup>, Huongfeng Li<sup>1,2</sup>,  
Markus Klein<sup>2,3</sup>, Matthias Stoeckle<sup>1</sup>, Parisa Monfared<sup>1,3</sup>, Rudolf Graf<sup>1</sup>, Stefan Vollmar<sup>1,2</sup>,  
Klaus Wienhard<sup>1,2</sup>, Wolf-Dieter Heiss<sup>1,2,3</sup>

<sup>1</sup>MPI For Neurological Research, Cologne, Germany, <sup>2</sup>Department of Neurology, University of Cologne, Cologne, Germany, <sup>3</sup>Centre for Molecular Medicine Cologne (CMMC), Cologne, Germany

**Introduction:** The combination of transgenes encoding for prodrug-activating enzymes is a promising approach in current gene therapy protocols. The enzymes *E. coli* cytosine deaminase and herpes simplex virus type 1 thymidine kinase have been shown to act synergistically. Using positron emission tomography (PET) we determined the *in vivo* transduction efficiency mediated by HSV-1 amplicons using the HSV-1-tk as PET marker gene to monitor the effects of prodrug therapy. **Methods:** Human Gli36dEGFR glioma cells were grown as s.c. tumors in 22 nude mice and transduced *in vivo* by HSV-1 amplicons carrying the genes for cytosine deaminase (cd), viral thymidine kinase (tk39) and gfp (HSV-cdIREStk39gfp). Non-transduced Gli36dEGFR tumors served as negative controls, retrovirally transduced Gli36dEGFR cells stably expressing cdIREStkgfp as positive control. Following transduction, therapeutic i.p. prodrug application was performed with 5-fluorocytosine and ganciclovir. Tumor sizes were measured using calipers and growth slopes were calculated. PET-imaging was performed in 11 mice. [18F]FHBG-PET was performed after *in vivo* transduction prior to therapy to evaluate transduction efficiency [%ID/g]. [18F]FLT-PET was performed as baseline evaluation prior to *in vivo* transduction and as therapy monitoring after 1 week of therapy. Background-corrected accumulation of [18F]FLT [%ID/g] was determined. Therapeutic efficiency was quantified by the difference of [18F]FLT-accumulation before and after therapy ( $\Delta$ FLT). **Results:** Positive control tumors were successfully treated with prodrugs leading to disappearance of tumors within 10 days. 15/22 *in vivo* transduced tumors responded to prodrug therapy; 4 tumors disappeared completely (complete responders) and 11 tumors showed decelerated growth compared to respective negative controls (partial responders). Growth slopes of tumors responding to gene therapy were significantly less steep compared to negative controls ( $p < 0.05$ ). Transduction efficiency as measured by [18F]FHBG-accumulation was  $1.22 \pm 0.83$  %ID/g for stably transfected tumors and  $0.37 \pm 0.30$  %ID/g for *in vivo* transduced tumors. In stably transduced tumors, therapeutic effects could be monitored by PET with significant differences in [18F]FLT-accumulation before ( $3.38 \pm 3.65$  %ID/g) and after therapy ( $0.06 \pm 0.19$  %ID/g;  $p = 0.01$ ). 8/11 *in vivo* transduced tumors showed a significantly lower [18F]FLT-accumulation after therapy ( $1.91 \pm 1.12$  vs.  $0.42 \pm 1.31$  %ID/g;  $p < 0.01$ ), while in 3 tumors [18F]FLT-accumulation was increased. For stably and *in vivo* transduced tumors, the level of exogenous gene expression or transduction efficiency as measured by [18F]FHBG-PET correlated well to the resulting therapeutic efficiency as measured by [18F]FLT-PET ( $r = 0.73$ ;  $p < 0.01$ , Fig.). Volumetric data did not correspond to [18F]FLT-PET data in assessment of therapeutic response. Consecutively, transduction efficiency in [18F]FHBG-PET did not correlate to therapeutic efficiency as measured by volumetry. **Conclusion:** Therapeutic efficiency can be non-invasively followed and quantified by microPET using [18F]FLT. Transduction with HSV-1 amplicon vectors *in vivo* causes distinct levels of gene induction, which correlate well to the effect of gene therapy as measured by [18F]FLT-PET imaging. Volumetry gives complementary information in assessing response to gene therapy.

**Grant support:** Supported in part by MSWF 516-400 002 99, ZMMK-TV46, DFG-Ja 981/1-2, EU-6thFW-EMIL



**NEURORECEPTOR EXPRESSION AS SURROGATE MARKERS FOR DEMENTIAS****Gitte M. Knudsen***NRU 9201, University Hospital Rigshospitalet, Copenhagen, Denmark*

According to international consensus, dementia is defined as a gradually onset of multiple cognitive deficit centered by memory disturbances, interfering with the daily life activities and related to organic brain lesions. The diagnosis of dementia can, particularly later in stages of the disease, be made with a reasonable certainty on the basis of neuropsychological testing. Yet, neuropsychological testing is not fully quantitative and objective and it does not allow for an objective and reproducible follow-up. For these reasons a search for biomarkers to identify and follow disease has been so actively pursued. The identification of reliable biomarkers (or surrogate markers) for dementia disorders is likely to contribute not only to a better understanding of the underlying pathophysiology, but may also work as an efficient tool to identify subjects at risk, for (sub)classification of disease, and to objectively monitor treatment response. With the increased prevalence of dementia with age, an aging population and the promise of disease-modifying therapies the characterization of the early stages of various types of dementia, in particular Alzheimer's disease (AD), biomarkers have become a topic of major research interest within dementia research. From human postmortem brain studies it is well documented that pronounced changes occur within several neurotransmitter system both in normal ageing and in dementia; for AD this is particularly well documented for the cholinergic transmitter system. With the new emerging techniques, including molecular imaging of the neurotransmitter systems with positron emission tomography (PET) or single photon emission tomography (SPET) the functional state of human central receptor systems brain can be assessed in vivo. When used with appropriate radioligands, PET and SPET can reveal the distribution of neuroreceptors in the living human brain, and their interactions with neurotransmitters or administered drugs. Based on previous imaging studies it seems that several- but not all - brain receptor densities decline with age but the rate of decline varies between the transmitter systems. Further, within one system the decline in density may also differ between different brain regions. These are important observations that necessitates a close matching between control and patient groups in imaging studies. In the presentation a review of neurotransmitter dysfunction in the most prevalent dementia disorders will be given. The focus will be primarily on Alzheimer's disease, but Lewy body dementia and frontotemporal dementia will also be discussed. Among the primary degenerative disorders, AD is the most extensively investigated when it comes to neuroreceptor studies. In postmortem studies marked reductions in some of the receptor systems, in particular 5-HT<sub>2</sub> receptors, nicotinic alpha<sub>4</sub>-beta<sub>2</sub>, and a preferential loss of M<sub>2</sub> as compared to M<sub>1</sub> muscarinic receptors have been found. Studies of muscarinic and dopaminergic receptors have shown conflicting results. Some of these findings have been partially replicated in in-vivo imaging studies: a decrease in 5-HT<sub>2</sub>, nicotinic, and possibly muscarinic receptors. As more and more radioligands become available, neuroreceptor imaging may become an important tool to diagnose, classify, and monitor dementia disorders.



**MONITORING STEM CELL MIGRATION IN THE NERVOUS SYSTEM BY IN VIVO MAGNETIC RESONANCE IMAGING**

**Mathias Hoehn**, Uwe Himmelreich, Ralph Weber, Pedro Ramos-Cabrer, Susanne Wegener,  
Dirk Wiedermann, Ekkehard Küstermann

*Max-Planck-Institute for Neurological Research, Cologne, Germany*

The fast growing understanding in stem cell biology has led to the exploration of the therapeutic potential of endogenous or implanted stem cells as a cell replacement therapy for stroke. Arvidsson et al. (1) demonstrated a significant activation of neurogenesis in the subventricular zone of ischemic rats while Helen Hodges (2) reported on migration of implanted embryonic stem cells towards the lesion periphery in ischemic rats, followed by outcome improvements relative to animals without cell implantations. These studies depended on established invasive techniques requiring the sacrifice of large groups of animals to investigate the temporal profiles of dynamical parameters such as migrational activity or cell differentiation in response to either cerebral lesion or (patho-)physiological factors. It is therefore highly desirable to exploit a noninvasive imaging technique such as MRI to observe (implanted) stem cells in a longitudinal study. A few laboratories (3,4) have begun to label stem cells with MRI contrast agents, preferably ultrasmall superparamagnetic iron oxide nanoparticles (USPIOs) to detect the cells with strong contrast against the background tissue of the host organ. Optimizing the MRI scanner hardware and the complete in vivo protocol we have recently succeeded in performing ultra-high MR imaging with isotropic resolution of 78 $\mu$ m, at an experimental time of only less than 70 min, thus making a longitudinal study with repetitive anesthesia sessions easily tolerable even for lesioned animals (5). The USPIO-induced hypointensity of the stem cells however leads to various situations making an unambiguous assignment for the contrast to the cells difficult. We have found that under ischemic conditions, a rather delayed vascular degradation leads to iron uptake by macrophages in the vicinity of the leaky vessels, thus producing an image contrast closely similar to that of stem cells spread out over the periphery of an ischemic lesion (6). Further, strategies will be discussed to distinguish hypointense contrast of vascular origin (BOLD effect) from that of stem cells by exploiting physiological modulation of the signal intensity and contrast mechanisms (7). Finally, new labeling strategies will be presented in an effort to avoid the confounding factors of the USPIO induced hypointensity and explore the potential of a new generation of MR contrast agents: Gd based chelates which can be used as enzyme activity or gene expression reporters. The presentation will discuss the potential and challenges of stem cell monitoring in the intact organism using highly resolved MR imaging. Particular focus will be given to cells implanted into rat or mouse brain. Chances for future applications of imaging not only localization of implanted cells but also their functional status (e.g. migration; differentiation; transformation) will be presented. 1) A. Arvidsson et al. *Nature Med.* 8, 963 (2002); 2) T. Veizovic et al. *Stroke* 32, 1012-1019 (2001); 3) J.W.M. Bulte et al. *Nature Biotechnol.* 19, 1141-1147 (2001); 4) M. Modo et al. *NeuroImage* 17, 803-811 (2002); 5) M. Hoehn et al. *Proc.Nat.Acad.Sci. USA* 99, 16267-16272 (2002); 6) R. Weber et al. *Magn.Reson.Med.* In press 2005; 7) U. Himmelreich et al. *Molec. Imag.* In press 2005



**GENE THERAPY FOR ISCHEMIC NEURONAL INJURY****Midori A. Yenari<sup>1</sup>, Heng Zhao<sup>2</sup>, Robert M. Sapolsky<sup>2,3</sup>, Gary K. Steinberg<sup>2</sup>**

<sup>1</sup>*Department of Neurology, University of California, San Francisco & San Francisco Veterans Affairs Medical Center, San Francisco CA, USA*

<sup>2</sup>*Department of Neurosurgery, Stanford University, Stanford CA, USA*

<sup>3</sup>*Department of Biological Sciences, Stanford University, Stanford CA, USA*

Advances in the area of stroke and other related disorders have identified a variety of molecular targets for potential therapeutic intervention. The use of modified viral vectors has now made it possible to introduce foreign DNA into central nervous system cells, permitting overexpression of a protein of interest. A particular advantage of the herpes simplex system is that the virus is neurotropic, and is therefore suited for relatively selective gene therapy to neurons. The vectors used by our group to date utilize an amplicon based bipromoter system which permits expression of both the gene of interest as well as a reporter gene. Using this strategy, we have shown that potentially neuroprotective genes can be transferred to individual central nervous system cells, and can confer a relative resistance to cerebral ischemic and excitotoxic insults. We previously reported that gene therapy using a neurotropic herpes simplex viral (HSV) vector system containing bipromoter vectors to transfer various protective genes to neurons. Using this system in experimental models of stroke, cardiac arrest and excitotoxicity, we have found that it is possible to enhance neuron survival against such cerebral insults by overexpressing genes that target various facets of injury. Of the genes studied by our labs, we have shown that glucose transporter (GLUT-1), the calcium binding protein calbindin D28K (CaBP), anti-oxidant genes glutathione peroxidase (GPx) and catalase (CAT), the anti-apoptotic protein Bcl-2 and the 70 kDa heat shock protein (HSP70) improve neuron survival after ischemia and excitotoxicity. Bcl-2, GPx and HSP70 also appear to protect when administered post insult. Because the extent of vector uptake is limited, it is not generally possible to affect overall infarct size or behavior. Regardless, we have demonstrated that for some cases, gene transfer may also improve cell function. Gene transfer can also be used in combination with other potential neuroprotective strategies with synergistic effects. For instance, mild hypothermia is well known to protect the brain from experimental brain ischemia provided brain cooling begins within hours of ischemia onset. This hypothermic neuroprotection is also associated with Bcl-2 upregulation in some instances, and hypothermia suppresses many aspects of apoptotic death. Our recent work has shown that two different kinds of protective therapies, Bcl-2 overexpression and hypothermia, both inhibit aspects of apoptotic cell death cascades, and combination of hypothermia with Bcl-2 gene transfer will prolong the temporal therapeutic window for Bcl-2 gene therapy. Some limitations of this technique exist, the main ones being that of delivery and extent and duration of transfection. Part of the limited duration of gene expression may be due to a localized tissue inflammatory response to the vectors themselves. This problem may be partially surmounted by the coadministration of anti-inflammatory treatments to prolong survival of transfected cells. While neuronal gene therapy for cerebral ischemia is still limited by the numbers of cells which vectors can transfect, it provides a powerful tool to understand mechanisms of cell death and identify potential molecular targets for therapy.



**GENE THERAPY USING ADENOVIRUS****Takeshi Hayashi**

*Department of Neurology, Okayama University Graduate School of Medicine and Dentistry, Okayama, Japan*

Glial cell line-derived neurotrophic factor (GDNF) has a strong neuroprotective property. It prevents neuronal cell death in various situations, and intracerebroventricular injection of this molecule actually reduced ischemic brain injury in vivo. However, GDNF needs to be given intracerebroventricularly because the blood-brain barrier inhibits its entry into the brain parenchyma from intravascular space. In order to get over this problem, gene transfer could be a promising method. Adenovirus is an appropriate vector to transfer genes into the brain, because this virus successfully infects non-dividing cells as neurons. In the ischemic brain, however, initiation of protein synthesis is inhibited, and thus, whether transferred gene becomes translated into protein remained uncertain. In an attempt to clarify this issue, we injected adenovirus containing lacZ gene into the brain after transient or permanent middle cerebral artery (MCA) occlusion. In the brain after transient MCA occlusion, lacZ activity was not or only minimally observed in the reperfused brain until 2 days. However, the activity dramatically increased at 7 days of reperfusion at a level similar to that of the control, which diminished by 21 days. In the brain with permanent MCA occlusion, lacZ activity was increased from 8 hour to 2 days in the MCA territory, which was less stronger than that of the control. Based on the finding of the successful expression of transferred lacZ gene, we injected adenovirus containing GDNF gene into the brain followed by making transient MCA occlusion. The infarction volume was measured with 2,3,5-triphenyltetrazolium chloride staining method, and it was revealed that GDNF-containing adenovirus reduced the infarction volume at 1 day of reperfusion. The numbers of TUNEL, immunoreactive caspase-3, and cytochrome c-positive neurons were markedly reduced in the GDNF gene transferred group, suggesting that amelioration of brain damage was caused by reduction of apoptotic signals activation. As the next step, we investigated therapeutic time window of GDNF gene-containing adenovirus. In the group of adenovirus injection at just before or just after the MCA occlusion, the infarction volume was significantly smaller than the control group. On the other hand, adenovirus injection at 1 hour after the reperfusion failed to reduce the infarction volume. This means that the GDNF gene transfer with use of adenovirus could be effective for treating stroke, if the vector was applied at an early time after the ischemic insult.



**CELL REPLACEMENT THERAPY AFTER STROKE BY RECRUITMENT OF ENDOGENOUS NEURAL PROGENITORS**

**Nobutaka Kawahara**<sup>1,5</sup>, Hirofumi Nakatomi<sup>1</sup>, Toshihiko Kuriu<sup>2</sup>, Shigeo Okabe<sup>2</sup>, Akira Tamura<sup>3,5</sup>,  
Masato Nakafuku<sup>4,5</sup>, Taaaki Kirino<sup>1,5</sup>

<sup>1</sup>*Department of Neurosurgery, The University of Tokyo Graduate School of Medicine, Tokyo, Japan*

<sup>2</sup>*Department of Anatomy and Cell Biology, Tokyo Medical and Dental University, Tokyo, Japan*

<sup>3</sup>*Department of Neurosurgery, Teikyo University School of Medicine, Tokyo, Japan*

<sup>4</sup>*Center for Developmental Biology, Cincinnati Children's Hospital Research Foundation, Cincinnati, USA*

<sup>5</sup>*SORST, Japan Science and Technology Corporation (JST), Japan*

Central nervous system injuries, such as stroke, lead to significant neuronal death in vulnerable regions of the brain, accompanied by corresponding loss of neuronal function. Recent evidence that neural stem cells or progenitors still persist in the adult mammalian brain has provided new possibility to repair such neuronal damage by recruitment of these progenitors. Here, we sought whether such neuronal regeneration could be achieved from endogenous neural progenitors in the hippocampal CA1 region following global ischemia. Rats were subjected to 6 minute global ischemia using 4—vessel occlusion and hypotension, and the growth factors (EGF and FGF-2) were infused into the ventricle from Day 2 to Day5 to augment the endogenous capacity. At Day 7, severe neuronal loss was observed even after the treatment, where only 2% of cells remained. Though these growth factors may have neuroprotective action, the treatment initiated from Day2 did not show neuroprotection. At Day 28, however, a significant increase in number of neurons, stained with cresyl-violet and neuronal marker NeuN, were observed in the treated animals, which amounted to 40 % of normal controls. These neurons were positively stained by BrdU after labeling during the treatment, indicating that they are newly produced neurons. Immunostaining for BrdU, progenitor markers (Pax 6, Mash 1), and Dil/retrovirus labeling, indicated that these newly produced neurons are derived from dormant neural progenitors residing in the paraventricular region above the CA1 field, a region that has not been recognized to harbor such progenitors. Morphologically, the regenerated neurons made synaptic connections with the existing neuronal circuit, as evidenced from electron microscopic studies. Electrophysiologically, fEPSP, which were lost after ischemia, was partially recovered, as well as long-term potentiation. In behavioral study using the water maze task, the treated animals exhibited higher performance compared with the untreated animal. Collectively, these data showed that dormant neural stem cells or progenitors exist in the periventricular region, where neurogenesis does not normally occur physiologically in the mature adult brain. Once neuronal death after ischemia takes place, these progenitors respond to the insult. However, endogenous capacity of this response is limited in the adult brain. Augmentation of the proliferation by growth factors after ischemia is capable of potentiating this endogenous capacity to replace the lost neurons, which also led to improved neuronal function. The data presented here showed a remarkable capacity of adult neural progenitors to repair ischemic injury in the hippocampal CA1. Accumulating evidence from other studies revealed that, in addition to classical neurogenic regions (subgranular layer of the hippocampal dentate gyrus and anterior subventricular zone), dormant or slowly proliferating neural stem or progenitors exist widely, such as around the third ventricle and the midbrain aqueduct. Recruitment of these progenitors to repair various ischemic injury may provide a new therapeutic approach for stroke.



**TAT FUSION PROTEINS AS INNOVATIVE TREATMENT STRATEGY IN STROKE**

**Ertugrul Kilic**

*University of Zurich, Department of Neurology, Zurich, Switzerland*

The delivery of proteins across the blood-brain barrier is severely limited by the proteins' size and biochemical properties. Thus, a large number of peptides have been characterized in recent years that efficaciously prevent neuronal death in vitro, but which may not be applied in vivo, since they are unable to cross cell membrane barriers. In the 1990ies, it had been shown that the HIV TAT protein is able to cross cell membranes even when coupled with larger peptides. Subsequent studies with fusion proteins of the 11-amino acid protein transduction domain of HIV-TAT revealed that TAT fusion proteins may successfully be used for therapeutic purposes in vivo, even when systemically applied. Indeed, intravenous delivery of TAT proteins linked with anti-apoptotic and neurotrophic factors resulted in a rapid and highly efficacious transduction of the brain tissue. When administered after focal cerebral ischemia, intravenous TAT-proteins significantly reduced brain injury, both when applied after severe and mild ischemic insults. These data provided the in vivo evidence of the efficacy of fusion proteins in the ischemic brain, thus raising new hopes that neuroprotection is feasible after stroke.



**STIMULATING BRAIN RECOVERY AFTER STROKE WITH CELL THERAPY**

**Michael Chopp**

*Neurology, Henry Ford Health Sciences Center, Detroit MI, USA*

I will describe experiments and data designed to induce restoration of neurological function after stroke and traumatic brain injury in rodents. Both cell and pharmacological therapies can evoke brain plasticity and improve functional outcome after stroke and brain trauma. Two types of cell therapy will be described, bone marrow stromal cell (MSC) therapy and administration of cells derived from the subventricular zone (SVZ). MSCs administered intravenously to young and old rodents with stroke significantly reduce neurological deficits, with benefit persisting for months after treatment. The functional benefits appear to arise from an MSC mediated activation of intact and compromised cerebral tissue, which induces angiogenesis, neurogenesis and synaptogenesis. MSCs produce and induce within the injured brain and microvasculature an array of neurotrophic factors and cytokines, which remodel brain. SVZs likewise restore neurological deficits after stroke. Both cell therapies can be non-invasively monitored by magnetically labeling the cells. In addition to cell mediated brain plasticity, data will be presented demonstrating that agents such as NO donors and compounds that increase brain cGMP and VEGF have a profound benefit on neurological function after stroke and these agents provide an additive therapeutic effect to cell therapy.



## FUNCTIONAL CEREBROVASCULAR ABNORMALITIES IN CADASIL

**Martin Dichgans**

*Department of Neurology, Klinikum Grosshadern, Munich, Germany*

CADASIL is a hereditary small vessel disease related to NOTCH3 mutations. Main vascular characteristics include: vascular smooth muscle cell degeneration, deposition of the extracellular domain of the Notch3 receptor, and deposition of electron dense material within the arterial wall. SPECT, PET, and perfusion MRI studies have demonstrated a reduction in cerebral blood flow (CBF) and cerebral blood volume (CBV) particularly within white matter regions that are hyperintense on T2-weighted images. Consistent with these findings, doppler sonography reveals diminished mean flow velocities in the MCA. These changes might in part relate to a rarefaction of the microvascular tree. Several studies found an impaired cerebrovascular reactivity. Thus, for example, the vasodilatory response to CO<sub>2</sub> and acetazolamide was found to be reduced whereas the vasodilatory response to L-Arginine was significantly enhanced in cerebral blood vessels. Again, altered cerebrovascular reactivity was most pronounced within WML. Treatment with statins over two months had no significant effect on cerebrovascular CO<sub>2</sub> reactivity and the response to L-Arginine. Isolated peripheral blood vessels from CADASIL patients show an enhanced vasoconstrictor response to angiotensin II and reduced tachyphylaxis in the presence of a normal vasodilatory response to acetylcholine and bradykinin. Both structural and functional vascular alterations might contribute to the occurrence of subcortical lesions. Yet, the exact mechanisms underlying such lesions in CADASIL are still unknown.



## TRANSGENIC MICE MODELING CADASIL ARTERIOPATHY HAVE IMPAIRED CEREBROVASCULAR REACTIVITY

Pierre Lacombe, Charleen Oligo, Valérie Domenga, Elisabeth Tournier-Lasserre, Anne Joutel

*Génétique Des Maladies Vasculaires INSERM U740; IFR-6 Lariboisière, Université Paris7, Paris, France*

**Background and Purpose:** CADASIL (cerebral autosomal dominant arteriopathy with subcortical infarcts and leukoencephalopathy) is an inherited small-vessel disease caused by highly stereotyped mutations in NOTCH3 (1,2). Clinical manifestations include recurrent lacunar strokes and cognitive impairment leading to subcortical dementia and premature death. The underlying vasculopathy is characterized by degeneration of vascular smooth muscle cells (VSMC), characteristic deposition of granular osmiophilic material (GOM) and accumulation of Notch3 protein at the cell surface of VSMC. We previously established that VSMC is the primary target of the pathogenic process (3,4). Yet, mechanisms of compromised cerebral hemodynamics in CADASIL remain to be elucidated. Herein, we tested the hypothesis that mutant NOTCH3 impairs the vasomotor function of cerebral vessels. **Methods:** We investigated the in vivo cerebrovascular reactivity in transgenic mice expressing a mutant NOTCH3 in VSMC (TgNotch3R90C). Two independent founder lines, TgMa and TgVe, expressing distinct level of mutant NOTCH3 in the brain (20 and 200% of endogenous murine NOTCH3, respectively) were analyzed. Notch3Tg mice develop an age-dependent arteriopathy similar to that seen in CADASIL patients, but no brain parenchyma lesions (4). Using Laser-Doppler flowmetry in awake TgNotch3R90C and wild-type littermates mice, we assessed the cerebrovascular reactivity to acetazolamide and hypercapnia, which are potent vasodilatory stimuli, and CBF autoregulation during stepwise blood pressure elevations and reductions. Mice were studied at 18 months of age when the CADASIL features are apparent, and at 10 months of age prior to their appearance. **Results:** At 18 month of age, both lines of Notch3Tg mice showed reduced responses to hypercapnia and acetazolamide. Notch3Tg mice also showed higher cerebrovascular resistance during hypertension, and their lower limit of CBF autoregulation was shifted to higher blood pressures. Cerebrovascular responses were similarly impaired in 10 month-old Notch3Tg mice. **Conclusion:** Cerebrovascular reactivity is early compromised in transgenic mice expressing a CADASIL mutant NOTCH3 in VSMC. Data are suggestive of an impaired myogenic response with a decreased relaxation and/or increased resistance. Our recent ex vivo analysis carried out on isolated caudal arteries from these same TgNotch3R90C mice showed a significant increase in pressure-induced contraction and a significant decrease in flow-induced dilation (5). Collectively, our data support that the cerebrovascular tone is increased in TgNotch3R90C mice, with a primary dysfunction of VSMC expressing a mutant NOTCH3. Whether functional deficits and brain parenchyma damages arise from chronic and/or acute hypoperfusions remains to be investigated. (1) Joutel et al. Notch3 mutations in CADASIL, a hereditary adult-onset condition causing stroke and dementia. *Nature* 383: 707-710, 1996. (2) Joutel et al. Strong clustering and stereotyped nature of Notch3 mutations in CADASIL patients. *Lancet* 350: 1511-1515; 1997. (3) Joutel A et al. The ectodomain of Notch3 receptor accumulates within the cerebrovasculature of CADASIL patients. *J Clin Invest.* 105: 597-605; 2000. (4) Ruchoux MM et al. Transgenic mice expressing mutant Notch3 develop vascular alterations characteristic of CADASIL. *Am J Pathol* 162: 329-342; 2003. (5) Dubroca C et al. Impaired vascular mechanotransduction in a transgenic mouse model of CADASIL arteriopathy. *Stroke.* 36:113-7; 2005.

**CBF AND METABOLISM IN DEMENTIA DURING ACTIVATION****Marc J. Mentis***Center for Neurosciences, North Shore - Long Island Jewish Research Institute, Manhasset NY, USA*

Background: Cortical dysfunction in Alzheimer's disease (AD) has cortical (plaque, tangle, cell death) and subcortical (neural modulators, i.e., cholinergic cell loss) causes. One hypothesis for the modest effect of anticholinesterase (AChE) drugs in AD is that augmenting cholinergic function cannot overcome the disruption from local cortical pathology. This hypothesis predicts that AChE drugs should have a profound restorative effect on cortical brain function in an area of brain that has minimal local pathology. The primary striate cortex is relatively free of local pathology. In healthy controls, its response to a pattern flash stimulus is augmented by endogenous muscarinic activity (Mentis et al. *Neuropsychopharmacology*, 2001). Therefore, if cholinergic deficiency is the major cause of dysfunction, AChE drugs should cause marked normalization of function in primary striate cortex of AD patients. Methods: Seven AD patients (mini-mental state exam (MMS)  $10.0 \pm 5$ ) were compared to 19 healthy controls (MMS  $29.0 \pm 5$ ). Each subject watched the pattern flash stimulus at various frequencies during Positron Emission Tomography, first off drug and then again while IV physostigmine was infused. Results: Replicating many studies, and indicative of integrated striate neural activity, the healthy controls showed a biphasic regional blood flow (rCBF) response as flash frequency increased. Compared to controls, the AD group before drug administration had a significantly smaller, but still biphasic rCBF response. After drug, the size of the rCBF response increased toward control levels, however, its biphasic nature (indicative of neural integration) was abolished. Conclusion: The AChE induced increase in primary striate rCBF rather than indicating a return of function toward normal, appeared to represent increased but dysregulated neural activity in the AD group. Thus, even with minimal cortical pathology, cholinergic augmentation alone was unable to markedly improve cortical function. Other neuromodulators (serotonin, norepinephrine, dopamine) are impaired in AD. Perhaps a strategy replacing multiple modulators simultaneously would more successfully restore cortical function in AD.

**CBF AS A DIAGNOSTIC TOOL IN DEMENTIAS: REVISION REQUIRED?**

**Olaf B. Paulson**

*Neurobiology Research Unit, Copenhagen University Hospital, Rigshospitalet, Copenhagen, Denmark*

Dementia has several aetiologies. Common to them all is that they lead to dysfunction of cerebral neurons and thereby to clinical symptoms, and that they disturb cerebral blood flow and metabolism. The causes of dementia may be divided into three categories: degenerative, e.g., Alzheimer's disease (AD), vascular dementias, and dementia due to other causes, e.g., sequela of head trauma. It is well known that advanced dementia irrespective of cause is accompanied by marked changes in cerebral perfusion and metabolism. In most instances the changes in perfusion and metabolism seem to be coupled. More controversial are the questions: 1) To which extent can measurements of CBF be used in the early diagnosis of dementia? and 2) Can CBF measurements be used to distinguish between different types of dementia, especially between vascular dementia and AD? The neural damage in a dementing disease may lead to tissue atrophy as well as to reduction in flow and metabolism. Of major interest is whether an observed flow reduction reflects only tissue loss (less tissue and thus lower total flow in the voxel) or reflects a true reduction of flow in the remaining tissue. With the classical inert gas clearance techniques, Kety Schmidt's original method and Lassen and Ingvar's later method using intraarterial injection of tracer, the measurements yield a direct value of perfusion per gram tissue. Thus, these measurements would be independent of any tissue loss and directly reflect flow in remaining tissue. In contrast, with the more modern tomographic methods the measurements depend heavily on the amount of tracer taken up in the tissue. Thus, in any given voxel the uptake will be proportional to the fraction of tissue present, the so-called partial volume effect. In dementia with atrophy the partial volume correction becomes essential if the aim is to calculate true flow in the remaining tissue. Though the evidence is not conclusive, it seems as if there is a flow and metabolism reduction in addition to the partial volume loss. Vascular dementia typically refers to dementia of vascular origin apart from sequela of major stroke. It might either be caused by multiple small ischemic lesions, potentially with infarction, or to more widespread and diffuse hypoperfusion leading to threatening ischemia. In threatening cerebral ischemia the circulation is often sufficient or only marginally reduced but with daily fluctuation of blood pressure insufficient perfusion may occur if there is no autoregulatory reserve. Also, vasodilatory stimuli like moderate accumulation of carbon dioxide might result in an adverse effect leading to insufficient perfusion in the threatened areas. Such abnormalities would be expected to distinguish vascular dementia from AD. There are many reports of such threatening ischemia, but most studies have been in smaller selected patient groups with signs of insufficient perfusion. In conclusion studies of cerebral blood flow and metabolism in dementing diseases have given us valuable information about pathophysiology. But at present it remains unclear to which extent flow measurement can be used more broadly in the clinical evaluation of patients with memory disturbances and dementing diseases.

## CAN THE PENUMBRA BE DETECTED: MR VERSUS PET IMAGING

Wolf-Dieter Heiss<sup>1</sup>, Jan Sobesky<sup>2</sup><sup>1</sup>Max Planck Institute for Neurological Research, Cologne, Germany<sup>2</sup>Department of Neurology, University of Cologne, Cologne, Germany

**Background and Purpose:** The concept of penumbra is based on animal experiments in which potentially reversible functional disturbances can be observed when blood flow decreases beyond a critical threshold. With reperfusion within a limited time window, these functional disturbances are reversible without leading to morphological damage and irreversible neurological deficits. In the last 20 years, surrogate markers of penumbra and irreversible tissue damage were studied, especially in regard to patients who could benefit from treatment in acute ischemic stroke. Positron emission tomography (PET) has been the gold standard but was replaced by diffusion- (DWI) and perfusion-weighted imaging (PWI) because of its wider distribution and the less complex logistics involved. There are some limitations with conventional DWI/PWI: increased diffusion signals can be reversible, and the determination of the threshold of critical perfusion by PWI is still a matter of ongoing debate. **Methods:** Comparative studies with PET and MRI were performed in 3 groups of patients: (1) In 12 acute stroke patients, results from DWI (median, 6.5 hours after symptom onset) and <sup>11</sup>C-flumazenil (FMZ) PET (median, 85 minutes between DWI and PET) were compared with infarct extension 24 to 48 hours later on T2-weighted MRI. (2) In 11 acute stroke patients, results from PWI (median, 8 hours after symptom onset) were compared with cerebral blood flow measurements obtained with [<sup>15</sup>O]H<sub>2</sub>O PET (interval, 60 minutes between PWI and PET). (3) In 13 patients with acute (n = 6) or chronic stroke (n = 7), results from PWI/DWI were compared with PET of cerebral blood flow and oxygen consumption to detect mismatch or increased oxygen extraction fraction as surrogate markers of penumbra. **Results:** (1) From regions with increased DWI intensity, decreased apparent diffusion coefficient (ADC) and decreased FMZ binding probability curves were computed for eventual infarction, and 95% prediction limits were determined. These limits predicted 83.5% (FMZ), 84.7% (DWI), and 70.9% /ADC) of the final infarct volume. However, the false-positive predictions were much higher for the DWI variables (5.1 and 3.6 cm<sup>3</sup> for DWI and ADC versus a median of 0 for FMZ). (2) The comparison of volumes generated by different time to peak (TTP) thresholds (PWI) and hypoperfusion <20 ml/100g per minute (PET) indicates that a TTP delay of 4 to 6 seconds yields a fair estimate of hypoperfusion. (3) The PWI/DWI mismatch with TTP >4 seconds did not reliably correspond to the penumbra as assessed by PET (oxygen extraction fraction >150%). Only 8 of 13 patients with a mismatch had areas of penumbra. In these cases, the penumbra volume was overestimated by MRI. **Conclusion:** DWI correlates with FMZ results and, with a few exceptions, yields a good estimate of acute tissue damage and final infarct volume. PWI measures seem to be less reliable; the TTP prolongation of >4 seconds assessed only 83% of the volume of hypoperfusion <20 ml/100g per minute. The mismatch volume imprecisely depicts increased oxygen extraction fraction, and, despite its clinical role for selection of patients for eventual therapy, it does not seem to be a reliable correlate of penumbra.

**HOW LONG DOES THE PENUMBRA SURVIVE? NECROTIC VERSUS APOPTOTIC INJURY****Anna M. Planas***Department of Pharmacology and Toxicology, IIBB-CSIC. IDIBAPS, Barcelona, Spain*

Penumbral tissue is subjected to blood flow reduction above the viability threshold. Neurons remain alive while they produce enough energy to maintain their membrane potential, at expenses of suppressing other energy-consuming functions, such as protein synthesis. Disturbances can be transient and not affect tissue viability, for instance protein synthesis inhibition can still reverse after 4h. Yet, this causes cellular stress as evidenced by strong induction of heat-shock proteins. Besides energy restriction, the penumbra is also subjected to dynamic changes generated by a progressively distorted environment. Alterations within the ischemic core propagate to the neighboring penumbra through various mechanisms, including spreading depression, release of soluble pro-inflammatory mediators to the extracellular space, and direct cell-matrix and cell-cell interactions. These factors may exacerbate ongoing changes in the penumbra and promote cell death. Subsequently, viable penumbral neurons become at risk of death if essential cellular functions do not recover in time and cell death programs are activated. The question that arises is: how long penumbral cells are viable? Penumbra viability likely depends on intrinsic cellular vulnerability as neurons are more vulnerable than other cells, and certain neurons are more vulnerable than others. Type of neurotransmitter receptors, cell size, morphology, cytoarchitectural features, networking connections, neuroprotective resources (e.g. antioxidant capacity, calcium binding proteins), and species peculiarities, among others, might contribute to selective neuronal vulnerability. Nonetheless, the duration of the ischemic insult highly determines penumbra viability. Reperfusion can rescue tissue at risk beyond the 3-hour time window established for thrombolysis with rt-PA. The duration of ischemia also determines cell death characteristics. Molecular and biochemical features of programmed cell death occur at core margins in inverse relationship to the duration of ischemia, as signs of apoptosis are more abundant than necrosis after short ischemic episodes. Fifteen to thirty-minutes middle cerebral artery (MCA) occlusion in rats is a good example of extensive signs of apoptosis. Also, after more severe ischemia programmed cell death is higher in regions with rich collateral circulation, whereas it is negligible in areas subjected to intense and prolonged blood flow restriction. Neuronal death can be delayed in several hours in the cortex compared with the striatum after transient MCA occlusion in rats. Heterogeneity in the neuronal reaction to moderate ischemic conditions might cause necrotic and apoptotic-like responses in neighboring cells. Moreover, the possibility that apoptotic-like signals might arise in cells that also show mild necrotic features cannot be excluded, but in this case inhibiting programmed cell death is unlikely to be beneficial. In transient focal ischemia, signs of programmed cell death have been reported from 4 to 24h, and they can persist during days. There is possibly a range of time-windows at which tissue at risk can still be rescued, and the efficacy of treatments targeting cell death programs will depend on whether some tissue remains salvageable. Imaging techniques approach the identification of tissue at risk with the diffusion-perfusion 'mismatch' concept, but cell death can occur long after reperfusion is restored. This calls for new imaging criteria aimed to identify salvageable tissue at protracted time.

**DOES THE PENUMBRA RECOVER: PHARMACOLOGICAL VERSUS HEMODYNAMIC INTERVENTIONS**

**Eng H. Lo**

*Massachusetts General Hospital & Harvard Medical School, Boston MA, USA*

The ischemic penumbra can be defined in many ways, based on measurements of electrophysiologic function, cerebral blood flow, metabolism, and gene expression. But perhaps the most clinically relevant definition is the pharmacologic penumbra, i.e. any brain tissue that can be salvaged after stroke. In theory, there are two non-mutually exclusive ways to salvage the penumbra: hemodynamic reperfusion and pharmacologic treatment. In this presentation, we will (1) review the experimental animal model data to verify how robust neuroprotection data really are for permanent versus transient focal cerebral ischemia, (2) examine the profiles of penumbral collapse as defined by spreading peri-infarct depolarizations with or without reperfusion, and (3) assess existing in vivo imaging data to see how the penumbra responds to reperfusion and therapy. If available, data from the SAINT trials that combine tPA with NXY-059 may also be discussed. Overall, these experimental and clinical data may give insight into the question of whether true neuroprotection in stroke is feasible in the absence of reperfusion.

**IS THERE ROOM FOR REGENERATION: SPONTANEOUS VERSUS INDUCED NEUROGENESIS****Zaal Kokaia**

*Lund Strategic Research Center for Stem Cell Biology and Cell Therapy, Section of Restorative Neurology,  
University Hospital, Lund, Sweden*

Stroke is a common disorder and one of the leading causes of death and disability in humans. In stroke, occlusion of a cerebral artery leads to focal ischemia in a restricted central nervous system region and death of different types of cells. Treatments to support efficient functional recovery in stroke patients are lacking. Cells from different sources have been tested for their ability to reconstruct the forebrain and improve function after transplantation in animals subjected to stroke. The transplanted cells can survive and partly reverse some behavioral deficits. However, the underlying mechanisms are unclear and there is little evidence for neuronal replacement. Recent findings in rodents that stroke leads to increased generation of neurons endogenous precursors in the subventricular zone, suggest an alternative approach to cell therapy in stroke based on regeneration. Stroke-generated new neurons, as well as neuroblasts probably already formed before the insult, migrate into the partially and severely damaged area of the striatum, where they express markers of developing and mature striatal medium-sized spiny neurons. Thus, the new neurons seem to differentiate into the phenotype of most neurons destroyed by the ischemic lesion. Majority of the new neurons die at early stages of their development most likely through apoptotic mechanism, and they only replace a relatively small fraction of the died mature striatal neurons. However, regeneration and re-establishment even of only a small part of damaged neuronal circuitries could have significant implications and support functional recovery. Several factors can induce or promote adult neurogenesis by stimulating formation and/or improving survival of new neurons, e. g., FGF-2, stem cell factor, erythropoietin, BDNF, caspase inhibitors, and anti-inflammatory drugs. Different hormones, environmental factors and physiological stimuli can also modulate adult neurogenesis. Whether the new neurons formed after stroke establish connections with other neurons is not known, though BDNF-generated new neurons in the intact striatum seem to form afferent and efferent connections. There is no significant formation of new neurons in the cerebral cortex after stroke. However, targeted apoptotic degeneration of cortical neurons in mice, leaving tissue architecture intact, leads to formation of new cortical neurons extending axons to the thalamus. Thus, restricted self-repair capacity in ischemically damaged cortex is probably due to lack of cues necessary to trigger neurogenesis from putative local parenchymal neural stem cells or migration of neuroblasts from subventricular zone. If new stroke-generated striatal neurons are fully integrated in the neuronal circuitry and their formation can be stimulated, this could lead to the development of a novel therapeutic strategy for stroke in humans.

**ENERGETIC COSTS ASSOCIATED WITH GLUTAMATERGIC AND GABAERGIC NEUROTRANSMISSION**

**Robin A. de Graaf**, Anant B. Patel, Graeme F. Mason, Douglas L. Rothman, Robert G. Shulman,  
Kevin L. Behar

*MRRC, Yale University, New Haven CT, USA*

Previous studies have shown that the glutamate/glutamine neurotransmitter cycle and neuronal glucose oxidation are proportional (1:1) with increasing neuronal activity above isoelectricity.  $\gamma$ -Aminobutyric acid (GABA), a product of glutamate metabolism, is synthesized from astroglial glutamine and contributes to total 'glutamate/glutamine' neurotransmitter cycling, although the fraction contributed by GABA is unknown. In the present study we used  $^{13}\text{C}$  NMR spectroscopy together with intravenous infusions of [1,6- $^{13}\text{C}_2$ ]glucose, and [2- $^{13}\text{C}$ ]acetate to separately determine rates of glutamate/glutamine and GABA/glutamine cycling and their respective TCA cycles in the rat cortex under conditions of halothane anesthesia and pentobarbital-induced isoelectricity. Under 1% halothane anesthesia GABA/glutamine cycle flux comprised 23% of total (glutamate + GABA) neurotransmitter cycling and 18% of total neuronal TCA cycle flux. In isoelectric cortex glucose oxidation was reduced >3-fold in glutamatergic and GABAergic neurons and neurotransmitter cycling was below detection. Hence, in both cell types the primary energetic costs are associated with neurotransmission, which increase together as cortical activity is increased. The contribution of GABAergic neurons and inhibition to cortical energy metabolism has broad implications for the interpretation of functional imaging signals.

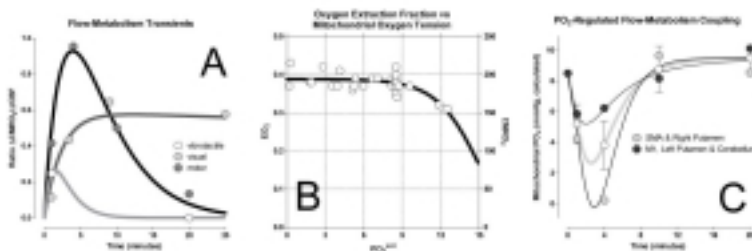
## BRAIN ENERGY METABOLISM: ROLE OF VARIABLE OXYGEN TENSIONS DURING NEURONAL ACTIVITY

Albert Gjedde<sup>1,2</sup>, Manouchehr S. Vafae<sup>1,2</sup>

<sup>1</sup>*PET Center, Aarhus University Hospitals, Aarhus, Denmark*

<sup>2</sup>*Center of Functionally Integrative Neuroscience, Aarhus University, Aarhus, Denmark*

We developed an equation which relates blood flow and oxygen metabolic rates in the brain to the oxygen tension in mitochondria (Gjedde et al. (2005) Cerebral metabolic response to low blood flow: Possible role of cytochrome oxidase inhibition. *J Cereb Blood Flow Metab* 25: in press). The equation is based on the assumption that net delivery of oxygen to brain tissue (J) is regulated by the tissue's conductivity of oxygen (L). Then, the difference between the respective average tensions of oxygen in brain capillaries and mitochondria (PO<sub>2cap</sub> for capillaries, PO<sub>2mit</sub> for mitochondria):  $J = L (PO_{2cap} - PO_{2mit})$ . This equation can be modified by the Hill equation of oxygen's saturations of hemoglobin in arteries and veins (SaO<sub>2</sub> and SvO<sub>2</sub>), which are functions of oxygen's tension in the capillaries, the Hill coefficient (h), and oxygen's half-saturation tension (P50):  $J = L (P50 [(SaO_2 + SvO_2)/(2 - SaO_2 - SvO_2)]^{1/h} - PO_{2mit})$ . This formula was used to evaluate the relationship between increments of brain work and average mitochondrial oxygen tensions. Increments of brain work were obtained by finger-tapping motions at the rate of 3 steps per second during PET-scanning for blood flow and oxygen consumption. Visual cortex stimulation sustains prolonged increases of oxygen consumption, but motor activity sustains a biphasic change of oxygen consumption in which the later decline correlates with exertion and fatigue (panel A). Oxygen's saturation of arteries and cerebral veins were computed from blood samples and the net extraction fraction of oxygen, and mitochondrial oxygen tensions were computed from the equation. The extraction fraction varied little (panel B), despite substantial focal changes of oxygen consumption, revealing matching relative increments of blood flow and oxygen consumption, and consequently declining mitochondrial oxygen tensions, at the highest rates of oxygen consumption measured in SMA and right putamen (panel C). The conclusion that declining oxygen tension in key centers of the brain limits activity is supported by evidence of declining oxygen tension in brain prior to central fatigue caused by exertion in athletes in whom energy reserves still exist in muscle (Nybo & Secher (2004) *Prog Neurobiol.* 72: 223-61, Nybo et al. (2003) *Acta Physiol Scand.* 179: 67-74). The progressive decline of oxygen tensions in brain mitochondria during activity, and the sensitivity of exertion to this decline, may explain fatigue in general and the need to sleep in particular.



INV-29

**THE DEGREE OF HETEROGENEITY IN METABOLIC DEMAND AND BLOOD FLOW  
AS MEASURED BY PET**

**Iida Hidehiro**, Hayashi Takuya, Watabe Hiroshi, Kudomi Nobuyuki, Piao Rishu, Teramoto Noboru, Youichirou Ota, Koshino Kazuhiro, Enmi Junichiro, Kim Kyeong-Min, Inomata Toru, Zeniya Tsutomu, Sato Sato, Yamamoto Atsushi, Yamauchi Miho

*Department Inv Radiology, National Cardiovascular Center Research Institute, Suita City, Japan*

It has been believed that direct and accurate assessment of local CMRO<sub>2</sub> and CBF is feasible using <sup>15</sup>O-labeled oxygen and PET in vivo. This is true, provided that the local radioactivity concentration is measured accurately, and that the kinetics of <sup>15</sup>O-oxygen is well modeled by a suitable model formulation. The fact is that the <sup>15</sup>O-oxygen is metabolized in the brain instantaneously to become a labeled-water, being cleared by CBF, and that the metabolized water contributes to the PET assessment, thus requiring a correction for this process. A recent technique has enabled shortening the examination time, and demonstrated a relationship of transient changes of oxygen demand and blood flow during various physiological and/or pathophysiological conditions. Experiments during neuronal activations or during decreased oxygen delivery demonstrated evidences that changes of CBF are not controlled to directly (or stoichiometrically) couple with those of CMRO<sub>2</sub>, and suggested that magnitude of the uncoupling depends on several physiological factors such as oxygen availability, capillary structure and hemoglobin contents. Effective oxygen diffusibility (EOD) has been proposed as an index to clarify the oxygen diffusion process between the capillary and cerebral tissue. Theoretical simulation also suggested possible error sources in the methodology which could be responsible to clarify the regional variation of the CMRO<sub>2</sub>/CBF uncoupling.

**NO WAY! O<sub>2</sub>/NO/BLOOD FLOW INTERACTIONS IN BRAIN**

**Donald G. Buerk**

*Physiology Department, University of Pennsylvania School of Medicine, Philadelphia PA, USA*

The role that NO plays in control of regional blood flow with increased neural activity in the brain is controversial. We have shown from direct electrochemical measurements with microelectrodes that there are transient decreases in tissue pO<sub>2</sub> (Ances et al. *Neurosci. Lett.* 306:106-110, 2001) and increases in tissue NO (Buerk et al. *NeuroImage* 18:1-9, 2003) that precede increases in blood flow during functional activation of the rat somatosensory cortex with electrical stimulation of the forepaw. More recent NO measurements have been made in mouse olfactory cortex in response to different odors. These observations prompt many other questions: Does inhibition of oxidative metabolism by NO play a role in mediating blood flow responses? Is there an increase in O<sub>2</sub> used by NO synthases to produce NO? Are there different sensitivities of nNOS and eNOS to O<sub>2</sub>? What role do astrocytes play in the control of blood flow? Does NO interact with cyclooxygenase and epoxygenase pathways? Can predictive dynamic mathematical models for coupled NO and O<sub>2</sub> transport incorporating nonlinear coupling of blood flow and metabolism with neural activity be developed based on experimental observations? (Supported in part by NIH 068164)

**PLASTICITY AND RECOVERY AFTER STROKE. INTRODUCTION**

**Barbro B. Johansson**

*Department of Clinical Neuroscience, Experimental Brain Research, Wallenberg Neuroscience Center,  
BMC A 13, Lund, Sweden*

The adult brain retains a capacity for plasticity and functional reorganization throughout the life span and most stroke surviving stroke patients improve to some extent with time. The mechanisms involved may vary with post-ischemic time, type and location of the lesion. Since the time of Hebb more than half a century it is known that environment and experience can enhance neuronal connectivity, and it was long ago proposed that reorganization of cortical representation areas, 'cortical maps', is a neuroanatomical basis for plasticity after stroke (Jenkins and Merzenich, Brain 1987). Nevertheless, surprisingly little research was directed towards brain plasticity after stroke before the last decade. Specific training methods have now been shown to induce cortical reorganization after stroke in humans. On the cellular and molecular level, experimental data indicate that post-ischemic housing in a stimulating (enriched) environment increases the number of dendritic spines, influences gene expression and endogenous stem cell proliferation and/or differentiation. The symposium includes two experimental and two clinical presentations. Mathias Hoehn will present rodent data on in vivo tracing and functional evaluating of exogenous stem cells, and the differentiation and possible integration of the cells as studied with immuno-histochemistry. Anis Mir will up-date how monoclonal antibodies to the neurite growth inhibitory molecule Nogo-A may improve functional after focal brain ischemia, and present evidence that corticospinal and subcortical plasticity may contribute to the beneficial effect. The development of clinical diagnostic and neuroimaging techniques has greatly improved the possibilities for longitudinal studies of the rehabilitation process in humans, and a challenge is how to correlate brain imaging with functional gains. Cathrin Bütefisch will review the diagnostic and therapeutic use of transcranial magnetic stimulation, and how the method may be used to elucidate potential mechanisms in brain plasticity. Richard Frackowiak will demonstrate how the dynamic plasticity of cortical maps after stroke can be elucidated with functional MRI, and how changes over time may relate to functional outcome.

**ANTI-NOGO-A ANTIBODY INFUSION IMPROVES BEHAVIORAL OUTCOME AND CORTICOSPINAL PLASTICITY AFTER EXPERIMENTAL STROKE****Anis K. Mir**<sup>1</sup>, Christoph Wiessner<sup>1</sup>, Martin Rausch<sup>1</sup>, Martin E. Schwab<sup>2</sup>, Gwendolyn L. Kartje<sup>3</sup><sup>1</sup>*Neuroscience Research, Novartis Institutes for BioMedical Research, Basel, Switzerland*<sup>2</sup>*Brain Research Institute, University of Zurich, Zurich, Switzerland*<sup>3</sup>*Neurology and Research Service, Hines VA Hospital, Hines IL, USA*

Stroke is associated with high incidence of mortality and functional disabilities. There is no specific treatment to improve functional recovery after the acute stage of stroke except extensive rehabilitation which results in limited improvement. The main reason for the limited recovery is that regeneration and plastic “hardware“ changes in the adult central nervous system are extremely restricted after injury. One of the most potent neurite growth inhibitory molecules in myelin is Nogo-A, a membrane protein comprising multiple inhibitory domains. There is a growing body of literature documenting the effects of Nogo-A neutralization on neuronal regeneration and plasticity and recovery of functional deficits after CNS lesions in adult rats. Monoclonal antibodies neutralizing the inhibitory effect of Nogo-A have been evaluated in experimental stroke. Intraventricular infusion of Nogo-A antibody resulted consistently in improvements in recovery of skilled forelimb reaching ability when treatment was initiated 24 hours after focal cerebral ischemia induced by photothrombosis or permanent middle cerebral artery occlusion (MCAO) in normotensive or spontaneously hypertensive adult rats, respectively. Nogo-A antibody treatment was also effective in 1.5 year aged rats with 7 days delayed treatment following MCAO. Improvement in function in these studies was associated with increased corticospinal mid line crossing fibers to cervical spinal cord and the thalamus from the intact hemisphere. Moreover, using functional magnetic resonance imaging a significant increase in activation was found in the thalamus during stimulation of the previously impaired forepaw in the animals that had recovered with anti-Nogo-A therapy. These results suggest that neuroanatomical changes in corticospinal plasticity and subcortical regions, ie the thalamus, may contribute to the functional recovery after Nogo-A antibody treatment. The mechanism of action of Nogo-A antibodies likely involves steric hindrance of the inhibitory domains of Nogo-A and down regulation of the protein by internalization of the Nogo-A-antibody complex. These results suggest that treatment with Nogo-A antibodies bears potential as a new rehabilitative treatment for ischemic stroke and the window of opportunity for treatment is much longer as compared to neuroprotective treatment approaches.

**CAN EXOGENOUS STEM CELLS IMPROVE OUTCOME AFTER EXPERIMENTAL STROKE?  
THE CHALLENGE OF COMBINED MRI IMAGING OF STEM CELL DYNAMICS, CELL  
DIFFERENTIATION AND FUNCTIONAL OUTCOME**

**Mathias Hoehn**, Ralph Weber, Pedro Ramos-Cabrer, Susanne Wegener, Dirk Wiedermann,  
Ekkehard Küstermann, Uwe Himmelreich

*Max-Planck-Institute For Neurological Research, Cologne, Germany*

Conventional therapies of stroke have so far demonstrated limited success. Cerebroprotective drugs have been extensively and rather successfully investigated in animal experiments. In the clinical environment, however, all drugs have failed so far. Thrombolysis is the only strategy with successful translation from experimental into clinical neurology. Experimental and clinical research on thrombolysis of stroke has extensively documented that it will prevent further expansion of the ischemic lesion by stabilizing the penumbral tissue but it will not reverse the damage of the early irreversibly damaged ischemic core area. The recent breath-taking developments in stem cell biology have motivated the evaluation of the therapeutic potential of endogenous or implanted stem cells as a cell replacement therapy for stroke. Arvidsson et al. (1) demonstrated a significant activation of neurogenesis in the subventricular zone of ischemic rats while the lab of Helen Hodges (2) reported on migration of implanted ES cells towards the lesion periphery in ischemic rats, followed by outcome improvements relative to animals without cell implantations. Using fMRI two groups investigated the spontaneous functional improvement and activation potential of the somatosensory cortex of rats following induction of stroke reporting a transient re-organization process, during which the representation area was shifted to the contralateral, undamaged hemisphere during a transition period (3,4). While some investigators looked at histological evolution of the lesion after treatment with stem cell implantation, no study focussed on the mechanisms of behavior improvements in these treated situations: restitution of function of the original representation area or plasticity dependent re-organization, enhanced by the stem cell interaction with the host organ. Such investigations present an enormous challenge on the design and execution of a complex experimental protocol. On the one hand, the evolution of the lesion must be characterized in parallel with the fate of the implanted stem cells (migrational dynamics to the target zone; cell specific differentiation). On the other hand, a potential therapeutical success must be evaluated in its temporal development. Finally, mechanisms explaining a potential outcome improvement are of great interest. Most recent investigations are exploring the potential contribution of molecular imaging techniques and have reported the in vivo monitoring of stem cell migration in rat (5) and mouse brain after stroke (6). The present contribution will demonstrate the possibilities (and limits) of non-invasive imaging modalities for the characterization of the lesion and the (implanted) cell mobility, while the functional fate (e.g. differentiation status) is described by way of immuno-histochemistry. Parallel investigations on the functional deficit and outcome improvement, respectively, are presented. Mechanisms responsible for a functional improvement (spatial reorganization vs recovery of primary representation field) can be studied by longitudinal fMRI studies of anesthetized animals, allowing the localization of activated brain areas. 1) A. Arvidsson et al. *Nature Med.* 8, 963 (2002); 2) T. Veizovic et al. *Stroke* 32, 1012-1019 (2001); 3) M. Abo et al. *NeuroReport* 12, 1-5 (2001); 4) R.M. Dijkhuizen et al. *JCBFM* 21, S310 (2001); 5) M. Hoehn et al. *Proc.Nat.Acad.Sci. USA* 99, 16267-16272 (2002); 6) D.E. Kim et al. *Stroke* 35, 952-957 (2004)

**MECHANISMS AND MODULATION OF PLASTICITY IN MOTOR CORTEX AND ITS  
IMPLICATION FOR RECOVERY AFTER STROKE. STUDIES WITH TRANSCRANIAL  
MAGNETIC STIMULATION**

**Cathrin M. Bütefisch**

*Department of Neurology, WVU, Morgantown, WV, USA*

The adult brain maintains the ability for plasticity throughout life. The underlying mechanisms are of major interest as plasticity plays an important role in learning and functional recovery after injury to the brain. An important concept derived mainly from stimulation experiments in animals is that of a distributed neuronal network where multiple overlapping motor representations are functionally connected through an extensive horizontal network. By changing the strength of horizontal connections between motor neurons, functionally different neuronal assemblies can form, thereby providing a substrate to construct dynamic motor output zones. Modulation of GABAergic inhibition and synaptic efficacy such as long-term potentiation (LTP) are mechanisms involved. Transcranial magnetic stimulation (TMS) provides means to study changes of the human corticospinal motor output system and intracortical inhibitory and excitatory networks in response to different stimuli in humans. In combination with drugs that either block or enhance TMS evoked responses, neurotransmitter systems mediating the observed effects can be identified. Using this combined approach we were able to identify NMDA receptor activation and GABAergic inhibition as mechanisms operative in use-dependent plasticity in intact human motor cortex. Further, d-amphetamine, a drug that operates by increasing monoaminergic transmission, enhances this process. Another approach is the application of TMS to motor cortex that is engaged in generating training movements in a Hebbian type paradigm. The important role of GABAergic inhibition was also demonstrated for other forms of plasticity in human motor cortex. Transient deafferentation of the forearm induced by a blood pressure cuff that is inflated above systolic blood pressure across the elbow results in a rapid reduction of GABAergic inhibition and increase of the motor cortical output to muscles proximal to the ischemic block. This approach was applied to patients after stroke. Motor practice of the paretic hand during deafferentation of the upper arm, produced by plexus anaesthesia, improved hand motor function dramatically. In addition to these processes involving intact neuronal tissue of motor cortex in the affected hemisphere, changes in excitability of contralateral homotopic motor cortex has been described. Specifically, the balance of excitatory and inhibitory activity was shifted towards an increase of excitatory activity. This shares similarities to mechanisms implicated as relevant for reorganizational processes after experimental brain injury and may be relevant for functional recovery after stroke.

**FUNCTIONAL AND STRUCTURAL NEUROIMAGING STUDIES OF PLASTICITY AND FUNCTIONAL RECOVERY****Richard S. Frackowiak***Wellcome Department of Imaging Neuroscience, UCL, London, UK*

Imaging neuroscience describes the functional organization of human brain at the level of large neuronal groupings, networks and systems. A systems level of description addresses how integrated brain functions are embodied in the physical structure of the brain. Magnetic resonance imaging (MRI) is now the modality of choice in structural and functional imaging neuroscience. The analysis of structural and functional brain images can nowadays be carried out automatically using statistical parametric mapping (SPM). The resultant ability to perform clinical-functional-anatomical correlative studies in life with complete objectivity and unparalleled sensitivity is providing powerful new opportunities for the study of brain pathology and plasticity. One of the most exciting and dramatic observations to come from human brain mapping with a wide range of structural and functional techniques is the dynamic plasticity of function in the brains of patients with strokes. Recent activation studies have provided interesting information about the brain's capacity to reorganise after such injury and in association with practice and learning that constitute the bedrock of rehabilitation. Though presently in the realm of basic physiology, the study of brain plasticity and its modulation by drugs and other therapies indicates a novel approach to the rehabilitation of stroke damaged adults. Brain maps must be viewed as dynamic, changing with development, disease progression and in the recovery of function after acute injury. The dynamic plasticity of functional brain maps provides an exciting opportunity to study these processes. References 1. Ward NS, Brown MM, Thompson AJ, Frackowiak RSJ. (2003) Neural correlates of motor recovery after stroke: a cross-sectional fMRI study. *Brain* 126, 1430-1448. 2. Ward NS, Brown MM, Thompson AJ, Frackowiak RSJ. (2003) Neural correlates of recovery after stroke: a longitudinal fMRI study. *Brain* 126: 2476-2496. 3. Ward NS & Frackowiak RSJ. (2003) Age-related changes in the neural correlates of motor performance. *Brain* 126, 873-888 4. Good CD, Johnsrude IS, Ashburner J, Henson RNA, Friston KJ, Frackowiak RSJ. (2001) A voxel-based morphometric study of ageing 465 normal adult human brains. *NeuroImage* 14, 21-36.

## PET IMAGING OF DA NEUROTRANSMISSION USING AGONIST VERSUS ANTAGONIST RADIOTRACERS

Nathalie Ginovart<sup>1,2</sup>, Matthaeus Willeit<sup>1</sup>, Ariel Graff<sup>1</sup>, Shitij Kapur<sup>1,2</sup>, Alan A. Wilson<sup>1,2</sup>

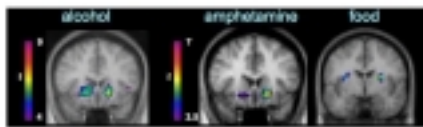
<sup>1</sup>*PET Centre, Centre for Addiction and Mental Health, Toronto, Canada,*

<sup>2</sup>*Department of Psychiatry, University of Toronto, Toronto, Canada*

An increasingly important and intriguing application of positron emission tomography (PET) is to measure endogenous levels of neurotransmitters in vivo in both man and animals. Direct measurement of neurotransmitter levels is not achieved; rather the technique hinges on the competition between the levels of endogenous neurotransmitter and the PET radiotracer. In this context, changes in endogenous levels of dopamine (DA) have been extensively studied using the antagonist PET radioligand [11C]-raclopride. However, even though, the “raclopride-displacement” technique is widely used and has already provided important empirical findings in diseases and normal neurophysiology, it suffers from major methodological limitations. Some of these limitations have led to a re-assessment of the simple competition model used in this PET paradigm. We recently obtained in vitro and in vivo preclinical data supporting a mixed competitive and non-competitive action of DA on [11C]-raclopride binding, a finding that can reconcile the short-lasting changes in DA levels and the long-lasting changes in “raclopride-displacement” observed after amphetamine. However, limitations to the model still exist and, in particular, it is noteworthy that a substantial portion of antagonist radiotracer binding is impervious to DA manipulations. The so-called “ceiling effect” to the “raclopride-displacement” can be related directly to the inability of the antagonist radiotracers to distinguish low- from high-affinity states D2-receptors. Currently, there is tremendous emphasis on developing agonist D2-radioligands to circumvent this limitation. By competing directly for the same high affinity sites as DA, a full agonist radiotracer at the D2-receptor should exhibit increased sensitivity to DA levels when compared to antagonists, and also should show full displacement at very high levels of endogenous DA. We are at a moment of opportunity for testing these hypotheses as we recently developed the D2-agonist radiotracer [11C]-(+)-PHNO for this purpose. Pre-clinical evaluation demonstrated that [11C]-(+)-PHNO is selective for D2-receptors and showed an increased sensitivity to endogenous DA when compared to [11C]-raclopride, making it a very promising radioligand for imaging the high affinity state D2-receptor using PET. Preliminary work in humans demonstrated that [11C]-(+)-PHNO has favourable in vivo kinetics and displays a high signal to noise ratio in brain. The aim of this talk is to describe some of our experiences in the field. The focus will be primarily on imaging DA neurotransmission using PET, comparing and contrasting [11C]-raclopride and [11C]-(+)-PHNO. The ability to selectively probe the functionally active state of D2-receptors with [11C]-(+)-PHNO should increase our understanding of critical pathophysiological changes that occur in a number of DA-related illnesses such as schizophrenia, Huntington’s disease and Parkinson’s disease.

**HUMAN DOPAMINE RESPONSE TO DRUGS AND NATURAL REWARDS****Alain Dagher***Montreal Neurological Institute, McGill University, Montreal QC, Canada*

The anhedonia hypothesis of drug addiction posits that drugs of abuse target the same neural systems as natural rewards such as food and sex. The most likely candidate brain region is the mesolimbic dopamine system. In animals, dopamine is released in the ventral striatum, or nucleus accumbens, in response to food, sexual mates, and to almost all drugs of abuse. There are several predictions one can make from the anhedonia hypothesis: (1) dopamine release in response to reinforcers will correlate with the degree of pleasure experienced; (2) natural reinforcers and drugs of abuse will release dopamine in the same brain areas; (3) aversive stimuli will not release dopamine. These predictions can be tested with PET experiments in human subjects. The method we use consists in comparing the binding potential of the D2 ligand [<sup>11</sup>C]raclopride in baseline and activation conditions. Studies in humans: Oral amphetamine and alcohol caused dopamine release in the ventral striatum in humans. The effect was greater in individuals with the novelty-seeking personality, a risk factor for addiction. The effect did not correlate with pleasure. However, while alcohol and amphetamine caused dopamine release in the ventral striatum, two natural rewards (money and food) targeted the main body and dorsal portion of the striatum. Thus there may be a dissociation between natural and drug rewards with respect to dopamine transmission. Another possibility is that conditioned rewarding stimuli target different brain regions than novel ones. We provided evidence for this second explanation by measuring dopamine release in response to smoking cigarettes in habitual smokers. Cigarette smoking caused dopamine release in the dorsal striatum. Finally, human and animal data suggest that hyper-responsiveness of the dopamine system may be a risk factor for addiction. How does dopamine hyper-responsiveness develop? We investigated this issue using two paradigms. We showed that poor parental bonding early in life was associated with a greater dopamine response to mental stress in adulthood. We also demonstrated sensitization in human subjects: we showed that repeated doses of oral amphetamine caused an enhanced response to subsequent amphetamine. This effect persisted after one year.



**EFFECTS OF TRANSIENT REDUCTION OF ENDOGENOUS 5-HT LEVELS ON 11C-DASB AND 11C-MDL100907 SPECIFIC BINDING: IMPLICATIONS FOR FINDING A SEROTONERGIC RADIOTRACER VULNERABLE TO ENDOGENOUS COMPETITION IN HUMANS**

**Peter S. Talbot**

*Department of Psychiatry, Columbia University College of Physicians & Surgeons, New York NY, USA*

Serotonin (5-HT) neurotransmission is involved in the normal regulation of affect and cognition, and its dysfunction is implicated in a range of mental disorders. However, there is currently no method to directly assess 5-HT synaptic levels in the living human brain. In the human dopamine (DA) system, baseline receptor occupancy by endogenous DA can be estimated by measuring the effects of DA depletion on the binding of certain radioligands through endogenous competition, particularly in striatum. For example, the measured increase in 11C-raclopride and 123I-IBZM binding following acute DA depletion implies a baseline D2 receptor occupancy of ~ 10% in healthy humans. Brain 5-HT can be transiently and safely reduced by rapid tryptophan depletion (RTD), a technique involving the ingestion of an amino acid mixture lacking L-tryptophan, the dietary precursor of 5-HT. We have used RTD in healthy humans in an attempt to demonstrate a measurable effect of reduced 5-HT on the specific binding of the selective 5-HT transporter (SERT) ligand 11C-DASB and the selective 5-HT<sub>2A</sub> receptor antagonist ligand 11C-MDL100907. However, values of regional specific binding were not significantly different between the reduced endogenous 5-HT and control conditions for either tracer. These results suggest that PET with 11C-DASB or 11C-MDL100907 is not sensitive to the decreased concentration of synaptic 5-HT following RTD, and that neither tracer has the potential for measuring changes in synaptic levels of 5-HT *in vivo*. Imaging techniques relying on endogenous competition would ideally require a brain region with high synaptic levels of, and significant baseline receptor occupancy by, endogenous neurotransmitter. However, *in vivo* microdialysis studies in non-human primates suggest that extracellular 5-HT concentration is very low (< 0.5 nM) across brain regions and is 1 – 2 orders of magnitude lower than striatal DA levels. In the case of the 5-HT<sub>2A</sub> receptor, this concentration is significantly below the estimated K<sub>D</sub> of 5-HT for the receptor configured in a state of high affinity for agonists (~ 1.3 nM). Moreover, *in vitro* studies suggest that the proportion of receptors configured in a state of high affinity for agonists, and therefore potentially available to endogenous 5-HT, is low (~ 13%). Together, these values suggest that baseline occupancy of 5-HT<sub>2A</sub> receptors by 5-HT may be only approximately 2%, making changes following increased or decreased 5-HT unmeasurable by current techniques in humans. Agonist serotonergic radioligands may be expected to be superior for endogenous competition studies, but have so far been unsuccessful in humans. Efforts to experimentally increase baseline receptor occupancy (for example by pretreatment with selective 5-HT reuptake inhibitor medication) prior to RTD may be of interest. However, the insensitivity of current tracers to endogenous competition implies that they may be used to measure differences in SERT or 5-HT<sub>2A</sub> receptor availability between populations or during therapy without the need to consider concomitant changes in neurotransmitter concentration.

## CAN WE MEASURE 5-HT RELEASE WITH PET?

Paul M. Grasby<sup>1,2</sup><sup>1</sup>*Imperial College London, London, United Kingdom*<sup>2</sup>*MRC CSC, London, United Kingdom*

Imaging of endogenous neurotransmitter release using PET is an exciting and valuable technique in understanding human in vivo neurochemistry (1). Endogenous neurotransmitter imaging has been demonstrated for dopamine and possibly for endogenous opioids, however the extension of this technique to other neurotransmitter systems remains to be established. The exact reasons why the binding of select radiotracers appear to be sensitive to endogenous neurotransmitter are not established although simple competitive occupancy or receptor internalisation models are predominant theories. Presently, we are investigating the possibility of imaging endogenous 5-HT release using selective PET radiotracers. In studies in man we have established that neither acute tryptophan depletion or tryptophan infusion (to putatively lower and raise central 5-HT respectively) had any effect on 11C-WAY 100635 binding to 5-HT<sub>1A</sub> receptors (2). Furthermore, acute and chronic treatment with SSRIs (expected to raise intrasynaptic 5-HT levels) did not alter 11C-WAY 100635 binding. Similarly, 5-HT<sub>1A</sub> occupancy by exogenous 5-HT agonist drugs has proved difficult to image in man (3, 4). However, such manipulations in man may be sub-optimal for altering central 5-HT levels and therefore the effect of substantial increases of endogenous serotonin on 11C-WAY 100635 and 11C-MDL 100907 binding was investigated in rat brain in vivo (5, 6). Binding studies were complemented by in vivo microdialysis to monitor 5-HT levels in similarly treated isoflurane-anaesthetised rats and by early gene expression studies. 11C-WAY 100635 and 11C-MDL 100907 proved to be generally insensitive to increased synaptic 5-HT in our rodent models. Theoretically, such minimal effects may be explained by many factors including a low baseline occupancy of the 5-HT<sub>1A</sub> and 5-HT<sub>2A</sub> receptor by 5-HT in vivo, a low proportion of high affinity sites to which endogenous 5-HT binds, or in the case of 11C-MDL 100907, the high concentration of 5-HT<sub>2A</sub> receptors located intracellularly and hence beyond interaction with synaptic 5-HT. A similar lack of sensitivity of other serotonergic radioligands (18F-Altanserin, 18F-MPPF, 11C-DASB) has been observed in some other PET centres. In summary, the characteristics of the 5-HT neurotransmitter system, rather than the radioligands per se, may partly explain the current difficulties in imaging 5-HT release. 1. Laruelle, J *Cereb Blood Flow Metab* 20: 423-451 (2000) 2. Rabiner et al. *NeuroImage* 15: 620-632 (2002) 3. Rabiner et al, *J Psychopharmacology*, 16:195-199 (2002) 4. Bantick et al. *Neuropsychopharmacology*, 29: 847-859 (2004) 5. Hume et al. *Synapse*, 41:150-159 (2001) 6. Harani et al. *Synapse* 50:251-60 (2003)